

Automotive Lubricants and Testing

Simon C. Tung
George E. Totten
Editors

SAE *International*[®]



Automotive Lubricants and Testing

Simon C. Tung and George E. Totten, EDITORS

ASTM Stock Number: MNL62



INTERNATIONAL
Standards Worldwide

ASTM International
100 Barr Harbor Drive
PO Box C700
West Conshohocken, PA 19428-2959

SAE*International*[®]

Copublished with SAE International
400 Commonwealth Drive
Warrendale, PA 15096-0001, USA
SAE Order Number R-428

Library of Congress Cataloging-in-Publication Data

Automotive lubricants and testing / [edited by] George E. Totten, Simon C. Tung.

p. cm. — (Automotive lubricants and testing handbook)

“ASTM Stock Number: MNL62.”

Includes bibliographical references and index.

ISBN 978-0-8031-7036-0 (alk. paper)

1. Lubrication and lubricants—Testing. 2. Automobiles—Lubrication—Testing. I. Totten, George E. II. Tung, Simon.

TL153.5.A976 2012

629.222—dc23

2012021696

Copyright © 2012 ASTM International, West Conshohocken, PA. All rights reserved. This material may not be reproduced or copied, in whole or in part, in any printed, mechanical, electronic, film, or other distribution and storage media, without the written consent of the publisher.

ASTM Photocopy Rights

Authorization to photocopy items for internal, personal, or educational classroom use of specific clients is granted by ASTM International provided that the appropriate fee is paid to ASTM International, 100 Barr Harbor Drive, PO Box C700, West Conshohocken, PA 19428-2959; Tel: 610-832-9634; online: <http://www.astm.org/copyright/>

ASTM International is not responsible, as a body, for the statements and opinions advanced in the publication. ASTM International does not endorse any products represented in this publication.

Copublishers:

ASTM International

100 Barr Harbor Drive

PO Box C700

West Conshohocken, PA 19428-2959, USA

Phone: 610-832-9585

Fax: 610-832-9555

E-mail: service@astm.org, Website: www.astm.org

ISBN: 978-0-8031-7036-0

ASTM Stock Number: MNL62

SAE International

400 Commonwealth Drive

Warrendale, PA 15096-0001, USA

Phone: 877-606-7323 (inside USA and Canada)

724-776-4970 (outside USA)

Fax: 724-776-0790

Email: CustomerService@sae.org

Website: www.sae.org

ISBN: 978-0-7680-7889-3

SAE Order Number R-428

Contents

Introduction	v
Part 1: Automotive Tribology and Lubrication Fundamentals	1
Chapter 1—Fundamental Principles of Contact and Lubrication	3
<i>Q. Jane Wang, Herbert S. Cheng</i>	
Chapter 2—Automotive Lubricants.	23
<i>Derek Mackney, Nick Clague, Gareth Brown, Gareth Fish, John Durham</i>	
Chapter 3—Lubricant Properties and Characterization.	47
<i>Kenneth O. Henderson, Chris J. May</i>	
Chapter 4—Controlling Lubricant Degradation through Performance Specification	61
<i>Malcolm F. Fox</i>	
Chapter 5—Elastohydrodynamic Lubrication Film Tests and Tribological Bench Tests.	85
<i>Q. Wang, Simon C. Tung, Y. Liu, Y. Zhang, D. Zhu</i>	
Chapter 6—Automotive Engine Hardware and Lubrication Requirements.	105
<i>Edward P. Becker, Simon C. Tung</i>	
Part 2: Automotive Lubricant Testing, Lubricant Performance, and Current Lubricant Specifications	117
Chapter 7—Gasoline Engine and Diesel Engine Powertrain Systems	119
<i>P. Silva</i>	
Chapter 8—Automotive Bearing Systems—Journal Bearings	129
<i>Omar Mian</i>	
Chapter 9—Testing and Evaluation of Lubricating Greases for Rolling Element Bearings of Automotive Systems	137
<i>Xinglin Li, Can Wu, Baojie Wu, Hongyu Zhang, Jianbin Luo, Qiang Feng</i>	
Chapter 10—The Drivetrain System	157
<i>Dave Simner</i>	
Chapter 11—Gear Oil Screen Testing with FZG Back-to-Back Rig	177
<i>Klaus Michaelis, Brian M. O'Connor</i>	
Chapter 12—Problems and Opportunities Regarding the Lubrication of Modern Automotive Engines	191
<i>E. S. Yamaguchi, G. A. Tanaka, K. Matsumoto</i>	
Chapter 13—Bench Performance Test Methods for Lubricated Engine Materials	215
<i>Peter Blau, Simon C. Tung</i>	
Chapter 14—Current and Future Specification of Lubricant Performance	231
<i>Malcolm F. Fox</i>	
Chapter 15—Automatic Transmission Lubricants	255
<i>Richard J. Vickerman, Craig Tipton</i>	
Chapter 16—Other Automotive Specialized Lubricant Testing Including Manual Transmission, Rear Axle, and Gear Box Lubricant Testing and Specification	273
<i>Dave Simner</i>	
Chapter 17—Design for Reduced Wear	293
<i>Roger Lewis, Tom Slatter</i>	
Chapter 18—Nonpetroleum-Based, No/Low-Sulphur, Ash, and Phosphorous, and Bio-No-Toxicity Engine Oil Development and Testing	317
<i>Mathias Woydt</i>	
Part 3: Specialized Automotive Lubricant Testing and Future Automotive Applications	331
Chapter 19—Current and Future Advances in Materials Development for Tribological Applications	333
<i>Barbara Rivolta, Lauralice Canale</i>	

Chapter 20—Surface Analysis and Tribochemistry of Automotive Engine Components	351
<i>Ardian Morina, Hongyuan Zhao</i>	
Chapter 21—Tribology and Fine Automotive Mechanical Systems	379
<i>Werner Friedrich Stehr</i>	
Chapter 22—Analysis of In-Service Automotive Engine Oils	399
<i>Jim C. Fitch</i>	
Chapter 23—Diesel Fuel Lubrication and Testing	417
<i>Jun Qu</i>	
Chapter 24—Filters and Filtration Testing of Automotive Fuels and Lubricants	427
<i>Gary Bessee, Erica Clark-Heinrich</i>	
Chapter 25—Dynamic Friction Characterization and Modeling of Tripod Constant Velocity Joints	437
<i>Chul-Hee Lee, Andreas A. Polycarpou</i>	
Chapter 26—Biobased Automotive Lubricants	455
<i>Lou A. Honary</i>	
Appendix: List of Referenced Documents	469
Index	481

Introduction

The automotive and petroleum industries are facing difficult international competition, government regulations, and rapid technological changes. Ever-increasing government regulations require improved fuel economy and lower emissions from automotive fuel and lubricant systems. Higher energy-conserving engine oils and better fuel-efficient vehicles will become increasingly important with increasing emphasis on saving resources and reducing engine friction. Identification of industry research needs for reducing friction and wear in transportation are critical for improving fuel economy and extended vehicle reliability. There are hundreds of tribological components, from bearings, pistons, transmissions, and clutches, to gears and drivetrain components. The application of tribological principles is essential for motor vehicle reliability and energy conservation.

Automotive Lubricants and Testing will provide a comprehensive overview of various lubrication aspects of a typical powertrain system, including the engine, transmission, driveline, and other components, and will address major issues and the current development status of automotive lubricant test methods. In North America, engine design engineers and tribologists are constantly challenged to create innovative products that meet more demanding emissions and fuel economy targets. Current research and development on engine cylinder components include new designs, materials, coatings, and surface treatments with the goals of weight reduction, longer life, higher operating temperatures, and reduced friction. To assist the automotive industry in achieving lower emission standards, higher fuel economy, and longer drain intervals, the petroleum industries and additive suppliers are developing low-SAP (sulphur, ash, and phosphorous) fuels and higher fuel-efficient performance lubricants.

Automotive Lubricants and Testing covers lubrication fundamentals and lubricant testing methods that are influenced by lubricant additive formulation and engine hardware changes. There are few existing publications that provide such a correlation between test methods and lubricant formulation technology. The most current ASTM specifications and all current International Lubricant Standards Advisory Committee approval systems for automotive engine lubricants are included in this text.

In addition, current standard test methods for automotive lubricants and the other bench test methods or test simulations developed for the powertrain system are reviewed. Although much of this handbook is focused on powertrain systems and engine lubricants, other automotive lubricants such as transmission oils, chassis lubricants, gear lubricants, and lubricating greases are also covered. Tribological bench test methods and automotive specialized lubricant testing to be used in a laboratory or mechanical devices for simulation of engine or powertrain system operating conditions are also described.

The lubricant in a powertrain system is subjected to very complex wear conditions in different parts of the engine. These conditions are due to variable patterns of driving behavior and lubricant contamination by reactive combustion gases and particulates that create difficulties in the correlation of actual engine/lubricant performance with simple bench tests. Therefore, a key feature of engine oil development and testing is the use of real engine tests to assess lubricant behavior in the complex combination of conditions present in an engine. *Automotive Lubricants and Testing* also covers the major test methods for typical engine components (gasoline and diesel), engine oil characteristics, engine material evaluations, and the current industrial standard test methods for chassis and drivetrain systems. Included are detailed descriptions of the tribological testing challenges associated with various automotive engine components, service effects on automotive lubricants, standard bench and engine sequence test development, and updated engine oil specifications for gasoline and diesel engine lubricants.

This handbook contains 26 chapters covering the powertrain, transmission, chassis, and drivetrain systems. In addition, the advanced lubrication and tribochemistry of powertrain systems have been included, such as diesel fuel lubrication, specialized automotive lubricant testing development, and biodegradable automotive lubricants. In addition, we have generated an appendix that includes abbreviations and technical terms, all ASTM reference documents, and updated standard test methods for engine oils, transmission lubricants, gear lubricants, and grease.

Simon C. Tung and George E. Totten, Editors

Part 1: Automotive Tribology and Lubrication Fundamentals

Fundamental Principles of Contact and Lubrication

Q. Jane Wang¹ and Herbert S. Cheng¹

1.1 INTRODUCTION

Tribological interfaces involving contact and relative motion are everywhere in modern machinery for power transmission and function accomplishment. Automotive power generation and drivetrain systems, as well as many other motion control systems, contain various tribological interfaces. The contact of components produces stresses and the relative motion between surfaces results in rubbing. Therefore, a tribological interface is an environment where energy is consumed and materials are worn out; it is also the critical location where many failures are initiated. Designing energy-efficient and robust mechanical systems requires understanding of tribological interfaces, and the theories of contact and lubrication are two fundamental areas. This chapter summarizes fundamental theories and practices of surface, contact and lubrication analyses.

1.2 ENGINEERING SURFACE AND SURFACE ANALYSIS

1.2.1 *Engineering Surfaces and Commonly Used Observation Instruments*

Engineering surfaces are complex and they are rough in nature, no matter which machining methods are used in finishing processes and how smooth they are polished. Surface irregularities representing the deviation of a real surface from an ideally smooth one compose a micro- or nanoscopic view of mountainous peaks and valleys. The peaks, or summits, are usually named as asperities; the overall surface appearance is referred to as topography and the structure of surface features as texture.

Engineering surfaces can be viewed with a scanning electron microscope (SEM), a scanning tunneling microscope (STM), and an atomic force microscope (AFM), as well as various optical microscopes. Surface details can be digitized with the assistance of an AFM, an STM, a white-light interferometer, a stylus profilometer, or a laser profilometer.

A SEM utilizes an electron beam focused to a sample surface spot of nanometer size. The image magnification is the ratio of the display size over the scanned surface area. Signals of interest include secondary electrons, backscattered electrons, and X-rays [1]. STM and AFM are scanning probe microscopes. STM uses an atomically sharp metallic tip and the sample to be studied as two electrodes of a tunnel junction. AFM also uses a sharp tip to probe a sample surface. However, it combines the principle of STM and stylus profilometry [2] and measures ultra-small

forces present between its probe tip and a sample surface by means of sensing the deflection of a flexible cantilever beam where the tip is attached. A stylus profilometer has a sharp diamond tip that “reads” surface height information and an amplifier that sends the signal to a receiving device. During a measurement, the tip moves on the surface to be characterized. The major advantage of this type of instrument is its convenience to use because the stylus profilometer may be portable and small enough to be attached to a machine surface for in situ and online surface inspection. However, profile distortion is inevitable because the stylus tip size is not atomically sharp. A white-light interferometer is one of the optical interferometers. However, it uses white light instead of a single-wavelength light because when a single short-wavelength light is used, measurement between adjacent depth points is limited to one quarter of the light wavelength, making the measurement of rougher surfaces difficult. The use of white light overcomes such difficulty.

Surfaces are not homogeneous. A surface may have several layers. The properties of surface layers may be different from that of the bulk material. Bhushan considers that, from the top to the bulk, there exist a physisorbed layer, a chemisorbed layer, a chemically reacted layer, a Beilby layer, and then a heavily deformed layer and a lightly deformed layer. He also indicated that the Beilby layer was produced by melting and surface flow during machining of molecular layers subsequently hardened by quenching as they were deposited on the cool underlying material [3]. Buckley [4] described a metal surface with three layers on a bulk metal: a worked layer next to an oxide layer, which is underneath an adsorbed layer of gases and water moisture. Although these considerations are not identically the same, they all indicate the complex nature of materials of engineering surfaces. Layer structure may be observed with a SEM, a transmission electron microscope (TEM), and X-ray diffraction (XRD). Material and chemical properties of layers may be characterized by means of an energy dispersive X-ray spectroscope (EDX), an X-ray photoelectron spectroscope (XPS), an Auger electron spectroscope (AES), an ion-scattering spectrometer (ISS), an electron probe microanalyzer (EPMA), X-ray fluorescence (XRF), and a secondary ion mass spectrometer (SIMS).

1.2.2 *Surface Statistical Analysis*

Digitization of an engineering surface results in a numerically represented surface, or profile. The size of the numerical

¹ Northwestern University, Evanston, IL, USA

surface is determined by the sampling range, and the datum interval reflects the measurement resolution. Although each measurement yields a deterministic map of a portion of a surface topography, surfaces of engineering components are random. Therefore, determining basic surface statistical parameters, surface height distribution, texture composition information, and asperity orientation is the goal of surface statistical analysis.

1.2.2.1 WAVINESS AND ROUGHNESS

A surface may have irregularities at different scales. Waviness and roughness explain some of them. Furthermore, the roughness shown in a larger scale may become the "waviness" in a smaller scale. The resolution of the measurement instrument used for surface digitization and the parameters used in the measurement determine the level of features to be observed.

1.2.2.2 SURFACE STATISTICAL ANALYSIS, STATISTICAL FUNCTIONS, AND PARAMETERS

A two-dimensional profile for height (z) taken along a traverse distance (x) may be used to illustrate statistical concepts and parameter determinations. Most of the analyses in this section are based on these types of profiles for simplicity.

1.2.2.2.1 Probability Density Function

In the following, z is the coordinate for surface profile height and x is the traverse direction. The entire z domain for the profile height analysis is first divided into several intervals for which the width is dz , or Δz for discrete data. Counting the heights within one of the intervals yields the number of frequency counts, and all frequency counts result in a histogram (or a bar chart) of height distribution.

The probability density function (PDF) is defined as frequency count $Fc_i(z)$ divided by the height datum interval, Δz .

$$\phi(z_i) = Fc_i(z)/\Delta z \quad (1.1)$$

Note that integration of the PDF over all z results in 1.

$$\int_{-\infty}^{\infty} \phi(z) dz = \sum_1^M \frac{Fc_i(z)}{\Delta z} dz = \sum_1^M Fc_i(z) = 1 \quad (1.2)$$

1.2.2.2.2 Mean, Centerline Average, and Standard Deviation or RMS Roughness

Several statistical parameters for a surface profile of N data can be readily analyzed from the corresponding digitized data matrix [5,6]. The mean, μ , or mathematical expectation, determines the centerline of surface texture heights.

$$\mu = \text{average}(z) = \int_{-\infty}^{\infty} z\phi(z) dz = E(z) = \sum_1^M z_i Fc_i(z) = \frac{1}{N} \sum_1^N z_i \quad (1.3)$$

Centerline average R_a is one of the indications of surface roughness. It reveals the degree of profile height deviation from the centerline.

$$R_a = \text{average} |z - \mu| = \frac{1}{N} \sum_1^N |z_i - \mu| = \int_{-\infty}^{\infty} |z - \mu| \phi(z) dz \quad (1.4)$$

The standard deviation, R_q , or the RMS roughness, is another measurement of surface roughness.

$$R_q = \sqrt{E(z - \mu)^2} = \left(\int_{-\infty}^{\infty} (z - \mu)^2 \phi(z) dz \right)^{1/2} = \left(\frac{1}{N} \sum_1^N (z_i - \mu)^2 \right)^{1/2} \quad (1.5)$$

The PDF for many engineering surfaces is Gaussian. With the assistance of mean and standard deviation, the normal and exponential distributions can be defined as follows:

$$\phi(z) = \frac{1}{R_q \sqrt{2\pi}} e^{-\frac{(z-\mu)^2}{2R_q^2}} \quad (1.6)$$

1.2.2.2.3 Probability Function, Cumulative Distribution Function, and Bearing Area

The cumulative distribution function, F , the probability function, Pr , and the bearing area, BA , at a particular height, z_0 , can be determined for a given PDF. The probability, Pr , for z to be in between z_1 and z_2 can be calculated by integrating the PDF from z_1 to z_2 , as given in eq. 1.7 below.

$$Pr(z_1 \leq z \leq z_2) = \int_{z_1}^{z_2} \phi(z) dz \quad (1.7)$$

The distribution function, F , at z_0 is the accumulative value of the PDF for $z \leq z_0$, or the probability of $z \leq z_0$.

$$F(z_0) = Pr(z \leq z_0) = \int_{-\infty}^{z_0} \phi(z) dz \quad (1.8)$$

The bearing area, BA , counts for percentage of asperities in "contact" with a flat surface of a rigid body at $z = z_0$.

$$BA(z_0) = \int_{z_0}^{\infty} \phi(z) dz = 1 - F(z_0) \quad (1.9)$$

1.2.2.2.4 Skewness and Kurtosis

Skewness and kurtosis are two commonly used parameters for an asperity height distribution function. Skewness, Sk , is defined as the third statistical moment of $(z - \mu)$. Continuous and discrete forms are as follows:

$$Sk = \frac{\int_{-\infty}^{\infty} (z - \mu)^3 \phi(z) dz}{R_q^3} = \frac{1}{R_q^3 N} \sum_1^N (z_i - \mu)^3 \quad (1.10)$$

Kurtosis, K , is defined as the fourth statistical moment of $(z - \mu)$. Continuous and discrete forms are as follows:

$$K = \frac{\int_{-\infty}^{\infty} (z - \mu)^4 \phi(z) dz}{R_q^4} = \frac{1}{R_q^4 N} \sum_1^N (z_i - \mu)^4 \quad (1.11)$$

The skewness of a surface may be positive or negative. It is zero if the surface topography is symmetric about its mean. However, kurtosis is always positive and nonzero. For a surface with a Gaussian height distribution, the skewness should be zero because of symmetry and kurtosis should be 3. Negative skewness can be related to deep valleys of a surface topography, which appear in the PDF as the tail to the left. Likewise, positive skewness is due to tall asperities, which result in a tail to the positive right side of the corresponding

PDF. On the other hand, a surface with kurtosis greater than that of a Gaussian distribution, which is 3, may have high peaks and deep valleys and is called leptokurtic whereas a surface with kurtosis less than 3 may have fewer sharp peaks and shallower valleys and is called platykurtic.

1.2.2.2.5 Autocorrelation Function, Correlation Length, and the Peklenik Number

The PDF, $\phi(z)$, yields statistical information about a surface, mainly on the deviation from the mean. However, surfaces having the same centerline average or RMS roughness values may possess very different topographic structure. Sinusoidal functions of the same amplitude but different frequencies, triangular and trapezoidal functions of the same peak-valley value but different spans are some of the examples. Autocorrelation function is a spatial structural function commonly used to reveal the structural information of a surface.

Mathematically, the autocorrelation function, $R(l)$, of height profile function $f(x)$ is the integration of the product of the latter by its shifted form over the entire domain of x . l is the distance of shift along the x direction. The autocorrelation function, $R(l)$, and its nondimensional form, $r(l)$, are as follows:

$$R(l) = E(z(x)z(x+l)) = \frac{1}{N - N_l} \sum_{i=1}^{N-N_l} (z_i(x)z_i(x+l))$$

$$= \lim_{L \rightarrow \infty} \frac{1}{L} \int_0^L z(x)z(x+l) dx \quad (1.12)$$

Here, L is the sampling length, l is the shift in x , and N_l is the number of data within l .

$$r(l) = R(l) / R_0^2 \quad (1.13)$$

It is easily seen that when $l = 0$, the autocorrelation function, $R(l)$, becomes the RMS roughness and the nondimensional autocorrelation function, $r(l)$, becomes 1.

The correlation length, l^* , measures how quickly a random event decays. It is the value of l over which $r(l)$ drops to $A\%$ of its value at the origin (which is 1, or the square of the RMS roughness when dimensional). Here, $A\%$ may be 10, 20, 37 (or 36.8%, which is $1/e$), or 50%, all commonly seen in research papers.

The correlation length may be used to determine the orientation of surface roughness. A parameter (Peklenik number), γ , is defined as the ratio of the correlation lengths in two orthogonal directions:

$$\gamma = l_x^* / l_y^* \quad (1.14)$$

The Peklenik number indicates surface texture orientation. $\gamma = 1$, or approximately 1, indicates an isotropic surface, and a transverse surface can be defined by $\gamma \ll 1$. The term “transverse” implies that the “ridges” of asperities characterized by the x -direction correlation length are perpendicular to the direction of the relative motion of the surfaces.

Therefore, three typical surface orientations— isotropic, longitudinal, and transverse—can be characterized with $\gamma = 1$, $\gamma \gg 1$, and $\gamma \ll 1$. Figure 1.1 illustrates the asperity footprints of such surfaces [7]. Note that the footprints of

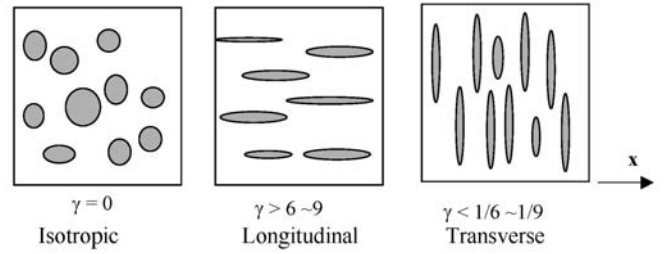


Figure 1.1—Illustration of asperity orientations.

longitudinal and transverse surfaces are similar. Rotating one for 90° results in the other. Patir and Cheng [7] used $\gamma = 9$ as the required large number to define a longitudinal surface. Later, Lee and Ren [8] found that $\gamma = 6$ should be sufficient for a clear longitudinal orientation.

Engineering surfaces may appear to be fractal. Similar to the length of a coastline as a function of the length of the ruler used to do the measurement, the surface topography is sensitive to the imaging resolution except that the scale of interest in the surface height and lateral directions are different. Readers may find detailed fractal theories for surface analyses in the work reported by Mandelbrot [9]; Majumdar and Bhushan [10]; Yan and Komvopoulos [11]; Borodich, Keer, and Harris [12]; and Wang [13].

1.3 CONTACT OF ENGINEERING SURFACES

Contacts of engineering surfaces are usually classified into two large categories: conformal and nonconformal (including counterformal). A conformal contact exists between a convex surface and a concave surface whereas a counterformal contact happens between convex bodies. The contact of two nominally flat surfaces is considered to be nonconformal. The contact area of a counterformal contact is usually much smaller than the dimension of the contacting bodies; therefore, the surface deformation can be described by the integral of a Green's function. Solutions to nonconformal contact problems may all be formulated by means of Green's functions. These solutions are also applicable to the interaction between the rolling elements and the races of a rolling-element bearing, where contacts are highly concentrated on small surface areas.

On the other hand, conformal contact involves a convex and concave surface of nearly the same radii of curvatures. The contact in a journal bearing is a good example. The finite element method is commonly used in conformal contact studies. Because the solution for a highly conformal contact is dependent on structure, no general formulas can be derived for contact area or contact pressure.

This section only discusses counterformal, or concentrate, contacts of homogeneous materials, where classic contact theories apply and solutions are in several groups of convenient formulas. Counterformal contacts may be further classified into line contact (cylindrical contact, Figure 1.2) and point contact (circular contact, Figure 1.3), and the latter may be more generally named as elliptical contact. A pair of spur gear teeth at contact may be simply considered as two equivalent cylinders with radii R_{e1} and R_{e2} of the curvatures of the two surfaces at the contact location. In Figure 1.3, each equivalent body has two radii, R_{e1}^1 and R_{e1}^2 , for body 1 and R_{e2}^1 and R_{e2}^2 for body 2, corresponding to two orthogonal principal curvatures.

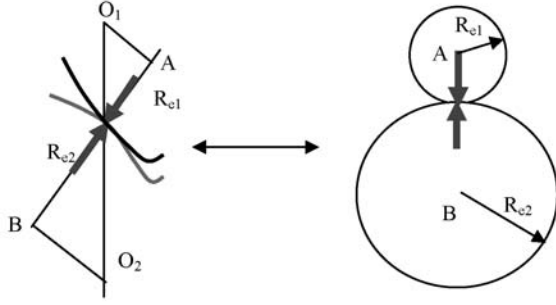


Figure 1.2—Spur-gear tooth contact and equivalent cylinders in contact.

1.3.1 Mechanics for the Contact between Two Elastic Cylinders (Line Contact)

Figure 1.4 shows two cylinders of infinite length under a load distributed along their entire length. Before any load is applied, the ideal contact footprint should be a line. When the load in a line-distribution, P , is applied, the contact area increases and becomes a rectangle with a width of $2a$. Increase in load widens the contact region. This is a plane strain problem, and in each cross section along the length direction, the contact geometry and pressure distribution are the same.

Figure 1.5 illustrates the deformations caused by a concentrated force at $x = 0$ and a distributed load, both acting on a unit length of a surface. The Flamant solution (eq. 1.15) is needed to describe the pressure-displacement relationship.

The left figure in Figure 1.5 is for the normal deformation, du_z , caused by a concentrated line load, P , at $x = 0$, which is mathematically expressed as [14]

$$du_z(x) = -\frac{2(1-\nu)P}{\pi E} \ln|x| + C \quad (1.15)$$

Here, C is an integration constant, E is the Young's modulus, and ν is the Poisson's ratio of the material. The core of this equation is the Green's function having a singularity at the point of the load application where the displacement tends to be infinite. One needs to select a reference point, x_r , which should be sufficiently far away from the region of interest. Therefore, the displacement is defined with respect to this reference point.

$$du_z(x) = du_z(x) - du_z(x_r) = -\frac{2(1-\nu)P}{\pi E} \ln\left|\frac{x}{x_r}\right| \quad (1.16)$$

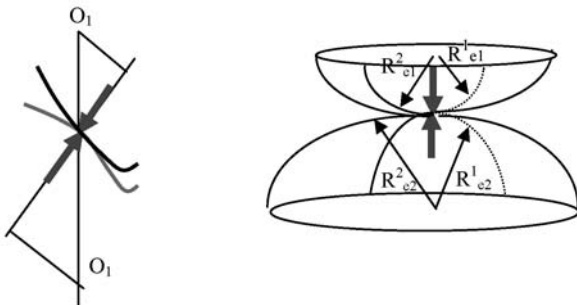


Figure 1.3—Helical-gear tooth contact and equivalent elliptical bodies in contact.

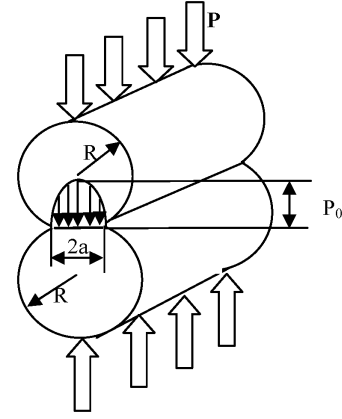


Figure 1.4—Pressure and deformation in a line contact.

The normal surface displacement, $u_z(x)$, at location x , due to the distributed load, $p(\xi)$, shown in the right plot in Figure 1.5 is the integration of eq. 1.16 over the loading region, Ω .

$$u_z(x) = -\frac{2(1-\nu^2)}{\pi E} \int_{\Omega} \ln\left|\frac{\xi-x}{\xi-x_r}\right| p(\xi) d\xi \quad (1.17)$$

Here, coordinate ξ corresponds to the load distribution. The stress components are as follows:

$$\begin{aligned} \sigma_x &= -\frac{4P}{\pi^2 a} \int_{-a}^0 \sqrt{1-\frac{\xi^2}{a^2}} \left[\frac{z(x+\xi)^2}{[(x+\xi)^2+z^2]^2} \right] d\xi \\ &\quad - \frac{4P}{\pi^2 a} \int_0^a \sqrt{1-\frac{\xi^2}{a^2}} \left[\frac{z(x-\xi)^2}{[(x-\xi)^2+z^2]^2} \right] d\xi \\ \sigma_z &= -\frac{4P}{\pi^2 a} \int_{-a}^0 \sqrt{1-\frac{\xi^2}{a^2}} \left[\frac{z^3}{[(x+\xi)^2+z^2]^2} \right] d\xi \\ &\quad - \frac{4P}{\pi^2 a} \int_0^a \sqrt{1-\frac{\xi^2}{a^2}} \left[\frac{z^3}{[(x-\xi)^2+z^2]^2} \right] d\xi \\ \tau_{xz} &= -\frac{4P}{\pi^2 a} \int_{-a}^0 \sqrt{1-\frac{\xi^2}{a^2}} \left[\frac{z^2(x+\xi)}{[(x+\xi)^2+z^2]^2} \right] d\xi \\ &\quad - \frac{4P}{\pi^2 a} \int_0^a \sqrt{1-\frac{\xi^2}{a^2}} \left[\frac{z^2(x-\xi)}{[(x-\xi)^2+z^2]^2} \right] d\xi \end{aligned} \quad (1.18)$$

1.3.2 Mechanics for the Contact between Two Elastic Balls (Point Contact)

Figure 1.6 shows two balls of equal sizes under a normal load, W . Before any load is applied, the ideal contact footprint should be a point. When load is applied, the contact area increases and becomes a circle of radius a . Increase in load enlarges the contact region. The surface of a half-space shown in Figure 1.7 is under normal loading in the area marked by S . Normal pressure $p(\xi, \eta)$ at point (ξ, η) is shown, and the deformation at point (x, y) is as follows:

$$u_z(x, y) = \frac{(1-\nu^2)}{\pi E} \iint_S \frac{p(\xi, \eta)}{\sqrt{(x-\xi)^2 + (y-\eta)^2}} d\xi d\eta \quad (1.19)$$

This is the Boussinesq equation for surface normal deformation due to the application of p , which can be solved

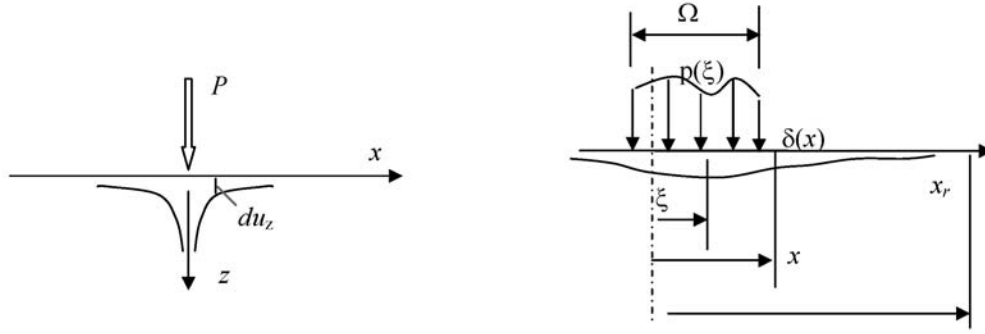


Figure 1.5—Two-dimensional elastic deformation caused by a concentrated line load, P , at $x = 0$ (left) and a distributed line load in region Ω (right).

through numerical integration once the distribution of p is known.

1.3.3 Solutions for Cylindrical and Spherical Contacts

Generally, a contact can be mathematically treated as an equivalent elastic body interacting with a rigid flat with the use of the equivalent radius of curvature R_e given in eq. 1.20 and the contact modulus, E' , or the equivalent Young's modulus, defined in eq. 1.21 in terms of the Young's modulus and Poisson's ratio of both contact materials:

$$\frac{1}{R_e} = \frac{R_1 \pm R_2}{R_1 R_2} \quad (1.20)$$

$$\frac{1}{E'} = \frac{1-\nu_1^2}{E_1} + \frac{1-\nu_2^2}{E_2} \quad (1.21)$$

For cylindrical line contact problems, the semicontact width, a , and the maximal contact pressure, p_0 , are

$$a = 2\sqrt{\frac{PR_e}{\pi E'}} \quad p_0 = \sqrt{\frac{PE'}{\pi R_e}} \quad (1.22)$$

For spherical point contact problems, the contact radius, a , and the maximal contact pressure, p_0 , are

$$a = \sqrt[3]{\frac{3WR_e}{4E'}} \quad p_0 = \frac{1}{\pi} \sqrt[3]{\frac{6WE'^2}{R_e^2}} \quad (1.23)$$

Here, P for line contact is load per unit length of contact, and W for point contact is the total load.

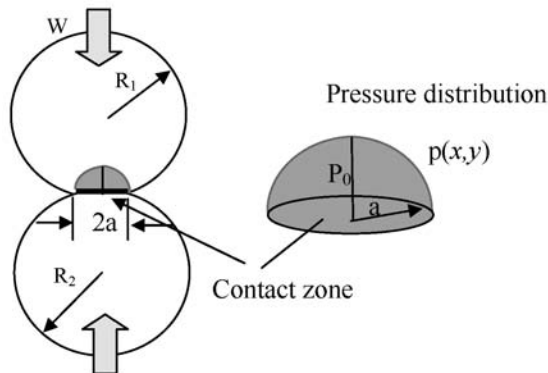


Figure 1.6—Contact of two equal elastic balls.

Figure 1.8 presents an example of the von Mises stress distribution due to the combined effect of pressure and frictional shear.

1.3.4 Contact between Nominally Flat Rough Surfaces

1.3.4.1 STATISTIC MODEL

Asperities may deform due to loading. The situation of the contact between two nominally flat surfaces may be simply viewed as many Hertzian contacts of asperities at the microscale. Ling [15] and Greenwood and Williamson [16] pioneered the investigation of contact involving a rough surface. In Greenwood and Williamson's analysis, asperities were assumed to have spherical summits of the same radius of curvature, β . The contact behavior of individual asperities was studied by using the Hertzian contact formulas mentioned in the previous section. A surface height probability density distribution function, $\phi(z)$, was then used to obtain the contact area and total contact load with respect to a prescribed surface separation, d . An elastic contact limit was derived, which indicated that material plastic flow occurred at the maximal Hertzian pressure to be 0.6 times the hardness of a metallic material. In this type of model, interaction between neighboring asperities, surface work hardening, surface layer properties, and friction are neglected.

Greenwood and Tripp [17] further investigate the statistical asperity contact models involving two rough surfaces of Gaussian height distributions. The profile height for surface 1 is z_1 and for surface 2 is z_2 . The composite RMS roughness is $R_q = [R_{q1}^2 + R_{q2}^2]^{1/2}$, where R_{q1} and R_{q2} are the RMS roughness values of the contact surfaces. The asperity peak density is η , and the apparent contact area is A . Therefore, the number of asperities in A is ηA . The asperity tip shape is assumed to be parabolic with a tip

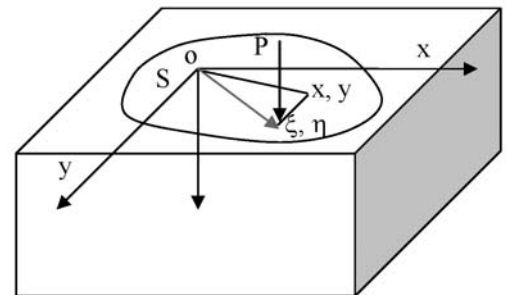


Figure 1.7—Half-space under normal loading p .

equivalent radius of curvature of $\beta/2$ because the geometry of asperities of both surfaces is assumed to be the same. The equivalent Young's modulus of materials is E' . The separation of the two surfaces, measured at the centerline of each surface roughness, is d .

The following basic relationships were derived by Greenwood and Trip, on the basis of the Hertz theory, for a given normal approach, δ , between one pair of asperities.

$$\text{Contact area for one asperity: } A_0 = \pi (\beta/2) \delta \quad (1.24)$$

$$\text{Load on the asperity: } P = \frac{4}{3} E' \sqrt{\frac{\beta}{2}} \delta^{3/2} \quad (1.25)$$

The total contact force and real contact area can then be obtained.

$$\text{Total contact force: } P(d) = 2\pi\eta^2 A \int_z \int_r P(\delta, r) \phi(z) r dr dz \quad (1.26)$$

$$\text{Total area of contact: } A(d) = 2\pi\eta^2 A \int_z \int_r A_0(\delta) \phi(z) r dr dz \quad (1.27)$$

They summarized the contact pressure for two rough surfaces with a normal surface height probability density distribution and a composite roughness of R_q in an elastic contact:

$$p(d) = 2 \cdot K \cdot E' \cdot F_{5/2} \left(\frac{d}{R_q} \right) \quad (1.28)$$

$$\text{where } K = \frac{8\sqrt{2}}{15} \pi (\eta\beta R_q)^2 \sqrt{\frac{R_q}{\beta}}.$$

Here, at a given height, z , the number of asperities in a differential area is $\eta(2\pi r) dr d\phi(z) dz$, and the number of asperities in the mating surface is $A\eta$.

Patir and Cheng [7] empirically treated eq. 1.28 with a further assumption that $\eta\beta\sigma$ is a constant within 0.03–0.05 on the basis of research of a number of engineering surfaces. This treatment results in a convenient form of the pressure-gap relationship:

$$\begin{cases} p(d) = 2KE'D(H^* - \frac{d}{R_q})^z & \text{for } d/R_q < H^* \\ p(d) = 0 & \text{for } d/R_q \geq H^* \end{cases} \quad (1.29)$$

where

$$D = 4.4086 \times 10^{-5},$$

$$z = 6.804,$$

$$H^* = 4, \text{ and}$$

$$K = 0.003 \text{ for } R_q/\beta = 0.01$$

$$\text{Note that in eq. 1.29 } \frac{2}{E'} = \frac{1-\nu_1^2}{E_1} + \frac{1-\nu_2^2}{E_2}.$$

1.3.4.2 DETERMINISTIC CONTACT SIMULATIONS AND NUMERICALLY DEVELOPED STATISTICAL MODELS

Numerical rough surface contact models have been developed to deterministically analyze contact pressure and area. These include isothermal contact simulations, such as the works done by Lee and Cheng [18], Lee and Ren [8], Ju and Farris [19], Yu and Bhushan [20], Nogi and Kato [21],

Hu, Barber, and Zhu [22], Ai and Sawamiphakdi [23], and Polonsky and Keer [24], and thermal-mechanical contact analyses, such as the works reported by Ting and Winer [25], Liu and Wang [26], and Liu and Wang [27]. Through analyzing many rough surfaces, statistical results can be obtained and convenient formulas can be curve fit. Lee and Ren's [8] deterministic-statistic approaches represent one group of such efforts. Because the numerical simulation models are built on eqs. 1.17 and 1.19, no asperity summit radius assumption is needed, and asperity interaction is automatically included. Empirical equations for contact pressure and contact area were obtained through mathematical regression from a sufficiently large number of numerical simulations. From Lee and Ren [8], the three-dimensional (3-D) contact pressure and the average gap for surfaces with a normal height distribution have the following relationships:

$$\frac{h_T(\lambda, H_Y, \bar{P}(\theta_j, z_k))}{R_q} = \exp \left\{ \sum_{i=0}^4 (\bar{\lambda}_G^T [G_i] \bar{H}_Y) (\bar{P}(\theta_j, z_k))^i \right\} \bar{P} < H_Y \quad (1.30a)$$

$$\frac{h_T(\lambda, H_Y, \bar{P}(\theta_j, z_k))}{R_q} = 0.0 \quad \bar{P} \geq H_Y \quad (1.30b)$$

The corresponding real contact area can be solved from the following relationships:

$$\frac{a_r(\lambda, H_Y, \bar{P}(\theta_j, z_k))}{a_{nom}} = \left\{ \sum_{i=0}^4 (\bar{\lambda}_A^T [A_i] \bar{H}_Y) (\bar{P}(\theta_j, z_k))^i \right\} \bar{P} < H_Y \quad (1.31a)$$

$$\frac{a_r(\lambda, H_Y, \bar{P}(\theta_j, z_k))}{a_{nom}} = 1.0 \quad \bar{P} \geq H_Y \quad (1.31b)$$

Here, $\bar{\lambda}_A^T = [1, \lambda, \lambda^2, \lambda^3]$, $\bar{\lambda}_G^T = [1, \lambda^{-1}, \lambda^{-2}, \lambda^{-3}]$, and the transpose of \bar{H}_Y is $\bar{H}_Y^T = [1, H_Y^{-1}, H_Y^{-2}, H_Y^{-3}]$. $[A_i]$ and $[G_i]$ are parametric matrices given by Lee and Ren [8]. Note that here the aspect ratio is expressed by λ in their work.

The asperity contact pressure and the real contact area can be expressed, respectively, as

$$P_c(\theta_j, z_k) = C_{pr} \cdot \bar{P}(\theta_j, z_k) \quad (1.32)$$

$$A_r = \sum_{A_{nom}} \left(a_r(\theta_j, z_k) R_B \Delta\theta_j \Delta z_k \right) \quad (1.33)$$

Here, C_{pr} is the pressure dimensional parameter.

1.3.5 Advanced Contact Analyses

1.3.5.1 CONTACT OF COATED SURFACES

Contact involving layered surfaces has become a common scenario because of the application of surface coatings. Ling [28] and Johnson [14] presented the mechanics ground for the analysis of contacts of coated bodies. Holmberg and Mathews [29] systematically described the tribological mechanisms pertinent to thin coatings in sliding contacts from the aspects of views of macromechanical, micromechanical, and tribochemical changes as well as material transfer. Their work defined four major parameters to model the tribological contact process: the coating-to-substrate hardness relationship, the thickness of the

coating, the surface roughness, and the size and hardness of any debris in contact, which may originate from external sources or be produced by wear.

Many have investigated contacts of layered materials and here are several examples. Plumet and Dubourg [30] investigated a multilayered body under normal and tangential loadings. Leroy, Floquet, and Villechaise [31] studied the thermomechanical behavior of multilayered surfaces. The effects of friction coefficient, layer thickness, and elastic modulus of coating materials on contact pressure distribution were studied by Cole and Sayles [32] and Mao, Sun, and Bell [33]. They found that soft coatings were beneficial to contact-pressure reduction. The influence of roughness and layer properties on contact stresses was investigated with the use of the Hankel transform. Goryacheva, Sadeghi, and Nickel [34] investigated the effect of a viscoelastic layer and surface roughness on normal pressure and internal stresses of an elastic indenter in sliding contact with a layered semi-infinite plane. In their studies, the surface roughness was described as a periodic system of cylindrical asperities. More research on the contact involving coated surfaces can be found in work done by Polonsky and Keer [24] and Liu and Wang [35]. Liu, Peyronnel, Wang, and Keer [36,37] recently developed convenient two- and 3-D extended Hertzian formulas for line, point, and elliptic contacts on the basis of full-scale numerical simulations.

1.3.5.2 ELASTO-PLASTIC CONTACT OF ROUGH SURFACES

Rough surfaces may deform plastically until the contact area becomes sufficiently large and the elementary pressure can hold the applied load [6]. The basic model of Greenwood and Williamson [16] was extended by Chang, Etsion, and Bogy [38] to take into account the volume conservation of the plastic zone. The finite element method (FEM) is widely used in elastic [39] or elastic-plastic [40–42] contact studies. Gao, Bower, Kim, Lev, and Cheng [43] conducted an extensive study on the plastic contact between a rigid, flat body and an elastic-perfectly-plastic solid with a one-dimensional sinusoidal surface by means of FEM. They identified two parameters for asperity contact performance characterization. On the other hand, Kim, Bhushan, and Cho [44] analyzed frictionless and frictional contacts between a rigid surface and an elastic-perfectly-plastic solid with a non-Gaussian rough surface generated by computer on the basis of different statistical parameters. Furthermore, Jacq, Nelias, Lormand, and Girodin [45] developed a fast, semianalytical method to study the elastic-plastic response of solid materials. Later, frictional heating was considered by Boucly, Nelias, Liu, Wang, and Keer [46] into the model mentioned above. Wang and Keer [47] investigated the effect of various strain hardening laws on the elasto-plastic indentation behaviors of materials. Chen, Liu, and Wang [48] further developed elasto-plastic models for the contact of nominally flat surfaces and for the line contact of 3-D rough surfaces.

1.3.5.3 FRACTAL CONTACT OF ROUGH SURFACES

The Weierstrass-Mandelbrot (W-M) fractal function may be used to characterize homogeneously and isotropically rough surfaces. For a continuous function $z(x)$ (with surface features slightly larger than those at the atomic scale), the W-M fractal function is defined as

$$z(x) = G^{(D-1)} \sum_{n=n_1}^{\infty} \frac{\gamma^n \cos 2\pi \gamma^n x}{\gamma^{(2-D)n}} \quad 1 < D < 2 \text{ and } \gamma > 1 \quad (1.34)$$

Here, G is a scaling constant; D is the dimension; γ^n is the n th frequency number (or simply, frequency), which is the reciprocal of the corresponding wavelength of roughness, and $\gamma^n = 1/\lambda_n$. The frequency ranges from γn_1 to infinity. Several fractal contact models are available [10–13,49]. Among these models, Yan and Komvopoulos [11] studied the contact of anisotropic surfaces through 3-D fractal characterization. Wang and Komvopoulos [49] introduced the concept of fractal-regular surface in elastic-plastic contact analysis that allows for the consideration of fractal domain decoupling. Wang [50] further demonstrated the construction of fractal-regular surfaces and presented an improved fractal contact model.

1.4 LUBRICATION AND LUBRICANT VISCOSITY

A layer of a lubricant, usually very thin (on the order of micrometers or even nanometers), between two solid surfaces can prevent direct solid-surface contact. A convergent wedge formed by two surfaces under a relative motion and a fluid with a certain viscosity are the essential physical conditions for the lubrication of a tribological interface. Mineral oils, synthetic fluids, and bio-based lubricants are commonly used in various applications, and viscosity is the major property determining their rheological behavior. The viscosity value reflects the resistance of a lubricant to shear. Although Newton's law of viscosity states the proportionality between fluid shear rate and shear stress, the viscosity may vary with temperature and pressure; it may also change with the share stress. Moreover, lubricant density can be a function of pressure.

1.4.1 Viscosity-Temperature Relationships

The dependence of viscosity on temperature is generally nonlinear [51]. The Walther equation for kinetic viscosity as a function of temperature is widely used:

$$\log(\log(\nu + a)) = A - B \lg T \quad (1.35)$$

Here, A , B , and a are constants; a is 0.7 if $\nu > 2$ CST; and T is temperature in Kelvin. A and B should be experimentally determined for a given lubricant.

The Eyring-Ewell equation modified by Andrade is also used because of its mathematical convenience.

$$\eta = k e^{-bT} \quad (1.36)$$

Two constants, k and b , are involved in this expression.

1.4.2 Viscosity-Pressure Relationships

A pressure-viscosity relationship plays an important role in elastohydrodynamic lubrication (EHL) because the viscosity of a fluid at the inlet has crucial influence on film formation. The equation below (eq. 1.37) is a convenient exponential expression widely used in EHL analysis. In eq. 1.37, α is the pressure-viscosity coefficient.

$$\eta = \eta_0 e^{\alpha p} \quad (1.37)$$

The exponential relationship mentioned above may result in excessively high viscosity at high pressure. The Cameron equation [52] (eq. 1.38) is preferred for this consideration [53].

$$\eta = \eta_0 (1 + cp)^\alpha \quad (1.38)$$

In both equations, η_0 is the viscosity under room conditions of pressure and temperature. α in eq. 1.37 depends on temperature [54]. Two other constants, c and η , are involved in eq. 1.38.

1.4.3 Viscosity-Temperature-Pressure Relationships

Several types of viscosity-temperature-pressure relationships may be used. Again, η_0 is the viscosity under room conditions of pressure, p_0 , and temperature, T_0 . Equation 1.39 is an extension of the pressure-viscosity relationship. Here, the pressure-viscosity coefficient, α , is the same as that in eq. 1.37 whereas β should be determined separately for the temperature effect.

$$\eta = \eta_0 e^{[\alpha(p-p_0) + \beta(T-T_0)]} \quad (1.39)$$

Cheng and Sternlicht [55] proposed another exponential equation for the viscosity-temperature-pressure relationship of a lubricant with three parameters: α , β , and γ :

$$\eta = \eta_0 e^{(\alpha p + \beta/T + \gamma/T_0 + \eta p/T)} \quad (1.40)$$

The linear relationship shown in eq. 1.41 is also a possible choice that uses two coefficients, c and β :

$$\eta = \eta_0 [1 + c(p - p_0) + \beta(T - T_0)] \quad (1.41)$$

The Roelands equation (eq. 1.42) is widely accepted for the temperature-pressure relationship [56]:

$$\eta = \eta_0 e^{(\ln \eta_0 + 9.76) \left[-1 + (1 + 5.1(10)^{-9} p)^Z \left(\frac{T - 138}{T_0 + 138} \right)^{S_0} \right]} \quad (1.42)$$

In this equation, Z and S_0 are the Roelands parameters to be defined for each lubricant.

1.4.4 Free-Volume Viscosity Models

The resistance to flow depends on the relative volume of molecules present per unit of free volume. Doolittle [57] explored the relationship between viscosity and the fractional free volume using an exponential function and developed the first free-volume viscosity model. A viscosity-pressure relationship represented by the Doolittle free-volume viscosity model [58] is as follows:

$$\bar{\eta} = \exp \left\{ B \frac{V_{occ}}{V_0} \left[\frac{1}{\frac{V}{V_0} - \frac{V_{occ}}{V_0}} - \frac{1}{1 - \frac{V_{occ}}{V_0}} \right] \right\} \quad (1.43)$$

In this equation, the volume variation is described by the Tait equation of state. V is the volume, V_0 is the volume at ambient pressure, V_{occ} is the occupied volume, and B is the Doolittle parameter.

$$\frac{V}{V_0} = 1 - \frac{1}{K'_0 + 1} \ln \left[1 + \frac{p}{K'_0} (1 + K'_0) \right] \quad (1.44)$$

In this equation, K_0 is the bulk modulus and K'_0 is the pressure rate of change of bulk modulus, both measured at ambient pressure. The density variation is the reciprocal of the volume variation in the above equation of state.

The following Yasutomi free-volume model [59] may also be used:

$$\bar{\eta} = \frac{\eta_g}{\eta_0} \exp \left[\frac{-2.3C_1(T - T_g)F}{C_2 + (T - T_g)F} \right] \quad (1.45)$$

Here, C_1 and C_2 are Yasutomi parameters, F is the relative free-volume expansivity, T_g is the Glass transition temperature in degrees Celsius, η_0 is the viscosity at ambient pressure, and η_g is the Glass transition viscosity. Expressions for T_g and F are given in eqs. 1.46 and 1.47 with additional Yasutomi parameters A_1 , A_2 , B_1 , and B_2 and the Glass transition temperature at ambient pressure, T_{g0} .

$$T_g = T_{g0} + A_1 \ln(1 + A_2 p) \quad (1.46)$$

$$F = 1 - B_1 \ln(1 + B_2 p) \quad (1.47)$$

1.4.5 Elastoviscous Effect

Under a heavy load, a lubricating fluid may perform like an elastic solid and show strong viscoelastic behavior [60,61]. A viscoelastic constitutive equation for such lubricants is given in the form of the well known nonlinear Maxwell type of model [62]:

$$\dot{\gamma} = \frac{d\tau}{Gdt} + F(\tau) \quad (1.48)$$

In this equation, $\dot{\gamma}$ is the shear rate, τ is the shear stress, and G is the shear modulus of a lubricant. The shear rate is related to the elastic (the first term) and the viscous (the second term) behavior of the fluid.

1.4.6 Shear Stress Effect

The Newtonian viscosity model assumes that viscous stress is proportional to shear rate and that the shear stress is continuous without wall slip. However, such conditions may not be satisfied all of the time by all fluids. Sometimes, wall slip may happen; that is, the wall shear stress is bounded by a limiting shear stress, τ_0 . The Prandtl-Eyring type of shear-thinning model [63] is widely used in traction analysis,

$$\eta = \frac{\tau_0}{\dot{\gamma}} \sinh^{-1}(\lambda \dot{\gamma}) \quad (1.49)$$

where η is the limiting viscosity at low shear rate, which may be a function of pressure p and temperature T . $\lambda = \mu/\tau_0$ with m as the limiting low-shear viscosity.

The viscosity function for a generalized Newtonian fluid is often described by the following Carreau model [64] for the shear stress-shear strain relationship expressed with the low-shear viscosity, η , the characteristic time, λ , and the power law exponent, n :

$$\tau = \eta \dot{\gamma} \left[1 + (\lambda \dot{\gamma})^2 \right]^{(n-1)/2} \quad (1.50)$$

A modification of the Carreau equation is also used for its convenience in application because in eq. 1.51 shear stress is the independent variable [65]:

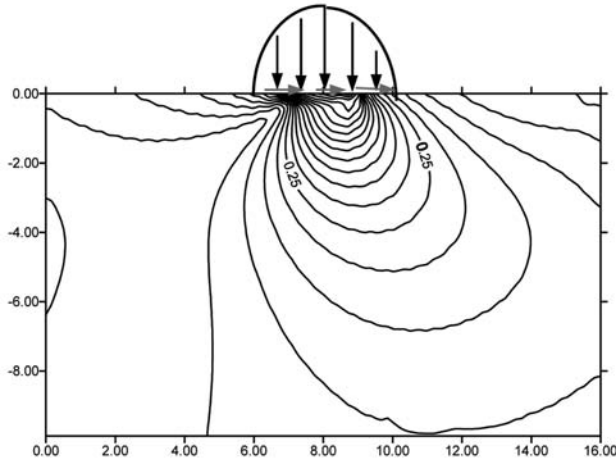


Figure 1.8—Illustration of the von Mises stress distribution due to the combined action of contact pressure and frictional shear.

$$\dot{\gamma} = \frac{\tau}{\eta} \left[1 + \left(\frac{\tau}{G} \right)^2 \right]^{(1-n)/(2n)} \quad (1.51)$$

The two models yield roughly the same results when $n > 0.6$ by allowing $\lambda = \mu/G$ [63].

Viscosity in ultrathin film lubrication has been found to be very different from that of the bulk; it may oscillate as a function of film thickness [66]. In research reported by Martini et al. [67], viscosity was characterized in terms of oscillation with film thickness and shear thinning. The following expression of this form was suggested from the molecular simulation of *n*-decane:

$$\eta(\dot{\gamma}, h, T) = \frac{\eta_0(T)}{\left[1 + (\dot{\gamma} / \dot{\gamma}_c(T))^2 \right]^{n/2}} - A_r e^{-h/r} \cos\left(\frac{2\pi h}{\lambda}\right) \quad (1.52)$$

In this equation, h is the film thickness, T is the temperature, $\dot{\gamma}$ is the shear rate, η_0 is the viscosity of the fluid subject to zero or low shear, $\dot{\gamma}_c$ is the critical shear rate, and n is the slope of the $\log \dot{\gamma}$ - $\log \eta(\dot{\gamma})$ curve in the shear thinning region. A_p , r , and λ are the amplitude, the rate of decay, and the oscillation wavelength, respectively, which can be obtained from fitting data.

1.4.7 Density as a Function of Pressure

Equation 1.44 is an expression of density variation. The density of a lubricant may be described as a function of pressure. The following is a density-pressure relationship for mineral oils [68] found in many lubricated analyses:

$$\frac{\rho}{\rho_0} = 1 + \frac{0.6p}{1 + 1.7p} \quad (1.53)$$

Here, η_0 is the viscosity under the ambient pressure, p_0 , and p is in gigapascals. It should be mentioned that molecular dynamic simulations of fluid molecules in a nanoscale gap reveal that the density of the fluid is not uniform across the liquid film thickness.

1.5 REYNOLDS EQUATION

1.5.1 Generalized Reynolds Equation and Hydrodynamic Lubrication

The generalized Reynolds equation describes the dynamics of fluid flow through a narrow clearance bounded by two solid surfaces (Figure 1.9). The following assumptions are made in deriving the generalized Reynolds equation: flows are laminar, the flow-surface interface is perfect without interfacial slipping, the lubricant is a Newtonian fluid, the body force is negligibly small, the lubricant thickness is so thin that the derivatives with respect to the film thickness direction are more important than those in other directions, the surface curvature effect is negligible, pressure across the fluid film is a constant, and the bounding solids are rigid and ideally smooth [69].

1.5.1.1 VISCOUS STRESS TENSOR

T_{ij} can be defined in terms of viscosity, η , pressure, p , and velocity gradient, $\partial_i V_j$:

$$T_{ij} = -\frac{2}{3}\eta\partial_k V_k\delta_{ij} + 2\eta\partial_{(i} V_{j)} - p\delta_{ij} \quad (1.54)$$

where:

$$\partial_i V_j = \frac{\partial V_x}{\partial x} + \frac{\partial V_y}{\partial y} + \frac{\partial V_z}{\partial z} \text{ and}$$

$$\partial_{(i} V_{j)} = \frac{1}{2} \left(\frac{\partial V_j}{\partial x_i} + \frac{\partial V_i}{\partial x_j} \right).$$

1.5.1.2 EQUATIONS OF MOTION

If $u = V_x$, then $v = V_y$, $w = V_z$, and the body force in a unit volume = $(X_F \mathbf{i} + Y_F \mathbf{j} + Z_F \mathbf{k})$. From Newton's second law, one should have the following equation:

$$\sum \mathbf{F} = m\mathbf{a} = \rho dV \left(\frac{Du}{Dt} \mathbf{i} + \frac{Dv}{Dt} \mathbf{j} + \frac{Dw}{Dt} \mathbf{k} \right) \quad (1.55)$$

The component in the x direction is

$$\rho dV \frac{Du}{Dt} = (\rho X_F + \frac{\partial T_{xx}}{\partial x} + \frac{\partial T_{xy}}{\partial y} + \frac{\partial T_{xz}}{\partial z}) dx dy dz$$

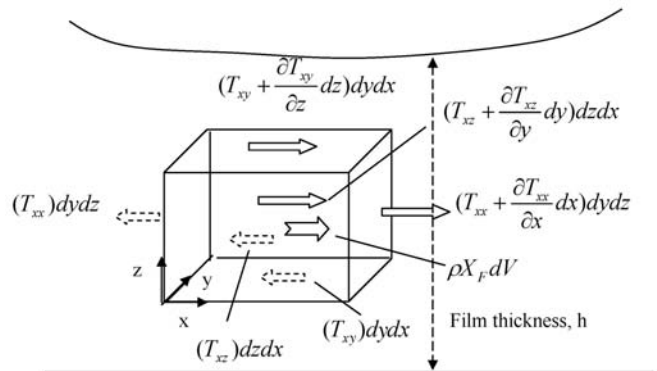


Figure 1.9—Forces in a fluid element along the x direction.

or

$$\begin{aligned}
 \rho \frac{Du}{Dt} &= \rho X_F + \frac{\partial T_{xx}}{\partial x} + \frac{\partial T_{xy}}{\partial y} + \frac{\partial T_{xz}}{\partial z} \\
 &= \rho X_F - \frac{\partial p}{\partial x} - \frac{2}{3} \frac{\partial}{\partial x} \left[\eta \left(\frac{\partial u}{\partial x} + \frac{\partial v}{\partial y} + \frac{\partial w}{\partial z} \right) \right] + 2 \frac{\partial}{\partial x} \left[\eta \frac{\partial u}{\partial x} \right] \\
 &\quad + \frac{\partial}{\partial y} \left[\eta \left(\frac{\partial u}{\partial y} + \frac{\partial v}{\partial x} \right) \right] + \frac{\partial}{\partial z} \left[\eta \left(\frac{\partial u}{\partial z} + \frac{\partial w}{\partial x} \right) \right] \\
 &= \rho X_F - \frac{\partial p}{\partial x} + \frac{2}{3} \frac{\partial}{\partial x} \left[\eta \left(\frac{\partial u}{\partial x} - \frac{\partial v}{\partial y} \right) \right] + \frac{2}{3} \frac{\partial}{\partial x} \left[\eta \left(\frac{\partial u}{\partial x} - \frac{\partial w}{\partial z} \right) \right] \\
 &\quad + \frac{\partial}{\partial y} \left[\eta \left(\frac{\partial u}{\partial y} + \frac{\partial v}{\partial x} \right) \right] + \frac{\partial}{\partial z} \left[\eta \left(\frac{\partial u}{\partial z} + \frac{\partial w}{\partial x} \right) \right] \quad (1.56)
 \end{aligned}$$

These relationships result in the generalized Reynolds equation using $p(x,y)$ for the average cross-film pressure:

$$\begin{aligned}
 &\frac{\partial}{\partial x} \left([F_2 + G_1] \frac{\partial p}{\partial x} \right) + \frac{\partial}{\partial y} \left([F_2 + G_1] \frac{\partial p}{\partial y} \right) \\
 &= h \left[\frac{\partial(\rho u)_2}{\partial x} + \frac{\partial(\rho v)_2}{\partial y} \right] - \frac{\partial}{\partial x} \left(\frac{(U_2 - U_1)(F_3 + G_2)}{F_0} + U_1 G_3 \right) \\
 &\quad - \frac{\partial}{\partial y} \left(\frac{(V_2 - V_1)(F_3 + G_2)}{F_0} + V_1 G_3 \right) + \int_0^h \frac{\partial \rho}{\partial t} dz + (\rho w)_2 - (\rho w)_1 \quad (1.57)
 \end{aligned}$$

where:

$$F_0 = \int_0^h \frac{dz}{\eta},$$

$$F_1 = \int_0^h \frac{z dz}{\eta} = \bar{z} F_0,$$

$$F_2 = \int_0^h \frac{\rho z(z - \bar{z}) dz}{\eta},$$

$$F_3 = \int_0^h \frac{\rho z dz}{\eta},$$

$$G_1 = \int_0^h z \frac{\partial \rho}{\partial z} \left(\int_0^z \frac{z}{\eta} dz - \bar{z} \int_0^z \frac{dz}{\eta} \right) dz,$$

$$G_2 = \int_0^h z \frac{\partial \rho}{\partial z} \left(\int_0^z \frac{z}{\eta} dz \right) dz, \text{ and}$$

$$G_3 = \int_0^h z \frac{\partial \rho}{\partial z} dz.$$

1.5.2 Simplification of the Generalized Reynolds Equation

Several commonly used forms of Reynolds equations can be derived through simplification of eq. 1.57.

1.5.2.1 INCOMPRESSIBLE REYNOLDS EQUATION

If the density of a fluid is not a function of position, then $\partial \rho / \partial z = 0$, $G_1 = G_2 = G_3 = 0$, $u_2 = U_2$, and $v_2 = V_2$. Furthermore, if density is not a function of time, then $\partial \rho / \partial t = 0$ and eq. 1.57 becomes

$$\begin{aligned}
 &\frac{\partial}{\partial x} \left(F_2 \frac{\partial p}{\partial x} \right) + \frac{\partial}{\partial y} \left(F_2 \frac{\partial p}{\partial y} \right) = h \left[\frac{\partial(u)_2}{\partial x} + \frac{\partial(v)_2}{\partial y} \right] - \frac{\partial}{\partial x} \left(\frac{(U_2 - U_1)F_3}{F_0} \right) \\
 &\quad - \frac{\partial}{\partial y} \left(\frac{(V_2 - V_1)F_3}{F_0} \right) + \rho(W_2 - W_1) \quad (1.58)
 \end{aligned}$$

1.5.2.2 ONE-DIMENSIONAL INCOMPRESSIBLE REYNOLDS EQUATION

For an infinitely wide bearing, $p = p(x)$, the Reynolds equation is

$$\frac{\partial}{\partial x} \left(F_2 \frac{\partial p}{\partial x} \right) = h \left[\frac{\partial(u)_2}{\partial x} \right] - \frac{\partial}{\partial x} \left(\frac{(U_2 - U_1)F_3}{F_0} \right) - \rho(W_2 - W_1) \quad (1.59)$$

1.5.2.3 COMPRESSIBLE REYNOLDS EQUATION

Neglecting all across-film property changes, $\partial \rho / \partial z = \partial \eta / \partial z = 0$ and $G_1 = G_2 = G_3 = 0$, the Reynolds equation becomes

$$\begin{aligned}
 &\frac{\partial}{\partial x} \left(\frac{\rho h^3}{12\eta} \frac{\partial p}{\partial x} \right) + \frac{\partial}{\partial y} \left(\frac{\rho h^3}{12\eta} \frac{\partial p}{\partial y} \right) = h \left[\frac{\partial(\rho u)_2}{\partial x} + \frac{\partial(\rho v)_2}{\partial y} \right] \\
 &\quad - \frac{\partial}{\partial x} \left(\frac{(U_2 - U_1)\rho h}{2} \right) - \frac{\partial}{\partial y} \left(\frac{(V_2 - V_1)\rho h}{2} \right) + \frac{\partial \rho}{\partial t} h + \rho(W_2 - W_1) \quad (1.60)
 \end{aligned}$$

1.5.2.4 ISOVISCOUS AND INCOMPRESSIBLE REYNOLDS EQUATION

The classic isoviscous and incompressible Reynolds equation is described by $\partial \rho / \partial z = \partial \eta / \partial z = 0$, and $\eta = \text{constant}$.

$$\begin{aligned}
 &\frac{\partial}{\partial x} \left(h^3 \frac{\partial p}{\partial x} \right) + \frac{\partial}{\partial y} \left(h^3 \frac{\partial p}{\partial y} \right) = 12h\eta \left[\frac{\partial U_2}{\partial x} + \frac{\partial V_2}{\partial y} \right] \\
 &\quad - 6\eta \frac{\partial}{\partial x} [h(U_2 - U_1)] - 6\eta \frac{\partial}{\partial y} [h(V_2 - V_1)] \\
 &\quad 12\eta(W_2 - W_1) \quad (1.61)
 \end{aligned}$$

which is

$$\begin{aligned}
 &\frac{\partial}{\partial x} \left(h^3 \frac{\partial p}{\partial x} \right) + \frac{\partial}{\partial y} \left(h^3 \frac{\partial p}{\partial y} \right) = -6\eta \frac{\partial h}{\partial x} (U_2 - U_1) + 12\eta \left[(U_2) \frac{\partial h}{\partial x} + V^* \right] \\
 &= 6\eta \left[(U_2 + U_1) \frac{\partial h}{\partial x} + 2V^* \right] \quad (1.62)
 \end{aligned}$$

1.6 LUBRICATION REGIMES

Full-film lubrication, or hydrodynamic lubrication, is the lubrication in which a lubricant film completely separates solid surfaces. Here, the term “hydrodynamic” indicates that the film is built through the use of motion. Partial-film lubrication, or mixed lubrication, means that the lubricant film is insufficient to completely cover all surfaces. In mixed lubrication, solid asperity contact occurs, and the lubricant film is no longer continuous in the interface region. When the lubricant film is further reduced, asper-

ity contact may become dominant. Surfaces may be covered only by a physically or chemically absorbed lubricant layer. This regime of lubrication is called the boundary-layer lubrication, or simply the boundary lubrication. Figure 1.10 presents these regimes of lubrication in terms of the well-known Stribeck curve [70], plotted as friction coefficient against a nondimensional factor, the Hersey number, $\eta N/P$, which is the viscosity, η , times the rotation speed, N , divided by the average pressure, $P = \text{load}/\text{projected area}$. The concept of friction variation in lubrication is attributed to a German professor, Richard Stribeck, who in 1902 confirmed the existence of a minimal friction through his extensive journal-bearing friction experiments. Later, in 1914, Ludwig Gumbel summarized the Stribeck results into a single curve by means of the dimensionless parameters mentioned above. Dowson reviewed the history of the development of the Stribeck curve concept [71]. The understanding and use of Stribeck curves have advanced from friction expressions to the division of lubrication regimes [72]. Reddy, Swarnamani, and Prabhu [73] presented a Stribeck diagram of friction for a tilting pad journal bearing. Xiao, Rosen, Amini, and Nilsson [74] studied the friction behavior of a rolling contact in terms of Stribeck curves.

The concept of the Stribeck curve reveals the insight of friction in lubrication. However, the nondimensional Hersey number only includes operating parameters; it does not consider the effect of bearing deformation and surface interaction related to material, surface roughness, and bearing structure. The recent trend of compact design demands mechanical components to work under higher load density, which may cause significant surface deformation and asperity interaction. The results of research on the frictional behavior of a journal-bearing conformal contact through numerical simulation suggest that additional factors (e.g., roughness, elasticity, and thermoelasticity) be included in Stribeck curve presentation [75]. A 3-D Stribeck surface is constructed to illustrate the load effect, which causes structural and surface deformations, on journal-bearing friction.

Because the Hersey number is the product of viscosity and rotational speed over the applied load, the variation in the Hersey number can be accomplished through speed

change without invoking the effect of load. However, load directly influences deformation and therefore film thickness. One can image that the same Hersey number can be constructed with different combinations of speed and load; different deformations may occur, resulting in different friction conditions.

Figure 1.11 shows a 3-D Stribeck surface and details constructed to indicate the relationship among friction coefficient, applied load, and rotational speed, where the first axis is load, the second axis is rotational speed, and the third (vertical) axis is friction coefficients in mixed and full-film lubrication regions under pairs of given load and rotational speed corresponding to Hersey numbers. In Figure 1.11a, the dotted line divides the Stribeck surface into two regions: the region above the curve is the mixed lubrication region whereas the bottom region is in the full-film lubrication region. Figure 1.11b is an enlarged view of the surface in the area where the rotational speed ranges from 10 to 16.67 r/s to better show the shape of the surface at high speeds.

1.7 EHL

It is known from elasticity that contact pressure can cause surface deformation. Such deformation enlarges the apparent contact area and increases the gap, or the film thickness, between surfaces. Therefore, the Reynolds equation should be solved with an elasticity component, and the lubrication involving surface elastic deformation is named elastohydrodynamic lubrication, or EHL.

1.7.1 Formulation and Solution for Line-Contact EHL Problems

1.7.1.1 BASIC EQUATIONS

- **Lubrication:** The Reynolds equation is used to express the relationship between film thickness and hydrodynamic pressure. Equation 1.63 is for line-contact EHL. Here, $U = (U_1 + U_2)/2$, the rolling velocity:

$$\frac{\partial}{\partial x} \left(\frac{\rho h^3}{\eta} \frac{\partial p}{\partial x} \right) = 12U \frac{\partial(\rho h)}{\partial x} \quad (1.63)$$

- **Lubricant:** The exponential viscosity-pressure relationship, eq. 1.37, repeated below may be used for simplicity:

$$\eta = \eta_0 e^{\alpha p} \quad (1.64)$$

The density-pressure relationship may follow the Dowson-Higginson formula:

$$\frac{\rho}{\rho_0} = 1 + \frac{0.6p}{1 + 1.7p} \quad (1.65)$$

- **Film thickness:** The film-thickness equation that considers body surface deformations is used. Note that for a line-contact EHL problem, the Flamant elastic equation discussed before should be used

$$h = h_0 + \frac{x^2}{2R^2} - \frac{2}{\pi E'} \int_0^{\xi} \ln \left| \frac{\xi - x}{\xi - x_r} \right| p(\xi) d\xi \quad (1.66)$$

For point-contact (or elliptic contact) problems, one only needs to add to the Reynolds equation a proper pressure flow term in the other direction and replace

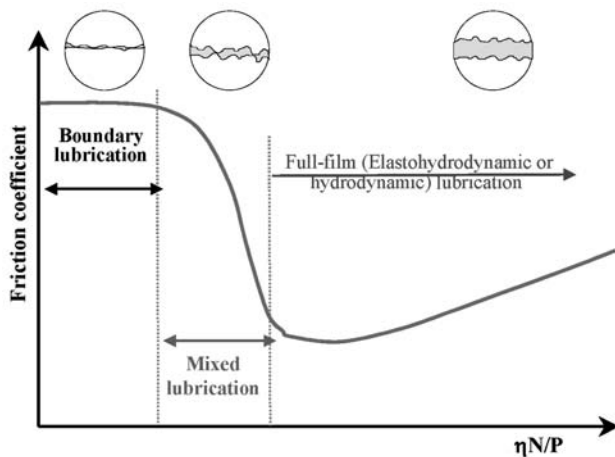


Figure 1.10—Lubrication regimes shown in the form of a Stribeck curve.

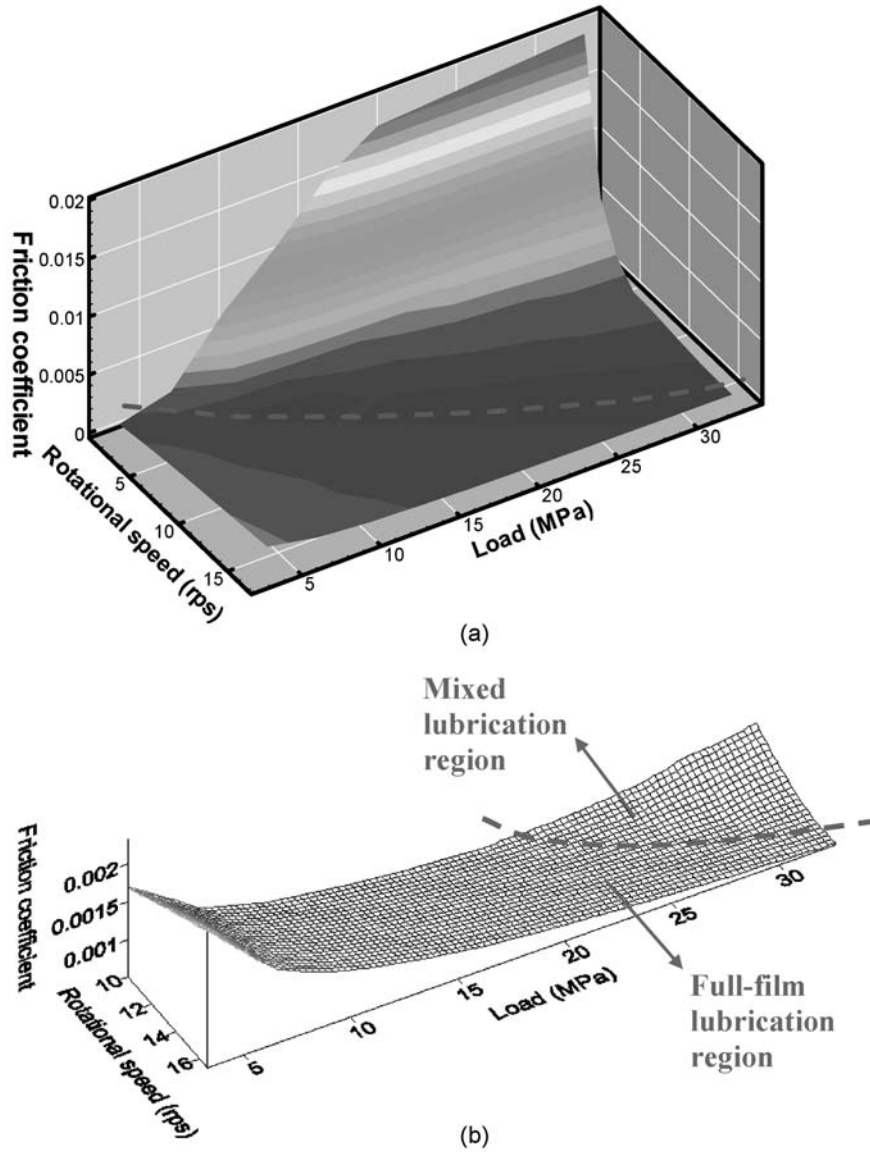


Figure 1.11—Stribeck surface—load, speed, and friction coefficient relationship [75]. (a) Rotational speed range 1.67–16.67 r/s. (b) Rotational speed range 10–16.67 r/s (enlarged view of panel a).

the displacement term in the film thickness equation by the following Boussinesq equation:

$$u_z(x, y) = -\frac{4}{\pi E'} \int_{\Omega} p(\xi, \zeta) \frac{d\xi d\zeta}{\sqrt{(x-\xi)^2 + (y-\zeta)^2}} \quad (1.67)$$

- **Load equation:** Integration of the pressure obtained from the Reynolds equation, which is now coupled with the elastic equation from film thickness, results in the load supported by the film:

$$W = \int p dx \quad (1.68)$$

The commonly used numerical methods are the relaxation iteration method (under-relaxation for EHL problems), the Newton-Raphson method, the multilevel multisummation method, and the progressive mesh densification method.

- **EHL solution:** Figure 1.12 illustrates a typical EHL solution, which is featured by necking at the outlet and flattening in the central region. Corresponding to necking, there is a pressure spike. In EHL problems, two film-thickness values are usually calculated—the minimal film thickness and the central film thickness—as illustrated in Figure 1.12 for a line-contact EHL problem. The former determines the worst lubrication condition whereas the latter indicates the film geometry at the central flattened region.

1.7.1.2 TYPICAL LINE-CONTACT EHL SOLUTIONS AND FORMULAS FOR MINIMAL FILM THICKNESS

The first solution to line-contact EHL film thickness was given by Grubin and Ertel [71,76] based on the fact that the central film is nearly flat. The inlet film shape can be prescribed with the assistance of the known elastic deformation, and the central film thickness can be solved through

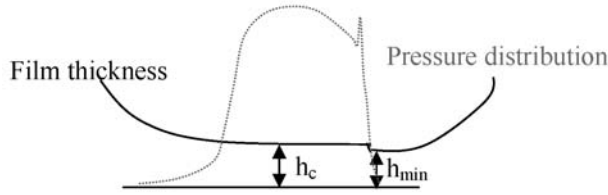


Figure 1.12—Typical EHL film thickness and pressure distribution.

integration of eq. 1.63. However, this type of solution can only yield the central film thickness if the mating surfaces become parallel in the EHL interface, and the film thickness value is higher than the accuracy solution [76].

Typical line-contact EHL solutions for minimal film thickness are Martin's rigid-isoviscous (RI) formulas, Blok's rigid-piezoviscous (RV) formulas, Herrebrugh's elastic-isoviscous (EI) formulas, and Dowson-Higgison's elastic-piezoviscous (EV) formulas. In the formulas, load $W = PB$ is used, where B is the length (width) of the contact) and P is the load per unit length [6].

- *Martin's solution:* This is for RI lubrication. This solution does not consider body elasticity and viscosity variation due to pressure rise.

$$h_{\min} = \frac{4.9}{\left(\frac{W}{\eta_0 URB} \right)} \quad (1.69)$$

- *Blok's solution:* This is for RV lubrication. This solution does not consider body elasticity but includes viscosity variation due to pressure rise.

$$\frac{Wh_{\min}}{\eta_0 URB} = 1.66 \left(\frac{W^{3/2} \alpha}{(\eta_0 U)^{1/2} R} \right)^{2/3} \quad (1.70)$$

- *Herrebrugh's solution:* This is for EI lubrication. This solution does consider body elasticity but ignores the viscosity variation due to pressure rise.

$$\frac{Wh_{\min}}{\eta_0 URB} = 3.0 \left(\frac{W}{B(URE')^{1/2}} \right)^{0.8} \quad (1.71)$$

- *Dowson-Higgison's solution:* This is for EV lubrication. This solution considers body elasticity and viscosity variation due to pressure change.

$$\frac{Wh_{\min}}{\eta_0 URB} = 2.65 \left(\frac{W^{3/2} \alpha}{(\eta_0 U)^{1/2} R} \right)^{0.54} \left(\frac{W}{B(URE')^{1/2}} \right)^{0.06} \quad (1.72)$$

1.7.2 Elliptical-Contact EHL

If the one-dimensional Reynolds equation is replaced by the two-dimensional Reynolds equation and the Flamant formula by the Boussinesq formula, then the formulation for point-contact EHL, or elliptical-contact EHL, which is more general, is constructed.

Dowson and Hamrock developed general solutions to typical EHL elliptical contact problems [54].

Nondimensional parameters for EHL of elliptical contacts are as follows:

Dimensionless film thickness: $\hat{H} = \frac{h}{R_x}$, where $\frac{1}{R_x} = \frac{1}{R_{x1}} + \frac{1}{R_{x2}}$

Dimensionless load: $\hat{W} = \frac{W}{E'R_x^2}$, where $\frac{2}{E'} = \frac{1-\nu_a^2}{E_a} + \frac{1-\nu_b^2}{E_b}$ (1.73)

Note that in almost all EHL formulas, the equivalent Young's modulus is defined differently from that in most elasticity work (see eq. 1.21).

Dimensionless speed: $\hat{U} = \frac{\eta_0 U}{E'R_x}$

Dimensionless material parameter: $\hat{G} = \alpha E'$

The minimal film thickness formula (EV) is

$$\hat{H}_{\min} = 3.36 \hat{U}^{0.68} \hat{G}^{0.49} \hat{W}^{-0.073} (1 - e^{-0.68k}) \quad (1.74)$$

where $k = a/b \approx 1.03 \left(\frac{R_y}{R_x} \right)^{0.64}$ is the contact elliptic ratio.

$$\frac{1}{R_x} = \frac{1}{R_{x1}} + \frac{1}{R_{x2}} \quad \frac{1}{R_y} = \frac{1}{R_{y1}} + \frac{1}{R_{y2}}$$

The corresponding Hamrock-Dawson central film thickness equation has the following form [54]:

$$\hat{H}_c = 2.69 \hat{U}^{0.67} \hat{G}^{0.53} \hat{W}^{-0.067} (1 - 0.61e^{-0.73k}) \quad (1.75)$$

1.8 MIXED LUBRICATION

When the film thickness falls into the same order of magnitude as that of the surface roughness, which is approximately $3Rq$, or the film thickness is approximately three times the RMS roughness of the surface, the rough-surface effect on lubrication has to be considered [77]. If the film thickness is greater than $3Rq$, a sufficient amount of fluid should flow through the interface. In thick-film lubrication, the main stream of the fluid does not "feel" surface irregularities.

Three approaches have been used in mixed-lubrication analyses: stochastic modeling, deterministic modeling, and interactive deterministic-stochastic modeling. Stochastic models use selected surface statistic parameters to deal with the influence of roughness on lubrication. They are powerful in drawing general features of rough surface behavior in lubrication. However, it is difficult to use these models for material and surface-finish studies because asperity-scale contact mechanics is not included, and the reality of surface topography is omitted. A stochastic model can be interactively implemented with a contact model to develop interactive deterministic-stochastic modeling, in which lubrication is analyzed with a macroscale average-flow model whereas the contact is calculated by means of an offline deterministic asperity contact model. Deterministic modeling of mixed lubrication directly analyzes the lubrication of rough surfaces and numerically links surface tribological performance to materials and surface topography.

1.8.1 Roughness Effect on Lubrication and Patir and Cheng's Average Reynolds Equation

Statistical flow models, such as those by Christensen [78], Patir and Cheng [7], and Harp and Salant [79], have been developed for considering the roughness effect on lubrication. In most of the statistical models, the Reynolds equation is modified by a set of flow factors related to surface roughness. Patir and Cheng's average flow model is presented below.

In deriving the average Reynolds equation, one can assume that the roughness is a Reynolds roughness, i.e., the asperities have small slopes, which is approximately a few degrees. A few terms are defined below based on Figure 1.13. Note that asperities are exaggerated. If there is no contact and deformation, the compliance and the average gap should be the same. The compliance and the average gap are not the same once deformation is involved. The concept of the average gap is defined on the separation of the centerlines of deformed surfaces.

1.8.1.1 AVERAGE REYNOLDS EQUATION

The Reynolds equation is valid to describe the flow between two surfaces with a Reynolds roughness, and the corresponding film thickness is the gap at a position of interest.

$$\frac{\partial}{\partial x} \left(\frac{h_T^3}{\eta} \frac{\partial p}{\partial x} \right) + \frac{\partial}{\partial y} \left(\frac{h_T^3}{\eta} \frac{\partial p}{\partial y} \right) = 6(U_1 + U_2) \frac{\partial \bar{h}_T}{\partial x} + 12 \frac{\partial \bar{h}_T}{\partial t} \quad (1.76)$$

If the corresponding flow rates are expressed over the average gap, one should have the terms of average flows:

$$\bar{q}_x = -\phi_x \frac{\bar{h}_T^3}{12\eta} \frac{\partial \bar{p}}{\partial x} + \frac{U_1 + U_2}{2} \bar{h}_T + \frac{U_1 - U_2}{2} R_q \phi_s \quad (1.77)$$

$$\bar{q}_y = -\phi_y \frac{\bar{h}_T^3}{12\eta} \frac{\partial \bar{p}}{\partial y} \quad (1.78)$$

Here, flow factors are introduced, and an additional term is added to the flow in the x direction. However, the original Patir and Cheng model defines the flows slightly differently because the term "compliance" is referred to as the film thickness.

$$\bar{q}_x = -\phi_x \frac{h^3}{12\eta} \frac{\partial \bar{p}}{\partial x} + \frac{U_1 + U_2}{2} \bar{h}_T + \frac{U_1 - U_2}{2} R_q \phi_s \quad (1.79)$$

U_1, U_2 :	Surface velocities
$\delta_1(x,y), \delta_2(x,y)$:	Surface deviations from the centerlines
$h_T(x,y)$:	Gap between two surfaces
$\bar{h}_T(x,y)$:	Average gap
$h(x,y)$:	Compliance (film thickness, by P&C), defined as the separation between two original centerlines.

$$\bar{q}_y = -\phi_y \frac{h^3}{12\eta} \frac{\partial \bar{p}}{\partial y} \quad (1.80)$$

Here, ϕ_x and ϕ_y are the pressure flow factors, and ϕ_s is the shear-flow factor. The additional term, $(U_1 - U_2)R_q\phi_s/2$, shows the flow due to surface roughness. For smooth surfaces, R_q is 0 and so is the additional flow. U_1 or U_2 has a different influence on the flow. For $U_1 = U_2$, no additional flow enters the region of interest. From the flow balance in a control volume one can obtain

$$\frac{\partial \bar{q}_x}{\partial x} + \frac{\partial \bar{q}_y}{\partial y} = -\frac{\partial \bar{h}_T}{\partial t} \quad (1.81)$$

Bringing in eqs. 1.79 and 1.80 results in the average Reynolds equation:

$$\begin{aligned} & \frac{\partial}{\partial x} \left(\phi_x \frac{h^3}{\eta} \frac{\partial \bar{p}}{\partial x} \right) + \frac{\partial}{\partial y} \left(\phi_y \frac{h^3}{\eta} \frac{\partial \bar{p}}{\partial y} \right) \\ & = 6(U_1 + U_2) \frac{\partial \bar{h}_T}{\partial x} + 6(U_1 - U_2) R_q \frac{\partial \phi_s}{\partial x} + 12 \frac{\partial \bar{h}_T}{\partial t} \end{aligned} \quad (1.82a)$$

If $U_2 = 0$ and $U_1 = U$, eq. 1.82a becomes

$$\frac{\partial}{\partial x} \left(\phi_x \frac{h^3}{\eta} \frac{\partial \bar{p}}{\partial x} \right) + \frac{\partial}{\partial y} \left(\phi_y \frac{h^3}{\eta} \frac{\partial \bar{p}}{\partial y} \right) = 6U \frac{\partial \bar{h}_T}{\partial x} + 6U R_q \frac{\partial \phi_s}{\partial x} + 12 \frac{\partial \bar{h}_T}{\partial t} \quad (1.82b)$$

1.8.1.2 PRESSURE FLOW FACTORS

Equation 1.82a defines the characteristics of the pressure flow factors. They may be large or small when h/R_q becomes small, but they tend to be unity when the film thickness is much larger than the height of surface asperities, or

$$\phi_x, \phi_y \rightarrow 1 \quad \text{as} \quad h/R_q \rightarrow \infty \quad (h \rightarrow \infty \text{ or } R_q \rightarrow 0) \quad (1.83)$$

Because x and y are orthogonal directions, one only needs to define one of these two flow factors. The other can be determined with the same method. The following defines ϕ_x first and only considers the pressure-driven flow.

ϕ_x = Pressure-driven flow between rough surfaces/pressure-driven flow between smooth surfaces = $\frac{\bar{q}_x(p)}{q_x(\bar{p})}$ (1.84)

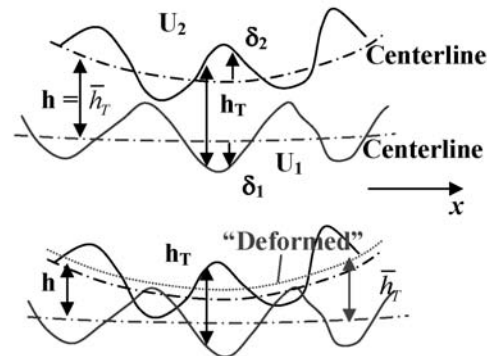


Figure 1.13—Flow between rough surfaces: gap and compliance.

The pressure-driven flow between rough surfaces means that the flow has a pressure, p , at the position of h_T whereas the pressure-driven flow between smooth surfaces is for the flow of the film thickness defined by the compliance corresponding to h_T and an average pressure, \bar{p} . Recall that to use the flow averaged across a calculation length, L_y , and for $U_1 = U_2$, the following can be derived:

$$\begin{aligned}\phi_x \frac{h^3}{12\eta} \frac{\partial \bar{p}}{\partial x} &= \frac{U_1 + U_2}{2} \bar{h}_T - \bar{q}_x \\ &= \frac{U_1 + U_2}{2} \bar{h}_T - \frac{1}{L_y} \int_0^{L_y} \left(\frac{h_T^3}{12\eta} \frac{\partial p}{\partial x} + \frac{U_1 + U_2}{2} h_T \right) dy = -\frac{1}{L_y} \int_0^{L_y} \left(\frac{h_T^3}{12\eta} \frac{\partial p}{\partial x} \right) dy\end{aligned}\quad (1.85)$$

Therefore, the pressure flow factor is defined as

$$\phi_x = \frac{\frac{1}{L_y} \int_0^{L_y} \left(\frac{h_T^3}{12\eta} \frac{\partial p}{\partial x} \right) dy}{\frac{h^3}{12\eta} \frac{\partial \bar{p}}{\partial x}} \quad (1.86a)$$

The pressure flow factor corresponding to the average gap (eqs. 1.79 and 1.80) is obviously

$$\phi_x = \frac{\frac{1}{L_y} \int_0^{L_y} \left(\frac{h_T^3}{12\eta} \frac{\partial p}{\partial x} \right) dy}{\frac{\bar{h}^3}{12\eta} \frac{\partial \bar{p}}{\partial x}} \quad (1.86b)$$

1.8.1.3 SHEAR FLOW FACTORS

The shear flow factor, ϕ_s , is found to be a function of the nondimensional film thickness, h/R_q , and the roughness orientation, γ , as well as a shear flow factor for a single surface, Φ . Obviously, ϕ_s is for the combined effect of two mating rough surfaces.

$$\phi_s = \left(\frac{R_{q1}}{R_q} \right)^2 \Phi_s \left(\frac{h}{R_q}, \gamma_1 \right) - \left(\frac{\sigma_2}{R_q} \right)^2 \Phi_s \left(\frac{h}{R_q}, \gamma_2 \right) \quad (1.87)$$

Physically, if one of the surfaces is smooth, $R_{q1} = 0$, eq. 1.87 becomes

$$\phi_s = - \left(\frac{R_{q2}}{R_q} \right)^2 \Phi_s \left(\frac{h}{R_q}, \gamma_2 \right) = -\Phi_s \quad (1.88)$$

Recall the term for the additional flow,

$$q = \frac{U_1 - U_2}{2} R_q \phi_s \quad (1.89)$$

If $U_2 > U_1$, the rough surface is moving faster, and there is an increase in the flow. On the other hand, if $U_2 < U_1$, the smooth surface is moving faster and there is a decrease in the flow.

Or, for $R_{q2} = 0$, then

$$\phi_s = \left(\frac{R_{q2}}{R_q} \right)^2 \Phi_s \left(\frac{h}{R_q}, \gamma_2 \right) = \Phi_s \quad (1.90)$$

In general, there is an increase in the flow if the rough surface moves faster.

1.8.1.4 FLOW FACTORS FOR SURFACES WITH A GAUSSIAN ASPERITY-HEIGHT DISTRIBUTION

The asperity height distributions of many of engineering surfaces may be simply expressed by a Gaussian distribution. One may further simplify the problem by assuming that one of the mating surfaces is ideally smooth whereas the other possesses the combined roughness of both and use the combined roughness value.

$$R_q = \sqrt{R_{q1}^2 + R_{q2}^2} \quad (1.91)$$

Patir and Cheng [7] published a set of empirical flow-factor equations for the surface with a Gaussian asperity-height distribution. These flow factors are summarized as follows.

1.8.1.4.1 Pressure Flow Factors

The pressure flow factor, ϕ_x , is found to be a function of a nondimensional film thickness, h/R_q , and the roughness orientation, γ .

$$\phi_x = \phi_x \left(\frac{h}{R_q}, \gamma \right) \quad (1.92)$$

$$\phi_x = 1 - Ce^{-r(h/R_q)} \quad \text{for } \gamma \leq 1 \text{ (isotropic and transverse)} \quad (1.93)$$

$$\phi_x = 1 + C \left(\frac{h}{R_q} \right)^{-r} \quad \text{for } \gamma > 1 \text{ (longitudinal)} \quad (1.94)$$

Coefficients, c and r , are given in Table 1.1.

Flow factors in two orthogonal directions are related through eq. 1.95.

$$\phi_y = \phi_y \left(\frac{h}{R_q}, \gamma \right) = \phi_x \left(\frac{h}{R_q}, \frac{1}{\gamma} \right) \quad (1.95)$$

1.8.1.4.2 Shear Flow Factors

One needs the following empirical relations to calculate the shear flow factor, ϕ_s :

$$\Phi_s = A_1 \left(\frac{h}{R_q} \right)^{\alpha_1} e^{-\alpha_2 \left(\frac{h}{R_q} \right) + \alpha_3 \left(\frac{h}{R_q} \right)^2} \quad \text{for } h/R_q \leq 5 \quad (1.96)$$

$$\Phi_s = A_2 e^{-0.25 \left(\frac{h}{R_q} \right)} \quad \text{for } h/R_q > 5 \quad (1.97)$$

The coefficients A_1 , A_2 , α_1 , α_2 , and α_3 are provided in Table 1.2.

TABLE 1.1—Coefficients c and r

γ	c	r	Range
1/9	1.48	0.42	$h/R_q > 1$
1/6	1.38	0.42	$h/R_q > 1$
1/3	1.18	0.42	$h/R_q > 0.75$
1	0.9	0.56	$h/R_q > 0.5$
3	0.225	1.5	$h/R_q > 0.5$
6	0.52	1.5	$h/R_q > 0.5$
9	0.87	1.5	$h/R_q > 0.5$

TABLE 1.2—Coefficients A_1 , A_2 , α_1 , α_2 , and α_3

γ	A_1	α_1	α_2	α_3	A_2
1/9	2.046	1.12	0.78	0.03	1.856
1/6	1.962	1.08	0.77	0.03	1.754
1/3	1.858	1.01	0.76	0.03	1.561
1	1.899	0.98	0.92	0.05	1.126
3	1.56	0.85	1.13	0.08	0.556
6	1.29	0.62	1.09	0.08	0.388
9	1.011	0.54	1.07	0.08	0.295

1.8.2 Deterministic Modeling of Mixed Lubrication of Counterformal Contact

Deterministic modeling and simulation of mixed lubrication has so far mainly been conducted for counterformal contact lubrication because of the consideration of computation burden. However, the deterministic approach has been proven to be powerful because the simulation allows detailed observation of microlubrication features related to surface topography. A deterministic mixed-lubrication model should describe the film thickness and pressure at every location at the interface between two rough surfaces.

$$h = h_0(t) + B_x x^2 + B_y y^2 + \frac{2}{\pi E^*} \int_{-\infty}^{\infty} \int_{-\infty}^{\infty} \frac{p(x'_1, x'_2) dx'_1 dx'_2}{\sqrt{(x_1 - x'_1)^2 + (x_2 - x'_2)^2}} + \frac{2}{\pi G^*} \int_{-\infty}^{\infty} \int_{-\infty}^{\infty} \frac{s(x'_1, x'_2) (x_1 - x'_1) dx'_1 dx'_2}{(x_1 - x'_1)^2 + (x_2 - x'_2)^2} + \delta_1 + \delta_2 \quad (1.98)$$

where:

$$\frac{2}{G^*} = \frac{(1-2\nu_1)(1+\nu_1)}{2\pi E_1} - \frac{(1-2\nu_2)(1+\nu_2)}{2\pi E_2} \quad \text{and}$$

δ_1 and δ_2 are asperities of surfaces 1 and 2, respectively.

The reduced Reynolds equation (eq. 1.99) and the zero film equation (eq. 1.100) have been used for contact determination [80–82].

$$U \frac{\partial(\rho h)}{\partial x} + \frac{\partial(\rho h)}{\partial t} = 0 \quad \text{at} \quad h \leq h_s \quad (1.99)$$

$$h = 0 \quad \text{at} \quad h \leq h_s \quad (1.100)$$

1.8.3 Interactive Deterministic-Stochastic Approach, or the Macro-Micro Approach, Mixed Lubrication of Conformal Contact

Conformal-contact lubrication problems involve structure analyses in lubrication solutions. Journal bearings are good examples. Here, one has to deal with different scales: macrogeometry and micro/nanoscale asperity interaction. An interactive deterministic-stochastic approach (or the macro-micro approach) may be a means to tackle such problems. Note that this method is less accurate if deeper asperity interaction is involved.

1.8.3.1 FILM THICKNESS

The film thickness is given by eq. 101. Here, surface deformation may be dissolved into two parts: the deflection of the middle surface of asperities (surface formed by the middle points across roughness heights of a 3-D topography, similar to the centerline for a two-dimensional roughness), u_{zMS} , and the deformation of the asperities with respect to the middle surface, δ_1 and δ_2 . The latter affects the microflows and may be considered by an average flow (AF) model whereas the former is a part of the structural deformation and should be analyzed through a macroscale elasticity computation [83].

$$h = h_0(t) + B_x x^2 + B_y y^2 + \underbrace{u_{zMS}(x, y, t)}_{\text{to be considered at the macro scale}} + \underbrace{\delta_1(x, y, t) + \delta_2(x, y, t)}_{\text{to be considered in the AF model}} \quad (1.101)$$

The macro-micro approach includes three components: (1) the macro middle-surface determination, u_{zMS} , (2) flow-factor and pressure calculation, and (3) microcontact analysis and embedment. An assumption has to be made to use the average-flow model: the distortion of asperities is negligibly small. The rough surfaces in interaction are placed according to the film thickness determined by considering the global elasticity. Therefore, the film thickness equation becomes

$$h = h_0(t) + B_x x^2 + B_y y^2 + u_{zCL}(x, y, t) \quad (1.102)$$

An offline asperity contact model has to accompany the analysis process.

1.8.3.2 ROUGHNESS EFFECT ON FLUID FLOW: THE AVERAGE REYNOLDS EQUATION

The average Reynolds equation is applied to each mesh grid where the film thickness can be treated as a constant. Flow factors are then determined corresponding to this film thickness.

1.8.3.3 ASPERITY CONTACT: AN ASPERITY CONTACT MODEL

Asperity contact can be obtained by applying an asperity contact model locally or at a given film thickness (which is the gap in a contact simulation) off the line of the lubrication analysis. A pressure-gap function can be prepared offline to be retrieved by the lubrication procedure. Therefore, the contact pressure, $p_c(x, y)$, can be related to this offline pressure-gap function as follows:

$$p_c(x, y) = f\left(\frac{h}{R_q}\right) \quad (1.103)$$

1.8.3.4 GLOBAL ELASTICITY

The geometry of the concave element in a conformal-contact system cannot be treated as an infinitely large body. Neither the Boussinesq nor the Flamant solution can be applied here. There is no simple solution for structure elasticity. The finite element method has to be used either

for the full solution or for the influence functions of the surface deformation.

Wang, Shi, and Lee [84] solved journal-bearing isothermal mixed lubrication with this approach. This method was then extended to the solution of mixed thermal EHL problems for journal bearings [85]. The model to solve EHL problems while taking heat transfer into account is called the mixed-TEHD (thermo-elasto-hydrodynamic) model. It describes a mixed-lubrication process that considers the effects of asperity and asperity contact, a heat-transfer process in the integrated journal-lubricant-bearing system to analyze the temperature changes, and a thermal-elastic process to evaluate the consequent deformations. Many researchers have contributed to the TEHD solutions of the journal-bearing problem [86–90]. Moreover, Khonsari, Jang, and Fillon [89] have computed a group of temperature maps and Pierre and Fillon [91] have developed a set of parametric maps for journal bearing design. Khonsari, Pascovici, and Kucinski [92] have included debris modeling in bearing lubrication analyses. Recently, Wang, Wang, and Lin [93] worked on modeling multiple bearings in one system, such as coupled journal and thrust bearings, motivated from drill-bit bearing design. The research on couple bearings raises two important issues: designing bearing systems with mutual enhancement and achieving bearing modularization.

1.9 BOUNDARY LUBRICATION

The far left side of Figure 1.10 is the regime of boundary lubrication, which usually corresponds to the low-speed, high-load conditions. The lubrication status of start of a systems falls into this regime, and the interfaces of heavily loaded machine components, as well as the tooling–work-piece contact in a metal forming processes, may also work in this regime of lubrication. Compared with the lubrication in the full-film and mixed-film regimes, no significant fluid exists in the interface to separate the interacting surfaces in boundary lubrication. Boundary layers, formed through physical or chemical adsorption, or surface tribochemical reaction, are the media to lubricate the interface. The Reynolds equation based on the pressure-driven and shear flows generally has limited use in boundary lubrication analyses. Instead, phenomenological studies have been conducted to unfold the nature and mechanisms of boundary lubrication (Hsu and Gates [94]; Martin, Le Mogne, Boehm, and Grossiord [95]; and many others), and molecular dynamics merges to be a useful analytical tool to model boundary lubricating films (Sham and Tichy [96]; Müser, Urbakh, and Robbins [97]; and many others).

A quantitative description of boundary lubrication requires understanding of lubricant chemistry; surface material composition and its mechanical and chemical properties; surface tribochemistry; and interfacial mechanical, thermal, and contact conditions. Boundary film formation and removal are two competing mechanics that determine the health of boundary lubrication. The resultant boundary film should be lubricious with low shear strength. Surface tribochemistry governs the process of boundary layer formation, and a working lubricant with additives is usually the means to replenish boundary films on a contacting surface. The effective thickness of a boundary film can be measured with an EHL apparatus [98], and the chemistry of a boundary film formation can be

examined [99] with the advanced surface analytical tools mentioned at the beginning of this chapter.

Boundary films are the last lines of defense against failure of tribological interfaces. Compared with the contact in a fluid lubrication, boundary lubrication may yield higher friction and wear. Seizure and scuffing are two commonly seen failure modes because of the possibly high magnitude of frictional heating. The mechanism of seizure may vary in accordance with material combinations and operating conditions. Most power cylinder systems involve aluminum-silicon alloy/steel interactions. Many experiments suggest that failures of these systems occur mainly during the running-in stage, in which element surfaces undergo severe changes, or in extreme working conditions in which some of the operating parameters become abnormal [100–102]. Scuffing and seizure are separate mechanisms of failure and may occur in sequence because in scuffing, severe wear tears off the protective boundary layer and exposes metallic surfaces in direct contact and rubbing.

1.10 CONCLUDING REMARKS

Tribological interfaces exist in all machines where surfaces of components are in contact and relative motion. Understanding surface tribological interaction has become essential to engineering design for compact structures and reliable service performance, which requires knowledge of the physical, material, and topographic nature of surfaces; the mechanics of contact of surfaces; and the evaluation of the lubrication effect on interfacial behavior. This chapter provides an overview of basic methods for surface characterizations and fundamental principles of contact and lubrication analyses.

Engineering surfaces are complex in nature. Surface topography can be inspected with the assistance of the SEM, STM, AFM, optical microscopes, and white-light interferometer. In-depth surface statistical or fractal analyses should result in parameters characterizing the major features of a surface.

Contact of engineering surfaces may be conformal or counterformal. A conformal contact exists between a convex surface and a closely related concave surface, whereas a counterformal contact happens between convex bodies. The FEM is commonly used in various conformal contact analyses. However, the interaction area of a counterformal contact is usually much smaller than the dimension of the contacting bodies. Therefore, the corresponding surface deformation can be described by the integral of pressure and a Green's function, which leads to the analytical formulas for the contact size, the normal deformation, and the maximal contact pressure, such as the Hertz formulas for the contact of spherical bodies.

The Reynolds equation is the foundation of lubrication. Solving the Reynolds equation together with an elastic equation results in elastohydrodynamics and the contribution of material elasticity to lubricating film formation. Modifying the Reynolds equation with flow factors related to surface roughness and allowing asperity contact leads to the theory and practice of mixed lubrication. On the other hand, boundary lubrication is a status in which no significant fluid exists in the interface to separate the interacting surfaces, and friction reduction is accomplished by boundary layers formed through physical or chemical adsorption, or surface tribochemical reaction. Boundary lubrication

analysis requires understanding of lubricant chemistry; surface material composition and its mechanical and chemical properties; surface tribochemistry; and interfacial mechanical, thermal, and contact conditions.

REFERENCES

- [1] Oura, K., Likshits, V.G., Saranin, A.A., Zotov, A.V., and Katayama, M., 2003, *Surface Science: An Introduction*, Springer, New York.
- [2] Bhushan, B., 1995, *Handbook of Micro/Nano Tribology*, CRC Press, Boca Raton, FL.
- [3] Bhushan, B., 1999, *Principles and Applications of Tribology*, Wiley Interscience, New York.
- [4] Buckley, D.H., 2000, "Properties of Surfaces." In *Handbook of Lubrication, Vol. II Theory & Design*, E.R. Booser, Ed., CRC Press, Boca Raton, FL.
- [5] Halling, J., 1971, 1978, *Principles of Tribology*, The McMillan Press, London.
- [6] Arnell, R.D., Davies, P.B., Halling, J., and Whomes, T.L., 1991, *Tribology, Principles and Designs*, Springer-Verlag, Berlin.
- [7] Patir, N., and Cheng, H.S., 1978, "An Average Flow Model for Determine Effects of Three Dimensional Roughness on Partial Hydrodynamic Lubrication," ASME J. Lubr. Technol., Vol. 100, pp. 12–17.
- [8] Lee, S.C., and Ren, N., 1996, "Behavior of Elastic-Plastic Rough Surface Contacts as Affected by the Surface Topography, Load and Materials," STLE Tribology Trans., Vol. 39, pp. 67–74.
- [9] Mandelbrot, B.B. and W.H. Freeman, 1982, *The Fractal Geometry of Nature*, Henry Holt and Co., New York.
- [10] Majumdar, A., and Bhushan, B., 1990, "Role of Fractal Geometry in Roughness Characterization and Contact Mechanics of Surfaces," J. Tribology, Vol. 112, pp. 205–216.
- [11] Yan, W., and Komvopoulos, K., 1998, "Contact Analysis of Elastic-Plastic Fractal Surfaces," J. Appl. Phys., Vol. 84, pp. 3617–3624.
- [12] Borodich, F.M., Keer, L.M., and Harris, S.J., 2003, "Self-Similarity in Abrasiveness of Hard Carbon-Containing Coatings," J. Tribology, Vol. 125, pp. 1–7.
- [13] Sasikanth, A. and Wang, S., 2007, "Fractal-Regular Surface Characterization Based on Experimental Data from Atomic Force Microscopy of Hard Disks," 2007 Proceedings of the STLE/ASME Joint Tribology Conference: Parts A&B, ASME, New York, pp. 585–587.
- [14] Johnson, K.L., 1996, *Contact Mechanics*, Cambridge University Press, Cambridge, UK.
- [15] Ling, F.F., 1958, "On Asperity Distributions of Metallic Surfaces," J. Appl. Phys., Vol. 29.
- [16] Greenwood, J.A., and Williamson, J.B.P., 1966, "Contact of Nominally Flat Surfaces," Proc. Royal Soc. London A, Vol. 295, pp. 300–319.
- [17] Greenwood, J.A., and Tripp, J.H., 1971, "The Contact of Two Nominally Flat Rough Surfaces," Proc. Inst. Mech. Eng., Vol. 185, pp. 48–71.
- [18] Lee, S.C., and Cheng, H.S., 1992, "On the Relation of Load to Average Gap in the Contact Between Surfaces with Longitudinal Roughness," STLE Tribology Trans., Vol. 35, pp. 523–529.
- [19] Ju, Y., and Farris, T.N., 1996, "Spectral Analysis of Two-Dimensional Contact Problems," ASME J. Tribology, Vol. 118, pp. 320–328.
- [20] Yu, M.M.H., and Bhushan, B., 1996, "Contact Analysis of Three-Dimensional Rough Surfaces under Frictionless and Frictional Contact," Wear, Vol. 200, pp. 265–280.
- [21] Nogi, T., and Kato, T., 1997, "Influence of a Hard Surface Layer on the Limit of Elastic Contact—Part I: Analysis Using a Real Surface Model," ASME J. Tribology, Vol. 119, pp. 493–500.
- [22] Hu, Y.Z., Barber, G.C., and Zhu, D., 1999, "Numerical Analysis for the Elastic Contact of Real Rough," Tribology Trans., Vol. 42, pp. 443–452.
- [23] Ai, X.L., and Sawamiphakdi, K., 1999, "Solving Elastic Contact between Rough Surfaces as an Unconstrained Strain Energy Minimization by Using CGM and FFT Techniques," ASME J. Tribology, Vol. 121, pp. 639–647.
- [24] Polonsky, I.A., and Keer, L.M., 2000, "A Fast and Accurate Method for Numerical Analysis of Elastic Layered Contacts," ASME J. Tribology, Vol. 122, pp. 30–35.
- [25] Ting, B.Y., and Winer, W.O., 1989, "Frictional-Induced Thermal Influences in Elastic Contact between Spherical Asperities," ASME J. Tribology, Vol. 111, pp. 315–322.
- [26] Liu, G., and Wang, Q., 2000, "Thermoelastic Asperity Contacts, Frictional Shear, and Parameter Correlations," ASME J. Tribology, Vol. 122, pp. 300–307.
- [27] Liu, S.B., and Wang, Q., 2001, "A Three-Dimensional Thermomechanical Model of Contact between Non-Conforming Rough Surfaces," ASME J. Tribology, Vol. 123, pp. 17–26.
- [28] Ling, F.F., 1973, *Surface Mechanics*, John Wiley & Sons, New York.
- [29] Holmberg, K., and Mathews, A., 1994, "Coatings Tribology: A Concept, Critical Aspects and Future Directions," Thin Solid Films, Vol. 253, pp. 173–178.
- [30] Plumet, S., and Dubourg, M.C., 1998, "A 3-D Model for a Multilayered Body Loaded Normally and Tangentially Against a Rigid Body: Application to Specific Coatings," ASME J. Tribology, Vol. 120, pp. 668–676.
- [31] Leroy, J.M., Floquet, A., and Villechaise, B., 1989, "Thermomechanical Behavior of Multilayered Media: Theory," ASME J. Tribology, Vol. 112, pp. 317–323.
- [32] Cole, S.J., and Sayles, R.S., 1921, "A Numerical Model for the Contact of Layered Elastic Bodies with Real Rough Surfaces," ASME J. Tribology, Vol. 114, pp. 334–340.
- [33] Mao, K., Sun, Y., and Bell, T., 1996, "A Numerical Model for the Dry Sliding Contact of Layered Elastic Bodies with Rough Surfaces," STLE Tribology Trans., Vol. 39, pp. 416–424.
- [34] Goryacheva, I., Sadeghi, F., and Nickel, D.A., 1996, "Internal Stresses in Contact of a Rough Body and a Viscoelastic Layered Semi-Infinite Plane," ASME J. Tribology, Vol. 118, pp. 131–136.
- [35] Liu, S., and Wang, Q., 2003, "Transient Thermoelastic Stress Fields in a Half-Space," ASME J. Tribology, Vol. 125, pp. 33–43.
- [36] Liu, S., Peyronnel, A., Wang, Q., and Keer, L., 2005a, "An Extension of the Hertz Theory for 2D Coated Components," Tribology Lett., Vol. 18, pp. 505–511.
- [37] Liu, S., Peyronnel, A., Wang, Q., and Keer, L., 2005b, "An Extension of the Hertz Theory for Three-Dimensional Coated Bodies," Tribology Lett., Vol. 18, pp. 303–314.
- [38] Chang, W.R., Etsion, I., and Bogoy, D.B., 1987, "Elastic Plastic Model for the Contact of Rough Surfaces," ASME J. Tribology, Vol. 109, pp. 257–263.
- [39] Komvopoulos, K., and Choi D.H., 1992, "Elastic Finite Element Analysis of Multi-Asperity Contacts," J. Tribology, Vol. 114, pp. 823–831.
- [40] Liu, G., Zhu, J., Yu, L., and Wang, Q.J., 2001, "Elasto-Plastic Contact of Rough Surfaces," Tribology Trans., Vol. 44, pp. 437–443.
- [41] Kogut, L., and Etsion, I., 2002, "Elastic-Plastic Contact Analysis of a Sphere and a Rigid Flat," J. Appl. Mech., Vol. 69, pp. 657–662.
- [42] Kogut, L., and Etsion, I., 2003, "A Finite Element Based Elastic-Plastic Model for the Contact of Rough Surfaces," Tribology Trans., Vol. 46, pp. 383–390.
- [43] Gao, Y.F., Bower, A.F., Kim, K.-S., Lev, L., and Cheng, Y.T., 2006, "The Behavior of an Elastic-Perfectly Plastic Sinusoidal Surface under Contact Loading," Wear, Vol. 261, pp. 145–154.
- [44] Kim, T.W., Bhushan, B., and Cho, Y.J., 2006, "The Contact Behavior of Elastic/Plastic Non-Gaussian Rough Surfaces," Tribology Lett., Vol. 22, pp. 1–13.
- [45] Jacq, C., Nelias, D., Lormand, G., and Girodin, D., 2002, "Development of a Three-Dimensional Semi-Analytical Elastic-Plastic Contact Code," ASME J. Tribology, Vol. 124, pp. 653–667.
- [46] Boucly, V., Nelias, D., Liu, S.B., Wang, Q., and Keer, L.M., 2005, "Contact Analyses for Bodies with Frictional Heating and Plastic Behavior," ASME J. Tribology, Vol. 127, pp. 355–364.
- [47] Wang, F., and Keer, L.M., 2005, "Numerical Simulation for Three Dimensional Elastic-Plastic Contact with Hardening Behavior," ASME J. Tribology, Vol. 127, pp. 494–502.

- [48] Chen, W.W., Liu, S., and Wang, Q., 2008, "Fast Fourier Transform Based Numerical Methods for Elasto-Plastic Contacts of Nominally Flat Surfaces," *J. Appl. Mechan.*, Vol. 75, 011022.
- [49] Wang, S., and Komvopoulos, K., 1994, "A Fractal Theory of the Interfacial Temperature Distribution in the Slow Sliding Regime: Part 1—Elastic Contact and Heat Transfer Analysis," *ASME J. Tribology*, Vol. 116, pp. 812–832.
- [50] Wang, S., 2003, "Real Contact Area of Fractal-Regular Surfaces and Its Implementations in the Law of Friction," *ASME J. Tribology*, Vol. 126, pp. 1–8.
- [51] Klaus, E.E., and Tewksbury, E.R., 1989, "Liquid Lubricants." In *Handbook of Lubrication: Theory and Practice of Tribology, Vol. II Theory & Design*, E.R. Booser, Ed., CRC Press, Boca Raton, FL.
- [52] Cameron, A., 1966, *The Principles of Lubrication*, Longman Press, London.
- [53] Briant, J., Denis, J., and Parc, G., 1989, *Rheological Properties of Lubricants*, Editions Technip, Paris.
- [54] Hamrock, B., 1994, *Fundamentals of Fluid Film Lubrication*, McGraw Hill, New York.
- [55] Cheng, H.S., and Sternlicht, B., 1965, "A Numerical Solution for the Pressure, Temperature, and Film Thickness between Two Infinitely Long, Lubricated Rolling and Sliding Cylinders, under Heavy Loads," *J. Basic Eng.*, Trans. ASME, Vol. 87, pp. 695–707.
- [56] Houppert, L., 1985, "New Results of Traction Force Calculations in Elastohydrodynamic Contacts," *J. Tribology*, Vol. 107, pp. 241–248.
- [57] Doolittle, A.D., 1951, "Studies in Newtonian Flow II the Dependence of the Viscosity of Liquids on Free-Space," *J. Appl. Phys.*, Vol. 22, pp. 1471–1475.
- [58] Cook, R.L., Herbst, C.A., and King, H.E., Jr., 1993, "High-Pressure Viscosity of Glass-Forming Liquids Measured by the Centrifugal Force Diamond Anvil Cell Viscometer," *J. Phys. Chem.*, Vol. 97, pp. 2355–2361.
- [59] Yasutomi, V., Bair, S., and Winer, W.O., 1984, "An Application of a Free Volume Model to Lubricant Rheology I—Dependence of Viscosity on Temperature and Pressure," *ASME J. Lubr. Technol.* Vol. 106, pp. 291–303.
- [60] Johnson, K.L., and Tevaarwerk, J.L., 1977, "Shear Behaviour of Elastohydrodynamic Oil Films," *Proc. Royal Soc. Lond. A*, Vol. 356, pp. 215–236.
- [61] Bair, S., and Winer, W.O., 1979, "A Rheological Model for Elastohydrodynamic Contacts Based on Primary Laboratory Data," *J. Lubric. Technol.*, Vol. 101, pp. 259–265.
- [62] Tevaarwerk, J.L., and Johnson, K.L., 1979, "The Influence of Fluid Rheology on the Performance of Traction Drives," *J. Lubr. Technol.*, Vol. 101, pp. 266–274.
- [63] Bair, S., and Qureshi, F., 2003, "The Generalized Newtonian Fluid Model an Elastohydrodynamic Film Thickness," *J. Tribology*, Vol. 125, pp. 70–75.
- [64] Carreau, P. J., 1972, "Rheological Equations from Molecular Network Theories," *Trans. Soc. Rheol.*, Vol. 16, pp. 99–127.
- [65] Bair, S., and Khonsari, M., 1996, "An EHD Inlet Zone Analysis Incorporating the Second Newtonian," *ASME J. Tribology*, Vol. 118, pp. 341–343.
- [66] Wang, J.C., and Fichtorn, K.A., 2002, "Influence of Molecular Structures on the Properties of Confined Fluids by Molecular Dynamics Simulation," *Colloids Surf.*, Vol. 206, pp. 267–276.
- [67] Martini, A., Liu, Y., Snurr, R. and Wang, Q., 2006, "Molecular Dynamics Characterization of Thin Film Viscosity for EHL Simulation," *Tribology Letters*, Vol. 21, pp. 217–225.
- [68] Dowson, D., and Higginson, G. R., 1977, *Elastohydrodynamic Lubrication*, Pergamon Press, Oxford, UK.
- [69] Pinkus, O., and Sternlicht, B., 1961, *Theory of Hydrodynamic Lubrication*, McGraw-Hill, New York.
- [70] Ludema, K., 1996, *Friction, Wear, Lubrication*, CRC Press, Boca Raton, FL.
- [71] Dowson, D., 1998, *History of Tribology*, Professional Engineering Publishing, London.
- [72] Luengo, G., Israelachvili, J., and Granick, S., 2002, "Generalized Effects in Confined Fluids: New Friction Map for Boundary Lubrication," *Wear*, Vol. 200, pp. 328–335.
- [73] Reddy, D.S., Swarnamani, S., and Prabhu, B.S., 2000, "Thermoelastohydrodynamic Analysis of Tilting Pad Journal Bearing—Theory and Experiments," *Tribology Trans.*, Vol. 43, pp. 82–90.
- [74] Xiao, L., Rosen, B.G., Amini, N., and Nilsson, P.H., 2003, "A Study on the Effect of Surface Topography on Rough Friction in Roller Contact," *Wear*, Vol. 254, pp. 1162–1169.
- [75] Wang, Y., Lin, C., Wang, Q., and Shi, F., 2006, "Development of a Set of Stribeck Curves for Conformal Contacts of Rough Surfaces," *Tribology Trans.*, Vol. 49, pp. 526–535.
- [76] Gohar, R., 2001, *Elastohydrodynamics*, Imperial College Press, London.
- [77] Winer, W., and Cheng, H.S., *Wear Control Handbook*, M.B. Peterson and W.O. Winer, Eds., ASME, New York.
- [78] Christensen H., 1970, "Stochastic Models for Hydrodynamic Lubrication of Rough Surfaces," *Proc. Inst. Mech. Eng.*, Vol. 184, pp. 1013–1026.
- [79] Harp, S., and Salant, R., 2001, "An Average Flow Model of Rough Surface Lubrication with Inter-Asperity Cavitation," *J. Tribology*, Vol. 123, pp. 134–143.
- [80] Hu, Y.Z., and Zhu, D., 2000, "A Full Numerical Solution to the Mixed Lubrication in Point Contacts," *ASME J. Tribology*, Vol. 122, pp. 1–9.
- [81] Zhao, J.X., Sadeghi, F., and Hoeprich, M.H., 2001, "Analysis of EHL Circular Contact Start Up: Part I—Mixed Contact Model with Pressure and Film Thickness Results," *ASME J. Tribology*, Vol. 123, pp. 67–74.
- [82] Holmes, M.J.A., Evans, H.P., and Snidle, R.W., 2005, "Analysis of Mixed Lubrication Effects in Simulated Gear Tooth Contacts," *J. Tribology ASME*, Vol. 127, pp. 61–69.
- [83] Wang, Q., Zhu, D., Yu, T., Cheng, H.S., Jiang, J., and Liu, S., 2004, "Mixed Lubrication Analyses by a Micro-Macro Approach and a Full-Scale Micro EHL Model," *ASME J. Tribology*, Vol. 126, pp. 81–91.
- [84] Wang, Q., Shi, F., and Lee, S., 1997, "A Mixed-Lubrication Study of Journal Bearing Conformal Contacts," *ASME J. Tribology*, Vol. 119, pp. 456–461.
- [85] Shi, F., and Wang, Q., 1998, "A Mixed-TEHD Model for Journal Bearing Conformal Contacts, Part I: Model Formulation and Approximation of Heat Transfer Considering Asperity Contacts," *ASME J. Tribology*, Vol. 120, pp. 198–205.
- [86] Pinkus, O., 1990, *Thermal Effects on Fluid-Film Lubrication*, ASME Press, New York.
- [87] Fillon, M., Bligoud, J., and Frêne, J., 1992, "Experimental Study of Tilting-Pad Journal Bearings-Comparison with Theoretical Thermoelastohydrodynamic Results. Trans. ASME J. Tribology, Vol. 114, pp. 579–587.
- [88] Tucker, P.G., and Keogh, P.S., 1994, "A Generalized Computational Fluid Dynamics Approach for Journal Bearing Performance Prediction," *Proc. Inst. Mech. Eng.*, Vol. 209, pp. 99–108.
- [89] Khonsari, M.M., Jang, J.Y., and Fillon, M., 1995, "On the Generalization of Thermoelastohydrodynamic Analyses for Journal Bearings," *ASME J. Tribology*, Vol. 118, pp. 1–9.
- [90] Paranjpe, R.S., and Han, T., 1995, "A Transient Thermohydrodynamic Analysis Including Mass Conserving Cavitation for Dynamically Loaded Journal Bearings," *Trans. ASME J. Tribology*, Vol. 117, pp. 369–377.
- [91] Pierre, I., and Fillon, M., 2000, "Influence of Geometric Parameters and Operating Conditions on the Thermohydrodynamic Behavior of Plain Journal Bearings," *Proc. Inst. Mech. Eng.*, Vol. 214, pp. 445–457.
- [92] Khonsari, M.M., Pascovici, M.D., and Kucinschi, B.V., 1999, "On the Scuffing Failure of Hydrodynamic Bearings in the Presence of an Abrasive Contaminant," *J. Tribology*, Vol. 121, pp. 90–96.
- [93] Wang, Y., Wang, Q., and Lin, C., 2003, "Mixed Lubrication of Coupled Journal-Thrust Bearing Systems Including Mass Conserving Cavitation," *ASME J. Tribology*, Vol. 125, pp. 747–755.
- [94] Hsu, S., and Gates, R.S., 2005, "Boundary Lubricating Films: Formation and Lubrication Mechanism," *Tribology Int.*, Vol. 38, pp. 305–312.
- [95] Martin, J.M., Le Mogne, Th., Boehm, M., and Grossiord, C., 1999, "Tribocchemistry in the Analytical UHV Tribometer," *Tribology Int.*, Vol. 32, pp. 617–626.

- [96] Sham, T.-L., and Tichy, J., 1997, "Scheme for Hybrid Molecular Dynamics/Finite Element Analysis of Thin Film Lubrication," *Wear*, Vol. 207, pp. 100–106.
- [97] Müser, M., Urbakh, M., and Robbins, M., 2003, "Statistical Mechanics of Static and Low-Velocity Kinetic Friction." In *Advances in Chemical Physics*, Vol. 126, I. Prigogine and S.A. Rice, Eds., John Wiley & Sons, Hoboken, NJ.
- [98] Johnston, G.J., Wayte, R., and Spikes, H.A., 1991, "The Measurement and Study of Very Thin Lubricant Films in Concentrated Contacts," *Tribology Trans.*, Vol. 34, pp. 187–194.
- [99] Hershberger, J., Ajayi, O.O., and Fenske, G.R., 2003, "X-Rays as a Tool for Investigation of Scuffing and Boundary Lubrication," *Tribology Trans.*, Vol. 46, pp. 550–555.
- [100] He, X., 1998, *Experimental and Analytical Investigation of the Seizure Process in Al-Si Alloy/Steel Tribocontacts*, Ph.D. Dissertation, Northwestern University, Evanston, IL.
- [101] Ye, Z., Zhang, C., Wang, Q., Cheng, H. S., Wang, Y., Tung, S., and He, X., 2004, "An Experimental Investigation of Piston Skirt Scuffing: Piston Scuffing Apparatus, Experiments, and Scuffing Mechanism Analyses," *Wear*, Vol. 257, pp. 8–31.
- [102] Wang, Y., Brogan K., and Tung, S. C., 2001, "Wear and Scuffing Characteristics of Composite Polymer and Nickel/Ceramic Composite Coated Piston Skirts against Aluminum and Cast Iron Cylinder Bores," *Wear*, Vol. 250, pp. 706–717.

Automotive Lubricants

Derek Mackney¹, Nick Clague¹, Gareth Brown¹, Gareth Fish², and John Durham¹

2.1 INTRODUCTION

A lubricant has to perform many functions to effectively lubricate the various parts of a vehicle. These functions include

- Reduction of friction and wear,
- Removal of heat,
- Removal of contaminants,
- Protection of surfaces from corrosion,
- Cleaning of surfaces, and
- Neutralization of acids formed during combustion.

Depending on the application, lubricants have to perform some or all of these functions across a wide temperature range and over an extended lifetime. Low temperatures can lead to gelation of the lubricant, which can lead to oil starvation at critical points in the machinery. High temperatures can lead to loss of viscosity and oil film collapse, resulting in excessive wear. The lubricant can also become oxidized, which causes oil thickening and the formation of insoluble sludge, lacquer, varnish, and carbonaceous deposits. Lubricants also need to be able to handle contaminants such as soot particles formed during combustion in an internal combustion engine. Even the most highly refined base oils or synthetic base oils cannot achieve all of these requirements alone. To effectively lubricate, the base oil needs additives to provide the properties that the base oil lacks. These properties include high- and low-temperature viscometrics, solvency, acid neutralization, oxidation resistance, corrosion resistance, and wear protection (in the mixed and boundary lubrication regimes).

Additives are normally sold as performance packages, a blend of components, each of which has a specific function or functions within the lubricant. However, it should be noted that to achieve the best results, high-quality base oils should also be used. It is unlikely that poor-quality base oil can be turned into a top-tier lubricant by adding a performance package.

2.2 ADDITIVES

The active part of an additive is often highly viscous or even solid at normal temperatures. Consequently, additives are usually prepared in a base oil to improve the manufacturing process and subsequent handling. Lubricant additives are often grouped into three basic categories:

1. *Performance additives* such as viscosity modifiers, pour-point depressants, seal swell agents, and antifoams that modify some physical property of the base oil.

2. *Oil protection additives* such as antioxidants that react chemically within the lubricant to reduce oil degradation.
3. *Surface protection additives* such as friction modifiers, antiwear additives, extreme pressure additives, detergents, and dispersants that act at the interface between the lubricant and machine components in the case of friction modifiers, antiwear agents, and detergents or contaminants in the case of dispersants.

2.2.1 Performance Additives

2.2.1.1 VISCOSITY MODIFIERS

The most fundamental properties of a lubricant are its viscosity [1] and the rate at which the viscosity changes with temperature. The viscosity of the lubricant should ideally not change with temperature. However, as the temperature decreases, the viscosity increases. Choosing a high-viscosity base oil to have the correct viscosity at high temperature generally means that at low temperature the oil does not flow adequately because it is too viscous, leading to oil starvation. Conversely, if low-viscosity base oil is chosen to allow low-temperature flow, then at high temperature the oil lacks sufficient viscosity to separate moving parts in the hydrodynamic lubrication regime. This can lead to oil film collapse, resulting in mixed or even boundary lubrication and subsequent wear. By combining low-viscosity base oil with a polymeric viscosity modifier (VM) it is possible to achieve the low- and high-temperature requirements (Figure 2.1). The VM is able to do this because of its large molecular size and its change in solubility with temperature. At low temperatures, the VM is sparingly soluble in the base oil and tends to curl itself into a small ball that occupies a small volume of oil. In this state, it has little influence on the viscosity of the oil, maintaining the low viscosity of the base oil. At higher temperatures, the solubility of the VM increases and the polymer molecules tend to unwind and occupy a larger volume of oil [2,3] (Figure 2.2). This has the effect of increasing the viscosity of the lubricant, thereby providing increased film thickness compared with the base oil alone, which allows the system to operate in the hydrodynamic lubrication regime rather than the mixed lubrication regime, thereby reducing wear. Under very high shear conditions the fluid can shear thin; that is, the fluid loses viscosity either because (1) the VM molecules are broken into smaller molecules with permanent viscosity loss or (2) the VM molecules align through the shear zone, which also leads to viscosity loss but this loss is temporary

¹ Lubrizol Limited, Hazelwood, Derbyshire, UK

² The Lubrizol Corporation, Wickliffe, Ohio, USA

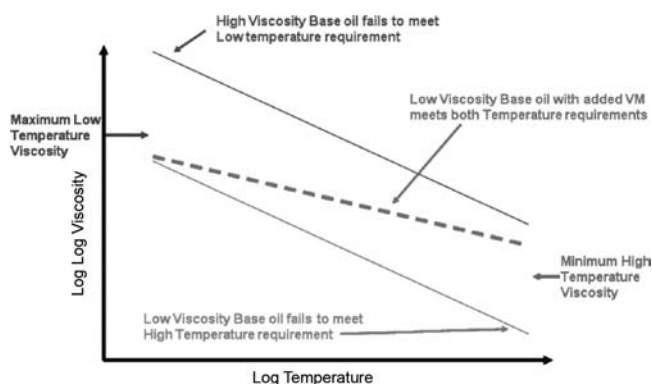


Figure 2.1—Schematic diagram of viscosity/temperature behavior of base oils with and without VMs.

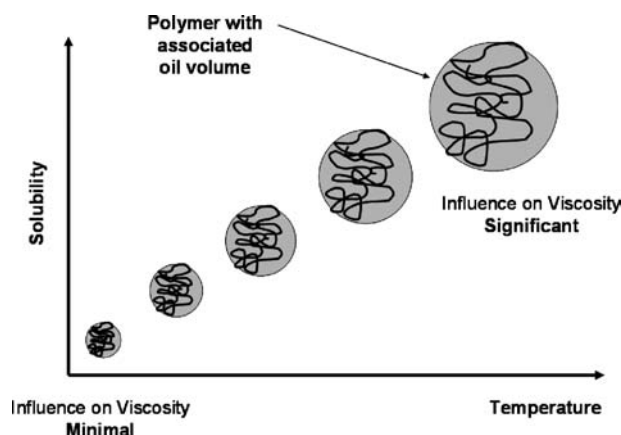


Figure 2.2—Mechanism of oil thickening by polymeric VMs [2].

and the original viscosity of the fluid will return outside of the shear zone. This property of lubricants is measured by the High-Temperature High-Shear Viscosity test (ASTM D4741 and D5481).

Specific viscometric requirements are shown in Table 2.6 (Section 2.3) and Table 2.10 (Section 2.4).

There are several different types of VMs. Most are high-molecular-weight ($M_n = 50,000$ to $500,000$) polymeric materials with varying degrees of branching prepared from individual monomers or groups of monomers. Figure 2.3 shows some of the VMs typically used in automotive applications.

2.2.1.1.1 Polyisobutylenes

Polyisobutylenes (PIBs) were the first type of VM used for engine oils. Although they have very good inherent shear stability, they have been superseded by other types because they do not provide the properties required for low-temperature operation. PIBs are also used as the backbone for many dispersants; consequently, dispersants of this type have viscosity-modifying properties. They generally cause an increase in traction in the elastohydrodynamic (EHD) lubrication regime that may adversely affect fuel economy. Lower-molecular-weight PIBs (2000–3000 MW) are used in gear oils; their excellent shear stability is essential in the high-shear environment of meshing gear teeth. However, because of the lower molecular weight, the thickening achieved per unit mass added is lower than for the high-molecular-weight materials used for engine lubricants; the concentration of polymer used in gear applications is typically much higher than that used in engine lubricants.

2.2.1.1.2 Olefin Copolymers

Olefin copolymers (OCPs) are typically ethylene-propylene copolymers and are widely used in engine lubricants

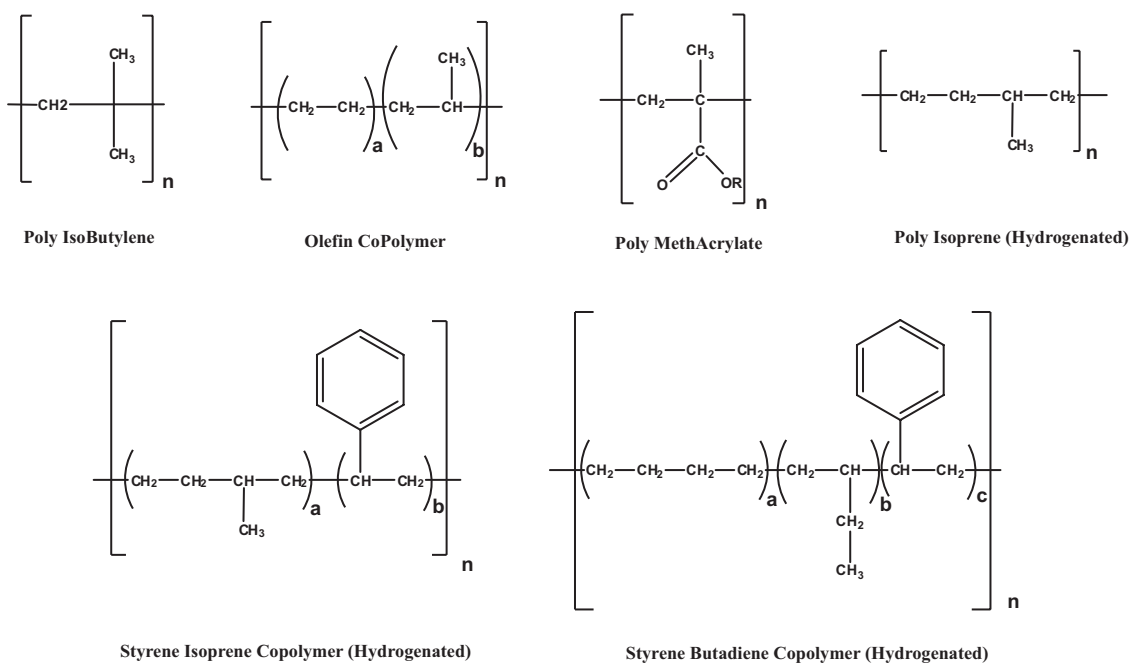


Figure 2.3—VMs typically used in automotive applications.

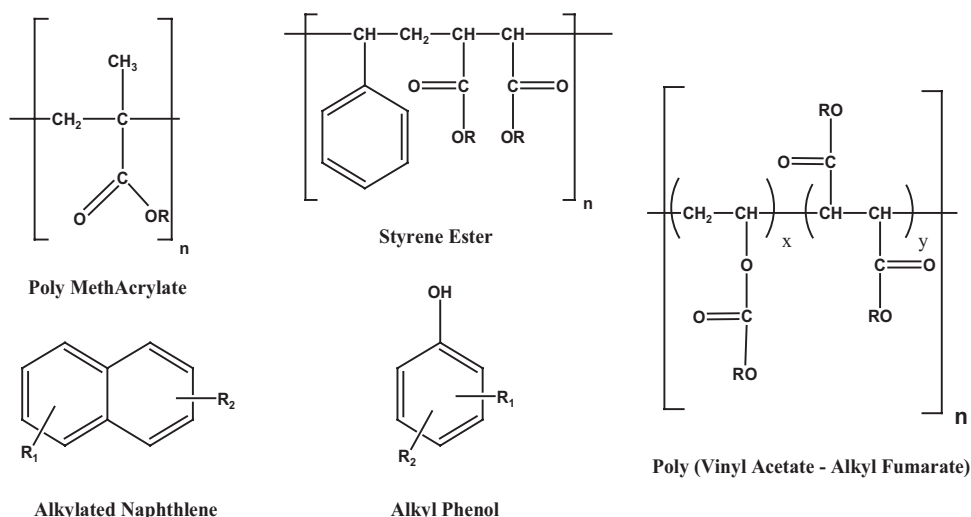


Figure 2.4—Pour-point depressants.

because of their cost-effectiveness and satisfactory engine performance. These polymers have good thermal stability and adequate low-temperature properties, but lubricants formulated with OCPs, as with other VMs, will often also need a pour-point depressant. Low-temperature properties can be adjusted by changing the ratio of ethylene to propylene in the polymer.

2.2.1.1.3 Hydrogenated Styrene Butadiene Copolymers

Hydrogenated styrene butadiene copolymers (SBCs) are widely used in high-performing engine oils because they provide good low-temperature properties, piston cleanliness, fuel economy benefits, and oil performance maintenance in the presence of high levels of soot. They are more expensive to produce than OCP-based polymers.

2.2.1.1.4 Hydrogenated Styrene Isoprene Copolymers

Hydrogenated styrene isoprene copolymers (SICs) are widely used in high-performing engine oils because of some unique properties. The high electron density in the styrene part of the molecule can interact with soot particles and it provides benefits for the oil in terms of cleanliness and performance maintenance in the presence of soot.

2.2.1.1.5 Hydrogenated Radial Isoprenes

Hydrogenated radial isoprenes (RIs) are VMs that exhibit good shear stability and thickening, which typically lead to lower treat rates than other VMs.

2.2.1.1.6 Polymethacrylates

Widely used in transmission applications, the alkyl sidechains found in polymethacrylates (PMAs) provide excellent low-temperature properties. These polymers tend not to be used in engine oils because they can lead to piston deposits. Changing the length of the alkyl sidechain from only short chains to variable chain lengths on the same molecule (4–20 C atoms) as well as reducing the length of the C backbone produces highly effective pour-point depressants.

2.2.1.2 POUR-POINT DEPRESSANTS

The pour point of a lubricant is the temperature at which the lubricant will no longer pour. A low pour point is

particularly important for proper performance in colder climates. As a lubricant is cooled, wax crystals begin to appear. Eventually, these crystals join to produce a gel-like structure that can lead to oil starvation due to blocking of oil-ways. Pour-point depressants act to reduce crystal growth and prevent gelling, thereby lowering the temperature at which the lubricant can effectively function. There are several types of chemistry used. Some are polymeric but of a lower molecular weight than those used for VMs, and some are smaller, nonpolymeric molecules. A structure with varying length linear alkyl sidechains on the polymer produces the best pour-point depressants. The polymeric types are generally more effective than the smaller, nonpolymeric types.

Figure 2.4 shows the different polymer architecture associated with pour-point depressants. Figure 2.5 compares pour-point depressant and VM structures, showing that VMs are generally long-chain polymers with short branches and the pour-point depressants are shorter-chain polymers with a mixture of long and short sidechains. This mixed side-chain structure effectively inhibits the growth of wax crystals, thereby allowing the operating temperature to be reduced.

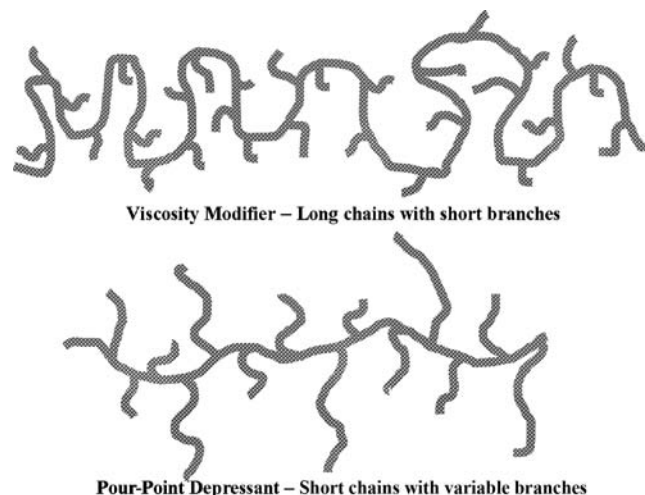


Figure 2.5—Comparison of pour-point depressant and VM structures.

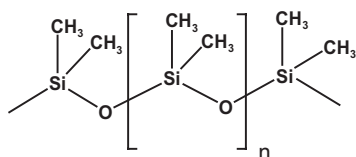


Figure 2.6—Polymethylsiloxane antifoam.

2.2.1.3 SEAL SWELL AGENTS

Many components of engines and transmissions are joined with the aid of seals that provide easy assembly of equipment and separation between different environments within the equipment. Contact with lubricating oils can result in shrinkage, brittleness, and cracking of these seals, which in turn can lead to leakage of the lubricant. To reduce these effects, certain chemicals are used at low levels, allowing the seal to retain its optimal size and hardness for sealing performance. Common chemicals used for this purpose include some phosphate esters and polyol esters.

2.2.1.4 ANTIFOAMS

Excessive agitation of lubricants can lead to air entrainment and foam formation. This can lead to increased rates of oxidation due to the intimate contact of large amounts of air with oil at elevated temperatures. In addition, an air/oil mixture is less able than a full oil film to support a given load. This can lead to oil film collapse, contacting surfaces, and consequent wear. Low-viscosity oils tend to produce foams that are less stable than higher viscosity oils. The presence of certain additives, such as detergents and dispersants, can increase foam formation. Good antifoam agents need low surface tension, to be essentially insoluble in the lubricant, and to have a good spreading coefficient. Polysiloxanes (Figure 2.6) are typically used because they are only sparingly soluble in the lubricant and tend to migrate to the air/oil interface where they act to reduce the surface tension of the bubbles, which then become unstable and collapse. These antifoams are extremely effective at very low treat rates (10–20 ppm Si) and at higher treat rates can cause stability issues with the oil and even increase the ability of the oil to foam. PMAs may also be used as antifoams in transmission applications; they operate in the same way as polysiloxanes, but they require higher treat rates (100–200 ppm).

2.2.2 Oil Protection Additives

2.2.2.1 ANTIOXIDANTS

All lubricating oils undergo oxidation in their working environments. Increasing temperature increases the rate of oxidation; the rate of oxidation will typically double for a 10°C increase in operating temperature. The pres-

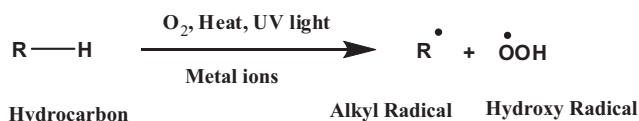


Figure 2.7—Initiation reaction.

ence of oxidation catalysts such as metal ions, oxygen, nitrogen oxides (NO_x), and some organic species will also increase the rate of oxidation. The mechanism of oxidation can be complicated for single species; the many different species that are found in any lubricating oil make oxidation an extremely complicated series of reactions. However, the oxidation process can be reduced to four basic steps: initiation, propagation, chain-branching, and termination [4,5].

1. *Initiation:* A C–H bond can be homolytically cleaved (Figure 2.7) under the influence of oxygen, heat, or ultraviolet light (from the combustion process) and can be catalyzed by the presence of metal ions to form free radicals.
2. *Propagation:* In the presence of oxygen, the alkyl radical will react very quickly and irreversibly to form the peroxy radical. This step is followed by the abstraction of a hydrogen atom from a second hydrocarbon molecule to form another alkyl radical and a hydroperoxide (Figure 2.8).
3. *Chain-branching:* At higher temperatures, hydroperoxide cleavage can result in the formation of alkoxy and hydroxy radicals. This step is relatively slow, but once it has occurred the newly formed radicals can easily react with more hydrocarbon molecules to generate further radicals and, depending on the exact nature of the molecule attacked, alcohols, aldehydes, ketones, acids, and water. Acids, aldehydes, and ketones can undergo various further reactions that can lead to polymeric species that eventually become oil-insoluble sludge, lacquer, and varnish (Figure 2.9).
4. *Termination:* Reaction of a radical with another radical will create a stable hydrocarbon molecule or another hydroperoxide, which can decompose further by the mechanisms listed above (Figure 2.10).

From the above series of reactions it becomes clear that reductions in the levels of peroxides and radicals will extend lubricant life by slowing down the rate of oxidation. The antioxidants used in lubricants fall into two categories: hydroperoxide decomposers and radical scavengers (Figure 2.11) [6]. Most lubricants use a combination of hydroperoxide decomposers and radical scavengers to effectively minimize oxidation. Radical scavengers tend to be aryl amines or alkylphenols. Different molecular-weight phenols and amines work at different temperatures, and

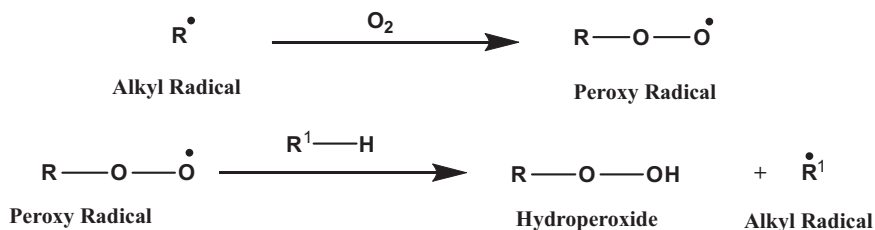


Figure 2.8—Propagation reactions.

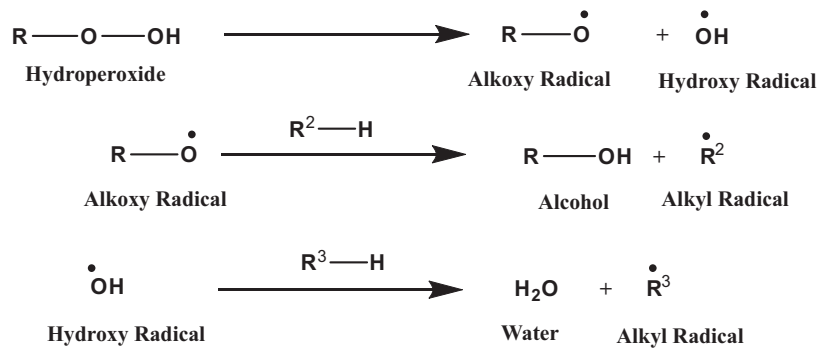


Figure 2.9—Chain-branching reactions.

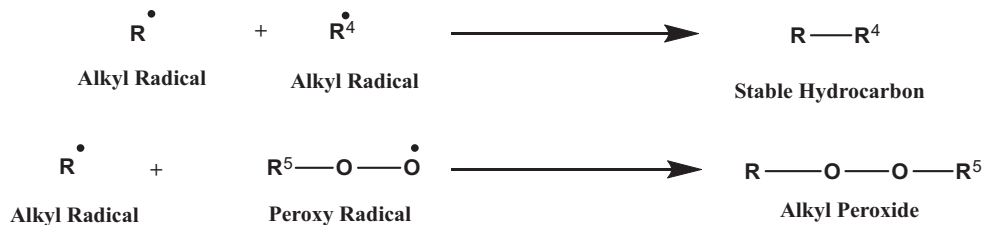


Figure 2.10—Termination reactions.

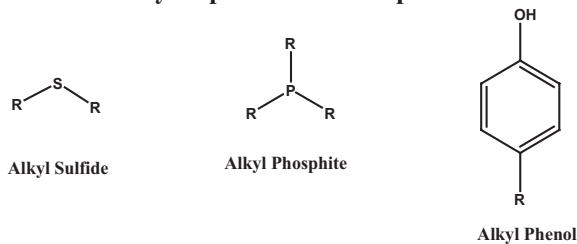
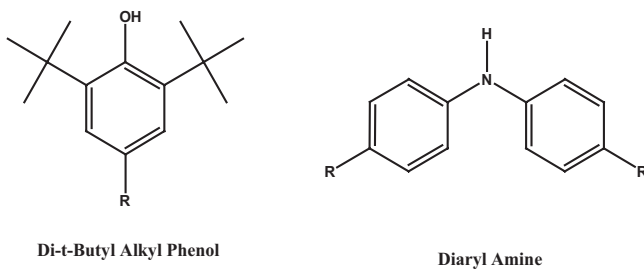
Hydroperoxide Decomposers**Radical Scavengers**

Figure 2.11—Typical antioxidants used in automotive applications.

in some applications mixtures will be used to provide the required oxidation performance for the lubricant. Zinc dialkyl dithiophosphate is a hydroperoxide decomposer and radical scavenger [6], and it provides excellent antiwear and corrosion prevention properties [7].

2.2.3 Surface Protection Additives

All surface protection additives work by combining a hydrocarbon tail with a polar head group that usually contains one or more elements from N, O, P, and S atoms. The hydrocarbon tail tends to be solubilized in the oil phase whereas the polar head group is attracted to metal surfaces or other

polar materials such as soot particles, oxidized oil sludge, and other deposits. By combining different polar heads with different hydrocarbon tails, different functions within the lubricant can be realized, such as friction modification, antiwear, and extreme pressure performance. It is the skill of the lubricant additive formulator that ensures the use of the correct ratio of all of these components to achieve the requirements of the lubricant in terms of friction reduction, wear protection, corrosion protection, and cleanliness.

2.2.3.1 FRICTION MODIFIERS

Friction occurs in lubricated systems either within the fluid because of its viscosity, commonly called viscous drag, or because of the relative motion of contacting components of the engine such as the piston ring on liner, piston skirt on liner, cam on follower, etc., which operate in the mixed or boundary lubrication regimes. Using a lubricant of lower viscosity can reduce viscous drag, but care must be taken not to reduce the viscosity to such an extent that normal hydrodynamic lubrication cannot be achieved in the main, big, and little end bearings. Friction modifiers are used in engines and gear boxes to reduce friction in more severe contact areas as mentioned above. This reduces power loss and thereby improves fuel efficiency. However, in the case of automatic transmission fluids, the need is to achieve the correct frictional properties to ensure smooth and timely engagement and disengagement of clutches and bands with no stick-slip or chatter.

There are two groups of friction modifiers that work in different ways to reduce friction: organic friction modifiers and organo-molybdenum friction modifiers. Organic friction modifiers are generally straight-chain hydrocarbons of approximately 18 C atoms with a polar head group that can be an amine, amide, carboxylic acid, ester, or phosphoric or phosphonic acid. The hydrocarbon chain solubilizes in the oil phase, and the polar head group attaches to the metal surface by physisorption or chemisorption. Further

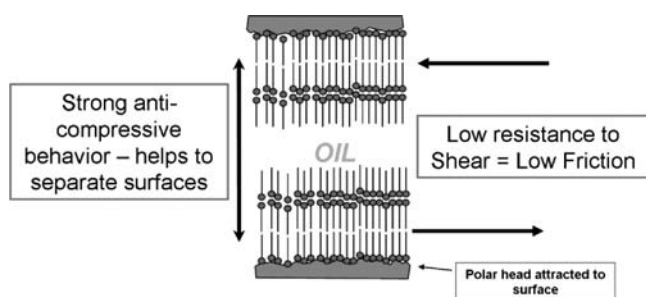


Figure 2.12—Organic friction modifier mode of operation.

stacking of molecules can produce multilayers as shown in Figure 2.12. The molecules stacked in this way are hard to compress and therefore help to separate the surfaces. In addition, there is little resistance to shear along the hydrocarbon tail to hydrocarbon tail boundaries resulting in

reduced friction [8]. Examples of organic friction modifiers are shown in Figure 2.13.

Once attached to the metal surface, organic friction modifiers begin to work immediately. Mo-containing friction modifiers, such as dithiocarbamates (Figure 2.14) and dithiophosphates, work in a slightly different way. Mo types rely on the energy generated in the contact to convert the Mo-containing species into MoS_2 . It is the MoS_2 that is the true friction modifier [9]. MoS_2 has a lamellar structure that enables its layers to slide past each other easily, resulting in very low friction (Figure 2.15). The need for a chemical reaction to take place means that these types of friction modifiers do not work efficiently under light loads or at low temperatures.

Friction modifiers are able to extend the working range of lubricants in terms of contact pressure, but only to a certain level, above which they become ineffective.

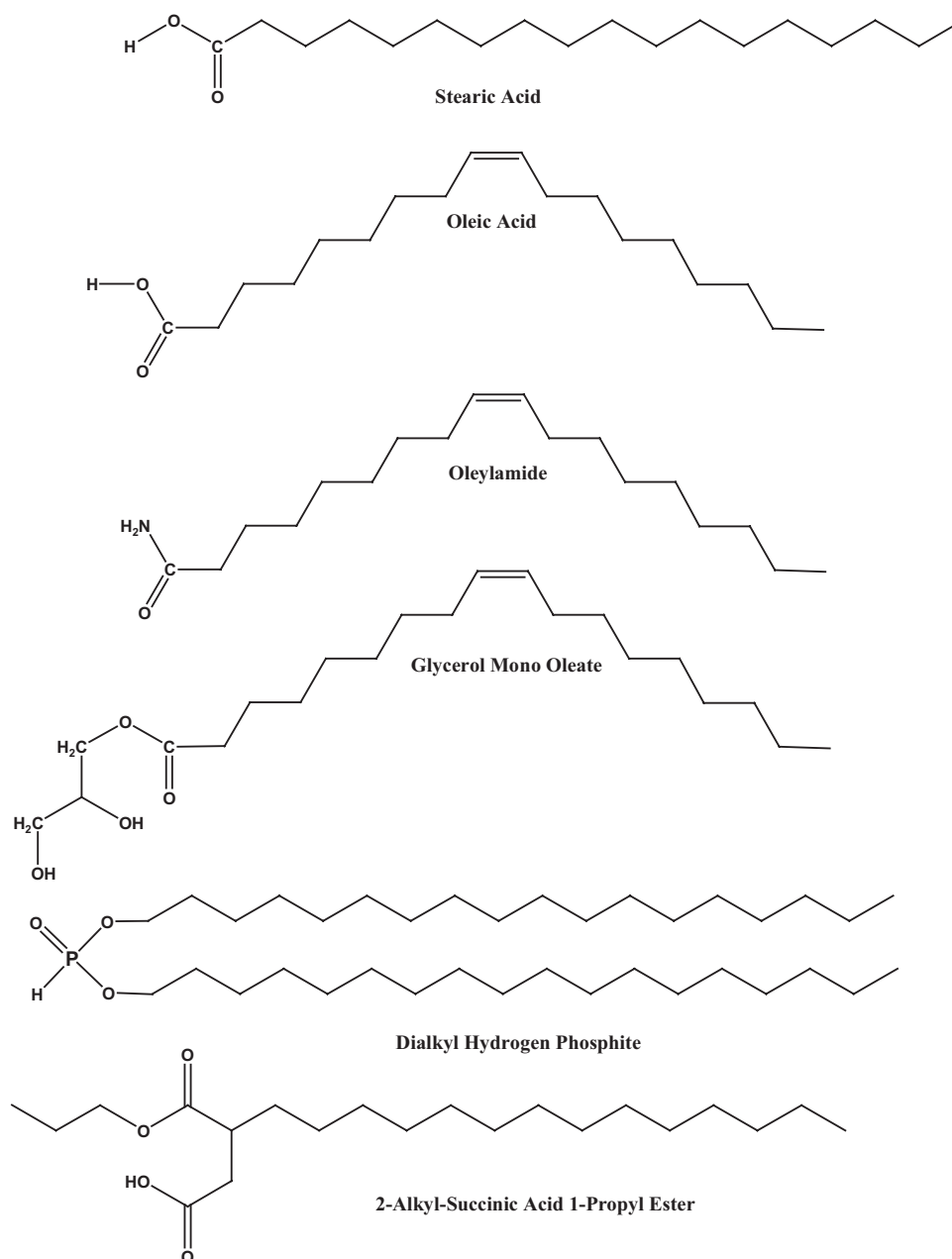


Figure 2.13—Examples of organic friction modifiers.

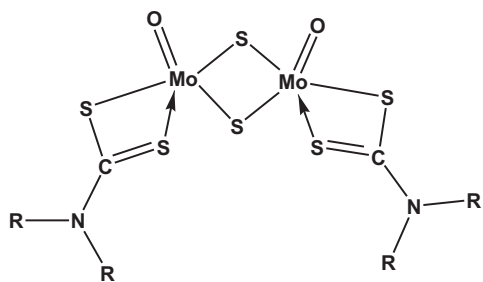
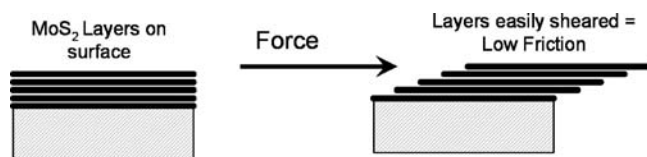
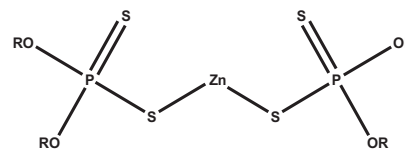


Figure 2.14—Molybdenum dithiocarbamate.

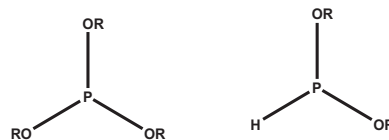
Figure 2.15—Mechanism of operation of MoS₂-containing friction modifiers.

2.2.3.2 ANTIWEAR AGENTS

Antiwear agents are used to reduce wear. To reduce wear under mild wear conditions, it is necessary to introduce antiwear agents into the lubricant. These are typically P-containing chemicals, of which the most widely used are zinc dialkyl dithiophosphates (ZDDPs), organic phosphates, and phosphites (Figure 2.16). These antiwear agents may increase friction. Antiwear agents work by reacting with metal surfaces under severe contact to form a polyphosphate protective reaction layer. The formation of the antiwear layer is still not fully understood but believed to be a multistep process involving degradation of the ZDDP, adsorption to the surface chemical change, and finally

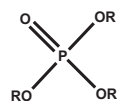


Zinc Dialkyl Dithio Phosphate

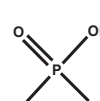


Trialkyl Phosphite

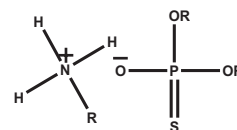
Dialkyl Hydrogen Phosphite



Trialkyl Phosphate



Dialkyl Hydrogen Phosphate



Amine Thiophosphate

Figure 2.16—Typical P-containing antiwear additives used in automotive applications.

growth of the reacted film to provide a protective barrier between moving surfaces (Figure 2.17) [6,10–14].

1. Break-in and mild wear removes the surface layers exposing metal or metal oxide.
2. Adsorption of the antiwear chemistry to the metal surface.
3. Reaction of the adsorbed antiwear chemistry to produce a pad-like protective reaction layer. However, this reaction will occur only when there is sufficient energy from frictional heating because of the high load.
4. Growth of the reaction layer to form a more substantial antiwear film.

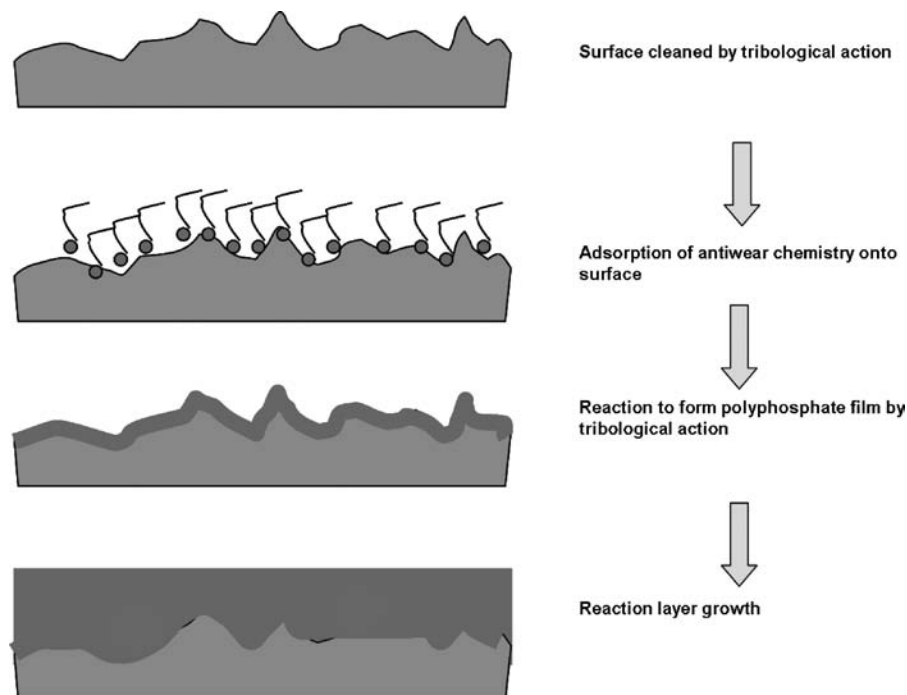


Figure 2.17—Antiwear mechanism: formation of zinc sulfide/polyphosphate film.

These films extend the range of operation further than the friction modifiers, but these also have an upper limit, often approximately 250°C. This temperature does not have to be the bulk temperature of the fluid, but it can be the friction-generated local temperature [7]. ZDDPs are formed by the reaction of an alcohol with P_2S_5 and then with ZnO. ZDDPs are made using different alcohols or alcohol mixtures, which can produce a mixture of different ZDDPs that can extend the operating temperature range of the antiwear protection.

The alcohol used to form the ZDDP will affect the temperature at which the molecule decomposes [15] to react with the metal surface to form a sacrificial zinc sulfide/polyphosphate coating. This coating then prevents metal-to-metal contact and wear of the surfaces passing over each other. Under normal conditions, metal surfaces have an oxide coating from reaction with the air. In an engine, this coating will be removed, and if metal-to-metal contact is observed, then these surfaces can microweld at asperities (adhesive wear). The microwelds are not strong enough to seize the equipment because the momentum of the equipment rips the surfaces apart causing metal transfer and wear debris to be formed. If antiwear chemistry is not present, seizure will ultimately occur.

B-containing detergents and dispersants as well as borate esters have been added to lubricants to provide antiwear properties. Typically, the B-containing species will liberate boric acid at the surface. The monoclinic crystal structure of the boric acid is such that the crystals are able to slide over each other and provide protection and reduced friction.

Alternatively, depending on the source of the B it can behave similarly to ZDDP. A surface tribochemical reaction takes place that results in a borate glass-like layer on the surface similar to the polyphosphate glass obtained by using ZDDP.

2.2.3.3 EXTREME PRESSURE AGENTS

Extreme pressure (EP) agents are additives used to prevent seizing under extreme conditions. EP agents are similar to antiwear additives because they both work to prevent or control wear. However, antiwear agents cannot adequately protect under more severe boundary conditions such as high temperatures, heavy or shock loading, and extended periods of operation.

The most commonly used EP additives are those using S as the reactive species. EP additives control wear in contrast to antiwear additives that reduce wear. The basic operation of EP additives is a four-step process that is similar to the operation of antiwear additives (Figure 2.17), although EP additives require higher temperatures or loads, or both to become activated compared with antiwear additives. The difference is in the final (fourth) step. Instead of the film increasing and forming a physical barrier to reduce wear, the iron sulfides produced at the asperities penetrate the surface and are easily sheared, removing iron sulfide from the metal component. This type of removal is controlled; there is no localized welding and subsequent tearing of metal into small fragments, which is characteristic of adhesive or scuffing wear. The final result of many of these occurrences is a gradual smoothing of the metal surfaces. This in turn leads to the load being carried on a much greater area and consequent reduction in wear due to the reduced severity of the contact [14,16–20]. In this way,

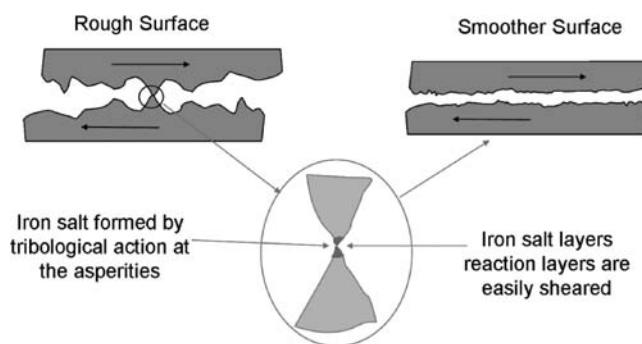


Figure 2.18—Smoothing of asperities by EP agent action.

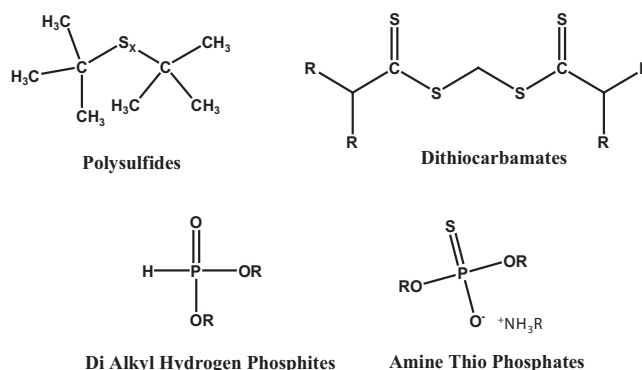


Figure 2.19—Typical EP additives used in automotive applications.

EP agents control wear (Figure 2.18). EP agents typically contain organic S, P (Figure 2.19), or Cl compounds, which can chemically react with the metal surface under high-pressure or high-temperature conditions, or both, to form metal salts. The hydrophilic chain is generally shorter than in friction modifiers and antiwear agents, which makes them more surface active.

Legislation affecting the use of Cl compounds as EP agents has now restricted its use to limited special applications, although Cl compounds are very effective at preventing wear under extreme conditions.

Table 2.1 compares the chemistries and modes of operation of friction modifiers, antiwear additives, and EP agents.

2.2.3.4 DISPERSANTS

Dispersants are used in most types of automotive lubricants. Engines produce small particles of highly carbonaceous material (soot) because of incomplete burning of the fuel. Soot, along with partly oxidized fuel, water, and acids that are the precursors to sludge formation, can reach the crankcase as blow-by gases. In addition, the oxidation of oil itself produces materials that can be rich in oxygen and are often polymeric in nature that eventually contribute to the formation of sludge, varnish, or lacquer. These materials can coat parts of the engine and block oil-ways, which can lead to oil starvation and equipment failure. In transmission systems, there is no combustion, but the oil can still be exposed to high temperatures and oxidation, and thermal degradation can still occur.

To handle these internally generated contaminants, it is necessary to introduce dispersants into engine oils, gear oils, and transmission fluids. Dispersants are typically polymeric hydrocarbons with a polar head; this polar head

TABLE 2.1—Comparison of Friction Modifiers, Antiwear Agents, and EP Agents

	Chemistry	Mode of Operation
Friction modifiers (operate at low loads to reduce friction)	<ol style="list-style-type: none"> 1. Long-chain organic acids, esters, amides, e.g., stearic acid, glycerol mono-oleate (GMO), oleylamide. 2. Organo-molybdenum compounds, e.g., molybdenum dithiocarbamates. 	<ol style="list-style-type: none"> 1. Physisorption or chemisorption to metal surface. Long chains allow low-friction movement over each other. 2. Under stress, heat, or pressure, breaks down to give solid, low friction, lubricant MoS_2 on surfaces.
Antiwear agents (operate under mixed boundary conditions to prevent wear)	Zinc dithiophosphate, other organic phosphates, and phosphates. Some use of borates.	Surface adsorption followed by chemical reaction with the surface under stress (load/temperature) to form polyphosphate layer, which can grow above the surface to form a protective film. Film can be eroded but underlying metal surfaces remain intact.
EP agents (operate under boundary conditions to control wear)	S- or P-containing materials, e.g., alkyl polysulfides, alkyl dithiocarbamates, alkyl phosphites, and alkyl phosphates.	Surface adsorption followed by reaction under severe stress to form metal sulfides or phosphides that have low shear strength and that shear to remove metal as its sulfide or phosphide but prevent metal-to-metal welding and tearing.

attaches to a soot or sludge particle by physisorption or chemisorption. The long hydrocarbon chains surrounding each particle can sterically interfere with each other, preventing the particle cores from contacting and forming larger particles (Figure 2.20). Dispersants do not contain any metallic elements and therefore do not contribute to ash.

The most commonly used dispersants are PIB succinimides, PIB succinate esters, and Mannich bases (Figure 2.21).

Polyisobutylene succinic anhydride (PIBSA) is reacted with polyamines, usually members of the homologous family of ethylenediamine, to produce PIB succinimides or with polyols to produce PIB succinate esters. By varying the molecular weight of the PIBSA, along with the amine or alcohol used and the ratio of reactants, it is possible to produce many final products from a relatively few starting materials. This ability means that it is relatively easy to modify a molecule to specifically target a particular class of contaminant. Using a high-molecular-weight PIBSA at a 1:1 molar ratio of PIBSA to polyamine produces a highly basic dispersant that is attracted to acidic soot particles. This type of dispersant is consequently excellent at soot dispersion. Use of a higher-molecular-weight PIBSA at a higher PIBSA-to-polyamine ratio results in a much larger dispersant molecule with less basicity that is better suited

to sludge dispersion. The effects of poor and good dispersancy are shown in Table 2.2.

Succinate esters are produced by the reaction of a PIBSA with alcohols, especially polyhydric alcohols, and result in the formation of succinate ester dispersants. Succinate ester dispersants are used in gasoline and diesel engine oils.

Mannich dispersants are produced by the condensation of a high-molecular-weight alkylphenol (e.g., polybutylphenol), an aldehyde, and alkyleneamines or alkylene polyamines. Mannich dispersants are generally only used in gasoline engine oils.

2.2.3.5 DISPERSANT VISCOSITY MODIFIERS

As the name suggests, a dispersant viscosity modifier (DVM) combines dispersancy and viscosity modification in one molecule. Using a monomer or grafting agent containing a functional group (e.g., maleic anhydride), it is possible to incorporate the functionality into the polymer chain. Further reaction of the maleic acid group with a suitable amine results in a polymer with imide and amine groups capable of imparting dispersancy (Figure 2.22).

2.2.3.6 DETERGENTS

Detergents are used in most types of automotive lubricants. Detergents are required to perform various functions within a lubricant depending on the specific application:

1. Suspend oil-insoluble oxidation or combustion products or both by adsorbing onto the surface in a similar way to dispersants.
2. Neutralize inorganic acids (formed during the combustion process) and organic acids (formed during oil degradation), thereby controlling the corrosive effects of these acids.
3. Reduce corrosion by forming a protective layer on metal surfaces.
4. Reduce deposit formation in high-temperature zones such as the piston ring pack.
5. Provide balanced friction for clutch and synchromesh performance in automatic transmission and manual transmission fluids in conjunction with a suitable friction-modifier system.

Detergents can be neutral or overbased. Neutral detergents are the salts formed by the stoichiometric reaction

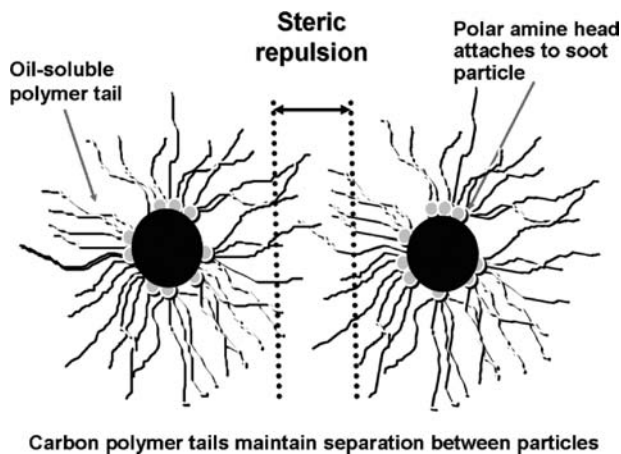
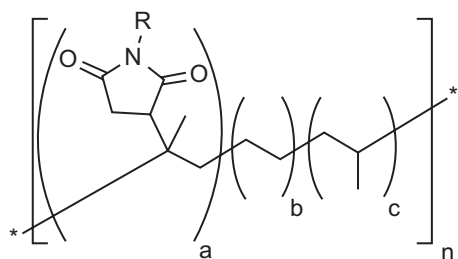


Figure 2.20—Steric stabilization of soot particles by dispersant.



where a, b, c, and n are integers.

Figure 2.22—Dispersant OCP.

between a metal (usually Ca, Mg, Na, or K) and an organic acidic species. The organic oil-solubilizing part of the detergent is usually sulfonic acids, phenols, or salicylic acids, which yield sulfonates, phenates, and salicylates, respectively (Figure 2.23). The alkyl chain used for detergents is typically approximately 24 C atoms and is much shorter than those used in dispersants. Neutral detergents are used to clean and keep clean high-temperature areas of equipment, such as the piston area of an internal combustion engine.

Neutral detergents are prepared by adding stoichiometrically equivalent amounts of base (as metal oxide or metal hydroxide) and organic acid. Overbased detergents are prepared by further reacting the neutral detergent with extra base and CO_2 to produce a detergent that contains a core of metal carbonate surrounded by the oil-solubilizing detergent substrate (Figure 2.24) [21].

The metal carbonate is then available to react, as needed, with acids formed during combustion or oil degradation to neutralize these acids before they can cause corrosion within the equipment. The amount of base within a detergent can be expressed as its total base number (TBN), measured in mgKOH/g. High-TBN fluids have a greater capacity to neutralize acids. Automotive fluids may contain a blend of detergent types (e.g., phenate and sulfonate) that can be neutral or overbased or both.

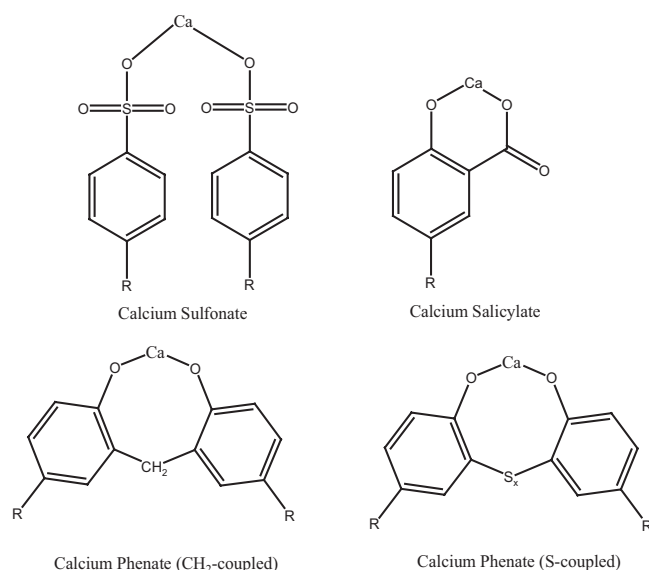


Figure 2.23—Detergents typically used in automotive applications.

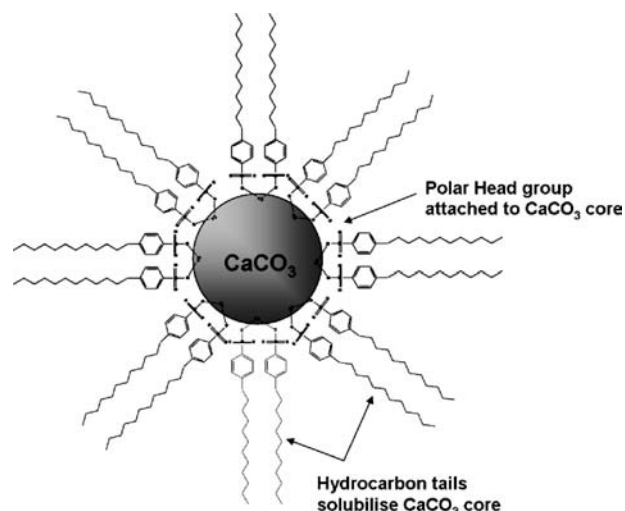


Figure 2.24—Schematic diagram of detergent molecules solubilizing CaCO_3 .

Transmission fluids may also contain detergent to help find the correct friction balance for smooth gear change. Friction modifiers have a tendency to reduce friction whereas detergents can be used to increase friction in oil. A balance of friction reduction and friction increase over a gear change is critical to the durability of a transmission over its lifetime. Table 2.3 lists the advantages and disadvantages of each type of detergent. Table 2.4 compares the properties of detergents and dispersants. Figure 2.25 shows examples of poor and good detergency in modern diesel pistons.

2.2.3.7 RUST AND CORROSION INHIBITORS

Rust is corrosion-specific to ferrous materials and requires the presence of water and a strong oxidant or acid. The term “corrosion inhibitor” tends to relate to the corrosion of other metals such as those containing Cu (e.g., brass or bronze) and Pb. Additives that protect ferrous materials from corrosion are usually referred to as “rust inhibitors”.

The use of detergents as rust inhibitors has already been discussed: Overbased detergents neutralize acidic species in the lubricant before they can cause corrosion. Neutral detergents are able to form a surface-covering barrier to prevent acidic species from directly contacting the metal components of engines and transmissions. Other rust inhibitors include long-chain alkyl phosphates, amine phosphates, and partial esters of succinic acid. These also adsorb onto the ferrous surface to form a barrier that prevents water from reaching the surface, thereby reducing corrosion.

Cu is susceptible to attack by reactive S compounds such as those found in high-S-content mineral oils and some EP agents. Prevention of Cu corrosion is achieved by using benzotriazole and substituted azoles and their derivatives that bond to the Cu surface and form a protective reaction film on the surface. By protecting the Cu, they also prevent Cu ions from being formed, which in turn reduces the catalytic effect that Cu ions can have on the oxidation rate of the lubricant. For this reason, these materials are also referred to as “metal deactivators.”

TABLE 2.3—Properties of Detergent Types

	Advantages	Disadvantages
Sulfonates	<ul style="list-style-type: none"> Excellent high-temperature detergency Can be overbased to very high level TBN ~500 mgKOH/g Cost-effective 	<ul style="list-style-type: none"> No antioxidant performance
Phenates	<ul style="list-style-type: none"> Good high-temperature detergency Provides antioxidant performance 	<ul style="list-style-type: none"> Maximum TBN achievable without co-surfactants ~300 mgKOH/g Detrimental to fuel economy Less cost-effective
Salicylates	<ul style="list-style-type: none"> Good high-temperature detergency Excellent antioxidants Sulfur-free 	<ul style="list-style-type: none"> Maximum TBN achievable ~280 mgKOH/g Less cost-effective
Neutral detergents	<ul style="list-style-type: none"> Excellent detergency Good corrosion protection 	<ul style="list-style-type: none"> Low acid-neutralization capability
Overbased detergents	<ul style="list-style-type: none"> Excellent acid-neutralization capability 	<ul style="list-style-type: none"> Low detergency

TABLE 2.4—Comparison of Detergents and Dispersants

	Detergents	Dispersants
Oil-soluble component	<ul style="list-style-type: none"> Alkylated sulfonates, alkylated salicylates, and alkylated phenates Alkyl chain contains up to 24 C atoms 	<ul style="list-style-type: none"> PIBSA Alkyl chain contains up to 150 C atoms
Polar component	<ul style="list-style-type: none"> Ca, Mg, or Na 	<ul style="list-style-type: none"> Polyamines or polyols
Ash	<ul style="list-style-type: none"> Contribute to ash 	<ul style="list-style-type: none"> Ashless
Function	<ul style="list-style-type: none"> High-temperature cleaning and suspension of deposits/contaminants Phenates and salicylates have antioxidant properties 	<ul style="list-style-type: none"> Low-temperature cleaning and suspension of deposits/contaminants

2.3 ENGINE OILS

Engine oils are used to lubricate engines running on different fuels, including diesel, gasoline, biodiesel, ethanol, natural gas, and dimethyl ether (DME). In general, engine oils can be split into two distinct categories: light duty and heavy duty. Light duty covers the typical engines used in passenger cars (gasoline and diesel). Heavy duty covers heavy-duty engines used in larger vehicles that typically use diesel fuel and with engine sizes varying from 2 up to 16 L.

Engine oils are typically designed to meet various specifications from original equipment manufacturers (OEM; e.g., Ford, PSA, Renault, etc.) or from industry associations (e.g., API, ACEA, etc.). Current performance requirements are mostly focussed on ensuring that the vehicle maintains its emissions performance for longer periods of time.



Figure 2.25—Examples of poor (left) and good (right) detergency.

Additive packages also play an important role in the performance of engine oil, and depending on the quality and performance requirements, treat rates of up to 25 % and higher are possible. This means that up to 25 % of the finished oil is made up of additive. VMs are also used in engine oils to help provide the correct viscosity grade. Typical components used in engine oils are shown in Table 2.5

TABLE 2.5—Typical Components of Heavy-Duty and Passenger Car Engine Oils

	Heavy-Duty Engine Oil	Passenger Car Engine Oil
Dispersant	2–12 % ^a	2–12 %
Detergent	1–5 %	1–5 %
Antiwear	0.5–2 %	0.5–1.5 %
Antioxidant	0–4 %	0–5 %
Friction modifier	0–1 %	0–2 %
Antifoam	20–200 ppm	20–200 ppm
Pour-point depressant	0–0.5 %	0–0.5 %
VM ^b	0–3 %	0–3 %
Base oil	55–96.5 %	54–96.5 %

^aIncludes DVM.

^bLevel of solid polymer in finished lubricant.

TABLE 2.6—SAE Viscosity Grades for Engine Oils^a (SAE J300 November 2007)

Low-Temperature Viscosities			High-Temperature Viscosities		
SAE Viscosity Grade	Cranking ^b (cP) Maximum at Temperature (°C)	Pumping ^c (cP) Maximum with no Yield Stress at Temperature (°C)	Low Shear Rate Kinematic ^d (cSt) at 100°C		High Shear ^e rate (cP) at 150°C Minimum
			Minimum	Maximum	
0W	6200 at -35	60,000 at -40	3.8	—	—
5W	6600 at -30	60,000 at -35	3.8	—	—
10W	7000 at -25	60,000 at -30	4.1	—	—
15W	7000 at -20	60,000 at -25	5.6	—	—
20W	9500 at -15	60,000 at -20	5.6	—	—
25W	13,000 at -10	60,000 at -15	9.3	—	—
20	—	—	5.6	<9.3	2.6
30	—	—	9.3	<12.5	2.9
40	—	—	12.5	<16.3	3.5 (0W-40, 5W-40, 10W-40 grades)
40	—	—	12.5	<16.3	3.7 (15W-40, 20W-40, 25W-40, 40 grades)
50	—	—	16.3	<21.9	3.7
60	—	—	21.9	<26.1	3.7

^aAll values are critical specifications as defined by ASTM D3244.

^bASTM D5293.

^cASTM D4684. The presence of any yield stress detectable by this method constitutes a failure regardless of viscosity.

^dASTM D445.

^eASTM D4683 and D4741, CEC-L-36-A-90.

and represent the complete performance range for passenger car and heavy-duty applications.

Typically the higher the levels of additives used in the formulation, the higher the levels of performance of the finished oil.

Engine oils are also provided with different viscosity grades that are recommended depending on the climatic conditions of where the vehicle operates. Lighter viscosity grades have also been shown to provide improved fuel economy performance through reduced churning losses, and the trend is toward vehicle engines being lubricated by these light viscosity grades (e.g., 0W-20 for passenger cars and 5W-30 for heavy-duty trucks). The viscosity grade is defined by SAE J300 and specifies requirements that must be met for that oil to be within a specific viscosity grade (Table 2.6).

A typical mainline heavy-duty engine oil would have a viscosity of 15W-40. The “15W” defines the low-temperature properties of the oil (see Table 2.6), and the “40” defines how the oil flows (or how viscous it is) at 100°C. Because this oil is a 15W-40, it is classed as a multigrade oil. SAE J300 allows for the definition of monograde oils (e.g., SAE 30), and these are defined by how viscous they are at 100°C.

As the viscosity grades have become lighter and oil film thickness reduced, there has been greater emphasis on the additive packages used. It is these oil films that help to provide the wear and durability protection of the lubricant. Therefore, when this oil film thickness is reduced, more robust additive packages must be developed.

Also, with this move toward lighter viscosity grades, we have seen a trend toward synthetic oils. These synthetic oils use more highly refined base oils, which improve the additive response in the oil. With traditional mineral oils, there

are many other compounds in the oil that compete with the additive for the surface. With these compounds removed, the additive chemistry is able to bond with the surface more easily and can provide the required protection.

Base oils used to make all finished lubricants are split into several categories on the basis of their chemical and physical characteristics. Mineral oil is classified as Group I; next is Group II, which is more highly refined base oil; and then there is Group III, which is highly refined. Group III base oil is classified as synthetic in most markets. PAO (polyalphaolefin) is Group IV base oil and is fully synthetic. Group VI is polyinternal olefin (PIO) and is fully synthetic. There are also esters and other basestocks that are classified as Group V. Esters are used widely in industrial and driveline fluids. If base oils are not included in Groups I–IV, then they are also classified as synthetic (Table 2.7).

TABLE 2.7—Base Oil Definitions (ATIEL Code of Practice Appendix B) [22]

Group	Saturates ^a	Sulfur ^b	Viscosity Index ^c
I	<90 %	>0.03 %	80–120
II	>90 %	<0.03 %	80–120
III	>90 %	<0.03 %	>120
IV	Polyalphaolefins (PAOs)		
V	All basestocks not included in Groups I, II, III, IV, or VI		

^aSaturates are measured using ASTM D2007.

^bSulfur content measured by ASTM D2622, D4294, D4927, or D3120.

^cViscosity index measured by ASTM D2270.

TABLE 2.8—API CJ-4 Performance Requirements and Associated Engine Tests

Valve train wear	Cummins ISB (ASTM D7484)
Valve train wear, filter plugging, and sludge	Cummins ISM (ASTM D7468)
Roller follower wear	RFWT (ASTM D5966)
Oil oxidation	Sequence IIIF (ASTM D6984) or IIIG (ASTM D7320)
Ring and liner wear, lead-bearing corrosion	Mack T12 (ASTM D7422)
Soot dispersancy	Mack T11 (ASTM D7156)
Piston deposits and oil consumption	CAT C13 and CAT 1N (ASTM D6750), Mack T12 (OC only)
Aeration	EOAT (ASTM D6894)
Used oil low-temperature pumpability	T11 Drain (180 h)

To be expected to work in the field, engine oils are subjected to rigorous engine testing to prove their performance before they can be used. These engine test requirements specify the limits that must be achieved for the oil to make that specific industry or OEM claim.

For example, oil that is to claim API CJ-4 must meet the engine test requirements as specified in ASTM D4485. The tests required are shown in Table 2.8.

The same applies for oil that is to make an ACEA claim (e.g., ACEA E6-08). Table 2.9 details the tests that are required for ACEA E6-08.

Other specifications will require different engine tests as they are required to provide specific performance criteria that are detailed in the specification. Some OEMs also have their own in-house engine tests that will be required. In some cases, OEMs will require field trials or additional engine testing if the oil is designed to be used in a factory fill application.

Not all oils will claim to meet just a single industry or OEM specification, and they usually make several claims. These claims will be based on a suite of engine testing, and some of this engine testing will be common to several specifications. For example, a European heavy-duty engine oil targeting mid-drain, high-sulfated ash may claim the following: API CI-4, ACEA E7-08, MB 228.3, MAN 3275, Volvo VDS-3, Renault RLD-2, Deutz DQC III-05, and MTU type 2. This is not an exhaustive list, and other OEM claims may be suitable for such oil. The claims made for such oil depend on the performance the additive is targeted for and how an oil company wants to market the oil.

TABLE 2.9—ACEA E6-08 Performance Requirements and Associated Engine Tests [23]

Valve train wear	OM646LA (CEC L-099-08)
Ring and liner wear, lead-bearing corrosion	Mack T12 (ASTM D7422)
Soot dispersancy	Mack T-8E (ASTM D5967)
Piston deposits, oil consumption, and sludge	OM501LA (CEC L-101-08)

Further details of engine oil specifications can be obtained directly from the OEM or from the relevant industry group (ASTM D4485 and API 1509 for API) and ACEA for the ACEA sequences [23].

There are also guidelines or codes of practice that must be followed for the oil to make a genuine claim with the industry specifications for ACEA and API. For the additive development for API performance claims, there is the ACC code of practice [24], which details any changes to the additive and the formulation that are allowed during the additive development but will be acceptable to support the final additive formulation. For the ACEA sequences, the ATC code of practice [25] exists, which has its own set of accepted modifications that can be used in the development of an oil. There are also rules that exist for the interchange of base oils and viscosity grades. For API, these are defined in API 1509 Appendices E and F [26]. For ACEA these are defined in the ATIEL code of practice [22]. All of the codes of practice are regularly updated and actual data are used to define the accepted additive changes and read-across guidelines. Representatives from oil and additive companies provide the input required to keep these documents up to date.

2.4 AUTOMOTIVE TRANSMISSION FLUIDS

2.4.1 Introduction

Automotive transmission fluids must perform in various operating conditions and provide a wide range of functionality to enable optimal transmission operation. As a result, these fluids are tailored very carefully to the hardware in which they are operating to ensure optimal performance.

Since the first automatic transmission, the Oldsmobile Hydra-matic, was brought to market in 1940, automobile transmissions have evolved and been diversified to produce the range of different technologies that are now available in the marketplace. From a choice between a conventional manual or planetary automatic transmission, new transmission types have been developed. The breadth of technology available in the marketplace today has widened to include manual transmission (MT), planetary automatic transmission (AT), wet and dry versions of the dual-clutch transmission (DCT), continuously variable transmission (CVT), and automated manual transmission (AMT), plus the recent addition of hybrid powertrains.

With this growth in choice of transmission types has come a divergence in the fluids used to lubricate them, with fluid being initially designed to lubricate a particular type of transmission and then more specifically designed to correctly match the performance criteria of a particular manufacturer or piece of hardware. This specificity has led to the transmission fluid being considered such an integral part of the performance of the transmission design that in some cases it is now considered to be a component that must be considered early in the development cycle of a new transmission.

To cover all aspects of modern transmission fluid performance, the current major commercial transmission types will be summarized, along with the fluid formulating approach and key performance areas for each of these transmission types.

In addition to the transmission, in nontransaxle vehicles, the axle(s) require a dedicated fluid to ensure protection of the highly loaded differential gears and to ensure the optimal performance of limited slip differentials, if fitted. A

comparison of the composition of these different lubricants is provided at the end of this section in Table 2.13.

2.4.2 Manual Transmission Fluid

In a conventional MT, the starting device is typically a dry clutch, which does not require a lubricant to operate. As a result, manual transmission fluid (MTF) performance is focussed on protection of the gears and bearings within the transmission. The fluid must also provide the correct frictional properties on the synchromesh materials to allow for smooth gear engagement and ensure a long service life because these are typically fill-for-life or extended-drain-interval fluids.

Most passenger car transmissions and an increasing proportion of commercial vehicle MTs use a cone-type synchronizer that Porsche developed and introduced in the 1952 Porsche 356. As a result, cone synchronizers were called Porsche-type for many years after this.

In the early synchronized transmissions, most cars were equipped with synchromesh only on the second-to-third shift, requiring only a single synchro and a simple linkage. Manufacturers often suggested that to shift from second to first it was best to come to a complete stop or double-declutch.

Beginning in the 1960s, there was a trend to provide a wider range of gears and to increase the number of synchronized shifts. Thus, there has been a progression through transmissions with three fully synchromeshed speeds, and then four speeds and five speeds, until today when six synchronized ratios are widely used. As a result, the lubricants for these transmissions were required to have the correct frictional profile on the synchromesh material to provide smooth gear engagement. Several materials may be used for synchronizer systems, with the most widely used systems being brass, sinter, Mo, and C.

In general, MTFs are developed according to OEM-driven specifications to meet the requirements of a particular family of transmissions. However, specifications exist for service fill fluids (although these are commonly focused on commercial vehicle transmissions) and include

- API MT-1,
- ZF TE-ML 02,
- Volvo 97305,
- Scania STO 1:0, and
- Daimler Chrysler 235.1 & 235.11.

2.4.3 Automatic Transmission Fluid

A planetary AT uses planetary gear sets, which have reduced loads compared with those in the MT but a more complex set of fluid operating conditions. The fluid must act as a traditional lubricant to provide wear and fatigue protection in the gears and bearings. In addition, it must also act as a hydraulic fluid to operate the shifting mechanisms in the transmission, act as a power transfer medium in the torque converter, and have the correct frictional performance to enable smooth engagement of the wet clutches for optimal shift quality.

ATs tend to have tightly defined performance criteria to ensure the correct frictional performance and protection of the contact surfaces. As a result, automatic transmission fluid (ATF) development is driven by OEM specifications to match the requirements of that OEM's hardware. This specificity can lead to complexity in the service fill marketplace because there may be significantly different

requirements for the different transmissions. To reduce this complexity, several oil marketers now offer multivehicle ATFs, which have wide-ranging performance claims, and can rationalize the need to stock multiple fluids to cover these specifications.

Selected representative ATF specifications in use include

- GM Dexron®,
- Ford Mercon®,
- Allison C-4,
- ZF TE-ML11 and TE-ML14,
- Daimler 236.X, and
- JASO 1-A.

2.4.4 Dual-Clutch Transmission Fluid

The DCT was invented by Adolphe Kégresse, a French automotive pioneer, who also developed the half-track vehicle. Unfortunately, despite conceiving the idea of a DCT, Kégresse did not produce a working transmission. Development of this transmission was restarted during the mid-1980s with Porsche and Audi developing the concept for motorsport with use in endurance racing and rallying. A commercial version of this transmission was not feasible until Volkswagen and Borg-Warner collaborated to bring DCTs to the market in 2003 [27]; since then, many other manufacturers have introduced their own transmissions to market.

The DCT requires a hybrid of MTF- and ATF-type performance to operate. The transmission contains conventional gear sets and bearings, which require MTF-like protection, and synchromeshes, which require MTF-like friction performance. The DCT also has a pair of clutches that enable starting and gear changes. These clutches may be of the dry variety, which currently are used in low-torque applications, or of the wet variety, which require ATF-like friction performance to ensure the correct torque capacity and smooth engagement. As a result, there are two categories of DCTs to meet the needs of these transmissions:

1. *Dry DCTs*: These do not require clutch performance and hence may be lubricated using a MTF for optimal gear, synchromesh, and bearing performance.
2. *Wet DCTs*: These have wet clutches and hence require hybrid performance, with MTF-like gear, synchromesh, and bearing protection but with ATF-like friction performance that is tuned to suit the clutch friction material to provide smooth shifts and optimal torque capacity.

Because it is a relatively new technology, DCT fluids are dominated by OEM-specific products with no service-fill specifications. However, in time this market is expected to mature, with service-fill specifications and fluids appearing in the marketplace.

2.4.5 Continuously Variable Transmission Fluid

The CVTs in commercial production are significantly different from any other transmission types on the market. They do not use gears to provide the transmission ratios but rather a pair of variable-diameter pulleys with a belt or chain to transfer the torque. Therefore, to provide proper power transfer without the risk of belt or chain slippage, the CVT fluid must provide the optimal level of grip, or traction, between the belt and pulleys. A CVT is also likely to contain a wet-clutch or torque converter as a starting device, so the fluid must also have the correct frictional properties to provide smooth starting.

2.4.6 Automotive Axle Fluids (or Automotive Gear Oils)

A typical automotive axle has to withstand extremely high loadings because the transfer of power from the gear box to the wheels occurs through the small contact region in the hypoid gear set. As a result of these high loadings, it is important for the fluid used to provide a high level of surface protection to prevent excessive wear, scuffing, and pitting. Consequently, automotive gear oils contain a high level of S-containing antiwear and EP agents to smooth asperities during break-in and to form a protective tribofilm on the mating surfaces during operation.

Automotive differentials may also include a limited-slip device, which may take several forms, using a clutch plate friction device or a geared “torsen” arrangement. These devices will require the correct lubricant properties for optimal performance. In the case of a plate-type unit, it is also critical to ensure the fluid has the correct friction response to allow for the optimal balance between grip and slip, which is tailored to the friction material used.

Selected representative specifications for automotive axle fluids include

- API GL-5, SAE J2360, and MIL-PRF-2105E;
- ZF TE-ML 05, TE-ML 12, and TE-ML 17;
- Daimler Chrysler 235.0, 235.8, and 235.20;
- Volvo 97310, 97311, and 97312;
- DANA SHAES 256 Revisions A and C;
- Mack GO-J and GO-J Plus; and
- Arvin Meritor 0-76N.

2.4.6.1 AUTOMOTIVE GEAR LUBRICANT VISCOMETRIC PROFILES

Automotive gear lubricant viscosity grades are defined by the SAE J306 standard [27], which is summarized in Table 2.10.

TABLE 2.10—Automotive Gear Lubricant Viscosity Grades (SAE J306) [27]

SAE Viscosity Grade	Maximum Temperature for Viscosity of 150,000 cP (°C) ^{a,b}	Kinematic Viscosity at 100°C (cSt) ^c	
		Minimum ^d	Maximum
70W	−55 ^e	4.1	–
75W	−40	4.1	–
80W	−26	7.0	–
85W	−12	11.0	–
80	–	7.0	<11.0
85	–	11.0	<13.5
90	–	13.5	<18.5
110	–	18.5	<24.0
140	–	24.0	<32.5
190	–	32.5	<41.0
250	–	41.0	–

^aUsing ASTM D2983 [28].

^bAdditional low-temperature viscosity requirements may be appropriate for fluids intended for use in light-duty synchronized MTs.

^cUsing ASTM D445 [29].

^dLimit must also be met after testing in CEC L-45-T-99, Method C (20 h) [30].

^eThe precision of ASTM D2983 has not been established for determinations made at temperatures below −40°C [28].

2.4.6.2 DRIVELINE FLUID SPECIFICATIONS

The following are the API automotive gear oil designations (see API publication 1560 for a full description):

- *Service designations in current use:*
 - **GL-4:** Lubricants for axles with spiral-bevel gears operating under moderate to severe conditions of speed and load or axles with hypoid gears operating under moderate speeds and loads. These oils may be used in selected MTs and transaxle applications in which API MT-1 lubricants are unsuitable.
 - **GL-5 (now adopted as ASTM D7450-08) [31]:** Lubricants for gears, particularly hypoid gears, in axles operating under various combinations of high-speed shock loads and low-speed/high-torque conditions. Lubricants qualified under MIL-L-2105E satisfy the requirements of the API GL-5 specification, although the API designation does not require military approval. The requirements of GL-5 are provided in Table 2.11.
 - **MT-1:** Lubricants intended for nonsynchronized MTs used in buses and heavy-duty trucks. Lubricants meeting the requirements of API MT-1 provide protection against the combination of thermal degradation, component wear, and oil seal deterioration that is not provided by lubricants meeting only the requirements of API GL-4 and API GL-5. API MT-1 does not address the performance requirements of synchronized transmissions and transaxles in passenger car and heavy-duty applications.
- *Service designations not in current use:* There are additional API designations that are no longer in current use but that may be referenced as performance requirements, particularly in developing markets. These include the following:
 - **GL-1:** Lubricants for MTs operating under such mild conditions that straight petroleum or refined petroleum oil may be used satisfactorily. Oxidation and rust inhibitors, defoamers, and pour-point depressants may be added to improve the characteristics of these lubricants. Friction modifiers and EP additives should not be used.
 - **GL-2:** Lubricants intended for automotive worm gear axles operating under conditions of load, temperature, and sliding velocity for which lubricants satisfying API GL-1 service will not suffice. Products suited for this type of service contain antiwear additives or film-strength improvers specifically designed to protect worm gears.
 - **GL-3:** Lubricants intended for MTs operating under moderate to severe conditions and spiral-bevel axles operating under mild to moderate conditions of speed and load. These service conditions require lubricants having good load-carrying capacities that exceed those satisfying API GL-1 service but are below the requirements of lubricants satisfying API GL-4 service. Lubricants designated for API GL-3 service are not intended for axles with hypoid gears.
 - **GL-6:** Lubricants intended for gears designed with very high pinion offsets. Such designs typically

TABLE 2.11—Tests Required in the API GL-5 (ASTM D7450-08) [31] Specification

Test	Requirements	SAE 70W and 75W	SAE 70W-xx and 75W-xx	All Other SAE Grades
High speed/shock load L-42 (standard) (ASTM D7452) [32]	Equal or better than reference oil	–	✓	✓
High speed/shock load L-42 (Canadian) (ASTM D7452) [32]		✓	✓	–
Low speed/high torque L-37 (standard) (ASTM D6121) [31], minimum	Ridging 8	–	✓	✓
Low speed/high torque L-37 (Canadian) (ASTM D6121) [33], minimum	Rippling 8	✓	✓	–
	Wear 5			
	Pitting/spalling 9.3			
	Scoring 10			
Rust test, merit rating (ASTM D7038) [34]	9.0 minimum	✓	✓	✓
Thermal stability (ASTM D5704) [35] Viscosity increase, % Pentane insolubles, wt Toluene insolubles, wt	100 maximum 3.0 maximum 2.0 maximum	✓	✓	✓
Foam, tendency maximum (ASTM D892) [36]	Seq I 20 Seq II 50 Seq III 20	✓	✓	✓
Copper corrosion, 3 h/250°F (ASTM D130) [37]	3 maximum	✓	✓	✓

TABLE 2.12—Automotive Gear Oil Tests

Test	Description	Characteristics Measured
ASTM L-33–1 (D7038) ^{a,b} [38]	Gear test using differential assembly	Resistance to corrosion in the presence of moisture
ASTM L-37 (D6121) [33]	Gear test using complete axle assembly	Resistance to gear distress under low-speed/high-torque conditions
ASTM L-42 (ASTM D7452) ^a [32]	Gear test using complete axle assembly	Resistance to gear distress (scoring) under high-speed/shock-load conditions
ASTM L-60 ^a (obsolete)	Bench test using spur gears	Oxidation stability
ASTM L-60–1 (D5704) [35]	Bench test using spur gears	Thermal and oxidative stability and deposits
ASTM D5662 [39]	Bench test	Seal compatibility
ASTM D5579 [40]	Gear test in a MT	Thermal stability in a cyclic durability test
ASTM D5182 [41]	Gear test using spur gears	Spur gear wear
ASTM D892 [36]	Bench test	Foaming tendencies
ASTM D130 [37]	Bench test	Stability in the presence of Cu and Cu alloys
^a Detailed test procedures for L-33, L-42 and L-60 can be found in ASTM STP 512A [42].		
^b ASTM D7038 [38] (L-33/1) or L-33 (obsolete).		

require protection from gear scoring in excess of that provided by API GL-5 gear oils. A shift to more modest pinion offsets and the obsolescence of original API GL-6 test equipment and procedures have greatly reduced the commercial use of these lubricants.

A representative overview of automotive gear oil test methods is provided in Table 2.12.

2.4.7 Summary of AT Fluids

In summary, this section has briefly outlined the key lubricant performance aspects of AT lubricants along with the key differences in lubricant requirements between each of the modern transmission types. The additive compositions used in these transmissions will be optimized to meet the performance requirements of each transmission, and typical fluid compositions are summarized in Table 2.13.

TABLE 2.13—Comparison of Typical Transmission Fluid Formulation					
Component Type	ATF (%)	CVT Fluid	DCT Fluid	MT Fluid	Automotive Gear Oil
Dispersant	1–5	1–5	1–5	0.1–1	0.1–1
Detergent	0.5–2	0.5–2	0.5–2	0.5–3	
Antiwear	0.1–1	0.1–1	0.1–1	0.1–2	0.1–2
EP agent			0.1–1	0.1–2.5	1–5
Oxidation inhibitor	0.1–1	0.1–1	0.1–1	0.1–1	0.1–1
Corrosion inhibitor	0.05–0.5	0.05–0.5	0.05–0.5	0.05–0.5	0.05–0.5
Friction modifier	0.1–3	0.1–3	0.1–3	0.1–1	0.1–5 ^a
Pour-point depressant	0–0.5	0–0.5	0–0.5	0–2	0–2
Foam inhibitor	0–0.1	0–0.1	0–0.1	0–0.1	0–0.1
VM	2–20	2–20	2–20	2–30	5–50
Base oils	65–96	65–96	64–96	57–97	34–94
Other ^b	0–1	0–1	0–1		
^a Only required where a limited slip device is present.					
^b “Other” may include seal swell agents and colored fluid dye.					

2.5 AUTOMOTIVE GREASES

Automotive applications for lubricating greases, either in service or as factory-filled components, account for approximately 37 % of all greases currently in use [43]. In the United States, heavy trucks and buses account for 55 % of the automotive grease use, 30 % relates to agriculture and construction use, and 15 % is used for passenger cars and light trucks. Most passenger car applications are now filled for life. For heavy trucks and buses, relubrication and maintenance intervals have been extended.

2.5.1 What Is Lubricating Grease?

Lubricating greases are liquid lubricants (e.g., mineral oils) that have been solidified with a thickening agent to produce a material that has a solid to semisolid nature, enabling it to remain in place at the area of lubrication. The NLGI, formerly known as the National Lubricating Grease Institute, is an organization that has been serving the grease industry since 1933. In their *Lubricating Grease Guide* [44], NLGI defines a lubricating grease as “[a] solid to semi-solid product of dispersion of a thickening agent in a liquid lubricant. Additives imparting special properties may be included.” Another more appropriate definition from Vold and Vold [45] is “[a] grease is a lubricant which has been thickened in order that it remain in contact with the moving surfaces and not leak out under gravity or centrifugal action, or be squeezed out under pressure.”

2.5.2 SAE J310—Basic Requirements of an Automotive Grease [46]

An automotive lubricating grease should

- Provide adequate lubrication,
- Provide rust and corrosion protection,
- Act as a sealant,
- Show minimal leakage or oil bleeding,
- Have reasonable resistance to shear softening,

- Not stiffen excessively and remain pumpable in cold weather,
- Be compatible with elastomer seals and other materials (e.g., yellow metals),
- Be tolerant to some degree of contamination, and
- Show good oxidation and thermal stability.

These performance-related properties show the demands placed on lubricating greases used in automotive service. There are other performance considerations that may be included (e.g., dampening of noise and vibration).

2.5.3 Why Use a Lubricating Grease?

The most immediate benefit is that the semisolid nature of a lubricating grease allows it to stay in place, resisting leakage and loss. At the outer surfaces of a bearing, the grease forms a physical barrier that acts as a seal against airborne contaminants, such as moisture and dirt. At the moving surfaces, greases typically form a thicker lubrication film than would be obtained from a lubricating oil of the same base oil viscosity, which is beneficial in terms of friction, wear, and operating life [47].

Greases can also be formulated with solid additives such as MoS₂ or graphite, which have good friction and antiwear properties. Another benefit is that compared with oil systems, the amount of grease required is significantly lower, and in many cases this small quantity of grease is used for the full service life of the application (fill for life).

2.5.4 Liquid Lubricants Used in Lubricating Greases

The liquid lubricant (base oil) component of a lubricating grease accounts for most of the formulation. For example, in a general-purpose Li lubricating grease formulation, the oil portion amounts to 80–90 %. The fluid also acts as a carrier for oil-soluble additives. For most applications, traditional mineral oils are used [48].

- *Naphthenic oils*: These are traditionally favored for grease formulations because of their better solvency, low-temperature properties, and additive compatibility.
- *Paraffinic oils*: These give the grease better high-temperature properties.
- *Re-refined oil*: This is used for some applications, generally as a proportion of the base oil.
- *Semisynthetic and synthetic oils blends*: These are used for special applications.
- *Vegetable oils*: These are often used for environmental applications.

The choice of base fluid depends on the application and temperature range, but for many automotive lubricating greases operating in the normal temperature range of -40 to 120°C , a 30 % naphthenic and 70 % paraffinic mineral oil blend would typically be used.

2.5.5 Grease Thickener

The solidifying agent, generally referred to as the thickener, exists as a three-dimensional network of fibers or surface-active particles dispersed in the liquid (oil) phase. This three-dimensional network is often regarded as acting like a sponge for the liquid lubricant.

2.5.5.1 SOAP-THICKENED GREASES

Soaps are by far the most commonly used thickener material in greases and account for approximately 75 % of all greases used today [48]. Soaps are metallic salts of fatty acids and are commonly produced in situ during the grease manufacturing process. The chemical reaction involves one or more alkali or other metal salts with one or more fatty acids.

- *Simple soap*: One alkali with one acid (e.g., lime and stearic acid).
- *Mixed soap*: Two or more alkali metals (e.g., lime and LiOH) with e.g., 12-hydroxystearic acid.
- *Complex soap*: A single alkali metal (e.g., LiOH) reacting with a long-chain acid (e.g., 12-hydroxystearic acid) and a complexing acid (e.g., azelaic acid). Complex soaps produce greases that are suitable for use at temperatures above the normal operating range (to 150°C).

2.5.5.2 NON-SOAP-THICKENED GREASES

Other types of thickener, generally referred to as non-soap thickeners, can be used to achieve the same thickening effect as soap thickeners, but they produce greases with different structural networks. For example, polyurea-thickened greases can look like rice pudding, whereas calcium sulfonate greases have very small blood-like platelets. The structural nature of the thickener in oil has an effect on the amount of thickener required to achieve the desired grease consistency (stiffness) and the texture (smooth, buttery, astringent, tenacious).

Urea greases (diurea, tetraurea, and polyurea) are formed in situ by the reaction of mixtures of amines or diamines both with di-isocyanates in the base fluid.

- *Sodium terephthalamate*: Na salts of (*N*-stearyl-amido)-terephthalic acid.
- *Calcium sulfonate greases*: Gels derived from highly overbased calcium sulfonate detergents.

2.5.5.3 HYBRID THICKENERS

Hybrid thickeners are a mixture of a soap and another thickener type:

- Urea complex greases are mixtures of urea and calcium complex thickeners.
- Calcium sulfonate complexes are a mixture of calcium sulfonate (gels) and calcium or calcium complex soap thickeners.

2.5.5.4 SPECIALTY THICKENERS/DISPERSIONS

Low volumes of other types of thickener are used for special applications:

- Fumed silica,
- Clay greases,
- Polymers,
- Carbon black, and
- Pigments.

2.5.6 Grease Additives

Additives used to improve the performance properties of lubricating greases can be segregated into three classes:

1. Chemically inert additives that undergo no chemical reaction, such as VMs to improve the base oil viscosity or provide adherence (tackiness). Functionalized polymeric materials that interact with soap thickeners are also used to improve the water resistance of lubricating greases. Solid additives (e.g., graphite and MoS_2) are also commonly used in grease formulations to provide antiwear and antiseizure properties.
2. Oil protection additives (e.g., antioxidants) are used in the finished grease to prevent degradation due to oxygen attack at high temperatures.
3. Surface protection additives (e.g., friction modifiers, antiwear additives, EP additives, and corrosion inhibitors) that chemically or physically interact at the metal surfaces to provide improved performance properties.

2.5.7 Types of Automotive Lubricating Greases

The main purpose of lubricating greases used in automotive applications is to address one or more of the following performance requirements:

- Corrosion protection,
- Lubrication of components,
- Antisqueak, and
- Water resistance.

2.5.7.1 GREASES FOR CARS AND LIGHT TRUCKS

There are essentially two application families of grease used in cars and light trucks: those used in the passenger compartment and those used on the exterior or underside of the vehicle. Lubricating greases used inside of the passenger compartment are subject to light-service general lubrication duties, such as providing smooth operation and antisqueak performance. These greases must be compatible with plastic components and are designed to be in service for the life of the component. Today, many components are lubricated with dry coatings. Lubricating greases used for external or underside applications are exposed to more severe operating conditions and must have good antioxidant properties and be water and corrosion resistant. Examples of these are shown in Figure 2.26.

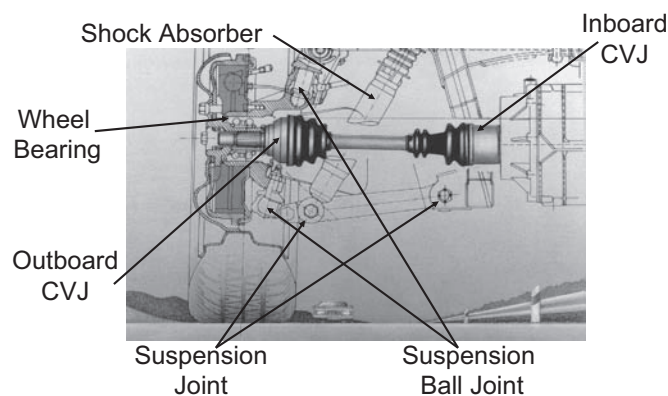


Figure 2.26—Diagram of front corner of a passenger car.
Source: Figure courtesy of GKN Driveline.

2.5.7.2 PASSENGER CAR AND LIGHT-TRUCK GREASE APPLICATIONS

- **Wheel bearings:** Greases used to lubricate wheel bearings must operate effectively over a wide temperature range (-40°C to $+150^{\circ}\text{C}$), which requires high-temperature thickeners. To deliver long-life service, semisynthetic base oils have now largely replaced mineral oil greases. The nature of the application often requires that different greases may be used (e.g., for ball and roller bearings) and their performance requirements are generally specified by the relevant equipment manufacturer (OEM).
 - **Constant velocity joints (CVJs):** CVJs are used on approximately 85 % of all cars and light trucks and require effective grease lubrication. Front-wheel and rear-wheel drive vehicles with independent rear suspension use four CVJs lubricated with up to 1.5 kg of grease. Four-wheel drive vehicles with independent suspension may have up to 13 joints with up to 3 kg of grease per vehicle, requiring the use of three or four differently formulated greases.
 - **Hooke's joints:** These are lubricated by one of four classes of grease—three that are serviceable (normal-, low-, and high-temperature applications) and one for filled-for-life applications that offer high-performance with a wide operating temperature range (-40 to $+120^{\circ}\text{C}$) and excellent durability.
 - **Window winders and sun (moon) roof mechanisms:** Lubrication requirements are minimal, but it is very important that these greases do not allow oil separation.
 - **Steering racks and suspension joints:** Grease needs to be water-, wear- and fretting-wear resistant, offer corrosion (rust) protection, and provide good shear stability and seal compatibility.
 - **Door hinges, locks, and handles:** These have general lubrication requirements, but it is important that water resistance and corrosion protection are effective.
 - **Brake mechanisms:** These require some corrosion protection and antiseize properties, but the most important thing is that they do not separate oil, which could interfere in the operation of the braking system.
 - **Shock absorbers:** These are typically used inside of the upper sealed part of the shock absorber, so water resistance is not typically an issue. Wear- and fretting-wear-resistant with good shear stability and seal compatibility are the main requirements.
- Small volumes of speciality products are also used in the following applications:
- **Electrical contact switches:** These use sophisticated high-cost products that are based on synthetic fluids (e.g., polyalkylethers or polyphenylethers). They must resist water, oxidation, corrosion, and wear and have uniform electrical conductivity/resistance.
 - **Pedal mechanisms:** There are two main facets to pedal mechanism greases. They must offer smooth movement of the pedal without squeak or stick-slipping and prevent seizure. The second main feature is that they must not separate oil or drip from where applied because this could stain the vehicle's carpeting or get onto the shoes or clothing of the driver.
 - **Accessory drive bearings:** Attached to the front end of most car engines are accessory components that are driven off the crankshaft. These include alternators/generators and water pumps. Because engine compartment temperatures have increased, the upper operating temperatures of greases for these applications have increased but without any compromise on the low-temperature requirement of -40°C . Therefore, for most accessory component applications, a higher quality mineral or semisynthetic oil must be used in the grease formulation. The primary issues for accessory drive bearings are long life and durability as well as no noise at high or low speeds or temperatures or on startup. In addition, for water pump bearings, the greases must be water and corrosion resistant with good sealing capabilities.
 - **Starter motors:** These only operate for a very short period of time, but they undergo significant shock loading. Greases for starter motors need to survive the high engine compartment temperatures as well as provide good EP and shock-load resistance. The components are also sealed for life, and higher viscosity EP greases are typically used, but the requirements are that they function without being too stiff at -40°C .
 - **Bearing greases for driveshafts, propshafts, or linkshafts:** In front-engine, rear-wheel drive vehicles the torque and speed need to be transmitted from the gear box to the rear differential. For most vehicles, a two- or three-piece propeller or driveshaft is used, and these need to be mounted to the underside of the vehicle via support bearings. The shaft can rotate at speeds of up to 10,000 r/min but has little torque loading on the bearing, with the main loading being the weight of the shaft itself. Durability of the bearings and greases due to loading is seldom an issue. The main challenges for the grease are related to noise and temperature. Sometimes the exhaust system is positioned adjacent to the propshaft, and this can create elevated operating temperatures for the grease and may lead to degradation of the bearing unless grease with good oxidation resistance and a high-temperature thickener are used. The bearing must also not make any noise or vibrate, so typically high-temperature/low-noise greases are used. For linkshaft bearings, similar bearings and greases as for propshafts are typically used, but they typically run at one third the speed of the propshaft, so high-speed noise is not an issue.

- *Sliding splines on propshafts:* Effective lubrication requires good antifretting, antiwear greases with some corrosion and oxidation resistance. Seal compatibility is also important.
- *Seat adjusters:* Here, very small quantities of grease are used, but the grease is typically there to prevent noise when the seat is moved backward or forward.

2.5.7.3 GREASES FOR COMMERCIAL VEHICLE APPLICATIONS

Greases used on commercial vehicles are formulated according to OEM specifications. For commercial vehicles, it is important that the service life of the lubricant is as long as possible, if not filled for life, which means that servicing and relubrication is minimized. However, for situations in which relubrication is necessary, use of multipurpose greases in the aftermarket instead of the specified OEM grease may occur.

For truck and tractor units, the main grease-lubricated components outside of the engine compartment are the wheel bearings, the kingpins, the universal or Hooke's joints, the sliding splines of the driveshafts linking the gear box output to the driving wheels, and the fifth-wheel and chassis components. The wheel bearing greases will be similar to those found on cars and light trucks in terms of temperature range and soap type, but because of the higher load in trucks, they may require higher levels of EP performance. However, if the bearing is correctly sized this should not matter. A more important consideration is that heavy trucks typically drive much slower than cars and so the film generated by the speed will not be as high. Therefore, slightly higher viscosity fluids may be necessary for optimal lubrication.

In tractors with single driving axle units, there is one shaft, and in vehicles with two or more driving axles there are multiple shafts. The number depends on the number of driving axles. The universal joints (UJs) are typically fitted with lubricators to facilitate easy relubrication. Sliding splines may have lubricators fitted or rely on the sealing gaiter being able to be unfastened, slid back, and grease applied to the splines before refitting the gaiter. The greases used on the UJs are typically similar to those described earlier, except that the sealed-for-life greases are often used as universal greases and periodically relubricated. The same grease used on the UJ is often used on the splines. Tribologically, this is not wholly satisfactory because the lubrication regimes are different, and solid lubricants are often used to prevent wear in splines, which could potentially cause issues with the needles in the UJ. For the UJ grease, a high level of corrosion and oxidation resistance is necessary. However, because the spline is typically well sealed, the corrosion inhibitor is somewhat superfluous.

Coupling (fifth-wheel) greases and chassis lubricants in trucks and tractor units were historically total loss systems. According to European Union figures published in 1990, more than 4000 tons of greases were deposited on Europe's roads from truck chassis total loss systems, which was deemed to be environmentally unsatisfactory [49]. In response to this, the industry moved to using greases with lower environmental impact. Cl, Pb, and other heavy metals were prohibited in total loss grease systems, and for some applications, biodegradable greases were mandated.

Chassis greases are used to lubricate suspension bushes and pivot points on the rear of the truck. The primary concerns with this type of grease are water/corrosion and oxida-

tion resistance and stability. Historically, OEMs specified the greases to be used, but, especially in North America, greases meeting the NLGI ASTM standard [50] are now more likely to be specified for relubrication. This is covered in a later section.

For trailer units, most applications are similar to those of the main tractor unit: wheel bearings, brake units, suspension, and chassis joints. Greases for these applications are typically the same as those used on the main tractor unit.

For buses, greases similar to those used on tractors and trailers are used. Depending on the position of the engine in the bus, this will define many of the performance requirements of the greases and the applications requiring grease lubrication. For example, rear-engine, rear-drive will have no propshafts and no UJs.

Reviewing the applications for current tractor and trailer unit greases, they are mostly similar to cars and light trucks except that they tend to be relubricated at intervals rather than sealed for life, and the loads that they carry are typically higher. One trend for today's tractor and trailer unit greases is that as the service intervals for the crankcase have increased, as have the relubrication intervals for the greases, and to sustain lubrication between services the use of higher quality greases is required.

2.5.8 Automotive Grease Specifications

On a typical vehicle, there are a wide variety of greases used, and most specifications applied to automotive greases come from the OEMs. Gaining OEM approval for a grease has historically been somewhat difficult, and OEM-approved greases are often difficult to find in the marketplace. Because of this, the use of multipurpose greases in the aftermarket is commonplace. Existing standards for automotive service greases are also not widely available. In North America there exists NLGI/ASTM D4950 [50], but in Europe, only industrial grease specifications (e.g., DIN 51825) exist. Japan, with its JIS K2220 Industrial Greases standard, is similar to Europe.

2.5.8.1 AUTOMOTIVE SERVICE-FILL GREASES

The NLGI and ASTM co-developed a new standard for automotive service-fill greases that was published in 1991 as ASTM D4950: Standard Classification and Specification for Automotive and Service Greases [50]. It was revised in 1995 and 2001 with some editorial changes in 2004 and 2008. The purpose of this specification was to describe the current categories of lubricating grease used in automotive service-fill applications, especially for passenger cars, trucks, and other vehicles operating under various service conditions. This was developed so that the quality of automotive lubricating greases could be standardized and guaranteed, and it focussed on the lubrication of chassis components and wheel bearings.

- *Chassis systems (LA and LB)*
 - The LA classification is for chassis components and UJs operating under mild service conditions that require a lubricant of basic performance. This is generally suited to noncritical components requiring frequent relubrication.
 - The LB classification is for chassis components and UJs operating under mild to severe service conditions that require a high-performance lubricant. This is generally suited to more critical components that require extended relubrication

TABLE 2.14—ASTM D4950 Specification: Testing Requirements

ASTM Test	Description	LA	LB	GA	GB	GC
D217	Penetration	+	+	+	+	+
D566 ^a	Dropping point	+	+	+	+	+
D1264	Water washout	—	—	—	+	+
D1742	Oil separation	—	+	—	+	+
D1743	Rust protection	—	+	—	+	+
D2266	Four-ball wear	+	+	—	+	+
D2596	Four-ball EP	—	+	—	—	+
D3527	High-temperature life	—	—	—	+	+
D4170	Fretting wear	—	+	—	—	+
D4289	Elastomer compatibility	+	+	—	+	+
D4290	Leakage	—	—	—	+	+
D4693	Low-temperature torque	—	+	+	+	+

^aASTM D2265 may be substituted.

intervals, those that operate under high loads and high vibration, and those that may be exposed to water or other contaminants or both.

- *Wheel bearings (GA, GB, GC)*
 - GA relates to wheel bearings operating under mild-duty conditions requiring a basic level of performance and likely to be used on noncritical applications or requiring frequent relubrication. The GA classification is now rarely used.
 - GB applies to wheel bearings operating under mild-to moderate-duty conditions and likely to be used for urban, highway, and off-highway applications.
 - GC applies to wheel bearings operating under mild-to severe-duty conditions and likely to be used in heavy-duty/high-temperature applications such as on trucks, buses, or vehicles that undergo extreme braking in service, such as in highly loaded vehicles and driving in mountainous regions. Lubrication is often fill for life, which requires a high-performance lubricating grease. GC is now the most commonly used and specified wheel bearing classification.
- *Multipurpose greases (GC-LB):* This is by far the most popular certification mark; it applies to the highest performance level for chassis and wheel bearing applications. Greases must be tested against a list of ASTM test methods by the submitting grease manufacturer (Table 2.14) and meet all of the required performance limits (Table 2.15). One additional requirement is that

TABLE 2.15—ASTM D4950 Acceptance Limits for the Various Automotive Grease Classes

Characteristic ^a	ASTM Method	LA	LB	GA	GB	GC	LB/GC
Worked penetration, W60	D217	220–340	220–340	220–340	220–340	220–340	220–340
Dropping point, °C	D566 or D2265	80	150	80	175	220	220
Four-ball Wear, mm max.	D2266	0.9	0.6	—	0.9	0.9	0.6
Four-ball EP,	D2596						
LWI, kgF, min.		—	30	—	—	30	30
Weld pt. kgF, min.		—	200	—	—	200	200
Elastomer Compatibility	D4289						
CR, % vol. change		0 to 40	0 to 40	—	—	—	0 to 40
CR, hardness change		0 to –15	0 to –15	—	—	—	0 to –10
NBR-L, % vol. change		—	—	—	–5 to 30	–5 to 30	–5 to 30
NBR-L, hardness change		—	—	—	+2 to –15	+2 to –15	+2 to –15
Oil separation, % max.	D1742	—	10	—	10	6	6
Rust, max. rating	D1743	—	Pass	—	Pass	Pass	Pass
Fretting protection, mg. loss	D4170	—	10	—	—	—	10
Low temp. torque	D4693						
@ –40°C, Nm		—	15.5	15.5	15.5	15.5	15.5
Water resistance	D1264						
@ 80°C, % max.		—	—	—	15	15	15
High temp. life, hrs., min.	D3527	—	—	—	40	80	80
Leakage tendency, g, max.	D4290	—	—	—	24	10	10

^aGrease must be within an NLGI consistency class (3, 2, or 1), which also must also be specified.



Figure 2.27—NLGI certification marks for automotive service greases.

although a 60-stroke worked penetration range of 220–340 units (tenths of a millimetre) at 25°C is permitted, the NLGI grade must be specified (i.e., 1, 2, or 3) and should be displayed on the container. A grease may have been tested to prove GC credentials and have a penetration range of 265–295 units so that it would be described as an NLGI No. 2 GC grease. An NLGI license approval and an annual certification fee are charged for the use of the NLGI certification mark (e.g., Figure 2.27).

As of June 2009, 213 products have been licensed by NLGI with no products approved under the LA, GA, or GB classifications: 44 products as LB (21 %), 3 products as GC (1 %), and 166 products as GC-LB (78 %).

Many OEMs currently specify LB or GC classifications or both for service or as requirements for initial fill specifications. In addition, the penetration range or NLGI classification of the grease to be used is also typically stated in the OEM documentation. The use of NLGI/ASTM service greases in off-highway applications is also now quite widespread, acknowledging the importance of the standard.

References

- [1] Hutchings I.M., 1992, "Viscosity." In *Tribology—Friction and Wear of Engineering Materials*, CRC, Boca Raton, FL, p. 59.
- [2] Selby, T.W., 1958, "The Non-Newtonian Characteristics of Lubricating Oil," *Trans. ASLE* Vol. 1, pp. 68–81.
- [3] Caines, A., and Haycock, R., 1996, "Constituents of Modern Lubricants." In *Automotive Lubricants Reference Book*, SAE, Warrendale, PA, pp. 72–73.
- [4] Aguilar, G., Mazzamaro, G., and Rasberger, M., 2010, "Oxidative Degradation and Stabilisation of Mineral Oil Based Lubricants." In *Chemistry and Technology of Lubricants*, 3rd ed., R.M. Mortier, M.F. Fox, and S.T. Orszulik, Eds., Springer, New York, pp. 108–117.
- [5] Migdal, C., 2003, "Antioxidants." In *Lubricant Additives: Chemistry and Applications*, L.R. Rudnick, Ed., CRC, Boca Raton, FL, pp. 8–9.
- [6] Aguilar, G., Mazzamaro, G., and Rasberger, M., 2010, "Oxidative Degradation and Stabilisation of Mineral Oil Based Lubricants." In *Chemistry and Technology of Lubricants*, 3rd ed., R.M. Mortier, M.F. Fox, and S.T. Orszulik, Eds., Springer, New York, pp. 118–134.
- [7] Spikes, H., 2004, "The History and Mechanisms of ZDDP," *Tribology Lett.*, Vol. 17, pp. 469–489.
- [8] Kenbeek, R., and Buenemann, T.F., 2003, "Organic Friction Modifiers." In *Lubricant Additives: Chemistry and Applications*, L.R. Rudnick, Ed., CRC, Boca Raton, FL, pp. 203–222.
- [9] Grossiord, C., Varlot, K., Martin, J.-M., Le Mogne, Th., Esnouf, C., and Inoue, K., 1998, "MoS₂ Single Sheet Lubrication by Molybdenum Dithiocarbamate," *Tribology Int.*, Vol. 31, pp. 737–743.
- [10] Spedding, H., and Watkins, R.C., 1982, "The Antiwear Mechanism of ZDDPs—Part I," *Tribology Int.*, Vol. 15, pp. 9–12.
- [11] Watkins, R.C., 1982, "The Antiwear Mechanism of ZDDPs—Part II," *Tribology Int.*, Vol. 15, pp. 13–15.
- [12] Willermet, P., Dailey, D.P., Carter, R.O., III, Schmitz, P.J., and Whu, W., 1995, "Mechanism of Formation of Antiwear Films from Zinc Dialkyldithiophosphates," *Tribology Int.*, Vol. 28, pp. 177–187.
- [13] Barnes, A.M., Bartle, K.D., and Thibon, V.R.A., 2001, "A Review of Zinc Dialkyldithiophosphates (ZDDPs) Characterisation and Role in Lubricating Oil," *Tribology Int.*, Vol. 34, pp. 389–395.
- [14] Bovington, C.H., 2010, "Friction, Wear and the Role of Additives in Controlling Them." In *Chemistry and Technology of Lubricants*, 3rd ed., R.M. Mortier, M.F. Fox, and S.T. Orszulik, Eds., Springer, New York, pp. 77–107.
- [15] Fuller, M., Yin, Z., Kasrai, M., Bancroft, G.M., Yamaguchi, E.S., Ryason, P.R., Willermet, P.A., and Tan, K.H., 1997, "Chemical Characterisation of Tribofilm and Thermal Films Generated from Neutral and Basic ZDDPs Using X-ray Absorption Spectroscopy," *Tribology Int.*, Vol. 30, pp. 305–315.
- [16] Papay, A.G., 1998, "Antiwear and Extreme-Pressure Additives in Lubricants," *Lubrication Sci.*, Vol. 10, pp. 209–224.
- [17] Farnig, L.O., 2009 "Ashless Antiwear and Extreme-Pressure Additives." In *Lubricant Additives: Chemistry and Technology*, 2nd ed., L.R. Rudnick, Ed., CRC, Boca Raton, FL, pp. 223–257.
- [18] Lara, J., Blunt, T., Kotvis, P., Riga, A., and Tysoe, W.T., 1998, "Surface Chemistry and Extreme-Pressure Lubricant Properties of Dimethyl Disulfide," *J. Phys. Chem. B*, Vol. 102, pp. 1703–1709.
- [19] Dacre, B., and Bovington, C.H., 1982, "The Adsorption of Dibenzyl Disulfide and Dibenzyl Sulfide on Steel," *ASLE Trans.*, Vol. 25, pp. 272–278.
- [20] Hiley, R.W., Spikes, H.A., and Cameron, A., 1980 "Polysulfides as Extreme-Pressure Lubricant Additives," *ASLE 80LC7A-3, ASME/ASLE International Lubrication Conference*, San Francisco, CA, August 18–21, 1980.
- [21] Seddon, E.J., Friend, C.L. and Roski, J.P., 2010, "Oxidative Degradation and Stabilisation of Mineral Oil Based Lubricants." In *Chemistry and Technology of Lubricants*, 3rd ed., R.M. Mortier, M.F. Fox, and S.T. Orszulik, Eds., Springer, New York, pp. 215–218.
- [22] "Code of Practice," <http://atiel.org/code-of-practice/code-of-practice>, accessed 2012.
- [23] "ACEA European Oil Sequences 2008," http://www.acea.be/index.php/news/news_detail/acea_european_oil_sequences_2008/, accessed 2012.
- [24] "American Chemistry Council," www.americanchemistry.com/s_acc/bin.asp?CID=368&DID=1361&DOC=FILE.PDF, accessed 2012.
- [25] "Technical Committee of Petroleum Additive Manufacturers in Europe," <http://www.atc-europe.org/publications.asp>, accessed 2012.
- [26] "American Petroleum Institute Publications," www.api.org/certifications/engineoil/pubs/index.cfm, accessed 2012.
- [27] SAE Standard J306_200506: Automotive Gear Lubricant Viscosity Classification, Fuels and Lubricants Tc3 Driveline and Chassis Lubrication, SAE, Warrendale, PA, 2005.
- [28] ASTM Standard D2983: Standard Test Method for Low-Temperature Viscosity of Lubricants Measured by Brookfield Viscometer, *Annual Book of ASTM Standards*, ASTM International, West Conshohocken, PA, 2009.

- [29] ASTM Standard D445: Standard Test Method for Kinematic Viscosity of Transparent and Opaque Liquids (and Calculation of Dynamic Viscosity), *Annual Book of ASTM Standards*, ASTM International, West Conshohocken, PA, 2009.
- [30] CEC Test Method CEC L-45-99: Viscosity Shear Stability of Transmission Lubricants, CEC Secretariat, Desford, UK, 2008.
- [31] ASTM Standard D7450: Standard Specification for Performance of Rear Axle Gear Lubricants Intended for API Category GL-5 Service, *Annual Book of ASTM Standards*, ASTM International, West Conshohocken, PA, 2008.
- [32] ASTM Standard D7452: Standard Test Method for Evaluation of the Load Carrying Properties of Lubricants Used for Final Drive Axles, Under Conditions of High Speed and Shock Loading, *Annual Book of ASTM Standards*, ASTM International, West Conshohocken, PA, 2009.
- [33] ASTM Standard D6121: Standard Test Method for Evaluation of Load-Carrying Capacity of Lubricants Under Conditions of Low Speed and High Torque Used for Final Hypoid Drive Axles, *Annual Book of ASTM Standards*, ASTM International, West Conshohocken, PA, 2009.
- [34] ASTM Standard D7038: "Standard Test Method for Evaluation of Moisture Corrosion Resistance of Automotive Gear Lubricants, *Annual Book of ASTM Standards*, ASTM International, West Conshohocken, PA, 2009.
- [35] ASTM Standard D5704: Standard Test Method for Evaluation of the Thermal and Oxidative Stability of Lubricating Oils Used for Manual Transmissions and Final Drive Axles, *Annual Book of ASTM Standards*, ASTM International, West Conshohocken, PA, 2009.
- [36] ASTM Standard D892: Standard Test Method for Foaming Characteristics of Lubricating Oils, *Annual Book of ASTM Standards*, ASTM International, West Conshohocken, PA, 2006.
- [37] ASTM Standard D130: Standard Test Method for Corrosiveness to Copper from Petroleum Products by Copper Strip Test, *Annual Book of ASTM Standards*, ASTM International, West Conshohocken, PA, 2004.
- [38] ASTM Standard D7038: Standard Test Method for Evaluation of Moisture Corrosion Resistance of Automotive Gear Lubricants, *Annual Book of ASTM Standards*, ASTM International, West Conshohocken, PA, 2009.
- [39] ASTM Standard D5662: Standard Test Method for Determining Automotive Gear Oil Compatibility with Typical Oil Seal Elastomers, *Annual Book of ASTM Standards*, ASTM International, West Conshohocken, PA, 2010.
- [40] ASTM Standard D5579: Standard Test Method for Evaluating the Thermal Stability of Manual Transmission Lubricants in a Cyclic Durability Test, *Annual Book of ASTM Standards*, ASTM International, West Conshohocken, PA, 2010.
- [41] ASTM Standard D5182: Standard Test Method for Evaluating the Scuffing Load Capacity of Oils (FZG Visual Method), *Annual Book of ASTM Standards*, ASTM International, West Conshohocken, PA, 2008.
- [42] *Laboratory Performance Tests for Automotive Gear Lubricants Intended for API GL-4, GL-5, and GL-6 Services*, Committee D02, Eds., ASTM International, West Conshohocken, PA, 1972.
- [43] Kline and co Research report 2008.
- [44] *Lubricating Grease Guide*, 5th ed., NLGI, Kansas City, MO, 2006.
- [45] Vold, M.J., and Vold, R.D., NLGI Spokesman 1952, Volume 16, p.8.
- [46] SAE J310: Automotive Greases Recommended Practice, SAE International, Warrendale, PA, 2005.
- [47] Cann, P.M., 1997, "Film Distribution in Grease Lubricated Rolling Contacts," NLGI Spokesman, Vol. 61, pp. 22-29.
- [48] *NLGI Grease Production Survey 2008*, NLGI, Kansas City, MO.
- [49] From a presentation given at the ELGI Annual Meeting, Heidelberg, Germany, 1992.
- [50] ASTM D4950: Standard Classification and Specification for Automotive and Service Greases, *Annual Book of ASTM Standards*, ASTM International, West Conshohocken, PA, 2008.

3

Lubricant Properties and Characterization

Kenneth O. Henderson¹ and Chris J. May²

3.1 INTRODUCTION

Lubricant physical properties are important in determining their suitability for the intended application and for comparing fluids. Some properties also provide insight into the remaining useful life of a fluid in service. In this chapter, we first review the components that go into making a lubricant. This is followed by a review of the most common ASTM International standard test methods used to measure a lubricant's physical properties. More information on the significance of tests for petroleum can be found in ASTM Manual 1, *Significance of Tests for Petroleum Products*, edited by Sal Rand [1].

3.2 COMPONENTS OF LUBRICANTS

An automotive lubricant can be broadly divided into four components: (1) a hydrocarbon base oil, (2) an additive package (DI), (3) a viscosity index improver (VII), and (4) a pour-point depressant (PPD). The base oil typically contributes more than 75 % of the oil composition and is often a blend of separate basestocks. For engine oils, the API five-group basestock classification system is used (see Table 3.1). This is based on saturates, sulfur, and the viscosity index of the material.

Group I basestocks include typical paraffinic solvent refined stocks.

Group II basestocks are produced by hydroprocessing, which raises the saturates level and reduces sulfur to very low concentrations.

Group III stocks are produced by more severe hydroprocessing, using slack wax (wax removed in the refining process), wax produced from Fischer-Tropsch processes, or other sources of feedstocks. The different feedstocks used to make Group III basestocks may have small amounts of residual molecules such as saturated polynuclear cyclic hydrocarbons, which can affect formulated oil performance. Or they may contain more residual wax, which can affect the finished oil low-temperature properties. Group III stocks are typically referred to as synthetic because of the high degree of molecular change effected during processing.

Group IV basestocks are synthetically derived from α -olefins. These are created by oligomerization of α -decene, α -dodecene, or both, followed by hydrogenation to remove any remaining unsaturation. Polyalphaolefins (PAOs) are sulfur-free stocks of high VI (>120) with low volatility and extremely good low-temperature properties.

Group V includes all other lubricant basestocks. These are typically either naphthenics (refined from naphthenic

crudes, VI < 80) or other synthetics such as esters and alkylated naphthalenes.

Within each basestock group a wide range of viscosity grades or cuts are available. Grades of Group I and II basestocks are commonly classified by their designation in the older SUS (Saybolt Universal seconds) viscosity units at 40°C. Thus, a basestock with a viscosity of approximately 150 SUS at 40°C will be labeled "150SN" or "150N," where SN and N refer to solvent neutral and neutral, respectively, which is old terminology referencing solvent extraction and pH neutral, respectively. For comparison, a 100N stock typically has a D445 kinematic viscosity of approximately 4 mm²/s at 100°C. Group III and IV stocks tend to be classified by their typical kinematic viscosity at 100°C; for example, a PAO-4 or PAO-6 stock will have a 100°C viscosity of approximately 4 and 6 mm²/s, respectively.

Mixtures of basestock types and viscosities are used by formulators to obtain the right combination of viscosity, volatility, additive solubility, and elastomer compatibility required in the finished lubricant.

3.2.1 DI Package

The DI package typically consists of up to 10 different components that give the lubricant its performance capability. Depending on the application, these can include ashless dispersants, metal detergents, antioxidants, antiwear agents, antifoamants, friction modifiers, rust inhibitors, metal passivators, and seal swell agents.

3.2.1.1 ASHLESS DISPERSANTS

Ashless dispersants are added to disperse insoluble oil contaminants. They are typically made from a moderately high-molecular-weight hydrocarbon for oil solubility coupled with a highly polar moiety for associating with the insoluble material.

3.2.1.2 DETERGENTS

Detergents included in the DI package are sulfonate, phenate, salicylate, or carboxylate surfactant salts commonly based on Ca, Mg, Na, or Ba. These detergents come in two forms: neutral detergents have a total base number (TBN) in the 20–30 range and overbased detergents incorporate an emulsified metal carbonate particle and have TBNs in the 300–400 range. Detergents are added to the oil to prevent the buildup of harmful deposits and, in the case of overbased detergents, to neutralize acidic combustion and oxidation byproducts that might harm the equipment.

¹ McEinri Associates, Port Matilda, PA, USA

² Retired, Priceville, Ontario, Canada

TABLE 3.1—API Base Oil Group Characteristics

API Base Oil Group	Saturates, %	Sulfur, % (S)	VI
Group I	<90	and/or S > 0.03	and 80 ≤ VI < 120
Group II	≥90	and/or S ≤ 0.03	and 80 ≤ VI < 120
Group III	≥90	and/or S ≤ 0.03	and VI ≥ 120
Group IV	Polyalphaolefins		
Group V	All other stocks not included in Group I–IV		

A formulation is likely to contain neutral and overbased detergents.

3.2.1.3 ANTIOXIDANT

Antioxidant is added to hinder the lubricant oxidation process. Common ashless antioxidants include hindered phenolics and diaryl amines whereas common ash-containing types include zinc dialkyl dithiophosphate (ZDDP) and complexes of Mo and Cu.

3.2.1.4 ANTIWEAR ADDITIVES

Antiwear additives are included to reduce wear on contacting surfaces where a complete oil film cannot form. The most common antiwear type is ZDDP, but other Zn, Mo, and ashless components may also be used depending on the application. For automotive gear oils (GOs), special S-P components are added to control wear under the extreme pressures and sliding contacts encountered in mating gear surfaces.

3.2.1.5 ANTIFOAMANTS

Antifoamants are typically polydimethyl siloxanes of various molecular weights and are only required at a few parts-per-million concentration to control lubricant foaming. It should be noted that the siloxanes are dispersed in the lubricant in the form of small particles or globules with specialized equipment. These small particles can be seen through the use of a phase contrast microscope similar to that used in clinical laboratories.

3.2.1.6 FRICTION MODIFIERS

Friction modifiers (FMs) are added to reduce lubricant-related energy losses and they broadly fall into two categories. Ashless FMs are typically derivatives of long-chain fatty acids, which are thought to adsorb onto the metal surfaces to lower the coefficient of friction. The most common ash-containing FMs are based on complexes of Mo and are thought to function by forming MoS₂ in situ, thereby reducing friction.

3.2.1.7 RUST INHIBITORS

Although overbased and neutral detergents offer protection against rusting, some formulations require supplemental ashless rust inhibitors. These may also be required in formulations in which the ash from a detergent would cause operational problems, but antirusting behavior is still important.

3.2.1.8 METAL PASSIVATORS

Metal passivators may be required to prevent lube component attack on yellow-metal components in the equipment

(copper, brass, bronze). Thiadiazoles are a class of commonly used passivators.

3.2.1.9 SEAL SWELL AGENTS

Seal swell agents include specialized synthetic esters and may be needed to balance the seal shrinkage tendencies of some base oil components such as PAOs.

3.2.2 Lube Oil Pour Depressant

Lube oil pour depressant (LOPD) is added to control the morphology of residual wax molecules below the cloud point of the basestock, where they crystallize out of solution. Subtle additive-wax interactions can also cause excessive low-temperature thickening or gelation if not controlled by proper LOPD selection, and results of the ensuing oil starvation can be disastrous to equipment operation. Pour depressants have the greatest impact on low-temperature, low-shear tests such as pour point and pumpability. These additives are lower-molecular-weight polymers of polymethacrylates, dialkyl fumarate-vinyl acetates, and styrene-ester, to name a few of the most common types. LOPDs are normally tailored to the specific formulation composition. Changes in basestock source or group may require a change in treat rate or even type.

3.2.3 VII

A VII is normally only present in multigraded engine lubricants to improve the viscosity-temperature properties of the lube. VIIs are hydrocarbon-soluble, relatively high-molecular-weight polymers. Common monofunctional VII types include ethylene-propylene, styrene-butadiene, and styrene-isoprene copolymers as well as polymethacrylates. Commercial VIIs are also available with additional functionality that imparts dispersant properties. Common types include multifunctional olefin copolymers (MFOCPs) and dispersant polymethacrylates (DPMAs). VIIs contribute to temporary and permanent viscosity loss (TVL/PVL) in multigrade oils, making the accurate measurement of these properties important. Discussion of these measurements is covered in greater detail in the viscosity measurement section of this review. VIIs in conjunction with suitable base oil components and pour depressants can help the formulator simultaneously meet the high- and low-temperature requirements for engine oils as laid out in the SAE J300 specification or for GOs in the SAE J306 classification [2,3].

3.3 PHYSICAL PROPERTIES OF LUBRICANTS

Physical properties covered in this chapter include

- Kinematic and dynamic viscosity
- Shear stability
- Pour point
- Cloud point
- Volatility
- Foaming characteristics
- Element content
- Ash
- Density
- Flash point
- Color
- Corrosiveness
- Water tolerance
- Elastomer compatibility
- Homogeneity and miscibility

Additional information on these tests can be found in two recent publications: *Fuels and Lubricants Handbook: Technology, Properties, Performance, and Testing*, edited by George E. Totten, Steven R. Westbrook, and Rajesh J. Shah, and *MNL 44 Guide to ASTM Test Methods for the Analysis of Petroleum Products and Lubricants*, 2nd edition, authored by R.A. Kishore Nadkarni [4,5]. These two publications are excellent sources of background information on the standard test methods in this chapter.

It is not uncommon to find ASTM International standard test methods used in evaluating petroleum products for other applications. In addition, several original equipment manufacturers (OEMs) have physical test requirements that are unique or derivatives of a standard test method. These OEM test requirements are typically required when a supplier is seeking to meet factory or service fill requirements.

3.3.1 Viscosity

Viscosity is a key property of any lubricant because the strength of the lubricant film is directly related to its viscosity at operating temperature. It is this film that lets two metal surfaces slide past one another without damage to either surface. For engine oils, the primary international specification is SAE J300, "Specification for Engine Oil Viscosity Classification" [2]. In addition to the criteria in SAE J300, additional requirements may apply depending on the lubricant's intended use. Examples of these additional requirements can be found in ASTM D4485 [6] and the ILSAC GF-5 specifications, which are included in ASTM D4485. Because of the various temperatures, shear rates, and shear stresses involved in automotive applications, various viscosity test methods are required.

Viscosity is a measure of a material's resistance to flow. Dynamic viscosity is a ratio of the force needed to push one plane past another where the annular space is filled with the material of interest. This applied force is referred to as shear stress. The rate of displacement and distance between the two planes yields the shear rate being applied to the material between the plates. For petroleum products the material is a fluid. Thus, dynamic viscosity is expressed by the following equation:

$$\eta = \tau / \gamma \quad (3.1)$$

where:

η = dynamic viscosity,
 τ = force per unit area, and
 γ = shear rate [7,8].

Another component of viscosity is its response to changes in shear rate. A Newtonian fluid is defined as a fluid for which the viscosity is independent of shear rate. Many basestocks approximate a Newtonian fluid. Once a VII or DI package is added to a basestock the fluid gains a non-Newtonian character. A non-Newtonian fluid's viscosity will change as the shear rate changes at a constant temperature. The addition of a VII is the greatest contributor to the non-Newtonian character of lubricants.

3.3.1.1 KINEMATIC VISCOSITY

Kinematic viscosity is related to dynamic viscosity by the density of the fluid:

$$\nu = \eta / \sigma \quad (3.2)$$

where:

ν = kinematic viscosity,
 η = dynamic viscosity, and
 σ = density of the fluid.

Kinematic viscosity is determined by measuring the time for a known volume of fluid to flow through a capillary tube of known length using gravity and the liquid head as the driving force. The specifics for measuring kinematic viscosity can be found in ASTM D445 [9], which uses the viscometers specified in ASTM D446 [10]. Most automotive fluid specifications include kinematic viscosity requirements at 100°C, although some also have requirements at 40°C.

The manual determination of kinematic viscosity is directly supported by the instructions in ASTM D445. With the advances in instrumentation, this measurement can be accomplished automatically. An automatic kinematic viscometer has the advantage of being able to measure the flow time more accurately than an operator can manually. Using the measured flow time, these devices calculate the viscosity, load the sample, and then clean and dry the capillary tube once the measurement is complete. The precision of kinematic viscosity measurements is very high whether it is done manually or automatically. Automatic determination has the advantage of a reduction in operator time and more consistent test conditions.

When comparing viscometric measurements between laboratories, the usual cause of discrepancies is due to a temperature difference between test locations. Controlling the bath temperature to within $\pm 0.01^\circ\text{C}$ can be a challenge when the bath temperature is close to room temperature (i.e., 40°C) or when the bath is significantly above 100°C . Other contributors to measurement differences include air drafts around the bath, insufficient stirring, and the viscosity of the bath fluid. Many of the contributors to poor kinematic viscosity results can be minimized or eliminated through the use of a high-quality commercial constant-temperature bath or an automatic instrument. This is because a user is assured that the device is fit for purpose.

Another contribution to poor precision is lack of viscometer tube cleanliness. Poor cleanliness can be due to inadequate rinsing or poor solvent selection. Poor cleanliness is a problem for manual and automatic measurements. Cleanliness issues are less obvious in automatic instruments because of less attention by the operator to flow in the capillary. Cleanliness problems can be the result of selecting the wrong solvent or the use of impure solvents. Technical-grade solvents can leave a residue on drying. This residue will alter the flow characteristics of the working capillary causing erroneous results. Measuring the viscosity of used lubricants will likely require a different or special solvent to adequately clean the viscometer. This is typically due to the presence of high molecular weight, an increase in polar components in the lubricant, or both.

3.3.1.2 CRANKING VISCOSITY

Cranking viscosity is the term used for a lubricant's dynamic viscosity when measured in the cold crank simulator (CCS) as described in ASTM D5293 [11]. Cranking viscosity

of automotive engine oils has been correlated with low-temperature engine cranking speed in several different studies conducted in CRC and ASTM programs [11–14]. Because engine cranking speeds relate to the ability of the engine to start, this is an important parameter and one that helps to define the “W” grade portion of the SAE J300 classification.

The CCS instrument is a constant shear stress rotational viscometer that measures dynamic viscosities at shear rates on the order of approximately 10^4 – 10^5 s⁻¹ and at temperatures ranging from –35 to –5°C. These approximate the temperature and shear rate ranges covered in vehicle cranking studies. The CCS effective viscosity range is approximately 900 to 25,000 mPa-s, although measurements can be made as high as 50,000 mPa-s.

Cranking viscosity is determined by turning a rotor with a constant shear stress and measuring the rotor speed turning in a stator. A constant shear stress is obtained by supplying an electric motor with a constant current. The narrow space between the rotor and stator is filled with the test oil. Test temperature is measured near the stator inner wall. The temperature is maintained by removing heat with a controlled process to keep a constant stator temperature during the test. By applying a constant stress, the speed of the rotor will vary as a function of viscosity. The instrument is calibrated by relating rotor speed to a series of reference fluids of known viscosity. The test sample's cranking viscosity is then calculated by inserting the test sample's measured rotor speed into the calibration equation.

3.3.1.3 PUMPING VISCOSITY

Pumping viscosity is a measure of an oil's ability to flow to the oil pump when an automotive engine is started at low temperature. Yield stress is the stress required to initiate flow and has been related to a particular engine phenomenon referred to as “air binding” [15]. SAE J300 has W grade pumping viscosity and yields stress limits as measured in the mini-rotary viscometer (MRV) and described in ASTM D4684 [16]. When an engine oil cools in a low-temperature environment, the rate and duration of cooling can affect the oil's yield stress and viscosity. The MRV test was developed to cover a large range of cooling conditions so that a determination can be made as to whether the lubricant's low-temperature properties are fit for purpose. To achieve this, fresh engine oil is slowly cooled through a temperature range at which wax crystallization is known to occur (–5 to –20°C), followed by relatively rapid cooling to the final test temperature.

An older test method, ASTM D3829 [17], uses a similar apparatus, but the cooling is a more rapid, nonlinear cooling profile. Its inability to detect some field failure oils is what prompted the development of ASTM D4684 and other techniques.

The MRV instrument is a constant shear stress rotational viscometer. The test procedure first measures yield stress by determining the minimum weight to induce rotation of a thread-wrapped rotor spindle. The procedure then measures viscosity from the time it takes for three revolutions after applying a shear stress of 525 Pa. These conditions result in an effective shear rate between 0.4 and 15 s⁻¹. The measurement of the engine oil's yield stress and viscosity is done after cooling at controlled rates over a period exceeding 45 h to a final test temperature between –10 and –40°C. The viscosity as measured at this shear stress was

found to produce the best correlation between the temperature at which the viscosity reached a critical value and an engine's borderline pumping failure temperature in several studies [18–22].

Procedure A has recently been added to test method D4684; it yields improved precision over the original method, now incorporated as Procedure B. The gain in precision is due to additional controls placed on cell calibration variance and better thermal isolation of the sample from ambient air. The current precision of Procedure A is stated for a yield stress range of less than 35–210 Pa and an apparent viscosity range from 4300 to 270,000 mPa-s. The test procedure can determine higher yield stress and viscosity levels.

This test method is suitable for unused oils, sometimes referred to as “fresh oils”, which are designed for light- and heavy-duty engine applications. It has also been shown to be suitable for used diesel and gasoline engine oils. ASTM D6896 [23] was developed specifically for used sooted diesel engine oils.

ASTM D5133, the Scanning Brookfield method, can also be used to determine low-temperature, low-shear viscosities, and some equipment manufacturers have specific viscosity/temperature limits for their factory and service fill engine lubricants. This method is discussed further under the gelation index (see Section 3.2.1.5).

3.3.1.4 HIGH-TEMPERATURE, HIGH-SHEAR VISCOSITY

High-temperature, high-shear viscosity (HTHSV) for engine lubricants refers to measuring dynamic viscosity at shear rates of 1 million reciprocal seconds or more. For automotive lubricants, the temperature of these measurements is at 100 or 150°C. Viscosity measured under these conditions is considered to be relevant to the temperatures and shear rates in the journal bearings of internal combustion engines at operating conditions. Oil specifications associated with the automotive industry are typically set at 150°C, whereas manufactures of engines for railroad prime movers or similar power units typically specify measurements at 100°C. The relationship between HTHSV and engine operation has been discussed in many papers published by SAE. A symposium held by ASTM D02.07 provides an excellent overview of the relationship between HTHSV and engine operation [24].

There are four ASTM test methods for measuring HTHSV. SAE J300 cites ASTM D4683, D4741, and D5481, the specification for which is 150°C [25–27]. For measurement of HTHSV at 100°C, ASTM D4741 and D6616 [28] are suitable. Test methods D4683, D4741, and D6616 are based on measuring the stress while turning a rotor in a stator at a constant speed. ASTM D5481 is a capillary method applying a constant force while measuring flow time to determine viscosity; shear rate for this method corresponds to an apparent shear rate of 1.4×10^6 s⁻¹, which has been found to decrease discrepancies with the other HTHSV methods operating at 1×10^6 s⁻¹. All four methods base their calibration on Newtonian reference fluids, which correlate stress or force to their certified viscosity.

3.3.1.5 GELATION INDEX

The gelation index is a derivative of the temperature-viscosity profile of a lubricant as it is cooled at a rate

of 1°C/h from -5 to -40°C per ASTM D5133 [29]. The viscosity measurements are made with a constant shear rate instrument operating at a shear rate of 0.2 s⁻¹. Two values are reported: gelation index and gelation index temperature. The gelation index is a special form of the first derivative relating the change in viscosity to temperature as temperature decreases. The gelation index temperature is the temperature at which the gelation index reaches a maximum. The ILSAC GF-5 specification (referenced in ASTM D4485) as well individual equipment manufacturer specifications include limits for gelation index as determined by ASTM D5133. This test is included in the above specifications as an additional safeguard. It is also one that can assist formulators in determining the appropriateness of formulation modifications on low-temperature properties.

In terms of test results, there can be perceived similarities between pumping viscosity by MRV and the viscometric values obtained by ASTM D5133. The viscosity typically obtained by ASTM D5133 will be higher than that measured by ASTM D4684. This is believed to be due to the differences in the measurement conditions of the two tests. ASTM D5133 operates at less than 20 % of the shear stress used in ASTM D4684.

Like the MRV for pumping viscosity, a variant of the Scanning Brookfield technique has been developed specifically for soot-containing engine oils. ASTM D7110 describes a method in which the oil is subjected to cooling at 3°C/h between -5 and -40°C; shear rate remains at 0.2 s⁻¹. Apparent viscosity and gelation index are measured as a function of temperature.

3.3.1.6 LOW-TEMPERATURE VISCOSITY OF DRIVELINE LUBRICANTS

The viscosity of driveline lubricants at low temperature is critical for gear lubrication and circulation of the fluid in automatic transmissions. For GOs, the concern is obtaining oil flow into the channel carved out by submerged gears as they begin rotating and then relubrication of the gears as they continue to rotate. For automatic transmission, power steering, torque, and tractor fluids, the issue is whether the fluid will flow to a pump and through the distribution system rapidly enough for the device to function as intended. Measurement of these lubricants' viscometric properties is often used to determine their acceptability for a given application. ASTM D2983 [30] is referenced in several industry and OEM specifications.

The low-temperature performance of GOs was originally evaluated by the channel test (FTMS 791 method 3456). Test Method D2983 replaced the channel test in 1971. In ASTM D2983, the sample is preheated, allowed to stabilize at room temperature, and then poured into a glass cell with a special spindle. The glass cell is then placed into a precooled cold cabinet set at a predetermined test temperature between +5 and -40°C and allowed to soak for 16 h. At the end of the soak period, the viscosity is measured by a Brookfield viscometer using a designated spindle (rotor) turning at a speed adjusted for suitable on-scale torque measurement. The viscosity is then calculated from the observed torque. This low shear rate method covers the viscosity range of 500 to 1,000,000 mPa-s.

ASTM D6821 [31] has the same temperature and viscosity range as ASTM D2983. However, the instrument

automatically does all of the sample preheating and thermal conditioning. An MRV configured for ASTM D6821 uses a different weight set and rotors than those used in ASTM D4684, although it is the same instrument. At the end of the thermal conditioning the sample is maintained at temperature and remains undisturbed until the shear stress is applied.

ASTM D2983 and D6821 were designed as replacements for the channel test to characterize the low-temperature viscosity of GOs and automatic transmission oils but with a higher degree of discrimination and less variance.

3.3.1.7 VISCOSITY OF SOOTED OILS

As discussed in the low-temperature pumpability methods above, variants have been developed to measure soot-laden used engine oil samples with MRV and Scanning Brookfield instruments. Measuring the 100°C kinematic viscosities of many of these oils can also be very challenging because of soot agglomeration. The standard engine tests such as the Mack T-8 and T-11 (ASTM D5967 and D7156) have developed specific pretreatment conditions to ensure more consistent results. An alternative method of viscosity analysis, ASTM D6895, was developed for use with standard laboratory rheometers at 100°C. After a preshearing step (10 s⁻¹ for 30 s), an increasing shear rate (approximately 10–300 s⁻¹) or shear stress (0.1–10 Pa) sweep is run followed by a decreasing sweep. The rotational viscosity for each step (increasing and decreasing) at a 100 s⁻¹ shear rate is interpolated from the viscosity versus shear rate data table. The rate index, as a measure of shear thinning, is calculated from a plot of ln(shear stress) versus ln(shear rate).

3.3.1.8 SHEAR STABILITY

Shear stability is a measure of a lubricant's resistance to viscosity loss due to the fluid passing through narrow passages at high shear rates. The high stresses experienced by the polymeric thickeners (VII) are sufficient to reduce the polymer's molecular weight and thus its effectiveness as a VII. The viscosity loss is expressed as a percentage and frequently termed "percent shear loss." To achieve the high shear rates needed to shear engine oils in a bench test, the fluid is circulated through a diesel injector nozzle, which results in the degradation of polymer molecules, reducing their molecular weight and the associated thickening efficiency. These test procedures are designed to minimize the thermal or oxidative effects of degrading the polymer molecules.

The engine oil shear stability bench tests are ASTM D5275, D6278, and D7109 [32–34]. Each of these test methods measures the percentage loss in 100°C kinematic viscosity. ASTM D6709 [35] (Sequence VIII engine test) includes a procedure for measuring the shear stability of an engine lubricant after 10 h of operation and the stripping of volatile fuel components before measuring 100°C kinematic viscosity. Industry and individual OEM specifications include shear stability requirements to ensure a minimum acceptable viscosity in service. Engine oil formulators typically use these tests during the development/qualification of a product. Manufacturers of VII typically use the bench tests for quality control.

An earlier shear stability bench test method ASTM D3945 [36] contained two separate procedures that used

different equipment. These were later separated into ASTM D5275 and D6278 because Procedures A and B did not give equivalent results for some formulations. The primary difference between the methods is in the type of diesel injector nozzle used to shear stress the oil. When the two methods were removed from ASTM D3945, there were changes made in the procedure. ASTM D6278 uses the test apparatus defined in CEC L-14-A-93 [37].

ASTM D2603 [38] (sonic shear) is used for shear stability evaluations but not for automotive lubricants. ASTM D7109 is very similar to ASTM D6278 and uses the same equipment. ASTM D7109 measures viscosity loss after 30 and 90 cycles whereas ASTM D6278 only measures viscosity loss after 30 cycles.

None of these test methods are intended to predict actual viscosity loss in field service because of the wide range of operating conditions, which may include significant thermal and oxidative contributions or soot contamination.

CEC L-45-A-99 (Method C) (KRL shear stability) [39] is a bench test designed to evaluate the shear stability of automotive gear and transmission fluids using a Four-Ball EP test machine equipped with a tapered bearing. Various OEM specifications for these types of fluids include KRL shear requirements after running for prescribed test times. The SAE J306 [3] viscosity classification for automotive GOs has a stay-in-grade kinematic viscosity requirement after 20 h of KRL shear. Mechanical shearing in this test is different than in the diesel injector tests and typically requires much more shear stable viscosity modifiers than those used in engine oils.

3.3.2 Pour Point

Pour point is one of the oldest automotive fluid tests still in use. ASTM D97 [40] was originally developed to assess dispensibility at low ambient temperatures. Subsequent studies have shown that it cannot be related to oil pumpability or startability in engines or other automotive equipment. In the test, the candidate fluid is placed in a stoppered glass jar and cooled via immersion of the jar in progressively colder baths until no movement is detected when the jar is removed from the bath and tilted perpendicularly (checks made at 3°C intervals). The pour point is defined as the temperature 3°C higher than the observed no-movement temperature. Sample preheating has been shown to be an important factor in removing thermal history, which improved the precision of pour point measurement.

Because ASTM D97 is a very labor- and time-intensive test, it has led to the development of various auto pour methods, each with a separate ASTM designation. These auto pour apparatuses generally can be set to detect pour points in 1 or 3°C intervals. The reasoning behind having multiple test methods is that some samples will yield significantly different results in different automatic devices. This approach gives the specification authors the ability to ensure products meeting their specifications are fit for purpose by controlling how the measurement is accomplished.

Each of the test methods using automatic instruments heats the sample to approximately 50°C before cooling the sample at the same rate used in ASTM D97. These automatic methods—ASTM D5949, D5950, D5985, D6749, and D6892 [41–45]—are accepted in most specifications as an

alternative to ASTM D97. In many cases, the specifications have retained ASTM D97 as the referee method.

ASTM D5949 uses a Peltier cooling device cooling at rate of 1.5°C/min. The pour point is measured by periodically applying a controlled burst of nitrogen gas over the oil surface and detecting movement with an optical device.

ASTM D5950 uses an optical device to detect movement of the cooled sample when it is tilted; the cooling profile in this case is nonlinear, similar to D97.

In ASTM D5985, the sample is continuously rotated at approximately 0.1 r/min against a stationary, counter-balanced pendulum as the sample cools (8°C differential between cooling block and test cell) until pendulum displacement is recorded (no flow point).

ASTM D6749 uses regulated, slightly positive air pressure applied to the sample surface, which causes an upward movement of the sample in a communicating tube as the sample is cooled (0.8–1.1°C/min from 40°C above the expected pour point).

ASTM D6892 uses a robotic tilt method and camera to periodically check for sample movement when it is removed from the controlled cooling medium. (Cooling is nonlinear, similar to ASTM D97.)

3.3.2.1 SPECIALTY POUR POINT TESTS

There are other pour point tests used in the industry. These are typically found in individual equipment manufacturers specifications and primarily differ from the above tests in the cooling profiles used before testing for pour. None are covered by ASTM methods. Examples include the John Deere shock cool and slow cool pour tests.

3.3.3 Cloud Point

Cloud point is defined as the temperature when observable wax crystals first begin to form in a fluid. To many observers this appears to be a whitish or milky cloud, which is the basis for the name of the method. This cloud appears when the temperature of the specimen is low enough to cause wax to begin to crystallize to form a two-phase sample. In many specimens, these crystals form at the lower circumferential wall of the test jar where the temperature is the lowest. The size and position of the cloud or cluster at the cloud point varies depending on the nature of the specimen. Some samples will form large, easily observable clusters whereas others are barely perceptible.

For automotive lubricants this property is usually only measured on unadditized basestocks because the color needs to be less than 3.5 by ASTM D1500 [71]. The results give an indication of whether the basestock material is fit for purpose.

ASTM D2500 [46] is the standard manual method for determining cloud point and uses similar equipment and cooling profiles to the ASTM D97 pour point. There are also three standard test methods using automatic instruments to measure cloud point: ASTM D5771, D5772, and D5773 [47–49]. Each method uses a different technique to optically detect the first appearance of the cloud of wax crystals as the sample is cooled under a controlled rate specific to the method. All of the methods preheat the sample to approximately 50°C before cooling.

3.3.4 Volatility

Volatility of engine oil lubricants in service has become of increasing concern to equipment manufacturers because of oil consumption, engine deposits, and air pollution effects. Two types of methods are used to assess volatility: The first is based on simulated distillation by gas chromatography (GCD), and the second, Noack volatility, measures bulk oil weight loss after heating at a prescribed temperature/time. Volatility was estimated using gas chromatography in many laboratories before the Noack method became the preferred method globally.

The first GCD method developed was ASTM D2887 [50]. It was created to measure the boiling point distribution of petroleum products, usually base oils, after calibrating the elution profile with reference hydrocarbon samples. As the need for more precise assessment of volatility in formulated oils grew, additional test methods were developed. The current GCD test method for measuring finished oil volatility is ASTM D6417 [51]. ASTM D5480 [52] continues to be referenced in some specifications but the method has been withdrawn; it differs from ASTM D6417 in the use of an internal standard. ASTM D6417 is used to estimate the amount of oil volatilized at temperatures between 126 and 371°C. This test method is limited to samples having an initial boiling point (IBP) greater than 126°C (259°F) or the first calibration point, as well as to samples containing lubricant base oils with end points less than 615°C (1139°F) or the last n-paraffins in the calibration mixture. The calculated results of the oil volatility estimation by this test method can be biased when some of the sample does not elute. These noneluting components are typically additives (polymeric materials) or heavier base oils. The results of this test method also may not correlate with other oil volatility methods for nonhydrocarbon synthetic oils.

A nonpolar open tubular (capillary) gas chromatographic column is used to elute the hydrocarbon components of the sample in order of increasing boiling point. The sample is diluted with a viscosity-reducing solvent before introduction into the chromatographic system. The column oven temperature is raised at a linear rate to effect separation of the hydrocarbon components in order of increasing boiling point. By knowing the retention times of known n-paraffins, the percent of hydrocarbons eluting below 371°C can be calculated.

ASTM D5800 [53], the Noack volatility method, has three procedures for determining evaporation loss. These three procedures differ in equipment and some operational details. In these tests a weighed sample is heated at 250°C for 60 min while passing air over it at a controlled rate. After 60 min at 250°C, the sample is weighed after cooling and the percent loss obtained from the weight difference. Procedure A is the original version of the test on which industry specifications have been based and uses Woods metal in the heating block—the toxicity of this material has caused many laboratories to turn to the alternate procedures. Procedure B is an automated version of Procedure A, which uses a non-Woods metal compound. Procedure C uses a different heating material along with a glass reaction vessel. Methods A and B show consistent differences in results that are related to the type of the sample being tested. For formulated oils, values obtained by Procedure B may be converted to comparable Procedure A values by the formula

$$\text{Value by Procedure A} = 0.970 \times \text{Value by Procedure B} \quad (3.3)$$

For basestocks, the relationship is opposite:

$$\text{Value by Procedure A} = 1.039 \times \text{Value by Procedure B} \quad (3.4)$$

3.3.5 Foaming Characteristics

Air entrainment and foaming are important lubricant performance concerns for several reasons:

- Air-lubricant mixtures disrupt the oil film between operating surfaces;
- They affect the compressibility of the fluid, hence the operation in hydraulic systems;
- They can increase lubricant losses in open systems; and
- They may increase the oxidation rate of the oil.

The distinction between entrained air and foam can be a subtle one, with the former referring to stable air-in-oil dispersions whereas the latter is associated with the bubble-rich layer that forms on top of the liquid phase. There are three test methods for assessing resistance to foaming or air entrainment. Two of these are bench tests and the third is an engine test.

ASTM D892 [54] measures foaming characteristics at 24°C (Sequence I), at 93.5°C (Sequence II), and at 24°C after testing at the 93.5°C temperature (Sequence III). ASTM D6082 [55] measures foaming characteristics only at 150°C because manufacturers have raised concerns about equipment operation at higher temperatures. In both tests a graduated cylinder holding the sample is immersed in a constant-temperature bath and then aerated with dry air at a controlled flow rate for a set amount of time. Both tests define a specific diffuser for the aeration step because porosity affects the bubble size. Once the aeration is complete, the height of the foam is measured at discrete time intervals. ASTM D892 differentiates between foam tendency (i.e., the height of the foam layer when the air supply is disconnected) and foam stability (the height of the foam layer after the sample has settled for 10 min). Foaming is influenced by interfacial tension properties and lubricant viscosity. In automotive fluids, this is typically controlled by the presence of a microdispersion of silicone polymers. Oils that give acceptable foam performance at the time of manufacture may possibly show changes on storage because of sequestering of the antifoam agent by polar dispersant additives. These same oils may again show good (low) foaming characteristics when operated for a short period of time in an engine, transmission, or gear box because the agitation redisperses the antifoam. To allow for this type of behavior, ASTM D892 includes an Option A, in which the oil is pretreated in a high-speed blender before being evaluated for foaming.

ASTM D6894 [56] was designed to evaluate used engine oil's resistance to aeration and is sometimes referred to as the Engine Oil Aeration Test (EOAT). The test is conducted using a specified 7.3-L, direct-injection, turbocharged, V-8 diesel engine on a dynamometer test stand. This test method was developed as a replacement for ASTM D892 for lubricants used in diesel engines after it was determined that this bench test did not correlate with oil aeration in actual service.

In this test the aerated oil samples are taken after 1, 5, and 20 h of defined engine operation and the percentage

of oil aeration is calculated from the initial volume and the final volume after settling for 30 min. The oil in this engine, in addition to lubricating the engine parts, also feeds a high-pressure oil system off of the main gallery. The high-pressure system increases oil pressure up to 20.7 MPa (3000 psi) in a plunger pump that in turn is used to operate fuel injectors. With the use of intensifiers, the fuel injection pressure increases up to 145 MPa (21,000 psi) independent of engine speed. This system can circulate all of the oil in the sump in approximately 8 s, and as a consequence, aeration is likely to be encountered with some engine oils. Data indicate that 8 % oil aeration was the limit beyond which engine operation and performance would be impaired in actual service.

3.3.6 Element Content

The element content of lubricants and their components is an essential part of monitoring fluid quality. For fresh lubricants, the primary elements of interest are Ba, Ca, Mg, P, and Zn. Some additives and formulations also contain B, Na, K, and Mo. Some analytic methods also have the ability to accurately measure B, P, and S. The measurement accuracy for S and P is lower than that obtained for other elements. The source of the alkali earths, Ba, Ca, and Mg is usually from detergents used in the formulations. Na and K may appear as contaminants in the Ca, Ba, and Mg source or be present as a separate detergent component (Na). Trace levels of these alkali earths can be used to indicate the source of detergents in the formulation or as a formulation marker.

The element content of used lubricants is invaluable in understanding the suitability of a lubricant formulation for its intended purpose. When measuring used lubricants, changes in the concentrations of elements such as Fe, Sn, Pb, Cu, and other wear metals are important in understanding lubricant life. The analysis of used lubricants creates some additional hurdles in obtaining accurate and repeatable results.

Element content can be determined by atomic absorption (ASTM D4628), X-ray fluorescence (ASTM D4927), or inductively coupled plasma atomic spectroscopy (ASTM D4951 and D5185) [57–60]. ASTM D4628, D4927, and D4951 are primarily for fresh lubricants, although good results can be obtained on used lubricants with ASTM D4628. The main limitation of ASTM D4628 is that each element must be tested for individually whereas ASTM D4951 and D5185 measure multiple elements per test.

The following summarizes the range, interferences, and potential limitations of the four methods.

The ASTM D4628 method is applicable for the determination of mass percent Ba from 0.005 to 1.0 %, Ca and Mg from 0.002 to 0.3 %, and Zn from 0.002 to 0.2 % in lubricating oils. Higher concentrations can be determined by increasing the sample dilution. If these four metals are measured at concentrations of 10 ppm or less, then it should be by prior agreement between the parties involved because of potentially conflicting results. When samples containing VIIs are measured, the observed results may be low unless the VII is included in the calibration samples.

ASTM D4927 has two test procedures that cover the determination of Ba, Ca, P, S, and Zn in unused lubricating oils at specific element concentration ranges. The range can be extended to higher concentrations by dilution of sample

specimens. The metal content of additives can also be determined after dilution. Two different methods are presented in these test methods. Test Procedure A (Internal Standard Procedure) uses an internal standard to compensate for interelement effects of X-ray excitation and fluorescence. Test Procedure B (Mathematical Correction Procedure) mathematically corrects for potential interference from other elements present in the sample.

The observed fluorescence of any one additive metal is affected by the presence of other elements in the sample. In some cases another metal can absorb the fluorescence, thus artificially reducing emission, whereas in other cases it can attenuate the measured intensity. The effect is that the metal concentration will be either understated or overstated, respectively. These effects are significant at concentrations varying from 0.03 mass % because of the heavier elements to 1 mass % for the lighter elements. The measured intensity for a given element can be mathematically corrected for when the absorption of the emitted radiation by the other elements present in the sample specimen is accounted for. Internal standards can also be used to compensate for X-ray interelement effects. If an element is present at significant concentrations and an interelement correction for that element is not used, the results can be low because of absorption or high because of enhancement.

ASTM D4951 covers the quantitative determination of Ba, B, Ca, Cu, Mg, Mo, P, S, and Zn in unused lubricating oils and additive packages. The sample dilutions must be held within a 1- to 5-mass % range of sample in the solvent to obtain the precision stated in the standard. The precision tables in the standard define the concentration ranges covered in the interlaboratory study, but concentrations that are outside of the ranges can be determined by this test method. Low concentration limits are dependent on the sensitivity of the inductively coupled plasma instrument and the dilution factor used. High concentration limits are determined by the product of the maximal concentration defined by the linear calibration curve and the sample dilution factor. S can be determined if the instrument is capable of operating at a wavelength of 180 nm.

ASTM D4951 can quantitatively measure more elements than ASTM D4628 and D4927 and thus provides more elemental composition data per test. ASTM D4951 also provides more accurate results than those obtained with ASTM D5185, which is intended for used lubricating oils and base oils.

There are no known spectral interferences between elements normally covered by the ASTM D4951 test method when the spectral lines listed are used. If a sample contains other elements that cause interference, then other spectral lines can be chosen to avoid the problem.

ASTM D5185 covers the determination of additive elements, wear metals, and contaminants in used lubricating oils by inductively coupled plasma atomic emission spectrometry (ICP-AES). This method has the advantage of measuring 22 elements that are found in used lubricating oils and are listed in the method. When spectral wavelengths below 190 nm are used, a vacuum or inert-gas optical path must be used. Also, the spectral limitations of some instruments can prevent the determination of Na and K.

ASTM D5185 does not determine element concentration when the elements are part of insoluble particulates.

Additionally, low values are seen when the sample mist entering the burner is too coarse. When element concentration is such that it saturates the detector or exceeds the calibration range, then further dilution can be made without a loss in precision.

Spectral interferences can usually be avoided by judicious choice of analytical wavelengths. When spectral interferences cannot be avoided, the necessary corrections should be made using the computer software supplied by the instrument manufacturer or the empirical instructions included in the method. Details of the empirical method are given in ASTM C1109 [61] and by Boumans [62]. This empirical correction method cannot be used with scanning spectrometer systems when the analytical and interfering lines cannot be precisely and reproducibly located. With any instrument, the analyst must always be alert to the possible presence of unexpected elements producing interfering spectral lines.

3.3.7 Sulfated Ash

Sulfated ash is used to determine the total metal content of a lubricant, the source of which is the additives used in compounding the formulation. Ash limitations are important in some lubricant applications in which this material may cause preignition or emission system plugging problems. Ash-forming metals are primarily associated with the detergents added to neutralize combustion byproducts (usually Ca or Mg) but may also include Ba, Zn, K, Na, and Sn. Mg sometimes does not react in this test the same way the other alkali earths or alkali metals do; therefore, if the Mg content in the sample is significant, then the data need to be interpreted with caution.

Sulfated ash by ASTM D874 [63] is obtained by the following procedure. A sample is ignited and burned until only ash remains. The ash residue is treated with sulfuric acid and then heated to 775°C until the carbon residue is converted to CO₂. The sulfuric acid treatment and subsequent heating to 775°C is repeated until the sample residue is a constant weight.

3.3.8 Density

Density is a fundamental physical property that is used in conjunction with other properties to characterize a product. For petroleum products, it is typically used in conjunction with volume or mass to convert from one measurement to another. It is also used to convert between kinematic viscosity and dynamic viscosity. An alternative way of expressing density is as a ratio to water at a specific temperature, and this is referred to as specific gravity. When quoting specific gravity, the temperature of the measurement and the reference temperature of water must be included.

Density is typically determined by measuring the mass of a precise volume of the product. Because density changes with temperature, the temperature must be specified and closely controlled during measurement. The manual methods are ASTM D1217, D1480, and D1481 [64,66,67]. Each method has some sample physical property limitations that need to be observed. When a precise measurement is not needed, a hydrometer can be used to determine specific gravity—ASTM D1298 [65]. ASTM D4052 [68] is an automatic method that is quite often used in today's laboratories because it is more convenient and the precision is equivalent to that obtained by manual

methods. The automatic method has a viscosity limitation that can be partially resolved by preheating viscous samples. Preheating is also used with manual methods ASTM D1480 and D1481.

ASTM D1217 is normally used for the measurement of the density of pure hydrocarbons or petroleum distillates boiling between 90 and 110°C, which can be handled in a normal fashion as a liquid at the specified test temperatures of 20 and 25°C. This test method was originally developed for the determination of the density of the ASTM Knock Test Reference Fuels *n*-heptane and *isooctane* with an accuracy of 0.00003 g/mL. Although this test method is not normally used for lubricants, it is useful whenever accurate densities of pure hydrocarbons or petroleum fractions with boiling points between 90 and 110°C are required.

ASTM D1480 describes two procedures using a Bingham pycnometer for determining the density of materials that are fluids at the desired test temperature. The procedures are restricted to liquids with vapor pressures below 600 mmHg (80 kPa) and viscosities below 40,000 cSt (mm²/s) at the test temperature. Although this method states precision for densities determined at any temperature between 20 and 100°C, it can be used at higher temperatures.

ASTM D1481 describes a procedure using a Lipkin bicapillary pycnometer for determining the density of fluids that have viscosity greater than 15 cSt at 20°C (mm²/s). It is not appropriate when the sample has a vapor pressure of 100 mmHg (13 kPa) or above.

ASTM D4052, the determination of density or relative density by a digital density meter, is suitable for petroleum distillates and viscous oils that can be handled in a normal fashion as liquids at test temperatures between 15 and 35°C. Some instruments conforming to this procedure have the ability to measure densities at temperatures up to 90°C. A small volume of sample is introduced into an oscillating sample tube and the change in oscillating frequency caused by the change in the tube mass is used with calibration data to determine sample density. The sample must be a liquid with vapor pressure below 600 mmHg (80 kPa) and viscosity below approximately 15,000 cSt (mm²/s) at the temperature of the test. This test method should not be applied to samples that are so dark as to obscure the presence of sample air bubbles that will affect the results. Testing of reference materials with certified density values established by pycnometry has confirmed the presence of bias with this method and users should be aware that this can be as much as 0.0006 g/mL.

3.3.9 Flash Point

Flash point is a measure of a test specimen's tendency to form a flammable mixture with air under controlled laboratory conditions. It is only one of several properties that should be considered in assessing the overall flammability hazard of a material. The flash point of a material is used to classify its shipping classification as flammable or combustible. The property is also used in safety regulations that define how to handle the material. Flash point can be used for the detection of contamination of relatively nonvolatile or nonflammable materials with volatile or flammable substances.

Two types of flash point tests are used for lubricants. Flash point by the Cleveland Open Cup (COC) is covered

in ASTM D92 [69]. Pensky Martens Closed Cup (PMCC) is covered in ASTM D93 [70].

Flash point is the temperature at which the vapors of the material will momentarily ignite when an ignition source is present. The COC is meant to simulate an open container whereas the PMCC is intended to simulate a closed container. A COC (ASTM D92) flash point will typically be higher than the PMCC (ASTM D93) flash point.

The COC and PMCC methods are manual methods for determining flash point. There are numerous instruments available in the marketplace that automate the testing of flash point. In both methods, the sample specimen is contained in a cup of specific dimensions and heated/stirred at defined rates. For ASTM D92, the cup has an open top. For ASTM D93, the cup is covered, except when testing for flash, at which time a small door opens for the period of the test. An ignition source is directed into the test cup at regular intervals (stirring interrupted) until a flash is detected.

The COC method is suitable for flash points above 79°C (175°F) and below 400°C (752°F). The COC method includes a procedure for determining a material's fire point.

The PMCC is suitable for flash points between 40 and 360°C. ASTM D93 has two procedures. Procedure A is applicable to fresh or new lubricants whereas Procedure B is commonly utilized with used lubricants. The two procedures differ in heating and sample stirring rates.

3.3.10 Color

The color of petroleum products is used mainly for manufacturing control purposes and can be an important quality characteristic because it is so readily observed by the user. Because most automotive lubricants are additized, color is not a good indicator of the degree of refinement of the material. However, when the color range of a particular product is known, a variation outside of the established range may indicate possible contamination with another product.

ASTM D1500 [71] covers the visual determination of color for petroleum products. This is accomplished by comparing the material's color against a set of colored glass standards when placed in a specified glass container using a defined light source. The closest match in color intensity is reported as the ASTM color with a number ranging between 0.5 and 8 in half-unit steps (very pale yellow to dark brown). If an exact match is not possible, the next darker color standard is referenced with an "L" preceding the number (e.g., "L7.5 ASTM color"). For very dark materials, the method allows for dilution (15 % by volume) of kerosine or a similar solvent meeting the color criteria. In this case, the color is reported as, for example, "L7.5 Dil ASTM color."

IP Method 17 [72] includes a procedure for measuring the color of undyed, refined petroleum products, but it also has a procedure for measuring petroleum products for tint and depth of color in Lovibond units using a series of red, yellow, and blue glasses.

3.3.11 Corrosiveness

Concerns over corrosive tendencies for oils with certain metals have led to the development of ASTM tests including ASTM D130, D5968, and D6594 [73–75]. ASTM D130 is applicable to automotive oils and other petroleum products and evaluates only copper corrosivity using carefully

prepared coupons immersed in the test fluid. After immersion at a prescribed temperature and time, the coupon is rated for appearance against the ASTM Copper Strip Corrosion Standard using a number/letter designation. Thus, a rating of "1a" would be close to a fresh copper strip appearance whereas a "4c" rating would indicate heavy corrosion with a glossy black appearance. ASTM D130 requirements are often cited in equipment manufacturer specifications, usually on the basis of a 3 h/100°C test time/temperature combination.

ASTM D5968 was developed to evaluate the corrosiveness of diesel engine oils and is based on a corrosion/oxidation test for gas turbine lubricants (FTM 791, Method 5308). It has also been referred to as the Cummins Bearing Corrosion Test and the Corrosion Bench Test (CBT). ASTM D5968 uses four different metal coupons (copper, lead, tin, and phosphor bronze) tied together with Nichrome wire and immersed in the fresh oil test fluid. Clean, dry air is bubbled into the oil at a controlled rate and the entire apparatus is immersed in a heating bath to maintain the test oil temperature at 121°C for 168 h. At the end of the test, the weight loss of each coupon (mg/cm² of surface); the increase in used oil copper, lead, and tin; and the ASTM D130 rating of the copper strip are reported. This test is a requirement of the API CF-4 (obsolete) and CG-4 heavy-duty engine oil classifications.

ASTM D6594 is somewhat similar to ASTM D5968 in that it uses the same four metal coupons, air bubbling, and test length. However, the coupons are separately suspended in the test fluid with stainless steel hangers, the test temperature is higher (135°C), and the end-of-test evaluation includes only a copper strip rating and an increase in used oil copper and lead concentration. ASTM D6594 was developed to evaluate corrosion in more modern, hotter-running diesel engines and is a requirement of API CH-4, CI-4, and CJ-4 classifications.

3.3.12 Water Tolerance/Filterability

ASTM D6794 and D6795 [76,77] methods measure the tendency of engine oil to form a precipitate when combined with water. It is normal for fuel combustion products to be absorbed into the lubricant and be retained. Formation of a precipitate can lead to oil filter plugging in service.

ASTM D6795 is based on the GM-9099P procedure developed by General Motors to simulate problems when a new engine was run for a short period of time followed by long-term storage. In this test, the oil is combined with 0.6 % water and an excess of dry ice (solid CO₂) and then blended at high speed for 30 s. After this treatment, the mixture is heated in an oven at 70°C for 30 min and then stored at room temperature for 48 h. The flow rate of the treated oil through a 25-μm porosity filter is determined using 69-kPa air pressure and compared to the flow rate of untreated oil. GM-9099P/D6795 has been included as a requirement in API "S" classifications API SH, ILSAC GF-1. A flow rate reduction of more than 50 % in the flow rate versus new oil is considered unacceptable.

ASTM D6794 is similar to ASTM D6795, but it does not use dry ice in the oil-conditioning phase and it increases the 70°C heating stage to 6 h. In addition, filterability is assessed separately for water contents of 0.6, 1, 2, and 3 %. This test was developed to address problems encountered with some oils that were prone to gelation in the presence

of water but that passed the GM-9099P/ASTM D6795 test. It was introduced as a "Report" requirement with API SJ/ILSAC GF-2 and a 50 % maximal flow rate reduction was specified for subsequent API "S" and ILSAC GF specifications.

3.3.13 Elastomer Compatibility

Effective sealing of automotive equipment requires compatibility of the elastomeric materials and the lubricants that come in contact with those materials. ASTM methods D7216 and D5662 [78,79] cover the elastomeric compatibility testing of engine oils and automotive GOs, respectively; these are static, bench seal tests that evaluate changes in physical properties of elastomeric coupons after they have been immersed in the lubricant for a specific time duration at specified temperatures. The changes in seal parameters include volume, hardness, and tensile properties (ultimate elongation, tensile strength, or both).

ASTM D7216 was developed to evaluate heavy-duty engine seal materials and references five seal types (fluoroelastomer, nitrile, polyacrylate, silicone, and Vamac), although it can be used to evaluate other seal/temperature/immersion time combinations. Results from this test are used to confirm acceptability of candidate fluids against API CI-4 and CJ-4 specifications. Because different elastomeric batches can exhibit differences in compatibility, ASTM D7216 requires a reference oil (TMC 1006-1) to be run at the same time as the candidate fluid(s). Reference oil test results are submitted to the ASTM Test Monitoring Center (TMC), which is responsible for determining if the results are operationally valid and by association the candidate results.

ASTM D5662 for GOs is similar to ASTM D7216, using specific seal materials of relevance (nitrile, polyacrylate, and fluoroelastomer) along with defined temperatures and test length. Again, a reference oil is run in parallel with the candidate(s) and data are submitted to TMC for validity confirmation. ASTM D5662 is used to evaluate candidate conformance for elastomeric compatibility as defined in GO specifications ASTM D5760 and SAE J2360.

Elastomeric compatibility is a common requirement in other industry lubricant specifications such as the ACEA engine oil classifications (which are based on the CEC-L-39-T-96 test method) and many individual OEM specifications that may use OEM specific seals or those identified by the SAE Committee on Automotive Rubber Specifications in SAE J2643.

3.3.14 Homogeneity and Miscibility

The standard test method for determining the homogeneity and miscibility of a fluid is ASTM D6922 [80]. On the basis of the Federal Test Method standard FED-STD-791/3470.1, it is used to determine whether a lubricant will remain homogeneous over a wide range of temperature conditioning and whether it is fully miscible with six reference oils (available from the ASTM TMC) over these same conditions. A separation of fluid components could affect the lubricant's performance in operating equipment. In addition, incidental mixing of different lubricants can occur during oil changes or top-ups, and it is important to ensure that the fluids remain miscible and homogeneous.

In ASTM D6922, the candidate oil along with 50/50 blends of the candidate with each reference oil are first

warmed to 46°C and inspected for separation. The oils are then subjected to an ASTM D97 type of cooling profile until the no-flow temperatures of all seven samples are reached (ASTM D6922 refers to this as the pour-point temperature) and are checked for separation after warming above their cloud points (disappearance of haze). Each oil is then heated until it reaches 232°C, cooled back to room temperature, and then stored in a cold box at the pour-point temperature of the undiluted candidate oil for 18–24 h. After warming each sample above its cloud point, a final check for separation is made by the operator.

3.4 HIGH-TEMPERATURE DEPOSITS

ASTM D6335 [81] is based on the Thermo-Oxidation Engine Oil Simulation Test, or TEOST-33C [82], and is used to assess high-temperature deposit tendencies of oils in turbocharged gasoline engines. The oil in these engines is exposed to very high contact temperatures in the turbocharger bearings, particularly after a hot engine shutdown; oil deposit buildup can lead to operational problems or even turbocharger failure. TEOST-33C was added as a requirement to Chrysler factory and service fill oil specifications in the 1990s and included in API SJ and GF-2 classifications. In ASTM D6335, a solution of the test oil and ferric naphthenate is maintained at 100°C and kept in contact with nitrous oxide and moist air. The solution is pumped at a controlled rate over a resistively heated depositor rod that undergoes 12 cyclic temperature events in which the rod temperature is ramped from 200 to 480°C. At the end of the approximately 2-h test, deposits on the rod are determined from rod weight gain. Oil deposits are also collected by filtration and their weight is measured; the applicable range of the test is reported to be 2–180 mg of total deposits. At the time of this writing, ASTM D6335 performance had been requested by ILSAC for inclusion in the GF-5 specification.

ASTM D7097 [83] is based on another Thermo-Oxidation Engine Oil Simulation Test, the TEOST MHT-4, which was developed to assess engine oil protection against piston ring zone deposits in modern gasoline engines. (The "MHT" designation refers to the Moderately High Temperature test to differentiate it from the turbo deposit test, TEOST-33C.) In this procedure, a very small amount of an organometallic catalyst containing Fe, Sn, and Pb is added to a small sample of test oil. This mixture is then circulated for 24 h over a special wire-wound depositor rod that has been heated to 285°C. During this time, air is also directed over the oil flowing down the depositor rod to enhance oxidation. At the end of the test, rod and oil deposits are determined by weight. The applicable range of the test is reported to be 1–150 mg or more. Engine oil requirements in this test were first introduced with API SL/GF-3, continued with API SM/GF-4, and they are expected to be included into the ILSAC GF-5 specification.

REFERENCES

Note: All ASTM publications are available from ASTM International, West Conshohocken, PA. Most but not all of the current version of the test methods are in Section 5 of the *Annual Book of Standards for Petroleum Products, Lubricants, and Fossil Fuels* (in five volumes).

- [1] ASTM, 2003, *Significance of Testing for Petroleum Products (7th Edition): (MNL 1)*, S. Rand, Ed., ASTM International, West Conshohocken, PA.
- [2] SAE J300, Specification for Engine Oil Viscosity Classification.

- [3] SAE J306, Surface Vehicle Standard for Automotive Gear Lubricant Viscosity Classification.
- [4] ASTM, 2003, *Fuels and Lubricants Handbook: Technology, Properties, Performance and Testing*, G.E. Totten, S.R. Westbrook, and R.J. Shah, Eds., ASTM International, West Conshohocken, PA.
- [5] Kishore Nadkarni, R.A., 2007, *Guide to ASTM Test Methods for the Analysis of Petroleum Products and Lubricants (2nd Edition): MNL 44-2nd*, ASTM International, West Conshohocken, PA.
- [6] ASTM D4485-07, Standard Specification for Performance of Engine Oil.
- [7] Wilkinson, W.L., 1960, *Non-Newtonian Fluids, Fluid Mechanics, Mixing and Heat Transfer*, Pergamon Press, London.
- [8] Schowalter, W. R., 1978, *Mechanics of Non-Newtonian Fluids*, Pergamon Press, London.
- [9] ASTM D445, Standard Test Method for Kinematic Viscosity of Transparent and Opaque Liquids (and Calculation of Dynamic Viscosity).
- [10] ASTM D446, Standard Specifications and Operating Instructions for Glass Capillary Kinematic Viscometers.
- [11] ASTM D5293, Standard Test Method for Apparent Viscosity of Engine Oils Between -5 and -35°C Using the Cold-Cranking Simulator.
- [12] CRC, 1968, *Evaluation of Laboratory Viscometers for Predicting Cranking Characteristics of Engine Oils at -0°F and -20°F* , CRC Report No. 409, Coordinating Research Council, Atlanta, GA.
- [13] Stewart, R.M., 1969, "Engine Pumpability and Crankability Tests on Commercial "W" Grade Engine Oils Compared to Bench Test Results," ASTM STP 621 ASTM 1967, 1968. 1969 *Annual Book of ASTM Standards, Part 17* (also published as SAE Paper 780369 in SAE Publication SP-429).
- [14] Shaub, H., Ed., 2000, *Oil Flow Studies at Low Temperature in Modern Engines*, ASTM STP 1388, ASTM International, West Conshohocken, PA.
- [15] ASTM, 1975, *Low Temperature Pumpability Characteristics of Engine Oils in Full Scale Engines*, ASTM DS-57, ASTM International, West Conshohocken, PA.
- [16] ASTM D4684, Standard Test Method for Determination of Yield Stress and Apparent Viscosity of Engine Oils at Low Temperature.
- [17] ASTM D3829, Standard Test Method for Predicting the Borderline Pumping Temperature of Engine Oil.
- [18] Smith, M.F., Jr., 1983, *Better Prediction of Engine Oil Pumpability through a More Effective MRV Cooling Cycle*, SAE Paper No. 831714, SAE, Warrendale, PA.
- [19] Henderson, K.O., Manning, R.E., May, C.J., and Rhodes, R.B., 1985, *New Mini-Rotary Viscometer Temperature Profiles That Predict Engine Oil Pumpability*, SAE Paper No. 850443, SAE, Warrendale, PA.
- [20] Rhodes, R.B., Ed., 1992, *Low Temperature Rheology Measurement and Relevance to Engine Operation*, ASTM STP 1143, ASTM International, West Conshohocken, PA.
- [21] ASTM, 1999, *Cold Starting and Pumpability Studies in Modern Engines*, ASTM Research Report RR: D02-1442, ASTM International, West Conshohocken, PA.
- [22] Shaub, H., Ed., 2000, *Oil Flow Studies at Low Temperature in Modern Engines*, ASTM STP 1388, ASTM International, West Conshohocken, PA.
- [23] ASTM D6896, Standard Test Method for Determination of Yield Stress and Viscosity of Used Engine Oils at Low Temperature.
- [24] Spearot, J.A., Ed., 1989, *High-Temperature, High-Shear (HTHS) Oil Viscosity Measurement and Relationship to Engine Operation*, ASTM STP 1068, ASTM International, West Conshohocken, PA.
- [25] ASTM D4683, Standard Test Method for Measuring Viscosity at High Shear Rate and High Temperature by Tapered Bearing Simulator.
- [26] ASTM D4741, Standard Test Method for Measuring Viscosity at High Temperature and High Shear Rate by Tapered-Plug Viscometer.
- [27] ASTM D5481, Standard Test Method for Measuring Apparent Viscosity at High-Temperature and High-Shear Rate by Multi-cell Capillary Viscometer.
- [28] ASTM D6616, Standard Test Method for Measuring Viscosity at High Shear Rate by Tapered Bearing Simulator at 100°C .
- [29] ASTM D5133, Standard Test Method for Low Temperature, Low Shear Rate, Viscosity/Temperature Dependence of Lubricating Oils Using a Temperature Scanning Technique.
- [30] ASTM D2983, Standard Test Method for Low-Temperature Viscosity of Lubricants Measured by Brookfield Viscometer.
- [31] ASTM D6821, Standard Test Method for Low Temperature Viscosity of Drive Line Lubricants in a Constant Shear Stress Viscometer.
- [32] ASTM D5275, Test Method for Fuel Injector Shear Stability Test (FISST) for Polymer Containing Fluids.
- [33] ASTM D6278, Standard Test Method for Shear Stability of Polymer Containing Fluids Using a European Diesel Injector Apparatus.
- [34] ASTM D7109, Standard Test Method for Shear Stability of Polymer Containing Fluids Using a European Diesel Injector Apparatus at 30 and 90 Cycles.
- [35] ASTM 6709, Standard Test Method for Evaluation of Automotive Engine Oils in the Sequence VIII Spark-Ignition Engine (CLR Oil Test Engine),
- [36] ASTM D3945, Test Method for Shear Stability of Polymer Containing Fluids Using a Diesel Injector Nozzle.
- [37] CEC L-14-A-93, Evaluation of the Mechanical Shear Stability of Lubricating Oils Containing Polymers, Co-ordinating European Council (CEC).
- [38] ASTM D2603, Test Method for Sonic Shear Stability of Polymer Containing Oils.
- [39] CEC L-45-99, Viscosity Shear Stability of Transmission Lubricants (Taper Roller Bearing Rig), Co-ordinating European Council (CEC).
- [40] ASTM D97, Standard Test Method for Pour Point of Petroleum Products.
- [41] ASTM D5949, Standard Test Method for Pour Point of Petroleum Products (Automatic Pressure Pulsing Method).
- [42] ASTM D5950, Standard Test Method for Pour Point of Petroleum Products (Automatic Tilt Method).
- [43] ASTM D5985, Standard Test Method for Pour Point of Petroleum Products (Rotational Method).
- [44] ASTM D6749-02(2007), Standard Test Method for Pour Point of Petroleum Products (Automatic Air Pressure Method).
- [45] ASTM D6892, Standard Test Method for Pour Point of Petroleum Products (Robotic Tilt Method).
- [46] ASTM D2500, Standard Test Method for Cloud Point of Petroleum Products.
- [47] ASTM D5771-05, Standard Test Method for Cloud Point of Petroleum Products (Optical Detection Stepped Cooling Method).
- [48] ASTM D5772-05, Standard Test Method for Cloud Point of Petroleum Products (Linear Cooling Rate Method).
- [49] ASTM D5773-05, Standard Test Method for Cloud Point of Petroleum Products (Constant Cooling Rate Method).
- [50] ASTM D2887, Standard Test Method for Boiling Range Distribution of Petroleum Fractions by Gas Chromatography.
- [51] ASTM D6417, Standard Test Method for Estimation of Engine Oil Volatility by Capillary Gas Chromatography.
- [52] ASTM D5480, Test Method for Motor Oil Volatility by Gas Chromatography.
- [53] ASTM D5800, Standard Test Method for Evaporation Loss of Lubricating Oils by the Noack Method.
- [54] ASTM D892, Standard Test Method for Foaming Characteristics of Lubricating Oils.
- [55] ASTM D6082, Standard Test Method for High Temperature Foaming Characteristics of Lubricating Oils.
- [56] ASTM D6894, Standard Test Method for Evaluation of Aeration Resistance of Engine Oils in Direct Injected Turbo-charged Automotive Diesel Engine.
- [57] ASTM D4628, Test Method for Analysis of Barium, Calcium, Magnesium, and Zinc in Unused Lubricating Oils by Atomic Absorption Spectrometry.
- [58] ASTM D4927, Test Methods for Elemental Analysis of Lubricant and Additive Components—Barium, Calcium, Phosphorus, Sulfur, and Zinc by Wavelength-Dispersive X-Ray Fluorescence Spectroscopy.

- [59] ASTM D4951, Standard Test Method for Determination of Additive Elements in Lubricating Oils by Inductively Coupled Plasma Atomic Emission Spectrometry.
- [60] ASTM D5185, Standard Test Method for Determination of Additive Elements, Wear Metals, and Contaminants in Used Lubricating Oils and Determination of Selected Elements in Base Oils by Inductively Coupled Plasma Atomic Emission Spectrometry (ICP-AES).
- [61] ASTM C1109, Test Method for Analysis of Aqueous Leachates from Nuclear Waste Materials Using Inductively Coupled Plasma-Atomic Emission Spectrometry.
- [62] Boumans, P.W. J.M., 1976, "Corrections for Spectral Interferences in Optical Emission Spectrometry with Special Reference to the RF Inductively Coupled Plasma," *Spectrochim. Acta*, Vol. 31B, pp. 147–152.
- [63] ASTM D874, Standard Test Method for Sulfated Ash from Lubricating Oils and Additives.
- [64] ASTM D1217, Standard Test Method for Density and Relative Density (Specific Gravity) of Liquids by Bingham Pycnometer.
- [65] ASTM D1298, Standard Test Method for Density, Relative Density (Specific Gravity), or API Gravity of Crude Petroleum and Liquid Petroleum Products by Hydrometer Method.
- [66] ASTM D1480, Standard Test Method for Density and Relative Density (Specific Gravity) of Viscous Materials by Bingham Pycnometer.
- [67] ASTM D1481, Standard Test Method for Density and Relative Density (Specific Gravity) of Viscous Materials by Lipkin Bicapillary Pycnometer.
- [68] ASTM D4052, Standard Test Method for Density and Relative Density of Liquids by Digital Density Meter.
- [69] ASTM D92, Standard Test Method for Flash and Fire Points by Cleveland Open Cup Tester.
- [70] ASTM D93, Standard Test Methods for Flash Point by Pensky-Martens Closed Cup Tester.
- [71] ASTM D1500, Standard Test Method for ASTM Color of Petroleum Products (ASTM Color Scale).
- [72] Institute of Petroleum Method 17, Determination of Colour, Lovibond Tintometer Method
- [73] ASTM D130, Standard Test Method for Corrosiveness to Copper from Petroleum Products by Copper Strip Test.
- [74] ASTM D5968, Standard Test Method for Evaluation of Corrosiveness of Diesel Engine Oil at 121°C.
- [75] ASTM D6594, Standard Test Method for Evaluation of Corrosiveness of Diesel Engine Oil at 135°C.
- [76] ASTM D6794-02(2007), Standard Test Method for Measuring the Effect on Filterability of Engine Oils after Treatment with Various Amounts of Water and a Long (6-h) Heating Time .
- [77] ASTM D6795-02(2007), Standard Test Method for Measuring the Effect on Filterability of Engine Oils After Treatment with Water and Dry Ice and a Short (30-min) Heating Time.
- [78] ASTM D7216-05, Standard Test Method for Determining Automotive Engine Oil Compatibility with Typical Seal Elastomer.
- [79] ASTM D5662-06a, Standard Test Method for Determining Automotive Gear Oil Compatibility with Typical Oil Seal Elastomers.
- [80] ASTM D6922-03, Standard Test Method for Determination of Homogeneity and Miscibility in Automotive Engine Oils.
- [81] ASTM D6335, Standard Test Method for Determination of High Temperature Deposits by Thermo-Oxidation Engine Oil Simulation Test.
- [82] Florkowski, D.W., and Selby, T.W., 1993, *The Development of a Thermo-Oxidative Engine Oil Simulation Test (TEOST)*, SAE Paper No. 932837, SAE, Warrendale, PA.
- [83] ASTM D7097, Standard Test Method for Determination of Moderately High Temperature Piston Deposits by Thermo-Oxidation Engine Oil Simulation Test - TEOST MHT.

Controlling Lubricant Degradation through Performance Specification

Malcolm F. Fox¹

4.1 INTRODUCTION

When lubricants are used they deteriorate by evaporation, oxidation, and contamination. Today lubricants are formulated to resist these causes of deterioration in a planned manner for a stated period of operation, extent of work, distance of travel, or other measures of use. The performance specification for formulations has direct implications for operational service use—the ultimate commercial objective of manufacturing lubricants—to protect machinery from internal wear. Lubricants also reduce energy consumption through reduced friction.

Individual methods of analyzing the degraded conditions of lubricants are described exhaustively and at length by Toms [1], Fox [2], and within the reference books by Haycock and Hillier [3], Mang and Dresel [4], and others. Analytical methods for measuring lubricant degradation are a mature technology, well reviewed and described elsewhere and not requiring repetition here. Instead, there is now a need to show how these analytical test methods contribute to building a coherent framework of lubricant performance specifications that can be relied upon to protect an automotive engine in service from lubricant degradation. These specifications essentially measure the utility of lubricant formulations to resist degradation by an organized array of individual tests. In addition to laboratory tests on fresh lubricant, there are tests on used lubricant samples from various engine tests, the assessment of deposits on specific engine parts as well as wear measurements on defined components (Figure 4.1). The degradation of lubricants is controlled for service use by two approaches:

1. *Defined laboratory tests:* On fresh samples of the candidate lubricant and used samples of the candidate lubricant from defined engine tests.
2. *Defined engine tests:* Assessed using deposit ratings of the candidate lubricant on components and the measured wear of engine components when using the candidate lubricant.

Controlling lubricant degradation has therefore moved up a league from defining individual laboratory analytical tests, as described previously [1–4]. It is now a series of parallel frameworks of performance specifications built up from those individual laboratory tests on fresh and used samples from engine tests, together with an objective assessment of deposits on test engine components from lubricant degradation as well as protection against wear that is given by the lubricant to essential engine components. Experience shows that laboratory tests on fresh, unused candidates can only give, at best, a very partial assessment of a candidate

lubricant performance in the field. Only very recently has a laboratory test, the ROBO (Romaszewski oil bench oxidation) test [5], replaced part of an engine test—in this case a form of oxidation test—in a lubricant performance specification, as will be described later in the ILSAC GF-5/API-SN specification. Experience shows that candidate lubricant samples from prescribed engine tests must also be tested together with other measures of degradation such as deposits on defined components within the engine and wear measurements on other critical components.

The formulation of lubricants for automotive engines for their lubrication and protection was successfully demonstrated and achieved several decades ago. But since the 1964 U.S. model year, when the first pollution control device was mandated for petrol/gasoline vehicles in California, there have been three main drivers of change for automotive engines that have fundamentally affected the ability of lubricants to control their degradation in use:

1. *The continual development of engine technologies for increased power densities from smaller engines, smaller lubricant sump volumes, and increased thermodynamic efficiencies for increased fuel economy:* The lubricant is now seen as an essential design component. The increased aerodynamic design of vehicles reduces natural cooling effects so that higher-power, increased-efficiency engines run at higher temperatures, increasing the severity of thermal degradative conditions for the lubricant. Increased engine speeds mean higher degradative shear rates of the lubricant in bearings. The overall effect is that smaller volumes of lubricants must resist exposure to greater intensities of degradation for longer periods.
2. *Changes in fuel composition:* These include drastic reductions in S content, which had a lubricity function, as well as the more recent introduction of bio-based extenders into fuels such as vegetable-oil-based fuels into diesel and various simple alcohols into petrol/gasoline.
3. *Introduction of environmental control measures for emissions:* This includes in-cylinder control of combustion processes through air/fuel mixtures, ignition timing, and exhaust gas recirculation (EGR). It also includes postcombustion control such as three-way catalysts (TWCs) for petrol/gasoline engines; catalytic converters, diesel particulate filters (DPFs), and selective catalytic reduction (SCR) for diesel engines; and their associated effects on the engine lubricant.

The aim is to control lubricant degradation and thus maintain its function for as long as possible to prolong the

¹ School of Mechanical Engineering, University of Leeds, UK

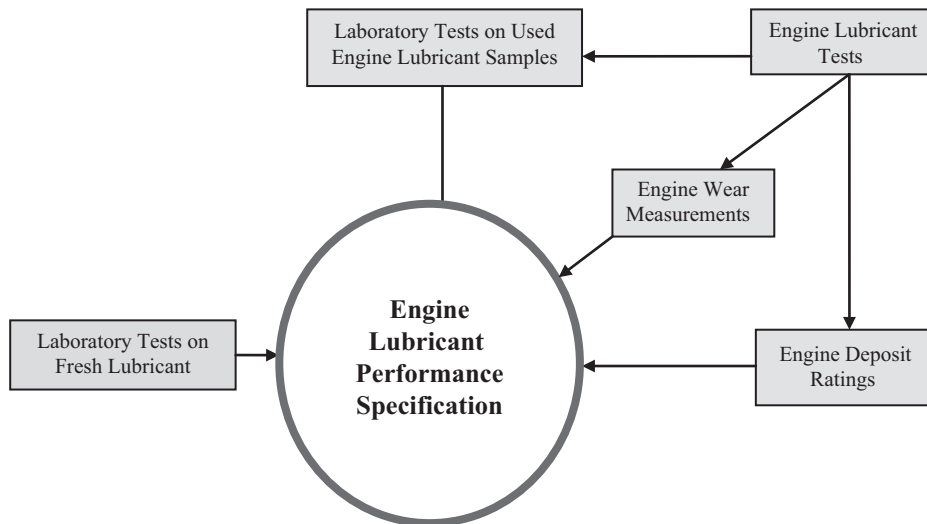


Figure 4.1—Laboratory and engine test contributions to controlling lubricant degradation through performance specification.

useful life of an automotive engine. To use the “bathtub curve” analogy—if lubricant degradation is controlled by formulation designed for the engine type, its operation, and its fuel, then the central section of the bathtub curve can be expanded before the final rapid wear and deterioration of the engine occurs (Figure 4.2). The length of that central section of the bathtub curve defines the operational life and reliability of the automotive engine. The organized and purposeful developments in controlling lubricant degradation have dramatically extended engine life. For example, a typical European 1950 sports saloon car engine of 2.4-L engine capacity required a lubricant change of 8 L every 2400 km because of degradation of the lubricant of that time. The sump needed removal and cleaning every 8000 km. The engine needed separate, different, monograde lubricants for summer and winter operation. Because of wear, the engine cylinder bores needed re-machining approximately every 50,000 km.

In 2011, an engine for an analogous new European car had a service interval lubricant change in the region of 20,000–30,000 km with the same lubricant used for winter and summer. Wear is much lower, and engine bore re-machining is essentially unknown. Many engines are

effectively “sealed for life”, lasting well over 150,000 km before being scrapped.

The extension of the ultimate service use life of vehicles through improvements in lubricant formulations obtained by lubricant performance specifications to reduce wear, emissions, and energy consumption has been a great achievement—indeed so successful as to be unremarkable. At the same time, as engine energy densities and maximal lubricant operating temperatures have increased, the volumes of lubricant used by vehicles have been reduced by 90 % and fuel consumption has been reduced overall by 50 % (Table 4.1). This achievement has been done by organized, concerted action over a period of 40 years jointly involving original equipment manufacturers (OEMs) of vehicles, fuel suppliers, and lubricant manufacturers. Within each of these areas, analytical test methods of assessing the degraded condition of lubricants have played a crucial role.

To give these analytical test procedures effective frameworks to control lubricant degradation, three substantial lubricant performance specification systems have been developed: the tripartite API system from North America; the European ACEA system; and the ILSAC system, which is

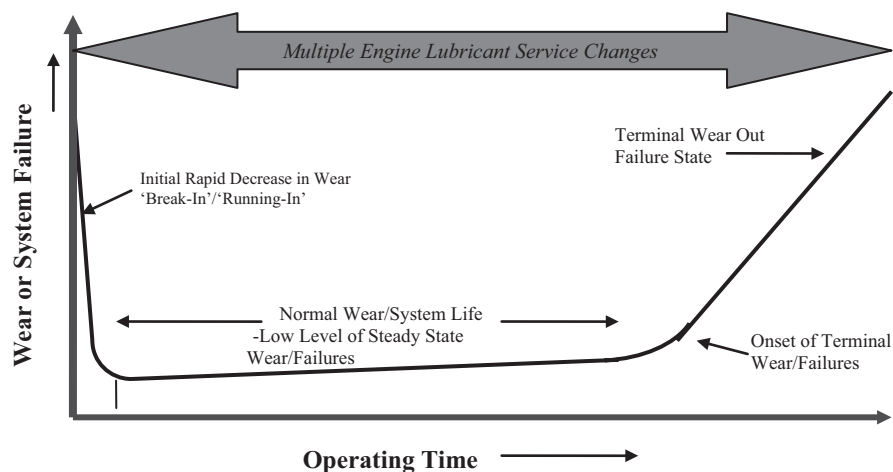


Figure 4.2—The bathtub curve related to engine wear and lubricant degradation.

TABLE 4.1—Lubricant Volumes, Operating Performance, and Engine Energy Density

Model Year	1991	2000	2010	1996	2010
Vehicle	GM Kadett	GM Astra	GM Astra	VW Golf	VW Golf
Engine type	C16NZ	X16XE	A16LET	A3 1.8	A6 1.4 TSI
Power, kW	55	77	132	66	118
Power density, kW/L	34	48	83	37	85
Max speed, km/h	150	180	221	178	220
Max lubricant temperature, °C	120	130	140	N/A	N/A
Lubricant change interval	5000 km or 6 months	15,000 km or 1 year	30,000 km or 1 year, max	15,000 km or 1 year	30,000 km or 1 year
Sump volume, L	3.5	3.5	4.5	3.8	3.6

Source: Table data compiled from Beercheck, R., 2011, "Evolution Pains." In *Proceedings of the Lubes 'N' Greases, Europe–Middle East Africa Conference*, p. 32, September 2011 and Hickl, T., 2011, "Funktions-Anforderungen an PKW-Motorenöle," *Proceedings of the UNITI Mineral Oil Technology Conference*.

now very close to the API system. Although they have tended to diverge in the past, they are now on a convergent course. Their format is very similar, and the overall lubricant performance specification is an assembly of laboratory tests and measurement of deposits and wear, as in Figure 4.3.

Each of the individual tests is specified to what are essentially international standards from ASTM, API, or SAE in North America or by CEC in Europe, as will be shown later. To consider the role of these standards in controlling the degradation of lubricants within performance bounds, it is useful to consider how they have developed over time because they were initially driven by the consequences of lubricant degradation; only more recently have they been

more proactive in anticipating the increased degradative demands on lubricants arising from changes in fuel composition, performance, and environmental emission controls.

4.2 THE FRAMEWORKS FOR CURRENT PERFORMANCE SPECIFICATIONS TO CONTROL LUBRICANT DEGRADATION

Since World War II, lubricant development has been driven by the automotive industries, initially for North America and Western Europe and now increasingly on a global level. The plain fact is that lubricant performance specifications set out to limit the extent of degradation in use, but their supporting tests have developed differently across separate continents.

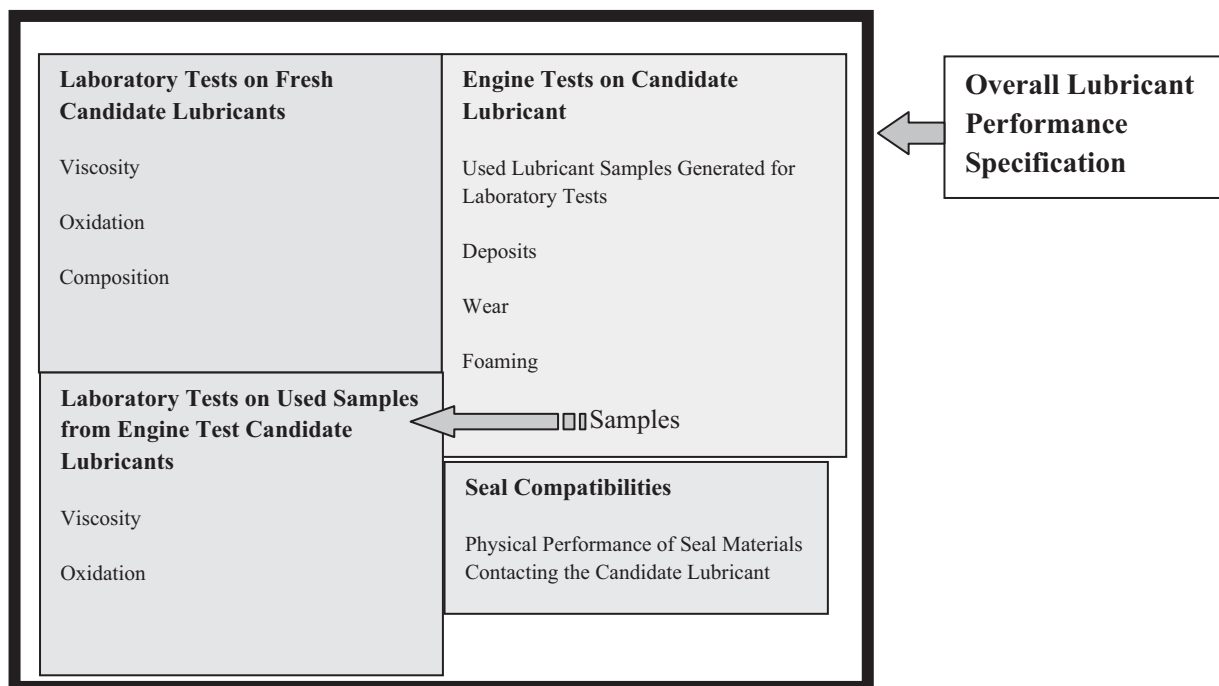


Figure 4.3—General format for lubricant performance specifications. Within each block the subheadings cover a range of individual tests.

Convergence toward a unified system is now occurring for the three major lubricant performance specification systems:

1. The API Tripartite system, which is based in North America;
2. The ILSAC system, which is “globalized” between North America and Japan, and originally a divergence from the API Tripartite system, but now very close to it; and
3. The ACEA system, which is based in Europe and is now converging slowly with the API Tripartite system.

Some individual lubricant degradation tests are shared between these specification systems. In addition, there are further individual OEM tests as required by Volkswagen (VW), Peugeot, and Daimler-Benz, as examples as well as a move toward individual OEM specifications such as the General Motors (GM) dexos™ specifications. Each system has its own philosophy and set of drivers to control lubricant degradation within a performance framework. The forms of the major lubricant performance specification systems have evolved from the interactions among the different “players” who have had varying influence over the years: lubricant suppliers, the additive industry, OEMs, and end users. However, OEMs have the final responsibility for their product’s performance warranties in an increasingly consumer-focused market. Other systems exist, but they are either for smaller markets or technically lag behind the three main systems. The genesis of the API Tripartite system is explained first because it was indeed the first specification system to evolve.

4.2.1 The North American API Tripartite System

The development of the API Tripartite has been described by Haycock and Hillier [3] and others recently [2]. Up to the mid-1930s there were no engine lubricant performance tests because lubricants were probably the least stressed component of overall engine systems. They were selected because they worked, however defined, and lubricant degradation was not significant. Then a new range of relatively high-powered Caterpillar engines caused lubricant degradation to produce heavy, adherent, carbon piston deposits that “stuck” piston rings and rapidly decreased engine efficiency: “clearly, engine design technology had moved significantly ahead of existing lubricant technology” [3].

Small amounts of a lubricant additive countered the deleterious “carbonization effect” on engine performance, but different lubricants gave different long-term field results leading to the first laboratory engine screening test, L-1 (1940), which was designed to rapidly screen lubricants for field use. This essentially became the U.S. Army MIL-2-104 specification in 1941. World War II accelerated lubricant development, driven by military engines and equipment operating at ever-higher power levels. Subsequent performance developments, increased service intervals, and environmental constraints and the interplay among them are a microcosm of the development of lubricant performance specifications [2]. The MIL-2-104A standard developed into the API C-(X) system, which has specified heavy-duty diesel North American lubricant performance standards for 40 years through to the current 2006 API CJ-4 specification. The API system has evolved through various additional requirements of changing fuel formulations, effects on the engines due to emission control systems, and higher power densities. It gave the United States an established

lead in engine lubricant quality standards for many years, but various concerns arose later. The Tripartite constitutional framework involved the SAE, ASTM, and API and had “virtue and weakness” because the relevant SAE and ASTM committees included automotive, lubricant, and additive industry representatives that could have conflicting organizational objectives. A parallel development for petrol engines produced the API Tripartite API –S(X) series of lubricant performance specifications. The API Tripartite system is composed of

1. ASTM, which defines the test methods and performance targets;
2. API, which develops and controls the service letter designations and “user” language; and
3. SAE, which defines the need and combines the information into an SAE “Recommended Practice” in the *SAE Handbook* for consumer use. The current document is the “Engine Oil Performance and Engine Service Classification” (other than “Energy Conserving”), SAE J183 JUN91 [5].

The API system is described in “Engine Service Classification and Guide to Crankcase Oil Selection”, API Bulletin 1509, in its current technical bulletins, not as an approval body but as certifying lubricant quality. The latest API 1509 bulletin can be found on the American Petroleum Institute website (<http://www.api.org>).

The API’s role has developed into its Engine Oil Licensing and Certification System (EOLCS). The strong growth of “quality procedures”, resulting from the success of Japanese industry and ISO 9000-series quality accreditation, caused fresh concerns about industrial lubricant formulation/testing practices that were strongly argued at the 1989 CEC Symposium. The additives industry supported these concerns, which lead to the five main features of the ACC Product Approval Code of Practice for lubricant performance tests:

1. Engine tests, registered with independent monitoring agencies before running, only run on “referenced (test) stands” with established, accepted, statistical criteria.
2. Test sponsors select the testing laboratory and must normally use the “next available” stand.
3. Multiple test acceptance criteria (MTAC), in which a lubricant must pass all controlled individual parameters on its first test. If a second test is needed, then each mean parameter value must be a pass. For three or more tests, one complete test can be discarded and the mean parameter values from the remaining tests must pass.
4. Details of changes to original formulations made as “minor” formulation modifications are documented in great detail such that all users of the code have a consistent set of working rules.
5. A “candidate data package” gives all of the test results together with an audit trail to demonstrate the nature and validity of formulation changes, plus details of all scheduled tests and severity changes.

The ACC Code of Practice is voluntary, but all major players have committed to all tests initiated by them and tests covered by the code are conducted in accordance with it.

EOLCS (API) arose from the problems and conflicts previously described and has five key elements:

1. Defined performance standards, which are defined similarly to the Tripartite system in which SAE, API,

and ASTM perform their previous traditional roles. If ASTM cannot achieve consensus, there is provision for ILSAC to take over. The system defines physical, chemical, and performance characteristics of engine lubricants for API SX and CX specifications.

2. Engine test protocol requires that each engine lubricant test must be run according to the American Chemistry Council Code of Practice. Although use of the code is generally voluntary, EOLCS mandates its use if the particular test has been covered by the code. The latest ACC Code of Practice is found at http://www.americanchemistry.com/s_acc/bin.asp?CID=368&DID=1361&DOC=FILE.PDF/.
3. A licensing procedure in which lubricant marketers are responsible for product performance and must certify that each viscosity grade of each brand meets requirements. Detailed rules allow for basestock interchange and engine test read-across in certain circumstances from one viscosity grade to another, described in API 1509.
4. Two licensed certification marks are available: the API symbol and Certification Mark.
5. Conformance audits for all licensed lubricant products: Manufacturers of failing products are liable to enforcement penalties, from license suspension to removal of the product from sale.

Engine lubricant test development is very time-consuming and ever-more expensive. Emphasis has moved toward commercial multicylinder engines of increasing size and complexity parallel to commercial engine development. However, larger engines require larger test beds and power absorption dynamometers, more fuel for longer periods, and more time for rating/rebuilding than the previous smaller engines, which contribute to rapid increases in lubricant evaluation costs.

4.2.2 ILSAC

Dissatisfaction with the rate of progress for new standards, the levels defined by those new standards, and the philosophy of waiting for component failure rather than preventing such failures lead to the formation of the International Lubricants Standardization and Approval Committee, or ILSAC, by the Japan Automobile Manufacturers Association, Inc. (JAMA), Chrysler, Ford, and GM. ILSAC has jointly developed, assembled, and approved ILSAC GF-(X), with the latest being GF-5 lubricant minimum performance standard for engine sequence and bench tests as well as chemical/physical properties for use in spark ignition internal combustion engines. ILSAC GF-5 lubricant performance specifications are now very close to API-SN.

4.2.3 ACEA

In contrast to the U.S. Tripartite specifications, Europe initially developed robust, single-cylinder, lubricant test methods using diesel and petrol engines originally designed for small construction vehicle/motive power for pump/electricity generation use, therefore cheap to buy and rebuild. In addition, European OEMs have different relationships with lubricant suppliers than in the United States, and furthermore a different attitude toward lubricant classification and approval. For example, the Daimler “Betriebsstoff-Vorschriften/Specifications for Service Products (Fuels, Lubricants, etc.)”, as regularly updated, are comprehensive

guides to lubrication requirements for Daimler vehicle products and components under a range of service conditions. Approved lubricants are listed, giving them considerable additional marketing value.

Although the need for individual OEM specifications/approvals has reduced in recent years because of the European ACEA (CCMC) classifications and others, further OEM specifications/approvals remain. Thus, VW initiated their own approvals, profoundly affecting other testing procedures by requiring that all approval tests be done within a limited group of independent laboratories. These must produce tests for several reference lubricants that demonstrate adequate discrimination between them. Candidate test lubricant results are assessed against reference oil results obtained on the same test stand, with VW arguing that these procedures enhance test quality. The initiatives taken by engine manufacturers benefit engine lubricants overall, engine development, and ultimately vehicle owners.

CCMC (“Comite des Constructeurs du Marché Commun” [Committee of Common Market Automobile Constructors]) was founded in 1972 as a trade association. ACEA (“Association des Constructeurs Européens d’Automobiles”) replaced it in 1991 with a different organizational constitution. CCMC crankcase lubricant sequence development was quite different from the U.S. tripartite system because the European Union (EU) motor industry privately developed plans, unrestricted by consensus with the lubricant industry. In response, and anticipating the need for dialogue with CCMC, the Technical Committee of Petroleum Additive Manufacturers (ATC) was formed in 1974. Equally, a lubricant marketers organization, “Association Technique de l’Industrie Européenne des Lubrifiants” (ATIEL), was formed in 1976 for discussion with CCMC, then ACEA.

The first CCMC Fuels and Lubricants Working Group sequences were published in 1975 and covered additional requirements beyond the API designations. These necessary additional tests covered the differences for small engine operation in Europe, mostly developed by the Coordinating European Council for the Development of Performance Tests for Transportation Fuels, Lubricants, and Other Fluids (CEC) from recommended engine manufacture prototype tests and extensively revised in 1984 and 1991. However, the internal tensions of CCMC led to its replacement by ACEA in 1996.

The differences between CCMC/ACEA Categories and API Test Sequences are that although U.S. classifications are backed directly by working groups monitoring test quality with only one recommended minimal quality for a specific application at any time, ACEA (previously CCMC) sequences are mainly based on CEC test procedures but with fewer formal links between the organizations. Further, European classifications include a substantial diesel light-vehicle market that does not exist in the United States. ACEA recognizes the provision of different classifications of lubricants for the same equipment, dependent on service interval, and is not involved in lubricant approvals, not wishing to incur development and maintenance costs for the necessary infrastructure. ACEA does not have legally enforceable powers, which is probably advantageous because it operates across several nation states whereas the U.S. system formally operates across one integrated federal state.

ACEA objectives are very similar to those of CCMC but with a different constitution. In addition to European manufacturers, it includes global (U.S.) companies manufacturing in Europe (e.g., GM and Ford) together with wider European companies (e.g., Volvo and Saab-Scania, the Scandinavian headquarters of the original European Community [Common Market] but have since joined the expanded European Union [EU]). ACEA issues “lubricant sequences” but does not give approvals, continuing to favor wherever possible multicylinder European engine tests developed by CEC. ACEA has common sequences for gasoline and light-duty diesel engines as well as heavy-duty diesel engines. Most recent developments have been the combination of the “B” light diesel and “A” petrol ACEA sequences to give the A/B sequences driven by current developments in European light-diesel engine technology and fuel composition.

CEC has a parallel but much more limited role in Europe than ASTM in the United States. Its scope is limited to performance tests on engine rigs with lubricant bench tests left to other organizations such as the Institute of Petroleum (IP; now the Energy Institute), establishing IP methods, or “Deutscher Normenausschuss”, awarding DIN (Deutsche Industrie Normen) classifications.

4.2.4 Some Universal Questions Concerning the Testing of Lubricant Degradation

4.2.4.1 SPECIAL OR UNIVERSAL LUBRICANT REQUIREMENTS?

Individual OEMs regarded their products as unique and wanted additional tests for their products over and above general lubricant tests, a view that still continues for certain manufacturers. However, this view initially proliferated standard test requirements, increased costs, and lengthened approval procedures. Formulating lubricants for vehicle fleets with different OEM engines was difficult. However, ILSAC, developed by U.S. and Japanese OEMs, has progressively rationalized lubricant tests on an international basis leading to the ILSAC GF-(X) series of petrol engine lubricant standards. An analogous diesel version, DHD-1, has not developed beyond the initial proposal. Lubricant development has not progressed within a constant reference framework because the qualities of base oil and additives used for lubricant product formulations are increasing (e.g., Group I base oils replaced by Group II or III or synthetic base oils); additive pack action is now much better understood, differentiated, and more robust. Resolving the conflicting properties and requirements of advanced lubricant formulations has given lubricant formulations that can be used across defined engine OEMs. However, this position is not really resolved. Although the API, ACEA, and ILSAC procedures are now well established and used extensively, many manufacturers still require their own lubricant performance standards in addition to those of API/ACEA/ILSAC. The move by GM in 2010 to introduce its own dexos1 specification for gasoline and light-duty brands of lubricant, although related to current standards with additional requirements, is a further challenge to the established systems. The reasons given for the GM dexos1 development include updating specifications with new technologies that the ILSAC GF-5 timeframe does not address. A global market specification is needed for lubricants for engine components designed in one continent and

manufactured in another continent for use in yet another continent.

4.2.4.2 SINGLE TESTS/MANY ENGINES OR MANY TESTS/SINGLE ENGINE?

Early engine tests were for one lubricant degradation test property/type of engine test (e.g., piston cleanliness for lubricant detergency, sludge formation for lubricant dispersancy, and engine component wear and component corrosion), which made these expensive and probably confusing. A wide range of physical or degradative tests is currently required for most specifications. To reduce costs, OEMs want the specification tests to be drawn from as restricted a range of typical engines as possible. New engine lubricant test development is expensive because the test itself requires extensive committee work to define, and tests of new hardware are expensive, followed by the purchase and installation of new equipment in the many engine lubricant test houses across the world. All of these procedures cause considerable expense and take substantial time to implement. This favors the evolution of existing test procedures with minor incremental changes. Engine testing is a mature technology and major developments are not expected. Realistic alternatives might be simple laboratory chemical/physical tests that may give rapid, much less expensive results. However, these tests are simplistic and do not reflect real on-road service conditions over several years. However, the ROBO laboratory test [5] for the oxidative degradation of candidate lubricants, ASTM D7528, evaluates the used lubricant low-temperature viscosity performance of candidate lubricants and simulates the ASTM Sequence IIIGA test in a shorter time at considerably less cost.

4.2.4.3 ACCELERATED TESTING

Engine lubricant tests use “accelerated” conditions, meaning, inter alia, “higher engine temperatures” than in normal service. Degradation rates increase by a geometric factor of 2–3 for each incremental 10°C. Higher power implies higher bearing loads, shear rates, increased valve spring loads, and cam/tappet loadings that produce the anticipated degradation effects in a much shorter time (e.g., the M111 sludge test, which reduces the engine run time necessary to show deposits and wear using an especially sensitive fuel). “Failure parameter levels” are set to be indicators, giving a testing philosophy that limits engine test length, thus limiting costs and preventing very expensive, potentially dangerous and unpredictable catastrophic engine failure. Meaningful relationships between engine test results and service performance may be strongly debated, but a better, more consistently related set of procedures has neither been developed nor found. The API/ACEA/ILSAC classification and specification systems, which are based on an assembly of standard varied tests that carefully assess the degradation of candidate lubricants, are proven to work for the overwhelming majority of automotive applications.

4.2.4.4 WHO SETS THE STANDARDS?

Should a new engine design use an existing lubricant that may limit its long-term performance level? Or should the new design require development of a new, higher quality lubricant for reliable performance? Two views flow from these points:

1. Lubricant companies may see this as engine manufacturers using them to solve equipment problems.
2. Alternatively, engine manufacturers regard the development of higher performance standard lubricants as part of total system technological development. The engine and lubricant are then considered together to develop advanced engine products. New vehicle aerodynamic design reduces the available engine space, lubricant volumetric capacity, and cooling effects.

U.S. and European situations have changed over the last 4 decades. Manufacturers initially designed engines to operate with the available good quality lubricants. However, sharp changes in emission control requirements, extended service intervals, reduced engine capacities, and higher power densities as well as fuel efficiency improvements have all severely increased the requirements for lubricant performance. Field problems together with enhanced lubricant requirements led U.S. engine manufacturers to work with lubricant and additive manufacturers.

The Japanese approach developed engines that can satisfactorily operate with a range of lubricants, the “robust” approach, which is particularly suited for a manufacturing industry strongly oriented to exporting products to all countries and the varying standards of service regimes found there. However, within Japan, the single automotive companies set stiff requirements for approval of preferred lubricants known as “Genuine” lubricants.

Europe had wider approaches to lubricant approval from different countries; thus, German OEMs set very comprehensive additional specifications with stringent targets. As field problems arise, specifications are amended.

4.2.5 A Summary of Attitudes and Philosophies

Different engine lubricant testing approvals arose in different continents from different attitudes and philosophies and, to a certain extent, different countries within those continents. Lubricant degradation issues are now addressed globally by new analytical test method development and procedures for specifying lubricant qualities. These benefit engine and equipment manufacturers, producers of lubricants and additives, and ultimately users of mechanical systems in an international marketplace. Moves toward merging separate lubricant performance specifications are slow, from built-in needs for agreement or majority voting to progress. This pace clearly does not satisfy large manufacturers such as GM, which introduced its dexos1 as a global specification, citing the need to respond quickly to new developments.

4.2.6 Testing Organizations, Their Roles, and Engine Tests

Various organizations are involved in lubricant degradation testing and specification procedures. Understanding lubricant classifications is complicated, with organizational acronyms that may seem to overlap or duplicate each other. The API Tripartite system is based in North America; ACEA initially for Western Europe but now including the rapidly developing Eastern European market; and JASO of Japan, including Asia and the Pacific Rim countries.

“Realistic” engine tests are only meaningful as field trials lasting 1 year, or more. But what is realistic? Engine use is extremely varied, and to address this, international committees have defined frameworks for engine tests

causing lubricant degradation that are practical, relevant, and reproducible under clearly defined conditions. Testing procedures, approvals, standardization, and performance limits for lubricants in the United States are defined by API, ASTM, and SAE. In Europe, responsibility is shared between CEC, which sets testing procedures, approvals, and standardizations, and performance limits set by ACEA, which are decided with the additive and lubricant industries. ILSAC has generally adopted the U.S. automobile specifications for a set of lower viscosity formulations with additional test requirements, in particular fuel efficiency tests.

4.2.7 General Principles of Controlling Lubricant Degradation

The general principles of controlling the degradation of engine lubricants through performance testing address issues of

- Oxidative and thermal stability,
- Control of contaminants via dispersion and detergency,
- Antiwear and anticorrosion protection,
- Shear stability and antifoaming tendency, and
- Fuel economy and fuel economy retention.

Each of these issues requires several analytical methods to measure their effectiveness and control.

4.3 VISCOSITY MEASUREMENT AND CLASSIFICATION: THE SAE J300 STANDARD

4.3.1 Viscosity Measurements

The major property of a lubricant is its viscosity; it must maintain that property within its design range during service use to effectively protect against system seizure. Various degradative processes of the lubricant in use will change its viscosity, usually related to changes in other parameters. The first, and effectively the only, engine lubricant viscosity classification is the SAE J300 viscosity classification. ISO viscosity values are used for machine oils, and cross-references can be made to the SAE system, but it is not particularly meaningful to do so.

Straightforward lubricant viscosities are measured within the SAE J300 specification using automated systems in which samples are injected into thermostatted kinematic viscometers at 40 and 100°C, respectively, from which the viscosity index (VI) is calculated. However, the measurement of viscosity has expanded considerably from simply measuring the viscosity of a fresh and used monograde lubricant. There are three issues:

1. The viscosity grade of the fresh lubricant and how it responds to decreased temperatures, set out in SAE J300,
2. How the lubricant responds to degradation caused by high-shear and high-temperature operation,
3. How the viscosity of the lubricant is affected by increasing levels of soot dispersed in it at ambient and lower temperatures.

A small increase in lubricant viscosity may be due to the volatilization of base oil “lighter ends” after prolonged high-level operation (i.e., the lubricant has become “thicker”). Significant increases in viscosity up to 20 % are regarded as severe, caused by incorrect addition of a higher viscosity lubricant, extensive soot contamination, and base oil oxidation. More recently, accumulation of the bio-based component from B05 diesel fuel in the lubricant will increase its viscosity by the biocomponent itself having

a higher viscosity and enhanced oxidation. Contamination by dispersed soot as well as extensive oil oxidation is readily seen; the black particulate degradation will obscure the increasing dark brown coloration of oxidation. Oxidation is distinctively seen in Fourier transform infrared (FTIR) sample spectra, and the pressurized differential scanning calorimetry (PDSC) antioxidant induction time reserve will decrease.

The converse, a decreased lubricant viscosity, is often due to fuel dilution, a characteristic occurrence when an engine idles for a prolonged period under cold conditions. Fuel and water condense in the lubricant in the sump. However, when the engine is subsequently used at normal, higher power duties, the increased temperatures evaporate the condensed fuel and water, and the viscosity returns to its previous value. However, a serious condition occurs when extensive fuel and water condense into the sump of a very cold engine at startup. For short journeys in severe cold the engine lubricant rarely warms up sufficiently to evaporate condensed fuel and water; the contaminants combine to precipitate the additive package from the lubricant. Substantial parts, if not all, of the additive pack “drop out” and accumulate in the bottom of the sump. The engine has an apparently satisfactory “oil” level, but it is one that is stratified and with drastically reduced protection against wear in the upper part of the lubricant sump volume.

Beyond the straightforward determination of viscosity, viscosity index improvers (VIIs) are polymers giving a degree of resistance to temperature thinning that is dependent on their chemical structure [6]. High rates of shear occur in high-speed engine bearings and at the ring pack/bore wall interface. At these very high shear rates ($>10^6 \text{ s}^{-1}$), there is a temporary loss of viscosity, but lubricants formulated with VIIs may permanently lose viscosity because of cleavage of sidechains and “backbones” of the polymer chains. Lubricant performance specifications include measures of how robust formulations must be able to resist degradation introduced by high-shear and high-temperature effects.

If a lubricant viscosity degrades during its service use, then its VI will necessarily change. Major causes of reduced VI are caused by cleavage of the VII polymer molecules to give smaller chains of less effect. Two effects follow: (1) reduction in the VII molecular weight reduces the lubricant viscosity at 40 and 100°C and (2) a reduction in the temperature-related VI effect, of which the latter is normally the greater.

SAE J300 is a fundamental component of lubricant performance specifications, and a major development has been its evolution from a single grade classification into a multigrade lubricant classification that measures viscosity at low (engine winter starting) temperatures and high (operating) temperatures for that approximately 90 % of the market that are multigrade lubricants. Viscosities are given by two numbers: the low-temperature viscosity by -W- (for Winter) is given first, and the second value is the minimal kinematic viscosity at 100°C. Put together, they become SAE xxW-yy (e.g., SAE 10W-30).

4.3.2 Comparative Viscosity Measurements of API CJ-4 and ACEA E9-08

Comparison across the different specification systems is not straightforward because API and ACEA operate to different time scales and quality development. The essential differ-

ence between the ACEA and API lubricant performance specifications is how they define different performance levels. The API C('X') system has built up a qualitative range across successive revisions of the specifications; hence, API CJ-4 is the latest at the time of writing. API and ACEA have a range of performance specifications, but they are arrived at by different routes; thus, for the heavy-duty diesel category,

- API has a range of lubricant performance specification levels that have arisen over time in the heavy-duty diesel category to give the current approved range of CF and CF-2 (1994), CG-4 (1995), CH-4 (1998), and CI-4 (2002) through to CJ-4 (2006), which represent a range of performance levels.
- ACEA has an analogous range of lubricant performance specifications that are reviewed and updated together as a block at each revision and designated as such (e.g., E4-08, E6-08, E7-08, and E9-08, where “-08” indicates that the specification was agreed and issued in 2008).

Therefore, it is not meaningful to directly compare API lubricant performance specifications with those for ACEA specifications because they have evolved differently in time. Thus, the API-CF performance specifications of 1994 should not be compared with ACEA E9-08. The time comparison, as existing for 2010, is

1994	1995	1998	2002	2006	2008
API	CF	CG-4	CH-4	CI-4	CJ-4
ACEA					E4-08
“					E6-08
“					E7-08
“					E9-08

The closest comparison that can be made is between API CI-4 and ACEA E9-08 as the current high-performance specifications of their respective systems, taking the first as the template.

Low-temperature viscosities in SAE J300 are measured by low-temperature cranking viscosity using the cold cranking simulator (ASTM D5293), and pumpability is now measured by the mini-rotary viscometer (MRV; ASTM D4684). Kinematic viscosities at 100°C are measured by very accurate capillary viscometers (ASTM D445).

The high-temperature/high-shear (HTHS) test (ASTM D4683) arises from the need to measure the candidate lubricant's ability to withstand high-shear conditions at high temperatures. This simulates the enhanced severity of conditions for smaller volumetric capacity but higher energy density and higher speed engines, as in continuous high-speed motorway/autobahn/interstate driving. Vehicle design is now increasingly more aerodynamic but with a reduced natural cooling of engines. The HTHS test measures the transmitted torque between a conical rotor in a tapered housing with a thin film of candidate lubricant between them—a tapered bearing simulator. Shear rates are high; the temperature is 150°C; and they are then brought together as HTHS viscosity measurements at 10^6 s^{-1} and 150°C (ASTM D4683, CEC-L-36-90-A, ASTM D4741, or ASTM D5481). API CJ-4 requires the candidate lubricant to demonstrate its ability to maintain a minimum 3.5-cP viscosity at 150°C after the ASTM D4883 HTHS test.

TABLE 4.2—API CJ-4 SAE J300 Viscosity Grades for Engine Oils

SAE Viscosity Grade	Low-Temperature (°C) Cranking Viscosity ^a (mPa/s) Maximum	Low-Temperature (°C) Pumping Viscosity ^b (mPa/s) Maximum, with No Yield Stress ^d	Low-Shear Rate Kinematic Viscosity ^c (mm ² /s) at 100°C (Maximum/Minimum)	High-Shear Rate Viscosity ^d (mPa/s) at 150°C (Minimum)
0W	6200 at -35	60,000 at -40	3.8/-	-
5W	6600 at -30	60,000 at -35	3.8/-	-
10W	7000 at -25	60,000 at -30	4.1/-	-
15W	7000 at -20	60,000 at -25	5.6/-	-
20W	9500 at -15	60,000 at -20	5.6/-	-
25W	13,000 at -10	60,000 at -15	9.3/-	-
20	-	-	5.6/<9.3	2.6
30	-	-	9.3/<12.5	2.9
40	-	-	12.5/<16.3	3.5 (for 0W-40, 5W-40, and 10W-40 grades), 3.7 (for 15W-40, 20W-40, 25W-40, and 40 grades)
50	-	-	16.3/<21.9	3.7
60	-	-	21.9/<26.1	3.7

From SAE J300, revised November 2007, with effect from May 2008.
^aBy ASTM D5293.
^bBy ASTM D4684 (any yield stress detectable by this method constitutes a failure regardless of viscosity).
^cBy ASTM D445.
^dBy ASTM D4683, CEC L-36-90 (ASTM D4741), or ASTM D5481.

These requirements are now included in SAE J300 for SAE 20 and above, effective May 2008 for engine oils (Table 4.2). The low-temperature viscosity measurements apply for the range 0W- through to 25W-, and the HTHS measurements apply for the grades of 20 and above.

The requirements for shear stability and HTHS stability in ACEA E9-08, SS.1.1 to 1.3, are very similar to API CJ-4 and use very similar or identical ASTM and CEC standard procedures. ACEA E9-08 has the requirement for lubricants to “stay in grade” for shear stability. Essentially, the API CJ-4 and ACEA E9-08 lubricant performance specifications are very similar on viscosity grades and shear stability tests after allowing for minor differences in interpretation, emphases, and the specification detail.

4.3.3 Shear Stability, API CJ-4 1.4, ASTM D7109

1.4 Shear Stability	ASTM D7109	KV at 100°C after 90 passes for XW-40, min	cSt	12.5	No MTAC
		KV at 100°C after 90 passes for XW-30, min	cSt	9.3	

The ASTM D7109 laboratory test measures the ability of a lubricant formulation to maintain its 100°C kinematic viscosity after 90 passes through a high-shear nozzle apparatus, essentially an adapted diesel fuel injector. It is a parallel method to ASTM D4683 and assesses the shear stability of a candidate lubricant by the shear effect alone, without the degradative effect of the high-temperature contribution. It evaluates the shear stability of polymer-containing fluids by measuring the viscosity loss (in mm²/s and as a percentage)

at 100°C using a diesel injector apparatus procedure. A reduction in high-temperature viscosity is a measure of polymer additive degradation by shear at the nozzle and minimizes thermal or oxidative effects. ASTM D7109 measures viscosity loss after 30 and 90 shear cycles, but API CJ-4 only requires the 90-cycle test for two different ranges of lubricant grades, XW-40 and XW-30. The method uses apparatuses defined in CEC L-14-A-93 and only differs from this in the calibration time period.

- *Comparison with ACEA E9-08:* The ACEA method uses ASTM D6709 after 90 cycles and is required to stay “in grade”.

4.3.4 HTHS Stability, S.1.6, API CJ-4, ASTM D4683

1.6 High-Temperature/High-Shear	ASTM D4683	Viscosity at 150°C	cP	3.5	No MTAC
---------------------------------	------------	--------------------	----	-----	---------

The High-Temperature/High-Shear (HTHS) test, ASTM D4683, arises from the need to measure the ability of the candidate lubricant to withstand high-shear conditions at high temperatures. These simulate the enhanced severity of conditions for smaller but higher energy density and higher speed engines, as in high-speed motorway/autobahn/interstate driving. As vehicle design becomes more aerodynamic there is less natural cooling of engines.

The ASTM D4683 test drives a conical rotor in a tapered housing at 150°C with a thin film of the test candidate lubricant between the two components, called a “tapered bearing simulator”. The shear rate is designed to be high, and the test temperature is 150°C, both simulating prolonged high-speed running under load. The test measures the transmitted torque between the top conical element,

rotated at a constant speed, and the lower element. CJ-4 requires the candidate lubricant to demonstrate its ability to maintain a minimum 3.5-cP viscosity at 150°C after the ASTM D4683 HTHS test. S1.6 of API CJ-4 duplicates the provisions in the SAE J300 specification by requiring a viscosity of 3.5 cP at 150°C.

- *Comparison with ACEA E9-08 1.3:* The European equivalent is the Ravensfield viscometer, CEC L-036-99, almost exactly the same as defined in ASTM D4741.

4.3.5 Sooted Oil MRV, API CJ-4, S.1.7, ASTM D6896

1.7 Sooted Oil MRV	ASTM D6896	180-h sample from Mack T-11 or T-11A	cP	25,000	No MTAC
		Viscosity at -20°C, maximum Yield stress	Pa	<35	

The Sooted Oil test, ASTM D6896, is a low-temperature viscosity test of a used, extensively sooted candidate lubricant and was a new requirement in API CJ-4 in 2006. It was perhaps foreshadowed by the “low-temperature pumpability test” requirement in API CI-4 Plus in 2002. It is well established that the rate and duration at which a used engine lubricant is cooled will affect its viscosity and yield stress (i.e., its viscosity will increase and the lubricant will tend to gel). The essential point is the effect that the presence and agglomeration of high soot levels in a degraded, used engine oil will have on its low-temperature viscosity and yield stress behavior.

One feature of recent engine emission technology has been to increase soot levels in the lubricant; therefore, its ability to withstand the deleterious effect of that soot on its viscometric behavior must be measured. The test lubricant sample is generated from the Mack T-11/11A engine after a 180-h test run and is carefully conditioned as specified in ASTM D6896. API CJ-4 requires that the degraded sample viscosity at -20°C does not exceed 25,000 cP with a yield stress of less than 35 using the MRV.

Low-temperature viscosity issues of sooted oil are addressed in the API CJ-4 engine tests at different soot levels. The related sooted oil test at ambient is given from an engine test, API CJ-4, S.2.1, by the Mack T-11 test, which produces samples with measured viscosities at 100°C for a range of soot levels (see Section 4.5).

- *Comparison with ACEA E9-08 2.2 and 2.3:* A difference is that ACEA E9-08 measures soot effects on lubricants by ASTM D5967 for a Mack T8E test duration of 300 h, producing samples with a relative viscosity limit of 4.8 %. An additional “soot-in-oil” test is the Mack T-11, identical to API CJ-4. The fundamental difference is that API CJ-4 measures the effect of soot levels on candidate lubricant viscosity at room temperature and at -20°C.

4.3.6 Sooted Oil Viscosities API CJ-4, S.2.1, ASTM D7156

2.1 Mack T-11	ASTM D7156	Soot at 4 cSt inc, min	%	3.5	3.4	3.3
		Soot at 12 cSt inc, min	%	6.0	5.9	5.9
		Soot at 15 cSt inc, min	%	6.7	6.6	6.5

The Mack T-11 test, ASTM D7156, evaluates the viscosity increase and soot concentration (loading) performance of degraded engine oils in turbo-charged and intercooled four-cycle diesel engines equipped with exhaust gas recirculation as a method of controlling emissions. The results for the test arise from viscometric analysis of the used candidate lubricants for specified maximal increments of kinematic viscosity of 4, 12, and 15 cSt at certain soot loadings of 3.5, 6.0, and 6.7 % (for the first test). Second and third tests have progressively higher increment requirements, as set out above. An abbreviated method, Mack T-11A, is identical but for a shorter test period.

- *Comparison with ACEA E9-08:* This issue has been addressed in the previous section 1.7 “Sooted Oils”.

4.4 LABORATORY TESTS ON FRESH AND DEGRADED HEAVY-DUTY DIESEL LUBRICANTS

4.4.1 Corrosion Tests, API CJ-4, S.1.2, ASTM D6594

1.2 High-Temperature Corrosion Bench Test	ASTM D6594	Cu in used oil increase, maximum	ppm	20	No MTAC
		Pb in used oil, increase, maximum	ppm	120	
		Cu strip rating, maximum		-30	

The purpose of the High-Temperature Corrosion Bench Test at 135°C, ASTM D6594, is to measure the increased corrosion of common nonferrous metals used in engines—in this case standard coupons of Cu and Pb—by used oils from the increased operating temperatures of modern engines. The emphasis is upon “increased corrosion” because Cu and Pb will be corroded by contact with a hot standard lubricant anyway. Air is blown through samples of used oil under specified conditions whereas the original method, ASTM5968, specified a temperature of 121°C. The increased temperature of 135°C in ASTM D6594, compared to the previous test, reflects the higher operating temperatures of modern diesel engines. Because this is a well-established test with low variance under laboratory conditions, there is no MTAC. The polished Cu strip from the test is rated as a visual index against an established standard bank of color and condition strips at the end of the test.

- *Comparison with ACEA E9-08 1.12:* API CJ-4 S.1.2 and ACEA E9-08 S.1.12 are next to identical, again with very slight differences in interpretation.

4.4.2 Foaming, API CJ-4, S.1.3, ASTM D892

1.3 Foaming	ASTM D892	Foaming/settling, maximum			
		Sequence I	%	10/0	No MTAC
		Sequence II	%	20/0	
		Sequence III	%	30/0	

The lubricant in the sump of an engine can be extensively aerated into foam, which, if it does not collapse rapidly, can be whipped up by the crankshaft into an extensive foam. The generated foam will seek escape from any convenient partially closed opening such as the oil filler cap, the dipstick tube, or any other partial opening it can find. The

lubricating effect of oil foam in a bearing against a heavy load is very low compared with the homogeneous oil. The compressibility of oil foam is very high compared with that of the “full” oil and will damage oil pumps and bearings. Therefore, prolonged foaming by aeration of lubricating oil must be avoided. Dealing with lubricant foaming is made more difficult by the detergent and dispersant components of the lubricant additive pack.

Silicones (polydimethylsiloxanes) or ester-based polymers are used to control foaming at very low concentrations. These must be carefully controlled because their concentrations are critical for these additives to work as intended. The ASTM D892 method creates foam in candidate oils by blowing air through a porous stone in a glass-measuring cylinder. The different standards set for the three sequences apply for the respective fixed times elapsed after the airflow is stopped for the foam to break and settle to zero foam volume.

- *Comparison with ACEA E9-08 1.9 and 1.10:* API CJ-4 Foaming Tendency and High Temperature Foaming test, S.1.3: API CJ-4, S.1.3 and ACEA E9-08, S.1.9 and S.1.10, measure the same laboratory-based foaming tendency performance at ambient temperatures. The difference between the specifications lies with their aims for measuring high-temperature foaming tendencies. ACEA E9-08 S.1.10 deals with this as a Sequence IV high-temperature extension to 150°C of ASTM D892, as ASTM D6082; API CJ-4 takes a different approach to measuring foaming at high temperatures through an engine test, S.2.7, ASTM D6894, described in Section 4.4.3, which measures the aeration of a candidate lubricant formulation when used as a lubricant and high-pressure hydraulic fluid in an engine. Thus, although almost identical at ambient temperatures, the API CJ-4 and ACEA E9-08 specifications diverge to measure different aspects of foaming tendency at high temperatures.

4.4.3 Oil Aeration, API CJ-4, S.2.7, ASTM D6894

2.7 Engine Oil Aeration	ASTM D6894	Oil aeration volume, maximum	%	8.0 (MTAC)	8.0 (MTAC)	8.0 (MTAC)
--	---------------	---------------------------------------	---	---------------	---------------	---------------

The need for the Engine Oil Aeration Test (EOAT) arose because the hydraulic unit electronic injection (HUEI) fuel system uses pressurized lubricant from the main lubricant distribution gallery as a hydraulic fluid. This actuates a high-pressure system, which, through sequential plunger pumps and pressure intensifiers, increases fuel injector pressures up to approximately 145 MPa, independent of engine speed and important for low-speed running. Injection timing and duration is varied electronically for optimal fuel economy and emission reduction, a very positive aspect of engine fuel management.

The aeration problem arises from the increased use of lubricant in that the total volume can be circulated in as short of a cycle time as approximately 8 s. This causes foam in some candidate lubricants, which does not have sufficient time to subside before it is recirculated. Consequently, aerated lubricant may be circulated to the injector pressure intensifiers and, because of its much higher

compressibility, adversely affect injector timing and therefore engine operation. Operating experience determined that 8 % oil aeration was the limit beyond which engine operation and performance would be impaired in actual service, hence the limit set. This test method is commonly called the EOAT and uses a specified 7.3-L direct-injection, turbo-charged diesel engine on a dynamometer test stand. ASTM D6894 is a replacement and complement for the ASTM D892 laboratory test after it was found that the latter bench test did not relate to oil aeration performance in actual service.

- *Comparison with ACEA E9-08:* There is no direct comparison between ACEA E9-08 and API CJ-4. The former uses a straightforward high-temperature extension of the conventional aeration test; the latter uses a separate engine foaming test, ASTM D6894, at high temperatures for candidate lubricants when used as a lubricant and hydraulic fluid for actuating fuel injectors.

4.4.4 Noack Volatility, API CJ-4 S.1.5, ASTM D5800

1.5 Noack Volatility	ASTM D5800	Evaporative loss at 250°C, viscosity grades other than 10W-30, maximum	%	13	No MTAC
		Evaporative loss at 250°C, 10W-30, maximum	%	15	

The Noack volatility test measures the evaporation loss from a candidate lubricant oil, an essential measurement for lubricant service at high temperature for prolonged periods. In addition to volume loss, evaporation contributes to air emissions and increases piston deposits. This issue has increased in importance with the move toward lower viscosity, higher volatility lubricant grades. ASTM D5800 requires the candidate oil to be held at 250°C in a container for a specified period while a gentle air stream removes the volatile components. The result is expressed as percentage weight loss. CJ-4 differentiates between 10W-30 grades and those above.

- *Comparison with ACEA E9-08 1.4:* The methods for measuring candidate lubricant volatility, ASTM D5800 and CEC L-040-93 for API CJ-4 and ACEA E9-08, are essentially identical. The difference is that API CJ-4 S.1.5 sets a limit of evaporative loss at 250°C of 13 % maximum loss for 10W-30 grades and below but allows a limit of 15 % maximum loss for grades above 10W-30. The volatility limit for ACEA E9-08, S.1.4, is set at 13 % maximum loss for all viscosity grades.

4.4.5 Chemical Limits, API CJ-4, S.1.8, ASTM D874 and D4951

1.8 Chemical Limits (Noncritical)	ASTM D874	Sulfated ash, maximum	%	1.0	No MTAC
	ASTM D4951	Phosphorus, maximum	%	0.12	
		Sulfur, maximum	%	0.4	

As the engine emission limits for particulates and nitrogen oxides decrease further (see Chapter 14), there is a need to reduce the lubricant contribution to the emissions. “Sulfated ash” is a measure of the amount of ash (as metals) in the lubricant. Reduction of sulfated ash limits the amount

of ash from the lubricant that is transferred from the engine into the exhaust system and is trapped by the particulate filters used to reduce overall particulate emissions. Because ash is inorganic, it cannot be burned off, in contrast to soot, which is also trapped. For this reason, a sulfated ash limit of 1 % has been set. P and S arise primarily from antiwear additives in the lubricant, and their use is limited because of their deactivating effect on catalytic converters over long periods of time.

Put together, “sulfated ash phosphorus sulfur” is known as SAPS, and the established trend is toward “low-SAPS” lubricant formulations, hence the limits set in CJ-4. Sulfated ash is determined by ignition using ASTM D874. The sulfated ash residue is the concentration of metal-containing additives within the candidate lubricant. P and S are determined by conventional inductively coupled plasma (ICP) atomic emission laboratory analytical procedures as defined in ASTM D4951.

- *Comparison with ACEA E9-08 1.5–1.7:* SS.1.5 through to 1.7 of ACEA E9-08 are equivalent to API CJ-4 requirements; the only slight differences of emphasis are the limits, being absolute limits for the latter and “up to” limits for the former.

4.4.6 Seal Compatibility, API CJ-4, S.1.9, ASTM D7216

1.9 Seal Compatibility	ASTM D7216	Volume Change	Hardness	Tensile Strength	Elongation
	Nitrile	+5/-3	+7/-5	+10/-TMC1006	+10/-TMC1006
	Silicone	+TMC1006/-3	+5/-TMC1006	+10/-45	+20/-30
	Polyacrylate	+5/-3	+8/-5	+18/-45	+10/-35
	FKM	+5/-2	+7/-5	+10/-TMC1006	+10/-TMC1006
	Vamac G	+TMC1006/-3	+5/-TMC1006	+10/-TMC1006	+10/-TMC1006

Seals are used in various configurations, but the most common and important seals used in engines are for sealing the junction between a rotating shaft and a stationary housing. Immersion of elastomer seal materials in modern lubricant formulations at engine operating temperatures over prolonged periods can lead to swelling, softening, and weakening of some seal materials. To guard against this, the various materials used as engine seals are exposed to the candidate lubricant at elevated temperatures for a given period of time. After exposure, the seal material specimens are tested for the physical properties of

- *Swell:* As a volume change, where a positive number indicates an increase in the seal volume. A negative number indicates a contraction in volume, which causes tension and ultimately cracking.
- *Hardness:* As a Shore A hardness measurement, in which softening is usually associated with swelling, slight swelling is allowable, and hardening is not.
- *Tensile strength:* As a measured percentage change, this assesses the ability of the seal to maintain its molded shape after exposure and thus its effectiveness.

- *Elongation at break:* As a measure of the elasticity of the material after exposure to the hot candidate lubricant, again an assessment of the seal to maintain its effectiveness.

The reference oil, TMC 1006-1, is aggressive for some seal material parameters under service conditions. The *relative* compatibility of the candidate and reference oils with seal materials allows predictive assessment of the candidate oil performance in service.

- *Comparison with ACEA E9-08:* The seal compatibility specifications have essentially the same objectives, but the elastomers are identified differently and the physical value limits arising from the tests are moderately different.

4.4.7 Additional Laboratory Requirement for ACEA E9-08 over API CJ-4

There are three additional requirements in the ACEA E9-08 laboratory tests compared with those for API CJ-4:

1. *An antioxidant reserve test, CEC L-085-99, by pressurized differential scanning calorimetry (PDSC):* A small quantity (<10 mg) of the candidate oil is weighed into a standard open sample pan. The configuration of the sample pan is such that a thin film is exposed to the pressurized atmosphere, thereby avoiding diffusion-controlled oxidation kinetics. The sample is placed in a test cell and pressurized with air to 35 bar. The cell is rapidly heated to a specified temperature, usually 190°C, and held at that regulated temperature and pressure while the antioxidant is consumed. When the antioxidant is exhausted, the hydrocarbon base oil is very rapidly oxidized, giving an exotherm. The onset time of the exotherm is measured and reported as the oxidation induction time. For E9-08, the pass limit must be more than 65 min.
2. *A provisional space left for a possible turbo-charger test, once adequate and reproducible data are available to establish a test standard.*
3. *A requirement for a total base number (TBN) of 7 mg or more KOH/g sample at the end of the Direct Injection Diesel Piston Cleanliness and Ring Sticking test, in the ACEA C4-08 S.2.8 and CEC L-078-99, as a test of lubricant longevity in service and measured by ASTM D2896:* The terms of this test are interesting because they differentiate between the lubricant TBN value and those that are retained at the end of test (EOT).

4.5 ENGINE TESTS FOR API CJ-4

In a similar manner to the laboratory tests, the number of engine tests has increased from six for CG-4 in 1995/1996 to nine for CJ-4 6 in 2006. The changes and additions are mainly due to dealing with the effects of increased soot levels in used lubricants that cause increases in viscosity and wear. Successive tests for the CJ-4 engine tests are described in the following subsections.

4.5.1 Sooted Oils, API CJ-4 S.2.1, ASTM D7156

2.1 Mack T-11	ASTM D7156	Soot at 4-cSt increments, minimum	%	3.5	3.4	3.3
		Soot at 12-cSt increments, minimum	%	6.0	5.9	5.9
		Soot at 15-cSt increments, minimum	%	6.7	6.6	6.5

The Mack T-11 test evaluates the viscosity increase and soot concentration (loading) performance of engine oils in turbo-charged and intercooled four-cycle diesel engines equipped with EGR as a method of controlling emissions. The results for the test arise from viscometric analyses of the used candidate lubricants for specified increments in kinematic viscosity of 4, 12, and 15 cSt at certain soot loadings of 3.5, 6.0, and 6.7 % (for the first test). An abbreviated method, Mack T-11A, is identical but for a shorter test period.

- *Comparison with ACEA E9-08:* This issue has been addressed in Section 4.3.6, 1.7 “Sooted Oils”.

4.5.2 Engine Wear, API CJ-4 S.2.2, ASTM D7422

2.2 Mack T-12	ASTM D7422	Merits, minimum	1000	1000	1000
---------------	------------	-----------------	------	------	------

The Mack T-12 test evaluates a candidate lubricant’s ability to minimize cylinder liner, piston ring, and bearing wear in engines using ultra-low-sulfur diesel fuel with EGR. The test simulates heavy-duty, on-highway truck operations after 2007 using a modified Mack E7 E-Tech 460 engine rated at 460 bhp and 1800 r/min with EGR. The first 100 h of the 300-h test is run at a rated speed and power to generate soot. For the last 200 h of the test run, the engine is overfueled at peak torque revolutions per minute to maximize ring and liner wear rates. The criteria evaluated at the end of the procedure are piston ring and cylinder liner wear, lead-bearing corrosion, oil consumption, and oxidation.

- *Comparison with ACEA E9-08 2.7:* Although the Mack T-12 test is used in ACEA E9-08, S.2.7, and the merit scoring system is the same, the ACEA test version is extended to include average liner and top ring wear units. The test pass/fail result is assessed using a score matrix, minimum 1000 units, as in Table 4.3.

4.5.3 Valve Train Wear, API CJ-4 S2.3, Cummins ISB

2.3 Cummins ISB	Tappet wear, maximum	mg	100	108	112
	Cam wear, maximum	microns	55	59	61
	Crosshead weight loss	mg	Rate/report	Rate/report	Rate/report

The Cummins ISB engine test procedure uses a common rail diesel fuel system engine equipped with EGR to evaluate a candidate lubricant’s ability to reduce camshaft lobe and valvetrain wear. The procedure simulates repetitive cyclic operation, as in field operation, with 2007 emission regulation engines. The 350-h procedure uses PC-10 test fuel and includes an initial 100 h of steady-state operation at 1600 r/min to accumulate 3.25 % soot content, and then operates for 250 h on a multistep, 28-s cycle to simulate cyclic operation. Although the full Cummins ISB test covers a matrix of wear on engine components as well as used lubricant degradation, CJ-4 only measures maximum

TABLE 4.3—Component Merit Ratings for the Mack T-12 Test

Parameter	Anchor Value	Merit Weight	Maximum	Minimum
Ring wear	70	200	105	35
Liner wear	20	250	24	12
Lead	25	200	35	10
Lead Δ	65	150	85	50
Oxidation	65	150	85	50
Merits	1000			

tappet wear, maximum cam wear, and maximum crosshead weight loss.

- *Comparison with ACEA E9-08:* The ACEA method uses a different engine, the OM646LA in the CEC L-099-08 test, for the cam wear outlet using a candidate lubricant. Differences of wear rates are not meaningful for different engines.

4.5.4 Engine Wear, Cummins ISM, API CJ-4 S.2.4

2.4 Cummins ISM	Merits, minimum		1000	1000	1000
	Top ring weight loss, maximum	mg	100	100	100

The Cummins ISM engine test replaces the Cummins M11-EGR engine test as a 200-h test procedure using 500-ppm S fuel to simulate high-load, heavy-duty field operating conditions with high soot and EGR flow rates using a 2007 emission-compliant engine. The engine has a variable geometry turbocharger, EGR cooler, and an electronically controlled EGR valve. The test procedure evaluates the effectiveness of a candidate lubricant’s ability to reduce soot-related overhead wear, sludge, oil filter plugging, injector adjusting screw weight loss, top ring wear and oil filter plugging, presented as a matrix. API CJ-4 uses the top ring wear and merits.

- *Comparison with ACEA E9-08:* The test parameters are essentially the same as API CJ-4.

4.5.5 Deposits and Oil Consumption, API CJ-4 S.2.5, ASTM D6750 SERVICE

2.5 Caterpillar 1N	ASTM D6750	Top land heavy carbon, maximum	%	3	4	5
		Top groove fill	%	20	23	25
		Weighted demerits, maximum	Demerits	286.2	311.7	323.0
		Average oil consumption (0–252 h), max	g/kWh	0.5	0.5	0.5
		Ring/liner scuffing		None	None	None

The Caterpillar 1N engine test, ASTM D6750, uses a four-stroke, single-cylinder diesel engine running on intermediate (400-ppm S) fuel for a 252-h steady-state run. It evaluates candidate lubricants for their ability to protect against carbon and lacquer deposit formation at high-temperature operation. The test relates to the operation of high-speed, supercharged diesel engines and their control of carbon and lacquer deposit on the piston. Evaluation includes deposit and lacquer ratings for the piston by visual inspection and rating, ring/liner/piston scuffing wear, and measurement of oil consumption.

- *Comparison with E9-08:* The closest comparison with ACEA is the CEC L-101-08 test using the OM501LA engine, which measures average bore polish, average piston cleanliness, lubricant consumption, and engine sludge. This engine is required to use B05 fuel to European Standard EN590 (i.e., diesel fuel with up to 5 % vegetable oil). The EN590 standard has since been increased to 7 % vegetable oil content, and this will probably be incorporated into future E9 standards.

4.5.6 API CJ-4, S.2.6, Piston Deposits and Control of Oil Consumption, ASTM D7549

2.6 Caterpillar C13	ASTM D7549	Merits, minimum	1000	1000	1000
		Hot stuck rings	None	None	None

The Caterpillar C13 multicylinder engine test assesses candidate lubricant performance for the control of piston deposits and oil consumption control under heavy-duty operating conditions. The test operating conditions are chosen to accelerate piston deposit formation in an engine design representative of many turbo-charged, intercooled, four-stroke-cycle diesel engines fitted with combustion systems that minimize exhaust gas emissions to controlled limits. The test method evaluates piston deposit formation by visual inspection and rating, piston ring sticking, and oil consumption control.

- *Comparison with E9-08:* Comparable in part to Mack T-12, as used in ACEA E9-08.

4.5.7 S.2.8, API CJ-4, Roller Follower Wear Test, ASTM D5966

2.8 Roller Follower Wear Test	ASTM D5966	Roller follower, pin wear, maximum	Microns	7.6	8.4	9.1
-------------------------------	------------	------------------------------------	---------	-----	-----	-----

ASTM D5966 determines the ability of a candidate lubricant to control wear under low/ moderate engine speeds and heavy engine loads in field use. Specific test operating conditions have been developed to correlate with lubricant field performance, and this engine lubricant test method is called the Roller Follower Wear test. The primary result of the test is wear of the roller follower shaft in the hydraulic valve actuator, as specified above, which correlates with wear in intermittent “stop/start” delivery vehicle engines, called the “6.2-L test”.

- *Comparison with E9-08:* No direct comparison with ACEA E9-08.

4.5.8 API CJ-4, S.2.9, Sequence IIIF—Viscosity at EOT, ASTM D6984

2.9 Sequence IIIF	ASTM D6984	Viscosity increase at EOT, maximum	%	275 MTAC	275 MTAC	275 MTAC
-------------------	------------	------------------------------------	---	----------	----------	----------

ASTM D6984, ASTM IIIF, is an interesting test method developed to evaluate petrol/gasoline and diesel automotive candidate lubricants’ performance in resisting oil viscosity increase and engine wear during moderately high-speed/high-temperature service. API CJ-4 only specifies the increase in viscosity at the EOT to be within an increment of 275 %. The engine used is a GM 3.8-L six-cylinder V6 gasoline engine, and the measured increase in viscosity is due to oxidation and not to soot accumulation. Therefore, the increase in candidate lubricant viscosity indicates its tendency to oxidize. The lubricant becomes substantially thickened and can cause oil pump starvation by insufficient liquid flowing toward the pump inlet on startup, leading to total sudden engine failure. Viscosities are measured by specified conventional laboratory means.

- *Comparison with ACEA E9-08:* ACEA uses a PDSC method to directly measure the antioxidant performance of a candidate lubricant whereas API uses an engine test, as above, to measure the oxidation resistance of a candidate lubricant as evidenced by an increase in viscosity.

4.5.9 API CJ-4/ACEA E9-08 Summary

The various engine tests in CJ-4 for candidate lubricants seek to cover all operational conditions, from steady-state, high-speed, and high-power running through to intermediate, stop/start operation. They separate multicylinder and single-cylinder effects and differentiate between thickening due to soot and oxidation and thickening due to oxidation alone. Aeration is assessed by laboratory and engine tests. API CJ-4 has evolved from previous lubricant performance specifications into a very robust specification that will last beyond its previously expected update in 2010. It is probable that this direction of lubricant performance specification has developed as far as it can to deal with emission control systems. Future developments, perhaps in API “CK-4”, will probably respond to different dimensions such as increasing levels of biofuels in diesel fuel. Low levels (up to 5 %, now up to 7 % in the EU) of biofuel in diesel are already causing problems of accelerated degradation in the form of sump biofuel accumulation, increased viscosity, enhanced gelation, and related issues of accelerated oxidation.

4.6 API SN/ILSAC GF-5 PASSENGER CAR ENGINE TEST CATEGORY FOR LUBRICANTS: COMPARISON WITH ACEA C(X)-08

ILSAC is the acronym for the International Lubricants Standardization and Approval Committee, composed of representatives from the Japan Automobile Manufacturers Association, Inc. (JAMA), Chrysler LLC, Ford Motor Company, and General Motors Corporation. Through ILSAC, these organizations have jointly developed, assembled, and approved minimal performance standards for engine sequence, bench tests, and chemical/physical properties for lubricants used in spark ignition internal combustion

engines. Although many OEMs recommend ILSAC GF-5 standards for lubricants, bearing in mind the qualification of “minimum performance standards”, individual OEMs may require compliance with additional performance parameters beyond the ILSAC GF-5 tests either set by themselves or require more stringent limits on certain tests included in the standard.

Therefore, ILSAC GF-5 is a minimum standard, the overall aims of which are improved fuel economy, improved protection for emission control systems, and improved lubricant robustness for petrol engines. GF-5 only applies to 0W(X), 5W(X), and 10W(X) multigrade oils for their energy-saving effects. It specifically does not apply to light-vehicle diesel engine use, a clear difference from ACEA C-(08) specifications. The development of ILSAC GF-5 has perhaps been more contentious than for previous GF formulations, probably because further improvements in performance have been required from performance specifications that are already very demanding indeed. As an example, this has particularly been the case for the Sequence VID fuel efficiency specification. There are several areas of ILSAC GF-5 that have been left as not definitive, and www.GF-5.com should be consulted for more information about the latest ILSAC specifications.

In that the earlier ILSAC GF-(X) lubricant performance specifications were a reaction to, and divergence from, the API S(X) series, then ILSAC GF-5 and API-SN represent almost a convergence. The essential remaining differences are that ILSAC GF-5 is concerned only with lubricant grades up to 10W-30 with the additional criterion of “energy conserving” whereas API-SN applies across a wider range of lubricant grades without the “Resource Conservation” requirement. To complicate issues further, an additional set of requirements combine API-SN with “Resource Conservation”. These are shown in Chapter 14 for “ILSAC GF-5” and “API SN Resource Conserving”, which also sets out the small differences between these and the “API SN for ILSAC Grades” and “API SN for non-ILSAC Grades”. The background to the main differences between these performance specifications is concerned with the low-viscosity grades, up to 10W-30. It is not meaningful and would be tedious to separately discuss ILSAC GF-5 and API-SN in detail when they are so similar; therefore, the former is used as a template and any differences between them commented upon appropriately.

The API S(X) petrol/gasoline light-vehicle specifications have evolved through standards now classified by the API as “obsolete”, SA to SH, for engines from earlier than 1930 up to 1996 through to those defined as “current”, from SJ (2001), SL (2004), and SM (2004) through to the latest specification, API-SN (2010), which is very closely associated with ILSAC GF-5. Therefore, it is convenient to consider ILSAC GF-5 and API SN together.

- *Comparison with ACEA C(X)-08:* Continuing the convention of examining and explaining the requirements of API-SN and ILSAC GF-5 and then comparing them with the analogous provisions of ACEA is more problematic than the previous comparison of API CJ-4 and ACEA E9-08. The light-vehicle markets in North America and Europe are different in that there is only a very small light-vehicle diesel sector in North America whereas diesel engine penetration of the European light-vehicle market is close to 50 %

and continues to increase. Therefore, the ACEA C-08 lubricant specification is for light-vehicle gasoline/petrol and diesel engines; comparisons are not entirely straightforward, and ACEA C4-08 is used as the highest quality grade.

4.6.1 ILSAC GF-5 Section 1—Viscosity Requirements

Using the ILSAC GF-5 requirements as a template, it can be seen that they are set out in a different order and sections than ACEA and API performance specifications. Thus, fresh oil specification requirements are listed in a separate Section 1 for viscosity and gelation index, SS.1a and 1b.

4.6.2 Fresh Oil Viscosity Requirements, ILSAC GF-5, 1.a & 1.b, SAE J300, and ASTM D5133

1.a Viscosity Requirements	SAE J300	Oils shall meet all of the requirements of SAE J300. Viscosity grades are limited to SAE 0W, 5W, and 10W multigrade oils for ILSAC, those and above for API-SN
1.b Gelation Index	ASTM D5133	12 maximum, to be evaluated from –5°C to the temperature at which 40,000 cP is attained or –40°C, or 2°C below the appropriate MRV TP-1 temperature (defined by SAE J300), whichever occurs first

1.a is described before in Section 4.3 for the API CJ-4 specifications but is limited for ILSAC to the lower viscosity grades, as specified above. It also applies to these and higher viscosity grades for API-SN.

- *Comparison with ACEA C4-08:* A more general approach is used that states no restrictions beyond those already defined within the latest active issue of SAE J300, except as defined by shear stability and HTHS requirements.

The Gelation Index, 1.b, ASTM D5133, measures the apparent viscosity of engine lubricants at low temperatures, a process that is not straightforward. It determines the temperature at which the candidate lubricant is unsuitable for an engine because of insufficient fluid flow to the coarse oil filter at the oil pump intake, which at low temperatures depends on the previous thermal history of the lubricant sample. This is a general problem for the apparent gelling temperature of mixed hydrocarbon fluids such as lubricants and diesel fuel and arises from their wide range of molecular weights and structures. Slower cooling rates give higher “gelling” temperatures; therefore, a standard rate is required.

A Scanning Brookfield temperature scanning viscometer applies a shear rate of approximately 0.2 s^{-1} at shear stresses below 100 Pa. Apparent viscosities are measured continuously as the sample is cooled at 1°C/h over the range of -5 to -40°C , or to the temperature at which the viscosity exceeds 40,000 cP, or to a 2°C decrement below the appropriate MRV TP-1 temperature as defined by SAE J300, whichever occurs first.

The physical manifestation of the slow rate of cooling is to maximize the formation of crystallites from the range of molecular weights in the base oil of the candidate lubricant formulation. The crystals/crystallites form interlocking networks and thicken the candidate lubricant as its

temperature slowly decreases, leading to gelation. Because a range of quite similar higher-molecular-weight hydrocarbons is present in the base oil, they give a broad spread of melting points. Hence, there is no definitive crystallization point and the eventual maximum rate of viscosity increase is the gelation index. The method also gives viscosity values and the temperature at which the gelation index occurs. The gelation index is not required for API-SN or for non-ILSAC-grade specifications.

- *Comparison with ACEA C4-08:* No gelation index test is specified.

4.7 ENGINE TEST REQUIREMENTS, ILSAC GF-5 SECTION 2

4.7.1 Wear and Oil Thickening, ILSAC GF-5 2a, ASTM D7320 Sequence IIIGA

2a Wear and Oil Thickening	ASTM Sequence IIIGA Test, ASTM D7320	Kinematic viscosity increase at 40°C, %	150, maximum
		Average weighted piston deposits, merits	4.0
		Hot stuck rings, number	None
		Average cam plus lifter wear, μm	60, maximum

The Sequence IIIGA test evaluates candidate lubricants for their resistance to thickening and engine wear under high-speed, relatively high-temperature operating conditions; it replaces the IIIF test method. After an initial 10-min running-in period, a 1996/1997 3.8-L GM V6 unleaded petrol engine ramps up over 15 min to 93 kW, 3600 r/min, and 150°C lubricant temperature and is run for 100 h.

Increased lubricant viscosities resulting from this test are indicative of a candidate lubricant's tendency to thicken because of oxidation. This may cause oil pump starvation due to insufficient lubricant flow to the pump intake in the sump and resulting in catastrophic engine bearing failure. The pass/fail limit is an increase in viscosity of 150 % over that of the fresh lubricant.

The deposit ratings for a candidate lubricant measure the tendency of the candidate lubricant to form deposits within the engine, particularly when those deposits accumulate to the extent of causing piston rings to stick in their grooves. "Stuck" rings cause loss of compression in the engine bore and thus reduce engine performance. Camshaft and lifter wear values measure the antiwear performance of a candidate test lubricant under high unit pressure contact. The IIIGA test was developed to rank oils having a range of performance as measured by oil viscosity increase and wear when run on unleaded fuels.

It is interesting to note the later development of the ROBO test, ASTM D7528, in S4.8.8 as a parallel, but possibly an alternative, bench test to the ASTM Sequence IIIGA engine test for the viscosity increase. The ROBO test is potentially attractive in giving comparable results but in a shorter time of 40 h and at a much lower cost.

- *Comparison with ACEA C4-08:* The comparison for ACEA is the CEC L-088-02 test using a Peugeot TU5JP-U petrol engine. The objectives are the same

as for the ASTM Sequence IIIGA, plus an oil consumption report but without the "cam lifter wear" provision, which is addressed in a separate test. Piston deposits, as varnish formed by a candidate lubricant, are assessed relative to those found when running a standard lubricant, RL 216, using the same test, not relative to the fresh lubricant as in the ASTM IIIGA sequence. The viscosity increase pass limit is set at 80 % or less of that for the RL216 reference lubricant.

4.7.2 Wear, Sludge, and Varnish Test, ILSAC GF-5 2b, ASTM D6593, Sequence VG

2b Wear, Sludge, and Varnish Test	Sequence VG, ASTM D6593	Average engine sludge, merits	8.0 minimum	None
		Average rocker cover sludge, merits,	8.3 minimum	
		Average engine varnish, merits,	8.9 minimum	
		Average piston skirt varnish, merits	7.5 minimum	
		Oil screen sludge, % area	15 maximum	
		Oil screen debris, % area	Rate and report	
		Hot stuck compression rings	None	
		Cold stuck rings	Rate and report	
		Oil ring clogging, % area	Rate and report	

The ASTM D6593 test method evaluates a candidate lubricant's ability to control engine deposits under operating conditions that are deliberately selected to accelerate deposit formation. The engine is a Ford 4.6-L SOHC V8, representative of many modern designs, with a test duration of 216 h, composed of 54 cycles, 4 h/cycle with three stages for each cycle. The test method correlates with field service data from comparative tests of two or more oils in intermittent, stop/go service such as police, taxi, and particularly delivery services. The same field service oils were then used in developing the operating conditions of this test procedure. The parameters measured are self-explanatory, concentrating on measuring varnish and sludge formation in different parts of the engine, and the effects of such deposits on the piston rings.

- *Comparison with ACEA C4-08:* ACEA uses the same ASTM Sequence VG test as the ILSAC GF-5 2b test and specifically states that it is a 'Low Temperature Sludge' test. Its format is the same but with very slight numerical differences for sludge and varnish values. Stuck ring requirements are the same. ACEA C4-08 specifies a limit of 20 % for oil screen sludge whereas ILSAC GF-5 states 15 % for the same, and 'rate and report' for oil ring clogging and oil screen debris.

4.7.3 Valvetrain Wear, ILSAC GF-5 2c, ASTM D6891 Sequence IVA

2c Valvetrain Wear	Sequence IVA, ASTM 6891	Average cam wear seven-position average), μm	90 maximum
---------------------------	-------------------------	---	------------

ASTM Sequence IVA, D6891, measures the candidate lubricant's ability to control valvetrain wear during stop/go, intermittent/short distance conditions and during extended idling, conditions that are representative of urban driving. The test evaluates cam lobe wear at low-temperature and low-speed conditions and cross-references to the ASTM Sequence IIIGA test. The 2.4-L Nissan engine design is a four-cylinder, in-line engine, and the test length is 100 h, with repetitively cycled stages of 50 and 10 min at 800 and 1500 r/min, respectively. Average cam lobe wear is determined by summing the measurements at seven positions for each of the 12 cams, then determining the average, maximal tolerance of 90 μm .

- *Comparison with ACEA C4-08:* The ACEA cam wear test is CECL-038-S4(TU3M), using the Peugeot TU3M engine configuration but sets maxima and average limits for cam wear and also average pad wear.

4.7.4 Bearing Corrosion, ILSAC GF-5 2d, ASTM D6709, Sequence VIII

2d Bearing Corrosion	Sequence VIII, ASTM D6709	Bearing loss Max. 26 mg 2266	
-----------------------------	---------------------------	------------------------------	--

ASTM D6709, Sequence VIII, evaluates the ability of a candidate to prevent corrosion of Cu and Pb bearings by a hot lubricant in a LABECO single-cylinder petrol engine. The test runs for 40 h at 3150 r/min with a candidate lubricant temperature of 143°C, which is an aggressive environment. The big-end bearing weight loss pass/fail parameter is 26 mg.

- *Comparison with ACEA C4-08:* There is no direct comparison.

4.7.5 Fuel Efficiency, ILSAC GF-5 2e, ASTM D7589, Sequence VID

2e Fuel Efficiency	Sequence VID ASTM D7589	SAE XW-20 viscosity grade	2.6 % fuel efficiency increase (FEI) SUM 1.2 % FEI 2 minimum after 100 h aging
		SAE XW-30 viscosity grade	1.9 % FEI SUM, 0.9 % FEI 2 minimum after 100 h aging
		SAE 10W-30 and all other viscosity grades not listed above	1.5 % FEI SUM, 0.6 % FEI 2 minimum after 100 h aging

The distinctive feature of the ILSAC GF-series is the fuel economy test, ASTM D7589, (Sequence VID), which is designed to give a comparative fuel-saving capability index of candidate lubricants. The test measures the fuel economy effects of automotive lubricants of passenger/

light-duty vehicles, defined as 3856 kg or less gross vehicle weight (GVW). The test compares a candidate lubricant against an established standard, fully formulated, SAE 20W-30 reference lubricant under repeatable laboratory conditions. The test measures fuel consumption over a simulated driving cycle, similar to the concept of the drive cycle for the automotive emissions test.

A 2008 3.6-L V6 GM gasoline engine/dynamometer system with an external oil temperature control system uses a “flying flush” system to change lubricants “on the fly” (i.e., without engine shutdowns). Fuel consumption is measured twice at each of six speed/load/temperature test conditions for the reference lubricant. The candidate lubricant is then introduced into the running engine and run under aging conditions for 16 h. Fuel consumption is then measured for each of the six test conditions. The candidate oil remains in the engine under aging conditions for a further 84 h, and the fuel consumption is measured again, as before. Finally, the reference lubricant is replaced in the engine, and the fuel consumption for the reference lubricant is measured again at the six test conditions.

The test results are given as a percentage change in fuel consumption for the candidate lubricant after Aging Phase I, relative to the reference lubricant, and similarly after Aging Phase II. The procedure addresses the longevity of the fuel efficiency effect, giving pass/fail values after 16 and then 100 h of testing for the separate levels of formulation viscosity as in the table for this subsection. A fuel efficiency requirement is not included in API-SN for ILSAC grades or for API-SN for non-ILSAC grades.

Comparison with ACEA C4-08 2.5: ACEA's approach is similar to GF-5 2e, but it is different in detail because it uses a Mercedes M111 engine under the CEC L 54-T-96 procedure with a 15W-40 RL191 reference lubricant. The engine test profile is based on the European emissions measurement procedure using a chassis dynamometer with a 2.0-L Mercedes-Benz M111 E20 four-cylinder gasoline engine. The 24-h test procedure runs a cycle commencing with the RL191 reference oil and uses a “flying flush” to change to the candidate oil, then runs the procedure cycle three times on the candidate oil. That part of the procedure using the candidate oil incorporates steady-state aging. The cycle has two parts composed of eight stages with varying speeds, loads, and coolant and oil temperatures over a period of 2 h, 24 min, and 10 s. Fuel consumption is measured under cyclic conditions over the two-part cycle. The remaining total time of the procedure is for a stabilization period between procedure cycles and flushing between reference and candidate lubricant. There is no used lubricant analysis. The pass requirement for fuel economy improvement is 1 % or greater increment for XW-30 grades over the duration of the test relative to the reference RL191 lubricant, but there is no longevity requirement of 0.9 % increment after 100 h of aging as in GF-5 2e. The formats of the ACEA/ILSAC fuel economy tests are similar but differ in detail (e.g., the reference lubricant grades are different, the two engines used reflect respective North American and European practice, and the engine cycles used are different). However, the similarities between the two tests are much greater than their differences, with the latter reflecting differences between continental practices.

4.7.6 Additional ACEA C4-08 Engine Test Requirements

There are four additional engine test requirements for ACEA C4-08 compared with ILSAC GF-5:

1. *Black Sludge test, ACEA C4-08 2.4:* CEC L-053-96, using the Mercedes M111 engine, evaluates the ability of a candidate lubricant to resist black sludge formation and deposition of sludge using a specially formulated fuel that exacerbates these problems. The full procedure also measures wear, but ACEA C4-08 only specifies black sludge measurement. The hardware specifies a four-cylinder 2.0L Mercedes-Benz M111 E20 gasoline engine/dynamometer, otherwise standard but for a water-cooled rocker cover, to simulate typical European urban, rural, and motorway driving use. The test protocol specifies a 5-L candidate lubricant fill and a complex 257-h procedure composed of four different phases, each with different operating cycles. The pass/fail criterion for ACEA C4-08 is $\geq \text{RL140} + 4\sigma$ or ≥ 9.0 , with RL140 being the reference lubricant.
2. *Medium-Temperature Dispersivity, ACEA C4-08 2.6:* CEC L-093-04 uses a Peugeot DV4TD four-cylinder, in-line, common rail diesel engine/dynamometer to evaluate the effect of combustion soot on increasing engine oil viscosity and piston cleanliness under simulated high-speed highway service in a diesel-powered passenger vehicle. After a 10-h run-in, the engine is operated continuously for 240 cycles of 30 min, with each cycle varying between 2 min of idling and 27 min of high power, with a 30-s ramp between each power level and with controlled engine coolant and lubricant temperatures. Lubricant samples are taken each 24 h during the 120-h test, and their 100°C kinematic viscosity, percentage soot, and iron contents are measured. The final lubricant sample is used together with the 24-h intermediate samples to interpolate the absolute viscosity increase at 6 % soot. Pistons and rings are rated for lacquer deposits and ring sticking. The viscosity increment pass/fail criterion is 0.60 of that for an RL 223 reference lubricant or less. The limit for the piston merit is 2.5 points or greater relative to RL223. There is no comparative test with ILSAC GF-5 because this is a test for candidate lubricants for light-vehicle diesel engines, for which there is no substantial market in North America. The test for increased sooted viscosity is analogous to the Sooted Oil test, ASTM D7156, in API CJ-4 S.2.1, but for much smaller engines. The (diesel) piston deposit measurement is analogous to the (petrol) ASTM D6593 Sequence VG, but with substantially different values.
3. *Wear, ACEA C4-08 2.7:* CEC L-099-08 is an interesting additional test that addresses valvetrain and bore wear in diesel engines fueled by a standard diesel containing 5 % fatty acid methyl ester (FAME). This is a particular EU concern where the EN590 diesel specification now allows up to 7 % FAME content and the test conditions will no doubt be increased in the future to reflect the increased fuel specification limit. It has required a new engine, the OM646LA, because the previous OM602 was no longer available and no longer representative of current European engine design. The test procedure has a 300-h alternating cycle with candidate lubricant sampled every 50 h. It evaluates inlet and outlet cam

and tappet wear, cylinder wear, and bore polish. Piston cleanliness and engine sludge are “report” items.

4. *Direct-Injection Diesel Piston Cleanliness and Ring Sticking, ACEA C4-08 2.8:* CEC L-078-99 evaluates candidate lubricant performance concerning piston cleanliness and piston ring sticking. The test simulates European high-speed highway operation, followed by idling, and uses a VW 1.9L in-line, four-cylinder, direct-injection, turbo-charged diesel engine/dynamometer known as “VW TDI”. The test format is 54 h, composed of 18 cycles, each of two power level phases of (1) idling for 30 min with a sump temperature of 40°C and (2) 4150 r/min and at full power for 150 min with a sump temperature of 145°C. Pass/fail criteria are based on the average piston cleanliness merit relative to the reference lubricant RL206, average ring sticking, and EOT TBN by ASTM D664 (“report”). An additional EOT TBN requirement reflects the increasing emphasis on the candidate lubricant to “stay in grade” during service use.

4.8 ILSAC GF-5 BENCH TEST REQUIREMENTS

4.8.1 Maximum Phosphorus Content and Volatility, Maximum Sulfur Content, ILSAC GF-5, 3a, ASTM D4951/7320/2622

3a Catalyst Compatibility	ASTM D4951	Phosphorus Content	0.08 % (mass) maximum
	ASTM D7320	Phosphorus Volatility	79 % phosphorus retention (Sequence IIIGB)
	ASTM D4951 or D2622	Sulfur content, 0W-XX, 5W-XX 10W-30	0.5 % (mass) maximum 0.6 % (mass) maximum

This requirement concerns the durability of the three-way catalytic converter emission control system for petrol/gasoline engines as it is affected by phosphorus and sulphur carried over from the candidate lubricant. These elements can cause deterioration of the catalytic converter and render it ineffective. Part of the test is a minor variant on the test used in 2a as the Sequence IIIGB (EOT) Bench Test. The first and third parts are concerned with phosphorus and sulphur contents in fresh candidate lubricants, respectively, and ASTM D4951 specifies how they will be analyzed using an ICP emission spectrophotometer.

The second part of 3a is concerned with the volatility of the phosphorus content of the additive. Higher molecular weight phosphorus compounds have lower volatility and will be more likely to be retained in the lubricant. The test measures the percentage ‘Phosphorus Retention’ in the End-of-Test, 100 hr, sample from the Sequence IIIGB test, and requires 79 % retention. Only ILSAC GF-5 and API-SN Resource Conserving specifications require the 79 % retention limit and also the 0.06 % minimum/0.08 % (by mass) maximum. API-SN for ILSAC GF-5 or non-ILSAC grades only set a 0.06 % phosphorus minimum and no sulphur limits for the 0W-and 5W-10X grades.

Comparison with ACEA C4-08 1.5 and 1.6: Apart from not requiring a measure of phosphorus retention, ACEA C4-08 1.5 and 1.6 are comparable to ILSAC GF-5 but the detail is different, where ACEA C4-08 sets a limit of

sulphur of ≤ 0.2 % m/m against 0.5 % or 0.6 % m/m dependent upon viscosity grade, for ILSAC GF-5. Phosphorus has a limit of ≤ 0.09 %, slightly higher than the 0.08 % value set by ILSAC GF-5. Further differences are that ILSAC GF-5 requires the ASTM D4951 method for phosphorus and sulphur determination, developed for the analysis of fresh lubricants using an internal standard whereas ACEA C4-08 requires ASTM D5185 using an optional internal standard method developed for used lubricants.

4.8.1.1 MINIMUM PHOSPHORUS CONTENT, ILSAC GF-5, 3b, ASTM D4951

3b Wear	ASTM D4951	Phosphorus Content	0.06 % (mass) minimum
----------------	------------	--------------------	-----------------------

Whilst **3a** sets an upper bound for phosphorus content of 0.08 % on the basis of catalytic convertor durability, **3b** sets a lower bound of 0.06 for the anti-wear concentration of phosphorus in additive compounds. The ASTM D4951, ICP emission spectrophotometer analytical method used is defined in 3a.

Comparison with ACEA C4-08: No lower bound is set for the phosphorus content of candidate lubricants.

4.8.1.2 VOLATILITY/EVAPORATIVE LOSS, ILSAC GF-5, 3c, ASTM D5800/6417

3c Volatility	ASTM D5800	Evaporation Loss	15 % maximum, 1 hr at 250°C
	ASTM D6417	Simulated Distillation	Note: Calculated conversions specified in D5800 are allowed.
			10 % maximum at 371°C

This requirement is, in part, the same as for API CJ-4, Section 1a for 10W-30 candidate lubricants, using the Noack method, ASTM D5800 and CEC L-40-93. The simulated distillation method, ASTM D6417 is an alternative using capillary gas chromatography but is not directly equivalent to ASTM D5800. The test measures the amount of the candidate lubricant volatilized at 371°C (700°F); the limit in this case is 10 %. Results from this method may be biased by polymeric additive materials or heavy base oil components not being completely eluted from the column and calculated conversions allow for this.

Comparison with ACEA C4-08, 1.4: The determination method is the same, CEC L-40-93, as the Noack test, but the limits are set lower at 11 % for ACEA C4-08 as compared with 15 % for ILSAC GF-5. The difference reflects the emphasis towards lower viscosity grades for ILSAC GF-5 and thus a higher level of volatility.

4.8.1.3 HIGH TEMPERATURE DEPOSIT FORMING TENDENCIES, ASTM D7097, D6335, ILSAC GF-5, 3d AND 3e,

3d High Temperature Deposits	TEOST MHT, ASTM D7097	Deposit Weight, mg	35 maximum
-------------------------------------	-----------------------	--------------------	------------

The **3d** TEOST MHT-4 and **3e**, TEOST 33C, are tests are both designed to evaluate the high temperature deposit forming tendencies of candidate lubricants but the procedures are

quite different. The different test conditions give different assessments of the candidate lubricant's high temperature deposit forming tendency. MHT-4, ASTM D7097, is a constant condition bench test which is run at 285°C for 24 hours in a specific apparatus. Its purpose is to predict the tendency of a candidate lubricant to form moderately high temperature piston deposits based on the deposits formed on a heated metal rod. The test limit in this case is 35 mg for ILSAC GF-5, API-SN Resource Conserving and API-SN for ILSAC grade specifications and 45 mg for API-SN for non-ILSAC grades.

3e High Temperature Deposits	TEOST 33C, ASTM D6335	Total Deposit Weight, mg,	30 maximum. Note: No TEOST 33C limit for SAE 0W-20
-------------------------------------	-----------------------	---------------------------	--

The Thermo-Oxidation Engine Oil Simulation (Bench) Test, ASTM D6335, assesses a candidate lubricants high temperature deposit forming tendency in a different manner. The test is known as 'TEOST® 33C' and is designed to protect turbochargers. These level of use of these engine components continually vary, and thus their operating temperature, the method cycles twelve times between 200°C and 480°C for two hours to simulate the cyclic temperatures encountered by a lubricant in a turbocharged, petrol/gasoline fueled, engine. Deposits accumulated over the test are measured as an increase in weight on a hollow heated rod (TEOST® Depositor Rod) over which the candidate lubricant oil flows at a specified rate. The limiting weight gain in this test is 30 mg and applies only to ILSAC GF-5 and API-SN Resource Conserving Grades. The apparatus used is the same as for **3d** above but with different conditions

Comparison with ACEA C4-08: No high temperature deposit forming tendency laboratory test requirement is set in ACEA C4-08.

4.8.1.4 FILTERABILITY, ILSAC GF-5, 3f, ASTM D6794 AND D6795

3f Filterability	ASTM D6794, "EOWTT"	with 0.6 % H ₂ O	50 % maximum flow reduction
		with 1.0 % H ₂ O	50 % maximum flow reduction
		with 2.0 % H ₂ O	50 % maximum flow reduction
		with 3.0 % H ₂ O	50 % maximum flow reduction
	ASTM D6795 "EOFT"	Test formulation with highest additive (DI/VI) concentration. Read-across results to all other base oil/viscosity grade formulations using the same or lower concentration of the identical additive (DI/VI) combination. Each different DI/VI combination must be tested.	
			50 % maximum flow reduction

These tests are closely related and assess the tendency of a candidate lubricant to plug an oil filter by forming precipitates by reaction with water present in the system. It simulates problems that may be experienced by a new engine that has been repeatedly operated for a series of very short periods, such as immediately after production, storage, or delivery movements. Combustion condensate water accumulates in the lubricant. After a long period of storage with some water or other combustion products present, these substances can affect the filterability of the lubricant to the extent that the oil filter is plugged, with catastrophic results to the engine.

EOWTT is the lubricant water tolerance test and consists of treating the candidate lubricant with the specified levels of water, heating it to 70°C for 6 h and then storing at room temperature for 48 h in the dark. The lubricant is then passed through a 25- μ m automotive filter and the flow rate is recorded and compared with those of a fresh oil sample and a reference oil. The levels of added water are set out in the test specification, from 0.6 to 3.0 %. EOFT is the filterability test and very similar to EOWTT, but the sample is only heated for 30 min.

- *Comparison with ACEA C4-08:* No filterability standard is set for ACEA C4-08.

4.8.2 Fresh Oil Foaming Characteristics, ILSAC GF-5, 3g, ASTM D892

3g Fresh Oil Foaming Characteristics	ASTM D892 (Option A and excluding paragraph 11).	Tendency/Stability*	
		Sequence I	10 ml maximum 0 ml maximum
		Sequence II	50 ml maximum 0 ml maximum
		Sequence III	10 ml maximum 0 ml maximum
		*After a 1-min settling period	

The fresh oil foaming characteristics for ILSAC GF-5 are determined using the same procedure for API CJ-4 but with different limits. The criterion of 1-min foam settling is for ILSAC-5, API SN (Resource Conserving) and API-SN for ILSAC grades; the foam settling time is 10 min for API-SN non-ILSAC grades.

- *Comparison with ACEA C4-08 1.11:* Identical requirements to ILSAC GF-5 3g.

4.8.3 Fresh Oil High-Temperature Foaming Characteristics, ILSAC GF-5 3h, ASTM D6082

3h Fresh Oil High-Temperature Foaming Characteristics	ASTM D6082 (Option A)	Tendency/stability* *After 1-min settling period	100 ml maximum 0 ml maximum
---	-----------------------	---	--------------------------------

A measured quantity of the candidate lubricant is pre-treated by heating to 49°C for 30 min and then cooled to room temperature. The sample is then heated to 150°C in a 1-L graduated cylinder and aerated with dry air through a metal diffuser at a rate of 200 mL/min for 5 min. For this

requirement the volume of foam generated before disconnecting the air and the volume amount of static foam after a 1-min settling period are recorded

- *Comparison with ACEA C4-08 1.12:* Identical requirements to ILSAC GF-5 3h.

4.8.4 ROBO Test, ILSAC GF-5, 3i, ASTM D7528

The ROBO test evaluates the used lubricant low-temperature viscosity performance of candidate lubricants. A sample is mixed with a ferrocene catalyst in a reaction vessel, heated, and then stirred with NO₂ and air for 40 h at 170°C. The introduction of this test is interesting because it simulates the ASTM Sequence IIIGA engine test and is quicker (40 vs. 100 h) and less expensive compared with the fired engine test. It produces comparable lubricant aging characteristics to those from the ASTM TMC Sequence IIIGA matrix ASTM reference oils 434, 435, and 438 after aging in the Sequence IIIG engine test. The aged oils are then tested for kinematic viscosity and for low-temperature pumpability properties as described in the Sequence IIIGA engine test, Appendix X1 of Test Method D7320. A range of conditions apply for the subsequent testing of the samples:

1. If the CCS viscosity measured is less than or equal to the maximum CCS viscosity specified for the original viscosity grade, then run ASTM D4684 (MRV TP-1) at the MRV temperature specified in SAE J300 for the original viscosity grade.
2. If the CCS viscosity measured is greater than or equal to the maximum viscosity specified for the original viscosity grade in SAE J300, then run ASTM D4684 (MRV TP-1) at 5°C higher temperature (i.e., at the MRV temperature specified in SAE J300 for the next higher viscosity grade).
3. The EOT ROBO sample must show no yield stress in the ASTM D4684 test. Its D4684 viscosity must be below the maximum specified in SAE J300 for the original viscosity grade, or the next higher viscosity grade, depending on the CCS viscosity, as outlined in 1 or 2 above, or "Aged Oil Low Temperature Viscosity," ASTM Sequence IIIGA Test, ASTM D7320.

The ROBO test does not apply to the API-SN for non-ILSAC-grade specifications.

Comparison with ACEA C4-08: The ROBO test is new to ILSAC GF-5 and has no comparative or analogous test in ACEA C4-08.

4.8.5 Shear Stability, ILSAC GF-5, 3j, ASTM D6709

3j Shear Stability	Sequence VIII, ASTM D6709	10-h stripped kinematic viscosity at 100°C	Kinematic viscosity must remain in original SAE viscosity grade.
--------------------	---------------------------	--	--

The ASTM D6709 test method evaluates lubricants for their ability to protect petrol engines against the effects of oxidation during high-temperature and severe service conditions. This is assessed by bearing weight loss and the 100°C kinematic viscosity of the lubricant at the end of the 40-h test, although ILSAC GF-5 only specifies the viscosity increase. The lubricant must remain in its original SAE grade at the end of the test; multigrade oils require a 10-h "stripped"

sample viscosity. Sequence VIII uses a carburetted, spark ignition, Cooperative Lubrication Research test engine using unleaded petrol/gasoline fuel.

- *Comparison with ACEA C4-08 1.2:* A diesel fuel-type injector apparatus is used to measure the 100°C viscosity of the candidate lubricant for shear stability after 30 passes through the test.

4.8.6 Homogeneity and Miscibility, ILSAC GF-5, 3k, ASTM D6922

3k Homogeneity and Miscibility	ASTM D6922	Shall remain homogeneous and, when mixed with TMC reference oils, shall remain miscible
---------------------------------------	------------	---

The aim of the ASTM D6922 test is to ensure that different lubricants from different sources can be homogeneous and miscible. Engine damage can occur if lubricants are combined that do not homogenize and function properly. ASTM D6922 defines a test method to determine if a candidate lubricant will remain homogenized with standard reference lubricants, in this case TMC reference lubricants, after subjection to a prescribed cycle of temperature variations.

- *Comparison with ACEA C4-08:* No analogous test.

4.8.7 Engine Rusting, ILSAC GF-5, 3l, ASTM D6557

3l Engine Rusting	Ball rust test, ASTM D6557	Average gray value	100 minimum
--------------------------	----------------------------	--------------------	-------------

The BRT (ball rust test), ASTM D6557, bench-test measures the ability of a candidate lubricant to prevent corrosion of internal engine parts in service when water and acid build-up occur. The test takes 18 h at 48°C during which a hydraulic tappet lifter ball is agitated and exposed to an acid/water solution in air. The measured parameter is the “gray value rating” of the ball using the reflective intensity as an indicator of surface area corrosion.

- *Comparison with ACEA C4-08:* No analogous test.

4.8.8 Emulsion Retention, ILSAC GF-5, 3m, ASTM D7563

3m Emulsion Retention	ASTM D7563 oil mixed with 10 % water, 10 % E85	The oil when blended* with a mixture of 10 % distilled water and 10 % E85 shall retain a fluid emulsion for the time and temperature specified. * Waring blender or equivalent—1 min maximum at room temperature. E85 solution = 85 % ethanol, 15 % gasoline	0°C, 24 h, no water separation 25°C, 24 h, no water separation
------------------------------	--	--	---

The Emulsion Retention test is a relatively new test included in response to the increasing use of biofuels such as E85, which is composed of 85 % ethanol and 15 % petrol/gasoline. These fuels may be used in “Flexible Fuel” vehicles. The alcohol/hydrocarbon mixture can retain water as an emulsion, but the water may separate out and cause problems, particularly when temperatures are below freez-

ing. The test procedure blends the candidate lubricant with 10 % water and 10 % E85 fuel using a domestic blender for 1 min. The pass criterion is that there is no subsequent water separation over 24 h at 0 and 25°C. This test does not apply to the API-SN for ILSAC or non-ILSAC-grade specifications.

- *Comparison with ACEA C4-08:* No analogous test, possibly because alcohol bio-petrol fuels do not have the market penetration in Europe that they have in North America.

4.8.9 Elastomer Compatibility, ILSAC GF-5, 3o, ASTM D7216 and SAE J2643

The Seal Compatibility bench test, ASTM D7216, evaluates candidate lubricant compatibility with typical automotive seal materials. It evaluates the physical properties of the seal materials after 336 h of immersion in the candidate oil to ensure that they will retain their shape, elasticity, and strength over the life of the vehicle. Seal compatibility is necessary to prevent lubricant passing through the many seals on rotating shafts for leak-free engines.

3o Candidate oil testing for elastomer compatibility shall be performed using the five standard reference elastomers (SREs) referenced herein and defined in SAE J2643. Candidate oil testing shall be performed according to ASTM D7216, which includes 336 h of immersion at 100°C for HNBR and 150°C for ACM, VMQ, FKM, and AEM. The postcandidate oil-immersion elastomers shall conform to the specification limits detailed herein (SAE J2643).

Elastomer Material	Test Procedure	Material Property	Units	Limits
Polyacrylate Rubber (ACM-1)	ASTM D471 ASTM D2240 ASTM D412	Volume Hardness Tensile Strength	% Δ points % Δ	–5, 9 10, 10 40, 40
Hydrogenated Nitrile Rubber (HNBR-1)	ASTM D471 ASTM D2240 ASTM D412	Volume Hardness Tensile Strength	% Δ points % Δ	–5, 10 –10, 5 –20, 15
Silicone Rubber (VMQ-1)	ASTM D471 ASTM D2240 ASTM D412	Volume Hardness Tensile Strength	% Δ points % Δ	–5, 40 –30, 10 –50, 5
Fluorocarbon Rubber (FKM-1)	ASTM D471 ASTM D2240 ASTM D412	Volume Hardness Tensile Strength	% Δ points % Δ	–2, 3 –6, 6 –65, 10
Ethylene Acrylic Rubber (AEM-1)	ASTM D471 ASTM D2240 ASTM D412	Volume Hardness Tensile Strength	% Δ points % Δ	–5, 30 –20, 10 –30, 30

- *Comparison with ACEA C4-08 1.10:* Although the aim of ACEA C4-08 1.10 is the same as ILSAC GF-5 3o, there are differences (1) because an additional measure of volume variation is included; (2) where the tests are conducted differently in respect to time and temperature of exposure; (3) elastomers are defined differently as RE1 through to RE4 plus AEM (Vamac) in VDA 675301; and (4) the values of changes in physical

properties after exposure are different for ACEA C4-08, 1.10. The Elastomer Compatibility physical test pass/fail values for ACEA C4-08 are slightly different from those for ACEA E9-08 for the same materials.

4.8.10 Additional ACEA C4-08 Engine Test Requirements

There are three additional laboratory test requirements for ACEA C4-08 compared with ILSAC GF-5:

1. *Sulfated Ash, ACEA C4-08 1.7*: As previously described in S4.4.5 for API CJ-4, (Section 1.8 “Chemical Limits” by ASTM D874 and D4951), “Sulfated Ash” is important from the heavy-duty diesel application part of C4-08 lubricants when applied to light vehicles. The determination method is the same, ASTM D874, but the pass/fail limit is set lower at 0.8 % m/m or less.
2. *Chlorine, ACEA C4-08 1.8*: The Cl content of a candidate lubricant is required as a “report” in parts per million, m/m, by ASTM D6443.
3. *TBN, ACEA C4-08 1.9*: The TBN of a candidate lubricant is required to be 6.0 mg KOH/g or greater by ASTM D2896. This lower bound reflects the need for an alkaline reserve, TBN, in the candidate lubricant although the conventional acidity generated by the sulfur of primarily diesel, but also petrol, fuels has decreased to very low levels.

4.8.11 Commonalities and Differences

The ILSAC GF-5 and API SN specifications on one hand and those for ACEA C4-08 on the other seek to ensure the suitability of lubricants for use in light-duty vehicles by setting limits for

- Oxidative and thermal stability,
- The effects of contaminants,
- Wear and corrosion of engine components,
- Viscosity stability and shear stability over time,
- Antifoaming tendencies under various conditions, and
- Fuel economy for fresh lubricants and its retention for degraded lubricants.

Where test performance specifications are very similar, the differences lie in the interpretation of detail or minor differences in values. In other cases, such as for some of the engine tests, the differences between ILSAC GF-5/API-SN and ACEA C(X)-08 reflect the differences in engine design and use between North America/Japan and Europe. As a subset of those differences, ACEA C(X)-08 performance specifications cover petrol- and diesel-fueled light vehicles whereas ILSAC GF-5/API-SN only applies to petrol light vehicles. These differences are reflected in the additional diesel engine tests specified within ACEA C(X)-08. Another aspect of this subset are the different emphases of fuel effects on lubricant degradation; ACEA C(X)-08 addresses the issue of “extender” oils derived from vegetable sources with a present test limit of 5 %, probably soon to be extended to the current 7 % in EU diesel fuel EN590, whereas ILSAC GF-5/API SN North America and Japan are concerned with the emulsion test for alcohol-extended petrol with water.

4.9 CONCLUSIONS—CONVERGENCE?

In both areas of heavy-duty diesel and light-vehicle lubricant degradation, the laboratory and engine tests assembled as the API Tripartite/ILSAC and ACEA lubricant

performance specifications are fundamentally similar. The ILSAC GF-5 and the API Tripartite SN lubricant performance specifications have converged after 2–3 decades of separation and are now the same for the lighter viscosity grades. There is substantial overlap between ILSAC GF-5/API SN and ACEA C4-08. The remaining minor differences arise from different engine design and use philosophies as well as different responses to the introduction of the different biofuels—either biodiesel or bioethanol.

The same convergence can be seen for the API CJ-4 and ACEA E(X)-09 lubricant performance specifications. Amongst other tests, both deal with the degradation of lubricants induced by environmental emission controls, primarily that of the effect of soot and biodiesel fuel dilution on the degradation of longer service period lubricant charges.

The improvements in lubricant performance over the previous specification required for the API CJ-4 and ACEA E(X)-08 specifications have been particularly difficult to achieve. This is because of the advanced nature of previous formulations and the effort necessary to deliver and reproducibly demonstrate the increasingly smaller performance increments. Minor details for ILSAC GF-5 and API SN were still being settled in mid-2010, a difference from previous lubricant performance specifications in which they had been essentially established at their time of publication. Further challenges are the effect of various biofuels, as additives to petrol/gasoline or as base fuel, in which the residual/partially burned products transfer to the sump and affect lubricant performance. The longer term intention is to further increase the percentage of bio-based material in fuels, which will exacerbate the problems they are already causing in lubricants, such as fuel contamination. Increased bio-fuel content may need review and extension of lubricant specifications.

However, the longer-term question posed is whether the separate API Tripartite and ACEA assemblies of lubricant tests on fresh and used candidate lubricants can continue to be justified. Tests proliferate even after stringent review of their need and test limits become more demanding; together these increase the already formidable cost of developing lubricants. Whereas multiple organizations, once well established, are always very difficult to rationalize, the escalating costs of candidate lubricant degradation testing and control may well take decisions away from the relevant bodies. The need to reduce costs and improve response times may lead the international automotive industry to look for global economies of scale by reducing lubricant performance specification systems to one encompassing system. The alternative is that very large automotive companies will produce their own global specification systems, as GM has with dexos. Other major automotive OEMs such as VW and Daimler-Benz are increasingly taking the current Tripartite API and ACEA specifications as de minimus standards and adding other more demanding operating requirement characteristics to meet increased lubricant service intervals to deal with direct-injection fuel systems, turbocharging, or other fuels such as compressed natural or liquid petroleum gases and biofuels. From the comparative commentary given above for heavy-duty diesel and light-vehicle systems for controlling the degradation of their respective lubricants, it is difficult to argue against a

unified system of performance specifications to control the degradation of lubricant in service life.

Bibliography

The API system is described in “Engine Service Classification and Guide to Crankcase Oil Selection,” API Bulletin 1509API, available at <http://www.api.org/publications/> and <http://www.api.org/certifications/engineoil/pubs/index.cfm>. Navigate to the “Engine Oil Licensing and Certification System” (EOLCS) to access the Engine Oil and Lubricants Publications.

The detailed information contained within the extensive references to ASTM test procedures can be accessed through [http://www.astm/Standards/D\(Relevant Standard Number Requested\)](http://www.astm/Standards/D(Relevant%20Standard%20Number%20Requested)).

CEC tests for ACEA are accessed via the CEC website at <http://www.cectests.org>; follow the link to “lubricants”.

ILSAC: follow <http://api-ep.api.org/filelibrary/15tech2rev.pdf>.

Infineum and Lubrizol provide excellent tabular summaries of current API and ACEA specification and testing sequences on their respective websites.

References

- [1] Toms, L.A., 1998, *Machinery Oil Analysis*, 2nd ed., Coastal Skills and Training, Virginia Beach, VA.
- [2] Fox, M.F., 2010, “Automotive Lubricant Specification and Testing.” In *The Chemistry and Technology of Lubricants*, 3rd ed., R.M. Mortier, S. Orszulik, and M.F. Fox, Eds., Springer, London.
- [3] Haycock, R.F., and Hillier, J.E., Eds., 2004, *Automotive Lubricants Reference Book*, 2nd ed., Professional Engineering Publications Ltd, London.
- [4] Mang T., and Dresel, W., Eds., 2001, *Lubricants and Lubrication*, Wiley-VCH, Weinheim, Germany.
- [5] ASTM D7528: Standard Test Method for Bench Oxidation of Engine Oils by ROBO Apparatus, *Annual Book of ASTM Standards*, ASTM International, West Conshohocken, PA, 2012.
- [6] Stambaugh, R.L., and Kinker, B.G., 2010, “Viscosity Index Improvers and Thickeners.” In *The Chemistry and Technology of Lubricants*, 3rd ed., R.M. Mortier, S. Orszulik, and M.F. Fox, Eds., Springer, London.

Elastohydrodynamic Lubrication Film Tests and Tribological Bench Tests

Q. Wang,¹ Simon C. Tung,² Y. Liu,³ Y. Zhang,⁴ and D. Zhu⁵

5.1 ELASTOHYDRODYNAMIC LUBRICATION EXPERIMENTAL TECHNIQUES, EXPERIMENTS, AND COMPARISON WITH SIMULATION RESULTS

Elastohydrodynamic lubrication (EHL) film thickness suggests the capability of a lubricant to support load under a set of hydrodynamic conditions. It is related to the rheological properties of a lubricant, contact geometry, materials properties, and operating conditions such as load, speed, and temperature. Film thickness variation with speed or load may follow the prediction made with the theory of EHL. Experimental techniques based on capacity [1-3]; electrical conductivity and contact resistance [4-6]; discharge voltage [7]; X-ray transmission [8]; indirect laser transmission [9,10]; R-C oscillation technique [11]; and optical interferometry [12-35] have been used in EHL experiments for film-thickness measurement. On the other hand, as a result of the rapid development of high-speed computers, in-depth and detailed numerical analyses of EHL problems intend to become a routine practice. More influential factors can be considered now in EHL calculations: several non-Newtonian properties of a lubricant [30,31,36-38], surface roughness [32,33,37,38], the thermal effect [34,39,40], and non-steady-state transitions [35,41,42] have been included in a number of simulation models. Moreover, mixed lubrication simulations based on digitized real rough surfaces have been conducted in wider ranges of speed and load [36,37]. This section reviews and discusses the existing techniques for EHL film-thickness measurements, views of measurement data, and comparisons of measurement results with EHL simulation solutions.

5.1.1 EHL Film Thickness and Measurement Techniques

5.1.1.1 CAPACITANCE METHODS

It is well known that capacitance is related to the areas of two plates and the distance between them. Therefore, the value of capacitance reflects the distance between two plates if the areas of the plates are known. The capacitance method has been widely used for the measurement of film-thickness in metal-metal EHL contacts, such as those in bearings and between piston liners and rings.

Crook [1] measured the film thickness between two surfaces by means of the capacitance between a pad and a disk. This capacitance value was related to the lubricant flux between these surfaces. However, the flux is a function of the film thickness between two surfaces. This method

is only suitable for measuring the film thickness in a full-film lubrication, and it is difficult to determine the film shape with this technique. The DC and AC conductivity techniques [2] were used to measure bearing electrical capacitance and to estimate the degree of surface separation in unmodified rolling bearings. To remove the possible filter action, a capacitive voltage divider was used to substitute the resistive voltage divider. The capacitance gaging method [3] was used to determine film shapes, in which a platinum stripe deposited on a disk formed one plate of the variable capacitor whereas the surface of a steel disk was the other. The change in thickness of the film separating the plates resulted in a change in capacitance. However, the resolution of the measured film shape was apparently coarse.

5.1.1.2 RESISTANCE METHOD

The ability of metal to conduct electric charge is better than that of a lubricant. When an oil film separates two moving metallic parts, the ability to conduct electric charge through the surfaces becomes low, resulting in a high electric resistance. On the other hand, the resistance is low if the lubricant does not separate the surfaces.

El-Sisi et al. [4] studied the influence of an applied potential on oil-film resistance and its variation with film thickness and oil temperature. Archard and Kirk [5] investigated the electrical resistance between crossed cylinders in which the maximum voltage applied between the specimens was controlled by means of a changing resistance. In the study by Zhang et al. [6], the contact resistance was used to understand the ratio of film thickness to the roughness of the contact surfaces in worm-gear lubrication. A group of formulas for this ratio was developed. However, the resistance method can hardly be used to measure the shape of an EHL film.

5.1.1.3 DISCHARGE-VOLTAGE METHOD

The value of discharge voltage is found to vary with film thickness. Macconochie and Cameron [7] indicated that once the calibration constant of voltage against film thickness was determined, the discharge-voltage method could be used for the film-thickness measurement in any type of machinery.

5.1.1.4 X-RAY TRANSMISSION METHOD

The X-ray transmission method for measuring lubricant film thickness consists essentially of directing a square, parallel, and monochromatic X-ray beam at the contact

¹ Northwestern University, Evanston, IL, USA

² RT Vanderbilt Company, Norwalk, CT, USA

³ Northwestern University, Evanston, IL, USA

⁴ Beijing University of Chemical Technology, Beijing, China

⁵ State Key Laboratory of Mechanical Transmission, Chongqing University, Chongqing, China

of lubricated rolling-disk surfaces [8]. Because the absorption characteristics of X rays in metal and lubricant are different, the amount of the X-ray beam passed through the lubricant-filled gap can be measured by a radiation counter and is thus related to film thickness.

5.1.1.5 INDIRECT LASER TRANSMISSION METHOD

The mean values of the central oil film thickness between helical gear tooth profiles were indirectly measured by Yang et al. [9], through measuring the gap variation for a pair of unloaded involute spur gears mounted outside of a gear box, by means of the laser transmission method. Calibration was conducted every step of the measurement to ensure major error elimination [9]. To reduce the effect of gear tolerance on measurement accuracy, a set of involute spur gears was mounted outside of the gear box and run-in together with the helical gears inside of the gear box before the scheduled measurement [10]. This method is suitable for the measurement of the central oil film thickness between the teeth of cylindrical spur and helical gears.

5.1.1.6 RESISTANCE-CAPACITANCE OSCILLATION METHOD

The resistance-capacitance (R-C) oscillation method applies the theory of the Wien oscillator [11]. The surface contact state is equivalent to that of a circuit of a variable capacitance and resistance in parallel. When the film thickness changes, capacitance and resistance change, which in turn modifies the output frequency. The film thickness can be found through the frequency measurement. The R-C oscillation technique can be used to measure the film thickness in partial- and full-film EHL contacts.

5.1.1.7 OPTICAL INTERFEROMETRY

The development of the optical interferometry method for film-thickness measurement dates back to 1962 when Kirk used Newton's fringes to inspect the film thickness in the contact between crossed cylinders lubricated with a mineral oil [12]. In 1963, Gohar and Cameron [13] used Newton's fringes to measure the film thickness between a 1-in. rotating steel ball and a plate of a special high-refractive index glass. The lubricant film shapes in the contact zone were evaluated. This was the first application of optical interferometry to a true elastohydrodynamic (EHD) contact (i.e., at pressures high enough to produce a piezoviscous response). Since then, many have used optical interferometry for film-thickness measurements and film-shape determinations under EHD conditions. This method has been applied to study the lubrication of engineering elements, such as rolling element bearings [15] and porous bearings [16]. It can also be used for film measurement at starved EHD conditions [17,18]. The disadvantage of the optical interferometry method, compared with electrical techniques, is that one of the surfaces must be made of an optically transparent material, such as glass or sapphire. Therefore, this method cannot be directly applied to realistic machine systems.

Different angles of the application of the basic film measurement principle have resulted in several different interferometry techniques.

5.1.1.7.1 Interferometry with a Stationary Glass Plate

The experimental apparatus reported by Gohar and Cameron [19,20] used a 25.4-mm-diameter steel ball of 39-nm centerline average surface finish and 1- μ m sphericity

mounted against a conical seat, which was rotated by a flexible 3.175-mm-diameter shaft. A glass of high refractive index was mounted against the ball. A microscope was located above the contact. A side illuminator was installed between the objective and the eyepiece to provide an almost-collimated light beam. Three sources were used: white light, sodium yellow, and mercury green. Because earlier glass plates could only stand for low velocities and low loads, diamond (or sapphire) was used. Diamond has excellent thermal properties and can satisfactorily conduct heat away. Sapphire can also sustain high loads and speeds, but it has a poor thermal conductivity. Because the plate was fixed, this experimental apparatus was only used for pure-sliding lubrication.

5.1.1.7.2 Interferometry with a Movable Glass Plate

A rotating glass plate was used to study rolling and sliding lubrication problems [21,22]. In these studies, a specially coated glass plate was mounted on an air bearing and driven by a super-finished 25.4-mm steel ball assembled in a polytetrafluorethylene cup. The ball was loaded against the lower surface of the plate by an air cylinder and rotated by a variable-speed electric motor. Oil was drip-fed onto the ball and drawn into the contact. With this technique, the reflectivity of the semireflecting coating layer determines the intensity distribution of the fringes. If the reflectivity is low, broad "two-beam" fringes can be produced. However, if the reflectivity is high, narrow "multiple-beam" fringes could be obtained. The amount of absorption in the semireflectivity layer must be low for multiple-beam fringes to produce fringes of good visibility. A chromium layer is often used. The ball and the glass disk can be independently driven by two sets of driving devices to facilitate the study the film thickness due to the variable ratio of sliding to rolling speed [14]. To create conditions similar to those encountered by the surfaces of rolling element bearing components and gear teeth, the contacting surfaces of a crowned roller of a hardened steel and a flat synthetic sapphire disk were used in the experiments reported in reference 23. In this work, the crowned roller and the synthetic sapphire disk were independently driven in the tests.

5.1.1.7.3 Interferometry with a Spacer Layer

In principle, optical interferometry is not capable of measuring films less than one quarter of the wavelength of a visible light (i.e., less than approximately 100 nm). The combination of a solid spacer layer with a spectrometric analysis of the reflected light from the contact enables the measurement of thin lubricant films [14]. The coating of a transparent solid with a known thickness is deposited on top of the semireflecting layer. This solid spacer layer thus permanently augments the thickness of any oil film present. The first interference fringe occurs at the separation induced by the spatial thickness of the spacer layer. This technique was reported to be capable of measuring separating films down to less than 5 nm [14,24].

5.1.1.7.4 Colorimetric Interferometry Technique

The colorimetric interferometry measurement technique uses a computer-aided color-matching method to evaluate the interference colors. Unknown EHL film thickness is determined by comparing interference colors between the interferograms and a standard reference image. Hartl et al. [25] used the $L^*a^*b^*$ model to define the color whereas

Molimard et al. [26] used the RGB model instead. The standard reference image is obtained from the Newton rings for a static contact. It was reported that this technique might yield very high film thickness resolution (~ 1 nm) whereas the spatial resolution is approximately $1\text{ }\mu\text{m}$. The measurement range can be from 800 nm down to a few nanometres [27].

5.1.1.7.5 Relative Optical Interference Intensity Technique

When the optical interference intensity varies from the minimum intensity to the maximum, the lubricant film thickness has a one-quarter wavelength change. Therefore, the lubricant film thickness at any point in the contact region can be determined by the location of the interference intensity between the minimum and maximum values and a pure phase change. Monochromatic interference fringe can be captured with a camera, and the optical image can be digitized for film calculation. The resolution of this technique could reach 0.5 nm in the vertical direction and $1.5\text{ }\mu\text{m}$ in the horizontal direction [28].

5.1.1.7.6 Combination with Total Reflection Technique

In mixed lubrication, the space between two surfaces can be divided into two regions of different lubrication mechanisms: the hydrodynamic mechanism and the boundary lubrication. Optical interferometry can be made into a powerful tool for the film-thickness measurement and film-shape observation in the field of mixed EHL. IC can be used to determine the contact area on the basis of the disturbance of the total reflection of the light at the points of contact between an optically transparent and an opaque material. Because the film thickness, the film shape, and the contact area can be observed at the same time, a combination of the optical interferometry technique with the total reflection technique may be an approach for investigating contact problems in mixed lubrication [29].

5.1.2 Fluid Behavior in Point-Contact EHL

Experimental investigations on counterformal-contact lubrication have resulted in a rich database for the understanding of the film thickness behavior in point-contact EHL problems. In many cases, the measured film thicknesses well follow the power-law relationship formulated by the Hamrock-Dowson (H&D) equation [43]. Deviations from the power-law straight line are usually observed for cases of low speed or very thin film. Figures 5.1–5.5 present several samples of measurement data from references [14] and [44–46] obtained by means of the optical interferometry technique. Several trends of film thickness variation at very thin film lubrications may be viewed as follows, although there might be other trends reported.

Figure 5.1, which is Figure 2 in reference 45, presents a set of measurement results that well follow the power-law relationship between film thickness and rolling speed. The lubricating fluid was hexadecane. The experiments were conducted at 20 N (0.48 GPa) and $25 \pm 0.5^\circ\text{C}$ in an EHL contact between a glass disk (with a silica spacer layer of 510 nm thick) and a steel ball. The lowest speed was 0.0002 m/s. The slope was found to be 0.68, and the power-law relationship was obeyed even when the film thickness were reduced down to about 0.5 nm.

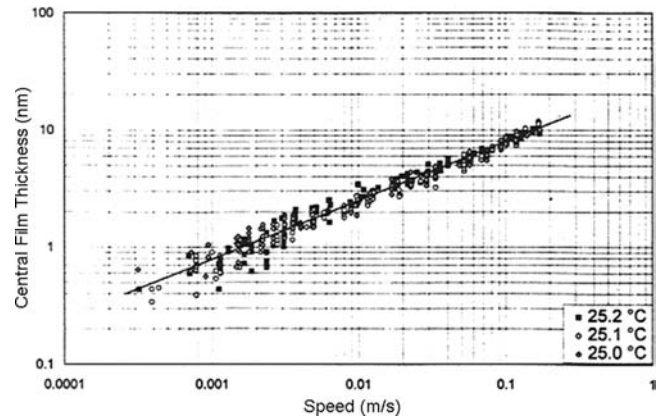


Figure 5.1—Power-law relationship between film thickness and rolling speed (Figure 2 in reference 45).

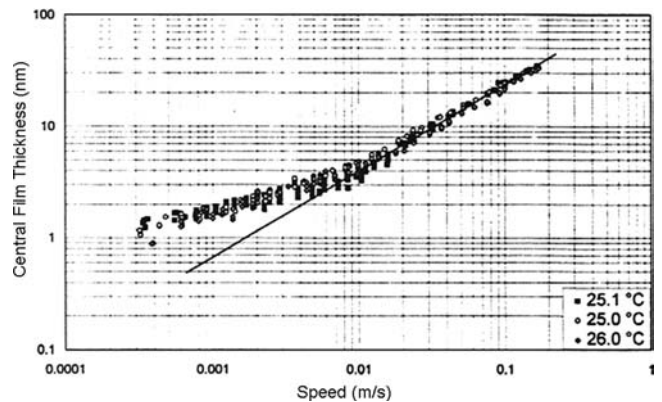


Figure 5.2—Upward deviation from the power-law relationship between film thickness and rolling speed when the rolling speed is very low (Figure 3 in reference 45).

Figure 5.2, which is Figure 3 in reference 45, for diisobutylate (2-ethylhexyl) ester presents a set of measurement results showing an upward deviation from the power-law relationship between film thickness and rolling speed when the rolling speed is very small. The experiment conditions are the same as those mentioned above. The log plot tends to become horizontal when the film thickness reduces to approximately 3 nm, suggesting the presence of some type of boundary film [45]. Such an upward deviation can also be found from Figures 5.3 and 5.4.

Figure 5.3 presents several cases showing downward deviations from the power-law relationship between film thickness and rolling speed when the speed is very low. Data in Figure 5.3a were obtained from Drs. Hartl and Krupka by using the colorimetric interferometry technique [27] from a sapphire disk/steel ball EHL contact at 23°C and a naphthenic base oil, SUN 2000N, was used as the lubricant. In Figure 5.3a, the downward deviation increased when the load was increased. Such a load-dependent trend of the downward film variation is also shown in Figure 5.3b for a few different lubricants: polyglycol oil JM65 (left); polyglycol oil JM68 (center); and white oils a-CN 13607, b-CN 13606, and c-CN 13603 (right) [46]. Here, the EHL contact was between a glass disk and a steel ball at 28°C . Data in Figure 5.3c were taken at 23 N (0.445 GPa) and $24 \pm 0.5^\circ\text{C}$ in an EHL contact between a

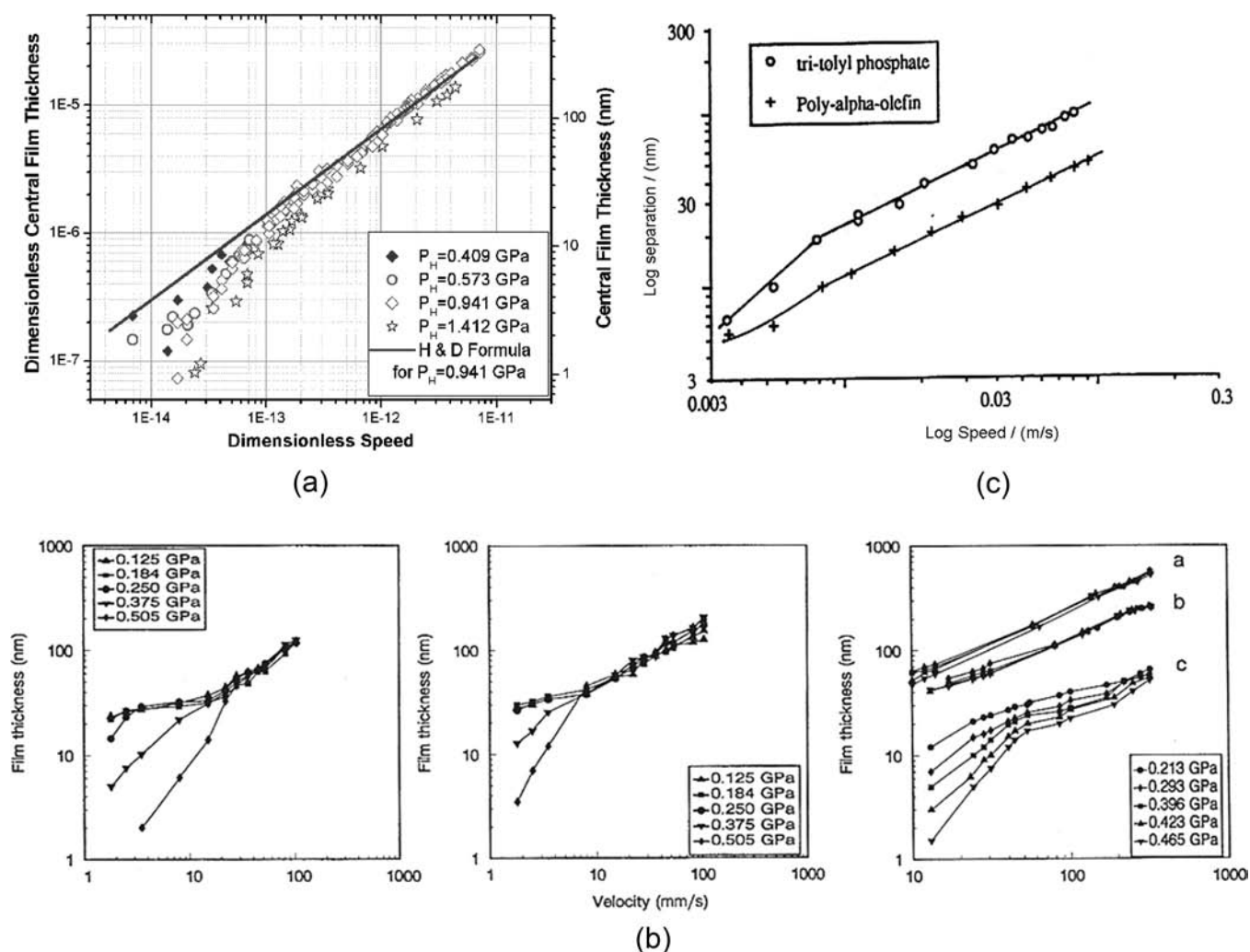


Figure 5.3—Downward deviations from the power-law relationship between film thickness and rolling speed when the rolling speed is very low. (a) Naphthenic base oil SUN 2000N. (b) Performance of a few lubricants: polyglycol oil JM65 (left); polyglycol oil JM68 (center); and white oil (a) CN 13607, (b) CN 13603 (right) (Figures 3, 4, and 8 in reference 46). (c) Tri-tolyl phosphate and synthetic hydrocarbon (PAO) (Figure 8 in reference 14).

glass disk (with a silica spacer layer of 100 nm thickness) and a steel ball [14]. In Figure 5.3c, tri-tolyl phosphate and polyalphaolefin (PAO) behaved slightly away from the power-law straight line at low speeds with downward deviations. Such downward trends of deviation are also shown by the lower portion of data plotted in Figure 5.4. Data in Figure 5.4a were also obtained at 23 N (0.445 GPa) with the same contact setup. In Figure 5.4a, the purified hexadecane fluid demonstrated a slightly downward film-variation trend, which suggested that no apparent residual film was formed [14]. Data in Figures 5.4, b and c, are from Figures 4 and 5 of reference 44 for different solutions of 6 wt % concentration of a polymer at 80 and 120°C.

Some data show three different behaviors—the power-law relationship, increased slope when the rolling speed is very small, and nearly constant film when the film is extremely thin—as suggested by the data for the squalane and the polyol ester shown in Figure 5.5, which are from Figures 7 and 9 of reference 14. The applied load and contact conditions were the same as those used in the experiments for Figures 5.3c and 5.4a. Here, the films

show a downward deviation from the power-law straight line first as the speed is reduced, and then the film thickness variation levels nearly horizontally when the speed is further reduced. The film thickness values of squalane and polyol ester, where the three slope behaviors were demonstrated, are obviously the thinnest among the films of the lubricants appearing in these figures under the same testing conditions. Evaluation of the lubrication film variation with respect to operating conditions allows lubricant engineers to assess the design of rheology built into a lubricant.

5.1.3 Simulation and Comparison between Numerical Results and Experimental Data

It is well known that an EHL model can be established mathematically with a set of equations, including the Reynolds equation for hydrodynamics, the elasticity equation for deformation considerations, the pressure-viscosity relationship for the lubricant behavior, and the film-thickness expression for the gap geometry. Such a formulation is strongly nonlinear and, in many cases, dependent on time.

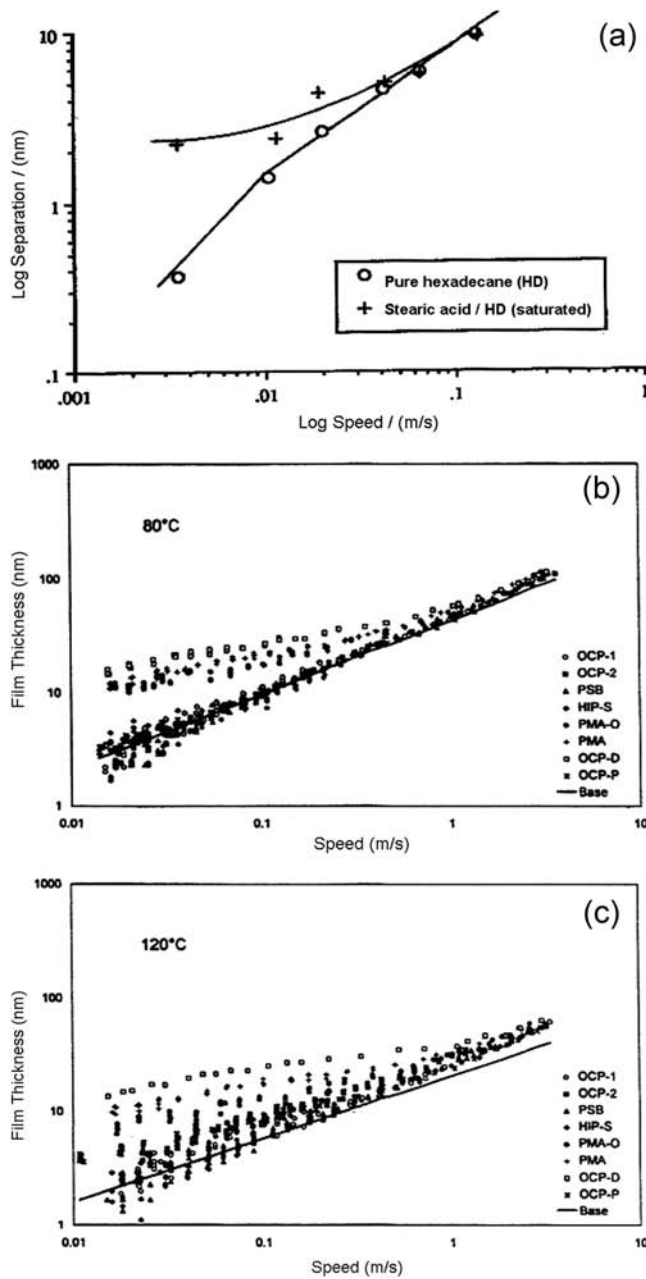


Figure 5.4—Upward and downward deviations from the power-law relationship between film thickness and rolling speed when the rolling speed is very low. (a) Figure 10 in reference 14. (b and c) Figures 4 and 5 in reference 44 for different solutions with 6 wt % concentration of viscosity index improver polymer at 80 and 120°C. The downward deviation could become clearer if straight lines were drawn through the middle of the data at higher speeds. The thinnest films under the same conditions were those in the downward deviation although additives were added.

5.1.3.1 RECENT EFFORTS ON EHL MODELING OF SMOOTH SURFACE LUBRICATION

EHL problems may involve a large amount of computation if the mesh size is small. The multigrid method with a considerably high mesh density was introduced to EHL by Lubrecht [47], Venner [48], and applied by Ai [49] and others to improve solution convergence and accuracy. The

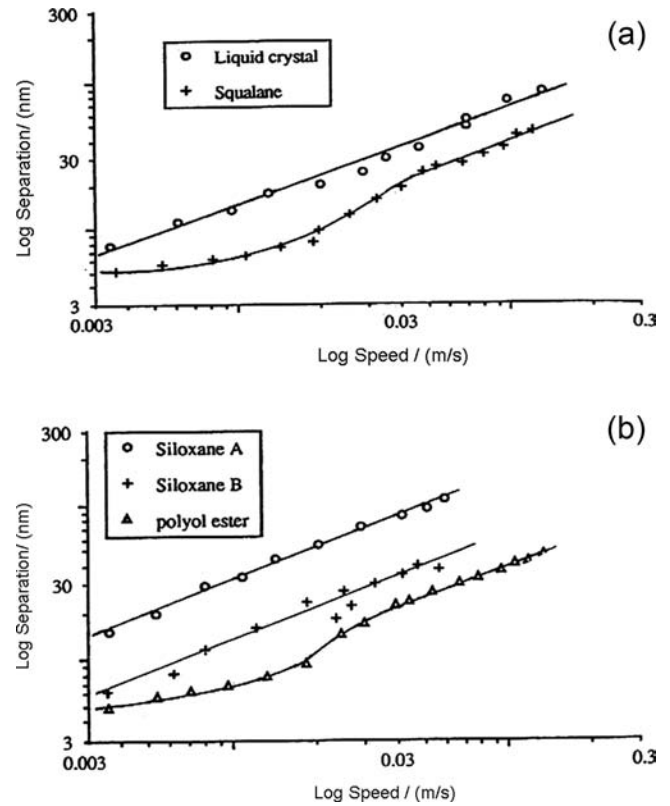


Figure 5.5—Three-slope behavior: the power-law relationship, increased slope when the rolling speed is very low, and nearly constant film when the film is extremely thin. (a) Figure 7 in reference 15; notice the behavior of squalane. (b) Figure 9 in reference 14; notice the behavior of polyol ester.

discrete convolution and fast Fourier transfer (DC-FFT) approach [50,51] and the multilevel multi-integration method [48] considerably accelerate the elasticity analysis in EHL computation. The semisystem method [48,49] ensures that the coefficient matrix of the Reynolds equation is strictly diagonally dominated by enhancing the leading diagonal element. With this method the solution convergence is further improved for cases under severe conditions. Holmes [52] developed a coupled deformation differentiation method aiming at better computation of the elastic deformation in EHL. Hu and Zhu [36–38] developed a unified solution approach that is based on the semisystem method. It can handle the entire transition from the full film and mixed EHL down to boundary lubrication by simultaneously solving the hydrodynamic pressure and the contact pressure. Using this robust approach, one can tackle problems in a wide range of operating conditions (e.g., from light to very heavy load and for the film thickness from several microns down to a practical zero).

5.1.3.2 RECENT MIXED EHL MODELING OF ROUGH SURFACE LUBRICATION

Engineering surfaces are rough, and the EHL analysis should consider the existence of surface asperities. Venner et al. [53] computed a single transverse ridge moving through the EHL conjunction subjected to a different slide-to-roll ratio by using the integrated multilevel method and

compared the results with the experimental observations in reference 54. Holmes et al. [55,56] investigated start-stop experimental observations [57,58] by using the coupled differential deflection method. Zhao and Sadeghi [59] and Zhao [60] simulated these two transient EHL experiments with a mixed lubrication model that separately handles the contact area and lubrication area. Felix-Quinonez et al. [61-63] investigated roughness effects of a single ridge and distributive three-dimensional flat-top defects passing through an EHL conjunction. The Hu-Zhu model [36-38] and its recent improvements [64-67] supported the investigations of a wide range of mixed EHL problems. The Hu and Zhu mixed lubrication model is briefly presented here and will be used for the simulation of several experimental measurements.

5.1.4 Hu and Zhu's Full-Scale Mixed EHL Model

Hu and Zhu's micro-EHL model [36-38] is a deterministic description of the EHL interface formed by two engineering surfaces.

In the regions of hydrodynamic lubrication, the pressure is governed by the Reynolds equation expressed as follows:

$$\frac{\partial}{\partial x} \left(\phi_x \frac{\rho h^3}{12\eta} \frac{\partial p}{\partial x} \right) + \frac{\partial}{\partial y} \left(\phi_y \frac{\rho h^3}{12\eta} \frac{\partial p}{\partial y} \right) = U \frac{\partial(\rho h)}{\partial x} + \frac{\partial(\rho h)}{\partial t} \quad (5.1)$$

The x -coordinate is chosen to coincide with the direction of motion. The instantaneous lubricant film thickness, h , or the gap between two surfaces, is calculated by a geometric equation,

$$h = h_0(t) + B_x x^2 + B_y y^2 + V(x, y, t) + \delta_1(x, y, t) + \delta_2(x, y, t) \quad (5.2)$$

where:

B_x and B_y = constants related to the original geometry of contacting bodies;

δ_1 and δ_2 = roughness amplitude of surface 1 and 2, respectively; and

V = surface deformation.

Two flow factors ϕ_x and ϕ_y were introduced in eq. 5.1 to describe the non-Newtonian lubricant properties. For example, for a lubricant with the Eyring constitutive model (τ_0 is the Eyring stress),

$$\gamma = \frac{\tau_0}{\eta} \sinh \left(\frac{\tau}{\tau_0} \right) \quad (5.3)$$

the two flow factors are [68]

$$\phi_x = \cosh \left(\frac{\tau_m}{\tau_0} \right) \quad \phi_y = \frac{\sinh(\tau_m / \tau_0)}{\tau_m / \tau_0} \quad (5.4)$$

where τ_m is the shear stress in the middle layer along the rolling direction. τ_m is determined by

$$\frac{\tau_m}{\tau_0} = \sinh^{-1} \left(\frac{\eta(u_2 - u_1)}{\tau_0 h} \right) \quad (5.5)$$

For a lubricant obeying the Newtonian model, $\gamma = \tau / \eta$, and the two flow factors are $\phi_x = \phi_y = 1$. The variation of viscosity with pressure is described by the power-law equation for simplicity:

$$\eta = \eta_0 \exp(\alpha p) \quad (5.6)$$

The variation of the lubricant density is a function of pressure, and a state equation is needed. Following Dowson and Higginson:

$$\rho = \rho_0 \left(1 + \frac{0.6 \times 10^{-9} p}{1 + 1.7 \times 10^{-9} p} \right) \quad (5.7)$$

The unified lubrication-contact approach in mixed lubrication developed by Hu and Zhu [36,38] consistently uses the same equation systems in hydrodynamic and contact regions. When the lubricant film thickness is smaller than a critical value, ϵ , the left-hand side of eq. 5.1, which represents the lubricant flow due to the hydrodynamic pressure gradient, vanishes because of the third power of the film thickness. As a result, the Reynolds equation is reduced to the following form:

$$U \frac{\partial h}{\partial x} + \frac{\partial h}{\partial t} = 0 \quad \text{at } h \leq \epsilon. \quad (5.8)$$

EHL practice has proven that contact pressure is the asymptotic solution of the film pressure when the film thickness is sufficiently small and the contribution from the pressure-driven hydrodynamic action then becomes negligible [36,48]. Analyses have proven that the model with and without the use of the reduced Reynolds equation yields the same pressure and film thickness [36,37,64].

5.1.5 Simulations and Comparisons

First, two experimental results, Figure 9 in reference 14 by Johnston et al. for a lubricant of siloxane A and Figure 2 in reference 32 by Choo et al. for another lubricant of HVI60, were modeled, and the experimental data were compared with the numerical solutions for steady-state performance evaluations. Second, the multitransverse ridge experiments by Kaneta et al. [33] were simulated, and the simulation results were compared with the experimental data to evaluate the model effectiveness on analyzing the EHL performance of rough surfaces in a transient state.

5.1.5.1 SIMULATION OF AND COMPARISON WITH THE EXPERIMENTAL RESULTS OF JOHNSTON ET AL. [14] AND CHOO ET AL. [32]

The working conditions used in the present calculations corresponding to the experiments by Johnston et al. [14] and Choo et al. [32] are listed Tables 5.1 and 5.2. For these two steady-state simulations, the solution domain of $-1.9 < x < 1.1$ and $-1.5 < y < 1.5$ was covered by a 512×512 mesh. The second-order backward differential scheme was used to discretize the wedge term. A grid test on 128×128 , 256×256 , 512×512 , and 1024×1024 meshes has shown that the discretization errors reflected by the variation of central film thickness using a mesh of 512×512 vary from 2.2 % at the lowest speed to 0.1 % at the highest speed. The reason for such a varying discretization error influenced by speed is due to the increasing pressure and film thickness gradients with decreasing speed in the inlet area [64].

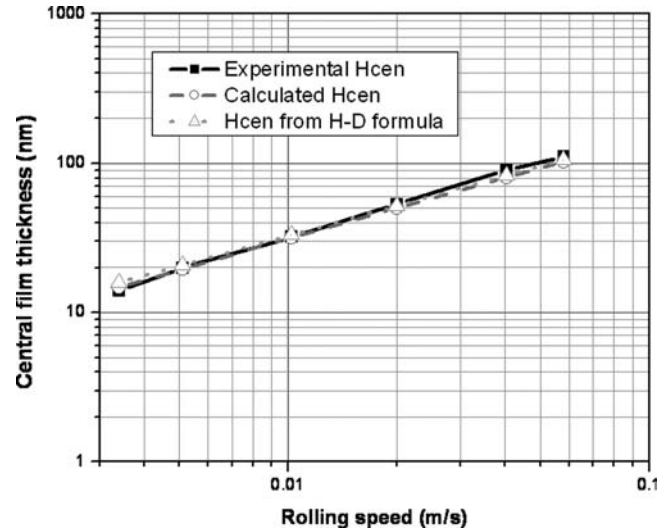
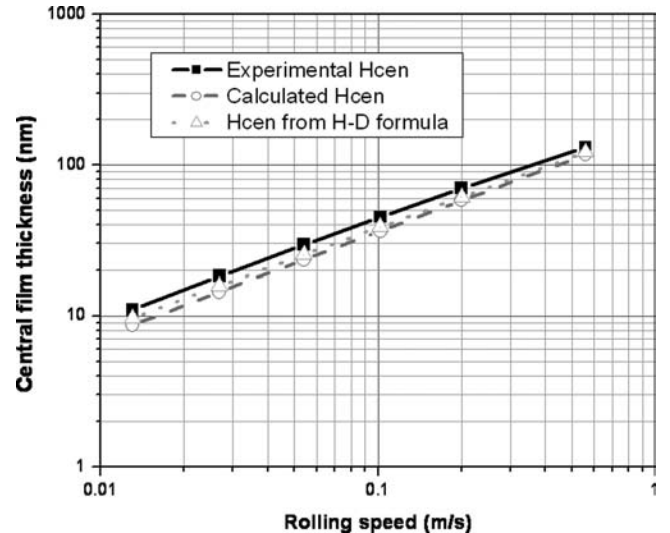
TABLE 5.1—Parameters to Calculate the Experiment by Johnston et al. [14]

Parameters	Value	Unit
Load, W	23	N
Young's modulus of steel ball, E_1	210	GPa
Poisson's ratio of steel ball, μ_{v1}	0.3	
Young's modulus of glass disk, E_2	75	GPa
Poisson's ratio of glass disk, μ_{v2}	0.17	
Ball radii, R	12.7	mm
Reduced Young's modulus, E	115.3	GPa
Hertzian contact radii, a	0.156	mm
Maximum Hertzian contact pressure, ρ_h	0.45	GPa
Inlet temperature, T_0	24.5	°C
Viscosity at inlet temperature, η_0	0.1536	Pa·s
Pressure-viscosity coefficient, α	18.3	1/GPa

Figure 5.6 presents the experimental results [14] and the data calculated by using the present model and the H&D formula for the experiment by Johnston et al. [14]. The comparison indicates that the central film thickness results, H_{cen} , from the experiment, the present calculation, and the H&D formula are nearly the same. Figure 5.7 plots another steady-state EHL comparison for the experiment by Choo et al. [32]. It is found that the numerical results from the present model are close to those from the H&D formula. However, the calculated film thickness is thinner than the experimental results by approximately 15%. Referring to the comparison mentioned previously, a large difference was observed in this case, and a major difference between these two cases lies in the pressure viscosity coefficient. In the case of the experiments by Johnston et al., the coefficient was extracted from the film-thickness measurement data using the H&D formula. However, in the experiment of Choo et al., the coefficient comes from viscometer measurement results. In practice, these two coefficients may be noticeably different [69]. A new coefficient definition for viscometer data was recently put forward

TABLE 5.2—Parameters to Calculate the Experiment by Choo et al. [32]

Parameters	Value	Unit
Load, W	20	N
Ball radii, R	9.525	mm
Reduced Young's modulus, E	117.3	GPa
Hertzian contact radii, a	0.1346	mm
Maximum Hertzian contact pressure, ρ_h	0.527	GPa
Inlet temperature, T_0	40	°C
Viscosity at inlet temperature, η_0	0.022	Pa·s
Pressure-viscosity coefficient, α	19.8	1/GPa

**Figure 5.6—Comparison of the calculated central film thickness, H_{cen} , with the experimental results by Johnston et al. [14].****Figure 5.7—Comparison of the calculated central film thickness, H_{cen} , with the experimental results by Choo et al. [32].**

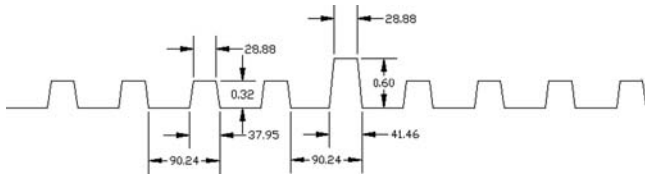
to unify these two coefficient determination approaches [70] with which a convincing agreement has been obtained in comparing experimental and simulation results for squalane [71].

5.1.5.2 SIMULATION OF AND COMPARISON WITH THE EXPERIMENTAL RESULTS FROM KANETA ET AL. [33]

The working conditions used in the simulation of the experiments by Kaneta et al. [33] are listed in Table 5.3. The physical dimensions of the multitransverse ridges extracted from Figure 1 in reference 33 are shown in Figure 5.8. There are nine total ridges, and the middle ridge is the highest one, the height of which is almost twice that of the others. Such a roughness pattern was incorporated into the upper surface to form an undulated rough surface. The rough surface gradually went into the contact zone from the left start of $x = -2.5$. The marching speed

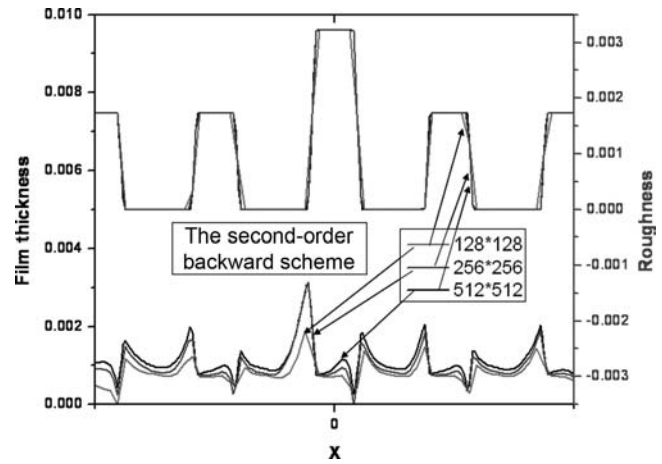
TABLE 5.3—Parameters to Calculate the Experiment by Kaneta et al. [33]

Parameters	Value	Unit
Load, W	39.5	N
Ball radii, R	12.7	mm
Reduced Young's modulus, E'	117	GPa
Hertzian contact radii, a	0.185	mm
Maximum Hertzian contact pressure, ρ_h	0.54	GPa
Inlet temperature, T_0	21	°C
Viscosity at inlet temperature, η_0	1.22	Pa·s
Pressure-viscosity coefficient, α	23.7	1/GPa
Rolling speed, u	0.024	m/s
Dimensionless load parameter, W^*	2.1×10^{-6}	
Dimensionless material parameter, G^*	2770	
Dimensionless speed parameter, U^*	2×10^{-11}	

**Figure 5.8—Simulated roughness profile using data from reference 33.**

depends on the slide-to-roll ratio, S . For $S = 0$, the marching speed equals the rolling speed, which is the average value of two surface speeds. For $S = 1$, the rough surface is slower than the smooth surface. For $S = -1$, the situation is reversed and the rough surface moves fast. For the case of $S = 0$, the Newtonian rheological model was assumed. For the other two cases with non-zero slide-to-roll ratio, the Eyring model expressed in eqs. 5.3–5.5 with an Eyring stress of $\tau_c = 5$ MPa was used.

In the simulations of the experiments by Kaneta et al., the second-order backward differential scheme was used for the discretization of both wedge and squeeze terms. The solution domain was enlarged to $-2.5 < x < 1.5$ and $-2.0 < y < 2.0$, which was divided into the 256×256 mesh. A discretization error comparison for the rough-surface case with a rolling speed $u = 0.024$ m/s is shown in Figure 5.9. In the comparison, a steady-state case in simple sliding ($S = 2$) with the stationary roughness was calculated, respectively, using different mesh sizes. The highest ridge of the roughness was adjusted to be at the center, $x = 0$. It is found that the discretization error using the second-order backward scheme and a mesh of 256×256 is approximately 5.8 % by comparing the average film thickness within a central circle with a radius of $2/3a$. In the time domain, the dimensionless time spacing equals the dimensionless space spacing, that is $\Delta t = \Delta x$. Holmes [52] studied the discretization error of the second-order backward differential

**Figure 5.9—Discretization error comparison for a rough case using the second-order backward scheme.**

for the squeeze term and indicated that $\Delta t = \Delta x$ was applicable via the comparisons of the centerline minimum and maximum values of the film thickness for different time steps.

Figure 5.10 shows a series of simulation results for $S = 0$ at different positions. The shapes of the film thickness in simulations resemble those of the films in experiments. As stated in reference 33, a divergent gap along the rolling direction is formed on each asperity whereas in the valley a convergent gap is formed because of the microsqueeze action. The deformed configuration remains invariant when passing the EHL conjunction. However, the average film thickness in simulations is somewhat lower than that in experiments. A similar difference was also observed in other comparative simulations [53,62, 72].

The simulation results for $S = 1$ and $S = -1$ are shown in Figures 5.11 and 5.12. The film thickness shapes in simulations are similar to those in experiments except at the positions where the roughness undergoes an abrupt change. These changes in roughness result in the corresponding pressure peaks in the pressure profile. Similar to the observations by Kaneta et al. [33], the microwedge effect intends to counterbalance the microsqueeze effect because the rough surface moves more slowly than the smooth surface at $S = 1$. This point is verified by the change of the gap. Opposite to the case of $S = 0$, the original divergent gap on each asperity turns into a convergent gap and vice versa for the geometry in the valley. However, for $S = -1$, a faster rough surface runs against a slower smooth surface, and the extents of the asperity wedge convergence and the valley wedge divergence become more complicated, meaning that the microwedge effect and the microsqueeze effect should strengthen each other. In addition, a disturbance in film thickness caused at the inlet area and propagated through the EHL conjunction can be observed for the case of $S = 1$, as stated in reference 33. However, for $S = -1$, the Couette-flow dominant phenomenon can hardly be found.

These results indicate that a proper EHL model, such as the unified Hu-Zhu EHL model mentioned here, can well simulate EHL experiments. However, the agreements still need to be further improved. EHL is essentially for the science of lubrication. The major difficulty

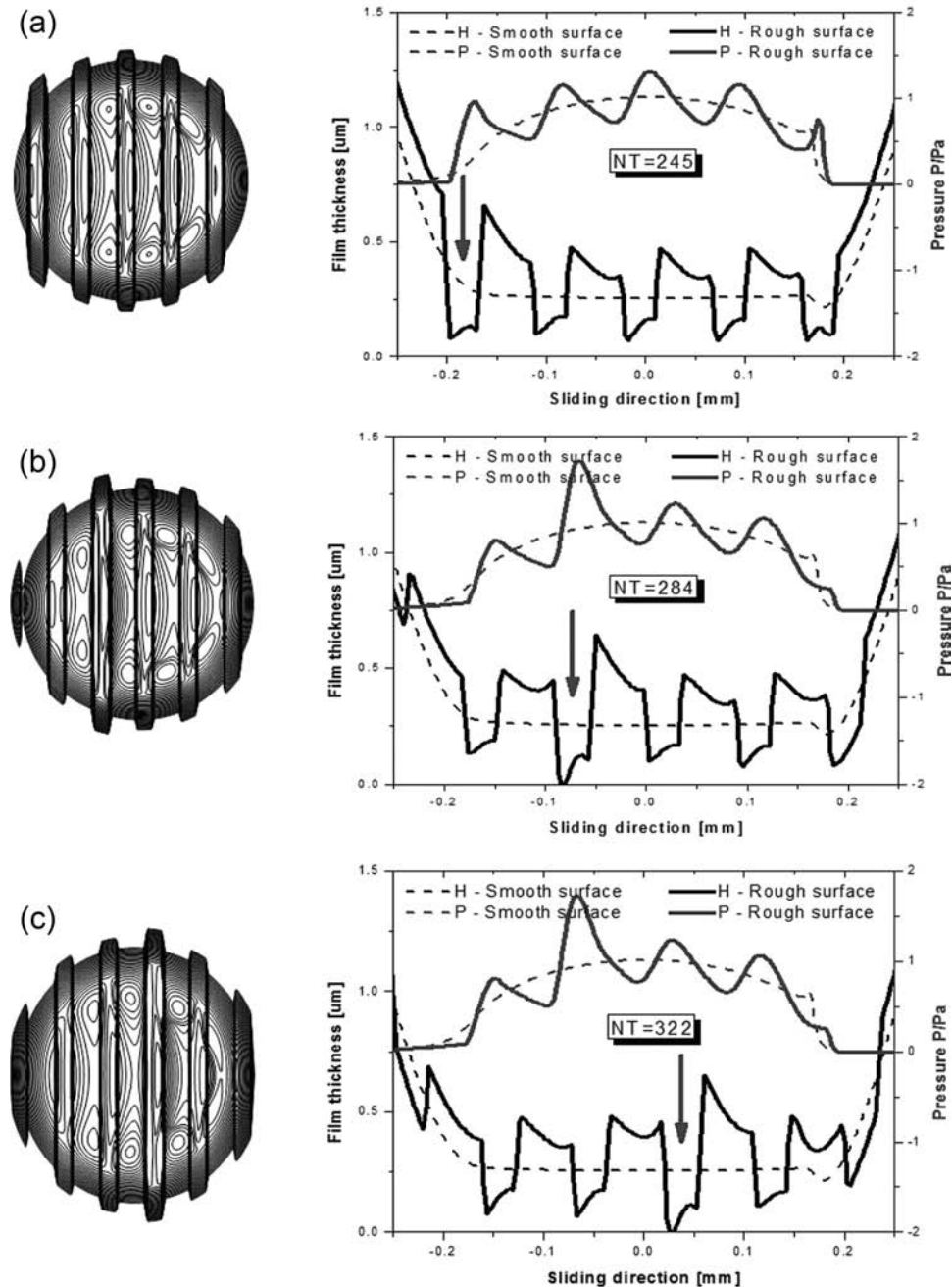


Figure 5.10—Simulation results well agree with the experimental data from Kaneta et al. [33] with multitransverse ridges at $S = 0$: (a) results at position a, (b) results at position c, and (c) results at position e.

in present simulations is the lack of accurate oil properties. A more accurate free-volume pressure-viscosity relationship and a Careau-type shear-thinning model are recently available for many lubricants [73]. The viscosity parameters in these models were regressed from realistic measurements for specific oil. Better agreement would be achieved if more accurate lubricant properties could be available. In addition, the thermal effect was not considered in the model reported in this section. The thermal effect can be neglected for pure rolling conditions unless the rolling speed is extremely high. The multiridge experiments by Kaneta et al. were at non-zero slide-to-roll ratios; however, the thermal effect

was not apparent because of the low rolling speed of 0.024 m/s. This is manifested by the fact that the average film thickness values were nearly constant in the three experiments of different slide-to-roll ratios [33].

5.2 TRIBOLOGICAL BENCH TEST METHODS AND TESTING RESULTS FOR MIXED FILM AND BOUNDARY LUBRICATION

The tribological bench testing approach can provide rapid and cost-effective information and is often used for screening or ranking lubricants in the process of developing new engine materials and lubricants. This section reviews the current developments of selected bench test methods using

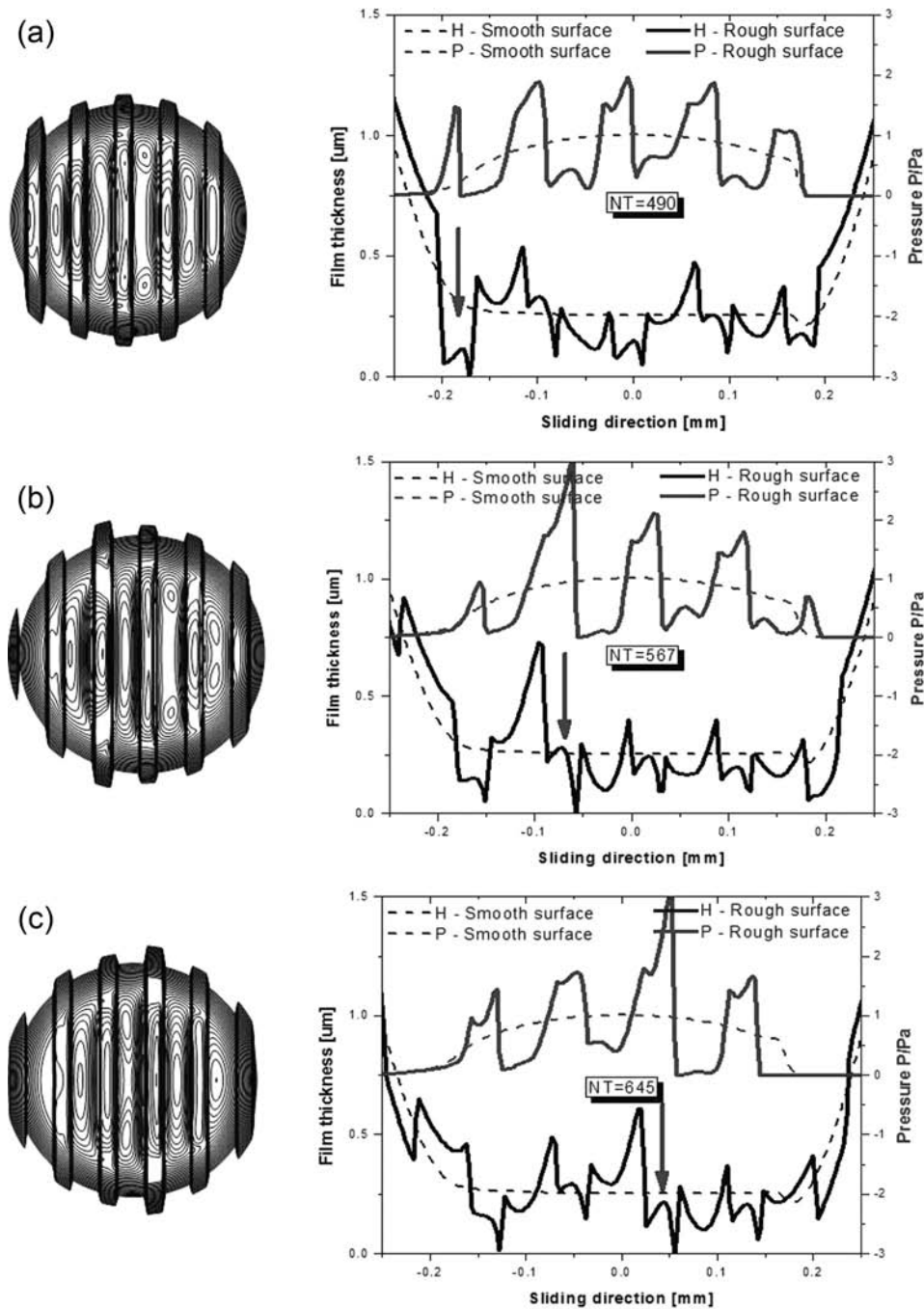


Figure 5.11—Simulation results well agree with the experimental data from Kaneta et al. [33] with multitransverse ridges at $S = 1$: (a) results at position a, (b) results at position c, and (c) results at position e.

rotary or reciprocating motion for evaluating the friction and energy-efficient characteristics of lubricants. The main advantage of the developed bench tests is that samples of real components (cylinder liners and piston rings) can be tested, preserving the geometry and metallurgy of the engine parts, thereby permitting a representative evaluation of surface finishes and oils. Results from materials and lubricant studies will be presented and correlated with vehicle testing.

Because the engine environment cannot be completely simulated in bench tests, engine tests are often needed to verify and validate findings. Several techniques have been developed by one of the authors to measure overall and

cycle-resolved, reciprocating component friction and wear in fired engines. These techniques and the current research and development efforts (including the investigation of new engine designs and energy-efficient lubricants) will be reviewed.

5.2.1 Overview of Current Bench and Simulation Tests for Engine Components

Over the years, a wide range of testing methods [74–80] has been developed for measuring lubricant properties and performance characteristics. There are generally three levels of lubricant testing, as shown in Figure 5.13. When

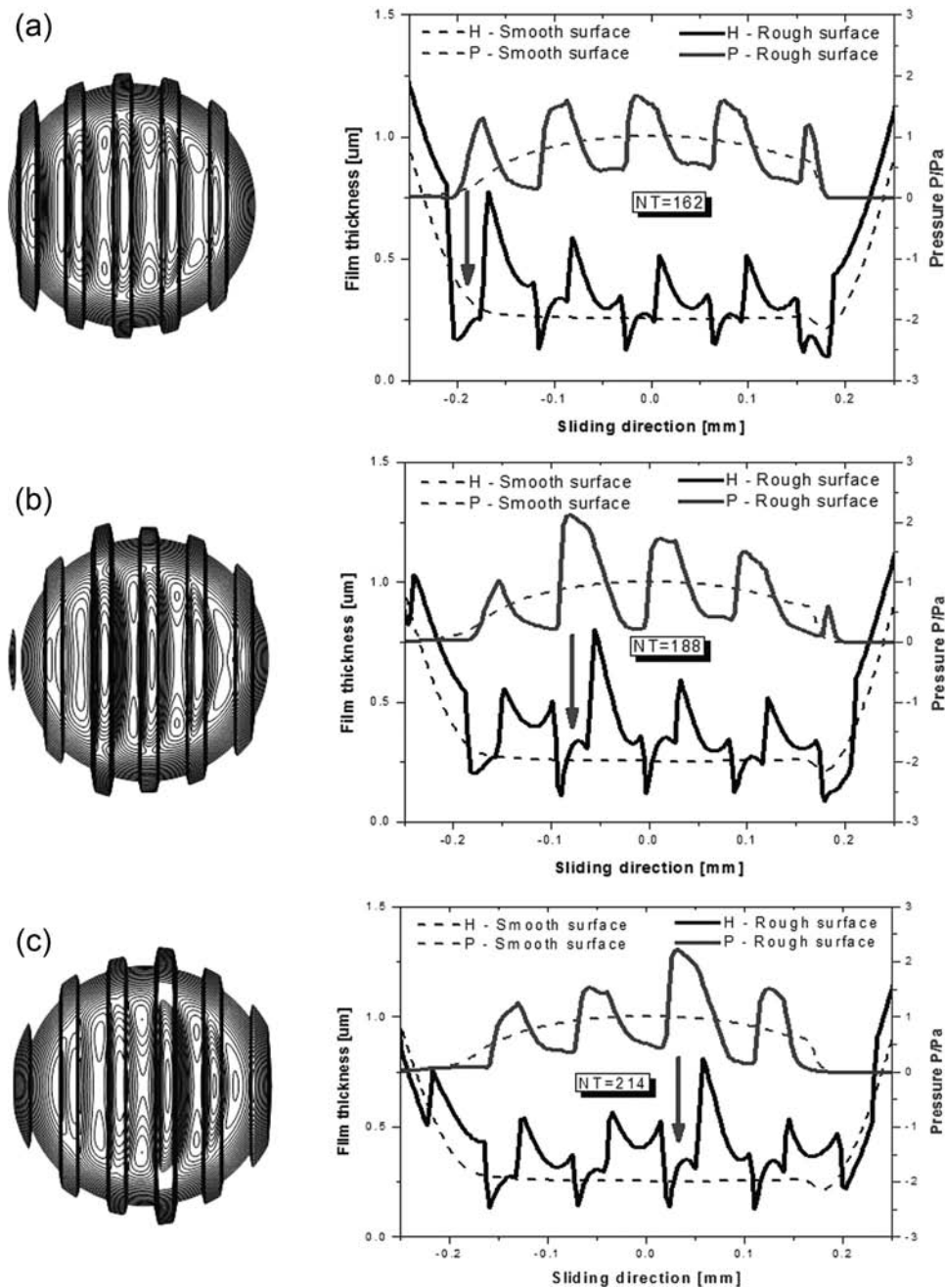


Figure 5.12—Simulation results well agree with the experimental data from Kaneta et al. [33] with multitransverse ridges $S = -1$: (a) results at position a, (b) results at position c, and (c) results at position e.

developing a lubricant, the lubricant manufacturer conducts the sequence tests shown in Figure 5.13 and several bench tests in each level before committing to more realistic, but costly and often time-consuming, application tests. After all three levels of tests, the engine lubricant or tested material can be accepted for final field tests to be in the marketplace.

5.2.1.1 INDUSTRIAL STANDARD BENCH TESTS

Most standard bench or engine simulation tests used in the United States and United Kingdom are

- *ASTM*: American Society for Testing and Materials
- *ISO*: International Organization for Standardization

- *SAE*: Society of Automotive Engineers
- *ILSAC*: International Lubricant Standard Committee
- *IP*: UK-based Institute of Petroleum
- *CEC*: Coordinating European Council

Most authorities consider that oxidation, metal corrosion, seal attack, viscosity, acidity tests, etc., give reasonably repeatable and meaningful measurements of corresponding lubricant properties. However, the usefulness of bench testing is often disputed in assessing wear resistance, friction, scuffing, and rolling contact fatigue of engine components under field driving conditions. Table 5.4 summarizes the results of a few important lubricating oil tests. There are many others. References 75–77 provide some further examples.

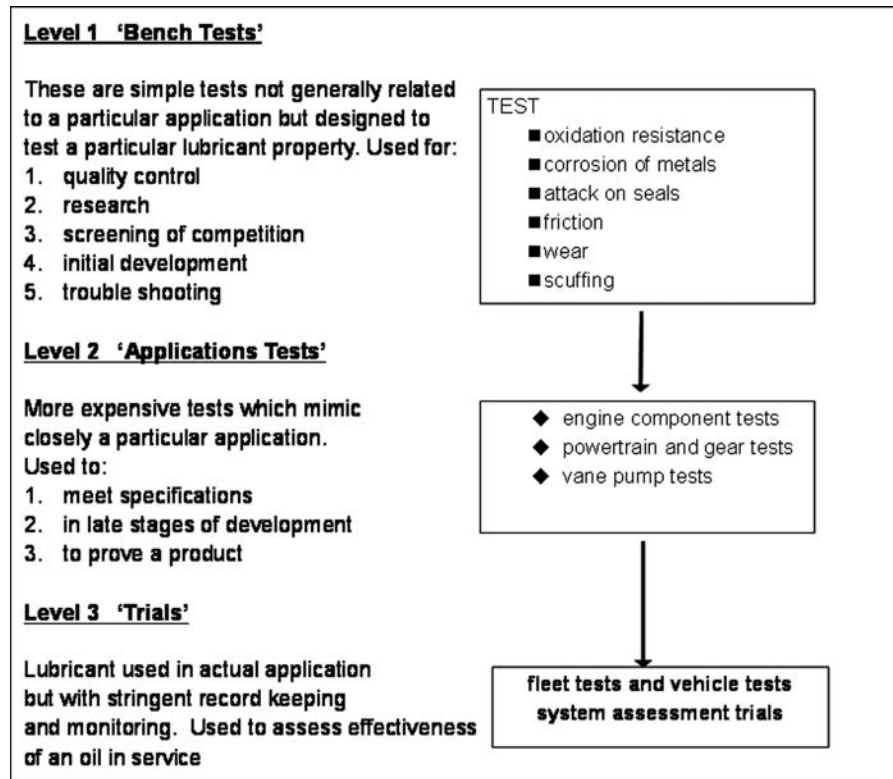


Figure 5.13—Three levels of testing of engine lubricating oils and materials.

5.2.2 Tribological Bench Test Methods

This section reviews the current bench testers using rotary or reciprocating motion for evaluating the friction and wear characteristics of surface materials and coatings. Several configurations, as shown in Table 5.4, are in common use for friction and wear evaluation [74,75]. General information is presented based on either a rotary (Falex type) or a reciprocating tester (two reciprocating testers such as the modified Cameron-Plint test machine or SRV test machine) developed in the authors' laboratory. The following describes several major bench test methods for the evaluation of tribological characteristics of engine and powertrain components.

5.2.2.1 ROTARY BENCH TEST METHODS

Standard rotary bench devices include pin-on-disk (ASTM G99), block-on-ring (ASTM G77), cross cylinders, and four-ball tests [75–77], as shown in Table 5.4. Although these tests can be designed for unidirectional, rotary, or reciprocating motion, they all involve a nonconformal contact geometry. In the last 25 years, the rotary block-on-ring tester [76,77] (designed as LFW-1, also referred to as a Falex friction and wear tester), shown in Figure 5.14, has been used in automotive laboratories for evaluation of piston rings, engine blocks, liners, and valve guides as well as their surface coatings. Scuff results have been obtained by incrementally increasing load until failure is detected by

TABLE 5.4—Common Bench Test Types and Design Details for Friction and Wear Testing

Geometry	Surface Contact	Loading Types	Types of Motion
Pin-on-disk	Point/conformal	Static or dynamic	Unidirectional sliding or oscillating
Pin-on-flat	Point/conformal	Static or dynamic	Reciprocating sliding
Pin-on-cylinder	Point/conformal	Static or dynamic	Unidirectional sliding or oscillating
Thrust washers	Conformal	Static or dynamic	Unidirectional sliding or oscillating
Pin-into-bushing	Conformal	Static or dynamic	Unidirectional sliding or oscillating
Flat-on-cylinder	Line	Static or dynamic	Unidirectional sliding or oscillating
Cross cylinders	Elliptical	Static or dynamic	Unidirectional sliding or oscillating
Four balls	Point	Static or dynamic	Unidirectional sliding

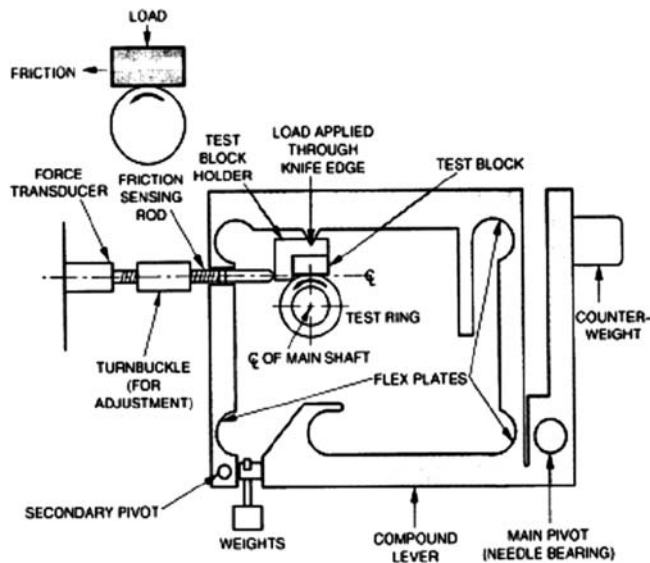


Figure 5.14—Schematic of Falex-type block-on-ring friction and wear tester [78].

the friction measurement. Several procedures have been used for wear testing with this device. These have involved variations in load, speed, lubrication, temperature, and duration. The coefficient of friction is determined at the beginning and end of each test from the load applied and the force transducer output. Block wear is most often evaluated by calculating the volume removed from the block wear scar area. The ring wear is evaluated by weight loss or a subjective evaluation of the visual appearance of the tested surface. Test procedures for this rotary block-on-ring tester, used extensively for piston ring and cylinder liner evaluations, have been described in the paper published by Patterson et al. [78]. The nonrealistic, nonconformal contact of standard specimens used in the block-on-ring test (vs. the conformal contact of the piston ring against the cylinder bore) limits the relevance of the test. In general, the main disadvantage of the rotary bench test methods is that real components cannot be tested; hence, the geometry of engine components is not preserved, and representative surface finishes cannot be evaluated.

5.2.2.2 RECIPROCATING TEST METHOD—MODIFIED CAMERON-PLINT FRICTION AND WEAR MACHINE

A Cameron-Plint high-frequency friction and wear tester has been modified, as shown in Figure 5.15, to serve as a tool for evaluating advanced lubricants or engine materials for possible use in the engine cylinder lubrication. The modified Cameron-Plint high-frequency friction and wear tester provides a reciprocating motion, which is suitable for simulating piston/cylinder liner dynamics [79,80]. The main advantage of this bench test method is that real components can be tested, and because the geometry of the engine is preserved, representative surface finishes can be meaningfully evaluated. A specimen holder can be moved back and forth across a cylinder segment as would occur in an engine. In addition, the holder has been modified to allow the piston ring to move in a slot, simulating the motion occurring in a piston ring groove. The friction and

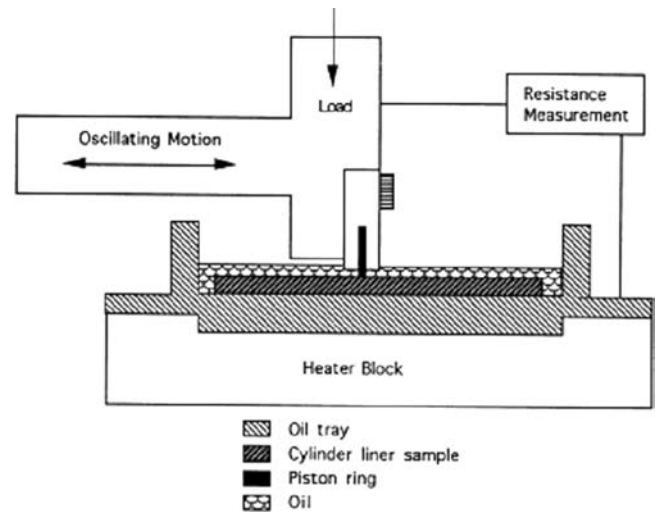


Figure 5.15—Schematic of Cameron-Plint high-frequency friction tester.

electrical resistance can be continuously measured during the test, and the wear of the cylinder liner and piston ring sections can be measured with a surface analyzer using standard techniques [80–82]. To evaluate the stable friction characteristics of engine bores, friction coefficient measurements can be performed after a sufficiently long sliding test time to ensure stabilization, typically 5 h. Friction force is reported as the root mean square (RMS) of the instantaneous friction force over one cycle. The reciprocating bench test procedures are described in detail in references 79–84. Selected results from representative studies of advanced engine materials, coatings, and energy-conserving lubricants are presented in the following subsection to illustrate the potential and use of this method [82–84].

5.2.2.3 BENCH WEAR TEST METHOD USING THE MODIFIED SRV TRIBOLOGICAL TEST MACHINE

The SRV 4 tribology test machine manufactured by Optimol Instruments was used in this bench wear study. A schematic of the system is shown in Figure 5.16. The SRV 4 machine operates by an electromagnetic drive motor, allowing for a controlled stroke at high frequency. The testing conditions developed by the authors are shown in Table 5.5. The SRV test machine has been used for oil sequence tests as well as for piston ring wear evaluation for the last few years in the literature [82–84]. This test machine has recently been modified with a new simulation test to determine the wear and tribological performance of valvetrain components [84]. The SRV 4 test machine can be used to evaluate specimens of camshaft lobe and follower materials subject to representative test conditions.

Five follower materials and eight lobe materials were selected based on their historical use and potential for success [84]. These were tested under sliding conditions against two different follower materials processed through different heat treatments. The same follower materials coated with a diamond-like coating (DLC) were also tested. The flat specimens were machined using the electric-discharge machining (EDM) method from a camshaft material having a representative surface finish of the shaft surface and used as the lower specimens. The lower specimens were

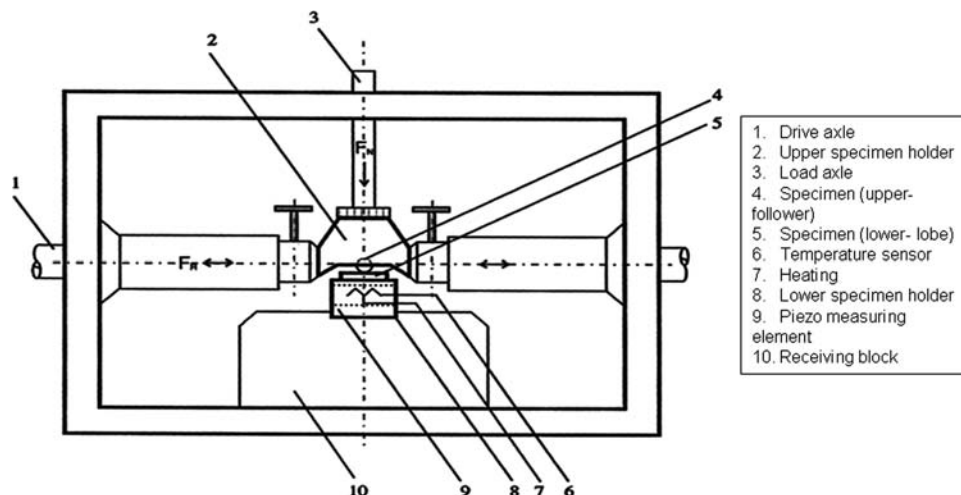


Figure 5.16—Schematic of Optimol SRV 4 high-frequency friction and wear tester.

8 × 6 × 4 mm (Figure 5.17a). The upper specimens, which represented the follower material, were machined from a SAE 52100 steel and 4130 steel bar stock to a cylindrical pin with a rounded tip. The upper specimen had a 10-mm diameter and a 10-mm length with a 35-mm radius on one end (Figure 5.17b). The rounded tip was polished to a surface finish of 0.3 Ra maximum. The 52100 and 4130 steel specimens were heat-treated to Rc 58-62. Thus, the effect due to chemistry, hardness, microstructure, and residual stresses is preserved. The lower specimens can exist with the original surface preserved or flat with a representative surface finish. The cam lobe geometry has an effect on the resultant contact stress for a given load. Custom upper and lower specimen holders were designed and manufactured. The holders are shown in Figure 5.18. The upper specimen holder (Figure 5.18a) is designed to hold the cylindrical specimen and the lower holder (Figure 5.18b) is designed to hold the rectangular block and 0.3 mL of oil to maintain lubrication. Exxon-Mobil 5W-30 oil with GF-4 designation was used for the test.

The test parameters were set to mimic actual operating conditions of a follower in contact with a cam lobe. The upper and the lower specimens are subjected to test conditions that can accelerate the testing under controlled conditions. The following parameters can be varied or kept constant: load, stroke, frequency, oil condition, oil temperature, and the amount of lubrication. Once oil is heated up to 130°C, the test then starts at 15 Hz at a stroke of 4 mm and a load of 50 N for 1 min. After this initial break-in period, the load is ramped up to the full load condition within another minute. The tests were 7 h and run at a frequency of 35 Hz, a stroke of 4 mm, and a load of 550 N. The bench is slightly different because there is oscillation instead of rotation. A 1-min break-in period was used to ensure the contacting surfaces were lubricated. A summary of the test conditions are listed in Table 5.5.

All possible material combinations were tested twice in a randomized fashion. Because of material availability issues, some tests were run in the last batch. Some tests were repeated because of data acquisition error.

Engine oil viscosity grade 5W-30 oil with GF-4 designation was used for the test. For the highly loaded contacts, the interaction between zinc dialkyl dithiophosphate

(ZDP), used as an antiwear and antioxidant additive, and the sliding materials is critical for wear-resistant film formation. The antiwear film formation mechanisms on camshaft materials other than steel, gray, and chilled iron have not been studied in detail, and hence their contribution to friction modification and ultimately to sliding wear properties is unknown. This bench test can be used to assess and select new camshaft/follower materials under sliding and rolling conditions as shown in Figure 5.19 using loads experienced by valvetrain components. This test can also be used to assess newer lubricant formulations using valvetrain components.

5.2.2.4 BENCH SCUFFING WEAR SIMULATION TESTS AND ENGINE DYNAMOMETER TESTS

Cameron-Plint reciprocating machines were used in evaluating the tribological behavior (scuffing wear) of coated pistons against 390 Al bore. The test setup is shown in Figure 5.15. Cold-scuffing simulation tests were conducted under conditions that lead to lubrication starvation. Wear simulation tests were performed under lubricated conditions. A special bench test fixture was used for the evaluation of scuffing and wear behavior of piston skirt against cylinder bore. A data acquisition system kept track of the coefficient of friction, the contact potential, and temperature. During the test, the cylinder bore sample was stationary. The motion of the piston sample was produced by a Scotch Yoke mechanism driven by a variable-speed motor. The piston sample was loaded against the cylinder bore sample by a spring balance. The load ranges from 0 to 250 N. The load can be translated into contact stress in two ways. The first-order estimate of the stress would be simply the load divided by the wear scar width multiplied by the length of the piston sample. The second approach more accurately reflects the true contact stress by using the Hertzian stress [78]. Because the radii of the two samples are deliberately different to allow for consistent alignment, a load divided by area process significantly understates the true contact stress, normally determined by elastic theory as the Hertzian stress. In this work, the Hertzian stress for the contact at 120 N was 17.2 MPa.

During the test, the tangential friction force is monitored and measured by a piezoelectric transducer attached

TABLE 5.5—Optimol SRV 4 Typical Lubricated Testing Conditions [84]

Load	1–2000 N
Test time	1 min to 999 h
Frequency	1–511 Hz
Stroke	0.2 to >4 mm
Temperature	Standard range: ambient to +290°C
	Low-range option: –35 to +290°C
	High-range option: ambient to +900°C
Test parameters	
Break-in test	
• Duration:	1 min
• Temperature:	130°C
• Frequency:	15 Hz
• Stroke:	4 mm
• Load:	50 N
• Contact stress:	900–1280 MPa
• Oil:	0.3 mL GF-4
Lubricated sliding test	
• Duration:	7 h
• Temperature:	130°C
• Frequency:	35 Hz
• Stroke:	4 mm
• Load:	550 N
• Contact stress:	900–1280 MPa
• Oil:	0.3 mL GF-4
Material size	
• Pin curvature:	35 mm
• Flat size:	8 × 6 × 4 mm

to the piston skirt fixture, a continuous recording of the “average” friction force. The electrical contact potential (or resistance) between piston and cylinder bore samples was also continuously measured during the test. The contact potential method is used to monitor lubricated contact conditions. This gives a qualitative indication of the degree of surface asperity interaction because asperity contact results in a great reduction in the electrical resistance (or potential) of the surface contact. In addition, these measurements can be used to monitor the lubricant film or surface coating changes at the interface and to determine the contact and wear mechanism of surface coatings. With the Talysurf analyzer, the wear scars for cylinder bore samples were analyzed in the longitudinal or transverse directions, or both, with respect to the sliding direction.

Physically, it is well known that the root cause of cold scuffing of the piston skirt and cylinder bore is the fuel dilution and high viscosity of oil that occurs at cold temperatures (approximately –20°C) in conjunction with high side forces. It is not practical to introduce the cold temperature and gasoline to the Cameron-Plint test environment, therefore a compromise was undertaken to have the lubricated conditions present during part of the test, with a transition to lubricant starvation similar to that of fuel dilution and high viscosity during the remainder of the test. This was accomplished by using a small amount of kerosine (0.2 cm³), a petroleum fraction that would have some of the tramp elements and a modest reaction at the interface during run-in similar to that of an engine oil but at a temperature (85°C) at which kerosine would decompose and evaporate. The wear simulation tests were conducted at 125°C with a load of 120 or 160 N. The stroke was 6.77 mm at a frequency of 10 Hz. The lubricant used was GF-4 SAE API SH Grade 5W-30.

To validate the scuffing bench tests, cold- and hot-scuffing engine dynamometer tests were designed to supplement for validation of the tested piston coatings against 390 Al bore with Saturn 1.9-L L-4 engines. For the cold-

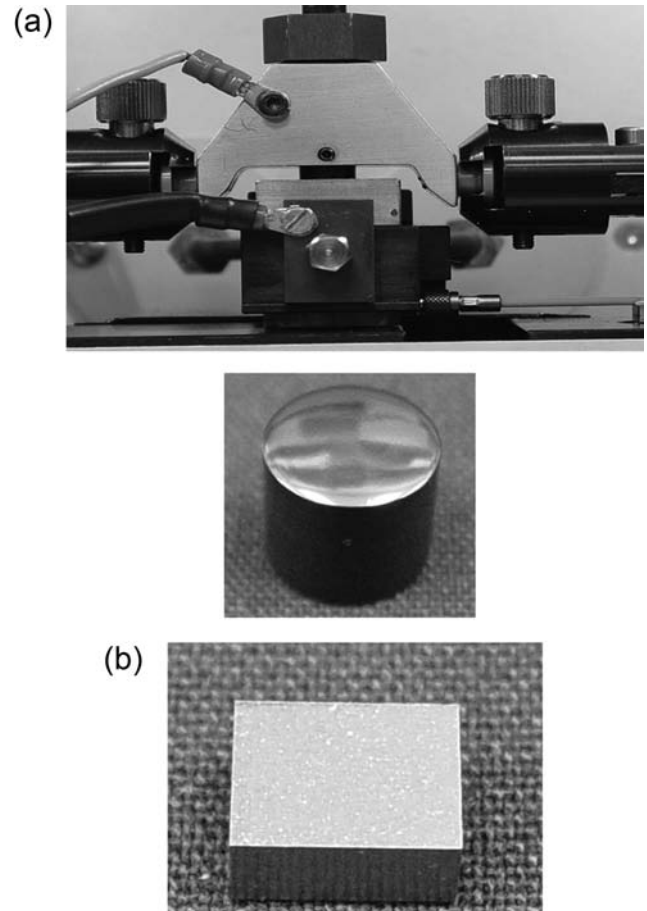


Figure 5.17—Test samples representing the follower material (upper specimen) and lobe material (lower specimen) [84]. (a) Upper specimen: cylindrical, 10 mm in diameter and 10 mm in length with a spherical contact surface at one end having a curvature of 35 mm. (b) Lower specimen: block measuring 8.0 × 6.0 × 4.0 mm.

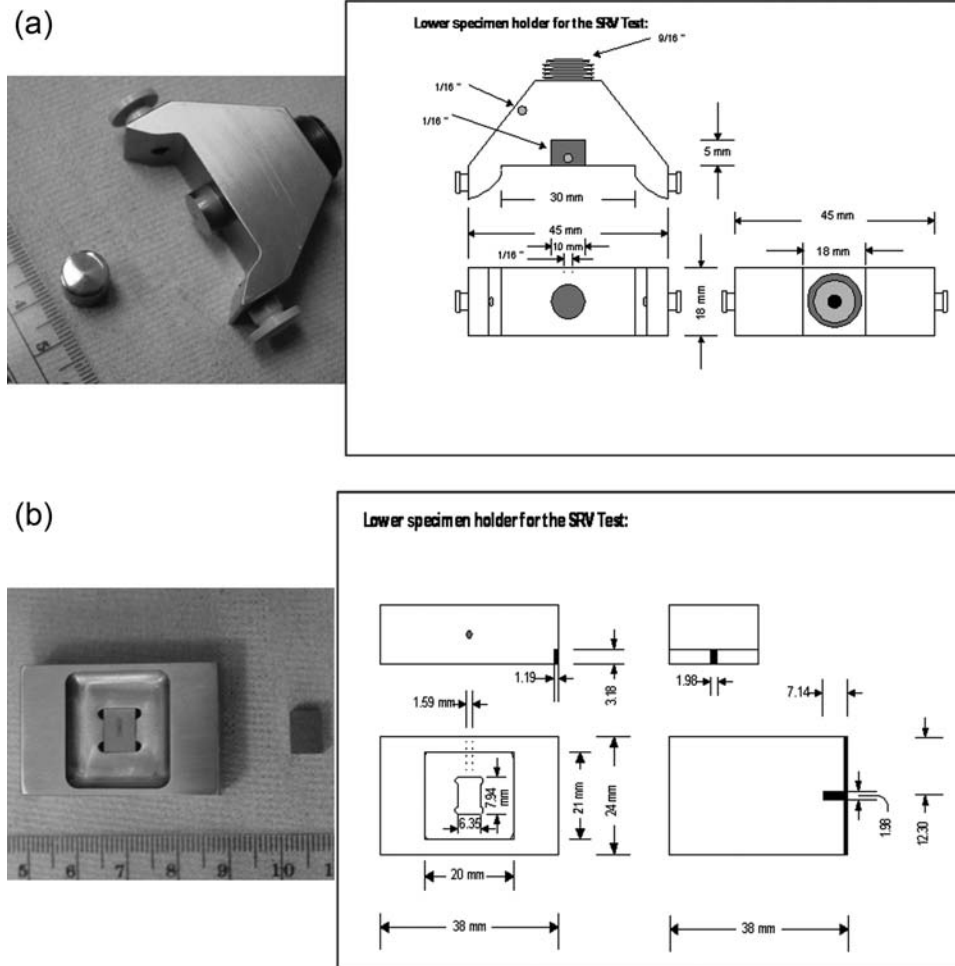


Figure 5.18—Custom specimen holders: (a) upper specimen and (b) lower specimen.

scuffing tests, the engines were installed on an eddy current dynamometer, set at 17 ft.·lbf of torques, and held at 2000 r/min for a period of 2.5 h. A 30HK chiller unit was used for the coolant, which had a setting of -4°C into the engine so that the outlet temperature was maintained at 0°C throughout the test. For the hot-scuffing tests, the engines were set to 5200 r/min WOT (wide-open throttle) until the coolant temperature reached a maximum of 110°C . The speed was then reduced to idle (1200 r/min at no load) so that the outlet coolant temperature reduced down to 30°C . The process cycle started over again until failure occurred or reached 9 h.

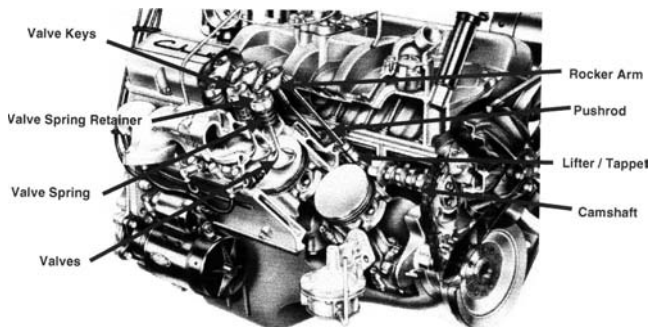


Figure 5.19—Valvetrain basic configuration.

5.3 EXPERIMENTAL METHODS FOR MEASURING WEAR AND SCUFFING

5.3.1 Wear and Scuffing Tests

Measurements of engine wear, scuffing, and surface fatigue are particularly complicated. The response of a lubricated, rubbing system critically depends on the precise conditions of a test. This means that different tests may render quite different results. Particularly important factors are

- The metallurgy and roughness of the rubbing specimens;
- The operation regime, whether full boundary or mixed EHD/boundary; and
- The temperature, which may change very significantly throughout a test because of bulk frictional heating.

The important issues for using wear and scuffing tests are always the awareness of their limitations and the thorough understanding of the capability of the tester, its design concepts, the regimes of lubrication present, and the contact pressure and temperatures involved.

The most widely used scuffing and wear testers are listed in Tables 5.4 and 5.5. Of these, the most common ones are probably the four-ball testers for scuffing and wear, the Timken block-on-ring scuffing tester, and the Falex pin-on-V-block wear/scuffing tester. For gear tests, FZG is the most widely used. The FZG is also used as a test for shear stability of polymer-containing oils to determine the extent of permanent viscosity loss during use (IP 351/81). Not

included in Table 5.4 are disc machines, which are used to simulate gear scuffing.

5.3.2 Assessment of Engine Wear and Scuffing Measurements

Engine components such as piston skirts, camshafts, and valvetrain components are subject to normal wear in the normal range of lubricated sliding. Then the wear mode will transfer into more severe scuffing after a higher loading and sliding condition. Earlier chapters in this handbook have reviewed how friction influences the temperature rise of a contact and how the thermal response of a rubbing system depends on the ability of the two rubbing bodies to remove heat. Because the viscosity and the additive response of a lubricant are crucially dependent on temperature, it is hardly surprising that different test machines give very different results. Another problem is that the contact area, and thus the contact pressure, can vary greatly because of wear throughout a test in a fashion that depends very strongly on the geometry of the test specimens.

Tribological bench testing in a laboratory can provide rapid and cost-effective information; it is often used for screening or ranking purposes in the process of developing new engine materials and lubricants. To determine the relative ranking of these materials under sliding conditions that are representative in terms of loading, specimens from the camshaft materials and the follower materials were specially heat-treated and then machined to a specific geometry such that the applied Hertzian loads were identical and the corresponding applied stresses for different materials could be calculated. Assessment of ranking can be done based on the selection of end-of-test (EOT) criteria. Thus, the test could be run for a specific duration with a limited amount of lubrication or it could be run to simulate response under fresh or degraded lubrication conditions. The lubrication regime can be chosen to be at full boundary or at mixed EHD/boundary conditions with a temperature range up to 135°C, so the effect of viscosity and oil additives can be similar as in an engine. The load could be ramped up slowly in the beginning, or the specimens could be subjected to the maximum load right from the beginning. The EOT criteria could be selected based on the percentage increase in friction coefficient or the EOT value of the friction coefficient. Determination of EOT response for acceptability of the sliding wear performance of each material was done by measuring the coefficient of friction and the wear scar depth as well as the wear volume of each mating surface [81–84]. The surface wear scar assessment was done using a Wyko machine.

Several examples of worn specimens are shown in Figure 5.20. The measurement technique for wear volume is shown in Figure 5.21. For the flat specimens, the

process is fairly straightforward. Figure 5.21a shows an image of a worn flat, including the surrounding unworn area. The image is then processed using the Veeco software. The unworn area is masked off, and then the unworn area is corrected for any tilt or curvature in the specimen. The worn area is then restored, and another feature of the Veeco software is used to calculate the worn volume. This feature calculates the volume below an arbitrary reference plane, which can be raised or lowered using the slider bar shown in Figure 5.21b. The reference plane is lowered until the unworn surface disappears from the view in Figure 5.21b, at which point the volume below the plane is the wear volume and is read directly from the screen [84].

The procedure for the pins is slightly more complicated. As shown in Figure 5.21c, the spherical pin is worn by contact with the flat, but the geometry of the contact is such that the wear area on the pin is not flat, which results in a wear area that is elliptical rather than circular. As a result, the use of a truncated sphere model to measure the wear volume would not be accurate. In this case, the image of the pin is leveled with respect to the worn area, and the spherical radius is subtracted from the image. The result is shown in Figure 5.21d, where the formerly spherical unworn region now appears flat and the worn region appears as a depression in the flat surface. Now the wear volume is measured using the same software feature as used previously for the flat samples.

The total wear volume of the different material combinations is shown in Figure 5.22 [84]. The total wear volume is the sum of the pin wear and the flat wear. Some combinations can be differentiated from others because they performed orders of magnitude better. Figure 5.22 shows the data for material combinations with less than 0.25 mm³ total wear. From this figure, one can see that overall lobe material D provided the least amount of total wear volume, and for the follower materials, 4 and 5 had the least total wear volume. Using the carburized steel 4130 plus DLC coating material showed the best wear resistance compared with the other material combinations. From these data, it was possible to select different material combinations that comparatively displayed the best results [84].

5.4 CONCLUSIONS

Several EHL film-thickness measurement techniques and some experimental data from point-contact lubrication investigations were reviewed. In many cases, the measured film thickness well follows the power-law relationship formulated by the H&D equation. Major deviations are usually observed when speed is low or film is very thin. A few trends of the film thickness variation with speed at low

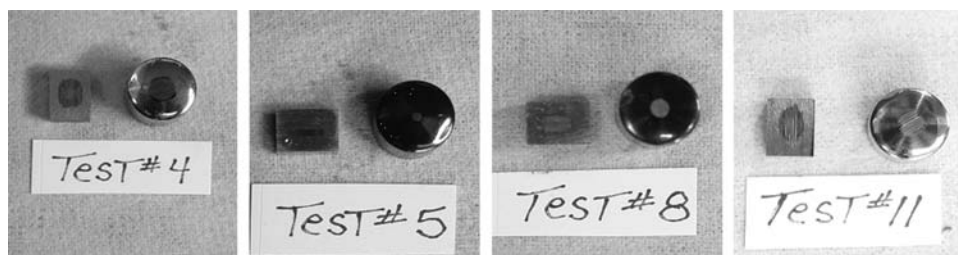


Figure 5.20—Examples of worn test specimens [84].

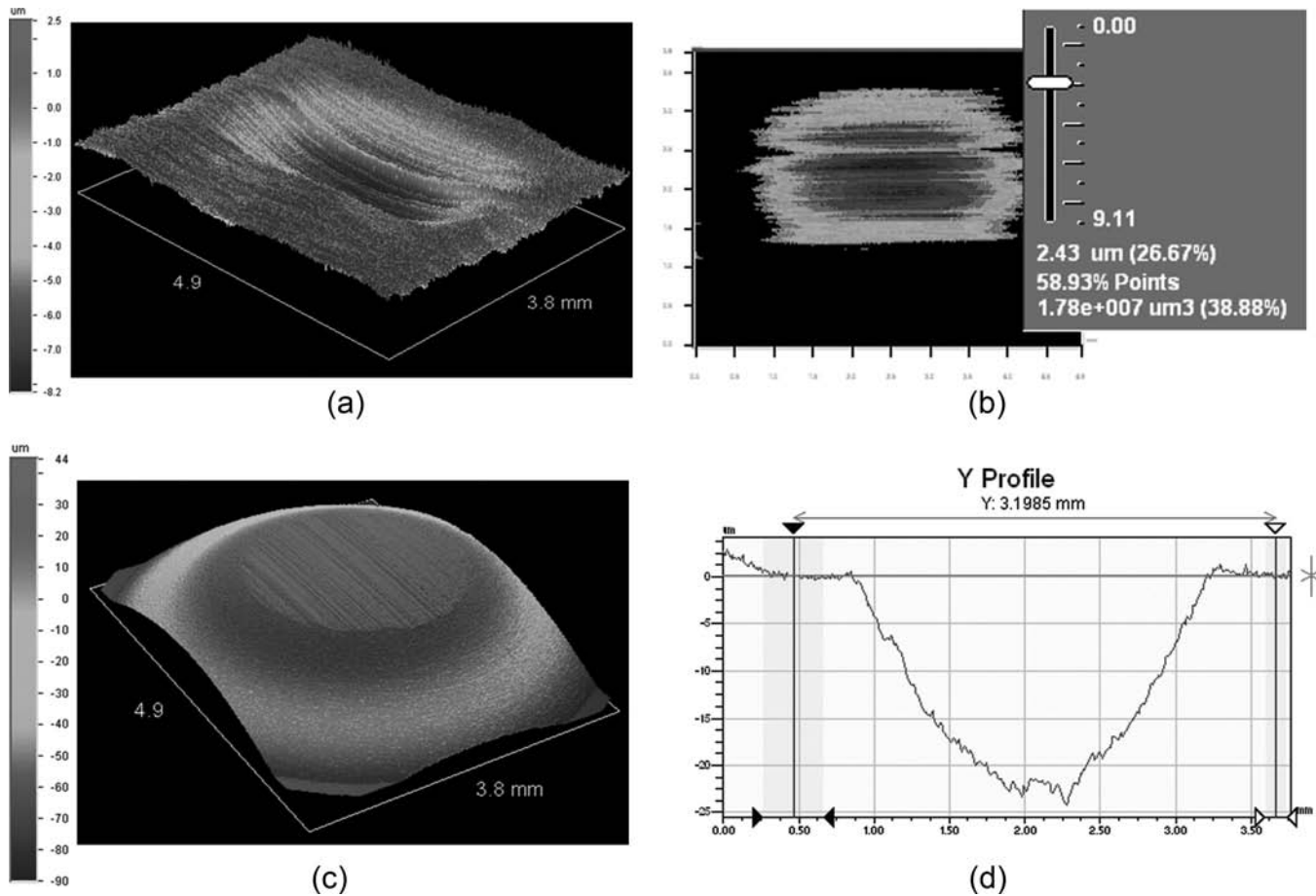


Figure 5.21—Wear analysis and wear three-dimensional profiles by Veeco images [84].

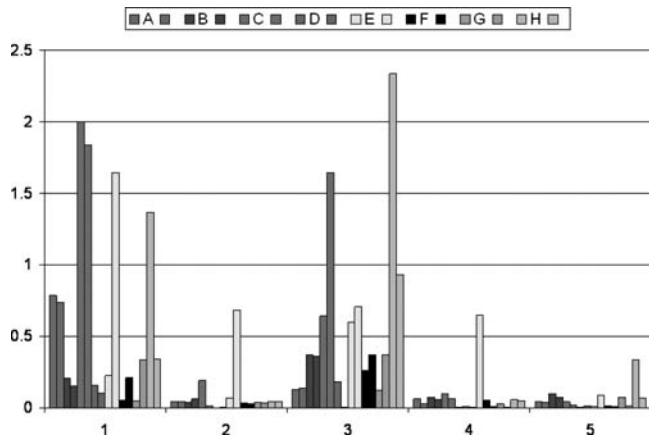


Figure 5.22—Wear volumes for different material combinations [84]. Note that wear volumes for different material combinations (A, B, C, D, E, F, G, H) with values >0.25 mm³ are removed for clarity. A = ADI, B = CCI, C = GCI, D = MCI, E = NCl, F = PFC 1D, G = PFC 1E, and H = PFC 2D. Material #1 = 52100 steel, Material #2 = 52100 steel + DLC, Material #3 = 4130 carburized steel, Material #4 = 4130 carburized steel + DLC, and Material #5 = 4130 carbonitrided steel.

speed and thin-film lubrication have been reported in the literature, which may be viewed as (1) power-law straight line, (2) upward deviation from the power-law straight line, (3) downward deviation from the power-law straight line, and (4) a three-slope behavior.

A few EHL film-thickness measurements are simulated by means of the Hu-Zhu modeling approach. The numerical results are compared with several groups of experimental data. The comparisons indicate that in most cases both sets of results are in reasonably good agreement.

This chapter also provided a comprehensive overview of various lubrication test methods for a typical engine system [79–84], including the bench wear and scuffing tests. Major technical issues related to wear mechanisms, lubricant degradation, and the current development status of automotive lubricant testing methods in North America and Europe were discussed. Tribological concerns associated with various automotive engine components, material effects on automotive lubricants, standard test development, and the updated bench test for wear and scuffing evaluation and simulation test development [84–92] for gasoline and diesel engines were investigated.

References

- [1] Crook, A.W., 1958, "The Lubrication of Rollers," *Phil. Trans. Roy. Soc. (London)*, Vol. 250, pp. 387–409.
- [2] Heemskerk, R.S., Vermeiren, K.N., and Dolfmsa, H., 1982, "Measurement of Lubrication Condition in Rolling Element Bearings," *ALSE Trans.*, Vol. 25, pp. 519–527.
- [3] Orcutt, F.K., 1965, "Experimental Study of Elastohydrodynamic Lubrication," *ALSE Trans.*, Vol. 8, pp. 381–396.
- [4] El-Sisi, S.I., and Shawki, G.S.A., 1960, "Measurement of Oil-Film Thickness between Disks by Electrical Conductivity," *ASME J. Basic Eng.*, Vol. 82, pp. 12–18.

- [5] Archard, J.F., and Kirk, M.T., 1961, "Lubrication at Point Contacts," *Proc. Royal Soc. Ser. A*, Vol. 261, pp. 532–550.
- [6] Zhang, Y.C., Meng, H.R., Fan, X., and Zhang, L.R., 1999, "Study on Contacting Electric Resistance Method to Determine Lubrication of Worm Drive," *Coal Sci. Technol.*, Vol. 27, pp. 23, 26–29 (in Chinese).
- [7] Macconochie, I.O., and Cameron, A., 1960, "The Measurement of Oil-Film Thickness in Gear Teeth," *ASME J. Basic Eng.*, Vol. 82, pp. 29–34.
- [8] Sibley, L.B., and Orcutt, F.K., 1961, "Elasto-Hydrodynamic Lubrication of Rolling-Contact Surfaces," *ALSE Trans.*, Vol. 4, pp. 381–396.
- [9] Yang, J.B., Qi, Y.L., and Chen, C.W., 1990, "Measurement of Oil Film Thickness between W-N Helical Gear Tooth Profiles Using Laser Transmission Method," *Chinese J. Mech. Eng.*, Vol. 26, pp. 68–71.
- [10] Zhang, Y.C., and Wen, S.Z., 1994, "Experimental Research of Measurement of Oil Film Thickness between Arc Profiles of Gear Tooth Using Laser Transmission Method," *Machine Des.*, Vol. 11, pp. 45–48 (in Chinese).
- [11] Zhang, P.S., Li, S.G., and Zhai, W.J., 1991, "A New Measurement Method of Oil Film Thickness in the EHL Condition: the R-C Oscillation Technique," *Wear*, Vol. 148, pp. 39–46.
- [12] Kirk, M.T., 1962, "Hydrodynamic Lubrication of 'Perspex,'" *Nature*, Vol. 194, pp. 965–966.
- [13] Gohar, R., and Cameron, A., 1963, "Optical Measurement of Oil Film Thickness under Elasto-Hydrodynamic Lubrication," *Nature*, Vol. 200, pp. 458–459.
- [14] Johnston, G. J., Wayte, R., and Spikes, H.A., 1991, "The Measurement and Study of Very Thin Lubricant Films in Concentrated Contacts," *Tribology Trans.*, Vol. 34, pp. 187–194.
- [15] Pemberton, J.C., and Cameron, A., 1979, "An Optical Study of the Lubrication of a 65 mm Cylindrical Roller Bearing," *ASME J. Lub. Technol.*, Vol. 101, pp. 327–337.
- [16] Yung, K.M., and Cameron, A., 1979, "Optical Analysis of Porous Metal Bearings," *ASME J. Lub. Technol.*, Vol. 101, pp. 99–104.
- [17] Wedeven, L.D., Evans, D., and Cameron, A., 1971, "Optical Analysis of Ball Bearing Starvation," *ASME J. Lub. Technol.*, Vol. 93, pp. 349–363.
- [18] Wedeven, L.D., 1975, "Traction and Film Thickness Measurements under Starved Elasto-hydrodynamic Conditions," *ASME J. Lub. Technol.*, Vol. 97, pp. 321–329.
- [19] Gohar, R., and Cameron, A., 1967, "The Mapping of Elasto-hydrodynamic Contacts," *ALSE Trans.*, Vol. 10, pp. 215–225.
- [20] Cameron, A., and Gohar, R., 1966, "Theoretical and Experimental Studies of the Oil Film in Lubricated Point Contact," *Proc. Royal Soc. Ser. A*, Vol. 291, pp. 520–536.
- [21] Foord, C.A., Wedeven, L.D., Westlake, F.J., and Cameron, A., 1969–1970, "Optical Elasto-hydrodynamics," *Proc. Inst. Mech. Eng.*, 1, Vol. 184, pp. 487–505.
- [22] Foord, C.A., Hammann, W.C., and Cameron, A., 1968, "Evaluation of Lubricants Using Optical Elasto-hydrodynamics," *ALSE Trans.*, Vol. 11, pp. 31–43.
- [23] Koye, K.A., 1981, "An Experimental Evaluation of the Hamrock and Dowson Minimum Film Thickness Equation for Fully Flooded EHD Point Contacts," *ASME J. Lub. Technol.*, Vol. 103, pp. 284–294.
- [24] Spikes, H.A., and Cann, P. M., 2001, "The Development and Application of the Spacer Layer Imaging Method for Measuring Lubricant Film Thickness," *J. Eng. Tribology*, Vol. 215, pp. 261–277.
- [25] Hartl, M., Krupka, I., and Liska, M., 1997, "Differential Colorimetry: Tool for Evaluation of Chromatic Interference Patterns," *Optical Eng.*, Vol. 36, pp. 2384–2391.
- [26] Molimard, J., Querry, M., and Vergne, P., 1998, "New Tools for the Experimental Study of EHD and Limit Lubrications," In *Proceedings of the 25th Leeds-Lyon Symposium on Tribology*, Institut National des Sciences Appliquées de Lyon, Lyon, France, pp. 101–109.
- [27] Hartl, M., Krupka, I., Poliscuk, R., Liska, M., Molimard, J., Querry, M., and Vergne, P., 2001, "Thin Film Colorimetric Interferometry," *Tribology Trans.*, Vol. 44, pp. 270–276.
- [28] Luo, J.B., Wen, S.Z., and Huang, P., 1996, "Thin Film Lubrication, Part I: Study on the Transition between EHL and Thin Film Lubrication Using a Relative Optical Interference Intensity Technique," *Wear*, Vol. 194, pp. 107–115.
- [29] Ai, X.L., and Zheng, L.Q., 1989, "A New Method for the Experimental Investigation of Contact in Mixed Lubrication," *Wear*, Vol. 132, pp. 221–233.
- [30] Sanborn, D.M., and Winer, W.O., 1971, "Fluid Rheological Effects in Sliding Elastohydrodynamic Point Contacts with Transient Loading: 1-Film Thickness," *ASME J. Lub. Technol.*, Vol. 93, pp. 262–271.
- [31] Chiu, Y.P., and Sibley, L.B., 1972, "Contact Shape and Non-Newtonian Effects in Elastohydrodynamic Point Contacts," *Lub. Eng.*, Vol. 28, pp. 48–60.
- [32] Choo, J.W., Glovnea, R.P., Olver, A.V., and Spikes, H.A., 2003, "The Effects of Three-Dimensional Model Surface Roughness Features on Lubricant Film Thickness in EHL Contacts," *ASME J. Tribology*, Vol. 125, pp. 533–542.
- [33] Kaneta, M., Tani, N., and Nishikawa, H., 2002, "Optical Interferometric Observations of the Effect of Moving Transverse Asperities on Point Contact EHL Films," In *Proceedings of the 29th Leeds-Lyon Symposium on Tribology*, University of Leeds, Leeds, UK, pp. 101–109.
- [34] Kaneta, M., Kawashima, R., Masuda, S., Nishikawa, H., Yang, P., and Wang, J., 2002, "Thermal Effects on the Film Thickness in Elliptic EHL Contacts with Entrainment along the Major Contact Axis," *ASME J. Tribology*, Vol. 124, pp. 420–427.
- [35] Sugimura, J., Jones, W.R. Jr., and Spikes, H.A., 1998, "EHD Film Thickness in Non-Steady State Contacts," *ASME J. Tribology*, Vol. 120, pp. 442–452.
- [36] Hu, Y.Z., and Zhu, D., 2000, "A Full Numerical Solution to the Mixed Lubrication in Point Contacts," *ASME J. Tribology*, Vol. 122, pp. 1–9.
- [37] Zhu, D., and Hu, Y.Z., 2001, "A Computer Program Package for the Prediction of EHL and Mixed Lubrication Characteristics, Friction, Subsurface Stresses and Flash Temperatures Based on Measured 3-D Surface Roughness," *Tribology Trans.*, Vol. 44, pp. 383–390.
- [38] Zhu, D., and Hu, Y.Z., 2001, "Effects of Rough Surface Topography and Orientation on the Characteristics of EHD and Mixed Lubrication in Both Circular and Elliptical Contacts," *Tribology Trans.*, Vol. 44, pp. 391–398.
- [39] Guo, F., Yang, P., and Qu, S., 2001, "On the Theory of Thermal Elastohydrodynamic Lubrication at High Slide-Roll Ratios—Circular Glass-Steel Contact Solution at Opposite Sliding," *ASME J. Tribology*, Vol. 123, pp. 816–821.
- [40] Zhu, D., and Wen, S.Z., 1984, "A Full Numerical Solution for the Thermoelasto-hydrodynamic Problem in Elliptical Contacts," *ASME J. Tribology*, Vol. 106, pp. 246–254.
- [41] Sugimura, J., Okumura, T., Yamamoto, Y., and Spikes, H.A., 1999, "Simple Equation for Elastohydrodynamic Film Thickness under Acceleration," *Tribology Int.*, Vol. 32, pp. 117–123.
- [42] Zhao, J., and Sadeghi, F., 2003, "Analysis of EHL Circular Contact Shut Down," *ASME J. Tribology*, Vol. 125, pp. 76–90.
- [43] Hamrock, B. J., and Dowson, D., 1976, "Isothermal Elastohydrodynamic Lubrication of Point Contacts, Part 1—Theoretical Formulation," *ASME J. Lub. Technol.*, Vol. 98, pp. 223–229.
- [44] Smeeth, M., Spikes, H., and Gunsell, S., 1996, "Boundary Film Formation by Viscosity Index Improvers," *Tribology Trans.*, Vol. 39, pp. 726–734.
- [45] Guangteng, G., and Spikes, H.A., 1996, "Boundary Film Formation by Lubricant Base Fluid," *Tribology Trans.*, Vol. 39, pp. 448–454.
- [46] Luo, J., Qian, L., Wen, S., Wen, L., Wen S., and Li. L., 1999, "The Failure of Fluid Film at Nano Scale," *Tribology Trans.*, Vol. 42, pp. 912–916.
- [47] Lubrecht, A.A., 1987, *The Numerical Solution of Elastohydrodynamic Lubricated Line and Point Contact Problems Using Multigrid Techniques*, Ph.D. Thesis, University of Twente, The Netherlands.
- [48] Venner, C.H., 1991, *Multilevel Solution of EHL Line and Point Contact Problems*, Ph.D. Thesis, University of Twente, The Netherlands.
- [49] Ai, X., 1993, *Numerical Analysis of Elastohydrodynamically Lubricated Line and Point Contacts with Rough Surfaces by Using Semi-System and Multigrid Methods*, Ph.D. Thesis, Northwestern University, Evanston, IL.

- [50] Liu, S.B., Wang, Q., and Liu, G., 2000, "A Versatile Method of Discrete Convolution and FFT (DC-FFT) for Contact Analyses," *Wear*, Vol. 243, pp. 101–110.
- [51] Liu, S., and Wang, Q., 2002, "Studying Contact Stress Fields Caused by Surface Traction with a Discrete Convolution and Fast Fourier Transform Algorithm," *ASME J. Tribology*, Vol. 124, pp. 36–45.
- [52] Holmes, M.J.A., 2002, *Transient Analysis of the Point Contact Elastohydrodynamic Lubrication Problem Using Coupled Solution Methods*, PhD Thesis, Cardiff University, Cardiff, UK.
- [53] Venner, C.H., and Lubrecht, A.A., 1994, "Numerical Simulation of a Transverse Ridge in a Circular EHL Contact Rolling/Sliding," *ASME J. Tribology*, Vol. 116, pp. 751–761.
- [54] Kaneta, M., Sakai, T., and Nishikawa, H., 1992, "Optical Interferometric Observations of the Effects of A Bump on Point Contact EHL," *ASME J. Tribology*, Vol. 114, pp. 779–784.
- [55] Holmes, M.J.A., Evans, H.P., and Snidle, R.W., 2002, "Comparison of Transient EHL Calculations with Start-Up Experiments," In *Proceedings of the 29th Leeds-Lyon Symposium on Tribology*, D. Dowson, M. Priest, G. Dalmaz, and A.A. Lubrecht, Eds., Elsevier, Amsterdam, pp. 79–89.
- [56] Holmes, M.J.A., Evans, H.P., and Snidle, R.W., 2002, "Comparison of Transient EHL Calculations with Shut-Down Experiments," In *Proceedings of the 29th Leeds-Lyon Symposium on Tribology*, D. Dowson, M. Priest, G. Dalmaz, and A.A. Lubrecht, Eds., Elsevier, Amsterdam, pp. 91–99.
- [57] Glovnea, R.P., and Spikes, H.A., 2001, "Elastohydrodynamic Film Formation at the Start-Up of the Motion," *J. Eng. Tribology*, Vol. 215, pp. 125–138.
- [58] Glovnea, R.P., and Spikes, H.A., 2001, "Elastohydrodynamic Film Collapse during Rapid Deceleration. Part I: Experimental Results," *ASME J. Tribology*, Vol. 123, pp. 254–261.
- [59] Zhao, J., and Sadeghi, F., 2003, "Analysis of EHL Circular Contact Shut Down," *ASME J. Tribology*, Vol. 125, pp. 76–90.
- [60] Zhao, J., 2005, "Analysis of EHL Circular Contact Start Up: Comparison with Experimental Results," WTC2005-63705, In *Proceedings of WTC2005 World Tribology Congress III*, September 12–16, 2005, Washington, DC.
- [61] Felix-Quinonez, A., Ehret, P., and Summers, J.L., 2003, "New Experimental Results of a Single Ridge Passing Through an EHL Conjunction," *ASME J. Tribology*, Vol. 125, pp. 252–259.
- [62] Felix-Quinonez, A., Ehret, P., and Summers, J.L., 2004, "Numerical Analysis of Experimental Observations of a Single Transverse Ridge Passing through an Elastohydrodynamic Lubrication Point Contact under Rolling/Sliding Conditions," *J. Eng. Tribology*, Vol. 218, pp. 109–123.
- [63] Felix-Quinonez, A., Ehret, P., and Summers, J.L., 2005, "On Three-Dimensional Flat-Top Defects Passing Through an EHL Point Contact: A Comparison of Modeling with Experiments," *ASME J. Tribology*, Vol. 127, pp. 51–59.
- [64] Liu, Y., Wang, Q., Hu, Y., Wang, W., and Zhu, D., 2006, "Effects of Differential Schemes and Mesh Density on EHL Film Thickness in Point Contacts," *ASME J. Tribology*, Vol. 128, pp. 641–653.
- [65] Liu, Y.C., Wang, Q.J., Wang, W.Z., Hu, Y.Z., Zhu, D., Krupka, I., and Hartl, M., 2006, "EHL Simulation Using the Free-Volume Viscosity Model," *Tribology Lett.*, Vol. 23, pp. 27–37.
- [66] Liu, Y., Wang, Q., Zhu, D., Wang, W., Hu, Y., (2009), "Effects of Differential Scheme and Viscosity Model on Rough-Surface Point-Contact Isothermal EHL," *J. Tribology*, Vol. 131, pp. 044501-1-5.
- [67] Wang, Q., Zhu, D., Zhou, R., and Hashimoto, F., 2008, "Investigating the Effect of Surface Finish and Texture on Mixed EHL of Rolling and Rolling-Sliding Contacts," *Tribology Trans.*, Vol. 51, pp. 748–761.
- [68] Ehret, P., Dowson, D., and Taylor, C.M., 1998, "On Lubricant Transport Conditions in Elastohydrodynamic Conjunctions," *Proc. Royal Soc. London A*, Vol. 454, pp. 763–787.
- [69] Bair, S., 2000, "On the Concentrated Contact as a Viscometer," *J. Eng. Tribology*, Vol. 214, pp. 515–521.
- [70] Bair, S., Liu, Y.C., and Wang, Q.J., 2006, "The Pressure-Viscosity Coefficient for Newtonian EHL Film Thickness with General Piezoviscous Response." Paper no. IJTC2006-12010. In *ASME Conference Proceedings*, ASME, New York, pp. 185–196.
- [71] Liu, Y.C., Wang, Q.J. and Bair, S., 2006, "EHL Simulation Using the Free-Volume Viscosity Model," *Tribology Lett.*, Vol. 23, pp. 27–37.
- [72] Krupka, I., Hartl, M., Poliscuk, R., Cermak, J., and Liska, M., 2000, "Experimental Evaluation of EHD Film Shape and Its Comparison with Numerical Solution," *ASME J. Tribology*, Vol. 122, pp. 689–696.
- [73] Bair, S., 2001, "Measurements of Real Non-Newtonian Response for Liquid Lubricants Under Moderate Pressures," *J. Eng. Tribology*, Vol. 215, pp. 223–233.
- [74] Benzing, R., and Peterson M., 1976, *Friction and Wear Devices*, ASLE Publication, Park Ridge, IL.
- [75] ASTM G99 Standard, 1990: Test Method for Ultra Testing with a Pin-On-Disk Apparatus, *Annual Book of ASTM Standards*, ASTM International, West Conshohocken, PA.
- [76] ASTM G77 Standard, 1983: Test Method for Ranking Materials to Sliding Wear Using Block-On-Ring Wear Tester, *Annual Book of ASTM Standards*, ASTM International, West Conshohocken, PA.
- [77] United States Steel (USS), 1971, *Lubrication Engineers Manual*, 1st ed., C. Bailey and J. Aarons, Eds., USS, Granite City, IL.
- [78] Patterson, D., Hill, S., and Tung, S., 1991, "Bench Wear Testing of Engine Power Cylinder Components," Presented at the ASME Technical Conference, Muskegon, MI.
- [79] Hartfield-Wunsch, S., Tung, S., and Rivard, C., 1993, "Development of a Bench Test for the Evaluation of Engine Cylinder Components and the Correlation with Engine Test Results," Paper No. 932693, *SAE Trans.*, pp. 1131–1138.
- [80] Hartfield-Wunsch, S., and Tung, S., 1994, "The Effect of Microstructures on the Wear Behavior of Thermal Sprayed Coatings," Reprint from the 1994 7th Thermal Spray Conference Proceedings, Boston, MA, June 20–24.
- [81] Fessenden, K.S., Zurecki, Z., and Slavin, T.P., 1991, *Thermal Sprayed Coatings: Properties, Processes, and Applications*, ASM International, Materials Park, OH.
- [82] Tung, S., and Tseregounis, S., 2000, "An Investigation of Tribological Characteristics of Energy-Conserving Engine Oils Using A Reciprocating Bench Test," Paper presented at the SAE Spring Fuels and Lubricants Conference, June 20.
- [83] Tseregounis, S., and McMillan, M., 1995, "Engine Oil Effects on Fuel Economy in GM Vehicles - Comparison with the ASTM Sequence VI-A Engine Dynamometer Test," SAE Paper No. 952347. Presented at the SAE Fuels and Lubricants Meeting, October 16–19.
- [84] Tung, T., Quintana, T., Wakade, S., Becker, E., and White, S., 2007, "A Test Method for Evaluating Automotive Camshaft and Follower Components Subjected to Lubricated Sliding Simulating Variable Valve Actuation," *JSAE/SAE Paper No. 20077324*. Paper presented at the JSAE/SAE International Fuels and Lubricants Conference, Kyoto, Japan, July 22–25.
- [85] Younggren, P.J., and Schwartz S.E., 1993, "The Effects of Trip Length and Oil Type (Synthetic Versus Mineral Oil) on Engine Damage and Engine-Oil Degradation in a Driving Test of a Vehicle with a 5.7L Engine," SAE Paper No. 932838. SAE, Warrendale, PA.
- [86] Smolenski, D.J., and Schwartz, S.E., 1994, "Automotive Engine Oil Condition Monitoring," *Lub. Eng.*, Vol. 50, pp. 716–722.
- [87] Rounds, F.E., 1987, "Effect of Lubricant Additives on Pro-Wear Characteristics of Synthetic Diesel Soots," *Lub. Eng.*, Vol. 43, pp. 273–282.
- [88] McDonald, J.E., 2011, "Oil Life Monitor for Diesel Engines," U.S. Patent 6327900, December 11.
- [89] Schwartz, S.E., 1986, "An Analysis of Upper-Cylinder Wear with Fuels Containing Methanol," *Lub. Eng.*, Vol. 42, pp. 292–299.
- [90] Schwartz, S.E., 1986, "Effects of Methanol, Water, and Engine Oil on Engine Lubrication System Elastomers," *Lub. Eng.*, Vol. 44, pp. 201–205.
- [91] ILSAC GF-4 and Sequence IIIG Performance Test Standard, 2004: ILSAC GF-4 Specification Draft.
- [92] Canter, N., 2004, "Development of a Lean, Green Automobile," *Tribology Lub. Technol.*, Vol. 60, pp. 15–16.

6

Automotive Engine Hardware and Lubrication Requirements

Edward P. Becker¹ and Simon C. Tung²

6.1 INTRODUCTION

The automotive industry is facing tough international competition, government regulations, and rapid technological changes. Ever-increasing government regulations require improved fuel economy and lower emissions from the automotive fuel and lubricant systems. Higher energy-conserving engine oils and better fuel-efficient vehicles will become increasingly important in the face of the saving of natural resources and the lowering of engine friction. Recently, industry research needs for reducing friction and wear in transportation are critical for saving fuel economy and extended vehicle reliability. There are many hundreds of tribological components, from bearings, pistons, transmissions, and clutches to gears and drivetrain components. The application of tribological principles is essential for the reliability of the motor vehicle and the energy conservation of our environment. This review chapter will provide a comprehensive overview of various lubrication aspects of a typical powertrain system including the engine, transmission, driveline, and other components as well as the major issues and the current development status for automotive engine lubricants in North America. This review chapter also describes the major functions of typical engines (gasoline and diesel), engine oil characteristics, and test methods. Included are descriptions of the tribological concerns associated with various engine components, service effects on engine oil, standard automotive tests for engine oil and the types of service they represent, and an overview of the current issues and future trends that needs to be addressed.

6.2 ENGINE OPERATION

Reciprocating internal combustion engines are the powerplant of choice for most automobiles and trucks on the road today [1]. The basic hardware of such an engine is illustrated in Figure 6.1. The basic principle of operation is to convert the chemical energy of a fuel first into heat and then into mechanical energy.

One of the most fundamental characteristics of an engine is the number of strokes, or reversals of direction, that the piston completes to generate power. Two- and four-stroke engines are common; however, for automotive transportation, the four-stroke cycle is typically used. The four strokes are

1. *Intake:* One of the valves (the intake) opens when the piston is near the top of the cylinder. As the piston moves downward, air (in a fuel-injected engine) or an air-fuel mixture (in a carbureted engine) is drawn into the cylinder.

2. *Compression:* As the piston moves upward, both valves are closed and the contents of the cylinder are compressed.
3. *Power:* As the piston nears the top of the cylinder again, fuel is added in a fuel-injected engine (the fuel is already mixed with air in a carbureted engine) and the mixture is ignited. The combustion process releases heat and generates various combustion products such as water vapor and carbon dioxide. The pressure rises rapidly within the cylinder, and the pressure forces the piston downward.
4. *Exhaust:* As the piston reaches the bottom of the cylinder, some of the energy generated by the combustion of the fuel has been transferred to the crankshaft by the piston via the connecting rod. Another valve (the exhaust) now opens, and the momentum of the crankshaft moves the piston upward again, sweeping the combustion products out of the cylinder. As the piston nears the top of the cylinder, the exhaust valve closes, the intake opens, and the cycle repeats.

In a two-stroke engine, intake and exhaust are typically accomplished simultaneously while the piston is near the bottom of the stroke, with only a compression and power stroke taking place before the cycle repeats. However, as the gases are simultaneously flowing in and out of the cylinder, there is usually considerable loss of unburned fuel into the exhaust, resulting in less efficient operation and an increase in undesired emissions.

6.3 ENGINE CHARACTERIZATION

As has already been noted, internal combustion engines can be characterized by the number of strokes the piston uses to accomplish the engine cycle. Several other characteristics are used to classify engines:

- *Number of cylinders:* Although single-cylinder engines were common in early automotive design, and engines with up to 16 cylinders are available in production models today, the most common choices are 4, 6, or 8 cylinders.
- *Cylinder arrangement:* The cylinders can be placed in various configurations, including in-line, V, horizontally opposed, or even radial. The most common arrangements by far are in-line four cylinders, or V6 or V8. Figure 6.2 is an example of a typical V6 engine.
- *Engine displacement:* The total volume swept by all of the cylinders from the bottom to top of their stroke.
- *Valve placement:* Various placements of the engine valves have been used during the development of the

¹ General Motors Corp., Brighton, MI, USA

² RT Vanderbilt Company, Norwalk, CT, USA

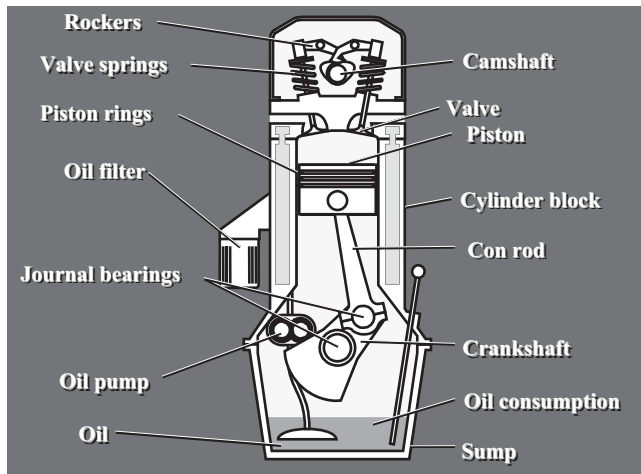


Figure 6.1—The main components in an internal combustion engine.

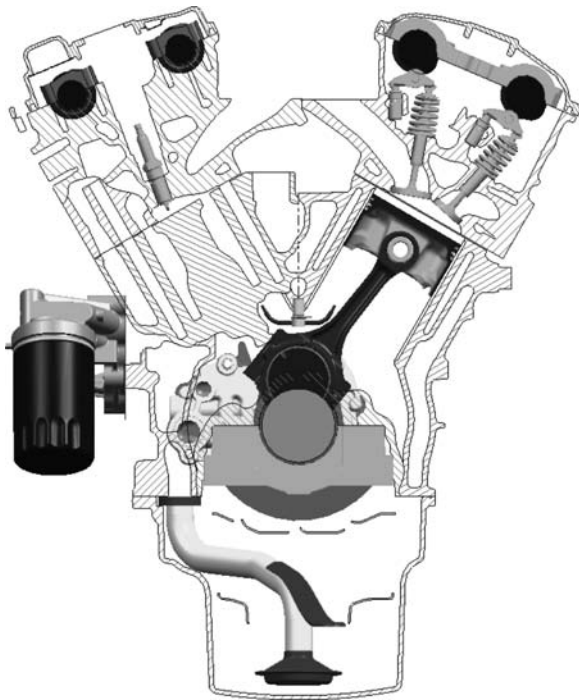


Figure 6.2—Cross-section view of a typical V6 engine.

modern engine, but nearly all modern engines have the overhead valve arrangements in which the valves are placed in the cylinder head.

- **Camshaft placement:** A camshaft is used to open and close the valves, and for many years the preferred placement of the cam was in the block, with pushrods used to operate levers that opened and closed the valves. The long mechanical arrangement required high operating loads and stiff springs for proper valve control. Modern design has tended toward overhead cams, in which the camshaft is much closer to the valves, allowing for lower loads and more precise control.
- **Means of initiating combustion:** In a spark-ignited engine, the fuel-air mixture requires an external source to begin the combustion process, usually an electric

spark from a spark plug. In a compression-ignited engine, the heat of compression is sufficient to begin the combustion process, therefore, no external energy source is required.

- **Fuel:** The fuel used will generally determine whether the engine is a spark-ignition or compression-ignition engine depending on the tendency of the fuel to ignite during the combustion process. Typical spark-ignition fuels are gasoline and alcohol (ethanol or methanol). Common compression-ignition fuels are diesel and biodiesel oils.

6.4 INTERACTING SURFACES AND LUBRICATION REQUIREMENTS

In general, the lubrication requirements of the internal combustion engine are determined by the various surfaces in relative motion within the engine. Each of these interactions has unique characteristics that must be accommodated by the lubricant. The goal in each case is to minimize the energy lost at these interfaces and minimize or eliminate wear.

Piston sets, rolling and sliding bearings, seals, the valve-train, and gears are part of an engine's portfolio of materials, and there are opportunities not only to use lighter-weight bulk materials, but also to apply new coatings and surface treatments that will extend service life, lower warranty costs, and boost reliability. In sliding bearings, the so-called Stribeck curve in Figure 6.3 [3] has been widely used to portray the inter-relationship between rotational speed (S), unit load (P), absolute viscosity (η), and friction coefficient (μ). As shown in Figure 6.3, as a bearing operates farther toward the upper left on the Stribeck curve, the more materials matter to its tribological performance. In fact, key engine components (e.g., piston rings, main bearings, and valve guides) operate in regions of the Stribeck curve in which other than full-film lubrication exists, so the proper selection of materials for contact surfaces is essential. Figure 6.3 also suggests that the highly loaded bearing surfaces that move slowly in a boundary lubrication condition (higher P and lower rotational speed will move to the boundary lubrication regime)

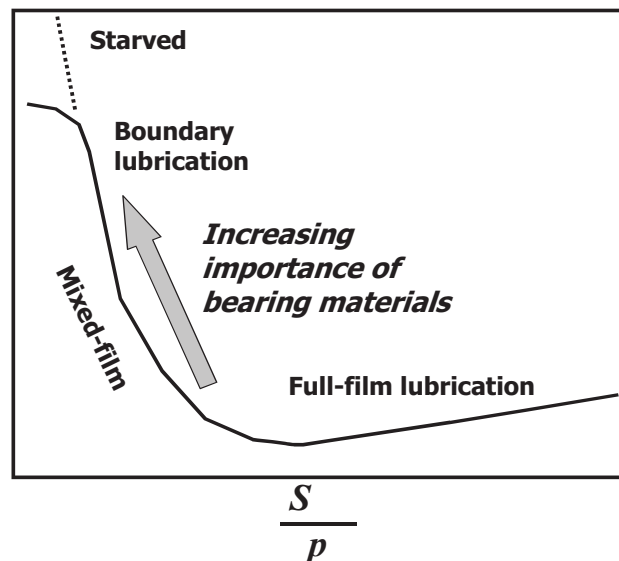


Figure 6.3—The importance of material increases as the lubricant film thickness decreases (Stribeck curve) [3].

will generate high friction as shown in the Stribeck curve. Valve train and gear components also face a major challenge due to a high load condition. In addition, there are certain valvetrain applications, as shown in Figure 6.4 (e.g., valves, camshafts, lifters, turbo-charger vanes, exhaust valve seats, and butterfly valves, in exhaust gas recirculation systems), in which the use of liquid lubricants becomes impractical. Such applications further increase the demand placed on bearing surfaces.

6.4.1 Crankshaft-to-Crankshaft Bearing

The crankshaft is the component that transfers rotational energy from the engine. As it turns, sliding occurs between the crankshaft and the engine block as well as between the crankshaft and the connecting rod. These two interfaces are journal bearings, designed to transfer forces under primarily hydrodynamic conditions. The space within these bearings is filled with engine oil, and the energy dissipated in these bearings is primarily a function of oil viscosity. Proper alignment and clearance of these bearings is required for good engine performance; therefore, these components are pro-

duced from strong and stiff materials to minimize deformation under load. Common choices for crankshaft materials are ductile cast iron or low-alloy steel. Connecting rods are usually steel, although titanium alloys have been used in a few cases. Engine blocks were traditionally produced from gray cast iron; however, cast aluminum has become the material of choice for modern engines because of weight savings.

Vehicle engines are generally shut down for long periods. During these times, the shaft will settle to the bottom of the journal and squeeze out of the oil film. Also, solid particles can become entrained in the oil. These can be from external sources such as dust or internal sources such as wear particles. If these particles are larger than the minimum clearance between the shaft and journal, they have the potential to damage the bearing. To prevent sticking during engine startup and provide the possibility of trapping a limited amount of debris, a soft, compliant bearing is desirable. The ability to trap debris is called embedability [2].

To meet these contradictory requirements, bearing inserts are used for the connecting rod and engine block.

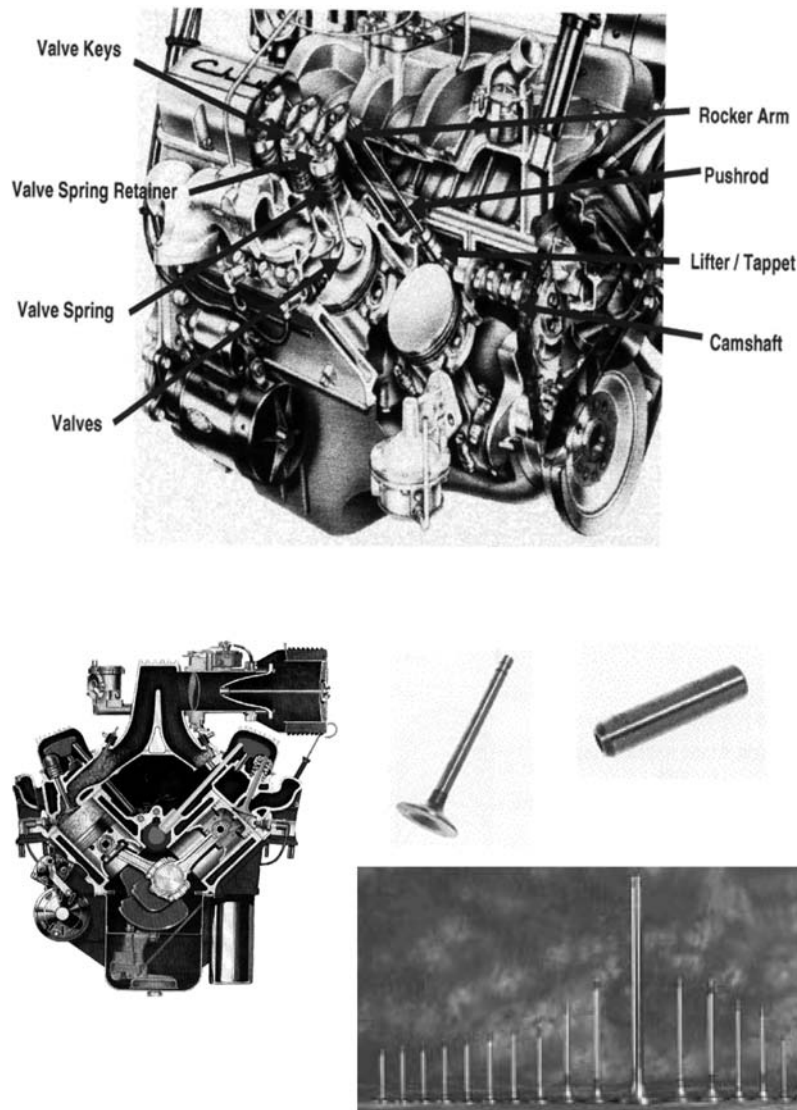


Figure 6.4—Valvetrain configuration and components: valvetrain basic configuration (top) and valvetrain components (e.g., valves, seat, and guides) (bottom).

These inserts are usually made of a steel backing (for strength and stiffness) with a soft coating (for embedability and to prevent adhesion when the engine is off). For many years, the coatings were lead-based babbitt alloys. However, environmental concerns have led to aluminum-based coatings becoming common.

In most engines, the oil is provided under pressure to these bearings, so in this case the most important properties of the lubricant are viscosity and heat capacity. The viscosity must be sufficiently high, even at high temperature, to maintain a hydrodynamic film between the surfaces and sufficiently low, even at low temperatures, to allow the pump to maintain oil flow into the bearings. Heat capacity is important because energy will be dissipated in the form of heat as the oil film is sheared, and the oil must absorb some of this heat without an unacceptable rise in temperature.

6.4.2 Piston-Skirt-to-Cylinder Block

The piston-skirt-to-cylinder block is one of the primary contributors to total engine friction [3]. The piston must fit within the cylinder with sufficient clearance to avoid seizure. However, too much clearance can result in unacceptable noise [4]. Most automotive engine pistons are cast from aluminum-silicon alloys, which are considerably lighter than the cast iron pistons of the past and have resulted in a significant reduction in engine mass and vibration. Also, the higher thermal conductivity of aluminum helps prevent overheating at the top of the piston. Most of the excess heat is conducted away by the cylinder block, and some oil is delivered to the pistons by the rotating crankshaft. However, sometimes pistons require additional cooling. This is usually provided by adding devices to direct a jet of oil onto the underside of the pistons.

Cylinder bores are usually made from gray cast iron, which has a lower coefficient of thermal expansion than aluminum. This creates a design challenge because a piston with adequate clearance at running temperature may be too loose (and hence noisy) at low temperature. To reduce friction and prevent scuffing of the piston, oil must be supplied to the cylinder bore walls. Oil flung from the crankshaft is usually sufficient for this purpose. The clearance between the piston skirt and cylinder wall is so small at high temperature that special coatings are applied to most pistons, such as nickel ceramic composites or molybdenum disulfide (MoS_2) [5,6]. These coatings also reduce the friction in the interface between the piston skirt and cylinder wall.

As the piston moves through the cylinder, the velocity changes from zero (at the top and bottom of each stroke) to a maximum value near the center of the stroke. The viscosity of the oil should be sufficient to generate a full hydrodynamic film over most of the stroke and have sufficient thermal conductivity to facilitate heat movement from the piston to the block.

6.4.3 Piston-Rings-to-Cylinder Block

The piston rings function as a set of sliding seals to separate the combustion gases above the piston from the crankcase environment below. The most common arrangement in automotive engines is a set of three rings. The upper compression ring, lower compression ring, and oil control ring can be seen in Figure 6.5. The ring-block sliding interface has been estimated to account for approximately 20 % of the total engine mechanical friction [7]. In addition, the

bearing and seal as shown in Figure 6.5 play an important role for engine friction and wear.

As with the piston skirt, oil usually reaches the cylinder bore surface by being thrown from the crankshaft after flowing through the bearings. Some oil is necessary for the compression rings to function properly, but oil that escapes past the top compression ring into the combustion chamber is lost. The oil control ring ensures that only the necessary amount of oil reaches the compression rings.

The upper compression ring experiences the highest loads and oil temperatures, and it must provide a good seal to the cylinder surface with very little engine oil. To provide acceptable durability, this ring is usually made from nitrided stainless steel or from steel coated with molybdenum.

Engine oil encounters the most severe conditions around the top compression ring. At the beginning of the power stroke, the load on the top compression ring is quite high and the velocity is near zero; hence, any liquid is effectively squeezed out between the ring and block at this point. The lubricant must have chemically reacted with the ring and block to provide a wear-resistant layer in this region. Certain antiwear additives (e.g., zinc dialkyl dithiophosphate, or ZDDP) can assist in forming these layers. The temperatures are also very high, and the oil must resist excessive breakdown and oxidation under these conditions. Antioxidant additives can provide some degree of protection here. Also, particulate matter can enter the engine at this interface through the air supply or incomplete combustion of the fuel. These contaminants must not settle out of the oil as it circulates through the engine. Maintaining such contaminants in suspension until the oil can be replaced is the function of detergent additives.

6.4.4 Piston Pin to Piston

The piston pin transfers force from the piston to the connecting rod. The interface between the pin and the piston is also a type of journal bearing; however, in this case, the motion is not full rotation. In engines with a fixed pin design, the pin is press-fit into the connecting rod, and the pin motion against the piston is fully reversed partial rotation. In the floating pin design, the pin is free to rotate within the rod and the piston, and the resulting motion is indeterminate. The floating pin has been shown to reduce the operating temperature of the pin boss and is therefore the preferred design [8]. In either case, the velocity of the pin is not sufficient to generate a full fluid film between the surface, and a condition of boundary lubrication results.

Automotive engine pistons are usually cast from aluminum-silicon alloys. Piston pins are made from low or medium carbon steel, which is usually carburized to generate a very hard surface. Lubricant is usually provided to this interface from two sources. Some oil is flung upward by the motion of the crankshaft and arrives at the underside of the piston. In addition, oil that is scraped from the cylinder walls by the oil control ring can flow down the piston into the pin bore. It has been shown that increasing the oil supply to this interface decreases the tendency for scuffing [8].

6.4.5 Camshaft to Follower

As the camshaft rotates, it presses against a flat or roller surface, which reciprocates to open and close the valve. The interface between the camshaft and follower is unidirectional sliding between nonconformal surfaces. Although

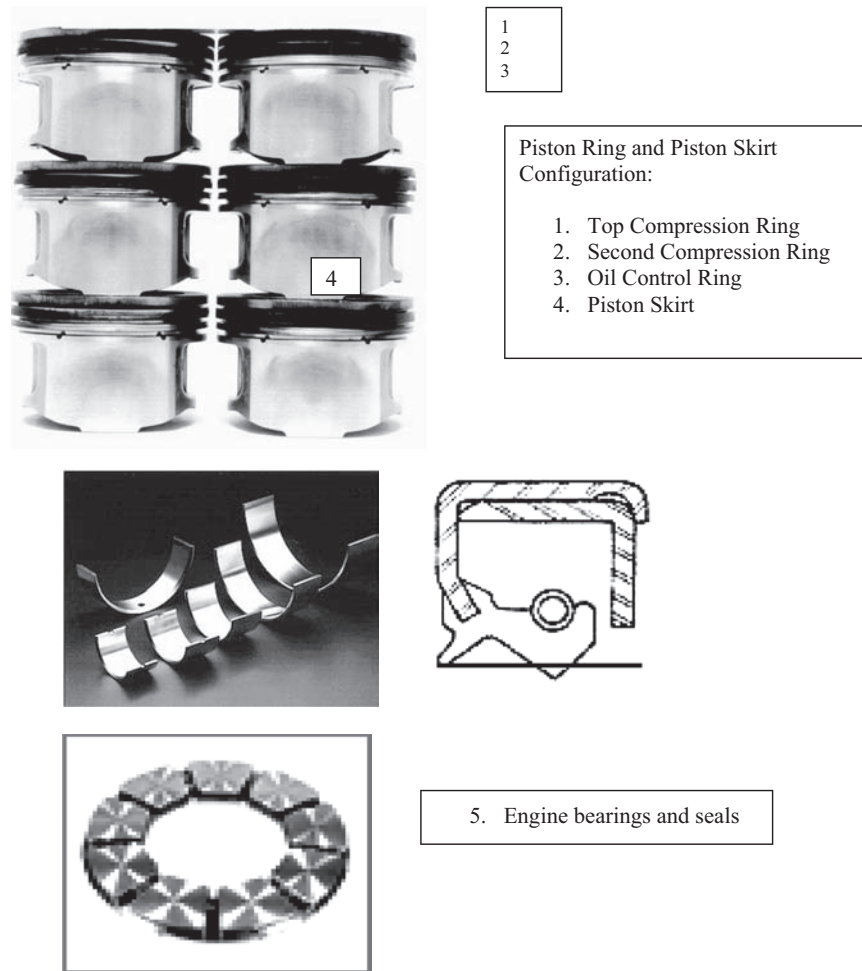


Figure 6.5—Piston ring, piston skirt, and engine bearing configuration: 1 = top compression ring, 2 = second compression ring, 3 = oil control ring, 4 = piston skirt, and 5 = engine bearings and seals.

engines are designed to provide oil to this interface, it is likely that oil will be scarce on occasion. For example, when starting a cold engine, the cams will begin turning before oil pressure is sufficient to pump the oil to the top of the engine. Only a few material combinations are used successfully in this application, and even those wear sufficiently during the life of an engine to require periodic adjustment or the use of self-adjusting hydraulic elements.

In this case, the lubricant functions primarily to reduce friction at the sliding interface; provide a chemical film to resist wear through the action of antiwear additives; and, in the case of engines with hydraulic valve lifters or hydraulic valve timing adjustments, to provide energy in the form of hydraulic pressure to actuate those systems.

6.4.6 Valve to Cylinder Head

A typical poppet valve is shown in Figure 6.4. The valves control the flow of gases into and out of the cylinder. The valve reciprocates within the valve guide. Engine valves are usually made of specialty steel alloys to resist oxidation and corrosion. In addition, wear-resistant coatings such as chromium are often used. Modern cylinder heads are usually made from cast aluminum alloys. The valve guides are typically made from steel by the powder metal process.

Only a very limited amount of engine oil reaches the valve guide because oil that flows through this area is ultimately lost. This small amount of oil contributes to the successful performance of the valve through additives that provide active chemical films in the guide under boundary lubrication.

6.4.7 Oil Pump

Most automotive engines use a pressurized lubrication system to ensure adequate distribution of lubricant throughout the engine and provide sufficient flow to maintain hydrodynamic conditions in the engine bearings. The oil circuit begins in the sump, from which oil is drawn into the pump. The pump delivers pressurized oil through a filter and then to passages in the block and head, to the crankshaft and camshaft bearings, and to the hydraulic valve lifters and variable valve actuation system in engines so equipped. The oil is then thrown from the rotating components onto the cylinder walls, valve lifters, and other components. As oil runs off of these surfaces, gravity directs it back to the sump through passages in the head and block.

Two types of pumps are commonly used—the spur gear pump and the gerotor—as shown in Figure 6.6. Spur gear pumps are the older design and have the advantage

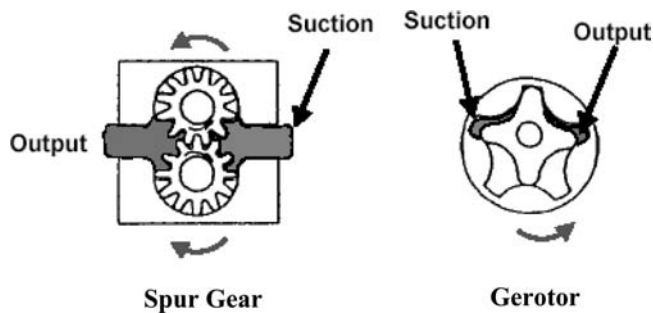


Figure 6.6—The two main types of oil pumps (spur gear pump and gerotor pump) in internal combustion engines.

of relatively quiet operation. However, the gerotor has the advantage of greater efficiency and can be made to take up less space in the engine compartment; therefore, most recent designs use the gerotor. The pump incorporates a relief valve for pressure regulation.

6.5 MECHANISMS OF WEAR AND DAMAGE IN ENGINE OPERATION

At one extreme of the spectrum of engine tribological problems is steady, cumulative damage. This could be wear or the development of fatigue cracks leading to rolling contact fatigue. In many types of components (e.g., cams, pistons, rolling element bearings) such damage is inevitable but predictable. The main cost is the regular inspection and replacement of parts to ensure that damage does not progress to failure. The engineer must use his or her understanding of damage accumulation mechanisms to select replacement periods consonant with the prevention of failure and to improve design so as to extend these periods. What is an acceptable risk of failure clearly depends on the application, and a greater safety margin is needed for a helicopter transmission than for something such as a conveyor belt.

The ability to reliably predict component life is becoming more important with the recent development and application of accounting techniques of life-cycle costing [2]. In these, the overall cost of a particular machine or component is evaluated over its whole life cycle (including metal extraction, manufacture, use, and disposal), which permits the direct comparison and optimization of the cost-effectiveness of different engineering designs.

There are many different possible types of surface damage [2,6] that can occur in rubbing systems, and many different names are used for the same types of damage.

6.5.1 Cumulative Plastic Deformation

When the asperities of rough surfaces come into contact (or even into near contact in mixed lubrication), the local stresses resulting from normal load and friction often exceed the yield strength of the material. This means that repeated asperity contact results in cumulative plastic strain of the surface and immediate subsurface.

This strain produces large changes in the metallurgical structure and properties of the material within a distance equivalent to approximately the root mean square roughness of the opposing surface with the accumulation of damage features such as voids, microcracks, and slip bands of very high dislocation density. In some cases, as a result of work-hardening, the cyclic plastic strain may become

contained and eventually lead to low cycle fatigue; in others it may continue through ratchetting until rupture occurs. The whole process of cumulative plastic deformation as a result of asperity contact and the consequent accumulation of material damage is now recognized to be the underlying cause of many types of wear processes.

The keys to reducing cyclic plastic strain [2] are

- Hard surfaces, so that plastic strain occurs only at the most severe asperity contacts;
- Smooth surfaces and low asperity slopes, so that asperity pressures are minimized;
- Thick lubricant films, so that pressure fluctuations are evened-out by the lubricant;
- Film; and
- Avoidance of adhesion and abrasion.

Note that the first two keys are quantitatively combined in the measure of plasticity index [2]. A low plasticity index should lead to low damage accumulation.

The above damage is produced by stresses resulting from asperity contact. In concentrated contacts, the overall contact also produces a Hertzian stress field [2]. This rarely exceeds the bulk plastic yield strength of the material, but it can still result in crack initiation at stress raisers and subsequent propagation to contact fatigue failure. This damage extends much deeper than asperity-related damage to a depth of the same magnitude as the Hertz radius.

6.6 ENGINE LUBRICANT ILSAC GF-5 STANDARD AND REQUIRED GF-5 ENGINE TESTS

6.6.1 Engine Lubricant ILSAC GF-5 Standard

Engine oil must clearly be capable of delivering acceptable performance under a wide variety of conditions and in contact with several different materials. One listing of publications applicable to the testing of oils is found in SAE J357 [9]. The International Lubricants Standardization and Approval Committee (ILSAC) establishes the minimum performance requirements for engine oils.

In the past 40 years, U.S. government regulations have brought about significant fuel economy and emission improvements through required mechanical and chemical component redesigns. Although these regulations were successful, more progress is needed. The number of vehicles on the road continues to increase, resulting in negative environmental effects. Furthermore, the cost of fuel continues to increase, resulting in amplified public demand for improved fuel economy. These factors accelerated the cycle of regulation and the performance upgrade of engine oils. The United States government has created a new regulation to further improve fuel economy and reduce greenhouse emissions. Based on the recent Obama administration's agreement for model years 2012–2016 vehicles, which will raise fuel efficiency to 35.5 mpg and begin saving families money at the pump this year, the next round of standards will require performance equivalent to 54.5 mpg or 163 grams/mile of CO₂ for cars and light-duty trucks by Model Year 2025 [17]. Regulation drives vehicle design, which in turn drives new enabling technology.

Automotive manufacturers will not be the only ones required to perform the regulation-driven redesign. Supporting industries and technologies, such as oil marketers and lubricant additive industries, are currently working together to develop and define a new motor oil specification known as ILSAC GF-5. The GF-5 oils will be designed

to improve the function and performance of the new engine and emission designs and to help ensure compliance with the new government regulations.

The GF-5 specification will have a global effect. As with the previous GF-4 specification, most of the developed countries immediately adopted GF-5 and global marketers of motor oils will add GF-5 to their requirements.

GF-5 oils equal the performance of GF-4 oils when it comes to volatility, oxidative thickening and wear protection. For all other performance parameters—emission system durability, seal compatibility, fuel economy, E86 rust protection, E85 emulsion retention, engine sludge protection, piston cleanliness, and turbo-charger protection—GF-5 clearly surpasses the older GF-4 specifications. To attain the required improvements to GF-5 performance parameters, lubricant manufacturers will have to include new performance attributes.

- Fuel economy and fuel economy retention.
- Enhanced oil robustness for spark-ignited internal combustion engines is required to ensure acceptable engine oil performance required for regional markets (North America, Japan, Europe, etc.) because of service requirements, fuel, environment, etc. Adjustment to chemical limits to allow improved performance while maintaining overall durability performance.
- Increase fuel economy throughout the oil change interval. Fuel consumption remains a critical issue for automotive and oil industry customers, and automotive manufacturers are facing increasingly stringent regulatory requirements.
- Improve overall vehicle fuel efficiency; automotive manufacturers are planning for increased numbers of smaller displacement, boosted intake engines that may be susceptible to low-speed preignition (LSPI). LSPI is an abnormal combustion event at low engine speeds and high loads.
- Provide wear protection for idle-stop engines (e.g., PHEV, EREV, and HEV; frequent starts, starts after extended periods of downtime, etc.) and for various engine components, including timing chains, valve-train components, etc.
- Enhance emulsion and rust protection for vehicle running on E85 (ethanol-based) fuel. Additional material compatibility with ethanol. Allow greater seal compatibility to help ensure seal longevity and prevent oil leaking in older vehicles.
- Enable a movement toward lower viscosity oils that enable better fuel economy.

Lower viscosity GF-5 oils (e.g., 0W-20 or 5W-20) will require lubricant formulations to incorporate more Group III base oils, which include other additives (e.g., polyalphaolefin and MoS₂) in viscosity modifiers (VMs) and pour-point depressants (PPDs). VM additives control the temperature-viscosity relationship of engine oils but are susceptible to shear degradation within engines. GF-5 requirements will necessitate VMs that provide good fuel economy and high-temperature deposit performance. Because PPDs play an important role in managing new and used low-temperature properties of finished oil, the GF-5 specification requires them to ensure fail-safe low-temperature performance. Using new GF-5 specification has some tradeoffs between fuel economy and robustness. A shift to lower viscosity grades will be driven by fuel economy, and base oil choices

will change. The required ILSAC GF-5 specification for engine oil performance is attached in Appendix 1 for the reader's information [16].

6.6.2 Required GF-5 Bench and Engine Tests

To comply with this new ILSAC GF-5 standard, performance-improving additive packages will require new technologies at higher costs. The higher costs of these additives will not only have to be offset by realized performance but also be accepted as valid by motorists. In the past, engine sequence and bench tests have been based on a range of base oils and additive technologies already proven to have satisfactory performance in service. Because GF-5 requires the introduction of new additive packages—a significant departure from existing past practice—new testing regimens, revised to reflect the changes needed to achieve the enhanced performance parameters, will be used. Examples include the following:

- The Sequence VI-D engine test, developed to measure the fuel economy performance of engine oil, has been revised to reflect the modern engine designs (e.g., the 3.6-L General Motors V6) used in most vehicles today.
- The methodology, test length, and calculation for the Sequence III-GB, which evaluates engine oil effect on catalysts used in emissions control systems, now tests emissions control system protection via an analysis of how much phosphorus remains in used oil, with anticipated phosphorus retention limits expected to be somewhere between 78 and 80 %.

Two new tests specifically developed for GF-5 to optimize seal compatibility and engine oil robustness. Some of these tests are performed in engines and others are bench tests.

6.6.3 Engine Tests

Sequence IIIG [10] involves running a General Motors 3.8-L V6 engine under specified conditions with the test oil for 100 h and evaluating several systems at the end of the test. Specifically related to the engine hardware, there are limits for the weight of material deposits on the pistons, the amount of wear on the camshaft and valve lifters, and whether the piston rings are stuck in their grooves.

Sequence IVA [11] is used to evaluate wear on the lobes of the camshaft. This test is performed using a Nissan 2.4-L L4 engine run under stop-and-go conditions for 100 h and then measuring the wear on the cams.

Sequence VIII [12] is run on a LABECO single-cylinder engine for 40 h at constant speed. The engine bearings are weighed before and after the test, and bearing wear, as indicated by weight loss, is the measured parameter.

Sequence VID [13] uses a General Motors 3.6-L V6 engine for testing the effect of friction modifier on fuel economy. The intent of this test includes discriminating between oils with and without friction modifiers and between new and “aged” oils by measuring their effect on fuel economy.

6.6.4 Bench Tests

The TEOST test [14] is designed to measure the tendency for the oil to form deposits at high temperature. Two versions of this test are commonly run. One test is performed at 285°C for 24 h and is intended to correlate with the tendency of the oil to form deposits on pistons. The other version involves cycling between 200 and 480°C for 2 h and is intended to indicate the tendency of the oil to form deposits on turbo-charger components.

The Ball Rust Test [15] involves exposure of a steel ball to an acid/oil solution and measuring the amount of corrosion that occurs in 18 h. The test is intended to indicate the ability of the oil to prevent rust on the iron and steel components in an engine.

6.7 CONCLUSIONS

The lubrication requirements for modern internal combustion engines are varied and complex. Different interfaces within the engine have widely different requirements. Engine oil must provide lubrication under hydrodynamic, mixed, and boundary conditions. The oil also protects engine components from oxidation and corrosion, holds contaminant particles in suspension, circulates at high and low temperatures, provides hydraulic pressure to actuate some engine components, and acts as a coolant for certain engine components. Modern engine oils are engineered to meet these and many other requirements.

This chapter also describes the major functions of typical engine components (gasoline and diesel), engine oil characteristics, the current industrial standard test methods, and oil specifications. Included are descriptions of the tribological concerns associated with various automotive engine components, interacting surface effects on automotive lubricants, standard test development, and the updated engine oil specification for gasoline and diesel engine lubricants in vehicles.

References

- [1] Taylor, C.M., 1985, *The Internal Combustion Engine in Theory and Practice*, MIT Press, Cambridge, MA.
- [2] Ludema, K.C., 1996, *Friction, Wear, Lubrication—A Textbook in Tribology*, CRC Press, Boca Raton, FL.
- [3] Goenka, P.K., Paranjpe, R.S., and Jeng, Y.R., 1992, *FLARE: An Integrated Software Package for Friction and Lubrication Analysis of Automotive Engines, Part 1: Overview and Applications*, SAE Paper No. 920487, SAE, Warrendale, PA.
- [4] Kageyama, H., Suzuki, T., and Ochia, T., 2001, *Numerical Study on the Three Dimensional Contact Pressure and Deformation of Piston Skirt*, SAE Paper No. 2001-08-0082, SAE, Warrendale, PA.
- [5] Funatani, K., Kurowawa, K., Fabiyi, P.A., and Puz, F.M., 1994, *Improved Engine Performance Via Use of Nickel Ceramic Composite Coatings (NCC Coat)*, SAE Paper No. 940852, SAE, Warrendale, PA.
- [6] Rao, V.D.N., Kabat, D.M., Yeager, D., and Lizzote, B., 1997, *Engine Studies of Solid Film Lubricant Coated Pistons*, SAE Paper No. 970009, SAE, Warrendale, PA.
- [7] Ting, L.L., 1985, *A Review of Present Information on Piston Ring Tribology*, SAE Paper No. 852355, SAE, Warrendale, PA.
- [8] Takiguchi, M., Oguri, M., and Someya, T., 1992, *A Study of Rotating Motion of Piston Pin in Gasoline Engine*, SAE Paper No. 938142, SAE, Warrendale, PA.
- [9] SAE, 2006, *Physical and Chemical Properties of Engine Oils*, SAE International Report J357, SAE, Warrendale, PA.
- [10] ASTM Standard D7320-09a, 2009: Standard Test Method for Evaluation of Automotive Engine Oils in the Sequence IIIG, Spark-Ignition Engine, *Annual Book of ASTM Standards*, ASTM International, West Conshohocken, PA.
- [11] ASTM D6891-09a, 2009: Standard Test Method for Evaluation of Automotive Engine Oils in the Sequence IVA Spark-Ignition Engine, *Annual Book of ASTM Standards*, ASTM International, West Conshohocken, PA.
- [12] ASTM Standard D6709-09a, 2009: Standard Test Method for Evaluation of Automotive Engine Oils in the Sequence VIII Spark-Ignition Engine (CLR Oil Test Engine), *Annual Book of ASTM Standards*, ASTM International, West Conshohocken, PA.
- [13] ASTM Standard D7589-09, 2009: Standard Test Method for Measurement of Effects of Automotive Engine Oils on Fuel Economy of Passenger Cars and Light-Duty Trucks in Sequence VID Spark Ignition Engine, *Annual Book of ASTM Standards*, ASTM International, West Conshohocken, PA.
- [14] ASTM Standard D7097-09, 2009: Standard Test Method for Determination of Moderately High Temperature Piston Deposits by Thermo-Oxidation Engine Oil Simulation Test-TEOST MHT, *Annual Book of ASTM Standards*, ASTM International, West Conshohocken, PA.
- [15] ASTM Standard D6657-09, 2009: Standard Test Method for Evaluation of Rust Preventive Characteristics of Automotive Engine Oils, *Annual Book of ASTM Standards*, ASTM International, West Conshohocken, PA.
- [16] ILSAC, February 2008: GF-5 Standard for Passenger Car Engine Oils, ILSAC Updated version.
- [17] President Obama Announces Historic 54.5 mpg Fuel Efficiency Standard. White House Announcement, July 29, 2011. <http://www.whitehouse.gov/the-press-office/2011/07/29/president-obama-announces-historic-545-mpg-fuel-efficiency-standard>.

APPENDIX 1

ILSAC GF-5 REQUIREMENTS [16]

1. FRESH OIL VISCOSITY REQUIREMENTS

1.a SAE J300

Oils shall meet all of the requirements of SAE J300. Viscosity grades are limited to SAE 0W, 5W, and 10W multigrade oils.

1.b Gelation Index: ASTM D5133

12 maximum

To be evaluated from -5°C to the temperature at which 40,000 cP is attained or -40°C , or 2°C below the appropriate MRV TP-1 temperature (defined by SAE J300), whichever occurs first.

2. ENGINE TEST REQUIREMENTS

2.a Wear and Oil Thickening: ASTM Sequence IIIG Test, ASTM D7320

Kinematic viscosity increase at 40°C , %	150 maximum
Average weighted piston deposits, merits	5.0 minimum
Hot stuck rings	None
Average cam plus lifter wear, μm	60 maximum

2.b Wear, Sludge, and Varnish Test: Sequence VG, ASTM D6593

Average engine sludge, merits	8.3 minimum
Average rocker cover sludge, merits	8.5 minimum

Average engine varnish, merits	8.9 minimum
Average piston skirt varnish, merits	7.5 minimum
Oil screen sludge, % area	5 maximum
Oil screen debris, % area	Rate and report
Hot stuck compression rings	None
Cold stuck rings	Rate and report
Oil ring clogging, % area	Rate and report

2.c Valvetrain Wear: Sequence IVA, ASTM D6891

Average cam wear (seven-position average), μm	90 maximum
--	------------

2.d Bearing Corrosion: Sequence VIII, ASTM D6709

Bearing weight loss, mg	26 maximum
-------------------------	------------

2.e Fuel Efficiency, Sequence VID

SAE 0W-20 viscosity grade:

X + 1.7 % FEI 1 minimum after 100 h aging

Y + 1.7 % FEI 2 minimum after 100 h aging

SAE 5W-20 viscosity grade:

X + 1.2 % FEI 1 minimum after 100 h aging

Y + 1.2 % FEI 2 minimum after 100 h aging

SAE 0W-30 viscosity grade:

X + 1.0 % FEI 1 minimum after 100 h aging

Y + 1.0 % FEI 2 minimum after 100 h aging

SAE 5W-30 viscosity grade:

X + 0.7 % FEI 1 minimum after 100 h aging

Y + 0.7 % FEI 2 minimum after 100 h aging

SAE 10W-30 and all other viscosity grades not listed above:

X % FEI 1 minimum after 100 h aging

Y % FEI 2 minimum after 100 h aging

X and Y are expected to be at least 0.5 % FEI (fuel efficiency increase) higher than GF-4 limits for comparable viscosity grades.

****Fuel Efficiency, Sequence VID, ASTM D7589 (updated version)**

SAE XW-20 viscosity grade:

FEI SUM 2.6 % minimum

FEI 2 1.2 % minimum after 100 h aging

SAE XW-30 viscosity grade:

FEI SUM 1.9 % minimum

FEI 2 0.9 % minimum after 100 h aging

SAE 10W-30 and all other viscosity grades not listed above:

FEI SUM 1.5 % minimum

FEI 2 0.6 % minimum after 100 h aging

2.f Used Engine Oil Aeration Test, ASTM D6894

Aeration volume, %	6, maximum
--------------------	------------

3. BENCH TEST REQUIREMENTS

3.a Catalyst Compatibility

Phosphorus content, ASTM D4951

Phosphorus volatility, test TBD

0.07 % (mass) maximum

TBD, Reduction in phosphorus volatility equivalent to what would be achieved by reducing the phosphorus content in oil containing higher volatility ZDDP from 0.07 to 0.05 %.

Sulfur content, ASTM D4951 or D2622

0.5 % (mass) maximum

3.b Wear

Phosphorus content, ASTM D4951

0.06 % (mass) minimum

3.c Volatility

Evaporation loss, ASTM D5800

(Note: Calculated conversions specified in D5800 are allowed.)

Simulated distillation, ASTM D6417

15 % maximum, 1 h at 250°C

10 % maximum at 371°C

3.d High-Temperature Deposits, TEOST MHT, ASTM D7097

Deposit weight, mg

30 maximum

3.e High-Temperature Deposits, TEOST 33C, ASTM D6335

Total deposit weight, mg	25 maximum
--------------------------	------------

3.f Filterability

EOWTT, ASTM D6794

with 0.6 % H ₂ O	50 % maximum flow reduction
with 1.0 % H ₂ O	50 % maximum flow reduction
with 2.0 % H ₂ O	50 % maximum flow reduction
with 3.0 % H ₂ O	50 % maximum flow reduction

Test formulation with highest additive (DI/VI) concentration. Additive (DI/VI) concentration is related to Dispersant/Viscosity Index Improver (DI/VI). Read-across results to all other base oil/viscosity grade formulations using the same or lower concentration of the identical additive (DI/VI) combination. Each different DI/VI combination must be tested.

EOLT, ASTM D6795	50 % maximum flow reduction
------------------	-----------------------------

3.g Fresh Oil Foaming Characteristics, ASTM D892 (Option A)

	Tendency	Stability*
Sequence I	10 mL maximum	0 mL maximum
Sequence II	50 mL maximum	0 mL maximum
Sequence III	10 mL maximum	0 mL maximum

*After 1-min settling period

3.h Fresh Oil High-Temperature Foaming Characteristics, ASTM D6082 (Option)

	Tendency	Stability*
	100 mL maximum	0 mL maximum

*After 1-min settling period

3.i Aged Oil Low-Temperature Viscosity, ROBO Test

Measure cold-cranking simulator (CCS) viscosity of the EOT ROBO sample at the CCS temperature corresponding to the original viscosity grade.

- If CCS viscosity measured is less than or equal to the maximum CCS viscosity specified for the original viscosity grade, run ASTM D4684 (MRV TP-1) at the MRV temperature specified in SAE J300 for the original viscosity grade.
- If CCS viscosity measured is higher than the maximum viscosity specified for the original viscosity grade in SAE J300, run ASTM D4684 (MRV TP-1) at 5°C higher temperature (i.e., at MRV temperature specified in SAE J300 for the next higher viscosity grade).
- The EOT ROBO sample must show no yield stress in the ASTM D4684 test and its ASTM D4684 viscosity must be below the maximum specified in SAE J300 for the original viscosity grade, or the next higher viscosity grade, depending on the CCS viscosity, as outlined in a) or b) above.

3.j Shear Stability, Sequence VIII, ASTM D6709

10-h stripped kinematic viscosity (KV) at 100°C
KV must remain in original SAE viscosity grade.

3.k Homogeneity and Miscibility, ASTM D6922

Shall remain homogeneous and, when mixed with SAE reference oils, shall remain miscible.

3.l Engine Rusting, Ball Rust Test, ASTM D6557

Average gray value	100 minimum
--------------------	-------------

3.m Emulsion Retention (DCX provide procedure):

Oil mixed with 10 % water, 10 % E85	
0°C, 24 h	No separation
25°C, 24 h	No separation

Note: Additives in the emulsified oil must not precipitate out when heated above 110°C.

3.n Rust Protection Test, ASTM D1748

100 h, sandblasted panel	No rust
--------------------------	---------

- Candidate oil testing for elastomer compatibility shall be performed using the four standard reference elastomers (SREs) referenced herein and defined in SAE J2643. Candidate oil testing shall be performed according to ASTM D7216, which includes 336 h of immersion at 100°C for HNBR, and 150°C for ACM, VMQ, and FKM. The postcandidate oil immersion elastomers shall conform to the specification limits:

Elastomer Material (SAE J2643)	Test Procedure	Material Property	Units	Limits
Polyacrylate rubber (ACM-1)	ASTM D471	Volume	% Δ	–5, 5
	ASTM D2240	Hardness	Points	–10, 10
	ASTM D412	Tensile strength	% Δ	–30, 30
	ASTM D412	Elongation at break	% Δ	–45, 5
	ASTM D412	Tensile stress at 50 % elongation	% Δ	–20, 65
Hydrogenated nitrile rubber (HNBR-1)	ASTM D471	Volume	% Δ	–5, 5
	ASTM D2240	Hardness	Points	–5, 5
	ASTM D412	Tensile strength	% Δ	–20, 10
	ASTM D412	Elongation at break	% Δ	–35, 0
	ASTM D412	Tensile stress at 50 % elongation	% Δ	–10, 35
Silicone rubber (VMQ-1)	ASTM D471	Volume	% Δ	–5, 40
	ASTM D2240	Hardness	Points	–20, 10
	ASTM D412	Tensile strength	% Δ	–45, 0
	ASTM D412	Elongation at break	% Δ	–40, 0
	ASTM D412	Tensile stress at 50 % elongation	% Δ	–50, 10
Fluorocarbon rubber (FKM-1)	ASTM D471	Volume	% Δ	–2, 3
	ASTM D2240	Hardness	Points	–4, 6
	ASTM D412	Tensile strength	% Δ	–65, 10
	ASTM D412	Elongation at break	% Δ	–60, 10
	ASTM D412	Tensile stress at 50 % elongation	% Δ	–30, 40

Part 2: Automotive Lubricant Testing, Lubricant Performance, and Current Lubricant Specifications

Gasoline Engine and Diesel Engine Powertrain Systems

P. Silva¹

7.1 INTRODUCTION

Reciprocating internal combustion engines have been studied since the middle of the 19th century, but their full industrial development began with their application for vehicle propulsion in the following century. By definition, reciprocating internal combustion engines are volumetric-type engines using internal combustion and their kinematic operation is based on the alternating motion of pistons inside of cylinders. There are two basic types of reciprocating engines: Spark ignition engines and compression ignition or diesel engines. Spark ignition engines for automotive application mainly use gasoline as fuel, but they can also work on ethanol or natural gas. Diesel engines operate on diesel fuel, but in principle they can run in a dual-fuel configuration that primarily burns natural gas with a small amount of diesel pilot fuel (e.g., in some city-bus applications or in cogenerative stationary applications) [1]. As a function of the modality with which the working cycle is performed, the engines can be referred to as two- or four-stroke engines according to the number of strokes of the piston in each working cycle. The present chapter will deal mainly with four-stroke engines, which are nowadays the widespread technology for vehicles. The two-stroke spark-ignited engine is only used in very small devices because of environmental constraints whereas the two-stroke diesel engine is limited to rare applications in slow, very large marine engines [2].

In addition to the automotive industry, internal combustion engines are currently used in many other sectors in marine propulsion, railway traction, and stationary applications such as motorpumps or air compressors, emergency gensets, peaking services, and cogeneration units for industrial users and residentially distributed generation. The size range of commercially available engines ranges from a few kilowatts to over 50 MW of mechanical power. They can be referred to as a mature industrial-developed technology, with good availability, high efficiency, and relatively low cost because of the high-volume series production. Weakness elements of internal combustion engines, with respect to alternative technologies such as, for example, gas turbines, can be identified in vibrations and acoustic emissions, lubricating oil consumption, relatively high maintenance costs, and pollutant emission levels. This last aspect has been solved in recent years with the adoption of catalytic reactors for the exhaust gases.

This chapter focuses on automotive applications of gasoline and diesel engine powertrain systems, even if many theoretical concepts and some considerations can be extended to different sizes and models.

7.2 THERMODYNAMICS AND WORKING PRINCIPLES

An internal combustion engine is a thermal engine, which is a machine that converts thermal energy (heat) coming from the combustion of a fuel into mechanical energy (work) after a cyclic transformation (i.e., a thermodynamic cycle). The efficiency of the thermal engine is defined as the ratio between the produced work, L , and the supplied heat, Q ($\eta = L/Q$).

The ideal thermodynamic cycle of a spark-ignited engine [3,4], the so-called Otto ideal cycle from the name of its first inventor as well as the ideal thermodynamic cycle of a compression ignition or diesel engine, consists of four transformations of an ideal gas that are represented in Figure 7.1:

- *Compression (the isentropic transformation 1–2):* The piston moves, reducing the volume occupied by a gas inside of a cylinder and causing the increase in its pressure and temperature. This phase is obtained through external work.
- *Combustion (the isochoric transformation 2–3 in the Otto cycle):* In this case, the combustion takes place instantaneously, without any motion of the piston. In the diesel engine, the combustion is not so fast, and in the ideal cycle it is well represented by the isobaric transformation 2–3'.
- *Expansion (the isentropic transformation 3–4):* The piston moves, increasing the gas volume inside of the cylinder and causing the decrease in pressure and temperature. This phase produces mechanical work.
- *Gas discharge (the isochoric transformation 4–1):* In the ideal cycle, it takes place instantaneously, without any motion of the piston. During this phase, the gas goes out from the cylinder.

The efficiency of the Otto ideal cycle is given by

$$\eta = 1 - \frac{|Q_n|}{|Q_c|} = 1 - \frac{(T_1 - T_4)}{(T_3 - T_2)} = 1 - \left(\frac{1}{r}\right)^{\gamma-1} \quad (7.1)$$

where γ is the ratio between constant pressure and constant volume-specific heat capacity and r is the volumetric compression ratio ($r = V_1/V_2$). The ideal diesel cycle, given the same compression ratio, has a lower efficiency than that obtained from eq. 7.1.

It must be noted that in an internal combustion engine, in contrast with the Carnot cycle, which is an ideal closed cycle (i.e., always operated with the same fluid), the evolving fluid, initially air or an air-fuel mixture, after a series of transformations is released back to the environment as

¹ Politecnico di Milano, Italy

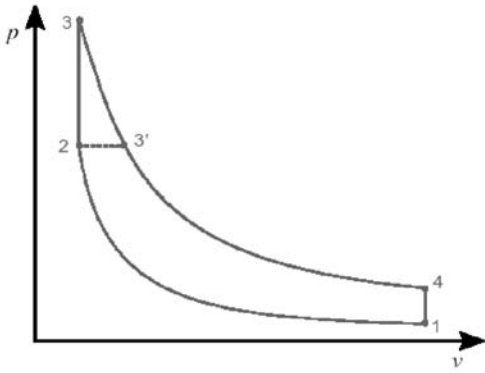


Figure 7.1—Otto and diesel ideal cycles.

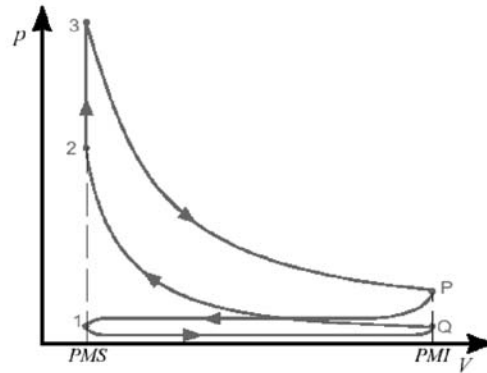


Figure 7.2—Otto real cycle.

exhaust gas, which results from the combustion of a fuel with air. Particularly the processed gas during the compression is air in the diesel cycle and generally an air-fuel mixture in the Otto cycle.¹ In the diesel cycle, the fuel is added to the combustion chamber a few instants before the combustion through an injection. In Otto and diesel cycles, the processed fuel during expansion is the exhaust gas, which is finally discharged to the environment.

The real cycle is therefore an open cycle made by irreversible transformations. In Figure 7.2, an Otto real cycle is reported as an example. Two further subsidiary transformations, the so-called “substitution cycle”, must be considered to complete the cycle:

- *Aspiration*: Aspiration is the transformation 1—Q, which takes place before the compression. It is necessary in the real cycle and allows for the air/air-fuel mixture intake inside of the cylinder by means of the opening of an appropriate intake valve. It is due to the movement of the piston, which causes an increase of volume and a slight decrease of pressure inside of the cylinder.
- *Forced gas discharge*: This is the transformation P—1 and takes place after the natural discharge phase. It is due to the movement of the piston, which causes a decrease of volume and a slight increase of pressure inside of the cylinder. During this phase, the exhaust valve is kept open.

The real Otto cycle is obtained starting from an air/fuel ratio that is near the stoichiometric value; the combustion of the air-fuel mixture is obtained by means of a spark-plug ignition between two electrodes, which takes place during the last instants of the compression phase. For this reason, the engine is often referred to as a “spark-ignited engine”. It is fundamental to avoid the autoignition of the mixture during the compression phase, the so-called “detonation” or “knock” due to high temperatures²; therefore, the volumetric compression ratio is limited to typical values of 8–12:1.

On the contrary, in the diesel cycle, fuel is injected into the cylinder at the end of the compression phase, and the combustion spontaneously starts because of the high

temperatures of air without any devices such as spark plugs. Moreover, the combustion is more gradual and occurs at nearly constant pressure. In contrast to spark-ignited engines, diesel fuel must have an easy ignition at temperatures occurring at the end of the compression. In fact, because of the compression phase processing only air, the volumetric compression ratio is always higher than in Otto cycles, typically 16–22:1.

As already mentioned, at a given volumetric compression ratio, the ideal efficiency is higher for the Otto cycle. However, in a real engine, the adopted compression ratio is higher for compression-ignited engines so that the nominal efficiency of a diesel real cycle is generally higher than a corresponding Otto cycle. In addition, the different regulation modality yields better partial load performances for diesel engines. In fact, in spark-ignited engines, the air/fuel ratio is kept nearly constant even at partial load simply by reducing the mass flow rate of the air/fuel mixture processed by the cylinders by means of a proper “throttle valve” or “butterfly valve” inserted in the intake manifold, which causes a pressure drop in the aspiration ducts. On the contrary, diesel engines always work with air/fuel ratios greater than stoichiometric³: At partial load, the fuel quantity is reduced with the constant air mass flow rate sucked by the cylinder without any additional pressure drop in the ducts.

For the abovementioned reasons, the architecture of Otto and diesel engines is different: The first requires a spark-plug circuit and a throttle valve for regulation; the latter needs a sophisticated high-pressure fuel ignition system and in general has a heavier structure because of the highest pressure ratios. In both cases, the fact that the combustion occurs inside of the cylinder on one hand simplifies the manufacturing because of the absence of heat exchangers with the benefit of fewer sources of losses. On the other hand, it brings limitations in the choice of fuels. In each case, these fuels must have the characteristics to achieve combustion in the required way and at the required times. The fuels generally used are gasoline (in alternative methanol or even natural gas) in spark-ignited engines and diesel fuel in compression-ignited engines. In general, the combustion can occur at very high temperatures because of its short duration and because the walls of the cylinder

¹ Sometimes modern spark-ignited engines can adopt direct gasoline injection, like in diesel engines. In these cases, the processed gas during the compression is air.

² The phenomenon can be eliminated by means of additive elements to the gasoline.

³ In diesel engines the combustion process is of a lean-burn type: the air/fuel ratio is always greater than stoichiometric and at partial load reaches very high values.

are cooled by a designated cooling circuit as well as by the new fluid that is taken in. High values of cycle maximal temperatures allow internal combustion engines to achieve extremely high efficiencies. This is even more remarkable because such efficiencies can be achieved by engines of modest power.

7.3 KINEMATICS AND GEOMETRIC PARAMETERS

The reciprocating internal combustion engine supplies work to a shaft by means of discontinuous compression; combustion; and expansion of fluids in a working chamber, the cylinder, the volume of which is varied by the alternate motion of a piston. As presented in Figure 7.3, the piston slides inside of the cylinder closed at the top by the cylinder head. The energy released by the combustion of fuel with air is transferred to the piston. The reciprocating motion of the piston is converted into the rotational motion of the engine crankshaft by means of the connecting rod-crankshaft mechanism. The produced work is extracted from the engine crankshaft. The combustion occurs inside of the working fluid, and therefore, the fluid, once burned, must be expelled and renewed by means of an appropriate distribution system (valves, discharge channel, or both) that periodically replaces the engine fluid.

For the purpose of completeness, another possible kinematic configuration can be obtained with the so-called rotary or Wankel engine [5], in which the volumetric variation of the working fluid is directly obtained through the shaft rotation without a reciprocating rod-crankshaft mechanism. However, the Wankel engine has very limited applications because of many unresolved technical problems as lubricating oil consumption or components wear.

The following parameters characterize the geometry of a reciprocating engine [6]:

- **Bore D :** Internal diameter of the cylinder.
- **Top dead center (TDC):** The point where the piston is nearest to the cylinder head.
- **Bottom dead center (BDC):** The point where the piston is farthest from the cylinder head.

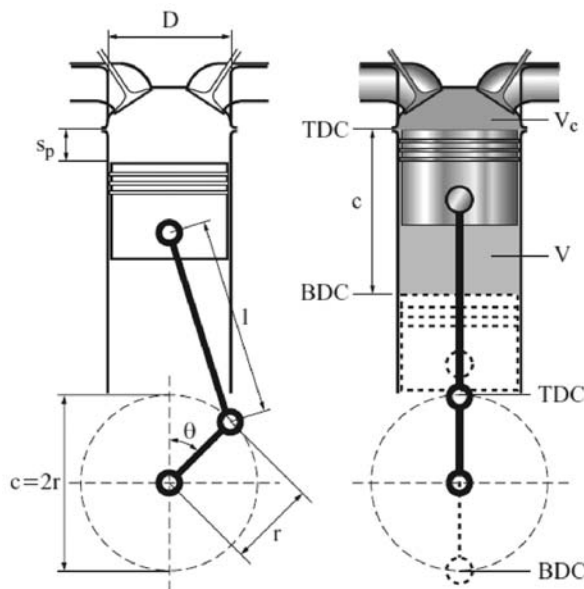


Figure 7.3—Normal centered crank mechanism.

- **Stroke c :** The distance covered by the piston in its movement between positions TDC and BDC. The stroke is twice the radius of the crank, $c = 2r$.
- **Ratio between bore D and stroke c , D/c (or its inverse c/D):** The typical value of the ratio D/c ranges from 0.25 for large, slow marine engines to approximately 1 for small- and medium-size engines and up to 1.4 for smaller, high-power motorcycle engines.
- **Ratio A :** The ratio between the length of the connecting rod and the radius of the crank, $A = r/l$ (or its inverse l/r). Typical values of A vary from 0.25 to 0.33 in small- and medium-size engines up to 0.11–0.17 in large, slow marine motors.
- **Volumetric compression ratio, ψ :** The ratio between the volume of the cylinder when the piston is at BDC (maximal volume, V_m) and the volume of the cylinder when the piston is at TDC (also called dead volume, V_c). As already mentioned, typical values of the compression ratio range from 8 to 12 for spark-ignited engines and 16–22 for compression-ignited engines.

$$\psi = \frac{V_m}{V_c} \quad (7.2)$$

- **Unit displacement, V_u :** The volume displaced by the piston in a complete stroke inside of the cylinder. It is equal to the product of the cross-section of the cylinder A_c and the stroke c . It is also equal to the difference between the volume of the cylinder when the piston is, respectively, at BDC and TDC.

$$V_u = A_c c = \frac{\pi D^2}{4} c = V_m - V_c \quad (7.3)$$

- **Total displacement, V :** The unit displacement multiplied by the number of cylinders q of the engine $V = qV_u$. (In the case of a single-cylinder engine, the total displacement coincides with the unit displacement.) The term “displacement” is often used instead of “total displacement” when there is no possibility of it being confused with unit displacement.
- **Instantaneous volume inside the cylinder, V_i :** It is the available volume for the working fluid inside of each cylinder, and it is expressed as a function of the crankshaft position:

$$V_i = V_c + V_u \frac{s_p}{C} \quad (7.4)$$

The parameters characterizing the kinematics of an internal combustion engine are the following:

- **Rotation speed ω of the engine crankshaft:** This is an angular speed and is proportional to the number of revolutions in the unit of time (n) according to $\omega = 2\pi n$.
- **Cycle frequency, f :** This parameter takes into account the fact that a work cycle may consist of one or more revolutions of the engine crankshaft. The parameter ϵ is introduced and is equal to 1 for two-stroke engines, which execute a full working cycle in one revolution of the engine crankshaft, and is equal to 2 for four-stroke engines, which require two engine crankshaft revolutions to perform the cycle. Cycle frequency $f = n/\epsilon$.
- **Crank angle, θ :** This is the angle between the crank at time t and the crank in its starting position, supposed

at TDC. It is a function of angular speed ω and time t :
 $\theta = \omega t = 2\pi n t$

- *Movement of the piston, s_p* : The distance covered by the piston starting from TDC:

$$s_p = (l+r) - \left(r \cos \theta + \sqrt{l^2 - r^2 \sin^2 \theta} \right) \\ = \frac{c}{2} \left(1 + \frac{1}{\Lambda} - \cos \theta - \frac{1}{\Lambda} \sqrt{1 - \Lambda^2 \sin^2 \theta} \right) \quad (7.5)$$

- *Velocity of the piston, v_p* : This is the instantaneous velocity of the piston. It is null at TDC and BDC (which is why they are called “dead” points). It is obtained by deriving s_p , where $v_{p,a}$ is the average velocity:

$$v_p = v_{p,a} \frac{\pi}{2} \left[\sin \theta + \frac{\Lambda \sin 2\theta}{2\sqrt{1 - \Lambda^2 \sin^2 \theta}} \right] \quad (7.6)$$

- *Average velocity of the piston, $v_{p,a}$* : This is the average velocity of the piston during a full revolution of the engine crankshaft, in which the piston covers a distance that is twice the stroke c . This velocity influences various phenomena characterizing the behavior of the engine, such as the fluid dynamic losses in the “substitution cycle” (i.e., during the cycle that permits renewal of the engine fluid in the cylinder), the energy losses due to the heat transfer toward the cooling system, and the inertial loads on different parts of the engine. The average velocity ranges from 7 m/s (slow marine engines) up to 20 m/s (spark-ignited engines for cars). The relationship is $v_a = 2cn$.
- *Acceleration of the piston, a_p* : This is the instantaneous acceleration of the piston. It is determined by deriving v_p . An acceptable approximation can be obtained by neglecting the term Λ^2 , which is very small:

$$a_p = \omega^2 \frac{c}{2} [\cos \theta + \Lambda \cos 2\theta] \quad (7.7)$$

7.4 PERFORMANCE CHARACTERIZATION

The main parameters characterizing engine performance are measured on an apposite test bench simulating the behavior of the end user, which can, in general, be a means of transport, a compressor, an electric generator, etc. The test bench permits coverage of the full range of shaft velocities and engine loads of a real engine application, and it is composed of a dynamometric brake capable of absorbing and dispersing the mechanical energy produced by the engine [7]. The brake measures the effective torque moment, M , that is available to the engine shaft. The actual power of the engine is given by multiplying the measured torque and the angular velocity ω under test conditions:

$$P = \omega M = 2\pi n M \quad (7.8)$$

An interesting parameter to describe engine performance that has increased alongside the development and downsizing of reciprocating engines is the power density. It is the ratio between the working power P and the total displacement V , and its constant trend toward higher values brings the decrease of fuel consumption and reduces emissions and costs.

In addition to torque and angular velocity, many other quantities are measured with the test bench. Pressure, p , in the cylinder is measured through a reaction pressure transducer on the wall of the combustion chamber. The measurement of instantaneous volume which is available inside of the cylinder for the working fluid, V_i , is directly related to the measurement of the crank angle, θ . The first instruments used to determine the state of the fluid inside of the cylinder were called indicators so that the thermodynamic cycle obtained in this way was called the “indicated cycle”.

An indicated cycle for a four-stroke, spark-ignited, nonsupercharged engine is depicted in Figure 7.2. The area obtained integrating the indicated cycle along the pressure-volume curve represents the indicated work, which is the work per cycle released to the piston from the working fluid in the consecutive phases of aspiration, compression, combustion, expansion, and discharge of combusted gas. In general, the contained area is positive if the cycle proceeds in a clockwise direction so that the work is executed on the piston by the fluid and is negative if the cycle proceeds in an anticlockwise direction so that the piston exerts the work over the working fluid. In the four-stroke engine, a full cycle is completed with two revolutions of the engine crankshaft: One revolution determines the upper positive area that proceeds clockwise and corresponds to the cycle transformations of compression, combustion, and expansion; the other revolution encloses the smaller lower negative area that proceeds anticlockwise and corresponds to the substitution cycle of the fluid. It should be noted that in a supercharged four-stroke engine even the substitution cycle normally gives a positive contribution to the engine work because the compressor supply pressure is greater than the exhaust pressure. In the two-stroke engine, the substitution cycle is not present; in fact, the exhaust gas is discharged at the end of the expansion and the fresh air-fuel mixture is aspired at the beginning of the compression phase so that the engine performs a complete cycle in only one revolution of the shaft [2].

Starting from indicated quantities (torque, work, power, etc.), measured or derived from the indicated cycle, we pass to actual quantities, taking into account that a part of the power given from the working fluid to the piston is used to overcome the friction of the engine's main couplings (pistons, bearings, etc.) and to drive all of the accessories that are essential to the working of the engine itself.

The system efficiency, η_s , is the ratio between the actual working power of the engine (i.e., the power $[P]$ measured on the dynamometric test bench) and the indicated power (i.e., the power $[P_i]$ calculated from the indicated cycle) ($\eta_s = P/P_i$). This efficiency decreases when the average velocity of the piston (which is related to the angular velocity) increases and when the load is reduced; typical values for a vehicle engine working at full load are approximately 0.94 at 1800–2400 r/min, decreasing to 0.80 at the highest rotation speed.

Another characteristic parameter of the engine is the air-fuel ratio, α , which is the ratio of the mass flow of air taken in (m_a) to the fuel flow (m_f): $\alpha = m_a/m_f$. The air-fuel ratio can be determined during the testing of the engine and characterizes the combustion under a specific working condition. It depends on the type of motor, the adopted fuel, and how the power is regulated [8]. The parameter can assume different values depending on the type of engine

and actual working conditions: It ranges from relatively low values of 13–14 in spark-ignited engines up to values of 70 or greater in diesel engines working at reduced loads [9]. The lambda coefficient (λ) is given by the ratio of the actual value of α in a specific operating condition to the stoichiometric ratio (α_{st}) that is the minimal value with which the complete oxidation of fuel is achieved ($\lambda = \alpha/\alpha_{st}$). Lambda is less than 1 for mixtures rich in fuel and is greater than 1 for lean mixtures. A typical stoichiometric ratio of 14.7 is required for gasoline and diesel fuel so that λ ranges from approximately 1 in spark-ignited stoichiometric engines⁴ up to 5 ($\alpha = 74$) in compression ignition engines working at partial loads.

Another performance parameter is the specific fuel consumption (c_s), defined as the ratio of the fuel flow to the actual power ($c_s = m_f/P$). Specific fuel consumption provides an indication of the efficiency with which the energy of the fuel is converted into the mechanical energy available to the shaft. The preceding factor can be properly referred to the chemical energy of the fuel, multiplying the fuel flow by its lower heating value (LHV), so that the ratio ($c_{se} = m_f \cdot LHV/P$) becomes the specific energy consumption whereas its reciprocal (η) is called efficiency ($\eta = 1/c_{se}$). The efficiency of a spark-ignited engine at full throttle varies between 0.30 and 0.40 whereas for a heavy-duty, large diesel engine it can exceed 0.50.

The power of the engine can be expressed as a function of the efficiency and the fuel flow ($P = \eta \cdot m_f \cdot LHV$).

The volumetric efficiency (η_v) is a coefficient that takes into consideration that the mass of fresh air actually aspired during each complete cycle of the engine (m_a) is generally different from the theoretical mass of air that should fill a volume corresponding to the total engine displacement ($m_{a,th}$). Therefore, its expression is

$$\eta_v = m_a / m_{a,th} = m_a / (\rho_a V) \quad (7.9)$$

where ρ_a is the density of air at the intake pressure and temperature. From the definition of volumetric efficiency, the air flow that feeds the engine has the following expression, remembering that ε is a parameter equal to 1 in a two-stroke engine and 2 in a four-stroke engine:

$$m_a = \eta_v \rho_a V (n/\varepsilon) \quad (7.10)$$

Finally, we can express the formula of the actual power of an engine as a function of the abovementioned coefficients:

$$P = \eta \eta_v \rho_a \frac{LHV}{\alpha} V \frac{n}{\varepsilon} \quad (7.11)$$

The characteristic curves (Figure 7.4) summarize the performance of an engine [10]. They give the trend of the mechanical power, the torque, and the specific fuel consumption as a function of the engine crankshaft angular velocity. They are generally given at full load; therefore, they correspond to the maximal performance supplied by the engine at different rotation speeds.

⁴ Engines working with rich mixtures ($\lambda < 1$) are no longer constructed because of pollutant emissions, especially CO and hydrocarbons.

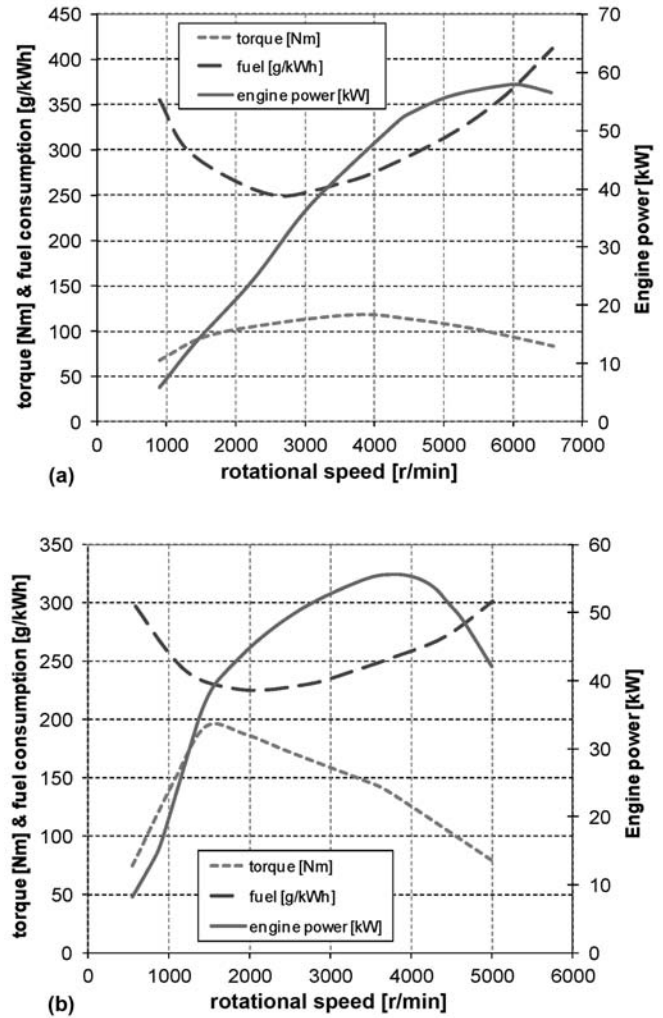


Figure 7.4—Characteristic curves: (a) spark-ignited engine and (b) diesel engine.

The example of Figure 7.4a refers to a typical automobile spark-ignited engine in which the power curve rapidly increases up to a maximum (~6500 r/min in the example shown). As a rule of thumb, the torque and the specific consumption have, respectively, a maximum and a minimum at an angular velocity that is approximately half of the rotation speed of the maximal power. Mechanical power is equal to the product of the torque and the angular velocity (see eq. 7.8); therefore, the power curve has an initial steep increase and a subsequent lower slope because of the decreasing torque. After the point of maximal power, the reduction of torque is such that it is no longer compensated for by the increase of engine speed, which causes a decrease of power. The maximal operating speed of the engine normally corresponds to its maximal power: With further increase of speed, lower power outputs would be obtained. These values of power could be also achieved at lower angular velocities with lower mechanical stress on the engine parts and with lower fuel consumptions.

The engine normally operates between this maximum speed and a minimum value imposed by mechanical constraints. In fact, below the minimum rotation, the fuel supply becomes irregular, the torque becomes unstable,

and the hydrodynamic lubrication of kinematic couplings becomes inefficient.

In the case of a diesel engine, a similar behavior is observed. Figure 7.4b shows an example of a typical automobile engine, with the only difference with respect to a corresponding spark-ignited engine being that the rotation speed at maximum power is lower (~ 4000 r/min in the example), mainly because of the larger masses of the parts in reciprocating movement so that the engine operation range is smaller.

As already mentioned, the characteristic curves are normally given for the engine at full load (nominal conditions). However, internal combustion engines are characterized by a great flexibility in use that is of particular importance in vehicle applications. They are requested to operate at different regimes and above all at different loads, rapidly passing from one working condition to another. Their performances depend on the position of the regulation device that changes the filling level of the cylinder in the case of spark-ignited engines (the throttle valve) or, in the case of a diesel engine, the quantity of the injected fuel. Moreover, their performances are influenced by environmental conditions, which can be very different.

In Figure 7.5, the efficiency variation with load at constant rotation speed is reported for a spark-ignited engine (nonsupercharged engine of 70 kW nominal power output) [1]. The rotation speed considered in the example is the value that minimizes the fuel-specific consumption (maximizes the efficiency), and, as already explained it is next to the speed that maximizes the torque. The load fraction refers to nominal full-load performance.

In the example, the efficiency drops from approximately 35 % at full load down to 25 % at 10 % load. This behavior is mainly due to the intervention of the throttle valve and to the relative increase of friction losses and heat losses of the engine.

In addition to this, engine performances are influenced by environmental conditions. Above all, temperature has an influence on power and efficiency. Figures 7.6a and 7.6b respectively report the power and efficiency curves as a function of temperature at full load for the same engine as shown in the example in Figure 7.5.

The main effect of temperature is on the engine power output because ambient temperature influences the air density and therefore the air mass flow aspired by the engine as well as the power produced at the shaft. It should

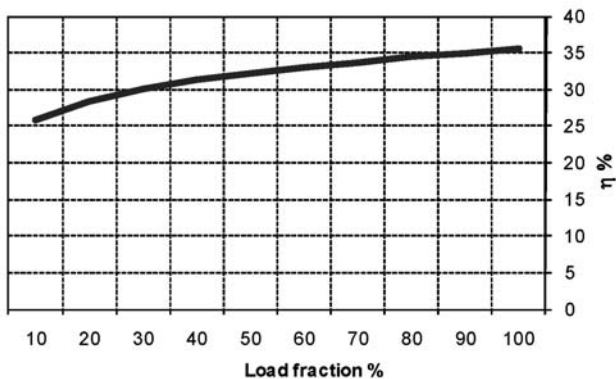


Figure 7.5—Partial-load performance (constant speed).

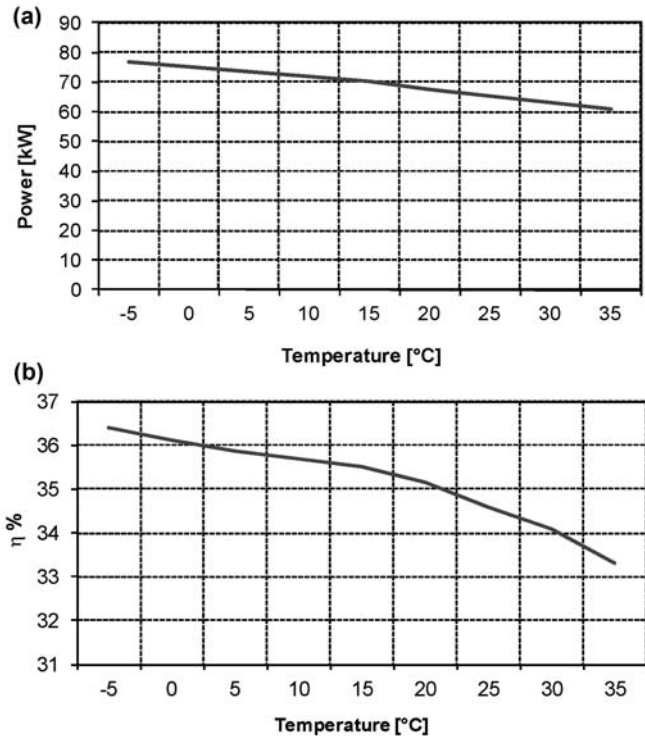


Figure 7.6—Power (a) and efficiency (b) variation with temperature (full load).

be noted that this effect is less evident in a supercharged engine.

7.5 CONFIGURATIONS AND MECHANICAL EQUIPMENT

An internal combustion powertrain system is generally arranged in a multicylinder configuration. The layout of the engine varies according to the adopted configuration [11]: With “in-line” architecture, the cylinders are exactly disposed on a single line and the crankshaft is on a single plane; in “V engines”, the cylinders are assembled on two V-shaped banks; in “radial engines” (used in historical aeronautic applications); they are positioned in a radial direction on one or more banks; and in “flat (or boxer) engines” they are on opposite sides of the crankshaft.

The ignition sequence is important because it defines the order with which the combustion is triggered in the cylinders. It is influenced by the engine’s configuration and the requirement of uniformity in ignition intervals.

In each configuration, the crankshaft-rod-piston connecting system induces forces and torques of centrifugal and reciprocating inertial types. The centrifugal forces are caused by the rotation of the engine cranks and of those parts of the rod that are connected to the crankshaft: The frequency is the same of the rotation of the shaft. These forces can be balanced through the application of counterweights or with an appropriate arrangement of the cranks in multicylinder configurations. The reciprocating inertial forces are due to the alternating motion of the pistons and the parts of the rods that are connected to them. The fundamental frequency is that corresponding to the rotation of the shaft, and even multiple harmonics of the fundamental are present.

In addition to these mechanical forces, the action of the gases inside of the cylinder during a complete cycle turns in forces generated on the piston. The main force, because of the combustion of the air-fuel mixture, acts on the crank mechanism producing the driving torque. The fluctuations of pressure inside of the cylinders and the reciprocating inertial forces during an engine cycle determine the cyclic variation of the supplied torque. Multicylinder configurations allow for a reduction in the torque fluctuation. A further attenuation of the consequences of torque variations is obtained by inserting an engine flywheel, thus limiting angular velocity variation, and by applying a filtering element, consisting of a torsion spring coupled to the clutch that acts as a flexible coupling.

7.5.1 Structural Elements

The main structural elements of a reciprocating engine powertrain system are the engine block, the cylinder head, the crankshaft, the connecting rod, the piston, the distribution system, the cooling circuit, and the lubrication circuit [6,10]. Figure 7.7 shows the expanded view of a turbo-charged diesel engine with five in-line cylinders. In general, the design of each component of the engine must consider the fatigue stresses caused by dynamic loads and the excursion caused by temperature variations.

The engine block is formed by two parts: The block itself and the base. The block contains the cylinder liner and the cooling circuit, and the base has the function of containing the crankshaft and housing the channels for the cooling fluid circulation, those for lubricant feeding for bearing

and sliding parts, and the lubricant reservoir. In automobile engines, the engine block is usually made of aluminum; therefore, the cylinder liners require specific surface treatments to improve the resistance to wear (co-deposition of Ni-based metallic deposit and silicon carbide). The materials used in the engine base are nodular or laminar cast iron or primary aluminum alloys of the type AlSi9.

The cylinder head is a very complex structure that includes the air feed and the exhaust gas manifolds, the actuating mechanism of the valves, the mixture ignition devices (spark plugs) or the fuel feed or both, and the circuits of the lubricating oil and of the cooling liquid. The connection to the engine block is made through screws or studs, and a gasket ensures the seal, preventing gas leaks from the combustion chamber toward oil and water circuits or vice versa.

The crankshaft has the primary function to ensure the conversion of the forces due to the gas pressure inside of the combustion chamber into the driving torque. Moreover, it must ensure the coupling to the clutch and the gear box, to drag auxiliary equipment as coolant and lubricating oil pumps, and at any time to generate a range of pressures that are right for hydrodynamic support with low-friction sliding, even in conditions with a limited meatus. They are generally made of nitride steels (Cr-Mo-Va alloys; e.g., 40CDV12) and hardened tempered steels (Cr-Mo, Ni-Cr-Mo alloys, such as 40NiCrMo₄).

The connecting rod connects the piston to the crankshaft, ensuring the transmission of motion. Its kinematics are the composition of a reciprocating motion (small end

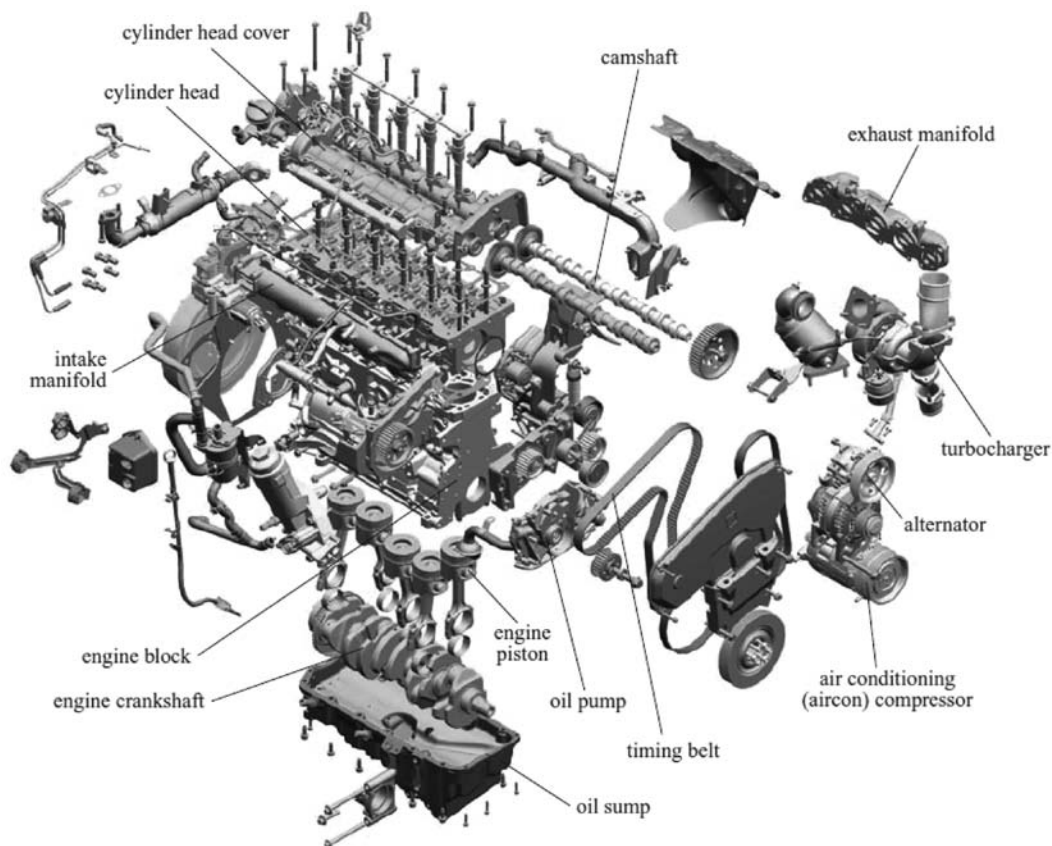


Figure 7.7—Expanded view of an engine (a turbo-charged diesel engine, FIAT 5 in-line cylinders). *Source:* Figure courtesy of FIAT.

of the connecting rod) and a rotary motion (big end). It must be designed to reduce as much as possible its mass and length to minimize the forces. The connection with the piston is performed by means of a pin at the base of the piston with the interposition of a bush assembled by interference. The lubrication of the bush is made by a hole that collects the oil sprayed to the crown of the piston. The connecting rods are generally made from steel (forged rods) or, for less-demanding applications, from nodular or malleable cast iron (cast rods). The most common solution is the forged rod, and the used materials are normally hardened and tempered steels or in some cases high-alloy steels. Some recent applications use “fractured rods”, which are obtained by a process in which, after forging, the rod beam is separated from the cap by fracture and then recomposed, ensuring increased accuracy in the centering of the cap and better roundness of the bearing saddle.

The piston performs the transmission of the force caused by gas pressure to the crank, at the same time ensuring the gas sealing by means of the piston rings and the heat disposal from the combustion chamber. In direct-injection diesel engines, part of the combustion chamber is created inside of the piston crown. In general, the piston is invested by large thermal gradients throughout the height, affecting the design of its profile. The piston materials have different requirements, including high static and fatigue resistance even at high temperatures, high thermal conductivity, a low thermal expansion coefficient, high rheological characteristics, and high resistance to wear. Aluminum alloys containing Si, Mg, and even Cu are normally used.

The distribution system ensures the renewal of the gas charge in the engine. It includes the intake and exhaust valves, the tappet rods and valve rockers with the device for setting the clearance and for automatic compensation, the springs ensuring their closure, and finally the camshaft operated by the crankshaft itself through the transmission system. Important parameters governing the renewal of the gas charge are the maximal valve lift (generally from 8 to 11 mm); its opening and closing profile; and the advance of the opening start with respect to TDC and BDC, respectively, for intake and exhaust valves, as well as the delay of their closure.

The cooling circuit permits the cooling of the materials heated up by the combustion process. It operates transferring the extracted heat to a circuit outside of the engine and includes the coolant pump, the channels inside of the cylinder head and engine block, and a thermostat for temperature control.

The lubrication circuit has the function of lubricating the engine parts, guaranteeing adequate hydraulic lifts in the couplings in relative motion, and at the same time contributing to their cooling. It consists of an oil pump, a filter for impurity removal, and the circuits for the oil distribution. A radiator for cooling and a thermostatic valve are sometimes present. There are two kinds of lubrication: Splash lubrication is used in less critical couplings whereas pressure lubrication is used in the other cases. The pressurized lubrication is obtained through the pump that sucks oil from the oil sump and distributes it under pressure to the circuit. In some cases, “dry-sump lubrication” is adopted (e.g., with off-road vehicles or high-performance sport vehicles) when it is difficult to guarantee the oil suction from the sump in all working conditions. In dry-sump

lubrication the oil is contained in a reservoir tank from which it is sucked by the pump, and the sump is kept dry by means of one or more pumps that ensure the recovery of oil and the delivery to the reservoir. Finally, the lubrication system is completed by an “internal ventilation system” that has the function of recovering the gas leaks occurring from the combustion chamber through the piston rings and transferring them to the engine intake after separating their lubricant content. It consists of a circuit inside of the engine with oil separators (labyrinth or cyclone types).

7.6 POLLUTANT FORMATION AND CONTROL

Pollutant formation in an internal combustion engine follows very complex mechanisms. (For complete studies, please refer to specialized texts [12,13].) Generally speaking, we can affirm that in an internal combustion engine pollutant emissions are higher than in external combustion plants or even in gas turbines, the combustion of which is internal similar to reciprocating engines, but it occurs as a continuous process that is easy to manage and control. In reciprocating engines, combustion takes place inside of the cylinders in short times and with variable temperatures. In particular, the cylinder's walls are relatively cold with respect to combustion temperatures, causing bad combustion conditions into the boundary layer next to the walls.

The principal pollutant emissions of an engine are carbon monoxide (CO), which originates at high temperatures and low lambda values (λ of air-fuel mixture [rich mixtures]; unburnt hydrocarbons (HCs), which originate at low temperatures and low lambda values (λ of air-fuel mixture); nitrogen oxides (principally nitric oxide [NO] and nitrogen dioxide [NO₂], generically indicated as NO_x), the formation of which is favored by high combustion temperatures and in the presence of oxygen; and particulate matter (PM), which originates from carbon particles that aggregate in bigger agglomerates. The formation of PM is related to the liquid fuel injection inside of the cylinder and is therefore a typical pollutant of diesel engines (lower concentrations of PM are even produced by gasoline direct injection [GDI] engines) [14].

With reference to a spark-ignited engine, Figure 7.8 qualitatively shows the relationship between the main pollutant emissions and the parameter λ [3]. Fuel consumption is also reported for clarity.

According to present environmental legislations, the adoption of specific measures is necessary to control pollutants from engines. Adoptable measures can be classified according to their type of application: Remedies “during combustion” and “after combustion”.

Among the remedies during the combustion process, in spark-ignited engines, it is common to use lean mixtures (high λ values), which at the same time allow for a reduction in CO emissions and flame temperatures, thus limiting NO_x formation [15]. In these so-called “lean-burn” engines, combustion chambers with a proper design must be adopted to create high-turbulence fluxes, thus also limiting HC formation, which would be favored by lower combustion temperatures [16,17]. Moreover, the adoption of a lean mixture permits increasing the volumetric compression ratio without incurring knock phenomena, resulting in higher efficiency values.

Another remedy adoptable during the combustion phase, mainly adopted in diesel engines, is the EGR valve

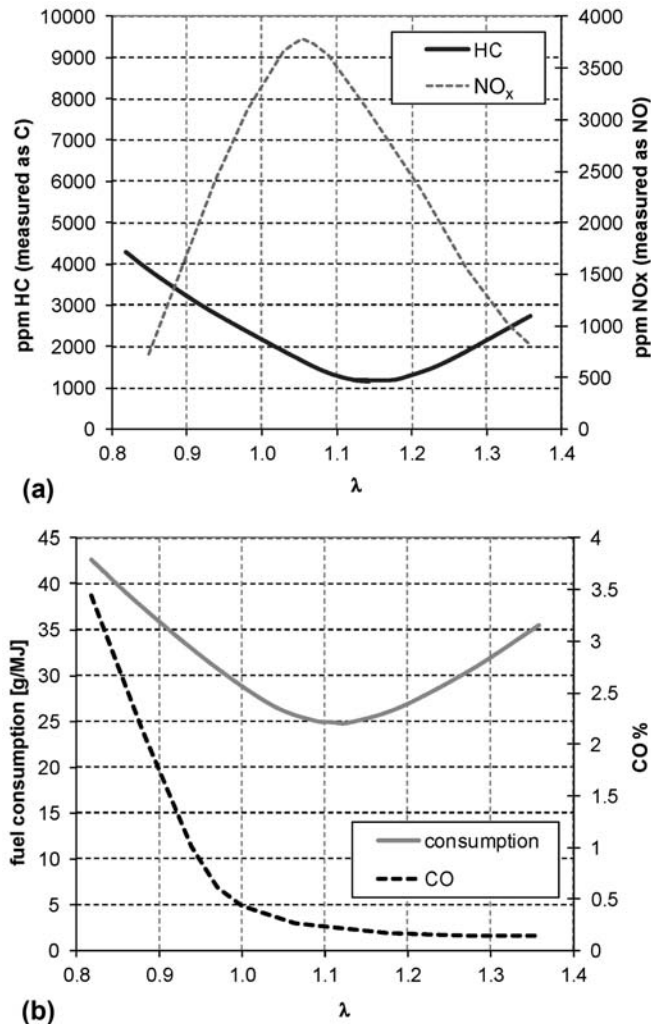


Figure 7.8—Qualitative concentration of pollutants as a function of λ for a spark-ignited engine.

(exhaust gas recirculation system), with which it is possible to recirculate a portion of the exhaust gases into the fresh mixture at the intake of the cylinder [18]. The exhaust gases act as an inertial mass and the dilution of the intake mixture is obtained, thus lowering combustion temperatures and NO_x emissions. In this process, the water content of the exhaust gases is important because it increases the heat capacity of the mixture. In stationary applications (e.g., in cogeneration systems), additional water is sometimes separately injected inside of the combustion chamber or in mixture with the fuel.

Finally, even the practice of overfeeding the engine by means of a turbo-charger has an effect in containing pollutants emissions: In general, all of the emissions are slightly reduced⁵ whereas efficiency is increased (especially for diesel engines), resulting in lower specific emission values [19].

Among the remedies after the combustion process, it is possible to adopt catalytic converters in the exhaust gas ducts. They are able to promote certain chemical

reactions, particularly oxidation and reduction, even at low temperatures with unfavorable kinetics, thus eliminating pollutants before the exhaust release to the atmosphere. For spark-ignited engines, a three-way converter can be adopted that is able to oxidize CO and HCs as well as to simultaneously reduce NO_x . It is characterized by high conversion efficiencies for air-fuel mixtures next to their stoichiometric value. For these reasons, a continuous measure of the oxygen content, the “lambda sensor”, and a closed circuit control on the fuel feeding in each cylinder are necessary. In Figure 7.9, the schematic principle of a three-way catalytic converter with a lambda sensor is reported, and Figure 7.10 shows the conversion efficiency as a function of λ [3].

As can be seen in Figure 7.10, to achieve the maximal efficiencies the converter must operate in a quite narrow range of the air-fuel ratio ($\lambda = 1 \pm 0.007$). In this way the two opposing functions of oxidation (CO and HC) and reduction (NO_x) are performed. Nowadays, using this technology, light vehicle exhaust emissions can reach very low levels [10]: Less than 1 g/km of CO and 0.1 g/km for HCs and NO_x .

For diesel engines and spark-ignited engines working with lean mixtures (lean-burn engines), an oxidative catalytic converter is used because a three-way converter would not be effective in NO_x reduction: The oxidative converter is active against CO and HCs and partially against PM in diesel engines [20]. Hence, in these engines, other remedies should be adopted during combustion, such as the EGR system, high-turbulence combustion, or stratified charge chambers. Modern injection systems adopt the so-called “common rail” system: A high-pressure volumetric pump processes a variable flow rate of compressed diesel fuel that is accumulated in a volume (rail) whereas the injection phase occurs separately through electronically operated electroinjectors. In this way, high injection pressures (up to 2000 bar) can be reached in a wide range of operating conditions independent of the speed of the engine and of the fuel quantity to be injected. In this way the injected fuel is finely atomized, resulting in low PM emissions.

Among remedies for after the combustion processes, especially for diesel engines, selective catalytic reduction (SCR) devices can be used, in which ammonia (NH_3) or urea are injected immediately before the converter. The SCR converter uses NH_3 as the agent for reducing NO_x to nitrogen and water. NH_3 injection is a solution applied in large stationary applications (e.g., cogeneration plants) and particular attention should be devoted to NH_3 dosing, avoiding its emission to stack, the so-called “ammonia slip”. In mobile applications such as in vehicles, urea is preferred and starting from it NH_3 is produced by decomposition inside of the converter.

There are also other solutions that are currently under development among car and truck manufacturers that exploit types of traps in which NO_x are adsorbed and periodically released. During the release, a regeneration process is performed using a reducing environment that is created by means of injecting small amounts of fuel or urea.

Finally, for PM abatement in diesel engines, traps can be used (diesel particulate filters [DPFs]). Their working principle is to entrap particles in a porous metallic or ceramic matrix that is periodically regenerated with autocombustion,

⁵ Even the NO_x emissions are limited if the supercharging is coupled with an intercooler, which limits the temperatures at the end of compression and during the combustion.

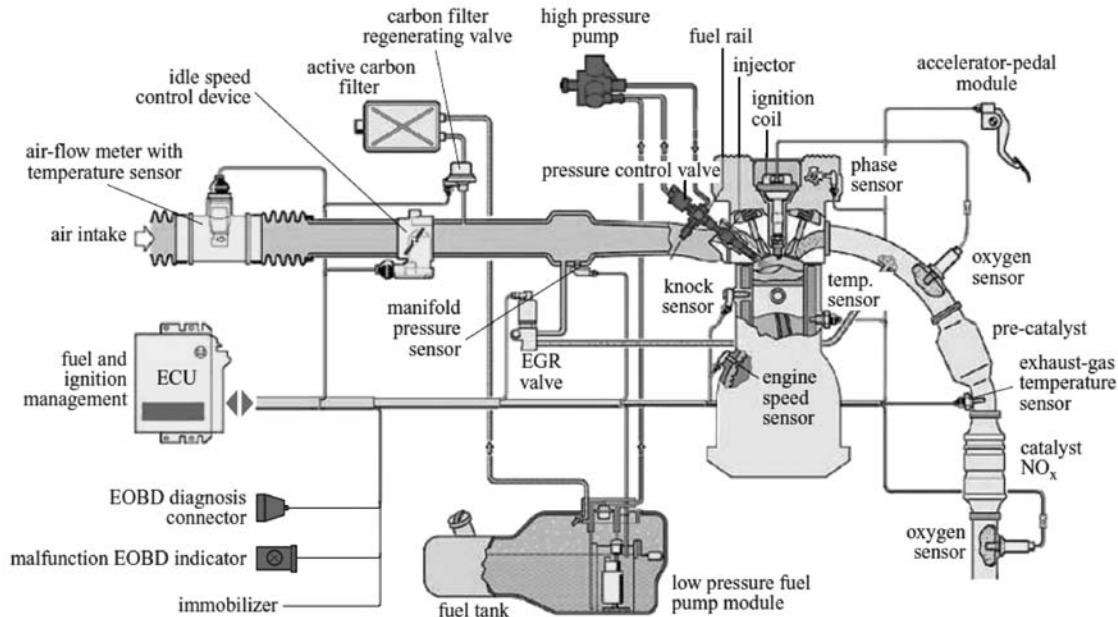


Figure 7.9—Schematic diagram of a three-way catalytic converter system with a lambda sensor. Source: Figure courtesy of Bosch.

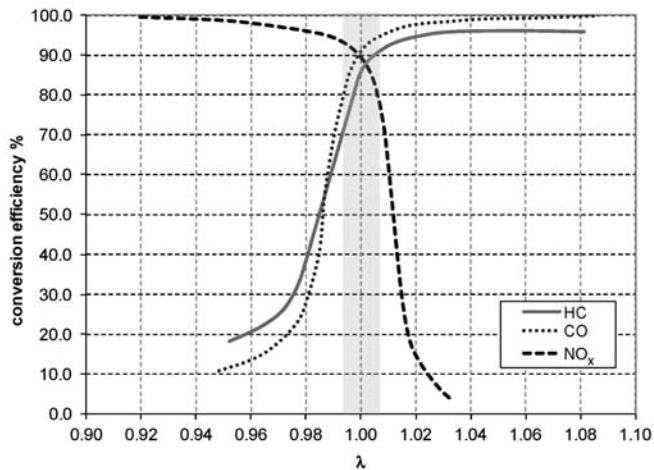


Figure 7.10—Conversion efficiency as a function of λ for a three-way catalytic converter.

which is caused by temporary air-fuel mixture enrichments or by small fuel injections before the filter itself.

Adopting all of these technologies, in a few years diesel engines, the weak points of which are mainly NO_x and PM emissions, should reach the already defined limits on the order of 0.5 g/km for CO, 0.05 g/km for HCs, 0.08 g/km for NO_x, and 0.0025 g/km for PM [10]. These limits would bring the diesel engine at the same level of emissions with respect to a gasoline engine but with still higher fuel efficiency.

References

- [1] Macchi, E., Campanari S., and Silva P., 2005, *La Micro-Cogenerazione a Gas Naturale*, Polipress, Milan, Italy.
- [2] Blair, G.P., 1996, *Design and Simulation of Two-Stroke Engines*, SAE, Warrendale, PA.
- [3] Ferrari, G., 2011, *Internal Combustion Engines*, Esculapio, Bologna.
- [4] Heywood, J.B., 1988, *Internal Combustion Engine Fundamentals*, McGraw-Hill, London.
- [5] Yamamoto, K., 1969, *Rotary Engine*, Mazda, Hiroshima, Japan.
- [6] Bosch, R., 2000, *Automotive Handbook*, 5th ed., SAE, Warrendale, PA.
- [7] Nunnery, M.J., 1974, *The Automotive Engine*, Newnes-Butterworths, London.
- [8] Ferguson, C.R., and Kirkpatrick A.T., 2001, *Internal Combustion Engines Applied Thermosciences*, 2nd ed., John Wiley & Sons, New York.
- [9] Goodger, E.M., 1975, *Hydrocarbon Fuels: Production, Properties and Performance of Liquids and Gases*, Macmillan, London.
- [10] Piccone, A., and Cornetti G., 2009, *Reciprocating Internal Combustion Engines*, Encyclopedia of Hydrocarbons, ENI-TRECCANI, Rome.
- [11] U.S. Environmental Protection Agency (EPA), 2002, *Technology Characterization: Reciprocating Engines*, CHP Partnership Report, EPA, Washington, DC.
- [12] Heck, R.M., and Farranto R.J., 1995, *Catalytic Air Pollution Control*, Van Nostrand, Reinhold, New York.
- [13] Sher, E., 1998, *Handbook of Air Pollution from Internal Combustion Engines: Pollutant Formation and Control*, Academic Press, San Diego, CA.
- [14] Zhao, F., Harrington D.L., and Lai M.C., 2002, *Automotive Gasoline Direct-Injection Engine*, SAE, Warrendale, PA.
- [15] Lenz, H.P., 1990, *Mixture Formation in Spark-Ignition Engines*, Springer-Verlag, New York.
- [16] Benson, R.S., 1982, *The Thermodynamics and Gas Dynamics of Internal Combustion Engines*, Vol. 1, J.H. Horlock and D.E. Winterbone, Eds., Clarendon Press, Oxford, UK.
- [17] Horlock, J.H., and Winterbone D.E., 1986, *The Thermodynamics and Gas Dynamics of Internal Combustion Engines*, Vol. 2, Clarendon Press, Oxford, UK.
- [18] Challen, B., and Baranescu, R., 1999, *Diesel Engine Reference Book*, 2nd ed., SAE, Warrendale, PA.
- [19] Watson, N., and Janota, M.S., 1982, *Turbocharging the Internal Combustion Engine*, John Wiley & Sons, New York.
- [20] Owen, K., and Coley T., 1990, *Automotive Fuels Handbook*, SAE, Warrendale, PA.

8

Automotive Bearing Systems— Journal Bearings

Omar Mian¹

8.1 INTRODUCTION

The principal use for journal bearings in automotive applications is for the crankshaft bearings, piston pin joint, balancer shafts, and crankshafts. These can either be half shells in which a split is required for assembly (e.g., crankshaft bearings) or bushes that can be inserted without a split (e.g., piston pin joints). For engine bearings, the oil is normally supplied at pressure from the oil pump via a filter/cooler assembly to a main oil gallery that runs along the side of the engine and then to the main bearing as indicated in Figure 8.1. The oil supply hole in the upper main bearing normally feeds into a groove so that a drilling in the crankshaft journal can transport the oil to the big-end bearing in the connecting rod. Oil supply to the pin joint small-end and piston pin boss is typically by “splash” from the sides of the or via internal drillings in the connecting rod or piston. During the design process, the assembly must be considered as a “system” with adequate lubricant supply and clearance shape—the bearings are often the “fuse” where any deficiencies become obvious in damage such as engine seizures. The normal design envelope for journal bearings is indicated by:

- **Maximum specific load (MSL):** MSL is the applied load divided by the projected area (length \times diameter). Typical values are 30–70 MPa for “bimetal” bearings and 60–100 MPa for “trimetal” bearings. Overloading can result in loss of the lining by fatigue mechanisms or “swaging”/plastic flow of material near edges.
- **Minimum oil film thickness:** This is where the oil film is not able to completely separate the surfaces and the opposing sliding surfaces or tips of surface asperities start to contact each other with potential wear, flash temperatures, or seizure. Typical surface roughness values (R_a) are approximately 0.2 μm for crankshaft journals and 0.05 μm for gudgeon/piston pins. High temperatures can result from “mixed” or “boundary” lubrication conditions because the friction coefficient for a lubricated contact is approximately 1 or 2 orders of magnitude less than that for “dry” friction. At high engine speeds (6000–7000 r/min, gasoline engines), localized thin film areas can result in heat generation and hot spots within the oil because of high shearing.
- **Shearing of oil within the clearance space:** This can further increase the bearing surface temperatures by up to approximately 20–50°C higher than the supply temperature, which can result in overheating of the bearing. During engine operation, the oil sump or bearing oil supply temperatures can reach approximately 100–155°C. Under some load-speed conditions, bearing

surface temperatures of 190°C or more are possible where some components within the bearing alloy such as tin can start to melt, causing engine seizures if the high temperatures are sustained. Prolonged periods of engine running at high temperatures can also lead to the degradation of oil where soot-like material or lacquers can clog up oil passages and leave a dark residue on the bearing running surface.

The ideal operation for journal bearings is when the surfaces of the journal (shaft) and bearing are separated by a film of oil as indicated by Figure 8.3 for the full range of normal operating conditions. The oil is entrained or squeezed into a wedge shape by relative movement between the surfaces, generating a pressure within the oil, which separates the surfaces [1,2]. However, there will always be situations such as at the starting and stopping of the engine where the pressure generated is insufficient to support the load, leading to some contact between the surfaces. The use of numerical computations allows the design to be checked by solutions of the Reynolds equation (a simplification of the Navier-Stokes equation). The design computations can generally be divided into two categories:

1. **Routine:** Considering rigid components with computation times of a few seconds [3,4], and
2. **Specialized:** Where computation times can be several hours or more but with more details being considered such as the elasticity of components [5].

8.2 DISCUSSION

8.2.1 Journal Bearing Design and Lubrication

Journal bearings rely on a film of oil in the clearance space between the journal (shaft) and the bush or bearing shells to generate film pressure and load capacity through “hydrodynamic” action. The load capacity is generated by pressurizing the film of oil in the clearance space between the journal (shaft) and the bearing due to the rotation entraining the oil into a wedge shape, or by “squeeze” film where the load capacity arises from the resistance of the oil as it tries to escape from the approaching surfaces when the applied load is changing dynamically. Typical clearances are 0.1 % of the diameter, and maintaining a desired clearance and clearance shape in the assembled system is critical to function. A typical construction and features of a half bearing are indicated in the example of a main bearing shell in Figure 8.4. The backing material in the multilayered construction is usually steel with a functional alloy layer on the running surface of approximately 10–20 % of the total thickness. For high-load applications, an additional

¹ MAHLE Engine Systems UK Ltd., Warwickshire, UK

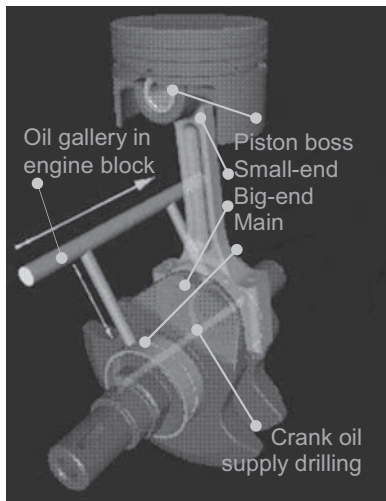


Figure 8.1—Typical crank mechanism with bearings.

layer of approximately $10\text{--}30\text{ }\mu\text{m}$ is also applied (“trimetal” construction).

Bearing shells and bushes are manufactured to a wall thickness tolerance of approximately $5\text{ }\mu\text{m}$ to control clearance and can have different wall thickness “grades” for assembly in individual locations to maintain low-assembled clearance tolerances because the tight wall thickness tolerance possible for bearing shells cannot be maintained on the housing or shaft. During assembly, the housing and journal (shaft) diameter can be measured so that the correct tolerance “grade” for the bearing is selected to achieve the desired clearance range. Important design features include

- “Nick” or “notch” to ensure correct assembly location in the housing,
- “Free spread” or gauge diameter that is bigger than the housing so that the bearing shells stay in position for the bolting operation during assembly,
- “Crush” or “overstand” to maintain desired interference and contact pressure with housing,

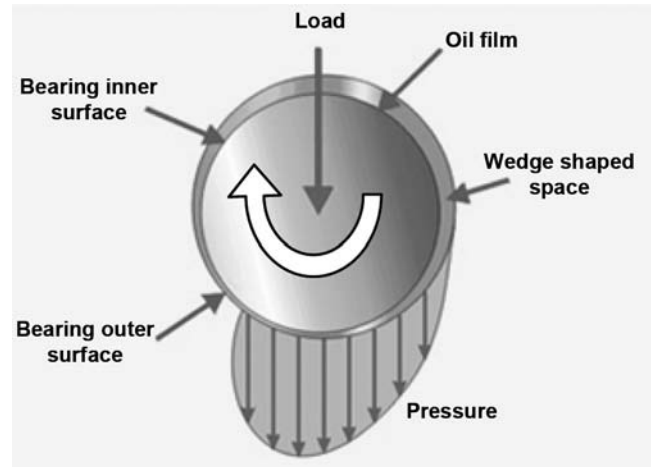


Figure 8.3—Hydrodynamic load capacity.

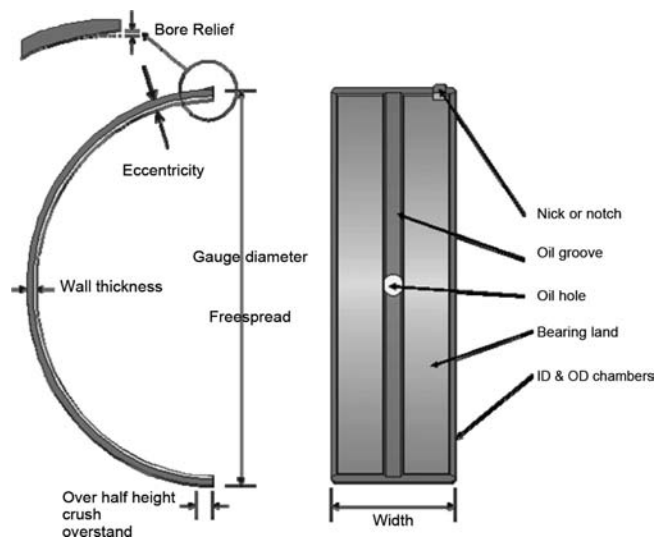


Figure 8.4—Bearing shell features (main bearing).

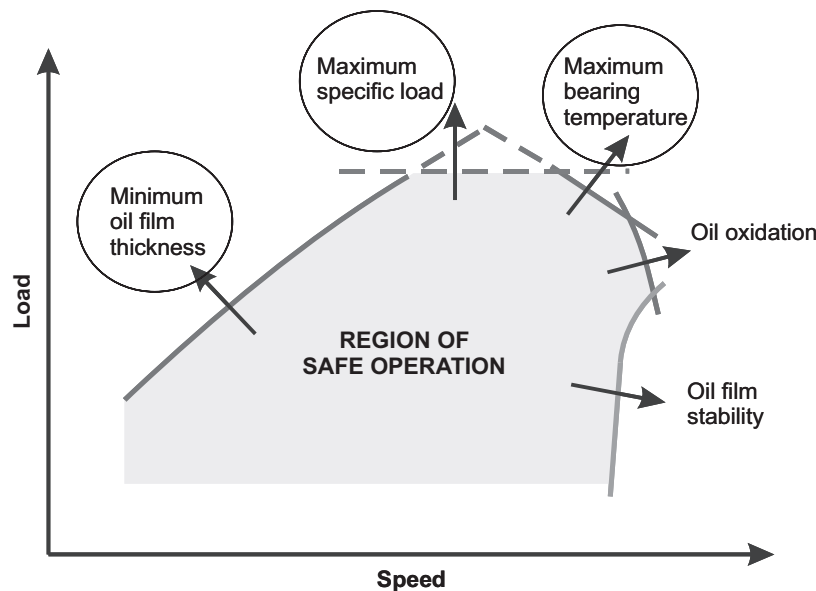


Figure 8.2—Safe area of operation.

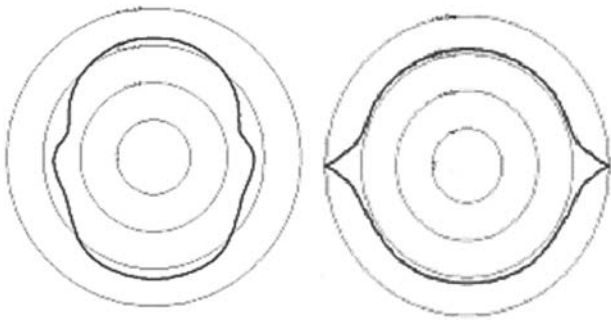


Figure 8.5—Typical big-end bearing-fitted clearance shape without and with eccentricity and bore relief (radial division = 5 μm).

- “Bore relief” to allow for misassembly (for connecting rods, a “fracture split” is better), and
- “Eccentricity” where the wall thickness near the joint is reduced.

A perfectly cylindrical bore shape after assembly or during running is not possible, in part because of the elasticity of components and assembly/manufacturing tolerances. For a bolted joint with half shells, the final boring operation of the bolted assembly is performed without the shells so that when they are inserted in the final assembly, the crush or overstand is designed to create a minimum value of contact pressure to minimize the risk of fretting damage and rotation. The assembled bearing bore shape is not circular if the wall thickness is uniform, as indicated in Figure 8.5 (left). The bearing wall thickness is usually reduced toward the edges by design (eccentricity) to maintain the desired clearance shape for a particular application.

The bore shape can be further influenced by the choice of housing materials and temperature because of differential thermal expansion, particularly for main bearings in which the block is typically made from a lighter alloy (usually aluminium) and the “cap” from cast iron or steel. Care is required to ensure that the housing bores are smooth and clean because trapped dirt particles can cause distortion and premature bearing fatigue damage. Geometrical features such as housing/bearing grooves can also influence thermal distortion of the final fitted bearing shape as indicated in Figure 8.6. However, for safe operation, the shape of the journal/shaft running surface is also important. From a design viewpoint, a “fitting” analysis is used to check for loss of interference with the housing at high temperatures and maintenance of a clearance at low temperatures. For bushes in which a split is not required for assembly, it is desirable to do the final boring operation after insertion.

Initial selection of bearing materials is by estimating the bearing MSL limits. The calculation of MSL should

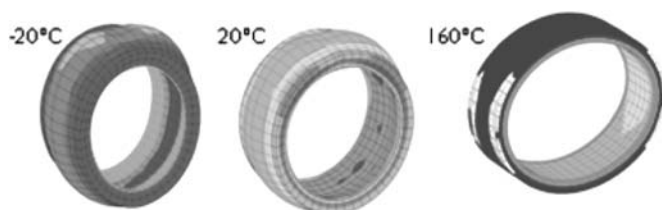


Figure 8.6—Fitted bearing shapes and stress for a main bearing shell in an alloy block with housing grooves (displacements magnified by 200 \times colors indicate stress variation).

include effects of component inertia in the load calculation for relevant components so the load calculation is generally the first step in the design process. The external loading for automotive bearings can arise from four main sources:

1. Combustion pressure acting on the top surface of the piston and then the transmission of the load through the crank-slider mechanism. The most important parameters here are the peak cylinder pressure and the crank angle at which this occurs. Highest combustion loading (upper bearing shells for rods, lower bearing shells for mains) is generally at the lower speeds at maximum torque condition and more critical for diesel engines
2. Inertia loading from the rotating and reciprocating components (rods, piston, rings, pin). Highest loading (lower bearing shells for rods, upper bearing shells for mains) is generally at the over-speed conditions and tends to coincide with higher bearing temperatures from the increased shearing in the oil. This is generally more critical for gasoline engines.
3. Direct loads from cam lobes, belt/chain drives, gears, power takeoff, starter motor, etc.
4. Bending moments and misalignment of bores in components such as crankshafts and camshafts.

The loads change throughout the 720° crank angle cycle for four-stroke engines and are normally displayed as a function of the crank angle as illustrated in Figure 8.7. For main-bearing-specific load calculations, the pin joint crank assumption at the main bearing journals is usually sufficient for design, but for enhanced accuracy in marginal operation, computationally expensive methods that include the stress analysis of the entire crank and engine block should be used. However, the engine in a typical application will be subjected to different thermal and load-speed conditions, which have been standardized into drive cycles such as the European Drive Cycle.

As indicated earlier, design techniques based on the Reynolds equation generally fall into two categories:

1. “Routine” simulations, usually based on the “mobility” solution method and “1D” assumptions in which the components are assumed to be rigid but allow many very rapid computations. Analysis of trends can be made with historical data, as indicated in Figure 8.8. The rapid nature of the design techniques means that a great deal of historical data are available for judging a new design, with any deviation indicating the use of more either more design iterations to obtain a robust solution or the use of more sophisticated analysis techniques to minimize expensive engine testing [6].
2. When a particular design application is close to the design limits, “specialized” and computationally expensive simulations with a full solution of the Reynolds and energy equation within the clearance space with elasticity of components are used (as indicated in Figure 8.9). These calculations are typically called thermoelasto hydrodynamic lubrication (TEHL). This allows much more detailed analyses of the oil film pressure, film thickness, temperatures, oil flow, power loss, and wear with further possibilities for optimizing bearing features, positioning of oil holes, and housing geometry.

Engine system parameters such as the engine oil supply pressure and temperature are also critical to bearing operation and can significantly affect the performance [7].

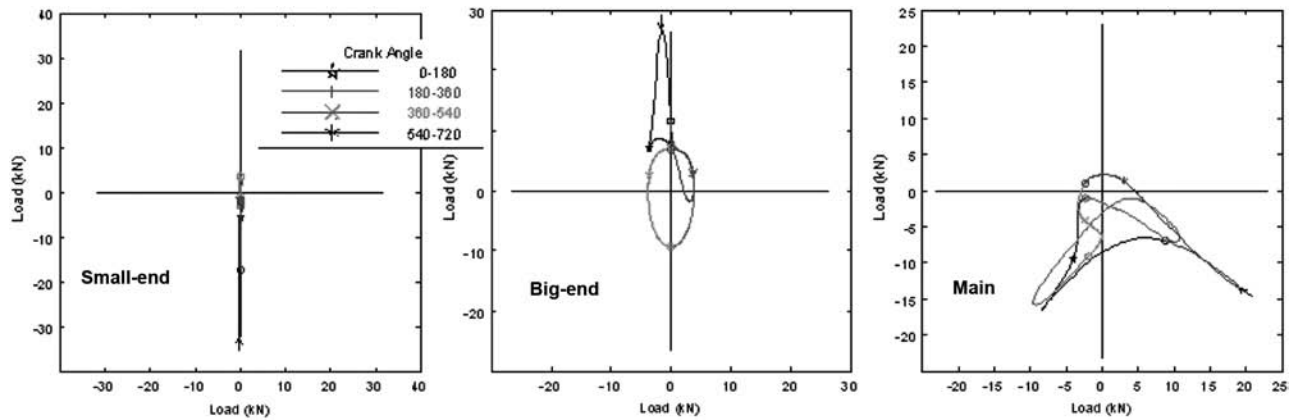


Figure 8.7—Typical polar load diagrams for a gasoline Vee engine at maximum torque load-speed condition or Koln City Drive Cycle. For engine testing in dynamometer cells rather than vehicles, the duty or “durability” cycle is often done according to standardized load-speed conditions to test different aspects of design.

Depending on operating conditions, oil supply temperatures can reach up to 155°C in gasoline engines and further shearing in the bearing can raise the temperature in the clearance space by approximately 40°C. If sustained, elevated bearing temperature conditions can lead to degrading of the oil and bearing materials with loss of function or seizure. The design of oil drillings within the crank to take oil from the main bearing grooves and supply the big-end bearings can also be critical to function, requiring calculations for the effect of inertia on the oil. At closest approach to the center of the crank, the oil pressure can fall below the vapor pressure, leading to a “bubble” and reduction in the oil supply through the crank drilling. Oil starvation at the big end can also occur if the feed main bearing does not have a crossdrilling at the journal [8].

The geometry and form of the surface roughness on the journals must be controlled to maintain an adequate oil

film to separate the surfaces to support the load. Instances of circumferential lobing (indicated in Figure 8.10) generally induced from vibration of machining from the finishing operation as indicated in the trace are detrimental to performance and lead to premature failure (lower load-carrying capacity).

8.2.2 Bearing Materials

Bearing materials are often chosen for specific applications on the basis of a combination of criteria. Apart from corrosion resistance, a balance between the “hard” properties (wear resistance, load-carrying capacity, fatigue resistance) and “soft” properties (compatibility, conformability, embedability, tolerance to dirt) is required at an acceptable cost. A selection from a range of material combinations in multi-layered architecture is therefore needed to suit a particular application. For “bimetal” construction, the base is usually

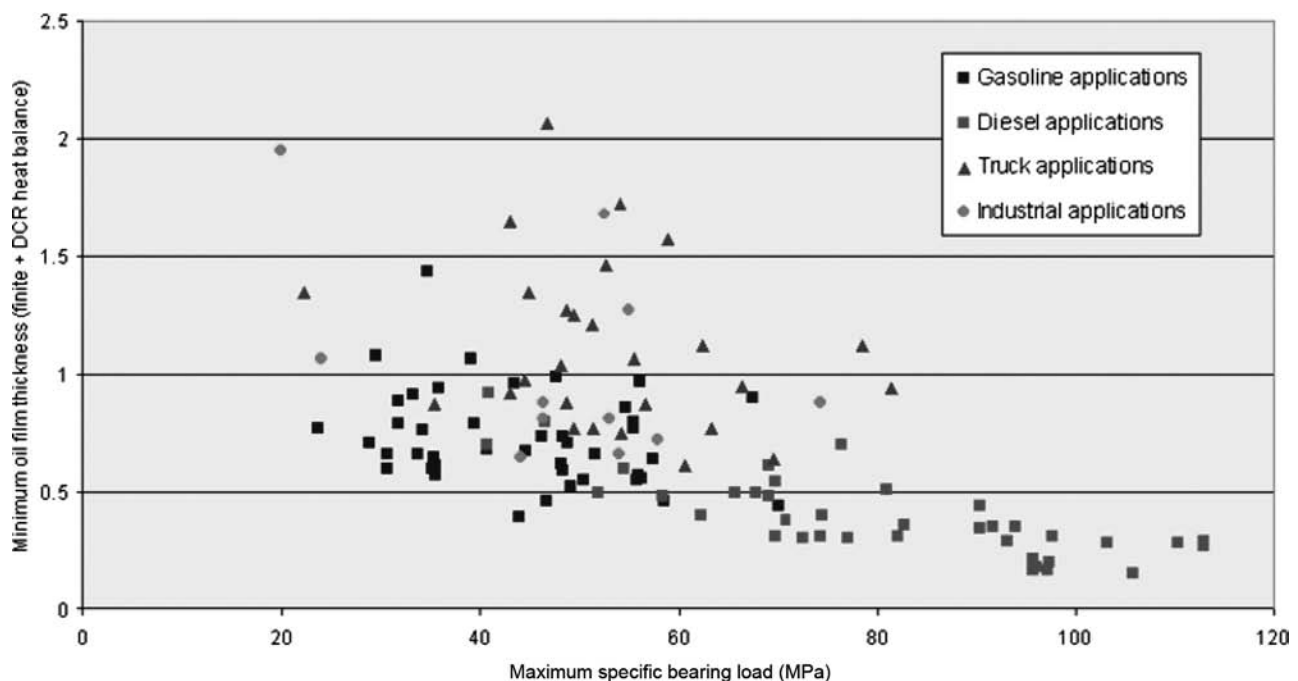


Figure 8.8—Analysis of trends from routine analyses.

Pressure, Film Shape, and Maximum Film Temperature Contour on Film Thickness

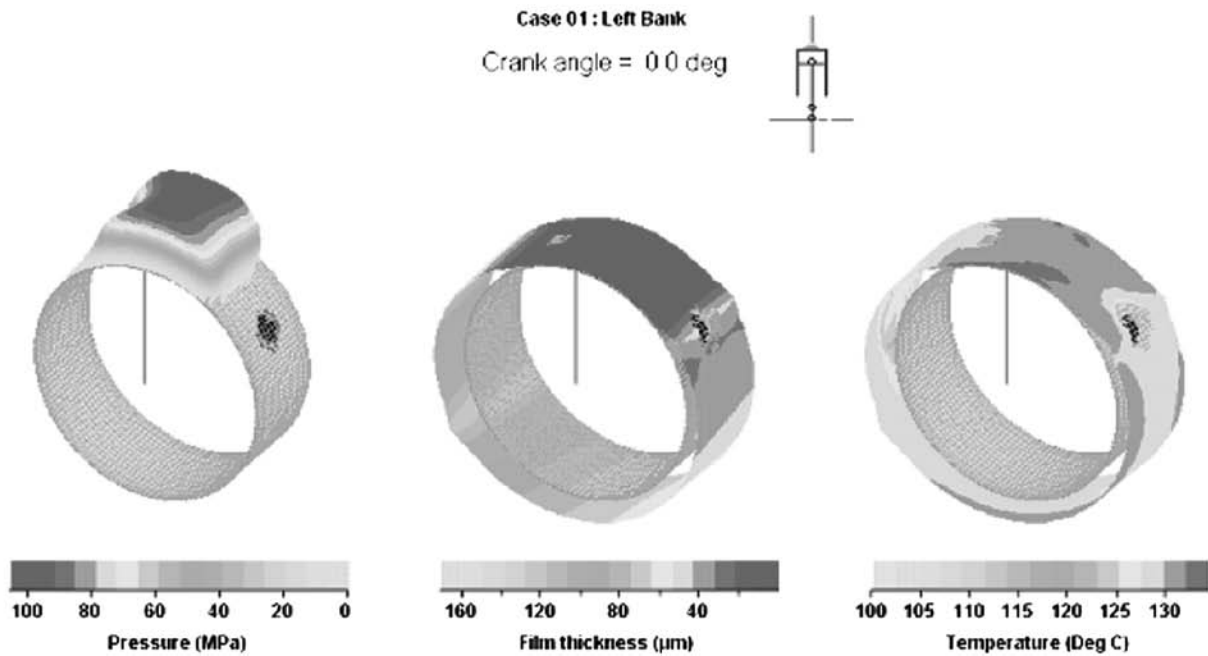


Figure 8.9—Typical TEHL output for a big-end bearing (0° crank angle).

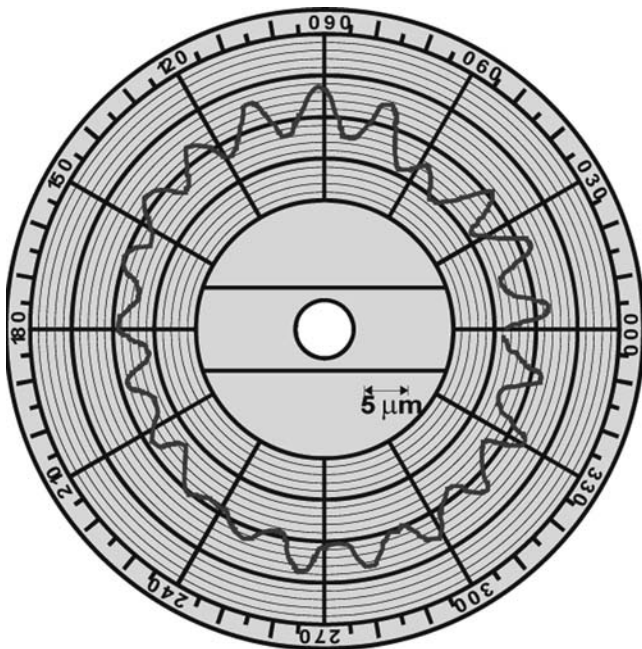


Figure 8.10—Detrimental journal lobing.

a mild steel grade with a “lining” of aluminium alloy of approximately 10–20 % of the thickness on the running surface for applications up to a MSL of approximately 70 MPa for half shells. The lining alloy usually contains tin, bismuth, zinc, and nickel with some fine hard silica particles to polish the journal or shaft to rectify misalignment or other “running-in” problems. Lead is still in use as an alloying component in automotive legacy and some heavy-duty applications, although legislation resulting from its hazardous nature means it is no longer a viable option. A typical

“roll-bonded” construction is shown in Figure 8.11, ready for forming and machining operations. For highly loaded applications to approximately 100 MPa, a further “overlay” of approximately 10–30 μm is applied for greater wear and fatigue resistance on cast or sintered bronze linings.

8.2.3 Surface Treatments

Bearing surface treatments are applied to the running surface of bearing shells after final machining to a thickness of approximately 10–30 μm to improve the scuff/seizure, fatigue, and wear resistance. The most common are electroplating and sputtering, allowing improved running-in and tolerance to edge-loading. In some cases, the final boring operation for bimetal bearings is controlled to produce circumferential “microgrooving” with some benefits in conformability and reduced running temperature in boundary lubrication situations. Diamond-like coatings (DLC) can also be applied to improve the surface finish and wear resistance of journals (e.g., piston pins) as well as case hardening, although the costs can be prohibitive. Good surface finish of journals to produce a smooth finish in the axial and circumferential direction is important to preserve the expected bearing load-carrying capacity. For cast iron crank journals, grinding and lapping/polishing must be done in the direction of rotation to avoid microburrs produced in the region of carbon nodules pointing in the wrong direction.

8.2.4 Testing Procedures for Lubrication

Most bearing tests are either rig tests or engine tests in the final stages of development. The latter are usually a drive cycle to simulate a driving style or durability cycle to check performance at different operating conditions in an engine dynamometer test cell. Rig and engine tests are more common because of the reduced cost and target-specific aspects

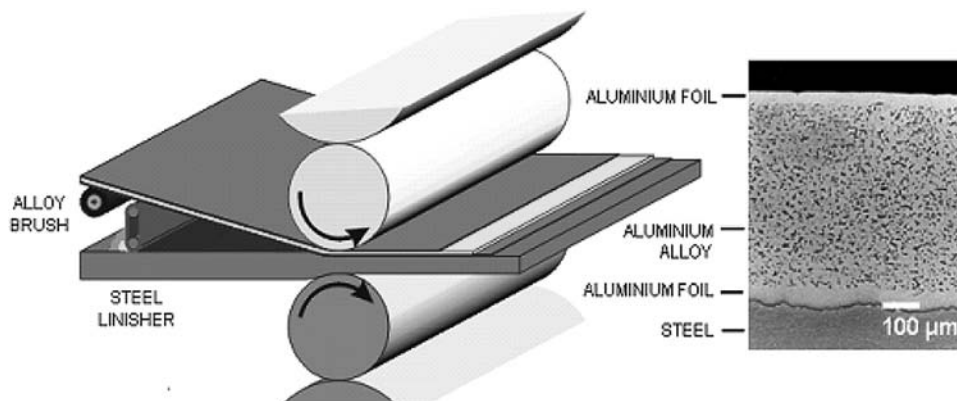


Figure 8.11—Bimetal material architecture example.

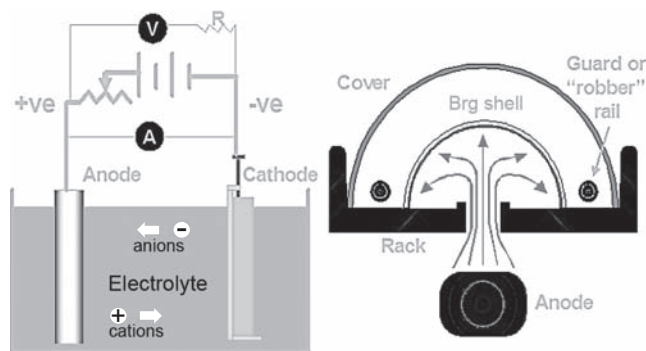


Figure 8.12—Electroplating of bearing shells.

of bearing performance [5], with the former being a more cost-effective solution. Engine testing for automotive applications is generally more severe in terms of durability; the reverse is normally true for large truck and generator set applications because of cost.

A typical test rig for testing product samples is shown in Figure 8.14, demonstrating the advantage of greater con-

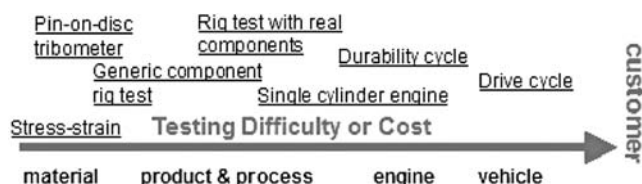


Figure 8.13—Testing and development flow.

trol of input variables such as specific load, oil temperature, and possible tests such as fatigue and seizure with measures including bearing temperature.

8.2.5 Wear and Damage Assessment

Evaluation of bearing damage is initially via visual inspection with the naked eye or microscope. With experience, it is possible to see signs of fatigue, overheating, low film thickness, particle contamination, signs of seizure, etc. Further detailed information is possible by sectioning samples and the use of electron microscope to examine, for example, the source of dirt contamination. Wear assessment normally requires the use of surface traces as shown in Figure 8.15. Assessment

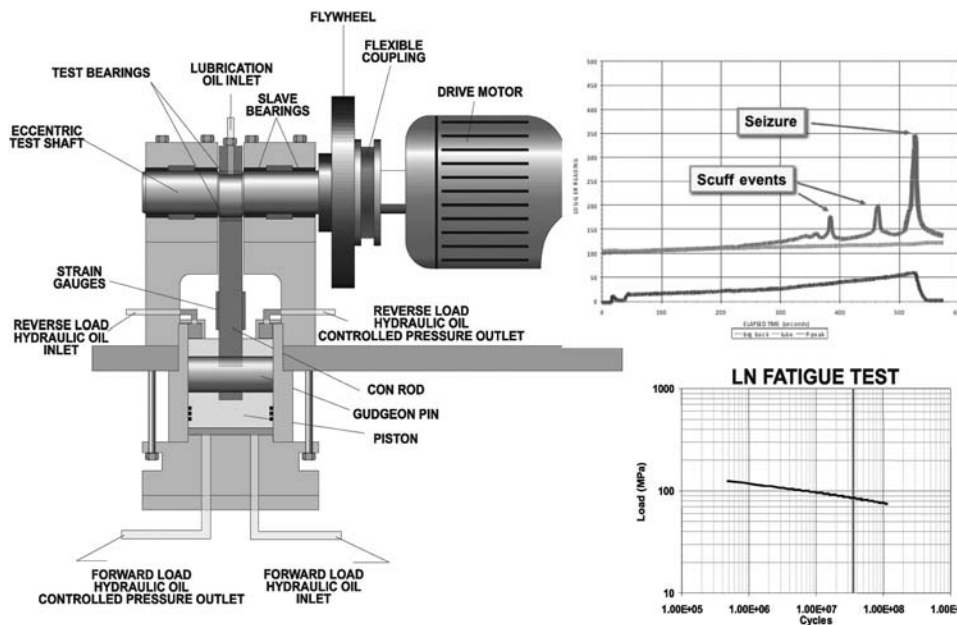


Figure 8.14—Typical rig/bench test and associated example of results.

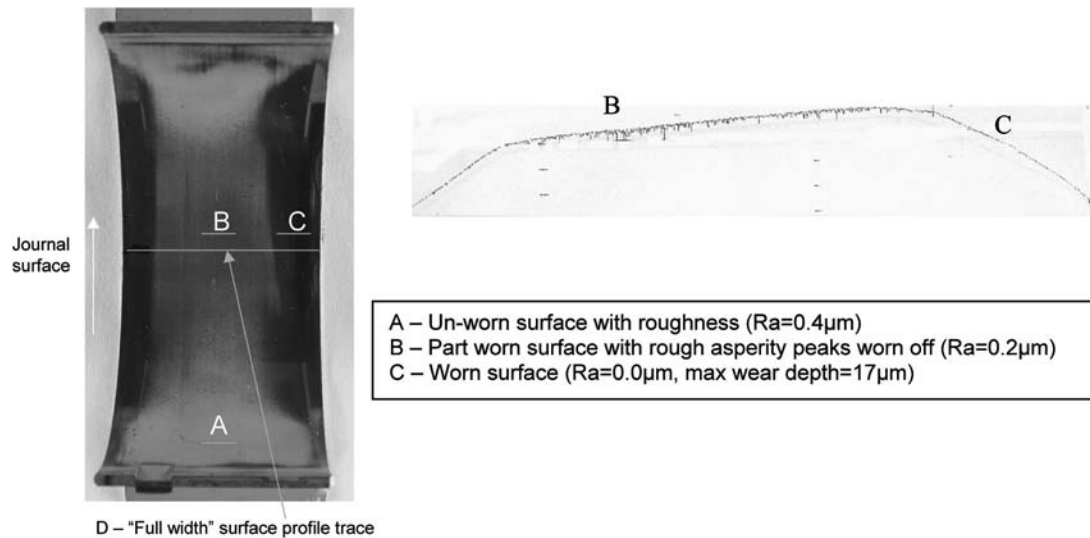


Figure 8.15—Example of wear assessment with surface profile measurement.

can be in terms of weight loss, maximum wear depth (e.g., through the electroplated overlay), or area affected.

8.3 CONCLUSIONS

Automotive bearings are part of a system that is apparently simple yet complex to analyze and design. Several levels of design are required, from the simple calculation of load and rig tests to engine tests and TEHL calculations. Although rarely seen, malfunction or incorrect design can have serious consequences such as complete engine failure.

REFERENCES

- [1] Cameron, A., 1976, *Basic Lubrication Theory*, Butterworth, London.
- [2] Barwell, F.T., 1979, *Bearing Systems: Principles and Practice*, Oxford University Press, London.
- [3] Martin, F.A., 1985, "Friction in Internal Combustion Engine Bearings," Paper C67/85, In *Proceedings of the Institution of Mechanical Engineers*, Institution of Mechanical Engineers, London, pp. 1–17.
- [4] Goenka, P.K. 1984, "Analytical Curve Fits for Solution Parameters for Dynamically Loaded Bearings", ASME J. Tribology F, Vol. 106, pp. 421–428.
- [5] Wang, D., Mian, O., Merritt, D., Praca, M., and Zhu, G., 2008, *Elasto-Hydrodynamic Lubrication Analysis and Wear Prediction for a Connecting Rod Small-End Bush and Piston Pin Interface*, SAE Paper 2008-36-008, SAE, Warrendale, PA.
- [6] Mufti, R.A., and Priest, M., 2009, "Theoretical and Experimental Evaluation of Engine Bearing Performance", J Eng. Tribology, Vol. 223, pp. 629–644.
- [7] Mian, A.O., Parker, D.D., and Williams, R., 2000, *Measured Crankshaft Bearing Oil Flow and Temperatures with Full and Partial Groove Main Bearings*, SAE Paper 2000-01-1341, SAE, Warrendale, PA.
- [8] Maasen, F., Koch, F., and Pischinger, F., 1998, *Connecting Rod Bearings Operating with Aerated Lube Oil*, SAE Paper 981404, SAE, Warrendale, PA.

Testing and Evaluation of Lubricating Greases for Rolling Element Bearings of Automotive Systems

Xinglin Li¹, Can Wu¹, Baojie Wu², Hongyu Zhang³, Jianbin Luo³, and Qiang Feng²

9.1 INTRODUCTION

A rapid development has been observed in the design and manufacturing of automobiles worldwide in the past few decades, and nowadays it is confronted with more challenges because of the requirement of saving energy and protecting the environment. Theoretically, this problem can be alleviated by further reducing automotive weight, optimizing driving configuration, and using the appropriate lubricants in a certain degree. All of these require that the bearings that support the operation of the automotive parts operate very well under the conditions of very high speed and high temperature. In most cases, lubricating grease is specifically capable for lubrication of the bearings. However, because of the limited space in rolling element bearings, lubrication technology is a key factor for improving the performance of automotive components [1,2].

On the basis of load-carrying capacity and utility, an automobile can be classified as a heavy-duty automobile, a medium-duty automobile, a light-duty automobile, a special-purpose vehicle, etc. Different types of driveline components have different lubricating requirements for the bearings. For example, the extreme pressure property of the lubricating grease is the most important characteristic in some cases whereas in other cases the lubricating grease should preferably maintain excellent lubricating properties under high temperature and for a long time [3,4]. Additionally, a vehicle is mechanically composed of four parts: the engine, chassis, body, and electrical parts. Each part has its own specific lubricating requirements such as antiwear, excellent extreme pressure properties, and good compatibility with the rubber components, etc. Therefore, different lubricating greases should be chosen based on the automotive components type and the specific part where lubrication is needed [5–7].

This chapter discusses in detail the use of different lubricating greases for automotive rolling element bearings, which are the hub bearing, constant velocity universal joint, auxiliary engine bearing, electrical part bearing, and the electric motor bearing [8].

9.2 AUTOMOTIVE SERVICE LUBRICATING GREASE [9,10]

9.2.1 Lubricating Grease for the Hub Bearing

The automotive hub bearing is the first important part where lubricating grease is widely applied; therefore, in this

section, we first discuss the use of lubricating grease for the automotive hub bearing.

9.2.1.1 DEVELOPMENT OF THE AUTOMOTIVE HUB BEARING

The automotive hub bearing has changed a great deal with the development of the automobile itself, and there are mainly two kinds of automotive hub bearings: the double-row tapered roller bearing (now the third-generation product) and the double-row angular contact ball bearing (now the fourth-generation product). The double-row tapered roller bearing is primarily used in the United States, and the double-row angular contact ball bearing is mostly used in Japan and across European countries. The basic configuration and characteristics of the two kinds of automotive hub bearings are summarized in Table 9.1.

9.2.1.2 CHARACTERISTICS OF AUTOMOTIVE FRONT-WHEEL HUB BEARINGS

The front-wheel hub bearing is a very important automotive part because it provides load support when rotating with the front axle; on the other hand, it is also involved in the steering motion with the steering joint. The double-row angular contact ball bearing with two-piece inner ring is widely used in China because it can carry very high radial load and biaxial load. The front-wheel hub bearing is lubricated through one-off filling of lubricating grease; therefore, the design of front-wheel hub bearing aims to obtain the largest rated load associated with small axial pulsation, excellent sealing capabilities, and dust-proof properties. The configuration of a typical double-row angular contact ball bearing is shown in Figure 9.1.

9.2.1.3 REQUIREMENTS OF LUBRICATING GREASE FOR AN AUTOMOTIVE HUB BEARING

The use of lubricating grease for an automotive hub bearing changes with the development of the hub bearing itself. The development trend of the wheel bearing can be expressed terms of the following features:

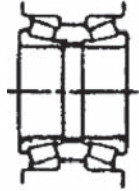

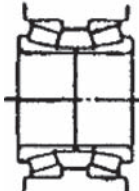
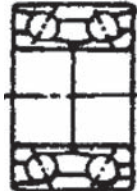
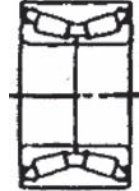

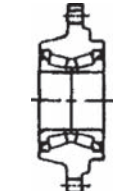
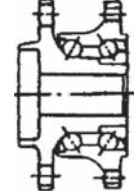
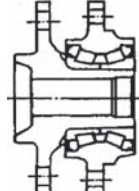
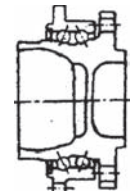
- Flexible compact structure, convenient maintenance, and lighter weight have been the developmental direction for the wheel bearing design concept. SKF put out the fourth-generation hub bearings, which integrated the universal joint. The integrated wheel bearings have higher load and higher temperature properties. Much

¹ National Testing Laboratory of Hangzhou Bearing Test and Research Center, Hangzhou, Zhejiang, China

² Sinopec Corp., Tianjin Branch, Tianjin, China

³ State Key Laboratory of Tribology, Tsinghua University, Beijing, China

TABLE 9.1—The Basic Configuration and Characteristics of the Two Kinds of Automotive Hub Bearing

Tapered Roller Bearing		Angular Contact Ball Bearing	
Previous configuration (single row) Clearance adjusted through spacer		Previous configuration (single-row deep-groove bearing) Clearance adjusted through spacer	
Previous configuration (light bearing) No need to adjust clearance		First generation (double-row angular contact bearing) No need to adjust clearance	
First generation (tapered roller bearing unit) No need to adjust clearance		Second generation (hub bearing unit) No need to adjust clearance	
Second generation (hub bearing unit) No need to adjust clearance		Third generation (hub bearing unit) No need to adjust clearance	
Third generation (hub bearing unit) No need to adjust clearance		Fourth generation (universal joint hub bearing unit) No need to adjust clearance	

effort has been put into ensuring that each part of the unit has the same lifespan.

- As the automobile increases speed the wheel bearings will have a higher temperature, and as the antilock brake system (ABS) produces much of the friction heat, wheel bearings that can endure both high temperature and high speed are undoubtedly needed.
- The requirements for the integral seal has been improved greatly, and includes rubber sealing, lubricant water resistance, leakage resistance, and the corresponding match of the rubber ring and lubricant.
- The lower fretting wear of the hub bearing.

Nowadays, the requirement of the lubricating grease can be summarized as the following four items because of the high integration of the hub bearing:

1. The lubricating grease should function well even longer than before.
2. The lubricating grease should function well at severe conditions, such as high speed and temperature.
3. The lubricating grease should have excellent water resistance, leakage resistance, and good compatibility with rubber.
4. The appropriate lubricating grease should be applied to reduce potential fretting wear of the hub bearing.

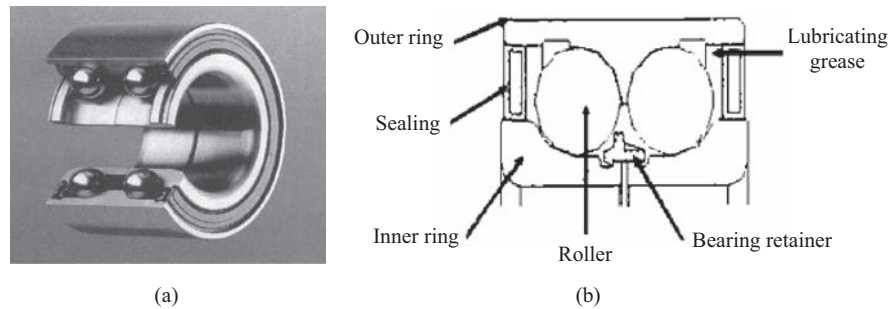


Figure 9.1—Typical front-wheel hub bearing: double-row angular contact ball bearing.

9.2.1.4 DEVELOPMENT OF LUBRICATING GREASE FOR AUTOMOTIVE HUB BEARINGS

Calcium-based lubricating grease was used as early as in the 1880s for the lubrication of the automotive hub bearing. However, this kind of lubricating grease is not suitable when the temperature is above 100°C because an amount of water (~1–2 %) should be added to keep the lubricating grease stable. This problem was solved in the 1930s by the introduction of sodium-based lubricating grease, which can work well at higher temperature. Since the 1940s, complex calcium-, lithium-, and barium-based lubricating greases were comprehensively used because of their better water-resistance and high-temperature property; therefore, sodium-based lubricating grease was gradually replaced by these kinds of lubricating grease. The introduction of complex lithium-based lubricating grease in 1962 represented a great improvement because it has the best high-temperature property, and this kind of lubricating grease is now widely used for the lubrication of automotive hub bearings at high-speed and high-temperature conditions. It is worth mentioning that recently more and more attention has been paid to polyurea-based lubricating grease, although in most cases it is applied for lubrication of angular contact ball hub bearings in which a longer time of service is required.

9.2.1.5 LUBRICATING GREASE FOR HUB BEARINGS AND RELATIVE STANDARDS

One important standard—ASTM D4950—was introduced in 1977 by ASTM, NLGI, and SAE in which the detailed

specification of the lubricating grease used for chassis and hub bearings was standardized. This was further updated in 1989 and in 1995, and the lubricating grease used for hub bearings can be classified into three categories: GA, GB, and GC (Tables 9.2 and 9.3). Generally, GC-LB lubricating grease is widely used for satisfying most requirements of automotive hub bearings. In addition, for the automotive companies themselves, they would prefer to know the lubricating grease properties under practical conditions (e.g., high-temperature life test [ASTM D3527], leakage tendency test [ASTM D4290], the EMCO rust protection test [DIN 51802], and the Timken load-carrying capacity test [ASTM D2509]).

Automotive companies would like to see some of the test data of the lubricants under simulated working conditions. The following tests are essential:

- *High-temperature life test*: Roller bearing operation time at 160°C, 1000-r/min speed, and 111-N load.
- *Wheel bearing leakage test*: Test the leakage of grease in the wheel weight after the wheel bearing is operated 20 h at 160°C and 1000-r/min speed.
- *EMCO rust test*: Install the bearing, which is the sample on the test machine, then inject the required amount of distilled water or synthetic seawater into the machine, and operate repeatedly. The bearing corrosion can be observed after a certain period of time.
- *Timken antiwear test*: Rotate the test rig at 123.71 m/min and remeasure the friction coefficient, wear coefficient, and wear surface morphology under different loads to evaluate the performance of the lubricating greases.

TABLE 9.2—ASTM D4950-1995 Standard Classification and Specification of Automotive Service Greases

Category	Grade	Property	Application
L	LA	Lubrication, antiwear, compatibility with rubber	Chassis components and universal joints from –20 to 60°C where frequent relubrication is practiced
	LB	Lubrication, low temperature, antiwear, antirust, compatibility with rubber	Chassis components and universal joints from –40 to 120°C over prolonged relubrication intervals
G	GA	Lubrication, low temperature	Wheel bearings over a limited temperature range (–20 to 70°C)
	GB	Lubrication, low temperature, water resistance, antiwear, antirust, stable at high temperature, long life, compatibility with rubber	Wheel bearings over a wide temperature range, (–40 to 120°C, occasional excursions to 160°C)
	GC	Lubrication, low temperature, water resistance, antiwear, antirust, stable at high temperature, long life, compatibility with rubber	Wheel bearings over a wide temperature range, (–40 to 160°C, occasional excursions to 200°C)

TABLE 9.3—ASTM D4950-1995 “G” Lubricating Grease

Category	Test	Property	Accepted Value
GA	D217 D566 or D2265 D4693	Worked penetration (mm/10) Dropping point (°C) Low-temperature performance, torque at –20°C (N·m)	220–340 Minimum 80 Maximum 15.5
GB	D217 D566 or D2265 D4693 D1264 D1742 D1743 D2266 D3527 D4289 D4290	Worked penetration (mm/10) Dropping point (°C) Low-temperature performance, torque at –40°C (N·m) Water resistance at 80°C (%) Oil separation, mass (%) Rust protection (rating) Wear protection, scar diameter (mm) High-temperature life (h) Elastomer SAE AMS 3217/2B compatibility Volume change (%) Hardness change (durometer-A points) Leakage tendencies (g)	220–340 Minimum 175 Maximum 15.5 Maximum 15 Maximum 10 Maximum pass Maximum 0.9 Minimum 40 –5 to 30 –15 to 2 Maximum 24
GC	D217 D566 or D2265 D4693 D1264 D1742 D1743 D2266 D3527 D4289 D4290 D2596	Worked penetration (mm/10) Dropping point (°C) Low-temperature performance, torque at –40°C (N·m) Water resistance at 80°C (%) Oil separation, mass (%) Rust protection (rating) Wear protection, scar diameter (mm) High-temperature life (h) Elastomer SAE AMS 3217/2B compatibility Volume change (%) Hardness change (durometer-A points) Leakage tendencies (g) Extreme pressure performance Load wear index, N (kgf) Weld point, N (kgf)	220–340 Minimum 220 Maximum 15.5 Maximum 15 Maximum 6 Maximum pass Maximum 0.9 Minimum 80 –5 to 30 –15 to 2 Maximum 10 Minimum 295 (30) Minimum 1960 (200)

9.2.2 Lubricating Grease for Constant Velocity Universal Joints

9.2.2.1 INTRODUCTION OF AUTOMOTIVE CONSTANT VELOCITY UNIVERSAL JOINTS

The constant velocity universal joint is a very important part of an automobile. It transfers the power generated by the engine from the transmission to the wheel. A constant velocity universal joint can be classified into a fixed ball joint and a plunging joint. A fixed ball joint is usually installed outside of the front axle (i.e., beside the hub bearing) whereas a plunging joint is fixed inside of the front axle and the two ends of the back axle. The most common type of automotive constant velocity universal joint is the rzeppa universal joint, as shown in Figure 9.2a. A Weiss universal joint and tripod universal joint are also sometimes used, as shown in Figure 9.2, b and c.

9.2.2.2 OPERATION CONDITIONS OF AUTOMOTIVE CONSTANT VELOCITY UNIVERSAL JOINTS

Because of its specific functions, a constant velocity universal joint usually works at extremely harsh conditions. The operation conditions can be summarized as follows:

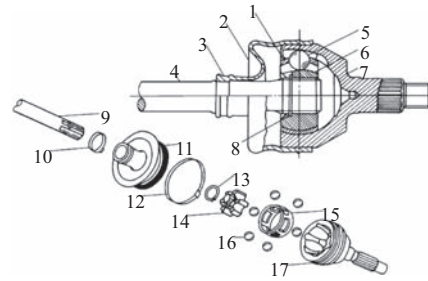
- A constant velocity universal joint carries high load with a contact pressure of up to 3–4 GPa at some parts; therefore, the wear of a constant velocity universal joint is relatively quite serious without good lubrication.
- The operation of a constant velocity universal joint is a very complicated mechanism including rotation, rolling, sliding, vibration, fretting, etc. All kinds of movement

can cause friction and its corresponding noise and loss of power.

- A constant velocity universal joint operates in an environment of high temperature because it is close to three major regions of automotive components that generate much heat (i.e., the engine, brakes, and hub bearing). The fourth generation of constant velocity universal joints combined with hub bearing components makes the dissipation of heat even worse.
- The protective cover of a constant velocity universal joint is easily damaged if an inappropriate lubricating grease is applied, which can cause swelling or hardening of the rubber.
- A constant velocity universal joint operates with mixed lubrication at high speed, and the lubrication mechanism cannot be described simply by traditional elastohydrodynamic (EHD) theory.
- A constant velocity universal joint may be damaged by corrosion of different media.
- A constant velocity universal joint is highly related to the NVH (noise, vibration, and harshness) characteristics of automotive components.

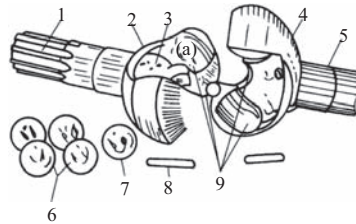
9.2.2.3 REQUIREMENTS OF LUBRICATING GREASE FOR AN AUTOMOTIVE CONSTANT VELOCITY UNIVERSAL JOINT

The operation conditions of a constant velocity universal joint make the choice of lubricating grease very rigorous. This issue is very important because recent statistical data



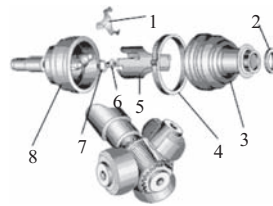
(a)

(1) ball-cage, (2) outer cover, (3) strip steel, (4) driveshaft, (5) steel ball, (6) inner race, (7) outer race, (8) snap ring, (9) driveshaft, (10) strip steel, (11) outer cover, (12) strip steel, (13) snap ring, (14) inner race, (15) ball-cage, (16) steel ball, (17) outer race



(b)

(1) stub shaft, (2) locking hole, (3) driven yoke, (4) drive yoke, (5) inner shaft, (6) propeller steel ball, (7) central steel ball, (8) striker, (9) Detent pin for ball-yoke slot



(c)

(1) locking tripod, (2) fastening piece, (3) protective cover, (4) protective cover hoop, (5) funneled shaft, (6) thrust plug, (7) gasket, (8) outer race

Figure 9.2—Three types of constant velocity universal joints for automobiles.

show that the use of lubricating grease for a constant velocity universal joint accounts for as much as 60 % of the total lubricating grease used for automobiles. To summarize, the requirements of lubricating grease for automotive constant velocity universal joints are

- The lubricating grease should have excellent antiwear and antivibration properties, which can attenuate energy when the constant velocity universal joint vibrates during operation.
- The lubricating grease should function well for a long time to prevent the occurrence of premature rolling contact fatigue of the constant velocity universal joint.
- The lubricating grease should have excellent extreme pressure properties and a low friction coefficient to reduce adhesive wear of the constant velocity universal joint when boundary lubrication dominates at the interface.
- The lubricating grease should function well at high temperatures as well as at low temperatures when the automobile is operated in winter or in cold regions.
- The lubricating grease should have good compatibility with rubber and other resins because the protective cover is usually made of these materials.
- The lubricating grease should have excellent mechanical stability, water resistance, and antirust properties, etc.

9.2.2.4 DEVELOPMENT OF LUBRICATING GREASE FOR THE AUTOMOTIVE CONSTANT VELOCITY UNIVERSAL JOINT

In 1959, lithium-based lubricating grease was used for lubrication of the constant velocity universal joint in the Austin Mini, and this kind of lubricating grease was later replaced by another special lubricating grease (bentone grease combined with 20 % molybdenum disulfide) for its relatively poor performances. In the 1960s the DKW company used gear oil with 10 % graphite in their reproduced F11 for the purpose of lubricating the constant velocity universal joint. However, this recipe was later abandoned because of its early fatigue damage and the loud noise it created during changes in speed. In 1967, NLGI No.1 or No.2 lubricating grease

was applied for the lubrication of the tripod universal joint by General Electric whereas the rzeppa universal joint was lubricated using NLGI No. 1 lubricating grease combined with molybdenum disulfide. In the 1970s, a new lubricating grease was invented in Germany composed of lithium-based grease, lead naphthenate, and molybdenum disulfide. In addition, the first generation of polyurea-based oil was used for special application for high-temperature environments in the United States, and polyurea-based lubricating grease was invented in Japan in the late 1980s. Since 1998, the tendency for miniaturization and integration has gradually dominated the development of the constant velocity universal joint, and the lubricating grease is generally composed of lithium- or polyurea-based grease, molybdenum disulfide, and SP additive. Nowadays, research has been focused on the development of lubricating grease that can function at high temperatures (e.g., 150°C) with the general composition of synthetic oil as the base oil and lithium complex soap or sodium amidate soap as the thickener.

9.2.3 Lubricating Grease for Auxiliary Engine Bearings and Electrical Part Bearings

9.2.3.1 INTRODUCTION TO AUXILIARY ENGINE BEARINGS AND ELECTRICAL PART BEARINGS

The engine is regarded as the “heart” of the automobile, and there are many auxiliary engine parts and electrical parts around the engine. Typical auxiliary engine parts include the timing belt stretcher, fluid coupling (used for fan cooling), water pump, etc. Typical electrical parts include the alternator, air conditioning compressor, etc. Generally speaking, the bearings involved in these parts are working at severe conditions of high temperature, high speed, and high loading, as shown in Table 9.4. Therefore, the lubricating grease used in the bearings should be of high quality. It is considered that auxiliary engine bearings and electrical part bearings are the third most important parts where lubricating grease is widely applied.

9.2.3.2 OPERATION CONDITIONS AND THE CORRESPONDING REQUIREMENTS FOR LUBRICATING GREASE

On the basis of the operation conditions of the auxiliary engine bearings and electrical part bearings, the

requirements of the lubricating grease can be summarized as follows:

- Auxiliary engine bearings and electrical part bearings usually work under high temperatures (e.g., 120°C), sometimes as high as 150°C because of the excellent sealing of the engine. Therefore, the lubricating grease should function well at high temperature.
- The lubricating grease should have small starting torque and operation torque at low temperatures (even at -40°C) to be used in winter or cold regions.
- The searing ring of the bearing cannot totally prevent the penetration of water, contamination, etc.; therefore, the lubricating grease should have excellent water resistance and antirust properties.
- The rotation speed of the bearing is usually as high as 10,000–20,000 r/min; therefore, the lubricating grease should function well at high speed and have relatively high viscosity to reduce the centrifugal effect. (There is less lubricating grease present in the inner ring and the retainer because of the centrifugal effect whereas 80–90 % of the lubricating grease is distributed in the areas around the outer ring the sealing ring.)
- The lubricating grease should have excellent colloid stability to prevent leakage from the sealing ring.
- The lubricating grease should function well for a long time.
- The noise should be as low as possible when the lubricating grease is used.
- The lubrication should be compatible with rubber to maintain good sealing performance.

9.2.3.3 CHARACTERISTICS OF THE LUBRICATING GREASE AND EVALUATION METHODOLOGY

The relationship between the characteristics of the lubricating grease used for auxiliary engine bearings and electrical part bearings and the corresponding evaluation methodology are summarized in Figure 9.3.

The 13 evaluation methods mentioned can generally be classified into two categories: one related to the basic physical and chemical properties of the lubricating grease (e.g., steel mesh oil separation and worked cone penetration) and the other related to the practical application of the lubricating grease (e.g., working time at high temperature and the

TABLE 9.4—Typical Auxiliary Engine Parts, Electrical Parts, and Their Working Conditions

	Parts	Bearing	Inner Diameter (mm)	Operation	Highest Speed (r/min)	Highest Temperature (°C)
Auxiliary engine	Timing belt stretcher	Single-row deep-groove bearing	25–30	Felloe	5000–8000	130
	Fluid coupling	Single-row deep-groove bearing	20	Inner wheel	5000	150–200
	Water pump	Ball bearing or roller bearing	—	Inner wheel	7000	120
Electrical parts	Alternator	Single-row deep-groove bearing	8–17	Inner wheel	18,000	130
	Electromagnetic clutch	Multi-row angular contact ball bearing	30–40	Felloe	7000–12,000	130
	Idler pulley	Single-row deep-groove bearing	12–20	Felloe	10,000–20,000	130

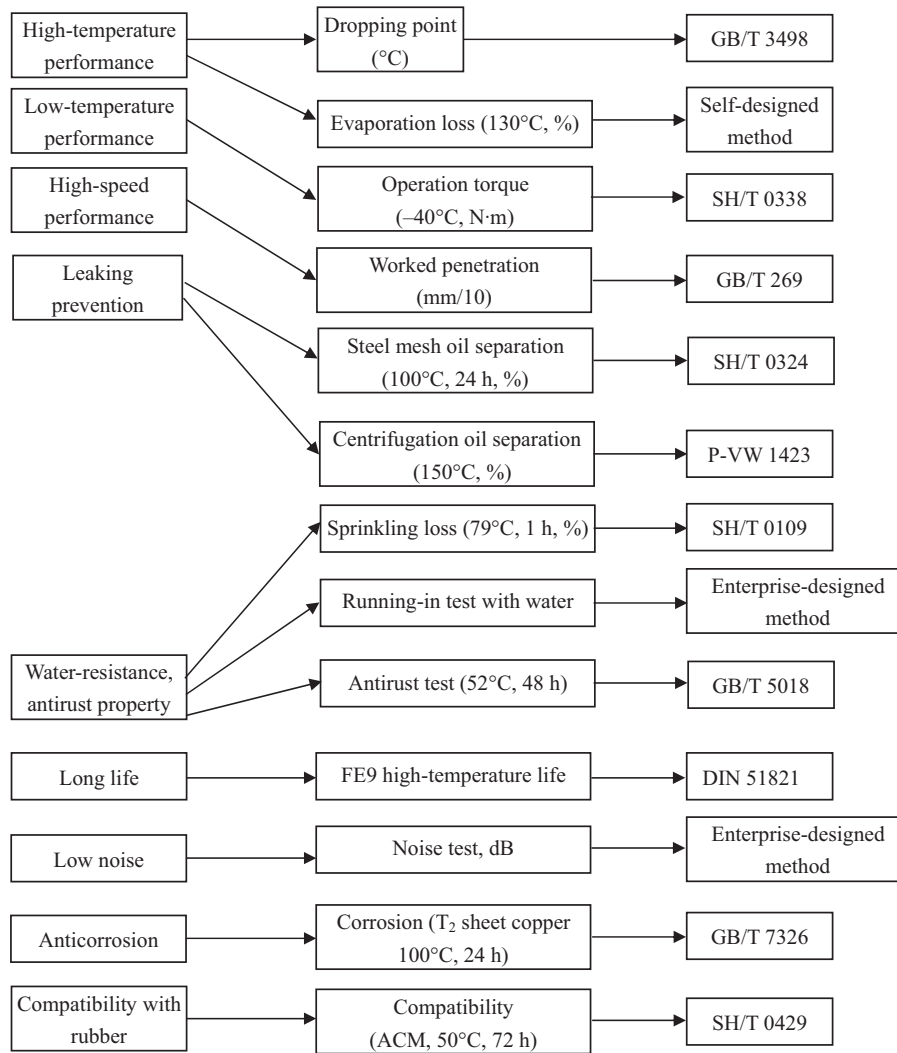


Figure 9.3—The relationship among the characteristics, lubricating grease, and the methodology.

low noise test). One typical example of the characteristics of the lubricating grease is shown in Table 9.5.

9.2.4 Lubricating Grease for Electric Motor Bearings

In addition to automotive hub bearings, constant velocity universal joints, auxiliary engine bearings, and electrical

part bearings, electric motor bearings are considered the fourth important part where lubricating grease is largely used. Electric motors mainly include those motors to drive or operate the fan, throttle valve, windshield wiper, rear-view mirror, etc.

The fan motor is located in the engine compartment and usually works at a temperature above 130°C. Carbon

TABLE 9.5—Lubricating Grease Used for Auxiliary Engine Bearings and Electrical Part Bearings

Parts	Fluid Coupling		Water Pump		Timing Belt Stretcher, Alternator, Idler Pulley, Electromagnetic Clutch	
	A	B	C	D	E	F
Grease No.	A	B	C	D	E	F
Thickener	PTFE	PTFE	Lithium soap	Polyurea	Polyurea	Polyurea
Base oil	Silicone oil	Fluorocarbon oil	Mineral oil	Poly-alpha-olefin	Ester oil	Alkylated biphenyl ether
Viscosity of base oil (mm ² /s, 40°C)	160	160	130	100–150	30	100
Worked cone penetration (NLGI No.)	2	2	3	2	2	2–3

PTFE = polytetrafluoroethylene.

wear debris may easily enter the bearing, worsening lubrication and resulting in agglomeration. Therefore, polyurea-based lubricating grease with poly-alpha-olefin as the base oil is generally used in this case. The bearings in the throttle valve motor require a small size to reduce the resistance during stirring at low temperature. Thus, the amount of the lubricating grease is relatively small, but the lifetime should not be compromised. The fluorocarbon oil polytetrafluoroethylene (PTFE) is suitable for this application because of its excellent fluidity at low temperature and stability at high temperature. With regard to the windshield wiper motor and rearview mirror motor, they have different characteristics according to their use, with low noise, low weight, low price, miniaturization, and quick response as their common requirements. Generally speaking, the bearings used in a rearview mirror motor or electric window motor are sliding bearings lubricated by oil, whereas when rolling bearings are used, lithium-based lubricating grease should be applied at steady cases and NLGI No.2 lubricating grease is suitable if quick response is specially required.

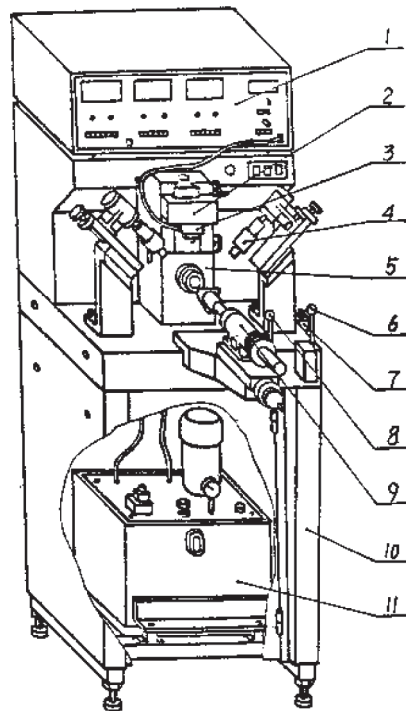
9.3 MEASUREMENT TECHNOLOGY OF VIBRATION, ABNORMAL SOUND, SEALED PERFORMANCE, AND FATIGUE LIFE OF AUTOMOTIVE BEARINGS

Nowadays, more and more attention has been paid to the measurement and control of automotive bearing vibration and abnormal sound because of the increased requirement of low noise and comfort. This section discusses in the detail the measurement of vibration (velocity and

acceleration), abnormal sound, and fatigue life of automotive bearings using the machines established in the National Testing Laboratory of the Hangzhou Bearing Test and Research Center (HBRC) with the assistance of the U.N. Development Program/U.N. Industrial Development Organization (UNDP/UNIDO) since the 1980s (CNAS No. L0309). The testing data generated by these machines are accepted worldwide; therefore, the test data are validated worldwide as a third position independent institute of bearing precision inspection and dynamic performance/fatigue life /reliability testing [11,12].

9.3.1 Testing of Bearing Vibration (Velocity) [13–16]

The bearing vibration (velocity) test can be performed using the BVT machines as shown in Figures 9.4 and 9.5 (e.g., BVT-5 and BVT-6). This series of instruments is mainly composed of a speed sensor, amplifier, driving shaft, loading cell, etc. The speed sensor converts the radial vibration signal of the bearing outer ring into an electrical signal, and the driving shaft is a newly developed hydrodynamic and hydrostatic shaft with the advantages of high rotation accuracy, good antivibration properties, and long life. The typical characteristics of the BVT series instruments are summarized in Table 9.6. The BVT series of machines was developed in a series of practice from BVT-1, BVT-2, BVT-3, BVT-4, BVT-5, and BVT-6. We also developed the latest version, BVT-7, for the bearing vibration (acceleration) tester of automatic clutch release bearings and belt tensioner pulley/idler bearings (vertical).



- (1) measuring amplifier, (2) transducer positioning device, (3) transducer, (4) radial loader device, (5) hydrodynamic-static spindle, (6) radial loader air valve, (7) three pneumatic,
- (8) axial loader air valve, (9) axial loader device, (10) body frame, (11) oil supply system

Figure 9.4—BVT-5 bearing vibration tester.

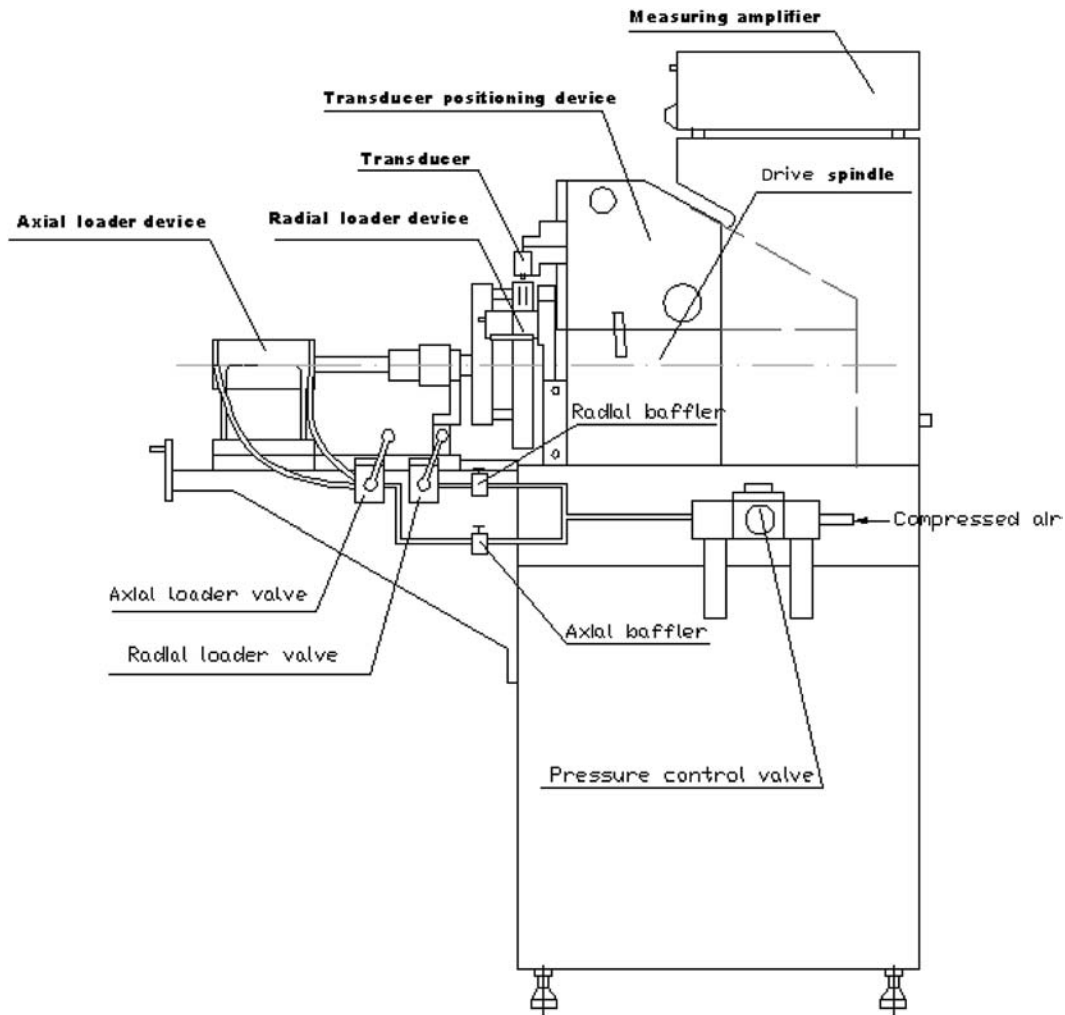
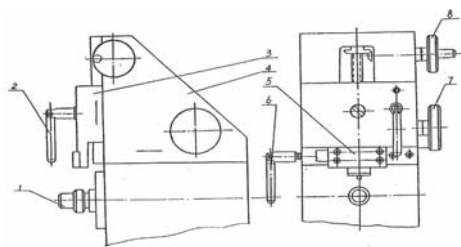


Figure 9.5—BVT-6 bearing vibration tester.

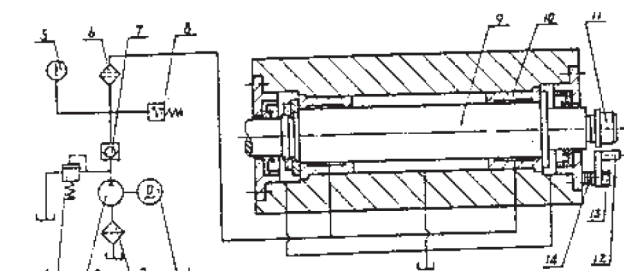


- (1) arbor, (2) vertical lock handle, (3) vertical sliding block, (4) horizontal sliding block, (5) transducer, (6) horizontal lock handle, (7) hand wheel, (8) hand wheel

Figure 9.6—Transducer positioning device.

The positioning device shown in Figure 9.6 is designed for precisely adjusting the transducer's horizontal and vertical position by turning hand wheel 7 and hand wheel 8.

Hydrodynamic-static bearings are used to axially and radially support the spindle; thus, good rigidity, good vibration-proof properties, high rotating accuracy, and long life are possible. A three-phase synchomotor drives the pulley and belt. No. 3 spindle oil is required, and the feed oil pressure ranges from 0.8 to 1.2 MPa. By adjusting the pressure relay, the spindle should not rotate when the oil pressure is under



- (1) motor, (2) rough filter, (3) oil pump, (4) overflow valve, (5) pressure meter, (6) fine filter, (7) one-way valve, (8) pressure relay, (9) spindle, (10) bearing, (11) arbor, (12) rubber column, (13) locking screw, (14) adjusting washer

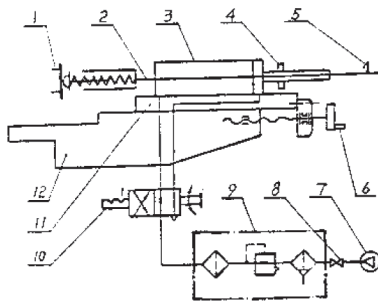
Figure 9.7—Spindle hydraulic mechanism.

0.3 MPa. The capacity of the oil box is approximately 30 L. The spindle hydraulic mechanism is shown in Figure 9.7.

The inlet pressure of 0.4 MPa (4 kgf/cm²) is used for the pneumatic loader illustrated in Figure 9.8. The stroke of the cylinder piston may be adjusted. The device has two kinds of loading plates, with the smaller one for bearing outer diameters (to be measured) from 20 to 80 mm and the bigger one from 80 to 130 mm. It also has two types of rubber loading columns, each for two kinds of loading plates.

TABLE 9.6—Typical Characteristics of the BVT Series Machines to Measure Automotive Bearing Vibration (Velocity)

BVT Instrument	BVT-1A	BVT-5	BVT-6
Types of tested bearing	Deep-groove ball bearing, angular contact ball bearing, tapered roller bearing	Deep-groove ball bearing, angular contact ball bearing, tapered roller bearing, cylindrical roller bearing, needle bearing, water pump bearing	Deep-groove ball bearing, angular contact ball bearing, tapered roller bearing, cylindrical roller bearing
Size range of tested bearing (mm)	Inner diameter: 3–60 Outer diameter: maximum 170	Inner diameter: 5–60 Outer diameter: Maximum 170	Inner diameter: 65–120 Outer diameter: Maximum 280
Measurement range ($\mu\text{m/s}$)	0–10,000		
Frequency range (Hz)	Low: 50–300; medium: 300–1800; high: 1800–10,000		
Shaft rotation speed (r/min)	1800	1800	900
Radial load (N)	–	150, 300	600
Axial load (N)	0–250	0–250	150–500
Power supply	Shaft motor: 380 V, 50 Hz, three phase, 370 W Oil pump motor: 380 V, 50 Hz, three phase, 180 W Amplifier: 220 V, 50 Hz		
Power (W)	600		
Temperature ($^{\circ}\text{C}$)	5–40		
Total weight (kg)	400	450	620
Total size (mm)	660 × 1030 × 1530	660 × 1030 × 1530	700 × 1200 × 1560



(1) load column, (2) piston rod, (3) cylinder, (4) position-adjusting nut, (5) position-adjusting screw, (6) hand wheel, (7) air-compressor engine, (8) cutoff valve, (9) three pneumatic, (10) rotary valve, (11) upper sliding block, (12) low sliding block

Figure 9.8—Axial loader pneumatic mechanism.

The inlet pressure of 0.4 MPa (4 kgf/cm²) is used for the pneumatic radial loader, and the pneumatic mechanism is shown in Figure 9.9.

We also developed a multiparameter test system [11,12] of vibration and abnormal noise of rolling bearings. Low-, middle-, and high-frequency band output signals of BVT can be obtained using a data acquisition card and feedback to a computer. Through testing and computing, the vibration waveform, peak value, crest factor, etc., are displayed on the screen. The device can be applied to bearing heterogeneity sound analysis, failure diagnosis, etc. The main functions are as follows:

- To display the vibrating signal time-domain waveform and frequency-domain waveform of low, middle, and high frequency.

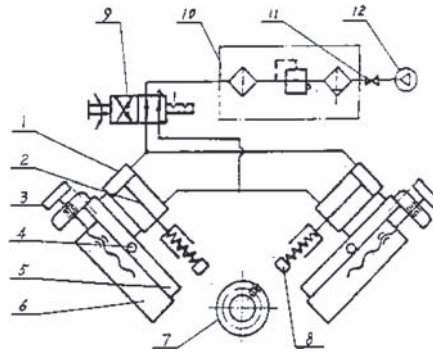
- To display multiple parameters, including peak value, root mean square, crest factor, pulse number, etc.
- The acquisition data can be saved and used. Meanwhile, the waveform parameters can be printed.
- The character frequency can be computed by inputting the testing bearing character dimensions, which can be consulted when analyzing.

9.3.2 Testing of Bearing Vibration (Acceleration) [13]

The bearing vibration (acceleration) can be tested using S0910-3, S3910-1, S9912-3, SL-2, SN-2 machines, etc., which are generally composed of an acceleration sensor, amplifier, driving shaft, loading cell, etc. The typical characteristics of these machines are shown in Table 9.7.

9.3.3 Testing of Abnormal Sound [13]

Abnormal sound of an automotive bearing is classified as a type of noise that is uncomfortable and can be induced by many factors, including damage to the bearing surface, involvement of contamination, vibration of the retainer, impingement between the retainer and the ball, etc. To date, there are no international standardized testing methods and specifications for abnormal sound. However, the occurrence of abnormal sound is usually associated with the presence of a spike signal. The BANT instrument was established based on this principle to measure the abnormal sound of automotive bearings. Generally, the BANT instrument is usually combined with the BVT instrument. The typical characteristics of BANT-1 and BANT-2 are shown in Table 9.8.



(1) cylinder, (2) plunger, (3) hand wheel, (4) locking screw, (5) upper sliding block, (6) low sliding block, (7) bearing, (8) load block, (9) rotary valve, (10) three pneumatic, (11) cutoff valve, (12) air compressor engine

Figure 9.9—Radial loader pneumatic mechanism (BVT-5).

9.3.4 Testing of Sealed Performance of Sealed Bearings [17]

9.3.4.1 SEALED BEARING GREASE LEAKAGE, TEMPERATURE RISE, AND DUSTPROOF PERFORMANCE

BGT-1A is a type of very useful equipment for testing the sealed bearing grease leakage, temperature rise, and dust-proof performance. The tester chiefly consists of a bearing housing, drive gearshift system, loading system, oil circulation system, and a computer control system. The monitor bearing temperature and spindle speed are controlled by the computer. It conforms to the specification JB/T 8571-2008 "Rolling Bearings—Sealed Deep-Groove Ball Bearings—Performance Test Rule of Dust-Proofing, Grease Leakage, and Temperature Rise" and JB/T 7752-2005 "Rolling Bearing—Specifications of Sealed Deep-Groove Ball Bearings."

- *Usage and application:* BGT-1A sealed bearing grease leakage temperature-rise dustproof performance tester is mainly for the bearings' sealing performance. The tester is composed of a test head, test spindle, driving system, loading system, lubricating system, and monitoring control system.
 - *Features about the life tester:*
 - Automatically monitors the bearing temperature rise, rotational speed, and loading;
 - Frequency control, convenient, reliable, high precision ($\leq \pm 3\%$);
 - Testing time can be preset;
 - Steady load; and
 - Automatically record and print testing data;
- Measure or analysis on the contrast test of sealed bearing grease leakage temperature-rise dustproof performance according to JB/T8571-2008.

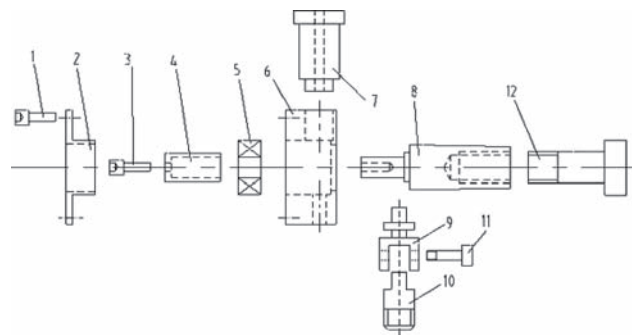
TABLE 9.7—Typical Characteristics of the Machines to Measure Automotive Bearing Vibration (Acceleration)

Machine	S0910-3	S3910-1	S9912-3	SL-2	SN-2
Types of tested bearing	Deep-groove ball bearing, angular contact ball bearing	Tapered roller bearing	Deep-groove ball bearing, angular contact ball bearing, tapered roller bearing, cylindrical roller bearing	Hub bearing	Cylindrical roller bearing
Size of tested bearing (mm)	Inner diameter: 3–60	Inner diameter: 15–60 Outer diameter: 35–130	Inner diameter: 65–140	–	Inner diameter: 15–60 Outer diameter: 35–130
Measurement range (dB)	Effective value: 0–100; Peak value: 0–115				
Frequency range (Hz)	50–10,000				
Shaft rotation speed (r/min)	1500	1500	1000 Radial loading: 600 N Axial loading: 225 N	1500 Axial loading: 127–240 N	1500
Power supply	380 V, 50 Hz, three phase, 500 W	380 V, 50 Hz, three phase, 500 W	380 V, 50 Hz, three phase, 2000 W	380 V, 50 Hz, three phase, 500 W	380 V, 50 Hz, three phase, 500 W

TABLE 9.8—Typical Characteristics of the Machines to Measure Automotive Bearing Abnormal Sound

Machine		Bant-1	Bant-2
Peak value ($\mu\text{m/s}$)	Pass band	0–3000	–
	Low-frequency band	–	0–2000
	Medium-frequency band	–	0–2000
	High-frequency band	–	0–2000
Impulse number		0–99,999	–
Crest factor	Low-frequency band	1–15	1–15
	Medium-frequency band	1–15	1–15
	High-frequency band	1–15	1–15
Wave display		Low-frequency band Medium-frequency band High frequency band Pass band, Null	–
Presetting and alarm		Yes	Yes

- Main technical specifications:**
 - Bore diameter = 8–60 mm
 - Spindle speed = 1200–1500 r/min
 - Measurement accuracy = $\pm 1^\circ\text{C}$ (for temperature rise)
 - Radial load = 0–600 N
 - Power supply:
 - Main engine = 380 V, 50 Hz, three phase
 - Computer = 220 V, 50 Hz, three phase
 - Power consumption = approximately 1.5 kW
 - Ambient temperature = 10–40°C
 - Weight = 300 kg
 - Dimensions = 650 × 500 × 1200 mm
- Description of components' test head, spindle, and driving system:**
 - The grease leakage temperature-rise test head (Figure 9.10) is composed of test arbor 8, tested bearing 5, load sleeve 6, fixing sleeve 4, end cap 2, holding screw, and so on.
 - The dustproof test head (Figure 9.11) is composed of test arbor 11, tested bearings 7 and 9, long-distance sleeve 8, short-distance sleeve 6, front sealed cover 2, rear sealed cover 10, wave shape washer 3, latch nut 5, and so on.
 - The spindle uses the 7208C/P4 and 7207C/P4 bearings as supporting bearings and drives through the high-speed belt (1.5 × 32 × 1000). The supporting bearings are lubricated with No. 10 spindle oil.
 - An electric motor, driveshaft, and spindle make up the driving system. It uses a V belt (A-900) for transmission between the motor and driveshaft, and a flat belt between the driveshaft and spindle. The drive ratio can be changed by adjusting the position of the V belt. The driveshaft uses two sets of 6006-2RZ/P5/Z2 bearings as supporting bearings. The drive ratio between motor and driveshaft can be determined. There are two drive ratios between the motor and driveshaft: $i_1 = 2$ or $i_1 = 1/2$.



(1) holding screw, (2) end cap, (3) socket head screw, (4) fixing sleeve, (5) tested bearing, (6) load sleeve, (7) thermometer holder, (8) test arbor, (9) tension rod holder, (10) loading tension rod, (11) bolt pin, (12) tension rod

Figure 9.10—Grease leakage temperature-rise test head.

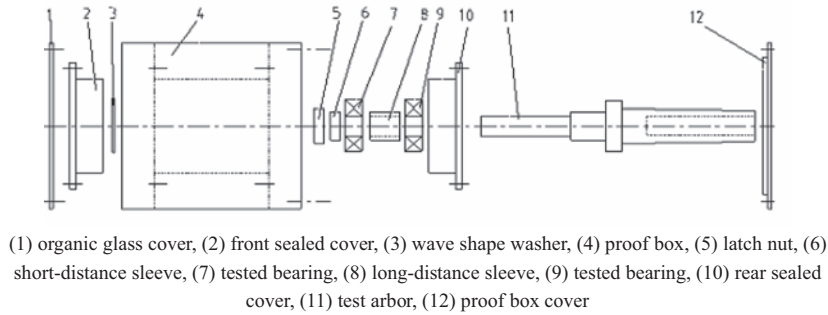


Figure 9.11—Dustproof test head.

The drive ratio i_1 can be determined according to the rotational speed n required by testing regulations. The V belt is mounted on the small belt wheel when the drive ratio $i_1 = 1/2$. The V belt is mounted on the large belt wheel when the drive ratio $i_1 = 2$.

- The loading system must apply the radial load during the test of grease leakage temperature rise. A tension transducer and spring screw rod should be adopted for loading and displaying the loading force on the computer.
- The computer control system is composed of an industrial computer, signal amplifier, temperature transducer, tension transducer, converter, velocity-measuring device, monitor software, and so on. The signal collected from the four temperature transducers and rotational speed transducer is converted into a digital signal through amplification. The tester will automatically stop when the bearing temperature rise exceeds the setting value. The tester will be also automatically stop when the testing time reaches the time set by the customer. The testing data of temperature rise and rotational speed are printed at any time.

9.3.4.2 ROLLING ELEMENT BEARING'S FRICTION TORQUE [18–20]

ABFT is a type of useful equipment to test the friction moment for first-, second-, and third-generation wheel hub bearings and units. An actuating motor to control the spindle speed and a high-accuracy air-flotation platform to load are adopted. Controlled by the computer, ABFT can

test the start moment and the dynamic moment and then record, export, and print the results.

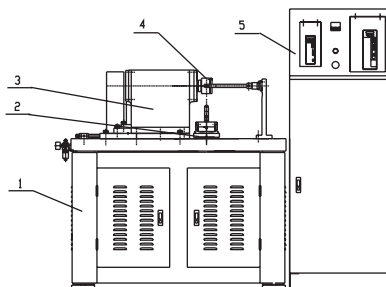
9.3.5 Testing of Fatigue Life and Reliability [21–23]

9.3.5.1 ROLLING ELEMENT BEARING'S STANDARD TESTING OF FATIGUE LIFE AND RELIABILITY [24–26]

The fatigue life of automotive bearings can be tested using an ABLT instrument (e.g., ABLT-1A, ABLT-2, ABLT-3, ABLT-4, ABLT-5, etc.). The typical characteristics of this series are summarized in Table 9.9. We also developed ABLT-6, the accelerated bearing life tester for the bearings with the outer ring rotating, and ABLT-7, the accelerated bearing life tester for the insert bearings with housing. We conduct the rolling element bearings' standard testing of fatigue life and reliability in terms of GB/T 24607-2009 "Rolling Bearing—Test and Assessment for Life and Reliability" [27–29]. Figure 9.13 of an ABLT-1A test rig is an example.

9.3.5.1.1 Usage and Application

The ABLT series automatic control accelerated life tester is mainly for the life test of rolling bearings in which the bore diameter of the bearings tested ranges from 5 to 240 mm. The tester is composed of a test head, test bed, driving system, loading system, lubricating system, electrical control system, and monitoring control system. The test head is mounted in a test bed. The driving system transfers the motion of the electric motor and makes the test shaft rotate at a certain speed. The loading system provides the needed



(1) testing system body, (2) load system, (3) transmission system, (4) testing part, (5) electrical and control system

Figure 9.12—ABFT-1 test rig.



Figure 9.13—ABLT-1A test rig.

load. The lubricating system makes the bearings tested well lubricated under normal conditions. The electrical control system provides the power and electric protection and controls the action of the electric engine and hydrocylinder. The monitoring control system records the test temperature and vibration information and monitors the running conditions of the machine.

It is called an “accelerated” test because the equivalent dynamic load added on the tested bearings is near or reaches half of the rated dynamic load C under the premise of maintaining a consistent rolling bearing contact fatigue failure mechanism for the purpose of shortening the test

period. Compared with conventional test methods, the accelerated life test considerably shortens the test time and saves on testing expenses. Features of the life tester include automatic steady load; automatic display of the outer ring temperature within an absolute error of 0.1°C ; automatic display of the test time with a time precision of 0.1 h ; automatic alarm and automatic stop; automatic recording; test data printing; and display of the main data illustration.

9.3.5.1.2 Description of Component Test Head, Test Bed, and Driving System

- *Test head:* The structure of the test head is shown in Figure 9.14. Piece 10 is the test shaft, and piece 3 is the middle load mass. Pieces 1 and 6 are end load masses that cannot be interchanged. Piece 4 is the middle bush. Pieces 2 and 5 are end bushes that can be interchanged.
- *Test bed:* This component is the main part of the tester. The radial load oil cylinder is located in the rear side, the axial load oil cylinder is located in the left side, the driving square shaft pass is on the right side, the thermometer supporter is on the top, and the lubricant passage way is surrounded.
- The driving system of the tester uses wedge belt transfer power and implements speed change with a replacing belt wheel. It has the advantages of simple speed change and accurate rotational speed. The test synchro-speeds of the motor are 3000 and 1500 r/min.

We also developed the latest versions ABLT-6 and ABLT-7 for the special rolling bearing life tester of automatic clutch release bearings and belt tensioner pulley/idler bearings (outer ring rotating), respectively.

TABLE 9.9—Typical Characteristics of the Machines to Test the Fatigue Life of Automotive Bearings

Test Machine		ABLT-1A	ABLT-2	ABLT-3	ABLT-4	ABLT-5
Types of tested bearing		Ball bearing, roller bearing		Ball bearing	Ball bearing, roller bearing	
Inner diameter of tested bearing (mm)		10–60	60–120	5–12	120–180	180–240
Amounts of tested bearing		2–4				
Rotation speed (r/min)		1000–10,000	500–5000	5000–36,000	500–3000	300–2500
Maximum radial load (kN)		100	250	1.5	400	800
Maximum axial load (kN)		50	125	0.4	200	300
Power supply	Shaft motor (kW)	3	7.5	1.5	10	15
	Oil pump motor (kW)	0.37	0.75	0.04	1.5	2
	Power (kW)	3.5	9	1.8	15	20
Temperature ($^{\circ}\text{C}$)		10–40				
Total weight (kg)		1000	2000	500	3500	4500
Total size (mm)		1500 × 720 × 1200	1750 × 900 × 1200	1100 × 650 × 1000	2000 × 1000 × 1500	2200 × 1100 × 1600

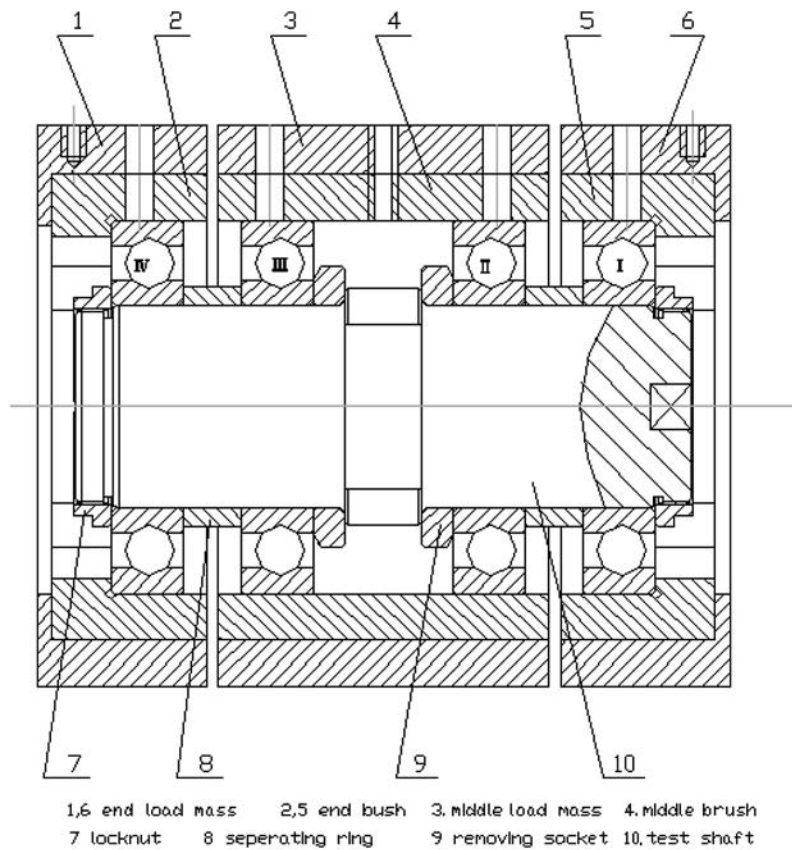


Figure 9.14—The structure of the test head.

9.3.5.2 TESTING OF LUBRICATING GREASE LIFE AND RELIABILITY

- SKF ROF lubricating grease life test (Figure 9.15)
 - The SKF ROF test can determine performance life and the high-temperature limit of lubricating grease.
 - Ten deep-groove ball bearings are fixed on five bearing blocks and filled with the quantitative lubricating grease, then the axial and radial loads are set. They spin at a predetermined speed (10,000 r/min) and at a predetermined temperature (130, 150, and 170°C) until failure. The running hours are recorded under each scenario.

- The Weibull life can be calculated to determine the lubricating grease's life.

FAG and SNR developed a similar test method.

- FAG FE8 lubrication grease life test rig (Figure 9.16)
For the FAG production system test rig FE8 operating instructions, we conduct the test in terms of the following:

- *DIN 51819-1*: Testing of Lubricants—Mechanical-Dynamic Testing in the Roller Bearing Test Apparatus Fe8 Part 1: General Working Principles
- *DIN 51819-2*: Testing of Lubricants—Mechanical-Dynamic Testing in the Roller Bearing Test Appara-



Figure 9.15—SKF ROF lubricating grease life test rig.



Figure 9.16—FAG FE8 lubrication grease's life test rig. 1 = workshop press, 2 = workshop carriages, 3 = test units, 4 = control cabinets, and 5 = PC with evaluation software.



Figure 9.17—FE9 test rig with five test units. 1 = frame, 2 = oil unit, 3 = test units (5 pieces), and 4 = control cabinet with actuator.

tus Fe8 Part 2: Test Method for Lubricating Greases, Oblique Ball Bearing or Tapered Roller Bearing

- *DIN 51819-3*: Testing of Lubricants—Mechanical-Dynamic Testing in the Roller Bearing Test Apparatus Fe8 Part 3: Test Method for Lubricating Oils, Oblique Axial Ball Bearing
- FAG FE9 lubrication grease life test rig (Figure 9.17)

For the FAG production system test rig FE9 operating instructions, we conduct the test in terms of DIN 51821, "Testing of Lubricants; Test Using the FAG Roller Bearing Grease Testing Apparatus FE9."

9.3.5.3 SIMULATION TESTING OF LIFE AND RELIABILITY

An environment simulation reliability test of a singular factor was applied for the appraisal and development tests

to deal with the production design in United States in the 1940s, checking on the quality and reliability of production design. A synthesized environment simulation reliability test, assignment section test, and check-and-accept test were applied in the 1970s. These testing methods henceforth have become the basic measures used to ensure product reliability and durability. However, because of the complexity of the environment, mechanical and electrical coupling factors, high costs, and the quality of test results, the simulation testing technologies have lost some predominance. Simulation test technology has received broad recognition in recent years. However, because of the factors listed above, the simulation test has moved more toward the building blocks and modularization.

The sketch map of sealed bearing simulation tester ABDT is in Figure 9.18. ABDT is a type of useful equipment to test the dustproof performance for deep-groove ball bearings; the first-, second-, and third-generation wheel hub bearings; and the unit. ABDT can simulate working conditions such as sand, dust, high temperature, etc., with tunable wind speed [30].

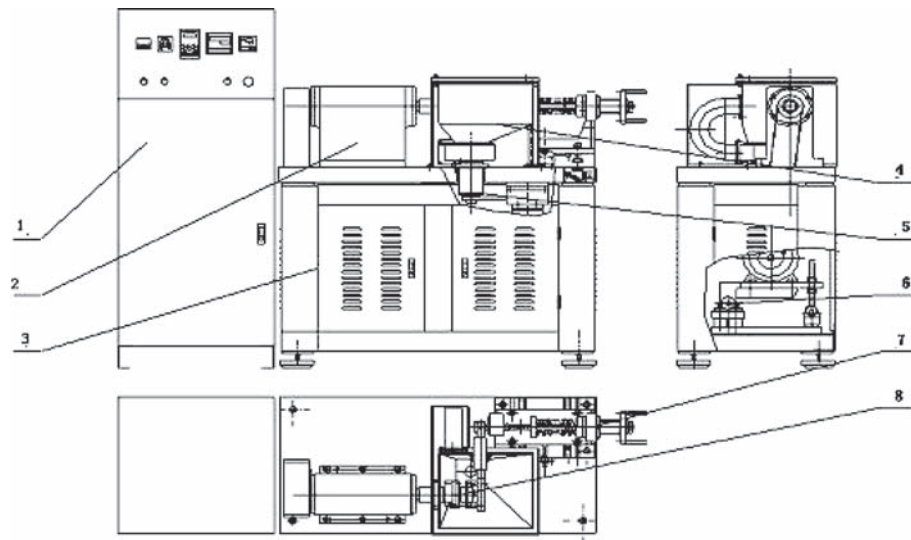
The reliability environment testing (RET) technology that has been widely used in the current bearing industry is derived from the failure of physics. To improve the reliability of the products, the failures have been observed and researched. It is believed that the major obstacles that prevented the products from being fixed can be found. It is proved in practice that the effect is very pronounced. It is equivalent and comparative to that of the general test technology [31]. To increase the testing load and accelerate the test process is widely adopted by many bearing companies. The test load applied in the deep-groove ball bearings accelerated testing in Japan has been approached or exceeded half of the rating load, as shown in Table 9.10.

9.3.5.4 STIMULATION TESTING OF LIFE AND RELIABILITY [32]

In opposition to the simulation test, the environmental stress stimulation test uses artificial methods to apply environmental stress to improve reliability by accelerating stimulation and removing product latency disfigurement. Stimulation testing in the early stage (e.g., high temperature, temperature circulation, and temperature impact, etc.) has been developed for simulation of high temperature change rate and broadband stochastic vibration. The test stress applied does not only need to simulate the real environment, but also to measure the higher stimulation testing efficiency. Along with the vigorous development of the stimulation test, researchers have tried to accelerate the development of this technology by standardization types. However, this consideration again pulls back to the track of the simulation test. Moreover, different stress filter solutions should be used in different failure modes and different defective mechanisms. It is not adopted to standardize the stimulation test rules. Nowadays, this test method is under the condition of no design defects, simply dealing with the defects formed during the production process. The defects cannot be removed from the design [33,34].

9.4 CONCLUSIONS

This chapter provides an overview of the testing and evaluation of lubricating greases for the rolling element bearings



(1) electricity box, (2) principal axis, (3) lathe bed, (4) heat-up dust box, (5) fan groupware, (6) main shaft motor, (7) loading wheel, (8) tested bearing

Figure 9.18—The sketch map of the ABDT-1 test rig.

of automotive systems. Automotive service lubricating greases are applied on the most important automotive parts, including hub bearings, constant velocity universal joints, auxiliary engine bearings, electrical part bearings, and electric motor bearings. This case study has described

the investigation and invention using characterization of the vibration (velocity/acceleration), abnormal sound, sealed performance, fatigue life, and reliability of automotive bearings. An overview on some of the laboratory's research outcomes/activities in fundamentals and industrial

TABLE 9.10—Accelerated Fatigue Life Test Parameters of Deep-Groove Ball Bearings

Bearing Company and Its Country	Test Bearing Types	Test Load P/N	Load Ratio P/C	Test Speed n (r·min ⁻¹)	Rotate Speed Ratio n/n_0	Calculate Life (h)	Maximum Contact Stress σ_{\max} (MPa)
BLA Japan	6206	9807	0.65	2000	0.15	29.9	4246
NTN Japan	6206	6860	0.45	2000	0.15	87.0	3817
NSK Japan	6206	5880	0.40	2800	0.22	96.7	3677
NACHI Japan	6308	19,600	0.63	1140	0.14	40.0	4103
SKF Sweden	6309	18,828	0.46	6000	0.75	27.8	3658
SKF United States	6309	17,040	0.46	1000	—	—	3181
SKF France	Variety	—	0.50	n_0	1	10 ⁷ revolutions	—
F&M United States	6207	9906	0.51	1800	0.18	70.0	3845
ASME United States	6208	11,024	0.44	—	—	98.2	3179
Romania	6308	15,000	0.46	1500	0.17	116.7	3746
RHP United Kingdom	6305	6556	0.41	4000	0.31	60.0	3565
Russia	Variety ^a	—	—	—	0.4–0.6	100–300	—
	6010 ^a	8100	0.50	4000	0.44	34.0	3836
FAG Germany	6204	7366	0.58	9000	—	—	2900
People's Republic of China	Variety	—	0.23–0.3	—	0.4–0.6	100–300	—

BLA = Bearing Life Association. ^aData before 1979. ^bData in 1985.

applications was conducted at the National Testing Laboratory of HBRC with the assistance of UNDP/UNIDO [35,36]. The testing data generated by these machines are accepted worldwide; therefore, the test data are validated worldwide for bearing precision inspection and dynamic performance/fatigue life/reliability testing [37,38]. Rolling element bearing practice in engineering is complex in nature. Rolling element bearing engineering science and technology must keep up with the times [39,40].

References

- [1] Li, X.L., 1991, *Rolling Bearing Tribology and Its Application, Final Report on Study Tour to Japan*, Project Number DG/CPR/83/001/32-07, U.N. Development Program/U.N. Industrial Development Organization, Geneva, Switzerland.
- [2] Li, X.L., 2009, "A,BLT+F,AST—Accelerated Automatic rolling Bearing fatigue Life and reliability Tester and Fast Failure Analysis System Technology in Hangzhou Bearing Test & Research Center with assistance of UNDP/UNIDO." P47, Paper presented at the Forum on Frontiers of Engineering, Chinese Academy of Engineering, June 28.
- [3] Liu, Z.J., He, S.Q., and Li, X.L., 2006, *The Application Handbook of Rolling Element Bearings* (2nd ed.), China Machine Press, Beijing, People's Republic of China.
- [4] Wang, H.J., Li, J.S., Ma, W., and Li, X.L., 2008, *The Inspection and Test of Rolling Element Bearings*. China Machine Press, Beijing, People's Republic of China.
- [5] Li, X.L., 1985, "A New Method for Computing the Static and Dynamic Characteristic Coefficients of Tilting-Pad Bearings," B.Sci. Thesis, Zhejiang University. Hangzhou, People's Republic of China.
- [6] Li, X.L., 1988, "Experimental Research and Theoretical Analysis on the Wear-In Process of the Point-Contact Rolling Friction Pairs," M.Sci. Dissertation, Zhejiang University. Hangzhou, People's Republic of China.
- [7] Li, X.L., 1995, "Test and Research on Accelerated Fatigue Life of Rolling Element Bearings," Ph.D. Dissertation, Zhejiang University. Hangzhou, People's Republic of China.
- [8] Li, X.L., 1999, "Test and Research on Hub Wheel Bearings Life of China Automobiles," Postdoctoral research project report, Shanghai Jiaotong University. Shanghai, People's Republic of China.
- [9] Li, X.L., 2009, "Keynote Speech in the 15th Conference of China Lubrication Grease Technology, Status in Quo and Progress of Lubrication Grease Testing Technology of Rolling Bearings Performance Life and Reliability." P1-6, *In Proceedings of the 15th Conference of China Lubrication Grease Technology*. The Petroleum Refining Branch of the Institute of China Petroleum, Shenzhen, October 19.
- [10] Li, X.L., Xue, J., Wu, B.J., Feng, Q., Zhang, Y.L., and Chen, Z.E., 2011, "Application of Rolling Bearings Lubrication Grease Testing." Available at <http://www.cnki.com.cn/Article/CJFDTOTAL-SYSA201106007.htm>.
- [11] Li, X.L., Quan, Y., and Jin, X., 1990, "Monitoring Test of the Wear Condition of Rolling Bearing Friction Pairs." In *Proceedings of the Japan International Tribology Conference*, ITC, Nagoya, Japan, pp. 803–808.
- [12] Li, X.L., Quan, Y., Jin, X., 1990, "Monitoring Test of the Wear Conditions of Ball Bearing Rolling Friction Pairs," J. Zhejiang Univ., Vol. 24, pp. 253–260.
- [13] Li, X.L., Chen, F.H., Shen, Y.T., Zhang, Y.L., and Zhang, Y.E., 2010, "The Principle of Rolling Bearing Measurement-Systematic Measurement Technology of Vibration, Noise and Abnormal Sound of Rolling Bearing." Available at <http://wenku.baidu.com/view/c83294244b35eefdc8d333e1.html>.
- [14] Shen, Y.T., and Chen, F.H., 2008, "The Bearing Vibration (Velocity) Tester," ZL 2007 2 0112720.2, China Patent.
- [15] ISO 15242-1, 2002: Rolling Bearings—Measuring Methods for Vibration—Part 1: Fundamentals.
- [16] ISO 15242-2, 2003: Rolling Bearings—Measuring Methods for Vibration—Part 2: Radial Ball Bearings with Cylindrical Bore and Cylindrical outside Surface.
- [17] Li, Y.L., Zhang, M.L., Cao, M.L., Zhang, Y.P., Lu, S.G., Li, J.P., Zhang, Y.J., and Shen, Y.T., 2010, "Multifunction Tester of Sealed Bearings," ZL 2007 1 0071492.1, China Invent Patent.
- [18] Sier, D., Li, X., Wang, J., Teng, H., 2011, "Frictional Torque Characteristic of Angular Contact Ball Bearings," Chin. Mech. Eng., Vol. 47, pp. 114–120.
- [19] Sier, D., Li, X., Wang, J., Wang, Y., and Teng, H., 2011, "Analysis on the Friction Torque Fluctuation of Angular Contact Ball Bearings," Chin. Mech. Eng., Vol. 47, pp. 104–112.
- [20] Sier, D., 2012, "Study on the Friction Torque Fluctuation of Angular Contact Ball Bearings," Postdoctoral research project report, Zhejiang University and Postdoctoral Research Workstation of Hangzhou Bearing Test and Research Center, Hangzhou, People's Republic of China.
- [21] Li, X.L., 2005, "Accelerated Rolling Bearing Life Testing Is Just Unfolding." Available at <http://www.cnki.net/kcms/detail/detail.aspx?dbcode=ccnd&dbname=ccnd2005&filename=jdsb20050620a062&uid=WEEvREcwSlJHSldRa1FiNlpKRzBzOE1UOWt5dVc3a2pQbkxTN2FzRFBkdTd5a2V3Q2RQcmJMYzF4N3lsUXdjPQ==&p=>.
- [22] Li, X.L., Li, J. Q., Zhang, Y. P., Chen, D.S., and Wang, X., 2006, "Status in Quo and Progress of Accelerated Testing Technology of Rolling Bearings Performance Life and Reliability," Bearing, No. 12, pp. 44–47.
- [23] Li, X., 2007, "Development and Status in Quo of Rolling Bearing Life Performance Testing Technology." Available at <http://www.cbia.com.cn/luntan/2007-1/5.htm>.
- [24] Li, X.L., Zhang, Y.L., Cao, M.L., Zhang, Y. P., Li, J.P., and Li, J.Q., 2008, "Accelerated Rolling Bearing Life and Reliability Tester and Its Test Method," ZL 2006 1 0052447.9 China Patent, No. 10052447.9.
- [25] Yin, J.J., 2010, "Study on System of the Accelerated Bearing Life Tester with Automatic Loading." Postdoctoral research project report, Zhejiang University and Postdoctoral Research Workstation of Hangzhou Bearing Test and Research Center, Hangzhou, People's Republic of China.
- [26] Lou, H.L., 2011, "Study on Life Testing and Reliability Evaluation Methods of Rolling Bearings." Postdoctoral research project report, Zhejiang University and Postdoctoral Research Workstation of Hangzhou Bearing Test and Research Center, Hangzhou, People's Republic of China.
- [27] Huang, R., Xi, L., Li, X.L., Liu, C.R., Qiu, H., and Lee, J., 2007, "Residual Life Predictions for Ball Bearings Based on Self-Organizing Map and Back Propagation Neural Network Methods," Mech. Syst. Signal Process., Vol. 21, pp. 193–207.
- [28] Huang, R., Li, X.L., Liu, C.R., Qiu, H., and Lee, J., 2007, "Residual Life Predictions for Ball Bearing Based on Neural Networks," Chin. Mech. Eng., Vol. 43, pp. 137–143.
- [29] Guo, L., Chen, J., and Li, X.L., 2009, "Rolling Bearing Fault Classification Based on Envelope Spectrum and Support Vector Machine," J. Vibration Cont., Vol. 15, pp. 1349–1363.
- [30] Li, X.L., Zhang, Y.L., Li, J.Q., Wang, Z.C., Cao, M.L., and Zhang, Y.P., 2009, "Dustproof Performance Simulation Test Rig and Its Test Method of Automotive Hub Bearing Units," ZL 2007 1 0067941.7, China Patent, No. 0067941.7.
- [31] Wu, C., Wang, W.R., Xu, B.-H., Li, X.L., and W.-G., 2011, "Chaotic Behavior of Hysteretic Suspension Model Excited by Road Surface Profile," J. Zhejiang Univ., Vol. 45, pp. 1259–1264, 1287.
- [32] Yin, J., Yu, Z., Li, X., and Wang, Z., 2008, "Process Adjustment and Quality Monitoring Method Based on Kalman Filter," J. Zhejiang Univ., Vol. 42, pp. 1419–1422.
- [33] Lou, H., Li, X., Zhuo, J., Zhang, Y., Zhang, Y., Yu, Z., and Zheng, Q., 2009, "Reliability Evaluation for Rolling Bearings with Small Sampling Based on Bayes Method." Paper presented at the 2009 8th International Conference on Reliability, Maintainability and Safety, *Proceedings of ICRMS*, Vol. 2, pp. 1112–1114, Chengdu, People's Republic of China, July 21–25.
- [34] Lou, H.L., Li, X.L., Xu, X.Z., Zhang, Y.P., and Yu, Z.H., 2011, "Study on Sequential Sampling Method Influenced by Shape Parameter for Weibull Distribution," Adv. Mat. Res., Vol. 189–193, pp. 4361–4364.

- [35] Pan, Y., Chen, J., and Li, X.L., 2010, "Bearing Performance Degradation Assessment Based on Lifting Wavelet Packet Decomposition and Fuzzy C-Means," *Mech. Syst. Signal Process.*, Vol. 2, pp. 559–566.
- [36] Pan, Y.N., Chen, J., and Li, X.L., 2009, "Spectral Entropy: A Complementary Index for Rolling Element Bearing Performance Degradation Assessment," *J. Mech. Eng. Syst.*, Vol. 5, pp. 1223–1231.
- [37] Su, L., He, S., Li, X., and Li, X., 2011, "Bio-Inspired Computational Techniques Based on Advanced Condition Monitoring," *Eng. Sci.*, Vol. 9, pp. 90–96.
- [38] Xu, D., Chen, X., Xu, Y., Li, X., and Yang, Y., 2011, "Fatigue Life Prediction of Rolling Element Bearings Based on Impact Energy Generated by Single Defect," *Adv. Sci. Lett.*, Vol. 4, pp. 1667–1672.
- [39] Chen, W., Ma, Z., Gao, L., Li, X., and Pan, J., 2012, "Quasi-Static Analysis of Thrust-Loaded Angular Contact Ball Bearings Part I: Theoretical Formulation," *Chin. J. Mech. Eng.*, Vol. 25, pp. 71–80.
- [40] Chen, W., Ma, Z., Gao, L., Li, X., and Pan, J., 2012, "Quasi-Static Analysis of Thrust-Loaded Angular Contact Ball Bearings Part 1, Part 2: Results and Discussion," *Chin. J. Mech. Eng.*, Vol. 25, pp. 81–87.

10

The Drivetrain System

Dave Simner¹

10.1 INTRODUCTION AND SCOPE

The aim of this chapter is to review the technology that might be found within the drivetrain of a vehicle and make the link to the lubricants used within those units. The lubricant is arguably the most important single component within the drivetrain, although it is often the most difficult to improve, modify, or develop. However, in investigating the drivetrain of the vehicle, some boundaries need placing around the problem. Before starting, it is also worth pointing out that the reader may well come across or be familiar with the term “driveline”. It is probably reasonable to say that “drivetrain” and “driveline” are terms that are interchangeable, although some engineers may have some subtle distinction between the two.

It is probably also reasonable to start by defining some of the other terms to be used within the chapter. “Powertrain” is a term used most widely to include all of the engine systems, the engine itself, the main gear box, and the rest of the drivetrain. One way to view this is to consider the whole system that goes from the fuel filler cap right through to the road wheels. This chapter focuses on one part of this system—the drivetrain. The engine and associated systems are not part of this discussion and are discussed in other chapters of this manual.

Therefore, the drivetrain takes us from the output of the engine at the flywheel to the hubs that support the road wheels. One of the major items within this part of the vehicle is clearly the gear box, although there are several other vital units. Other chapters within the manual consider the automatic gear box in its various guises; therefore, these are not considered here. Most of the material is taken from the automotive industry, although some consideration will be given to the commercial truck and military vehicle industries.

One term that can cause some ambiguity is “transmission”. You will undoubtedly see the word “transmission” used to refer to the drivetrain as described above. For the purposes of this chapter, the author will try and avoid such use and therefore may use the word “transmission” to refer to just one unit within the drivetrain. Such use is not as specific as “gear box”, “transfer case”, or “final drive unit”, and as such is useful in some contexts.

To understand the use of a lubricant within any one transmission unit, what those units do within the vehicle must be understood. In doing this, the function of the units is considered, and mention may be made as to how these have developed over the years as well as how they are developing in the current industry. In understanding this, the importance of the lubricating fluid used can be established.

The first subsections of the chapter will consider the entire drivetrain and some of the factors involved in match-

ing the system to the vehicle. After this, the various types of transmission unit will be discussed. Finally, several technology areas essential to the integrity of the drivetrain will be analyzed. As mentioned, in each area, the interrelationship between function and impact of the lubricant will be discussed.

10.1.1 What Does the Drivetrain Actually Do?

The drivetrain essentially transmits the power from the engine to the wheel, and in doing so it actually makes the vehicle usable. If the engine were to be directly connected to the wheels, then the vehicle would be difficult to start from rest because the engine would also need to be started as the vehicle begins to move. Assuming such an engine was capable of driving the vehicle at low speed, up gradients, or when under load, then the chances are that the engine would not then rotate quickly enough to move the vehicle at high speed. Internal combustion engines have a limited speed range; therefore, the reverse of this situation is that an engine that can match the high speed requirement would not be able to produce the torque required at low speed to make the vehicle usable. Therefore, the functions that enable the driveline to perform the required task include

- Allowing the vehicle to start and stop by disconnecting the drive when appropriate;
- Enabling the vehicle to start from rest at varied acceleration rates in a controlled manner;
- Altering the speed ratio between the engine and wheels;
- Allowing this ratio to change when required;
- Perform all of the above functions (and others) in a refined manner;
- If required by the type of vehicle, the functions should occur in a manner transparent to the driver; and
- Working in conjunction with the suspension system to allow optimal traction to be delivered to the ground.

Figures 10.1 and 10.2 provide an overview of the drivetrain. Figure 10.1 shows some of the considerations that may be considered when specifying a transmission unit. If an engineer needed to write out the requirements for a unit, then the data shown would probably be required by the transmission manufacturer to ensure that it satisfactorily did the job. These guidelines could, perhaps, be applied to any transmission system, not just one from the automotive industry. Figure 10.2 shows the function of an automotive powertrain, with the engine and its systems shown for completeness. The efficiency of a transmission, mentioned here, is discussed later in the chapter. The performance requirements of the vehicle are also introduced briefly to provide some background to the design problem.

¹ Cranfield University, Defence Academy, Swindon, Wiltshire, UK

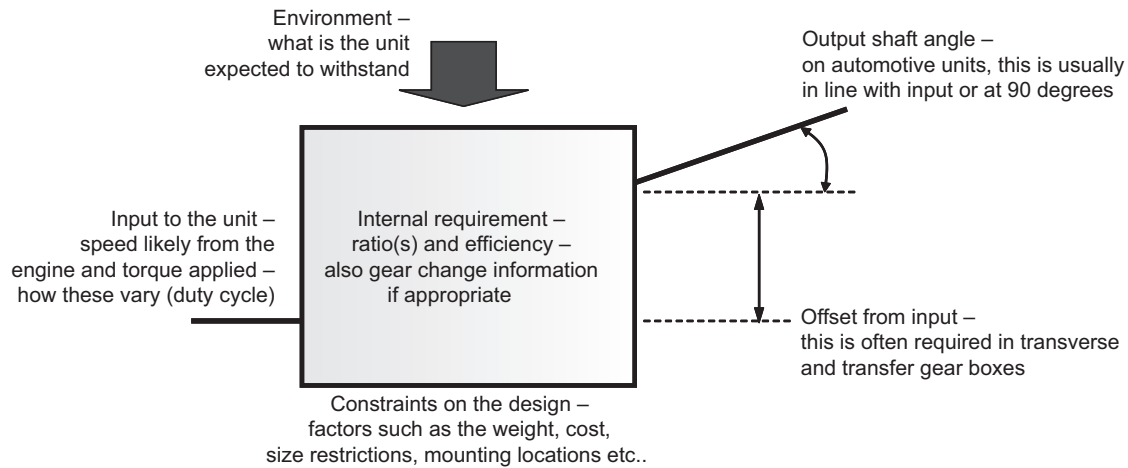


Figure 10.1—The role of a transmission unit—an abstract illustration to show some of considerations when specifying a transmission.

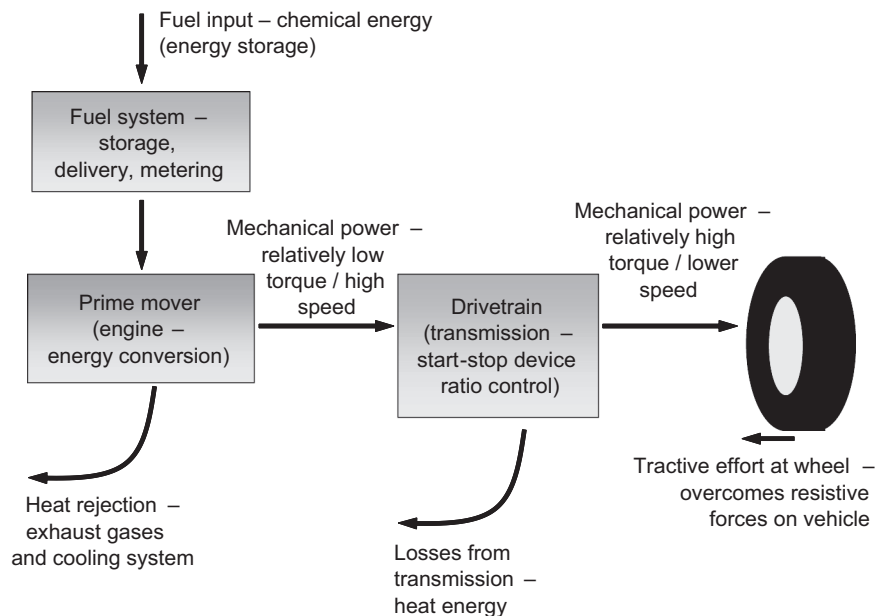


Figure 10.2—The role of the transmission /drivetrain within the vehicle system—a diagrammatic overview.

10.2 THE DRIVETRAIN AND COMPONENT UNITS

10.2.1 The Drivetrain—Design Options

This first topic is very likely to be familiar to most readers; however, it may be useful to just recap the various vehicle package options open to the automotive industry. There are many options, and only the more common will be considered here. The most common in current production is probably the transverse installation illustrated in Figure 10.3. The first diagram in the set shows this concept.

Once vehicles increase in size, it becomes more difficult to package a larger powertrain across the front of the vehicle; therefore, the longitudinal drivetrain installation becomes dominant in the market. This applies to larger cars, performance cars, 4×4 vehicles, and trucks. The rear-wheel drive layout was also historically used for small vehicles, although it does then have limitations for

package efficiency. This is because the front of the vehicle becomes extended to accommodate the in-line engine, and the central drivetrain and rear axle installation impinge on the interior of the vehicle. These limitations, and the overall lower cost of the front-wheel drive solution, have led the industry to where it is today.

One slightly unusual package option illustrated here is the last one. This rear-wheel drive design has been used by several manufacturers, including Toyota and MG. This mid-engine design allows for the use of components and powertrain units from front-wheel drive vehicles to be fitted behind the passengers, providing good weight distribution. However, the design does need careful consideration of the cooling requirements because providing airflow over the powertrain is not as straightforward as if the units were at the front. This would clearly have implications for the lubricant choice because high

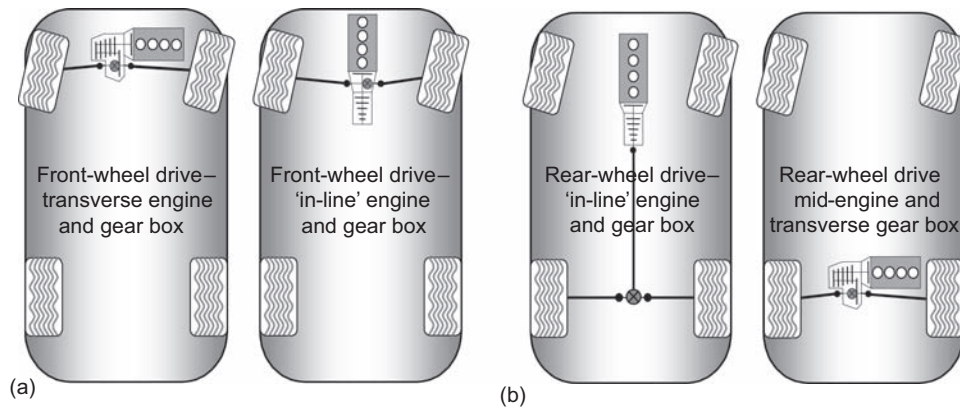


Figure 10.3—Driveline diagrams—overall layout of the powertrain: (a) two options for front-wheel drive vehicles and (b) two rear-wheel drive options.

temperatures are arguably more likely than in a front-engine installation.

The second front-wheel drive layout is interesting and indeed much less common than the first. This has been used in Honda (Acura) and Audi vehicles. Although it does little to shorten the length of the front of the vehicle (engine bay), it does reduce the intrusion of the drivetrain into the cabin of the vehicle and allows for the use of a larger engine than can be packaged transversely.

In brief, it can be seen that the main gear box is invariably attached directly to the engine, with then some sort of connection between the output and the wheels. In the case of front-wheel drive vehicles, this is quite straightforward and involves nothing more than the use of driveshafts. However, in all-wheel drive vehicles, the connection to the wheels is not so straightforward and requires the use of a transfer gear box and final drive units or axles. This can be seen diagrammatically in Figure 10.4. The following sections will review these different parts of the system and some of the different designs used in each area.

The most basic versions of the drivetrain are two-wheel drive. By definition, these drive either the front or rear wheels of the vehicle. The essential advantage of these layouts is the cost and the commonality across different vehicles. On cars, it is not unusual for different models or even different manufacturers to share common engine and gear box assemblies. This drives up production volumes and thus reduces the cost base of the vehicle. In the truck industry, specialist gear box manufacturers supply standard units to a range of vehicle original equipment manufacturers (OEMs). In this way, specialist vehicles can be manufactured for certain applications without the high investment costs associated with manufacturing transmission units specifically for that one vehicle.

Two-wheel drive is sufficient for small- and medium-sized vehicles that operate on roads or firm surfaces. Driving two of the wheels is not sufficient where a vehicle needs to operate in difficult terrain or is used for heavy-duty operations (such as towing) or for larger trucks. If only two wheels were used in such situations, then insufficient traction would be available from those two tires alone to propel the vehicle. Figure 10.4 shows an all-wheel drive layout as may be found on a 4×4 (sport utility vehicle) or small off-road truck.

In this example, the transfer gear box is fitted directly behind the main gear box and provides the facility to drive the front and rear wheels. In doing so, permanent, full-time, four-wheel drive systems and part-time, two-/four-wheel drive systems are possible. The disconnect for part-time four-wheel drive would be found within the transfer gear box. For example, for heavy-duty vehicles, the traction required on steep gradients requires a lower ratio than normally provided by the main gear box. This is discussed more fully later, but suffice to say here that some transfer gear boxes will have two gears—a high and a low range.

Shafts are then used from the front and rear of the transfer gear box to drive the axles. These axles can be either rigid, “live” axles or independent suspension arrangements. The latter have the inherent advantage that the final drive unit is fixed to the chassis of the vehicle, are hence kept “out of harms way”, and do not contribute to the unsprung mass of the vehicle. In defense of the live axle, it should be said that some engineers would prefer this arrangement off-road because the axle is inherently robust and keeps the rotating components enclosed. Of course, this would also help to keep those components lubricated, and the number of rotating shaft seals is reduced from seven to three. For reference, a live axle is one in which the wheels are driven, as opposed to a “dead” axle where the wheels are undriven.

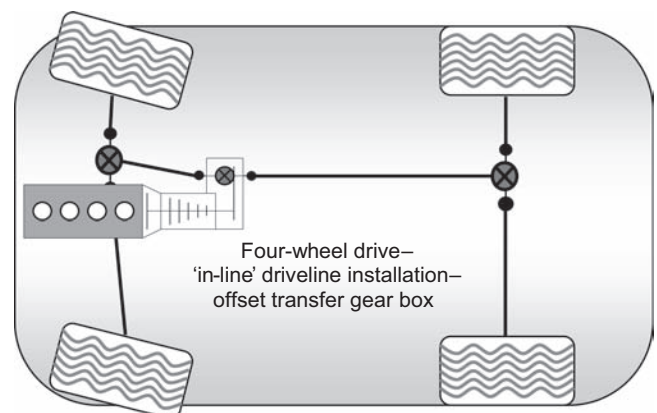


Figure 10.4—Four-wheel drive—drivetrain layout showing gear box, transfer gear box, and front and rear axles.

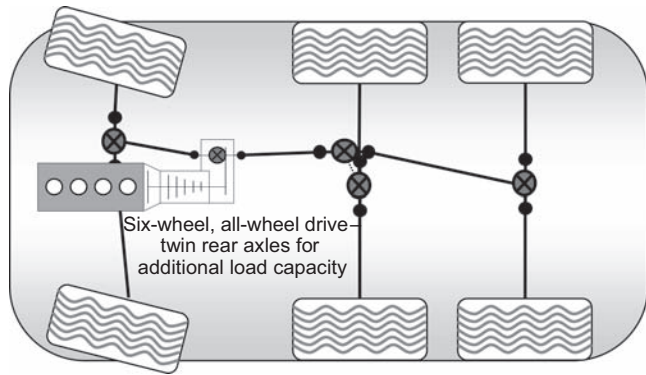


Figure 10.5—All-wheel drive layout typical of that used on military vehicles and some off-road trucks.

The concept can be extended to more axles if the vehicle requires this. This is common in off-road trucks because they require several axles to distribute the load of the vehicle onto more than four tires and equally need most, if not all, of them to be driven. Figure 10.5 shows how this could be achieved on a 6×6 vehicle. Differentials are located within the transfer gear box and axles as indicated by the crossed circles on the figure. In permanent, all-wheel drive systems, the wheels need to be allowed to rotate at slightly different speeds when the vehicle is, for example, driven around a corner. This means that the inner wheels during cornering rotate slower than the outer wheels that have further to travel in any given time. The same principle applies to front and rear wheels because the front of a vehicle travels further than the rear. Long, articulated trucks demonstrate this well if observed while traveling around a bend or turn. Following this discussion one step further, it can be seen that on a 6×6 vehicle such as that illustrated here, the middle and rear axles need a differential between the axles. This interaxle differential is often located within the middle axle, allowing a difference in speed between that and the rear axle.

10.2.2 Trends in Transmissions and the Drivetrain

Having provided a brief overview of the parts of the drivetrain system, it is perhaps useful to observe some of the trends within the industry and suggest what effect they may have on the engineering and design.

10.2.2.1 HYBRID VEHICLES

With the commentary in the press regarding hybrid and electric-drive vehicles, it is difficult to avoid this discussion. Although outside of the scope of this chapter, it is worth observing that some, if not most, hybrid and electric vehicles will contain some mechanical transmission system. Although vehicles have been produced using in-wheel hub drive motors, many organizations and engineers think this not the appropriate way to proceed; therefore, many concepts and vehicles retain much of the system being discussed in this chapter. This is the case in the passenger car and heavy-vehicle industry. From the perspective of the lubricant, the operating temperature of some of the components will certainly present interesting challenges to the engineer and would perhaps be worth consideration in another forum.

10.2.2.2 OPERATING ENVIRONMENTS

The environments within which transmission units operate have much higher operating temperatures than those experienced by the equivalent vehicles from, say, the 1970s and before. The drivetrain and chassis on these earlier vehicles would have had much more “open” architectures that allowed a greater airflow around the transmission than we find today. There are probably a few reasons for this, but we can point to greater packaging efficiency being one key factor, thus leading to less space around the engine and gear box. In addition to this, the more careful management of noise emissions on vehicles has led to covers and noise shields being used underneath vehicles to manage the radiation of noise. These shields can reduce the airflow around the gear cases and therefore reduce the natural heat loss. This needs to be managed, but along with these changes, the industry has seen a significant growth in engineering capability. For example, modern computational fluid dynamics (CFD) systems allow for accurate airflow prediction before the vehicle design is complete. Thus, the airflow over the gear box, final drives, etc., can be managed to maximize the cooling effect where possible. Again, operating temperature is a key aspect within the lubrication system. One vital fact is that the lubricant is the essential element in the cooling system. It will transfer the heat generated in the gears and bearings to the gear cases or cooling system. It is for this purpose that most of the fluid is required; only a very small amount is needed to provide the fluid film within the lubricated contacts.

10.2.2.3 TORQUE CAPACITY

Nobody reading this book will need to be told that vehicle engines have become far more powerful as time has progressed. It is probably outside of the scope of this chapter to attempt to chart this increase, but we only need to compare a typical family car from the 1970s with perhaps 60 kW (~80 hp) to one from today with perhaps double or even triple that figure. In parallel with this increase in engine power we have seen the capacity of transmission units increase significantly for any given size. For this to happen, we have, of course, seen an improvement in materials, gears, bearings, and lubricants. In addition, the manufacturing accuracy, consistency, and hence quality has improved significantly.

10.2.2.4 PACKAGE SIZE

One example to illustrate this is the package of transverse gear boxes in front-wheel drive cars. The increasing emphasis on crash protection has been driven by many issues, including the NCAP independent testing in Europe and similar testing in North America. This has led to vehicle structures having to become stiffer and probably straighter at the front of the vehicle around the powertrain assembly. As this has occurred, the overall width available within the engine bay has reduced for a given width of car. This trend has probably not been assisted by the increase in tire sizes that has also occurred during the same time period. These structural developments within the chassis of the vehicle have led to narrower engine bays and therefore less space for the powertrain across the car.

10.2.2.5 OTHER DEVELOPMENTS AND OBSERVATIONS

All of these developments have an effect on the lubrications system and the choice of oil that has to be made. To complete this aspect, it is probably worth including a few other trends:

- *Quality systems:* These have undoubtedly reduced variation in the product and helped in increasing the demand from designs—less spare capacity in the design perhaps.
- *Service intervals have increased:* This means the lubricant has to remain in the unit longer.
- *Fill for life:* An extension of the above point—some transmission units are designed to retain the lubricant for the design life of the vehicle.
- *Size increase on vehicles:* For any one family of vehicle (particularly passenger cars), it can be seen that the size and weight has increased. Largely because of customer demand, this has increased the load on the drivetrain system.

10.2.3 The Gear Box

Earlier in the chapter, the observation was made that the gear box needs to have a range of ratios to allow the engine to operate at different speeds relative to the wheels of the vehicle. The overall ratio also reduces the speed of rotation because the engine tends to produce a higher speed at lower torque than required to drive the vehicle. In this section, the development of the manual gear box will be considered. Automatic gear boxes are considered in Chapter 15.

Very early on in the development of the automobile, the different gear ratios would be selected by moving the whole gear along the shaft to engage with the mating gear on the next shaft. This can be seen in Figure 10.6. This was a very crude method of gear selection that relied on significant driver skill or brute force to select different ratios. Here, the engine drive is at the top of the picture, starting with the bevel gear pair that turns the drive through 90°. The intermediate shaft then carries four gears, two of which slide along the shaft to allow engagement with the appropriate gears on the output shaft (shown along the bottom of the picture).

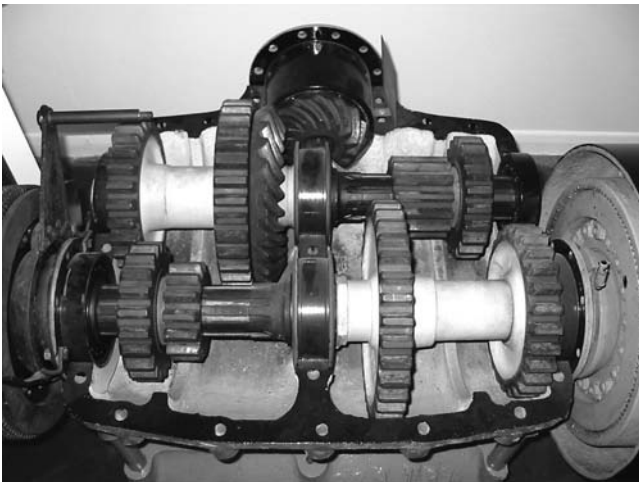


Figure 10.6—A historic gear box out of a T34 tank showing sliding gear selection for the different gear ratios.

Clearly, the need to be able to change ratio within the gear box is vital; therefore, the automotive industry very rapidly developed the synchromesh gear box to overcome the significant limitations of sliding gear ratio engagement [1,2]. Because of the packaging of the drivetrain in different configurations for different vehicles, as discussed earlier, essentially two types of gear boxes evolved: the transverse and the longitudinal, in-line gear boxes. In many texts, this type of gear box is referred to as the “manual” gear box. As will be seen, with automation of the gearshift and clutch, it is debatable whether the word “manual” is now appropriate for this area of automotive technology.

The following section introduces the transverse and in-line designs of gear boxes. It is reasonable to say that the transverse gear box is more widely used on small vehicles and the in-line gear box used on larger vehicles. Of course, there are exceptions to this general rule. Section 10.4 of this chapter will expand on the need for different ratios within the gear box. Until a few years ago, the trend worldwide was for a lower percentage of manual/synchromesh gear boxes to be fitted, but the percentage of automatic gear boxes was increasing. Although traditionally a predominantly manual market, even Europe was seeing this trend, and the larger cars increasingly became fitted with automatics. With the increase in automated synchromesh gear boxes (especially the dual clutch transmission), it will be interesting to see how the market develops over the next decade.

10.2.3.1 SYNCHROMESH GEAR BOXES

With the synchromesh gear box, the driver has to change between one gear ratio and another (ignoring for one moment the more recent automated versions). The different gears have different ratios that allow different relative speeds between the engine and road wheels. As has already been stated, there are several distinct types of these transmissions, including “transverse” or “transaxle” front-wheel drive gear boxes and “in-line” gear boxes used in rear- and four-wheel drive vehicles. These gear boxes have the following advantages:

- Usually have high mechanical efficiency,
- Arguably the most fuel-efficient type of transmission (when driven well),
- Relatively cheap to produce—possibly only half of the equivalent conventional automatic,
- Lightweight—typically 50–70 % of the equivalent automatic, and
- Smaller and hence usually easier to package in the vehicle.

Disadvantages of these advantages include

- Some driver skill required (ask anyone who only drives automatic cars),
- Emissions and fuel consumption can be heavily influenced by the driver’s gear selection,
- Clutch operation and changing gears can be tiring and annoying in heavy traffic, and
- Some drivers find it difficult or even impossible to use a manually operated, synchromesh gear box.

Figures 10.7 and 10.8 show the gear layout and general principle of the transverse gear box. More complex versions of the gear box also exist with two alternative intermediate gear shafts. These allow a little more flexibility with the gear ratios and can have a shorter package length. The lubrication

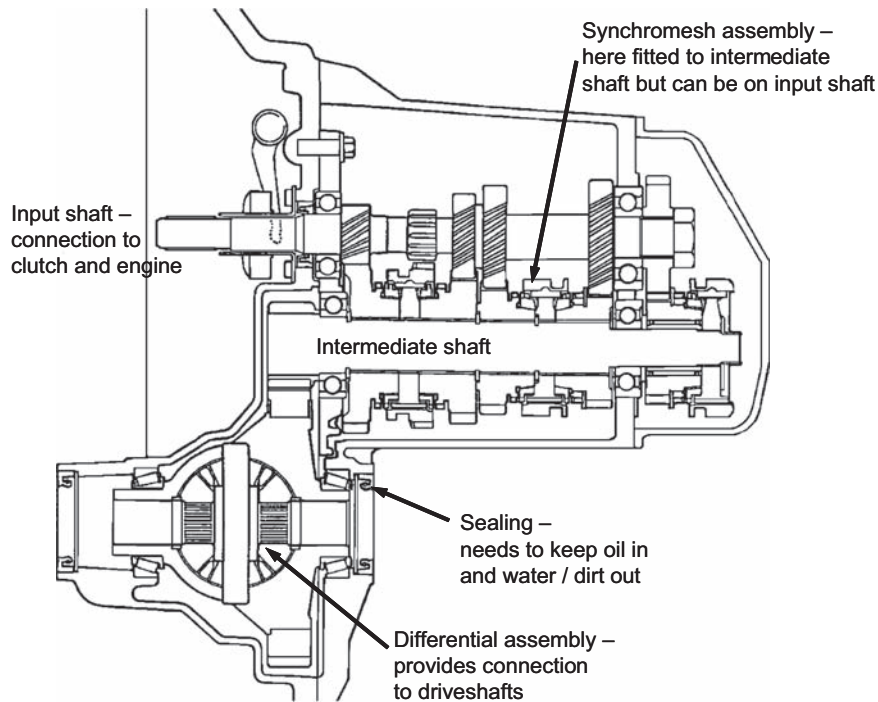


Figure 10.7—Schematic of a transverse synchromesh gear box.

of the gear box is usually by splash or oil bath lubrication. Rarely do these gear boxes have oil pumps unless they require external oil coolers. One care point with the oil system is ensuring that the upper parts of the gear and bearing system get lubrication as soon as the vehicle starts. The differential assembly and final drive gear are often rather lower than the input gears and the oil bath is around these gears. Hence, when the vehicle is stationary, even with the engine running, the intermediate shaft and differential shaft will

also be stationary. This will depend on the position of the synchromesh assemblies, although the example illustrated would have this situation because the synchromesh is fitted on the intermediate shaft for all of the gears. The synchromesh mechanism is discussed in Section 10.3.

The type of gear box illustrated in Figure 10.9 is used in longitudinal powertrain installations. In some cases, as here, a transfer gear box is fitted to the output of the main gear box to allow all-wheel drive to be utilized.

The picture in Figure 10.9 is useful (despite the gear box being rather old) because it illustrates that the use of sliding gear engagement persisted on reverse (and sometimes first gear) through to the 1960s and 1970s. The use of spur and helical gears can also be seen in the transfer gear box section of the unit on the right-hand side. The spur gears

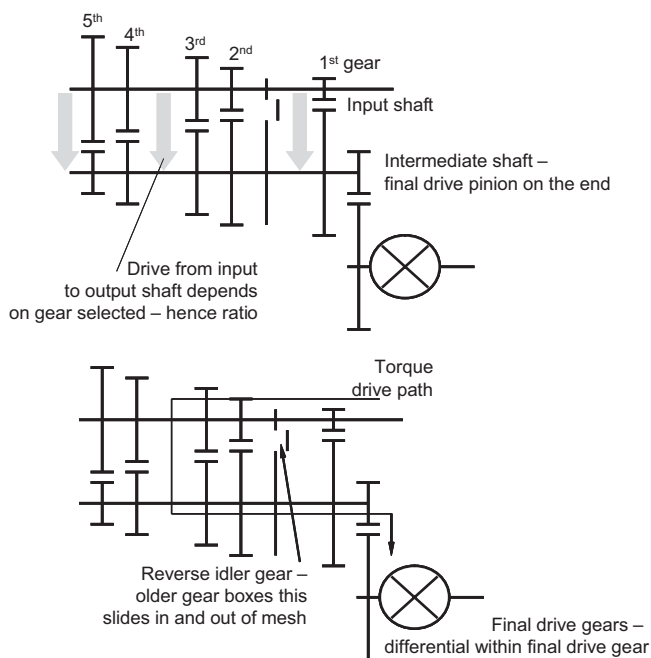


Figure 10.8—Diagrammatic representation of a transverse gear box such as illustrated in Figure 10.7.

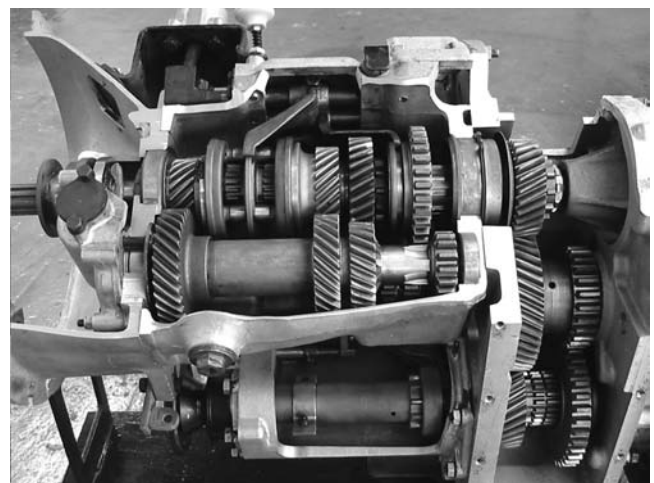


Figure 10.9—Cutaway gear box and transfer gear box assembly from an early Land Rover vehicle (circa 1970).

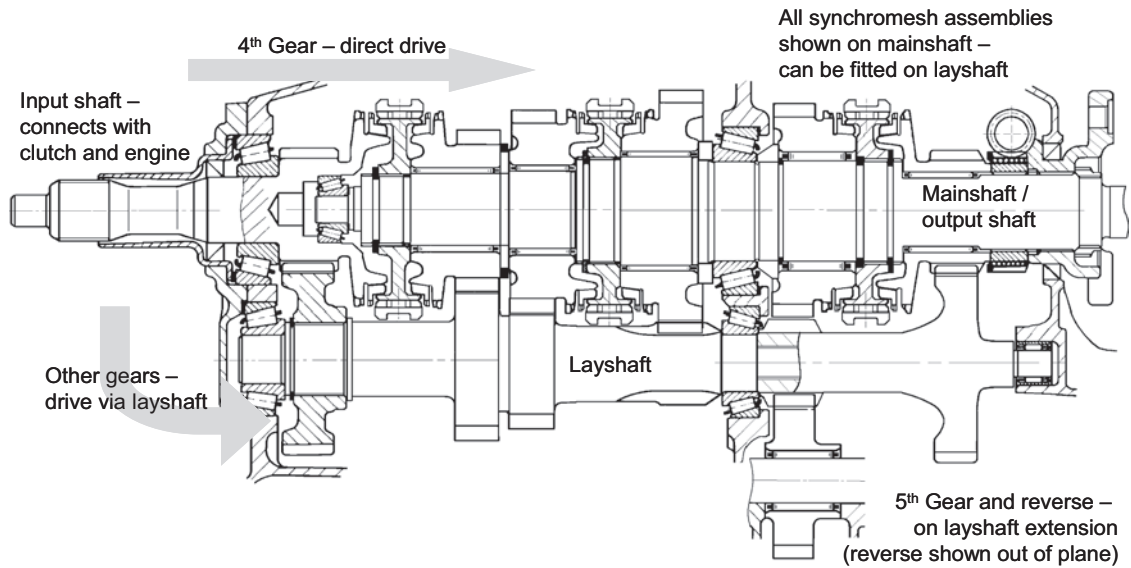


Figure 10.10—Cutaway diagram of an in-line synchromesh gear box.

are used for the low range ratio because the additional noise created by their use would have been acceptable to the customer in that era. The lubricant in these gear boxes was often the same as the axle, typically an extreme pressure (EP) 90 grade. Although not ideal for the gear change/synchromesh, it would have given adequate protection to the gear surfaces. Some years ago, the use of engine oil in some gear boxes would also have been considered normal despite the lack of appropriate additives for gear box use. Today, most synchromesh gear boxes would use a lighter oil, possibly an automatic transmission fluid (ATF). The

manufacturers and oil companies are increasingly developing manual transmission fluids that are similar in viscosity to ATFs while having an additive package more suited to the synchromesh mechanism.

Recent in-line gear box designs have allowed the use of constant mesh, helical gears for all gears, including reverse. In such designs, synchromesh is also fitted to all gears. Figure 10.10 shows a typical layout, whereas Figure 10.11 indicates the principles of operation. It is interesting to note that traditionally fourth gear was the direct gear, as illustrated. This does not have to be the case, and some

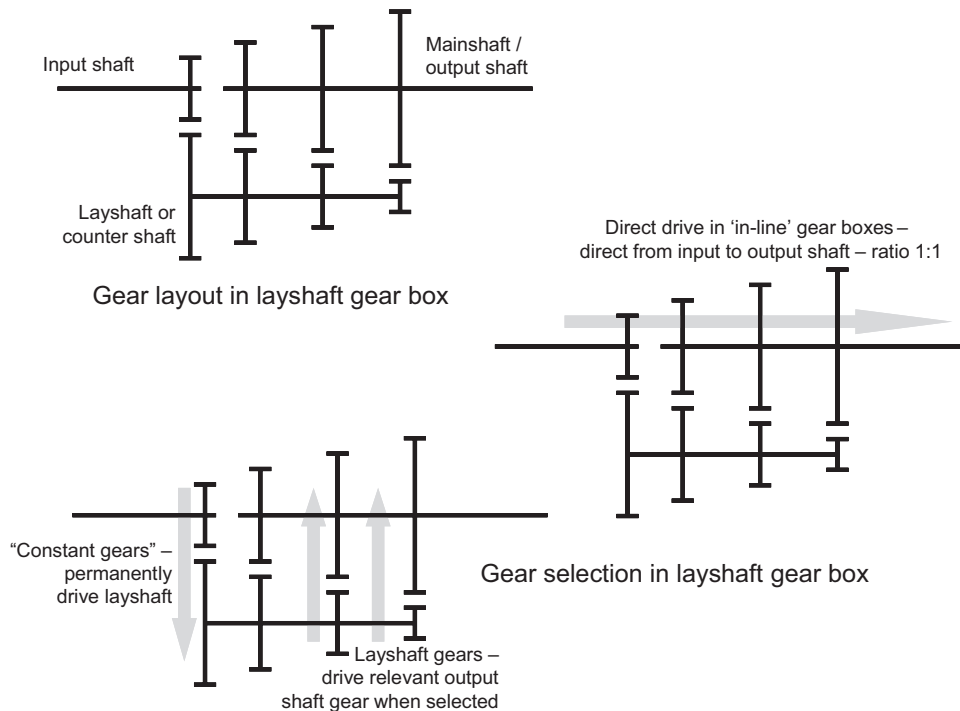


Figure 10.11—Diagram to show power flow through gear box.

manufacturers have configured the unit so that fifth gear is 1:1. This is the most efficient operating point for the gear box and can lead to slightly better fuel consumption on the open road. As with the transverse gear box, more than one layshaft can be fitted to give a wider range of ratios, and this is often done on versions for heavier vehicles. Again, similar to the transverse gear box, the gear box is often dip/splash lubricated. However, with this type of gear box construction, whenever the gear box input is rotating, the layshaft is also rotating and is therefore able to distribute the oil around the gear box. Testing with clear gear cases, as illustrated in Chapter 16, can show where the oil is moving and if any parts of the gear box are running with little oil.

Figure 10.12 shows the gear and synchromesh arrangement in an old in-line gear box. In this closer view, synchromesh assemblies can be seen on second gear, third gear, and the direct gear selection (fourth gear). This is discussed later. Again, spur gears can be seen used for first gear; as a result, selection of first would have been difficult unless the vehicle was stationary. The gear box is this time from a Morris unit dated around the early 1960s. The gear box would be installed in the vehicle with the layshaft (lowest gears in the photo) in the lowest part of the casing. This would ensure good distribution of the oil around the gear box.

This dip lubrication means that there is no real need for pressure-fed oil supply as in an automatic or continuously variable transmission (CVT) gear box; therefore, there is no hydraulic system as such. However, some gear boxes may have small oil pumps to ensure lubrication of components that are installed in the gear box well above the normal oil level or to supply external oil cooling systems. These oil pumps only operate at very low pressures and as such will not affect the parasitic losses to any significant degree.

10.2.3.2 AUTOMATED SYNCHROMESH AND DUAL CLUTCH GEAR BOXES

The detail of the design is not really required in this chapter because the lubrication principles are similar to conventional synchromesh gear boxes. However, the compactness of many of the designs does mean that there is possibly an increased likelihood of needing external cooling. This



Figure 10.12—Another gear box from the same era as Figure 10.9.

would clearly be considered during the specification of the lubricant. One engineering problem that is eased is the shift feel. Additives can have an effect on the operation of the synchromesh, and the customer can perceive this when manually changing gear. What manifests itself as a roughness during the gear shift can be improved by different oil selection, although objective testing can be complex. By taking away the human interface of the gear selection mechanism, this subjective “roughness” may not be a problem at all.

Figure 10.13 shows the move from the early sliding gear, nonsynchronized gear boxes, such as the T34 tank gear box shown earlier, through to the latest dual clutch “automated manual” gear boxes. The latter are becoming ever more popular today because, arguably, they offer better efficiency and a lower cost base than conventional automatic gear boxes. The cost advantage of the simple automated manual gear box, retaining a conventional single-plate dry clutch mechanism, will probably ensure that this type of gear box continues in vehicles where cost is key to the marketing effort. As dual clutch gear boxes develop, they appear to be successfully replacing not only manual gear boxes, but also conventional automatics. The key aspect the dual clutch arrangement provides is the ability to perform a “hot shift”. This is where the two clutches allow a gear ratio change without any discontinuity of power delivery by swapping the drive from one clutch to the other. This provides better performance and better shift comfort.

10.2.3.3 TRANSFER GEAR BOXES

Many vehicles have a switchable all-wheel drive system in which while on the road the vehicle will be driven through just (usually) the rear wheels. Once mobility over loose terrain is required, the driver can then engage the drive to the remaining wheels. This obviously provides greater traction. There are many different options and embodiments of this system depending on the vehicle type, function, and manufacturer. One trend it is probably reasonable to point to is that on smaller 4×4 vehicles (passenger car type and small pickups), more and more manufacturers are producing permanent all-wheel drive systems. These essentially simplify the system for the driver and provide the additional grip in adverse conditions without any manual intervention. However, larger, all-wheel drive trucks and military vehicles are tending to retain the ability to disengage drive to the front wheels. These are therefore driven on normal, hard surfaces in rear-wheel drive, albeit this may still mean that drive is applied to more than one axle if the truck has three or four total axles.

10.2.4 Driveshafts, Propeller Shafts, Driveshaft Joints, and Final Drives

Several other vital components and subsystems are required to complete the driveline on a vehicle in addition to the gear box itself. These include

- Driveshafts for front-wheel drive;
- Driveshafts for rear engine/rear-wheel drive cars;
- Propeller (“prop”) shafts, which are used on rear-wheel and four-wheel drive vehicles;
- Axles—rear-wheel drive, front-engined vehicles;
- Transfer gear boxes—four-wheel drive vehicles; and
- Driveshaft joints—component parts of the various types of shafts.

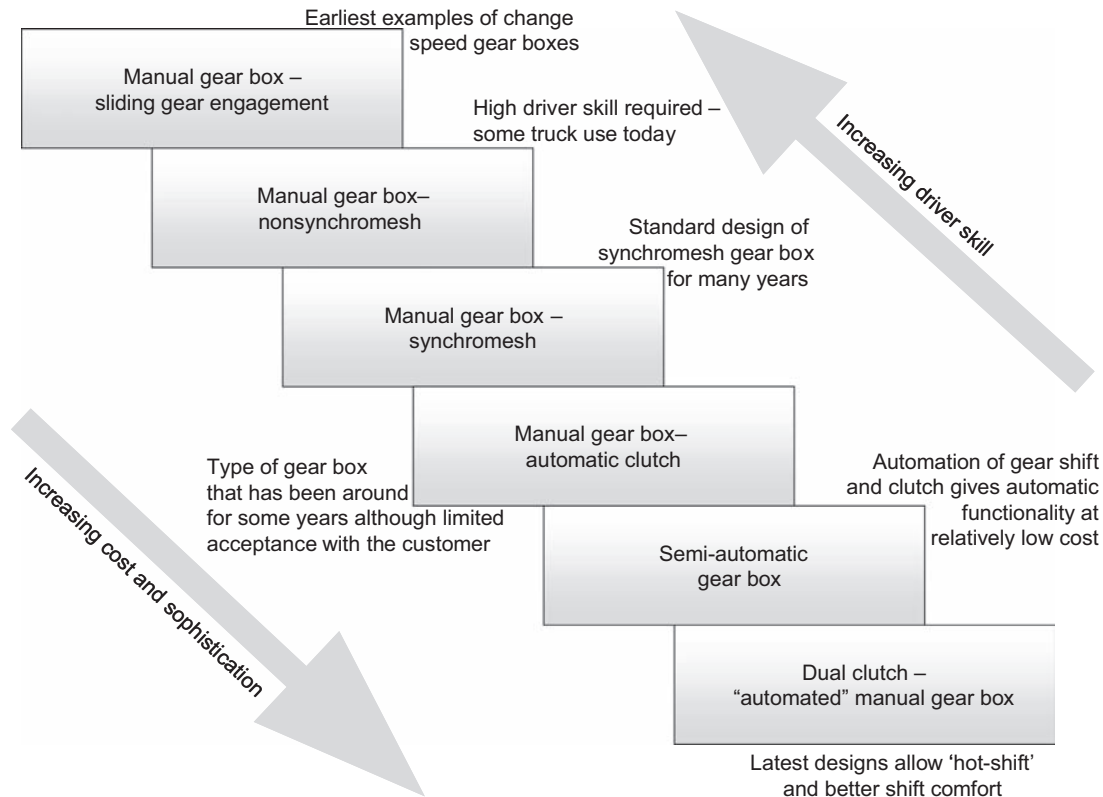


Figure 10.13—Gear box design and development trends.

10.2.4.1 DRIVESHAFTS

To allow for relative movement between the powertrain assembly and the wheel, the driveshaft has to allow for changes in the operating angle of each joint and for changes in the length of the shaft. The latter is normally referred to as “plunge” and is allowed for by letting a section of the shaft or

one of the joints slide axially as well as articulate. The inner and outer driveshaft joints operate at different angles. As the inner joints commonly operate at smaller angles they also allow for any length variation in use. This is referred to as “plunge.” Therefore, the outer joints only have to accommodate angular articulation and can then allow for the steering

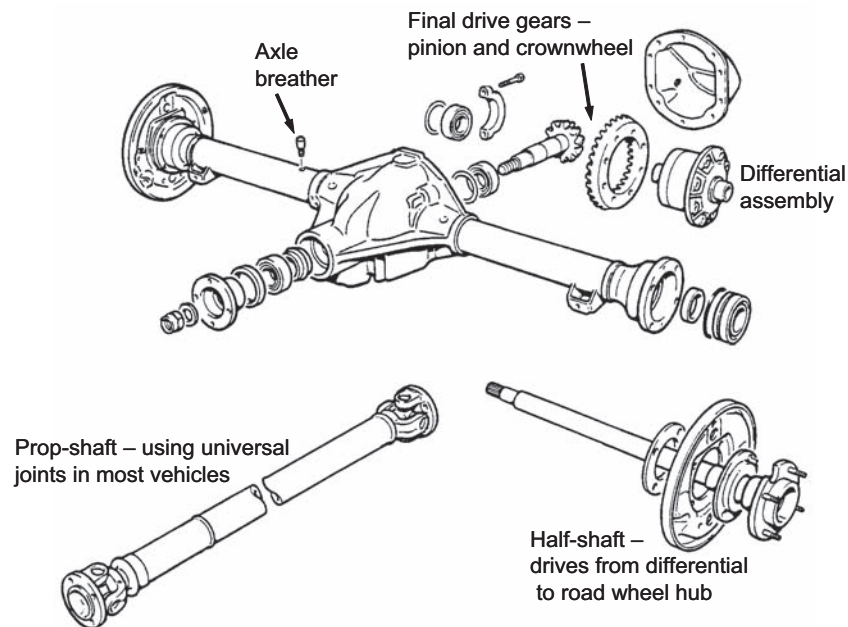


Figure 10.14—Axle and prop shaft components from a rigid axle vehicle.

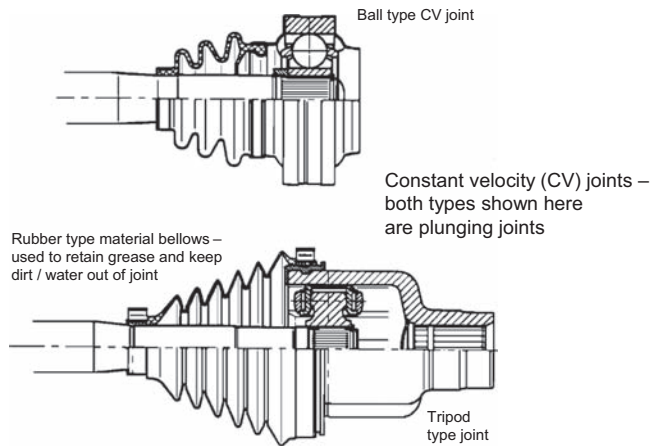


Figure 10.15—Constant velocity joints.

angles that occur at the hubs. Typical angles at the gear box end of the shaft are approximately 20° whereas those that occur at the hubs can be in excess of 45° at their maximum. The driveshaft joints are lubricated for life on most modern vehicles, and therefore, the sealing bellows retain the grease required and prevent contamination from outside.

10.2.4.2 PROPELLER ("PROP") SHAFTS

These transmit the power along the vehicle, typically from gear box to axle, in four-wheel drive and rear-wheel drive vehicles. They have historically used simple universal joints. However, the use of constant velocity joints (CVJs) has more recently increased because of the better refinement they can provide. Using simple universal joints introduces cyclic speed fluctuations. The use of two universal joints can theoretically eliminate or reduce this. Alternatively, CVJs can be used. The components shown in Figure 10.14 are the prop shaft and rigid axle such as may be used on a truck or utility 4x4 vehicle. In the past, such designs would have also been found on smaller, passenger

cars as discussed in the first section of this chapter. The prop shaft shown has universal joints fitted.

CVJs are becoming more widespread within the industry (Figure 10.15). As their design has developed, it has been made able to cope with higher powers and heavier vehicles. There is also a trend to replace the traditional universal joint on the central prop shaft. This is particularly the case on 4x4 vehicles as customer demands call for better noise and vibration levels.

Independent suspension is being used on far more vehicles today than in the past (Figure 10.16). In the 4x4 market, the demand for better refinement and handling is driving this trend and can be seen on the latest Land Rover, Volvo, and Mercedes off-road vehicles. More utilitarian 4x4 vehicles have also seen this on front axles in some cases, although many retain a live, rigid rear axle to support the higher payload at the back. This trend can also be observed in the truck market, although to a lesser degree. One manufacturer using independent suspension quite widely on trucks is Oshkosh, the military trucks of which use double wishbone suspension. Some engineers consider independent suspension beneficial for off-road mobility, and it can certainly improve ride quality because of its lower unsprung mass. However, one comment often made is that as both wheels can move up on the suspension, this can allow the center of the chassis and the final drive assembly to hit the ground (i.e., the central ground clearance is not constant as it is with a rigid axle).

While discussing final drive units, it should be noted that they contain final drive reduction gears and the differential assembly. It is easy to overlook the role of the reduction gears because they clearly need to turn the drive through 90° to drive the wheels and reduce the speed of rotation significantly to turn the wheels at the required rate. Of course, the differential has a different role, as discussed earlier.

The differential gears can be difficult to see on many real units, so the model in Figure 10.17 shows the separate components more clearly. The side gears are connected to

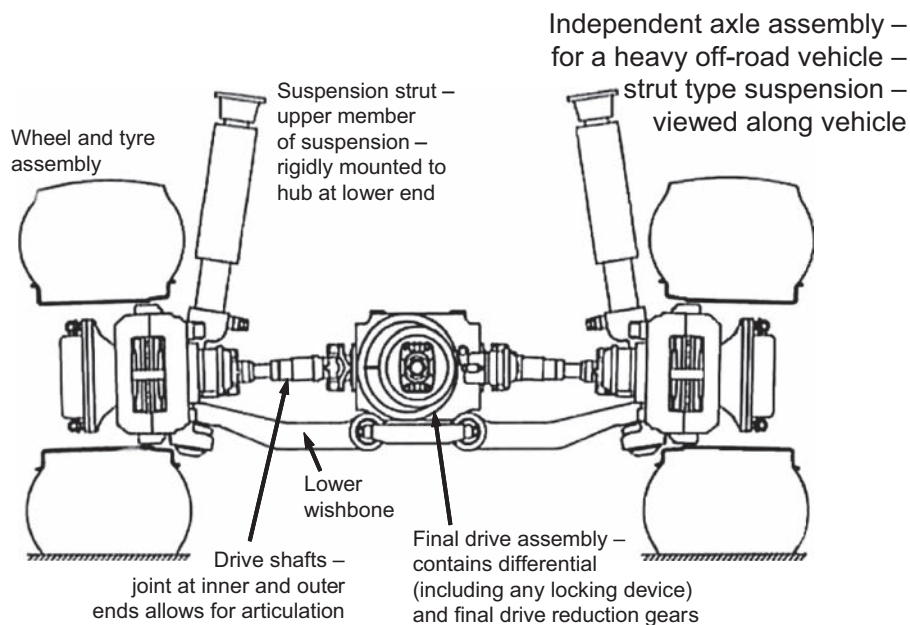


Figure 10.16—Independent axle from a heavy truck using strut suspension.

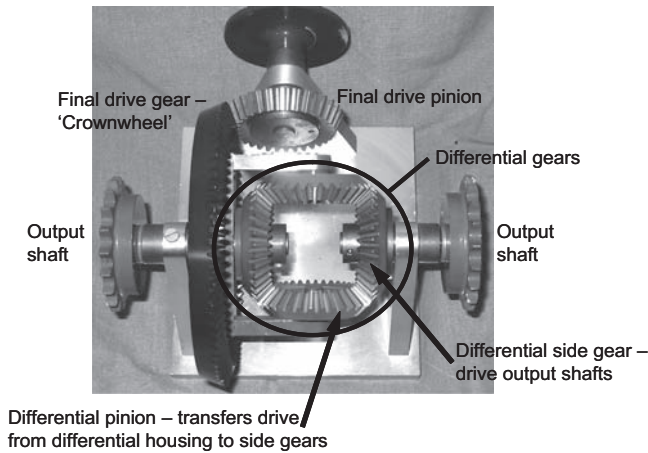


Figure 10.17—Photo of a model final drive and differential assembly.

the half shafts driving the wheels when the differential is fitted within an axle. The lubrication issues depend on the choice of final drive gears. Below a ratio of approximately 3.5 to 4:1, spiral bevel gears can be used whereas higher ratios require the use of hypoid gears. The higher relative sliding speeds within the hypoid gear mesh mean that an oil with a better EP performance is required. The detail of this lubrication regime is covered in another chapter.

To summarize, there are many types of axles used for different vehicles; however, the main requirements of axle assemblies are

- Allow the drive to turn through 90°.
- Support the required mounting and suspension positions and loads.
- Allow the wheel and hub assemblies (on independent suspension) to move with the suspension.
- On live, rigid axles, the whole assembly needs to move in response to loads at the wheels vertically (bounce) and to articulate (roll).
- Support the wheel hub and brake assemblies.
- House the differential assembly, which is located within the final drive bevel gears.
- Allow differential speeds between the wheels on opposite sides of the vehicle.
- Limited slip or torque biasing differential assemblies can also be used on performance or off-road vehicles. These reduce or eliminate wheel slip, which would reduce the performance of the vehicle.

10.3 DISCUSSION—GEARS, BEARINGS, AND SYNCHROMESH ASSEMBLIES FOR DRIVETRAIN UNITS

To delve deeper into the implications for lubricants within the drivetrain, some discussion is required on the components that go to make up the transmission units. More detail on the bearings is contained within Chapter 9 and the gears within Chapter 11. For completeness, the use of spur and helical gears will be considered here because those are used widely within the gear boxes discussed in this chapter.

The use of spur and helical gears can be clearly seen in Figure 10.18. The use of spur gears is very limited today because of the noise associated with them. The lower

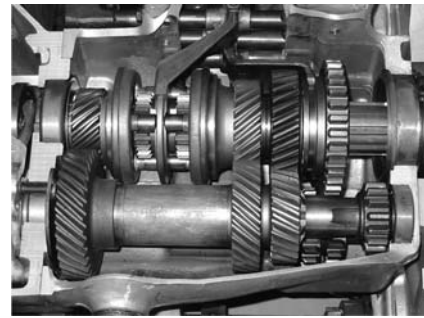


Figure 10.18—A closer view of the Land Rover gear box shown in Figure 10.9.

transmission error associated with helical gears, especially when under load, is key to reducing the vibration produced within the gear mesh. It is this vibration that is transmitted through the shafts, bearing, and casing into the vehicle structure. The customer will perceive this as noise, and as customer expectation increases, this noise becomes less acceptable. Helical gears are better at giving lower transmission error under a wide range of loads as the helical teeth allow the contact condition to adjust with the load. The load will deflect the tooth shape, effectively introducing errors, and spur gears are less accommodating of this deflection. As may be imagined, there are drawbacks associated with helical gears. A minor point is they may be a little more expensive to produce, although this is debatable. In addition to this, helical gears need to have a reasonable face width to allow for the overlap on the helical teeth without using very large helix angles. In the extreme, it is not worth producing helical gears on narrow face width gears because there would be no overlap of the helix. This is sometimes the case within motorsport gear boxes because the gears tend to be of large diameter and small face width.

The other key components are the bearings. If we look back in history, plain journal bearings would be found in a range of transmission units; however, it would be fair to say that rolling element bearings are used almost universally today, although they do produce axial loading onto the gear shafts. This cannot be ignored and means that the bearing system must be designed to accommodate these loads. Looking back at Figures 10.7 and 10.10, two bearing arrangements can be seen. Modest axial loads can be accommodated by “normal” deep groove ball bearings; therefore, as long as the axial load is within limits, these bearings can be used, as shown in Figure 10.7. These bearings tend to be less costly. Once the proportion of axial load to radial load increases, the use of different bearings is required. These can be taper bearings as shown in the longitudinal gear box in Figure 10.10 or angular contact bearings. As mentioned, Chapter 9 contains more information.

10.3.1 Gears

The design of the involute gear can be something of a mystery, but a brief explanation is useful in understanding the demands of the lubrication system. Although other gear tooth shapes are used for some types of gearing, automotive transmissions use the involute. The involute system has several advantages:

- Provides continuous smooth drive from one shaft to another;
- Flexibility in manufacture, allowing several dissimilar gears to be produced from the same tooling;
- Standard system allows easy specification and dimensioning [3]; and
- Internationally recognized and used.

10.3.1.1 BASIC GEAR GEOMETRY—AN INTRODUCTION

This section will introduce the design of spur and helical involute gearing. The main requirement of any gearing is to transmit uniform motion from one shaft to another. Of course this can be done by other means, such as a belt drive. Considering the action of the belt as it unwraps from one pulley and wraps onto another (as in a crossed belt drive perhaps) can provide an understanding as to how the involute curve is formed.

10.3.1.1.1 The Involute Curve

This is the basis for most gearing and can be defined as the curve that is described if a line is unwrapped from a circle (called the base circle). Each of the tangential lines taken from the base circle is the same length as the part of the circumference of the circle between its contact with the circle and the origin of the curve (Figure 10.19). Virtually, all gears used use the involute principle.

Figure 10.20 shows two involute teeth in contact as they pass through the gear mesh. The tangential line represents the line of action of the gears (i.e., the contact point for the two gear teeth as they move through the mesh). The contact point can be seen to move as shown on the diagram:

Start—root end of the driving gear contacts the tip end of the driven gear

→ end—tip of driving gear contacts the root end of the driven gear.

The contact occurs with a mixture of rolling and sliding. At the midpoint of the contact (where the contact crosses the line of centers), the action is pure rolling. As the contact approaches either end point, the amount of sliding increases. This can be illustrated by considering the

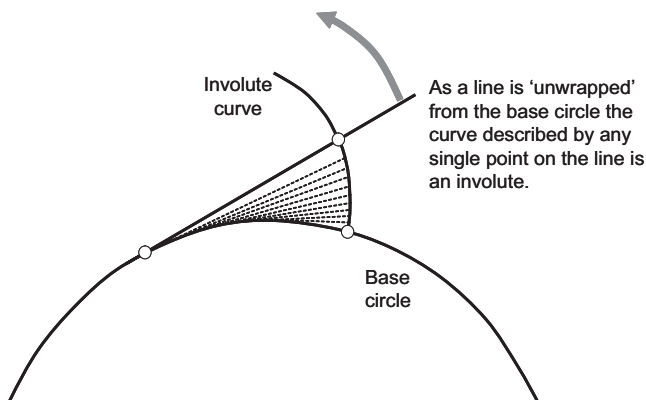


Figure 10.19—Creation of an involute curve by unwrapping a “string” from around a circle (the base circle).

instantaneous direction of motion of the contact point on each gear (Figure 10.21).

In theory, involute gears do not introduce any variation in speed on the driven gear—hence the smooth continuous drive. Of course, in practice, the situation is a little different because deflection under load and manufacturing errors do introduce errors in the smooth rotation and hence noise and vibration. It is this contact condition that the lubricant must cope with. The contact in the center of the contact near the pitch point is nominally elastohydrodynamic lubrication (EHL) and as long as the surfaces of the gears are well finished, lubricated, and the speed of rotation reasonable (above ~5 m/s) [2]. When operating at low speeds, near the tip and root of the teeth, the likely regime will be mixed, or boundary, lubrication. In these conditions, the additives within the oil become important in preventing metal-to-metal contact and possible surface damage.

As can be seen from Figure 10.21, only at the “pitch point”—where the contact between the gears occurs on the line of centers—is there no sliding. In the first half of the gear mesh, the sliding of the surfaces is moving toward each other. As can be seen from the figure, in the second half of the gear action, the sliding at the surfaces is in the opposite direction. In spur and helical gears, the relative sliding speeds are fairly modest. However, in some gear types, significant sliding takes place and the lubricant has to be chosen accordingly. For example, it would be expected that a hypoid gear set in an axle would need an oil with an EP additive in it to prevent wear, surface damage, and possible premature failure.

10.3.2 Bearings—System Design

Most bearing manufacturers produce catalogues that detail the design process involved in choosing a bearing for a particular application. These notes usually start with the premise that the designer has already worked out what type of bearing they want and know the loads. However, starting from the beginning leads to a process that may look something like this:

- At the scheme stage of the transmission, investigate the layout of the shafts, bearing positions, and approximate sizes (usually limiting diameters and widths to fit within the casing).
- Ensure the bearing set can take axial and radial loads from the gears.
- Calculate bearing loads taking into account duty cycle of unit (i.e., the “average” load as well as peak and possible abuse loads).
- Knowing the bearing size, type, and loads, calculate the life of the bearing—compare with the required life of the unit.
- Optimization of the bearing set will be a process that takes into account several factors, including
 - Cost of bearings versus cost effect on other parts of the unit,
 - Package space available,
 - Lubricant and operating temperatures,
 - Production volumes, and
 - Availability/manufacturer chosen, etc.

The latter stages of the process will almost certainly involve the bearing manufacturer(s), and because of the

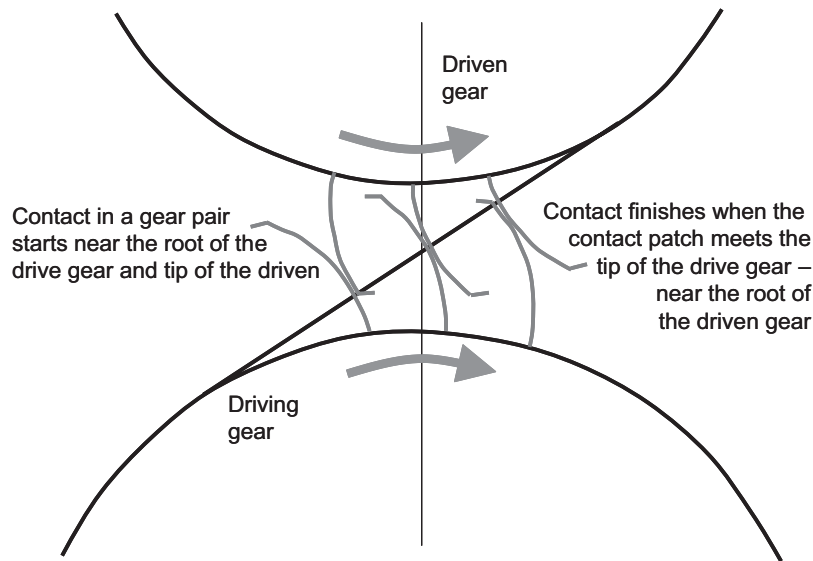


Figure 10.20—Using involute curves gives a smooth continuous drive from one shaft to another.

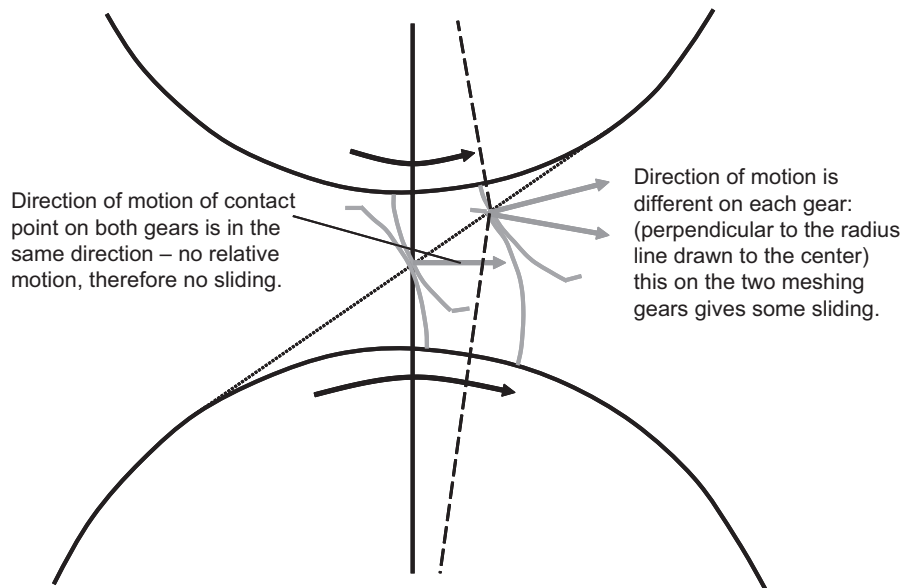


Figure 10.21—Gear motion through the gear mesh.

specialist design packages and detail performance data they have available, this should definitely be encouraged.

10.3.3 Synchromesh Assembly

This section briefly introduces the synchromesh assembly to complete the review of the key components within a manual gear box and to suggest some of the factors related to the lubricant. A starting point for synchromesh design must be the paper written by Socin and Walters [4]. This not only explains the function of the synchromesh used in many gear boxes, but it also takes the reader through the main calculations that may be required during the design of single-cone synchros.

Earlier in the chapter, the power flow through a gear box was described (e.g., in Figures 10.10 and 10.11). In the example here, the mainshaft gears are free to rotate on the shaft unless connected via the synchromesh assembly when

that gear ratio is selected. Figure 10.22 considers the gear arrangement on first and second gear. One fundamental assumption when considering gear changing is that the output stage of the gear box does not alter in speed during the gear shift. During the short duration of the shift, the vehicle will not really slow down or speed up to any great extent as the result of a gear change under normal road-going conditions.

The resultant speeds of the layshaft (and hence the input of the gear box) are different in the two gears. Therefore, in changing gear (e.g., from first to second), the layshaft, input shaft, and clutch must slow down so that the second mainshaft gear can go at the same speed as the mainshaft. It is this speeding up and slowing down of the input side of the gear box that the synchromesh does. The work done by the synchromesh assembly is to change the speed of the inertia on the layshaft, input shaft, and

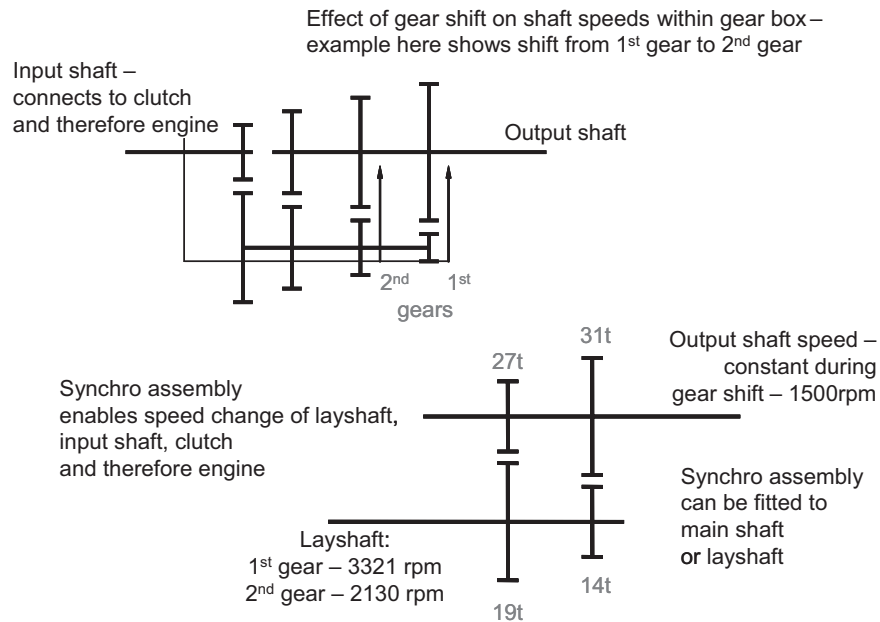


Figure 10.22—Diagrammatic illustration of the different gear speeds during a gear shift.

the clutch driven plate. Most of the inertia is found in the clutch plate.

The diagram below is a cross section of a synchromesh assembly. The baulk ring is essentially a small cone brake, and it is the friction between this and the cone on the gear that completes the synchronization. Of course, this is a lubricated contact and under normal conditions is a fluid film, although in repeated gear changes and under high load the fluid film will break down and the components then rely on boundary lubrication to prevent wear. The additives in the fluid can also have an influence on the gear selection feel and hence the quality of the gear change felt by the customer. In much the same way as clutch engagement is refined for automatic gear boxes (discussed in

Chapter 15), the additive package can have an effect on this aspect of synchromesh performance. One of the key aspects here is the relative values of the dynamic and static coefficients of friction. The dynamic friction is important while the synchronization is taking place (dynamic condition), although during the final engagement with the gear the baulk ring is stationary relative to the gear and then has to move slightly to allow alignment (static condition).

Figure 10.23 shows a single-cone synchromesh for clarity using one friction surface to achieve synchronization before gear engagement. The friction surface is conical in shape and is between the baulk ring and the gear. However, most gear boxes now use double and triple cones (with two and three friction surfaces).

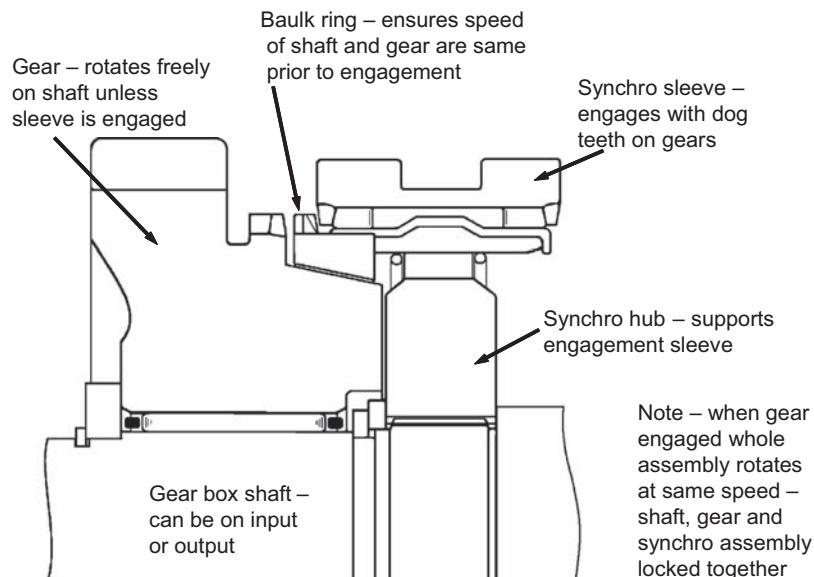


Figure 10.23—Diagram of a typical synchromesh device.

10.3.4 Sealing

Some years ago it would be probably quite normal for a gear box to leak a little. This could have been from the rotating shaft seals or from the joints in the gear box casing. Today, this would be unacceptable to the customer and on environmental grounds. Rotating seals have become much more sophisticated and as a result not only perform better and more reliably but also continue to do so for much greater mileages. Chapter 16 makes some mention of seal testing, and the effect of a lubricant on the seal material is quite key to its performance. For example, many oil-seal material combinations will cause some swelling of the material. It is clearly important to control the degree to which this occurs. Lubricant and seal manufacturers will provide further information on this aspect when required.

The lubricant must be retained within the gear box, but the dirt and water outside also need to be kept outside. One aspect that is easy to overlook is the sealing of the spline on the inside of a drive flange. Oil will easily seep between the two components, and the o-ring shown stops this oil from escaping around the fixing used to hold the flange in place (Figure 10.24).

10.4 DISCUSSION—PERFORMANCE ATTRIBUTES OF THE DRIVETRAIN

10.4.1 Efficiency—A Key Design Aspect for Drivetrain and Drivetrain Lubricants

The efficiency of a transmission is important for two reasons. First, any losses in the system will increase the amount of fuel that the vehicle uses, and second, the lost energy must go somewhere; nominally, this will be in the form of heat. As fuel prices have increased over the last few years, there has been a renewed interest in all forms of technology that improve fuel efficiency, and although the transmission efficiency aspects will only ever be a minor contributor, the improvements are worth doing because in many cases the cost impact may be negligible. The heat input to the transmission unit from any losses also must be

dissipated so that the oil temperature does not continue to climb and ultimately cause damage. The lubricant plays a vital part in the process as it carries the heat from the gear mesh or bearings (where the heat is predominantly generated) to the casings or oil cooler.

There are several ways that this subject can be broken down, including considering the transmission unit as a “black box” that is simply installed in the vehicle so that the overall efficiency of the unit can simply be represented as a percentage. However, this percentage varies greatly as the conditions change within the unit. At steady state, the losses in the unit will equal the heat dissipated. Most of this heat is radiated from the cases of transmission units that do not have external coolers and from the cooler matrix in the case of those that do have such systems (Figure 10.25). As mentioned earlier, the lubricant is actually the coolant in this mechanism.

The variation of losses depends on the operating conditions of the transmission. As already discussed, these operating conditions also vary greatly; therefore, to understand the implications of the efficiency, the use of simulation is arguably essential to fully understand the situation. Such simulation is required because the natural variation within a vehicle during testing makes it very difficult to measure small variations in the performance, especially fuel consumption.

Before continuing with this section, an important point to appreciate is that the efficiency (or losses) of a transmission unit can be considered in three ways:

1. The load (torque)-related efficiency, which occurs largely as a result of the friction losses at the gear mesh and can be considered in the form of a percentage efficiency or loss figure (i.e., a loss of 3 % would be an efficiency of 97 %), whichever is the most convenient.
2. The parasitic losses can be considered to be independent of the applied torque. These losses can be considered to be “negative and speed- and temperature-related torque” and take the form of a resistance within the transmission.

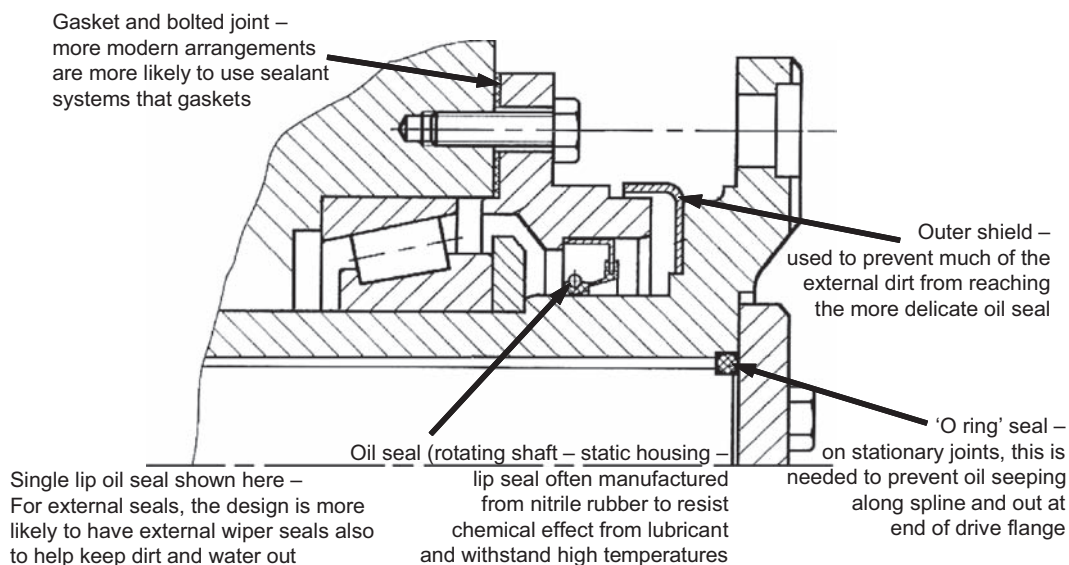


Figure 10.24—Diagram of a typical sealing arrangement on the output of a gear box.

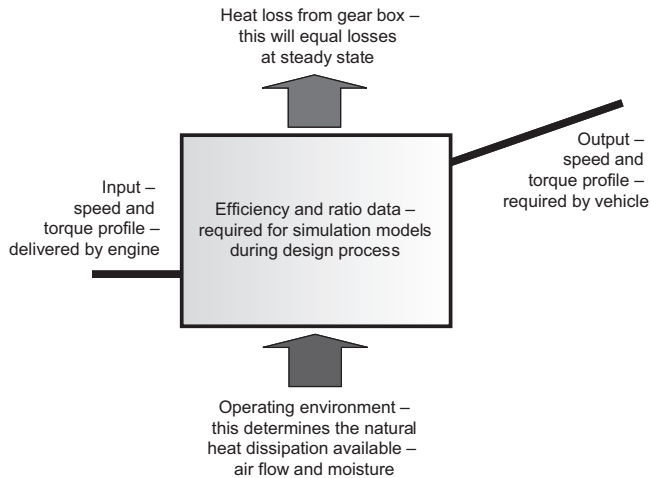


Figure 10.25—Diagrammatic representation of system losses in the form of heat that must be dissipated to ensure that the temperature of the unit does not continually rise until destruction.

3. The slip losses that may occur in transmission elements that do not involve a fixed gear ratio. Where the drive is transmitted by gear pairs, the input/output speed ratio is obviously fixed by the tooth numbers on the gears. Where the drive is transmitted by another means, the output speed is not necessarily a fixed ratio to the input. Such CVT transmissions are considered elsewhere in this manual.

The overall efficiency of a transmission unit needs to take all three aspects into account to arrive at an overall efficiency figure.

Although several authors in the literature consider all of the losses in a transmission together, others have considered either the load-related or parasitic losses in isolation. In common with this approach, we will separately consider the losses. Merritt [3] uses the definitions of oil-churning losses and “tooth friction” when discussing gear losses. He and other authors have chosen to elaborate on the friction losses at the gear mesh and assume that the parasitic losses are small by comparison. However, the parasitic losses can be significant and need to be considered in a wide variety of transmission units. This is particularly the case when the gear box is operated from a cold start, where the lubricant is at or near the ambient air temperature. In winter, this could obviously be well below freezing.

In automatic units, the losses associated with the oil pump are often the largest cause of parasitic loss. When the gear box requires a high oil pressure, the torque required to drive the pump can be a significant proportion of the torque being transmitted. Fortunately, as discussed earlier, most synchromesh gear boxes have no oil pump and typically little loss contribution as in an automatic transmission or CVT.

Most transmission units use rolling element bearings rather than plain bearings. As with the gears, bearings will have load-related friction losses and parasitic losses due to the oil movement rotation of the bearing. For prediction and comparison purposes, the bearing loss can often be treated as part of the gear system losses. It can be assumed that they are small and either constant or behave in a similar way as the gear losses (relative to the “control”

variables of speed, torque, and viscosity). Usually, the bearing losses are considered to be an order of magnitude smaller than the corresponding gear losses.

The efficiency of a transmission unit is particularly important during two operating conditions of the vehicle:

1. *Cold-start, urban drive cycles, low-speed driving, etc.:* The parasitic losses will have an effect on fuel economy because they are significant compared with the traction required by the vehicle.
2. *Heavy-duty use, high speed, towing, etc.:* The friction (load-related) losses are roughly proportional to the torque transmitted and can cause very high heat build-up within the unit. This can lead to very high oil temperatures and even breakdown of the oil or component failure due to thin oil films.

In summary, the loss mechanisms that may be encountered can be described in terms of the three categories discussed above:

1. Load related losses:
 - Friction losses at the gear mesh
 - Load-related bearing friction losses
2. Parasitic losses:
 - Oil churning where gears and shafts dip in the oil bath or rotate in foamed oil
 - Oil entrainment at the point where the gear teeth enter the mesh point
 - Windage losses if the gears operate in air or oil mist
 - Oil seal drag
 - Oil pump parasitic losses
 - Parasitic losses in bearings due to oil displacement in the bearings
 - Drag in clutch packs in automatic transmissions and CVTs (those not engaged)
3. Slip losses:
 - Slip in the contact patch where drive is transmitted by friction (i.e., belt-pulley contact in a CVT)
 - Slip that occurs in a fluid drive such as a torque converter.

In most nonpumped automotive transmissions, the large proportion of the load-related and parasitic losses comes from the gear friction losses and the oil churning losses, respectively. The pump losses must always be considered if the transmission has a high-pressure hydraulic circuit. In other transmissions and torque converters the slip losses can also be significant.

10.4.2 Matching of the Drivetrain to the Vehicle

There are several forces acting on the vehicle when it is in motion. The force applied by the powertrain needs to overcome

- The rolling resistance of the tires,
- The aerodynamic drag of the vehicle body,
- Any resistance due to the climbing of an incline, and
- Overcoming the inertia of the vehicle (as a whole) and the rotating parts while the vehicle is accelerating.

The engine obviously provides the mechanical energy, and the drivetrain then converts this to a usable value. As discussed earlier, the torque from the engine tends to be too low to use directly at the wheels while the speed of the engine is too high. As the last point above states, the engine

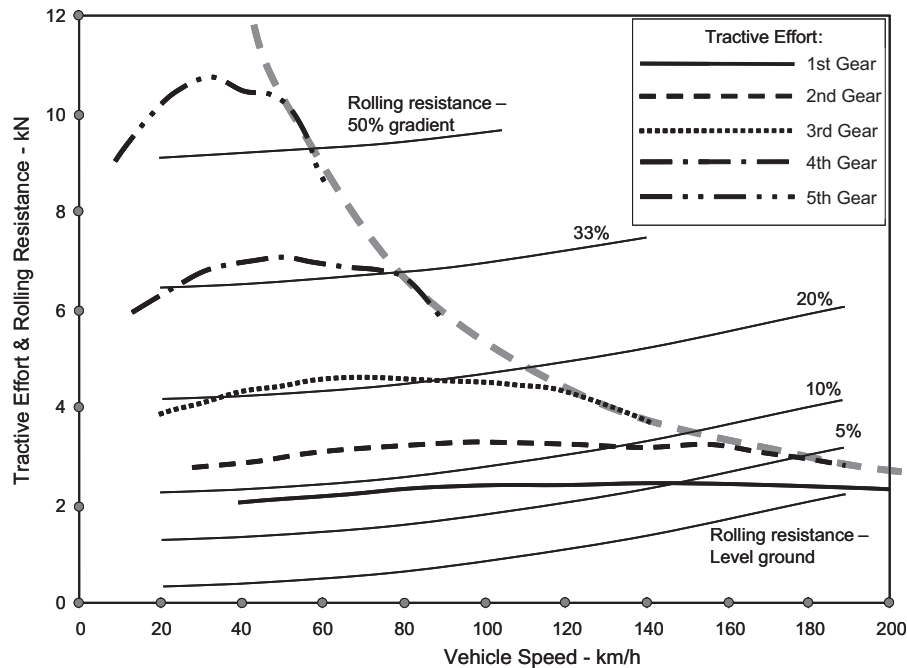


Figure 10.26—Tractive effort graph showing the rolling resistance on different gradients and the tractive effort produced by a 4×4 vehicle in the different gear ratios.

also needs to accelerate its own inertia. This is particularly significant in the lower gears. However, while at steady state, these inertia forces are zero.

The above forces are seen in normal, road-going vehicles. In addition to these, heavy-duty and off-road vehicles also need to overcome additional forces, including

- Resistance because of soft ground;
- Trailer towing; and
- Specialist equipment such as ploughs or dozer blades that may be used in construction, agriculture, or the military environment.

It should be noted that these forces can become so large that the vehicle is slowed down or even completely prevented from moving.

Figure 10.26 shows the forces acting on a large passenger car (medium-sized 4×4) and how they change with speed and gradient. A few comments can be made on the graph.

- The heavier the vehicle, the more pronounced would be the difference between the forces required on different gradients.
- Aerodynamic resistance really only starts to be important at motorway speeds and above.
- Although not shown on this graph, abrupt driving styles can give much higher resistance to motion because of the effects of the inertia of the vehicle.

Illustrated in Figure 10.27 are examples of how the rolling resistance and aerodynamic forces add up with increasing road speed for a range of vehicles. These figures assume zero wind speed on level road. Several things can be observed when comparing the overall resistance of the different cars. It can be seen that the overall magnitude and the difference between vehicles increases significantly with speed.

- Note the difference between the older design of the (Austin/Rover) Mini and the more recent city car; this becomes exaggerated at speed. The drag coefficients have a more pronounced effect as the speed increases.

- A large load is produced by the high weight combined with the large frontal area of the 4×4 vehicle.
- The difference between the medium and large car can be seen to cross over as the speed increases, with the heavier, large car having the highest resistance load at low speeds. However, this larger vehicle then gains the advantage at higher speeds because of the better aerodynamics, and this is almost certainly helped by the longer length of the body and the body style.

10.4.3 The Load on the Transmission

As can be seen, the total rolling resistance that has to be overcome is the resistive load acting on the vehicle. This can be seen as a torque requirement at the driving wheel(s),

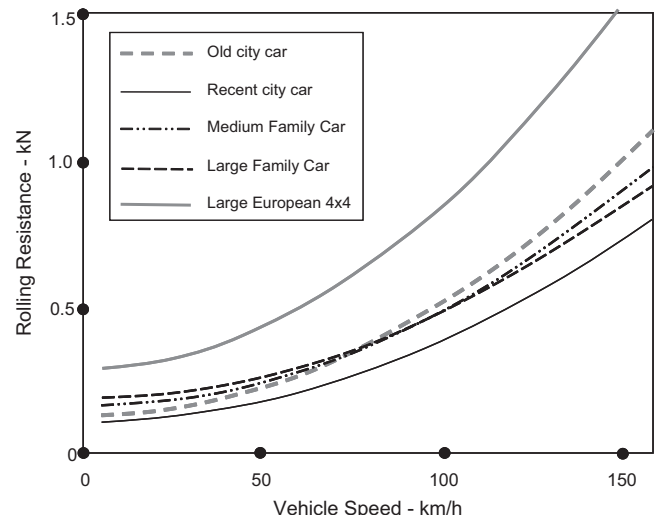


Figure 10.27—The comparative rolling resistance of a range of passenger vehicles.

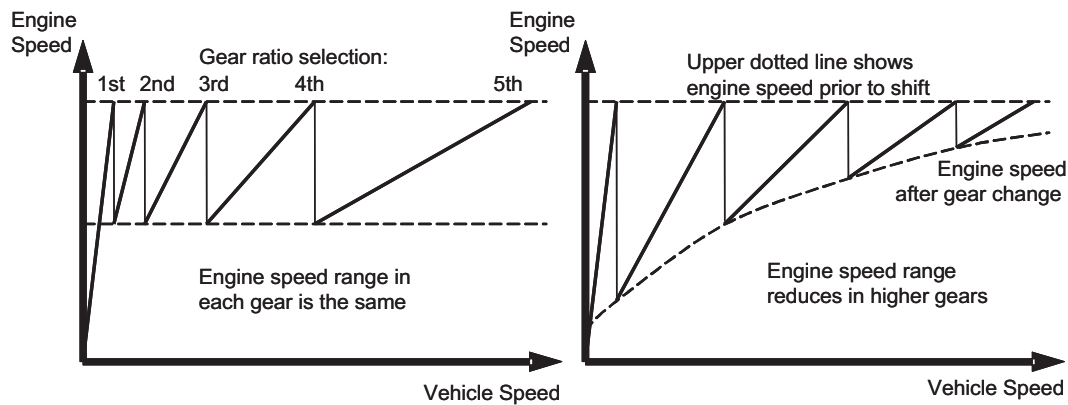


Figure 10.28—The gear ratio progression for different options of ratio selection. The left graph shows geometric progression whereas the right shows an alternative used more widely on passenger cars.

which in turn can be calculated if the dynamic rolling radius of the tire(s) is known.

Without considering numerical examples here, suffice to say there are many references that provide a treatment of this problem, including the *Bosch Automotive Handbook* [5] and *Automotive Transmissions—Fundamentals, Selection, Design, and Application* [2], both of which provide a basic insight. More detailed analysis of the vehicle performance would require the use of a computer simulation package to ease the calculation workload, and such analysis is really outside of the scope of this book. The changing effect of the inertia load can be usefully addressed by the use of such packages. This is because of the dynamic nature of the forces involved.

It is important to appreciate that the choice of gear ratios in a transmission is often dictated in practice by what is available or what is already in production (Figure 10.28). This situation is because of the large cost involved in engineering new gear assemblies and modifying or installing the manufacturing plant required to make those newly engineered parts.

The decision to be made by the engineers and management of any vehicle company is whether the changes to a vehicle are significant enough to warrant a new version of a transmission unit. Clearly, the financial situation will be a major factor. Minor changes can sometimes be made by amending one or two ratios within a gear box. This may leave the intermediate ratios as is and hence perhaps not optimized. A further factor in the decision process is the gear design itself. For example, the input pinion in first gear is often the smallest diameter gear in the gear box. This can be the ultimate limit on the torque capacity because this gear needs to withstand the shock loads applied to the vehicle. The testing that may be considered for this aspect is discussed in Chapter 16, but it is true to say here that these can be very challenging.

In summary, there are several decisions needed during the engineering process. These, in addition to the gear ratios, influence the effective, overall ratio at any point in the operating regime. These factors include

- The required performance of the vehicle;
- The weight, rolling resistance, aerodynamic performance, and other parameters of the vehicle;
- Any commercial restrictions that may exist on the design of the transmission;

- Packaging restrictions in the vehicle—if the gear cases have to be altered this can be costly; and
- Availability of any particular transmission—as discussed above.

Selection of the first gear ratio governs the starting performance of the vehicle and will be influenced by

- The steepest gradient required,
- The fully laden weight of the vehicle,
- The gross train weight for vehicles with trailers, and
- Characteristics of the engine at low engine revolutions (i.e., the required engine speed for effective air inlet “boost” on turbo-charged engines).

Selection of top gear ratio:

- Engine characteristics,
- Economy requirements at cruising speed,
- In-gear performance (e.g., is the driver expected to change gear on overtaking?), and
- The maximum speed to be achieved in top and the next gear down (i.e., is top gear an “overdrive” ratio?).

The intermediate gears are usually spaced to provide an even, comfortable spread between the top and first ratio. Often on commercial vehicles the ratios are often chosen to give constant speed increments between the gears, therefore keeping a fairly consistent speed range in each gear. Passenger cars often have a larger spread in the lower gears than the higher ratios. It is important to point out that such progression is, at best, a theoretical aspiration because the practicalities of obtaining specific ratios rely on the gears having an integer number of teeth. Performance requirements will also influence the choice of gear ratios in performance vehicles. For example, second gear may be chosen in a car so that 100 km/h can be attained without resorting to a change into third, thus avoiding the time lag associated with a gear shift. The commercial pressures mentioned above will also have an influence.

10.5 CONCLUSIONS

This chapter provides a brief introduction to the vehicle drivetrain. The drivetrain is the part of the powertrain of a motor vehicle, excluding the engine and engine systems. The drivetrain includes all of the hardware that carries the drive from the flywheel of the engine to the road wheel hubs. Outside of the scope of the material in this chapter are conventional automatic gear boxes and CVTs. These are discussed elsewhere in this manual.

The premise is made in writing this chapter that to ensure the lubricant system fulfills its job within the vehicle, the engineers should not only know some aspects of the tribology within the unit but should also know how the designed hardware is intended to function.

Included in the discussion are synchromesh gear boxes, transfer gear boxes, and final drive/axle units. The shafts that are used to connect these units together are also included. Where options are available to the designer or engineer, these have been discussed. For example, the chapter starts by discussing the reasons why a particular drivetrain layout may be selected over another, why are some vehicles front-wheel drive, and while others are rear-wheel drive. However, especially at the more detailed level, there is often no single right answer, only several options, each with their own advantages and disadvantages. The appropriate engineering judgment can only be made with the requisite data and a good understanding of the technology.

In the second half of the chapter, the different areas of relevant technology have been introduced and discussed. Although gears and bearings are both covered in other chapters, this chapter attempts to set this in the context of the gear box or drivetrain. Likewise, a brief introduction to vehicle performance is provided so that the implications for the lubricant choice can be assessed.

Read in conjunction with the other chapters in this manual, this should provide the drivetrain context for much of the detailed information on the hardware (e.g., gears and bearings) and on the lubricants. These lubricants are arguably one of the most important components within the transmission, but one of the more challenging to specify correctly.

References

- [1] Gott, P.G., 1991, *Changing Gears: The Development of the Automotive Transmission*. SAE, Warrendale, PA.
- [2] Lechner, G., and Naunheimer, H., 1999, *Automotive Transmissions—Fundamentals, Selection, Design, and Application*. Springer, New York.
- [3] Merritt, H.E., 1971, *Gear Engineering*, Pitman, London. Unfortunately out of print but should be possible to find it in good technical/college libraries or online.
Note that the gear standards such as ISO and AGMA also contain much useful information regarding gears and gear design.
- [4] Socin, R.J., and Walters, L.K., 1968, *Manual Transmission Synchronizers*, SAE Paper 680008, SAE, Warrendale, PA.

- [5] *Bosch Automotive Handbook*, (7th ed.), 2007, Robert Bosch GmbH, Plochingen, Germany.

Bibliography

The following references contain information that may prove useful to readers in providing background information or more detail of the topics covered in this chapter. The following books also contain some useful background information appertaining to transmission unit design and the choice of lubricant.

- ASTM L-42, 2006: Standard Test Method for Evaluation of the Load Carrying Properties of Lubricants Used for Final Drive Axles under Conditions of High Speed and Shock Loading, ASTM Test Monitoring Center, Pittsburgh, PA.
- ASTM STP512A, 1986: Laboratory Performance Tests for Automotive Gear Lubricants Intended for API GL-5 Service, ASTM Committee D-2 on Petroleum Products and Lubricants. Subcommittee B on Automotive Lubricants, ASTM International, West Conshohocken, PA.
- BS-ISO-12925-1, 1996: Lubricants, Industrial Oils and Related Products (Class L). Family C (Gears). Specifications for Lubricants for Enclosed Gear Systems. British Standards Institution, London. Retrieved from <http://www.bsigroup.com>.
- Genta, G., and Morello, L., 2009, *The Automotive Chassis* (Vols. 1 and 2), Springer, New York.
- Happien-Smith, J. (Ed.), 2001, *An Introduction to Modern Vehicle Design*. Oxford, UK, Butterworth-Heinemann.
- Heisler, H., 2002, *Advanced Vehicle Technology*. Oxford, UK, Butterworth-Heinemann.
- Ludwig, Jr., L.G., 2004. "Properties of Enclosed Gear Drive Lubricants, Schaeffer Manufacturing Company" Machinery Lubrication, May-June. Retrieved from <http://www.machinerylubrication.com/>.
- SAE J2360: Automotive Gear Lubricants for Commercial and Military Use. At the time of writing, this standard had been issued some years ago but was in the process of being updated. It is to be the equivalent of Military Specification MIL-PRF-2105E, although available globally. SAE, Warrendale, PA. Retrieved from <http://www.sae.org/>.
- Stokes, A., 1992, *Manual Gearbox Design*. Oxford, UK, Butterworth-Heinemann.
- Syed, R., and Committee: D02 (Eds.), 2009. *A Comprehensive Review of Lubricant Chemistry, Technology, Selection, and Design*, ASTM International, West Conshohocken, PA. Several chapters are of use in providing an understanding of different aspects of lubricant performance and testing.
- Totten, G.E., Westbrook, S.R., Shah, R.J., and Committee D02 (Eds.), 2003. *Fuels and Lubricants Handbook: Technology, Properties, Performance, and Testing*. ASTM International, West Conshohocken, PA. Particularly useful are Chapters 16 and 17.
- Zeroshift website. Retrieved from <http://www.zeroshift.com> on March 31, 2011. Comparison of shift times with different transmission types.

Gear Oil Screen Testing with FZG Back-to-Back Rig

Klaus Michaelis¹ and Brian M. O'Connor²

NOMENCLATURE

a	mm	center distance
b	mm	face width
C_2	–	weight factor
C_{lt}	mm/rev	linear wear coefficient
d	mm	pitch diameter
d_a	mm	tip diameter
d_b	mm	base pitch diameter
d_w	mm	working pitch diameter
F	N	load
F_{bt}	N	normal tooth load
F_N	N	normal force
f_{tm}	μm	mean profile deviation
f_H	–	relative pressure distribution
f_L	–	relative load distribution
H_V	–	tooth loss factor
h_{min}	μm	minimum film thickness
m	mm	module
N	–	number of cycles
n	min^{-1}	speed
P_a	kW	transmitted power
P_{VZP}	kW	load dependent mesh power loss
p_C	N/mm^2	Hertzian stress at pitch point
R_a	μm	arithmetic mean roughness
S	–	safety factor
s	–	slip rate
T	Nm	Torque
T_1	Nm	pinion torque
v	m/s	speed
v_g	m/s	sliding speed

v_t	m/s	pitch line velocity
v_Σ	m/s	sum velocity
w_1	mm	linear wear amount
w_{lp}	mm	permissible linear wear amount
X_{LL}	–	load loss factor
x	–	profile shift factor
z	–	number of teeth
α	°	pressure angle
β	°	helix angle
η	mPas	dynamic oil viscosity
λ	–	relative film thickness
μ	–	coefficient of friction
μ_{mz}	–	mean coefficient of gear tooth friction
$\vartheta_{fla\ int}$	°	mean flash temperature
ϑ_{int}	°	integral temperature
$\vartheta_{int\ P}$	°	permissible integral temperature
$\vartheta_{int\ S}$	°	scuffing integral temperature
ϑ_M	°	gear bulk temperature
ϑ_{oil}	°	oil temperature
ρ	mm	relative radius of curvature
σ_H	N/mm^2	contact stress
ζ_w	–	wear relevant specific sliding
Indices		
1		pinion
2		gear
C		pitch point
n		normal plane
T		Test

¹ FZG Gear Research Centre, Technische Universitaet Muenchen, Garching, Germany

² The Lubrizol Corporation, Wickliffe, Ohio, USA

11.1 INTRODUCTION

For better efficiency in transmissions, lower viscosity grades of gear oils and reduced oil volumes are often used. With increasing power density and extended oil drain intervals, the demands on the lubricant as a design element increase accordingly. The introduction of lubricant properties in load-carrying capacity rating requires not only knowledge of their physical properties such as viscosity, viscosity-temperature, or viscosity-pressure behavior, but also the quantitative influence of the performance additive on scuffing, wear, micropitting, and pitting of gears.

Numerous test methods have been developed to describe lubricant properties. They range from simple, low-cost bench tests on the one end to full-scale field testing on the other end [1]. The aim is a test method that produces

comparable results to practical applications as simple, cheap, and quick as possible.

Figure 11.1 shows some test arrangements developed for the prediction of scuffing and wear properties of gear oils. The best test configuration for full comparability is the actual gear box under typical operating conditions. For industrial gear applications, this is usually too expensive, and for automotive gear applications, this is often too time consuming. The second-best choice includes test methods using defined test gears with high reproducibility in geometry, heat treatment, and surface finish being exposed to exaggerated operating conditions to reduce test time. Parameters that are modified compared with actual operating conditions have to be chosen very carefully for the best simulation. Methods on disk type rigs often simulate one point on the path of contact of a gear mesh with its local pressure, rolling, and sliding velocity. Many other bench test rigs use a simple specimen geometry under pure sliding conditions.

Figure 11.2 shows scuffing results on some of these rigs for different "lubricants" including milk and beer [2]. In the often specified four ball and Timken tests, milk and beer are rated with higher scuffing load capacity as a non-EP mineral oil ISO VG 220 or a hydraulic oil with zinc dithiophosphate (ZDTP) additives, ISO VG 46. Only the FZG test using test gears gives a correct relative rating of these lubricants. Even results from twin disk machines with a close simulation of the kinematics of one point on the path of contact can be quite misleading. Two standard hypoid gear oils and one with an additional MoS_2 content were evaluated in a hypoid gear, a spur gear, and a twin disk test (Figure 11.3). Although the two gear tests showed rather poor performance for the MoS_2 -containing lubricant of less than 50 % of the standard oils, the twin disk result was at 300 %.

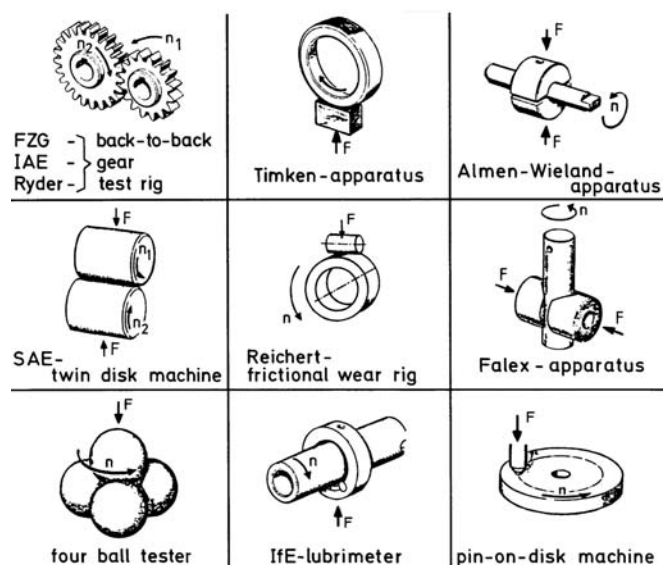


Figure 11.1—Lubricant test arrangements (schematic).

11.2 TEST RIG AND TEST GEARS

With this experience, several test methods for gear lubricants were developed using the FZG back-to-back gear test rig. More than 500 FZG machines are available worldwide [3].

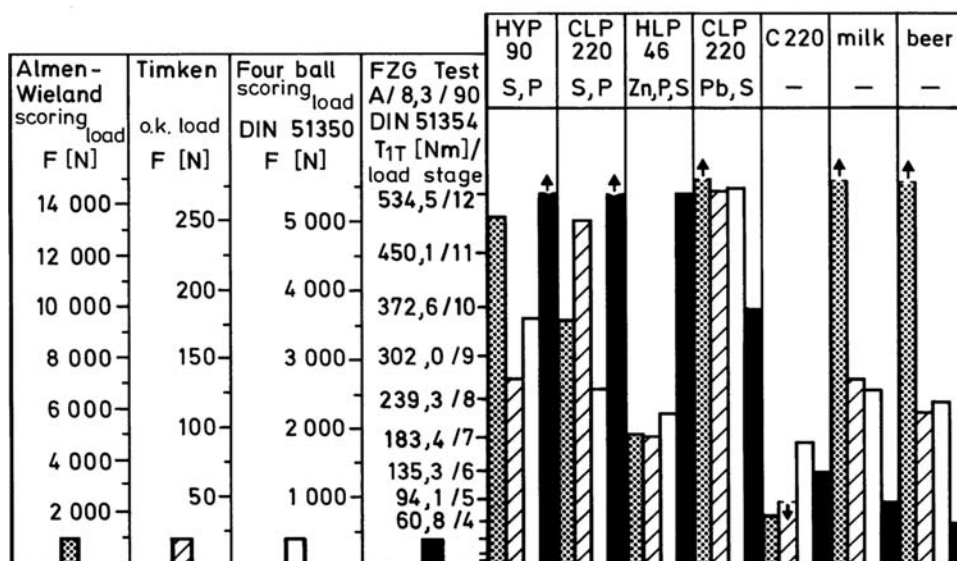


Figure 11.2—Scuffing results for different lubricants [2]. HYP 90 S,P = hypoid gear oil SAE 90 with sulfur-phosphorus extreme pressure (EP) additive, CLP 220 S,P = industrial gear oil ISO VG 220 with sulfur-phosphorus EP additive, HLP 46 Zn, P,S = hydraulic oil ISO VG 46 with ZDTP additive, CLP 220 Pb, S = industrial gear oil ISO VG 220 with lead-naphthenate EP additive, C 220 = industrial gear oil ISO VG 220 without EP additive.

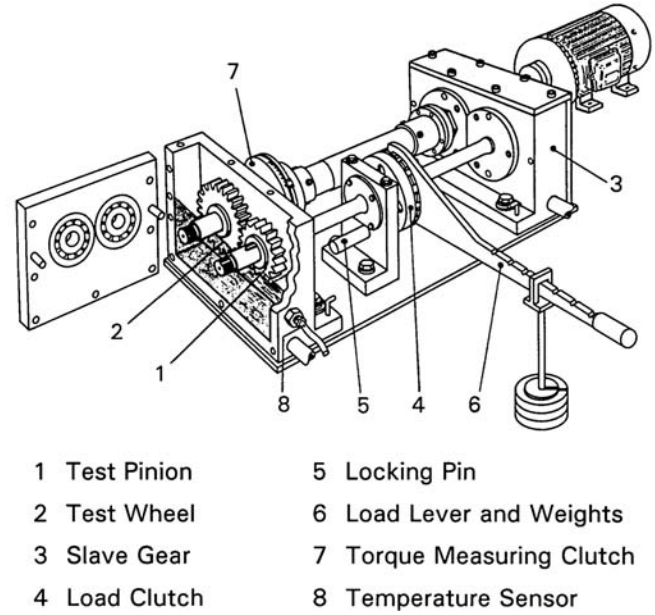
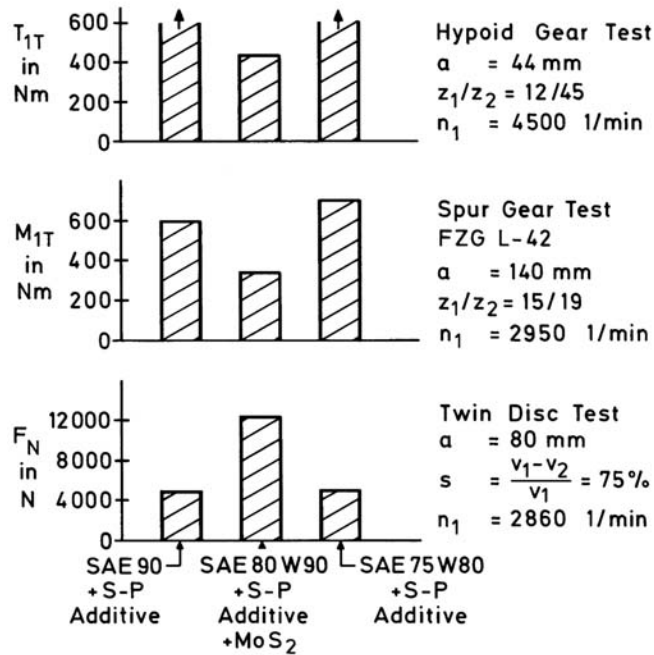


Figure 11.4—FZG back-to-back gear test rig.

Figure 11.3—Scuffing results in disk and gear tests. Arrows indicate results outside of test range.

11.2.1 Test Rig

The FZG gear test rig is a back-to-back rig with center distance a of 91.5 mm [3] (Figure 11.4). Two shafts connect test gears and slave gears. One shaft is divided in two parts with the load clutch in between. One half of the load clutch can be fixed to the foundation with the locking pin whereas the other half is twisted, for example, by means of a lever and weights. After bolting the clutch together, the load can be removed and the shaft has to be unlocked. Thus, a static torque is applied to the system that can be checked in the torque-measuring clutch as the twist of a calibrated torsion shaft.

The rig can be operated either with a two-speed alternating current motor at 1500/3000 r/min or a variable-speed motor between $n = 100$ and 3000 r/min. The gears are normally dip-lubricated with a heater and a cooling coil in the test head for temperature control. With an additional oil supply device, spray or jet lubrication can be applied.

11.2.2 Test Gears

For the different standard tests, there are two standard test gear geometries in use [3]. For scuffing tests, gear type A with high sliding at the pinion tip is used whereas gear type C with balanced sliding is used for wear, micropitting, and pitting tests. The main data of the test gears are summarized in Table 11.1.

Table 11.1—Main Data of Test Gears

	Symbol	Unit	A Type	C Type
Center distance	a	mm	91.5	91.5
Number of teeth pinion	z_1	—	16	16
Number of teeth gear	z_2	—	24	24
Module	m	mm	4.5	4.5
Pressure angle	α	°	20	20
Helix angle	β	°	0	0
Face width	b	mm	20	14
Profile shift factor pinion	x_1	—	0.8532	0.1817
Profile shift factor gear	x_2	—	-0.5	0.1715
Working pitch diameter pinion	d_{w1}	mm	73.2	73.2
Working pitch diameter gear	d_{w2}	mm	109.8	109.8
Tip diameter pinion	d_{a1}	mm	88.8	82.5
Tip diameter gear	d_{a2}	mm	112.5	118.4
Material	MAT	—	20MnCr5	16MnCr5
Heat treatment	—	—	Case carburized	

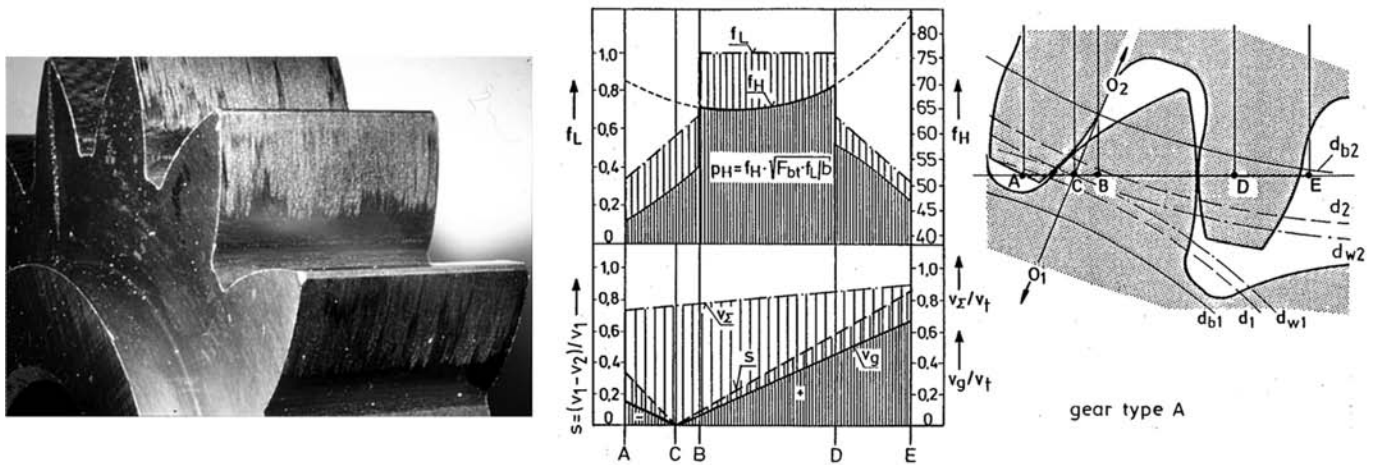


Figure 11.5—A-type test gears for scuffing tests.

Test gears are case-carburized with a surface hardness of $HRC = 60 \pm 2$ and a case depth of $E_{ht} = 0.6\text{--}0.9$ mm. The surface roughness is controlled to the required values of the respective test procedure. Test gears are manufactured in batches of 100 pairs by one manufacturer and closely controlled for gear accuracy, surface finish, and metallurgical properties.

11.3 TEST METHODS

For the different gear failure modes that can be influenced by the lubricant type, viscosity, and additive system, adequate test methods were developed in close cooperation with industry. In some cases different modifications of the test methods are available adjusted to the specific application. The following subsections describe often-used methods.

11.3.1 Scuffing Load Capacity Tests

Scuffing is an instantaneous failure in which gear flanks are welded together in the contact zone under pressure and temperature, typically at medium- or high-speed conditions without any protecting layers on the surfaces (Figure 11.5). Scuffing can be prevented by a thick separating lubricant film from the oil viscosity or by physically adsorbed or chemically reacted surface layers from the additive system. Figure 11.6

shows profile and lead measurements in corresponding contact areas of a scuffed pinion and gear. It is obvious that during scuffing material was transferred from the dedendum area of the gear with negative specific sliding to the addendum area of the pinion with positive specific sliding.

A widely used test method for the evaluation of the scuffing properties of industrial gear lubricants is the FZG gear oil test A/8.3/90 according to ISO 14635-1 [4], which is equivalent to other standards such as IP 334 [5], ASTM D5182 [6], and CEC L-07-A-95 [7]. A-type gears are used and designed for high sliding at the pinion addendum for high scuffing risk (Figure 11.5). The gears are loaded stepwise in 12 load stages between pinion torques T_1 of 3.3 and 534.5 Nm corresponding to Hertzian stress values of p_c of 150–1800 N/mm². They are operated for 15 min at a pitch line velocity of 8.3 m/s and a starting oil temperature, ϑ_{oil} , of 90°C in each load stage under conditions of dip lubrication without cooling. In the visual test, the gear flanks are inspected after each load stage for scuffing marks. Failure load stage is indicated when the faces of all pinion teeth show a summed total width of damaged areas that is equal or exceeds one pinion face width.

Table 11.2 shows typical results of gear lubricants in this test. It is obvious that for industrial applications with high scuffing demands such as for light rail (e.g., street

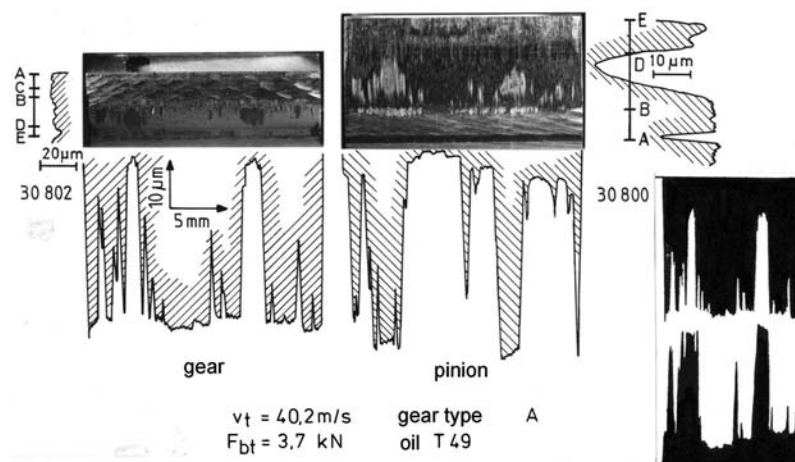


Figure 11.6—Corresponding scuffing failures on pinion and gear.

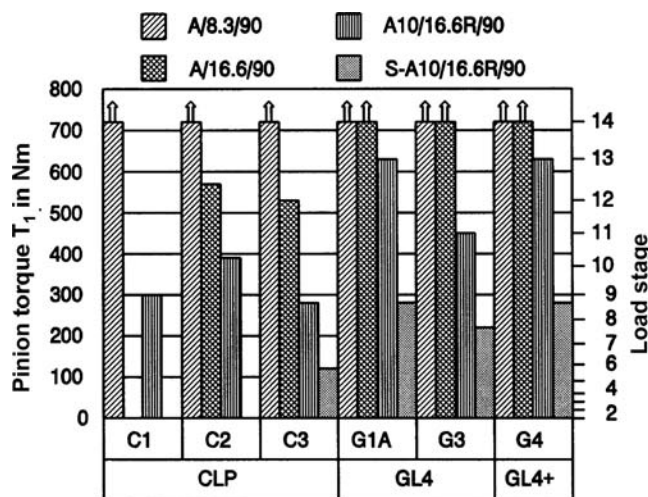
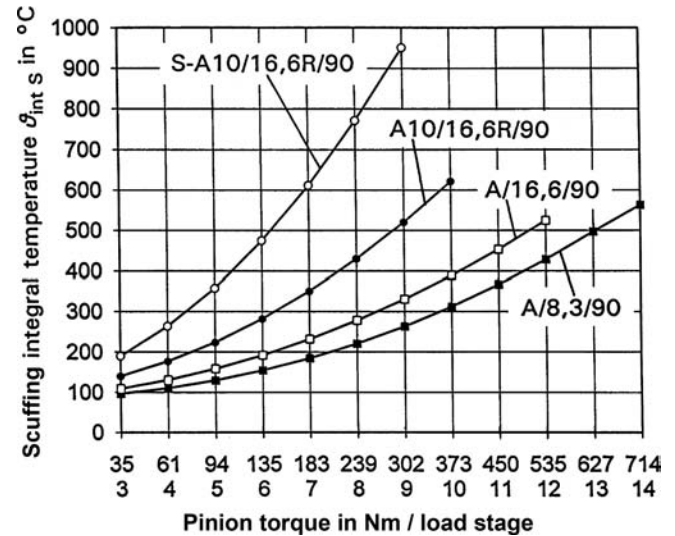
TABLE 11.2—Typical Results of the Standard Scuffing Test

Lubricant Type	Typical ISO VG	Typical Scuffing Load Stage		
		Non-EP	Mild EP	EP Oil
ATF	32-46	NA	5-8	9-11
Turbine oil	32-68	NA	6-8	9-11
Industrial gear oil	100-320	NA	8-12	>12
Transmission oil	100-220	NA	NA	>12
Axle oil	150-220	NA	NA	>12
NA = not applicable.				

cars) or wind turbines as well as in automotive applications such as manual transmissions or hypoid rear axles, the standard A/8.3/90 scuffing test does not have sufficient discriminating power.

For automotive gear oils requiring API GL-4 quality level, no standardized scuffing test method is available. For API GL-5 oils, the CRC L-42 test [8] is required, but there are very few test stands available to the industry. In systematic investigations with the standard FZG gear test rig, the scuffing risk of the standard procedure was increased by varying speed and specific load, load application, and direction of rotation. A step test identified with the shorthand designation A10/16.6R/90 can be used for lubricants up to the level of API GL-4. A shock test, designated S-A10/16.6R/90, for discrimination between API GL-4 and GL-5 has also been developed. A-type test gears with a reduced pinion face width, b , of 10 mm (A10) are used at increased speed of 16.6 m/s (16.6) and reversed sense of rotation (R), at oil temperature, ϑ_{oil} , of 90°C (90). In the step test, load is stepwise increased until scuffing occurs. In the shock test (S), the gears are directly loaded in the expected load stage and “pass” or “fail” is stated. A detailed description of the test procedures can be taken from the FVA Information Sheet [9].

With the standard test method A/8.3/90, lubricants of API GL-1 and GL-2 can be discriminated. Lubricants of higher scuffing level GL-3 to GL-5 can be discriminated in the A10/16.6R/90 and S-A10/16.6R/90 tests. A comparison

**Figure 11.7—Scuffing results for different lubricants.****Figure 11.8—Comparison of scuffing test methods.**

of results from different scuffing test methods is shown in Figure 11.7. With these tests, it is possible to cover the whole range of scuffing load capacity between API GL-1 and GL-5. In addition to a relative ranking of lubricants with respect to their scuffing performance, the results of these tests can also be recalculated to critical scuffing temperatures and be introduced into the DIN [10] and ISO [11] standards of scuffing load capacity rating. For the integral temperature criterion, the integral temperature ϑ_{int} must be less or equal to the permissible integral temperature $\vartheta_{int p}$:

$$\vartheta_{int} = \vartheta_M + C_2 \cdot \vartheta_{fla int} \leq \vartheta_{int p} = \frac{\vartheta_{int s}}{S_{s min}} \quad (11.1)$$

where:

ϑ_{int} = integral temperature (°C),

ϑ_M = gear bulk temperature (°C),

C_2 = weight factor,

$\vartheta_{fla int}$ = mean flash temperature along path of contact (°C),

$\vartheta_{int p}$ = permissible integral temperature (°C),

$\vartheta_{int s}$ = scuffing integral temperature (°C), and

$S_{s min}$ = minimum scuffing safety factor.

The critical scuffing temperature is the lubricant strength value with respect to scuffing failures. On the basis of this critical scuffing temperature, different scuffing test methods can be compared as shown in Figure 11.8. For a lubricant with a failure load stage 12 in the standard scuffing test A/8.3/90 corresponding to a scuffing integral temperature of approximately 420°C, a scuffing load capacity of load stage 8 would be expected in the step test A10/16.6R/90 and of load stage 6 would be expected in the shock test S-A10/16.6R/90.

11.3.2 Slow-Speed Wear Test

Wear is a continuous process especially under thin film conditions, typically at slow pitch line velocities, where asperity interaction can occur. This leads to material removal from the mating surfaces with each load cycle (Figure 11.9).

ASTM method D4998, commonly referred to as the Chevron Test [12], is one method used to assess wear at low speeds. It is run with A-type gears at a pitch line velocity, v , of 0.57 m/s (150 r/min at the pinion), at load stage 10 (pinion torque $T_1 = 372.6$ Nm), and at an oil temperature,

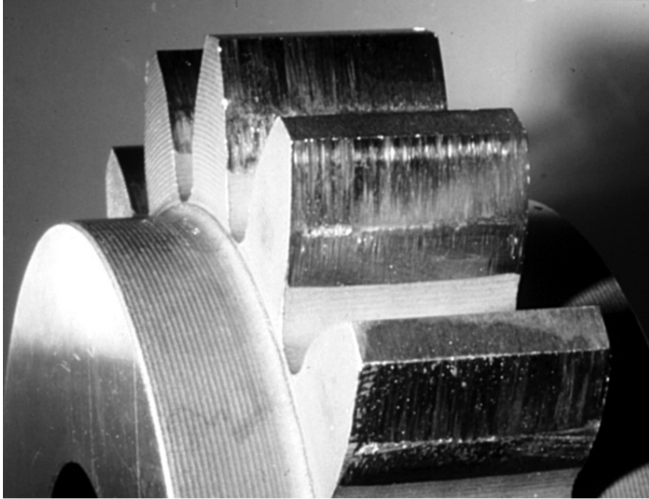


Figure 11.9—Typical wear failure on test pinion.

ϑ_{oil} of 120°C. The weight loss of the pinion and gear is determined after 20 h. Test results are used as a relative ranking of different oils. The test was developed for tractor hydraulic fluids of low viscosity grade and can often not discriminate between different industrial and automotive gear oils of higher viscosity. Therefore, a new universal wear test C/0.05/90:120/12 was developed (see Table 11.3) to define the low-speed, thin-film wear characteristics of gear oils. Pitting test gears, type C-PT (C), with balanced sliding between pinion and gear tip are used at a pinion speed of 0.05 m/s (0.05) (13 r/min at the pinion) at oil temperatures, ϑ_{oil} of 90 and 120°C (90:120) and at load stage 12 (12) (pinion torque of $T_1 = 378.2$ Nm). The test method is conducted with a minimum of two parts. Running the test on the standard FZG rig requires a speed reducer between the driving motor and slave gear box. A detailed description of the test procedure can be taken from the DGMK Information Sheet [13].

11.3.2.1 PART 1: C/0.05/90/12

Part 1 runs two 20-h segments with intermediate weighing of pinion and gear. The pitch line velocity, v , is maintained at 0.05 m/s, and the oil sump temperature at ϑ_{oil} is 90°C.

TABLE 11.3—Test Conditions of the Wear Test C/0.05/90:120/1

Test Conditions	C/0.05/90/12	C/0.05/120/12	C/0.57/90/12
Pitch line velocity	0.05 m/s	0.05 m/s	0.57 m/s
Pinion speed	13 r/min	13 r/min	150 r/min
Gear speed	8.7 r/min	8.7 r/min	100 r/min
Oil temperature	90°C	120°C	90°C
Pinion torque	378.2 Nm	378.2 Nm	378.2 Nm
Running time	2 × 20 h	2 × 20 h	1 × 40 h
Revolutions of shaft 2	2 × 10,400	2 × 10,400	1 × 240,000
Test result	Weight loss of pinion and gear		

This condition gave the highest wear rates for all tested lubricants.

11.3.2.2 PART 2: C/0.05/120/12

Part 2 runs also two 20-h segments with intermediate weighing of pinion and gear. The oil sump temperature, ϑ_{oil} , is increased to 120°C with the other parameters kept constant to check the additive reaction at elevated temperature.

These two parts must always be performed when evaluating a lubricant. Part 3 can be added for more detailed information in one operating condition.

11.3.2.3 PART 3: C/0.05/90/12 OR C/0.05/120/12 OR C/0.57/90/12

Part 3 runs 40 h without intermediate weighing using one of the following conditions:

- C/0.05/90/12: Repeating the test conditions of part 1 can show how mechanical and chemical changes on the flank surface are relevant under changing operating conditions.
- C/0.05/120/12: Repeating the test conditions of part 2 can be appropriate when the operating conditions in practice are predominantly at a higher temperature level and the results of part 2 are not yet sufficient or have not yet arrived at a steady-state level.
- C/0.57/90/12: Changing the pitch line velocity, v , to 0.57 m/s, corresponding to a pinion speed, n_1 , of 100 r/min, can show the influence of higher speed and thus higher film thickness and better lubricating conditions on the wear behavior. The oil temperature, ϑ_{oil} , of 90°C was chosen because in most cases at the lower temperature higher wear rates were found.

Different gear lubricants such as hydraulic oils, automatic transmission fluids (ATFs), turbine oils, industrial gear oils, and automotive gear oils of GL-4 and GL-5 performance were tested under these conditions. Typical test results are shown in Figure 11.10. It can be seen from Figure 11.10 that different categories of wear behavior can occur:

- High or medium wear rate in parts 1 and 2 (e.g., Dexron 32 D),
- High or medium wear rate in part 1 and low wear rate in part 2 (e.g., GL-5-SP 80W),
- Low wear rates in parts 1 and 2 (e.g., UTTO-Z 46).

Predictions of wear results from viscosity parameters or additive content are not possible. The experimental results of the wear test can be introduced as specific wear rate values c_{lt} into the wear calculation method according to Plewe [14]:

$$W_l = c_{lt} \cdot \left(\frac{\sigma_H}{\sigma_{HT}} \right)^{1.4} \cdot \left(\frac{\rho_c}{\rho_{CT}} \right) \cdot \left(\frac{\zeta_W}{\zeta_{WT}} \right) \cdot N \leq W_{lp} \quad (11.2)$$

where:

W_l = linear wear amount (mm),

c_{lt} = linear wear coefficient (mm/rev),

σ_H = contact stress (N/mm²),

σ_{HT} = test contact stress (N/mm²),

ρ_c = relative radius of curvature at pitch point (mm),

ρ_{CT} = relative radius of curvature at pitch point for test gear (mm),

ζ_W = wear relevant specific sliding,

ζ_{WT} = wear relevant specific sliding in the test,

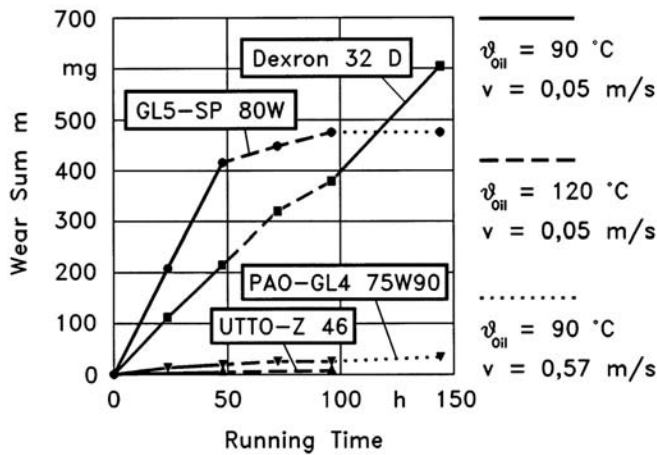


Figure 11.10—Results from the FZG wear test. Dexron 32 D = automatic transmission fluid ISO VG 32, GL5-SP 80W = axle gear oil API GL5 SAE 80W with sulfur-phosphorus EP additive, PAO-GL4 75W90 = polyalphaolefin gear oil API GL4 SAE 75W90, UTTO-Z 46 = universal tractor transmission oil ISO VG 46 with ZDTP additive.

W_{lp} = permissible linear wear amount (mm), and
 N = number of cycles (rev).

For pure mineral oils without additives, the linear wear coefficient, c_{lt} , can be taken from Figure 11.11. For candidate oils, the linear wear coefficient can be recalculated from the wear test result for the relevant film thickness at test conditions and be introduced in Figure 11.11. As a first approximation, a parallel line to curve 2 for case-

carburized gears with oil lubrication from Figure 11.11 is drawn through the test point and applied as the linear wear coefficient, c_{lt} , for the candidate oil in eq. 11.2.

11.3.3 Micropitting Test

Micropitting is a fatigue failure of the surface that occurs predominantly in the areas of negative sliding (i.e., in the dedendum below the pitch circle). Microcracking leads to an ongoing breakout of material from the surface, which can eventually result in a large profile error (Figure 11.12). These micropits can reach a material depth of some 5 μm in the early stages, but they can also progress deeper layer by layer to 30 or 50 μm (Figure 11.13).

For low churning losses and high efficiency in many applications, low-viscosity grade lubricants are often used. To compensate for the wear and scuffing performance loss due to a lack of viscosity, various antiwear and EP additives are used in the finished fluid. The type of the base oil and the additive type show a large influence on micropitting failure of gears [15]. A test method identified as C-GF/8.3/90 for the evaluation of the micropitting performance of lubricants was established to help quantify the performance of lubricants against micropitting. The test requires an oil-spray device for a constant oil temperature, ϑ_{oil} , of 90°C (90) at an oil flow rate, V , of 2 l/min. Gear type C with a specified high surface roughness, R_a , of $0.5 \pm 0.1 \mu\text{m}$ (C-GF) is run at a pitch line velocity, v , of 8.3 m/s (8.3). A 1-h run-in in load stage 3 ($p_c = 500 \text{ N/mm}^2$) is followed by a step load evaluation in load stages 5–10 (lever arm moment length = 0.35 m resulting in $p_c = 800\text{--}1500 \text{ N/mm}^2$). Running time is 16 h per load stage. After every load stage, the gears are

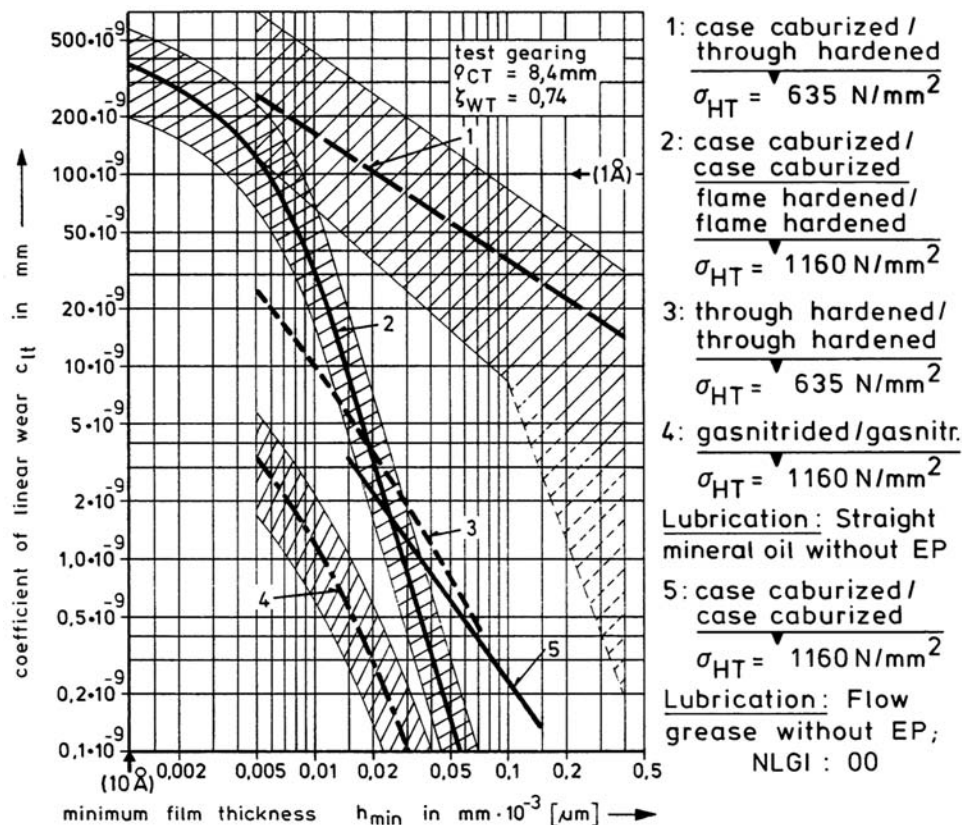


Figure 11.11—Linear wear coefficient c_{lt} for pure mineral oils.

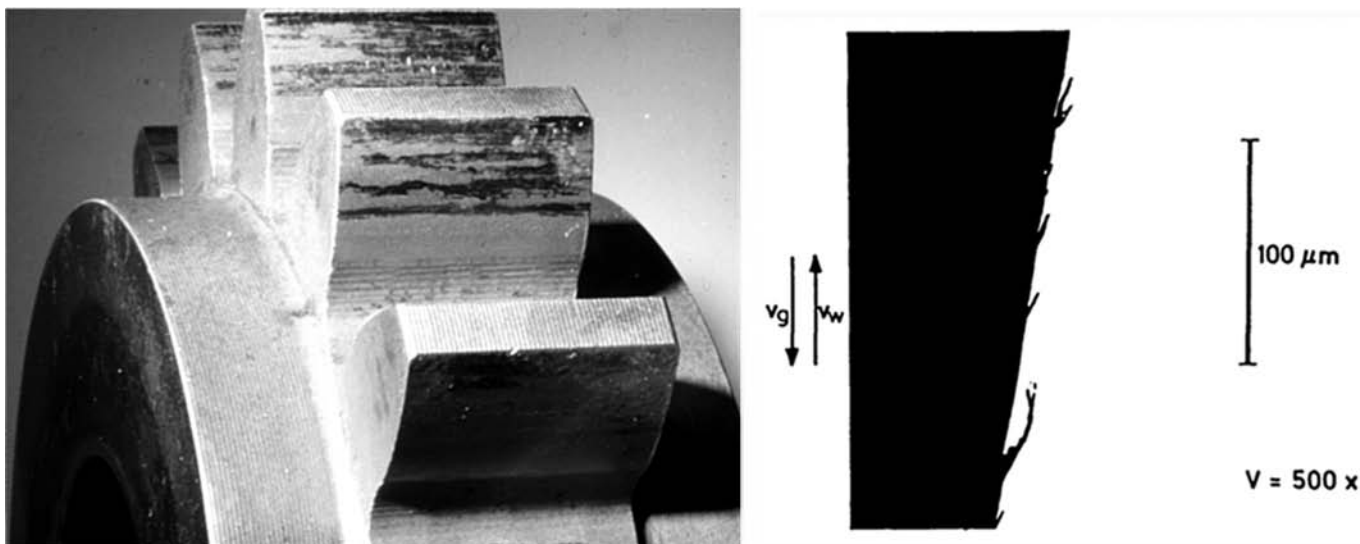


Figure 11.12—Typical micropitting failure on pinion.

dismounted and the profile deviation is measured. If the profile deviation exceeds $7.5 \mu\text{m}$ (corresponding to a change of AGMA accuracy grade from 12 to 11), the test is terminated, and the failure load stage is reported.

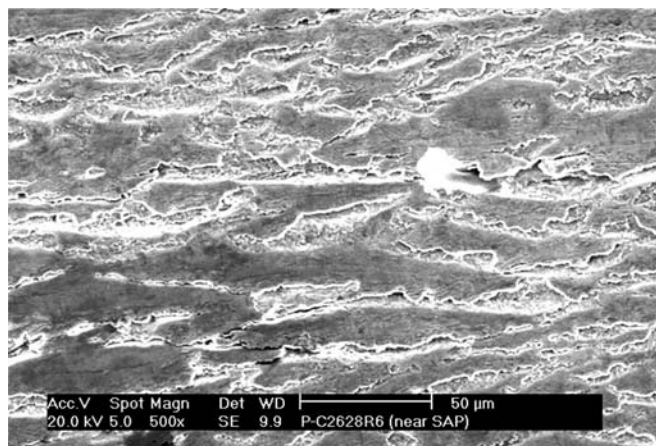


Figure 11.13—Close-up view of a micropitting failure.

After the step load test is completed, an endurance test with the same gear pair is performed. This consists of one 80-h segment in load stage 8 followed by a maximum of five 80-h segments in load stage 10. The gears are inspected after every test sequence, and the profile deviation is again measured. When the profile error exceeds $20 \mu\text{m}$ (corresponding to a change of the AGMA accuracy grade to 8) or if macropitting occurs, the endurance test is terminated. A detailed description of the test method can be found in FVA Information Sheet 54/I-IV [16]. Figure 11.14 shows examples of lubricants with different micropitting capacity.

Because of the very long running time of this micropitting test, a shorter micropitting test designated C-GFKT/8.3/90 was developed for screening purposes [17]. This shorter test is run with dip lubrication conditions and uses a step load procedure. A 1-h run-in at load stage 3 is followed by 16 h each in load stages 7 and 9. This test evaluates micropitting in a qualitative manner for the micropitting performance of a gear lubricant. When the failure criterion of $7.5\text{-}\mu\text{m}$ profile deviation is exceeded after load stage 7, then the lubricant is rated in micropitting class “low”; if $7.5\mu\text{m}$ is exceeded after load stage 9, then

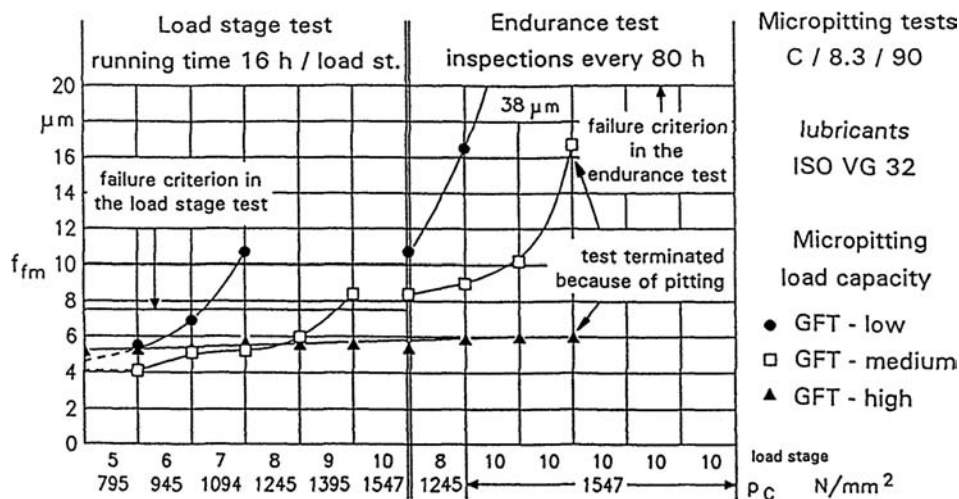


Figure 11.14—Typical micropitting test results.

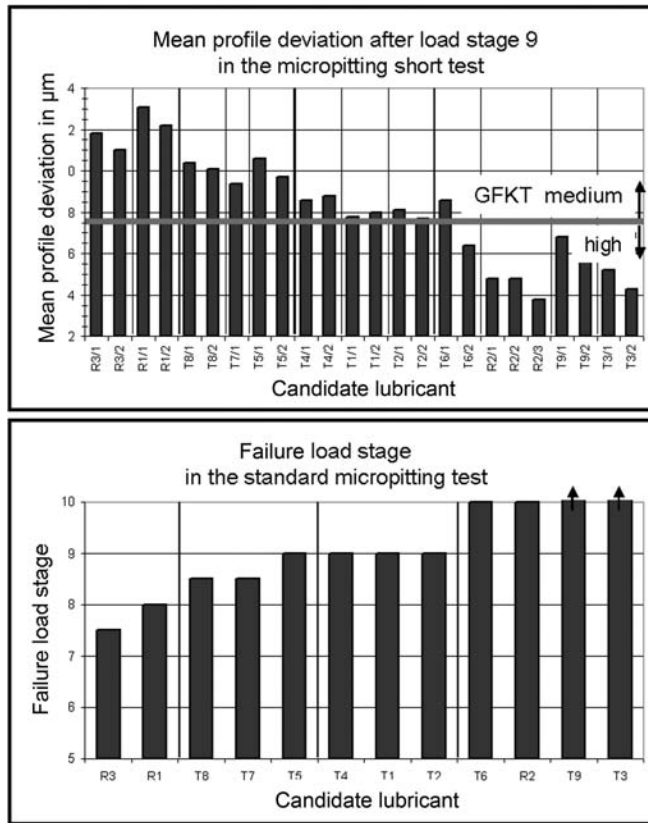


Figure 11.15—Results of short and standard micropitting test.

the rating is micropitting class “medium”; and if the profile deviation after load stage 9 is below $7.5 \mu\text{m}$, then the rating is micropitting class “high.” A comparison between results of the standard test and the short test showed good correlation (Figure 11.15).

Predictions of micropitting results from viscosity parameters or additive content are not possible. The experimental results of the tests can be introduced into a micropitting capacity rating method according to Schrade [18]. From the failure load stage in the micropitting test, a permissible relative film thickness, λ_{GFp} , can be derived (Figure 11.16). Together with the relative film thickness at operating conditions, λ_{GF} , a micropitting safety factor is evaluated:

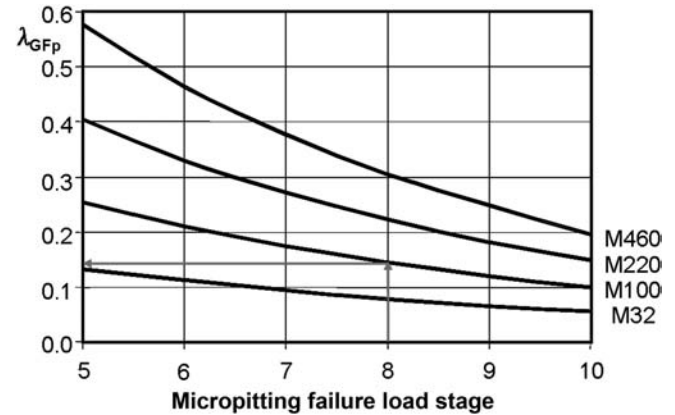


Figure 11.16—Permissible relative film thickness from a micropitting test. M460 = mineral oil ISO VG 460, M220 = mineral oil ISO VG 220, M100 = mineral oil ISO VG 100, and M32 = mineral oil ISO VG 32.

$$S_{GF} = \frac{\lambda_{GFp}}{\lambda_{GF}} \geq S_{GFmin} \quad (11.3)$$

where:

S_{GF} = micropitting safety factor,

λ_{GFp} = permissible relative film thickness,

λ_{GF} = relative film thickness for operating conditions, and

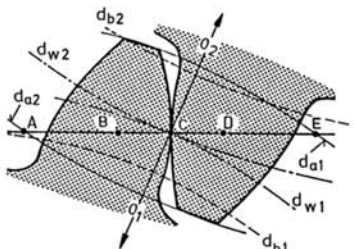
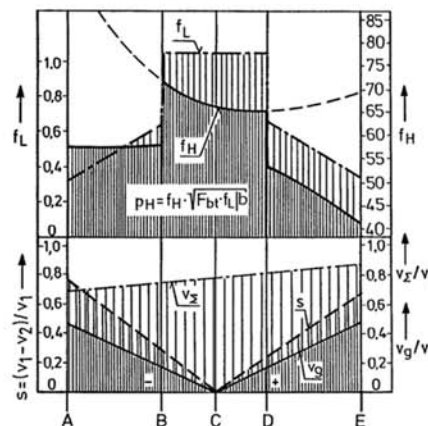
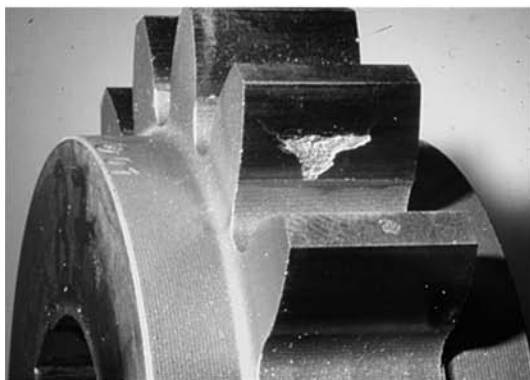
S_{GFmin} = minimum micropitting safety factor.

A high micropitting risk at operating conditions is expected for a micropitting safety factor below 1.0, a medium micropitting risk for safety factors between 1.0 and 2.0, and a low micropitting risk for safety factors above 2.0.

11.3.4 Pitting Tests

Pitting is a fatigue failure in the area of negative sliding in the dedendum of the pinion, which often originates from surface cracks that propagate into the material and progress further under high subsurface shear stress levels. In some cases and especially for larger sizes, the crack initiation can also originate subsurface with crack propagation toward the surface (Figure 11.17).

Lubricant type, viscosity, and additive system influence the pitting life of gears. Especially for automotive gear oils, a single-stage test method C-PT/9:10/90 for the evaluation of the relative pitting life was developed. Running an oil in



gear type C

Figure 11.17—C-type test gears for pitting tests.

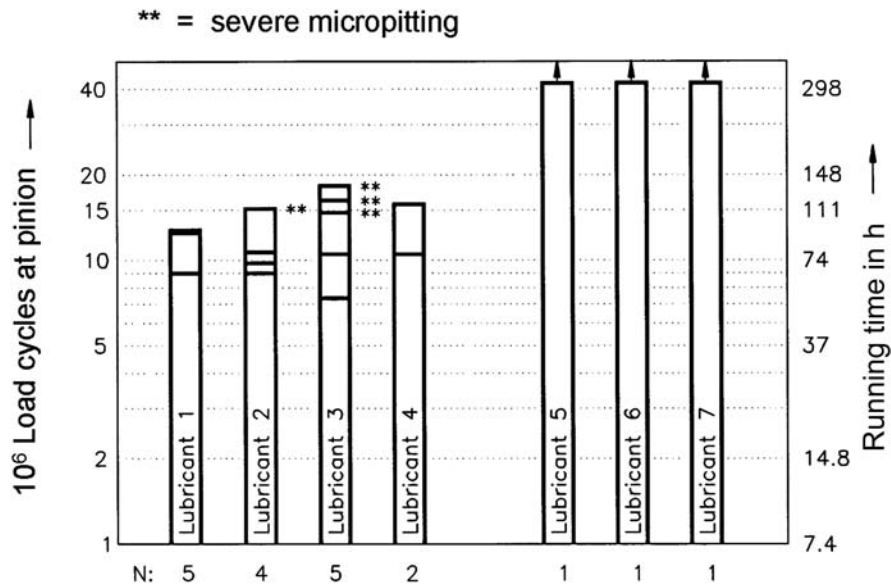


Figure 11.18—Pitting results in load stage 9 for different lubricants. N = number of test runs for each lubricant.

the pitting test requires a minimal scuffing load stage of at least load stage 9 ($T_1 = 302.0$ Nm); otherwise, the gears will experience scuffing under the conditions of the pitting test. C-type gears are used, which are designed for balanced sliding at the pinion and gear tip (Figure 11.17) and a specified low surface roughness, R_a , of $0.3 \pm 0.1 \mu\text{m}$ (C-PT) to avoid micropitting failures. The gears are run at a pitch line velocity, v , of 8.3 m/s in load stage 9 ($T_1 = 302.0$ Nm; $p_c = 1650$ N/mm²) for low-viscosity gear oils below ISO VG 100 and at load stage 10 ($T_1 = 372.6$ Nm; $p_c = 1830$ N/mm²) for medium- and high-viscosity gear oils of ISO VG 100 or higher (9:10). The gears are dip lubricated with a constant oil temperature, ϑ_{oil} , of 90°C (90). A cooling coil with water supply has to be mounted on the top cover of the test gear box.

A run-in of 2 h in load stage 6 ($p_c = 1100$ N/mm²) is followed by the test run in the respective load stage until the failure criterion is reached. The failure criterion is either 4 % pitted area on any single tooth flank of the pinion or 1 % total pitting damage for all 16 pinion teeth. The number of load cycles until failure is reported and compared to the pitting life of a reference oil. Because of the rather large scatter of pitting life, at least three test runs with one lubricant are required for statistically meaningful results. For the pitting failure life, a Weibull distribution is assumed and the load cycles for 50 % (L50) failure probability are reported [19]. This value is compared with the L50 values of reference lubricants. Figure 11.18 shows results of different gear lubricants in the standard single-stage test C-PT/9/90.

The result of the standard pitting test is often strongly influenced by the occurrence of micropitting. Therefore, a practice-relevant pitting test C-PTX/10/90 was developed using modified test gears C-PTX with tip and root relief as well as lengthwise crowning at the wheel together with superfinished surfaces of pinion and wheel to suppress micropitting. The application test C-PTX/SNC/90 [20] extends the test method to two different load levels dependent on the result of the single-stage test in load stage 10. If the mean pitting life of three runs in load stage 10 is equal to or less than 15 million pinion cycles, then at least two more test runs are added in load stage 9. If the result in load

stage 10 is over 15 million cycles, then the test is followed by additional test runs in load stage 11. Figure 11.19 shows the result of a lubricant in the application test.

Test results from the pitting test can be introduced into the ISO calculation procedure [21] by defining a new time strength branch of the SN-curve compared to the standard SN-curve for the non-EP oil of same viscosity (Figure 11.20). The approach is very conservative because the endurance level is kept constant. Improvements are therefore only calculated for gear pairs with limited life.

11.3.5 Efficiency Test

In addition to adequate load-carrying capacity, the power loss of a transmission becomes increasingly important. A simple way to improve transmission efficiency is the choice of a low-friction lubricant. No load losses due to churning and squeezing effects and load-dependent losses due to shear in the contact of gears and bearings are related to lubricant properties. A test method was developed that allows a comparison of the efficiency behavior of candidate oils with a mineral reference oil in the different lubrication regimes of full elastohydrodynamic (EHD) flank separation, mixed film lubrication, and boundary lubrication.

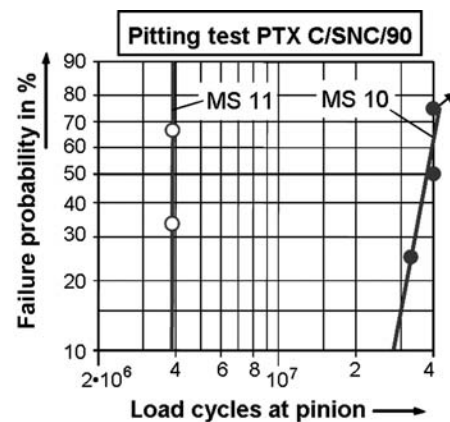


Figure 11.19—Result of the application test.

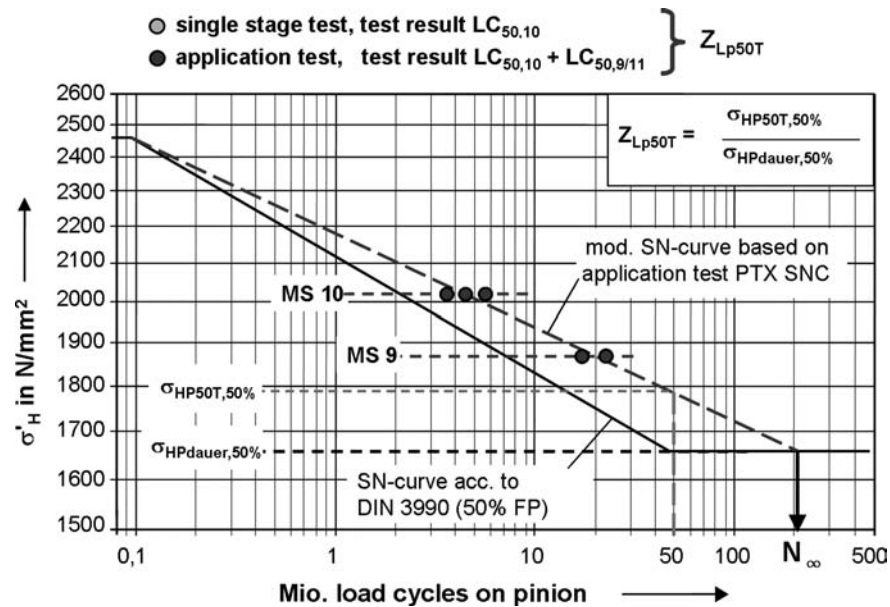


Figure 11.20—Modified SN-curve from results of the pitting application test.

The standard rig requires modifications with a speed increaser between motor and slave gear box, a torque meter at the input shaft to the slave gear box, and a torque meter in the power circulation for exact transmitted power measurements. The efficiency test designated E-C/0.5:20/5:9/40:120 [22] uses C-type gears (C-PT) in the speed range between 0.5 and 20 m/s (0.5:20) at different load stages between load stage 5 and 9 (5:9) with oil temperatures ranging between 40 and 120°C (40:120). At different combinations of operating conditions, full-film lubrication, mixed lubrication, and boundary lubrication occurs, and the frictional behavior of the candidate lubricant can be evaluated in all relevant lubrication regimes. With measurements at no load and different high-load levels, no-load losses and load-dependent losses can be separated. Type C-PT test gears are mounted in the test and the slave gear box, followed by a run-in sequence so that a uniform distribution of the power loss between the two gear boxes can be assumed. The candidate oils are compared to the results of the reference oil, mineral oil ISO VG 100 with 4 % of a sulfur-phosphorus EP additive package.

Figure 11.21 schematically shows the test sequence. After each reference or candidate oil test, a so-called “check test” with a pure mineral oil ISO VG 32 is performed to check for possible changes in the test equipment and to create neutral gear tooth surfaces. The test of the reference or a candidate oil then follows at different speed levels. In the first test sequence, the load is varied between load stage 5 and 9 at a constant oil temperature of 90°C. In the second sequence, the temperature is varied between 40 and 120°C at constant load (load stage 7), and in the third sequence, the no-load losses at all speed and temperature levels are measured.

Measured power loss results of candidate oils are related to the results of the reference oil as a function of temperature in the no-load loss factor X_{Lo} for no-load conditions, in the load loss factor X_{LL} predominantly at EHD and mixed lubrication conditions, and in the boundary loss factor X_{LG} predominantly at mixed and boundary lubrication. The loss factors represent the relation of the measured

power loss for the reference and the candidate oil at the different lubrication regimes. The no-load loss factor is mainly influenced by the viscosity of the oil, the load loss factor by the base oil type, and the boundary loss factor by the additive system. Figure 11.22 shows load loss factors for different base oil types. In the range of EHD and mixed lubrication conditions, polyalphaolefins (PAO 68) typically reduce friction to 80–90 % and polyglycols (PG 68) from 80 to 60 % of the values of mineral oils (MIN 100). A polyether-type lubricant (PETH 68) even showed friction values of 40–50 % of a mineral oil.

In addition to the loss factors, the steady-state temperature at mean operating conditions is evaluated as well as the total energy loss during the test. Ranking tables for candidate oils can be evaluated in which the relevant oil prop-

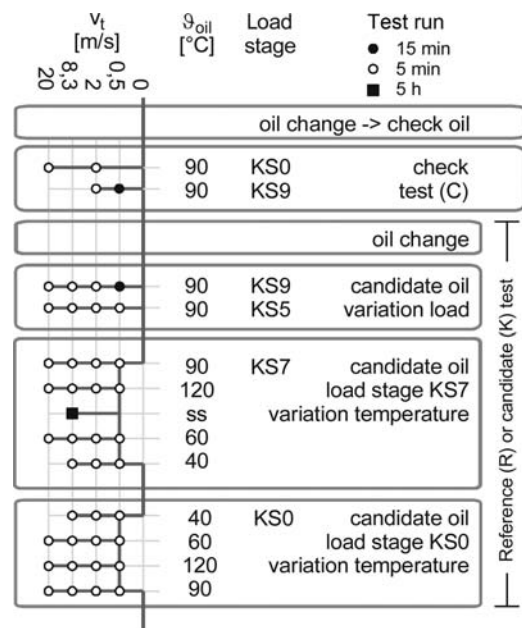


Figure 11.21—Efficiency test procedure.

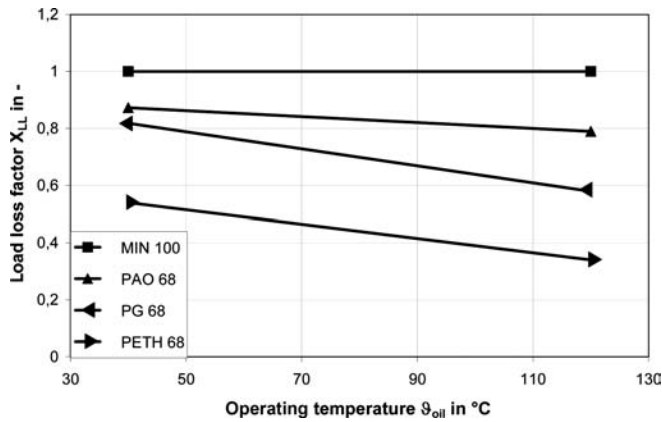


Figure 11.22—Load loss factor for different base oils.

erties in different applications are taken into consideration. With the test results, equations for the mean coefficient of gear tooth friction are derived for application in practical gear boxes. A simple approximation is [22]:

$$\mu_{mz} = 0,048 \cdot \left(\frac{F_{bt}/b}{v_{\Sigma C} \cdot \rho_{red C}} \right)^{0,2} \cdot \eta_{oil}^{-0,05} \cdot R_a^{0,25} \cdot X_{LL} \quad (11.4)$$

where:

μ_{mz} = mean coefficient of gear tooth friction,

F_{bt} = normal tooth load (N),

b = face width (mm),

$v_{\Sigma C}$ = sum velocity at pitch point (m/s),

$\rho_{red C}$ = reduced radius of curvature at pitch point (mm),

η_{oil} = dynamic oil viscosity at oil temperature (mPas),

R_a = arithmetic mean roughness of pinion and gear $R_a = 0.5 \cdot (R_{a1} + R_{a2})$ (μm), and

X_{LL} = load loss factor at operating oil temperature.

The load-dependent power loss P_{VZP} in the gear mesh can then be calculated from [22]:

$$P_{VZP} = \mu_{mz} \cdot H_V \cdot P_a \quad (11.5)$$

where:

P_{VZP} = load-dependent mesh power loss (kW),

μ_{mz} = mean coefficient of gear tooth friction,

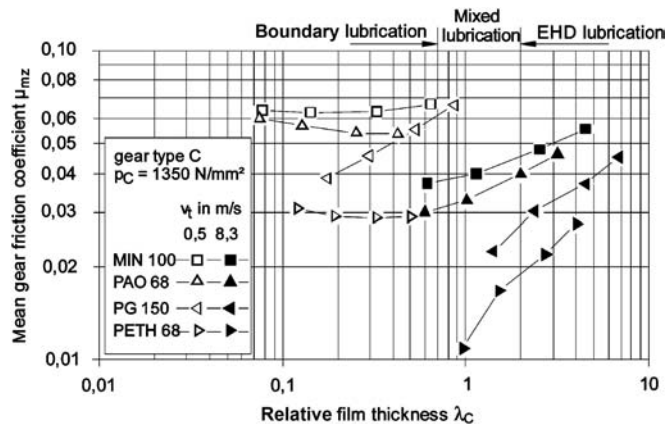


Figure 11.23—Mean friction coefficients of different gear lubricants.

H_V = tooth loss factor, and

P_a = transmitted power (kW).

Figure 11.23 shows the results of the mean coefficient of friction for different base oils. The highest friction is measured for the mineral oil (MIN 100). Lower friction is found for the polyalphaolefin (PAO 68) and even lower for the polyglycol (PG 150). The lowest friction in the gear mesh could be evaluated for a low-friction lubricant on polyether basis (PETH 68) with average values at 50 % of the values of a mineral oil.

11.4 SUMMARY

The influence of lubricants on gear failure modes and gear efficiency can be quantified in methods using appropriately designed test gears. The FZG back-to-back gear test rig is widely available globally and used extensively in the lubricant industry. Numerous methods have been developed and are widely accepted in industry for the quantification of the influence of lubricants on gear failures such as scuffing, wear, micropitting, and pitting as well as on frictional performance. The results of such test methods can be introduced into calculation algorithms for universal application to gears in practice.

REFERENCES

- [1] Höhn, B.-R., Michaelis, K., and Doleschel, A., 2001, "Limitations of Bench Testing for Gear Lubricants," In *ASTM STP 1404: Bench Testing of Industrial Fluid Lubrication*, ASTM International, West Conshohocken, PA.
- [2] Wirtz, H., Presented at Technical Academy, Wuppertal, 1980, unpublished, "Schmierstoffe und anwendungsbezogene Schmierstoffprüfung."
- [3] Höhn, B.-R., Oster, P., and Michaelis, K., 2004, "Influence of Lubricant on Gear Failures—Test Methods and Application to Gearboxes in Practice," *Tribotest*, Vol. 11, pp. 53–56.
- [4] ISO 14635-1, 2000: Gears—FZG Test Procedures—Part 1: FZG Test Method A/8.3/90 for Relative Scuffing Load-Carrying Capacity of Oils. International Organization for Standardization, Geneva, Switzerland.
- [5] IP 334, 1990: Determination of Load Carrying Capacity of Lubricants, FZG Gear Machine Method, Institute of Petroleum, London, UK.
- [6] ASTM D5182, 2008: Standard Test Method for Evaluating the Scuffing (Scoring) Load Capacity of Oils, *Annual Book of ASTM Standards*, ASTM International, West Conshohocken, PA.
- [7] CEC L-07-A-95, 1995: FZG Gear Machine: Load Carrying Capacity Test for Transmission Lubricants. Coordinating European Council, Desford, UK.
- [8] Winter, H., and Michaelis, K., 1982, *Scoring Load Capacity of EP-Oils in the FZG L-42 Test*, SAE Technical Paper 821183, SAE, Warrendale, PA.
- [9] FVA Information Sheet No. 243, 1995: Scuffing Test EP-Oils, Method to Assess the Scuffing Load Capacity of Lubricants with High EP Performance Using an FZG Gear Test Rig, Forschungsvereinigung Antriebstechnik, Frankfurt, Germany.
- [10] DIN 3990, Teil 4, 1987: Tragfähigkeitsberechnung von Stirnrädern: Berechnung der Fresstragfähigkeit, Deutsches Institut für Normung, Berlin, Germany.
- [11] ISO DTR 13989, 2000: Calculation of Scuffing Load Capacity of Cylindrical, Bevel and Hypoid Gears, International Organization for Standardization, Geneva, Switzerland.
- [12] ASTM Standard D4998-89, 1989: Standard Test Method for Evaluating Wear Characteristics of Tractor Hydraulic Fluids, *Annual Book of ASTM Standards*, ASTM International, West Conshohocken, PA.
- [13] DGMK Information Sheet No. 377, 1996: "Method to Assess the Wear Characteristics of Lubricants in the FZG Gear Test Rig," *Deutsche Wissenschaftliche Gesellschaft für Erdöl, Erdgas und Kohle*, Hamburg, Germany.

- [14] Winter, H., and Plewe, H.J., 1982, "Calculation of Slow Speed Wear of Lubricated Gears," AGMA Paper, p. 219.16 presented at the AGMA Fall Technical Conference, New Orleans, LA.
- [15] Winter, H., and Oster, P., 1987, *Influence of the Lubricant on Pitting and Micro Pitting (Grey Staining, Frosted Areas) Resistance of Case Carburized Gears - Test Procedures*, AGMA Technical Paper 87FTM10, AGMA, Alexandria VA.
- [16] FVA Information Sheet No. 54/I-IV, 1993: Test Procedure for the Investigation of the Micro-Pitting Capacity of Gear Lubricants, Forschungsvereinigung Antriebstechnik, Frankfurt, Germany.
- [17] DGMK Information Sheet, 2005: Short Test Procedure for the Micropitting Load Capacity of Gear Lubricants, Deutsche Wissenschaftliche Gesellschaft für Erdöl, Erdgas, und Kohle, Hamburg, Germany.
- [18] Höhn, B.-R., Michaelis, K., Oster, P., Schrade, U., and Tobie, T., 2005, "Calculation of the Micropitting Load Capacity of Case Carburized Gears," Paper presented at the COST 532 Conference, Porto, Portugal, Triboscience and Tribotechnology, pp. 55–71.
- [19] FVA Information Sheet No. 2/IV, 1997: Influence of Lubricant on the Pitting Capacity of Case Carburized Gears in Load-Spectra and Single-Stage-Investigations, Forschungsvereinigung Antriebstechnik, Frankfurt, Germany.
- [20] FVA Information Sheet No. 371, 2003: Practice Relevant Pitting Test, Forschungsvereinigung Antriebstechnik, Frankfurt, Germany.
- [21] ISO DIS 6336, 2006: Calculation of Load Capacity of Spur and Helical Gears, International Organization for Standardization, Geneva, Switzerland.
- [22] Höhn, B.-R., Michaelis, K., and Doleschel, A., 2004, "Evaluation of the Frictional Properties of Transmission Lubricants," Paper presented at the 14th International Colloquium Tribology, Technische Universität Esslingen, January 13–15, Vol. 1, pp. 337–346.
- [23] FVA Information Sheet No. 345, 2002: Method to Determine the Frictional Behaviour of Lubricants Using a FZG Gear Test Rig, Forschungsvereinigung Antriebstechnik, Frankfurt, Germany.

12

Problems and Opportunities Regarding the Lubrication of Modern Automotive Engines

E.S. Yamaguchi¹, G.A. Tanaka¹, and K. Matsumoto²

12.1 INTRODUCTION

For those readers who have been involved with diesel and passenger car engine oils for many years, this chapter may not seem to cover all aspects of this broad topic in great detail. However, for those readers who are interested in the topic and who have not lived through the development of engine oil categories, this chapter is meant to convey an understanding of the challenges and the excitement that practitioners are now facing. The goals of this chapter are to give the reader a full understanding of the lubrication of diesel and gasoline engine oils and their present U.S. categories, and then to concentrate on what makes these oils perform so well today. That role is fulfilled by the additives that are put into these oils, and this chapter will describe the function of these remarkable components.

12.2 REQUIREMENTS FOR GASOLINE ENGINE OILS TODAY

Gasoline engine oils today are very complex mixtures of primarily base oil (along with their subcomponents) and secondary lubricating oil additives. This chapter will focus on mineral-oil-based lubricants. Table 12.1 shows the latest gasoline engine oil category, which is the International Lubricants Standardization and Approval Committee (ILSAC) GF-5 [1]. In addition to these engine test types listed in Table 12.1, which must be passed to currently qualify as this highest quality gasoline engine oil, there are several bench tests that need to be passed to claim GF-5 performance; these tests are enumerated in Table 12.1. The qualifications for the next level will likely be even more rigorous, as each successive level has historically been. There are several different exhaust after treatment systems in current use [2], and the development of new ones continues. For gasoline engines, the most widely used is the three-way catalyst (TWC). This oxidizes carbon monoxide (CO) and hydrocarbons (HCs) to carbon dioxide (CO₂) while reducing oxides of nitrogen (NO_x) to N₂. The TWC is suited to engines operating close to stoichiometry, but it is unable to satisfactorily reduce NO_x to N₂ in a lean-burn engine where there is a surplus of oxygen in the exhaust gas. For such engines, which are common in Japan, NO_x storage-reduction catalysts are used that store NO_x during lean engine operation and reduce it to N₂ during periodic stoichiometric operation [3].

Phosphorus, particularly the phosphorus delivered by zinc dialkyldithiophosphate (ZDDP), has been the predominant antiwear agent in fully formulated lubricants for the

past 50 years. Several studies have suggested that phosphorus may poison the catalytic converters used on gasoline-fueled engines to reduce exhaust emissions of unburned HCs and NO_x [4–6]. This negatively alters the fuel efficiency achieved by these engines. As the environmental regulations governing tailpipe emissions (CO, HCs, and NO_x) have tightened, the allowable concentration of phosphorus in engine oils has been significantly reduced. Engine oil category GF-5 maintains the same phosphorus level as the GF-4 category, but reduces the phosphorus volatility so that the amount of phosphorus deposited on the catalyst will be equivalent to an oil containing 0.05 % phosphorus. A brief summary of the engine tests required for the GF-4 category follows (consult reference 1).

It is interesting to note that a recent study by Bishop and Stedman [7] showed that dramatic reductions in emission rates have been achieved for the metropolitan areas of Chicago, Denver, Los Angeles, and Phoenix since 1997: 56–71 % for CO, 27–63 % for HCs, and 48–68 % for NO_x. All cities used fuels that have been changed chemically so that the potential for making ozone or other toxic materials is decreased. In the cities of Tulsa, OK, and Omaha, NE, where no fuel reformulation programs existed, the same levels of reductions were observed. Thus, the authors attribute the observed reductions to the sensors that monitor the exhaust and control the combustion in the engine. During this period, sensors to control the air/fuel ratio on a cylinder-by-cylinder basis were introduced, and large emission reductions followed.

12.3 GASOLINE ENGINE TESTS FOR GF-5/SL PERFORMANCE

12.3.1 Sequence IIIG Test (ASTM D7320)

For the Sequence IIIG engine tests, the candidate oil is run in a General Motors fuel-injected engine (3.8-L), V6 231 cubic inch displacement (CID). The primary objective of the test is to measure oil oxidation by way of viscosity increase. Second, the cam and lifter wear is measured, as well as an evaluation of the high-temperature piston deposits (piston varnish). The limits for the Sequence IIIG test are shown in Table 12.1. The viscosity increase level is measured at 40°C and compared to the new oil every 20 h.

12.3.2 Sequence IIIGA Test (ASTM D7528)

In this test, an end-of-test engine oil is subjected to cold-temperature viscosity measurements. Using an oil from a 1996/1997 General Motors V6, 3.8L, 231 CID engine, the oil has the following break-in: a 10-min oil-leveling procedure

¹ Chevron Oronite Co., LLC, Richmond, CA, USA

² Honda R & D Co., Ltd. Automobile R & D Center

TABLE 12.1—ILSAC Approved GF-5 Performance Category and Test Methods[1]

PERFORMANCE PARAMETER	TEST METHOD	ILSAC STANDARD	
		GF-4	GF-5
1. Fresh Oil Viscosity Requirements	SAE J300—Viscosity grades limited to SAE 0W, 5W, 10W Multigrade Oils		All of J300
2. Gelation Index To be evaluated from -5°C to the temp at which 40,000 cP is attained or -40°C, or 2 Celsius degrees below the appropriate MRV TP-1 temperature (Defined by SAE J300), whichever occurs first.	ASTM D 5133		12 max
3. Wear and Oil thickening: - Kinematic Viscosity Increase @ 40°C, % - Avg. weighted piston deposits, merits - Hot stuck rings - Avg. cam plus lifter wear, μm	IIIG, ASTM D7320	150 max 3.5 min None 60 max	150 max 4.0 min None 60 max
4. Wear, Sludge, Varnish Test: - Avg. engine sludge, merits - Avg. rocker cover sludge, merits - Avg. engine varnish, merits - Avg. piston skirt varnish, merits - Oil screen sludge, % area - Oil screen debris, % area - Hot stuck compression rings - Cold stuck rings - Oil ring clogging, % area	Sequence VG, ASTM D6593	7.8 min 8.0 min 8.9 min 7.5 min 20 max Rate, report None Rate, report Rate, report	8.0 min 8.3 min 8.9 min 7.5 min 15 max Rate, report None Rate, report Rate, report
5. Valvetrain wear: Avg. cam wear, 7 position avg. μm	Sequence IVA, ASTM D6891	90 max	90 max
6. Bearing corrosion: Bearing weight loss, mg	Sequence VIII, ASTM D6709	26 max	26 max
7. Fuel Efficiency SAE XW-20 viscosity grade: FEI Summary FEI 2 minimum after 100 hours aging SAE XW-30 viscosity grade: FEI Summary FEI 2 minimum after 100 hours aging SAE 10W-30, all other viscosity grades not listed above: FEI Summary FEI 2 minimum after 100 hours aging	Sequence VID, ASTM D7589		2.6 1.2 1.9 0.9 1.5 0.6
8. Catalyst Compatibility: Phosphorus Content	ASTM D4951	0.08% (mass) max	0.08% (mass) max
9. Catalyst Compatibility: Phosphorus Volatility	Sequence IIIGB, ASTM D7320		79% phosphorus retention
10. Catalyst Compatibility: Sulfur Content - 0W-XX, 5W-XX - 10W-30	ASTM D4951 or D 2622	0.5% (mass) max 0.7% (mass) max	0.5% (mass) max 0.6% (mass) max
11. Wear - Phosphorus content	ASTM D4951	0.06% (mass) min	0.06% (mass) min
12. Volatility - Evaporation loss - Simulated distillation	ASTM D5800 ASTM D6417	15% max, 1 h, 250°C 10% max 371°C	15% max, 1 h, 250°C 10% max 371°C
13. High-Temperature Deposits Deposit weight, mg	TEOST MHT, ASTM D7097	35 max	35 max
14. High-Temperature Deposits Total deposit weight, mg <i>NOTE: No TEOST 33C limit for SAE 0W-20</i>	TEOST 33C, ASTM D6335 (Note: No TEOST 33C limit for SAE 0W-20)	30 max	30 max

TABLE 12.1—ILSAC Approved GF-5 Performance Category and Test Methods[1] (Continued)			
		ILSAC STANDARD	
PERFORMANCE PARAMETER	TEST METHOD	GF-4	GF-5
15. Filterability EOWTT With 0.6% H ₂ O With 1.0% H ₂ O With 2.0% H ₂ O With 3.0% H ₂ O	ASTM D6794	Max Flow Reduction	
		50%	50%
		50%	50%
		50%	50%
16. EOFT	ASTM D6795	50%	50%
17. Fresh Oil Foaming Characteristics Sequence I Sequence II Sequence III	ASTM D892 (option A, no paragraph 11)	Tendency: 10 mL max 50 mL max 10 mL max Stability, after one min: 0 mL max stability for all	Tendency, Stability: 10, 0 mL max 50, 0 mL max 10, 0 mL max Stability, after one min: 0 mL max stability for all
18. Fresh Oil High-temperature Foaming Characteristics	ASTM D6082 (Option A)	Tendency: 100 mL max Stability, after one min: 0 mL max	Tendency, Stability: 100, 0 mL max Stability, after one min: 0 mL max
19. Aged Oil Low-Temperature Viscosity Measure CCS visc of EOT ROBO sample @ CCS temp corresponding to original visc grade: - If CCS ≤ max CCS visc for original visc grade, run ASTM D4684 at MRV temp specified in SAE J300 for original visc grade - If CCS visc measured is higher than max visc specified for the original visc grade in J300, run ASTM D4684 at 5°C higher temp - The EOT ROBO sample must show no yield stress in D4684 test and its D4684 visc must be below the max specified in SAE J300 for the original visc grade or the next higher visc grade, depending on the CCS visc	ROBO Test or ASTM Sequence III GA Test, ASTM D7528		
20. Shear Stability 10-hour stripped KV at 100°C	Sequence VIII, ASTM D6709	KV must remain in original SAE visc grade	KV must remain in original SAE visc grade
21. Homogeneity and Miscibility	ASTM D6922	Shall remain homogeneous and when mixed with TMC reference oils shall remain miscible	Shall remain homogeneous and when mixed with TMC reference oils shall remain miscible
22. Engine Rusting Average gray value	Ball Rust Test, ASTM D6557	100 min	100 min
23. Emulsion Retention Oil mixed with 10% water, 10% E85 0°C, 24 Hours 25°C, 24 Hours	ASTM D7563		No water separation No water separation
24. Elastomer Compatibility Elastomer material, SAE J2643: Polyacrylate Rubber (ACM-1)	ASTM D471, Volume, %Δ ASTM D2240, Hardness, pts. ASTM D412, Tensile strength, %Δ		-5, 5 -10, 10 -30, 30

(Continued)

TABLE 12.1—ILSAC Approved GF-5 Performance Category and Test Methods[1]

PERFORMANCE PARAMETER	TEST METHOD	ILSAC STANDARD	
		GF-4	GF-5
Hydrogenated Nitrile Rubber (HNBR-1)	ASTM D471, Volume, %Δ ASTM D2240, Hardness, pts. ASTM D412, Tensile Strength, %Δ		-5, 5 -5, 5 -20, 10
Silicone Rubber (VMQ-1)	ASTM D471, Volume, %Δ ASTM D2240, Hardness, pts. ASTM D412, Tensile Strength, %Δ		-5, 40 -20, 10 -45, 0
Fluorocarbon Rubber (FKM-1)	ASTM D471, Volume, %Δ ASTM D2240, Hardness, pts. ASTM D412, Tensile Strength, %Δ		-2, 3 -4, 6 -65, 10
Ethylene Acrylic Rubber (AEM-1)	ASTM D471, Volume, %Δ ASTM D2240, Hardness, pts. ASTM D412, Tensile Strength, %Δ		-5, 30 -10, 10 -30, 30

and then a 15-min slow ramp up to speed (high) and load conditions of 125 bhp, 3600 r/min, and 150°C oil for 100 h. Every 20 h, there is an oil check at the end of the test, the Cold Crank Simulator (CCS) ASTM D5293 is run, and the yield stress (ASTM D4684) is determined.

12.3.3 Sequence VG Test (ASTM D6593)

This is an engine dynamometer test that is a replacement for the Sequence VE engine test, the ASTM D5302 Sludge and Varnish Test. It uses a 2000 Ford 4.6-L, eight-cylinder, fuel-injected gasoline engine in a 216-h test with unleaded gasoline. This test simulates stop-and-go city driving (e.g., in a taxicab). Only sludge and varnish are evaluated, although several other parameters are measured and recorded.

12.3.4 Sequence VID (ASTM D7589)

This test uses a 2008 3.6-L, GM V6 gasoline engine, and it is used to determine the fuel economy of the test oil, which includes aging conditions consisting of two phases of long-term aging—one for 16 h and the other for 84 h. The test is run in such a way so that the oil to be evaluated is used after the reference baseline oil BL, and the fuel consumption of the candidate oil is determined after both aging periods at six different test conditions. Then the BL is run again. The required improvements of the candidate oil over the BL are given in the table and show dependence of the fuel economy of the test on the viscosity grades.

12.3.5 Sequence VIII Test (ASTM D6709)

The Sequence VIII test is a modified version of the CRC L-38 copper, lead, and bearing corrosion test that uses a Labeco single-cylinder test that lasts for 40 h. The CRC L-38 used leaded fuel, and later, it was determined that the current Sequence VIII test should be conducted using unleaded fuel. The Sequence VIII test determines the extent of shear stability of the viscosity index improver (VII), as well as the properties regarding the candidate oil on bearing corrosion using unleaded gasoline with no greater than 0.08 % phosphorus.

12.3.6 Sequence IVA Test (ASTM D6891)

This particular test uses a Nissan 2.4-L, KA 4E model engine. It is a four-cylinder, in-line, overhead camshaft engine with two intake valves and one exhaust valve per cylinder. The goal here is to measure the amount of cam wear in this particular engine test. Cam lobes are measured before and after the engine test to determine how much wear is observed on 7 positions around 12 lobes, which are averaged to obtain the final results. Unleaded fuel is used for the Sequence IVA test.

Passing several bench tests is also required. To maintain proper engine operation as per original equipment manufacturer (OEM) specifications, the Catalyst Compatibility Test mandates no greater than 0.08 % phosphorus maximum. This is based on research [5] indicating catalyst performance degradation with higher phosphorus levels. Still, the concern for satisfactory wear performance specifies a 0.06 % phosphorus minimum. Some researchers think that formulating with low levels of ZDDP may not be possible [8–10]. There is much effort around the development of nonphosphorus-containing supplemental wear inhibitors today; however, this is a difficult challenge [11,12]. Crompton scientists have developed silicon-containing additives that are claimed to be partial or full replacements of ZDDP in automotive lubricants formulations. There are other scientists that have developed additives that are ashless but still contain phosphorus or sulfur or both. Their performance is generally not primarily targeted for wear protection in automotive engine oil formulations [13].

12.4 REQUIREMENTS FOR DIESEL ENGINE OILS TODAY

As for the diesel engine arena, the highest level of performance is claimed by API CJ-4. To qualify for an API CJ-4 level diesel engine oil, a prospective candidate oil must pass all of the tests shown in Table 12.2 [14]. Although the GF-5 category concentrated on fuel economy, the CJ-4 category for diesel engine oils stresses particulate emissions. In diesel engines, a combination of exhaust gas recirculation (EGR), an oxidation catalyst, and a diesel particulate filter (DPF) are generally

TABLE 12.2—Engine and Bench Test for API CJ-4

Test Type	Purpose	Parameter	Requirement				
Caterpillar 1N	Evaluates performance of crankcase lubricants	Piston deposits Ring sticking Piston scuffing Ring scuffing Liner scuffing Oil consumption	Weighted demerits, max 286.2/311.7/323.0 Top groove fill, max 20/23/25 Top land heavy carbon, max 3/4/5 Oil consumption (0–252 h) g/kWh, max 0.5 Piston/ring/liner scuffing None Piston ring stick None				
Caterpillar C13	Evaluates performance of crankcase lubricants for piston deposits and oil consumption	Liner (1Y-4107) Piston (1Y-4106) Top ring (1Y-4108) Second ring (1Y-4109) Oil ring (1Y-4110)		Max	Merit Weight	Anchor	Min
			Delta O/C	31	300	25	10
			ATLC	35	300	30	15
			ATGC	53	300	46	30
			R2TCA	33	100	22	5
			Merits 1000				
Cummins ISB	Evaluates a crankcase lubricant's ability to reduce valvetrain and camshaft lobe wear	Camshaft Mushroom-style slider tappets Crosshead	MTAC				
			1 2 3				
			ACSX 55 55 59 61				
			ATWL 100 100 108 11				
Cummins ISM	Evaluates a lubricant's effectiveness at reducing soot-related overhead wear, sludge, oil filter, plugging	Injector adjusting screw Sludge Crosshead Top ring wear Oil filter plugging	Parameter	Anchor	Merit Weight	Max.	Min.
			XHD	5.7	350	7.1	4.3
			RWL	100	0	100	0
			Ofdp	13	150	19	7
			IAS	27	350	49	16
			Sludge	9	150	9.3	8.7
			Merits 1000				
Engine Oil Aeration Test	Determines effectiveness of engine lubricating oils at minimizing air entrainment in large pickups and medium-duty trucks	Oil evaluation	At 20 h, the maximal allowable amount of air entrainment in the oil is 8 % for API CJ-4, CI-4, and CH-4 and 10 % for API CF-4				
Mack T-11	Evaluated soot handling performance	Oil filter plugging	Viscosity at 12 cSt Viscosity at 15 cSt Viscosity at 4 cSt		6.0 TGA soot min 6.7 3.5		
			New oil MRV at –20°C 180-h used MRV		20,000 all grades 25,000, yield stress <35 D4684M		
Mack T-11A	Evaluates soot handling performance of lubricating oils operating in diesel engines equipped with EGR	Oil samples	180-h sample soot New oil MRV at –20°C 180-h used MRV		4.82/5.16/5.49 20,000 all grades 25,000, yield stress <35 D4684M		
Mack T-12	Evaluates an oil's ability to minimize cylinder liner, piston ring, and bearing wear in engines with EGR	Piston ring wear, Cylinder liner wear, Lead bearing corrosion, Oil consumption, and Oxidation	Parameter	Anchor	Merit Weight	Max.	Min.
			RWL	70	200	105	35
			LWS	20	250	24	12
			Lead	25	200	35	10
			Lead Delta	10	200	15	0
			O/C	65	150	85	50
			Merits 1000				

(Continued)

TABLE 12.2—Engine and Bench Test for API CJ-4 (Continued)

Test Type	Purpose	Parameter	Requirement		
Roller Follower Wear Test	Determines effects of lubricating oils on camshaft roller follower axle wear	Roller follower axes	<u>Average Pin Wear</u> mils, max or µm, max		<u>MTAC Limits</u> 0.30/0.33/0.36 7.6/8.4/9.1
Sequence IIIF	Measures oil thickening and piston deposits under high temperature conditions	Pistons inspected for deposits and varnish; cam lobes, lifters measured for wear; oil screen plugging is evaluated	<u>Parameter</u> Viscosity increase		<u>Pass Limit</u> 275 %
Sequence IIIG	Measures oil thickening and piston deposits under high-temperature conditions	Pistons inspected for deposits and varnish; cam lobes and lifters measured for wear; oil screen plugging is evaluated	<u>Parameter</u> Viscosity increase		<u>Pass Limit</u> 150 %
Chemical and Bench Tests					
Foaming	Determines the foaming characteristics of lubricating oils	Foaming volumes	<u>Foaming/Settling</u>		
			Sequence I, max Sequence II, max Sequence III, max		10/0 % 20/0 % 10/0 %
High-Temperature Corrosion	Evaluates diesel engine lubricants to determine tendency to corrode various metals	Four metal coupons	Copper Lead Copper	Used oil increase Used oil increase Strip rating	Max 20 ppm Max 120 ppm Max 3—
High-Temperature High-Shear Viscosity	Covers the laboratory determination of the viscosity of engine oils	Viscosity	Viscosity at 150°C, min 3.5 cP		
NOACK Volatility	Examines the evaporation loss of engine oils	The loss in mass of oil is determined	Evaporation loss at 250°C 13 % Viscosity grade other than 10W-30, max evaporation loss at 250°C 10W-30, max 15 %		
Seal Compatibility	Evaluates the compatibility of automotive engine oils with four reference elastomers	Effects of test oils on elastomers, measurement of changes in volume, hardness, tensile properties	Nitrile		
			Volume change		+5/−3
			Hardness		+7/−5
			Tensile strength		+10/−TMC 1006
			Elongation		+10/−TMC 1006
			Silicone		
			Volume change		+TMC 1006/−3
			Hardness		+5/ −TMC 1006
			Tensile strength		+10/−45
			Elongation		+20/−30
			Polyacrylate		
			Volume change		+5/−3
			Hardness		+8/−5
			Tensile strength		+18/−15
			Elongation		+10/−35
			FKM		
			Volume change		+5/−2

TABLE 12.2—Engine and Bench Test for API CJ-4 (Continued)

			Hardness	+7/–5
			Tensile strength	+10/–TMC 1006
			Elongation	+10/–TMC 1006
			Vamac G	
			Volume change	+TMC 1006/–3
			Hardness	+5/–TMC 1006
			Tensile strength	+10/–TMC 1006
			Elongation	+10/–TMC 1006
Sooted Oil Mini-Rotary Viscometer	Measures yield stress and viscosity of engine oils	Viscosity and yield stress	180-h sample from Mack T-11 or T-11A Viscosity at –20°C, max 25,000 mPa·s Yield stress <35 Pa	

used. The DPF collects soot, which is burned. To meet the newest emissions requirements, NO_x-removal devices such as selective catalyst reduction (SCR) using urea injection or NO_x storage-reduction catalysts are extensively implemented [15].

In this category, for the first time, DPFs are to be used in trucks to trap the particulates, which largely consist of soot additive elements and calcium sulfate from the detergent as well as zinc pyrophosphates (Zn₂P₂O₇) from the ZDDP. Engineers have devised methods of controlling the peak cylinder temperature by retarding fuel injection timing to lower the peak flame combustion temperatures. Adding EGR is the other method used to reduce NO_x emissions. This has been used in the CJ-4 type engine category. The use of these new requirements, including what is called the “chemical box,” which is used to limit the amounts of certain chemical elements derived from diesel engine oil additives in the formulation, have given rise to several new engine tests and bench tests. The limits include 1 % sulfated ash, 0.4 % sulfur, and 0.12 phosphorus [16]. The bench tests and engine tests are discussed below.

12.5 DIESEL ENGINE TESTS FOR API CJ-4 PERFORMANCE

12.5.1 Mack T-11 Test (ASTM D7146)

The Mack T-11 procedure includes the use of a Mack E-Tech V-Mack III 728 CID engine, which is equipped with a fuel (500 ppm sulfur) injection system that uses electronically controlled unit injectors using low-swirl cylinder heads. This test is meant to emulate heavy-duty engines in stop-and-go operations with high soot loading. The engine is an in-line, six-cylinder, four-stroke, turbo-charged engine that uses cooled EGR to meet 2004 emissions regulations. The test length is 252 h, and during this time the soot production is measured at the following times during the test: 96, 192, and 228 h of engine testing. This is done to make sure that soot production is controlled. In addition to the low-temperature pumpability characteristics, the MRV (Mini-Rotary Viscometer test at –20°C, the viscosity at 100°C, and the soot amount are measured at the end of the test. There are some conditions under which a test oil may fail this MRV procedure but still pass the T-11 viscosity limits, in which case another set of tests is run.

12.5.2 Mack T-11A Test (ASTM D8696)

The T-11A test is a replacement for the Mack T-10A test and evaluates the soot handling performance of CJ-4 candidate

oil. It is measured by viscosity increase measurements of used diesel engine oils (MRV at –20°C) and soot. Listed below are the pass/fail criteria:

- 180-h sample soot: 4.82/5.16/5.49
- New oil MRV at –20°C: 20,000 all grades
- 180-h used MRV: 25,000, yield stress <35 D4684M

12.5.3 Sequence IIIF/IIIG Tests

The same hardware and procedures are prescribed for both tests, but the IIIF has a more relaxed viscosity limit and no other ratings, such as weighted piston demerits (see discussion about the IIIG in Section 12.3).

12.5.4 Mack T-12 Test

The Mack T-12 engine test is a test with heavy EGR, and this test measures wear occurring in certain parts of the engine (e.g., the cylinder liner, the piston rings, and bearing wear). The test simulates heavy-duty diesel trucks driving on highways. The Mack T-12 procedure uses a modified Mack E7 E-Tech 460 engine, rated at 460 bhp, running at 1800 r/min, and using 15-ppm sulfur fuel. The combustion system features the 2002 low-swirl cylinder head design. This is a 300-h test in which the first 100 h are used to produce soot. This is done at a certain speed (800 r/min) and varies power, after which the engine is overfueled at peak torque to maximize the wear rates on the rings and cylinder liners. The pass/fail criteria are evaluated using a 1000-point merit system: the piston ring wear, the cylinder liner wear, the lead bearing corrosion, the oil consumption, and oxidation are all measured. Although the oil gallery temperature is controlled at 116°C to produce oxidation, this is also the main source of lead corrosion from the bearings. At the end of the test, the amount of soot produced is approximately 6 %.

12.5.5 Engine Oil Aeration Test

The Engine Oil Aeration Test (EOAT) uses a 7.3-L, V8, four-stroke, turbo-charged, compression ignition engine using a hydraulically actuated electronically controlled unit injector (HEUI) fuel injection system. This 1994 Navistar Truck test engine simulates a large pickup and medium-duty trucks under high speeds and high-load applications, and this procedure tests the engine oil's ability at minimizing air entrainment, which may influence the engine fuel injection timing. The engine itself is rated at 215 bhp at 3000 r/min.

At test hours 1, 5, and 20, the entrainment of air into the oil is measured. The lubricant is also analyzed for wear metals at 0 and 20 h. The CJ-4 limit is 8 % aeration in the Navistar 7.3-L HEUI. The CJ-4 category includes a limit on aeration due to Navistar's problems with oil aeration in 1994. Rough running might be a problem with substantial aeration.

12.5.6 *Roller Follower Wear Test*

A General Motors 6.5-L indirect-injected diesel engine that is rated at 160 hp at 3400 r/min is used in this 50-h test. The engine test evaluates the effects of engine oils on camshaft roller follower axle wear. It is run at 1000 r/min with near-maximum load and without an oil change. However, make-up oil is added at 25 h. The oil gallery and coolant-out temperatures are set to 120°C.

12.5.7 *Cummins ISB Test*

The Cummins ISB procedure is used for testing the diesel engine crankcase lubricant's ability to protect against wear of the valvetrain components. In evaluating valvetrain wear performance, it is important to have a repetitive cyclic operation, and this is what the Cummins ISB procedure provides. It is a 350-h procedure using a Cummins ISB 5.9-L 2004 engine equipped with EGR. After 100 h of steady-state operation at 1600 r/min to accumulate 3.25 % soot in the oil, the engine is operated another 250 h on a very fast (28-s) cycle that simulates the cyclic operation known to give rise to camshaft wear. The engine in this second 250 h actually completes 32,000 cycles. It is certified at 2.0 g NO_x/bhp·h, and the test uses 15-ppm sulfur fuel. The CJ-4 procedure stipulates a measurement of the rotating tappet and camshaft as the wear parameters measured in this test.

12.5.8 *Cummins ISM Test*

This procedure evaluates valvetrain wear, ring wear, sludge, and filter plugging. It is more complex than the ISB procedure. This procedure uses a 2002 model-year 11-L engine with cooled EGR and a variable geometry turbocharger. The engine is a replacement for the Cummins M-11 EGR test and simulates high-load, heavy-duty field conditions with high EGR flow rates. This is a 200-h test and cycles between 1600 and 1800 r/min with 50 h at each speed. The target soot level is 6.5 % at 150 h, which is achieved by retarded timing and overfueling. The parameters measured on this test are (1) average crosshead weight loss, (2) average top ring weight loss, (3) average adjusting screw weight loss, (4) sludge rating on rocker cover and oil pan combined, and (5) oil filter delta pressure at 150 h.

12.5.9 *Caterpillar 1N Test*

This diesel engine test simulates a high-speed, turbo-charged diesel engine in service before 1998 with low-sulfur fuel (0.03–0.05 % sulfur). The unique feature about this test is that it uses an aluminum piston in a Caterpillar 1Y 540 single-cylinder diesel test engine with a four-valve arrangement having a 149 CID. There is also a keystone top ring and a rectangular second ring. The compression ratio is 14.5:1. The test is run at 2100 r/min, 70 bhp, 1800 bmep, 7999 Btu/min fuel input, 200°F coolant temperature, 225°F oil temperature, 260°F inlet air temperature, and a 29:1 air/fuel ratio for 252 h. The test procedure measures piston deposits, ring sticking, piston scuffing, ring scuffing, liner scuffing, and oil consumption. The deposit measurements

are conducted using the CRC weighted demerits system. The top groove fill and the top land heavy carbon deposit are the carbon deposits on top of the piston of interest, and the brake-specific oil consumption is also rated. The Caterpillar 1N test engine does not use EGR.

12.5.10 *Caterpillar C13 Test*

This engine test procedure evaluates piston deposits and oil consumption in a similar manner to the 1-N test, and it does not use EGR. The engine used for this test is an in-line six-cylinder Caterpillar C-13 engine with one-piece steel pistons with a turbo-charged air system utilizing advanced combustion emission reduction technology (ACERT). The test runs for 500 h at 1800 r/min and has a 40°C intake manifold temperature, 88°C coolant-out temperature, 40°C fuel-in temperature, a 98°C oil temperature, and a 280-kPa intake manifold pressure. This test is intended to simulate the heavy-duty diesel engines configured to meet 2007 on-highway emission regulations and uses the ultralow-sulfur diesel fuel (15 ppm). The actual parameters that are measured on the pistons are top-land carbon, top-groove carbon, carbon on the top face of the second rectangular ring, and liner scuffing/wear. Also, the oil consumption is measured by averaging data at the 100- and the 150-h points and comparing these to the average oil consumption for 450–500 h to determine the delta increase.

A summary of the performance characteristics that are evaluated for the API CJ-4 category is given in Table 12.3 [16]. Table 12.4 lists all tests that must be passed for CJ-4 approval. It is a formidable challenge to pass all 15 tests at the highest level of diesel engine oil performance because, for example, the increase in injection pressures has raised contact stresses at the camshaft in the fuel pump (Hertz stress) to levels as high as 250,000–300,000 psi and above [17] since 1988 when regulation of diesel emissions started. Clearly, the bench tests are significantly cheaper than the engine tests, so one should be fairly confident about an oil formulation before spending nearly \$100,000 for a diesel engine test.

12.6 ADDITIVE FUNCTIONS

By design, the additives used in CJ-4 formulation are not emphasized, but rather the functions of these component types are discussed. The reader may read several excellent reviews of the chemistry and tribology of these additives [18–22]. Table 12.5 shows the typical use levels described by Bell [23]. It also describes the functions of the various additive groups in descriptive terms. Each function will now be addressed (see Table 12.6).

12.6.1 *Controlling Wear [24,25]*

It was in the first half of last century (1940s) when H.C. Freuler of Union Oil discovered ZDDPs [26,27]. At the time, he thought they would be useful as oxidation and corrosion inhibitors for engine oils, but the advent of competition to produce greater acceleration without increasing engine size produced a valvetrain wear problem that was readily solved by the multifunctional ZDDP. Later, it was found that the secondary ZDDP gives better wear performance than the primary, which gives better wear performance than the alkaryl ZDDPs in engine tests [28]. This pattern of behavior has been linked to the thermal stability of these materials [29]. Today, it is known that the secondary ZDDP is adsorbed more readily than the primary ZDDP, which is adsorbed even more readily than

TABLE 12.3—API CJ-4 Engine Tests and Performance Criteria

Performance	Cummins ISM	Cummins ISB	GM 6.5L	Cat C13	Cat 1N	Mack T-12	Mack T-11(A)	Gasoline I/II/III/IV	Navistar 7.3L
Valvetrain wear	X	X	X						
Liner wear						X			
Ring wear	X					X			
Bearing corrosion						X			
Oxidation						X		X	
Oil consumption				X	X	X			
Iron piston deposits				X					
Aluminum piston deposits					X				
Soot viscosity increase							X		
Sludge	X								
Filter plugging	X								
Aeration									X
Low-temperature pump at 5.2 % soot ^a							X		

^aAt 180 h. GM = General Motors, Cat = Caterpillar.

the alkaryl ZDDP. These data were gathered by inelastic electron tunneling experiments, in which it was shown that the alkaryl ZDDP was actually hydrolyzed on adsorption to a metal oxide surface [30,31].

Subsequently, many studies [32,33] using X-ray absorption near-edge structure spectroscopy (XANES) showed that the neutral version of the ZDDP structure was better adsorbed than the basic version of the same ZDDP salt in tribochemical and thermal films as determined by the length of the polyphosphate chain; the longer the polyphosphate chain, the better. This suggested that in a commercial material, which contains neutral and basic salt, it is the neutral ZDDP that would give rise to better wear performance [32]. This was in fact shown to be the case in several Sequence VE experiments, in which a secondary neutral ZDDP was tested three times in this sequence engine test and compared to a secondary basic ZDDP. In all three times, the neutral ZDDP structure passed the wear requirement for that test whereas the basic structure failed

the wear requirement [34]. What this suggests is that the wear performance of the ZDDP for commercial materials is dominated by the neutral ZDDP structure. The basic ZDDP structure is needed for other properties [35], and it is an important part of the commercial manufacturing process. A recent patent application from Lubrizol discloses a technique to boost the efficiency of the emission system by using the basic salt of low-molecular-weight ZDDPs [36].

Today's ZDDPs provide the wear performance that is required in the modern cam and lifter contacts. In particular, it has been shown that if one takes a 2.3-L overhead camshaft engine and isolates the valvetrain oil from the crankcase oil and its blowby using a separated oil sump, then (1) with engine blowby camshaft wear was high; (2) without

TABLE 12.4—API CJ-4 Bench Test Schedule

Test Number	Name	Property
1	ASTM D892 (Non-Option A)	Foam sequence I, II, III
2	Noack D5800	Volatility
3	ASTM D7216	Elastomer compatibility
4	Viscosity after shear ASTM D4683	High temperature/high shear
5	HTCBT 135°C D6594	Corrosion
6	Kurt-Orbahn ASTM D7109	Shear stability—90 cycles

TABLE 12.5—Typical Ranges of Composition of Engine Crankcase Lubricants

Function	Component	Concentration, mass %
Friction and wear	Viscosity index improver	0–6
	Antiwear additive	0.5–2
	Friction reducer	0–2
	Rust/corrosion inhibitors	0–1
Contamination and cleanliness	Antioxidant	0–1
	Detergent	1–10
	Ashless dispersant	2–9
Maintaining fluid properties	Pour-point depressant	0–0.5
	Antifoam additive	0–0.001
	Base oil (mineral or synthetic or both)	75–95

TABLE 12.6—Lubricating Oil Additive Type and Purpose

Additive Type	Additive Purpose
Antioxidants	<ul style="list-style-type: none"> • Prevent oil thickening because of oxidative process • Slow oxidation processes to prevent accumulation of oil-insoluble products
Viscosity improvers	<ul style="list-style-type: none"> • Reduce viscosity loss at higher temperatures • Reduce viscosity loss at higher temperatures to maintain hydrodynamic lubrication
Dispersants and detergents	<ul style="list-style-type: none"> • Solubilize oxidation products and neutralize acidic oxidation products
Antiwear agents	<ul style="list-style-type: none"> • Reduce wear rates to control wear debris • Reduce wear rates in mild antiwear applications
Antirust agents	<ul style="list-style-type: none"> • Prevent oxidation of ferrous metals to control corrosion debris
Corrosion inhibitors	<ul style="list-style-type: none"> • Prevent oxidation of nonferrous metals to control corrosion debris
Demulsifiers	<ul style="list-style-type: none"> • Promote rapid separation of bulk water from oil
Extreme pressure agents	<ul style="list-style-type: none"> • Prevent seizure and reduce wear rate
Pour-point depressants	<ul style="list-style-type: none"> • Prevent low-temperature thickening from wax in mineral oil
Antifoam agents	<ul style="list-style-type: none"> • Prevent foaming and maintain pumpability of lubricant
Friction modifiers	<ul style="list-style-type: none"> • Lower friction coefficients and reduce wear rates

engine blowby the camshaft wear was low; and (3) with engine blowby piped back into the isolated camshaft sump, the wear became high again, with 10W-30 formulated engine oils containing 0.05 % phosphorus from ZDDP. Later, studies also identified nitric acid as the primary cause of the camshaft wear. It is derived from the NO_x reacting with the water in the blowby. However, even in the presence of blowby, camshaft wear could be controlled by the proper selection of ZDDP and detergent type. Thus, there is a strong link between engine blowby and wear performance [37].

In this era of ever-decreasing allowed amounts of ZDDP, it has been found in bench tests that it is possible to combine ZDDP and other phosphorus-containing additives to give rise to good wear performance as determined by a Cameron-Plint bench test and studied by XANES spectroscopy. This spectroscopy showed that the film formed from a mixture of 20 % of the ZDDP and 80 % of the ashless phosphorus material still gave rise to an effective film and good wear performance [38,39]. Although reduction of phosphorus is the goal for engine oils going forward,

it does not appear that there is a suitable substitute for ZDDP with the same cost/performance profile at this time. ZDDP forms a very effective boundary film between the two moving metal surfaces, and these boundary films protect the underlying metal in a way that no other additive has been able to do so far.

As for the films on engine test parts or bench test tribocouple surfaces, their thickness has been measured in several ways. A common method consists of using X-Ray photoelectron spectroscopy (XPS). Through argon ion bombardment of a given boundary film, it is possible to measure the physical thickness of those films. This is a common technique used today, and it gives films on the order of approximately 50–100 nm or so for ZDDP boundary films. Unfortunately, this and other techniques [40–44] permanently change the physical appearance of that surface, destroying it for further analysis. Surface analytical techniques such as electron-probe microanalysis (EPMA) [45,46], secondary electron microscopy with energy-dispersive X-ray analysis (SEM/EDX) [47–49], particle-induced X-ray emission (PIXE) [50], and XANES spectroscopy [51–53] are nondestructive in nature. They yield a mass film thickness; therefore, provided that the film density is known, a physical thickness can be calculated. Jahanmir [54] determined that ZDDP-derived antiwear films are greater than 400 nm in thickness by atomic emission spectroscopy (AES)-depth profiling. Willermet et al. [46,55] also used that technique, along with surface profilometry, to confirm physical film thickness estimates from SEM/EPMA measurements. They found the average thickness of a film formed from ZDDP to be 53 nm. Suominen Fuller et al. [56] used X-ray absorption spectroscopy to determine the tribofilm thickness to be approximately 50 nm, on average, for the conditions of that particular experiment.

Another way to measure the film's thickness is by using the unique surface force apparatus (SFA) in Lyon, France. This technique allows one to measure force distance curves of various films that are made on an oxide surface, and film thicknesses of ZDDPs have been determined [57,58]. This is based on a capacitance measurement, as was the film thickness work of Williamson and Bell [59].

Another technique that has been successfully exploited by H. A. Spikes' group [60–64] and others [65,66] is interferometry, and it allows for the determination of the thickness of boundary films made from various lubricating oil additives. The Imperial group has written many papers using this type of technique, concluding that the boundary films are between approximately 80 and 120 nm thick.

There is plenty of activity aimed at reducing or displacing ZDDP or both. For example, a supplemental wear inhibitor that contains no phosphorus is described in U.S. Patent No. 2003/0148899 Al [67]. This disclosure provides a lubricant oil composition, having enhanced wear-preventive characteristics for a diesel engine operating with large quantities of soot in the oil (soot content: 0.20–4.0 wt %) and is especially suitable for a pressure-accumulating (common rail) type diesel engine equipped with an EGR system. The claimed lubricant oil composition contains a base oil composed of a mineral or synthetic oil or both incorporated with at least three additives that are a sulfurized oxymolybdenum dithiocarbamate at 0.03 to 0.50 wt % as molybdenum; a ZDDP at 0.04 to 0.05 wt % as phosphorus; at the least one metallic salt of alkyl salicylate

selected from the group consisting of a calcium salt of alkyl salicylate at 0.004–1.0 wt % as calcium, magnesium salt of alkyl salicylate at 0.002–0.60 wt % as magnesium, and zinc salt of alkyl salicylate at 0.006–1.60 wt % as zinc, with all percentages being based on the whole composition. Bench tests in a SRV friction/wear tester were conducted.

ZDDP provides excellent antiwear performance and mild extreme pressure (EP) performance. When more EP performance is called for, as in the injector screws from a 400-h Cummins M11 HST with 9 % soot [68], then a more robust EP additive is required. Some EP additives used today for engine oil applications are molybdenum dithiocarbamate (MoDTC), molybdenum dithiophosphate (MoDTP), and dibenzyldisulfide-type structures; sulfurized olefin structures; overbased detergents (and modifications thereof); and sulfurized esters [13,69,70].

12.6.2 Controlling Oxidation [71]

It is well known that HCs, oxygen, and heat will give rise to an increased rate of oxidation. These are the exact conditions operating in an internal combustion engine. This means that the automotive engine oil formulation must contain some antioxidants to make sure that the engine oil does not oxidize too quickly. There are several types of oxidation inhibitors on the market today, but the most cost-effective type of oxidation inhibitor is the ZDDP. Various researchers have shown that the ZDDP does its oxidation inhibition by two mechanisms of controlling the growth of the radical chain and hydroperoxide decomposition [72]. Although this is the most cost-effective antioxidant, most modern formulations contain additional antioxidants (e.g., the aromatic amines and hindered phenolic compounds) that contribute to oxidation control. In fact, the combination of the aromatic amine compound and the hindered phenol has been shown to be quite effective in controlling oxidation in an automotive engine oil. A synergism develops, and this gives rise to long increases in oxidation induction times. In addition, there are several advantages observed for these alkyldiphenylamines with regard to base-stock selection. Because of the reduction in the amount of ZDDP allowed in gasoline and diesel engine formulations, the use of the alkylphenolic- and the alkyldiphenylamine-type antioxidant will increase in the near future. A table summarizing the main classes of antioxidants is shown in Table 12.7 [72].

V. J. Gatto and coworkers have written a relevant review article about oxidation fundamentals for the interested

reader, and they developed several mechanistic insights that are quite apt for any HC system in which oxidation occurs. They are as follows [73]:

- Select a base stock with as little sulfur and aromatics as possible.
- Use sulfur-containing additives and arylamines sparingly to suppress sludge and deposit formation.
- Minimize, as practical as possible, metal contamination.
- Capitalize on homosynergism and heterosynergism effects by using combinations of hindered phenolics, arylamines, and peroxide decomposers.

Gatto et al. [73] point out that numbers 2 and 4 are contradictory. It is here that the expertise of the formulator is called upon to achieve a passing formulation. This automotive engine oil arena is totally performance driven and generally uses (see Table 12.5) far more additives in different proportions than used by Gatto's turbine oils. As shown by the discussion on diesel versus gasoline engine oil requirements, the amount of allowable ZDDP, for example, is now lower and quite different for each, which will naturally affect the supplemental antioxidant systems required for the Sequence IIIG engine test, which must be passed by both kinds of oils. Modern engine oils use preferentially Group II or III oils as base oils, in part to reduce the amount of sulfur or aromatic constituents, the latter of which are easily oxidizable. Elimination of base oil-derived sulfur may require reintroduction in the form of another additive.

Finally, the consumer prefers longer drain intervals, producing greater thermal and oxidative stress on the oil. Also, passenger cars are hotter because the gradual trend toward smaller but more powerful engines [74], and the oil is stressed by the reduction of sump volumes and locally higher temperatures as in turbobearings.

12.6.3 Controlling Friction [75]

A mandated federal increase in the U.S. corporate average fuel economy (CAFE) standards in 2007 has set the stage for further friction reductions in automotive engine oils (Federal Energy Independence and Security Act), meeting 35.5 mpg by 2016. A full 15 % of the energy input to an automotive engine is lost through mechanical events, and according to Hoshi [76], the valvetrain accounts for 7.5–21 % of the total engine frictional loss. Viscous drag of the lubricant (hydrodynamic lubrication) and boundary lubrication contribute to frictional losses. In particular, the viscous drag effect is observed in some parts of the piston ring/liner assembly travel and sleeve bearings. Estimates suggest that the friction loss happening in this piston assembly accounts for 40–50 % of the total frictional losses in the engine [77]. Boundary lubrication occurs between the rings and liner at the top of the piston travel and at the bottom of the piston travel. At these points, the pressure behind the rings is greatest; therefore, movement from these positions incurs the greatest frictional drag. The valvetrain is another area where boundary lubrication prevails. In these places (e.g., the camshaft/follower tribocontact), the protective film is a boundary film. The tribocontact is nearly devoid of oil. This protective additive film is able to absorb all of the cyclic stresses that are incurred in the camshaft/follower assembly, and the frictional drag experienced in this type of tribocontact will be larger than the piston ring and liner contact during hydrodynamic lubrication.

TABLE 12.7—Oxidation Inhibitors for Engine Oils [72]

• Sulfur compounds
• Phosphorus compounds
• Sulfur-phosphorus compounds
• Aromatic amine compounds
• Hindered phenolic compounds
• Organo-alkaline earth salt compounds
• Organo-zinc compounds
• Organo-copper compounds
• Organo-molybdenum compounds

Good fuel efficiency can be achieved by two mechanisms in gasoline and diesel engines. Friction reduction may be achieved by choosing a low-viscosity engine oil, which depends on the property of the base stock and VII. This type of base oil will give rise to good hydrodynamic lubrication, which occurs mostly in the bearings. Modern engine oils now have this feature built into them. When choosing base oils, it is important to choose one with a low pressure-viscosity coefficient, α , which would provide low friction at the contact. Other features that must be considered are low kinematic viscosity, high viscosity index, high temperature, and high shear viscosity, all of which will be addressed in the next section. In addition, the fluid must not be easily oxidized, which was discussed previously.

The second means of reducing friction is by using friction-modifying additives. These additives affect the overall coefficient of friction by lowering the boundary coefficient of friction. The friction modifying agents for automotive engine oils are meant to reduce friction in the mixed and the boundary lubrication regimes. In practice today, the friction modifiers that are most commonly used are long-chain carboxylic acid derivatives, especially long-chain amides, organic partial esters, organic polymers, and MoDTC [78]. Phosphoric or phosphonic acid derivatives are not the first choice because of the ongoing reduction of phosphorus in engine oils. The mechanism of action of the carboxylic acid derivatives is probably related to their reaction on the surface—to form a carboxylate salt. Korcek and his colleagues have found that the MoDTC functions by an exchange of functional groups with the ZDDP [79]. The mechanism of action with respect to the MoDTC is related to its ability to form molybdenum disulfide (MoS_2) on the surface during rubbing [80,81]. Morina and coworkers studied the effects of temperature and the ZDDP/MoDTC ratio on MoS_2 film formation under boundary lubrication conditions on AISI type 52100 steel surfaces. Using energy-dispersive X-ray analysis and XPS, the authors found that the ratio of MoS_2 /molybdenum trioxide (MoO_3) in the wear scar is an important factor that governs the decrease in friction when using MoDTC additive. The ratio was dependent on the temperature and amount of ZDDP in the original oil.

Note how MoDTC may behave as a friction modifier and an effective EP agent. The reader has already been exposed to the multifunctional aspect of some of the most useful (ZDDP, MoDTC) additives. Other additives that can form MoS_2 on the surface in the presence of ZDDP are the molybdic acid-treated succinimides. Recent work has shown that these succinimide post-treated dispersants, in the presence of ZDDP, also produce MoS_2 in the contact, which gives rise to the low friction [82,83] and low wear in a bench test. According to Harperscheid and Omeis, fuel savings of 3–4 %, using various friction modifiers and lowering viscosity, are achievable today. Most of the energy losses are due to thermal losses, followed by mechanical losses in the drivetrain of the engine [84].

12.6.4 Controlling Viscosity during Engine Speed and Temperature Changes [85–89]

Viscosity is defined as internal resistance of a fluid to flow, and it was first discovered by Sir Isaac Newton. It is quite arguably one of the most important physical properties of a lubricant. Consider that engine oil must be able to form a fluid film between moving parts of an engine. Such ability

of a lubricant to form a film depends largely on viscosity. The viscosity also controls engine friction and oil circulation, which in turn influence oil consumption, oil leakage, engine noise, engine coolant flow, fuel consumption, power output, starting, and warm-up.

Consider what happens if the proper viscosity is not chosen for automotive engine oil. If the lubricant is too viscous, then engine starting can be difficult, giving rise to increased fuel consumption and perhaps even wear that is not good for the long-term life of the engine. If the oil is not viscous enough, the wear in the engine increases. Thus, selecting the proper viscosity for the lubricant is vitally important.

12.6.4.1 NEWTON'S DEFINITION OF VISCOSITY [89]

Viscosity is the proportionality constant, η , between the shear stress, S , and the shear rate, R , and is given in the following equation:

$$S = \eta R \quad (12.1)$$

The schematic in Figure 12.1 shows the definition of viscosity for Newtonian liquids. It relates the shear stress, defined as the force divided by the area, A , and the shear rate, R . The shear rate, R , is defined as the ratio of velocity of the moving surface, V , and the film thickness, H . Thus, viscosity, η , is equal to the force times the film thickness divided by the area times the velocity. The viscosity measured by this equation is referred to as the absolute (or dynamic) viscosity. In addition to the absolute viscosity, the kinematic viscosity is also used to characterize the fluids. The kinematic viscosity is the absolute viscosity divided by the density of the Newtonian fluid. Commonly used units of viscosity are poise for the absolute viscosity, generally reported in cP (10^{-2} poise), and stokes for the kinematic viscosity, generally reported in cSt (10^{-2} stokes). The dimensional unit of poise is dyne-s/cm² whereas that of stokes is square centimetres per second.

Empirically, the viscosity of Newtonian mineral oils when plotted against temperature between the cloud

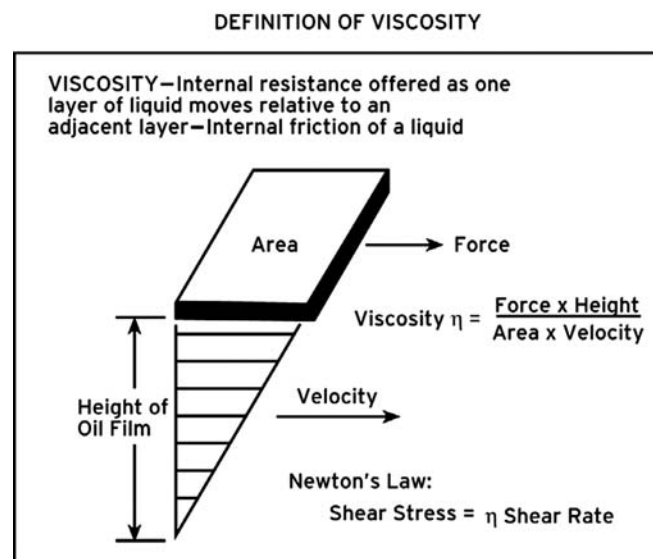


Figure 12.1—Definition of viscosity.

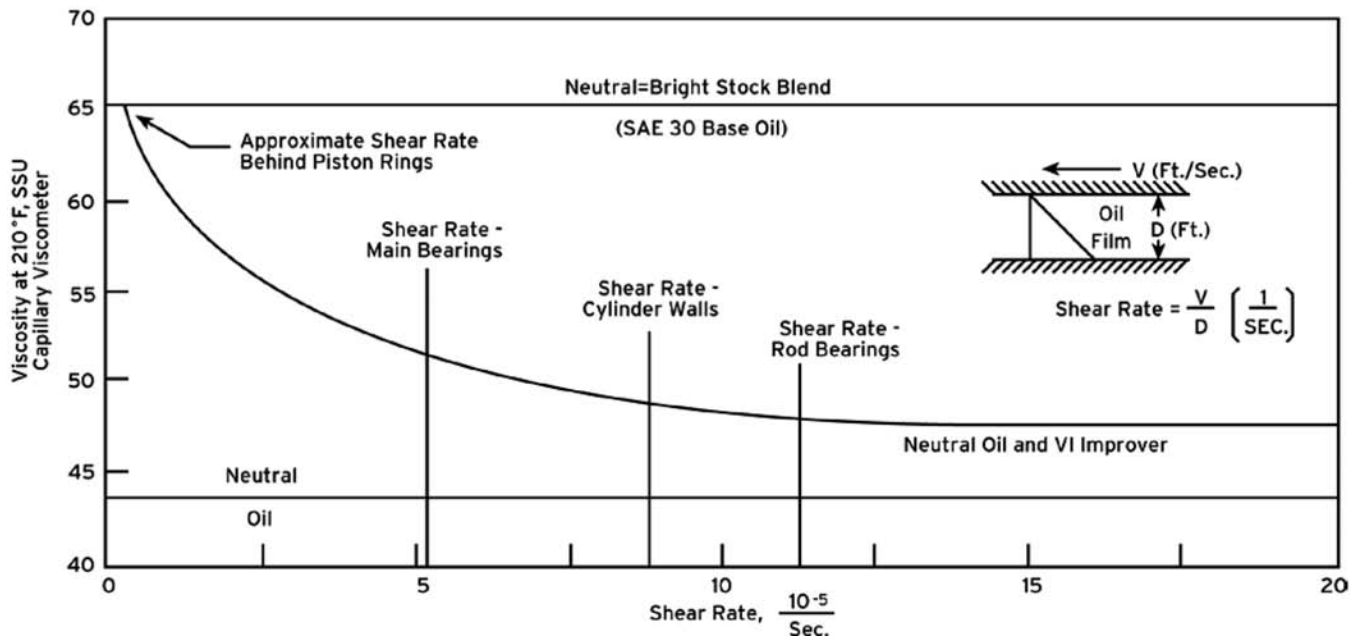


Figure 12.2—Effect of shear rate on viscosity laminar flow.

point and flash point of the oil yields a straight line on a vertical log scale. However, most formulated automotive engine oils are non-Newtonian because of the presence of a VII in the oils. The viscosity of VII-containing oils varies directionally with the shear rate (i.e., decreases as the rate of shear increases), resulting in non-Newtonian behavior. (See Figure 12.2 and note how differently the parts of the engine behave viscosity-wise when varying the shear rate.) Lower viscosity grade engine oils typically contribute to increased fuel efficiency and possibly an increase in wear. Up in the ring belt zone at low shear rates (Figure 12.2), a multiviscosity-numbered or multigrade oil (e.g., 10W-30 made possible by use of a VII) maintains a measured high viscosity. According to Figure 12.2, as the shear rate increases at the bearings and cylinder walls, oil viscosity lowers almost to that of the unthickened base oil (10W) because the VII molecules are completely aligned in the direction of motion. Once shearing is ended, the viscosity of the SAE 10W-30 oil returns to its high viscosity as long as the VII molecules have not been permanently sheared to smaller sizes. If the latter has occurred, then the oil will not return to its high viscosity and shear losses contribute to reducing shear friction whereas at the high shear rates, lower viscosity produces lower friction and lower energy consumption. Many excellent reviews [18,85,89] have been written about VIIs. The common types of commercially available VIIs are given in Table 12.8 and include olefin copolymers, acrylates, and others.

12.6.4.2 VISCOSITY AND TEMPERATURE RELATIONSHIPS

An important property of the oil is an empirical number called the viscosity index (VI), which indicates how the oil's viscosity responds to a change in temperature. Oil with a low VI describes a relatively large change in viscosity with temperature whereas oil with a high VI has a much smaller change in viscosity with temperature. Historically, VI was developed by a comparison with the behavior of

TABLE 12.8—VII Types

General Class	Dispersant Type Available	Monomers Used
Hydrocarbon type		
PIB (polyisobutylene)	No	Isobutylene
OCP (olefin copolymer)	Yes	Ethylene and propylene
SB or SI (olefin copolymers)	No	Styrene with butadiene or isoprene
Ester type		
Styrene ester	Yes	Styrene and maleic ester
Polymethacrylate	Yes	Methacrylic acid and alcohol

naphthenic oils, which thinned out with an increase in temperature more than paraffinic oils. The oils were given values between 0 and 100 VI, with the former for naphthenic and the latter for paraffinic. The VI of the oil is calculated from kinematic viscosities at 40°C (or 104°F) and 100°C (or 210°F) using equations or VI tables published by ASTM.

12.6.4.3 USING VII TO CONTROL VISCOSITY CHANGE WITH TEMPERATURE

To control viscosity change with temperature more effectively in automotive engine oils, one formulates the lubricating oils with VIIs, which are polymers such as ethylene-propylene copolymers, polymethacrylates, and hydrogenated polystyrene-isoprene, among various others. Multigrade oils are thus made by thickening low-viscosity oil with these polymeric VIIs. The VIIs are large polymeric molecules that increase the viscosity of the oil to a much larger

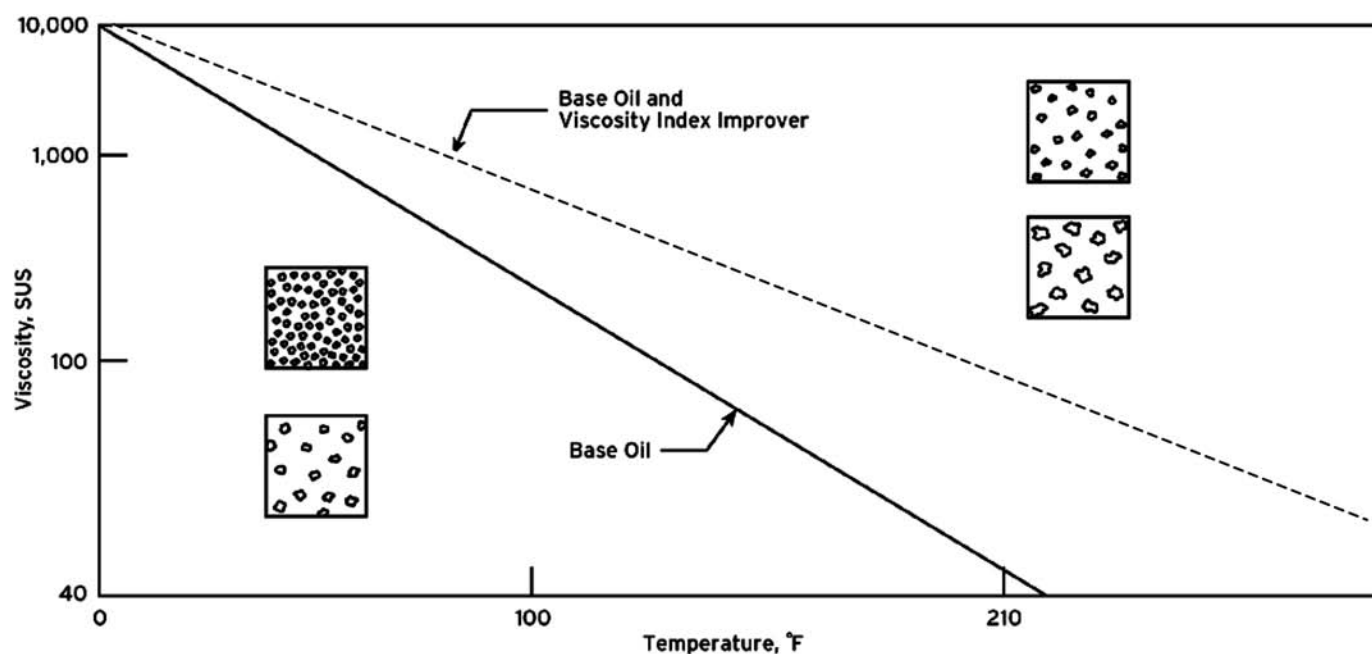


Figure 12.3—Effects of VIIs on temperature.

degree at higher temperatures compared with lower temperatures. Thus, VII affects the change in viscosity with temperature and thereby increases the VI of the oil (Figure 12.3). Base oil itself has high viscosity at low temperatures and thus the movement of the molecules is slow. (See left curve and schematics in Figure 12.3.) For the case of base oil + VII (Figure 12.3), the VII molecules do not significantly add to the viscosity of the base oils at low temperatures as compared with high temperatures. At high temperatures (right-hand side of Figure 12.3), the base oil molecules have higher kinetic energy and start to move around fast. However, such movement of the base oil molecules is affected by the presence of the VII, resulting in high oil viscosity at higher temperatures. Thus, for a given increase in temperature, the base oil + VII case improves the VI by thickening the oil at higher temperatures as compared with the base oil only case. In addition, the multigrade oils are non-Newtonian because the viscosity varies with the shear rate and decreases as the shear rate increases because of the polymeric contribution from VIIs. Current viscosity grades used for engine oils are shown in Table 12.9, which is derived from an SAE J300 specification [90].

12.6.4.4 SHEAR STABILITY OF ENGINE OILS

As one can imagine, polymeric VIIs, with their large molecular structures, may be degraded in engine use because of mechanical action and in some case because of thermal degradation. Both mechanisms give rise to a loss of viscosity in the oil. Such loss of viscosity is commonly characterized by the shear stability index (SSI) of the oil. The SSI of the VII is given by the following equation:

$$SSI = \frac{m_i - m_f}{m_i - m_o} \times 100$$

where:

m_i = the initial viscosity of the lubricant with the VII (cSt),

m_f = the final viscosity of the lubricant after shear (the shear is given by the Kurt-Orbahn fuel injector rig; see RCL38 Engine Test, Sonic Shear Device, and the KRL Tapered Bearing Rig), and

m_o = the viscosity of the lubricant without the VII (cSt).

SSI allows one to quantitatively define the shear stability of the VII. A VII is more shear stable when it has a low SSI number and less shear stable when it has a high SSI number. The higher molecular weight VIIs generally have the higher SSI and the lower molecular weight VIIs have lower SSI. An SSI is typically measured by the Kurt-Orbahn (Bosch Injector) 30-cycle shear test for automotive engine oil formulations and ranges from 24 to 50 for modern engine oil. The newest trend in VIIs is to build extra functionality into these materials. It is possible to add dispersant functionality to the VIIs. The topic of dispersancy will be addressed in Section 12.6.5. Examples of the functional VIIs are given in Table 12.8.

12.6.4.5 BOUNDARY FILMS FROM VIIS

From the initial observation of friction and wear reduction via boundary film formation from a polymethacrylate VII [91], Spikes and collaborators did a series of elegant experiments regarding structure/performance relationships using the ultrathin film interferometric approach. Müller, Fan, and Spikes synthesized a series of functionalized polyalkylmethacrylates (PAMAs) and studied their friction and wear properties [92]. Although these materials are primarily used as VIIs, the authors found that these materials can adsorb onto the surfaces and form thick boundary films in a rolling/sliding high-pressure lubricated contact. These films have significant effects on reducing friction as well as controlling wear. The test methods they used were a high-frequency reciprocating rig (HFRR) and the Mini-Traction Machine (MTM®) from PCS Instruments. The MTM was also used in the bidirectional mode in conjunction with inductively coupled plasma atomic emission spectroscopy

TABLE 12.9^{a,b}—SAE Viscosity Grades for Engine Oils

SAE Viscosity Grade	Low-Temperature (°C) Cranking Viscosity ^c (mPas max)	Low-Temperature (°C) Pumping Viscosity ^d (mPas max) with No Yield Stress ^d	Low-Shear-Rate Kinematic Viscosity ^e (mm ² /s) at 100°C (min)	Low-Shear-Rate Kinematic Viscosity ^e , (mm ² /s) at 100°C (max)	High-Shear-Rate Viscosity ^f (mPas) at 150°C (min)
0W	6200 at -35	60,000 at -40	3.8	—	—
5W	6600 at -30	60,000 at -35	3.8	—	—
10W	7000 at -25	60,000 at -30	4.1	—	—
15W	7000 at -20	60,000 at -25	5.6	—	—
20W	9500 at -15	60,000 at -20	5.6	—	—
25W	13,000 at -10	600,00 at -15	9.3	—	—
20	—	—	5.6	<9.3	2.6
30	—	—	9.3	<12.5	2.9
40	—	—	12.5	<16.3	3.5 (0W-40, 5W-40, and 10W-40 grades)
40	—	—	12.5	<16.3	3.7 (15W-40, 20W-40, 25W-40, and 40 grades)
50	—	—	16.3	<21.9	3.7
60	—	—	21.9	<26.1	3.7

^a1 mPas = 1 cP; 1 mm²/s = 1 cSt

^bAll values are critical specifications as defined by ASTM D3244.

^cASTM D5293.

^dASTM D4684: Note that the presence of any yield stress detectable by this method constitutes a failure regardless of viscosity.

^eASTM D445.

^fASTM D4683, CEC L-36-A-90 (ASTM D4741), or ASTM D5481.

Significance and use: The limits specified in Table 12.9 are intended for use by engine manufacturers in determining the engine oil viscosity grades to be used in their engines and by oil marketers in formulating, manufacturing, and labeling their products. Oil marketers are expected to distribute only products that are within the relevant specifications in Table 12.9. Disputes between laboratories as to whether a product conforms with any specification in Table 12.9 shall be resolved by application of the procedures described in ASTM D3244. For this purpose, all specifications in Table 12.9 are critical specifications to which conformance based on reproducibility of the prescribed test method is required. The product shall be considered to be in conformance if the assigned test value (ATV) is within the specification. Two series of viscosity grades are defined in Table 12.9: (1) those containing the letter W and (2) those without the letter W. Single viscosity-grade oils ("single grades") with the letter W are defined by maximum low-temperature cranking and pumping viscosities and a minimum kinematic viscosity at 100°C. Single-grade oils without the letter W are based on a set of minimum and maximum kinematic viscosities at 100°C and a minimum high-shear-rate viscosity at 150°C. The shear rate will depend on the test method used. Multiviscosity-grade oils ("multigrades") are defined by both of the following criteria: (1) maximum low-temperature cranking and pumping viscosities corresponding to one of the W grades and (2) maximum and minimum kinematic viscosities at 100°C and a minimum high-shear-rate viscosity at 150°C corresponding to one of the non-W grades.

(ICP-AES) with the latter monitoring wear. The interesting effects that the authors saw for these block copolymers, not random, were significant reductions in friction coefficient relative to the reference base oil. From this work, it was shown that a dramatic decrease in the wear in the HFRR was observed for the functionalized PAMA synthesized from the MoEMA (morpholinoethylmethacrylate) material in base oil Group I SN150.

12.6.5 Controlling Contaminants: Sludge, Varnish, Soot, and Other Deposit Precursors [18,19]

Ashless dispersants, which have been described extensively in several review articles [18,19,87,93], perform the functions of solubilization and peptization in automotive engine oils. These materials are uniquely capable of solubilizing approximately 10 times the amount of insoluble material that can be handled by, for example, a metal detergent, and they are effective at peptizing soot particles, which have recently become of great concern. The soot particles normally have a fundamental size of approximately 40 nm, and this is in the critical size (1–50 nm) range covered by these dispersants. These materials can also peptize large particles between 500 and 1500 nm by charge repulsion. This may have been the case for some soot research on oil thickening from Kornbrekke et al. [94]. "Small" size or "nano" particulates have been shown to pose added cardio-

vascular and pulmonary health hazards according to recent findings; therefore, it is particularly important that the dispersants function effectively and trap as many soot particles as possible [95,96]. Recently, Su et al. conducted an in vitro study of the inflammatory and cytotoxic potential of soot particles from current low-emission (Euro IV) diesel engines toward human peripheral blood monocyte-derived macrophage cells. Surprisingly, they discovered that soot derived from the low-emission diesel engine showed higher toxic and inflammatory potential than particulate matter from an older diesel engine ("black smoke") at the same mass concentration. The percentage of dead cells was approximately 2–3 times greater for the low-emission diesel engine than the older one. Thus, the authors concluded that the structure and function of the soot are important factors because the reduction of soot mass alone fails to produce less negative effects in this in vitro experiment [97]. Please recall how the Mack T-11 engine test uses a minimum 6 % soot increase at 12 cSt as its passing criteria for soot dispersancy control. In fact, many of the functional properties that we have been discussing can be seen in Table 12.3. The performance areas that are addressed by the various engine tests of the CJ-4 category are listed.

Dispersants are especially suited for dealing with precursors to sludge or varnish generated in a used oil at the relatively low temperatures of a gasoline engine. The initial motivation for such materials was to prevent sludge—"cold"

sludge made at relatively low temperatures—and varnish originating from dirty fuel and lubricant oxidation products [98]. In addition, the amounts of sludge and varnish precursors are significantly affected by the blowby from the crankcase oil. Quillian et al. [98] significantly reduced varnish and sludge deposits by diverting the blowby from the crankcase oil. Vineyard and Coran [99] collected the liquid products of blowby and implicated these materials as deposit precursors. Their analysis showed that α,β -nitronitrates were present in the blowby. Dimitroff et al. [100] measured NO_x (nitric oxide [NO] and nitrogen dioxide [NO_2]) in the blowby and found that its level was dependent on spark timing.

Many researchers have been studying the fundamentals of colloid science that relate to soot-induced viscosity increases and wear in diesel engines [101–112]. Most of these studies are bench tests because engine tests are quite costly, and many studies were done before the higher soot levels produced by EGR [103–105,107,108,111,112].

Today, topics of major concern include how to provide extra dispersancy for handling the soot derived from diesel engines because of EGR. Very recently, a ball-on-disc sliding wear test, using a PCS Instruments MTM tribometer, was used as a bench test for this wear problem [113,114]. Sliding conditions at high pressure are required for soot polishing wear. Conditions that correlate tribometer test results with M-11 engine results at high soot concentrations (~9 %) have been found. Soot is quite dominant in sludge collected from used diesel engine oils. Ball wear and Stribeck curves were determined in these tests. The high wear oil progresses from mixed lubrication conditions to boundary lubrication at higher sliding speeds than the low-wear oil. The oils differ only in the type of VII used.

Scientists formerly at Ethyl Corporation, now the Afton Chemical Company, have also been interested in this topic, as shown in an SAE paper in which they show an advantage for functionalized dispersant VIIs regarding film formation properties in a bench test (ASTM D1169) [115]. They also show that engine soot-containing oils gave measurable resistivity whereas carbon black gives none. Obviously, the latter indicates a fundamental difference between carbon black and engine soot.

12.6.5.1 CONTROLLING CONTAMINANTS: ACIDS AND DEPOSITS [18,33,116]

Another form of contamination control is performed by metallic detergents. Detergents are capable of controlling contaminants such as acids, produced on combustion, by neutralization so that these acidic materials do not cause rust in the engine. Detergents are also able to control contamination by the formation of micelles, which are capable of solubilizing one unit of liquid deposit precursor for each unit of additive present. Second, they peptize solids of the size range 0–20 nm. They are also capable of forming films around deposit particle precursors to which they are physically adsorbed. For example, they impart a surface charge to the particles in the size range of 500–1500 nm, and coagulation of these particles is prevented by repulsion by like charges. The detergents utilized today in engine oils are sulfonates, phenates, and salicylates, and they are either neutral or overbased to different degrees. The overbased materials are especially effective at neutralizing the acid

precursors such as nitric acid from the gasoline engines and the sulfuric acid produced by the diesel engines, thereby reducing corrosive wear [116–124]. Total base number (TBN) retention is the topic of a paper that argues for TBN and total acid number (TAN) measurements because some detergents may not effectively neutralize all of the acidic species in the lubricant [125].

Calcium sulfonate detergents, similar to many of the other additives, have been found to serve several functions. In a very recent paper by Topolovec-Miklozic, Forbus, and Spikes [126], the authors studied the film-forming and frictional properties of some overbased calcium sulfonate detergents. These additives formed solid calcium carbonate films on the rough surfaces of 100–150 nm in thickness. These films have been shown to provide wear protection in accordance with previous studies [69]. In addition, the authors found that the sulfonate materials that they tested had large differences in boundary friction coefficients. Two of them gave very low boundary friction coefficients of 0.06–0.08, and the other two gave higher friction coefficients more typical of the boundary regime. The authors believe that these performance differences lie in the structural arrangement of the sidechains of the alkylsulfonate detergents. Thus, these overbased sulfonate detergents do more than merely neutralize acids in the bulk oil or clean up deposits on high-temperature surfaces (e.g., piston and valve seats) by displacing deposit precursors and keeping them apart by a charge particle repulsion mechanism. This paper and others are striving to elicit the very best performance of this class of additive as well as any favorable secondary attributes. This is particularly important today because the levels of allowable sulfated ash, phosphorus, and sulfur are decreasing in engine oils.

In another study of overbased calcium sulfonates, with ZDDP or MoDTC, Costello and Urrego [127] found that the films formed in a tribometer contact showed that the overbased sulfonate reduced the phosphate film thickness whereas in the second case it reduced the MoS_2 film thickness. An advantage was also observed by XPS studies for the use of the crystalline overbased calcium sulfonate versus the amorphous overbased calcium sulfonate with likely more calcium carbonate for the former. It is known to be an effective EP film (250 kg weld point) [69]. Again, this study is aimed at eliciting the advantageous surface behaviors of the MoDTC or ZDDP in the presence of different types of calcium sulfonate. In the Four-Ball EP tests, the crystalline overbased calcium sulfonate with ZDDP gave the best results in this comparison; however, the combinations of sulfonates plus sulfurized olefin gave even better results in this test with a weld point greater than 800 kg. It is clear that some of these lubricating oil additives function at the surfaces and the bulk oil as shown in Table 12.10.

12.6.5.2 CONTROLLING RUST [137,138]

“Rust,” a corrosion product, can occur under a low-temperature, air oxidation environment in the presence of water, which is available especially in very short trips taken in passenger car engines. This kind of travel (i.e., stop-and-go) gives rise to water from the combustion, and this is blown past the rings into the crankcase where it mixes with the engine oils. A hot engine, with evaporation of water, eliminates the problem; however, under less ideal circumstances,

TABLE 12.10—Surface Activity of Various Classes of Lubricant Additives

Additive Type	Surface Active	Bulk Solution Active	Reference
Dispersants	X	X	128–132, 135
Detergents	X	X	133, 134
Antiwear agents	X		20, 21
Antioxidants		X	19, 136
Corrosion inhibitors	X		135–137
Viscosity modifiers	X	X	89, 92
Pour-point depressants		X	19, 85
Foam inhibitors		X	19, 85
Friction modifiers	X		19, 85

the air, the water, and sometimes organic acids that are present due to combustion may give rise to rust unless the engine's surface is protected from this type of wear. This can be done using overbased sulfonates, which act as rust inhibitors. The overbased sulfonates that are effective include those that neutralize the acids that are catalyzing the rusting and those overbased sulfonate structures that can adsorb tightly onto the iron surface and form a protective and stable film. The rationale for design of such materials is to make the size of the HC groups as small as possible without having them precipitate out of solution. The omnipresent ZDDPs also give some corrosion protection. Because of the high solubility of water in ethanol fuels, rust is of some concern. In particular, alcohol-based fuels can produce water or aldehydes or both during engine operation.

12.6.5.3 CONTROLLING FOAM [19–21]

The polar nature of the engine oil additives gives rise to their foam-stabilizing properties. The splashing action or the mechanical agitation, or both, of the crankcase oil during engine operation causes air and other vapors to be whipped around, resulting in foam generation. In extreme cases, the oil actually can be lost because of the foam. The entrainment of the air in the oil can also decrease the ability of the oil to provide an effective hydrodynamic lubricating film because of the air bubbles that compromise the integrity of the film. The control of foam in modern-day engines is accomplished using silicon-based foam inhibitors, particularly the polymethylsiloxanes, which are used in parts-per-million quantities and exhibit very low solubility in oil.

12.6.5.4 CONTROLLING WAX FORMATION [22, 139]

Wax formation is always a possibility with mineral oils because they may contain wax that can precipitate out of the solution at approximately 0°C as crystals, and crystals may form a substantial network. By definition, the pour point of an oil is the lowest temperature at which the oil will flow. Pour-point depressants (PPD) are components that co-crystallize with or adsorb onto the waxes, thereby also preventing the wax growth and limiting the wax network growth. There are many kinds of PPDs: the polymethylacrylate esters of waxy alcohols, wax alkylated naphthalene materials, styrene esters, polyvinyl acetate,

alkylphenols, coupled alkylphenols, and poly(ethylene/vinyl acetates). Using the ASTM D97 and the pour point procedure, “Mini-Rotary Viscometer (MRV) SAEJ300,” it is possible to determine the pour point in degrees Celsius response to the percentage of PPD. PPD molecules are waxy materials; therefore, it is very important to take care in using the proper amount and type for the best result. Also, caution must be exercised to maintain the ability of the oil to flow properly to the oil pump and the bearings in the engine at low temperature and low shear rates. This is a normal part of the specifications for multigrade oils.

12.7 PROLONGING ENGINE OIL LIFETIME

It is clear from the preceding discussions that engine oils have the following functions:

- To maintain oil film, to supply additives, and to wash out debris such as wear metal from lubricated parts;
- To remove heat from sliding surfaces and the related parts;
- To seal the parts of piston rings and cylinder;
- To clean engine internals and to disperse sludge in oil; and
- To protect engine internals from rust and corrosion.

It is required that engine oils maintain all of the above functions for a finite period of time. However, with engine operation, engine oils degrade. This is because the engine oil is subject to shearing of molecules, oxidation, nitration, and polymerization by heat plus contamination by fuel and blowby gas during circulation in an engine, all of which leads to deterioration. Continuous use of the deteriorated engine oil for a long period will cause engine problems. Therefore periodic oil change is required. Engine oil deterioration will be judged by criteria such as neutralization number (TAN and TBN), kinematic viscosity, water contents, and carbon residue. However, carmakers usually recommend that car owners change oil on the basis of driving hours or driving distance.

Engine oil filters may assist the additives to delay the time of oil replacement. They have the construction as shown in Figure 12.4. Engine oil filters are designed on the basis of full flow of the oil delivered by the oil pump, but a portion of the oil will return to the oil pan by a pressure-regulating valve located at the entrance of the oil filter

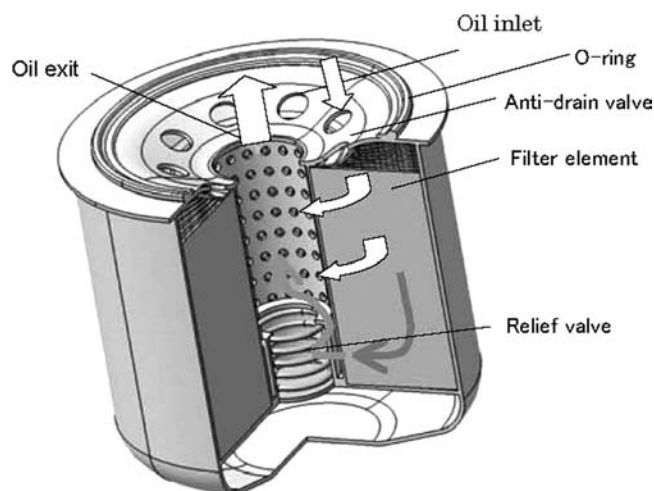


Figure 12.4—A schematic figure of an engine oil filter.

to regulate the oil pressure in the oil gallery. The oil that comes into the filter element through the antidrain valve will be cleaned through the filter element, go out to the center core through the punched holes, and will be delivered to the lubricating parts.

To prevent oil starvation, highly viscous oil will be directly delivered to the lubricating parts through the relief valve without passing through the filter element when the engine is started from a cold condition. When the filter element is clogged, the contaminated oil will also be delivered to the lubricating parts through the relief valve. Therefore, it is important to change filter elements as recommended. The guideline for this particular filter element replacement is set to 30,000 km in consideration of the holding capacity of contaminants by the filter element until the pressure reaches the preset pressure loss value at the maximal oil flow rate and the driving distance multiplied by a safety factor.

Apart from the oil filter system described above, one also has systems that only take a portion of the flow to not lose too much pressure and power. Please note that the 30,000-km filter change interval is not a generic number for all engines, but it usually goes with the oil drain interval and is very OEM, engine design, and usage pending. Small, older cars can still be at 5000 km whereas trucks may go to as far as 150,000 km.

Filter performance is examined in accordance with ISO 4548-12 (see Figure 12.5):

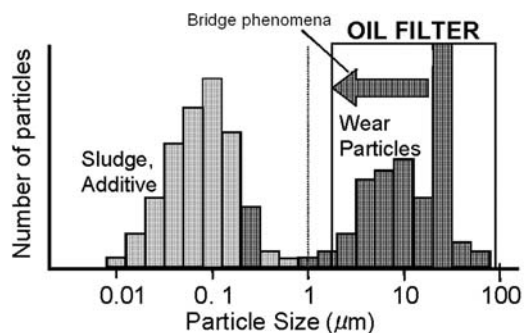


Figure 12.5—Bridge phenomena.

- To remove more than 70 % of particles smaller than 30 μm ,
- To remove more than 85 % of particles smaller than 40 μm , and
- To remove 85 % of contaminants by the gravimetric method.

In this way, oil filters can control wear particles sized from approximately 2 to 100 μm whereas additives can control particles sized less than 1 μm . This system may effectively control the number and size of particles as long as the engine oil filters are replaced at proper time intervals. The so-called “bridge phenomena” involves oil oxidation products that have polar groups. Metal particles have free electrons inside, although they are covered by metal oxide, which is dielectric. Therefore, the polar groups of oil oxidation products will adhere on such metal particles and coat them. The HC parts of the polymerized oil oxidation products are sticky. Therefore, they will glue other contaminants when they cover the surfaces of filter media. They have “flypaper” effects to cause the bridge phenomena. There is some concern about particles less than 1 μm in diameter sticking to the filter; vide infra.

Pleated paper with 0.5- to 0.7-mm thick phenol resin treatment must be used for the filter element to improve the performance and to optimize the life of the filter element. Modern engine oils use good detergent and dispersant additives to prevent carbonaceous materials, silicon dioxide (SiO_2), and wear particles from agglomerating or from depositing on the lubricating surfaces by keeping them in suspension in oil. In this manner, the engine oil filter will also clean the engine oil by removing the suspended particles, including soot, which may come into the engine during the assembly and running-in operation.

Figure 12.6 gives an example of the sludge particle count, as determined by a standard particle counter, at the time of engine commission. ASTM is currently in the process of developing a new standard for particle counting because the current method is not effective for heavily contaminated and very viscous oils [140].

There are some reports that sludge smaller than 1 μm has an influence on wear [141]. If manufacturers reduce the pore sizes of a filter element to remove such small contaminants, the pressure drop of the filter element will become large and the filter element will be clogged soon. Periodic oil change is therefore recommended for removing very fine sludge from the engine, otherwise risking

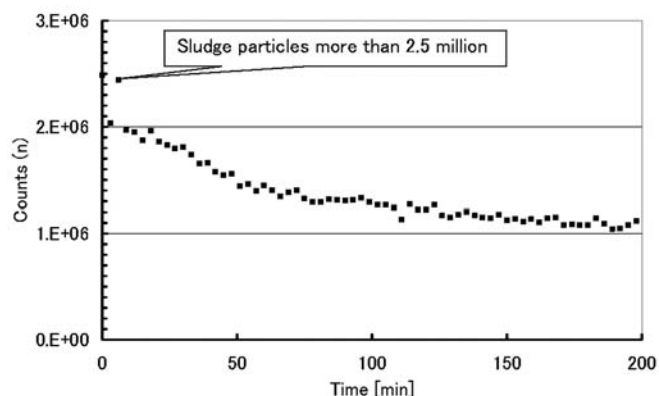


Figure 12.6—An example of generation of fine sludge particles at the time of engine commission.

larger wear particles circulating in the oil, because of a high backpressure.

Automobile makers recommend that automobile users periodically change the oil filter and engine oil. In general, automobile makers recommend changing engine oil every 10,000 km or once a year. In the case of severe conditions, oil change at every 5000 km or every 6 months is recommended.

In the case that one of the following conditions continues more than 30 % of the total driving distance, it is considered “severe conditions”:

- Frequent driving on the unpaved road,
- Long touring in severe environmental conditions,
- Frequent driving on hilly roads,
- Repetitive short-distance driving,
- Driving in cold conditions below 0°C,
- Frequent engine idling and frequent driving at low speed, and
- Frequent towing of another vehicle.

12.8 MEETING 21ST CENTURY CHALLENGES

12.8.1 System Compatibility Issues

Engine manufacturers often develop their own requirements to which additive makers must adhere. An example of this is in the area of elastomer compatibility developed by Volkswagen. There is one bench test called the DC AK6 Elastomer Compatibility Test that requires the use of seals made of Viton, which is a Fluorel-Caoutchouk polymer. It is referred to as FPM and is sometimes called Fluorel or Tecnoflon. The test is run for 168 h at 150°C, and an oil formulation is assessed in the areas of hardness, volume change, tensile strength, and elongation at breakage [142]. This particular type of test requires the lubricating oil additive chemists and formulators to devise formulations that not only lubricate the metal parts of the engine but also do no harm to this type of seal. This is a compatibility issue, and nitrogen-containing molecules may be harmful to this seal type.

Another system compatibility issue is presented by the current use of biodiesel and its effect on engine wear. Some diesel engine operators have recently been using various combinations of biodiesel fuel with regular mineral diesel fuel. Recall that pure biodiesel fuel (B100) is made from fatty acid methyl esters (FAMES). FAMES have different physical properties when compared with regular diesel fuel, such as higher surface tension, lower volatility, and higher specific gravity. These differences lead to larger droplet size and thus more wall impingement of the fuel during injection in the combustion chamber. This then gives rise to greater levels of fuel dilution as the oils break down into the crankcase. Mixing of the fuel with the oil can give rise to compatibility issues, and in a recent study, it was shown that by using various amounts of biodiesel in combination with the normal diesel fuel, partially oxidized biodiesel components may compete with the ZDDP antiwear additives for the metal surface. Thus, the wear characteristics of the biodiesel-contaminated oil were evaluated by electrical contact resistance experiments, HFRR experiments, and Four-Ball wear tests. It was found that the wear bench tests showed a higher level of wear caused by the interaction of the oxidized biodiesel components and the ZDDP. Lube oil dilution with aged biodiesel may increase wear even at concentrations of 5 % or less in these bench tests [143].

Obviously, another possible negative interaction may be the change in viscosity that the lubricant could experience because of the dilution factor.

On the other hand, some studies have found that there are reductions in particulate emissions with the use of biodiesel fuel as compared with regular diesel fuel [144]. This decrease is due to reduced soot formation and enhanced soot oxidation. The reader may recall that many of the diesel engines used today operate with EGR, which increases the amount of soot formed and therefore increases the stress on the lubricant system, especially dispersants. Thus, there are many issues that engine oil formulators must keep in mind when formulating a new oil. He or she has no idea what kind of oil or fuel the engine operator will decide to use; thus, the formulator must develop robust formulations that can be successful in all environments.

12.8.2 Environmental Issues

The problem associated with the use of ZDDP is that the phosphorus- and sulfur-containing compounds poison the catalyst components of the catalytic converters. This is a major concern because effective catalytic converters are needed to reduce pollution and to meet governmental regulation designed to reduce toxic gases such as HCs, CO, and NO_x in internal combustion engine exhaust emissions. Such catalytic converters generally use a combination of catalytic metals (e.g., platinum and metal oxides) and are installed in the exhaust streams (e.g., the exhaust pipes of automobiles) to convert toxic gases to nontoxic gases. As previously mentioned, these catalyst components are poisoned by the phosphorus and sulfur components or the decomposition products from these ZDDPs. Accordingly, the use of engine oils containing these elements may substantially reduce the life and effectiveness of catalytic converters. However, it is even more complicated than that. The study of Ueda et al. in 1994 showed that the calcium and magnesium from the detergents prevented phosphorus from adhering to the catalyst and the sensors, thereby forming a dense coating. Therefore, some of the additives that are typically used in the formulation are actually ameliorating the effect of the phosphorus poisoning [6]. The authors found that the calcium and magnesium detergents as well as MoDTC improved the vehicle NO_x emissions.

However, recently Krocher et al. reported on a characterization study of a V₂O₅/WO₃-TiO₂/SCR catalyst that was deactivated by calcium and potassium [145]. This study was done using ammonia (NH₃) temperature programmed desorption (TPD), diffuse reflectance infrared Fourier transform (DRIFT) spectroscopy, and XPS as well as theoretical density functional theory (DFT) calculations. The authors discovered that NH₃-TPD experiments showed that elements such as potassium or calcium affected the acidity of the catalyst surface. Subsequent DRIFT spectroscopy showed that the poisoning agents interacted with the Bronsted acid sites of the V₂O₅ active phase, thereby affecting NH₃ adsorption. This is important now because heavy-duty diesel engines frequently use SCR to decrease NO_x levels and diesel-catalyzed particulate filters (DCPFs). The addition of EGR is also a particularly effective way to reduce NO_x levels. Engine combustion can be optimized to provide maximal fuel efficiency but at the cost of high NO_x. It is anticipated that SCR will give lower fuel consumption as well as lower emissions. The DCPFs address the particulate

matter problem; therefore, it is expected that engines with DPFs will require retarded timing and EGR to attain low NO_x levels. Thus, in this complicated world with diesel and gasoline engines, the entire system has to work together to attain the best environmental consequence, especially for the human population. The recent finding that diesel exhaust streams contain particles that may be particularly more damaging to human tissue than originally thought is a challenge that must be met in this century [97].

12.9 CONCLUSIONS

Today's automotive engine oils call for the utmost performance from the additives that combine with the base oils to make this technically complex product. These additives and the oil filters function to give the long life consumers expect from today's products. This chapter was written to clarify the role of the different additive types and engine oil filters vis-à-vis the current demanding environment. It is hoped that the reader has a better appreciation for the challenges that additive chemists now face—emission concerns, better fuel economy, and a trend to increase drain intervals in the passenger car motor oil and heavy-duty diesel engine oil markets.

ACKNOWLEDGMENTS

The authors acknowledge the generous help given by Dr. Akira Sasaki of the Kleentek Corporation and Drs. Kirk Nass and Pritesh Patel of Chevron Oronite. We also appreciate the close reading of the manuscript by Mr. Peter Kleijwegt.

References

- [1] International Lubricant Standardization and Approval Committee, 2009, Document for GF-5 Requirements.
- [2] Koltsakis, G.C., and Stamatelos, A.M., 1997, "Catalytic Automotive Exhaust After Treatment," *Prog. Energy Combust. Sci.*, Vol. 23, pp. 1–39.
- [3] Matsumoto, S., 2004, "Recent Advances in Automobile Exhaust Catalysts," *Catalyst Today*, Vol. 90, pp. 183–190.
- [4] Spearot, J.A., and Caracciolo, F., 1977, *Engine Oil Phosphorus Effects on Catalytic Converter Performance in Federal Durability and High Speed Vehicle Tests*, SAE Technical Paper 770637, SAE, Warrendale, PA.
- [5] Caracciolo, F., and Spearot, J.A., 1979, *Engine Oil Additive Effects on the Deterioration of a Stoichiometric Emissions Control (C-4) System*, SAE Technical Paper 790941, SAE, Warrendale, PA.
- [6] Ueda, F., Sugiyama, S., Arimura, K., Hamaguchi, S., and Akiyama, K., 1994, *Engine Oil Additive Effects on Deactivation of Monolithic Three-Way Catalysts and Oxygen Sensors*, SAE Technical Paper 940746, SAE, Warrendale, PA.
- [7] Bishop, G.A., and Stedman, D.H., 2008, "A Decade of On-Road Emissions Measurements," *Environ. Sci. Technol.*, Vol. 42, pp. 1651–1656.
- [8] Colclough, T., Marsh, J.F., and Robson, R., 1991, *Laboratory and Field Performance of Zero Phosphorus Oils*, SAE Technical Paper 910868, SAE, Warrendale, PA.
- [9] Chamberlain, W.B., and Zalar, F.V., 1984, *Balancing Crankcase Lubricant Performance with Catalyst Life*, SAE Technical Paper 841407, SAE, Warrendale, PA.
- [10] Spikes, H.A., 2008, "Low- and Zero-Sulphated Ash, Phosphorus and Sulfur Anti-Wear Additives for Engine Oils," *Lub. Sci.*, Vol. 20, pp. 103–136.
- [11] Migdal, C.A., Rowland, R.G., Sikora, D.J., and Osterholtz, F.D., 2005, "Silane Additives for Lubricants and Fuels," U.S. Patent 6,887,835 B1, May 3.
- [12] Grabowski, W., Migdal, C.A., and Hull, S., 2005, "Polysiloxane Additives for Lubricants and Fuels," Publication Number WO 2005/010133 A1, February 3.
- [13] Rudnick, L.R. (Ed.), 2003, *Lubricant Additives*, Marcel Dekker, New York, pp. 45–112 and 223–258.
- [14] Table 2, www.southwestresearch.org. API CJ-4 Summary of Tests. For more information contact Ben Weber, Director SWRI, bweber@swri.org.
- [15] Gristede, I., Bremm, S., Müller, W., Leyrer, J. and Gröger, M., 2006, "NO_x Aftertreatment Systems for Diesel Engines for Series Introduction in North America," In *Proceedings of the 15th Aachener Kolloquium Fahrzeug- und Motorentechnik 2006*, Aachen, publ. FKA mbH, Aachen 2006.
- [16] McGeehan, J.A., Moritz, J., Shank, G., Kennedy, S., Stehouwer, D., Urbank, M., Belay, M., Goodier, S., Cassim, A., Runkle, B., DeBaun, H., Harold, S., Chao, K., Herzog, S., Stockwell, R., Passut, C., Fetterman, P., Taber, D., Williams, L., Kleiser, W. M., Zalar, J., Scinto, P., Santos, E., and Rutherford, J.A., 2007, *API CJ-4: Diesel Oil Category for Pre-2007 Engines and New Low Emission Engines Using Cooled Exhaust Gas Recirculation and Diesel Particulate Filters*, SAE Paper No. 2007-01-1966, SAE, Warrendale, PA.
- [17] McGeehan, J.A., and Ryason, P.R., 2000, *Preventing Catastrophic Camshaft Lobe Failures in Low Emission Diesel Engines*, SAE 2000-01-2949, SAE, Warrendale, PA.
- [18] Myshkin, N.K., Kim, C.K., and Petrokovets, M.I., 1997, *Introduction to Tribology*, Cheong Moon Gak, Seoul, Korea, pp. 1–32 and 204–220.
- [19] Rizvi, S.Q.A., "Additives—Chemistry and Testing," In *Tribology Data Handbook*, Bouser, E.R., Ed., CRC Press, Boca Raton, FL, pp. 117–137.
- [20] Mang, T., and Dresel, W. (Eds.), 2007, *Lubricants and Lubrication*, Wiley-VCH, Weinheim, Germany, pp. 88–118.
- [21] Roby, S.H., Yamaguchi, E.S., and Ryason, P.R., 2000, "Lubricant Additives for Mineral Oil Based Hydraulic Fluids," In *Handbook of Hydraulic Fluid Technology*, Totten, G.E., Ed., Marcel Dekker, New York, pp. 795–823.
- [22] Rudnick, L.R. (Ed.), 2003, *Lubricant Additives*, Marcel Dekker, New York, pp. 1–705.
- [23] Bell, J.C., 1993, "Engine Lubricants," In *Engine Tribology*, Taylor, C.M., Ed., Elsevier Science, Amsterdam pp. 287–301.
- [24] Papay, A.G., 1996, "Antiwear and Extreme Pressure Additives in Lubricants," *Technische Akademie Esslingen 10th International Tribology - Solving Friction and Wear Problems, Colloquium*, Vol. 2, pp. 1093–1099.
- [25] Papay, A.G., 1998, "Antiwear and Extreme Pressure Additives in Lubricants," *Lub. Sci.*, Vol. 10, pp. 209–224.
- [26] Freuler, H.C., 1944, "Modified Lubricating Oil," U.S. Patent 2364283.
- [27] Freuler, H.C., 1944, "Modified Lubricating Oil," U.S. Patent 2364284.
- [28] McGeehan, J.A., Graham, J.P., and Yamaguchi, E.S., 1990, *Camshaft Surface Temperatures in Fired-Gasoline Engines*, SAE Paper No. 902162, SAE, Warrendale, PA.
- [29] Dickert, J.J., Jr., and Rowe, C.N., 1967, "Thermal Decomposition of Metal O,O Dialkyl Phosphorodithioates," *J. Org. Chem.*, Vol. 32, pp. 647–653.
- [30] Yamaguchi, E. S., and Ryason, P. R., 1993, "Inelastic Electron Tunneling Spectra of Lubricant Oil Additives on Native Aluminum Oxide Surfaces," *Tribology Trans.*, Vol. 36, pp. 367–374.
- [31] Yamaguchi, E.S., Ryason, P.R., and Labrador, E.Q., 1995, "Inelastic Electron Tunneling Spectra of Neutral and Basic Zinc Dithiophosphates on Native Aluminum Oxide Surfaces," *Tribology Trans.*, Vol. 38, pp. 243–252.
- [32] Fuller, M., Yin, Z., Kasrai, M., Bancroft, G.M., Yamaguchi, E.S., Ryason, P.R., Willermet, P.A., and Tan, K.H., 1997, "Chemical Characterization of Tribochemical and Thermal Films Generated from Neutral and Basic ZDDPs Using X-Ray Absorption Spectroscopy," *Tribology Int.*, Vol. 30, pp. 305–315.
- [33] Pawlak, Z., 2003, "Tribocchemistry of Lubricating Oils," In *Tribology and Interface Engineering Series*, No. 45, Briscoe, B.J., Ed., Elsevier, Amsterdam, The Netherlands, pp. 1–214.
- [34] Yamaguchi, E.S., 1999, "The Relative Wear Performance of Neutral and Basic ZnDTPs in Engines," *Tribology Trans.*, Vol. 42, pp. 90–95.
- [35] Yamaguchi, E.S., Onopchenko, A., Francisco, M.M., and Chan, C.Y., 1999, "The Relative Oxidation Inhibition Performance of Some Neutral and Basic Zinc Dithiophosphate Salts," *Tribology Trans.*, Vol. 42, pp. 895–901.

- [36] Wilk, M.A., DiBiase, S.A., and Schroeck, C.W., "Lubricating Oil Composition and Method of Improving Efficiency of Emissions Control System," PCT Int. Appl. WO 2008/011338A2.
- [37] McGeehan, J.A., and Yamaguchi, E.S., 1989, *Gasoline—Engine Camshaft Wear: The Culprit Is Blow-By*, SAE Paper No. 892112, SAE, Warrendale, PA.
- [38] Zhang, Z., Yamaguchi, E.S., Kasrai, M., Bancroft, G.M., 2005, "Tribofilms Generated from ZDDP and DDP on Steel Surfaces. Part 1: Growth, Wear, and Morphological Aspects," *Tribology Lett.*, Vol. 19, pp. 211–220.
- [39] Zhang, Z., Yamaguchi, E.S., Kasrai, M., Bancroft, G.M., Liu, X., and Fleet, M.E., 2005, "Tribofilms Generated from ZDDP and DDP on Steel Surfaces. Part 2, Chemistry," *Tribology Lett.*, Vol. 19, pp. 221–229.
- [40] Smith, G.C., 2000, "Surface Analytical Science and Automotive Lubrication," *J. Phys. Appl. Phys.*, Vol. 33, pp. R187–R187.
- [41] Minfray, C., Martin, J. M., Esnouf, C., Le Mogne, T., Kersting, R., and Hagenhoff, B., 2004, "A Multi-Technique Approach of Tribofilm Characterization," *Thin Solid Films*, Vol. 447–448, pp. 272–277.
- [42] Choa, S. H., and Ludema, K., Potter, G., DeKoven, B., Morgan, T., and Kar, K., 1995, "A Model for the Boundary Film Formation and Tribological Behavior of a Phosphazene Lubricant on Steel," *Tribology Trans.*, Vol. 38, pp. 757–768.
- [43] Evans, R.D., More, K.L., Darragh, C.V., and Nixon, H.P., 2005, "Transmission Electron Microscopy of Boundary-Lubricated Bearing Surfaces, Part II: Mineral Oil Lubricant with Sulphur and Phosphorus-Containing Gear Oil Additives," *Tribology Trans.*, Vol. 48, pp. 299–307.
- [44] Glaeser, W.A., Baer, D., and Engelhardt, M., 1993, "In Situ Wear Experiments in the Scanning Auger Spectrometer," *Wear*, Vol. 162–164, pp. 132–138.
- [45] Bell, J.C., Delargy, K.M., and Sweeney, A.M., 1992, "The Removal of Substrate Material through Thick Zinc Dithiophosphate Anti-Wear Films." In *Wear Particles*, D. Dowson, C.M. Taylor, T.H.C. Childs, M. Godet, and G. Dalmaz, Eds., Elsevier Science, Amsterdam, The Netherlands, pp. 387–396.
- [46] Willermet, P.A., Dailey, D.P., Carter, R.O., III, Schmitz, P.J., Zhu, W., Bell, J.C., and Park, D., 1995, "The Composition of Lubricant-Derived Surface Layers Formed in a Lubricated Cam/Tappet Contact II. Effects of Adding Overbased Detergent and Dispersant to a Simple ZDTP Solution," *Tribology Int.*, Vol. 28, pp. 163–175.
- [47] Garten, R.P.H., and Werner, H.W., 1994, "Trends in Applications and Strategies in the Analysis of Thin Films, Interfaces and Surfaces," *Anal. Chim. Acta*, Vol. 297, pp. 3–14.
- [48] Palacios, J.M., 1986, "Thickness and Chemical Composition of Films Formed by Antimony Dithiocarbamate and Zinc Dithiophosphate," *Tribology Int.*, Vol. 19, pp. 35–39.
- [49] Palacios, J.M., 1987, "Films Formed by Antiwear Additives and Their Incidence in Wear and Scuffing," *Wear*, Vol. 114, pp. 41–49.
- [50] Johansson, S.A.E., Campbell, J.L., and Malmqvist, K.G. (Eds.), 1995, "Particle-Induced X-Ray Emission Spectrometry (PIXE)." In *Chemical Analysis: A Series of Monographs on Analytical Chemistry and Its Applications*, Vol. 133, Wiley, New York.
- [51] Martin, J.M., Grossiord, C., Le Mogne, T., Bec, S., and Tonck, A., 2001, "The Two-Layer Structure of ZNDTP Tribofilms Part I: AES, XPS and XANES Analyses," *Tribology Int.*, Vol. 34, pp. 523–530.
- [52] Najman, M.N., Kasrai, M., and Bancroft, G.M., 2004, "Chemistry of Antiwear Films from Ashless Thiophosphate Oil Additives," *Tribology Lett.*, Vol. 17, pp. 217–229.
- [53] Najman, M.N., Kasrai, M., and Bancroft, G.M., 2004, "Investigating Binary Oil Additive Systems Containing P and S Using X-Ray Absorption Near-Edge Structure Spectroscopy," *Wear*, Vol. 257, pp. 32–40.
- [54] Jahanmir, S., 1987, "Wear Reduction and Surface Layer Formation by a ZDDP Additive," *J. Tribology*, Vol. 109, pp. 577–586.
- [55] Lindsay, N.E., Carter, R.O., Schmitz, P.J., Haack, L.P., Chase, J.E., DeVries, R.E., and Willermet, P.A., 1993, *Characterization of Films Formed at a Lubricated Cam/Tappet Contact*, *Spectrochim. Acta*, Vol. 49A, pp. 2057–2070.
- [56] Suominen Fuller, M.L., Rodriguez Fernandez, L., Massoumi, G.R., Lennard, W.N., Kasrai, M., and Bancroft, G.M., 2000, "The Use of X-Ray Absorption Spectroscopy for Monitoring the Thickness of Antiwear Films from ZDDP," *Tribology Lett.*, Vol. 8, pp. 187–192.
- [57] Georges, J.M., Tonck, A., Poletti, S., Yamaguchi, E.S., and Ryason, P.R., 1998, "Film Thicknesses and Mechanical Properties of Adsorbed Neutral and Basic Zinc Diisobutyl Dithiophosphates," *Tribology Trans.*, Vol. 41, pp. 543–553.
- [58] Tonck, A., Bec, S., Georges, J.M., Coy, R.C., Bell, J.C., and Roper, G.W., 1999, "Structure and Mechanical Properties of ZDTP Films in Oil." In *Lubrication at the Frontier*, D. Dowson, Ed., Elsevier Science, Amsterdam, The Netherlands, pp. 39–48.
- [59] Williamson, B.P., and Bell, J.C., 2006, *The Effects of Engine Oil Rheology on the Oil Film Thickness and Wear Between a Cam and Rocker Follower*, SAE Paper 962031, SAE, Warrendale, PA.
- [60] Taylor, L.J., and Spikes, H.A., 2003, "Friction-Enhancing Properties of ZDDP Antiwear Additive: Part I—Friction and Morphology of ZDDP Reaction Films," *Tribology Trans.*, Vol. 46, pp. 303–309.
- [61] Taylor, L.J., and Spikes, H.A., 2003, "Friction-Enhancing Properties of ZDDP Antiwear Additive: Part II—Influence of ZDDP Reaction Films on EHD Lubrication," *Tribology Trans.*, Vol. 46, pp. 310–314.
- [62] Spikes, H.A., and Cann, P.M., 2001, "The Development and Application of the Spacer Layer Imaging Method for Measuring Lubricant Film Thickness," *Proc. Inst. Mech. Eng.*, Vol. 215, pp. 261–278.
- [63] Glovnea, R.P., Olver, A.V., and Spikes, H.A., 2005, "Lubrication of Rough Surfaces by a Boundary Film-Forming Viscosity Modifier Additive," *J. Tribology*, Vol. 127, pp. 223–229.
- [64] Spikes, H.A., 2006, "Origins of the Friction and Wear Properties of Antiwear Additives," *Lub. Sci.*, Vol. 18, pp. 223–230.
- [65] Marklund, O., and Gustafsson, L., 2001, "Interferometry-Based Measurements of Oil Film Thickness," *Proc. Inst. Mech. Eng.*, Vol. 215, pp. 243–260.
- [66] Shiomi, H., Makino, S., and Sugimura, J., 2007, "Measurement of Oil Film Thickness and Wear of Nanometer Scale under Pure Sliding Conditions with Ultrathin Film Interferometry," *Jap. J. Tribology*, Vol. 52, pp. 635–648.
- [67] Kuribayashi, T., Kawagoishi, N., and Ogano, S., "Lubricant Oil Composition for Diesel Engines," U.S. Patent No. 2003/0148899 A1.
- [68] McGeehan, J.A., Yeh, S.W., Couch, M.C., Hinz, A., Otterholm, B., Walker, A., and Blakeman, P., 2005, *On the Road to 2010 Emissions: Field Test Results and Analysis with DPF-SCR System and Ultra Low Sulfur Diesel Fuel*, SAE Paper No. 05FFL-43, SAE, Warrendale, PA.
- [69] Hong, H., Riga, A.T., Cahoon, J.M., and Vinci, J.N. 1993, "Evaluation of Overbased Sulfonates as Extreme-Pressure Additives in Metalworking Fluids," *Lub. Eng.*, Vol. 49, pp. 19–24.
- [70] McGeehan, J.A., Alexander, W., Ziemer, J.N., Roby, S.H., and Graham, J.P., 1999, *The Pivotal Role of Crankcase Oil in Preventing Soot Wear and Extending Filter Life in Low Emission Diesel Engine*, SAE Paper 1999-01-1525, SAE, Warrendale, PA.
- [71] Rasberger, M., 1997, "Oxidative Degradation and Stabilization of Mineral Oil Based Lubricants." In *Chemistry and Technology of Lubricants*, 2nd ed., R.M. Mortier and S.T. Orszulik, Eds., Springer, New York, pp. 98–143.
- [72] Rudnick, L.R. (Ed.), 2003, *Lubricant Additives*, Marcel Dekker, New York, pp. 1–44.
- [73] Gatto, V.J., Moehle, W.E., Cobb, T.W., and Schneller, E.R., 2006, "Oxidation Fundamentals and Its Application to Turbine Oil Testing," *J. ASTM Int.*, Vol. 3, pp. 1–20.
- [74] Canter, N., 2008, "Use of Antioxidants in Automotive Lubricants," *Tribology & Lub. Technol.*, Sept., pp. 12–19.
- [75] Papay, A.G., and Devlin, M.T., 1996, "Friction and Friction Modifiers in Lubricants," *Technische Akademik Esslingen*

- 10th International Tribology—Solving Friction and Wear Problems Colloquium, Vol. 2, pp. 1073–1078.
- [76] Hoshi, M., 1984, “Reducing Friction Losses in Automobile Engines,” *Tribology Int.*, Vol. 17, pp. 185–189.
- [77] Wakuri, Y., Soejima, M., Kitahara, T., Fujisaki, K., and Nuki, K., 1995, “Effect of Lubricating Oils on Piston Ring Friction and Scuffing,” *Jap. J. Tribology*, Vol. 40, pp. 437–449.
- [78] Rudnick, L.R. (Ed.), 2003, *Lubricant Additives*, Marcel Dekker, New York, p. 208.
- [79] Korcek, S., Johnson, M.D., Jensen, R.K., and McCollum, C., 1998, “Retention of Fuel Efficiency of Engine Oils,” *Technische Akademie Esslingen 11th International Industrial and Automotive Lubrication, Colloquium*, Vol. 2, pp. 1281–1288.
- [80] Arai, K., Yamada, M., Asano, S., and Yoshizawa, S., 1995, *Lubricant Technology to Enhance the Durability of Low Friction Performance of Gasoline Engine Oils*, SAE Paper 952533, SAE, Warrendale, PA.
- [81] Morina, A., Neville, A., Priest, M., and Green, J. H., 2006, “ZDDP and MoDTC Interactions in Boundary Lubrication—The Effect of Temperature and ZDDP/MoDTC Ratio,” *Tribology Int.*, Vol. 39, pp. 1545–1557.
- [82] Zhang, Z., Yu, L.G., Yamaguchi, E.S., Kasrai, M., and Bancroft, G.M., 2007, “Effects of Mo-Containing Dispersants on the Function of ZDDP: Chemistry and Tribology,” *Tribology Trans.*, Vol. 50, pp. 58–67.
- [83] Komvopoulos, K., Pernama, S.A., Yamaguchi, E.S., and Ryason, P.R., 2006, “Friction Reduction and Antiwear Capacity of Engine Oil Blends Containing Zinc Dialkyl Dithiophosphate and Molybdenum-Complex Additives,” *Tribology Trans.*, Vol. 49, pp. 151–165.
- [84] Mang, T., and Dresel, W. (Eds.), 2007, *Lubricants and Lubrication*, Wiley-VCH, Weinheim, Germany, p. 215.
- [85] Mang, T., and Dresel, W. (Eds.), 2007, *Lubricants and Lubrication*, Wiley-VCH, Weinheim, Germany, pp. 23–33, 94–106.
- [86] Kragelsky, I.V., and Alisin, V.V. (Eds.), 2001, “Tribology—Lubrication, Friction, and Wear,” In *Tribology in Practice Series*, Mar Publishers, Moscow, Russia, pp. 278–300.
- [87] Kajdas, C., 1993, “Engine Oil Additives: A General Review,” In *Engine Oils and Automotive Lubrication*, W.J. Bartz, Ed., Expert Verlag, Ehningen, Germany, pp. 149–175.
- [88] Sethuramiah, A., 2003, *Lubricated Wear: Science and Technology*, D. Dowson, Ed., Elsevier, Amsterdam, The Netherlands.
- [89] Kinker, B.G., 2000, “Fluid Viscosity and Viscosity Classification,” In *Handbook of Hydraulic Fluid Technology*, G.E. Totten, Ed., Marcel Dekker, New York.
- [90] SAE J300 Specification, 2007: Engine Oil Viscosity Classification: SAE International Surface Vehicle Standard. SAE, Warrendale, PA.
- [91] Günsel, S., Smeeth, M., and Spikes, H.A., 1996, *Friction and Wear Reduction by Boundary Film Forming Viscosity Index Improvers*, SAE Paper 962037, SAE, Warrendale, PA.
- [92] Müller, M., Fan, J., and Spikes, H.A., 2007, “Design of Functionalized PAMA Viscosity Modifiers to Reduce Friction and Wear in Lubricating Oils,” *J. ASTM Int.*, Vol. 4.
- [93] Liston, T.V., 1992, “Engine Oil Additives—What They Are and How They Function,” *Lub. Eng.*, Vol. 48, pp. 389–397.
- [94] Kornbrekke, R.E., Patrzyk-Semanik, P., Kirchner-Jean, T., Galic Raguz, M., and Bardasz, E.A., 1998, *Understanding Soot Mediated Oil Thickening Part 6. Base Oil Effects* SAE Paper 982665, SAE, Warrendale, PA.
- [95] Dockery, D.W., and Stone, P.H., 2007, “Cardiovascular Risks from Fine Particulate Air Pollution,” *New Eng. J. Med.*, Vol. 356, pp. 511–513.
- [96] Araujo, J.A., Barajas, B., Kleinman, M., Wang, X., Bennett, B.J., Gong, K.W., Navab, M., Harkema, J., Sioutas, C., Lulis, A.J., and Nel, A.E., 2008, “Ambient Particulate Pollutants in the Ultrafine Range Promote Early Atherosclerosis and Systemic Oxidative Stress,” *Circ. Res.*, Vol. 102, pp. 589–596.
- [97] Su, D.S., Serafino, A., Müller, J.-O., Jentoft, R.E., Schlögl, R., and Fiorito, S., 2008, “Cytotoxicity and Inflammatory Potential of Soot Particles of Low-Emission Diesel Engines,” *Environ. Sci. Technol.*, Vol. 42, pp. 1761–1765.
- [98] Quillian, R.D., Jr., Meckel, N.T., and Moffitt, J.V., 1964, *Cleaner Crankcases with Blow-By Diversion*, SAE Paper No. 801B, Warrendale, PA.
- [99] Vineyard, B.D., and Coran, A.Y., 1969, *Gasoline Engine Deposition: Blow-By Collection and the Identification of Deposit Precursors*, American Chemical Society, Washington, DC, pp. A25–A32.
- [100] Dimitroff, E., Moffitt, J.V., and Quillian, R.D., Jr., 1968, “Why, What, and How: Engine Varnish Formation,” Preprint, ASME and ASLE Lubrication Conference, October 8–10.
- [101] Bovington, C., and Castle, R., 2002, “Lubricant Chemistry Including the Impact of Legislation,” *Tribology Series*, Vol. 40, pp. 141–146.
- [102] Spikes, H.A., and Oliver, A.V., 2003, “Basics of Mixed Lubrication,” *Lub. Sci.*, Vol. 16, pp. 3–28.
- [103] Narita, K., 1997, “The Effects of Diesel Soot on Engine Oil Performance,” *Jap. J. Tribology*, Vol. 42, pp. 677–683.
- [104] Ryason, P.R., and Hansen, T.P., 1991, *Voluminosity of Soot Aggregates: A Means of Characterizing Soot-Laden Oils*, SAE Paper 912343, SAE, Warrendale, PA.
- [105] Georges, E., Georges, J. M., and Hoffinger, S., “Contact of Two Carbon Surfaces Covered With a Dispersant Polymer,” *Langmuir*, 13, pp. 3454–3463 (1997).
- [106] Ratoi, M., Castle, R.C., Bovington, C.H., and Spikes, H.A., 2004, “The Influence of Soot and Dispersant on ZDDP Film Thickness and Friction,” *Lub. Sci.*, Vol. 17, pp. 25–43.
- [107] Spikes, H.A., and Chiñas-Castillo, F., 2000, “Behavior of Colloidally-Dispersed Solid Particles in Very Thin Film Lubricated Contacts,” In *Thinning Films and Tribological Interfaces*, Elsevier B.V., Amsterdam, The Netherlands, pp. 719–731.
- [108] Chiñas-Castillo, F., and Spikes, H.A., 2000, “The Behavior of Colloidal Solid Particles in Elastohydrodynamic Contacts,” *Tribology Trans.*, Vol. 43, pp. 387–394.
- [109] Yamaguchi, E.S., Wilson, D.M., Kasrai, M., and Bancroft, G.M., 2002, “XANES Analysis of Used Engine Oils and Relationship to Wear,” *Tribology Trans.*, Vol. 45, pp. 437–443.
- [110] Ryason, P.R., Chan, I.Y., and Gilmore, J.T., 1990, “Polishing Wear by Soot,” *Wear*, Vol. 137, pp. 15–24.
- [111] Chiñas-Castillo, F., and Spikes, H. A., 2004, “The Behavior of Diluted Sooted Oils in Lubricated Contacts,” *Tribology Lett.*, Vol. 16, pp. 317–321.
- [112] Rounds, F.G., 1987, “Effect of Lubricant Additives on the Prowear Characteristics of Synthetic Diesel Soots,” *Lub. Eng.*, Vol. 43, pp. 273–282.
- [113] Yamaguchi, E.S., 2002, “Friction and Wear Measurements Using a Modified MTM Tribometer,” *IP.com J.*, Vol. 7, pp. 57–58.
- [114] Yamaguchi, E.S., Untermann, M., Roby, S.H., Ryason, P.R., and Yeh, S.W., 2006, “Soot Wear in Diesel Engines,” *J. Eng. Tribology Proc. Inst. Mech. Eng.*, Vol. 220, pp. 463–469.
- [115] Devlin, M.T., Li, S., Burgess, T., and Jao, T.-C., 2002, *Film Formation Properties of Polymers in the Presence of Abrasive Contaminants*, SAE Paper 2002-21-2793, Warrendale, PA.
- [116] O'Connor, S.P., Crawford, J., and Cane, C., 1994, “Overbased Lubricant Detergents—A Comparative Study,” *Lub. Sci.*, Vol. 6, pp. 297–305.
- [117] Roman, J.P., Hoornaert, P., Faure, D., Biver, C., Jacquet, F., and Martin, J.-M., 1991, “Formation and Structure of Carbonate Particles in Reverse Microemulsions,” *J. Colloid Interface Sci.*, Vol. 144, pp. 324–339.
- [118] Griffiths, J.A., Bolton, R., Heyes, D.M., Clint, J.H., and Taylor, S.E., 1995, “Physico-chemical Characterisation of Oil-Soluble Overbased Phenate Detergents,” *J. Chem. Soc. Faraday Trans.*, Vol. 91, pp. 687–696.
- [119] Arndt, E.R., and Kreuz, K.L., 1988, “Characterization of Calcium Alkylaryl Sulfonates Containing Encapsulated Solids,” *J. Colloid Interface Sci.*, Vol. 123, pp. 230–237.
- [120] Mansot, J.L., Hallouis, M., and Martin, J.M., 1993, “Colloidal Antiwear Additives. 1. Structural Study of Overbased Calcium Alkylbenzene Sulfonate Micelles,” *Colloids Surf. A Physicochem. Eng. Aspects*, Vol. 71, pp. 123–134.
- [121] Giasson, S., Espinat, D., and Palermo, T., 1993, “Study of Microstructural Transformation of Overbased Calcium Sulfonates during Friction,” *Lub. Sci.*, Vol. 5, pp. 91–111.

- [122] Giasson, S., Palermo, T., Buffeteau, T., Desbat, B., and Turllet, J.M., 1994, "Study of Boundary Film Formation with Overbased Calcium Sulfonate by PM-IRRAS Spectroscopy," *Thin Solid Films*, Vol. 252, pp. 111–119.
- [123] Chiñas-Castillo, F., and Spikes, H.A., 2000, "Film Formation by Colloidal Overbased Detergents in Lubricated Contacts," *Tribology Trans.*, Vol. 43, pp. 357–366.
- [124] Tavacoli, J.W., Dowding, P.J., Steytler, D.C. Barnes, D.J., and Routh, A.F., 2008, "Effect of Water on Overbased Sulfonate Engine Oil Additives," *Langmuir*, Vol. 24, pp. 3807–3813.
- [125] van Dam, W., Broderick, D.H., Freerks, R.L., Small, V.R., and Willis, W.W., 2000, "The Impact of Detergent Chemistry on TBN Retention," *Tribotest J.*, Vol. 6, pp. 227–240.
- [126] Topolovec-Miklozic, K., Forbus, T.R., and Spikes, H.A., 2008, "Film Forming and Friction Properties of Overbased Calcium Sulphonate Detergents," *Tribology Lett.*, Vol. 29, pp. 33–44.
- [127] Costello, M.T., and Urrego, R.A., 2007, "Study of Surface Films of ZDDP and MoDTC with Crystalline and Amorphous Overbased Calcium Sulfonates by XPS," *Tribology Lub. Technol.*, Vol. 63, pp. 20–24, 57–61.
- [128] Pugh, R.J., Matsunaga, T., and Fowkes, F.M., 1983, "The Dispersibility and Stability of Carbon Black in Media of Low Dielectric Constant. 1. Electrostatic and Steric Contribution to Colloidal Stability," *Colloids and Surfaces*, Vol. 7, pp. 183–207.
- [129] Pugh, R.J., and Fowkes, F.M., 1984, "The Dispersibility and Stability of Carbon Black in Media of Low Dielectric Constant. 2. Sedimentation Volume of Concentrated Dispersions, Adsorption, and Surface Calorimetry Studies," *Colloids and Surfaces*, Vol. 9, pp. 33–46.
- [130] Pugh, R.J., and Fowkes, F.M., 1984, "The Dispersibility and Stability of Coal Particles in Hydrocarbon Media with a Polyisobutylene Succinamide Dispersing Agent," *Colloids and Surfaces*, Vol. 11, pp. 423–427.
- [131] Forbes, E.S., and Neustadter, E.L., 1972, "The Mechanism of Action of Polyisobutenyl Succinimide Lubricating Oil Additives," *Tribology*, Vol. 5, pp. 72–77.
- [132] Endo, K., and Inoue, K., 1993, "Effects of the Structure on Various Performances of Polyisobutenylsuccinimides," *Mech. Eng.*, Vol. 80, pp. 242–252.
- [133] Yamaguchi, E.S., Ryason, P.R., Yeh, S.W., and Hansen, T.P., 1997, "Boundary Film Formation by ZnDTPs and Detergents Using ECR," *World Tribology Congress 1997*, Preprint 97-WTC-17.
- [134] Yamaguchi, E.S., Ryason, P.R., Yeh, S.W., and Hansen, T.P., 1998, "Boundary Film Formation by ZnDTPs and Detergents Using ECR," *Tribology Trans.*, Vol. 41, pp. 262–272.
- [135] Papke, B.L., 1988, "Neutralization of Basic Oil-Soluble Calcium Sulfonates by Carboxylic Acids," *Tribology Trans.*, Vol. 31, pp. 420–426.
- [136] Schilling, G.J., and Bright, G.S., 1977, "Fuel and Lubricant Additives—II. Lubricant Additives," *Lubrication*, Vol. 63, pp. 13–24.
- [137] Hamblin, P.C., Kristen, U., and Chasan, D., 1990, "Ashless Antioxidants, Copper Deactivators, and Corrosion Inhibitors: Their Use in Lubricating Oils," *Lub. Sci.*, Vol. 2, pp. 287–318.
- [138] Ries, H.E., and Gabor, J., 1967, "Chain Length Compatibility in Rust Prevention," *Chemistry and Industry*, Vol. 37, pp. 1561–1562.
- [139] RohMax Additives, 1996, *Pour Point Depressants*, Technical Report RM-96-12-02.
- [140] ASTM D296: Particle Count Standard.
- [141] Snyder, K.E., Gschwender, L.J., and Sharma, S.K., 2007, "Effects of Contamination on Aerospace Hydraulic Components and System Performance." Paper presented at the Contamination Control Symposium of ASTM.
- [142] Mang, T., and Dresel, W., Eds., 2007, *Lubricants and Lubrication*, Wiley-VCH, Weinheim, Germany, pp. 279–281.
- [143] Fang, H.L., Whitacre, S.D., Yamaguchi, E. S., and Boons, M., 2007, *Biodiesel Impact on Wear Protection of Engine Oils*, SAE Paper 2007-01-4141, SAE, Warrendale, PA.
- [144] Lapuerta, M., Armas, O., and Rodriguez-Fernandez, J., 2008, "Effect Of Biodiesel Fuels on Diesel Engine Emissions," *Prog. Energy Combustion Sci.* Vol. 34, pp. 198–223.
- [145] Nicosia, D., Czekaj, O., and Kröcher, O., 2008, "Chemical Deactivation of V_2O_5/VO_3-TiO_2 SCR Catalysts by Additives and Impurities from Fuels, Lubrication Oils and Urea Solution Part II. Characterization Study of the Effect of Alkali and Alkaline Earth Metals," *Appl. Catal. B*, Vol. 77, pp. 228–236.

13

Bench Performance Test Methods for Lubricated Engine Materials

Peter Blau¹ and Simon C. Tung²

13.1 INTRODUCTION

Internal combustion engines are made from a wide variety of materials. These materials must contain the fuel and combustion pressures, transmit forces to the drivetrain, deliver electrical power, and give form and structure to the engine. In the context of this chapter, some of those materials must withstand bearing pressures and rub smoothly and reliably, without seizing or excessive wear, for thousands of hours. Although bronzes and other nonferrous alloys are used, by far, iron-based metals and alloys, particularly gray cast iron, have comprised the major bearing materials. Cast iron remains available in bulk quantities, is relative inexpensive, and is familiar to engine makers. However, with a density of 7.1–7.7 g/cm³, cast iron parts are more than 1.6 times heavier than titanium, 2.5 times heavier than aluminum, and 4.2 times heavier than magnesium parts of equal size. With a drive toward reducing the weight of engines to improve fuel economy, vehicle designers are motivated to find cost-competitive, lighter weight materials for engines and drivetrains that function well in advanced engines and drivetrains. Engine designers have historically been interested in finding workable alternatives to cast iron for more than three quarters of a century. As early as 1923, Audi announced an aluminum alloy engine and became an early leader in applying lightweight alloys to engines [1]. By 2006, the average aluminum content in U.S. automobiles was 319 lb (149 kg), a nearly 24 % increase over the preceding 5 years [2]. Most of this substitution was in the area of structural materials, but lightweight alloys are not ideally suited for tribocomponents such as engine castings, valvetrains, fuel injector plungers, roller followers, and disc brakes. This is mainly because of high contact pressures for the valvetrain components.

Piston sets, rolling and sliding bearings, seals, the valvetrain, and gears are part of an engine's portfolio of materials, and there are opportunities not only to use lighter-weight bulk materials, but also to apply new coatings and surface treatments that will extend service life, lower warranty costs, and boost reliability. In sliding bearings, the so-called Stribeck curve, which was in fact developed earlier by another German engineer named Martens [3], has been widely used to portray the inter-relationship between rotational speed (S), unit load (P), absolute viscosity (η), and the friction coefficient (μ). As shown in Figure 13.1, as a bearing operates farther toward the upper left on the Stribeck curve, the more materials matter to its tribological performance. In fact, key engine components, such as

piston rings, main bearings, and valve guides, operate in regions of the Stribeck curve in which other than full-film lubrication exists, so the proper selection of materials for contact surfaces is essential. As the combined parameter on the horizontal axis of Figure 13.1 suggests, highly-loaded, slow-moving bearing surfaces, like those in gears, need higher-viscosity lubricants in order to provide low friction. In addition, there are certain valvetrain applications as shown in Figure 13.2, such as valves, camshafts, lifters, turbo-charger vanes, exhaust valve seats, and butterfly valves in exhaust gas recirculation systems, in which the use of liquid lubricants becomes impractical. Such applications further increase the demand placed on bearing surfaces.

Test methods described elsewhere in this book focus on the properties of lubricants, and most of the standards that are used to measure friction and wear-related characteristics of lubricants use steel or cast iron coupons. However, selecting new materials or surface treatments for engines requires using tests that evaluate not only the lubricants, but also the bearing materials that support them. The selection and use of such material-based tests is the focus of this chapter.

13.2 FIELD TESTING VERSUS LABORATORY BENCH TESTS

In a perfect world, all candidate materials for engines should be tested under field conditions with a sufficient number of replicates to establish, with high statistical confidence, the reliability of those materials. However, field tests are realistically not only expensive, but to a large extent, the results of field trials also depend on the driver, weather conditions, road conditions, geography, and duty cycle. Developing a representative field test protocol presents significant challenges because once a new vehicle leaves the dealership, the operating conditions for that vehicle are completely out of the control of the manufacturer, who must still honor the warranty. Warranties are carefully written for that reason, but the robustness of vehicle systems is necessary nonetheless. An ability to rank engine materials by bench testing can reduce the need for expensive, full-scale engine tests. This becomes vitally important for cost-effectively moving vehicle technology forward to meet 21st century competition, regulatory requirements, and developments in alternative fuels. Therefore, the test methods should mimic the interfacial conditions of applications, and wherever possible, baseline data should be cross-correlated with field data to establish the test method's validity.

¹ Oak Ridge National Laboratory, Materials Science and Technology Division, Oak Ridge, TN, USA

² RT Vanderbilt Company, Norwalk, CT, USA

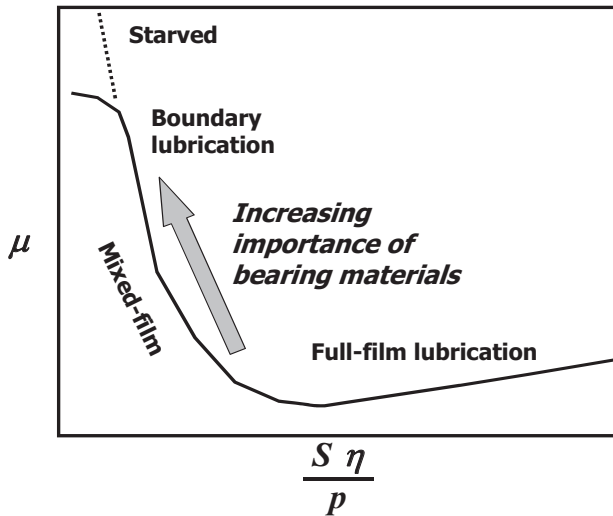


Figure 13.1—The importance of materials increases as the lubricant film thickness decreases.

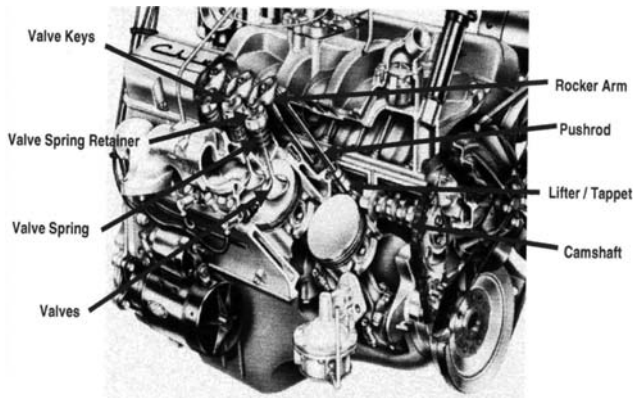


Figure 13.2—Valvetrain basic configuration.

13.3 TEST METHOD SELECTION

There is no such thing as a “generic” friction or wear test because the tribological performance of materials is strongly affected by the context in which those materials are used. As Czichos demonstrated more than 30 years ago [3], surface treatments can rank in opposite merit of wear resistance depending on the type of wear to which they are subjected. Therefore, for example, if one is attempting to evaluate materials for a piston ring, the test should simulate the key contact conditions of that application, and a simple, unidirectional pin-on-disk sliding test conducted at room temperature will simply not do.

Tribosimulation applied to engine research and other tribosystems has been the subject of several publications (e.g., references 4–6). Simulations need not mimic every aspect of the ultimate application, but they should at least embrace the key elements to obtain an initial ranking of performance that eliminates some obviously unsuitable candidates and identifies one or more promising choices for subsequent engine or field tests.

Over the years, a wide range of tests has been developed for measuring lubricant properties and performance characteristics (e.g., reference 7). There are generally three levels of lubricant testing, as shown in Figure 13.3. When developing a lubricant, the lubricant manufacturer passes through the sequence shown in the figure, performing numerous bench tests before committing to more realistic, but costly and often time-consuming applications tests.

Tribotesting conditions include the considerations and parameters listed in Table 13.1. Unlike tensile tests or other bulk material tests in which the specimen geometry and boundary conditions are well established, tribotests involve open systems in which the boundaries themselves are the concern. They can change with time because of factors such as running-in and changes in lubricant chemistry. The

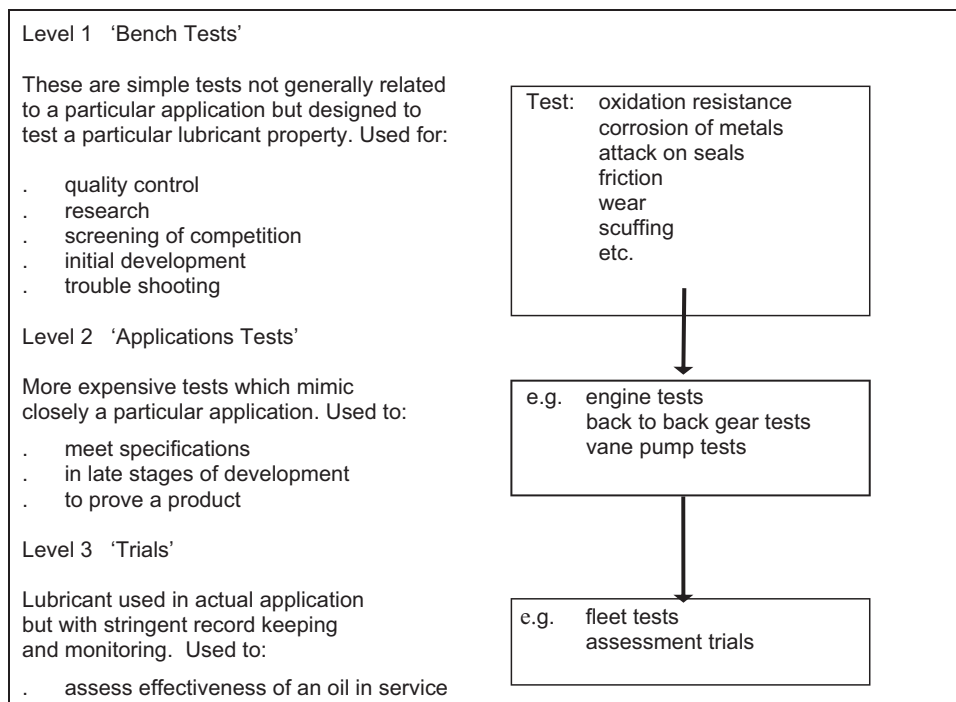


Figure 13.3 —Three levels of testing of engine lubricating oils and materials.

TABLE 13.1—Considerations in Selecting or Designing Bench-Scale Tests for Engine Materials

Category	Variables	Effects or Examples
Macrogeometry	Dimensions of bearing surfaces, conformal or nonconforming contact surfaces	Lubricant fluid flow, debris entrainment, film thickness, heat flow, and contact stress distribution
Microgeometry	Surface texture: roughness, waviness, and lay (directionality of features)	Film thickness-to-composite-roughness ratio, running-in characteristics, lubricant flow, wear pattern, finishing cost
Motion	Direction: unidirectional or reciprocating motion. Constancy: continuous or start/stop accelerations or other variations in speed	Stability of lubricant film thickness, third-body entrainment, directionality and shear rates applied to material surfaces, mechanical mixing or formation of wear debris deposits
Contact pressure	Applied load (constant or variable)	Contact pressure distribution on the bearing surface, elastic or plastic deformation of materials, degree of retention of initial surface finish, wear-in, squeeze-out of lubricants
Thermal environment	Surrounding temperature, frictional heating (function of friction force and velocity)	Lubricant viscosity, lubricant cavitation or volatilization, additive reactivity and thermal degradation, flash and bulk surface temperatures, scuffing characteristics, localized material softening and deformation
Lubrication	Composition, viscosity, method of supply or recirculation, method of filtration, aging and stability, contamination (water content, wear debris, acidity, soot, etc.)	Regime of lubrication (boundary, mixed film, full film), reactivity with material surfaces, ability to remove third bodies, load-carrying capacity
Contact damage—current materials	Type(s) of wear on the surfaces of interest; characteristic contact features and their evolution, experience with current materials in related applications	Surface examination serves as a basis to compare laboratory results with on-engine behavior
Evolution of design and history of material performance	Why the original engine materials were selected and how they performed	Do new operating requirements push existing materials into regimes for which they were not originally selected?
Candidate materials or surface treatments	List of bulk materials, coatings, or surface treatments for this application	Considerations of cost, availability, and experience from similar applications. Which options have a solid engineering history and which are more experimental?

kind of lubricant used and its means of supply are only one element in the larger universe of test parameters [8]. Fortunately, not every variable in Table 13.1 must be precisely matched to the application of interest for bench tests to be useful in material selection. Despite improvements in computational models, designers of engines may not know a priori the exact contact conditions for key interfaces in a new engine configuration, especially when there is little or no service history for a concept that is still on the drawing board.

As indicated in Table 13.1, the alternative means to establish the validity of a laboratory test is to examine surfaces of the test specimens to determine whether they show the same features that occur in components removed from an engine environment. This requires attention to detail and experience in examining surfaces from the engine components of interest. For example, microwelding may be a concern in the wear of upper piston ring grooves; light abrasion or burnishing may suggest the downstream potential for scuffing on a piston skirt; and micropitting may be an indication of acid attack or, depending on pit shapes and orientation, rolling contact fatigue.

Internationally, standard bench or engine simulation tests are published by

- DIN EN—German Institute for Standards
- ISO—International Organization for Standardization
- SAE—Society of Automotive Engineers
- ILSAC—International Lubricants Standardization and Approval Committee
- IP—United Kingdom-based Institute of Petroleum
- CEC—Coordinating European Council
- ASTM International
- JASO—Japanese Automotive Standards Organization

Note that JASO and DIN EN are just relevant standardization organizations for engine lubrication, not major organizations to develop engine oil specifications.

Standardized tests for oxidation, metal corrosion, seal attack, viscosity, and acidity give reasonably repeatable and meaningful measurements of lubricant properties. On the other hand, the usefulness of bench testing to assess wear resistance, friction, scuffing, and rolling contact fatigue is controversial. Therefore, it is incumbent on tribologists to find tests for friction and wear that correlate best with engine operating experience. Table 13.1 summarizes some

of the important lubricating properties and test parameters to consider when selecting bench tests for engine materials or lubricating oils. There are others as well (e.g., references 8–10).

If a tribosystem operates under boundary lubrication, the friction coefficients typically range from approximately 0.08 to 0.13, but that estimate may not be sufficiently accurate for designers or those who must select reliable low-friction surface treatments to enhance fuel economy energy. Certain engine design choices can be facilitated with the help of bench testing. For example, the specified surface texture (roughness, waviness, and lay) affects the cost of manufacturing, and it is desirable to determine whether tighter tolerances for surface finish would achieve any benefits beyond what a good running-in practice might more cost-effectively provide.

The advent of alternative fuels such as biodiesel, gas-to-liquid, hydrogen, natural gas, and ethanol may force changes in engine materials. Some of these fuels are more lubricative than gasoline or conventional diesel fuel, but others are less so [9,10]. Such motivations support the development and use of reliable bench tests, but the number of one-of-a-kind bench-scale tests has proliferated [11]. The development of standards, whether for in-house use by a certain engine builder or as consensus documents for industry-wide use, helps to improve the ability of one organization to compare its results with those of others or to benchmark its own test results over time.

13.4 SELECTION AND USE OF BENCH TESTS FOR SPECIFIC ENGINE SUBSYSTEMS

The following sections exemplify how certain bench-scale friction and wear tests can rank engine materials in a cost-effective manner relative to full-sized engine tests. There are so many friction and wear interfaces in engines that these descriptions cannot be all-inclusive. Rather, they are intended to provide practical examples of bench-scale testing and illustrate some basic principles that can be more widely applied. The mention of specific commercial machines and lubricant products was done to document these case studies and is not intended to be a commercial product recommendation.

13.4.1 Bench Tests for Engine Cylinder Components and Valvetrain Subsystems

Typical bench-scale tribotesting geometries include the pin-on-disk [12], block-on-ring [13], crossed-cylinders, and four-ball test method [14]. These geometries are listed in Table 13.2. Variants of such tests can be conducted under unidirectional, rotary, or reciprocating motion. All of these also involve a “nonconformal” contact geometry, in which the shapes of opposing surfaces do not match at the outset of the test. Nonconformity also means that wear of one or both counterfaces can change the nominal contact area, and thus the nominal contact pressure, over time.

Over the past 25 years or more, the block-on-ring tester, once referred to as an “LFW-1” or “Falex Model 1” (see Figure 13.4), was used in automotive laboratories to evaluate materials and surface coatings for piston rings, engine blocks, liners, and valve guides. Scuffing resistance was determined by incrementally increasing the load until failure was detected by a sudden change in the measured

TABLE 13.2—Common Bench-Test Types

Test Geometry	Type of Contact	Contact Geometry	Relative Motion
Pin on disc	closed	non-conformal (1)	unidirectional
	open (2)	non-conformal	reciprocal
Block on ring	closed	non-conformal	unidirectional
	closed	non-conformal	reciprocal
Crossed cylinders	closed	non-conformal	unidirectional
	open	non-conformal	reciprocal (3)
Four balls	closed	non-conformal	unidirectional
Ring on cylinder bore (4)	closed	conformal	reciprocal

- (1) If the pin surface is initially curved.
- (2) If the sliding track forms a spiral.
- (3) Common in fretting studies.
- (4) Modified Cameron-Plint High Frequency Tester.

friction force. Block-on-ring machines were also used for wear testing under different combinations of load, speed, lubricant type, temperature, and sliding duration. The coefficient of friction is determined based on the applied load and the tangential force transducer output. Block wear is commonly reported in terms of the volume removed. This can be done using stylus profiling, wear scar width measurements, or mass loss. The ring specimen wear is evaluated by weight loss, or more subjectively, by visual inspection.

Block-on-ring tests for piston ring and cylinder liner evaluations have been used, but the initial, nonconformal contact geometry of this test is unlike the conformal

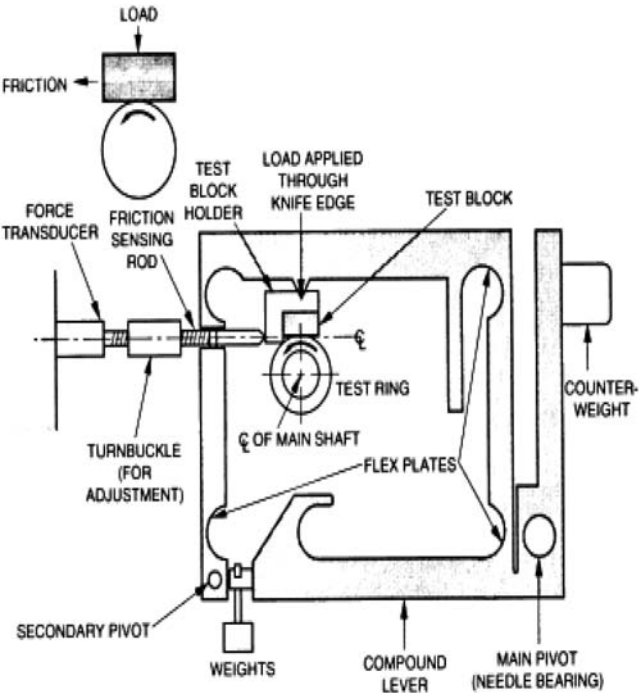


Figure 13.4—Schematic of Falex-type block-on-ring friction and wear tester.

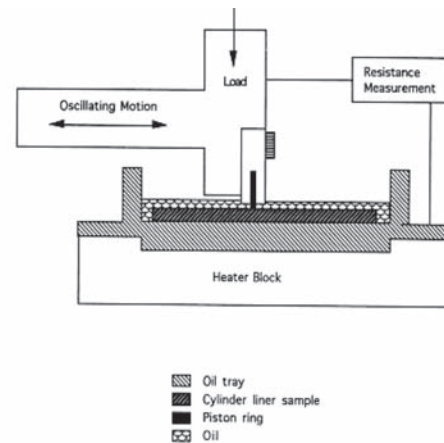
contact of a piston ring against the cylinder bore that occurs quickly after run-in, and that shortfall limits its relevance. Other disadvantages of nonconformal bench test methods, such as those listed in Table 13.2, are that full-sized components cannot readily be tested and that the chemical environment, such as the presence of engine-conditioned oil, exhaust gas environments, and unburned fuel or moisture in the oil, are not well simulated.

Many kinds of internal combustion engine components slide back and forth during operation. Examples include piston rings inside cylinder bores, valve stems in their guides, fuel injector plungers in nozzles, and piston wrist pins as the connecting rods articulate about the crankshaft. The reversal of relative motion means that the sliding velocity and resulting lubrication regimes do not remain constant. Materials and surface finishes experience reversed tractions, and as a result, wear is worst at the locations where the direction of motion changes, such as the top dead center position of a piston stroke. Therefore, reciprocating-motion tests are better than unidirectional tests for screening materials for such applications. Examples, using modified, commercially manufactured tribotesters, follow.

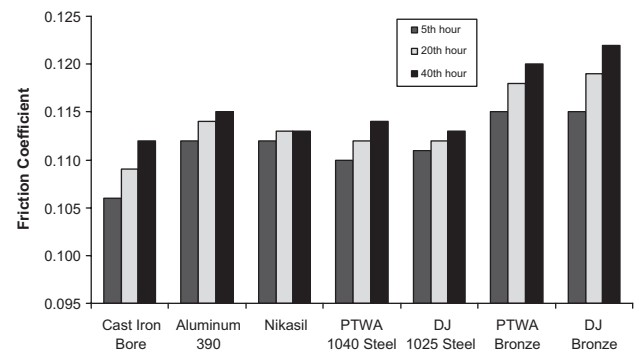
13.4.1.1 RECIPROCATING BENCH TESTS FOR PISTON RINGS ON CYLINDER BORES

A commercially made, reciprocating tribotester (commonly called a “Cameron-Plint,” Model TE-77, although it is no longer manufactured under that tradename) was configured as shown in Figure 13.5. The purpose of the tests was to evaluate advanced lubricants and engine materials for possible use on engine cylinder bores. The reciprocating motion of the modified machine to some extent simulates piston/cylinder liner dynamics [15,16]. The main advantage of this bench test is that specimens cut from real engine components can be used. Because the contact geometry of the engine is preserved, representative surface finishes can be meaningfully evaluated. A ring segment in a specimen holder is moved back and forth across a cylinder segment as would occur in an engine. In addition, the upper (moving) specimen holder was modified to allow the piston ring segment to move in a slot, simulating the movement that occurs in a piston ring groove. Friction force and electrical resistance are continuously measured during the test, and the wear of the cylinder liner and piston ring sections are measured with the use of a surface roughness analyzer [16]. To evaluate the stable friction characteristics of engine bores, friction coefficient measurements are performed after a sufficiently long sliding test time to ensure stabilization, typically 5 h. In reporting the results, friction force is given as the root mean square (RMS) of the instantaneous friction force over each forward and back cycle. The reciprocating bench test procedures are described in detail in references 17 and 18. Selected results from representative studies of advanced engine materials, coatings, and energy-conserving lubricants [18] are presented in Figure 13.5 to illustrate the results obtainable by this method.

More recent work on reciprocating bench-scale testing has recognized that fresh lubricants do not rank materials similarly in friction and wear as do lubricants that have been conditioned by exposure to fired-engine conditions [19]. This was the basis for development of ASTM standard



(A) Cameron-Plint High Frequency Friction Machine



(B) Friction Characteristics of Different Cylinder Bore Coatings Lubricated Against Piston Rings

Figure 13.5—Schematic of Cameron-Plint high-frequency friction machine and friction test results.

G181 [20], with support from the U.S. Department of Energy, to improve fuel economy in heavy-duty diesel engines. Special step-loading techniques, explained in the standard, were developed to run-in the contact surfaces before friction measurements [21,22]. The repeatability and reproducibility of the ASTM method were determined by interlaboratory testing. It was shown that by correctly conducting the procedure, it was possible to distinguish between the frictional characteristics of drain oils obtained from a series of standard diesel engine tests.

13.4.1.2 BENCH TESTS FOR CAM LOBE AND FOLLOWER MATERIALS

The friction and wear of candidate cam lobe and follower materials were measured using a customized test method and a specially modified SRV 4 tribology test machine manufactured by Optimol Instruments Prüftechnik GmbH, Germany. Technical data for the machine that was used is shown in Table 13.3, and a schematic diagram and picture of the system are shown in Figure 13.6. The SRV 4 uses an electromagnetic drive motor to oscillate specimens at high frequency. In addition to the current example, this type of machine has also been used for oil sequence testing and piston ring wear evaluations [23–25].

TABLE 13.3—Optimol SRV 4 Technical Data

Load	1–2000 N
Test time:	1 min to 999 h
Frequency:	1–511 Hz
Stroke:	0.2 to >4 mm
Temperature:	Standard range: ambient to +290°C Low-range option: –35°C to +290°C High-range option: ambient to +900°C
Test parameters used by the authors to simulate valvetrain lubricated sliding conditions in the cited paper [23].	
Break-in	
• Duration:	1 min
• Temperature:	130°C
• Frequency:	15 Hz
• Stroke:	4 mm
• Load:	50 N
• Contact stress:	900–1280 MPa
• Oil:	0.3 mL GF-4
Test	
• Duration:	7 h
• Temperature:	130°C
• Frequency:	35 Hz
• Stroke:	4 mm
• Load:	550 N
• Contact stress:	900–1280 MPa
• Oil:	0.3 mL GF-4
Material size	
• Pin curvature:	35 mm
• Flat size:	8 × 6 × 4 mm

Five follower materials and eight lobe materials were selected based on their historical use, and in the case of nontraditional materials, their potential for success. These were tested under sliding conditions against two different follower materials that had different heat treatments. The same follower materials, but coated with a diamond-like coating, were also tested. Flat specimens, measuring 8 × 6 × 4 mm, were cut by electric-discharge machining (EDM) from camshaft material having a representative production surface finish (see Figure 13.7a). The upper specimens, which represent the follower material, were machined from SAE 52100 steel and 4130 steel bar stock into cylindrical pins with a rounded tip. The upper specimen had a 10-mm diameter, 10-mm length, and a 35-mm radius on the tip (see Figure 13.7b). The rounded tip was polished to a maximum arithmetic average (Ra) surface finish of 0.3 mm. The 52100 and 4130 steel specimens were heat-treated to HRC 58–62 to preserve the material chemistry, hardness, microstructure, and residual stresses typical in the application. Lower specimens can be tested with original surface curvature or used as a flat specimen but with a representative

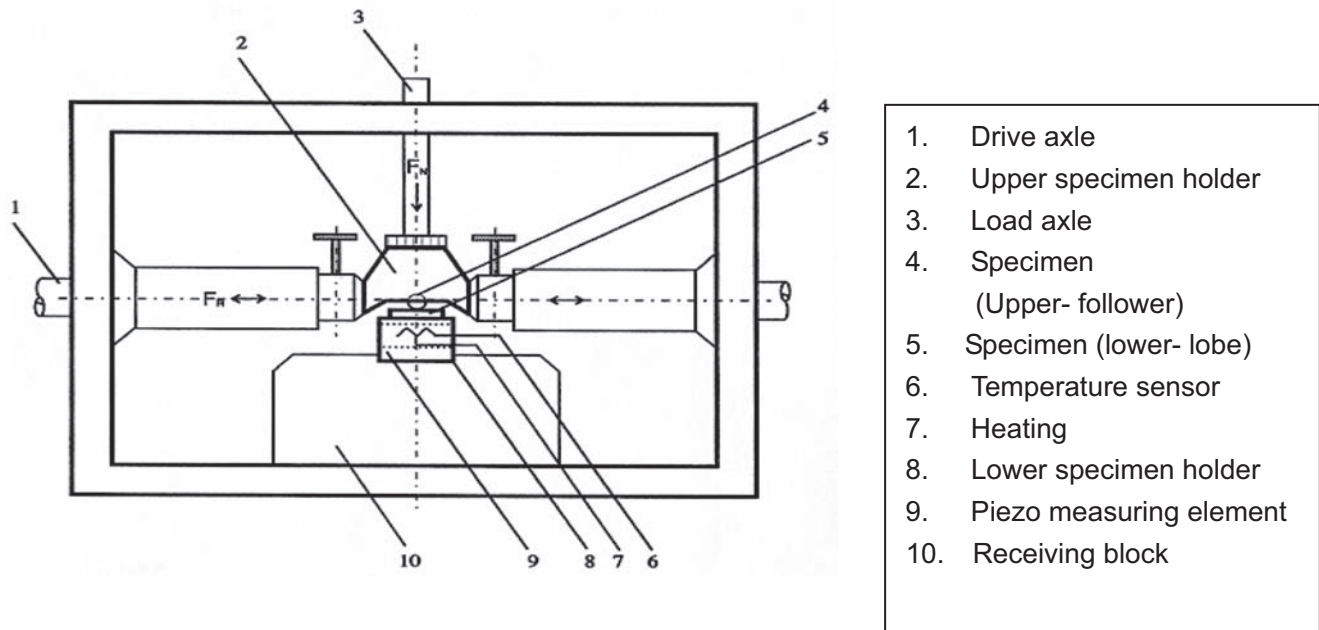
surface finish. Because the cam lobe geometry has an effect on the resultant contact stress for a given load, this was also considered.

Custom specimen holders were designed for this test. The upper holder, Figure 13.8a was designed to hold the cylindrical specimen. The lower holder, Figure 13.8b, was designed to hold a rectangular block. Approximately 0.3 mL of oil was placed on the lower specimen to maintain lubrication. Test parameters were set to mimic the actual operating conditions of a follower in contact with a cam lobe, but parameters were chosen to accelerate testing under controlled conditions. The following parameters could be varied or held constant during the test: load, stroke, frequency, oil condition, oil temperature, and the amount of lubrication. A break-in procedure was applied to ensure that contacting surfaces were lubricated. Once the oil was heated to 130°C, the test started at 15 Hz at a stroke of 4 mm and a load of 50 N for 1 min. After this initial break-in period, the load was ramped up to the full-load condition within another minute. Tests were run for 7 h with a frequency of 35 Hz, a stroke length of 4 mm, and a normal force of 550 N. Here, the bench test is different than the application because there is oscillation instead of rotation. A summary of the test conditions is given in Table 13.3. Each material combination was tested twice, in randomized order.

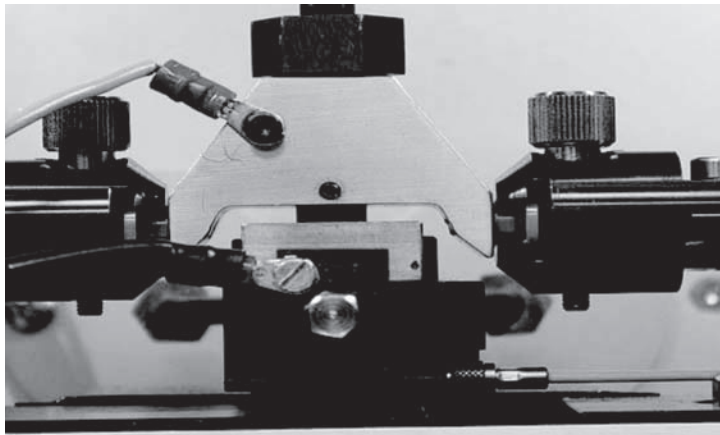
Engine oil with viscosity grade 5W-30 oil (SAE SM) was used for the test. For the highly loaded contacts, the interaction between zinc dialkyl dithiophosphate (ZDDP), used as an antiwear and antioxidant additive, is critical for wear-resistant film formation. Antiwear film formation mechanisms on camshaft materials, other than steel and gray and chilled iron, have not been extensively studied, and hence ZDDP's contribution to friction modification, and ultimately to sliding wear properties, is unknown for this application. Nevertheless, this kind of bench test can be used to assess and select new camshaft/follower materials under sliding and rolling conditions. This test can also be used to assess effects of newer lubricant formulations on the performance of valvetrain components.

13.4.1.3 PISTON SKIRT SCUFFING SIMULATION TESTS

A study of piston skirt scuffing was conducted in which results from bench tests were compared with those from dynamometer tests. For the bench testing portion of the work, the same type of reciprocating test machine, as was used in example 13.4.1.1, was used to evaluate the tribological behavior of coated pistons against an aluminum alloy 390 cylinder bore. The test setup is shown in Figure 13.5. Cold-scuffing simulation tests were conducted under conditions that lead to lubrication starvation. Wear simulation tests were performed under lubricated conditions. A special bench test fixture was used. A data acquisition system recorded the coefficient of friction, the electrical contact potential, and the temperature. During the test, the cylinder bore sample was stationary. The motion of the piston sample was produced by a Scotch yoke mechanism driven by a variable-speed motor. The piston sample was loaded against the cylinder bore sample by a spring balance. The load ranged from 0 to 250 N and can be translated into contact stress in two ways. The first-order estimate of the



(a) Upper specimen: cylindrical, 10 mm in diameter and 10 mm in length, with a spherical contact surface at one end having a curvature of 35 mm



(b) Picture of SRV tribological test apparatus

Figure 13.6—(a) Schematic of Optimol SRV 4¹ and (b) picture of SRV tribological test apparatus.

stress would be simply the load divided by the wear scar width multiplied by the length of the piston sample. The second approach computes the elastic contact stress using the Hertz equations. Because the radii of the two samples are deliberately different to allow consistent alignment, a load divided by area process significantly understates the true contact stress, normally determined by elastic theory as the Hertz stress. In this work, the Hertz contact stress at 120 N was 17.2 MPa.

During the test, the tangential friction force is continuously monitored and measured by a piezoelectric transducer attached to the piston skirt fixture. The electrical contact potential (or resistance) between piston and cylinder bore samples was also continuously measured. The contact potential method is used to monitor lubricated contact conditions. This gives a qualitative indication of

the degree of surface asperity interaction because asperity contact results in a great reduction in the electrical resistance (or potential) across the interface. In addition, these measurements can be used to monitor the lubricant film or surface coating changes at the interface and to determine the contact and wear mechanism of surface coatings. Wear scars for cylinder bore samples were analyzed in the longitudinal or transverse directions, or both, with respect to the sliding direction using a mechanical stylus surface profiling instrument (TalysurfTM).

It is well known by engine makers that three root causes of cold scuffing of the piston skirt and cylinder bore are fuel dilution, the high viscosity of engine oil that occurs at cold temperatures (approximately -20°C), and high side forces. It was impractical to introduce the cold temperature and gasoline to the current bench-testing environment, so

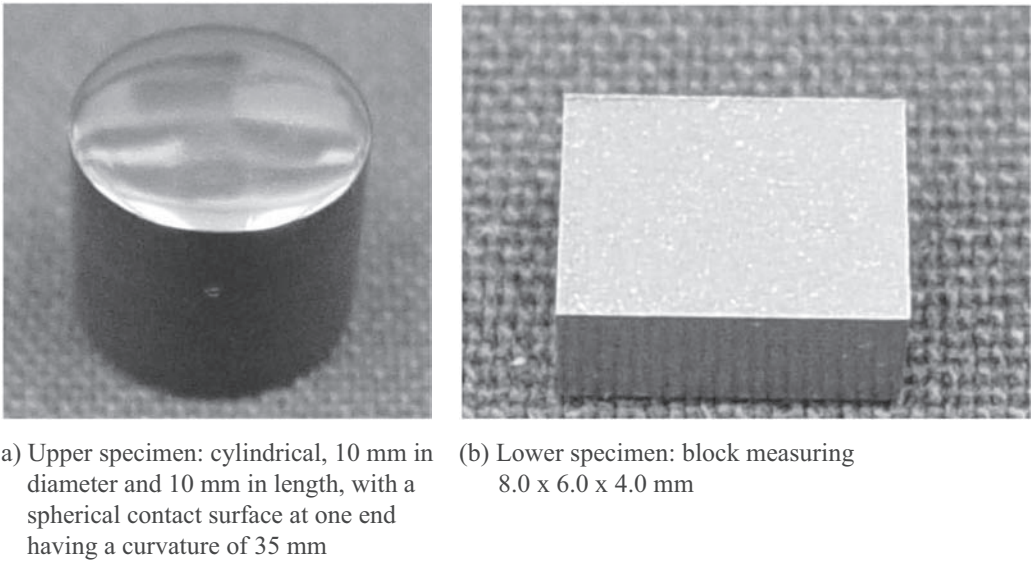


Figure 13.7—Test samples representing the follower material (upper specimen) and lobe material (lower specimen).

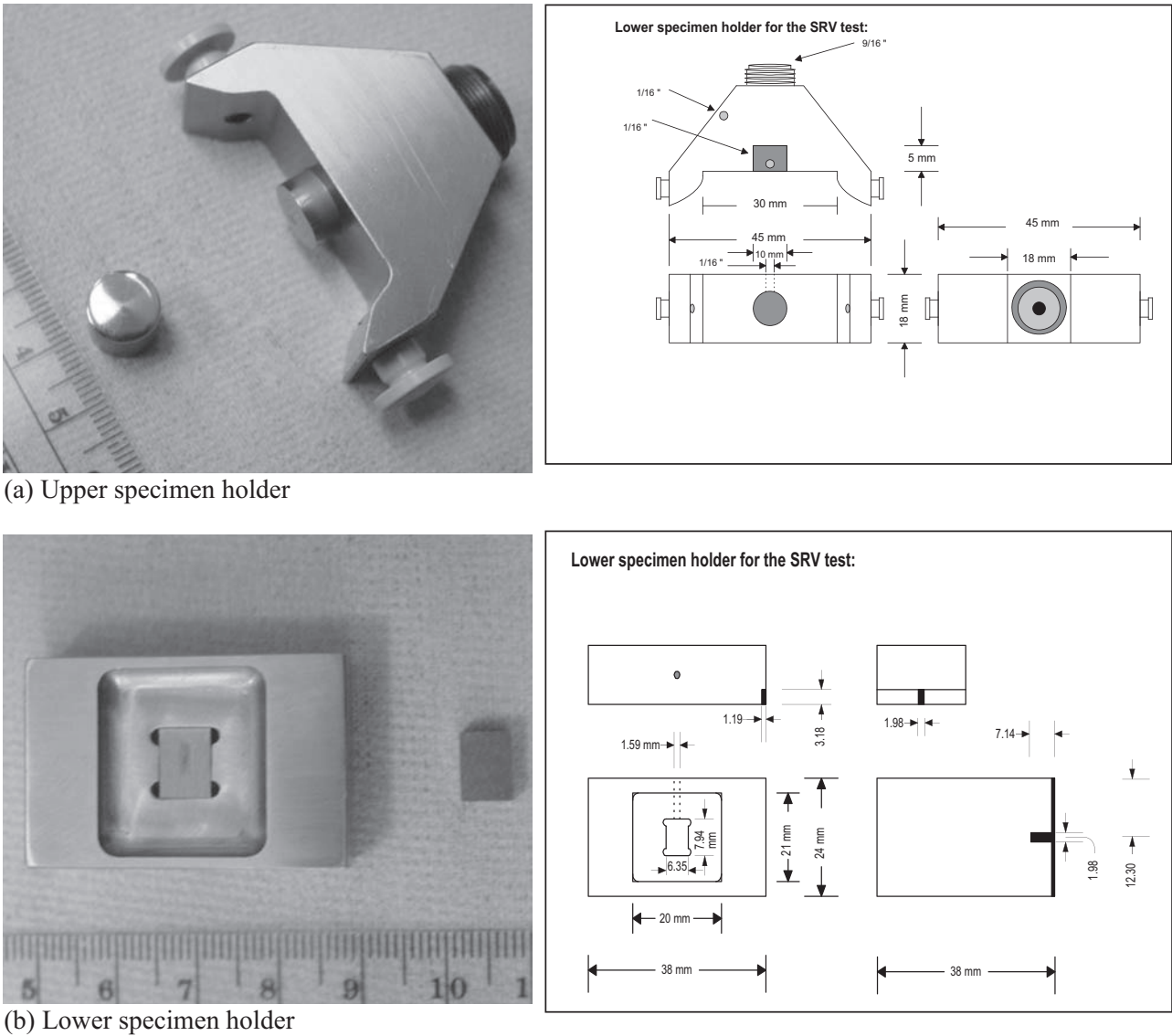


Figure 13.8—Custom specimen holders.

an alternative strategy was devised to produce a similar effect. Lubricated conditions were present during the first part of the test, and then there was a transition to lubricant starvation, similar to that of fuel dilution and high viscosity, for the remainder of the test. This was accomplished using a small amount of kerosine (0.2 mL), a petroleum fraction that would have some of the tramp elements, and a modest reaction at the interface during run-in similar to that of an engine oil but at a temperature of 85°C, at which the kerosine would decompose and evaporate. These simulative wear tests were conducted at 125°C, with loads of 120 or 160 N. The stroke was 6.77 mm at a frequency of 10 Hz. The lubricant used was SAE API SH, Grade 5W-30.

Bench tests must provide a means to rank lubricant and materials performance or result in a metric linked to component durability. However, wear is commonly measured differently in full-scale engines than in the laboratory. For example, the diametrical clearance inside of a bearing or cylinder liner, the lash in a valvetrain, or the concentration of wear particles in engine oil are used in practice, but laboratory measurements are reported in terms of mass loss or wear scar volume. How can these units of measure be linked? Physically, volume units are related to length units cubed; therefore, the relationship between contact pressure (load) and linear wear rate is not expected to be the same as between pressure and volumetric wear rate. Section 13.4.2 describes how bench-test wear data are quantified, and Section 13.4.3 compares these measures with dynamometer test results in the case of scuffing.

13.4.2 Methods for Measuring Wear in Bench Tests

13.4.2.1 SIMULATION OF CAMSHAFTS AND FOLLOWER WEAR

To determine the relative ranking of materials and surface treatments under sliding conditions that are representative of the loading on camshafts and followers, specimens of currently used materials were heat-treated and machined to a specific geometry. This allowed calculation of applied Hertzian stresses for different materials of interest. Ranking was done based on the selection of end-of-test (EOT) criteria. Tests could be run for specific durations with a limited amount of lubrication, or they could be run to simulate interfacial response under fresh or degraded lubrication conditions. The lubrication regime can be chosen to be at full boundary or at mixed elastohydrodynamic (EHD)/boundary conditions with temperatures up to 135°C, so the effects of viscosity and oil additives can be similar to those in an engine. The load could either be ramped up slowly,

or the maximum load could be applied at the start. Various EOT criteria are possible. For example, EOT criteria could be selected based on the percent increase in friction coefficient or the EOT value of the friction coefficient. In the present example, the determination of EOT response for acceptability of the sliding wear performance was done by measuring (1) the coefficient of friction, (2) the wear scar depth, and (3) the wear volume of each mating surface. The surface wear scar assessment was done using a noncontact, scanning optical interferometer (Wyko™, Veeco Corporation, USA) that enables the measurement of surface feature dimensions.

Several examples of worn specimens are shown in Figure 13.9. The measurement technique for wear volume is illustrated in Figure 13.10. For flat specimens, the process is fairly straightforward. Figure 13.10a shows an image of a worn flat, including the surrounding unworn area. The image is then processed, using commercial software, by first masking off the unworn area. Then the unworn region is corrected for any macroscale tilt or curvature. The worn area is then restored to the image, and another subroutine is used to calculate the volume below an arbitrary reference plane, which can be raised or lowered using the slider bar shown in Figure 13.10b. The reference plane is lowered until the unworn surface disappears from the view, at which point the volume below the plane is in effect the wear volume and is read directly from the screen display.

The procedure for the test pins is slightly more complicated. As shown in Figure 13.10c, the spherical pin is worn by contact with the flat, but the geometry of the contact is such that the wear area on the pin is not flat. That results in an elliptical wear area. As a result, the use of a truncated sphere model to measure the wear volume would not be accurate. In this case, the image of the pin is leveled with respect to the worn area, and the spherical radius is subtracted from the image. The result is shown in Figure 13.10d, where the formerly spherical unworn region now appears flat and the worn region appears as a depression in the flat surface. Now the wear volume is measured using the same software feature as used previously for the flat samples.

13.4.2.2 PISTON RING AND CYLINDER LINER TESTS

The wear depths of cylinder bore segments and piston rings can be measured in bench-scale tests [26,27]. Figure 13.11 shows wear results when tests were run at a normal load of 80 N, a temperature of 60°C, and a reciprocating frequency of 10 Hz for 10 h. Because of contact curvature effects, the wear depth varies with the contact length. A three-dimensional (3D) profile of a wear scar is shown in Figure 13.11. It can be

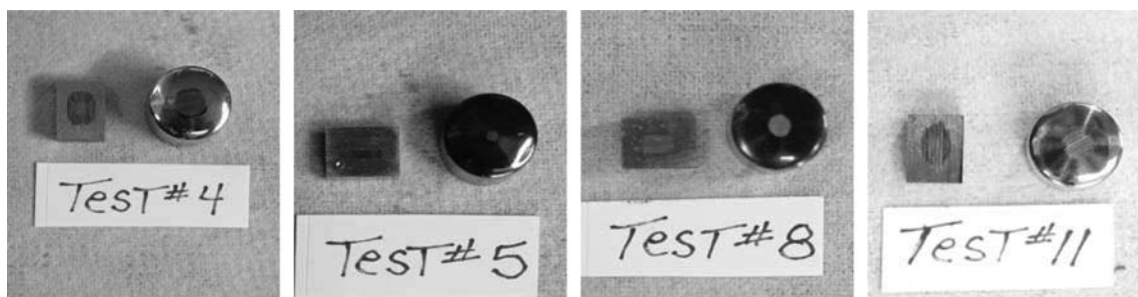
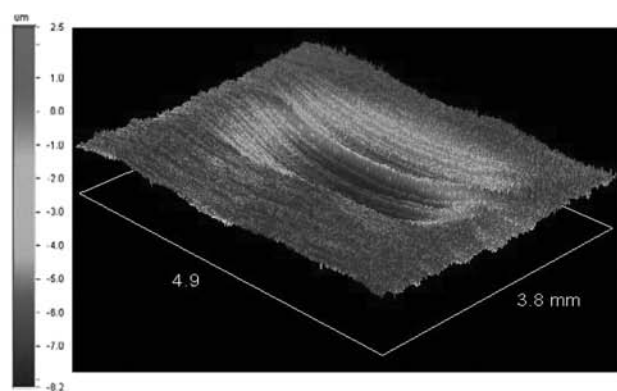
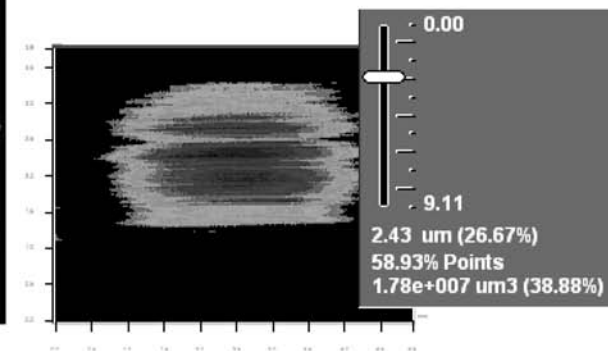


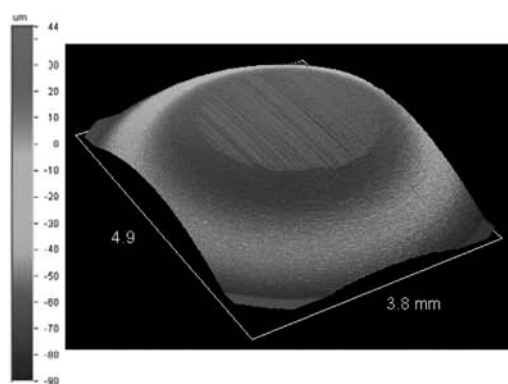
Figure 13.9—Examples of worn test specimens.



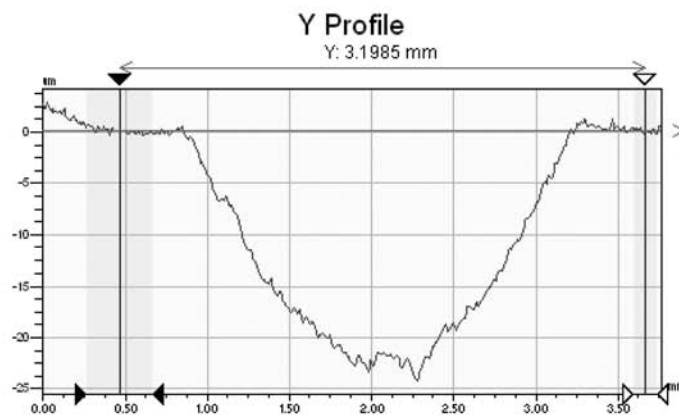
(a) Flat specimen



(b) Flat specimen volume calculation



(c) Pin specimen



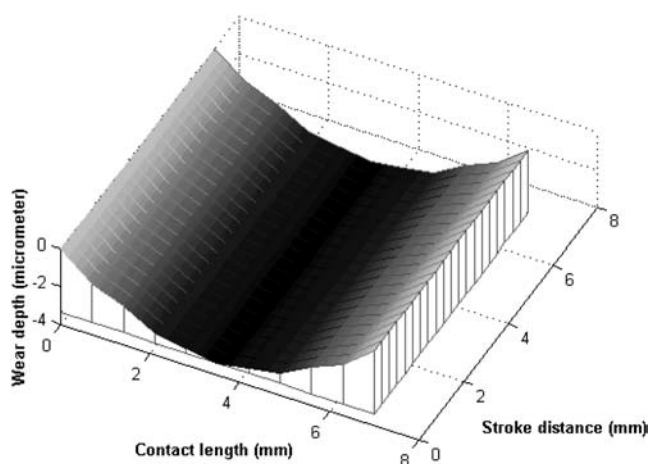
(d) Corrected pin specimen

Figure 13.10—Wear analysis and wear 3D profiles by Veeco images.

seen that the wear depth changes with the contact length in the radial direction. The wear volume was calculated in accordance with the 3D wear profile, as in the foregoing example.

Figures 13.12 and 13.13 show a comparison of wear volumes for cast iron cylinder bores running against different ring treatments and materials: (1) nitrided stainless steel rings, (2) chromium nitride (CrN)-coated rings, and

(3) diamond-like carbon (DLC)-coated rings. The cast iron cylinder bore running against the DLC coating had the lowest wear, and the most severe wear occurred with the CrN coating. However, the wear volumes of the nitrided stainless steel piston rings and for the coated rings are similar. Furthermore, the wear for the piston ring running in an engine oil containing molybdenum dithiocarbamate (MoDTC) is much lower than that running in oil without MoDTC. This indicates that MoDTC can reduce wear in addition to friction for nitrided stainless steel rings with and without coatings. The base engine oil studied in this example contained ZDDP, an additive used to provide good antiwear and antioxidation. As suggested by others [9], the interaction of MoDTC with ZDDP may produce a protective tribofilm that acts to reduce wear between the piston ring and cast iron cylinder.

**Figure 13.11**—3D wear profile of cast iron cylinder bores running against a nitrided steel ring.

13.4.2.3 SCUFFING MEASUREMENTS

Scuffing is a form of surface damage that alters the topography of mating parts but may or may not result in a net loss of material. Therefore, some investigators do not consider scuffing to be a form of wear because material is not progressively removed. It is merely displaced. Tung et al. [25] developed a test method to rank scuffing and wear resistance of various piston coatings against 390 Al cylinder bores. Piston coatings were grouped according to relative scuffing resistance. Those showing very good scuffing

Different Coated Piston Ring Wear Volume Comparison

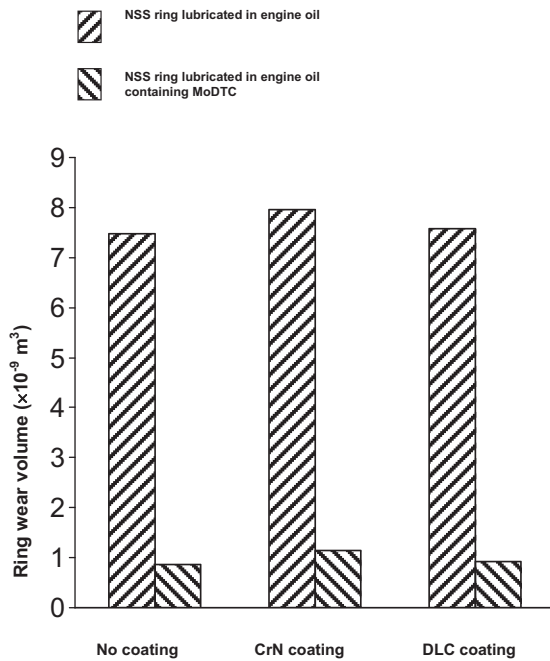


Figure 13.12—Comparison of wear volumes of coated piston rings (nitrided stainless steel ring, CrN-coated ring, and DLC-coated rings) against cylinder bores.

Cylinder Bore Wear Volume Comparison against Different Ring Coatings

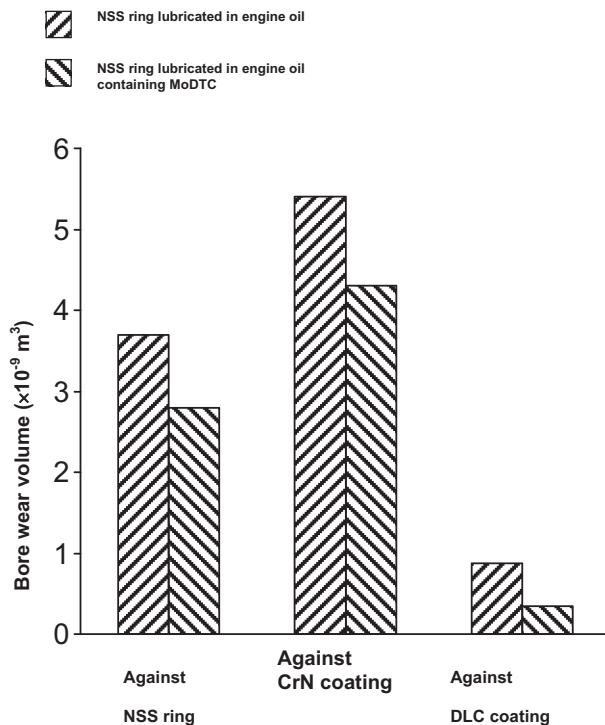


Figure 13.13—Comparison of wear volumes of cylinder bores against different piston ring coatings (nitrided stainless steel ring, CrN-coated ring, and DLC-coated rings).

resistance included a Ni-P-BN coating, an Fe plating, and a Ni-W plating. Those with moderate scuffing resistance included DLC, electroless Ni plating, and Ni-P-SiC coating. The group with marginal scuffing resistance included Ni-P-Si₃N₄ and TiN coatings. The least well-performing group included a TiN PVD coating. Counterface wear is also important. Hard anodizing, DLC, Ni-P-SiC, and Ni-Si₃N₄ coatings produced less severe wear on the 390 Al bore samples than did the TiN coating, and the Ni-W plating, electroless Ni plating, Fe plating, and Ni-P-BN coatings produced the least wear on the counterface, along with very good wear resistance themselves.

13.4.3 Dynamometer Tests for Scuffing

To validate the results of the bench-scale scuffing tests described in Section 13.4.1.3, cold- and hot-scuffing tests were conducted using a Saturn 1.9-L L4 engine dynamometer. Most of the bench-tested piston coatings were run against an Al alloy 390 bore. For the cold-scuffing tests, the engines were installed on an eddy current (EC) dynamometer and set at 17 ft.lbf of torque and held at 2000 r/min for a period of 2.5 h. (Eddy current defines the localized induced currents in parts that are rotating in a magnetic field. These currents produce heat and absorb power in the intake gas flow.) A 30HK chiller unit was used for the coolant, which had a setting of -4°C into the engine so that the outlet temperature was maintained at 0°C throughout the test. For the hot-scuffing tests, the engines were set to 5200 r/min wide-open throttle (WOT) until the coolant temperature reached a maximum of 110°C . The speed was then reduced to idle (1200 r/min at no load) so that the outlet coolant temperature reduced down to 30°C . The process cycle starts over again until failure is observed or the running time reached 9 h.

In this example, engine dynamometer results showed the same ranking as the simulation test results in terms of scuffing and wear performance. Some of the coating tribological behavior found in the simulation tests was also shown in the engine dynamometer tests. In summary, with proper care, and by recognizing the limitations of simulative testing, scuffing and wear bench simulation tests can be used as a rapid, low-cost, and repeatable means of initial, first-order screening and studying the tribological behavior of candidate engine materials and lubricants.

13.5 ENGINE SEQUENCE TESTS FOR EVALUATING ENGINE OIL PERFORMANCE

13.5.1 Engine Sequence Test Methods

The lubricant in a crankcase engine is subjected to very complex conditions, with many different conditions in different parts of the engine, variable patterns of driving behavior, and, critically, the contamination of the lubricant by reactive combustion gases and particulates. This makes it very difficult to relate engine/lubricant performance to simple bench tests, and a key feature of engine oil development and testing is the use of engine tests to assess the behavior of the lubricant in the complex combination of conditions present in a firing engine.

Engine tests involve running freestanding engines under standardized conditions in test cells. The engine is rebuilt before each test using new components, and the test is performed according to a precise schedule. Engine conditions are normally chosen to reflect some pattern of

driving use that stresses the engine/lubricant in a particular way as follows:

- Running at low-speed, low-temperature conditions to simulate stop-start driving and regular commuting. This places particular stress on the dispersant and anti-rusting properties of the oil and is used to measure the effectiveness of these.
- Running under high-speed, high-temperature conditions to simulate motorway driving. This stresses the oil with respect to antioxidancy and anticorrosion properties and is used to mainly assess these and any accompanying cam wear.

Almost all tests are designed to be more severe than conditions generally encountered in service. Table 13.4 shows the procedure for ASTM sequence engine test “VE”. At the end of this test, the quantity and type of deposits on the filter, pistons, and valve gear are compared with standard charts and given a “merit rating” from 1 (lousy) to 10 (“clean or untarnished”). Wear of cams is also measured.

Various classes of standard engine sequence tests as shown in Table 13.5 are available to confirm that current automotive engine oils provide the desired protection, including long oil life, corrosion and wear protection, resistance to the formation of sludge and deposits, the ability to remain within an appropriate viscosity range, etc. ILSAC and API are two organizations that play a major role in overseeing the availability of standard engine-oil-related test methods. ASTM is typically one of the organizations that publish standard procedures to be used when conducting an automotive test. Such standard tests are prepared in painstaking detail so that there will essentially be no chance

of incorrectly conducting a standard test if one has followed the written directions. Automotive companies tend to be the ones who develop such tests. In general, different tests are used for gasoline-fueled engines than those used for diesel engines. Tests typically need to be updated periodically for various reasons. In some cases, test components, such as a specific type of engine, may no longer be available. Changes in the chemical nature of the fuel, such as the transition from leaded to unleaded fuel, may mean that a former test is no longer pertinent to current engine wear, corrosion, and sludge characteristics. Future engine designs that differ from current test engines mean that standard tests will have to be created using the newer types of engines because the older engines may not be predictive of current performance. If it is possible to legitimately substitute a bench test for an engine test (such that the fundamental mechanisms of oil and engine damage correlate strongly with the results from the bench test), the bench test becomes far less labor-intensive and expensive. A brief overview of the evolution of standard engine oil test methods and the status of current automotive engine oil test method development is provided in the following paragraphs.

Early test methods for engine oils were far less sophisticated and less specialized than the tests of today. It can be anticipated that the tests of the future may be even more specialized. Wherever possible, bench tests will be substituted for engine dynamometer tests, such as was the case for development of the Ball Rust Test, a bench test that replaced the Sequence IID (i.e., Sequence 2D) engine test, which measured the ability of an engine oil to protect against the kind of corrosive damage that can occur during

TABLE 13.4—Sequence VE Engine Test

Parameter	Sequence VE
Engine type Engine displacement cm ³ Fuel	Ford Pinto four-cylinder 2290 Unleaded fuel
Test conditions Phase 1: Duration, engine speed air/fuel ratio, load kW Coolant outlet temperature, °C Oil-to-bearing temperature, °C Phase 2: Duration, engine speed Air/fuel ratio, load kW Coolant outlet temperature, °C Oil-to-bearing temperature, °C Phase 3: Duration, engine speed Air/fuel ratio, load kW Coolant outlet temperature, °C Oil-to-bearing temperature, °C	Total test 288 h with 72 cycles of the following sequence: 2 h, 2500 r/min Stoichiometric, 25 kW 51.7 68.3 75 min, 2500 r/min Stoichiometric, 25 kW 85 98.9 45 min, 750 r/min Stoichiometric, 0.75 kW 46.1 46.1
At EOT assessment: Average engine sludge Average piston skirt varnish Average engine varnish Percentage oil ring filling Percentage oil screen clogging Any piston ring sticking Average and maximum cam wear	
Test evaluates:	Sludge, varnish, wear

TABLE 13.5—U.S. and European Gasoline Engine Sequence Tests [31]

Test	Engine	Assesses
L-38 (ASTM D5119)	Labeco single-cylinder, leaded fuel	Bearing corrosion, sludge, varnish, oil oxidation, viscosity change
IID (ASTM D5844)	GM V8 engine, leaded fuel	Low-temperature rust and corrosion
IIIE (ASTM D5533)	GM Buick V6, leaded fuel	High-temperature sludge, varnish, cam wear, viscosity change
IIIF (ASTM D6984)	GM 3.8-L	High-temperature engine test, oil thickening, high-temperature piston deposits, and cam wear
IIIG (ASTM D7320)	GM 3.8-L, V6 engine	High-temperature engine test, piston deposits, and cam wear
IVA (ASTM D6891)	Nissan KA24E four-cylinder, finger followers	Low-temperature engine test, cam wear
VE (ASTM D5302)	Ford four-cylinder, unleaded fuel	Mixed conditions, sludge, varnish, cam wear
VG (ASTM D6593)	Ford V8, 4.6-L, roller followers	Mixed conditions, sludge, varnish, cam and piston wear
VIA (ASTM D6202)	Ford 4.6-L	Fuel efficiency
VIB (ASTM D6202)	Ford V8, 4.6-L, roller followers	Fuel efficiency (before and after engine oil ageing)
VID (ASTM D7589)	GM 3.6-L engine	Engine Oil Fuel Economy Test
VIII (ASTM D6709)	Labeco single-cylinder engine for 40 hours at constant speed	Bearing weight loss and shear stability of oil in engine
Peugeot TU3	Four-cylinder, unleaded fuel	Wear
Petter W-1	One-cylinder	Bearing corrosion, wear, viscosity increase
Volkswagen 1449	Four-cylinder, 2.0-L	Gasoline engines
Volkswagen 1452	Four-cylinder, 1.8-L	Diesel engine test for ring sticking and piston cleanliness
Volkswagen 1481	1.4 L VW FSI L4 engine	Direct-injection gasoline engines
CEC-L-88-T-02 (TUP5J-L4)	PSA engine L4, 72-hour test	High-temperature deposits, ring sticking, oil thickening
CEC-L-54-T-96 (M111)	Ref: ASTM D6975	Fuel economy
CEC-L-38-A-94 (TU3M)	Ref: CEC-L-38-A-94	Valve train scuffing wear
CEC-L-51-A-98 (OM602A)	Ref: CEC-L-51-A-98	Wear, viscosity, stability, and oil consumption
CEC-L-78-T-99 (VW TDI)	Ref: CEC-L-78-T-99	Direct-injection piston cleanliness and ring sticking

extended short-trip winter service in which water and corrosive chemicals (derived from the partial combustion of the fuel) enter and remain in the engine oil for extended periods and cause engine corrosion.

At the fundamental level, oil analyses can determine whether a given engine oil has all of the required additives in its formulation (and thus is not deficient, such as an “SA” quality oil would be). Such information can be pertinent to engine durability field problems because most vehicle warranties are invalidated if the wrong grade of engine oil has been used in an engine.

As of early 2006, the only two designations widely used to describe light-duty gasoline engine oil performance were API SM and ILSAC GF-4. In 2009, API SN and ILSAC GF-5 oils became available in the marketplace. The engine test and bench test performance requirements for API SM are similar to those for ILSAC GF-4, but ILSAC GF-4 oils must also meet energy-conserving requirements. Similarly, API SN requirements as well as energy-conserving requirements must be passed before engine oil can be designated as ILSAC GF-5 [26].

The appropriate test methods for engine oils must be conducted in accordance with the requirements outlined in the American Chemistry Council Product Approval Code of Practice. These requirements include test registration of all tests, use of only calibrated equipment and facilities, and guidelines for acceptable modifications during program development. At present, these new requirements were implemented when API SN and ILSAC GF-5 designations for engine oil were adopted in 2009, and the requirements have been continued as new performance categories have evolved [31].

13.6 CURRENT ISSUES AND FUTURE TRENDS

13.6.1 Issues Related to Conservation of Fuel and Test Compatibility

Government regulations mandate improvements in fuel economy. Vehicle weight reduction is one way to address this mandate. If aluminum components are used in an engine or in any automotive wearing surface, it becomes important to identify a design such that aluminum oxide (which can form on an aluminum surface) is not rubbed

off and allowed to enter the lubricant because aluminum oxide is abrasive and can act as a severe polishing agent, which will increase the wear rate. Lubricant additives that are optimal for use with an iron surface do not necessarily provide the same wear and scuffing protection for an aluminum surface. Aluminum engine blocks with cast iron cylinder bores must be designed such that differences in the rate and magnitude of thermal expansion of these metals do not cause unacceptable gaps to open between contacting surfaces.

13.6.2 Insights Gained from Tests with an Alternative Fuel

Hydrocarbon fuel supplies from fossil sources are finite. To ensure future mobility capability, various alternatives to hydrocarbon fuels have been tested, such as solar power, batteries, hydrogen, alcohol fuel (such as methanol or ethanol), and “flexible fuels”, which may contain up to 85 % alcohol but also incorporate enough hydrocarbon (at least 15 %) to permit a cold start. Suitable performance has been obtained in most cases. However, each type of alternative fuel may also have its unique disadvantages. In addition, the transition from one fuel to another often requires important modifications to any automotive materials that touch the fuel or its reaction products to avoid incompatibility problems. Thus, use of alternatives to hydrocarbon fuel typically requires a significant development effort to ensure the appropriate durability of materials.

Several years ago, at a time of heightened interest in finding a substitute for gasoline, experiments using methanol-containing fuel were performed by various car companies. The fuel (termed M85) consisted of 85 % methanol and 15 % unleaded gasoline. City and freeway driving tests were conducted on a chassis dynamometer so that each vehicle that was tested experienced exactly the same road and weather conditions as the other test vehicles [27,28]. A flexible-fuel vehicle that ran on gasoline was also part of the test so that a quantitative assessment of the effects caused solely by differences in the fuel could be obtained. The findings from that test were as follows.

In freeway service, there was no difference in the rate of engine oil degradation or engine damage between the methanol fuel and unleaded gasoline. This suggested that, under conditions in which the combustion of the fuel is complete, the nature of the fuel was not a factor in the extent of engine oil degradation. In city service, the engine oil used with gasoline degraded approximately 2.5 times faster than oil in the methanol-fueled vehicles that had been tested under identical conditions; that is, methanol was significantly milder to the oil than gasoline during city driving. The reason for this difference in severity was because the molecular weight of methanol is considerably lower than that of gasoline so that the products of partial combustion of methanol boiled out of the oil and thus were not available to inactivate the engine oil's additives. The investigators were surprised by this result because, at that time, it was assumed that alcohol's effects on engine oil would be more aggressive than those of gasoline under all types of service conditions.

In extremely cold short-trip winter service, methanol was harsher to the oil than was gasoline because combustion of methanol produces approximately twice as much water per kilometre of service than does gasoline. Toward

the end of short-trip testing with methanol fuel the engines were being lubricated with a mixture that contained less than 50 % engine oil and slightly more than 50 % contamination (water, fuel, and fuel reaction products). When gasoline fuel entered the engine oil during short-trip winter service, the viscosity of the engine oil decreased. When methanol fuel entered the engine oil, the methanol formed an emulsion, which caused the viscosity of the oil to increase. Although extreme short-trip driving in a winter climate is not representative of most trips, it is desirable to learn about any potential problems before the vehicles are in the hands of the general public. These results indicate that when using a nontraditional fuel, an investigator must confirm that engine materials are not endangered.

An additional concern that needs to be explored when using alternatives to gasoline is to make sure that engine and seal materials are compatible with the alternative fuel of interest. For example, in studies conducted by exposing polyacrylate, silicone, and nitrile seals to methanol fuel, it was found that methanol was able to extract beneficial protective additives out of some seals so that the susceptible seals might become prone to hardening [28]. To conduct such a seal test, a thin segment of the elastomer of interest is immersed in the desired test fluid (here, M85 fuel) and allowed to remain in contact with the fluid at a temperature of interest for whatever duration the investigator deems important. Analyses can determine whether beneficial additives have been extracted out of the elastomer by the test fuel. In addition, an alternative fuel may enter a seal and soften it. Thus, any seal that had become softened by an alternative fuel would be at risk of accelerated wear or failure. Although some types of seals had become soft in the short-trip study with methanol fuel, seal failure did not occur.

Solubility relationships between engine materials and engine fluids can usually be identified in handbooks or tables incorporating titles such as “solubility parameters” or “cohesion parameters”. The solubility parameters include three numerical terms. One of the terms indicates the extent to which the substance of interest is soluble in hydrocarbons such as gasoline. A second term indicates the extent to which the substance of interest is soluble in mildly polar materials such as a compound that has a chain of several carbon atoms linked to a polar atom such as chlorine at one end of the hydrocarbon chain. A third term indicates the extent to which the molecule of interest is soluble in a hydrogen-bonding fluid such as water. If any engine material interacts adversely with a fuel of interest, the engine material needs to be replaced or the material needs to be coated or in some way protected. Use of these solubility parameters to determine material compatibility before attempting a vehicle test with an alternative fuel can sometimes allow an investigator to avoid an engine failure.

If piston rings have a molybdenum fill (or another kind of potentially removable fill), it is worthwhile to conduct a bench test to determine whether the fuel interacts with the fill material. In the case study cited above, M85 fuel was capable of removing the molybdenum fill in piston rings, which caused the rings to contact the cylinder bore on the sharp edges at the center of the rings. The sharp edges of the rings (where the molybdenum was removed) contacted and abraded the cylinder bore. It is also important to determine that bearings are not damaged in the presence of

an alternative fuel. A simple immersion of the material of interest in the alternative fuel, followed by analysis of the elements that have entered the fuel by being extracted from the engine component, provides an assessment of compatibility. In addition, the amount of fuel in an elastomer sample should be measured. If analysis indicates a problem, it becomes prudent to identify an alternative material composition for the component that exhibited the incompatibility.

These driving tests with an alternative fuel provided results that were sometimes at odds with conventional automotive wisdom. Because of this divergence, the investigators were able to gain an enhanced understanding of several mechanisms of oil degradation and their relationship to engine wear and corrosion for gasoline and alcohol fuels. In addition, these results highlighted the fact that it may be risky to make assumptions about durability of engine materials in city and short-trip service when using an alternative fuel because the alternative fuel may behave differently than hydrocarbons when in contact with engine materials.

The kinds of issues related to alternative fuels, as described above, need to be investigated, understood, and resolved before alternative fuels and the engines in which they are used are placed in the public domain. Useful information in this regard can sometimes be gained from bench tests (e.g., wear tests), but unanticipated interactions between the fuel and engine oil may occur under actual operating conditions that may be outside of the domain of a simplified or single parameter bench test. In addition, valuable insights regarding fundamental causes of various engine effects may be derived when comparing test results from different kinds of fuels.

These tests indicate that, by paying attention to material compatibility and recognizing the needs that are specific to a given fuel, alternatives to gasoline can become highly successful automotive power sources. If at some future date supplies of hydrocarbon fuels begin to dwindle significantly, many major automobile companies already have test results in their archives [29,30] that will permit them to successfully use alternative fuels.

13.7 CONCLUSIONS

This chapter has provided the reader with a comprehensive overview of various lubrication test methods for a typical engine system including the bench wear tests, engine sequence tests, and real field tests as well as the major technical issues on lubricant degradation and the current development status for automotive lubricant testing methods in North America and Europe. This chapter also describes the major functions of typical engine components, engine oil characteristics, and the current industrial standard bench and engine tests methods. Included are descriptions of the tribological concerns associated with various automotive engine components, service effects on automotive lubricants, standard test development, and the updated engine oil specification for gasoline engine lubricants in vehicles. In addition, this chapter provides an overview of the current issues and future trends for these automotive lubricants that need to be addressed.

REFERENCES

- [1] Audi, 2002, "Historical background on Use of Aluminum at Audi," available at <http://www.audiworld.com/news/02/aluminum/content1.shtml>.
- [2] "Aluminum Content for Light Non-Commercial Vehicles to Be Assembled in North America, Japan and the European Union in 2006," Drucker Worldwide report, available at <http://aluminumtransportation.org/downloads/duckerppt.pdf>.
- [3] Woydt, M., and Wäsche, R., 2010, "The History of the Stribeck Curve and Ball Bearing Steels: The Role of Adolf Martens," *Wear*, Vol. 268, pp 1542–1546.
- [4] Blau, P.J., 1997, "Design and Validation of Laboratory-Scale Simulations for Selecting Tribomaterials and Surface Treatments." In *New Directions in Tribology*, I.M. Hutchings, Ed., Institution of Mechanical Engineers, London, pp. 177–190.
- [5] Blau, P.J., 1993, "A Retrospective Study of the Use of Laboratory Tests to Simulate Internal Combustion Engine Materials Tribology Problems." In *ASTM Special Technical Publication 1199*, A.W. Ruff and R.G. Bayer, Eds., ASTM International, West Conshohocken, PA, pp. 133–148.
- [6] Ludema, K.C., 1996, *Friction, Wear, Lubrication—A Textbook in Tribology*, CRC Press, Boca Raton, FL.
- [7] SAE J300, 2001: Engine Oil Viscosity Classification, SAE, Warrendale, PA.
- [8] Tung, S.C., and McMillan, M.L., 2004, "Automotive Tribology Overview of Current Advances and Challenges for the Future," *Tribology Int.*, Vol. 37, pp. 517–536.
- [9] Schwartz, S.E., and Smolenski, D.J., 1987, *Development of an Automatic Engine Oil-Change Indicator System*, SAE Paper No. 870403, SAE, Warrendale, PA.
- [10] Schwartz, S.E., 1992, "A Model for the Loss of Oxidative Stability of Engine Oil during Long-Trip Service. Part 1. Theoretical Considerations," *STLE Tribology Trans.*, Vol. 35, pp. 235–244.
- [11] Benzing, R., and Peterson, M.B., 1976, *Friction and Wear Devices*, ASLE Publication, Park Ridge, IL.
- [12] ASTM G99, 2005: Standard Test Method for Wear Testing with a Pin-on-Disk Apparatus, *Annual Book of Standards*, Vol. 3.02, ASTM International, West Conshohocken, PA.
- [13] ASTM G77, 2005: Standard Test Method for Ranking Resistance of Materials to Sliding Wear Using Block-on-Ring Wear Test, *Annual Book of Standards*, Vol. 3.02, ASTM International, West Conshohocken, PA.
- [14] ASTM D4172, 2004: Standard Test Method for Wear Preventive Characteristics of Lubricating Fluid (Four-Ball Method), *Annual Book of Standards*, Vol. 5.02, ASTM International, West Conshohocken, PA.
- [15] Hartfield-Wunsch, S., Tung, S., and Rivard, C., 1993, *Development of a Bench Test for the Evaluation of Engine Cylinder Components and the Correlation with Engine Test Results*, SAE Paper No. 932693, SAE 1993 Trans., Section 3, pp. 1131–1138.
- [16] Hartfield-Wunsch, S., and Tung, S., 1994, "The Effect of Microstructures on the Wear Behavior of Thermal Sprayed Coatings," Reprint from the 1994 7th Thermal Spray Conference Proceedings, Boston, MA, June 20–24.
- [17] Fessenden, K.S., Zurecki, Z., and Slavin, T.P., 1991, *Thermal Sprayed Coatings: Properties, Processes, and Applications*, T.F. Bernecke, Ed., ASM International, Materials Park, OH.
- [18] Tseregounis, S., and McMillan, M., 1995, *Engine Oil Effects on Fuel Economy in GM Vehicles - Comparison with the ASTM Sequence VI-A Engine Dynamometer Test*, SAE Paper No. 952347, SAE Fuels and Lubricants Meeting, October 16–19.
- [19] Truhan, J.J., Qu, J., and Blau, P.J., 2005, "A Rig Test To Measure Friction And Wear Of Heavy Duty Diesel Engine Piston Rings And Cylinder Liners Using Realistic Lubricants," *Tribology Int.*, Vol. 38, pp. 211–218.
- [20] ASTM G181, 2009: Standard Practice for Conducting Friction Tests of Piston Ring and Cylinder Liner Materials Under Lubricated Conditions, *Annual Book of Standards*, Vol. 3.02, ASTM International, West Conshohocken, PA.
- [21] McGeehan, J.A., 1978, *A Literature Review of the Effects of Piston and Ring Friction and Lubricating Oil Properties*, SAE Paper No. 780673, SAE, Warrendale, PA.
- [22] Younggren, P.J., and Schwartz, S.E., 1993, "The Effects of Trip Length and Oil Type (Synthetic Versus Mineral Oil) on Engine Damage and Engine-Oil Degradation in a Driving Test of a Vehicle with a 5.7L Engine," SAE Paper No. 932838, SAE, Warrendale, PA.

- [23] Tung, S.C., Quintana, A., Wakade, S., Becker, E., and White, S., 2007, *A Test Method for Evaluating Automotive Camshaft and Follower Components Subjected to Lubricated Sliding Simulating Variable Valve Actuation*, JSAE/SAE Paper No. 0077324. Presented at the JSAE/SAE International Fuels and Lubricants Conference, Kyoto, Japan, and publication in the 2007 SAE Transactions, July 22–25.
- [24] Lin, P., Barber, G., Zou, Q., Anderson, A.H., Jr., Tung, S., and Quintana, A., 2008, “Friction and Wear of Low-Phosphorus Engine Oils with Additional Molybdenum and Boron Compounds, Measured on a Reciprocating Lubricant Tester,” *Tribology Trans.*, Vol. 51, pp. 659–672.
- [25] Tung, S.C., and Gao, H., 2003, “Tribological Characteristics and Surface Interaction Between Piston Ring Coatings and a Blend of Energy-Conserving Oils and Ethanol Fuels,” *Wear*, Vol. 255, pp. 1276–1285.
- [26] ILSAC GF-4 and Sequence IIIG Performance Test Standard, 2004: ILSAC GF-4 Specification Draft.
- [27] Schwartz, S.E., 1986, “An Analysis of Upper-Cylinder Wear with Fuels Containing Methanol,” *Lub. Eng.*, Vol. 42, pp. 292–299.
- [28] Schwartz, S.E., 1986, “Effects of Methanol, Water, and Engine Oil on Engine Lubrication System Elastomers,” *Lub. Eng.*, Vol. 44, pp. 201–205.
- [29] Canter, N., 2004, “Development of a Lean, Green Automobile,” *Tribology Lub. Technol.* Vol. 60, pp. 15–16.
- [30] Hoogers, G., 2003, *Fuel Cell Technology Handbook*, CRC Press, Boca Raton, FL.
- [31] ILSAC GF-5 Standard, 2008, GF-5 Engine Oil Standard. Issued by API International Lubricant Standard Advisory Committee (ILSAC).

Current and Future Specification of Lubricant Performance

Malcolm F. Fox¹

14.1 INTRODUCTION

For the past 50 years the specification and testing of lubricant performance has successfully protected engines and powertrains against wear, internal deposit formation, and corrosion while reducing friction. Lubricant systems have systematically evolved in concert with increased performance requirements arising from

- Higher engine operating temperatures from increased power densities and reduced aerodynamic cooling;
- Extended service drain periods in response to consumer expectation and market expansion;
- Improvements and changes in fuel quality, mainly for reductions in sulfur but also gradual reformulations, then inclusion of biofuels at (currently) low percentages; and
- The consequences of increasingly stringent environmental emission controls.

These developments are set out in Chapter 4. The purpose of this chapter is to describe the 2010 performance specifications and to explain why they have developed as they are. The specifications have reached a plateau of performance, and further changes will be made to meet new challenges, with the introduction of biofuels being the most immediate. Therefore, this chapter looks forward and assesses what probable challenges that lubricants will have to meet in the near future.

For the current lubricant performance specifications, the dominant issue for diesel engine lubricants is the parabolic relationship between particulate and nitrogen oxide (NO_x) emissions, given diagrammatically in Figure 14.1. This plot will vary numerically between different engine designs, as shown in Figure 14.1, but it demonstrates that although the overall sum of particulate and NO_x can be reduced, within an individual configuration of an engine design one pollutant emission cannot be reduced without increasing the other. Thus, retarding the ignition timing will give a good reduction in particulate emissions, but, at the same time, it increases the overall combustion temperature and therefore increases NO_x emissions. Alternatively, advancing the ignition timing will reduce the overall combustion temperature and decrease NO_x emissions but increase particulate emissions. For a given engine design, the overall sum of these two pollutants cannot be reduced below a certain level at the same time and other means of emission control must be used.

For particulate emissions, control is exercised by retarding the ignition timing using exhaust gas recirculation

(EGR) and diesel particulate filters (DPFs). On the other hand, for NO_x emission control, a selective catalytic reduction (SCR) device is used. However, in the limit, both control measures may need to be used for both emissions to meet Euro V and U.S. 2007 and 2010 requirements (Figure 14.2).

The ability of formulations to lubricate engines, reduce wear and friction, and last longer is not in doubt. The current issue is for lubricant formulations to protect engines against wear and maintain lower friction over longer periods at the same time as ever-higher levels of soot accumulate within that lubricant. The strategies used to reduce diesel engine emissions are set out in Figure 14.2 and show how the Euro IV and V together with the U.S. 2007 and 2010 emission limits are achieved.

Every aspect of engine design, fuel composition, and emission control systems has substantially changed during the last 50 years. The North American Tripartite API; the European ACEA; and the ILSAC systems (U.S. and Japan, increasingly international) and their precursors have responded to these changes by improving lubricant formulations in an increasingly concerted manner. Technical inconsistencies among engine, fuel, and emission control systems that could potentially cause engine damage have been minimized or eradicated. On reflection, the success of these systems has been so thoroughly universal that it has become an unremarkable commonplace. In contrast, it is shown later that for markets in which lubricant specification, fuel quality, and engine performance systems are not in concert and in which environmental emission requirements are more noted than adhered to, lubricant drain intervals must be very short to minimize engine damage.

The successful development of lubricant performance specification and testing systems arises from first ensuring that lubricant formulations are matched to engine performance to minimize wear and degradation and second that lubricants continue to work effectively under the increasingly severe engine conditions arising from required environmental emission standards. The last not only includes enhanced soot levels building up in the lubricant but also reduced SAPS (sulfated ash, phosphorus, and sulfur) levels to prevent particulates from clogging the increasingly sophisticated emission control systems such as three-way catalytic (TWC) converters, SCR converters, and DPFs. In addition, contemporary lubricant formulations must deal with increased soot loadings arising from engines

¹ School of Mechanical Engineering, University of Leeds, Leeds, West Yorkshire

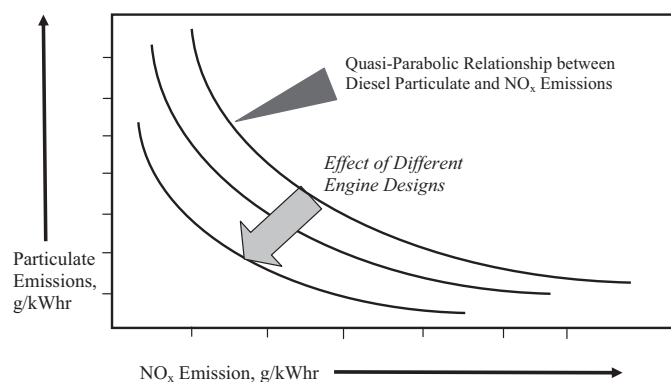


Figure 14.1—Quasi-parabolic relationship between diesel particulate and NO_x emissions.

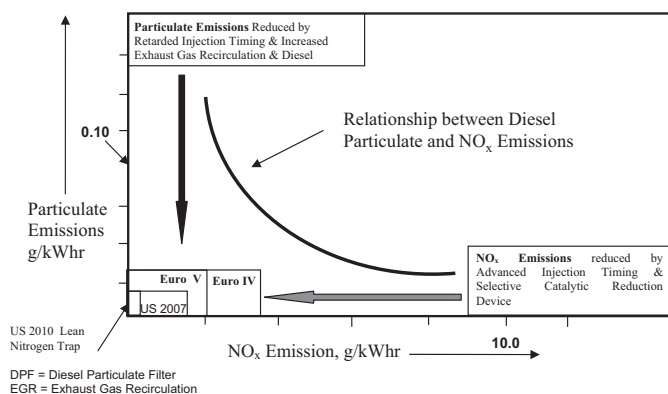


Figure 14.2—Control measures to reduce diesel emissions of particulate and NO_x .

configured for current and immediate-future emission control regulations that could otherwise increase lubricant viscosity and in-cylinder component wear rates during the service life of the lubricant charge.

As set out in Chapter 4, the three major strands of specification and testing of lubricant performance systems are the API system originating in North America, the European ACEA system, and the increasingly international ILSAC system of the United States and Japan. These separate strands arise from developments in different continents, with different approaches and driving forces. In addition, two-stroke lubricant specifications for engines used in motorcycles, portable industrial equipment, and marine outboard motors are discussed.

A characteristic of each of these specification and performance systems is their acceptance across national and continental boundaries. Only the most iconoclastic nations attempt to keep their own lubricant performance specification and testing systems, but maintaining their technical relevance is increasingly time-consuming and very expensive.

This chapter describes the respective current 2010 forms of API, ACEA, and ILSAC lubricant specifications as well as the two-stroke engine systems and how they may develop further to meet the next challenging issues. In the following sections, the current requirements for each system are presented as well as the technical issues that are addressed by the specifications. The lubrication

of industrial machine gears is described by Kadjas et al. in Chapter 8 of *The Chemistry and Technology of Lubricants* (3rd ed.) [1] as American Gear Manufacturers Association (AGMA) 9005-D94, now superseded by ANSI/AGMA 9005-E02.

14.2 AN OVERVIEW OF THE ACEA 2008 EUROPEAN LUBRICANT SEQUENCES

The thrust of this chapter is not so much as to describe the ACEA lubricant sequences and, in turn, in subsequent sections the API and ILSAC sequences because they and their eventual successors are set out on various websites (see the bibliography to this chapter), but to describe how they have changed with time, what the current (at the time of writing) sequences seek to address, and how they may change in the near future.

The ACEA 2008 European lubricant sequences were launched just before the end of that year and replaced the ACEA 2004 and 2007 lubricant sequence revisions. After extensive discussions with ATC and ATIEL, the substantial changes of the ACEA 2008 sequences aim to meet the Euro V engine emission standard requirements for 2009. They should also meet the Euro VI emission standards of 2013 with possibly only minor revisions. All new lubricant formulations must meet the new ACEA 2008 sequence requirements by the end of 2009; after the end of 2010, it will not be possible to claim lubricant performance meeting ACEA 2007. The ACEA 2008 lubricant sequences are minimum standards, and individual original equipment manufacturers (OEMs) may, and often do, set additional tests for a formulation to meet their approval.

The driving force of the ACEA 2008 sequence revisions was to meet the lubricant requirements of the new engine technologies for light vehicles and heavy-duty trucks. This requires substantial reformulations for the A/B and C sequences. For all of the ACEA 2008 sequences, major changes have involved the replacement of obsolete engine tests. These changes have made the ACEA 2008 lubricant test sequences very robust so that they will meet the Euro VI requirements beyond Euro V in due course, around 2013, other than minor changes that may become necessary.

The overall trend for the 2008 light-duty A/B and C sequences was to increase the severity of the performance requirements. In addition, the 2008 sequences improved requirements for reduced wear and sludge, increased cleanliness, and enhanced fuel economy. The effects of biofuels on light-duty engines and their lubricants are covered because the European EN590 diesel standard pump fuel allows 7 % FAME (fatty acid methyl ester) content, and the new OM646 engine test, which replaces the previous OM441LA engine, is required to use these 7 % biofuels and has reduced wear test limits. A new requirement is an end-of-test (EOT) level for total base nitrogen (TBN) to show that lubricants meeting this standard can maintain an adequate level of acid-neutralizing reserve.

The ACEA Heavy-Duty Diesel (HDD) E-sequences for 2008 withdrew the obsolete E2 sequence category. The E4, E6, and E7 sequences were changed only necessarily where obsolete tests were replaced by modern versions of equivalent severity levels. The ACEA E-sequences were extended to a new E9-08 sequence that was based on the API CJ-4 sequence (see Section 14.3) to meet the requirements of

low-SAPS formulations compatible with DPFs, a movement toward compatibility of the ACEA and API sequences. Additional European tests regarded as representing European engine designs replace some of the U.S. engine tests in API CJ-4. No turbo-charger deposit test was included because no lubricants were yet available to discriminate between good and bad performance. A meaningful relationship had yet to be demonstrated with real engine operating experience, and the turbo-charger tests under consideration do not give information about lubricant quality.

For the light-duty engine sequences, the Volkswagen (VW) intercooled turbodiesel was replaced by the VW turbo-charged direct injection (TDI) engine test. For the HDD sequences, natural progression introduced two new engines, the OM646 and OM501, to replace outgoing engines that were regarded as not being representative of modern engine technologies and that were becoming obsolete and difficult to source essential test replacement spares. The Mack T12 test has more stringent limits for the E9 category.

14.2.1 The ACEA A/B Gasoline/Diesel Light Vehicle Lubricants

The A/B petrol and diesel engine lubricant categories are all “stable, stay-in-grade” lubricants. The subdivisions are

- **A1/B1:** For extended drain intervals in petrol and diesel light-vehicle (car and light van) engines, specifically designed for low-friction, low-viscosity lubricants. A high-temperature/high-shear-rate (HTHS) viscosity is specified of 2.6 mPa·s for xW-20 and 2.9–3.5 mPa·s for all other viscosity grades.
- **A3/B3:** For high-performance petrol and diesel light-vehicle engines, for extended drain intervals when specified by the engine manufacturer, for year-round use of low-viscosity lubricants, or for severe operating conditions as defined by the engine manufacturer.
- **A3/B4:** Intended for use in high-performance petrol and direct-injection diesel engines, but also suitable for applications described under A3/B3.
- **A6/B6:** For use at extended drain intervals in high-performance petrol and diesel light-vehicle engines designed for low-friction, low-viscosity lubricants with a HTHS viscosity of 2.9–3.5 mPa·s.

It is essential that for each application the vehicle manual or handbook is consulted because these lubricants may be unsuitable for some engines.

Laboratory and engine test requirements for A/B and C ACEA 2008 European Oil Sequence for petrol and diesel engine service-fill lubricants are defined in Tables 14.1 and 14.2, respectively. A new engine test is introduced into the A/B-08 specifications, the OM646LA, a light-duty diesel engine test replacing the OM602A, for the purpose of giving increased wear protection. This was also the first ACEA test to run on 7 % biodiesel, known as B05, also introduced across the C(X)-08 and E(X)-08 series, described later.

14.2.2 The ACEA C Gasoline/Diesel Light-Vehicle Lubricants

The C catalyst-compatible lubricant category was introduced in 2004 to be compatible with “after-use” pollution control systems. It represents stable, stay-in-grade, catalyst-compatible lubricants for diesel- and petrol-fueled light vehicles.

- **C1:** For use with either DPFs or petrol TWCs requiring low-friction, low-viscosity lubricants with an HTHS minimum of 2.9 mPa·s. These lubricants will increase DPF and TWC life, maintain fuel economy, and have the lowest SAPS limits.
- **C2:** For high-performance car and light van diesel/gasoline engines with either DPFs and TWCs designed to use low-friction, low-viscosity oils with an HTHS viscosity higher than 2.9 mPa·s. These lubricants will increase DPF/TWC operating lifetimes and maintain vehicle fuel economy.
- **C3:** For high-performance car and light van diesel/gasoline engines vehicles with DPFs and TWCs with a minimum HTHS viscosity higher than 3.5 mPa·s. These lubricants will increase DPF/TWC operational life.
- **C4:** For high-performance car and light van diesel/gasoline engines vehicles with DPFs and TWCs with a minimum HTHS viscosity greater than 3.5 mPa·s. These lubricants increase DPF/TWC operational life.

It is essential that for each application the vehicle manual or handbook should be consulted because these lubricants may be unsuitable for some engines.

14.2.2.1 ACEA C SEQUENCE LABORATORY TESTS

The laboratory A/B sequence requirements for 1.1, 1.2, and 1.10–1.12 in Table 14.1 are close to those for the C(X) sequences. The different requirements are set out in Table 14.3. Compared to the A/B-08 series, the C-08 requirements are

- Marginally more stringent for high-temperature viscosity and high shear rate (Table 14.3, section 1.3),
- Two percentage points less for evaporative loss (Table 14.3, section 1.4),
- Tighter limits for SAPS (Table 14.3, subsection 1.5–1.7) to protect the TWC and emission control system, and
- Lower TBN levels for C3- and C4-08 as a result of lower SAPS.

14.2.2.2 ACEA C SEQUENCE ENGINE TESTS

The requirements for subsections 2.1–2.3 and subsection 2.6 are the same as for the A/B sequences in Table 14.2; the further differences are set out in Table 14.4. Relative to the previous sequences, the ACEA C(X)-08 engine sequences have reduced limits in C1–C3 for the M111SL engine sludge test. The fuel economy requirement in the M111FE test for the C1 sequence is increased. Replacement of the OM441LA engine test pass limits by those for the OM646LA test engine will give enhanced protection against diesel wear.

14.2.3 The ACEA E Sequence Heavy-Duty Diesel Lubricant Specification System

The 2008 ACEA heavy-duty diesel lubricant specification system has an E-designation of E4–E9, plus the year date when the test was instituted, thus E9-08 as an example. First introduced in 1996, the ACEA E(X)-(date) series of specifications were based on the Mercedes-Benz classification system. This is a clear difference from the U.S. API system, in which current standard specifications are separate from individual OEMs. Individual U.S. tests contributing to overall specifications can be associated with individual OEMs but not the overall specification. The major changes compared with the previous ACEA

TABLE 14.1—Laboratory Tests for the A/B-08 ACEA Sequences

Requirement	Test Method	Properties	Unit	Limits				
				A1/B1-08	A3/B3-08	A3/B4-08	A5/B5-08	
1.1 Viscosity Grades		SAE J 300 Latest active issue		No restriction except as defined by shear stability and HT/HS requirements. Manufacturers may indicate specific viscosity requirements related to ambient temperature.				
1.2 Shear Stability	CEC L-014-83 or ASTM D6278	100°C viscosity after 90 cycles	mm²/s	xW-20 stay-in grade, xW-30 ≥ 9.3 xW-40 ≥ 12.0	All grades to be stay-in grade.			
1.3 Viscosity at High Temperature and High Shear Rate	CECL-036-90 (2nd ed.) (Ravenfield)	Viscosity at 150°C and 10 ⁶ s ⁻¹ shear rate	mPa·s	≥2.9 and ≤3.5; xW-20: 2.6 min	≥3.5	≥3.5	≥2.9 and ≤3.5	
1.4 Evaporative Loss	CECL-040-93 (Noack)	Maximum weight loss after 1 h at 90°C	%	≤15	≤13			
1.5 TBN	ASTM D2896		mg KOH/g	≥8.0				
1.6 Sulfated Ash	ASTM D874		%m/m	≤1.3	≤1.5	≤1.5	≤1.6	
				Note that the following sections apply to all sequences.				
1.7 Sulfur	ASTM D5185		% m/m	Report				
1.8 Phosphorus	ASTM D5185		% m/m	Report				
1.9 Chlorine	ASTM D6443		ppm rn/m	Report				
1.10 Oil/Elastomer Compatibility	CECL-039-96	Maximum variation of characteristics after immersion for 7 days in fresh oil without pre-aging. Hardness DIDC Tensile strength Elongation at rupture Volume variation	Points	Elastomer Type				
				RE1	RE2-99	RE3-04	RE4	AEM/ VAMAC
			%	−1/+5	−5/+8	−22/+1	−5/+5	As per Daimler
			%	−40/+10	−15/+18	−30/+10	−20/+10	
	%	−50/+10	−35/+10	−20/+10	−50/+10			
			%	−1/+8	−7/+5	−1/+22	−5/+5	
1.11 Foaming Tendency	ASTMD892 without option A	Tendency–stability	mL	Sequence I (24°C) 10 to nil Sequence II (94°C) 50 to nil Sequence III (24°C) 10 to nil				
1.12 High-Temperature Foaming Tendency	ASTM D6082 High-temperature foam test	Tendency–stability	mL	Sequence IV (150°C) 100 to nil				

E 2007 sequences are deletion of the previous E2 category, regarded as technically obsolete, and the introduction of the E9-08 category, a welcome move toward convergence of the ACEA and API sequences. Each of the following grades is required to be stable and to stay in grade. However, recommendations may differ among OEM engine manufacturers; therefore, driver manuals or dealers should be consulted if in doubt. The 2008 ACEA E(X)-08 series are as follows:

- **E4:** Introduced in 1999 as a definition of an ultra-high-performance diesel (UHPD) lubricant for high-performance engines used under severe operating conditions, including long drain intervals. It therefore

provides excellent control of piston cleanliness, wear, soot handling, and lubricant stability. Recommended for highly rated diesel engines meeting Euro I–V emission requirements and running under very severe conditions (e.g., significantly extended oil drain intervals) according to the manufacturer's recommendations. Suitable for engines without particulate filters, for some EGR engines, and for some engines fitted with SCR NO_x reduction systems.

- **E6:** As for E4 but with reduced levels of permitted SAPS to prevent damage to emission control aftertreatment devices. It is suitable for EGR engines, with/without particulate filters, and for engines fitted with SCR NO_x

TABLE 14.2—Engine Tests for the A/B-08 ACEA Sequences

Requirement	Test Method	Properties	Unit	Limits			
				A1/B1-08	A3/B3-08	A3/B4-08	A5/B5-08
2.1 High-Temperature	CECL-088-02 (TU5JP-U)	Ring sticking (each part)	Merit	≥9.0			
Deposits		Piston varnish (six elements, average of four pistons)	Merit	≥RL 216			
Ring Sticking	72-h test	Absolute viscosity increase at 40°C between minimum and maximum values during test	mm²/s	≤0.8 × RL 216			
Oil Thickening		Oil consumption	kg/test	Report			
2.2 Low-Temperature Sludge	ASTM D6593-00 (Sequence VG) under protocol and requirements for API	Average engine sludge	Merit	≥7.8			
		Rocker cover sludge	Merit	≥8.0			
		Average piston skirt varnish	Merit	≥7.5			
		Average engine varnish	Merit	≥8.9			
		Comp. ring (hot stuck)	%	None			
		Oil screen clogging		≤20			
2.3 Valvetrain Scuffing Wear	CECL-038-S4 (TU3M)	Cam wear, average	µrn	≤10			
		Cam wear, max	µm	≤15			
		Pad merit (average of eight pads)	Merit	≥7.5			
2.4 Black Sludge	CECL-053-95 (M111)	Engine sludge, average	Merit	≥RL140	≥RL140 + 4σ or ≥9.0	≥RL140 + 4σ or ≥9.0	≥RL 140 + 4σ or ≥9.0
2.5 Fuel Economy	CECL-054-96 (M111)	Fuel economy improvement versus reference oil RL1S1 (15W-40)	%	≥2.5	–		≥2.5
2.6 Medium-Temperature Dispersivity	CEC L-093-04 (DV4TD)	Absolute viscosity increase at 100°C and 6 % soot	mm²/s	≤0.60 × RL223 result			
		Piston merit	Merit	≥(RL223 – 2.5 points)			
2.7 Wear	CEC L-099-08 (OM646LA)	Cam wear outlet (average maximum wear eight cams)	µm	≤140		≤120	
		Cam wear inlet (average maximum wear eight cams)	µm	≤110		≤100	
		Cylinder wear (average four cylinders)	µm	≤5.0		≤5.0	
		Bore polishing (13 mm)	%	≤3.5		≤3.0	
		Tappet wear, inlet (average wear eight cams)	µm	Report			
		Tappet wear, outlet (average wear eight cams)	µm	Report			
		Piston cleanliness, four pistons,	Merits	Report			
		Engine sludge, average	Merits	Report			
2.8 Direct-Injection Diesel Piston Cleanliness and Ring Sticking	CEC L-078-99 VW TDI	Piston cleanliness	Merit	≥RL206 – 4 points		≥RL206	
		Ring sticking (rings 1 and 2)					
		Average for all eight rings	ASF	≤1.2		≤1.0	
		Maximum for any first ring	ASF	≤2.5		≤1.0	
		Maximum for any second ring	ASF	0.0			
		EOT TBN (ISO 3771)	mg KOH/g	4.0			
		EOT TAN (ASTM 2896)	mg KOH/g	Report			

TAN = total acid number.

TABLE 14.3—Different Requirements for the ACEA C-08 Laboratory Tests Compared with A/B-08 Sequences

Requirement	Test Method	Properties	Unit	Limits			
				C1-08	C2-08	C3-08	C4-08
1.3 Viscosity at High Temperature and High Shear Rate	CEC L-036-90 (2nd ed.) (Ravenfield)	Viscosity at 150°C and 10^6 s^{-1} shear rate	mPa·s	≥2.9		≥3.5	≥3.5
1.4 Evaporative Loss	CEC L-40-93 (Noack)	Maximum weight loss after 1 h at 250°C	%	≤13			≤11
1.5 Sulfur	ASTM D5185		%m/m	≤0.2	≤0.3		≤0.2
1.6 Phosphorus	ASTM D2896		% m/m	≤0.05	≤0.07–0.09		≥0.090
1.7 Sulfated Ash	ASTM D874		%m/m	≤0.5	≤0.8		≤0.8
1.8 Chlorine	ASTM 6443		ppm m/m	Report			
1.9 TBN	ASTM 2896		mg KOH/g			≥6.0	

TABLE 14.4—Different Requirements for the ACEA C-08 Engine Test Sequences Compared with A/B-08

Requirement	Test Method	Properties	Unit	Limits			
				C1-08	C2-08	C3-08	C4-08
2.4 Black Sludge	CEC L-053-96 M111	Engine sludge, average	Merit	≥RL140 + 4σ or ≥9.0			
2.5 Fuel Economy	CEC L-054-96 M111	Fuel economy improvement vs. reference oil RL191(15W-40)	%	≥3.0≥	≥2.5	≥1.0 (for xW-30 grades)	
2.7 Wear	CEC L-099-08 OM646LA	Cam wear outlet, average wear eight cams	μ	≤120			
		Cam wear inlet, average wear eight cams	μ	≤100	Report	≤100	
		Cylinder wear, average four cylinders	μ	≤5.0			
		Bore polishing (13 mm), maximum value of four cylinders	%	≤3.0			
		Tappet wear inlet (average maximum wear eight cams)	μ	Report			
		Tappet wear outlet (average maximum wear eight cams)	μ	Report			
		Piston cleanliness (average four pistons)	Merits	Report			
		Engine sludge, average	Merits	Report			
2.8 Direct-Injection Diesel Piston Cleanliness and Ring Sticking	CEC L-078-99	Piston cleanliness	Merit	≥RL206			
	VW TDI	Ring sticking, rings 1 and 2, average of all eight rings	ASF	≤1.0	≤1.2	≤1.0	
		Maximum for any first ring	ASF	≤1.0	≤2.5	≤1.0	
		Maximum for any second ring	ASF	0.0			
		EOT TBN (ISO 3771) and EOT TAN (ASTM D664)	mg KOH/g	Report			

reduction systems. E6 quality is strongly recommended for engines fitted with particulate filters combined with low-sulfur diesel fuel.

- *E7*: A “super high-performance diesel lubricant” that provides effective control of piston cleanliness and

bore polishing as well as excellent wear control, soot handling, and lubricant stability. Recommended for highly rated diesel engines meeting Euro I–V emission requirements under severe conditions (e.g., extended oil drain intervals according to the manufacturer’s rec-

ommendations). Suitable for engines without particulate filters, for most EGR engines, and for most engines fitted with SCR NO_x reduction systems.

- **E9:** A new specification introduced for 2008 that is based on the API CJ-4 sequence, but with additional European engine performance tests that replace some U.S. engine models not representative of European design practice. It is as for E6 but is also suitable for engines with/without particulate filters, most EGR engines, and for most engines fitted with SCR NO_x reduction systems. E9 is strongly recommended for engines fitted with particulate filters and is designed for use in combination with low-sulfur diesel fuel.

It is essential that for each application the vehicle manual or handbook should be consulted because these lubricants may be unsuitable for some engines.

There are substantial changes in the E4, E6, and E7 engine tests for 2008 from the previous sequences in which (1) the OM646LA engine replaces the OM602A, used to measure diesel cam wear, lubricant viscosity increase, bore polish, cylinder wear, and lubricant consumption; and (2) the OM501LA engine replaces the OM441L, used for diesel bore polishing, piston cleanliness, boost pressure loss, and lubricant consumption with the important requirement that these engines are run using B05 diesel (i.e., with 7 % biodiesel, reflecting that EN590 diesel fuel in the European Union can contain up to 7 % biodiesel). The Cummins ISM engine replaces the Cummins M11 and the Mack T12 replaces the Mack T10. The laboratory and engine test sequences for the E(X)-08 sequences are set out in Table 14.5 with the SAPS requirements in subsections 1.5–1.7; the effects of soot in the lubricant on viscosity are in subsections 2.2 and 2.3; soot-induced wear specifically set out in subsection 2.5; and wear generally in subsections 2.1, 2.4, and 2.6.

Across the sequence spectrum, different emphases are laid on bore polish, piston cleanliness, valvetrain wear, turbo-charger deposits, and soot-induced wear. Various engine test combinations are used for the different E-quality levels with the Mercedes-Benz tests being used for long duration with varying power level cycles on a repetitive basis. The Mack T11, T12, and Cummins ISM give comparability to the API CJ-4 series.

14.2.4 Trends for Future ACEA Sequences

The robust changes introduced by the ACEA 2008 sequences should meet the Euro VI engine emission requirements up to 2013/2014. Beyond that, possibly before if higher biofuel content is mandated, the major issue for the next ACEA review will probably be experience of the longer term use of biofuels interacting with the particulate filter emission control system used by engine OEMs. After the initial introduction and establishment of the (up to 7 % vegetable oil) B05, it is envisaged that the vegetable oil content of diesel will increase further (e.g., to 10 %, to 15 %, etc.). However, for B05 fuel at present, the emission control systems can be progressively blocked by carbonaceous deposits. The rate of blocking buildup may be different for different engine designs, but eventually the coarse ceramic filters used as particulate traps are blocked and must be replaced. The carbonaceous deposits are burned off by a periodic thermal regeneration strategy using a temporary

delay in fuel-injection timing. In effect, this acts as excess fuel injection and raises the exhaust temperatures to burn off the carbonaceous particulate in the trap. The strategy works well, but a certain amount of inorganic, incom-bustible ash will build up in time and the trap must be replaced eventually.

The unintended consequence of delaying the injection timing is an accumulation of unburned fuel splashed onto the bore wall, which is then swept into the sump oil. The vegetable oil component of biodiesel is much less volatile than the diesel component and accumulates in the sump. Being less chemically stable than either diesel fuel or the lubricant formulation, it then causes lubricant degradation evidenced as a rapid increase in lubricant viscosity after an induction period. This effect is related to the decline in anti-oxidancy of a lubricant, which is accelerated with biodiesel accumulation in the engine sump. An associated effect is a decrease in deposit control with biodiesel. The alternative strategy of exhaust fuel postinjection may be favored by OEMs because of the fuel dilution problems associated with in-cylinder postinjection. Fuel dilution by EN590 diesel fuel containing 7 % FAME is not a major issue at present except for vehicles with consistently short journey operation in which lubricant gelation under cold starting conditions is becoming an increasing problem. A physical problem can be an increase in apparent lubricant volume level in the sump due to extensive fuel dilution. The higher level of fuel-diluted lubricant can be beaten to a froth when it contacts the rotating big ends on the crankshaft and the wear protection properties of a lubricant froth are minimal. Higher levels of a different biocontent material may cause lubricant degradation/dilution problems in the future. There is no particular technical significance to the previous level of 5 % FAME in diesel and the current level of 7 %; the political environmental agenda is to drive these levels to ever higher values. The previous 5 % and the current 7 % FAME levels are but “stops on the way” to higher levels following the concept of “sustainability”. The 5 % and 7 % FAME levels in diesel were set at their time in terms of what was felt to be the sufficient availability of FAME and the capability of engines to deal with its longer term effects. As said, lubricant gelation under certain adverse environmental conditions is emerging as a problem for low-temperature cold starts. However, that problem is referred back to OEMs and lubricant formulators as their problem to resolve.

14.3 NORTH AMERICAN LUBRICANT SPECIFICATION AND APPROVALS—THE API TRIPARTITE SEQUENCES

14.3.1 The API Tripartite Sequences

Lubricant performance specification and approvals in the United States and North America have been developed by a tripartite arrangement of the American Petroleum Institute (API), the Society of Automotive Engineers (SAE), and the American Society for Testing Materials (ASTM) as described in Chapter 4. For the reasons stated there, the API Tripartite sequences have different emphases than those for ACEA.

14.3.2 The SAE Viscosity Classification

The U.S. SAE J300 viscosity classification was the very first engine lubricant property classification and applied

TABLE 14.5—Laboratory Tests for ACEA E(X)-08 Laboratory Engine Sequence Tests

	Test Method	Properties	Unit	Limits				
				E4-08	E6-08	E7-08	E9-08	
1.1 Viscosity		SAE J300 latest active issue		No restriction except as defined by shear stability and HTHS requirements. Manufacturers may indicate specific viscosity requirements related to ambient temperature.				
1.2 Shear Stability	CEC L-014-93 or ASTM D6278	Viscosity after 30 cycles measured at 100°C	mm²/s	Stay in grade				
	ASTM D6278	Viscosity after 90 cycles measured at 100°C	mm²/s			Stay in grade		
1.3 Viscosity High Temperature/ High Shear Rate	CEC L-036-90 (2nd ed.) Ravenfield	Viscosity at 150°C and 10 ⁶ s ⁻¹ shear rate	mPa·s	≥3.5				
1.4 Evaporative Loss	CEC L-040-93 Noack	Maximum weight loss after 1 h at 250°C	%	≤13				
1.5 Sulfated Ash	ASTM D874		% m/m	≤2.0	≤1.0	≤2.0	≤1.0	
1.6 Phosphorus	ASTM D5185		% m/m		≤0.08		≤0.12	
1.7 Sulfur	ASTM D5185		% m/m		≤0.3		≤0.4	
1.8 Oil Elastomer Compatibility	CEC L-039-96	Maximum variation in properties after immersion for 7 days in fresh oil without pre-aging Hardness DIDC Tensile Strength Elongation Rupture Volume Variation	Points	Elastomer Type				
				RE1	RE2-99	RE3-04	RE4	AEM/ VAMAC
			%	-1/+5	-5/+8	-25/+1	-5/+5	As per Daimler
			%	50/+10	-15/+18	-45/+10	-20/+10	
1.9 Foaming Tendency	ASTM D892 without option A	Tendency – stability	mL	Sequence I (24°C) 10 to nil				
			mL	Sequence II (94°C) 50 to nil			Sequence II (94°C) 20 to 0	
			mL	Sequence III (24°C) 10 to nil				
1.10 High-Temperature Foaming Tendency	ASTM D6082	Tendency – stability	mL	Sequence IV (150°C) 200-50				
1.11 Oxidation	CEC L-085 -99 (PDSC)	Oxidation induction time	min	R&R	R&R	≥65	≥65	
1.12 Corrosion	ASTM D6594	Copper increase	ppm	R&R	R&R	R&R	≤20	
		Lead increase	ppm	R&R	R&R	≤100	≤100	
		Copper strip rating	max	R&R	R&R	R&R	3	
1.13 Turbo-Charger Performance	Should a test become available before the next document update, ACEA reserves the right to set performance limits providing adequate data are available.							
1.14 TBN	ASTM D2896		mg KOH/g	≥12	≥7	≥9	≥7	
R&R = rate and report.								

R&R = rate and report.

to monograde lubricants. It has now evolved into a multigrade lubricant classification that indicates viscosity at low (engine winter starting) and high (summer and operating) temperatures for multigrade lubricants. These lubricants have 90 % of the market share, and the respective viscosities are indicated by two numbers with the low-temperature viscosity given first as -W- (winter), with the second value showing the minimum kinematic viscosity at 100°C, given together as SAE xxW-yy, (e.g., as SAE 10W-30).

Low-temperature viscosities were initially extrapolated from measurements at higher temperatures. Low-temperature cranking viscosities are now measured by the Cold Cranking Simulator (ASTM D5293) and pumpability by the Mini-Rotary Viscometer (ASTM D4684). Kinematic viscosities at 100°C (ν_{100}) are HTHS viscosity measurements at 10⁶ s⁻¹ and 150°C, ASTM D4683 (CEC L 36-90-A, ASTM D4741, or ASTM D5481) are representative of lubricant conditions in modern vehicle bearings and are now

TABLE 14.6—Engine Tests for the E(X)-08 ACEA Sequence Tests

Requirements	Test Method	Properties	Unit	Limits			
				E4-08	E4-08	E7-08	E9-08
2.1 Wear	CEC L-099-08 OM646LA	Cam wear outlet (average maximum wear eight cams)	μ	≤ 140		≤ 155	
2.2 Soot in Oil	ASTM D5967	Test duration 300 h		≤ 2.1/2.2/2.3			
	Mack T8E	Relative viscosity at 4.8 % soot 1 test/2 test/3 test average					
2.3 Soot in Oil	Mack T-11	Minimum TGA soot at 4.0 cSt (100°C)	%				3.5/3.4/3.3
		Minimum TGA soot at 12.0 cSt (100°C)					6.0/5.9/5.9
		Minimum TGA soot at 15.0 cSt (100°C)					6.7/6.6/6.5
2.4 Bore Polishing Piston Cleanliness	CEC L-101-08 OM501LA	Bore polishing, average	%	≤1.0		≤1.0	
		Piston cleanliness, average	Merit	≥26		≥17	
		Oil consumption	kg/test	≤9			
		Engine sludge, average	Merit	Rate and report			
2.5 Soot-Induced Wear	Cummins ISM	Merit rocker pad average weight loss at 3.9 % soot, 1/test/2 test/3 test average	mg			≤7.5/7.8/7.9	≥1000
		Oil filter differential pressure at 150 h, 1 test/2 test/3 test average	kPa			≤55/67/74	≤19
		Engine sludge, 1 test/2 test/3 test average	Merit			≥8.1/8.0/8.0	≥8.7
		Adjustment screw weight loss	mg				≤49
2.6 Wear-Liner- Ring-Bearings	Mack T12	Merit average liner wear	μ		≥1000		
		Average top ring weight loss	mg		≤26 ≤117		≤24 ≤105
		EOT lead	ppm		≤42		≤35
		Delta lead 250–300 h	ppm		≤18		≤15
		Oil consumption (Phase II)	g/h		≤95		≤85

TGA = thermogravimetric analysis.

TGA = thermogravimetric analysis.

included in SAE J300 for SAE 20 and above, measured by very accurate capillary viscometers (ASTM D445). HTHS viscosity measurements at 10^6 s^{-1} and 150°C , ASTM D4683 (CEC L 36-90-A, ASTM D4741, or ASTM D5481), are representative of lubricant conditions in modern vehicle bearings and are now included in SAE J300 for SAE 20 and above. SAE viscosity grades effective since May 2008 for engine oils are given in Table 14.7.

The SAE viscosity classification system has global domination of automotive lubricant formulations. The alternative ISO classification is used for industrial oils and lubricants.

14.3.3 The Achievements of the API Tripartite System

The API system, and similarly the ACEA system, as in the previous section, have worked well because, overall, an integrated approach has taken developments in engine design, fuel, and lubricant together. A range of lubricant specifications are available for engines and fuels developed over 10–20 years by a successful, continuing, technocratic process. If this seems obvious, it is instructive to consider

where such technical transitions have not been so well managed. For the largest national lubricant market in the Middle East [2], locally constructed vehicles are now supplemented by more modern vehicles locally assembled but designed by multinational manufacturers to international standards. Imported vehicles are built to the same international standards. However, high levels of impurities in the available fuels rapidly degrade predominantly obsolete lubricant formulations. Two thirds of those lubricants for passenger car and light vehicles are API-SC standard, declared obsolete by API a decade ago and not suitable for North American engines built after 1967. A further 26 % of lubricants are graded SE, SF, and SG and were also declared obsolete and not suitable for vehicles constructed after 1979, 1988, and 1993, respectively. For heavy-duty diesel trucks, 50 % of lubricant volume is API CD (ca. 1955) and API CE (ca. 1985). Locally assembled European trucks and buses are very popular and require at least API CI-4 plus (ca. 2002). Locally manufactured light vehicles require at least API SL.

Fuel quality in this market is the major problem; the official sulfur content of diesel is 10,000 ppm (i.e., 1 %),

TABLE 14.7—SAE Viscosity Grades for Engine Oils

SAE Viscosity Grade	Low-Temperature (°C) Cranking Viscosity ^a (mPa·s), Maximum	Low-Temperature, (°C) Pumping Viscosity ^b (mPa·s), Maximum, with No Yield Stress	Low Shear Rate Kinematic Viscosity ^c (mm ² /s) at 100°C, Maximum/Minimum	High Shear Rate Viscosity ^d (mPa·s) at 150°C, Minimum
0W	6200 at -35	60,000 at -40	3.8/–	–
5W	6600 at -30	60,000 at -35	3.8/–	–
10W	7000 at -25	60,000 at -30	4.1/–	–
15W	7000 at -20	60,000 at -25	5.6/–	–
20W	9500 at -15	60,000 at -20	5.6/–	–
25W	13,000 at -10	60,000 at -15	9.3/–	–
20	–	–	5.6/<9.3	2.6
30	–	–	9.3/<12.5	2.9
40	–	–	12.5/<16.3	3.5 (0W-40, 5W-40, 10W-40 grades)
40	–	–	12.5/<16.3	3.7 (15W-40, 20W-40, 25W-40, 40 grades)
50	–	–	16.3/<21.9	3.7
60	–	–	21.9/<26.1	3.7

From SAE J300, revised November 2007, with effect from May 2008, supersedes SAE J300 of May 2004.

^aBy ASTM D5293; ^bBy ASTM D4684—note that the presence of any yield stress detectable by this method constitutes a failure regardless of viscosity;

^cBy ASTM D445; ^dBy ASTM D4683, CEC L-36-90 (ASTM D4741), or ASTM D5481.

probably higher in practice whereas Europe and North America have either capped, or will shortly cap, diesel sulfur content at 10–20 ppm or lower. The very high sulfur fuel degrades lubricants very quickly so that service interval lubricant drains for trucks average 4500 km (cf. 30,000–160,000 km in Europe) and 2000 and 2500 km for passenger and light vehicles (cf. 25,000 km in Europe), respectively. These fuel quality levels are particularly active in degrading low-SAPS oils, as for API SM. In addition to sulfur, fuels also contain high levels of phosphorus, which deactivate the TWC converters of new vehicles within their first hour or so of operation.

14.3.4 The API C-(Series) Specifications for Heavy Duty Diesel Engines to API CJ-4

The API C-(X) Series specifications have evolved from the CA/CB/CC specifications through to the current CJ series as

- *Now obsolete*
 - *CA/B/C*: For naturally aspirated engines built up to 1959, 1961, and 1990, respectively.
 - *CD (1955)*: For certain naturally aspirated and turbo-charged engines.
 - *CD-II (1985)*: For two-stroke cycle engines.
 - *CE (1985)*: For high-speed, naturally aspirated, and turbo-charged engines (can replace CC and CD lubricants).
- *Current*
 - *CF (1994)*: For off-road, indirect-injection, and other diesel engines including those using fuel containing more than 0.5 % sulfur. Can replace CD lubricants.
 - *CF-2 (1994)*: For severe-duty two-stroke engines. Can replace CD-II lubricants.

- *CF-4 (1990)*: For high-speed, four-stroke, naturally aspirated, and turbo-charged engines. Can replace CD and CE lubricants.
- *CG-4 (1995)*: For severe-duty, high-speed, four-stroke engines using fuel containing less than 0.5 % sulfur. Required for 1994 emission standards and can replace CD, CE, and CF-4 lubricants.
- *CH-4 (1998)*: For high-speed, four-stroke engines designed to meet 1998 emission standards. Specifically formulated for fuel containing up to 0.5 % sulfur w/w. Can replace CD, CE, CF-4, and CG-4 lubricants.
- *CI-4 (2002)*: For high-speed, four-stroke engines designed to meet 2004 emission standards implemented in 2002. Formulated to sustain engine durability in which EGR is used. Some CI-4 lubricants may qualify for CI-4 PLUS status. Intended for fuels containing up to 0.5 % sulfur. Can replace CD, CE, CF-4, and CG-4 lubricants.
- *CJ-4 (2006)*: For high-speed, four-stroke engines designed to meet 2007 emission standards. Formulated for use with fuel containing up to 0.05 % sulfur (500 ppm w/w). Use of these lubricants with fuels with more than 15 ppm sulfur (0.0015 % w/w) may affect the durability of exhaust aftertreatment systems or oil drain service intervals or both. These lubricants will sustain emission control systems using particulate filters and other advanced aftertreatments. Optimal protection for catalyst poisoning, particulate filter blocking, engine wear, piston deposits, low- and high-temperature stability, soot handling, oxidative thickening, foaming, and viscosity loss due to shear. These lubricants exceed the

performance criteria of CI-4, CI-4 PLUS, CH-4, and CG-4 and can effectively lubricate engines requiring these API service categories. However, when using CJ-4 lubricants with fuel with more than 15 ppm w/w sulfur, consult the OEM for service interval.

- **CK-4:** Although the logical expectation might have been CK-4 at, or after, 2010, CJ-4 has been continued on. It may well be that emission-related issues may have reached their technical limits, but the effect of biofuels on lubricants will become a separate issue to be seen.

“Obsolete” lubricant grades can still be obtained from specialist manufacturers for older, “classic” vehicles. For “current” grades, from the sequence of outline requirements set out above, the major influences driving their recent development are the effects of decreased fuel sulfur content and the requirements of the various forms of emission control systems.

It is essential that for each application the vehicle manual or handbook should be consulted because these lubricants may be unsuitable for some engines.

14.3.5 The API CJ-4 HDD Engine Specification

The API CJ-4 specification for HDD lubricants has two sections—for laboratory tests and for engine tests—set out in

Tables 14.8 and 14.9. The purposes of the CJ-4 laboratory tests are

- **1.1 Viscosity Grades:** From Table 14.7, giving lubricant manufacturers freedom to develop “lighter grades,” such as the 0W-20 developed for truck fuel economy [2].
- **1.2 High-Temperature Corrosion Bench Test at 135°C:** Measures increased corrosion by used oils of common metals in engines (e.g., copper and lead) from increased operating temperatures.
- **1.3 Foaming:** To measure the foaming tendency of the candidate lubricant formulations.
- **1.4 and 1.6 Shear Stability:** First, ability of lubricant to maintain its 100°C viscosity after 90 passes by ASTM D7109; second, ability to maintain 3.5-cP viscosity minimum at 150°C after the High-Temperature/High-Shear test as in SAE J300.
- **1.5 Noack Volatility:** Evaporative loss by the Noack test, or its simulation, limited to 13 % (15 % for lighter grades), reflecting 15–20 % tightened limits introduced in API CH-4, according to grade.
- **1.7 Sooted Oil Maximum Relative Viscosity:** To measure the viscosity and yield stress at –20°C of used lubricants from a 180-h Mack T-11/11A test. An increased requirement from API CI-4 for a 75-h sample from (a less severe) Mack T-10 test.

TABLE 14.8—Laboratory Tests for HDD Engine Category API CJ-4

Requirement	Test Method	Properties	Unit	Limits		
				1 Test	2 Tests	3 Tests
1.1 Viscosity Grades		SAE J300		Manufacturer specifies viscosity within SAE J300 specification		
1.2 High-Temperature Corrosion Bench Test	ASTM D6594	Copper in used oil increase, maximum Lead in used oil increase, maximum Copper strip rating, maximum	ppm ppm –	20 120 30	No MTAC	
1.3 Foaming	ASTM D892	Foaming/settling, maximum Sequence I Sequence II Sequence III	% % %	10/0 20/0 30/0	No MTAC	
1.4 Shear Stability	ASTM D7109	KV at 100°C after 90 passes for xW-40, minimum KV at 100°C after 90 passes for xW-30, minimum	cSt cSt	12.5 9.3	No MTAC	
1.5 Noack Volatility	ASTM D5800	Evaporative loss at 250°C, viscosity grades other than 10W-30, maximum Evaporative loss at 250°C, 10W-30, maximum	% %	13 15	No MTAC	
1.6 High Temperature/High Shear	ASTM D4883	Viscosity at 150°C	cP	3.5	No MTAC	
1.7 Sooted Oil MRV	ASTM D6896	180-h sample from Mack T-11 or T-11A Viscosity at –20°C, maximum yield stress	cP Pa	25,000 <35	No MTAC	
1.8 Chemical Limits (noncritical)	ASTM D874 ASTM D4951	Sulfated ash, maximum Phosphorus, maximum Sulfur, maximum	% % %	1.0 0.12 0.4	No MTAC	
1.9 Seal Compatibility	ASTM D7216 Nitrile Silicone Polyacrylate FKM Vamac G	Volume Change +5/–3 +TMC1006/ –3 +5/–3 +5/–2 +TMC1006/–3	Hardness +7/–5 +5/–TMC1006 +8/–5 +7/–5 +5/–TMC1006	Tensile Strength +10/–TMC1006 +10/–45 +18/–45 +10/–TMC1006 +10/–TMC1006	Elongation +10/–TMC1006 +20/–30 +10/–35 +10/–TMC1006 +10/–TMC1006	

KV = kinematic viscosity, MTAC = multiple test acceptance criteria, MRV = Mini-Rotary Viscometer.

TABLE 14.9—Engine Tests for HDD Engine Category CJ-4

Requirement	Test Method	Properties	Unit	Limits		
				1 Test	2 Tests	3 Tests
2.1 Mack T-11	ASTM D7156	Soot at 4 cSt increase, minimum	%	3.5	3.4	3.3
		Soot at 12 cSt increase, minimum	%	6.0	5.9	5.9
		Soot at 15 cSt increase, minimum	%	6.7	6.6	6.5
2.2 Mack T-12		Merits, minimum		1000	1000	1000
2.3 Cummins ISB		Tappet wear, maximum	mg	100	108	112
		Cam wear, maximum	Microns	55	59	61
		Crosshead weight loss	mg	Rate/ report	Rate/ report	Rate/ report
2.4 Cummins ISM		Merits, minimum	mg	1000	1000	1000
		Top ring weight loss, maximum		100	100	100
2.5 Caterpillar 1N	ASTM D6750	Top land heavy carbon, maximum	%	3	4	5
		Top groove fill	%	20	23	25
		Weighted demerits, maximum	Demerits	286.2	311.7	323.0
		Average oil consumption (0–252 h), maximum	g/kWh	0.5	0.5	0.5
		Ring/liner scuffing	–	None	None	None
2.6 Caterpillar C13		Merits, min	–	1000	1000	1000
		Hot stuck rings	–	None	None	None
2.7 Engine Oil Aeration	ASTM D6894	Oil aeration volume, maximum	%	8.0 (MTAC)	8.0 (MTAC)	8.0 (MTAC)
2.8 Roller Follower Wear Test	ASTM D5966	Roller follower pin wear, maximum	Microns	7.6	8.4	9.1
2.9 Sequence IIIF4	ASTM D6984	Viscosity increase at EOT, maximum	%	275 MTAC	275 MTAC	275 MTAC

- **1.8 Chemical Limits:** A new limit test introduced into API CI-4 for SAPS for low SAPS.
- **1.9 Seal Compatibility:** Essentially the same as for API CH-4 when it was introduced but with an extended material test range.

The purposes of the API CJ-4 engine tests in Table 14.9 are

- **2.1 Mack T-11:** To generate a substantially sooted lubricant sample, for viscosity limit measurements up to 6.7 %, from this severe engine test.
- **2.2 Mack T-12:** Merit rating of components for deposit control.
- **2.3 Cummins ISB:** A new engine test in API CJ-4, to measure tappet, cam, and crosshead component wear, which partially replaces the Cummins M-11-EGR test in API CI-4 and CH-4.
- **2.4 Cummins ISM:** A new engine test in API CJ-4, for merit rating of deposit control and top ring weight loss, as a measure of wear.
- **2.5 Caterpillar 1N:** A continuation of the Caterpillar 1MPC, 1P, 1K, and 1R tests used in successive API C-X tests since API CF-CF-2 for the measurement of deposits and wear through top land heavy carbon, top

groove fill (by deposits), weighted demerits, average oil consumption, and ring/liner scuffing.

- **2.6 Caterpillar C13:** A new engine test for the measurements of deposit merits and hot stuck rings.
- **2.7 Engine Oil Aeration:** An engine test that complements the laboratory foaming test (1.3).
- **2.8 Roller Follower Wear Test:** A long established wear test since API CG-4.
- **2.9 Sequence IIIF4:** Measures viscosity at EOT, 275 %, slightly tighter than 295 % maximum at 60 h for API CH-4, different emphasis from 67.5 minimum hours to 375 % increase in viscosity in API CG-4.

14.3.6 Comparative Discussion of the AP-C(X) Series

The previous commentary of the Heavy-Duty Diesel engine test category for API CI-4 shows that successive test categories gradually revise the nature of the tests, either as bench tests or engines, and the passing limits for these tests. This evolutionary process is expected to continue with the next API-C(X) series when the CJ- series is revised in due course.

Viewing these test requirements in the context of previous HDD engine test categories, from API CG-4 through to API CJ-4, the increasing number of tests for each successive specification becomes evident (Table 14.10). New engine tests, or versions of tests, are included in the new specifications (Table 14.11), and the test engines (or their regimes used) are revised or replaced to respond to the perceived new issues.

In addition, the “properties” column becomes divided into subcategories and the “limits set” decrease, the test for the soot-induced thickening of the lubricant changes in several parameters (Table 14.12). The engine test becomes progressively more severe, from the Mack T-8 to the Mack T-11. At the same time, as an example, the viscosity properties for each specification become more differentiated, from a viscosity increase at 3.8 %, maximum, of 11.5 cSt for one test for CG-4 by ASTM 5967 through to increases of 3.5, 6.0, and 6.7 % soot for viscosities at 4, 12, and 15 cSt for one test of CJ-4 by ASTM 7156.

14.4 THE API SM PASSENGER CAR ENGINE TEST CATEGORY

14.4.1 Evolution of the API S(X)

Specifications

The petrol passenger car API S(X) specifications (also including light vehicles such as vans and mini-buses) have evolved through

- *Now obsolete*
 - SA for engines built up to 1930, contains no additives, and can damage more modern equipment.
 - SB for engines up to 1951.
 - SC for engines up to 1967.
 - SD for engines up to 1971.
 - SE for engines up to 1979. (Use of SA–SE lubricants can damage more modern equipment.)
 - SF suitable for engines up to 1988.
 - SG suitable for engines up to 1993.
 - SH suitable for engines built up to 1996.

TABLE 14.10—Changes in Laboratory Test Requirements through API CG-4 to API CJ-4

TABLE 14.10—Changes in Laboratory Test Requirements through API CG-4 to API CJ-4			
CJ-4, 2006	CI-4 and CI-4 PLUS, 2002	CH-4, 1998	CG-4, 1995
Laboratory Tests			
1.1 Viscosity Grades	1.1 Viscosity Grades	1.1 Viscosity Grades	1.1 Viscosity Grades
1.2 High-Temperature Corrosion, 135°C	1.2 High-Temperature Corrosion Bench Test	1.2 High-Temperature Corrosion Bench Test	1.2 Cummins Bench Corrosion Test
1.3 Foaming	1.3 Foam Test	1.3 Foam Test	1.3 Foam Test
1.4 Shear Stability	1.4 Shear Stability	1.4 Shear Stability	
1.5 Noack Volatility	1.5 Noack Volatility	1.5 Volatility	
1.6 High Temperature/ High Shear	1.6 High Temperature/ High Shear		
1.7 Sooted Oil MRV	1.7 Low-Temperature Pumpability		
1.8 Chemical Limits	1.8 Elastomer Compatibility		
1.9 Seal Compatibility			

TABLE 14.11—Changes in Engine Test Requirements through API CG-4 to API CJ-4

CJ-4, 2006	CI-4 and CI-4 PLUS, 2002	CH-4, 1998	CG-4, 1995
Laboratory Tests			
2.1 Mack T-11	2.1 Mack T-8E	2.1 Mack T-8E	2.1 Mack T-8
2.2 Mack T-12	2.2 Mack T-10	2.2 Mack T-9	2.2 Caterpillar 1N
2.3 Cummins ISB	2.3 Cummins M11-EGR	2.3 Cummins M-11	2.3 Roller Follower Wear Test
2.4 Cummins ISM	2.4 Caterpillar 1R	2.4 Caterpillar 1-P	2.4 Sequence IIIE
2.5 Caterpillar 1N	2.5 Caterpillar 1K or 1N	2.5 Caterpillar 1-K	2.5 CRC L-38
2.6 Caterpillar C13	2.6 Roller Follower Wear Test	2.6 Roller Follower Wear Test	2.6 HEUI Air Entrainment Test
2.7 Engine Oil Aeration	2.7 Engine Oil Aeration Test	2.7 Engine Oil Aeration Test	
2.8 Roller Follower Wear Test	2.8 Sequence IIIF	2.8 Sequence IIIF	
2.9 Sequence IIIF			

TABLE 14.12—Changes in Soot Loading Viscosity Tests, CJ-4 to CG-4

Test	Requirement	Test Method	Properties	Unit	Limit		
					1 Test	2 Tests	3 Tests
CJ-4	Mack T-11	ASTM D7156	Soot at 4-cSt increase, minimum	%	3.5	3.4	3.3
			Soot at 12-cSt increase, minimum	%	6.0	5.9	5.9
			Soot at 15-cSt increase, minimum	%	6.7	6.6	6.5
CI-4	Mack T-8E	ASTM D5967	Relative viscosity at 4.8 % soot, max. (RV = viscosity at 4.8 % soot/ viscosity of new oil sheared in ASTM D6278)		1.8	1.9	2.0
CH-4	Mack T-8E	ASTM 5967-96 Ext	Relative viscosity at 4.8 %, maximum	cSt	2.1	2.2	2.3
			Viscosity increase at 3.8 %, maximum	cSt	11.5	12.5	13.0
CG-4	Mack T-8	ASTM 5967	Viscosity increase at 3.8 %, maximum	cSt	11.5	12.5	13.0
			Filter plugging, differential pressure, maximum	kPa/psi	138/20	138/20	138/20
			Oil consumption, maximum	g/kWh/ lb/bhp·h	0.304/ 0.0005	0.304/ 0.0005	0.304/ 0.0005

- *Current*

- SJ for 2001 and older automotive engines. (The SI and SK specifications were intentionally omitted by AP.)
- SL for 2004 and older automotive engines.
- SM for all automotive engine engines currently in use, introduced in 2004, for improved oxidation resistance, improved deposit protection, better wear protection, and better low-temperature performance of the service life of the lubricant. Some SM formulations may meet the latest ILSAC specification as “Energy Conserving.”
- SN (2010) continues the convergence with ILSAC and is discussed in that section with ILSAC.
- GF-5.

A characteristic of automotive petrol lubricant specifications is the inclusion of the performance properties of each previous category; thus, the SM specification gives full protection for SJ or SL requirements. This differs from the diesel engine specifications that usually, but not necessarily, include the performance properties of an earlier specification.

The API-SM specification, as shown in Tables 14.13 and 14.14, has mainly similar aims to that of CJ-4. The differences are that the CJ-4 Heavy-Duty Diesel specification has a major preoccupation with the effect of combustion soot-induced thickening of the oil arising from relatively recently introduced environmentally associated emission controls whereas API-SM uses the ASTM Sequences IIIG and IIIGA to measure the ability of the lubricant formulation to withstand (mainly) oxidative thickening. Limits of lubricant formulations are set for phosphorus and sulfur content. The major part of the API SM specification is concerned with in-cylinder component and valve gear wear.

14.5 ILSAC AND API SN

ILSAC is the acronym for the International Lubricants Standardization and Approval Committee, which is composed of representatives from the Japan Automobile Manu-

facturers Association, Inc. (JAMA) and representatives from Chrysler LLC, Ford Motor Company, and General Motors Corporation. Through the ILSAC committee, these organizations have jointly developed and approved an ILSAC GF-5 lubricant minimum performance standard for use in spark ignition internal combustion engines. The GF-5 standard specifies lubricant minimum performance requirements for engine sequence and bench tests as well as chemical/physical properties. Although many OEMs will recommend ILSAC GF-5 standards for lubricants, individual OEMs may require compliance with performance parameters beyond the tests included or require more stringent limits on certain of the tests included in the standard. Therefore, ILSAC GF-5 should be regarded as a minimum standard. In addition, any lubricant bearing the GF-5 designation must necessarily comply with all of the legal and regulatory requirements that apply on the restriction of use of substances, labeling, and relevant health and safety data.

Overall, ILSAC GF-5 aims to improve fuel economy, protection for emission control systems, and lubricant robustness for petrol engines. It only applies to 0W(X), 5W(X), and 10W(X) multigrade oils for their energy-saving effects; it specifically does not apply to light-vehicle diesel engines use. The development of ILSAC GF-5 has perhaps been more contentious than for previous formulations, probably because more improvements in performance have been attempted from performance specifications that are already very demanding indeed. As an example, this has particularly been the case for the Sequence VID fuel efficiency specification in ILSAC GF-5 S.2e. There are several areas of ILSAC GF-5 that have been left as not definitive, and www.GF-5.com should be consulted for more information about the latest ILSAC specifications.

14.5.1 ILSAC GF-5 Requirements

The ILSAC GF-5 requirements, as shown in Tables 14.15 and 14.16, are set out in a different order and sections than the previous ACEA and API performance specifications. Thus, fresh oil specification requirements are separated

TABLE 14.13—Passenger Car Engine Test Category for API SM: Laboratory Tests

Requirements	Test Method	Properties	Unit	Limits SM/EC GF4
1.1 Viscosity Grades		All of those that apply, typically SAE 0W-20, 0W-30, 5W-20, 5W-30, and 10W-30		Manufacturer sets targets within SAE J300 specification
1.2 Foam Test (Option A)	ASTM D892	Sequence I Sequence II	mL initial,	10/0 50/0
	ASTM D6082	Sequence III Sequence IV	Foam, mL/mL, after settling	10/0 100/0
1.3 Phosphorus	ASTM D4951	Phosphorus content	%	0.06 minimum, 0.08 maximum
1.4 EOFT	ASTM D6795	0.6 % Water-dry ice percentage reduction in flow	% reduction	50 maximum
1.5 EOWTT	ASTM D6794	With 0.6 % water	% reduction	50 maximum
		With 1.0 % water	% reduction	50 maximum
		With 2.0 % water	% reduction	50 maximum
		With 3 % water	% reduction	50 maximum
1.6 TEOST (MHT4)	ASTM D6922	Total deposits	mg	35 maximum
1.7 Homogeneity and Miscibility	ASTM D5133	Oil compatibility		Pass
1.8 Scanning Brookfield		Gelation index		12 maximum
1.9 Volatility	ASTM D5800	Volatility (Noack)	% off at 250°C	15 maximum
	ASTM D6417	Volatility (GCD)	% off at 371°C	10 maximum
1.10 Ball Rust Test	ASTM D6557	Rust rating	Average gray value	100 minimum
1.11 Sulfur	ASTM D4951 or D2622	Sulfur content of 0W and 5W multigrades	%	0.5 maximum
		Sulfur content of 10W multigrades	%	0.7 maximum

out in a separate Section 1 for viscosity and gelation index, Subsections 1a and 1b, and used oil specifications are within Section 2, “Engine Test Requirements” within Subsection 2a for “Wear and Oil Thickening” as well as in considerable detail in Section 3 for “Bench (Laboratory) Test Requirements” and Subsection 3i for “Aged Oil Low Temperature Viscosity”. Seal material testing is again described in great detail within subsection 3o “Candidate Oil Testing for Elastomer Compatibility”.

14.5.2 Relationship of ILSAC GF-5 to API SN (and API SN Resource Conserving)

In that the ILSAC GF-(X) lubricant performance specifications were a reaction to, and divergence from, the API S(X) series, ILSAC GF-5 and API-SN represent almost a convergence. The essential remaining differences are that ILSAC GF-5 is concerned only with lubricant grades up to 10W-30 with the additional criterion of “Energy Conserving”, whereas API-SN applies across a wider range of lubricant grades without the “Resource Conservation” requirement. To complicate issues further, an additional set of requirements combine API-SN with “Resource Conservation.” These differences for all four combinations are succinctly set out in Table 14.18; there are no differences shown for ILSAC GF-5 and API SN Resource Conserving and small differences between these and the “API SN for

ILSAC Grades” and “API SN for non-ILSAC Grades.” The background to the main differences between these performance specifications are concerned with the low-viscosity grades up to 10W-30.

Some minor details for ILSAC GF-5 and API SN had yet to be settled in mid-2010, a difference between previous lubricant performance specifications in which they have been essentially established at their time of publication. It is probable that ILSAC GF-5 and API SN represent a significant turning point in lubricant performance specifications, in which the improvements required have been particularly difficult to meet because of the (already established) advanced nature of the formulations and the effort required to reproducibly deliver those further improvements. The further challenges beyond ILSAC GF-5 and API SN may come from new dimensions, such as the effect of various biofuel additives to petrol and their residual or partially burned products transferred to the sump and their effects on the performance of lubricants. The biofuels may be part-ethanol/petrol, biobutanol fuel mixtures or other bulk, bio-based, cheap organics that can be mixed with petrol.

14.6 MOTORCYCLE AND SMALL-ENGINE LUBRICANT PERFORMANCE SPECIFICATION

Lubricant systems for small engines are divided into their cycle type as either two or four- stroke. The term “small

TABLE 14.14—Engine Tests for API SM

Requirements	Test Method	Properties	Unit	Limits SM/EC GF4
2.1 Sequence IIIG		Viscosity increase of 100 h	%	150 maximum
		Average weighted piston deposits	Merits	3.5 minimum
		Hot stuck rings	#	None
		Average cam plus lifter wear	μ	60 maximum
2.2 Sequence IIIGA	ASTM D4684	Aged oil low-temperature viscosity	Cp	Meets requirements of original grade or the next higher grade
2.3 Sequence IVA	ASTM 6891	Cam wear average	μ	90 maximum
2.4 Sequence VG	ASTM 6593	Average engine sludge	Merits	7.8 minimum
		Rocker arm cover sludge	Merits	8.0 minimum
		Average piston skirt varnish	Merits	7.5 minimum
		Average engine varnish	Merits	8.9 minimum
		Oil screen clogging	%	20 maximum
		Hot stuck rings	#	None
		Cold stuck rings	#	Rate & report
		Oil ring clogging	%	Rate & report
		Follower pin wear, cylinder #8 average	μ	Rate & report
		Ring gap increase, cylinder 1 and 8, average	μ	Rate & report
		Oil screen debris	% area	
2.5 Sequence VIII	ASTM 6709	Bearing weight loss 10-h stripped viscosity	mg cSt	26 max. Stay in grade
2.6 Sequence VIB (Required for ILSAC GF-4 only)	ASTM 6837	SAE 0W-20 and 5W-20 grades	All	2.3/2.0 minimum
		SAE 0W-30 and 5W-30 grades	%FE11	1.8/1.5 minimum
		SAE 10W-30 and all other grades	%FE12	1.1/0.8 minimum

TABLE 14.15—ILSAC GF-5 Fresh Oil Viscosity Requirements

1.a Viscosity Requirements	SAE J300		Oils shall meet all of the requirements of SAE J300. Viscosity grades are limited to SAE 0W, 5W, and 10W multigrade oils.
1.b Gelation Index	ASTM D5133	12 maximum	To be evaluated from –5°C to the temperature at which 40,000 cP is attained or –40°C, or 2 Celsius degrees below the appropriate MRV TP-1 temperature (defined by SAE J300), whichever occurs first.

engines” applies to motorcycles, snowmobiles, outboard motors, and other water sports equipment as well as portable light equipment such as chainsaws for outdoor woodworking.

14.6.1 Lubricating Two-Stroke Engines

Two-stroke engines have a relatively simple construction compared with four-stroke engines that gives them low initial cost and high power/weight ratios. Widely used in power motorcycles and portable, on-site apparatus, by design they use a “total loss” system in which each cycle feeds a small amount of lubricant into the engine where it burns with the main petrol fuel. Lubricant is either premixed with fuel in the vehicle tank or a small metering

delivery pump injects directly into the engine. From the different use and delivery method of lubricant between two- and four-stroke engines, the important issues for two-stroke engine are deposits on pistons, rings, and in the crankcase; spark plug “whisker” formation; exhaust port and silencer blocking; excessive wear due to piston/bore scuffing; exhaust smoke; and preignition.

14.6.2 Two-Stroke Automotive Lubricant Specifications

Although API, ASTM, TISI, CEC, and JASO established standards for two-stroke lubricants, the dominance of the Japanese motorcycle industry lead to the JASO M345 standard

TABLE 14.16—ILSAC GF-5 Engine Test Requirements

2a Wear and Oil Thickening	ASTM Sequence IIIG Test, ASTM D7320	Kinematic viscosity increase at 40°C, %	150 maximum
		Average weighted piston deposits, merits	4.0
		Hot stuck rings	None
		Average cam plus lifter wear, μm	60 maximum
2b Wear, Sludge, and Varnish Test	Sequence VG, ASTM D6593	Average engine sludge, merits	8.0 minimum
		Oil ring clogging, % area	Rate and report
		Cold stuck rings	Rate and report
		Hot stuck compression rings	None
		Oil screen debris, % area	Rate and report
		Oil screen sludge, % area	15 maximum
		Average piston skirt varnish, merits	7.5 minimum
		Average engine varnish, merits	8.9 minimum
		Average rocker cover sludge, merits	8.3 minimum
2c Valve-train Wear	Sequence IVA, ASTM D6891	Average cam wear (seven-position average), μm	90 maximum
2d Bearing Corrosion	Sequence VIII, ASTM D6709	Bearing weight loss, mg	26
2e Fuel Efficiency	Sequence VID	SAE xW-20 viscosity grade	2.6 % FEI SUM 1.2 % FEI 2 minimum after 100 h aging
		SAE xW-30 viscosity grade	1.9 % FEI SUM 0.9 % FEI 2 minimum after 100 h aging
		SAE 10W-30 and all other viscosity grades not listed above	1.5 % FEI SUM 0.6 % FEI 2 minimum after 100 h aging

being the most important. It ranks lubricant performance and benefits relative to low (JATRE 3) and high (JATRE 1) reference lubricants as in Table 14.19. Higher weighted values for each entry indicate a better lubricant performance such that the high reference position, JATRE 1, has a value of 100 in each test. The parameters scored are

- Smoke, as visible exhaust smoke;
- Detergency, by piston cleanliness and ring sticking;
- Exhaust system blocking, by restricted exhaust flow leading to power loss; and
- Lubricity, by resistance to piston seizure.

14.6.3 Composition of Two-Stroke Lubricants

Two-stroke lubricant formulations have several key components (Table 14.20) each having a specific role, dependent on specification and performance requirements.

Table 14.21 combines Tables 14.19 and 14.20 to give the relative importance of the formulation components from the first table with the composition of those components for the different performance levels. JASO FA, although obsolete, is included to demonstrate how increased performance JASO FA through FD is achieved by relative changes in formulation. Thus, performance additives and PIB increase whereas base oil decreases.

14.6.3.1 PERFORMANCE ADDITIVES

Two-stroke engines do not have highly loaded surfaces such as valve cams and followers, and their lubricants do

not need zinc dialkyldithiophosphate (ZDDP) antiwear additives. The base oil in the two-stroke lubricant formulation acts as the major antiwear component. Given the “once through, short residence time, total loss” system, the short time that lubricant is in the engine it must have sufficient inherent viscosity to prevent piston scuffing, and JASO recommends a 6.5-cSt (100°C) minimum lubricant viscosity.

Two-stroke engines are very sensitive to ash levels. If high-ash-level lubricants (e.g., four-stroke lubricant formulations) are used (Table 14.22), then deposits rapidly accumulate on spark plugs, cylinder heads, piston crowns, and exhaust ports. Ash deposit buildup on spark plugs eventually stops the engine as an alternative discharge route for the spark by conductive “whisker” formation across the spark plug electrodes. Ash deposit buildup on cylinder heads and piston crowns retains heat and cause preignition/detonation or melts the piston crown. Exhaust port ash deposits throttle gas transfer and reduce power generation. Altogether, ash deposits in two-stroke engines are undesirable. Where highly stressed engines run cool, as for marine outboard engines, very low ash or ashless systems are used (Table 14.22). The choice and treat rate of detergents/dispersants used in two-stroke lubricant formulations and the ash deposition from them must prevent engine failure from preignition/detonation, short-circuiting of the spark electrode gap, piston damage, or clogging of the exhaust port/silencer.

TABLE 14.17—ILSAC GF-5 Bench Test Requirements

3a Catalyst Compatibility	ASTM D4951	Phosphorus content	0.08 % (mass) maximum
	ASTM D7320	Phosphorus volatility	79 % phosphorus retention (Sequence IIIGB)
	ASTM D4951 or D2622	Sulfur content, 0W-XX, 5W-XX, 10W-30	0.5 % (mass) maximum 0.6 % (mass) maximum
3b Wear	ASTM D4951	Phosphorus content	0.06 % (mass) minimum
3c Volatility	ASTM D5800	Evaporation loss	15 % maximum, 1 h at 250°C <i>Note:</i> Calculated conversions specified in D5800 are allowed.
	ASTM D6417	Simulated distillation	10 % maximum at 371°C
3d High-Temperature Deposits	TEOST MHT, ASTM D7097	Deposit weight, mg	35 maximum
3e High-Temperature Deposits	TEOST 33C, ASTM D6335	Total deposit weight, mg	30 maximum <i>Note:</i> No TEOST 33C limit for SAE 0W-20
3f Filterability	EOWTT, ASTM D6794	With 0.6 % H ₂ O	50 % maximum flow reduction
		With 1.0 % H ₂ O	50 % maximum flow reduction
		With 2.0 % H ₂ O	50 % maximum flow reduction
		With 3.0 % H ₂ O	50 % maximum flow reduction
	EOFT, ASTM D6795		Test formulation with highest additive (DI/VI) concentration. Read-across results to all other base oil/viscosity grade formulations using the same or lower concentration of the identical additive (DI/VI) combination. Each different DI/VI combination must be tested.
			50 % maximum flow reduction
3g Fresh Oil Foaming Characteristics	ASTM D892 (Option A and excluding paragraph 11)	Tendency stability*	
		Sequence I	10 mL maximum, 0 mL maximum
		Sequence II	50 mL maximum, 0 mL maximum
		Sequence III	10 mL maximum, 0 mL maximum *After 1-min settling period
3h Fresh Oil High-Temperature Foaming Characteristics	ASTM D6082 (Option A)	Tendency stability*	100 mL maximum 0 mL maximum *After 1-min settling period

3i Aged Oil Low-Temperature Viscosity, ROBO Test

Measure CCS viscosity of the EOT ROBO sample at the CCS temperature corresponding to original viscosity grade.

(a) If CCS viscosity measured is less than or equal to the maximum CCS viscosity specified for the original viscosity grade, run ASTM D4684 (MRV TP-1) at the MRV temperature specified in SAE J300 for the original viscosity grade.

(b) If CCS viscosity measured is greater than the maximum viscosity specified for the original viscosity grade in SAE J300, run ASTM D4684 (MRV TP-1) at 5°C higher temperature (i.e., at MRV temperature specified in SAE J300 for the next higher viscosity grade).

(c) The EOT ROBO sample must show no yield stress in the ASTM D4684 test, and its ASTM D4684 viscosity must be below the maximum specified in SAE J300 for the original viscosity grade, or the next higher viscosity grade, depending on the CCS viscosity, as outlined in (a) or (b) above, *or*

Aged Oil Low-Temperature Viscosity, ASTM Sequence IIIGA Test, ASTM D7320

(a) If CCS viscosity measured less than or equal to the maximum CCS viscosity specified for the original viscosity grade, run ASTM D4684 (MRV TP-1) at the MRV temperature specified in SAE J300 for the original viscosity grade.

(b) If CCS viscosity measured is greater than the maximum viscosity specified for the original viscosity grade in SAE J300, run ASTM D4684 (MRV TP-1) at 5°C higher temperature (i.e., at MRV temperature specified in SAE J300 for the next higher viscosity grade).

(c) The EOT IIIGA sample must show no yield stress in the ASTM D4684 test and its ASTM D4684 viscosity must be below the maximum specified in SAE J300 for the original viscosity grade, or the next higher viscosity grade, depending on the CCS viscosity, as outlined in (a) or (b) above.

TABLE 14.17—ILSAC GF-5 Bench Test Requirements (Continued)

3j Shear Stability	Sequence VIII, ASTM D6709	10-h stripped kinematic viscosity at 100°C	Kinematic viscosity must remain in original SAE viscosity grade.	
3k Homogeneity and Miscibility	ASTM D6922		Shall remain homogeneous and, when mixed with TMC reference oils, shall remain miscible.	
3l Engine Rusting	Ball Rust Test, ASTM D6557	Average gray value	100 minimum	
3m Emulsion Retention	Oil mixed with 10 % water, 10 % E85	The oil when blended* with a mixture of 10 % distilled water and 10 % E85 shall retain a fluid emulsion for the time and temperature specified.	0°C, 24 h, no water separation 25°C, 24 h, no water separation *Waring blender or equivalent – 1 min maximum at room temperature. E85 solution = 85 % ethanol and 15 % gasoline	
3o Candidate oil testing for elastomer compatibility shall be performed using the five Standard Reference Elastomers (SREs) referenced herein and defined in SAE J2643. Candidate oil testing shall be performed according to ASTM D7216, which includes 336 h of immersion at 100°C for HNBR and 150°C for ACM and VMQ.				
FKM and AEM. The postcandidate-oil-immersion elastomers shall conform to the specification limits detailed herein (SAE J2643).				
Elastomer Material	Test Procedure	Material Property	Units	Limits
Polyacrylate rubber (ACM-1)	ASTM D471 ASTM D2240 ASTM D412	Volume Hardness Tensile strength	% Å Points % Å	–5, 9 –10, 10 –40, 40
Hydrogenated nitrile rubber (HNBR-1)	ASTM D471 ASTM D2240 ASTM D412	Volume Hardness Tensile strength	% Å Points % Å	–5, 10 –10, 5 –20, 15
Silicone rubber (VMQ-1)	ASTM D471 ASTM D2240 ASTM D412	Volume Hardness Tensile strength	% Å Points % Å	–5, 40 –30, 10 –50, 5
Fluorocarbon rubber (FKM-1)	ASTM D471 ASTM D2240 ASTM D412	Volume Hardness Tensile strength	% Å Points % Å	–2, 3 –6, 6 –65,10
Ethylene acrylic rubber (AEM-1)	ASTM D471 ASTM D2240 ASTM D412	Volume Hardness Tensile strength	% Å Points % Å	–5, 30 –20, 10 –30, 30

TABLE 14.18—Differences among API-SN, API-SN “Resource Conserving,” and ILSAC GF-5

Specification Requirements	Specific SAE Grade	API SN for ILSAC Grades	API SN for Non-ILSAC Grades	API SN Resource Conserving	ILSAC GF-5
Foam Test Option A		1-min set	10-min set	1-min set	1-min set
Phosphorus, % minimum/maximum		0.06 min/no	0.06 min/no	0.06 minimum/0.08 max	0.06 minimum /0.08 max
Phosphorus retention, %		No	No	79 minimum	79 minimum
TEOST MHT-4, mg		35 maximum	45 max	35 maximum	35 max
TEOST 33C, mg	Excluding 0W-20	No	No	30 maximum	30 max
Gelation index		12 maximum	No	12 maximum	12 max
Emulsion retention		No	No	Yes	Yes
Sulfur, % maximum	0W and 5W/10W	No/no	No/no	0.5/0.6	0.5/0.6
Sequence IIIGA (ROBO)		Yes	No	Yes	Yes
Sequence VID, FE1Sum/FE12	0W-X 5W-X 10W-X	No No No	– – –	2.6/1.2 minimum 1.9/0.9 minimum 1.5/0.6 minimum	2.6/1.2 minimum 1.9/0.9 minimum 1.5/0.6 minimum

TABLE 14.19—JASO M345 Indices by Performance Area

		Performance		
		Lowest		Highest
Area of interest	Index	JASO FB	JASO FC	JASO FD
Smoke	'SIX'	45	85	85
Blocking	'BIX'	45	90	90
Lubricity	'LIX'	95	95	95
Detergency	'DIX'	85	95	>125 ^a

The JASO FA standard is obsolete. ^aThree-hour test.

TABLE 14.20—Major Components in Two-Stroke Lubricants

Component	Weight, %	Function
Performance additives	to 6 %	Cleanliness
Bright stock	to 10 %	Lubricity, antiwear
Solvent	10–30 %	Reduce exhaust blocking, fuel miscibility, "pumpability"
PIB (Polyisobutene)	10–30 %	Clean combustion, low smoke emission levels
Base Oil	to 95 %	Enhanced lubricity, antiwear, carrier fluid

TABLE 14.21—Typical Two-Stroke Lubricant Formulations for Different Performance Specifications

	JASO FA	JASO FB	JASO FC	JASO FD
Performance additives	▽	▽▽	▽▽▽	▽▽▽▽
Bright stock	▽▽	▽	–	–
Solvent	–	▽	▽▽▽	▽▽▽
PIB	–	–	▽▽▽	▽▽▽
Base oil	▽▽▽	▽▽	▽	▽

14.6.3.2 BASE OILS

Bright stock, for lubricity, plus a 500-N base oil are used to formulate standard quality two-stroke lubricants. Where very high oil film strength is required for high-performance

loads and high temperatures for two-stroke racing engines or intermittent high power of chainsaw engines, then ester synthetic base oils may be used. Another application of complex ester lubricant technology is the formulation of biodegradable lubricants for outboard marine engines, snowmobiles, and chainsaws used in environmentally sensitive areas.

14.6.3.3 POLYISOBUTENE

Polyisobutene (PIB) substitution for the mineral base oil component of two-stroke lubricants substantially reduces visible smoke emissions. The PIB burns very cleanly but has to be chosen carefully by formulation and by molecular weight. Very-low-molecular-weight PIBs lack lubricity, yet very-high-molecular-weight PIBs have detergency problems and engine starting difficulties from the increased formulation viscosity. Typical PIBs for low-smoke-emission lubricant formulations are in the 450–1250 amu range. Another formulation approach mixes higher and lower molecular weight PIBs as a dumbbell system.

14.6.3.4 SOLVENTS

Where two-stroke lubricant formulations are mixed with fuel in the vehicle tank before use, the solvent assists with that mixing process. For auto-lube pump systems, the solvent reduces the lubricant viscosity and improves "pumpability". The solvent is usually a dearomatized light hydrocarbon with a flash point of approximately 80°C, but kerosine is often used for the same purpose.

14.6.4 The Constraints of Two-Stroke Emissions

Although images of two-stroke vehicles trailing plumes of light blue smoke are now unusual, nevertheless the major issue with two-stroke engines are a high level of hydrocarbon and carbon monoxide emissions. These arise from excess heavier hydrocarbons in the fuel/air mixture, a rich mixture combustion giving the carbon monoxide component of the emission. High hydrocarbon and smoke emissions arise from incomplete combustion of the lubricant oil component, a combination of unburned oil hydrocarbons passing straight through the engine together with an unburned fuel/lubricant mixture "short circuiting" between inlet and exhaust ports. Excessive emissions also occur because of high (up to 3 %) lubricant treat rates in premix systems. When the engine is idling, as at traffic lights, "lubricant pooling" can build up in the crankcase giving very high smoke emissions during subsequent acceleration.

Against these debits, rich combustion of two-stroke engines gives low NO_x emissions together with lower combustion temperatures from an element of EGR because of "port scavenging." This occurs when a portion of the exhaust gas is drawn back into the crankcase during

TABLE 14.22—Lubricant Ash Deposits by Comparative Application

Engine Cycle	Two Stroke		Four Stroke		
Application	Outboard marine	Motorcycle	Motorcycle	Car	Truck
Typical ash, %	Very low "ashless"	<0.25	<1.2	<1.2	<2.0

each induction cycle. Technical improvements to reduce emissions from two-stroke engines include “low smoke lubricants” as JASO FC/D, “auto-lube” related to engine revolutions per minute to minimize oiling at low speed, timing of fuel-injection systems when the transfer ports are covered to prevent short circuiting, and oxidation catalysts. Notwithstanding these developments, two-stroke engines are now essentially restricted to off-road racing, small (50 cm³) scooters, marine outboard, and portable equipment. The four-stroke engine has become the engine for contemporary motorcycles.

14.6.5 Four-Stroke Motorcycle Lubricants

Lubricants for four-stroke petrol light-vehicle engines and four-stroke motorcycle engines have similarities. There are additional physical stresses on the motorcycle engine lubricants arising from their high operating speed (to 16,000 r/min), high specific power (to 150 kW/L), small sump volumes, integral wet clutch, and gear boxes lubricated by the engine lubricant and lightweight engine construction.

14.6.5.1 SPECIFICATIONS

API gasoline specifications were the most widely used standards for four-stroke motorcycle engine lubricants until the mid-1990s. Since that time, trends in fuel-efficient light vehicle lubricants through low-viscosity base oils and friction modifier formulations were unsuitable for motorcycles. A dedicated four-stroke motorcycle specification, JASO T903, was developed that addressed motorcycle engine specific issues of wet clutch performance, gear box protection, and specific physical and chemical concerns.

14.6.5.2 WET CLUTCH PERFORMANCE

This is assessed by comparison of a candidate lubricant's friction characteristics to JAFRE A, a high-friction reference

oil, and JAFRE B, a low-friction reference oil, under the JASO T904-98 procedure as a modified SAE No. 2 friction test for motorcycle applications. Three main clutch friction performance characteristics are assessed: static friction (SFI, clutch slip); dynamic friction (DFI, clutch take-up/feel); and stop time (STI, synchronization time). From these assessments, a clutch performance index is calculated for the candidate oil that then classifies it (Table 14.23) as either:

- JASO MA, MA1, or MA2 (high friction, suitable for wet clutch applications) or
- JASO MB (low friction, more suited to dry clutch or scooter applications).

To meet JASO MA1 or MA2, all indices for a candidate lubricant must be within that specified for the category. If indices are shared between JASO MA1 and MA2, then the candidate lubricant meets JASO MA. To meet JASO MB, at least one or more of the indices must meet JASO MB criteria.

14.6.5.3 SHEAR LOSS

Integral motorcycle gear boxes give higher shear loss for multigrade lubricant formulations compared with light-vehicle engines. After-shear viscosity targets are set for four-stroke engine lubricants with sufficient base viscosity to protect gear boxes from pitting/scuffing wear. Table 14.24 compares the shear loss requirements for SAE J300 (light vehicle engine) and JASO T903 2006 (four-stroke motorcycle engine).

JASO T903 2006 has additional physical and chemical specifications:

- Minimum API SG quality level;
- Minimum 2.9 cP HTHS viscosity for bearing protection;
- 1.2 % maximum ash level;
- 0.12 % maximum phosphorous for catalyst longevity; and

TABLE 14.23—JASO T903T 2006 Clutch Friction Specifications

Parameter	Index	JASO T 903 2006 Indices			
		High Friction			Low Friction
		JASO MA	JASO MA2	JASO MA1	JASO MB
Dynamic friction index	DFI	1.45 ≤ DFI < 2.5	1.8 ≤ DFI < 2.5	1.45 ≤ DFI < 1.8	0.5 ≤ DFI < 1.45
Static friction index	SFI	1.15 ≤ SFI < 2.5	1.7 ≤ SFI < 2.5	1.15 ≤ SFI < 1.7	0.5 ≤ SFI < 1.15
Stop time index	STI	1.55 ≤ STI < 2.5	1.9 ≤ STI < 2.5	1.55 ≤ STI < 1.9	0.5 ≤ STI < 1.55

Source: Reprinted with permission from J-SAE.

TABLE 14.24—Comparison of J300 and T903 2006 Shear Loss Requirements for Multigrade Lubricants

Viscosity Grade	Aftershear Kinematic Viscosity at 100°C (30 Cycles, ASTM 6278)			
	Other Grades	xW-30	xW-40	xW-50
SAE J300	Stay in grade	≥9.3	≥12.5	≥16.3
JASO T903	Stay in grade	≥9.0	≥12.0	≥15.0

Source: Reprinted with permission from J-SAE.

- 0.08 % minimum phosphorus, to protect gear boxes, compared with the downward trend in modern low-phosphorous passenger car engine oils.

14.6.5.4
LUBRICANT COMPOSITION AND CLUTCH PERFORMANCE

Although four-stroke motorcycle engine lubricant formulations use very similar additive components as petrol light-vehicle engine lubricants, there are differences. The choice and treat rates of additives levels are different for the four-stroke motorcycle lubricant to deal with increased high-temperature performance. It must also ensure proper operation of wet clutch systems, both lubricated and cooled by the engine lubricant. Each additive component in the lubricant formulation can affect clutch performance. An overview of typical responses to clutch performance is given in Table 14.25. This is not definitive because different clutch friction materials, lubricant feed rates, and clutch spring rates also affect a single clutch system’s performance.

14.6.6
Lubricant Classifications for Nonautomotive Two-Stroke Engines Applications

Although automotive two-stroke applications concentrated on the Japanese classifications, this engine cycle is used for many small, portable, powered applications such as chainsaws and garden power machinery such as trimmers, etc. In addition, there is the far larger U.S. marine outboard motor industry that also covers winter vehicles such as snowmobiles. Classification of engine lubricants for these applications is as necessary as for automotive use.

There is an important division between land-use and marine-use engine lubrication applications. The first land-use application service classification for two-stroke oils applies to many engine applications, from mopeds, small generators, motor scooters, motorcycles, chainsaws, etc., up to approximately 500 cm³, is SAE J2116. The API designations are TA (obsolete) and TC (current). The second application is under the aegis of the National Marine Manu-

facturing Association (NMMA) for two-stroke outboard engine lubricants.

The first application, under SAE J2116, had four designations, from TA through to TD, of which only TC is current, the others being declared obsolete. The TC designation is designed for various high-performance engines up to 500 cm³, as used on motorcycles, snowmobiles, and chainsaws with high fuel/oil ratios, but not outboard marine engines, as noted previously. ASTM-TC two-cycle lubricants are designed to address ring sticking, preignition, and cylinder scuffing problems. The ASTM D4859-08 specification is specifically for two-stroke petrol engines prone to ring scuffing, preignition caused by deposit formation, scuffing of pistons, fouling of spark plugs, and piston varnish. The lubricants are primarily tested for ring sticking, piston deposit formation, lubricity, and preignition caused by deposits. The specific subsidiary ASTM standards for this purpose are

- D4857, which assesses the ability of the lubricant to minimize ring sticking and piston deposit formation (other than outboard marine engines). This uses a Yamaha RD 350B engine to measure
 - Ring sticking and deposits in two crossover test runs,
 - Second ring sticking,
 - Piston skirt varnish,
 - Plug fouling,
 - Preignition,
 - Exhaust blocking, and
 - Piston scuffing/seizure
 with results relative to a standardized reference lubricant;
- D4858, which assesses the tendency of a lubricant to promote preignition for these engines using a Yamaha CE50S engine, measuring the occurrence of preignition; and
- D4863, which assesses the lubricity of two-stroke gasoline lubricants using the same engine as in D4858, the Yamaha CE50S, by means of measuring the drop in torque relative to the standardized reference lubricant.

TABLE 14.25—Effects of Formulation Additive Classes on SAE No. 2 Clutch Friction			
Constituent	Impact on Wet Clutch Performance		
	Negative	Neutral	Positive
Detergent	Type specific		
Dispersant	Type specific		
ZDDP	Type specific		
Friction modifier	*		
Antioxidant	Type specific		
Viscosity modifier	Dispersant viscosity modifiers	OCP type	
Mineral base oils		*	
Synthetic base oils	Type/viscosity specific		
Antifoam		*	
Pour-point depressants		*	
Dye		*	

JASO standards have been described previously in Table 14.2.1 and were found not to meet the latest European two-stroke engine test requirements. ISO now divides two-stroke lubricants into four categories—ISO-L-EGB through to -EGE—that mirror the JASO tests but with increasingly demanding standards such as increased piston cleanliness after a 3-h test and lowered smoke emissions.

Two-stroke outboard marine lubricants have developed to meet the water-cooled engine technologies for powering boats whereas the automotive two-stroke engines tend to be air-cooled. The additives used are all non-ash forming because almost all marine two-stroke outboard engines have a tendency to “coke” various parts of the combustion chamber, such as piston rings. NMMA has developed performance categories for two-stroke marine engines over time, now consolidated into the TCW-3R category. The test criteria to achieve this classification are given in Table 14.26.

The comprehensive NMMA TC-3WR test criteria cover a range of engine designs and size capacity. The cost of this test causes increasing concern (of approximately \$250,000–300,000) for what is a relatively small market compared with automotive lubricants. On the other hand, failure of a two-stroke outboard engine in service could be a safety-critical issue.

An additional issue that outboard two-stroke engines must address is compatibility with the environment. As well as satisfying the NMMA TW-3WR requirements, a two-stroke lubricant must meet minimal requirements for toxicity standards to wildlife and rapid degradability. The International Council of Marine Industry Associations (INCOMIA) set Standard 27-97 for “environmentally friendly” outboard engine lubricants. To meet this standard, the marine two-stroke lubricants are formulated with rapidly biodegradable, fully synthetic, ester base oils. In this way, high performance is matched with environmental compatibility.

14.6.7 Effects of Future Emission Controls

Light vehicle engines have been subject to increasing environmental emission controls since 1964. Motorcycle engines are subject to the same controls, and the technical

advances of closely controlled fuel injection systems, multi-valve technology, and TWCs are common for higher performance motorbikes as they must, in turn, meet increasingly stringent emissions targets.

Emerging markets regard fuel economy as important, and it is a driver for change to lower viscosity lubricants, with 10W-30 grades increasingly accepted for modern engines. In this respect, motorcycle engine lubricants lag behind light vehicle engines by a decade. Motorcycle engines have, in general, small sumps with some as small as 0.75 L. The two trends of higher operating temperatures and longer service drain intervals put additional stress on the lubricant.

The two strands of lubricant performance specifications for automotive light-vehicle petrol engines and for four-stroke motorcycle engines are now clearly separate. There will be continued interaction between them, but developments in four-stroke motorcycle engine and powertrain design now have sufficiently critical differences for their lubricant specifications to develop separately. This is necessary to ensure that lubricant performance specification protects these highly stressed applications.

14.7 FUTURE SPECIFICATIONS FOR GASOLINE/PETROL AND DIESEL ENGINE LUBRICANT PERFORMANCE

The next update of API-SM, as -SN, was established in 2010. The update to HDD CJ-4 as CK-4 appears to be delayed because of the comprehensive nature of CJ-4, reasonably expected to last possibly until 2014.

It is reasonable to speculate on the drivers for further revision of the lubricant performance specifications. The 2010 baseline has established lubricant specifications for extremely low-emission engines, and there is probably little further to be gained there. Future issues will come from new directions.

14.7.1 Biofuels

By 2012, the initial interest in biofuels as either both gasoline/petrol and diesel replacements or extenders should

TABLE 14.26—NMMA TCW-3R Test Criteria

A. Engine Tests	
Test Engine	Criteria of Test
Yamaha 50S	Seizure/lubricity
Yamaha 50S	Preignition, causing power loss
Mercury 15HP	Compression loss, ring sticking, piston cleanliness
OMC 40HP	Ring sticking, piston cleanliness
OMC 70HP	Ring sticking, piston cleanliness
B. Laboratory Tests	
Low-temperature viscosity	Limited viscosity at –25°C
Miscibility	Mixing with fuel at –25°C
Corrosion protection	Standard rust tests compared to reference lubricant
Compatibility	Stability after mixing with reference fuel
Filterability	Flow rate compared to pure fuel

have matured into a more stable market. The second phase of biofuels, such as ethanol or butanol from non-food cellulosic sources or FAMEs from jatropha plants and many other nonfood sources, will supplement phase one biofuels. Future performance specifications must address the effects of the respective biofuels for gasoline/petrol and diesel engines on lubricants. Use of vegetable-based diesel fuel oil or hydrocarbon diesel fuels with various levels of vegetable oils (e.g., 5 or 10 %), leads to fuel condensation/deposition in the sump of the engine and dilution of the lubricant by accumulation of the relatively low volatility vegetable oil. Drives to increase the biocontent of biofuel to higher percentages may cause lubrication problems. The vegetable oil-derived fuel dilution leads to enhanced viscosities and enhanced oxidation rates of the lubricant. One physical aspect of the fuel dilution effect is an increased lubricant volume that can be stirred into a foam by rotating big ends. A foamed lubricant gives very low protection of bearing surfaces and dramatically enhanced wear results.

Ethyl alcohol (100 %) as a spark ignition engine fuel or alcohol substituted at low levels in petrol can interact with, and cause problems with, the additive pack in the current type of lubricant formulations. Reformulation of lubricants to deal with the effects of these fuels will be necessary, but the relevant technology is available from South America where, for example, Brazil has operated light vehicles on total alcohol fuels for more than a decade. The longer term effects of higher alcohol fuel additives, such as biobutanol (C_4), on lubricant performance is not fully known at present.

14.7.2 Efficiency Standards

The existing Corporate Average Fuel Efficiency (CAFE) standards have improved fuel efficiency in the United States. These standards only apply to petrol-fueled vehicles at present; the strongly competitive market for diesel engine efficiency appears not to need standards. At the end of the first decade of this century the urgency to improve petrol automotive energy efficiency was further emphasized by changes in government policy. Lubricants have a role in improving fuel efficiency through reduced friction loss in bearings, in-cylinder and valvetrain, possibly by formulating lower SAE grade products. This will require the development of higher fuel efficiency specifications as in API SM 2.6 and ILSAC GF-5.

The use of hybrid vehicle propulsion in its various forms will require new lubricant performance specifications. The different use cycle of the internal combustion engine part of the hybrid system will pose challenges for smaller engines that are intermittently used.

14.7.3 Extended Service Intervals

U.S.-oriented lubricant formulations traditionally have had a shorter service lubricant change interval than European

formulations. The development of new formulations to meet extended service intervals is straightforward. The challenge may lie with the introduction of EOT test specifications, as in the ACEA 2008 specifications. The cost of extended service interval lubricants is not linear—one rule of thumb advanced is that doubling the service life of a lubricant doubles its cost.

14.8 CONCLUSIONS

The purpose of this chapter is to demonstrate the dynamic changes of lubricant performance specifications with time. As discussed, these specifications may have come close to their current limits in dealing with the effects of emission control systems. The new drivers for change will probably be the requirements to work with biofuels of various compositions.

The pressures and drivers for changes in lubricant performance specifications can be followed through the relevant technical press. Some useful, but not exclusive, publications are given in the bibliography; some give original contributions and assessments of developments, others feed off them and disseminate those developments to a wider audience. Regular reading of these publications will indicate how the pressures for change are developing and how the industry is responding.

References

- [1] Kadjas, C., Karpińska, A., and Kulczycki, A., 2010, "Industrial Lubricants." In *The Chemistry and Technology of Lubricants* (3rd ed), Ed. R. M. Mortier, S. Orszulik, and M. F. Fox, Eds., Springer, New York.
- [2] Vajedi, M., 2008, "A Slow Road to Better Engine Oils," *Lubes 'n' Greases*, November/December, pp.14–30.

Bibliography

- [1] CEC tests for ACEA are accessed via the CEC website at <http://www.cectests.org> and follow the link to "Lubricants".
- [2] For ACEA European Oil Sequences, see <http://www.ACEA.be>, <http://www.info@acea.be>, or <http://www.communications@acea.be>.
- [3] API—The API website is very extensive. Navigate to the "Engine Oil Licensing and Certification System (EOLCS)" to access the engine oil and lubricants publications.
- [4] ILSAC—Follow <http://api-ep.api.org/filelibrary/15tech2rev.pdf> and <http://www.GF5.com>.
- [5] Infineum and Lubrizol provides an excellent tabular summaries of current API and ACEA specification and testing sequences on their respective websites.
- [6] Dresel, W., and Mang, T., Eds., 2001, *Lubricants and Lubrication*. Wiley-VCH, Weinheim, Germany.
- [7] Technical magazines such as *Lubes 'n' Greases* and *Insight*, published by Infineum, *Petroleum News*, published by the Energy Institute, and *Lube Magazine* all publish articles on trends in lubricant performance requirements and commentaries on the relevant specifications.

15

Automatic Transmission Lubricants

Richard J. Vickerman¹ and Craig Tipton²

15.1 INTRODUCTION

This chapter will cover the functions, properties, and composition of automatic transmission fluids (ATFs), along with a brief description and history of original equipment manufacturer (OEM) ATF specifications for passenger cars. The cited works include an eclectic mixture of materials designed to give the reader interested in further study some historic and some more modern information, along with information from different points of view when possible. By no means is this meant to be a comprehensive review; it is only meant to be a small window into the world of transmission lubricant technology.

ATFs are probably the most complex lubricant in automobiles today—a consequence of the range of functions they must perform during a long service life. Functionally, all transmission fluids fulfill the following requirements:

- Torque transfer medium in the torque converter and at clutch-to-metal and metal-to-metal interfaces;
- Hydraulic control medium for actuation of the valve body and clutch systems;
- Lubrication, cleaning, and protection of gears, synchronizers, belts, chains, pulleys, bushings, bearings, and seals, among other parts; and
- Heat transfer medium for the removal of excess heat generated in, for example, the torque converter and during shifting clutch engagements.

These requirements vary in degree and importance depending on the type of transmission concerned. To accomplish these functions, several critical physical and chemical properties are required:

- Thermal stability and resistance to oxidation,
- Correct friction characteristics and friction durability,
- Proper viscometric profile over the anticipated operating conditions of the transmission and service life of the fluid,
- Compatibility with all of the various materials contained in a transmission,
- Antiwear performance,
- Anticorrosion and antirust performance, and
- Antifoaming performance.

The functions most notably associated with the transmission in a conventional internal combustion engine powered vehicle are

- To allow the engine to be connected and disconnected from the remainder of the drivetrain (the engine needs to idle),
- To allow the best match between the engine's delivered speed and torque and the vehicle's required speed and torque based on the inputs from the driver and the responses from the vehicle, and
- To allow the vehicle to travel in reverse.

15.2 TRANSMISSION CLASSIFICATION

Historically, transmissions were classified into two main categories: manual transmissions (MTs) and automatic transmissions (ATs), which referred to the level of involvement of the vehicle's driver in the operation of the transmission. A MT, or stick-shift transmission, requires the driver to control practically all functions of the transmission: launch, gear selection, shift point, etc. Gear ratios are selectable by the driver through a hand-operated gear shift lever [1]. With an AT, once the car is put in the desired operating mode (e.g., forward or reverse), the operator need only press the accelerator pedal or brake and the transmission system takes care of the rest [2]. ATs use epicyclic (planetary) gearing controlled by clutch packs or brake bands to engage a gear ratio. ATs that allow the driver to manually select a specific gear are often called manumatics, first popularized by Porsche in the 1990s under the tradename Tiptronic® [3–5]. A manual-style transmission operated by a computer is often called an automated-manual transmission rather than an AT [6].

Contemporary automobile ATs typically use four to six forward gears and one reverse gear, although they have been built with as few as two and are now being built with as many as nine gears [7]. In contrast, transmissions for heavy trucks and other heavy equipment are typically MTs and usually have at least nine gears so that the transmission can offer a wide range of gears and close gear ratios to keep the engine running in the power band. Some heavy-vehicle MTs have dozens of gears, but many are duplicates, introduced as an accident of combining gear sets, or introduced to simplify shifting. MTs are generally referred to by the number of forward gears they offer (e.g., five-speed) as a way of distinguishing them from ATs or other available MTs. Likewise, a five-speed planetary AT is typically referred to as a “five-speed automatic.”

15.3 TRANSMISSION HARDWARE

The ability to separate the engine from the wheels in a vehicle powered by a conventional internal combustion engine is at the root of some very complex and innovative transmission designs. For the basic MT and AT this function is accomplished by the manual clutch and torque converter or start-clutch [8] systems, respectively. These are also considered the “launch” devices for the vehicle.

15.4 CONVENTIONAL ATs

The conventional planetary AT (see Figure 15.1) incorporates a series of planetary gear sets along with flat plate or band clutches or both to match engine-delivered power to vehicle-required power [2,9].

¹ The Lubrizol Corporation, Wickliffe, OH, USA

² Retired, The Lubrizol Corporation, Wickliffe, OH, USA

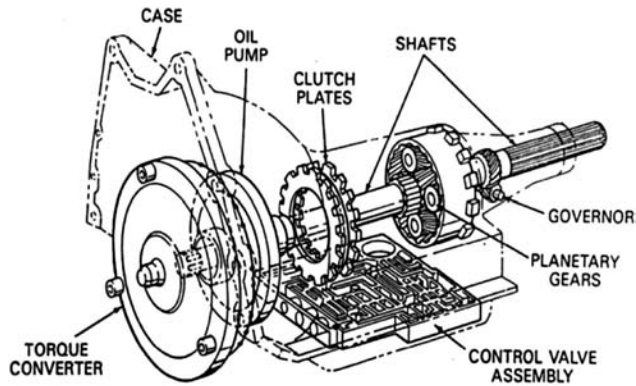


Figure 15.1—Diagram of an AT.

15.4.1 The Torque Converter

The AT has historically used a torque converter [10] as a coupling device with the engine and as a launch device. The torque converter is a hydraulic device shaped like a doughnut, filled with ATF, consisting of a pump, turbine, stator, and converter clutch (see Figures 15.2 and 15.3).

The operation of a torque converter can be explained by comparison with a child's pinwheel and an electric fan. In this comparison, the fan takes the place of the converter pump and the pinwheel behaves like the turbine. When the fan is turned on, it creates a flow of air that, when directed at the pinwheel, causes it to rotate. This airflow is analogous to the flow of fluid created when the running engine rotates the converter's pump. When the flowing fluid

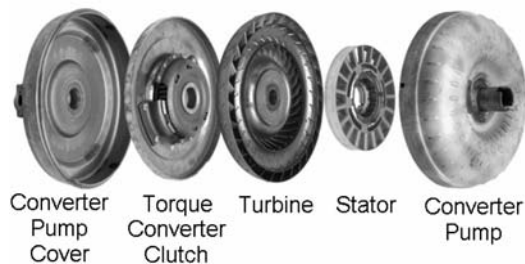


Figure 15.2—Expanded view of the torque converter.



Figure 15.3—Cutaway view of a torque converter.

impacts the turbine it will cause it to rotate and in turn the transmission and drivetrain, ultimately moving the vehicle.

To stop the vehicle, the operator applies the vehicle's brakes, which in turn stops the wheels, driveshaft(s), transmission components, and ultimately the converter's turbine. The fluid connection through the torque converter allows the engine to idle when the vehicle is stopped [11]. This is very much the same as holding the blades of a pinwheel stationary while within the flow of air. In this situation, the fan air continues to flow and press on the pinwheel blades, but with the pinwheel held stationary, the air simply moves around the blades. When the pinwheel is released, it will resume its rotation.

The pinwheel analogy also helps illustrate the inefficiencies of the torque converter. The mechanical energy from the engine is converted to hydraulic fluid energy via the converter pump. This hydraulic energy must then be converted back to mechanical energy via the turbine. To help improve the converter's efficiency, a clutch was added connecting the pump and turbine, providing a mechanical coupling, when engaged, between the engine and transmission analogous to the MT clutch system. There are many styles of converter clutches, but at their basic level, they consist of a friction material surface along with a mating steel reaction surface [12].

15.4.2 Planetary Gears

Most conventional ATs obtain their gear ratios through the use of planetary, or epicyclic, gear sets (see Figure 15.4), which consist of an inner sun gear, an outer internal gear (internal gear as the teeth are on the inside), and a series of planet gears, connected to each other by a carrier assembly that is located between the sun and internal gear [13,14].

The sun gear, planet carrier, and internal gear can either be the input to the gear set, be held stationary, or be the output of the gear set. Various gear ratios can be obtained depending on how this is done. There are numerous versions and configurations for a planetary gear set, but in its simplest form, it can provide two forward gear ratios, a direct drive ratio, and a reverse direction ratio on the basis of the manner in which the power is routed through the assembly.

15.4.3 Flat Plate and Band Clutches

The power through the planetary gear set is controlled by a series of plate or band clutches or both [15–24]. The plate clutch system consists of alternating friction plates and steel reaction plates (see Figures 15.5 and 15.6). A common configuration has the friction plate with an inner spline pattern and the steel separator with an outer spline. When the clutch is engaged, power is transferred via friction



Figure 15.4—Expanded view of planetary gear set.



Figure 15.5—Cutaway of an AT with a good view of the torque converter clutch, shifting clutches, and planetary gear set.

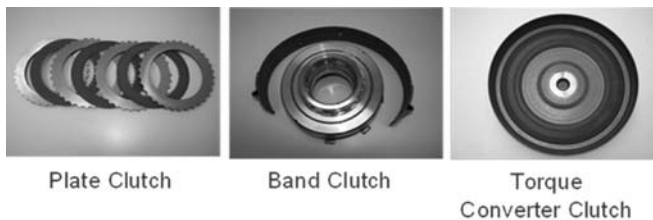


Figure 15.6—AT clutch types.

between the mating surfaces of the clutch and separator plates. If one of the plates is splined to a nonrotating component, then the engagement of the clutch will result in the other part also being held stationary.

A band clutch consists of a steel band lined with friction material wrapped around a steel drum. With this style of clutch, one end of the band is held fixed to the transmission case and an apply pin is used to wrap the other end around the drum. Because the band is fixed to the case, it can only serve to stop the drum's rotation during engagement [25].

15.4.4 Automatic Control

An AT, by definition, controls when and to which gear it shifts via sensors for vehicle and driver inputs, which send signals to the vehicle's on-board processor. When the shift point is determined, the transmission control unit will actuate control solenoids causing transmission fluid to flow through the appropriate circuit to apply the correct clutches routing power as needed through the planetary gears.

With the advent of sophisticated electronic controls, the driver can choose between many driving options from economical and sport driving modes to pseudomanual options that use "paddle shifters" to allow the driver to manually choose when to change gears.

15.4.5 Planetary Gear ATF

Planetary gear ATFs are one of the most complex lubricants made today—a consequence of the broad range of performance requirements necessary for the proper functioning of a typical AT [26–28]. Functionally, all transmission fluids fulfill the following four major requirements:

1. A torque transfer medium in the torque converter and at clutch-to-metal and metal-to-metal friction interfaces;

2. Hydraulic control medium for actuation of the valve body and clutch systems;
3. Lubrication, cleaning, and protection of gears, synchronizers, belts, chains, pulleys, bushings, bearings, and seals, among other parts;
4. A heat transfer medium for the removal of excess heat generated in, for example, the torque converter and during clutch engagements.

Depending on the specific application, transmission lubricants must perform all of this over a bulk temperature range of -40°C to as high as 180°C , and in some cases over the lifetime of the vehicle [29–31].

OEMs are constantly striving to increase the overall fuel efficiency of their vehicles [8,32–39]. This has led to the development of ATs that are smaller and lighter with increased power density, compared with their predecessors, and more available gear ratios of up to and including nine ratios to date [7,40].

Torque converter clutches were introduced to improve the fuel economy of vehicles equipped with ATs [10,41]. Locking torque converter clutches were first and were designed to engage at higher speeds when the two halves of the torque converter reach a similar relative rotational velocity. They effectively lock the two halves of the torque converter together, forming a rigid connection between the engine and transmission, eliminating the inherent inefficiency of a fluid coupling. A locking torque converter clutch works well at highway speeds, but it offers no benefit under city driving conditions where the two halves are connected only through the fluid.

Continuously slipping torque converter clutches (CSTCCs), further improving efficiency, soon followed [41–46]. The CSTCC reduces losses in the torque converter by slipping under partial actuator load during city driving conditions and retains the ability to completely lock up under highway driving conditions. These torque converter clutch systems can experience a low-frequency vibration (20–40 Hz) during operation that results from a stick-slip event between the friction material and the reaction plate, commonly called "shudder" [47,48]. Shifting clutch systems can also experience stick-slip events that, for example, can manifest as a harsh shift engagement or a squawk noise (~ 430 Hz) [49]. To ensure the correct frictional performance and to eliminate shudder, the fluids must be designed accordingly. Often the various clutches in an AT use different friction materials regardless of whether they are torque converter or shifting types [15,19,50–52].

15.5 NONCONVENTIONAL ATs

With the introduction of nonconventional AT options (e.g., continuously variable transmissions [CVTs] and dual-clutch transmissions [DCTs]), the term AT is no longer sufficient to describe a specific type of device. The conventional AT is now often referred to as a "planetary automatic", sometimes a stepped ratio planetary AT.

15.5.1 DCTs

The DCT can be thought of as two independent MTs combined into one unit in which each independent section is activated by one of two clutches (hence the name dual clutch) located on two separate transmission input shafts (see Figure 15.7). These two clutches are typically configured concentrically and located between the engine

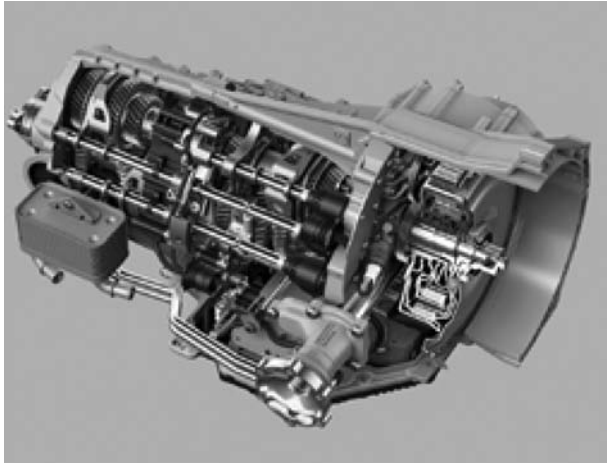


Figure 15.7—DCT cutaway view.

and input shafts of the transmission. Within the gear box, one of the two input shafts has the ability to route power through the odd-numbered gears (1, 3, 5, etc.) whereas the other drives the even-numbered gears (2, 4, 6, etc.). Shifting between the odd and even gears is accomplished by alternating power flow from the one clutch to the other and back again. The odd-gear clutch, when routing power through first gear, is also used for the important task of launching the vehicle [53–55].

When the vehicle is prepared for launch, the synchronizers for first and second gears will both be engaged. The launch clutch will apply as the driver operates the accelerator and the vehicle will begin moving forward via power through first gear. At the appropriate time, the outer clutch will disengage and the inner clutch will apply, diverting power through second gear. If the driver continues to accelerate in second gear, then the transmission synchronizers will disengage first gear and engage third gear in anticipation of the next upshift, which is accomplished by releasing the inner clutch and applying the outer. This carefully choreographed selection of clutches and synchronized gears continues throughout the drive cycle.

Shifts can take place either manually, via Formula-1-style shift paddles on the steering wheel, or under automatic control when the driver places the shift selector into drive mode. Under automatic control, the computer preselects the next appropriate gear in the unengaged half of the gear set. The result is a very fast, but completely smooth, gear shift, free from interruption in torque flow to the driving wheels.

DCTs can be either wet or dry, referring to the manner in which the clutch system is lubricated. A wet DCT uses lubricated, multiplate clutches much like those found in a conventional AT [56]. A dry DCT uses a pair of nonlubricated clutches consisting of pressure plates and dry clutch disks similar to a conventional MT. Which option is chosen is a matter of design preference and vehicle requirements.

In terms of mechanical efficiency, a DCT will never quite be able to match the theoretical efficiency of a standard MT because the necessary hydraulic systems will inevitably absorb some energy, especially on a wet clutch DCT. Also, by using the helical cut spur gears of a MT, the gear train has greater fuel efficiency over its planetary counterparts [12,14].

15.5.1.1 DCT FLUID

Neither a conventional ATF, nor a standard manual transmission fluid (MTF) is up to the task of lubricating all of the various systems in a DCT. The wet clutch-dual clutch transmission fluid (DCTF) requires a hybrid of performance to operate manual-style gears and synchronizers and the AT-type wet clutches [57]. When the clutches are the dry variety, the transmission may be lubricated using a MTF. The critical performance requirements for a DCTF are

- Lubrication of the clutches, gears, shafts, bearings, and synchronizers;
- Heat dispersal for the entire system;
- Hydraulic actuation of the clutches and gear system; and
- Protection of components against wear and corrosion.

Running in a permanent lubricant bath with fluid being pumped through, wet clutches are critical components, and precise control of their engagement and disengagement is central to the transmission's smoothness and refinement. The DCT's fluid must sustain consistent launch and shift friction characteristics with antishudder performance for, ideally, the lifetime of the transmission. DCT-specific lubricants require a specialized additive technology to guarantee the DCT's technical advantages and its durability in service. Synchronizer components also depend on the correct frictional performance for their smooth operation with no evidence of wear that can cause synchronizer clash or baulk.

Helical gears of the DCT have a higher torque density compared with an AT because the AT's epicyclic gear arrangement allows the load to be shared between multiple planets. As a result, DCT fluids generally need a higher degree of gear and bearing protection relative to a conventional ATF [2].

Because it is a relatively new technology, DCT fluids are dominated by OEM-specific products, which are still evolving along with the transmission technology, with no published service-fill specifications as yet. However, this market is expected to mature in time, with service-fill specifications and fluids appearing on the market.

15.5.2 CVT

In theory, a CVT has an infinite number of available gear ratios between some fixed minimum and maximum, and the shift steps are imperceptible and unnoticed by the driver. The most common CVT relies on a belt or chain looped around two variable diameter pulleys, called variators, which is the type that will be discussed here [58–67].

Unlike a conventional fixed diameter pulley, the width of the CVT pulley varies as the two halves move toward and away from each other via hydraulic control. As the pulley opens up, the contact line of the belt/chain moves toward the rotation axis, creating a smaller effective radius for the pulley. When the pulley halves squeeze toward each other, the contact line of the belt/chain is pushed outward, creating a larger effective radius. These changing effective radii work with each other in that as one pulley increases its effective radius, the other decreases, creating a range of ratio combinations between the input and output pulleys [58].

15.5.2.1 CVT FLUIDS

CVT fluids are designed to lubricate this metal-to-metal contact zone, effectively maintaining a high friction



Figure 15.8—Van Doorne push-belt CVT variator pulley and belt arrangement.

coefficient for efficient torque transfer while protecting the system from wear [62,68]. Figure 15.8 shows a Van Doorne [69] style push belt and variator arrangement and Figure 15.9 shows a Luk chain arrangement [65,66,70,71].

CVTs are connected to the engine via either a wet start clutch or locking torque converter and have the same friction requirements as their counterparts in other ATs, respectively. Balancing the different needs of the metal-to-metal friction zone between the belt (or chain) and the pulleys and the wet clutch system is certainly a challenge to the formulator [72].

To meet the requirements of these functions in a wide range of operating conditions, bulk fluid temperatures ranging from -40°C in cold climates to 180°C or even higher in extreme conditions of mountain trailer-towing or idling in traffic when ambient temperatures are high, many properties, physical and performance, often occur in specifications for specific reasons [64,69,73–79].

With all of these different types of transmissions and different, often contradictory performance requirements, the field of transmission fluid formulating is a challenging one. Next, the chemistry of ATFs will be covered.

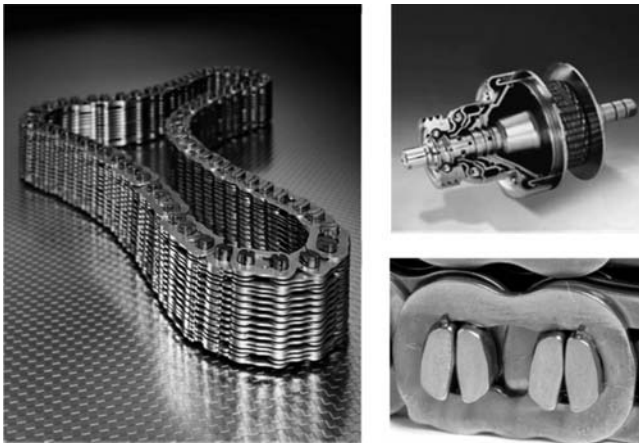


Figure 15.9—Luk CVT chain and pulley arrangement.

15.6 ATF CHEMICAL CONSTRUCTION

Transmission fluids consist of three essential components:

1. An oil of the appropriate viscosity, also called a basestock or base oil, which composes up to 90 % of the fluid;
2. The additive package, which composes up to approximately 15 % of the fluid; and
3. Viscosity index improvers (VIIs), or viscosity modifiers (VMs), which can typically be present from 2 to 15 %.

How these various components find their way into the formulation depends on the application and the geographical location of the OEM [29,31,39,80–82].

In North America, lubricant additive companies have been largely responsible for developing the lubricant performance package, a mixture of additives blended together in a “concentrate” [34,83–89]. This concentrate is purchased by oil companies, which in turn blend it at the appropriate level with a basestock and, if required, a VII. Sometimes the oil company will add additional additives to the fluid to alter the performance for a specific application. Finally, the oil company will typically supply the finished lubricant that has been designed to meet specific performance specifications to the OEM.

In Asia and Europe, the situation is somewhat different than in North America, although is hard to generalize and harder to document because each region’s OEMs have each maintained different levels of interaction with additive suppliers and oil companies. One generalization that is based on personal experience is that in Asia and Europe, overall, the oil companies are more involved in the development of the performance package. In some cases, the additive companies may not fully understand the specific requirements of the application, and the OEM may work directly with the oil company to develop a fluid that meets their performance requirements [32,37].

In all cases, the oil company will ultimately purchase a complete or a partial additive package plus other components from one or more additive suppliers and use these to create the final lubricant formulation.

15.6.1 Base Oils

Base oils used in transmission fluids are normally mineral oils (see Figure 15.10) refined from crude oil, preferably paraffinic crude, or synthetic oils made by chemically reacting compounds of specific chemical composition [90].

The manufacturing process of mineral oils for ATFs has greatly improved over the last several decades [91–93]. Conventional solvent refining and solvent dewaxing have given way to the use of hydrocracking and hydrotreating followed by various catalyst-based dewaxing methods. Conventional solvent refining uses solvent extraction to remove unwanted fractions, such as aromatic compounds and waxes. In contrast, hydrocracking and hydrotreating, hydrodenitrogenation, and hydrodesulfurization processes involve various degrees of hydrogenation, which remove colored contaminants and unsaturated components, nitrogen, and sulfur, respectively [94,95]. Improvements in dewaxing methods have made available mineral oils with improved oxidative stability and low temperature fluidity [96].

API has classified base oils into five groups, shown in Table 15.1, covering a range of physical and chemical properties. Mineral oils fall into three groups—Groups I, II, and III—which are defined by sulfur content, concentration of saturated hydrocarbons, and viscosity index [97].

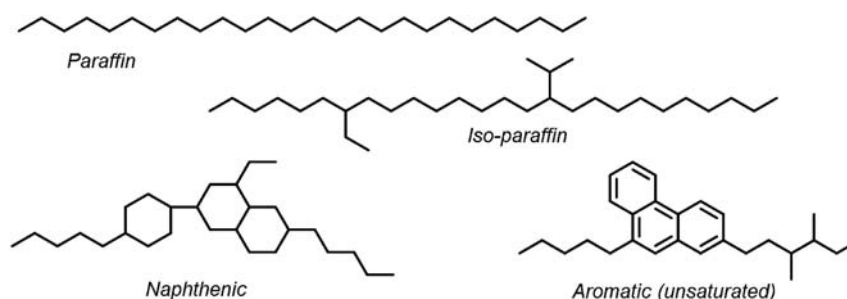


Figure 15.10—Chemical species found in base oils derived from crude oil.

TABLE 15.1—API Classification of Basestocks

Base Oil Group	Sulfur (%)		Saturated (%)	Viscosity Index
I	> 0.03	and / or	< 90	80 to 120
II	< 0.03	and	> 90	80 to 120
III	< 0.03	and	> 90	>120
IV	All polyalphaolefins (PAOs)			
V	All other basestocks not included in Groups I, II, III, or IV			

Synthetic oils fall into two groups—Group IV is for poly(alphaolefins) (PAOs) and Group V is for all other synthetic oils (e.g., poly[esters] and poly[ethers]) (see Figure 15.11).

The effect of the recent improvements in physical and chemical properties of base oils has been mostly beneficial to ATFs. These improvements significantly increase an ATF's ability to meet higher lubricant performance requirements overall. At the same time, these changes have had some negative effect on performance in some areas [91,98].

15.6.1.1 EFFECT ON LOW-TEMPERATURE PROPERTIES

Base oil quality directly affects the low-temperature fluidity of the oil itself and, as a result, also the fully formulated oil [96,99]. Generally, the more highly refined the oil, the better its low-temperature fluidity; in essence, the refining process either removes or chemically alters the constituents responsible. The introduction of more highly refined base oils has enabled OEMs to set more stringent lower temperature viscosity requirements, thus improving the operation of their transmissions in colder climates. For example, when DEXRON® II was introduced in the early 1970s [88,100,101], ATFs could be readily formulated with conventional solvent-refined Group I base oil because the maximum allowable Brookfield viscosity at -40°C was

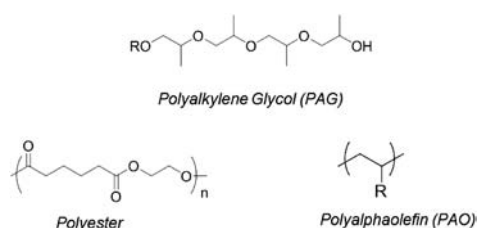


Figure 15.11—Group IV synthetic base oils.

50,000 cP. When MERCON® and DEXRON® IIE [102–104] specifications were introduced in 1987 and 1989, respectively, the maximum Brookfield viscosity at -40°C was reduced to 20,000 cP. This radical change in low-temperature viscosity requirements made it difficult to use conventional Group I solvent neutral base oils. Volatility limits preclude the use of low molecular weight materials, e.g. kerosine, as fluidizers. When MERCON® V [105] was introduced in 1996, a blend of Group II and Group IV was needed to meet the maximum Brookfield viscosity at -40°C of 13,000 cP [91,92]. When Chrysler's MS 9602 (ATF+®4) was introduced in 1998 [106], Group III or higher grade base oils were required to meet the specification of less than or equal to 10,000 cP at -40°C [89]. A Group IV base oil was necessary to satisfy General Motors' Allison Division's TES-295 specification, which stipulates a Brookfield viscosity at -40°C to be equal to or less than 8700 cP [107].

15.6.1.2 EFFECT ON ATF OXIDATION STABILITY

Along with OEMs' increasingly stringent requirements in low-temperature fluidity is their demand for better oxidation stability. Good oxidation stability is essential to achieve longer drain intervals or fill-for-life performance [96,108,109].

Unsaturated components in the base oil tend to have poor oxidation stability as compared with saturated hydrocarbons. The more highly refined base oils have fewer of these oxidatively unstable components and exhibit higher oxidation stability compared with their less refined cousins. However, even highly refined hydrocarbon base oils when subjected to the oxidative conditions found in transmissions will eventually reach a point beyond which they are unfit for service. Additive chemistry can make significant contributions to controlling oxidation processes, but not even conventional antioxidants can indefinitely stave off catastrophic oxidation of the base oil. There is an abundance of available energy and chemical oxidizers in these systems.

15.6.1.3 EFFECT ON SEAL COMPATIBILITY

Various elastomeric materials such as poly(acrylate), nitrile rubber, fluoro-elastomer (Viton®), and silicone-elastomer are used as seal materials to prevent internal and external leakage of fluid. Transmission leaks can occur when the seal materials shrink, harden, or become too soft, in some cases due to the plasticizer leaching into the oil. The base oil used in a fluid formulation has a large effect on the physical properties of elastomeric seals because certain base oil constituents such as aromatic compounds can act as replacement plasticizers. The ability to act as a plasticizer is in the order of Group I > Group II > Group III > PAO [110].

Naphthenic (cycloparaffin) and aromatic base oils are good plasticizers, for silicone, Viton®, and nitrile elastomers. Highly paraffinic hydrocracked base oils or PAOs are not as good and tend to shrink some seal materials by leaching out the original plasticizer. Replacement plasticizers, or seal swell agents (e.g., esters, aromatic compounds, or sulfones), are added to the formulation to counter this behavior. This is the main disadvantage of synthetic base oils and unconventional base oils. The dosage for seal swell agents can vary from zero to several percent by weight depending on the base oil [111,112].

15.6.2 Transmission Fluid Additive Package Components

- *Performance additives:* These are composed of molecules that have a polar head group (ionic or nonionic moieties containing oxygen, nitrogen, sulfur, or phosphorus atoms) and a nonpolar tail (long hydrocarbon chain) and include friction modifiers (FMs), antiwear (AW) additives, extreme-pressure (EP) additives, detergents and dispersants, and seal conditioning agents (see Table 15.2).
- *Oil protection additives:* These have antioxidant functionality that inhibits chemical reactions that occur when oils and additives are exposed to oxidizing conditions, especially at elevated temperatures.
- *Bulk fluid property additives:* These include VMs, pour-point depressants (PPDs), and antifoaming agents that modify the physical properties of the base oil.

FMs, AW additives, EP additives, detergents, dispersants, corrosion inhibitors, and seal swell agents are typically surface-active in nature and perform their main function while adsorbed to the various internal surfaces of the transmission. For example, FMs adsorbed on the mating surfaces of the clutch plates and corresponding steel reaction plates will affect the coefficient of friction of that system [113–118].

Surface-active compounds, or surfactants, are organic molecules that are amphiphilic, meaning they contain hydrophobic (water fearing) groups (hydrocarbon tails) and hydrophilic (water loving) groups (polar

TABLE 15.2—Functions and Treat Rate Ranges for ATF Components

Component	Percent Volume	Function
Additive package	5–15 %	
Friction modifiers		Friction durability/shudder resistance
Oxidation inhibitors		Oxidation resistance
Detergents/dispersants		Sludge resistance and friction
Corrosion inhibitors		Metal protection
Antiwear		Decreased component wear
Seal swell agents		Better seal compatibility
Antifoam		Reduce foaming tendency
Viscosity modifier	2–15 %	Improves viscometric profile
Base oil	80–90 %	Solvent, lubricant, heat transfer agent

heads). Surface-active compounds often interfere with each other by competing for the same surface; for example, a particular corrosion inhibitor or FM may enable the fluid to meet anticorrosion or friction targets, respectively, by adsorbing onto surfaces. However, those same additives may also adsorb so strongly that the AW agents necessary for gear protection are excluded from the surface, resulting in fatigue or wear failures or both [119]. Successful lubricants of all types need to have a carefully balanced additive system to achieve the required overall performance. This balance can be disturbed by the addition of aftermarket top-treatments (additives marketed as enhancements and added to the fully formulated lubricant). Top-treatments may enhance one attribute of the fluid (as advertised) but likely at the expense of another attribute.

15.6.3 Viscosity and VIs

VIIs (viscosity index improvers), or VMs (viscosity modifiers), are polymers added to mineral oils to maintain viscosity at higher temperatures (see Figure 15.12). At low temperatures these polymers curl upon themselves and

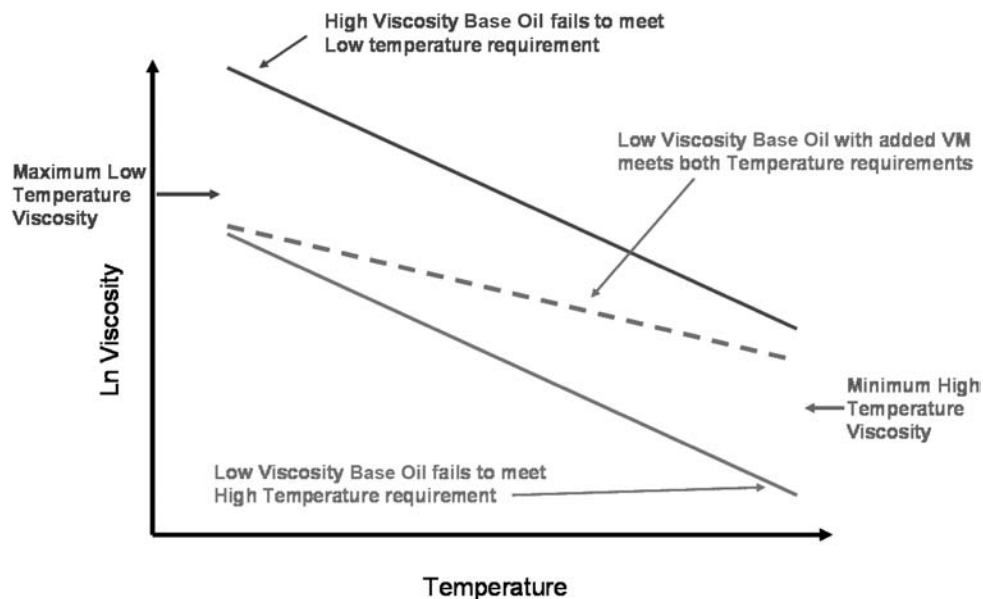


Figure 15.12—Idealized schematic of the viscosity-temperature relationship.

occupy a small volume and consequently interact little with the bulk oil. This results in little change in the viscosity of the bulk oil. As the temperature is increased, the polymer uncurls and interacts to a greater extent with the bulk oil, effectively increasing the viscosity of the fluid. The major effect of these additives is in improving low-temperature viscometrics while maintaining appropriate viscometrics at high temperature [120]. PMAs are preferred for AT and DCT applications as well as for CVT and MT fluids [121–129].

Globally, most specifications call for specific viscometric properties at high and low temperature, but they may differ as to viscosity retention during use. Low-temperature fluidity is important because of the effect on hydraulic system pressure rise times, viscous drag on the engine starting system, and maintenance of flow to the hydraulic pump to supply oil pressure [130].

15.6.3.1 EFFECT OF SHEAR ON VISCOSITY

The viscosity of base oil, either mineral or synthetic, is not expected to change significantly when it is subjected to shear. However, high-molecular-weight VIIs are often added to the ATF formulation and these are affected by shear [121,122]. The introduction of relatively high-molecular-weight VIIs to ATF can introduce permanent or temporary viscosity loss. Permanent viscosity loss occurs when the high-molecular-weight polymer breaks down as a result of shearing. Temporary viscosity loss occurs when a fluid is under high shear rate and the viscosity is reduced reversibly, meaning the viscosity will be restored as soon as shearing returns to the low shear rate [131–133].

15.6.4 PPDs

The pour point of a lubricant is the lowest temperature at which the lubricant will no longer pour. It is a rough indication of the lowest temperature at which the lubricant is readily pumpable and is particularly important for proper performance in colder climates.

As a lubricant is cooled, wax crystals begin to form. These crystals eventually join to produce a gel-like structure, which thickens the oil, which can lead to oil starvation because of blocking of oilways. Pour point depressants (PPDs) act to reduce crystal growth and prevent gelling, thereby lowering the temperature at which the lubricant can effectively function (see Figure 15.13). These are typically polymers similar to VIIs but of a lower molecular weight [134].

15.6.5 FMs and Friction Performance Criteria

The selection of proper friction characteristics for an ATF is of paramount importance for the drivability of the vehicle. Whereas in an engine the goal is usually to decrease the

friction on sliding parts as much as possible to improve efficiency, in a transmission the goal is usually to maintain a specific level of friction in the clutch systems over the service life of the fluid [50,52,98,135–138].

FMs are long-chain molecules with polar head groups and nonpolar hydrocarbon tails. The polar head group is designed to adsorb on (i.e., form a physical bond with) metal and composite friction material surfaces and, together with the length and structure of the hydrocarbon tail, creates a friction-modifying film. There are many useful friction-modifying additives; in general, they include fatty amines, carboxylic acids, alcohols, esters, and amides. Important structural variations include the number, type, and oxidation state of the heteroatoms that make up the polar head. These head-group variations dictate the FM's degree of association with the various surfaces, and the length, number, and shape of the hydrocarbon tail(s) connected to the polar head group play a role in determining the overall FM solubility and the nature of the surface film [113,114,116,139–143].

Design and control philosophies as well as transmission torque density requirements dictate the selection of the friction material and fluid properties. The coefficient of friction is a characteristic of the entire clutch system, and the observed friction depends on the nature of the composite friction material; the steel reaction member; and the characteristics of the fluid at various speeds, pressures, and temperatures [56,57,144–149].

Smooth clutch engagements are typically associated with a friction characteristic known as “positive Mu-v.” This term describes the slope of the coefficient of friction versus sliding speed curve of the clutch system (see Figure 15.14). When the Mu-v curve has a positive slope, the coefficient of friction increases as relative sliding speed increases, or it decreases as relative speed decreases. A “negative Mu-v” in a clutch system suggests inadequate friction modification and may result in harsh clutch engagements. In such a case it is possible to set up a stick-slip condition that may result in noise, such as a squawk or squeal audible to the driver, or a vibrational shudder that can be felt by the driver [56,147,150–152].

Durability of the friction characteristics are related to several factors, including the chemical stability of the FM system and the propensity of the fluid to degrade on and within the friction interface [153,154]. Like all components in the ATF, FMs can be thermally or oxidatively degraded. If sufficient modifier is degraded, then the friction performance of the fluid will also degrade.

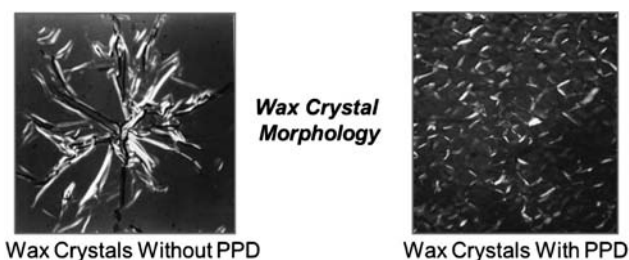


Figure 15.13—Wax crystals in oil with and without a pour-point depressant.

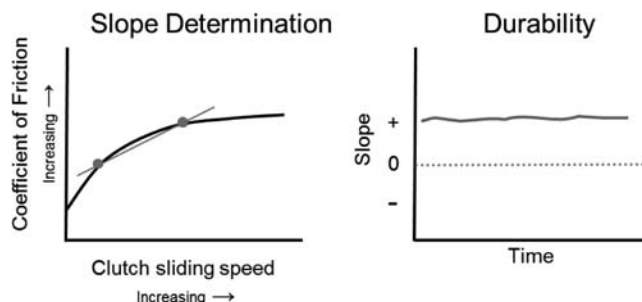


Figure 15.14—Illustration of a positive slope in a coefficient of friction vs. sliding speed curve along with slope durability with time.

If the fluid degrades at the friction interface, even when the FM concentration is largely unchanged, then friction performance may also suffer. In such cases, degradation products deposit on the friction material surfaces because of high temperatures at the friction interface or the propensity of particular additives to form glaze deposits [21,155].

The remaining classes of additives all behave, to varying degrees, as FMs. Some are considered part of the primary FM system; for others, the formulator needs only account for their effect, positive or negative, on the overall friction characteristics of the fluid.

15.6.6 Dispersants

Dispersants are part of the primary FM system; their effects are largely on dynamic friction. Like FMs, rust inhibitors, and detergents, dispersants also consist of polar head groups combined with nonpolar tails, generally consisting of 50–150 carbon atoms. Dispersants also suspend oil-insoluble degradation products, small particulates, and water, thereby reducing the deposition of solids within the transmission. The polar groups surround degradation products, which are themselves polar in nature, whereas the nonpolar tails keep the entire assembly soluble in the oil [156,157].

The most commonly used dispersants are polyisobutylene succinimides, polyisobutylene succinate esters, and Mannich bases (see Figure 15.15).

15.6.7 Detergents

Detergents are metal salts of organic acids (soaps) made by neutralizing the acid with a metal oxide or metal hydroxide. Detergents can contain more oxide or hydroxide than necessary to neutralize the acid and the excess is referred to as the overbase. This overbase is available to neutralize acids that

may form through oxidation of the oil, which may be surface active or degrade elastomers like silicone based seals. The soap portion of the detergent operates by dispersing fluid degradation products and preventing the deposition of these materials from adhering to active surfaces. In transmission fluids they primarily provide balanced friction for clutch and synchromesh performance in ATFs and MTFs in conjunction with a suitable FM system [158].

The organic acid part of the detergent is usually a sulfonic acid or phenol or salicylic acids, which yield sulfonates, phenates, and salicylates, respectively (see Figure 15.16). The “R group,” in this case an alkyl chain, for detergents is much shorter than those used in dispersants, typically 24–30 carbon atoms total. Neutral detergents are used to clean and keep clean high-temperature areas of equipment.

Overbased detergents are prepared by adding more metal oxide or hydroxide than is necessary to neutralize the acid moiety. This excess base is reacted with carbon dioxide to produce an oil-soluble material that contains a core of metal carbonate surrounded by the oil-solubilizing detergent substrate (see Figure 15.16).

15.6.8 AW and EP Agents

Unlike FMs, AW and EP agents chemically react with metal surfaces and are important at elevated loads and reduced speeds in which the viscosity of the oil is insufficient to maintain a hydrodynamic lubrication film [120] and the system moves to boundary lubrication [81,119,159–166]. Under these conditions of mixed to boundary contact, interfacial temperatures between metal parts rise high enough to activate AW and EP additives. AW components generally contain phosphorus esters or thioesters and are activated at contact temperatures of approximately

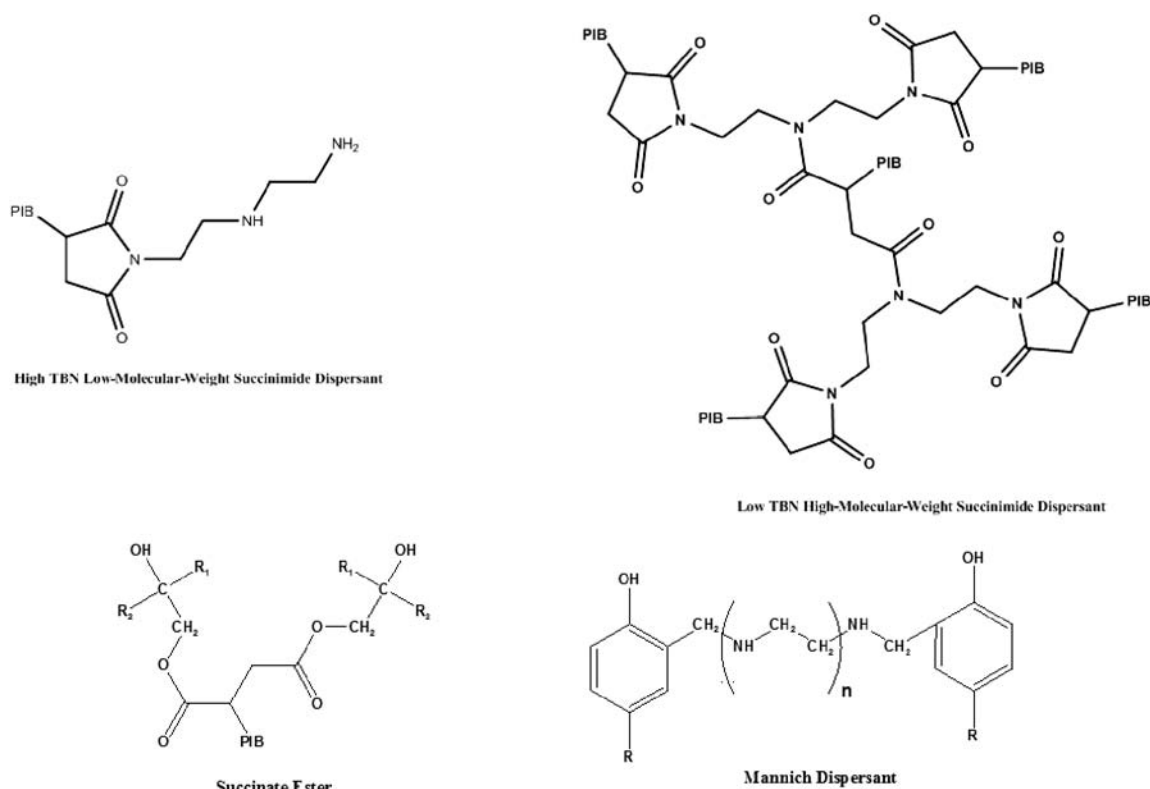


Figure 15.15—Dispersants typically used in automotive applications.

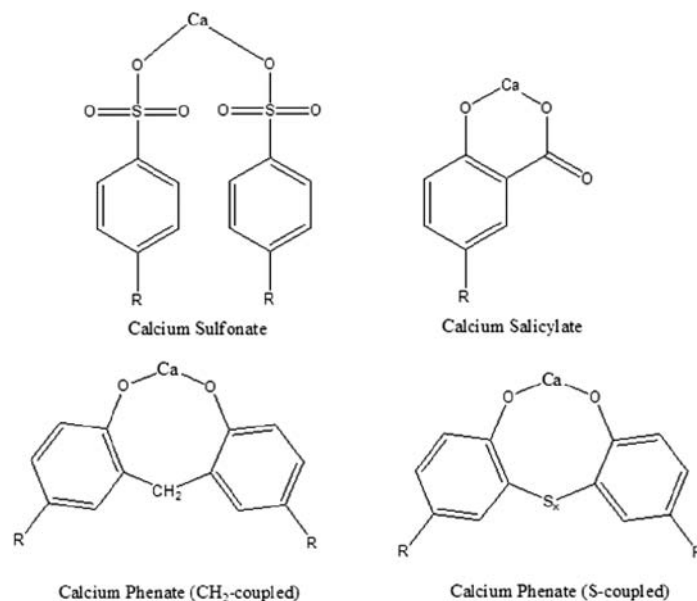


Figure 15.16—Detergents typically used in automotive applications.

80–100°C. EP components generally contain alkyl sulfides and are activated at contact temperatures of approximately 100°C [119]. Whereas this affords good protection for metal parts, the activation of these additives at the clutch interface can lead to a loss of torque transfer quality through the deposition of thermal degradation products on and within the clutch plate.

EP agents are additives used to prevent seizing under boundary lubrication conditions. EP agents are similar to AW additives because they both work to protect gears and bearings, among other components. However, AW agents perform under mixed boundary conditions; EP agents perform under more severe boundary conditions and create controlled wear that polishes the metal surface, increasing the real contact area, which reduces friction and surface stress [119,167].

EP agents typically contain organic sulfur, phosphorus, or chlorine compounds (see Figure 15.18), which can chemically react with the metal surface under high-pressure or high-temperature conditions or both to form metal salts. With increased oil and chemical industry legislation, the use of chlorine compounds as EP agents is now restricted to special applications, although chlorine compounds are very effective at preventing wear under extreme conditions.

Because EP and AW additives are very surface-active, they can interfere with the performance of other surface-active additives, even other EP and AW additives, which are competing for the same surfaces. Copper corrosion inhibitors are known to outcompete EP additives, lowering their effectiveness. A good balance of AW and EP additives with each other, and with the rest of the components of the formulation, is generally critical for good overall performance.

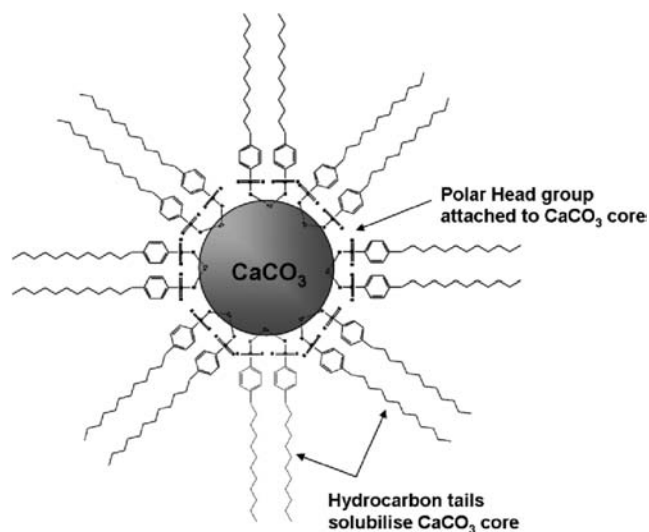


Figure 15.17—Schematic diagram of detergent molecules surrounding calcium carbonate.

15.6.9 Rust and Corrosion Inhibitors

Corrosion protection is required for ferrous metal rusting when moisture inevitably enters the transmission as well as for copper and other alloys used in bushings, thrust washers, and electrical control contacts and wires (see Figure 15.19). Corrosion of ferrous materials is typically called rust and requires the presence of water and a strong oxidant or acid. The term corrosion tends to relate to other metals such as those containing copper (e.g., brass or bronze) and lead. Additives that protect ferrous materials from corrosion are usually referred to as rust inhibitors.

Overbased detergents neutralize acidic species in the lubricant before they can cause corrosion, whereas neutral detergents are able to form a surface-covering barrier to prevent acidic species from directly contacting the metal components of engines and transmissions. Other rust inhibitors include long-chain alkyl phosphates, amine phosphates, and partial esters of succinic acid. These adsorb onto the metal surface to form a barrier that excludes water reaching the surface, thereby reducing corrosion.

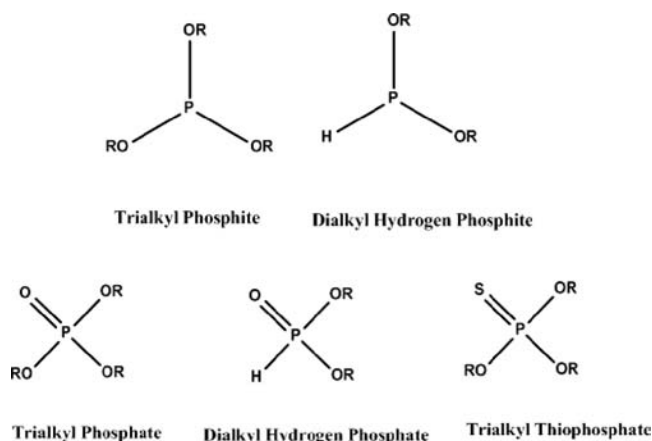


Figure 15.18—Typical phosphorus-containing AW additives used in automotive applications.

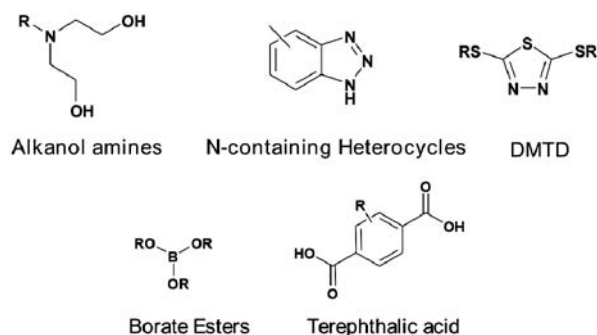


Figure 15.19—Typical rust and corrosion inhibitors used in automotive applications.

Copper is susceptible to attack by reactive sulfur compounds such as those found in high-sulfur-content mineral oils and some EP agents. Copper corrosion inhibitors (e.g., benzotriazole and substituted azoles and their derivatives) adsorb on the copper surface, forming a tenacious surface layer that protects the surface from chemical attack. By doing so, they also reduce the catalytic effect of copper on the oxidation rate of the lubricant. For this reason, these materials are also referred to as metal deactivators [156].

15.6.10 Oxidation Inhibitors

All lubricating oils undergo oxidative degradation in their working environments [108,168]. The mechanism of oxidation can be complicated for single species, and trying to account for the vast number of different species that are found in any lubricating oil makes understanding the effects of oxidation extremely difficult. The oxidation process itself can fortunately be reduced to four basic steps: initiation, propagation, chain branching, and termination [156]. These are free radical reactions, and the oxidation inhibitors (antioxidants) are molecules that either scavenge free radicals or decompose hydroperoxides, interrupting one or more steps in the process.

15.6.11 Seal Swell Agents

Elastomers and elastomeric seals may be formulated with a plasticizer to give them flexibility, softness, and other properties much like phthalates are used in vinyl plastics such as automobile dashboards. These plasticizers can be

leached out into the lubricant over time. The effects of heat and time also may cause changes in the elastomer's chemical structure, causing contraction in volume and hardening. The net effect of the shrinkage can be the loss of proper sealing and leakage of the fluid around the seal.

By putting a seal swelling or seal conditioning additive into the lubricant, these effects can be counteracted. Seal swelling agents have a high affinity for the rubber, penetrate into the body of the elastomer to counteract the shrinkage, and will preferentially remain in the elastomer functioning as a replacement plasticizer [156].

15.6.12 Foam Inhibitors

Controlling foam and air entrainment is important to retard unwanted fluid volume growth and fluid ejection from the transmission as well as loss of incompressibility of the fluid for hydraulic function. The difference between foam and entrained air is that air entrainment is the result of extremely small bubbles dispersed throughout the bulk of the oil, and foam is a dispersion of a gas in a liquid in which the individual gas bubbles are separated by thin liquid films called lamellae.

Foam inhibitors are generally silicones, fluorinated silicones, or acrylate esters that work by disrupting the film around the bubble, facilitating film breakage. These additives are present in very small concentrations (<15 ppm Si is typically observed in a fully formulated driveline fluid). Acrylates are used at somewhat higher concentrations [169–171].

15.6.13 Other Additives

When needed, additives such as dyes, emulsifiers, or demulsifiers may be incorporated into a driveline fluid.

15.7 A BRIEF HISTORY OF TRANSMISSION FLUID SPECIFICATIONS

All transmission fluid specifications include information on the following:

- Physical and chemical properties that define the fluid;
- Friction performance criteria;
- Wear performance criteria;
- Oxidation, rust, and corrosion performance criteria; and
- Antifoam and seal compatibility requirements.

Transmission fluid specifications are established by the OEMs (i.e., the vehicle or the transmission manufacturer) and define a series of performance criteria that the fluid must meet to ensure acceptable in-vehicle performance. In some cases (e.g., Chrysler's MS-9602), a particular additive package will be specified [89,172].

When a new fluid specification is developed, a series of performance targets are generally established. These targets are generally set such that the stress on the fluid is significantly more severe than that anticipated in the actual application. The proper mixture of additive chemistry, VIIs, and base oil(s) are formulated and tested against these targets. During the development cycle, things can change as new information is generated and, as a result, the actual test methods for evaluating the fluids may change. The end result is a fluid well matched to a particular type or group of transmissions capable of ensuring acceptable performance and a long, trouble-free operation over the fluid's service life.

When ATs were first introduced in the late 1930s and until about 1949, they were generally lubricated with engine oil [84]. However, transmissions had different performance requirements than engines, and the use of engine oils for this application was soon found to be inadequate. Some specialized fluids were used in ATs during this time period, but the first specification to standardize the requirements for ATFs was introduced in 1949 by General Motors. This first specification for a mineral-oil-based ATF was designated as "Type A" [84]. Importantly, the Type A specification also provided a process for qualification of service-fill ATFs through a trademark and licensing procedure. Further advances in this specification occurred when it was found that some Type-A-qualified ATFs showed deficiencies in oxidation resistance, which led to the introduction of the Type A, Suffix A (or TASA) specification in 1957 [173]. During this time period, many manufacturers used Type A or TASA fluids for their AT-equipped vehicles [86]. The Ford Motor Company's factory-fill fluids met specification ESW M2C33-A-B that described a fluid with the TASA characteristics [174].

Ford introduced the ESW M2C33-C-D specification in 1961 after it was approved for service fluid use in 1960 vehicles [175]. This change was driven by the need for better oxidation control that was measured by the new Merc-O-Matic Oxidation Test. Also, the AW and torque capacity performance improvements were included in this specification [86].

In 1967 Chrysler, Ford, and General Motors introduced upgraded specifications. Ford had the objective of a fluid with improved antioxidation, wear, and friction

performance that would be "fill-for-life." This new fluid was described by the ESW M2C33-E-F specification and was conventionally called "Type F" [86]. In Ford specifications ESW M2C33-A-B, ESW M2C33-C-D, and ESW M2C33-E-F, the first suffix letter refers to the natural, undyed fluid and the second to red-dyed fluid [176]. ESW M2C33-F was also a service-fill specification, and Ford granted approvals under the specification along with qualification numbers. Differences included a six-pack clutch friction test that required a high static coefficient of friction. It was believed at Ford that an ATF with a friction curve similar to base oil would undergo less frictional change with time than a fluid that incorporated a chemical FM. The rationale was that the FM could degrade, and the friction characteristics would revert to those of the base oil. Another driving force was to reduce the number of plates in the clutch pack to get a more consistent shift characteristic. Oxidation resistance performance was increased through raising the temperature of the Merc-O-Matic Oxidation Test from 300 to 325°F [83,85,86].

Also in 1967, General Motors introduced the DEXRON® Specification [177]. The primary issues addressed by this new specification included longer shift-time retention and clutch plate durability. Also addressed were improvements in low-temperature viscosity, antifoam characteristics, oxidation resistance, and seal and nylon compatibility with the fluid. DEXRON also became a registered trademark and included qualification procedures and testing protocols to ensure the quality of service fill DEXRON fluids in the marketplace.

Chrysler also upgraded its requirements for ATF in this time period with a new specification for factory fill, MS-4228 [178], replacing the older MS-3256 [179] that had described a TASA-type fluid [87]. Particular attention was given to low-temperature viscosity in this specification to provide for adequate time to start and time to shift at low temperatures. Oxidation resistance of fluids was improved under the new specification by the use of a special Chrysler bench oxidation test.

Ford deviated from the Type F concept of a high static friction fluid with the introduction of the ESW M2C138-CJ specification in 1974, which called for a friction-modified fluid with lower static friction [180]. This type of fluid was introduced to alleviate the difficult engineering task of reducing gear engagement noise with fluids designed for high static friction. A new friction test was introduced that called for a narrow band of acceptability in the ratio of static to dynamic friction in the ESW M2C138-CJ fluids. DEXRON® II was introduced in 1973 with improved wear performance and improved low-temperature fluidity [100].

Ford introduced its ESP M2C166-H [181] specification for factory-fill fluids requiring improved friction characteristics in lock-up torque converters for factory-fill fluids. In this specification, Ford introduced the Aluminum Beaker Oxidation Test (ABOT) [182] to replace the oxidation test performed in a motored transmission. Ford then introduced the MERCON® Service Fill Transmission Fluid Specification in January 1987 to match the performance expected from the ESP M2C166-H factory-fill fluid. MERCON® was a trademarked fluid with procedures for qualification and licensing of fluids to ensure quality in the marketplace [102,183]. In September 1992, Ford revised the MERCON® performance limits changing low-temperature viscosity

requirements, volatility requirements, viscosity difference limits after exposure to high temperatures, and improved oxidation performance [183]. In 1989, General Motors introduced the DEXRON® IIE specification [103], the DEXRON® III in 1993 [109], and a series of upgrades—DEXRON® IIIG in 1990 and DEXRON® IIHH in 2004 [184–186].

By 1987, service fill fluids were developed that met all major ATF specifications, MERCON®, DEXRON® II and III, and Chrysler's MS-7176 (ATF+®3) [187]. These were generally called “DEXRON/MERCON” fluids [188]. ATF specifications started to diverge [189] in 1996 with the release of Ford's MERCON® V (Roman numeral 5, not the letter ‘V’) [105] specification and DaimlerChrysler's MS-9602 (ATF+®4) specification. The MERCON® V specification included new friction requirements because of the development of modulated and continuous slipping torque converter clutches and requirements for verifying AW performance and antishudder characteristics [3]. Chrysler's new ATF represented a complete performance upgrade including improved viscosity retention, oxidative stability, low-temperature viscosity, AW performance, and friction durability [89,106].

Ford introduced their MERCON® SP specification in 2004 describing a lower viscosity fluid specifically for their six-speed, rear-wheel-drive applications [190]. In 2007, the MERCON® LV (Low Viscosity, not 55) was designed to be fill for life and offered stable friction performance, potential fuel economy benefits, improved antishudder performance, greater oxidation resistance, and improved antifoaming and aeration performance [191,192].

In early 2005, General Motors unveiled a new ATF for all of their GM Powertrain stepped gear ATs called DEXRON® VI [34,172]. Improvements included friction durability [108], oxidation resistance, aeration and foam control, viscosity stability, and the fluid has the potential to enable improved fuel economy and extended drain intervals. A few significant tests have been added to the specification. The cold crank simulator is now required as a measure of low-temperature pumpability and a film thickness evaluation, which at the time had to be done at Imperial College, London, UK. Also included in the new specification were viscosity stability as measured by a 40-h KRL tapered roller bearing shear test and the replacement of the GM Foam Test with ASTM D892.

Table 15.3 provides a progression of the ATF specifications from the major North American manufacturers during this time period.

15.8 CONCLUSIONS

When ATs were first introduced in the late 1930s and until about 1949, they were generally lubricated with engine oil. However, transmissions had different performance requirements than engines, and the use of engine oils for this application was soon found to be inadequate. Some specialized fluids were used in ATs during this time period, but the first specification to standardize the requirements for ATFs was introduced in 1949 by General Motors. Since that time, ATFs have evolved from their engine oil heritage into one of the most highly engineered and carefully crafted components in the modern automobile. OEM specification requirements ensure that approved fluids perform in several tests designed to simulate conditions that often exceed anything the fluid will be exposed to in actual service. To not

TABLE 15.3—History of the Specification of ATF Viscosity in North America

Specification	Number	Year	Company
Type A		1949	GM
Type A, Suffix A		1957	GM
Type F		1959	Ford
MS-3256		1964	Chrysler
MS-4228		1966	Chrysler
DEXRON®		1967	GM
DEXRON®-II*	6137M	1973	GM
M2C138-CJ		1974	Ford
DEXRON®-II	6137M	1978	GM
MS-7176D		1980	Chrysler
M2C166-H		1981	Ford
MERCON®		1987	Ford
DEXRON®-IIE	6137- M	1990	GM
DEXRON®-IIE-Rev.	6137- M	1992	GM
DEXRON®-III	6297- M	1993	GM
MERCON® V	M2C185-A	1996	Ford
DEXRON®-IV	6301- M	1997	GM
DEXRON®-IIIG**	6417- M	1997	GM
DEXRON®-III***	6418- M	1997	GM
MS9602, Change C		1999	DaimlerChrysler
MS9602, Change E		2002	DaimlerChrysler
DEXRON®-IIHH	GMN10055	2004	GM
MS9602, Change F		2003	DaimlerChrysler
MERCON® SP		2004	Ford
DEXRON®-VI	GMN10060	2005	GM
MS9602, Change G		2006	DaimlerChrysler
MERCON® LV		2007	Ford

just meet, but often exceed, these performance requirements, quality ATFs contain various components including FMs, dispersants, detergents, AW additives, oxidation inhibitors, seal conditioning agents, rust and corrosion inhibitors, antifoaming agents, and VIIs all dissolved or dispersed into highly refined mineral oils or a synthetic lubricating oil or both. The technology of ATs will continue to evolve in response to the desires of the automobile consumer. New and innovative transmission designs (e.g., DCTs and CVTs) create unique and interesting challenges that will drive innovation in lubricant technology.

References

- [1] Wikipedia, 2011, “Manual Transmission.” Available at http://en.wikipedia.org/wiki/Manual_transmission (accessed October 30, 2011).
- [2] Wikipedia, 2011, “Automatic Transmission.” Available at http://en.wikipedia.org/wiki/Automatic_transmission (accessed September 1, 2011).

- [3] Wikipedia, 2011, "Manumatic." Available at <http://en.wikipedia.org/wiki/Tiptronic> (accessed September 2, 2011).
- [4] Wikipedia, 2011, "Porsche." Available at <http://en.wikipedia.org/wiki/Porsche> (accessed January 5, 2012).
- [5] "Porsche Automobile Holding SE." Available at <http://www.porsche-se.com/pho/en/> (accessed January 5, 2012).
- [6] Wikipedia, 2011, "Transmission (Mechanics)." Available at [http://en.wikipedia.org/wiki/Transmission_\(mechanics\)](http://en.wikipedia.org/wiki/Transmission_(mechanics)) (accessed September 6, 2011).
- [7] "ZF Friedrichshafen AG." Available at <http://www.zf.com/corporate/en/homepage/homepage.html> (accessed June 23, 2011).
- [8] Kao, C.-K., Smith, A.L., and Usoro, P.B., 2003, *Fuel Economy and Performance Potential of a Five-Speed 4T60-E Starting Clutch Automatic Transmission Vehicle*, SAE Technical Paper 2003-01-0246, SAE, Warrendale, PA.
- [9] How Stuff Works, 2011, "How Automatic Transmissions Work." Available at <http://www.howstuffworks.com/automatic-transmission.htm> (accessed March 3, 2011).
- [10] Wikipedia, 2011, "Torque Converter." Available at http://en.wikipedia.org/wiki/Torque_converter (accessed July 25, 2011).
- [11] Bosch, R., 1993, "Hydrodynamic Couplings and Converters." In *Automotive Handbook*, 3rd ed., Wiley, New York, p. 539.
- [12] Kluger, M.A., and Long, D.M., 1999, *An Overview of Current Automatic, Manual and Continuously Variable Transmission Efficiencies and their Projected Improvements*, SAE Technical Paper 1999-01-1259, SAE, Warrendale, PA.
- [13] Wikipedia, 2011, "Epicyclic Gearing." Available at http://en.wikipedia.org/wiki/Epicyclic_gearing (accessed August 16, 2011).
- [14] Lynwander, P., 1983, *Gear Drive Systems: Design and Applications*, Marcel Dekker, New York.
- [15] Anderson, A.E., 1972, *Friction and Wear of Paper Type Wet Friction Elements*, SAE Technical Paper 720521, SAE, Warrendale, PA.
- [16] Stebar, R.F., Davidson, E.D., and Linden, J.L., 1990, *Determining Frictional Performance in Automatic Transmission Fluids in a Band Clutch*, SAE Technical Paper 902146, SAE, Warrendale, PA.
- [17] Lam, R.C., and Kowal, S., 1992, *Fluid Transport Phenomena During the Engagement of Fiber-Reinforced Polymeric Friction Materials*, SAE Technical Paper 922097, SAE, Warrendale, PA.
- [18] Kitahara, S., and Matsumoto, T., 1994, "Present and Future Trends in Wet Friction Materials," *Jap. J. Tribology*, Vol. 39.
- [19] Ito, K., Barker, K.A., Kubota, M., and Yoshida, S., 1998, *Designing Paper Type Wet Friction Material for High Strength Durability*, SAE Technical Paper 982034, SAE, Warrendale, PA.
- [20] Kimura, Y., and Otani, C., 2005, "Contact and Wear of Paper-Based Friction Materials for Oil-Immersed Clutches—Wear Model for Composite Materials," *Tribology Int.*, Vol. 38, pp. 943–950.
- [21] Newcomb, T., Sparrow, M., and Ciupak, B., 2006, *Glaze Analysis of Friction Plates*, SAE Technical Paper 2006-01-3244, SAE, Warrendale, PA.
- [22] Haviland, M.L., Rodgers, J.J., and Davison, E.D., 1963, *Surface Temperatures and Friction in Lubricated Clutches*, SAE Technical Paper 630028, SAE, Warrendale, PA.
- [23] Matsumoto, T., 1993, *A Study of the Influence of Porosity and Resiliency of a Paper-Based Friction Material on the Friction Characteristics and Heat Resistance of the Material*, SAE Technical Paper 932924, SAE, Warrendale, PA.
- [24] Miura, T., Sekine, N., Azegami, T., Murakami, Y., Itonaga, K., and Hasegawa, H., 1998, *Study on the Dynamic Property of a Paper-Based Wet Clutch*, SAE Technical Paper 981102, SAE, Warrendale, PA.
- [25] Grzesiak, A., and Lam, R.C., 1992, *Application of Fluid Transport Phenomenon to Transmission Band Friction Material*, SAE Technical Paper 922098, SAE, Warrendale, PA.
- [26] Fein, R.S. 1992, "Liquid Lubricants," *ASM Handbook, Friction Lubric. Wear*, Vol. 18, pp. 81–88.
- [27] Kemp, S.P., and Linden, J.L., 1990, *Physical and Chemical Properties of a Typical Automatic Transmission Fluid*, SAE Technical Paper 902148, SAE, Warrendale, PA.
- [28] Klaus, E.E., and Tewksbury, E.J., 1984, "Liquid Lubricants." In *Handbook of Lubrication, Theory and Practice of Tribology* Vol. 2, E.R. Booser, Ed., CRC Press, Boca Raton, FL, pp. 229–254.
- [29] Caines, A.J., and Haycock, R.F., 1996, *Automotive Lubricants Reference Book*, SAE, Warrendale, PA.
- [30] Tipton, C.D., 2006, "Automatic Transmission Fluids." In *Handbook of Lubrication and Tribology*, 2nd ed., G.E. Totten, Ed., CRC, Boca Raton, FL.
- [31] Abraham, W.D., Lann, P.L., Ikeda, M., and Tipton, C.D., 2007, *Future Automatic Transmission Fluids Now! The Melding of New Technology with Global OEM Needs*, SAE Technical Paper 2007-01-3975, SAE, Warrendale, PA.
- [32] Kurosawa, O., Matsui, S., Komiya, K., Morita, E., and Kawasaki, Y., 2003, *Development of the Fuel Saving Low Viscosity ATF*, SAE Technical Paper 2003-01-3257, SAE, Warrendale, PA.
- [33] Ito, M., Kurosawa, O., and Matsuoka, T., 2004, *The Evaluation of the Fuel-Economy Performance of Low-Viscosity Drive-Train Lubricants and the Development of Oils with Improved Fatigue Life*, SAE Technical Paper 2004-01-3029, SAE, Warrendale, PA.
- [34] Fewkes, R., Calcut, B., and Willis, A., 2006, *General Motors DEXRON-VI Global Service-Fill Specification*, SAE Technical Paper 2006-01-3242, SAE, Warrendale, PA.
- [35] Kurihara, I., 2007, *Design and Performance of Low-Viscosity ATF*, SAE Technical Paper 2007-01-3974, SAE, Warrendale, PA.
- [36] Lewis, C., and Bollwahn, B., 2007, *General Motors Hydra-Matic & Ford New FWD Six-Speed Automatic Transmission Family*, SAE Technical Paper 2007-01-1095, SAE, Warrendale, PA.
- [37] Yamamori, K., Saitou, K., Kobiki, Y., Ogawa, A., 2003, *Development of New Automatic Transmission Fluid for Fuel Economy*, SAE Technical Paper 2003-01-3258, SAE, Warrendale, PA.
- [38] Kluger, M., and Greenbaum, J.J., 1993, *Automatic Transmission Efficiency Characteristics and Gearbox Torque Loss Data Regression Techniques*, SAE Technical Paper 930907, SAE, Warrendale, PA.
- [39] Ward, W.C., and Copes, R.G., 1993, "The Next ATF Challenge—Meeting Fuel Efficiency Needs and Providing Driver Satisfaction." Paper presented at the NPRA Annual Meeting, Paper ID AM-93-06.
- [40] Ota, H., Nozaki, K., Honda, A., Kinoshita, M., Aoki, T., Todo, M., and Iwase, M., 2007, *Toyota's World First 8-Speed Automatic Transmission for Passenger Cars*, SAE Technical Paper 2007-01-1101, SAE, Warrendale, PA.
- [41] Kamada, Y., Wang, N., Kotanigawa, T., Kawabata, J., Araki, M., and Mukaida, K., 1998, "Wet Friction Materials for Continuous Slip Torque Converter Clutch—Fuel Economy Improvement of Passenger Cars Equipped with Automatic Transmission." *Tribology Series*, Vol. 34, pp. 527–533.
- [42] Kono, K., Itoh, H., Nakamura, S., Yoshizawa, K., and Osawa, M., 1995, *Torque Converter Clutch Slip Control System*, SAE Technical Paper 950672, SAE, Warrendale, PA.
- [43] Throop, M.J., and McWatt, D.G., 1997, *Slipping Torque Converter Clutch Interface Temperature, Pressure and Torque Measurements Using Inductively Powered Radiotelemetry*, SAE Technical Paper 970679, SAE, Warrendale, PA.
- [44] Guan, J.J., Willermet, P.A., Carter, R.O., Melotik, D.J., 1998, *Interaction between ATFs and Friction Material for Modulated Torque Converter Clutches*, SAE Technical Paper 981098, SAE, Warrendale, PA.
- [45] Chen, Y.F., 1998, *Friction Material for Slip Clutch Applications*, SAE Technical Paper 981101, SAE, Warrendale, PA.
- [46] Lam, R.C., and Chen, Y.-F., 1994, *Friction Material for Continuous Slip Torque Converter Applications: Anti-Shudder Considerations*, SAE Technical Paper 941031, SAE, Warrendale, PA.
- [47] Slough, C.G., Everson, M.P., Jaklevic, R.C., Melotik, D.J., and Shen, W., 1996, "Clutch Shudder Correlated to ATF Degradation through Local Friction vs. Velocity Measurements by a Scanning Force Microscope," *Tribology Trans.*, Vol. 39, pp. 609–614.
- [48] Berger, E.J., Sadeghi, F., and Krousgrill, C.M., 1997, "Torque Transmission Characteristics of Automatic Transmission Wet Clutches: Experimental Results and Numerical Comparison," *Tribology Trans.*, Vol. 40, pp. 539–548.
- [49] Lam, R.C., Chavdar, B., and Newcomb, T., 2006, *New Generation Friction Materials and Technologies*, SAE Technical Paper 2006-01-0150, SAE, Warrendale, PA.

- [50] Devlin, M.T., Li, S., Tersigni, S.H., Turner, T.L., Jao, T.-C., Yatsunami, K., and Cameron, T.M., 2003, *Fundamentals of Anti-Shudder Durability: Part II—Fluid Effects*, SAE Technical Paper 2003-01-3254, SAE, Warrendale, PA.
- [51] Li, S., Devlin, M.T., Tersigni, S.H., Jao, T.-C., Yatsunami, K., and Cameron, T.M., 2003, *Fundamentals of Anti-Shudder Durability: Part I—Clutch Plate Study*, SAE Technical Paper 2003-01-1983, SAE, Warrendale, PA.
- [52] Cameron, T.M., 2004, *ATF Friction Properties and Shift Quality*, SAE Technical Paper 2004-01-3027, SAE, Warrendale, PA.
- [53] Wikipedia, 2011, "Dual Clutch Transmission." Available at http://en.wikipedia.org/wiki/Dual_clutch_transmission (accessed November 9, 2011).
- [54] "BorgWarner Inc." Available at <http://www.borgwarner.com/en/default.aspx> (accessed January 8, 2012).
- [55] The Lubrizol Corporation, 2012. "DCTfacts." Available at <http://www.dctfacts.com/> (accessed January 8, 2012).
- [56] Lam, R.C., Chen, Y.-F., and Newcomb, T., 2001, "Wet Start Clutch and Related Slip Clutch Designs: Friction Interface Considerations." In *Proceedings of the 2001 International Symposium on the Tribology of Vehicle Transmissions*, pp. 24–33.
- [57] Hurley, S., Tipton, C.D., and Cook, S.P., 2006, *Lubricant Technology for Dual Clutch Transmissions*, SAE Technical Paper 2006-01-3245, SAE, Warrendale, PA.
- [58] Abo, K., Kobayashi, M., and Kurosawa, M., 1998, *Development of a Metal Belt-Drive CVT Incorporating a Torque Converter for Use with 2-Liter Class Engines*. SAE Technical Paper Series 980823, SAE, Warrendale, PA.
- [59] Kawabara, S., Fujii, T., and Kanehara, S., 1998, *Power Transmitting Mechanisms of CVT Using a Metal V-Belt and Load Distribution in the Steel Ring*, SAE Technical Paper Series 980824, SAE, Warrendale, PA.
- [60] Mozer, H., Piepenbrink, A., and Sommer, S., 2001, *The Technology of the ZF CVT-CFT 23*, SAE Technical Paper 2001-01-0873, SAE, Warrendale, PA.
- [61] Nishigaya, M., Tamura, T., Yasue, H., Kasuga, S., and Sugaya, M., 2001, *Development of Toyota's New "Super CVT."* SAE Technical Paper 2001-01-0872, SAE, Warrendale, PA.
- [62] Abo, K., Sugano, K., Shibayama, T., and Hayasaki, K., 2003, *Development of New-Generation Belt CVTs with High Torque Capacity for Front-Drive Cars*, SAE Technical Paper 2003-01-0593, SAE, Warrendale, PA.
- [63] Hohn, B.-R., Pflaum, H., and Tomic, D., 2006, *Fuel Consumption and Energy Balance of "Optimized CVT-Hybrid-Driveline,"* SAE Technical Paper 2006-01-3259, SAE, Warrendale, PA.
- [64] Narita, K., and Priest, M., 2007, "Metal-Metal Friction Characteristics and the Transmission Efficiency of a Metal V-Belt Type Continuously Variable Transmission," *Proc. IMechE J. Eng. Technol.*, 2007, Vol. 221, pp. 11–26.
- [65] Wikipedia, 2011, "Continuously Variable Transmission." Available at http://en.wikipedia.org/wiki/Continuously_variable_transmission (accessed October 15, 2011).
- [66] Fischetti, M., 2006, "No More Gears," *Scientific American*. Vol. 294, p. 92.
- [67] Singh, J., Berger, K., Mack, P., Piorkowski, P., Hogan, T., and Wong, A., 2003, *General Motors "VTi" Electronic Continuously Variable Transaxle*. SAE Technical Paper 2003-01-0594, SAE, Warrendale, PA.
- [68] Wada, H., and Matsuoka, T., 2003, "Initial Wet Clutch Friction Characteristics of ATF/B-CVTF Under Low Speed Sliding Conditions." Paper presented at the JSAE/SAE International Spring Fuels and Lubricants Meeting, Paper ID JSAE 20030172.
- [69] Pennings, B., van Drogen, M., Brandsma, A., van Ginkel, E., and Lemmens, Marlene, 2003, *Van Doorne Fluid Test – A Test Method on Belt-Pulley Level to Select Fluids for Push Belt CVT Application*, SAE Technical Paper 2003-01-3253, SAE, Warrendale, PA.
- [70] LuK GmbH & Co. KG, 2012, "LuK Chain." Available at http://www.luk.de/content.luk.de/en/products/transmission_components/cvt/luk_kette_sv/LuK_Kette_sv.jsp (accessed January 8, 2012).
- [71] Luk GmbH & Co. KG, 2012, "LuK CVT—Components for Continuously Variable Transmissions." Available at http://www.luk.com/content.luk.de/en/products/transmission_components/cvt/cvt.jsp (accessed January 8, 2012).
- [72] Fewkes, R., Gunsing, J., and Sumiejski, J.L., 1993, *Lubricant as a Construction Element in the VDT Push-Belt CVT System*, SAE Technical Paper 932848, SAE, Warrendale, PA.
- [73] Nakazawa, K., Mitsui, H., Kakegawa, K., Murakami, Y., Ishikawa, T., and Yauchibara, R., 1998, *Performance of CVT Fluid for High Torque Transmitting Belt-CVTs*, SAE Technical Paper 982675, SAE, Warrendale, PA.
- [74] Kobayashi, D., Mabuchi, Y., and Katoh, Y., 1998, *A Study on the Torque Capacity of a Metal Pushing V-Belt for CVTs*, SAE Technical Paper 980822, SAE, Warrendale, PA.
- [75] Huston, M.E., Tipton, C.D., Qureshi, F., Sumiejski, J.L., Derevanik, T.S., Flask, C.A., Whitticar, D.J., and Ward, W.C., 1999, *Shifting from Automatic to Continuously Variable Transmissions: A Look at Fluid Technology Requirements*, SAE Technical Paper 1999-01-3614, SAE, Warrendale, PA.
- [76] Tersigni, S.H., Iyer, R.N., McCombs, T.A., Jones, M.S., and Yatsunami, K., 2002, *Comparing a CVT to a Four-Speed Automatic Transmission on Stress to the ATF*, SAE Technical Paper 2002-01-1694, SAE, Warrendale, PA.
- [77] Thomas, J., Constans, B., Gresser, E., Maillard, M., Naganuma, N., Nishino, T., and Itoh, F., 2004, *Testing the Torque Capacity of CVT Fluids*, SAE Technical Paper 2004-01-2007, SAE, Warrendale, PA.
- [78] Nishizawa, H., Yamaguchi, H., Suzuki, H., Osawa, M., Iwatuki, K., and Oshiumi, Y., 2005, *Friction Characteristics Analysis for Clamping Force Setup in Metal V-Belt Type CVT*, SAE Technical Paper 2005-01-1462, SAE, Warrendale, PA.
- [79] Ward, W.C., Copes, R.G., Sumiejski, J.L., and Fewkes, R., 1996, *Performance Features of Fluids for CVT Applications*, JSAE paper number 9636457.
- [80] Papay, A.G., 1991, "Formulating Automatic Transmission Fluids," *Lubric. Eng.*, Vol. 47, pp. 271–275.
- [81] Joseph, I., 2010, "Driveline Fundamentals and Lubrication." In *Chemistry and Technology of Lubricants*, 3rd ed., R.M. Mortier, M.F. Fox, and S.T. Orszulik, Eds., Springer Science, New York, pp. 325–344.
- [82] Ward, W.C. Jr., Nunnari, J.J., and Schullo, F.J., 1999, "Innovative ATF Technology that Bridges Global OEM's Specification." Paper presented at the NPRA Meeting, Paper ID LW-99-131.
- [83] Stanek, J.M., and Smith, D.B., 1968, *Considerations in Design of a Type F Automatic Transmission Fluid*, SAE Technical Paper 680040, SAE, Warrendale, PA.
- [84] Anderson, R.L., and Hunstad, N.A., 1968, *DEXRON® Automatic Transmission Fluid*, SAE Technical Paper 680038, SAE, Warrendale, PA.
- [85] Coleman, L.E., 1968, *Development of Type F Automatic Transmission Fluids*, SAE Technical Paper 680039, SAE, Warrendale, PA.
- [86] Ross, W.D., and Pearson, B.A., 1968, *ATF—Type F Keeps Pace with Fill-for-Life Requirements*, SAE Technical Paper 680037, SAE, Warrendale, PA.
- [87] Kobe, R.A., and Wagner, J.C., 1968, *The Chrysler TorqueFlite and Automatic Transmission Fluid*, SAE Technical Paper 680036, SAE, Warrendale, PA.
- [88] Haviland, M.L., Anderson, R.L., Davison, E.D., Goodwin, M.C., and Osborne, R.E., 1974, *Dexron®-II Automatic Transmission Fluid Performance*, SAE Technical Paper 740053, SAE, Warrendale, PA.
- [89] Florkowski, D.W., King, T.E., Skrobol, A.P., and Sumiejski, J.L., 1998, *Development and Introduction of Chrysler's New Automatic Transmission Fluid*, SAE Technical Paper 982674.
- [90] Wikipedia, 2011, "Petroleum." Available at <http://en.wikipedia.org/wiki/Petroleum> (accessed November 1, 2011).
- [91] Henderson, H.E., and Swinney, B., 1998, *Higher Quality Base Oils for Next Generation Automatic Transmission Fluids*, SAE Technical Paper 982666, SAE, Warrendale, PA.
- [92] Watts, R.F., Noles, J., Pujara, N., and Trautman, T., 2001, *The Impact of Evolving Automatic Transmission Fluid Specifications on Base Oil Selection*, SAE Technical Paper 2001-01-1992, SAE, Warrendale, PA.

- [93] Kwon, W.-S., Kim, K.-W., and Henderson, H.E., 2005, *Base Stock Developments in Automatic Transmission Fluid Design*, SAE Technical Paper 2005-01-3858, SAE, Warrendale, PA.
- [94] Helton, T.E., Degnan, T.F. Jr., and Mazzone, D.N., 1998, "Mobil's Lube Hydroprocessing Technologies—A Legacy of Catalytic Innovation and Commercial Success." Paper presented at the AIChE Spring Meeting, Paper ID 25D.
- [95] Mack, P.D., Zaugg, T.D., and Cohen, S.C., 1996, "Severely Hydro-Cracked/Hydro-Isomerized Base Oils—The Key to Enhanced Performance Levels." Paper presented at the NPRA Meeting, Paper ID FL-96-114.
- [96] Hamilton, G.D.S., Lanthier, R., and Markin, A.D., 1990, *Development of Automatic Transmission Fluids Having Excellent Low Temperature Viscometric and High Temperature Oxidative Properties*, SAE Technical Paper 902145, SAE, Warrendale, PA.
- [97] "American Petroleum Institute." Available at <http://www.api.org/> (accessed November 1, 2011).
- [98] Cavdar, B., and Lam, R.C., 1997, *Wet Clutch Performance in a Mineral-Based and in a Partially-Synthetic-Based Automatic Transmission Fluid*, SAE Technical Paper 970976, SAE, Warrendale, PA.
- [99] Schodel, U.F., 1991, "Automatic Transmission Fluids (ATFs)—The Improvement of Low Temperature Characteristics," *J. Soc. Tribologists Lubric. Eng.*, Vol. 47, pp. 463–467.
- [100] GM, 1973, *DEXRON®-II Automatic Transmission Fluid Specification, GM-6137-M*, General Motors Research Labs, Fuels and Lubricants Department, Warren, MI.
- [101] Haviland, M.L., and Davison, E.D., 1971, *Automatic Transmission Fluid Viscosity Requirements*, SAE Technical Paper 710838, SAE, Warrendale, PA.
- [102] Ford Motor Company, 1987, *MERCON® Automatic Transmission Fluid Specification*, Ford Motor Company, Dearborn, MI.
- [103] GM, 1989, *DEXRON®-III Automatic Transmission Specification GM-6137-M*, General Motors Research Labs, Fuels and Lubricants Department, Warren, MI.
- [104] Linden, J.L., and Kemp, S.P., 1987, *Improving Transaxle Performance at Low Temperature with Reduced-Viscosity Automatic Transmission Fluids*, SAE Technical Paper 870356, SAE, Warrendale, PA.
- [105] Ford Motor Company, 1996, *MERCON® V, Automatic Transmission Fluid Specification*, Ford Motor Company, Dearborn, MI.
- [106] Engineering Specification MS-9602, DaimlerChrysler Corporation. (Change C, 1999), (Change E, 2002), (Change F, 2003), (Change G, 2006).
- [107] Johnson, T.L., 1998, *Introducing TRANSYND, A New Severe Duty Extended Drain Interval Fluid for Allison Heavy Duty Automatic Transmissions*, SAE Technical Paper 982798, SAE, Warrendale, PA.
- [108] Calcut, B., and Fewkes, R., 2006, *The Oxidative Stability of GM's DEXRON-VI Global Factory Fill ATF*, SAE Technical Paper 2006-01-3241, SAE, Warrendale, PA.
- [109] Kemp, S.P., and Linden, J.L., 1992, *The Oxidation Stability of General Motors Proposed Factory-Fill Automatic Transmission Fluid*, SAE Technical Paper 922371, SAE, Warrendale, PA.
- [110] Macnaught Pty Ltd., 2012. "Materials Compatibility of Synthetic Lubricant Base Oils." Available at http://www.macnaught.com.au/files/graphs_-_compat.pdf (accessed February 10, 2012).
- [111] Mang, T., and Dresel, W., Eds., 2007, *Lubricants and Lubrication*, 2nd ed., Wiley, Weinheim, Germany.
- [112] Roslaili, A.A., Nor Amirah, A.S., Nazry, S.M., and Nihla, K.A., 2010, "Determination of Structural and Dimensional Changes of O-Ring Polymer/Rubber Seals Immersed in Oils," *Int. J. Civil & Environ. Eng.*, Vol. 10, pp. 1–15.
- [113] Okabe, H., and Kanno, T., 1980, "Behavior of Polar Compounds in Lubricating-Oil Films," *ASLE Trans.*, Vol. 24, pp. 459–466.
- [114] Papay, A.G., 1983, "Oil-Soluble Friction Reducers—Theory and Application," *Lubric. Eng.*, Vol. 39, pp. 419–426.
- [115] O'Connor, B.M., Van Mellekom, J.H., Gahagan, M.P., Rank, R., and Jahn, W., 2002, *Influence of Additive Chemistry on Manual Transmission Synchronizer Performance*, SAE Technical Paper 2002-01-1697, SAE, Warrendale, PA.
- [116] Hsu, S.M., 2004, "Molecular Basis of Lubrication," *Tribology Int.*, Vol. 37, pp. 553–559.
- [117] Mosey, N.M., Muser, M.H., and Woo, T.K., 2005, "Molecular Mechanisms for the Functionality of Lubricant Additives," *Science*, Vol. 307, pp. 1612–1615.
- [118] Papay, A.G., 1990, "Effect of Chemistry on Performance of Automatic Transmission Fluids," *Lubric. Eng.*, Vol. 46, pp. 511–518.
- [119] Papay, A.G., 1998, "Antiwear and Extreme-Pressure Additives in Lubricants," *Lubric. Sci.*, Vol. 10, pp. 209–224.
- [120] Spikes, H.A., 2006, "Sixty Years of EHL," *Lubric. Sci.*, Vol. 18, pp. 265–291.
- [121] Sprys, J.W., Vaught, D.R., and Stephens, E.L., 1994, *Shear Viscosity of Automatic Transmission Fluids*, SAE Technical Paper 941885, SAE, Warrendale, PA.
- [122] Sprys, J.W., Doi, J., Furumoto, M., Hoshikawa, N., King, T., Kurashina, H., Linden, J.L., Murakami, Y., and Ueda, F., 1998, *Shear Stability of Automatic Transmission Fluids – Methods and Analysis. A Study by the International Lubricants Standardization and Approval Committee (ILSAC) ATF Subcommittee*, SAE Technical Paper 982673, SAE, Warrendale, PA.
- [123] Sarkar, R., Devlin, M.T., Li, S., Glasgow, M.B., and Jao, T.-C., 2002, *Low and High Temperature Non-Newtonian Behavior of Automatic Transmission Fluids*, SAE Technical Paper 2002-01-1695, SAE, Warrendale, PA.
- [124] Umamori, N., and Kagimiya, T., 2003, *Study of Viscosity Index Improver for Fuel Economy ATF*, SAE Technical Paper 2003-01-3256, SAE, Warrendale, PA.
- [125] Dardin, A., Hedrich, K., Muller, M., 1967, Topolovec-Miklozic, K., and Spikes, H., *Influence of Polyalkylmethacrylate Viscosity Index Improvers on the Efficiency of Lubricants*, SAE Paper 2003-01-1967, SAE, Warrendale, PA.
- [126] Callais, P., Schmidt, S., and Macy, N., 2004, *The Effect of Controlled Polymer Architecture on VI and Other Rheological Properties*, SAE Technical Paper 2004-01-3047, SAE, Warrendale, PA.
- [127] Stohr, T., Eisenberg, B., and Muller, M., 2008, *A New Generation of High Performance Viscosity Modifiers Based on Comb Polymers*, SAE Technical Paper 2008-01-2462, SAE, Warrendale, PA.
- [128] Vickerman, R.J., Streck, K., Schiferl, E., and Gajanayake, A., 2009, *The Effect of Viscosity Index on the Efficiency of Transmission Fluids*, SAE Technical Paper 2009-01-2632, SAE, Warrendale, PA.
- [129] Stoehr, T., Eisenberg, B., Suchert, E., Spikes, H., and Fan, J., 2011, *Advances in Tribological Design of Poly(alkyl methacrylate) Viscosity Index Improvers*, SAE Technical Paper 2011-01-2123, SAE, Warrendale, PA.
- [130] Watts, R.F., and Szykowski, J.P., 1990, *Formulating Automatic Transmission Fluids with Improved Low Temperature Fluidity*, SAE Technical Paper 902144, SAE, Warrendale, PA.
- [131] Bartz, W.J., 1994, *Evaluation of Reversible and Irreversible Viscosity Losses Using the Viscosity Loss Trapezoid*, SAE Technical Paper 941980, SAE, Warrendale, PA.
- [132] Selby, T.W., 1993, *The Viscosity Loss Trapezoid - Part 2: Determining General Features of VI Improver Molecular Weight Distribution Using Parameters of the VLT*, SAE Technical Paper 932836, SAE, Warrendale, PA.
- [133] Bair, S., 2001, "The Variation of Viscosity With Temperature and Pressure for Various Real Lubricants," *J. Tribology*, Vol. 123, pp. 433–436.
- [134] Rizvi, S.Q.A., 1992, "Lubricant Additives and Their Functions," *ASM Handbook, Friction, Lubric. Wear*, Vol. 18, pp. 98–112.
- [135] Tipton, C.D., and Schiferl, E.A., 1997, *Fundamental Studies on ATF Friction, Part I*, SAE Technical Paper 971621, SAE, Warrendale, PA.
- [136] Tipton, C.D., Huston, M.E., and Wetsel, W.R., 1998, *Fundamental Studies on ATF Friction, Part II*, SAE Technical Paper 982670, SAE, Warrendale, PA.
- [137] Eguchi, M., and Yamamoto, T., 2005, "Shear Characteristics of a Boundary Film for a Paper-Based Wet Friction Material:

- Friction and Real Contact Area Measurement," *Tribology Int. Bound. Lubric.*, Vol. 38, pp. 327–335.
- [138] Marty, S., and Carpenter, B., 1993, *Intricacies of SAE#2 Computerized Clutch Friction Durability Testing*, SAE Technical Paper 932847, SAE, Warrendale, PA.
- [139] Hopkins, A.G., and Anderson, J.N., 1983, *Effect of Commercial Oil Additives on Wet Friction Systems*, SAE Technical Paper 831312, SAE, Warrendale, PA.
- [140] Beltzer, M., and Jahanmir, S., 1986, "An Absorption Model for Friction in Boundary Lubrication," *ASLE Trans.*, Vol. 29, pp. 423–430.
- [141] Belzer, M., and Jahanmir, S., 1986, "The Effect of Additive Molecular Structure on Friction Coefficient," *J. Tribology*, Vol. 108, pp. 109–116.
- [142] Yoshizawa, H., Chen, Y.-L., and Israelachvili, J., 1993, "Fundamental Mechanisms of Interfacial Friction 1. Relation between Adhesion and Friction," *J. Phys. Chem.*, Vol. 97, pp. 4128–4140.
- [143] Yoshizawa, H., and Israelachvili, J., 1993, "Fundamental Mechanisms of Interfacial Friction. 2. Stick-Slip Friction of Spherical and Chain Molecules," *J. Phys. Chem.*, Vol. 97, pp. 11300–11313.
- [144] Friihauf, E.J., 1974, *Automatic Transmission Fluids – Some Aspects on Friction*, SAE Technical Paper 740051, SAE, Warrendale, PA.
- [145] Papay, A.G., and Hartley, R.J., 1989, *Frictional Response of Automatic Transmission Fluids in Band and Disc Clutches*, SAE Technical Paper 890712, SAE, Warrendale, PA.
- [146] Frey, D., Brugel, E., and Wetzel, A., 1997, "Test Procedures for Slip-Controlled Multi-Disc Clutches." Paper presented at the Fifth CEC International Symposium on the Performance Evaluation of Automatic Fuels and Lubricants, Goteborg, Sweden, Paper ID CEC97-TL11.
- [147] Noles, J., Watts, R.F., Ishikawa, M., and Saito, H., 2007, *Test Methods for Determining Anti-Shudder Durability of Automatic Transmission Fluids*, SAE Technical Paper 2007-01-1974, SAE, Warrendale, PA.
- [148] Chen, Y.-F., Newcomb, T., and Lam, R.C., 2001, *Friction Material/Oil Interface for Slipping Clutch Applications*, SAE Technical Paper 2001-01-1153, SAE, Warrendale, PA.
- [149] Devlin, M.T., Tersigni, S.H., Senn, J., Turner, T.L., Jao, T.-C., and Yatsunami, K., 2004, *Effect of Friction Material on the Relative Contribution of Thin-Film Friction to Overall Friction in Clutches*, SAE Technical Paper 2004-01-3025, SAE, Warrendale, PA.
- [150] Kugimiya, T., Mitsui, J., Yoshimura, N., Kaneko, H., Akamatsu, H., Ueda, F., and Akiyama, S., 1995, *Development of Automatic Transmission Fluid for Slip-Controlled Lock-up Clutch System*, SAE Technical Paper 952348, SAE, Warrendale, PA.
- [151] Kugimiya, T., Yoshimura, N., Kuribayashi, T., Mitsui, J., Ueda, F., Ando, Y., Nakada, T., and Ohira, H., 1997, *Next Generation High Performance ATF for Slip-Controlled Automatic Transmission*, SAE Technical Paper 972927, SAE, Warrendale, PA.
- [152] Murakami, Y., Linden, J.L., Flaherty, J.E., Sprys, J.W., King, T.E., Kurashina, H., Furumoto, M., Iwamoto, S.I., Kagawa, M., and Ueda, F., 2000, *Anti-Shudder Property of Automatic Transmission Fluids—A Study by the International Lubricants Standardization and Approval Committee (ILSAC) ATF Subcommittee*, SAE Technical Paper 2000-01-1870, SAE, Warrendale, PA.
- [153] Ward, W.C., Sumiejski, J.L., Castanien, C.J., Tagliamonte, T.A., and Schiferl, E.A., 1994, *Friction and Stick-Slip Durability Testing of ATF*, SAE Technical Paper 941883, SAE, Warrendale, PA.
- [154] Watts, R.F., Nibert, R.K., and Tandon, M., 1996, "Anti-Shudder Durability of Automatic Transmission Fluids: Mechanism of the Loss of Shudder Control." Paper presented at the 10th International Colloquium on Tribology.
- [155] Newcomb, T., Sparrow, M., Ciupak, B., Hadad, Y., and Hassert, J., 2008, *The Effect of Lower Viscosity Automatic Transmission Fluid on Glaze Chemistry*, SAE Technical Paper 2008-01-2395, SAE, Warrendale, PA.
- [156] Gergel, W.C., 1984, "Lubricant Additive Chemistry." Paper presented at the International Symposium Technical Organic Additives and Environment.
- [157] Kugimiya, T., 2000, "Relationship between Chemical Structures of Dispersant and Metallic Detergent and Mu-v Characteristics," *Tribologist*, 2000, Vol. 45, pp. 396–405.
- [158] Glasson, S., Espinat, D., and Palermo, T., 1993, "Study of Microstructural Transformation of Overbased Calcium Sulfonates During Friction," *Lubric. Sci.*, Vol. 5, pp. 91–111.
- [159] Caracciolo, F., 1990, *Development of a Sprag Wear Test Procedure for Evaluating the Antiwear Performance of ATFs*, SAE Technical Paper 902149, SAE, Warrendale, PA.
- [160] Papay, A.G., and Sunne, J.P., 1989, *Antiwear Characteristics of Automatic Transmission Fluids*, SAE Technical Paper 892157, SAE, Warrendale, PA.
- [161] Dowson, D., 1995, "Elastohydrodynamic and Micro-Elastohydrodynamic Lubrication," *Wear*, Vol. 190, pp. 125–138.
- [162] Chiu, Y.P., 1997, *A Reassessment of Lambda Ratio as a Bearing Surface Fatigue Performance Indicator*, SAE Technical Paper 972714, SAE, Warrendale, PA.
- [163] Chiu, Y.P., 1997, "The Mechanism of Bearing Surface Fatigue—Experiments and Theories," *Tribology Trans.*, Vol. 40, pp. 658–666.
- [164] Reyes, M., and Neville, A., 2003, "The Effect of Anti-Wear Additives, Detergents and Friction Modifiers in Boundary Lubrication of Traditional Fe-Based Materials," *Tribology Ser.*, Vol. 41, pp. 57–65.
- [165] Hohn, B.R., and Michaelis, K., 2004, "Influence of Oil Temperature on Gear Failures," *Tribology Int.*, Vol. 37, pp. 103–109.
- [166] Jao, T.-C., Henly, T., Carlson, G.W., Ved, C., Carter, R.O., Hildebrand, D.H., and Ogorek, W., 2006, *Planetary Gear Fatigue Behavior in Automatic Transmission*, SAE Technical Paper 2006-01-3243, SAE, Warrendale, PA.
- [167] Lyashenko, I.A., Khomenko, A.V., and Metlov, L.S., 2011, "Thermodynamics and Kinetics of Boundary Friction," *Tribology Int.*, Vol. 44, pp. 476–482.
- [168] Calcut, B.D., and Sarkar, R., *Estimating the Useful Life of an ATF Using an Integrated Bulk Oxidation and Friction Degradation Model*, SAE Technical Paper 2004-01-3028, SAE, Warrendale, PA.
- [169] Dixon, L.T., and Korcek, S., 1976, *Foaming and Air Entrainment in Automatic Transmission Fluids*, SAE Technical Paper 760575, SAE, Warrendale, PA.
- [170] Friesen, T.V., 1987, *Transmission-Hydraulic Fluid Foaming*, SAE Technical Paper 871624, SAE, Warrendale, PA.
- [171] Duncanson, M., 2003, "Effects of Physical and Chemical Properties on Foam in Lubricating Oils," *J. STLE*, Vol. 59, pp. 9–13.
- [172] GM, 2005, *Dexron®-VI Automatic Transmission Fluid Specification, GMN10060*, General Motors Corporation, Warren, MI.
- [173] GM, 1957, *Automatic Transmission Fluid, Type A, Suffix A Identification Specification* (Revisions issued August, 1958, and April, 1959), General Motors Research Labs, Fuels and Lubricants Department, Warren, MI.
- [174] Ford Motor Company, 1959, *ESW-M2C33 A-B Automatic Transmission Fluid, Manufacturing Standard*, Ford Motor Company, Dearborn, MI.
- [175] Ford Motor Company, 1961, *ESW-M2C33 C-D Automatic Transmission Fluid, Manufacturing Standard* (Revised 1964), Ford Motor Company, Dearborn, MI.
- [176] Ford Motor Company, 1967, *ESW-M2C33 E-F Automatic Transmission Fluid*, Ford Motor Company, Dearborn, MI.
- [177] GM, 1967, *DEXRON® Automatic Transmission Fluid Specification, GM6032M*, General Motors Research Labs, Fuels and Lubricants Department, Warren, MI.
- [178] Chrysler, 1966, *Fluid, Automatic Transmission, High V.I., Chrysler Corporation Material Standard MS-4228 (Change B)*, Chrysler, Auburn Hills, MI.
- [179] Chrysler, 1964, *Fluid, Automatic Transmission, Type A, Chrysler Corporation Material Standard, MS-3256 (Change F)*, Chrysler, Auburn Hills, MI.
- [180] Ford Motor Company, 1974, *ESP-M2C138-CJ, Automatic Transmission Fluid Specification*, Ford Motor Company, Dearborn, MI.
- [181] Ford Motor Company, 1981, *ESP-M2C166-H, Automatic Transmission Fluid Specification*, Ford Motor Company, Dearborn, MI.

- [182] Willermet, P.A., Mahoney, L.R., Kandah, S.K., and Sever, A.W., 1980, *The Prediction of ATF Service Life from Laboratory Oxidation Test Data*, SAE Technical Paper 801363, SAE, Warrendale, PA.
- [183] Willermet, P. A. and Kandah, S. K., *The Aluminum Beaker Oxidation Test for MERCON World-Wide Service ATF*, SAE Technical Paper 881673, SAE, Warrendale, PA.
- [184] GM, 2003, *DEXRON®-III Automatic Transmission Fluid Specification*, GMN10055, General Motors Corporation, .
- [185] Papay, A.G., 1998, "Automatic Transmission Fluids *Dexron®-II and Beyond." Paper presented at the 43rd Annual Meeting of the STLE, May.
- [186] Linden, J.L., Stebar, R.F., and Kemp, S.P., 1994, *Friction Characteristics of DEXRON®-III Automatic Transmission Fluids*, SAE Technical Paper 941887, SAE, Warrendale, PA.
- [187] Chrysler Corporation, 1997, *Engineering Specification, MS-7176 Change E*, Chrysler, Auburn Hills, MI.
- [188] Arakawa, Y., Yauchibara, R., and Murakami, Y., 2003, *Development of a Multi-purpose ATF Meeting DEXRON®-III, MERCON® and JASO M315 Specifications*, Paper ID 20030055, JSAE Review, JSAE, Tokyo, Japan.
- [189] Fewkes, R., and Willis, A., 2007, *Comparison of OEM Automatic Transmission Fluids in Industry Standard Tests*, SAE Technical Paper 2007-01-3987, SAE, Warrendale, PA.
- [190] Ford Motor Company, 2004, *MERCON® SP, Automatic Transmission Fluid Specification*, Ford Motor Company, Dearborn, MI.
- [191] Ford Motor Company, 2007, *MERCON® LV, Automatic Transmission Fluid Specification*, Ford Motor Company, Dearborn, MI.
- [192] Tocci, L., 2007, "Ford Unveils New Transmission Fluid," *Lube Report*, April 24.

16

Other Automotive Specialized Lubricant Testing Including Manual Transmission, Rear Axle, and Gear Box Lubricant Testing and Specification

Dave Simner¹

16.1 INTRODUCTION

Having discussed the fundamentals of the various transmission units in Chapter 10, the potential tests that would be required to prove that the lubricant is satisfactory for service are considered here. It is clear that there is a vast choice of tests available for this purpose, and equally, there is a whole range of performance indicators to ensure that the transmission is fit for the duty required. In certain circumstances, only one specific function of the lubricant will need to be proven to specify that fluid; at other times, there is a whole host of different functions that need to be tested and signed off. In this chapter, the options for testing transmission units and their lubricants are discussed. Most of these options will affect or be affected by the lubricant. However, for completeness, some testing in which the fluids are unlikely to have much of a part to play is included.

Chapter 10 discussed the technology that goes into making up the transmission and driveline of a vehicle. The role that lubricants play in ensuring that these units adequately perform their task and last the life of the vehicle was also considered. Therefore, the question arises as to what is a suitable life for the vehicle. In addition to this question, a few years ago it would be considered normal for a transmission to be refurbished during the life of the vehicle. Certainly, wear items such as clutch plates may have needed to be replaced, and bearings, seals, and possibly gears would have been exchanged during mid-life rebuilds. Today, the customer expectation for most transmission units is that they will last the life of the vehicle. Consider this for one moment from the perspective of the manufacturer: If 7-year unlimited mileage warranties are offered (as sold with some cars in Europe now), then factoring in replacement transmission units will make the economics of these arrangements prohibitively expensive. This is not just the preserve of European car sales because similar warranty offerings are also appearing for North America and other regions. In addition to this, parts of the industry are moving to a position in which the lubricants are also “filled for life.” It is probably a safe wager that the trends of longer warranties and more fill-for-life fluids will continue and migrate from the light automotive world toward the heavier, commercial market.

It is interesting to consider that if a key part within a gear box is modified (e.g., a gear or bearing), then once assured

of the strength and durability of that part, it can then be considered for introduction into production. This might be confirmed with a limited range of testing just focusing on the component in question. It is potentially possible to demonstrate the improved performance outside of the transmission in question using a rather simple bench test. However, if the effect of changing a lubricant is considered, then it can be seen that there are many ways that the fluid can influence the way the transmission will function. This could include the way it is stored, through its initial operation, to its ongoing operation in a range of environments. It is difficult to envisage another “component” within the transmission that has a greater and more diverse effect on its operation than the lubricant.

Most of the testing that falls into our remit for this chapter is developed by the company either producing the transmission unit or it is specified by the vehicle manufacturer installing the unit into a vehicle. The existence of universally accepted standard tests is fairly rare. Therefore, most of the tests used around the industry are proprietary. Where standard tests have been agreed upon, those will be discussed together with what performance aspects they demonstrate.

In this chapter, the small bench tests for lubricants will not be considered in any depth because although these can be used very successfully to provide screening of fluids, they do not fully replicate the functions or conditions within any particular transmission unit. They are also considered in another chapter of this manual.

16.2 DISCUSSION: WHOLE DRIVETRAIN TESTING

16.2.1 *Testing the Vehicle Driveline System*

If the testing of whole transmission units is considered to begin with, then the most obvious factor is the mechanical durability of the unit (i.e., the life of the gears and bearings). Several different types of tests are applicable here because they can either apply to entire drivetrains or be adapted to test specific transmission units.

Perhaps the most obvious method of testing a transmission unit against a requirement is to fit the system to a vehicle and expose that vehicle to extensive road testing covering the design mileage of the vehicle. What mileage the design life should be can be debated at length. Looking from the customer perspective, a car mileage of 400,000–500,000 km can

¹ Cranfield University, Defence Academy, Swindon, Wiltshire, UK

be suggested. The customer would clearly like the vehicle to last a very long time because they intend to keep it or they want it to retain a good resale value. In arriving at this figure, it could be envisaged that a very-high-mileage customer who wanted to keep a vehicle in excess of 10 years would complete many thousands of miles of driving every year. However, if vehicles were designed for this level of durability, then it can be argued that the more typical customer would be paying for durability, robustness, and longevity that they are never likely to need. Therefore, should the design perhaps be aimed at a more “average” driver? Looking around the world, many examples of “typical” or “average” drivers can probably be found. For example, is a family an average “customer”, or a taxi driver, sales representative, or farmer? Of course, what is decided on for one type of vehicle may or may not carry across the whole range of vehicles. It is probably reasonable to expect a higher mileage “design life” on larger cars than smaller ones because they typically get used regularly for longer “out-of-town” trips and typically clock up a higher total mileage. Without having access to individual manufacturers’ test programs, it is difficult to be specific here, but a typical figure for passenger cars is likely to be around half of the above figure—in the region of 150,000–250,000 km. One observation can be made regarding the design life: that the mileage expected by the customer and designed for by the manufacturer is steadily increasing.

To establish the limits of the transmission in question, data clearly need to be obtained from vehicles in the field. With modern datalogging techniques this can easily be done from development vehicles and real customers. The data that are established will inform the engineer about torque levels delivered by the engine in various different driving conditions. Gear selection is also critical for the transmission engineer; not just for the gear box, but also to establish the applied torque to the driveline downstream of the gear box. Figure 16.1 shows typical data: gear selection, percentage time in each gear, and torque levels used by the vehicle. It is interesting to note on the latter figure just how low the torque delivered by the engine is for most of the time. Only very rarely does the torque approach the maximum of which the engine is capable.

Commercial vehicles and heavy-goods vehicles need to be considered separately because it is likely that they will be used for transportation of goods and as such spend many hours a day on the road most days of the year. Of course, this presents a problem if commercial vehicles (e.g., a delivery van) are derived from a car platform. The commercial customer will accumulate mileage far more rapidly than a private car driver would be likely to do. Fortunately, a mitigating factor is that the commercial customer will probably expect to replace the vehicle more frequently.

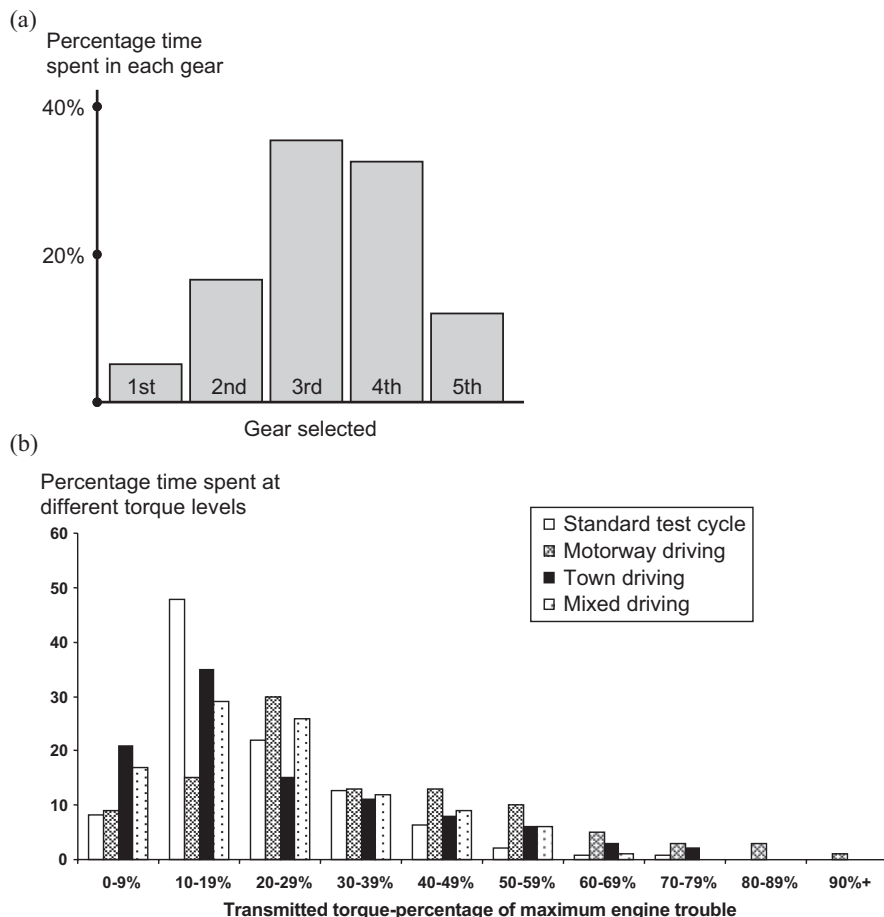


Figure 16.1—Data collected on vehicle in use can provide information regarding how the transmission is loaded during in the lifetime of the vehicle: (a) gear selection (based on information from reference 1) and (b) torque levels recorded in a vehicle in various different types of vehicle tests.

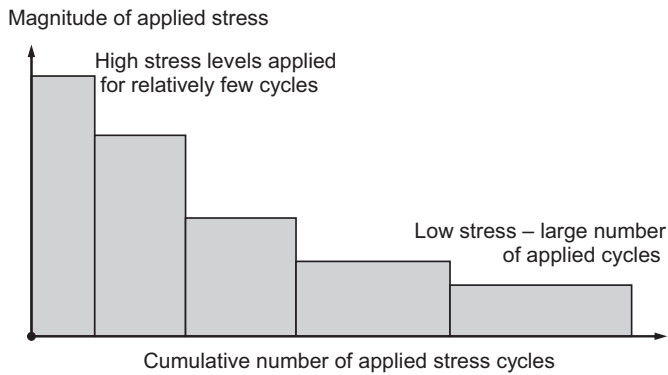


Figure 16.2—Measured data from tests or vehicle dataloggers can show how many stress cycles are applied to particular components at the various levels of stress. Typical data show relatively few cycles at the highest stress/loads.

If the standard theory for the fatigue of metals is considered, then it is known that the higher the applied stress, the fewer application cycles a component can endure. Of course, such a high load could ultimately be applied that the component would fail under a single application. At the other extreme, a light load can be applied many times with little or no damage to the component, such that the part will last a very long time. If this is considered in the context of the transmission system, then examples of all of these situations can be found:

- **Overload:** The application of one overwhelming load that instantly breaks a component—the stress exceeds the ultimate stress limit. This could be the result of some unforeseen load case or simply abuse.
- **Short-term strength:** A very high load that is somewhat unusual, possibly because of some abuse from the driver. This may not cause immediate failure, but repeated occurrence (perhaps up to 100 or so) can cause failure.
- **Low cycle fatigue:** Reducing the loading will increase the life of the component, although failure will still occur at a relatively low number of cycles.
- **Normal fatigue loading:** The application of a high but manageable and foreseeable load case that would cause failure if allowed to occur too often and become the norm during the entire life of a vehicle. In this condition, the result is a finite life in which failure will occur at some point given a high enough frequency of the load pattern.
- **Infinite life:** The application of a load case that is within the infinite life load limit of the component. Therefore, the transmission can withstand the very high numbers of load applications encountered during the life of a vehicle. Under some load conditions, this could be many millions of cycles.

In most whole-unit testing, it is probably fair to say that of the most interest is the durability of the gears and bearings. The lubricant is a crucial part of this system. As discussed in Chapter 10, within the transmission, the strength of the components and the surface durability (wear pitting, micropitting, abrasion, scuffing) need to be proven. Clearly, the lubricant directly influences, if not controls, the wear. In addition to this, the lubricant needs to be present in the unit if it is to be operated in any meaningful way (and therefore be subjected to load). A static test of some sort could be envisaged that would allow load to be applied to the gear train without any lubricant being present, but this is probably unlikely.

At this point in the discussion it is useful to establish that there are several fundamental methods for testing transmission units. Of course, a test can either be in the vehicle or on a test rig, and even if the system is indeed installed in a vehicle, the tests can still be performed with the vehicle itself mounted on a rig and not on the road. If durability testing rather than performance testing is considered, then the options can be categorized as follows:

- Open loop testing with the entire driveline system installed in a representative vehicle and then the vehicle driven in some form of test on a road, test track, or off-road if appropriate.
- Open loop testing with a full or partial vehicle system installed on a test rig or rolling road. This potentially has

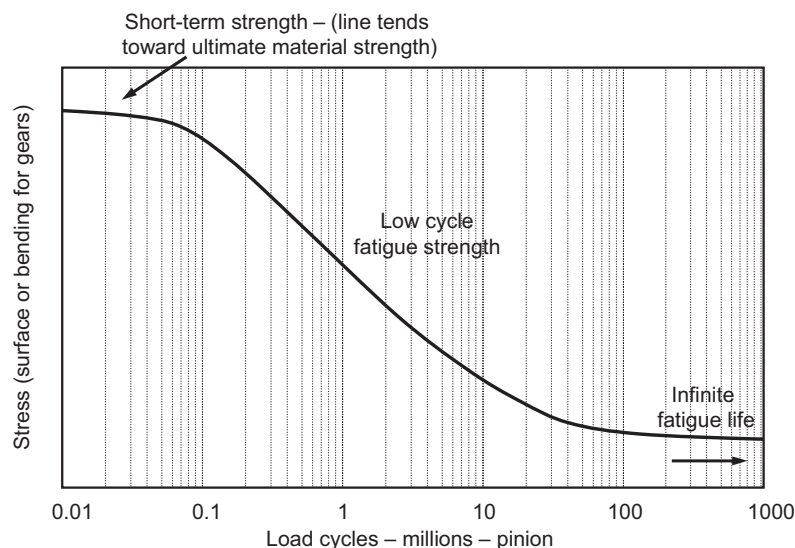


Figure 16.3—A typical gear *s/n* curve—fatigue damage reduces the allowable stress as the number of applied cycles increases. The position of the curve is indicative of the surface fatigue performance of gear steels—the curve would be further to the left on the graph for bending strength of the gear teeth. The stress limits are obviously different for different materials. Good data on gear materials, particularly for surface stress, can be expensive to obtain.

the advantage that the test conditions and environment can be more closely controlled than if the vehicle is driven.

- Open loop testing on a test rig using just a partial transmission system or a single transmission unit. In this test, setup of an engine or drive motor provides the input to the transmission unit, and another device (usually a brake dynamometer) absorbs the power at the output shaft.
- Closed loop or “four-square” testing in which the output and input of a transmission system are connected via a slave test unit. By physically applying the required torque to this closed system, there is no need to provide the total power put through the transmission, but just to make up the losses in the test and slave unit. This four-square test principle is discussed in more detail in Section 16.3. Although it is quite possible to construct a four-square-type rig for the entire driveline of a vehicle, the resulting rig would be complex, expensive, and probably quite inflexible. Such a rig is likely to be specially designed for a particular transmission and possibly difficult to adapt for another.
- Closed loop testing using electrical feedback. Traditional electric drive rigs have absorbed the power output of the system under test by converting the energy into heat (in the dynamometer) and then expelling that heat from the rig in some way. With an electric dynamometer, the resulting output electrical energy can be used to help drive the test rig. In this way, the net electrical input to the system only needs to make up for the losses, not provide the total power required at the input to the transmission. Such a rig does require quite expensive electric control equipment but clearly results in large savings in running costs.

16.2.2 In-Vehicle Durability Testing

The largest drawback of testing complete transmission systems is arguably the cost. The testing of this type tends to be time-consuming and therefore expensive. This issue is compounded by the large, expensive facilities required for such testing. If there is a need to test the driveline at a representative load, then perhaps the first choice would be to conduct the test in a vehicle. However, there are several drawbacks to this approach, including

- The cost and availability of a representative vehicle (especially early in the vehicle development program when many of the other vehicle systems will be at the prototype stage).
- The cost of supporting vehicle testing for extended durations.
- The timing of results availability—extended road tests can potentially last beyond the normal development period and only achieve the required high mileage once the vehicle has gone into production.
- The variability of external factors such as driver variability, weather, road conditions, failure of other vehicle systems, etc.
- Variation in the environmental factors such as ambient temperature, presence of water, road salt, etc.
- Potential of a premature test failure due to accidental damage to the vehicle or failure of another unrelated system.

The decision to use this type of lengthy and costly testing would ultimately have to be made by the company

management. They would need to weigh the risk involved in the program against the cost of completing this type of test.

To reduce the cost of a test, one option is to accelerate the process by making the conditions or loading more severe. This can have advantages in cost and time, but care needs to be taken not to cause untypical failures due to these conditions or loads. One example of this would be the problems caused by high-speed testing. It may be decided to conduct this on a test track rather than a public road, and this gives us an advantage in terms of quicker mileage accumulation. However, if one consequence is, for example, unusually high lubricant temperatures, then premature failures caused by lubricant breakdown rather than fatigue damage to the gears or bearings will occur. Even local temperatures can obviously cause unrepresentative failures; for example, perhaps a bearing that is fed with an adequate but relatively small flow of oil, which then proves to be marginal during extreme conditions. This might be presented as a bearing that overheats, although only under extreme high-speed, high-ambient conditions. The development engineers would then need to decide if such a failure justifies a potentially costly engineering modification or not.

In any durability testing, the key aim is to be able to build the number of test cycles as quickly as possible. This rapid testing can provide rapid feedback to the development program of the vehicle and, of course, help to keep costs down. As indicated above, the danger with increasing the speed of testing is that although it helps reduce the test time, the process can also cause problems. Looking at a whole vehicle example for a moment, it is possible that undesirable side effects occur. If rough roads are used to test the vehicle to increase the vibration input to a vehicle structure and driveline, then a benefit can be a reduction in the time taken to prove the durability of the structure. However, by driving a vehicle over rougher roads than the vehicle would usually be exposed to, components such as suspension dampers can get overheated, tires behave differently than normal, and suspension bushes can also suffer premature failure. Therefore, it can be envisaged that such accelerated testing can cause issues for the vehicle the normal driver will not encounter.

16.2.3 Accelerated Testing

As indicated, it is clearly very difficult to build up “normal” mileage to the level matching the design life of the vehicle or transmission. There are several options potentially available to the development engineer that could provide confidence in the durability rather quicker than mileage accumulation. These include

- *High-speed testing:* This has the advantage of building up mileage quickly and is usually more severe than normal use. Given some degree of validation with earlier vehicles, it could be assumed that 80,000 km of high-speed use is perhaps similar to 240,000 km of normal driving. Data gathered on the vehicle can be analyzed to allow some degree of comparison of the relative fatigue damage on gears and bearings through the transmission system. The level of torque applied to the gears can be considered against known stress limits within a gear analysis software tool.
- *Heavy-duty trailer towing:* Similar to the above case, the increase in load will increase the fatigue damage within the rotating parts for any given distance traveled.

- *Off-road driving:* Many vehicles are capable of being used either on or off-road. It is probably an obvious observation, but off-road is more severe, and therefore if testing exclusively in such environments, then again there will be a build up of damage to the vehicle more quickly than on-road testing.

The danger with any accelerated testing such as this is that conditions could conceivably be allowed that are unrealistic. As an example, consider the case of high-speed testing. This is very often completed at high ambient temperatures in areas of the world such as the Mediterranean countries in Europe, the southern states of the United States, desert regions, or similar areas. Again, this high-temperature condition could be seen as simply the worst-case scenario for the vehicle in question. However, if the lubricant temperature is allowed to climb to an unrealistic maximum, then there is a danger of causing failures that would not be encountered when the vehicle is used by the typical user. The danger of this approach is clearly that overtesting can lead to engineering a solution that is too complex, heavy, or just too costly. A case can clearly be made that the vehicle does need to operate satisfactorily in such conditions, but whether such testing should be part of a durability test program depends on the type of vehicle and its intended market.

16.2.4 The Difficulty of Off-Road Testing

The case of off-road vehicles is more difficult to get right than many other real-world tests. It is not common to design such a vehicle and then be able to stipulate that the user is only meant to drive in certain environments, only on some terrains, or with limits on the vehicle use under defined conditions. An off-road vehicle should arguably be suitable for any situation in which it is able to maintain progress. This can potentially lead to problems.

- *Rough road:* This is perhaps where a road surface has many rocks or potholes, which might occur where a road has been created for large, heavy construction vehicles and is then used for testing light-passenger 4×4 vehicles. It is easy to imagine excessive use of speed damaging the vehicle, introducing unrealistic levels of vibration into the structure or driveline and ending in test results that are difficult to equate to the normal user. Single, unrepresentative events such as large potholes can also cause unrealistic damage. There are many anecdotal stories of potholes appearing in test routes that then give unexpected results or unexpected problems during testing. One such example was found during the testing of an army patrol vehicle in the United Kingdom when large shock loads were measured during testing. The cause turned out to be a large pothole actually just outside of the test area on the approach road. The air suspension had meant that the drivers had not noticed anything out of the ordinary.
- *Soft sand:* Assuming that the vehicle is capable of maintaining progress in such terrain, the torque levels required are very high because of the resistance to motion that is imposed by the sand. Given the relatively slow speeds that most vehicles are able to maintain, the available air-blast cooling is typically low, leading to high powertrain lubricant temperatures. This situation is compounded by the length of time this situation can continue compared with, for example, gradient climbing.

Again, it is difficult to say whether such use is reasonable or indeed, usual. Such a decision can only be made by the engineers in consultation with those who market the vehicle and the user if ready access exists.

- *Very rocky terrain:* Terrains such as dry riverbeds are perhaps the preserve of very capable off-road vehicles. To maintain progress, the vehicle needs to be able to keep most if not all wheels in contact with the ground, requiring extremely good wheel articulation and possibly the use of controlled differentials to prevent individual, lightly loaded wheels from spinning uselessly. The challenge here for the strength and durability of the driveline is especially the high potential for shock loading of the axle components. Whether such use is really a major issue for the lubricant is debatable, but it remains a severe test of the vehicle system.
- *Littoral environment:* This application is common for military vehicles, and in certain parts of the world exposure to the marine environment is not uncommon with other users. The presence of salt in the atmosphere as well as saltwater during wading can be challenging for materials and lubricants. The difficulty for some development engineers is that if such environments are not mandated, the exposure to such conditions can lead to expensive solutions for something that is applicable to few owners.
- *General off-road use:* Within this category consideration needs to be made of trailer-towing, heavy loading within the vehicle, the speed at which it is expected the vehicle will be driven, etc. It might be reasonable for a rugged utility vehicle to operate in a similar manner off-road as on-road. With the lighter end of the 4×4 market, some manufacturers are sometimes arguably selling “an image” rather than a real capability in some vehicles. If this is the case, how do the engineers “downgrade” the capability during testing? This is clearly a decision for each manufacturer. Situations such as recovering another vehicle and towing are expected in the more rugged 4×4 vehicle, but they are probably not designed for with the light, compact off-road vehicles or the more recent “crossover” style of vehicle.

16.2.5 Cooling Tests

One of the key issues for the lubrication system is that of temperature. For example, with many mineral-based oils there can be many more problems if the bulk oil temperatures are allowed to attain temperatures near 120°C or above than if those temperatures are kept down below 100°C. Therefore, manufacturers will want to make sure that temperature measurements are taken during a wide range of road testing to ensure that no one case will find an unforeseen weakness in the system. Typical problem areas are high-speed driving, heavy slow-speed trailer-towing, and in some cases heavy urban traffic. For other vehicles, there will be other circumstances that tax the development engineers. Cognizance of the likely uses to which a user or customer will put their vehicle is vital for the manufacturer, particularly within the engineering team.

To fill out some of the detail, it is worth pointing out why particular driving styles can cause temperature difficulties.

- *High-speed driving:* High-speed testing is very often performed at high ambient temperatures. The cooling performance of the system is dependent on the

differential between the oil temperature and the air that is cooling it. High ambient temperatures reduce this differential. At high speed, the power that is being transmitted by the driveline is high; therefore, the load-dependent losses will be high, and those losses result in high heat going into the oil. With efficient air-blast cooling, this may not be a problem, but if airflow under the vehicle is relied upon to provide cooling, then measures such as noise shields or aerodynamic aids (e.g., spoilers) can be counterproductive.

- *Heavy-duty trailer-towing:* Again, this is a condition in which high power is required to drive the vehicle. The problem with trailer-towing is that there may not be sufficient airflow, because of reduced road speeds, to provide airflow for cooling.
- *Urban driving:* Again, the issue here is the lack of airflow for natural cooling of the transmission. If the vehicle is fitted with a separate oil cooler as part of the cooling group at the front of the vehicle, then this can be enough to keep oil temperatures in the gear box low, especially if a temperature-switched fan is able to provide the required additional airflow. One of the main problems in vehicles over the last few years has been the proximity of the exhaust catalyst to the gear box and the high temperature at which these devices operate. After a period of high-speed driving, the catalyst can be very hot, and the subsequent “soak” of that heat into other parts of the powertrain can be significant.

In the past, maximum oil temperatures have been limited to perhaps 120°C for applications using mineral oils. It was also common to specify a maximum temperature for “excursions” and a lower limit for continuous operations. The difficulty found with this approach is that it is impossible to really limit the frequency and duration of such excursions. Essentially, if a transmission unit is capable of reaching a particular lubricant temperature, then it is probably capable of operating for extended periods at this same temperature. Warning lights can be fitted to alert the driver of high temperatures, or diagnostic systems can record such excursions for consideration later in the workshop. Arguably, a better solution is to engineer the vehicle system so that such temperatures are unlikely under normal operating conditions. In other words, our maximum continuous operating oil temperature is the same as the maximum allowable temperature excursion. However, as has been discussed, the words “normal operating conditions” can be difficult to define.

16.2.6 Extreme Operating Conditions

In addition to the durability of the transmission units, there are several different performance attributes in which the lubricant would be expected to have little or no influence. Some of them will be included here for completeness. For example, during the life of a vehicle, the transmission can be expected to encounter load cases that could be considered outside of the norm. These may occur because of driver error, incompetence, or just simply unusual driving circumstances.

One such case is “the idiot start.” Almost certainly, every automotive company has their own name for this, but essentially what is meant here is when the driver revs the engine to either the maximum speed of the engine or the maximum torque condition and, with first gear engaged

in a manual vehicle, simply slides their foot off the clutch pedal. As can be imagined, this entails the clutch rapidly engaging and the stationary mass of the vehicle reacting against the rotating inertia of the engine. The vehicle will jump forward, and then the (now probably) stalled engine will bring it rather abruptly to a halt. It is unlikely that the lubricant in this case will have any bearing on the outcome of the test—either the driveline is robust enough to endure such abuse or it will fail somewhere. A typical failure would be when one of the gear shafts breaks at the weakest point. The effect on the design of such tests is that the engineer may wish to ensure that the “weakest link” is a component that can be easily replaced. One of the axle half shafts can be selected on a 4×4 vehicle or one of the driveshafts on a front-wheel-drive vehicle. Either of these is somewhat preferable to the main gear box, final drive gears, or the differential gears.

Having discussed the case of the idiot start, perhaps a few other tests not necessarily directly related to the lubricant or the durability of the transmission can be suggested:

- *Heavy-duty trailer-towing:* This should be something considered on commercial or 4×4 vehicles. It is clearly possible to engineer a vehicle that is capable of towing or pulling far more than the normal legal on-road limit. Each manufacturer needs to consider what sort of “overload” they are prepared to design their vehicle to withstand. This will vary greatly, but it could be 3 or 4 times the legal limit on some utilitarian vehicles.
- *Oil-out testing:* This is probably more important and common in the aerospace industry where some geared systems have to perform for a set time having lost all of the lubricant. In some automotive applications, this can be a consideration, and testing needs to be considered to see if the failure is sudden and catastrophic, whether there is a gradual failure accompanied with some audible warning for the driver (squealing from bearings or a loud rattle for example), or perhaps a failure mode that just “disconnects” the drive, allowing the vehicle to roll to a standstill.
- *Water immersion:* There will be mention of the possible problem of water ingestion in the discussion of transmission breathers later in this chapter. A key aspect of off-road vehicles is to understand the implications of immersion in sea- and freshwater and what precautions the operator needs to take if the vehicle is driven in deep water. Of course, “deep water” for a family car will not be same as deep water for a military or off-road vehicle. The latter will need to be able to operate, without preparation, in perhaps 0.5–1 m of water. Military vehicles operating in the littoral environment will be expected to wade to depths in excess of 1.5 m if driven off a landing craft onto a beach. This requirement will need to be agreed upon by the user, the vehicle manufacturer, and the suppliers of the driveline components.
- *Off-road use:* This is probably the most difficult to predict the use cases that need to be designed for. For family 4×4 vehicles, there is an even greater dilemma. The vast majority of such vehicles never leave the tarmac. In the United Kingdom, there is a name for such vehicles—the “Chelsea tractor”—referring to a select part of London where many such vehicles are simply used to ferry the children to school and spend most of their life in traffic queues. If off-road testing is

a serious consideration, then the final result will be a vehicle capable of towing large trailers, accessing severe terrain and gradients, and perhaps driving across one desert or another. Such capability comes at a cost and with a significant weight penalty. This topic has already been covered in earlier sections.

16.3 DISCUSSION: TESTING OF GEAR BOXES, AXLES, AND OTHER INDIVIDUAL TRANSMISSION UNITS

The gear and bearing durability of the driveline for a vehicle has already been discussed in the previous section, and the concepts apply to all transmission units collectively or individually. In addition to this topic, the synchromesh mechanism within the gear box needs to be considered. As discussed in Chapter 10, these have only been associated with manual gear boxes in the past, but the current trend is to automate this type of gear box. This is providing a degree of ambiguity in the marketplace as the customer is presented with a driver interface that mimics a conventional automatic. Conventional automatic gear boxes present very specific engineering challenges because of the clutch mechanisms within the gear train and the hydraulic system within the gear box. These issues are dealt with in Chapter 15. In this section, the testing of separate gear boxes and the methods used will be discussed.

16.3.1 Square Rig Testing

In testing the durability of a gear box (or axle) on a test rig, the essential requirement is to apply a suitable torque at the input, react that torque on the output, and then rotate the transmission for the required number of cycles. As discussed previously, perhaps the most straightforward way of performing this is to fit the unit to a vehicle. However, a test rig that provides a similar loading condition is more repeatable, capable of being run 24 h/day, and probably more dependable overall.

For durability testing, the development engineers normally need to be able to apply torque levels at least equal to the maximum that will be experienced in the vehicle. Manufacturers will often achieve this by mounting the transmission on a rig powered by a combustion engine. This approach gives the benefit of realistic torque transients as well as average torque levels, although running costs can be high. In addition to this, the equipment required to provide several hundred kilowatts of power using an electrically driven test rig is very costly in terms of the initial installation and the running costs.

However, the approach to rig testing taken with many geared systems is to use a “four-square” configured test rig. With this type of test rig the output of the unit being tested is fed back into the input via a slave gear box with the opposite gear ratio. In this configuration, torque can be wound into the test rig while it is stationary, and when rotated the only power input required is to compensate for the losses in the system. Figure 16.4 shows this principle.

In practice, these test rigs can be costly to set up because a slave gear box is required that mimics the gear box under test. The detail that causes the most difficulty is that the ratio has to be opposite to the test unit. For example, if the test gear box has a 2:1 reduction ratio, the test rig slave gear box needs to have a 0.5:1 speed increasing ratio. Another way of looking at this is that in the test gear

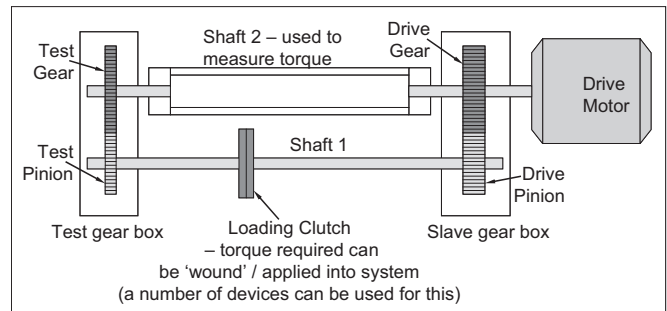


Figure 16.4—The principles of a four-square test rig. The FZG-type test rig shown here is typical of the four-square rigs used for gear testing, although other configurations are available.

box if the pinion is the drive gear, the slave pinion will be the driven gear. One expedient that can be used is to utilize another test gear box as a slave gear box. This will rotate in the same direction as the test gear box, although the torque will be applied in the opposite direction. Assuming this slave gear box can be run under more favorable conditions than the one under test, the fact that the rotating parts are operating counter to the design intent can be acceptable. Precautions that could be taken include ensuring that the slave gear box is kept cooler than the test gear box and using a lubricant with a better load-carrying capacity. Care must be taken that the bearings within the slave gear box can be loaded in the opposite sense than intended.

This principle of power recirculation is also used in the FZG and similar gear test rigs [2]. These tests are discussed in detail in Chapter 11. Using these test rigs, a large torque can be applied to the test gears without needing large drive motors on the input of the test rig or large brakes (power absorption devices) on the output of the test rig. This helps to keep down the initial cost of the test rig and the ongoing running costs.

An alternative configuration to the FZG test rig is used by the National Aeronautics and Space Administration (NASA) Glenn Research Center in their gear fatigue test apparatus [3]. With this, as with other similar rigs, the load can be applied using a hydraulic circuit that potentially allows load levels to be changed during a test. This helps to speed-up testing and lower costs, and it gives more flexibility over load cycles.

16.3.2 Gear Box Testing—Gear Changing

The external gear-change mechanisms are discussed later. In this section, the mechanism within the gear case is considered. As discussed in Chapter 10, the synchromesh is the mechanism in the gear box that enables the change in gear to be accomplished. During a gear shift, the input side of the gear box, the clutch assembly and the engine crank, has to alter its speed to match the speed of the vehicle. Of course, the output of the gear box and the rest of the driveline is nearly held at constant speed during the short time taken to shift gear under normal conditions. The components within the synchromesh assembly are effectively a brake mechanism and are therefore subject to wear in the same way as most friction mechanisms of this type. For intermittent use, an oil film within the assembly can perform various functions, but the issue of interest here is the control or elimination of wear. Winding the clock back a few years, it

was not unusual to drive a high-mileage car and find that changing gear from third down into second gear would be accompanied by an assortment of noises—most of them not very pleasant. The work done by the synchromesh of second gear tended to be rather more than by the other gears; therefore, the mechanism tended to suffer in some cars. The reason for this problem was the wear that had taken place to the baulk (blocking) ring within the synchromesh. Because this problem does not surface on modern cars, it is reasonable to assume that the wear on the parts is controlled sufficiently or eliminated.

Depending on the type of vehicle, taking data from vehicles used in the field and using these to assess a typical gear-change pattern is one possibility. It is likely that a vehicle used around the city or a delivery vehicle would be the worst-case scenario; therefore, data could be taken from that environment. It is reasonable to assume this would be a typical, normal, but challenging target against which to assess the durability of the gear selection mechanism. As discussed elsewhere in this chapter, each manufacturer will have their own targets, or engineering standards, for this type of characteristic. Once it is known how often the “target” driver changes gear, a decision can then be taken as to how many cycles to test to and hence the resultant figure for upshifts (first gear into second gear; second gear into third gear; and so on) and downshifts. Although these gear shifts will take place at all sorts of road speeds and engine speeds, it is reasonable to assume just a few typical test conditions. Summarized, synchromesh testing needs to address several issues and has several variables needing definition as shown in Figure 16.5. Standardization of testing would be very difficult because of the variation in applications and requirements between vehicles and manufacturers.

Each manufacturer will have used their own measured data to decide on the number of shift cycles for any given mileage (i.e., the shift frequency). The design intent mileage will also vary from around perhaps 250,000 km for a passenger car to in excess of 1,500,000 km for a heavy commercial vehicle. This obviously has an effect on the total number of cycles just as the frequency of shifting does.

In addition to durability testing such as illustrated above, manufacturers may also consider whether there is a need for additional test cases such as

- *Skip shifts (e.g., first to third to fifth)*: Should these be used as part of the tests, and if so, what percentage of the test should these constitute? It is worth noting that new drivers (on manual cars) are now taught this technique because of the improved fuel consumption that it can lead to.
- Using robotic shift test rigs, tests can be performed to a set pattern to mimic realistic driving yet still achieve the numbers of cycles required.
- Should the testing be performed using the maximum clutch inertia used on that gear box, or should there be a range of clutch parts used?
- *Abusive tests*: Applying an excessive shift force (i.e., a very short shift time) can overwhelm the synchromesh mechanism in some circumstances. Is it reasonable to test for this to see if the mechanism is damaged beyond further use? If so, how many times should this happen, and should it apply to all gears? The second gear synchromesh in car gear boxes has traditionally displayed signs of distress earlier than other gears. This is particularly the case when undertaking rapid downshifts from third gear into second gear.

The latter question is perhaps particularly important with some types of baulk ring materials because there are

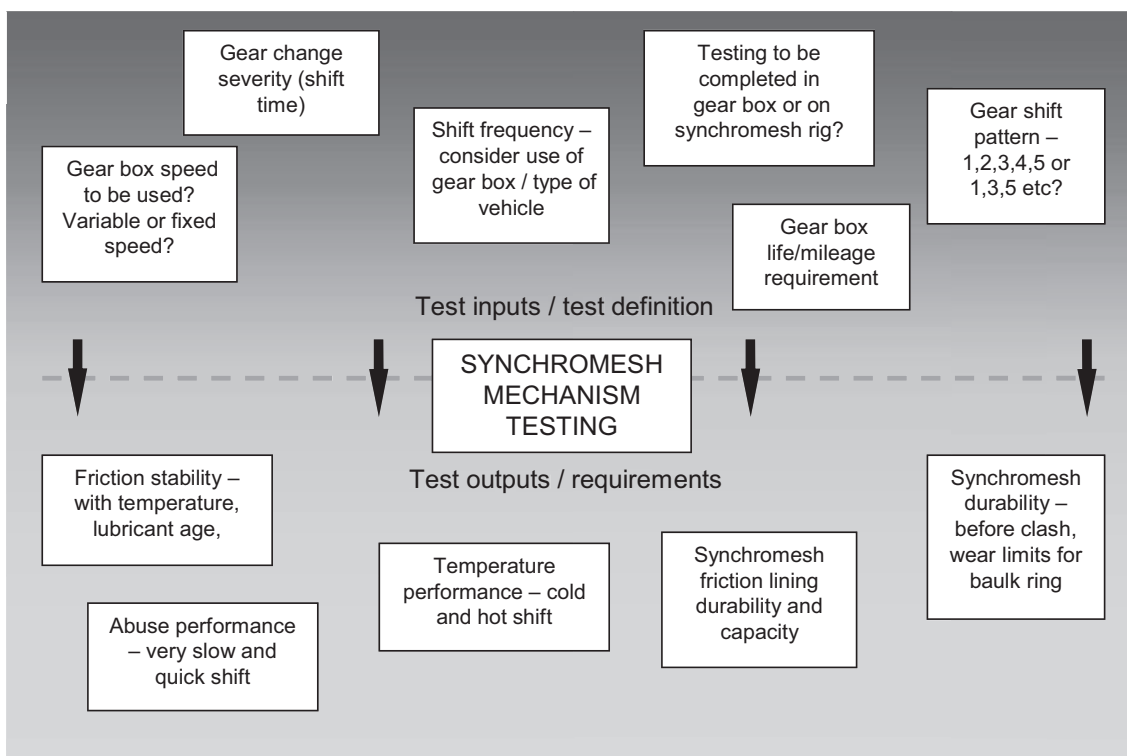


Figure 16.5—Flowchart diagram showing required decision points and outputs of synchromesh testing.

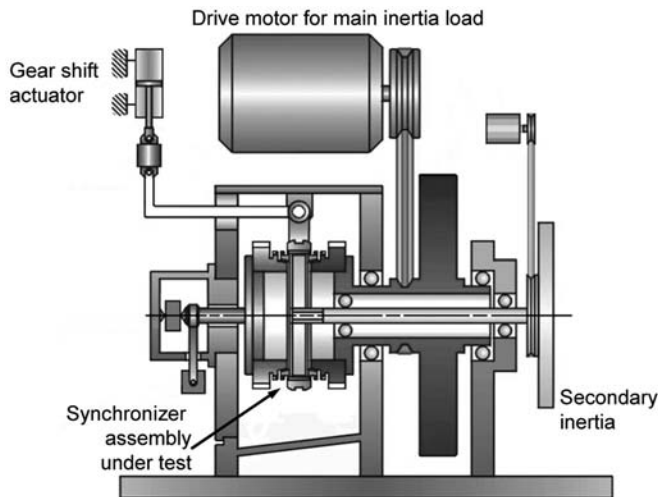


Figure 16.6—FZG SSP synchronizer test rig.

friction lining materials that perform excellently up to a limit and then if pushed over that limit they can fail quite suddenly. This issue is probably becoming less of an issue because sintered metallic and other robust friction linings are becoming more common. The standard material for this component used to be brass, aluminum bronze, or something similar. The friction surface would have oil-clearing grooves machined into them. For some years, various resin-bonded organic lining materials were used. When used well lubricated in normal conditions, they exhibit very good wear performance and wear properties. However, it is possible, in theory at least, to do so much work with them that the lining material can fail quite suddenly because of excessive heat buildup. It is debatable if this could be considered a reasonable use case or not, but the advent of the more recent metal-sprayed, sintered, or other new linings has led to rather more abuse-tolerant components. Again, the question for the development engineer is to establish what reasonable use is and what is simply abuse.

Several bodies have investigated a standard test machine over the years, and one such device is used by the FZG institute in Germany. In some references, this type of test rig may be referred to as a “Hurth” rig.

Another issue with synchromesh testing is the question of the shift feel. This is not a problem for the durability of the components because problems can occur at any mileage and component condition from new. Ironically, this has become more of a problem in recent years because of the advent of more powerful synchromesh mechanisms. A full discussion of the problem is included in Chapter 10, but specialist test rigs are needed to assess the shift feel. These sense the magnitude of the shift load and the instantaneous variation in that shift load as the gear is engaged. These rigs may not be the same as those used for durability testing, but the results can be invaluable to ensure that the customer has a gear shift that is not only light in load but also feels smooth, without undue rough “notches” as the gear is selected. This issue is clearly more important for the passenger car rather than the heavy commercial market.

16.3.3 Final Drive and Differential Testing

Much of the testing for these units falls into the above category of durability of the gears and bearings. However,

final drive gears will operate at rather lower speed than the main gear box, and if the vehicle is fitted with a two-speed transfer gear box, then the vehicle can be capable of applying huge torque levels at the axle or wheel or both. The following is an example to illustrate this:

- Consider a 4×4 vehicle with a maximum engine torque of 500 Nm.
- A typical gear box first gear ratio would be approximately 3.5:1; therefore, the output torque is 1750 Nm.
- A two-speed transfer gear box is likely to have a high range ratio around unity and a reduction ratio in a low range of approximately 2.5:1; therefore, output torque is 4375 Nm.
- Assuming a ratio of 3.5:1 in the axle final drive gears, the torque at the wheels is 15,313 Nm.

The torque levels at the axle are clearly very high, and it is probably debatable whether the vehicle will be capable of mobilizing this force without the tires losing traction. (Indeed, assuming this figure, a tire radius of 0.4 m, and a rather high tire traction coefficient of 1, a vehicle weight of ~4 t would be required to deliver this traction without wheel slip.) Such high torques, coupled with the slow speed, present a challenge to the lubricant and some headaches for the test engineer.

The key engineering challenge in the axle is that there are two systems operating here. Within the axle, the drive is turned through 90° and the speed of rotation is reduced; the final drive gears do this. The differential is also installed within the assembly. The lubricant will need to perform adequately in both mechanisms.

16.3.3.1 FINAL DRIVE GEARS

In many front-wheel-drive car and van transmissions the final drive gears serve two purposes: to reduce the speed of rotation from the output of the gear change gear set to the output of the gear box and to provide much of the required offset between the engine crankshaft and the driveshafts to the wheels. The output, of course, rotates at wheel speed. Typical ratios for these gears are between 3.0:1 and 5.0:1, and they are invariably helical gears. Chapter 10 contains diagrams and more detail. The key aspect here is that there is little difference in the lubrication requirements between the change speed gears and the final drive gears. The torque levels are higher because of the reduction ratio; therefore, a higher facewidth would be expected on the final drive, and the location in the gear box can mean the oil levels are increased around the final drive gears. However, the lubrication regime is less onerous than the bevel gears found in most axles, especially compared with the hypoid gears commonly found in larger vehicles.

With rear-wheel-drive or all-wheel-drive vehicles, the final drive gears are nearly always within the axle assembly and therefore are usually spiral bevel or hypoid gears; more detail is contained in Chapter 10. The key aspect with bevel gears is that the contact condition is often not as conducive to easy lubrication as in helical gears; there is more sliding within the gear mesh. This especially the case with hypoid gears because the offset on the gear mesh is the cause of this sliding. The greater the offset, the higher the sliding speeds for any given pitch line speed. Later in this chapter, GL-4 and GL-5 gear oils are considered; suffice to say here that the latter have greater extreme-pressure properties. In some circumstances, the use of GL-4 oil may be considered for

helical and spiral bevel gears; therefore, antiwear performance is probably adequate in such a case. However, if the axle is fitted with hypoid gears, then the higher sliding speeds mean that the lubricant will require an extreme-pressure additive package, and a GL-5 oil or something similar would be required. As will be seen, recent developments of these longstanding specifications have given the transmission engineer higher performance lubricants to choose from.

16.3.3.2 THE DIFFERENTIAL

The differential is fitted within the transmission to allow the wheels on opposite sides of the vehicle to rotate at different speeds when the vehicle travels around a corner. Under normal use the differential gears are stationary, and the whole differential assembly rotates as a single unit. This presents a dilemma for the development engineer when testing because in a test rig the two output shafts will often rotate at similar if not the same speeds. For convenience and cost, on some test rigs the differential will be locked in some way so that the output can only be taken from the axle assembly on one side. Clearly, in this condition only the final drive gears (or the effectiveness of the lubricant) can be tested and not the performance of the differential gears.

The differential mechanism itself is clearly the more awkward part of the axle to test because a different output condition needs to be applied at the two driveshafts or wheels. Clearly, this is going to happen when tested in the vehicle, but if more control over the test conditions is desired, a test rig is more appropriate. The decisions that need to be made by the development engineer include what are the most arduous conditions that the differential will reasonably encounter and as such what testing needs to be completed in addition to the normal road mileage, etc. There will be several conditions that need to be built into these tests, including high and low speed and the situations in which there is a significant speed differential across the axle.

It is probably the case that each vehicle manufacturer will have in-house tests to satisfy themselves on the adequate durability and abuse resistance of the differential assembly. These tests are likely to be rather more stringent for 4x4 or off-road vehicles than family cars or road-going commercial vehicles. Without speculating as to what the detail of these tests may or may not be, it is likely that two conditions will be of interest:

1. *High-speed, low-torque conditions on the differential:* This would be similar to when driving a performance vehicle and one wheel lifts on cornering, allowing it to spin quickly compared with the other wheel that still maintains traction on the road surface.
2. One can envisage that in tight off-road situations a slow-speed, high-torque condition will occur in which a large torque is applied to both wheels, although there is a reasonable differential in the wheel speed. Similar circumstances can occur when the vehicle is maneuvering while towing.

In years gone by, the data to enumerate the speed difference between wheels and be able to correlate these with engine or transmission torque would have been difficult, probably expensive, and in some cases simply not possible. With modern data gathering techniques, the engine and transmission data available within the vehicle databus, and information on individual wheel speeds from the vehicle

antilock brake controller, the vehicle engineer has much more opportunity to be able to identify the operating conditions. These data can be gathered during "normal" road use or during specific, presumably damaging, test conditions. Armed with these data, the opportunity to devise targeted test regimes is much better now than even a few years ago. For differential testing, the engineer would clearly be trying to establish what percentage of time was spent either with a high-speed difference (and the associated torque magnitude) or with a significant speed difference during periods of large applied torque.

16.3.3.3 EFFICIENCY TESTING

Although some discussion in Europe and the United States has suggested that standard methods be developed for efficiency testing, there appears to be little widespread agreement as yet. The main problem with the efficiency of transmission systems in vehicles is that the effect on the vehicle performance is difficult to measure. The effect that would be hoped for as a result of improvements in efficiency is, of course, an improvement in fuel economy. Unfortunately, the variation in fuel consumption that occurs in vehicle testing is likely to be of a similar magnitude as the improvement hoped for, if not greater. This will be the case even on a rolling road under the controlled conditions that exist within this type of facility. Of course, this does not mean that small improvements in efficiency should not be pursued because they can be beneficial given the correct circumstances. What the relatively small changes do mean is that accurate test data and validated simulation models are crucial if there is a need to understand the end result of lubricant or efficiency changes on the vehicle system.

Chapter 10 discussed the various mechanisms that are responsible for the losses in the transmission. Because there are several different mechanisms, it is difficult to envisage a single test condition that would give an overall indication of the efficiency performance of a fluid within a particular transmission. This problem is then compounded if considering the variation that exists between different transmission units. Therefore, there is arguably a need to test for these different contributions, and this would mean performing several tests, possibly using different test setups or utilizing different instrumentation. For example, one might envisage a situation when comparing two fluids in which a beneficial effect from the base fluid in one of them is mimicked by improvements in the additive package of the other. Although the result from some testing might mean the overall result is similar, there is arguably a need to differentiate between the two to optimize the result.

There appears to be little widespread acceptance or use of specific testing described in the technical literature. It has been found in some engine tests that the availability of test units for several years can be problematic. With testing that utilizes a complete transmission unit, the continued availability of consistent test units can also be an issue. Manufacturers are always looking to improve the specification and the design, take cost out, or improve the durability, etc. The possibility of exactly the same specification of transmission unit being manufactured for many years is unlikely. The other issue of one test unit being widely agreed upon is that because designs vary, the validity of results gained from any one design of gear box or axle is likely to be quite different from results gained from another unit.

To pursue this topic, the various methods of measuring the loss in a geared system need to be considered. Several ways of doing so can be suggested, and Table 16.1 indicates some of those methods as well as the advantages and limitations.

The most common method probably used in recent years is to measure the efficiency via torque measured on the input and output shaft of a test bed transmission. This can only be done when testing the unit in question on an open-loop test bed as the torque is “wound in” to the transmissions on a four-square test rig as discussed earlier in the chapter. This means the losses in the system are not clearly delimited between the slave and test units. Indeed, the way these rigs are set up (i.e., with heavier duty gears, bearings, and oils in the slave gear box) probably means greater losses will be obtained in that unit than the test one. However, despite these drawbacks, four-square rigs do offer a good standardized opportunity for comparative testing, and one may choose to use the test fluid in both gear boxes. A set of test conditions could be envisaged that would cover low-load, low-temperature, variable-speed tests to assess the

effect of parasitic losses, and high-power (torque) conditions that would assess the load-dependent losses within the system.

Researchers have used indirect measurement of transmission losses in the past. If the assumption is made that the energy lost from the system is turned into heat, then one indirect method that can be used is to measure the heat taken from the system. A rather more difficult embodiment of this method is to measure the warm-up of a unit when on a test rig and run either under load or under free-running conditions with no load. The record of the temperature increase can then be compared to an artificially applied heat input via an electrical element, with the premise being that if the temperature rise in the “dummy” test with no load or no rotation of the transmission equals the live test of the unit, then the electrical heat input in the former equals the losses in the latter. In this way, no real torque measurement is required, and it is argued that the electrical input is easier to control and measure than the mechanical input/output of the transmission unit. Over the last few years, accurate torque-measuring equipment has become

TABLE 16.1—Various Methods of Assessing Efficiency, Including Lubricant Effects

Test description	Advantages	Limitations
No-load “spin” test—measuring the torque to turn at the input shaft.	Relatively cost-effective and requires little instrumentation except an accurate torque transducer and thermocouples. Accurately discriminates parasitic losses (i.e., oil churning) at different speeds and oil temperatures.	No account taken of load-related (friction) losses within the gear mesh; therefore, it provides an incomplete picture of overall losses. Loads on bearings can also be influential.
Test on rig measuring input and output speed and torque.	Nearly direct picture of power in and out of the transmission. Test unit is in potentially realistic test conditions—under load.	Care needed to ensure that the torque measured is accurate—losses can be quite small (1–2 %) and errors in transducers can be similar. Output torque can vary greatly in different gears; therefore, instrumentation choice is critical. Care needs to be taken regarding the temperature of the environment, the unit bulk, and the lubricant temperature.
Measure heat output from the test unit. (Note: There are several variations on this theme in the literature, and some are quite complex.)	Can potentially be cheaper than acquiring the accurate instrumentation required for the method above.	The need to measure heat to oil means accurate flow measurement as well as accurate temperature measurement. Difficult to perform unless oil is pumped through an external cooling circuit perhaps. Need to ensure that temperature has reached equilibrium because heat can be lost in warming up the test unit and rig structure. Need to account for all heat losses.
Use standard test rig such as FZG gear tester. Need to measure losses in both test and slave gear boxes. Rig input measured at drive motor.	Potential for tests that can be repeated and validated in different locations. Good potential for accurate differentiation between test fluids. Different gear designs allow friction losses to be investigated under different lubrication conditions (e.g., high sliding conditions).	Can be difficult to ascertain which loss mechanisms are influenced by a change in fluid. The influence of the slave gear box needs to be carefully considered. Parasitic/churning losses are relatively low compared with many transmissions.
Test in vehicle by measuring fuel consumption.	The key advantage is that this gives a direct indication of our desired end result—better fuel economy. Easy test setup if vehicles are available.	Fuel economy testing is particularly prone to variation. Fuel usage in vehicle can be difficult to measure accurately because of temperature variation, return (spill) fuel lines on some vehicles, and level of accuracy required.

more readily available and rather more cost-effective. It is debatable whether the complexity of the temperature-controlled test mentioned here is now sensible.

Relating improvements to the effect on the vehicle is the real “end game” of this topic. As has been suggested, the actual fuel economy benefits can be awkward to ascertain. The improvement in vehicle simulation over the last decade or so has given the development engineer the tools to be able to assess potential changes to the vehicle performance at modest cost. However, this does need the careful validation of the computer models used. It is important to accurately model the resistances to motion that occur so that the transmission losses do not make up an unrealistic proportion compared with other losses such as the rolling resistance of the tires or the aerodynamic losses. Such computer models are now the norm for vehicle development. It can be particularly useful where active thermal management can be used within the vehicle to provide the most efficient overall system. For example, such developments can prove beneficial where waste heat is used from one part of the vehicle (e.g., the engine) to warm up the gear box, for example, to improve the total efficiency of the vehicle. Only simulation can provide the system optimization of such developments because it is possible that a positive effect in one area will have a negative effect in another. Care is clearly needed to ensure the best outcome in such complex problems.

16.4 DISCUSSION: OTHER TRANSMISSION TESTING, INCLUDING BENCH TESTS

In this section, the testing that may be considered to prove some of the peripheral items on the transmission system will be discussed. Some of these items will seem to be quite insignificant, but without them the whole system would simply not function. Equally, as will be seen, there are aspects that can be quite challenging to engineer. These aspects appear to be minor, but the amount of effort involved within the development process, and the implications of getting the wrong solution, can be disproportionate.

16.4.1 Breathers

The breather system of any transmission unit plays a vital role as seen in Chapter 10. There is a need to ensure that oil cannot be expelled from the unit and conversely that debris or water cannot enter the unit. This can be awkward to achieve on any unit, but on off-road vehicles it can be particularly demanding because the customer is more likely to immerse the unit in deep water and expose it to sandy, dusty, or dirty conditions. The outlet of the gear box or axle where the breather will fit should, fairly obviously, be toward the top of the gear box, away from the fluid. However, it is important to consider how it can be ensured that nothing untoward gets in or out. Unfortunately, it is almost impossible to specify a series of simple standard tests that would ensure satisfactory performance; almost all configurations will be unique. However, what can be done is to suggest some conditions that need to be considered when testing the vehicle.

- Consider the different installation angles at which the unit is fitted. Does this vary in different versions of the vehicle(s)? Do any one of these installations place the breather lower than any other?
- Some testing with no breather fitted may help to understand the likelihood of problems—perhaps with

an oil catcher of some description to see what oil, if any, does come out and, more importantly, when. Safety considerations clearly mean this is more likely to be performed on a test rig rather than in-vehicle.

- The development team needs to consider whether high-speed, low-speed, level-road, uphill, or downhill driving is more likely to cause oil expulsion than any other condition. Cornering, and the lateral accelerations this creates, also needs to be considered.
- What will happen when a hot transmission unit is immersed in water needs to be considered with any vehicle. This could happen when the vehicle needs to ford a river or encounters an area of road that is flooded. Clearly, this is more likely for off-road vehicles, although even road-going vehicles may reasonably be expected to cope with some degree of immersion.
- With the main gear box of a vehicle, the engineer needs to consider whether any particular gear selection is more likely to cause problems of oil expulsion than another. This might occur where the breather is fitted at one end of the unit, and the oil tends to gather at this location when one gear or another is selected.
- It can be useful to consider what testing can be performed on a test rig rather than in-vehicle. Rig testing will clearly be quicker and cheaper and will probably also have the advantage that it can be performed earlier in the development program than in-vehicle testing.
- Rig testing can also be performed with a transmission unit where steps are taken to be able to see inside of the unit. A few years ago this would entail cutting “windows” in the gear case to see where and when the oil flowed under different conditions. Over the last few years, the availability of temperature-resistant, optically clear resins has enabled covers or cases to be manufactured so that the oil flows can be viewed within a test transmission.

16.4.1.1 AIR RELEASE AND AIR ENTRAINMENT CHARACTERISTICS OF THE FLUID

One characteristic of the lubricant that has an influence on the performance of the breather in a transmission is the air retention properties. As the lubricant is churned

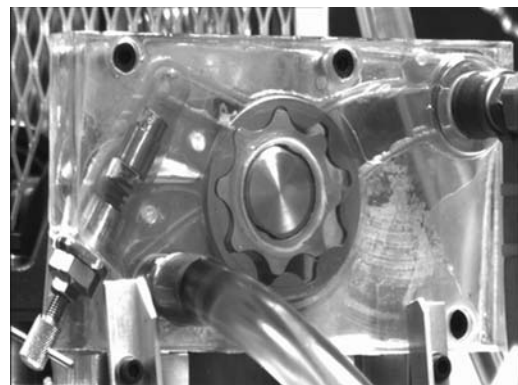


Figure 16.7—Example of flow visualization work. The photograph shows an oil pump such as might be fitted to either an engine or transmission unit. The use of cases made from clear resins helps in the development of the lubricant system. Such work allows the variation in flow to be viewed and measured over a range of input conditions.

by the motion of the internal components, air is mixed in with the fluid, and this increases the effective fluid volume. In the extreme, the fluid “foam” could conceivably increase in volume to an extent that it exceeds the internal volume of the transmission; testing of the breather system would hopefully show this. In addition to testing the whole transmission, the fluid can be tested using standard bench tests. These will be discussed in Section 16.5. In the event of knowing one fluid has a satisfactory performance, the available bench tests can be used to compare the performance of the known, existing fluid and the new one. At the very least, this would give greater confidence in a new fluid and potentially reduce the amount of testing needed for the sign-off of the engineering change.

16.4.2 Linkages

Earlier in the chapter the issues surrounding the establishment of a test regime for the gear box synchromesh devices were discussed. The part of the gear-change mechanism external to the gear box has similar development needs; the typical shift pattern needs to be established as well as the number of gear shifts and the severity of those shifts. It is possible to use similar test specifications for synchromesh assembly and linkage. Also, if the synchromesh tests are to be performed in a production or near-production standard gear box, it is conceivable that the same tests could cover both mechanisms. The essential system failure of interest is probably one that falls outside of the scope of this chapter in that the linkage is likely to use cables or linkages with dry, composite bearings. As such, the wear life required to be investigated is not a lubricant issue as such, but simply a matter of wear rate. If the failure mode is simply wear, then it needs to be decided what free play can be tolerated, and this probably comes down to a subjective measurement at the gear knob. This will depend on several inputs, including the overall movement of the lever, the perceived quality level of the vehicle, and ultimately the amount of movement before accurate gear selection becomes difficult.

The environmental effects on the linkages need to be established. These mechanisms tend to operate within the engine bay of the vehicle and therefore will be exposed to high temperatures in excess of 150°C, which could be even higher if the linkage needs to be routed near the catalyst of the exhaust system. Now that close-coupled catalysts (those near the exhaust manifold of the engine) are required to meet new emissions standards, such close routing will be increasingly common. Should any polymer materials be used within the linkage joints or bearings, they then clearly need to withstand any temperature exposure. Equally, if any applied lubricant is relied upon, that would also have to be retained within the mechanism and withstand the same temperature exposure. Testing at realistic temperatures is clearly required.

Another aspect of the environmental effect is the presence of water or debris. It is easy to imagine that road dirt (sand, grit, salt, etc.) would get on the mechanism, but if considering an off-road application, then the linkage actually operating completely immersed in water or possibly with dried-on, baked mud could be envisaged. If it is decided that one aspect of particular concern is the possible effect of corrosion, then salt-spray enclosures can provide a suitable test environment. Although these do not exactly mimic real life as such, they can be very useful in providing an

indication of comparative performance between an existing, known system and a new, revised one. Equally, many companies will have set particular salt-spray test durations as the criteria for acceptance of the corrosion of components to be fitted within the engine bay or underneath the vehicle.

16.4.3 Seals and Sealing

High temperatures within transmissions are a major worry for gear box manufacturers and the vehicle original equipment manufacturer (OEM). High lubricant temperatures cause all sorts of problems for the fluid itself and the other components within the unit. This is nowhere more significant than for the seals. Although minor, low-cost items compared with other parts, they can fail rapidly and by allowing massive leakage of the working fluid can cause catastrophic failure in very short time. The failure mode could be argued to be more of a failure of the fluid than the seal itself. This is because high temperatures with some fluids cause the fluid to degrade, and hard deposits form on the lip of the seal. It should be remembered that the lip of an oil seal is actually a very fine edge of rubber-like material. It is then easy to envisage that any hard deposits will interfere with the function of that lip. In turn, this failure increases the local temperature buildup at the seal lip, which of course then increases the rate of failure. Many modern seals are made from fluorocarbon or polytetrafluoroethylene materials that are far more able to withstand temperatures in excess of 100–120°C; however, this may not be the case for the fluid. With the seal material and perhaps more so with the lubricant, cost is the key issue. Technology exists to reduce or possibly eliminate this problem unless the temperature buildup in the transmission is beyond that expected for some reason. However, some of the newer technologies come with a high cost associated with them.

In addition to the lip build-up problem that can cause leakage in transmissions, the lubricant can affect the material used for the seals. This can cause degradation of the material and again ultimately loss of lubricant and failure of the unit. In the next section, some of the bench tests available will be considered, and the effect of a lubricant on the seal materials is the focus for some of these tests. A typical response of some materials is to swell in the presence of hot oil, and this characteristic can be measured. Again, a known, satisfactory material-fluid combination can be useful in allowing comparative testing.

16.4.4 Driveshaft Joints

Because of the overwhelming number of front-wheel-drive vehicles manufactured worldwide, most driveshafts manufactured are for this type of vehicle and therefore of the constant-velocity type. Heavier vehicles are still more likely to use the universal (Hookes) joints. In the past, the joints used in most situations required the regular reapplication of lubricant, although nearly all light-car joints now are now sealed for life; therefore, the manufacturer is responsible for the lubricant choice, application, and sealing. The trend in heavier vehicles, in which periodic relubrication may still be expected, is for the service intervals to increase, similar in principle to the oil changes in the main transmission units. The testing of the grease for this application is a specialist task, as is the design of the joint itself. As with many transmission systems, one of the key concerns is

TABLE 16.2—Review of ASTM Standards That Could Be Considered during the Development of a Transmission Fluid for In-Vehicle Use

ASTM Test	Comment
D665-06 Rust-Preventing Characteristics of Inhibited Mineral Oil in the Presence of Water	A test such as this can be useful to confirm if a new lubricant will potentially be able to control corrosion within a transmission unit should it be contaminated with water. If a fluid is known to be satisfactory, then it could be that a comparison made using such a test is used to provide some confidence in this specific characteristic.
D892-06 Foaming Characteristics of Lubricating Oils	The importance of correct design of the breather for a gear box was discussed earlier in the chapter. Foaming of the oil is a major contributor to performance of the breather system, and tests such as this can give some confidence in a new fluid before embarking on the testing of the system in the unit, on a test rig or in-vehicle. Test method D6082 can also be used to determine the foaming characteristics.
D2266-01 Wear-Preventative Characteristics of Lubricating Grease (Four-Ball Method) (D2783-03 is a similar method used for extreme-pressure performance of oils, and D4172 is used for the wear performance of oils.)	The load-carrying capacity of a lubricant is one of the key aspects likely to be of interest. Wear between contacting components is clearly a vital aspect to get correct, and manufacturers often quote the four-ball test as an indicator. However, it is worth pointing out that the contact conditions within a transmission are somewhat different than those found within the four-ball test; therefore, this type of test is again useful for screening fluids rather than proving their application in a particular transmission. The test method points out that there has been no correlation between the test and field service. It should be noted that there is more than one version of the four-ball test machine, and each different test requires the use of a particular type.
D2782-02 Measurement of Extreme-Pressure Properties of Lubrication Fluids (Timken method) (There are several other test methods for extreme-pressure performance.)	The four-ball method above uses four ball bearings in contact that are rotated against each other under load to find the point of seizure. Likewise, this test uses a tapered roller-bearing component running against a test block under high load to determine the amount of scoring of the contacting surface. As with the four-ball test, the contact conditions are different than normal gear and bearing contacts, although the test can be used to indicate the extreme-pressure performance.
D2893-04 Oxidation Characteristics of Extreme-Pressure Lubrication Oils	This test assesses the oxidation performance of gear oil by exposing it to air (bubbled through the fluid) at high temperatures. The degradation of the fluid is assessed by measuring any change in viscosity and by looking at any precipitation during the test. When oils are operating in transmission units, the heat generated means that the fluid gets hot. These high temperatures can mean that the oil degrades, and this can lead to premature failure. Although tests like this do not replicate the conditions within a gear box, they can be used successfully to assess the performance of a new oil against a known fluid.
D3427-07 Air-Release Properties of Petroleum Oils	This test measures the ability of oil to release air bubbles that have become mixed into the fluid. It is linked to the foaming test in some ways because both mechanisms will have an effect on the breather performance within a transmission unit.
D3527-07 Life Performance of Automotive Wheel Bearing Grease	This is a laboratory procedure for testing the high-temperature durability influence of greases used within the wheel-bearing assembly. Much of the discussion here has been aimed at the larger transmission units, but the final part of the drivetrain system is the wheel-bearing assembly. In practice, these can be separate hub units or be built into an axle. Some examples can also be oil—rather than grease—lubricated.
D4289-03 Elastomer Compatibility of Lubricating Greases and Fluids	This test evaluates the compatibility of an elastomer with oils and greases. An assessment is made of any change in the volume of the material and any effect on the hardness. The test is performed at high temperatures, which can be varied depending on the application and type of oil. D5662-09 also addresses elastomer compatibility with automotive gear oils.
D5183-05 Determination of the Coefficient of Friction of Lubricants Using the Four-Ball Wear Test Machine	As the title suggests, this is a procedure for measuring the friction using the standard test machine. The test is performed under lighter loads than would be used in the extreme-pressure tests and requires a version of the four-ball tester with greater sensitivity.

(Continued)

TABLE 16.2— Review of ASTM Standards That Could Be Considered during the Development of a Transmission Fluid for In-Vehicle Use (Continued)

ASTM Test	Comment
D5704-09 (L-60-1) Evaluation of the Thermal and Oxidative Stability of Lubricating Oils Used for Manual Transmissions and Final Drive Axles	This test in some ways follows on from D2893 and similar tests but uses a simplified test gear box to provide a representative environment for the test fluid to test its stability at raised temperature. The test rig contains a gear pair run under load, allows for heating of the oil, and has air blown through the fluid. This test also forms part of the suite of tests for the GL-5 service designation and is referred to as the "L-60-1" test. Because this test uses a relatively complex test gear box as part of the rig, the question does need to be posed as to whether it can be classified as a bench test; nonetheless, it does not use a standard production gear box.
D6425-05 (DIN 51834) Measurement of Friction and Wear Properties of Extreme-Pressure Lubricating Oils	This test uses an SRV test machine, which assesses the oil's coefficient of friction and its ability to protect against wear when subjected to high-frequency oscillating motion. As with several of the tests discussed in this section, it does not attempt to mimic a real gear box but can be useful to assess candidate oils, especially when compared against existing known good oils. It must be pointed out here that tests such as these reproduce a contact condition that simply does not occur within a real transmission unit; therefore, care must to be taken in assessing the relevance of the results.
Note that the date indications were correct at the time of writing but may have been subsequently updated. Another discussion of the ASTM tests can be found in ASTM Manual 37 [4].	

temperature, and the environment near the gear box can be extremely hot, especially if the exhaust is allowed to influence this to an undue degree. The variables that would need to be taken into account if considering the testing of shaft assemblies or joints would include

- *Environment:* Particularly temperature, presence of water, salt, mud, etc.
- *Speed of rotation:* Profile of test speeds or is testing to take place all at the maximum speed encountered?
- *Load profile:* As with all transmission units, the torque applied during the service life varies greatly; therefore, the testing needs to reflect this, which means that testing can be reduced if the fatigue damage is calculated as being largely a result of just part of the load spectrum.
- *Possible failure modes:* Testing needs to reflect wear damage and surface fatigue damage within the joint.
- *Angle of installation:* Nominal angle of the vehicle design at the nominal suspension or axle position.
- *Variation of the angle with suspension motion.*
- *Degree of plunge:* As the suspension or axle moves, the installed length of the shaft is likely to change, which means one of the joints on the shaft needs to move axially to accommodate this.
- *Steering influence:* The outboard joints of front-wheel-drive vehicles or front axles need to accommodate the movement of the road wheels when the vehicle is steered, which will mean that these joints are likely to experience the highest angle.

16.5 DISCUSSION: ASTM TEST METHODS

In this section, the relevant standard lubricant tests available from ASTM are considered. Many of these are bench tests intended for screening of lubricants, as has already been discussed elsewhere in this manual. These can provide very useful insight into the relative performance of different lubricants. This is especially the case if an existing fluid has proven performance in the transmission unit in question. A reasonable degree of confidence can conceivably be obtained in a new fluid if it is similar to the existing one and perhaps is just a marginally different viscosity or

maybe has a slightly modified additive package. However, where there has been a significant change to the lubricant, these simple "bench" tests will not give a complete picture of the effect on a transmission unit. This is also the case where a new or revised transmission is being developed, and there is no close baseline to work from. It is impossible to suggest when such a change becomes significant enough to warrant testing beyond the bench tests discussed in this section. This decision has to be made by the engineer in consultation with the lubricant supplier. As will be seen, there are also ASTM tests that provide more information than the simple bench tests. Although these use rather more sophisticated test rigs, they are still aimed at proving out a particular characteristic of the lubricant and therefore cannot provide proof that any one lubricant will be completely satisfactory if used in any particular transmission unit.

16.5.1 Bench Tests

These tests are invaluable for the industry. They provide a relatively quick, straightforward, and cost-effective indication of a small range of performance aspects of a lubricant. A few examples have been chosen here of this type of test with a few observations on the usefulness and limitations.

16.5.2 Unit Tests

Although the major advantage of bench tests is that they are relatively inexpensive, there is also a clear need to perform tests on whole transmission units or even in a vehicle. Several test methods have been developed that use standardized units to assess a more holistic performance. Some of the test methods of this type will be reviewed here.

16.5.2.1 GEAR BOX TESTS—D5579 AND D5704 (L-60-1)

These tests are performed in specifically designed or modified test gear boxes rather than a standard vehicle transmission. One of the key issues with using standard gear boxes is the continued availability of proven test units. It is unlikely today that gear box manufacturers will wish to retain a particular specification for a period of many years

when ongoing cost reductions or quality improvements are likely to dictate fairly regular engineering changes to standard production units.

Standard D5579 is a test of fluid performance within a synchromesh assembly. The test is performed in a modified Mack truck transmission using the high-low shift mechanism (rather than the main gear selection synchromesh assemblies).

Mention has already been made of D5704 in the previous section. It is arguably not really a bench test because it uses a complete gear box, although it also does not use a production specification gear box or parts. Test rigs such as this are arguably a good way to specify a test because special rig components can be made available long after any standard production gear box has gone out of manufacture. This ensures that the test method can endure, thus providing continuity as developments in materials and fluids are made.

16.5.2.2 AXLE TESTS—D6121 (L-37), D7038 (L-33), D7450 (GL-5), AND D7452 (L-42)

Several ASTM methods are performed using axle assemblies. These tests vary from low-speed, high-torque applications to the reverse: high speed at lower torque. The key advantage of these tests is the “close-to-real-life” results gained from the results. The fluid is being used in a realistic situation, the failure modes are probably those that would be seen in service, and there are several aspects of the tests that can be used to provide confidence in an oil selection.

Standard tests using a complete transmission unit, as one might expect, would cost a great deal more to perform than the simple laboratory “bench” tests referred to in the previous section. The industry has a dilemma here because the tests that use a complete unit should, by definition, give a more holistic view of the performance of that fluid. However, such testing comes at a price and presents a significant problem in controlling the repeatability of test results from one year to the next. There would not appear to be a straightforward solution to this problem.

16.5.3 Lubricant Specifications

16.5.3.1 AXLE AND TRANSFER GEAR BOX LUBRICANTS

As has been seen, some manufacturers are happy to allow customers to fill transmission units with a lubricant as

long as it complies with one of the standard gear oil specifications. The most common ones are the API grades GL-4, GL-5, and the more recent grade, MT-1. However, the approach taken by others is that the customer should use particular fluids that have been approved for use. The reason for this may be that the transmission requires a particular characteristic within the fluid that is not tested for within the above service designations. A full discussion of these grades is undertaken in Chapter 16 of ASTM Manual 37 [4]. Note that GL-1, GL-2, GL-3, and GL-6 have been withdrawn, although it is still possible to find product packaging that refers to them. The three current grades above are lubricating oils that may be used in axles or heavy-duty, nonsynchronized transmissions. This type of fluid can conceivably be used within a transfer case unless, perhaps, the unit has a synchronized high-low shift mechanism. It is probably worth commenting that the heavy-duty parts of the automotive market are moving toward large synchronized transmissions or epicyclic-type “conventional” automatics. As such, fewer nonsynchronized gear boxes are in production, and this type of transmission could become obsolete in time. Manufacturers such as ZF, Eaton, and Allison are typical in this respect.

To qualify a lubricant as GL-4, GL-5, or MT-1, the fluid must comply with certain physical characteristics:

- *Load-carrying capacity:* Tests D7452 (L-42) and D6121 (L-37).
- *Stability:* D7038 (L-33—Corrosion) and D5704 (L-60—Oxidation).
- *Physical characteristics:* ASTM D892—Foaming Test.
- *Additional tests for MT-1:* For example, copper material and seal material compatibility.

All of these tests are bench tests or standardized unit tests. A summary of this situation is shown diagrammatically in Figure 16.8.

16.5.3.2 VISCOSITY GRADES

It is worth noting at this point that there are several different viscosity grade “systems”. Industrial gear oils tend to be known by the ISO grades, whereas engine oils have their own grading systems (SAE), and transmission fluids again have their own SAE classification system. These are discussed elsewhere in this manual. It should be noted that many of these oils are actually similar viscosity to, for

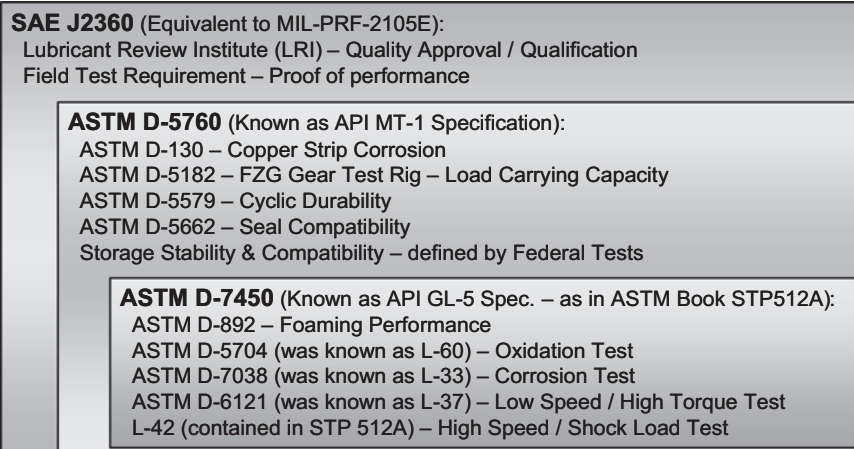


Figure 16.8—Development of gear oil specifications.

example, some engine oils. Any comparison can be difficult because the methods of testing and the temperature at which the viscosity is reported are different across the different systems. One trend that can arguably be observed is the general reduction in viscosity as new developments occur. There are several reasons for this, including the need for an improvement in efficiency already discussed. As additive packages and base fluids become more highly developed, then the same load-carrying and wear performance can be achieved.

16.5.3.3 STP512

In addition to the methods that have been issued as ASTM standards, a document was issued several years ago that covered a range of tests to assess an oil as able to pass GL-5. (The earlier version of STP512—STP512EB, 1972—covers GL-4, GL-5, and the now obsolete GL-6 test regimes.) In addition to various physical characteristics, an oil needs to pass various tests performed in an axle. STP512A [5] was published in 1986 to detail these tests. Those same tests are also included within the later MT-1 and SAE J2360 specifications. These later specifications add additional requirements to the base provided by the test suite from STP512A. A full discussion of these is included in the previous chapter in this manual and other ASTM manuals.

16.5.4 Manual Transmission Lubricant Specifications

Over the years there has been discussion regarding the introduction of a service designation for manual, synchronized transmission units. Sometimes referred to as PM-1, this was to include a test of synchromesh durability in addition to the performance tests and physical tests one would expect for most transmission lubricants. In the absence of an internationally recognized specification for these transmissions, several manufacturers have issued their own specifications whereas others have approved particular fluids following their own tests. Examples of manufacturer-issued specifications include Eaton PS164—revision 7, which was issued a few years ago; Mack TO-A; and ZF Meritor O-81.

Oils that satisfy these requirements have been produced by a wide range of oil companies, and a search of the Internet would produce several potential suppliers. These fluids have a lower viscosity than typical axle fluids and different physical properties. Perhaps as important to fluids used in manual transmissions is the compatibility with copper-based metals because these can be used within the synchromesh assemblies. Modern synthetic base fluids and additive packages ensure good performance, long drain intervals, and good efficiency without having to resort to the high viscosity associated with traditional gear or axle fluids. The detailed requirements and procedures to satisfy these specifications are proprietary to the companies involved.

As mentioned above, with other manual transmission fluids some manufacturers have reached the conclusion that standard oils do not provide the level of performance required. The very specific testing of the transmission units required to prove certain aspects of performance means that it is difficult to ensure that all similar fluids will, for example, provide the shift comfort expected in certain classes of vehicles. Although “standard” oils may well surpass the durability requirement for the gears and bearings,

several subjective measures can exist for the gear change in which one oil “feels right” whereas another does not. This does not mean a “second-place” fluid is in anyway inferior; it just means there is a difference or perhaps a difference is perceived. When a transmission or vehicle manufacturer finds their selves in this position, one course of action open to them is to approve a particular blend of lubricant or indeed to market a fluid through their own spares network. It can be argued that with many gear boxes moving toward “fill for life”, this is acceptable because replacement oil is no more likely to be required by the dealer network than many other spares. The reverse of this argument is that some people take the view that lubricants should be a readily and widely available “standard” consumable. Obviously, unless the suite of tests available can completely assess all aspects of performance, standard tests can never completely cover the sign-off for some demanding applications.

16.6 CONCLUSIONS

From this discussion, it is clear that there is a choice of small, defined bench tests for lubricant screening or more expensive, elaborate tests for the whole transmission unit under consideration. However, standardization of the testing of complete gear boxes does prove to be expensive and leaves an ongoing issue of the supply of consistent assemblies and components for the test gear boxes.

To try and summarize the testing aspects for automotive transmissions needing consideration is difficult, but perhaps a few bullet points can be noted.

- *Gear and bearing durability:* The key decision is to ensure that an appropriate amount of testing on rig and in-vehicle is performed. The testing needs to be able to provide confidence and evidence that the system will perform adequately for the design life. The lubricant has a major influence on surface durability.
- *Lubricant durability:* Ensure that the fluid will perform to a satisfactory level for the time required by the application. Is a fill-for-life application being considered or not?
- *Abuse testing:* What tests are required to ensure that most transmissions survive most drivers? It is this aspect of the performance that may not have very much bearing on the lubricant.
- *Bench testing:* What lubricant screening can be used to provide confidence in a new fluid or even possibly allow some degree of sign-off? The more of this type of testing, the lower the development costs will be.

ASTM provides a large range of standard test methods—particularly bench tests—that can be used to great effect within the development program of a lubricant or a transmission system. Where the outcome of these tests can be added to experience from existing fluids and gear boxes, the results from standard tests can provide good confidence in proposed new lubricants.

A key consideration in the testing of transmission units is that there is a huge range of potential tests available to manufacturers. It is not possible to perform all of the permutations every time an existing gear box is introduced into a new variant of vehicle, or with every change in the specification of the transmission, or to find that the use of the vehicle has evolved. To do so would be a huge financial burden on the companies involved—both the vehicle OEMs and the transmission manufacturers. The engineers within

the organization must establish what level of testing needs to be performed to provide confidence that the system will perform satisfactorily. With a new design, there can be a standard set of tests expected, but even this might be rather costly. As established during this chapter, the lubricant is possibly the most influential component within the transmission. It influences the performance and durability of the transmission system. The lubricant also serves many purposes and influences the performance of the entire system.

Because any specification that is chosen is likely to be a compromise, there not only needs to be high confidence of an improvement in the one desired area but also an understanding of where the resulting tradeoffs occur. In summary, it is hoped that this discussion will help engineers to decide what testing may be required on their system without incurring too high of a risk or indeed cost. There is clearly no common, easily defined solution to the problem of proving satisfactory performance; however, this discussion aims to raise awareness of the issues. This awareness should then allow the development team to exercise their engineering judgment to find the most appropriate test and development program.

REFERENCES

- [1] Lechner, G., and Naunheimer, H., 1999, *Automotive Transmissions—Fundamentals, Selection, Design, and Application*. Springer, New York.
- [2] Van De Velde, F., Willen, P., De Baets, P., and Van Geetruyen, C., 1999, "Substitution of Inexpensive Bench Tests for the FZG Scuffing Test—Part II: Oil Tests," *Tribology Trans.*, Vol. 42, pp. 71–75.
- [3] Krantz, T.L., Cooper, C.V., Townsend, D.P., and Hansen, B.P., 2007, "Increased Surface Fatigue Lives of Spur Gears by Application of a Coating," *Gear Solutions*, June, Available at <http://www.gearsolutionsonline.com>.
- [4] *Fuels and Lubricants Handbook: Technology, Properties, Performance, and Testing*, ASTM Manual 37, G.E. Totten, S.R. Westbrook, and R.J. Shah, Eds., ASTM International, West Conshohocken, PA.
- [5] ASTM Committee D-2 on Petroleum Products and Lubricants. Subcommittee B on Automotive Lubricants, 1986, *STP512A Laboratory Performance Tests for Automotive Gear Lubricants Intended for API GL-5 Service*, ASTM International, West Conshohocken, PA.

RECOMMENDED READING

The following references contain information that may prove useful to readers in providing background information or more detail on the topics covered in this chapter. The ASTM standards listed have been referred to in this chapter.

- Hargreaves, D.J., and Planitz, A., 2009, "Assessing the Energy Efficiency of Gear Oils via the FZG Test Machine," *Tribology Int.*, Vol. 42, pp. 918–925.
- Hohn, B.R., and Michaelis, K., 2004, "Influence of Oil Temperature on Gear Failures," *Tribology Int.*, Vol. 37, pp. 103–109.
- Ludwig, L.G., Jr., 2004, "Properties of Enclosed Gear Drive Lubricants, Schaeffer Manufacturing Company," *Machinery Lubrication*, May–June. Available at <http://www.machinery-lubrication.com/>.

The following books and standards also contain some useful background information appertaining to transmission unit design and the choice of lubricant.

- BS-ISO-12925-1, 1996: Lubricants, Industrial Oils and Related Products (Class L). Family C (Gears). Specifications for Lubricants for Enclosed Gear Systems.

- BS-ISO-14635-3, 2005: Gears. FZG Test Procedures. FZG Test Method A/2, 8/50 for Relative Scuffing Load-Carrying Capacity and Wear Characteristics of Semifluid Gear Greases.

- Genta, G., and Morello, L., 2009, *The Automotive Chassis*, Vols. 1 and 2, Springer, New York.

- Gott, P.G., 1991, *Changing Gears: The Development of the Automotive Transmission*. SAE, Warrendale, PA.

- Happien-Smith, J., Ed., 2001, *An Introduction to Modern Vehicle Design*. Butterworth-Heinemann, Oxford.

- SAE J2360: Automotive Gear Lubricants for Commercial and Military Use. At the time of writing, this standard had been issued some years ago but was in the process of being updated. It is to be the equivalent of Military Specification MIL-PRF-2105E, although available globally.

- Stokes, A., 1992, *Manual Gearbox Design*. Butterworth-Heinemann, Oxford.

The reader may also find some details of tests or requirements made available by the transmission manufacturer. This varies according to the company and their policy. In some cases, the specifications are only made available on request and not published on the company website. In other cases, the information is freely available.

The following ASTM documents are referred to in this chapter.

- STP 512A: See reference 5.

- ASTM D130-10: Standard Test Method for Corrosiveness to Copper from Petroleum Products by Copper Strip Test.

- ASTM D665-06: Standard Test Method for Rust-Preventing Characteristics of Inhibited Mineral Oil in the Presence of Water.

- ASTM D892-06: Standard Test Method for Foaming Characteristics of Lubricating Oils.

- ASTM D2266-01 (reapproved 2008): Standard Test Method for Wear Preventive Characteristics of Lubricating Grease (Four-Ball Method).

- ASTM D2782-02 (reapproved 2008): Standard Test Method for Measurement of Extreme-Pressure Properties of Lubricating Fluids (Timken Method).

- ASTM D2893-04 (reapproved 2009): Standard Test Methods for Oxidation Characteristics of Extreme-Pressure Lubrication Oils.

- ASTM D3427-07: Standard Test Method for Air Release Properties of Petroleum Oils.

- ASTM D3527-07: Standard Test Method for Life Performance of Automotive Wheel-Bearing Grease.

- ASTM D4289-03 (reapproved 2008): Standard Test Method for Elastomer Compatibility of Lubricating Greases and Fluids.

- ASTM D5182-97, 2008: Standard Test Method for Evaluating the Scuffing Load Capacity of Oils (FZG Visual Method).

- ASTM D5579-09a: Standard Test Method for Evaluating the Thermal Stability of Manual Transmission Lubricants in a Cyclic Durability Test.

- ASTM D5662-09: Standard Test Method for Determining Automotive Gear Oil Compatibility with Typical Oil Seal Elastomers.

- ASTM D5704-09 (L-60-1): Standard Test Method for Evaluation of the Thermal and Oxidative Stability of Lubricating Oils Used for Manual Transmissions and Final Drive Axles.

- ASTM D5760-09: Standard Specification for Performance of Manual Transmission Gear Lubricants.

- ASTM D6121-09 (L-37): Standard Test Method for Evaluation of Load-Carrying Capacity of Lubricants Under Conditions of Low Speed and High Torque Used for Final Hypoid Drive Axles.

- ASTM D6425-05 (DIN 51834): Standard Test Method for Measuring Friction and Wear Properties of Extreme Pressure (EP) Lubricating Oils Using SRV Test Machine.

- ASTM D7038-09a (L-33-1): Standard Test Method for Evaluation of Moisture Corrosion Resistance of Automotive Gear Lubricants.

- ASTM D7450-08 (GL-5): Standard Specification for Performance of Rear Axle Gear Lubricants Intended for API Category GL-5 Service.
- ASTM D7452-09a (L-42): Standard Test Method for Evaluation of the Load-Carrying Properties of Lubricants Used for Final Drive Axles, Under Conditions of High Speed and Shock Loading.
- ASTM Committee D-2 on Petroleum Products and Lubricants. Subcommittee B on Automotive Lubricants, 1986, *STP512A*

Laboratory Performance Tests for Automotive Gear Lubricants Intended for API GL-5 Service, ASTM International, West Conshohocken, PA. Particularly useful are Chapters 16 and 17.

Rizvi, S.Q.A., 2009, *A Comprehensive Review of Lubricant Chemistry, Technology, Selection, and Design*, Manual 59-EB, ASTM International, West Conshohocken, PA. Several chapters are of use in providing an understanding of different aspects of lubricant performance and testing.

Design for Reduced Wear

Roger Lewis¹ and Tom Slatter¹

17.1 INTRODUCTION

Wear is the progressive damage, involving material loss, which occurs on the surface of a component as a result of its motion relative to the adjacent working parts. Most contacting components in an engine are provided with a supply of lubricant to avoid excessive wear and subsequent damage, which may occur if they were allowed to contact in dry conditions. The consequences of wear in an engine can be severe and can lead to complete engine failure in some cases. Other effects can be loss of performance, an increase in oil consumption, a decrease in fuel economy, and an increase in emissions.

Demands on engine performance are continually increasing. To help meet emission targets, oil consumption is being reduced and service intervals are rising, which is leading to more contamination (e.g., soot) in the lubricant, both of which lead to more wear occurring. Lead, sulfur, and other friction-reducing agents are being removed from fuel and lubricants because of their harmful effects to the environment. There is also pressure to reduce engine weight and the total number of components to improve economy and drive down cost. This has meant that lighter, and typically less durable, materials are being introduced. Where previously inserts made from harder wearing materials may have been put in place to reduce wear problems, alternative solutions are now being sought to reduce the numbers of components and their associated manufacturing costs. Re-engineering the components can prove to be difficult, and then the existing lubricants that were designed to work with ferrous materials may now not be as effective when any new materials are introduced.

It is evident from the rest of this publication that there are many models available for lubrication and friction, but wear modeling tools are less prevalent. This means that engine and component manufacturers have to run engine tests to compare a range of wear-reducing solutions, which is expensive and time-consuming. Such a short-term approach does not help develop an understanding of the problem, so a similar approach would have to be taken should the problem occur again.

In this chapter, a wear analysis process will be described that can be used to address potential wear issues with a new design or to find solutions to wear problems that have occurred in an existing piece of equipment. The stages of the process will be outlined in the first section. Subsequent sections will provide some of the basic theoretical and practical background needed to work through the stages. The later sections include a case study in which a wear analysis process has been used to solve a wear problem and develop design tools to help avoid similar problems occurring again

in the future, more dedicated information on design tools, and finally a section on ways to help mitigate wear problems, including surface modification and thin surface coatings, which are increasingly being used in automotive applications.

17.2 WEAR ANALYSIS PROCESS

17.2.1 The Process

A wear analysis process has been proposed to help engineers in industry to solve wear problems with existing equipment or to resolve concerns with new designs [1]. The process is outlined in the flow chart in Figure 17.1 and some examples in which it may be applied are shown in Table 17.1. It is a blend of experimental, theoretical, and analysis techniques. Wear testing may or may not be needed (i.e., it could be performed purely using available data). However, the key to the method is to consider all aspects of the problem, not just look at one issue. In industry, timescales are often short, and solving a problem will involve performing a set of tests to find the best material combination to reduce a wear problem. With this process, contact geometry, level of lubrication, component dynamics, etc., are all considered. It should be noted that the process need not be complex and that rudimentary and approximate wear relationships may be adequate.

The wear analysis process essentially involves developing an engineering model of the wear process under consideration. This can then be used to understand and optimize the parameters that will ensure acceptable wear performance. It starts with examination and ends with verification.

17.2.2 Examination

This is the data-gathering phase and involves consideration of the whole tribosystem, not just the worn component or component in which wear is anticipated in new designs. The reason for the wear problem may be related to a different part of the overall system under consideration.

In most applications, it is possible to identify two types of systems: a microtribosystem and a macrotribosystem [1]. A microtribosystem is basically a specific wear point or wearing contact and a macrotribosystem is the mechanism by which wear takes place. This concept can be seen in Figure 17.2, which illustrates a valve drive system from an automotive engine.

Several microtribosystems can be identified, such as those for the wear between the valve and seat insert, rocker arm and valve tip, and the cam and rocker arm. The macrosystem in this case would be the whole assembly. Microsystem parameters are related to macrosystem parameters. For example, a change in the cam profile alters the valve-closing velocity and hence wear of the valve and seat.

¹ The University of Sheffield, Sheffield, UK

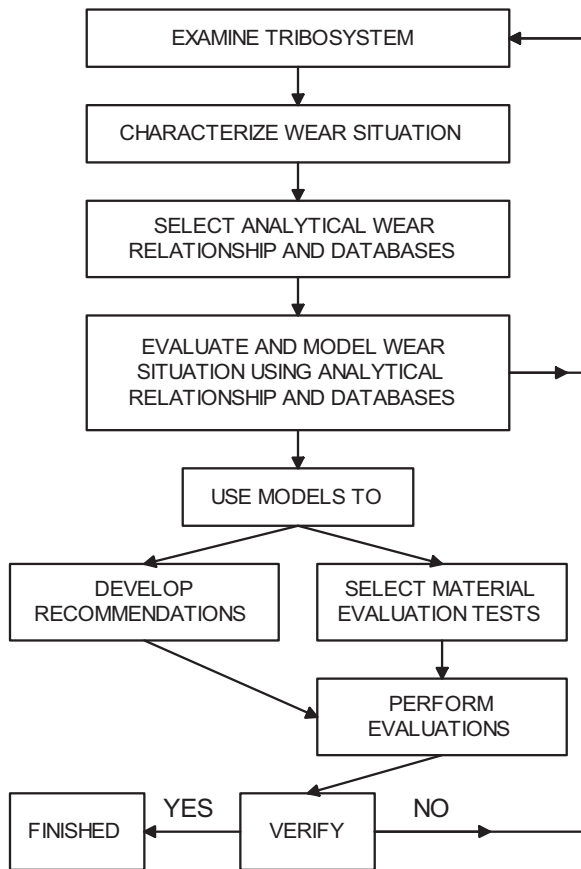


Figure 17.1—The wear analysis process.

When performing a wear analysis, micro- and macro-tribosystems should be included. First, wear relationships used in a wear analysis are based on the parameters of the microsystem, and these parameters, as well as the location of wear points within the macrosystem, are determined by conditions associated with the macrosystem. Second, wear problems can be resolved or avoided by appropriate selection of micro- and macrosystem parameters. Typical data that might be collected during this stage are shown in Table 17.2.

Clearly not all of this information will be available, but the minimum required data for wear in existing components include the amount of wear and the usage (this may be in time or number of cycles). Other parameters such as load, operating speed, and environmental conditions (e.g.,

temperature and humidity) are very useful because they play a significant role in wear processes.

17.2.3 Characterization

Wear behavior is very complex, and there are many different relationships to describe wear processes; therefore, characterization is essential. It provides the basis for selecting appropriate models for wear behavior to use in the modeling and evaluation stage of the wear analysis process. It also aids in the application of these models to the wear situation under analysis. It basically involves collating all of the data gathered on the wear issue into a useful description of the wear situation.

Characterization should contain the following elements:

- Description of the motion causing wear,
- Description of the contact geometry,
- Nature of the loading,
- Description of the materials,
- Type of lubrication,
- Predominant wear features,
- Surface roughness,
- Description of the operating environment,
- Wear magnitude, and
- Associated usage.

It is not necessary for the characterization to provide all of the information to perform a wear analysis; however, it should serve to limit the number of possibilities to consider.

Wear mechanisms and their characteristic features will be outlined in Section 17.3; Section 17.4 will cover simple lubrication modeling (for determining lubrication regimes and minimum film thicknesses), and the contact mechanics theory needed to calculate contact geometries and pressures will be discussed in Section 17.5.

17.2.4 Modeling and Evaluation

This stage is the core of the wear analysis. It involves selecting an appropriate analytical relationship to describe wear and select design parameters. There are four steps in this stage:

1. Determine which relationships to use,
2. Develop a mathematical model relating wear life to design parameters,
3. Verify the model to check accuracy (if not acceptable modify or use alternative), and
4. Use the model to optimize parameters and establish the design changes required.

Examples of analytical relationships used to predict wear are given in Section 17.6, in which other aspects of wear modeling are discussed as well as wear maps and other tools to predict wear.

It should be noted here that although tests may not be required, many of the analytical relationships for predicting wear are semiempirical and need data from tests that may not be available for the materials under consideration.

17.2.5 Testing

This is not an intrinsic part of the process, but it may be significant if material data are not available. It may be done for several of reasons:

- As part of the verification process,
- To evaluate materials because available data are not adequate, and
- To define wear coefficients for analytical models.

TABLE 17.1—Application of the Wear Analysis Process

In Existing Equipment	During Design Process
Occurrence of reduced wear life in established hardware	Design of new equipment
Wear life differences in different installations	Evaluation of the effect of design change
Poor or unacceptable wear life with prototype or development hardware	Evaluation of the effect of new or extended applications
	Design enhancement

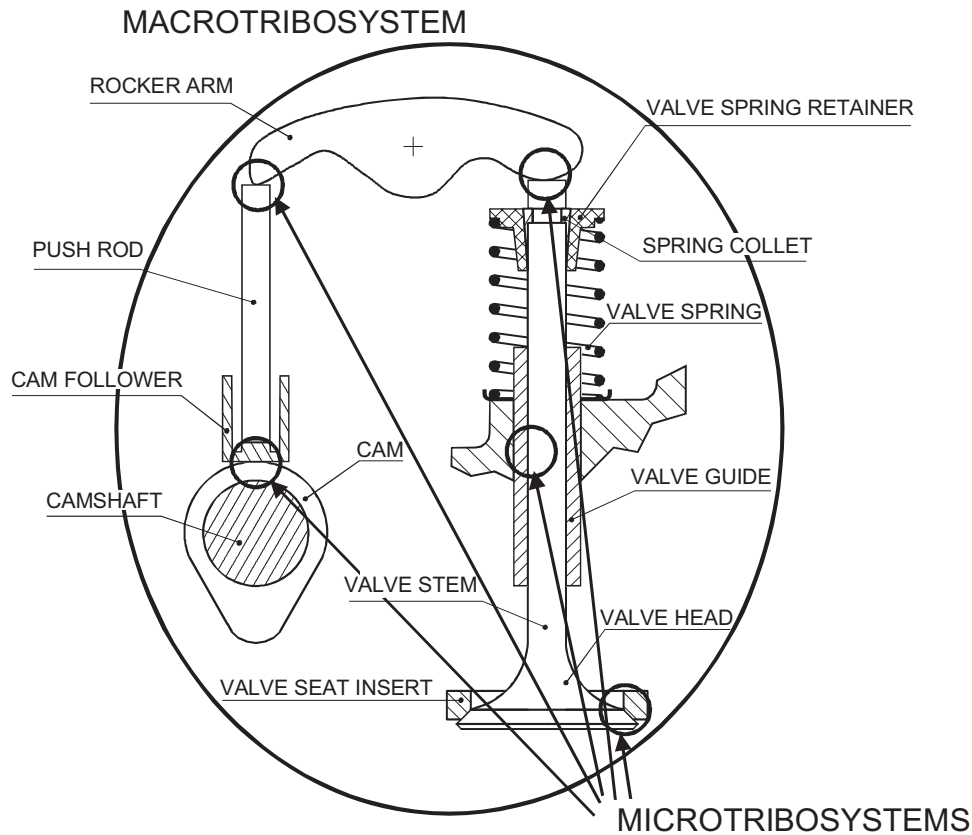


Figure 17.2—A valvetrain system illustrating macro- and microtribosystems.

Testing must generally conform to available standards, and a key element is some kind of simulation to ensure that the wear is the same in the test as it is in the actual application.

Generic elements to be considered in a wear test include

- Simulation
- Control
- Data acquisition
- Data analysis
- Documentation

Tests can be performed using standard commercial test apparatuses conforming to test standards (e.g.,

those issued by ASTM), or they can be performed using bespoke apparatuses designed to test actual components. More information on testing and standards is given in Section 17.7.

17.2.6 Process Implementation

The wear analysis process can be used for short-term problem solving (e.g., if a piece of equipment is out of service and needs to be resolved as soon as possible) or for longer term design problems when models will be developed for integration into design codes and a deeper understanding of the problem is necessary. An example of the latter is given in the valve recession case study outlined in Section 17.8, which is about the development of a predictive model for valve recession and design tools for reducing the likelihood of wear occurring.

It should be noted here that other resources are available to help solve wear problems or select materials for reducing wear. Some, such as *Bearings: A Tribology Handbook* [2], are for quite specific applications, and the *Materials Selector* [3] is for more general information.

17.3 WEAR MECHANISMS

In examining worn surfaces during the examination and characterization phases of a wear analysis process, it is essential to understand which wear mechanisms may have led to the features seen. Equally, when designing a component to reduce the likelihood of wear occurring, it is important to understand what wear mechanisms may result from certain contact conditions. This section aims to give a brief overview of wear, related to automotive examples, and to

TABLE 17.2—Typical Data That Might Be Gathered during the Examination Stage of the Wear Analysis Process

Component Information	Contact Condition Information	Lubrication Information
Geometry Dimensions Materials	Orientation Location Loading Motion	Type of lubrication Lubricant Conditions
Environmental Information	Wear Information	
Temperature Humidity Atmosphere Contamination	Amount of wear Usage Appearance Location of wear	

give an engineer the tools needed to perform a failure analysis or identify wear mechanisms to design out.

17.3.1 Wear Situations

Before looking at actual wear mechanisms, it is necessary to first characterize possible wear situations [1]. These are related to the nature of the motion during contact and the number of contact cycles.

17.3.1.1 SLIDING

In terms of potential to cause wear, motion that is tangential to the surface, or sliding motion, is more severe than motion perpendicular to the surface, such as occurs with impact or rolling. Several wear mechanisms can occur as a result of sliding, including oxidative wear in mild contact conditions (e.g., those with a low load and sliding velocity), and in more severe conditions adhesive or galling wear. If reciprocating motion is apparent, then fretting wear may occur. This can be a problem in nominally stationary contacts, such as two plates bolted together, where vibrations cause small-amplitude oscillatory motions. If particles are present in the contact, possibly generated by the initial wear mechanism, abrasive wear may also occur.

Very severe sliding conditions can lead to seizure and high heat generation in the contact, which may cause a thermal breakdown of the surface material. Typical sliding contacts in the engine include the piston/liner and piston ring/liner contacts and valve/valve guide, etc. In addition to occurring independently, sliding is very likely to occur in combination with other wear situations such as rolling and impact.

17.3.1.2 ROLLING

With rolling motion the principal mechanisms that dominate wear behavior are fatigue mechanisms. Generically, these are referred to as surface fatigue and are forms of repeated-cycle deformation mechanisms. Surface fatigue mechanisms involve the formation and propagation of cracks, which ultimately lead to the loss of particles from the surface. These cracks tend to form below the surface and propagate to the surface. However, in cases in which significant traction is involved, cracks form at the surface. Traction is generated in a rolling contact, when sliding occurs as well as rolling. Sliding is caused by slip as a result of the two components moving at different velocities. Examples of rolling/sliding contacts in an engine include several in the valvetrain: cam/follower, rocker arm, roller/cam, etc. Surface wear features that are apparent with surface fatigue are spalls or pits on the material surface.

17.3.1.3 IMPACT

Predominant wear mechanisms are deformation, either by a single cycle or repeated cycles. Impact wear can either be percussive, in which a large body hits another large body, or erosive in nature, in which many small particles impact against a large body.

Percussive wear, in which the impacting body approaches perpendicular to a counterface, is much less severe than a tangential approach or perpendicular approach with a moving counterface. In these situations, a sliding motion also occurs in the contact as shown in Figure 17.3. An example in the engine is the valve impact during closure against a seat insert.

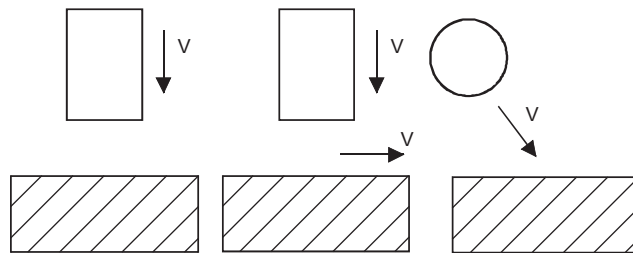


Figure 17.3—Percussive wear mechanisms.

If the wear situation is known, information has been collated that can be used to identify wear mechanisms that may occur, as shown in Table 17.3 [1].

17.3.2 Wear Mechanisms

There is virtually an endless list of wear mechanisms that have been defined (see glossary in reference 1). Despite this, there are a few generic terms that cover the main types of wear behavior. Some of these are described below.

17.3.2.1 ADHESIVE WEAR

The basic concept for adhesive mechanisms is that actual contact between surfaces occurs at discrete points within the apparent area of contact. At these spots, called junctions, bonding occurs between surface asperities. When the surfaces move relative to each other, these junctions are broken and new ones are formed. The tip is usually plucked off the softer asperity, leaving them adhering to the harder surface and forming a “transfer film.” They can subsequently become loose and give rise to wear debris. Ductile or brittle fracture can occur in the asperity contact, as shown in Figure 17.4 [4]. Severe damage can sometimes result in the tearing away of macroscopic chunks of material, and this situation is known as galling. If adhesive wear results from the breakdown of lubrication in a contact, then the term scuffing is used to describe the onset of wear. This can be seen in engine component contacts that are indirectly lubricated and may experience starvation of lubricant [5].

17.3.2.2 ABRASIVE WEAR

Abrasive wear is damage to a component surface that arises because of the motion relative to that surface of either harder asperities, known as two-body abrasive wear, or because of hard particles trapped between the surfaces, known as three-body abrasive wear. Examples of both of these are shown in Figure 17.5. Such particles may be introduced between the two softer surfaces as a contaminant from the outside environment, or they may have been formed in situ by oxidation or by some other chemical or mechanical process.

Abrasive wear gives a characteristic surface topography consisting of long parallel grooves running in the sliding direction as shown in Figure 17.6. The volume and size of the grooves varies considerably from light scratching at one extreme to severe gouging at the other. Industrial surveys have shown that abrasive wear accounts for up to approximately 50 % of wear problems.

One particular abrasive wear problem that is becoming more prevalent in engines is that caused by soot contamination in lubricants. Car, engine, and lubricant manufacturers are facing increasing pressure to lengthen service

TABLE 17.3—General Operational Classification of Wear Situations for Use in Wear Analysis

Motion	With or Without Slip	Lubed or Unlubed	With or Without Particles	Typical Mechanisms ^a				
				Adhesive	Single-Cycle Deformation	Repeated-Cycle Deformation	Chemical	Thermal
Rolling ^b	With slip	Lubed	Without			×		
		Unlubed	Without	×		×		
		Lubed	With		×	×		
		Unlubed	With	×	×	×		
	Without slip	Lubed	Without			×		
		Unlubed	Without			×		
		Lubed	With			×		
		Unlubed	With			×		
Impact ^c	With slip	Lubed	Without			×		
		Unlubed	Without	×		×		
		Lubed	With		×	×		
		Unlubed	With	×	×	×		
	Without slip (compound impact)	Lubed	Without			×		
		Unlubed	Without			×		
		Lubed	With			×		
		Unlubed	With			×		
Sliding ^d	Unidirectional	Lubed	Without			×		
		Unlubed	Without	×		×	× ^e	× ^f
		Lubed	With		×	×		
		Unlubed	With	×	×	×	× ^e	× ^f
	Reciprocating (large amplitude)	Lubed	Without			×		
		Unlubed	Without	×		×	× ^e	× ^f
		Lubed	With		×	×		
		Unlubed	With	×	×	×	× ^e	× ^f
	Reciprocating (small amplitude)	Lubed	Without			×		
		Unlubed	Without			×	× ^e	
		Lubed	With		×	×		
		Unlubed	With		×	×	× ^e	

^aExcept in hostile environments, where thermal and chemical wear mechanisms can be significant and dominate the wear behavior.

^bMildest wear situation; repeated-cycle deformation mechanisms tend to be dominant; wear increases with slip and particles; with particles and slip, abrasive wear can be dominant; smooth-surface particles preferred.

^cRepeated-cycle deformation mechanisms tend to be dominant; gross plastic deformation generally unacceptable, unless in short-life applications; stresses should be in the elastic range for lives >10⁶ impacts; wear increases with slip.

^dRepeated-cycle deformation mechanisms tend to be dominant, but chemical mechanisms can be significant; with particles, abrasive wear can be dominant; mild to severe wear transitions with load and speed common in unlubricated situations; lubrication generally required for metal and metal-ceramic pairs; galling and fretting are forms of sliding wear.

^eWith metals.

^fWith polymers.

intervals and therefore oil life to reduce lifetime vehicle costs for the customer and the overall effect the vehicles have on the environment, in particular a reduction in the amount of engine oil discarded. However, increasing sump drain intervals means that oil is becoming contaminated with high levels of soot and increasingly more degraded.

Additionally, the use of exhaust gas recirculation (EGR), in which a portion of the exhaust gases are recirculated into the inlet manifold, is increasing to reduce the peak combustion temperature and therefore reduce nitrogen oxide emissions. EGR also leads to combustion products being recirculated rather than passing out of the engine in the

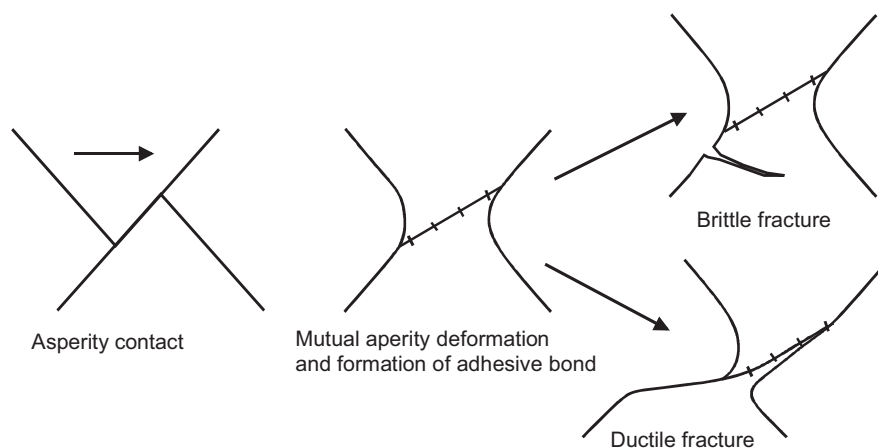


Figure 17.4—Ductile and brittle fracture in adhesive wear. *Source:* Figure adapted from [6].

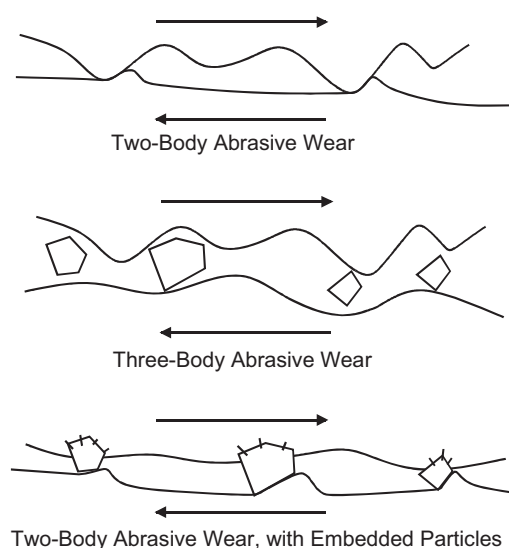


Figure 17.5—Abrasive wear mechanisms.

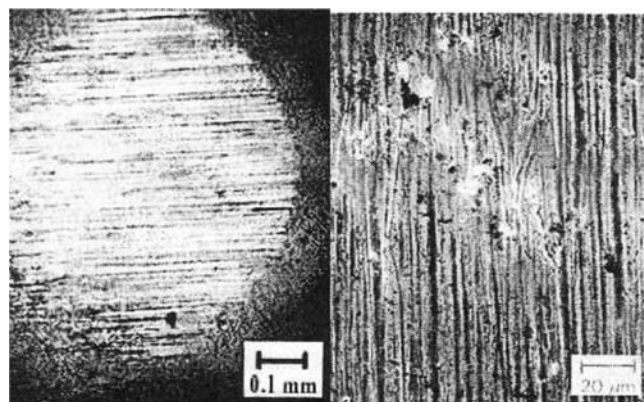


Figure 17.6—Abrasive wear features (resulting from severe three-body abrasion) [7].

exhaust gases, which leads to further oil contamination. Soot in oil increases wear of engine components [8,9], and the most affected are shown in Figure 17.7. Several mechanisms contribute to this. In contacts in which the loading and sliding is less severe and soot concentrations are low,

three-body abrasion is seen; when soot concentrations go above 3–4 %, the soot can actually cause the contact to become starved of lubricant and a transition in wear occurs to give a much higher rate of material loss.

Lubricants are being designed to disperse particles within the lubricant and keep them in suspension. Vehicle service intervals are currently dictated by the length of time that lubricants can maintain their physical properties, but also, and possibly more importantly, by the length of time that they can hold particles in suspension. The soot particles are contained within the lubricant by dispersant additives. However, current lubricant technology has reached a limit on the amount of dispersants that can be added because too much will result in a corrosion problem in the engine due to the free amines associated with the dispersant [10,11].

A different approach to addressing the problem would be to design component contacts to avoid soot entrainment. Some work has been performed to visualize soot entering a ball-on-flat contact [12] and a greater understanding of the wear mechanisms using tests related to component contacts. This is particularly important with this problem because simple specimen tests that do not resemble the actual contact will not necessarily entrain soot in the same way as the real components and give misleading results. Work by Green and Lewis [13] related wear tests to the valve tip/elephant's foot contact and compared test wear features with actual components. They found that a good correlation existed. This work also highlighted where transitions occurred in wear due to changes in soot concentration.

Another issue that comes out of this problem is that typical wear test standards involved the use of new lubricant and took no account of lubricant contamination and degradation. Truhan et al. [14] have now proposed a new standard that starts to deal with this problem. This is focussed on the piston ring/cylinder liner contact, but it could be rolled out to other contact tests.

Engine testing standards have been set up to look at soot contamination. Standard tests are defined for Europe (ACEA [European Automobile Manufacturers Association]/CEC [Co-ordinating European Council] tests) and the United States (API tests). The main engine tests for assessing the effects of soot are outlined in references 15 and 16.

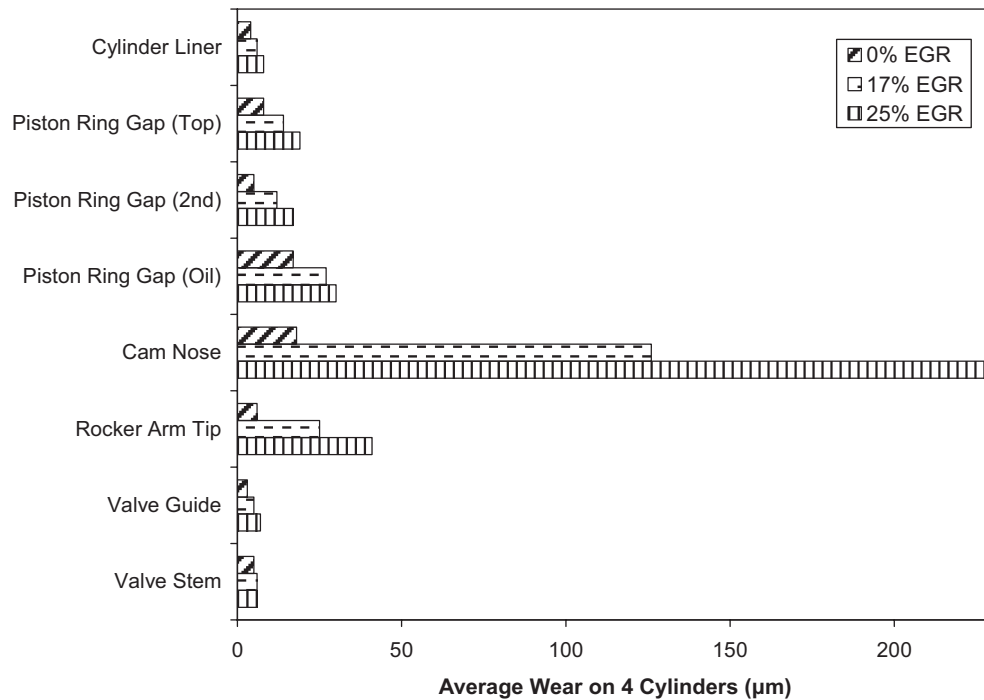


Figure 17.7—A reproduction of 4d55t engine wear data showing relative component wear levels [9].

Of these, the Cummins M-11 EGR test appears to provide the most useful standard soot-induced wear engine test because it focuses on the main areas of potential wear and gives more opportunities for analyzing and understanding the effect of soot. This is also the test that appears to be most commonly used in industry.

17.3.2.3 PERCUSSIVE IMPACT

The mechanism of impact wear involves elastic and plastic deformation when impact energy is high or fatigue

accompanied by wear debris release due to crack formation or both. If oxygen is present, then an oxidative mechanism may also take place. The mechanisms of impact wear are illustrated in Figure 17.8.

In general, the wear is dependent on the formation of deformed layers, particularly when wear by fatigue or crack formation is predominant. In such cases, subsurface cracks extend parallel to the surface causing material to delaminate. Superimposing sliding can cause an acceleration of wear.

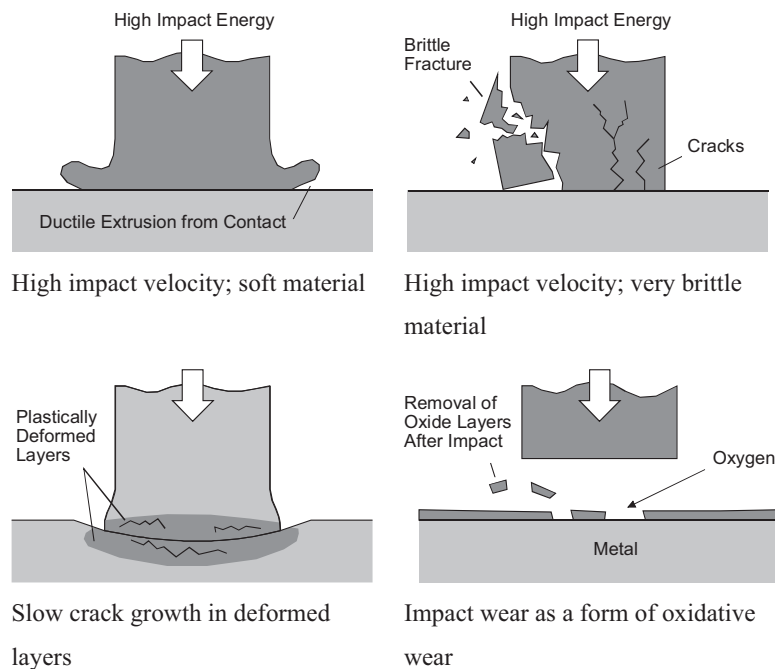


Figure 17.8—Impact wear features. Source: Figure adapted from [6].

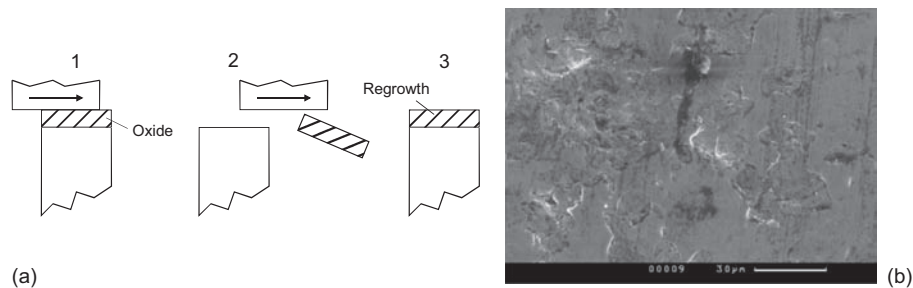


Figure 17.9—Oxidative wear: (a) mechanism and (b) features.

17.3.2.4 OXIDATIVE WEAR

This process involves the formation of oxides on the surface of the material. It is clearly related to the ability of the wearing material to undergo oxidation and the availability of oxygen. Whether it occurs depends on the temperatures generated in the contact; therefore, it is associated with higher sliding velocities. Wear rates are lower than those seen with mechanical wear processes. The material removal process is shown in Figure 17.9, along with a typical oxidative wear surface.

17.3.2.5 THERMAL WEAR

Thermal wear processes are those directly associated with the increase in temperature caused by frictional heating in the contact. The principal type of wear process in this category is when a material melts or softens to such an extent that it can be displaced like a viscous fluid. Other mechanisms, such as adhesive wear, are also accelerated by a reduction in hardness. Other types are linked with thermal stresses that can cause thermal fatigue and cracking, which lead to loss of material.

17.3.2.6 CORROSIVE WEAR

Corrosive wear is fundamentally caused by a reaction between the material being worn and a corroding medium, which could be a chemical reagent or reactive lubricant. Corrosion alone may not be particularly damaging. When combined with adhesive or abrasive processes, brought about because of corroded surfaces sliding against one another and the possible presence of particulate matter, wear rates can quickly accelerate. The surface film formed during corrosion is broken away by an abrasive/adhesive mechanism exposing fresh material, which is subsequently corroded and so on. Several scenarios can occur if a material is corroded and a film forms on its surface [17]:

- A durable lubricating film is formed.
- A weak film may form that has a short life under sliding conditions, and a high wear rate may result from regular formation and destruction of the film (most prevalent form of corrosive wear).
- The protective surface film may be worn (e.g., by pitting) and a galvanic coupling between the remaining film and underlying substrate could cause rapid corrosion of the worn surface area.
- The corrosive and wear processes may act independently to cause material loss.

Typical examples of corrosive wear can be found where overly reactive extreme pressure additives are used in oil

[18] or when methanol, used as fuel, is contaminated by water and the engine experiences wear [19]. Corrosive wear can also occur when oxygen is present in oil [20].

17.3.3 Interaction of Mechanisms

Different wear mechanisms often coexist, interact, and compete. When examining wear scars it is typical to find evidence of different mechanisms.

These could be different wear mechanisms acting independently or they could be features indicating different stages of a complex wear process. These could result from variations in contact conditions. For example, in lubricated sliding, a high spot may cause local lubrication failure, resulting in adhesive wear. At junctions where there is no lubrication failure, a different mechanism will be evident. Alternatively, the different types of wear could have occurred at different times, such as the result of an occasional hard particle being drawn through the contact.

17.3.4 Wear Rates and Transitions

When lubricated machine components are run together for the first time, their ultimate load-carrying capacity is often reduced because they have not been preconditioned by running them at low load. This process, during which the components improve in conformity, topography, and frictional compatibility before full-load conditions are applied, is known as “running-in.” The wear rate is usually initially quite high, but as the surfaces become smoother, the wear rate falls. After a suitable period full-load conditions can be applied without any sudden increase in wear rate. A typical component history is shown in Figure 17.10. Once running-in is complete, a steady low-wear-rate regime is

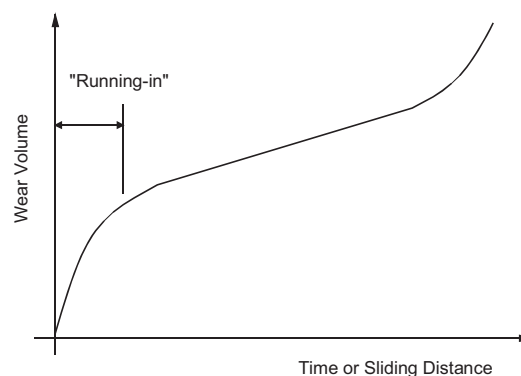


Figure 17.10—Wear transitions.

TABLE 17.4—Mild Vs. Severe Wear

Mild Wear	Severe Wear
Results in extremely smooth surfaces—often smoother than the original	Results in rough, deeply torn surfaces—much rougher than the original
Debris extremely small, typically only 100-nm diameter	Large metallic wear debris, typically up to 0.01-mm diameter
High electrical contact resistance, little true metallic contact	Low contact resistance, true metallic junctions formed

maintained for the life of the component until, for example, fatigue processes take over and a further wear transition occurs leading to high wear rates. Several mechanical wear processes may occur during running-in, such as abrasion and adhesion.

Wear is often classified as being mild or severe. This is not based on any particular numerical value of wear rate, but on the general observation that for any pair of materials, increasing the severity of the loading (e.g., by increasing either the normal load, sliding speed, or bulk temperature) leads at some stage to a comparatively sudden jump in the wear rate. The differences in the two regimes are shown in Table 17.4.

Normalized wear rates of 10^{-4} to 10^{-3} are typical for mild wear, with wear rates for severe wear reaching levels in the range of 10^{-3} to 10^{-2} . The mechanisms most associated with severe wear are adhesive or thermal mechanisms. Increasing temperatures in the contact and the resulting thermal softening can lead to a further transition into a catastrophic wear regime.

17.4 LUBRICATION

This chapter will not focus heavily on lubrication and its theory because this is covered in depth in the rest of the book. However, it is an important aspect of a component contact, and the level of lubrication will determine how much wear occurs and which wear mechanism is prevalent.

A good starting point for analyzing a particular contact during the design process is a Stribeck curve [21],

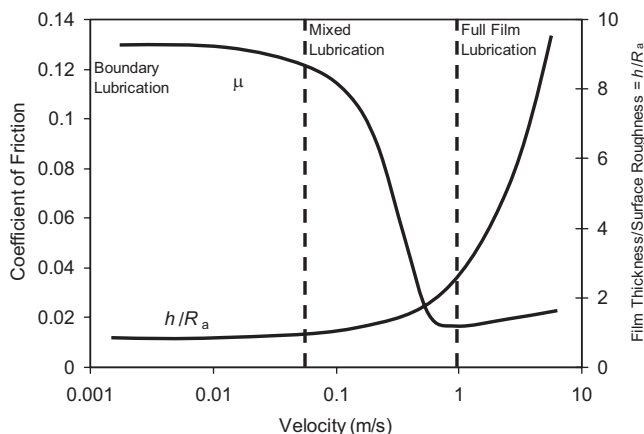


Figure 17.11—A generalized Stribeck curve (friction) and separation.

as shown in Figure 17.11, and the associated lubrication regimes:

- *Boundary lubrication (BL)*: There is physical contact between surface asperities and they support the load. Shearing of the boundary layers accommodates the velocity difference between the surfaces.
- *Mixed lubrication (ML)*: In this regime, the lubricant film supports some of the load and as such ML is sometime called the partial lubrication. The remainder of the load is still supported by contacting asperities.
- *(Elasto)hydrodynamic lubrication (EHL)*: The contact surfaces are now completely separated. The velocity difference is accommodated by shearing in the lubricant film.

Friction coefficient can be plotted against velocity as shown in Figure 17.11 or against Stribeck number ($\eta U/W$, where η is dynamic viscosity, U is the sliding velocity, and W is the load).

The parameter h/R_a (film thickness/combined surface roughness) is also used to determine lubrication regime. EHL or hydrodynamic lubrication exists if h/R_a is greater than 3, ML if it ranges from 1 to 3, and BL if it is less than 3. However, these definitions do not work for smooth surfaces. Here, a method has been proposed that uses h/R_a and h/R_g (where R_g is the lubricant molecule size) [22].

For low wear and friction, it is desirable to be at the lowest point on the Stribeck curve where full-film lubrication has just initiated. Moving away from this point (i.e., to higher velocity) is not detrimental in terms of wear, but it will lead to higher friction. The separation is significant because it is possible to calculate this for contacts to see what lubrication regime may be apparent. For example, minimum film thicknesses for model contacts can be calculated using equations found in Hamrock [23]. This was done in reciprocating wear testing of sooty oils by Green et al. [24].

As will be seen in Section 17.6, one key to designing for low wear is knowledge of where wear transitions occur. Andersson and Sala-Russo [25] defined transition loads, from mild to severe wear, for mixed lubricated contacts, of which there are several in an engine, with different surface roughness and for different oil viscosities. An example can be seen in Figure 17.12, and more information on wear mechanisms, transitions, etc., can be found in Sections 17.3 and 17.6.

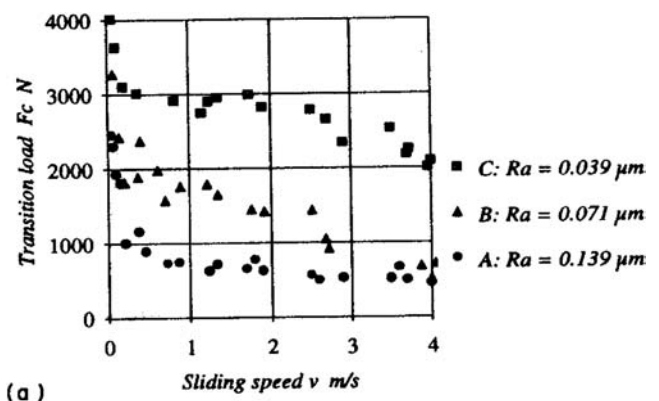


Figure 17.12—The influence of surface roughness on the transition load of a lubricated sliding steel ball-on-flat [25].

17.5 CONTACT MECHANICS

An automotive engine relies on the integrity of components with interacting surfaces, such as gears, bearings, or cams. Loads are often supported on a small surface area of the component. Contact pressures and stresses therefore tend to be high. Engineers need to design the components to withstand these high contact stresses to avoid wear. Excessive contact stress or deformation can lead to component failure by

- *Overload*: Components yield or fracture from excessive contact loading.
- *Wear*: Material removal from the surfaces.
- *Rolling contact fatigue*: Cyclic contact stresses may cause fatigue crack initiation.
- *Seizure*: Component surfaces locally weld under high contact stress.
- *Loss of tolerance*: By excessive deformation of the components.

17.5.1 Hertz Theory of Elastic Contact

When two curved bodies are brought into contact, they initially contact at a single point or along a line. With the smallest application of load, elastic deformation occurs and contact is made over a finite area. An analytical method for determining the size of this region was first described by Heinrich Hertz in 1881 [26], and this still forms the basis for calculations today. His model of contact stress is based on the following simplifying assumptions:

- The materials in contact are homogeneous, and the yield stress is not exceeded.
- Contact load is caused by the load that is normal to the contact, which effectively means that there are no tangential forces acting between the solids.
- The size of the contact is small compared with the size of the curved bodies.
- The contacting solids are at rest and in equilibrium.
- The effects of surface roughness is negligible.

Elastic bodies in contact deform and the contact geometry, load, and material properties determine the contact area and stresses. The contact geometry depends on whether the contact occurs between surfaces, which are both convex or a combination of flat, convex, and concave.

The effect on the contact conditions when the Hertz assumptions are not met is discussed in Section 17.5.6.

17.5.2 Contact Parameters and Geometry

The shape of the contact area depends on the shape (curvature) of the contacting bodies. For example,

- Point contacts occur between two balls;
- Line contacts occur between two parallel cylinders; and
- Elliptical contacts occur when two cylinders are crossed, or a moving ball is in contact with the inner ring of a bearing, or two gear teeth are in contact.

It is defined by convention that convex surfaces possess a positive curvature and concave surfaces have a negative curvature. The following general rule can be applied to distinguish between these surfaces: If the center of curvature lies within the solid, then the curvature is positive; if it lies outside of the solid, then the curvature is negative. This distinction is critical in defining the parameter characterizing

the contact geometry, which is known as the reduced radius of curvature, R' .

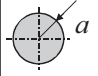
The most frequently used contact parameters are

- Contact area dimensions,
- Maximum and average contact pressure,
- Stress distribution in the contact, and
- Position of the maximum shear stress below the surface.

The following sections will look at these parameters for several typical contacts.

17.5.3 Contact between Two Spheres (Circular Point Contact)

The contact equations for a circular point contact (see Figure 17.13) are as follows:

Reduced Radius	Contact Area Dimensions	Maximum Contact Pressure	Average Contact Pressure	Contact Pressure Distribution
$\frac{1}{R'} = \frac{1}{R_1} + \frac{1}{R_2}$	$a = \sqrt[3]{\frac{3PR'}{4E^*}}$ 	$p_0 = \frac{3P}{2\pi a^2}$	$p_{avg} = \frac{P}{\pi a^2}$	$p(r) = p_0 \sqrt{1 - \frac{r^2}{a^2}}$

where:

- a = radius of the contact area (m),
- P = normal load (N),
- p = contact pressure (N/m²),
- E^* = reduced elastic modulus (N/m²),
- R' = reduced radius of the contact, and
- R_1 and R_2 = radii of the contacting bodies 1 and 2, respectively.

The reduced elastic modulus, E^* , is given by

$$\frac{1}{E^*} = \left(\frac{1 - \nu_1^2}{E_1} + \frac{1 - \nu_2^2}{E_2} \right)$$

where ν_1 and ν_2 are the Poisson's ratios of the contacting bodies 1 and 2, respectively, and E_1 and E_2 are the elastic moduli of the contacting bodies 1 and 2, respectively.

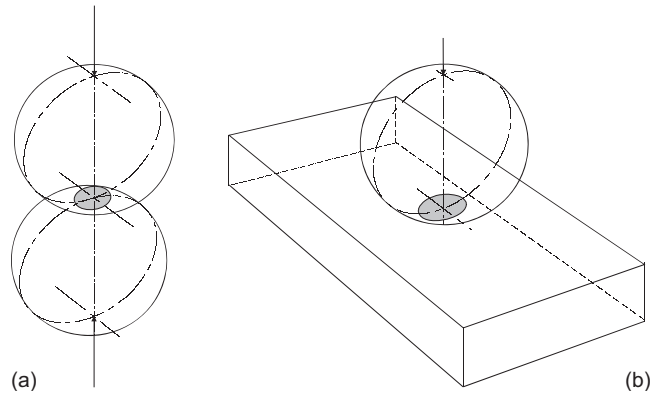


Figure 17.13—A circular point contact (a) resulting from a ball-on-ball contact and (b) a ball-on-flat contact.

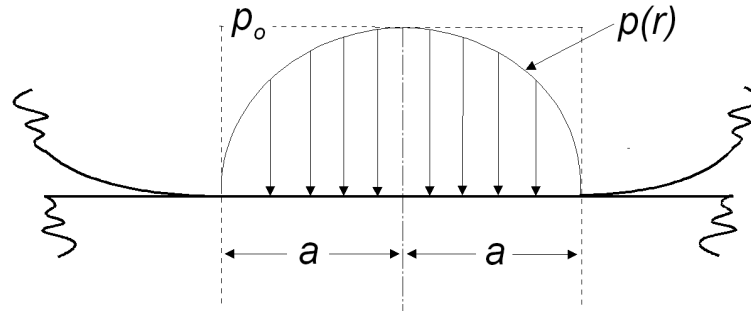


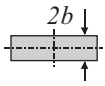
Figure 17.14—Contact pressure distribution in a point contact.

For the case in which a ball is loaded against a flat (see Figure 17.13b), the radius of the flat is taken as ∞ .

The diagram in Figure 17.14 shows the contact pressure distribution. The form is elliptical with a maximum value of p_0 at the axis of symmetry ($r = 0$). The contact pressure falls to zero outside of the area of contact.

17.5.4 Contact between Two Parallel Cylinders (Line Contact)

The contact equations for a line contact (see Figure 17.15) are as follows:

Reduced Radius	Contact Area Dimensions	Maximum Contact Pressure	Average Contact Pressure	Contact Pressure Distribution
$\frac{1}{R'} = \frac{1}{R_1} + \frac{1}{R_2}$	$b = \sqrt{\frac{4P'R'}{\pi E^*}}$ 	$p_0 = \frac{2P'}{b\pi}$	$p_{avg} = \frac{P'}{2b}$	$p(x) = p_0 \sqrt{1 - \frac{x^2}{b^2}}$

where b is the half width of the contact rectangle (m) and P' is the load per unit length (N/m).

The contact pressure distribution is the same as that shown diagrammatically for a circular point contact in Figure 17.15.

17.5.5 Elliptical Point Contact

The contact equations for an elliptical contact (see Figure 17.16) are as follows:

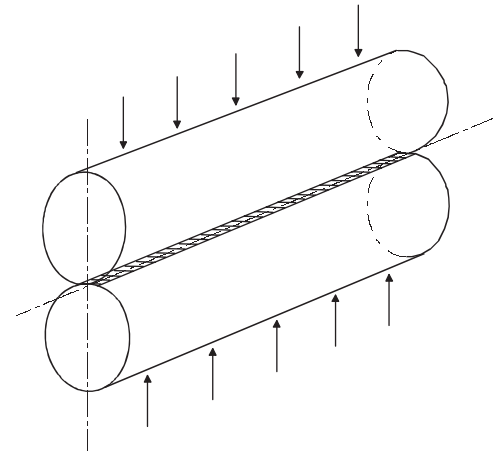
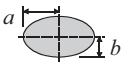


Figure 17.15—A line contact between two parallel cylinders.

where k is the ellipticity parameter ($k = a/b$) and E is an elliptic integral of the second kind. The elliptic integral may be obtained from tables of mathematical data. Alternatively, an approximate solution is given by

$$k = 1.0339 \left(\frac{R_y}{R_x} \right)^{0.6360} \quad \text{and} \quad E = 1.0003 + \frac{0.5968 R_x}{R_y}$$

Other important issues to consider are related to what happens subsurface because this can be where some failures initiate. For example, maximum shear stresses are at a peak subsurface under some contact conditions, and it can be here that yield first occurs. Equations for determining subsurface stresses can be found in several publications (see, for example, [27]).

Reduced Radius	Contact Area Dimensions	Maximum Contact Pressure	Average Contact Pressure	Contact Pressure Distribution
$\frac{1}{R'} = \frac{1}{R_x} + \frac{1}{R_y}$ where: $\frac{1}{R_x} = \frac{1}{R_{1x}} + \frac{1}{R_{2x}}$ and $\frac{1}{R_y} = \frac{1}{R_{1y}} + \frac{1}{R_{2y}}$	$a = \sqrt[3]{\frac{3k^2 E P R'}{\pi E^*}}$ $b = \sqrt[3]{\frac{3 E P R'}{\pi k E^*}}$ 	$p_0 = \frac{3P}{2\pi ab}$	$p_{avg} = \frac{P}{\pi ab}$	$p(x, y) = p_0 \left\{ 1 - \frac{x^2}{a^2} - \frac{y^2}{b^2} \right\}^{1/2}$

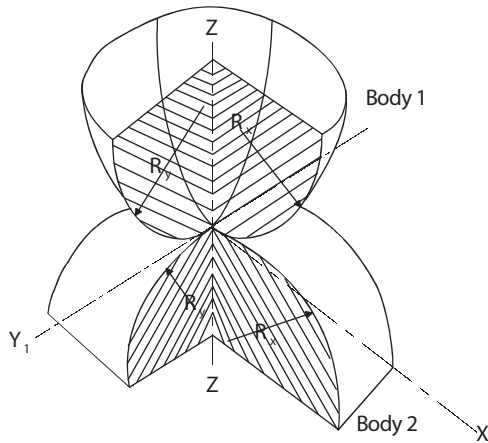


Figure 17.16—Elliptical contact parameters.

17.5.6 Non-Hertzian Contact

Most engineering contacts violate the Hertz assumptions. Contact mechanics under these conditions become complex and numerical methods are needed. The following sections look at the trends observed when the assumptions are relaxed.

17.5.6.1 THE EFFECT OF FRICTION—SLIDING ELASTIC CONTACTS

Hertz assumes that loading is normal to the contact and that the contact is static. In many contacts this will not hold true. There will be a tangential force, Q , applied to one of the contacting bodies in addition to the normal load, P . If $Q < \mu P$ (where μ is the coefficient of friction), then no incipient sliding of the bodies will occur. The bodies will remain in static contact, but regions of stick and microslip are seen within the contact region.

If the tangential force is increased, such that $Q > \mu P$, then sliding will occur. The contact stress distributions are now due to pressure and frictional tractions.

17.5.6.2 ONSET OF YIELD—PLASTIC CONTACT

The shear stress is at a maximum at a location subsurface. The Tresca yield criterion tells us that yield occurs when

$$\tau_{\max} = k = \frac{Y}{2} \quad (17.1)$$

where k is the yield stress in pure shear and Y is the yield stress in tension. Applying this criterion gives expressions for the load and contact pressure at which first yield will occur.

	Line Contact	Point Contact
Maximum shear stress	$\tau_{\max} = 0.3p_0$	$\tau_{\max} = 0.31p_0$
Depth of maximum shear stress	$z = 0.78b$	$z = 0.57a$
Load for first yield	$P'_y = \frac{\pi R (1.67Y)^2}{E^*}$	$P_y = \frac{\pi^3 R^2}{6E^*} (1.60Y)^3$
Peak contact pressure at first yield	$(p_0)_y = 3.3k = 1.67Y$	$(p_0)_y = 3.2k = 1.60Y$

Yield will initially occur at a location subsurface. The region of plasticity is initially contained by an elastic

region. If the load is increased further, then the plastic region grows. The state of “full plasticity” is defined when the plastic region reaches the surface.

The hardness test is a fully plastic indentation process. Empirically, the hardness, H (in pascals), may be related to the material stress by $H \approx 2.7Y$. Therefore, a useful rule of thumb is that yield will occur when $p_{\text{avg}} > 0.4H$.

17.5.6.3 CONTACT OF ROUGH SURFACES

When two spheres with rough surfaces are pressed together, the rough interface acts like a compliant layer. The asperity peaks outside of the nominal Hertzian contact areas may touch. Thus, the region of microcontacts will extend beyond that predicted by smooth surface analysis. There will be local pressure peaks at each asperity contact, but the average pressure acting over the contact will be reduced. For a random rough surface, the probability of contact decreases remotely from the contact center. It is difficult to precisely define the boundary of this extended contact area.

17.6 WEAR MODELING AND MAPPING

This stage is the core of the wear analysis. It involves selecting an appropriate analytical relationship to describe the anticipated wear in the design of a new or modified component or model wear seen in a worn component and select design parameters to overcome the problem.

There are four steps in this stage:

1. Determine relationships to use.
2. Develop a mathematical model relating wear life to design parameters.
3. Verify the model to check accuracy (if not acceptable modify or use alternative).
4. Use to optimize parameters and establish the design changes required.

The best known wear model is that for sliding contacts, attributed to Archard [28] but developed initially by Holm [29]:

$$V = \frac{KPS}{h} \quad (17.2)$$

where:

V = wear volume,
 P = normal force,
 S = sliding distance,
 h = penetration hardness, and
 K = empirical coefficient.

Lim and Ashby [30] used this model to develop their widely referenced wear map for a steel-on-steel unlubricated contact (see Figure 17.17). The thick lines on the map delineate different wear mechanisms and thin lines are contours of equal wear rate. The map is based on the following parameters: normalized wear $\tilde{Q} = \frac{V}{A_n}$, normalized pressure $\tilde{F} = \frac{F_N}{AH}$, and normalized sliding velocity $\tilde{v} = \frac{vr_0}{a_0}$, where V is the wear volume, A_n is the apparent contact area, F_N is the normal load, H is the hardness of the softer material in the contact, v is the sliding velocity, r_0 is the radius of the pin, and a_0 is the thermal diffusivity of the material.

The wear map is a very useful way of assessing during a design process for a contact with known conditions in which wear regime may occur. Of critical importance is

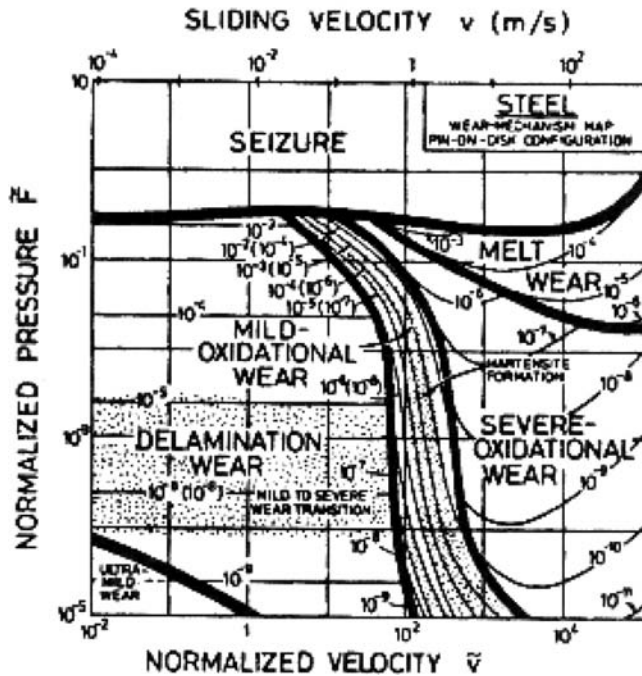


Figure 17.17—Lim and Ashby wear map for unlubricated sliding of a steel-steel couple.

to avoid passing through the transition between mild and severe wear.

A look through the literature will reveal many other wear maps built to study individual materials (cast iron [31], ceramics [32], etc.), mainly for sliding wear situations, although some exist for rolling/sliding contacts [33]. Maps have also been developed for specific applications, such as gears [34] and some linked to automotive engineering [35].

Clearly within the various wear regimes very different wear mechanisms will be apparent. This has led to the development of wear models more specific to these regimes, including the delamination wear theory proposed by Suh [36], which explains how the flake-like wear debris associated with this regime is generated, and the oxidative wear mechanism put forward by Quin [37].

Several other models have been derived from the Archard sliding wear model, including those for predicting wear due to abrasion and impact wear. Several of these and other models are outlined in Table 17.5.

Another model of interest is the Bayer zero wear model [38]. The model states that wear can be reduced to a minimum, or eliminated, by keeping the stress in the vicinity of the region of contact below a certain value. This value is a function of the materials and lubricants used as well as the lifetime. This came from work performed using a large range of material combinations to establish at which conditions there was zero wear.

It should be noted here that although tests may not be required as part of the wear analysis process, many of the analytical relationships for predicting wear are semiempirical and need data from tests that may not be available for the materials under consideration. Some data have been published in the literature. A good example being the Archard wear coefficients collated by Rabinowicz [39], shown in Figure 17.18. Wear coefficients for more specific material pairs can be found in Table 17.6.

TABLE 17.5—Wear Models

Wear Mechanism	Model	Parameters
Sliding adhesive wear	$V = \frac{KPS}{h}$	V is the wear volume P is the normal force S is the sliding distance h is the penetration hardness K is an empirical coefficient
Percussive impact wear	$V = KNv^n$	V is the wear volume v is the impact velocity N is the number of impacts K and n are empirical wear constants
Zero wear-relationship for compound impact	$N_0 = \frac{2000}{1+\beta} \left(\Gamma_r' \frac{\sigma_y}{\sigma_m} \right)^9$	N_0 is the number of impacts to exceed zero wear σ_y is the yield stress in tension σ_m is the maximum contact stress Γ_r' and β are empirical constants
Abrasive wear	$V = \frac{2k \tan \theta PS}{\pi h}$	V is the wear volume P is the normal force S is the sliding distance h is the penetration hardness 2θ is the included angle of the abrasive k is an empirical coefficient

17.7 WEAR TESTING

As mentioned in Section 17.1, wear testing is not necessarily always included in a wear analysis process. However, they may be required for the following reasons:

- Evaluation of the function, performance, maintainability, reliability, life, or efficiency of engineering tribosystems or components;
- Quality control of components;
- Characterization of the tribological behavior of materials and lubricants;
- Investigation of tribological processes; and
- Validation of modeling approaches.

Wear experiments must be carefully designed to meet the objectives of the tribotesting to be performed. The type of test, the equipment to be used, the test conditions, and the data that must be collected have to be selected precisely with respect to the aims of the testing.

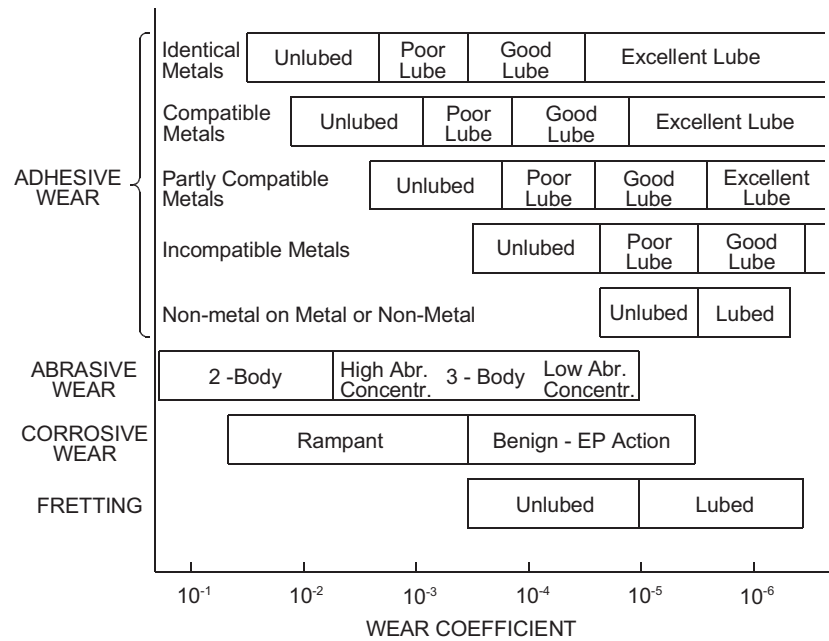


Figure 17.18—Wear coefficients to be anticipated in various sliding situations [39].

TABLE 17.6—Archard Wear Coefficients for Mild Steel Vs. a Range of Different Materials [27]

Material	Archard Wear Coefficient, K
Mild steel (on mild steel)	7×10^{-3}
α/β brass	6×10^{-4}
Polytetrafluoroethylene	2.5×10^{-5}
Copper-beryllium	3.7×10^{-5}
Hard tool steel	1.3×10^{-4}
Ferritic stainless steel	1.7×10^{-5}
Polythene	1.3×10^{-7}
Poly(methyl methacrylate)	7×10^{-6}

TABLE 17.7—Categories of Tribotest

Test Type	Description
<i>Machinery field tests</i>	Testing of actual tribomachinery under practical operating conditions
<i>Machinery bench tests</i>	Testing of actual tribomachinery under practical-orientated (simplified, simulated, or accelerated) operating conditions
<i>Systems bench tests</i>	Testing of specific tribosystems under practice-orientated operating conditions
<i>Component bench tests</i>	Testing of specific tribocomponents under practice-oriented operating conditions
<i>Specimen tests</i>	Testing of arbitrary test specimens under practice-oriented or laboratory-operating conditions

17.7.1 Categories of Test

Depending on the structure and function of the tribomachinery, tribosystem, tribocomponents, or specimen to be studied, tribotests can be categorized as shown in Table 17.7.

The complexity of these tests clearly decreases in going down the list. The test categories at the top utilize actual operating systems and components along with actual loading regimes and environmental conditions, but they offer little control over variables. As the tests are simplified, they move to using actual components but with simulated operating systems right down to simple specimens with simulated loading and environmental conditions. However, the simpler the test, the more control there can be over variables, so tests can be performed to study the influence on wear of different parameters.

In deciding which test type to use, other factors come into the equation, such as the time taken to run the tests and the cost. In general, the more complex the test category selected the longer the tests take to run and the greater the cost.

Table 17.8 shows a selection of different methods including some standard ASTM tests, shown in order of increasing complexity, which could be used to test engine components. The test conditions that can be used and the types of wear measurement that can be taken are also given.

17.7.2 Designing a Wear Test Methodology

When investigating any type of wear problem, it is important to proceed in an organized manner to avoid missing important information that could help to solve the issue in question. An obvious route would be to replicate the system in a laboratory and test all permutations of material, geometry, operating conditions, and the like to attempt to replicate the unwanted wear and to find the cause. This method is cumbersome, expensive, and the complexity of many tribological systems means that the root cause of the problem can be hidden by many other issues.

Therefore, it is good practice to generate an overall wear testing methodology to give a framework for any

TABLE 17.8—The Increasing Complexity of Different Types of Wear Test for Automotive Engine Components

	Test Method	Type of Test	Test Conditions	Measured Quantity
INCREASING COMPLEXITY	Crossed Cylinder (ASTM G83-83)	Adhesive wear	High contact stress High sliding velocity No lubrication	Weight loss
	Block-on-Ring (ASTM G77-83)	Adhesive (sliding)	High contact stress Sliding speed High Temperature No lubrication	Weight loss Friction
	Thrust Washer	Adhesive/abrasive	High contact stress Sliding speed High temperature No lubrication	Weight loss Wear depth Wear profile Cycles to failure
	Bench Test-Rigs	General	Valve gear lube Speed Temperature Spring load Seating velocity	Oil residue analysis Wear depth Wear profile
	Motorized or Fired Engine Tests	General	Engine operating Conditions Speed Torque	

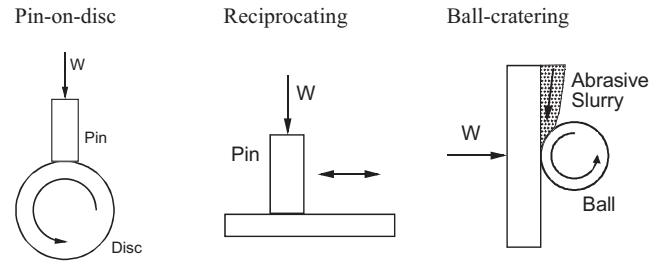
individual tests or experiments that are performed, regardless of complexity, to fit into.

ASTM has developed a guide to developing and selecting wear tests. This is a useful document because it refers to many of the ASTM standards for wear testing. When possible, it is best to adhere to the standards because this allows comparison with previous testing using the standards. Clearly, it will not always be possible to do this, particularly because most standards are for specimen tests, and if component testing is required, it is highly unlikely a test will have been defined.

17.7.3 Standard Test Apparatus

If the test category selected is that of specimen tests, then a wide range of standard test apparatuses is available that can be bought off of the shelf. This wide variety has arisen from a desire to ensure appropriate controls and test convenience and a need to simulate the wear conditions for the intended application. These test rigs use a range of simple specimen contacts depending on the type of motion and wear mechanism to be simulated. Some of these are listed below and shown in Figure 17.19:

- Four-ball (rolling/sliding—used for lubricant evaluation),
- Pin-on-disc (unidirectional sliding—used for materials testing),

**Figure 17.19—Some standard wear test configurations.**

- Ball-on-flat (unidirectional/linearly reciprocating—used for materials/coating testing),
- Twin disc (rolling/sliding—used for wear/RCF testing, e.g., wheel/rail materials, gear materials, etc.), and
- Dry sand/rubber wheel (used for abrasion testing).

ASTM publishes standard test methods for such apparatuses (for example, ASTM G133 Test Method for Linearly Reciprocating Ball-on-Flat Sliding Wear, ASTM G99 Test Method for Wear Testing with a Pin-on-Disc Apparatus, etc.)

17.7.4 Design of Laboratory Tests

When designing an experimental strategy, several factors must be considered. Some of these are linked to practical considerations, particularly with component or specimen bench tests, such as how to best simulate the component contact under consideration, but others applicable to all types of tests include which parameters to control and measure and how this can be achieved, how many tests to run (repeatability vs. parameter variation), selection of parameter ranges, and how to determine that the test is a valid simulation of the actual component contact or how to use the data collected as an input to or to validate a wear model.

The basic characteristics and relevant parameters of laboratory and simulative tests are shown in Figure 17.20.

The design of laboratory wear tests should be performed in the following steps:

1. Choose a suitable test configuration for the test specimens of triboelement (1) and triboelement (2) and specify the geometry of the test configuration, materials characteristics, and properties as well as surface characteristics.
2. Characterize the interfacial element (3) (e.g., the lubricant) and the environmental medium or atmosphere (4) in terms of their chemical nature, composition, and chemical and physical properties.
3. Choose a suitable set of operational parameters, including type of motion, load, velocity, temperature, and test duration (the range of parameters used is discussed further later on).
4. Perform the tests as functions of varied structural parameters (e.g., hardness or roughness) and operational parameters (e.g., varying load and velocity). This is more appropriate for exploratory testing.
5. Measure interesting tribometric characteristics (e.g., friction, wear, temperature rise, noise, or vibrations).
6. Characterize the worn surfaces.

It may be necessary to control, via feedback, particular test parameters, such as load or velocity. This adds complexity to the test setup, but it will allow more confidence in the test method. Data may need to be recorded during the testing (e.g., dimensions, temperature etc.) so appropriate

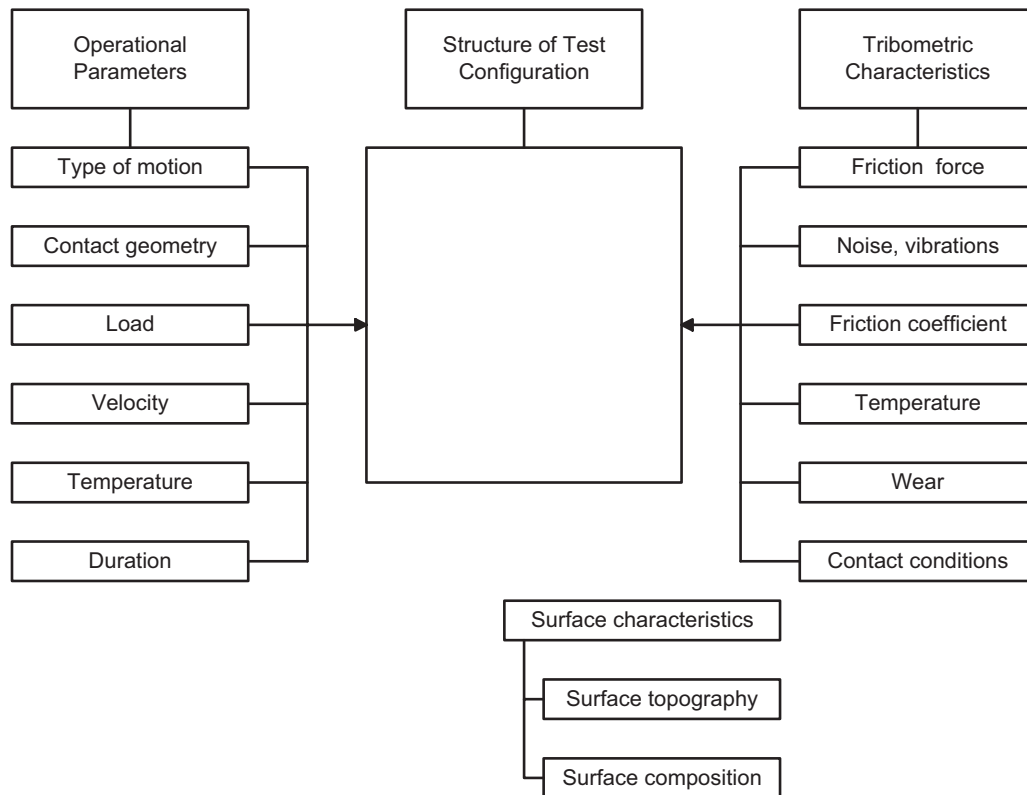


Figure 17.20—Test design flow chart. Source: Figure adapted from [1].

instrumentation will be required. During and after testing, wear will need to be quantified, by mass loss or geometry change.

It is important to consider the number of tests that are required to obtain good quality results. The number of tests may be constrained by costs and time allocation; therefore, it must be decided whether to test many different configurations of test parameters or to repeat tests at a few configurations to study variability. For example, using many different configurations will allow the performance of a component or model validation to be explored over a wider range of conditions, but not take into account the possible scatter at one set of conditions. Repeating at a few configurations will lead to a higher overall confidence in the results; however, knowledge of the overall parameter space will have to be sacrificed.

Parameter ranges selected should reflect the range of possible conditions in the actual application. It should

be noted here that using results interpolatively is better than using them extrapolatively, as shown in Figure 17.21, particularly if using the experimental data to validate a model.

It is very important that the condition and the preparation of specimens are kept under tight control. Lack of attention to this detail can cause scatter in the results and a lack of repeatability. Specimen preparation varies with the test and the materials involved, but in general surface roughness, geometry, microstructure, and hardness must all be controlled. It should be noted that the specimen under consideration, the counterface, and the wear-producing medium (e.g., a third body abrasive) must all be controlled with equal vigor.

The accuracy of a test simulation can be assessed qualitatively using visual and optical inspection to compare wear features from the tested components or specimens with those from actual field operation. This can give confidence in the test method, but more information is needed in the form of wear rates to quantitatively assess the test in terms of how well it ranks materials or for validation of a wear model. An important aspect is the repeatability of the results. It is impossible to validate anything with one set of results, and the potential scatter must be assessed.

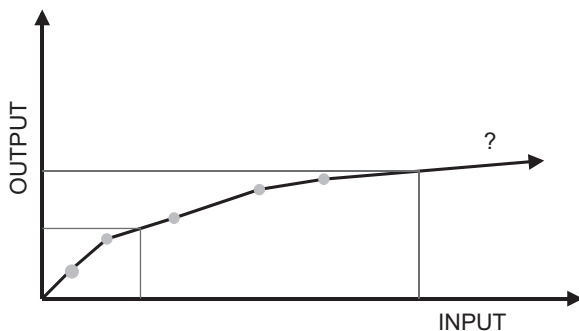


Figure 17.21—Extrapolation vs. interpolation.

17.8 CASE STUDY: COMBATING ENGINE VALVE RECESSION

17.8.1 Introduction

Valve recession occurs when wear of the valve or seat inserts in an automotive engine have caused the valve to

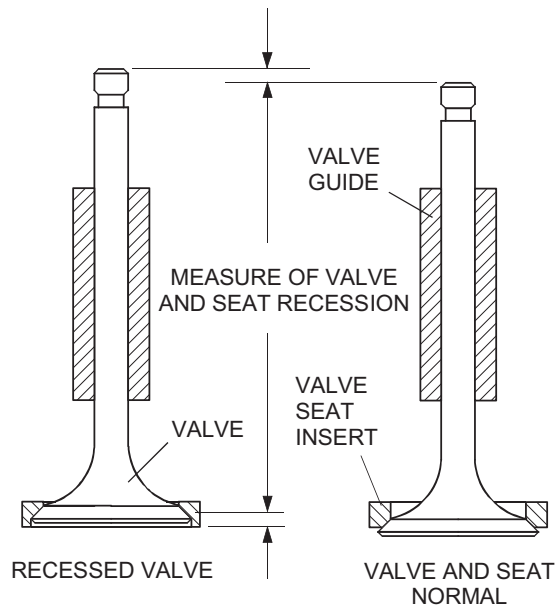


Figure 17.22—Valve recession.

sink or recede into the seat insert, as shown in Figure 17.22. Excessive recession leads to valves not seating correctly and cylinder pressure loss. Leaking hot combustion gases can also cause valve guttering or torching, which will accelerate valve failure.

Although new valve materials and production techniques are constantly being developed, these advances have been outpaced by demands for increased engine performance, and wear-related problems remain an issue. Dynamometer engine testing is often used to establish short-term solutions. This is time-consuming and does not necessarily reveal the actual causes of wear.

A long-term approach is required to understand fundamental wear mechanisms and the effect of varying engine-operating conditions or design changes to the valvetrain. This information can then be used to develop tools for predicting wear and for solving problems more quickly if they do occur. In this case study, such tools were developed using a combination of component failure analysis, bench test work, and wear modeling.

17.8.2 The Problem

The failures that initiated the investigation involved an eight-valve, 1.8-L, direct-injection diesel engine with direct-acting cams. The engine was undergoing design upgrades, one of which was the change from indirect to direct injection. This meant the inclusion of holes in the cylinder head between the inlet and exhaust ports to accept the fuel injector. A new seat insert material was also being trialed in the tests. The material had solid lubricants incorporated, which were thought to help improve machinability and reduce sliding wear problems at the valve/seat interface. The valve, seat insert, and operating system are shown in Figure 17.23.

Several problems occurred during preproduction dynotesting. The new seat insert material exhibited excessive wear (0.3 mm of recession in 100 h). Further analysis also revealed that uneven wear of the seat

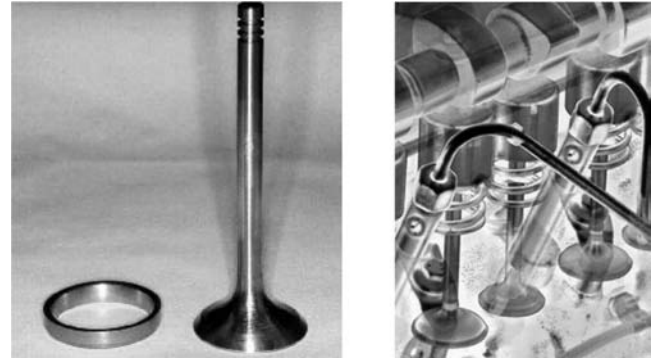


Figure 17.23—Valve, seat insert, and valve-operating system.

inserts was occurring. This was found to be a result of thermal distortion of the seat inserts thought to be due to enforced changes in cooling channels to incorporate the fuel injectors. The seat inserts returned to their original shape upon cooling, which meant on restarting the valves were unable to seat properly and cylinder pressure loss resulted.

17.8.3 Laboratory Investigations

17.8.3.1 TEST APPARATUS

Figure 17.24 shows a suite of laboratory test equipment that has been developed to study the valve recession problem, covering the range of test methods outlined in Table 17.7. Table 17.9 indicates where the different rigs fit in the different levels of testing. At the least-complex end, an impact wear tester has been developed that uses an actual cam to study impact wear properties of head and seat insert materials [40]. A rig that uses actual seat inserts and valves is used in hydraulic-loading apparatuses to simulate the effects of combustion loading as well as the impact on valve closure (using simulated valvetrain dynamics) [41]. A motorized cylinder head [42] and a modular test rig that uses actual valve drive components (able to take any size of valve and seat insert) have been designed to study component impact wear using actual valvetrain dynamics. These rigs were used to investigate the fundamental wear mechanisms and the effect of critical engine operating parameters.

17.8.3.2 WEAR MECHANISMS

The laboratory investigations showed that the inlet valve and seat insert wear problem involves two distinct mechanisms:

1. Impact as the valve strikes the seat on closure, and
2. Microsliding at the valve/seat interface caused by elastic deformation of the valve head as it is pressed into the seat by the combustion pressure.

Impact on valve closure causes plastic deformation of the seating face surface and the formation of a series of circumferential ridges and valleys. It also led to surface cracking and subsequent material loss from seat inserts at high closing velocities. Sliding caused the formation of radial scratches on the seat insert seating faces.

Figure 17.25 illustrates some of these features and compares wear surfaces on valves and seats run in the test apparatus (Figure 17.25, a and b) with those examined

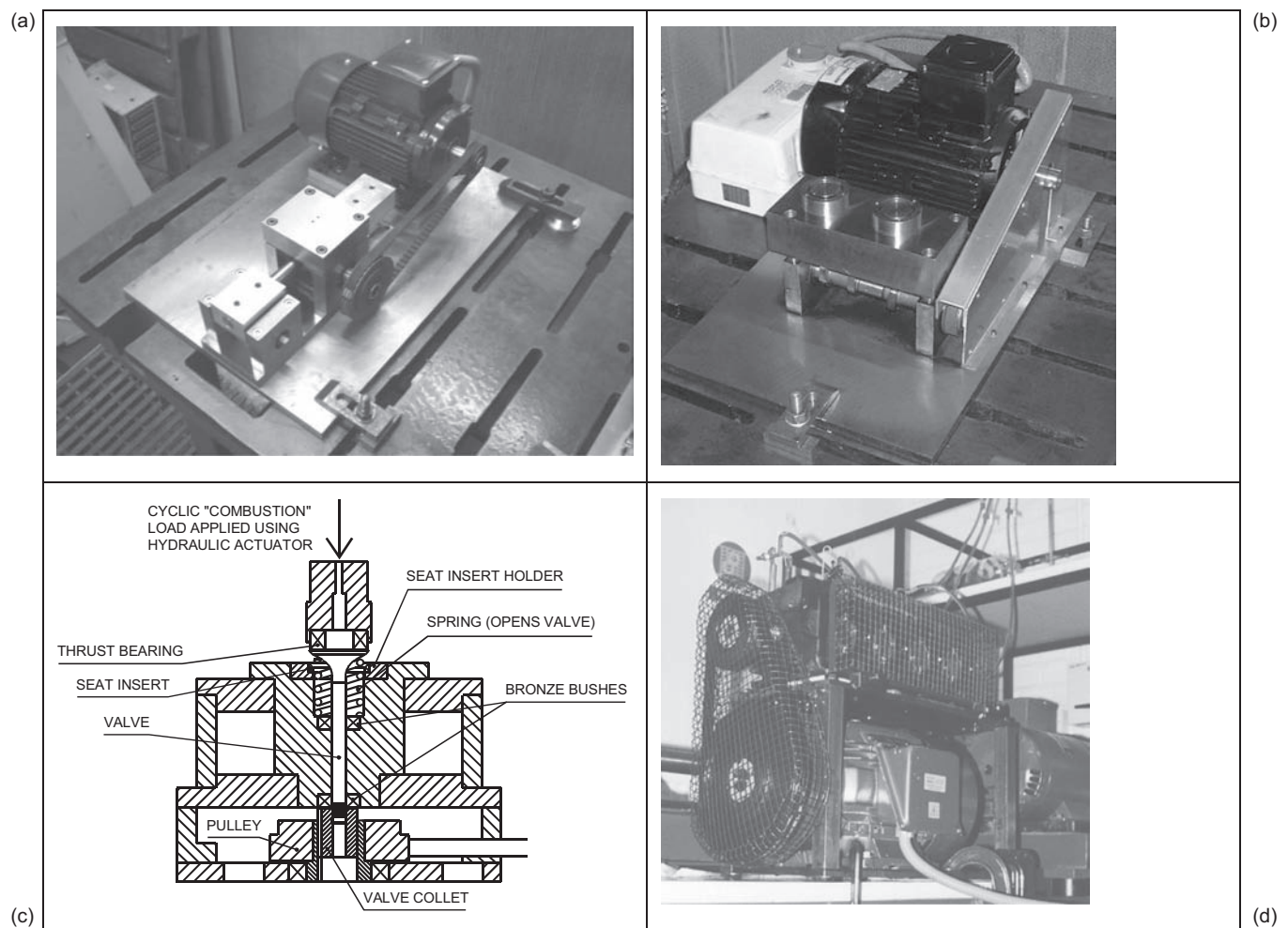


Figure 17.24—(a) Specimen impact wear tester, (b) modular test rig, (c) rig mounted in hydraulic test apparatus, and (d) motorized cylinder head.

during failure analysis of valves and seats from engine tests (Figure 17.25, c and d).

17.8.3.3 EFFECT OF ENGINE-OPERATING PARAMETERS

The test work showed that recession was strongly dependent on valve-closing velocity, combustion load, and valve/seat insert misalignment, as shown in Figure 17.26 [43].

17.8.4 Development of Predictive Models

A valve recession prediction model has been developed using the results of the bench testing [43,44]. The model separately considers impact and sliding because they occur as two separate load events. Parameters were derived either directly from the valve and seat design and engine operating conditions or from bench test results. The model has the form

TABLE 17.9—Levels of Experimental Testing		
Level	Aims of Test/Experiment	Types of Test/Experiment
1 <i>Material level</i>	Investigation of primary material properties	Impact wear testing of “thick shim” test specimens of modified cylinder head and valve seat insert materials
2 <i>Component level</i>	Investigation of interactions between geometry and materials	Hydraulic cylinder head rig to investigate the wear due to valve sliding due to combustion pressure and impact on closure
3 <i>System level</i>	Investigation of individual wear mechanisms or the effect of system dynamics or both	Motorized cylinder head rig to investigate wear due to impact from valvetrain dynamics Modular test rig to investigate the wear due to different valve and valve seat material combinations and the effect of contact geometry
4 <i>Integrated level</i>	Investigation of interaction between wear mechanisms at realistic operating conditions	Firing single-cylinder test engine to recreate actual pressures, temperatures, environment, etc.
5 <i>Actual level</i>	Investigation at “real-world” level	Engine durability dynamometer test

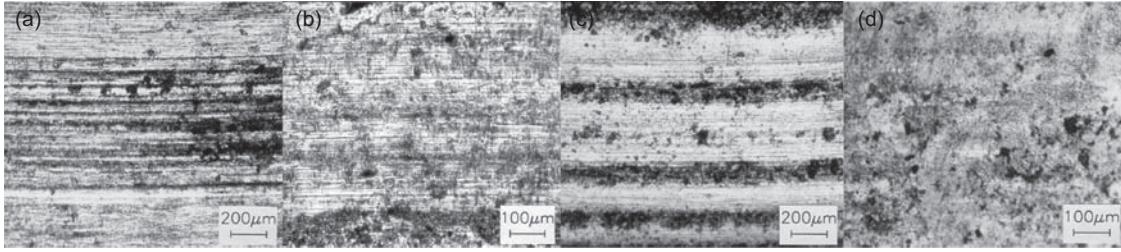


Figure 17.25—Laboratory tested valve (a) and seat insert (b) compared with engine tested valve (c) and seat insert (d).

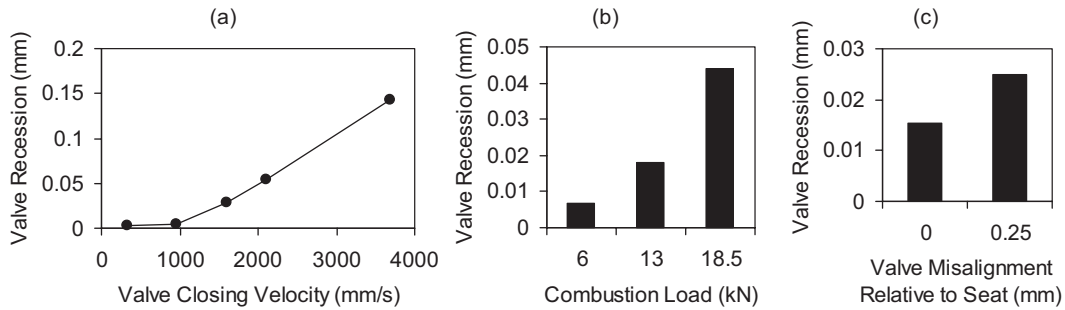


Figure 17.26—Valve recession with cast tool steel seat inserts for increasing (a) valve-closing velocity (after 100,000 cycles), (b) combustion load (after 25,000 cycles), and (c) valve misalignment (after 25,000 cycles).

$$V = \left(\frac{k\bar{P}N\delta}{H} + KN \left(\frac{1}{2} mv^2 \right)^n \right) \left(\frac{A_i}{A} \right)^j \quad (17.3)$$

where:

V = wear volume,

\bar{P} = average load at the valve/seat interface,

N = number of cycles,

δ = slip at the valve/seat interface,

H = seat hardness,

k = sliding wear coefficient determined during wear tests,

m = mass of valve and follower,

v = valve-closing velocity, and

K and n = impact wear constants determined during wear testing.

The factor, consisting of the ratio of the initial valve/seat contact area, A_i , to the contact area after N cycles, A , to the power of a constant j , was included to incorporate the change in pressure at the interface, and other effects likely

cause a reduction in the wear rate with time, such as work hardening. The constant j was determined empirically using bench and engine test data.

The wear volume can readily be converted into a linear recession from the seat geometry

To provide a tool for running the wear modeling code, software called RECESS has been developed. Figure 17.27 shows RECESS predictions against measured data for engine dynotests run using cast and sintered tool steel inserts. As can be seen, the model produces a good prediction of valve recession.

Knowledge built up during failure analysis, bench testing, and modeling has been combined to develop a flow chart for use in solving valve recession problems that do occur, more quickly, as shown in Figure 17.28 [44].

17.8.5 Adopted Solution

The short-term solution for the recession problem outlined was to replace the seat insert material with a material exhibiting higher toughness to reduce the effect of impact wear on valve closure. The structure of the original material meant it had good resistance to sliding wear, but low fracture toughness. The impact issue was also addressed by slightly altering the inlet cam profile to reduce the valve-closing velocity.

The problem of uneven wear caused by thermal distortion of the seat inserts was remedied by reconfiguring the cylinder-head cooling channels to promote uniform cooling around the seat inserts.

A new long-term approach to combating valve recession is now possible. As new engine design changes are made, the prototype valvetrain systems are typically modeled in multibody simulation packages. The output from these, the loads, and deformations are used as inputs to RECESS to predict recession rates for a given design. In this way it may be possible to design out the causes of valve recession.

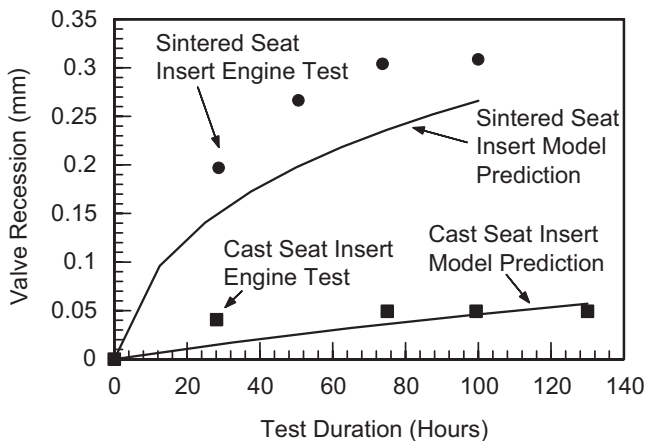


Figure 17.27—Model predictions vs. engine test data.

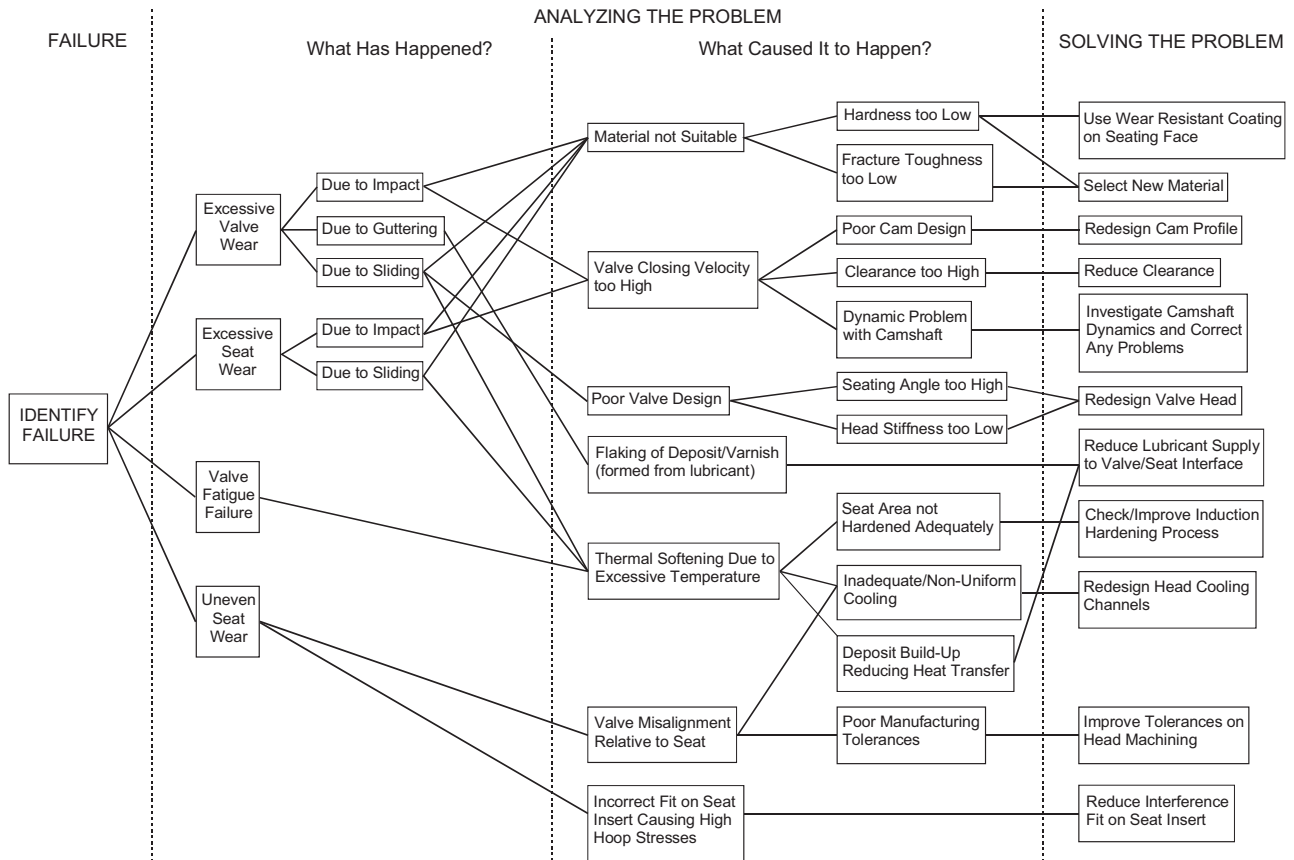


Figure 17.28—Solving valve/seat failure problems.

17.9 OPTIONS FOR REDUCING WEAR

17.9.1 Review Previous Investigations

Clearly before embarking on a lengthy investigation based around a process as outlined in this chapter it would be wise to see what has been done before. Have the wear

mechanisms of the components you are interested in been investigated previously? Table 17.10 shows a snapshot of the results of a review performed on recent work in wear of automotive engine components. There are many more publications not listed here. This work has focussed on a

TABLE 17.10—Recent Work on Wear of Automotive Engine Components

Engine Component	Reference	Focus of Work
Piston pins	45	Reducing wear (coatings)
Piston ring and cylinder wall	46	Wear testing/measurement
Piston ring and cylinder wall	47	Wear testing Identifying wear mechanisms
Piston ring and cylinder liner	48	Reducing wear (coatings)
Piston ring and cylinder liner	14	Wear testing method
Cylinder liners	49	Reducing wear (surface finish)
Piston rings	50	Reducing wear and friction (laser texturing)
Piston rings	51	Reducing wear (coatings)
Valve lifters	52	Reducing wear (coatings)
Cam	53	Reducing wear (design)
Cam followers	54	Reducing wear (coatings)
Valves/seat inserts	43,44	Identifying wear mechanisms Reducing wear (design/materials)
Valve guides	55	Wear testing of new material
General	56	(Surface texturing)
Whole engine	57	(Materials)

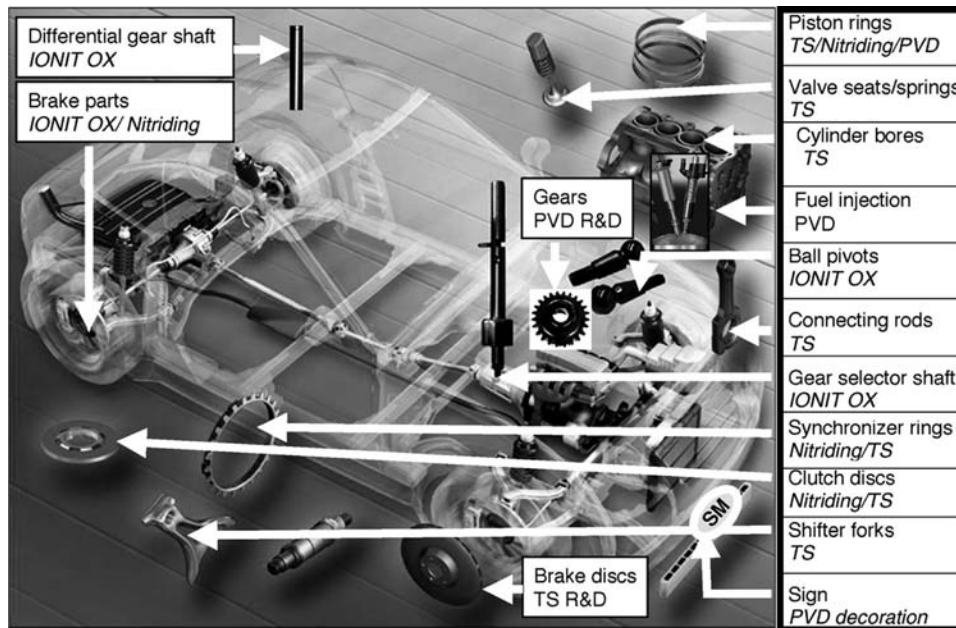


Figure 17.29—Selected parts that could be treated by surface technologies [60].

range of issues, but the focus of the work can be broken down into several broad themes: wear-testing methods; understanding of wear mechanisms; and by far and away the largest body of work is on reducing wear by changing the design of components, using new materials, or applying surface treatments or coatings. This final issue—surface treatments and coatings—is very much in vogue at the moment, with a great deal of research effort going into automotive applications of such technology. This is being driven by the need to reduce the amount of lubricant used and because lighter materials with less wear resistance are being introduced.

17.9.2 Design Tools

The work outlined in Table 17.10 is very much specific to certain applications. Unfortunately, there are not many generic tools for engine components to help predict or reduce wear occurring for use in a design process. One good example is the model outlined in Section 17.8 for estimating valve recession and the accompanying wear reduction design tools.

Another example is the computational model developed by Mukras et al. [58] for studying wear in oscillating pin joints. Some work has also been performed by Kim and Kotkoff [59] using the zero-wear model [38] to design out the excessive wear of a new injector coupling.

This is clearly an area in which a great deal of work can be done by researchers and academics to improve knowledge transfer and produce usable wear prediction tools.

17.9.3 Surface Coatings

As mentioned above, it is evident in Table 17.10 that one of the key methods for reducing wear in the near future will be by the application of surface coatings technology. Surface coatings can have an effect all over an automobile as highlighted by Vetter et al. [60] in their review of surface treatment selections for automotive applications. The potential areas of interest are illustrated in Figure 17.29. They focussed on coating techniques rather than actual coatings, but the

potential is clear, and the field has developed considerably in the years since they published their paper.

This section is not intended to provide details on which coatings should be used because several textbooks exist that can give much better information. For example, Holmberg and Matthews [61] provide detailed information on coatings and their application methods as well as a guide to selecting the correct coating for the application of concern.

17.9.4 Surface Treatments

Alongside surface coatings, the texturing of surfaces using lasers to create surface dimples or other features is finding more applications (see Table 17.10). These are primarily to improve retention of lubricants with the aim of reducing friction and hence saving energy, but they will also have an effect on wear. This technology is mainly aimed at piston rings and liners. In fact, this is where most attention has been paid in terms of addressing tribological problems. However, as shown in Figure 17.7, the biggest wear problems occur elsewhere in the valvetrain on the cam nose and rocker arms.

References

- [1] Bayer, R.G., 2002, *Wear Analysis for Engineers*, HNB Publishing, New York.
- [2] Neale, M.J., 1993, *Bearings: A Tribology Handbook*, Butterworth-Heinemann, Oxford, UK.
- [3] Watermann, N.A., and Ashby, M.F., Eds, 1991, *Materials Selector*, Elsevier Science Publishers, London.
- [4] Vingsbo, O., 1979, "Wear and Wear Mechanisms." In *Proceedings of the International Conference on Wear of Materials*, Dearborn, MI, April 16–18.
- [5] Querlioz, E., Ville, F., Lenon, H., and Lubrecht, T., 2007, "Experimental Investigations on the Contact Fatigue Life under Starved Conditions," *Tribology Int.*, Vol. 40, pp. 1619–1626.
- [6] Stachowiak, G.W., and Batchelor, A.W., 2001, *Engineering Tribology*, Butterworth-Heinemann, Boston.
- [7] Swanson, P., and Klann, R., 1981, "Abrasive Wear Studies Using the Wet Sand and Dry Rubber Wheel Tests." In *Proceedings of the International Wear of Materials Conference*, ASME, New York, pp. 379–389.

- [8] Green, D.A., and Lewis, R., 2008, "The Effects of Soot Contaminated Engine Oil on Wear and Friction: A Review," *J. Auto. Eng.*, Vol. 222, pp. 1669–1689.
- [9] Nagai, I., Endo, H., Nakamura, H., and Yano, H., 1983, *Soot and Valve Train Wear in Passenger Car Diesel Engines*, SAE Paper No. 831757, SAE, Warrendale, PA.
- [10] Dennis, A.J., Garner, C.P., and Taylor, D.H.C., 1999, *The Effect of EGR on Diesel Engine Wear*, SAE Paper No. 1999-01-0839, SAE, Warrendale, PA.
- [11] Li, S., Csontos, A.A., Gable, B.M., Passut, C.A., and Jao, T., 2002, *Wear in Cummins M-11/EGR Test Engines*, SAE Paper No. 2002-01-1672, SAE, Warrendale, PA.
- [12] Chinas-Castillo, F., and Spikes, H.A., 2004, "The Behaviour of Diluted Sooted Oils in Lubricated Contacts." In *Proceedings of the 30th Leeds-Lyon Symposium on Tribology*, Elsevier Tribology Series No. 43, pp. 37–43.
- [13] Green, D.A., and Lewis, R., 2007, "Effect of Soot on Oil Properties and Wear of Engine Components," *J. Physics D, Appl. Physics*, Vol. 40, pp. 5488–5501.
- [14] Truhan, J.J., Qu, J., and Blau, P.J., 2005, "The Effect of Lubricating Oil Condition on the Friction and Wear of Piston Ring and Cylinder Liner Materials in a Reciprocating Bench Test," *Wear*, Vol. 259, pp. 1048–1055.
- [15] Japan Automobile Manufacturers Association (JAMA), 2001, *Global Performance Specification for Diesel Engine Oil (Global DHD-1)—Recommended Guideline*, JAMA, Tokyo.
- [16] Groff, W.P., 1997, *Evaluation and Qualification of Gasoline and Diesel Engine Lubricants*, Southwest Research Institute, San Antonio, TX.
- [17] Rengstorff, G.W., Miyoshi, K., and Buckley, D.H., 1986, "Interaction of Sulphuric Acid Corrosion and Mechanical Wear of Iron," *ASLE Trans.*, Vol. 29, pp. 43–51.
- [18] Benedict, G.H., 1968, "Correlation of Disk Machines and Gear Tests," *Lubrication Engineering*, Vol. 4, pp. 591–596.
- [19] Yahagi, Y., and Mizutani, Y., 1984, "Corrosive Wear of Steel in Gasoline-Ethanol-Water Mixtures," *Wear*, Vol. 97, pp. 17–26.
- [20] Masuko, M., Itoh, Y., Akatsuka, K., Tagami, K., and Okabe, H., 1983, "The Influence of Sulphur-Based Extreme Pressure Additives on Wear under Combined Rolling and Sliding." In *Proceedings of the Annual Conference of the Japan Society of Lubrication Engineers*, pp. 273–276.
- [21] Streibeck, R., 1902, "Die Wesentlich Eigenschaften der Gleit-und-Rollen-lager," *Zeits. Ver. Deutscher Ing.*, Vol. 46, pp. 1341–1348.
- [22] Luo, J.B., Lu, X.C., and Wen, S.Z., 2001, "Developments and Unsolved Problems in Nano-Lubrication," *Prog. Nat. Sci.*, Vol. 11, pp. 173–183.
- [23] Hamrock, B.J., 1994, *Fundamentals of Fluid Film Lubrication*, McGraw-Hill Series in Mechanical Engineering, McGraw Hill, New York.
- [24] Green, D.A., Lewis, R., and Dwyer-Joyce, R.S., 2006, "The Wear Effects and Mechanisms of Soot Contaminated Automotive Lubricants," *J. Eng. Tribology*, Vol. 220, pp. 159–169.
- [25] Andersson, S., and Salas-Russo, E., 1994, "The Influence of Surface Roughness and Oil Viscosity on the Transition in Mixed Lubricated Sliding Steel Contacts," *Wear*, Vol. 174, pp. 71–79.
- [26] Hertz, H., 1881, "Über die Berührung Fester Elastischer Körper" (On the Contact of Elastic Solids), *J. Reine Angewandte Mathematik*, Vol. 92, pp. 156–171.
- [27] Williams, J., 1994, *Engineering Tribology*, Oxford University Press, Oxford, UK.
- [28] Archard, J.F., 1953, "Contact and Rubbing of Flat Surfaces," *J. Appl. Physics*, Vol. 24, pp. 981–988.
- [29] Holm, R., 1946, *Electric Contacts*, Almqvist & Wiksells Boktryckeri AB, Uppsala, Sweden.
- [30] Lim, S.C., and Ashby, M.F., 1987, "Wear Mechanism Maps," *Acta Metal.*, Vol. 35, pp. 1–24.
- [31] Riahi, A.R., and Alpas, A.T., 2003, "Wear Map for Grey Cast Iron," *Wear*, Vol. 255, pp. 401–409.
- [32] Adachi, K., Kato, K., and Chen, N., 1997, "Wear Map of Ceramics," *Wear*, Vol. 203, pp. 291–301.
- [33] Lewis, R., and Olofsson, U., 2004, "Mapping Rail Wear Regimes and Transitions," *Wear*, Vol. 257, pp. 721–729.
- [34] Taki, T., 2007, "Study on Constructing Wear Maps of Gears," *J. Japan. Soc. Tribologists*, Vol. 52, pp. 615–621.
- [35] Wilson, S., Riahi, A.R., and Alpas, A.T., 2000, "Wear Maps for Manufacturing and Automotive Engineering." Paper presented at the International Symposium on Ecomaterials held in conjunction with the 39th Annual Conference on Metallurgists of CIM, Ottawa, Canada, August 22–23.
- [36] Suh, N.P., 1973, "The Delamination Theory of Wear," *Wear*, Vol. 25, pp. 111–124.
- [37] Quin, T.F.J., 1962, "Role of Oxidation in the Mild Wear of Steel," *Brit. J. Appl. Physics*, Vol. 13, pp. 33–37.
- [38] Bayer, R.G., Clinton, W.C., Nelson, C.W., and Schumacher, R.A., 1962, "Engineering Model of Wear," *Wear*, Vol. 5, pp. 378–391.
- [39] Rabinowicz, E., 1981, "The Wear Coefficient—Magnitude, Scatter, Uses," *J. Lubric. Technol.*, Vol. 103, pp. 188–194.
- [40] Slatter, T., Lewis, R., and Broda, M., 2007, "The Influence of Induction Hardening on the Impact Wear Resistance of Compacted Graphite Cast Iron." In *Proceedings of the DGM International Symposium on Friction, Wear, and Wear Protection*, Aachen, Germany, April 9–11.
- [41] Lewis, R., Dwyer-Joyce, R.S., and Josey, G., 2000, "Design and Development of a Bench Test-Rig for Investigating Diesel Engine Inlet Valve and Seat Wear," *Trans. Mech. Eng. IEAust*, Vol. 24, pp. 39–46.
- [42] Lewis, R., and Dwyer-Joyce, R.S., 2001, "An Experimental Approach to Solving Valve and Seat Insert Wear Problems." In *Proceedings of the 27th Leeds-Lyon Symposium on Tribology*, Elsevier Tribology Series No. 39, pp. 629–640.
- [43] Lewis, R., and Dwyer-Joyce, R.S., 2002, "Wear of Diesel Engine Inlet Valves and Seat Inserts," *J. Auto. Eng.*, Vol. 216, pp. 205–216.
- [44] Lewis, R., and Dwyer-Joyce, R.S., 2002, "Design Tools for Predicting Inlet Valve Recession and Solving Valve Failure Problems," *J. Engines, Trans. SAE* 2001, pp. 105–114.
- [45] Morgenstern R., Kiessling, W.G., and Reichstein, S., 2008, "Reduced Friction Losses and Wear by DLC Coating of Piston Pins." In *Proceedings of the Spring Technical Conference of the ASME Internal Combustion Engine Division*, ASME, New York, pp. 289–297.
- [46] Donghui, H., Wang, P., Tian, W., Zhao, D., Cao, G., Ni, B., Zhang, X., Li, L.; Zhang, G., Liu, C., Li, D., 2008, "Study on Real Time Wear Measurement of Piston-Ring and Cylinder Bore in an Engine using Thin Layer Activation Method," *Appl. Radiat. Isot.*, Vol. 66, No. 8, pp. 1073–1078.
- [47] Papadopoulos, P., Priest, M., and Rainforth, W.M., 2007, "Investigation of Fundamental Wear Mechanisms at the Piston Ring and Cylinder Wall Interface in Internal Combustion Engines," *J. Eng. Tribology*, Vol. 221, pp. 333–343.
- [48] Skopp, A., Kelling, N., Woydt, M., and Berger, A.M., 2007, "Thermally Sprayed Titanium Suboxide Coatings for Piston Ring/Cylinder Liners under Mixed Lubrication and Dry-Running Conditions," *Wear*, Vol. 262, pp. 1061–1070.
- [49] Tomanik, E., 2008, "Friction and Wear Bench Tests Of Different Engine Liner Surface Finishes," *Tribology Int.*, Vol. 41, pp. 1032–1038.
- [50] Etsion, I., and Sher, E., 2009, "Improving Fuel Efficiency with Laser Surface Textured Piston Rings," *Tribology Int.*, Vol. 42, pp. 542–547.
- [51] Kawai, K., 2006, "Tribological Properties of Nanomultilayer Coatings for Piston Rings," *J. Japan. Soc. Tribologists*, Vol. 51, pp. 633–638.
- [52] Lindolm, P., and Svahn, F., 2006, "Study of Thickness Dependence of Sputtered-Carbon Coating for Low Friction Valve Lifters," *Wear*, Vol. 261, pp. 241–250.
- [53] Flocker, F.W., 2008, "Addressing Cam Wear and Follower Jump in Single-Dwell Cam Follower Systems with an Adjustable Modified Trapezoidal Acceleration Cam Profile." In *Proceedings of the Spring Technical Conference of the ASME Internal Combustion Engine Division*, ASME, New York, pp. 327–335.
- [54] Lawes, S.D.A., Fitzpatrick, M.E., and Hainsworth, S.V., 2007, "Evaluation of the Tribological Properties of DLC for Engine Applications," *J. Physics D Appl. Physics*, Vol. 40, pp. 5427–5437.

- [55] Blau, P.J., Dumont, B., Braski, D.N., Jenkins, T., Zanoria, E.S., and Long, M.C., 1999, "Reciprocating Friction and Wear Behaviour of a Ceramic-Matrix Graphite Composite for Possible Use in Diesel Engine Valve Guides," *Wear*, Vol. 225, pp. 1338–1349.
- [56] Borghi, A., Gualtieri, E., Marchetto, D., Moretti, L., and Valeri, S., 2008, "Tribological Effects of Surface Texturing on Nitriding Steel for High-Performance Engine Applications," *Wear*, Vol. 265, pp. 1046–1051.
- [57] Becker, E.P., 2008, "Trends in Tribological Materials and Engine Technology," *Tribology Int.*, Vol. 37, pp. 569–575.
- [58] Mukras, S., Kim, N.H., Sawyer, W.G., Ackson, D.B., Berquist, L.W., 2007, "Numerical Integration Schemes and Parallel Computation for Wear Prediction using Finite Element Method," *Wear*, Vol. 266, pp. 822–831.
- [59] Kim, J.S., Kotkoff, D.N., 1990, "Zero Wear Analysis of an Injector Coupling," SAE paper 902239.
- [60] Vetter, J., Barbezat, G., Crummenauer, J., and Avissar, J., 2005, "Surface Treatment Selections for Automotive Applications," *Surface Coatings Technol.*, Vol. 200, pp. 1962–1968.
- [61] Holmberg, K., and Matthews, A., 1994, *Coatings Tribology: Properties, Techniques and Applications in Surface Engineering*, Elsevier Tribology Series No. 28, Elsevier, Amsterdam.

Nonpetroleum-Based, No/Low-Sulphur, Ash, and Phosphorus, and Bio-No-Toxicity Engine Oil Development and Testing

Mathias Woydt¹

18.1 INTRODUCTION

More and more, engine oils must minimize or avoid their effect on the durability of particulate filters and catalysts, and in the future, on terrestrial and aquatic environments. They must also maximize their contribution to fuel economy. Replacing hydrocarbon-based oils with environmentally friendly products is one of the ways to reduce the adverse effects on the ecosystem caused by the use of lubricants. By analyzing recent technological evolutions and future trends in engine oil specifications, with the associated consequences for the functional properties performed by base oils and individual additives, the need and potential application of alternative base oils with intrinsic properties will be displayed. The focus of this chapter is on alternative base oils.

The “competition” between hydrocarbons and alternative base oils is not yet technologically decided in favor of hydrocarbons, esters, or polyglycols. In the past, the beneficial contribution of the additive technology and progress in hydrocarbon base oil technology could be demonstrated by an increasing ability to support thermal and oxidative loads of hydrocarbon-based engine oils. From the end of the 1960s until now, the specific loading has increased from approximately 35,000 to more than 480,000 kW/km/L² (kW power/km drain/litre of displacement), which will further increase by heavily supercharged diesel passenger car engines reaching 85 kW/L and upward in the near future (downsized engines).

18.1.1 General Context

The drain intervals in passenger cars have increased in the last 35 years from approximately 3000–5000 km up to 50,000 km. The associated reduction in oil consumption and drained oil volume was compensated for by much higher prices for the formulations and a steady-state increase of the total vehicle fleet, stabilizing today at approximately 65 % of the population in G7 countries. A drain interval of 50,000 km already can be interpreted as “lifetime” fill because for many passenger car customers it means 5 years and more, but the original equipment manufacturers’ (OEMs) wording today is 50,000 km or 2 years. It is also important to know if manual or automatic top-ups are foreseen are not for the chemical and technical evaluation of the figure of 50,000 km. The effect of fuel and biofuel dilution must also be considered.

Leasing offers that include all maintenance represent a trend today. Therefore, the OEM will tend to minimize

costs related to this incentive by increasing the drain/maintenance intervals.

A drain interval of 50,000 km and higher per se for passenger cars does not define a technical limit, even with respect to “bio-no-tox” criteria, as was demonstrated by the Renault “Ellypse” demonstrator [1,2] seeking a drain interval between 70,000 and 100,000 km.

OEMs are more and more interested in passenger car motor oils (PCMOs) with reduced metal-organic additives, thus contributing to the vision of an environmentally friendly and sustainable car. This is necessary to reduce the ash buildup in the aftertreatment system caused by engine oils and therefore improve its filter efficiency and lifetime. High fuel efficiency retention and long drain intervals are also expected from the engine oils. Easy removal of bio-no-tox fluids and recycling support a sustainable development.

As displayed by the Renault Ellypse demonstrator and the Ford Model U, additional requirements may be demanded in the future, including biodegradability, non-toxicity, and renewable content.

The criteria for receiving the environmental label “Euro-marguerite” require hydraulic fluids to have a content of more than 50 % renewables. A smaller figure of 10 % was proposed for crankcase oils (engine oils) [3] by the U.S. Department of Agriculture (USDA). High fuel efficiency retention, preferably over the drain interval, and long drain intervals (reduced waste volume) also have an environmental impact.

One of the questions for OEMs is as follows: Are the hydrocarbon technologies (base oil + additive packages) as well-established products still robust enough to fulfill all of these requirements, or do they need to look toward nonconventional base stocks, such as ester or polyglycol base oils? These have more intrinsic properties resulting in a lower additive treat level, or “more simple” formulations, which grant a durable application for future decades with respect to the EC directive [4] 1999/45/EC regarding the symbol “N” labeling of preparations and USDA [5] and U.S. Environmental Protection Agency (EPA) [3] policies.

Fuel economy targets will also increase the demand for low-viscosity grades, especially at low temperatures, with high viscosity indices (VIs). Direct-injecting engines favor formulations without polymeric VI improvers.

Pure hydrocarbons alone can be U.S. Food and Drug Administration (FDA)-proof. It is the additive packages, which make hydrocarbons functional, that determine

¹ Federal Institute for Materials Research and Testing (BAM), Berlin, Germany

the eco-tox, bio-no-tox, or ash formation properties of hydrocarbon-based formulations. Therefore, it is obvious to substitute toxicologically critical additives with others or new functional concepts, such as

- Extreme pressure (EP)/antiwear (AW) properties by triboactive materials and coatings,
- Viscosity improvers by the high VI of base oils, such as esters and polyglycols, and
- Polar base oil molecules.

One of the key questions is as follows: What will the 2012+ engine oil look like?

If the alternative engine oils currently represent one direction, what will the engine oil specification for them look like, because the existing items and the individual values are based on long experience defined by the chemical profile of hydrocarbons and the related additive packages?

18.1.2 Engine Oil Specification

The recent new engine oil specifications of Renault SAS (RN 0720), Daimler Chrysler AG (DC 229.31), Ford WSS-M2C934-A, and Volkswagen AG (VW 504.00) display an interest in PCMOs with reduced metal-organic additives targeting mid-SAP (sulfur, ash, and phosphorus) or low-SAP (RN 0720) demands or both. The European oil sequence ACEA-C1-04 limits sulfated ash to 0.5 wt % (low SAP) and ACEA-C2-04/C3-07 to less than 0.8 wt % (mid SAP).

This is necessary to reduce the ash buildup in the particulate filter, which affects the fuel economy retention through an increase of the exhaust backpressure, to improve its catalytic system efficiency, and to guarantee lifetime. The ash built-up in the aftertreatment devices increases the exhaust backpressure, leading to a worse effect or penalty on fuel economy [6].

Phosphorus and sulfur are partly related to the AW and EP properties of a hydrocarbon-based formulation, but also

to the endurance and efficiency of exhaust aftertreatment devices. Figure 18.1 compiles the SAP factors with their evolution, potential associated strategies, and other factors and trends. Figure 18.1 also presents the whole variety or spectrum of trends, needs, or wishes of OEMs for future engine oils.

The introduction of a “chemical box” will restrict the chemical freedom of engine oil formulations. The chemical box for passenger cars limits phosphorus (ca. <800 ppm [P]), sulfur (<0.3 [%] [S]), ash (<0.5–1.0 wt %), and the NOACK volatility (<10 % or <13 %) as general criteria. In addition, the fragmentation of standardized oil specifications among Europe, Asia, and the United States persists, and the diversification in OEM specifications is spreading more and more because engine designs requiring specific oil formulations or using specific combustion processes, such as nonconventional combustion modes (e.g., Toyota’s Low-Temperature Combustion, Homogeneous Charge Compression Ignition [HCCI], or “Combined Combustion System” [CCS], and Volkswagen AG; Diesotto [Daimler AG], etc.) have been released. In general, all specifications are being and will be replaced by new ones on shorter notice, thus spiralling the development costs.

By 2012, carbon dioxide (CO₂) emission fines will increase in Europe from 20 €/g of CO₂ above the limits to 95 €/g of CO₂ in 2015. These figures draw a clear economical frame for engine oils contributing to fuel economy. In consequence, the engine oil concepts need to be more robust to buffer future developments well, and meaningful tribological test procedures outside of engines to cut engine bench test costs are needed.

The hydrocarbon-based engine oil formulators have recently reduced the ash content to 0.7–0.8 wt % (mid SAP), some with the help of an ester content. Prototype engine oils blended with 30–60 wt % esters having 0.5 wt % (low SAP) are under evaluation.

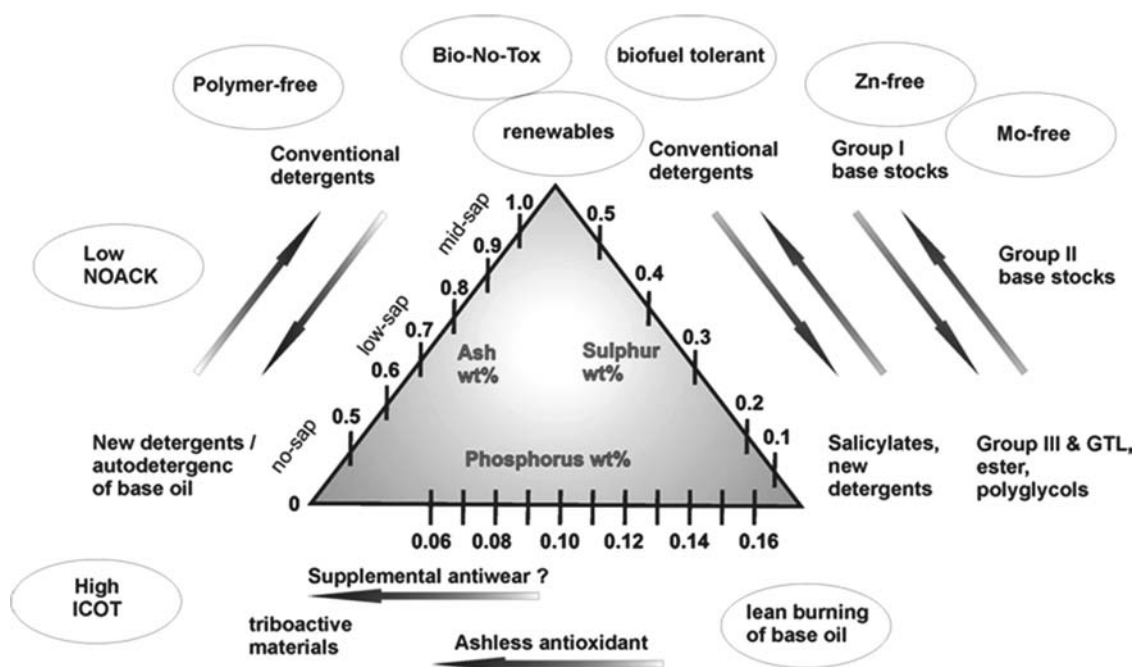


Figure 18.1—What will engine oil look like in 2015 or 2018?

18.1.3 Viscosimetrics

The engine oil specifications of standardization bodies and OEMs refer to kinematic viscosities at 40–100°C in square millimetres per second and the high-temperature, high shear (HTHS) viscosity in millipascal seconds determined at a shear rate of 10^6 s^{-1} at 150°C (see ASTM D4683 and D4741).

The kinematic viscosity and the HTHS viscosity are seen by OEMs as key properties for safe and durable operation, especially for the crankshaft bearings, because two main tasks for engine lubricants are energy saving (friction) and wear prevention. The dependency of the hydrodynamic design on specific values of the kinematic and HTHS viscosities may be true if only polymer-containing hydrocarbon-based formulations were considered.

The pressure-viscosity coefficient has until now not been mentioned in engine oil specifications, but it has a strong influence on the film thickness (see Section 3.1.1) and in consequence on the frictional losses associated with film shearing. It was recently shown that the fuel efficiency [7–9] of an engine is correlated with the pressure-viscosity coefficient of the hydrocarbon-based formulations. Further correlations exist with viscosity and with the coefficient of friction under mixed/boundary lubrication. Another aspect represents the influence of shear rate on the viscosity or the stability of the viscosity as function of shear rates above 10^6 s^{-1} (see Section 3.1.2). Here, polymer-free formulations mainly present no shear losses. To compare different base oil chemistries (e.g., hydrocarbons, esters, and polyglycols), the pressure-viscosity coefficients and the dependency of viscosity on temperature up to 150°C must be considered (Table 18.1).

18.2 EXPERIMENTS

18.2.1 Tribotesting Outside of Engines

The tribological performance of “bio-no-tox and low-ash” oils interacting with the materials of the piston ring/cylinder liner was characterized in several application-oriented simulation tests outside of engines on the basis of the BAM [10] and the SRV[®] test [11].

Piston ring/cylinder liner simulation tests were performed under mixed/boundary lubrication conditions with different lubricants at 170°C and 0.3 m/s of continuous sliding, in which a thermal-sprayed piston ring segment was pressed with 50 N against a cylinder liner segment (or flat disk) up to a sliding distance of 24,000 m. An oil amount of 0.3–0.5 L was used for each test. The test rig and the piston ring/cylinder liner configuration are shown in reference 10 using liner segments.

SRV tests were additionally performed according to a new ASTM Dyyyy-xx draft method [11] under development as cross-check (under evaluation). The SRV sample configuration with piston ring segments and the wear scars used here are shown in reference 11. The BAM and SRV tests characterize the friction and wear behavior in the top dead center region.

The resistance against seizure of an iron-based steel alloy (100Cr6H = AISI 52100) was determined for different lubricants with the SRV test rig according to ASTM

D5706-05 [12] under conditions of mixed lubrication and quoted as Hertzian contact pressure (last okay pressure before failure). As a measure for the resistance against seizure, the critical Hertzian contact pressure is compiled in Figures 18.8 and 18.9.

18.2.2 Testing Oxidative Stability Outside of Engines

Oxidation resistance is one of the limiting factors for long drain intervals and the factor for high-temperature lubrication [13]. The French ICOT test [14] (ICOT = iron-catalyzed oxidation test) using 40-ppm iron acetylacetonate ($\text{C}_{15}\text{H}_{25}\text{FeO}_6$) as a diluted catalyst defines the oxidation resistance at 170°C under an aeration of 10 L/h by three properties:

1. The viscosity increase (e.g., max. $\Delta\eta < 100 \%$),
2. The increase of an individual total acid number (TAN; e.g., max. $< 7.5 \text{ mg KOH/g}$), and
3. The percentage evaporation loss at $\Delta\eta = 100 \%$ because of oxidation (e.g., maximum 10 %).

These set values can differ among OEMs. The ICOT test indicates only the oxidative resistance and gives no hint about the AW/EP retention of a formulation. The test setup is similar to DIN 51352 or comparable to IP48. For actual factory-fill oils, one ICOT test hour corresponds to approximately 270–330 km of driving. Comparing the experiences from the field with the test results achieved with the ICOT test using hydrocarbon-based formulations [15], ACEA A3/B3 high-performance grades display an induction time between 72 and 96 h and have a target oil drain interval of approximately 30,000 km (ACEA A5/B5 $> 96 \text{ h}$). This relation must be established for esters and polyglycols.

18.2.3 Substitution of EP/AW Additives by Triboactive Materials

Wear protection represents another concern when using mid- or low-SAP oils as well as oils with or without low contents of EP and AW additives associated with bio-no-tox properties according to directive EC/1999/45. The EP/AW functions of additives, even the proven molybdenum-based piston ring coatings, may be substituted by means of triboactive or triboreactive materials/coatings.

Lubricious oxides (LOs) and triboactive materials appeared recently in scientific literature [16] and display estimated functional properties by different approaches. No official consensus about their meaning exists within the scientific community.

The term “lubricious oxides” was created in 1989 by Michael N. Gardos [17,18] for TiO_{2-x} as well as thematized by reference 19. LOs aimed for low wear that may also be associated with low dry coefficients of friction. The correct term for TiO_{2-x} is “Magnéli phases of titania,” $\text{Ti}_n\text{O}_{2n-1}$ with $4 \leq n \leq 9$, whereas TiO_{2-x} with $x \leq 0.01$ describes “Wadsley” defects.

The term “triboactive materials” appeared in Europe in the late 1990s and described a more beneficial reaction between the surface and the lubricant or the ambient environment, thus indicating a more overall functional approach. Oxides, hydroxides, or hydrates cover this understanding.

Novel and noncommercial triboactive or triboreactive materials were selected from Magnéli-type phases (e.g., $\text{TiO}_{1.93}$, $\text{Ti}_n\text{O}_{2n-1}$, and $\text{Ti}_{n-2}\text{Cr}_2\text{O}_{2n-1}$); substrates such as (Ti,Mo)(C,N)+23NiMo-binder, which forms by tribo-oxidation on

¹ SRV, n – Schwingung, Reibung, Verschleiß (German); oscillating, friction, wear (English translation). Optimol Instruments GmbH, Westendstr. 125, D-80339 Munich, Germany. See ASTM D5706, D5707, D6425, D7217, and D7421.

the surfaces, $\gamma\text{-Ti}_3\text{O}_5$, Ti_5O_9 , Ti_9O_{17} , and $\text{Mo}_{0.975}\text{Ti}_{0.025}\text{O}_2$; and double oxides such as NiTiO_3 and $\beta\text{-NiMoO}_4$. For more details about the triboactive materials $\text{TiO}_{1.93}$, $\text{Ti}_n\text{O}_{2n-1}$, $\text{Ti}_{n-2}\text{Cr}_2\text{O}_{2n-1}$, and $(\text{Ti},\text{Mo})(\text{C},\text{N})+23\text{-}30\text{NiMo}$ -binder deposited by thermal spraying on piston rings and liner samples, please refer to references 20–22.

18.2.4 Alternative Fluids

Despite the potential future evolution of hydrocarbons by synthesizing novel molecules to combine low volatility with low-temperature fluidity and increased VIs, esters and polyglycols were identified as alternative base oils and blended into environmentally friendly prototype engine oils meeting all or most of the following properties:

- Low viscosity at 40°C and NOACK volatility,
- Low contributions to exhaust emissions (lean burning),
- High oxidative stability in the ICOT test,
- High biodegradability (>60 % in OECD 301x),
- Low toxicity (bio-no-tox),
- Low ash or ash-free,
- Zn- and Mo-free, and
- Polymer-free.

Synthetic esters are characterized by their polar structure, often low friction, high wear resistance, and good viscosity-temperature behavior (high VI). Their miscibility with most hydrocarbon-based oils and most esters can be classified as environmentally friendly and biodegradable (bio-no-tox) and can be synthesized based on renewable resources.

In addition to synthetic hydrocarbon lubricants, another promising class includes polyglycol-based lubricants, which present an “oxygen” polarity in every monomer, and some have high biodegradability and low aquatic toxicities. The criticism of “thermolysis” [23] and the bad ecotoxicity [24] of polyglycols could recently not be confirmed using new polyglycol base stocks optimized for engine operation [22] and a new additive chemistry. The U.S. Air Force first lubricated their piston engines with polyglycols in World War II [25].

Three factory-fill hydrocarbon-based engine oils considered modern high-performance formulations—Fuchs Titan SL PCX (0W-30), Castrol SLX 0W-30, and Total HC (5W-30) factory-fill (FF) oil—served as reference oils with a HTHS viscosity of approximately 3.0 mPa·s (target for

TABLE 18.1—Viscosimetric and Ecotoxicological Properties of Engine Oils and Alternative, Prototype Formulations (*CEC)

Formulations	$\eta_{40^\circ\text{C}}$ (mm ² /s)	$\eta_{100^\circ\text{C}}$ (mm ² /s)	VI	PP (°C)	HTHS Viscosity (mPa·s)	NOACK (%)	Algae (mg/L)	Daphnie (mg/L)	Fish (mg/L)	OECD 301x (%)
HC FF SAE 5W-30	55.15	9.57	159	−42	3.0	12.8				
Titan PCX SyperSyn	53.19	9.44	162	−45	2.95	9				
Castrol SLX 0W-30	57	10.2	168	−57	3.0	8.1				
Ester formulations										
Total HTX 822	111	17.4	184	−36	5.3	5				>60 ^a
Greentec LS 5W30	59.3	11.5	187	−39	4.0	5.5				68
BP Vistra 7000	86.9	14.0	167	−45	4.1	10.7	>50	>100	>1000	~80 ^a
Fuchs 100E HDDO	62.8	11.3	173	−42	3.5	6.0	>100	>1000		>60
Total 100E	40.93	7.6	225	<−42	2.93	4.8	1.780		10,000	62
Fuchs 100E	43.26	8.23	144	−39	2.95	5.5	>100	256		45–55
Total HCE	46.32	8.41	159	<−42	2.95		>120	>1000	>1000	62
Titan GT1	46.5	8.9	160	−45	2.95	6	>1000	>1000	>1,000	61
Total HCE mid-SAP	57.8	10.4	176	<−48	2.99	6.6	>100	>1000		~28
Fuchs HCE low-SAP	44	8.8	184	−45	2.9	6	>1000	>100		78–87
Polyalkylene glycols										
PPG 32-2+2,6Phopani	34.5	6.7	156	−45	2.78	4.8	>100	600		70,5
PPG B46	48,25	9,03	172	−39	3.59	3.9	>100	>100		61
PAG B32-3 b.o.	35.1	7.8	210	−51	3.6	16.0	>100		>100	>60
PAG 46-2	47.4	9.94	203	−31	4.3	19.2	>100	688		64
PAG 46-4+2,6Phopani	49.6	8.44	146	−33	3.6	6.2	>100	301		80
PAG D21	68.5	11.5	160	−32	4.81	2.5	>100	>100		68

^aSet limit for biodegradation according to OECD is ≥60 %, set limits for the aquatic toxicities are ≥100 mg/L. HCE = hydrocarbon-ester blends, 100E = 100 % ester b.o. b.o. = base oil.

the prototype oils) for tribological properties under mixed/boundary lubrication and for viscosimetrics.

Castrol Greentec LS 5W-30 and Total HTX 822 15W-50 represented the fully formulated 100 % ester-based engine oils developed in the mid 1990s, and BP Vistra 7000 5W-40 was a blend of hydrocarbons with esters also commercialized in the mid-1990s, as can be concluded from the HTHS viscosities. They may be considered as fully formulated and biodegradable engine oils of the first generation.

The commercially available Fuchs Titan GT1 0W-20 with a portion of 50 % ester is listed on the positive list of the German Market Introduction Programme (MIP) for “Biolubricants and Biofuels,” funded by the Ministry of Consumer Protection, Food and Agriculture (BMVEL). The ester-based formulation of HCE low-SAP of Fuchs conforms with the requirement of more than 50 % renewables and with the toxicity criteria of the European directive EC/1999/45 (symbol “N” criteria). Also, fully ester-based prototype Fuchs Titan 100E SAE 0W-20 and Total 100E were blended also as Fuchs 100E HDDO formulation. Comparison of the different data of the biodegradation of the ester formulations shows that the types of ester base oils must be carefully selected to meet the biodegradability target.

The polyalkylene glycols PAG 46-2 and PAG 46-4, in which the base oils are basically formulated at BAM according to the philosophy stated in U.S. 6,194,359 (Daimler AG) and FR 2 792 326 (Renault SAS), are free of polymers, zinc, and calcium and need no labeling with the symbol “N” (UBA-number 5369, PAGs as EO-PO polymers). PAG46-2 presents a VI above 200 without using polymeric VI improvers. The high NOACK volatilities represent a disadvantage of the PAG46-2 base oil formulations, but they can be tailored below 13 %. The formulations PPG32-2, PPG B46, and PAG 46-4 presented NOACK volatilities below 6.2 %.

The recent example of the base oil PAG B32-2 shown in Table 18.1 demonstrates that even with using ethylene oxide in the molecular backbone of the base oil, low pour points associated with VIs above 200 are realizable.

Additionally, the oxidation resistance of the PAG 46-4 and of PPG 32-2 was boosted at BAM by proprietary additive packages “Phopani” and “Phepani,” which addressed the chemical solution to the specific oxidation reaction steps in polyglycols. The polymer-free polyalkyleneglycols (PAGs) cover a wide range of VI exceeding 200 (see also PAG B32-3 b.o.) whereas the polymer-free polypropyleneglycols (PPG 32-2) exhibit as “30” viscosity at 40°C associated with a NOACK below 5 %. For example, the polymer-free PPG 32-2 contained 1700 ppm sulfur and 200 ppm of organic phosphorus with respect to bio-no-tox criteria. Polypropyleneglycol monobutylethers (PPGs) are classified in WGK 1 as “slightly hazardous” to water (WGK = Wassergefährungsklasse = Water Hazard Classes) by the German Environmental Agency (UBA, www.umweltbundesamt.de) under the number 3530.

All polyglycols used here are ash-free. The PAG D21 and PAG D46 base oils had a content of ethylene oxide much above 50 mol %. The amount of phosphorus and sulfur is reduced to approximately 780 ppm [P] and 650 ppm [S] for the PAG46-3/PAG46-2 and for the PAG46-4 to approximately 650 ppm [P] and 800 ppm [S]. The PAG46-4 and

PPG32-2 prototype formulations meet the ACEA-C1 SAP criteria. The VIs in Table 18.1 of the polyglycols are stated in *italic*, as the in a logarithmic (40°C to 150°C) plot the polyglycols not follow a linear regression.

All prototype formulations respond to the symbol “N” criteria and most to a Zn-and-Mo-free philosophy (all polyglycols as well as Fuchs GT1 and HCE low-SAP). Ester-based formulations can fail to respect to the biodegradation of more than 60 % (see Table 18.1). Most recent ester-based formulations have a 40 viscosity [mm²/s] at 40°C associated with a NOACK evaporation loss below 7 % and a VI greater than 175.

A high VI selecting a 30 viscosity [mm²/s] at 40°C (see PPG32-2 and PAG B32-2) is a fine and right approach for city driving cycles and hybrid propulsion systems if it can be realized by hydrocarbons as a polymer-free formulation to meet a HTHS viscosity of more than 2.6 or 2.9 mPa·s?

18.3 RESULTS

18.3.1 Film-Forming Behavior

18.3.1.1 OIL FILM THICKNESS

To differentiate the hydrodynamic film-forming behavior of alternative oils (hydrocarbons, esters, and polyglycols), the dynamic viscosity taking into account the differences in density and the pressure-viscosity coefficients must be used. All properties should be determined at least at 150°C. For safe and durable engine operation, the film-forming behavior of polyglycols is compared to those of ester- and hydrocarbon-based engine oils. The test methodology and data for densities, viscosities, and piezo-viscosities (pressure-viscosity coefficients) measured between 22 and 150°C are discussed in detail elsewhere [26].

The dynamic viscosity considers the range of densities presented by the alternative oils. The report of the viscosity itself to rank different engine oil chemistries cannot be considered sufficient because the exponents applied to the different parameters for the estimation of film thicknesses are not identical and are not only limited to viscosity. Three different equations from literature [27,28] are referenced to calculate the oil film thicknesses. Two of them describe a line contact ($h_{L,1}$ and $h_{L,2}$) and one a point contact (h_p). The proportionalities used are

$$h_{L,1} \propto \alpha^{0.6} \cdot \eta^{0.7} \text{ (Dowson and Higginson)}$$

$$h_{L,2} \propto \alpha^{0.54} \cdot \eta^{0.7} \text{ (Dowson and Dyson)}$$

$$h_p \propto \alpha^{0.49} \cdot \eta^{0.68} \text{ (Fromm)}$$

For all tested fluids, the relative film thicknesses have been calculated on the basis of the temperature. The value for the factory-fill oil “HC” SAE 5W-30 at 150°C was taken as a reference. Most formulations in Figures 18.2 and 18.3 have a HTHS viscosity between 2.8 and 3.0 mPa·s, with exception of PAG46-2, PAG 46-3, PAG46-4, and PPG 32-2. The different approaches for film thicknesses produce the same ranking of the formulations [29].

In Figure 18.2, the differences in film thickness seem to be minor at 150°C whereas the enlargement in Figure 18.3 reveals a reduced film thickness of up to approximately 20 % at 150°C for some polyglycols, which fits with the minimal bottom line of 12 hydrocarbon and ester-based formulations as well as blends of hydrocarbons with esters. These results are congruent because these differ in density

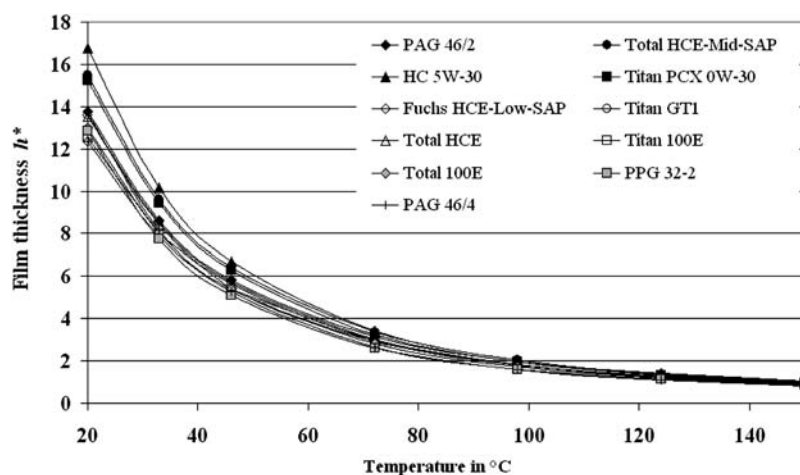


Figure 18.2—Relative film thickness h^* for a line contact over a full range of temperatures.

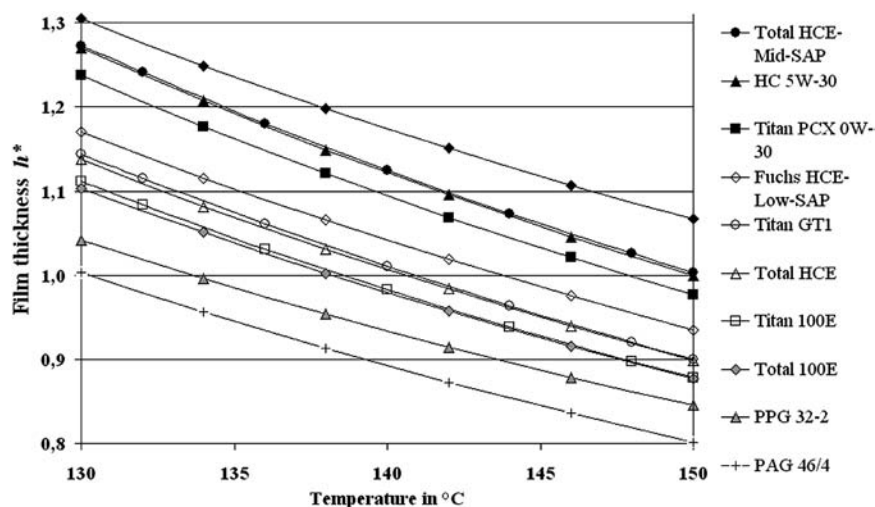


Figure 18.3—Relative film thickness h^* for a line contact for "high" temperatures (enlargement of Figure 18.2).

and pressure-viscosity coefficient. Figure 18.2 also shows that at low temperatures the film thicknesses are unnecessarily high. Thus, engine oils with reduced low-temperature viscosities associated with high intrinsic VI (e.g., >200) are desirable to improve fuel economy for city driving, short trips, and hybrid applications.

Only an increased dynamic viscosity can compensate for the lower pressure-viscosity coefficients (α) of the polyalkylene glycol PAG 46-4 (compare with PPG32-2 and PAG 46-2 in Table 18.2), a reduced oil sump temperature, or the retention of a smoother surface roughness. As for PPG 32-2 with a kinematic viscosity at 40°C of 34.5 mm²/s, the quite "high" film thickness factor is surprising, which at 150°C is only approximately 10 % lower than those of the hydrocarbon-based factory-fill oils. This must be validated in view of the lower coefficients of friction of 0.04–0.06 under mixed/boundary lubrication (see Figure 18.9 and Figure 18.10), the higher volumetric heat capacity [26,29], and the very small sensitivity of the viscosity to high shear rates. PPG32-2 meets the pressure-viscosity coefficients of hydrocarbon-based factory-fill oils at room temperature.

Table 18.2 compiles the viscosimetric properties and pressure-viscosity coefficient α determined in a falling ball viscosimeter at 1000 bars for polymer-containing hydrocar-

bons and hydrocarbon-ester engine oils as well as for polymer-free, polyglycol-based, and ester-based prototype engine oils. The data show that the lower pressure-viscosity coefficient of polyalkyleneglycol PAG must be compensated for by the higher HTHS viscosity to provide the same film thickness formation behavior of hydrocarbon-based FF engine oils. This should also apply for engine oils composed of 100 % esters, which have a pressure-viscosity coefficient equivalent to the polypropyleneglycol monobutylether PPG32-2 at 150°C.

Comparing the values in the column "HTHS Viscosity at 150°C" with those of the dynamic viscosity " ν at 150°C," it can be seen that the following qualitative relations exist:

- Polymer-blended hydrocarbons: HTHS viscosity + 9–10 % = dynamic viscosity,
- Polymer-free polyglycols, hydrocarbon/ester and ester blends: HTHS viscosity + <3 % = dynamic viscosity, and
- Polymer-blended hydrocarbon/ester blends: HTHS viscosity + 12–16 % = dynamic viscosity.

These are much smaller than comparing the kinematic viscosity $\eta_{150^\circ\text{C}}$ with the HTHS viscosity at 150°C, except here also for polymer-free blends.

Table 18.2 shows that HTHS viscosity is not necessary for describing the viscosimetric behavior of polymer-free alternative engine oils, and the dynamic viscosity at 150°C

TABLE 18.2—Viscosimetric Properties of Different Factory-Fill and Prototype Engine Oils

Lubricants	VI	η_{40} (mm ² /s)	η_{100} (mm ² /s)	η_{150} (mm ² /s)	HTHS Viscosity 150°C (mPa·s)	ν_{150} (mPa·s)	α_p^{1000} 22°C (GPa ⁻¹)	α_p^{1000} 150°C (GPa ⁻¹)
HC 5W-30 FF	159	55.15	9.57	4.197	3.0	3.22	19.8	119
Fuchs Titan SL PCX	162	53.19	9.44	4.14	2.95	3.23	18.3	11.8
Castrol SLX 0W-30	168	57.0	10.2	4.42	3.0	3.34	18.2	11.86
Ester formulations								
100E HDDO	150	56.2	9.4	4.03	3.0	3.34	16.6 ^a	11.3
Total 100E	156	40.93	7.60	3.46	2.93	2.94	16.9	10.63
Titan 100E	166	45.0	8.40	3.64	2.95	2.91	16.9	10.8
Total HCE	159	46.32	8.41	3.73	2.95	2.98	17.3	11.1
Titan GT1	164	47.03	8.90	3.78	2.95	2.90	17.6	11.1
Fuchs HCE low-SAP	184	44.0	8.8	4.26	2.9	3.3	16.8	11.0
Fuchs HCE low-SAP2	193	42.5	8.8	4.12	2.9	3.26	18.2	11.1
Total HCE mid-SAP	170	57.8	10.4	4.53	2.99	3.53	17.96	11.6
Polyglycol formulations								
PPG 32-2	156	34.3	6.7	3.2	2.78	2.87	19.2	10.56
PAG 46-2	203	47.4	9.94	4.81	4.3	4.44	14.6	8.8
PAG 46-4	146	49.6	8.44	3.7	3.6	3.61	11.76	7.32

^aAt 40°C; 100E = 100 % ester base oils, HCE = blend of hydrocarbons with esters.

appears sufficient for the film thickness in combination with the pressure-viscosity coefficient. The determination of viscosities at shear rates much above 10^6 s^{-1} with low film heating during testing is desired for the future because much higher values occur in the crank shaft/shell and piston ring/cylinder liner tribosystems. The loss in viscosity by high shear rates will be lowest or quasi-nonexistent for polymer-free formulations.

18.3.1.2 SHEAR THINNING

The instruments described in ASTM D4624, D4741, and D4683 allow viscosity measurements at shear rates up to $1 \times 10^6 \text{ s}^{-1}$. This shear rate figures in engine oil specifications. A much higher shear rate will cover the situation in the tribosystems of engines. The determination of HTHS viscosity under a shear rate of 10^6 s^{-1} using a capillary viscosimeter is standardized in ASTM D4624 for capillaries made of glass or stainless steel. The experience shows that the rotational method (ASTM D4741 and D4683) has better repeatability and reproducibility compared with the capillary method. However, it is by far easier to extend the measuring range to high shear rates using the capillary method.

PTB (www.ptb.de) has modified a high-shear viscometer HVA 6, manufactured by Anton Paar (www.anton-paar.com), to reach a shear rate of $3.5 \times 10^6 \text{ s}^{-1}$; this is described in detail in reference 30. The heating of the oil passing through the PTB capillary viscometer under very high shear rates is limited to 2–3 K.

The maximum Reynolds value ($Re = 1256$) occurred in the measurement series on 100 E 0W-20. This is in accordance with reference 31 or ASTM D4624, where a Reynolds value less than 2000 is stated.

The polyalkylene glycol PAG 46-4 shows an almost perfect Newtonian behavior with no indications for shear thinning. The polymer-free Fuchs HCE 0W-20 and 100E 0W-20 are quite similar. The shear thinning of the polymer-containing Fuchs HCE-low-SAP and Titan SL PCX 0W-30 is visible. All four liquids show a very weak pseudo-plastic behavior. In rheology, Figure 18.4 is normally shown with a double logarithmic axis. As a result, five nearly horizontal curves are obtained.

Especially regarding low-viscosity oils, one conclusion is that the ranking by HTHS viscosity depends on their shear rate. At shear rates above 10^6 s^{-1} , the HTHS viscosity values of polymer-containing formulations will drop to the values or fall below those of the polymer-free formulations with an initially lower HTHS viscosity value. No drop of the viscosity under high shear conditions can compensate for a lower pressure-viscosity coefficient or lower HTHS viscosity values with respect to oil film thickness and the stated HTHS viscosity in a specification, which was established for hydrocarbons.

18.3.2 Oxidative Stability (ICOT Test)

The ICOT test used here was introduced in Section 18.2.2. For actual factory-fill oils, 1 ICOT test hour correspond to approximately 270–330 km of driving. This relation must be validated for esters and polyglycols. The ICOT life for a 30,000-km drain-interval PCMO that is based on hydrocarbons lies between 120 and 140 h. Thus, in comparison with Table 18.1, the oxidation resistance of alternative oils can be much improved with respect to the bio-no-tox criteria.

The custom-made base oils for the polyglycols PPG32-2 and PAG46-4 with the proprietary “boosters” for oxidation

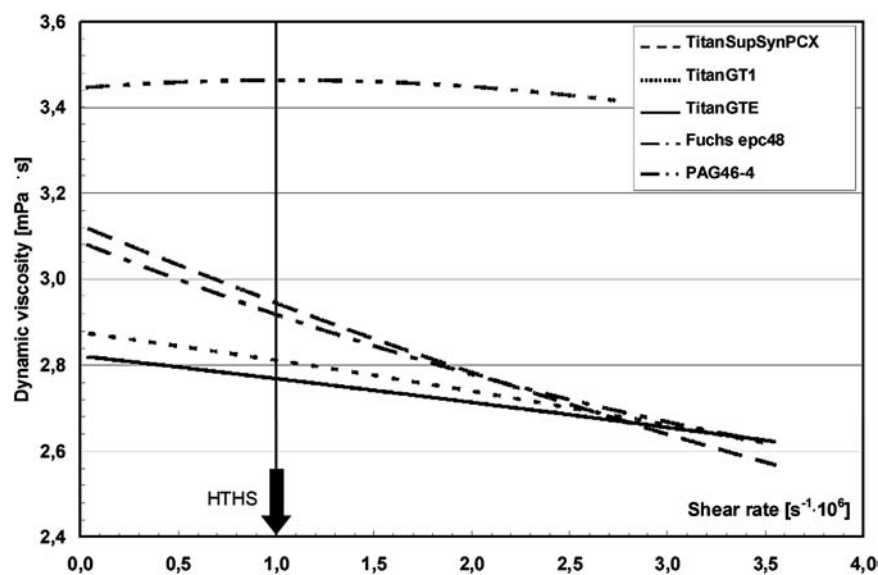


Figure 18.4—Viscosity curves depending on the shear rate for five different liquids at 150°C.

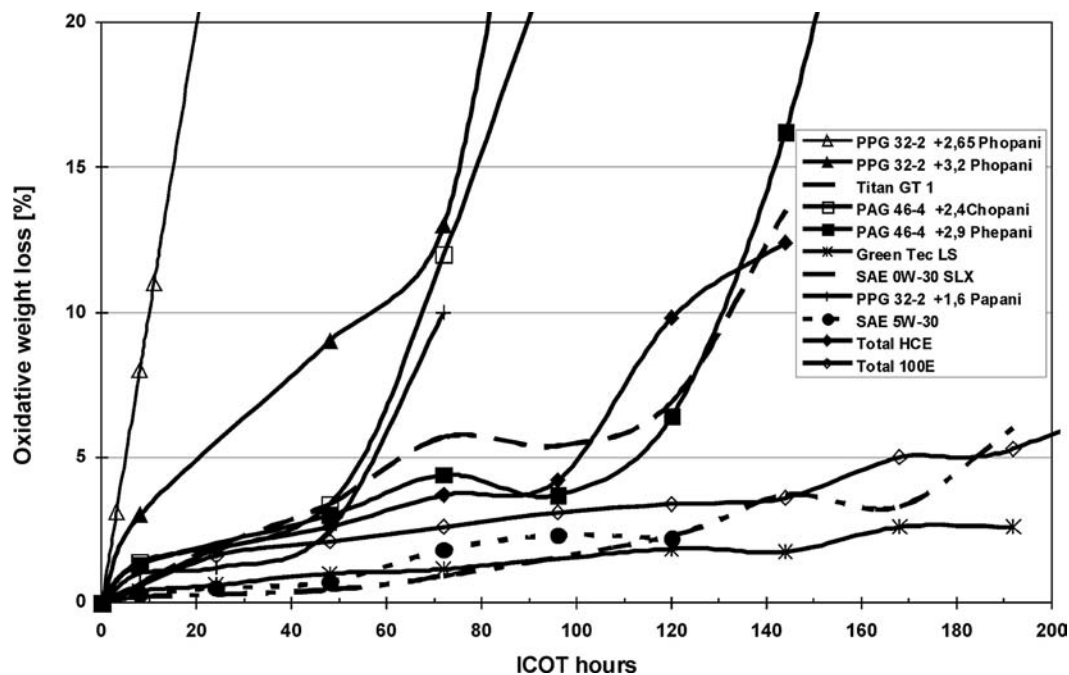


Figure 18.5—Oxidative evaporation losses of different engine oil formulations in ICOT test vw. test time ($T_{oil} = 170^{\circ}\text{C}$).

resistance have an ICOT lifetime of at least 96 h respecting the bio-no-tox criteria. Overall, “Phopani” is good for 100 h and above and “Phepani” for 130 h and above. The custom-made PAG 46-4 base oil reached the individual set limit of D+7 mg KOH/g at approximately 48 h without additives. The evolution of TAN over the test time of the PAG46-4+2,9 Phepani confirmed that until 130 h, even until 192 h, the set limit of 7.5 mg KOH/g was not passed.

The PAG 46-4+ 2,6 Phepani reached the same test time for viscosity increase as the ester-based Titan GT1 SAE 0W-20 and presented the same evolution in oxidative weight loss. In contrast, the excessive oxidative weight loss for the “Papani” package is unacceptably high; even the viscosity increase remained stable over test time (see Figure 18.5 and Figure 18.7).

The lowest oxidative weight losses until 200 h (see Figure 18.5) were determined for Greentec LS (100 % ester) and Total 100E, and even the PAO-based formulation (SAE 0W-30 SLX) reached earlier the drain interval criteria for TAN and viscosity increase. The highest stability in viscosity until 200 h was determined for Total 100E (see Figure 18.7).

18.3.3 EP Behavior in SRV Test

The resistance against seizure of an iron-based steel alloy (ball bearing 100Cr6H = AISI 52100) was determined for different lubricants with an SRV test rig according to ASTM D5706-05 under the conditions of mixed/boundary lubrication and quoted as Hertzian contact pressure (last okay pressure before failure [see Figure 18.8] with the pass

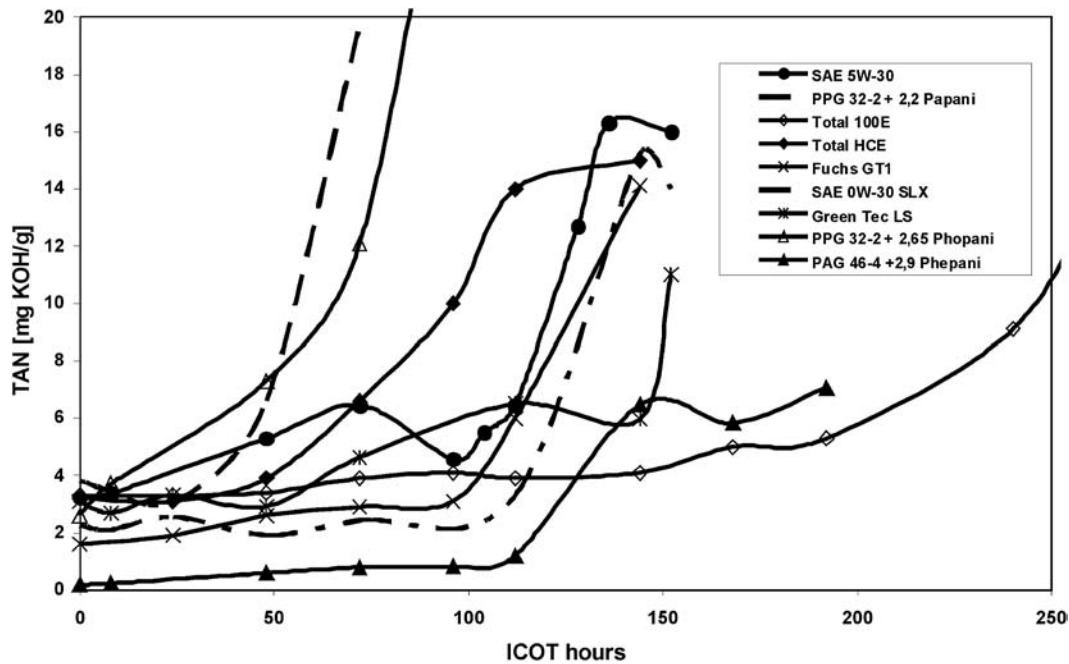


Figure 18.6—Evolution of TAN vs. ICOT test time of engine oil formulations ($T_{oil} = 170^{\circ}\text{C}$).

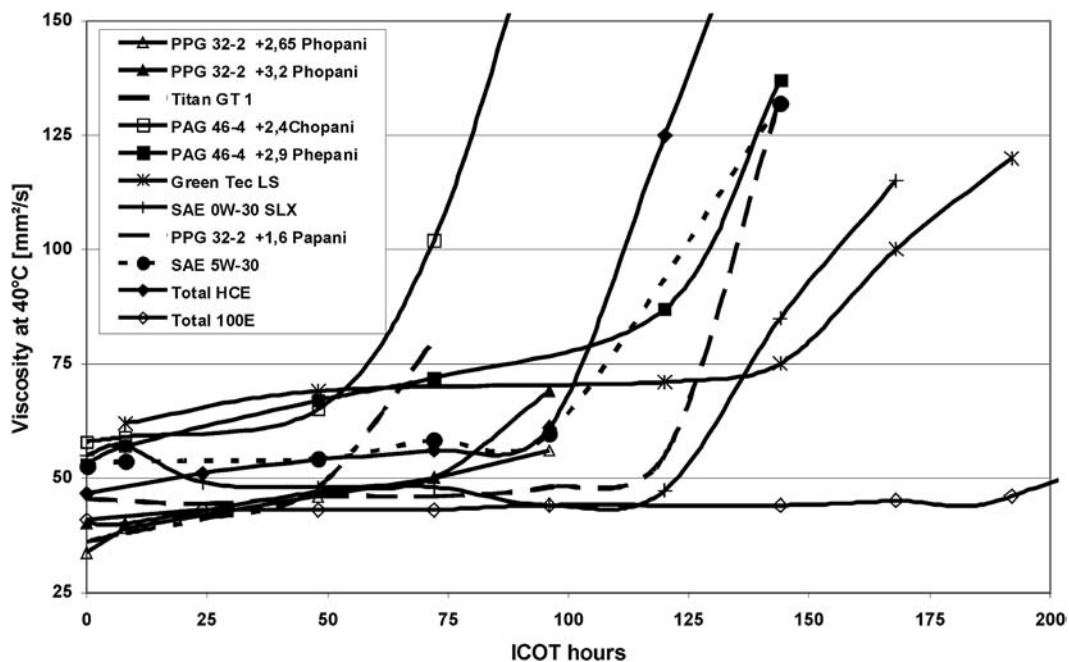


Figure 18.7—Viscosity increase vs. oxidation test time ($T_{oil} = 170^{\circ}\text{C}$).

load). At 135°C , the factory-fill oils ranged from 3000 to 3500 MPa.

The unadditivated polyglycols PAG46-4 and PPG32-2 achieved the highest values of approximately 3700 MPa, which were lowered by antioxidants, and they were on the same level as the ester-based formulations Fuchs 100E and Total HCE.

The formulations using polyglycols with a low content of EP additives or free of “classic” EP additives displayed no disadvantages exceeding the maximum design limit of today of 2000 MPa. This was confirmed by the SRV test using a different test condition (higher stroke of 3 mm

and 200°C) with coated piston rings sliding under linear oscillation against a globular cast iron liner specimen (see Figure 18.9). The unadditivated PAG46-4 base oil, HCE low-SAP, presented the highest EP pressures at 135 and 200°C .

18.3.4 Friction and Wear Behavior in BAM Test

Figures 18.10 and 18.11 summarize in a plot the coefficient of friction under mixed and boundary lubrication versus the wear rate of different triboactive and state-of-the-art ring and liner coatings in five oils using the BAM test procedure described in reference 10. The two polyglycols without a friction modifier and the Fuchs PCX containing

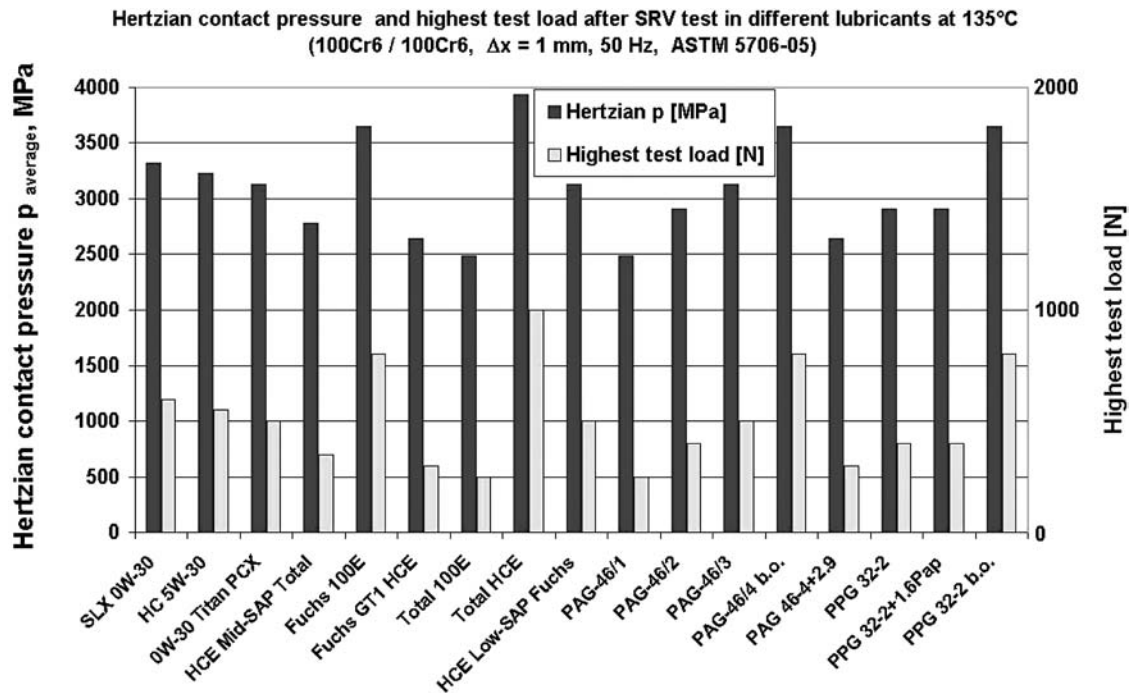


Figure 18.8—Resistance against seizure for different lubricants according to ASTM D5706-05 using 100Cr6H/100Cr6H (AISI 52100) at 135°C.

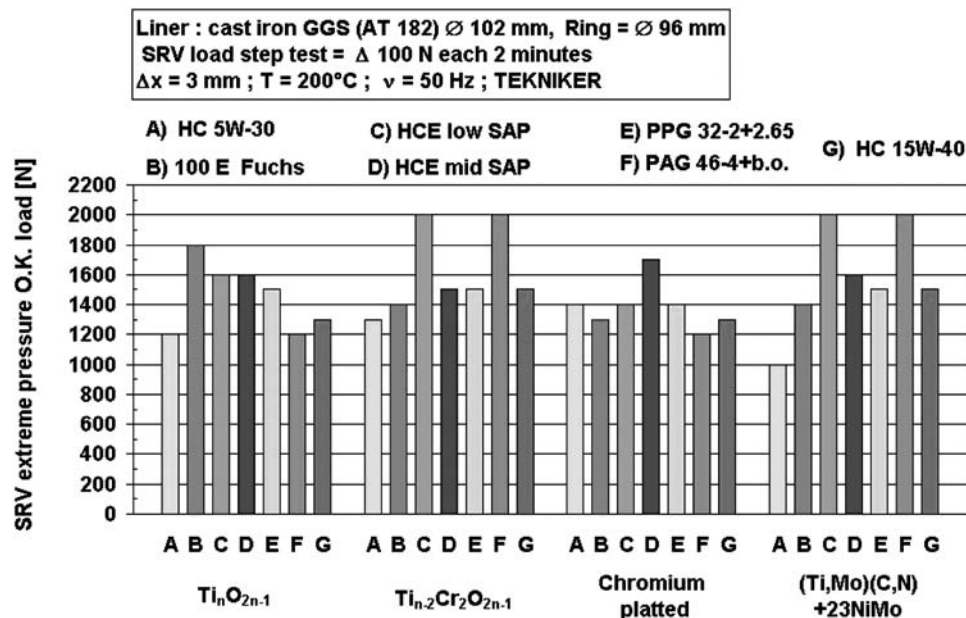


Figure 18.9—SRV EP step-load test using samples prepared from engines. Note: The HC 15W-40 is an industrial engine oil with 11,630 ppm and a HTHS viscosity of 4.2 mPa·s.

an organic friction modifier displayed as a trend the lowest coefficients of friction.

The PPG32-2, PAG46-4, and the PCX offer, when lubricating the appropriate materials, a potential for zero liner wear, although they are polymer-, zinc- and molybdenum-free and meet bio-no-tox criteria (except bio-no-tox for PCX). More individual details about the friction and wear behavior of alternative oils lubricating triboactive and state-of-the-art materials/coatings can be found in references 20–24.

Figures 18.9 and 18.10 show that the response to friction and wear rate depends not only on the oil formulations

but also on the interaction with the surface of the material couple.

18.3.5 Internal Friction of Engines

One aspect of the EC-funded project “EREBIO” was the validation of the reduction of engine friction by means of alternative lubricants. The measurements of the friction were performed using an entrained turbo-diesel engine of Renault SAS (1.9 L, R4, 2 V, 89 kW, F9Q 764, cast iron block) according to the “strip” method. The precision of this IAV test procedure is ± 0.1 Nm (IAV = Ingenieurgesellschaft

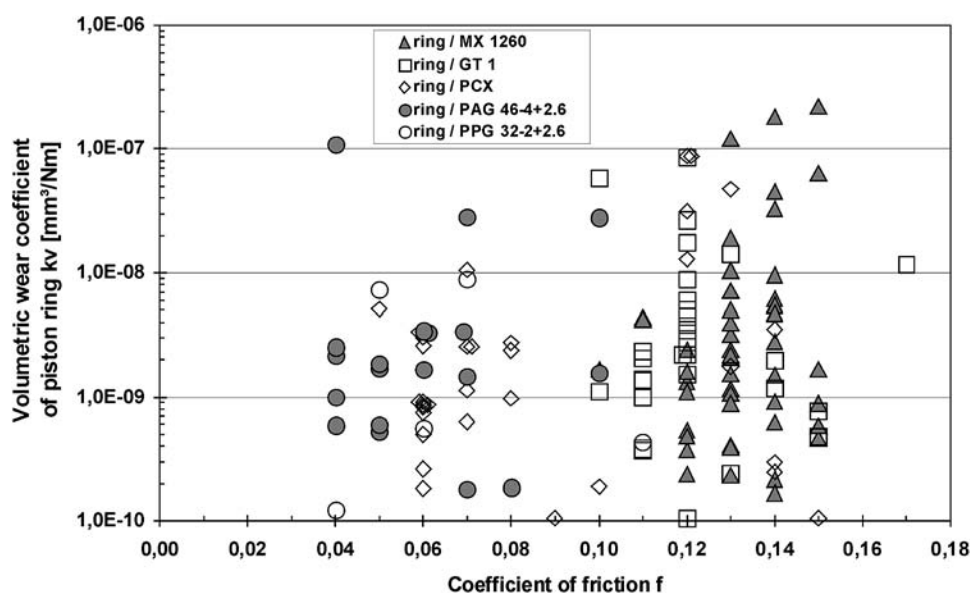


Figure 18.10—Summarizing plot of coefficient of friction at test end vs. wear rate for ring of sets of different tribocouples in PAG 46-4+2,6 Phopani, PPG32-2+2,6 Phopani, SAE 5W-30 (HC), PCX 0W-30, and GT1 using the BAM test ($F_N = 50$ N; $v = 0.3$ m/s; $T = 170^\circ\text{C}$; $s = 24$ km).

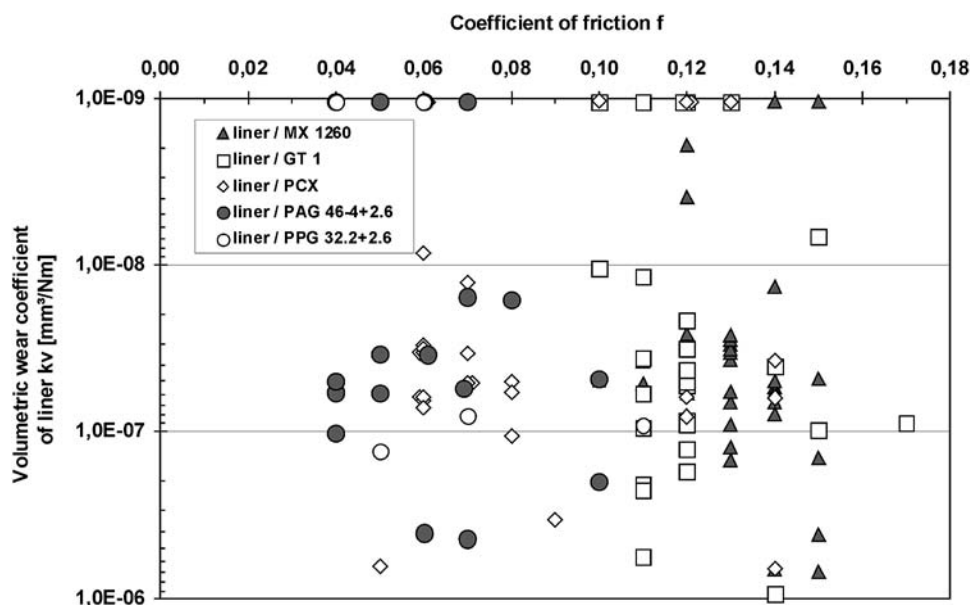


Figure 18.11—Summarizing plot of coefficient of friction at test end vs. wear rate for liner of a set of different tribocouples in PAG 46-4+2,6 Phopani, PPG32-2+2,6 Phopani, SAE 5W-30, PCX 0W-30, and GT1 using the BAM test ($F_N = 50$ N, $v = 0.3$ m/s, $T = 170^\circ\text{C}$, and $s = 24$ km).

Auto und Verkehr; <http://www.iav.de>). The results emphasized that, especially at idle speed (a frequent operating regime in city driving), considerable reduction of engine friction can be achieved with the PPG 32-2 (see Figure 18.12), thus improving the fuel economy. A similar reduction in engine friction, but less pronounced, was observed at high speed.

18.3.6 Substitution of Molybdenum and Scuffing Resistance

In view of the human toxicity and the strong increases in stock exchange prices of ferromolybdenum and molybdenum oxide (more than 10 times since 1999), the substitution of molybdenum-based ring coatings was another object of

the EC-funded project EREBIO. This was validated by Cie Tarabusi using a 100-h durability fired engine test under hot scuffing conditions (Tarabusi Specification AT M 8/33). The piston rings were coated and finished by Tarabusi with novel spray powders developed and produced in pilot plants in the frame of the EREBIO project using as a reference the molybdenum-based plasma coating PL72. The components were measured before and after the test. In Figure 18.13, the differences among measurements are presented.

The engine test data under severe operation revealed that the substitution of molybdenum-based piston ring coatings by means of different triboactive/reactive coatings is feasible. Good wear and antiscuffing properties were shown by $\text{Ti}_n\text{O}_{2n-1}$, followed by the $(\text{Ti},\text{Mo})(\text{C},\text{N})+23\text{NiMo}$

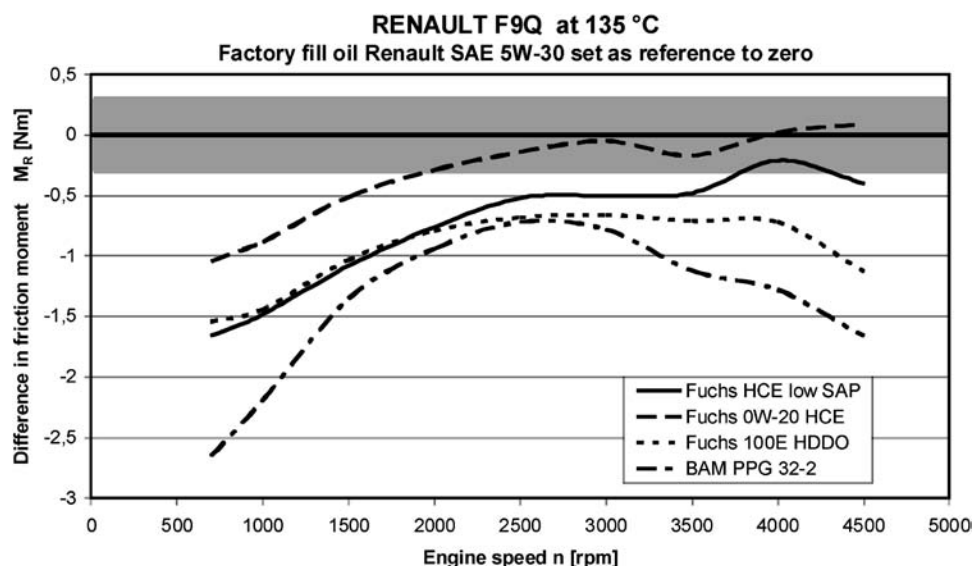


Figure 18.12—Contribution of alternative engine oils to internal engine friction. Test data from IAV GmbH, full engine [24].

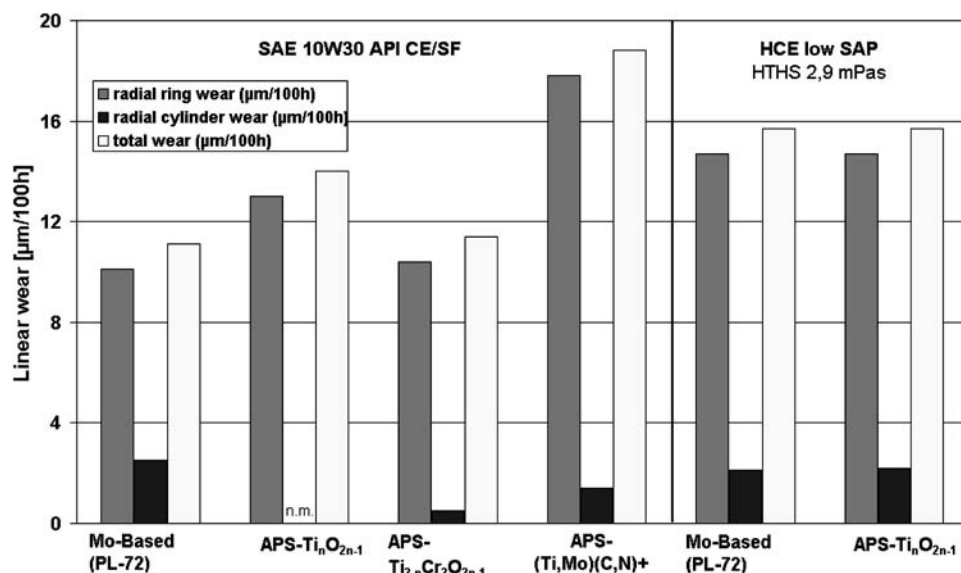


Figure 18.13—Durability testing (100 h) under scuffing conditions. Test data from Cie Tarabusi; Nissan 2.7-L, four-cylinder turbo-diesel engine (stroke = 92 mm, bore = 96 mm, rings 2 mm in height); water = 140°C; oil = 155°C, 4000 r/min; cylinder in gray cast iron AT182 (3.1–3.4 wt % carbon) [24].

coating. The wear resistance of the Ti_nO_{2n-1} coating is similar to standard molybdenum base coating for standard and HCE low-SAP oil. The best tribological properties were found for the $Ti_{2-n}Cr_2O_{2n-1}$ coating, but it spalled-off on some edges during the engine tests.

All triboactive/reactive coatings presented no tendency for adhesive wear or scuffing and offered a potential for wear reduction or simple isowear of the system. The data also underline that low-SAP formulations that are based on a blend of hydrocarbons with esters had no adverse effects regarding wear and scuffing resistance of the molybdenum-based ring or the triboactive Ti_nO_{2n-1} ring coating.

18.4 SUMMARY

Overall, the different nonhydrocarbon-based, polymer-free, bio-no-tox, and low-ash or no-ash prototype engine oils with reduced additive contents displayed isoperformance

regarding the tribological behavior against cast iron with high carbon content and the new triboreactive materials. They can shift the low-wear/high-wear transition of aluminium/silicon liner alloys to higher combustion pressures or engine speeds or both. The polymer-free, alternative prototype formulations revealed the directions, future feasibilities, and values for tentative functional improvements of engine oils in the future.

The results presented here revealed that in engine oil specifications, the dynamic viscosity at 150°C (especially measured under higher shear rates than 10^6 s^{-1}) and the pressure-viscosity-coefficients must be introduced, especially when alternative oils of different chemistries must be ranked with hydrocarbons. With these data, the oil film thickness of an individual formulation can be estimated and compared within the different base oil types, such as esters, hydrocarbons, blends of esters with hydrocarbons,

and polyglycols. To differentiate viscosimetric properties of alternative oils, the dynamic viscosity taking into account the differences in density must also be used. All viscosimetric lubricant properties should be determined at least up to 150°C.

The coefficient of friction under mixed/boundary lubrication is, as a black and white painting, more determined by the lubricants than by the materials or by an individual interaction between lubricants and a specific material or tribo pairing. In contrast, the wear resistance is more likely to be determined by the material couples and the initial surface finishing.

References

- [1] Renault SAS, 2002, *Ellypse: Direction de la Communication, Pressemappe zum Mondial de l'Automobile in Paris*. Available at <http://www.planeterenault.com> or www.renault.com > protos > Ellypse.
- [2] Renault SAS, 2002, *Dossier Zukunftssichere Entwicklung—“ELLYPSE”, Radikal Konstruiert, R&D—Wege der Innovation, Das Magazin für Forschung und Entwicklung*, Number 26, Renault SAS, Boulogne-Billancourt, France.
- [3] U.S. Environmental Protection Agency, 2000, “Oil Pollution Prevention and Responses, Non-Transportation-Related Facilities, Final Rule,” June 30, 40 CFR Part 112, pp. 40776–40817.
- [4] EC Directive 1999/45/EC, 1999, “Concerning the Approximation of the Laws, Regulations, and Administrative Provisions of the Member States Relating to the Classification, Packaging, and Labelling of Dangerous Preparations,” Off. J. Euro. Comm. L200/1.
- [5] U.S. Department of Agriculture, 2003, “Guidelines for Designated Biobased Products for Federal Procurement,” 7 CFR Part 2902, Fed. Regist., Vol. 68, No. 244, pp. 70730–70746.
- [6] Sutton, M., 2006, “Continued Investigations of Lubricants Effects on Diesel Particulate Filters,” In *Proceedings of the 17th International Colloquium on Tribology*, January 17–19, Technische Akademie Esslingen, Ostfildern, Germany.
- [7] Sorab, J., Korcek, S., McCollum, C.B., and Schriewer K.W., 1998, *Sequence VIB Engine Test for Evaluation of Fuel Efficiency of Engine Oils. Part II: Stage Selection and Time Factor Determination*, SAE Technical Paper 982624, SAE, Warrendale, PA.
- [8] Igarashi, J., 2002, “The Mineral Oil Industry in Japan.” In *Proceedings of the 13th International Colloquium on Tribology*, January 15–17, Technische Akademie Esslingen, Ostfildern, Germany, pp. 13–17.
- [9] Taylor, R.I., Dixon, R.T., Wayne, F.D., and Gunsell, S., 2004, “Lubricants and Energy Efficiency: Life-Cycle Analysis.” In *Proceedings of the 31st Leeds-Lyon Symposium on Tribology*, September 7–10.
- [10] Woydt, M., and Kelling, N., 2003, “Testing the Tribological Properties of Lubricants and Materials for the System “Piston Ring/Cylinder Liner” outside of Engines,” *Ind. Lubric. Tribology*, Vol. 55, pp. 213–222.
- [11] Woydt, M., and Ebrecht, J., 2008, “SRV-Testing of the Tribosystem Piston Ring and Cylinder Liner Outside of Engines,” *TriboTest*, Vol. 14, pp. 113–126.
- [12] ASTM D5706-05, 2006: Standard Test Method for Tribological Characterization of Piston Ring and Cylinder Liner Materials and Lubricants using SRV® Test Machine, *Annual Book of ASTM Standards*, ASTM International, West Conshohocken, PA.
- [13] Lansdown, A.R., 1993, “High Temperature Lubrication.” In *Proceedings of the 6th International Congress on Tribology*, Vol. 1, Budapest, Hungary, pp. 56–64.
- [14] GFC Lu T 02, 2004: Test D'Oxydation Catalysé par l'Acétyl Acétonate de fer (ICOT), Groupe Français de Coordination (GFC). Available at <http://gfc@gfc-tests.org>.
- [15] Fitamen, E., Tiquet, L., and Woydt, M., 2007, “Validation of Oxidative Stability of Factory Fill and Alternative Engine Oils Using the Iron Catalysed Oxidation Test,” *J. ASTM Int.*, Vol. 4.
- [16] Woydt, M., 2004, “Review on Lubricious Oxides and Their Practical Importance.” In *Handbook of Surface Modifications and Processing: Physical & Chemical Tribological Methodologies*, Totten, G.E., Ed., Marcel Dekker, New York.
- [17] Gardos, M.N., 1989, “The Effect of Anion Vacancies on the Tribological Properties of Rutile (TiO_{2-x}),” *Tribology Trans.*, Vol. 32, pp. 30–31.
- [18] Gardos, M.N., 1993, “The Effect of Magnéli Phases on the Tribological Properties of Polycrystalline Rutile.” In *Proceedings of the 6th International Congress on Tribology*, Vol. 3, pp. 201–206.
- [19] Woydt, M., Kadoori, J., Hausner, H., and Habig, K.-H., 1990, “Development of Engineering Ceramics According to Tribological Considerations (Bilingual),” *J. German Ceramic Soc.*, Vol. 67, pp. 123–130.
- [20] Woydt, M., Skopp, A., Kelling, N., Hartelt, M., and Berger, L.-M., 2007, “Thermal Sprayed TiO_{2-x}-Coatings under Mixed Lubrication and Unlubricated Sliding Conditions,” *Wear*, Vol. 262, pp. 1061–1070.
- [21] Landa, J., Illarramendi, I., Kelling, N., Woydt, M., Skopp, A., and Hartelt, M., 2007, “Potential of Thermal Sprayed TiO_{2-x} Coatings for Substituting Molybdenum Based Ring Coatings,” *Ind. Lubric. Tribology*, Vol. 59, pp. 217–229.
- [22] Desplanches, G., Criqui, B., Linnemann, T., and Woydt, M., 2006, “Tribological Performances of New Triboactive Ti_{n-2}Cr₂O_{2n-1} and (Ti,Mo)(C,N) as Piston Ring and Cylinder Liner Coatings Interacting with Bio-No-Tox Lubricants.” In *Proceedings of the 17th International Colloquium on Tribology*, January 15–17, Technische Akademie Esslingen, Ostfildern, Germany.
- [23] Kussy, S., 1985, “Chemical, Physical and Technological Properties of Polyethers As Synthetic Lubricants,” *J. Synth. Lubric.* Vol. 2, pp. 63–84.
- [24] Igartua, A., Fernández, X., Areitiaurtena, O., Luther, R., Seyfert, C.H., Rausch, O.J., Illarramendi, I., Berg, M., Schultheib, H., Duffau, B., Plouseau, S., and Woydt, M., 2009, “Biolubricants and Triboreactive Materials for Automotive Applications.” *Tribology International* 42 (2009), 561–568.
- [25] Kratzer, C., Green, D.H., and Williams, D.B., 1946, “New Synthetic Lubricants,” *SAE J. Trans.*, Vol. 54, pp. 228–238.
- [26] Schmidt, R., Klingenberg, G., and Woydt, M., 2006, “Thermophysical and Viscosimetric Properties of Environmentally Acceptable Lubricants,” *Ind. Lubric. Tribology*, Vol. 58, pp. 210–224.
- [27] Jones, D.A., 1993, “Elastohydrodynamic Lubrication Theory.” In *Engine Tribology*, C.M. Taylor, Ed., Elsevier Science, Amsterdam, The Netherlands, pp. 15–50.
- [28] Hamrock, B.J., and Dowson, D., 1981, *Ball Bearing Lubrication, The Elastohydrodynamics of Elliptical Contacts*, John Wiley & Sons, New York.
- [29] Schmidt, R., and Woydt, M., 2006, “Viskosimetrische und Thermophysikalische Eigenschaften Umweltverträglicher Motorschmierstoffe,” *Tribologie Schmierungstechnik*, Vol. 2006, pp. 16–20.
- [30] Schmidt, R., Klingenberg, G., and Woydt, M., 2006, *New Lubrication Concepts for Environmentally Friendly Machines—Tribological, Thermophysical, and Viscosimetric Properties of Lubricants Interacting with Triboactive Materials*, BAM Research Report 277, BAM, Bremerhaven, Germany.
- [31] DIN 53014 Part 2: Viscosimetry, Capillary Viscometers with Circular and Rectangular Cross Section for Determination of Flow Curves; Systematic Deviations, Sources and Corrections.

Part 3: Specialized Automotive Lubricant Testing and Future Automotive Applications

Current and Future Advances in Materials Development for Tribological Applications

Barbara Rivolta¹ and Lauralice Canale¹

19.1 INTRODUCTION

Improvements in the tribological performance of engines can produce many benefits, the most important of which are

- A reduction in fuel and oil consumption;
- A reduction in maintenance requirements and no longer of service intervals;
- An increase in engine power output;
- Harmful exhaust emissions reduction; and
- Improved durability, reliability, and engine life.

Considering the many internal combustion engines in service today, even the smallest improvements in the engine efficiency, emission levels, and durability could produce a significant effect on the global fuel economy and environment.

A paper by Andersson [1] shows the distribution of fuel energy for a medium-sized passenger car during an urban cycle: Only 12 % of the available energy in the fuel is available to drive the wheels, with 15 % being dissipated as mechanical losses (mainly frictional). According to his publication, a 10 % reduction in mechanical losses would lead to a 1.5 % reduction of fuel consumption.

Regarding energy consumption within the engine, friction loss is the most important portion, being 48 % of the energy consumption [2]; the other portions are the acceleration resistance (35 %) and the cruising resistance (17 %). If we look into the engine friction loss, piston rings and bearings represent 66 % of the total friction loss, and the valvetrain, crankshaft, transmission, and gears represent approximately 34 %. Regarding only powertrain friction loss, sliding of the piston rings and piston skirt against the cylinder wall is undoubtedly the largest contribution to friction. Frictional losses from the rotating engine bearings (notably the crankshaft and camshaft journal bearings) are the next most significant, followed by the valvetrain (principally at the cam and follower interface) and the auxiliaries such as the oil pump, water pump, and alternator. The total amount and the relative proportions of these losses vary with the engine type, component design, operating conditions, choice of engine lubricant, and service history of the vehicle (i.e., worn condition of the components). Auxiliaries should not be neglected because they can be responsible for 20 % or more of the mechanical friction losses.

In recent years, energy-saving and pollutant-reduction requirements induced carmakers to design more efficient engines. The most important contribution to the engine efficiency can be attained by reducing the weight of the rotating and reciprocating engine parts. In a special way, lighter materials such as titanium, aluminum, and magnesium alloys are among

the best candidate materials to manufacture engine components. However, once those materials show poor tribological properties, a major role can be played by surface modification, conferring on them wear and surface damage resistance [3].

The tribological operating environment is complex and different for specific applications. Figure 19.1 shows the range of temperature and friction coefficients required for specific applications. In most cases, component contacts that rely on the presence of a lubricating fluid film are used to produce low friction ($\mu < 0.1$) during operational use. In addition to friction and temperature, contact pressures are also present, and according to Dearnley et al. [4], values of 10–60 MPa are found for autoengine piston ring cylinder liners and journal bearings. Other components such as engine cam/cam followers achieve contact pressures of 800–1500 MPa. Such requirements promote the necessity to modify the surface of the components.

19.2 SURFACE ENGINEERING

Surface modifications can be obtained by surface treatments and surface coatings. There is a wide range of treatments in each area. Figure 19.2 provides this picture of possibilities [5].

Surface treatments involve altering the surface properties of the base metal by thermal or thermochemical diffusion. Such treatments do not involve the use of coatings, and they do not build up or alter the dimension of the component [6,7]. These treatments are ideal for machined or high-tolerance components where machining to final dimensions is performed before the treatment methods. Almost all of these treatments are performed in components that will be used in areas of lubricated wear [5].

On the other hand, surface coatings can be described as processes that build up and in some way alter the dimensions of the original component. Machining may or may not be required after coating. The depth of coating is dependent on the process used and on the requirements for that application. The depth range is from micrometres for physical vapor deposition (PVD) and chemical vapor deposition (CVD) to millimetres for thermal spraying and welding. The thermal spray method is able to deposit a wide range of materials, metals, and ceramics. The density of the coating also depends on the process [5]. Details on surface treatments and coatings for friction and wear and surface hardening of steel can be found in references 8 and 9, respectively.

Induction hardening, flame hardening, and the other surface thermal treatments are promoted by heating of the surface, modifying it by increasing the surface wear resistance

¹ Politecnico di Milano, Italy

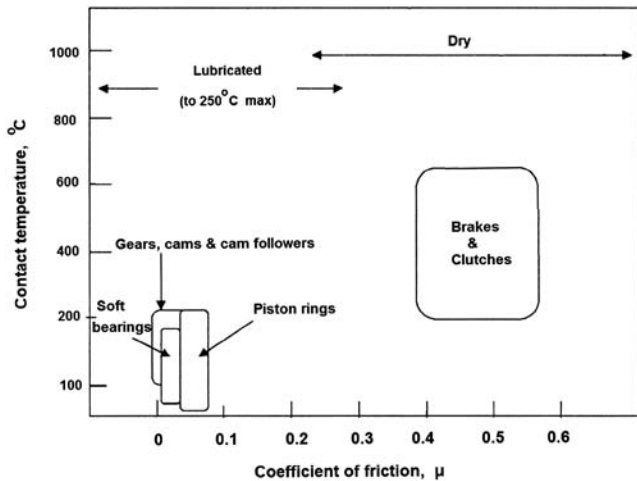


Figure 19.1—Friction-temperature regimes for automotive components. *Source:* Figure adapted from [4].

while the base material is not affected past the treatment zone. Laser heat treatment uses high-power direct diode lasers (HPDLs), carbon dioxide (CO_2) lasers, and continuous-wave neodymium-yttrium-aluminum-garnet (CW ND: YAG) lasers to provide energy to heat the surface metallic materials. Application includes gears, bearing journals, engine cylinder liners, valves, seats, bearing race keyways, and others. If performed properly, laser transformation hardening produces a case that is superior in hardness and fatigue properties, typically 1–2 RC points harder than other surface thermal treatments. The power density (watt/area) used to perform laser heat-treating is generally between 500 and 5000 W/cm^2 , and case depths from a few thousandths to more than 0.1 in. can be achieved [5]. Because the heating is restricted, laser heat treatment is often self-quenching

and does not require external quenchants, which are only used when deep cases are required or if treated materials are of poor hardenability [10].

There are various surface modifications that can be accomplished by electron beam treatments, and surface hardening is among them. Similar to laser treatments, in the hardening of steel by electron beam treatment, the results are dependent on controlling the surface heating to produce austenite, which transforms to martensite on cooling. Electron beam surface modification technologies require application in vacuum whereas laser treatment is applied in air. Laser and electron beam heating have been widely applied to steel and cast iron to improve surface hardness and wear resistance [11].

Carburizing is one of the most common of the case methods. It is a well-known process in which low-carbon steels ($<0.25\% \text{ C}$) are surface-enriched with carbon ($\sim 0.8\% \text{ C}$), thereby promoting the increase of surface hardness and maintaining the toughness of the core. Hardening and tempering complete this process that also gives compressive stress to the surface. Typical carburizing temperatures are in the range of 900–950°C, and the process can take several hours [11]. Vacuum carburizing is a modified gas carburizing process in which the carburizing is done at pressures far below atmospheric pressure (760 Torr). The current typical pressure range for low-pressure vacuum carburizing is 3–20 Torr. The advantage of this method is that the steel surface is cleaned during heatup, and the vacuum environment makes the transfer of carbon to the steel surface faster (i.e., higher carbon transfer values). This happens because the atmospheric interactions such as those found in the water gas reaction cannot take place. The main advantage is the absence of intergranular oxidation [12]. The carburizing process is well detailed in reference 8.

Nitriding is another surface treatment having the objective of increasing the surface hardness. An important

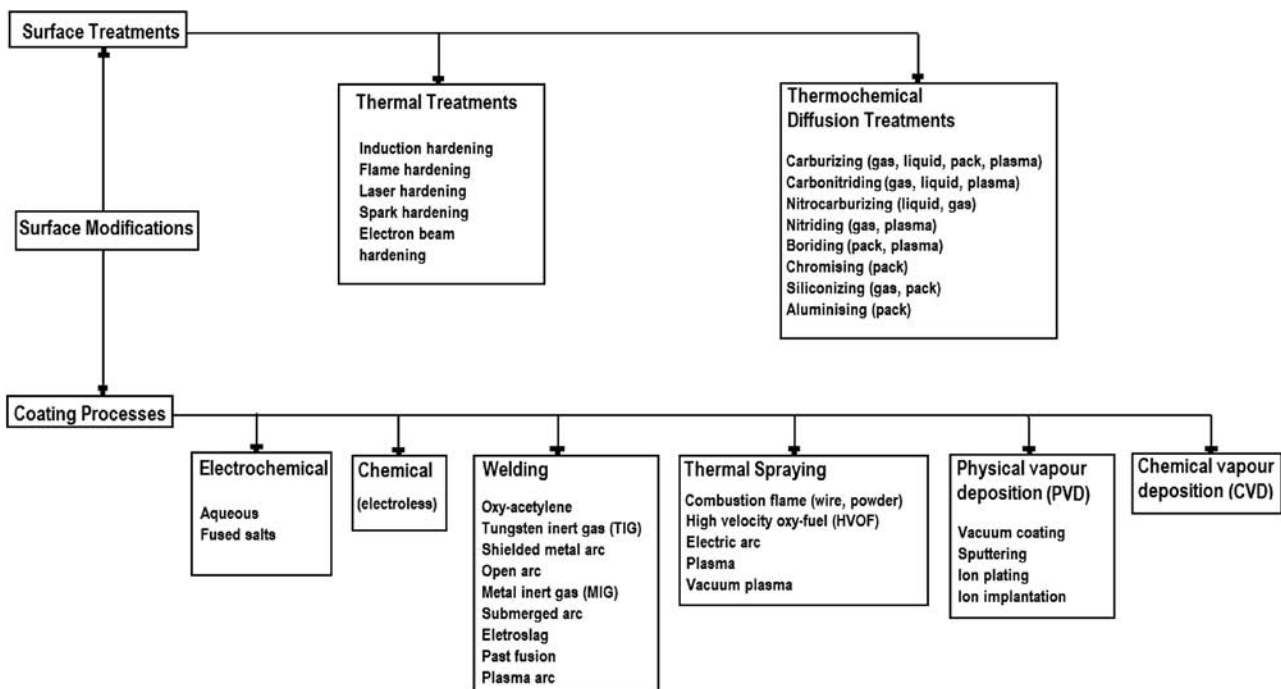


Figure 19.2—Range of surface modifications. *Source:* Figure adapted from [5].

review about this subject can be found in Hoffmann and Mayer [13]. This process was developed in the 1920s, having ferritic steel as a substrate and involving nitrogen introduction in the ferrite structure traditionally at temperatures between 495 and 565°C. There are no phase modifications as in carburizing and carbonitriding, and it is used as the last process for the component manufacture. Maximum nitrogen solubility in the ferrite is 0.1 %; higher amounts provoke the intermetallic phase formation, called nitrides. The first nitride to be formed is γ' (Fe_4N), which is stable through 6.1 % nitrogen. The ϵ nitride, (Fe_{2-3}N) formation, which dissolves until 11.0 % nitrogen, occurs at greater values. The nitride layer has a high hardness compound from the γ' and ϵ nitrides in the substrate's surface, which is called the white layer or compound layer. While nitriding continues, nitrogen goes toward the substrate interior, forming a diffusion layer. Although there are many nitriding processes, plasma nitriding (PN) has been growing in the industry because of its flexibility and control. For example, the process can be designed so that a layer only gets the ϵ nitride, which results in less toughness but extreme hardness, or only the γ' nitride, which provides better toughness with lower hardness. Before nitriding, the component must be quenched and tempered [11,12].

Carbonitriding, which is the alternative process for carburizing and nitriding, is one of the most common thermochemical processes used in industry to improve mechanical properties of the surface layer. During the process, carbon and nitrogen atoms diffuse into the surface layer. The process is similar to carburizing in that the austenite composition is enhanced and the high surface hardness is produced by quenching to form martensite. This process is a modified form of gas carburizing in which ammonia is introduced into the gas carburizing atmosphere. Carbonitriding is typically done at lower temperatures than carburizing, but at the austenitizing condition, between 700 and 900°C, and for a shorter time. Combined with the fact that nitrogen inhibits the diffusion of carbon, what generally results is a shallower case than is typical for carburized parts, usually between 0.075 and 0.75 mm deep. The surface hardness and abrasive wear are increased after carbonitriding, and the fatigue strength of the parts is also improved. In addition to gas carbonitriding, other alternative technologies have been pursued, including molten salt (bath cyaniding), which, although efficient, is extremely toxic [11–16].

Nitrocarburizing is also referred to as ferritic nitrocarburizing because the nitrogen and carbon are introduced to the surface of ferrous materials at temperatures completely within the ferritic phase field (i.e., at a temperature below that of the austenite formation during heating) [17]. A very thin layer is formed during the process, as well as an underlying “diffusion” zone. Similar to nitriding, rapid quenching is not required. Nitrocarburizing is normally performed at 550–600°C and can be used to produce an equivalent 58 HRC minimum hardness, with this value increase dependent on the base material. White layer depths range from 0.0013 to 0.056 mm, with diffusion zones from 0.03 to 0.80 mm being typical [12,18]. A detailed review regarding gaseous and plasma nitrocarburizing can be found in reference 19.

The boriding process is applied to component parts when high abrasive resistance or a good adhesive performance

is required because it renders the possibility of producing layers with excellent wear properties. In most cases, boriding is performed in powders consisting of boron carbide (B_4C) with an activator (KBF_4) and a diluent (SiC). Another technique is the application of boron-containing pastes on the surface. The boriding treatment temperature is between 800 and 1050°C. In the case of iron and steel substrates, FeB and Fe_2B are formed in the layer. These borides have a high hardness (~1500 HV). Nowadays, plasma boriding is also used and is an alternative to the conventional boriding process [7].

Aluminizing or aluminum diffusion alloying is an economical process that resists high-temperature oxidation and “hot corrosion.” Hot corrosion results mainly from sodium and sulfur in the fuel and gas stream at high temperatures. Protection of the surface of steels, stainless steels, and nickel alloys operating in severe high-temperature environments is obtained with this coat. This chemical process is performed at high temperatures, and aluminum diffuses into the surface of the base metal forming new metallurgical aluminide alloys. In the pack aluminizing process, the workpiece is packed in a container containing a mixture of aluminum powder, a halide (e.g., ammonium chloride) serving as a chemical activator, and an inert filler such as alumina. In the temperature range of 820–980°C, aluminum chloride vapor is formed by the reaction of aluminum and the ammonium chloride. Aluminum is deposited on the component surface by the decomposition of aluminum chloride. The layered microstructures consist of an upper aluminum-rich single phase approximately 35 μm thick, followed by a mixed microstructural zone of approximately 50 μm [16]. Low-carbon steel surfaces that are aluminized before being nitrided reveal a higher hardness than nitrided plain low-carbon steel, partly because of the formation of aluminum nitride (AlN) in the surface structure [20].

Galvanic or electrochemical coatings are based on a donor anode, an electrolyte, and an electric power source. In the coating process, metal ions from the anode move through the electrolyte to the substrate at a rate that is defined by the electric current density [21]. In electrochemical chromium plating, chromic acid (H_2CrO_4), or the aqueous solution of chromium trioxide (CrO_3), acts as the chromium donor, whereas an inert anode is used. Chromium is the hardest of the various metals that are commonly applied and it can be as thick as 1 mm, but it is most economical if it can be applied as a thick layer (1–2 μm). In this thickness range, it can be applied to finish machined parts. Vickers hardness values between 600 and 1000 kg/mm^2 are usually obtained [22]. The modification of electrochemical coatings with particles of disperse phases allows for improving their properties and widening the areas of their application. Because of its wear resistance, chromium is a promising material as a matrix for such composite coating. Using ultradispersive diamond particles, the microhardness of the chromium coating can be increased by a factor of 1.4 [4,23–25]. In electrochemical plating, the components to be coated act as cathodes and locations for hydrogen gas formation. Precautions in the deposition process or post-treatment may be necessary for avoiding hydrogen embrittlement of the coated surface material [26].

Ion implantation is a surface modification process in which ions are driven into a substrate by very high-energy ion beams. This process changes the surface chemistry of

a substrate, and it is performed at room temperature. However, significant surface temperature increases, up to 400°C, have been measured during high current density implantation of Type 304 stainless steel; therefore, ion implantation may be considered to be a thermochemical process [11]. This procedure exposes a metal surface to accelerated metal ions, such as nitrogen or titanium, which diffuse into a certain depth of the material. The case depths produced by ion implantation are very shallow, on the order of 0.2 μm , compared with nitride depths of 100 μm and a carburized case depth of 1 mm or more. Because chemical gradients are gradually incorporated into the substrate, an ion-implanted surface system does not have adhesion problems associated with coatings and their discontinuous interfaces with substrates [11]. Ion implantation increases the hardness of metals without significantly affecting the microgeometry of the surface, which has proven successful in several applications. However, studies by Qui et al. have shown by pin-on-disk and reciprocating tests that nitrogen ion implantation alone is insufficient for providing improvements in the tribological performance of aluminum piston materials [27].

CVD produces coatings or layers, sometimes referred to as plating, on a substrate surface. A chemical reaction between gaseous reactants occurs, and the reaction products are deposited on the substrate. Typical CVD applications include the deposition of alloy carbide or nitride layers on tool steels or cemented carbides. CVD coatings producing moderate or low substrate temperatures (700–900°C) are under active consideration [11].

PVD is another surface modification technology used to deposit coatings or layers on substrates. Atoms or molecules are physically generated from target materials in vacuum chambers and are deposited on substrates. Pure atom layers or metal nitrides, carbides, or oxides may be deposited by introducing appropriate gases to PVD installations. There are many types of PVD systems, classified roughly by the methods used to generate the depositing atoms and the substrate environment. Types of PVD systems include those based on evaporation, sputtering, and ion plating. The properties and structures of the thin (typically between 5 and 10 μm thick) coatings applied by PVD processing are very sensitive to processing conditions. The

coatings consist of titanium nitrides or other alloy nitrides, carbides, and carbonitrides and have hardness values of 2500 HV or higher. The major advantage of the PVD coatings is that they are applied at substrate temperatures of approximately 500°C [11].

Thermal spray is a continuous, directed melt-spray process in which particles of virtually any materials are melted and accelerated to high velocities impinging on the substrate and rapidly solidified to form a thin “splat.” Types of thermal spray processes include combustion flame spraying and high-velocity oxy-fuel (HVOF) spraying. The chemistry of the coating is determined by the composition of the feedstock. The spray materials range from low- to high-melting-point metals and alloys, ceramics, and polymers. The integrity and quality of the coating deposition are measured by three fundamental factors: oxide content, porosity, and bond strength. The torch can be based on the combustion process or on an electric arc, the choice of which will be determined by the type of spray material used and the specific application [28]. Table 19.1 gives the characteristics of various thermal-spray processes.

Many coatings are antiwear, showing high lubricity and allowing for an important improvement of the power efficiency, decreasing the mechanical losses due to friction.

In recent years, because of the increase in engine power, the operating conditions of components have become severe, leading to worsening of the component performance. The use of tribological coatings implies many advantages for the automotive industry because it can allow for the production of vehicles with considerably improved performance, reliability, environmental sustainability, and operation economy [3,29].

Surface enhancement engineering solutions are increasingly becoming the goals of the automotive industry in the reduction of wear, friction, and corrosion for powertrain parts and engine interiors. In addition to solutions such as thermal spray, PVD, plasma-enhanced CVD (PECVD), and thermochemical heat treatments such as nitriding, there are also combined processes such as IONITOX [30]. IONITOX is a combination of gas nitriding and plasma activation processes that is performed before oxidation. Corrosion stability is reached because of a 2- μm thickness

TABLE 19.1—Characteristics of Various Thermal-Spray Processes and Their Material Characteristics

Spray Type	Feed Type	Flame Temperature (°C)	Particle Velocity (m/s)	Materials	Microstructural Features	Applications
Combustion	Wire powder	~3000	~40–100	Metals, polymers, ceramics	Relatively high porosity and oxidation	Reclamation, corrosion, protection
HVOF	Powder	~3000	~400–800	Metals/cermets, Low-melt ceramics	High density, excellent adhesion, compressive stresses	Wear protection
Two-wire Arc	Wire	~3000–6000	50–150	Metals, cermets (cored wires)	Reasonably dense, thick	Reclamation, wear protection
Plasma	Powder wire	~5000–25,000	80–300	Ceramics, metals	Porosity in ceramics deposits	Thermal barriers, insulators
Cold Spray	Powder	Room temperature	400–800	Metals	Dense, compressive stresses	Conductors, reclamation, cladding

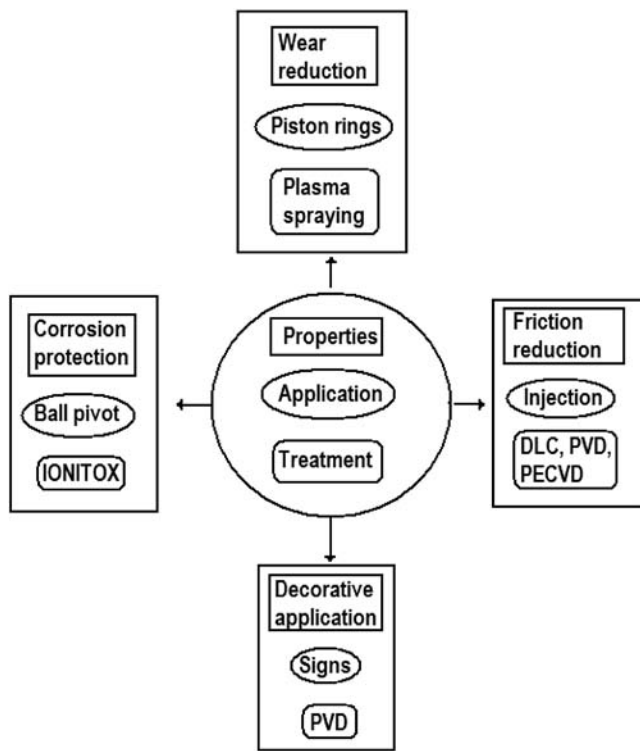


Figure 19.3—The main functional properties required on automotive applications. *Source:* Figure adapted from [30].

of dense oxide layer (Fe_3O_4), which also increases the wear resistance, decreasing the friction [30,31].

Various surface treatments are required for the different functional surface properties of automotive parts. Figure 19.3 shows a rough classification of the four main required properties and the respective surface deposition technique [30,31]. Some requirements such as low friction and low wear are overlapping but within the above-mentioned groups of surface treatments cover a wide range of properties: mechanical, electrical, tribological, and corrosive properties.

Because the coatings are generally applied using the atmospheric plasma spray (APS) method, a certain degree of oxidation can be formed during the coating. The formation of the correct oxides on ferrous base bulk materials such as FeO (wustite) and Fe_3O_4 (magnetite) was demonstrated to improve the tribological properties for their lubricant effects [32].

Different techniques for surface modifications for wear resistance promote several hardness ranges. Figure 19.4 shows a hardness value range of the various surface-engineering processes commonly used for wear protection [22].

As already mentioned, among the required properties for automotive components, wear resistance and corrosion resistance are very important. Table 19.2 (from reference 18) shows the most used surface modification methods applied for automotive components.

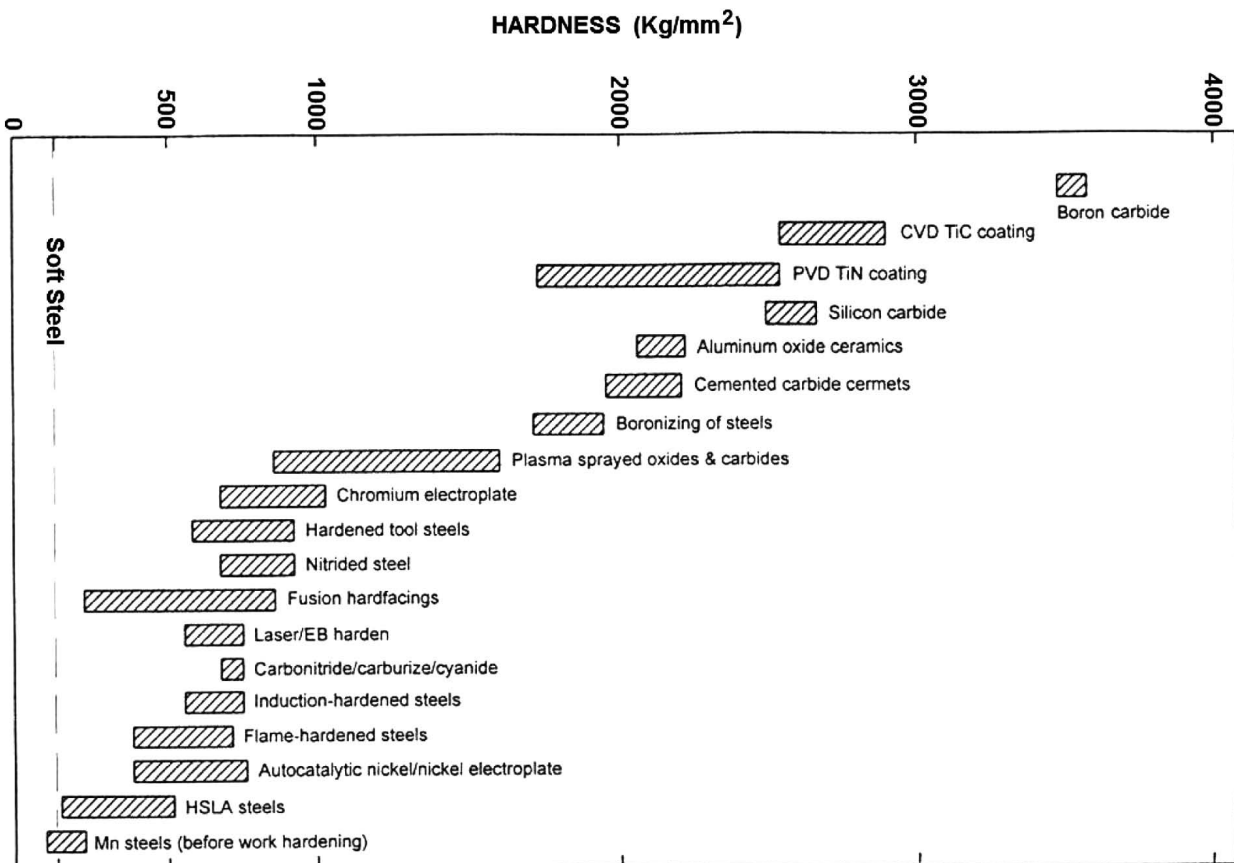


Figure 19.4—Hardness ranges of common surface-engineering processes. *Source:* Figure adapted from [22].

TABLE 19.2—Surface Modification Methods Applied for Automotive Components

Methods	Modification Type	Thickness (μm)	Property	Typical Application
Electrolytic plating	Cr, Cu, Ni, Zn-Fe, Zn-Ni, Ni-P-SiC, BN, Fe, Sn, Ni-P-B	100–300 10–100 5–20	Resistance to corrosion, wear, microwelding	Bumper, body component panels, cylinder bores, piston
Electroless conversion	Ni-P-SiC, phosphate coat	3–20	Wear resistance	Brake cylinder pistons
Electrolytic deposition	FeS, Fe ₂ S, phosphate coat	3–8 20–50	Reduce friction, Lubrication	Cold forming blanks
Coat quench	Phosphate, MoS ₂ , etc.	4–7	Prevent rusting, adjust friction coefficient	Fasteners, spring retainers, etc.
Solid lubricant coat	MoS ₂ , graphite, etc.	3–100	Reduce friction, dry lubrication	Piston rings, gears, pistons
Painting	Color parts	30–500	Outlook, corrosion resistance	Body and panels and other components
Plasma spray	Fe, Cr, Al, Mo, ceramics, W, WC, Cu, Cu-Zn	100–400	Wear resistance, thermal insulation	Piston rings, O ₂ sensor, cylinder bore
CVD	DLC	2–10	Reduce wear and friction	Piston rings
PVD	TiN, CrN, TiAlN, TiAlCN	4–20	Wear, seizure resistance	Piston rings, etc.

19.3 AUTOMOTIVE ENGINE COMPONENTS

19.3.1 Piston Assembly

To improve the tribological properties, especially adhesion, solutions such as diamond-like carbon (DLC), other carbon films (WC/C), molybdenum disulfide (MoS₂), and multilayer coatings (CrN/MoS₂) have been used. PVD, magnetron sputtering, and plasma-assisted chemical vapor deposition technologies, including hybrid deposition systems, have been also suggested to coat piston and piston rings with self-lubricant coatings to improve their friction properties. As hybrid technologies, a double-layer coating made out of PVD WC/Co as a base coat and a top layer of MoS₂ and WC/Co was deposited and tested. With this coating, aluminum cylinder liners showed better friction behavior than cast iron lines [3].

19.3.2 Cylinder Bores/Piston Skirt

The optimizations of the tribological behavior of piston skirts versus the cylinder bore system is considered important for the reduction of noise and for the improvement of wear and scuffing resistance. For example, the choice of a good clearance between the piston and block is considered fundamental because it must be as small as possible for decreasing noise and vibration but at the same time sufficient to avoid seizure of the parts.

19.3.2.1 CYLINDER BORES

Cylinder bores are generally manufactured from gray cast iron (either plain or with the addition of alloying elements) or from Al-Si alloy. The surface treatment and coating of cylinder walls is less common than with pistons in industry even if some wear-resistant coatings such as Nikasil plating or thermal-sprayed coatings [33,34] have been applied to aluminum bores.

Nowadays, the most frequently used solution regarding tribology for engine blocks in aluminum cast alloys is the insert of cast iron sleeves. However, such a solution has some disadvantages, including irregular heat flow from the cylinder bore to the cooling system, oxide formation between the cast iron sleeves and the Al cast material, and

so on. A solution using hard chromium has a deleterious effect on the environment. Because of these facts, internal plasma spray coatings are used today in various engines. Among the advantages over cast iron sleeves are friction reduction of the piston groups by approximately 30 % leading approximately 3 % fuel reduction, oil consumption reduced 2 times, and low wear rate [31,32].

Several thermal spray processes were developed for the cylinder bore application, but only the plasma spray process has reached the status of high-volume manufacturing [30]. A porosity volume between 1 and 3 % finely distributed provides good tribological properties once micropores are filled up with lubricating oil, ensuring the safe lubrication of the process [32]. The thermal spray process allows for the use of a large range of materials. Antiwear coatings are based on metallic carbide containing ceramic or composite material. Three main coating processes for cylinder bores in Al-Si cast alloys are basically used: wire arc (wire), HVOF (wire or powder), and rotating plasma (powder). Table 19.3 shows a comparison among these processes [30,35].

ASTM C633-79 recommends 40–50 MPa as the bond strength for aluminum cast alloy and 50–70 MPa when the substrate is gray cast iron. Although in terms of performance 80- μm coating thickness is enough, typical values for a sprayed coat are between 160 and 240 μm [35]. The maximum coating thickness depends on the heat expansion coefficient and the mechanical properties of the coat. The thickness allowance for a tested, stabilized, coating process is between 100 and 150 μm in the bore diameter. The recommended thickness is 125 μm [32,35–37]. To obtain a reasonable bond strength of the sprayed coating on the cylinder wall, the surface must be active shortly before the spray operation. Grind blasting with Al₂O₃-based materials are traditionally used for this operation. In this case, a cleaning operation after blasting reduces the contamination with embedded particles and a bond strength can be achieved [37].

In the specific case of the coating of cylinder bores, the transfer of heat into the substrate unit must be considered

TABLE 19.3—Comparison of the Thermal Spray Processes for the Coating Deposition in Engine Cylinder Bores

Criteria	Wire Arc (Wire)	HVOF (Wire or Powder)	Rotating Plasma (Powder)
Versatility in the choice material	Low, metallic alloys	Medium, metallic alloys, carbides, composites	High, metallic alloys, ceramics carbides, composites
Heat transfer into the engine block	Medium	Very high	Low
Reliability of the melting process	Medium, formation of the melted particle is difficult to control	High (powder) Medium (wire)	High
Coating thickness as sprayed	500 μm	200 μm	200 μm
Coating properties for cylinder bores	Medium	High	High
Process cost	Low	High	Low

with priority because the engine blocks are in Al-Si cast alloy and overheating during the coating can result in a nonacceptable distortion or metallurgical change in the microstructure. To keep the heat transfer under control, it is necessary to select the correct size of the plasma gun, spray parameters, traversing speeds during spraying, and cooling methods [37].

There are many advantages associated with the plasma coating of cylinder bores on an aluminum cast alloy engine block in comparison with the conventional method of using a cast iron liner in the aluminum cast. Among them are the higher wear resistance and reduced oil consumption. Fuel consumption reduction is more than 2 % [34,36]. In comparison with other coating processes for cylinder bores (e.g., nickel dispersion coatings, HVOF, and electric arc wire spraying), plasma is less expensive and more efficient [32].

19.3.2.2 Cylinder

Chromium nitride (CrN) coatings show excellent wear, corrosion, and oxidation resistance, also exhibiting a low coefficient of friction, high hardness, and good adhesive

properties on the substrate. With very thin coating thicknesses ($\sim 2 \pm 0.2 \mu\text{m}$), it does not require additional machining. Because these coatings can be applied at relatively low temperatures, no warping occurs on the base material. Table 19.4 gives the general properties of CrN coatings [38].

Öner, Hazar, and Nursoy [38] performed experimental studies to verify the behavior of a CrN coating in a cast iron cylinder of a diesel-injection engine. The thickness obtained was $1.8 \pm 0.2 \mu\text{m}$. The technique used was PVD under temperatures of 250–300°C. Figure 19.5, a–d, shows comparative results between a coated and uncoated cylinder

TABLE 19.4—Properties of a CrN Coating Material [38]

Thickness range (μm)	1.0–10.0
Hardness (HV)	2200 \pm 400
Oxidation temperature ($^{\circ}\text{C}$)	700
Surface roughness (R_a)	0.20

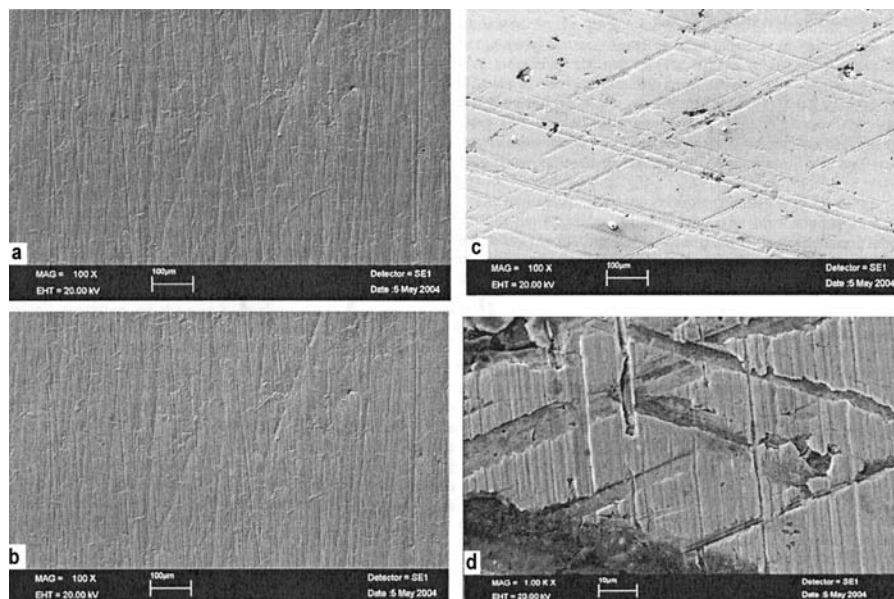


Figure 19.5—Micrographs showing a coated and uncoated cylinder before and after test runs: coated cylinder (a) before and (b) after test; uncoated cylinder (c) before and (d) test [38].

before and after test runs. Cylinder surfaces were tested under normal operating conditions [38].

It is clear that compared with Figure 19.5, a and b, Figure 19.5, c and d, shows an intense worn surface. The main purpose of the ceramic coating is to make the cylinder tube more resistant to wear when the lubrication system is not completely separating the mating surfaces under hydrodynamic lubrication. Because at the coated cylinder there are less wear particles flowing with oil, less abrasive particles are available to cause wear. The coating also helps to prevent wear in the whole cylinder-piston-ring system [38].

19.3.2.3 CYLINDER BLOCK

A cylinder block is generally made of cast iron because of its economic advantages, ease of processing, and excellent tribological qualities. In recent years, high-weight cast iron cylinders are being gradually replaced by Al-Si-Cu alloys with an insert of a cast iron cylinder liner. A more recent trend is to develop an integral cast aluminum alloy block using hypereutectic alloys, including high silicon of 16–18 %.

19.3.2.4 PISTONS SKIRTS

Gray cast iron was originally used for automotive pistons, but now Al-Si cast alloys are preferred because lighter pistons reduce the total engine weight and the reciprocating mass, thereby reducing the engine vibration. Furthermore, the higher thermal conductivity of aluminum helps to prevent overheating of the top of the piston with no requirement for specific cooling. The major disadvantage is that aluminum has a higher coefficient of thermal expansion than cast iron, which must be considered in the designing phase to avoid, for example, that a piston designed to have adequate clearance at operating temperature may be too loose (and hence noisy) at low temperature. Additions such as copper and nickel to aluminum can modify the thermal expansion coefficient; for example, the 336 alloy has a thermal expansion coefficient 13 % lower than pure aluminum, even if 70 % greater than cast iron. Nowadays, piston skirts are usually coated with materials such as nickel-ceramic composites or MoS₂, which also reduce the friction between the piston skirt and cylinder bore.

Piston skirt coatings that are based on materials such as polytetrafluoroethylene (PTFE) or graphite are also applied. In contrast to piston ring and cylinder liner coatings, piston skirt coatings are generally intended to reduce friction rather than wear [34].

Toyota has been using composites for engine pistons since 1981 [39]. Diesel engine pistons have been produced by the development of alumina-silica fibers that were squeeze-cast into the top portion of an aluminum alloy piston.

Aluminum-based metal matrix composites (MMCs) have been used for several years [32,40]. These MMCs are fabricated by the addition of a reinforcement phase to the matrix by the use of several techniques such as powder metallurgy, liquid metallurgy, and squeeze casting. The reinforcement phase is generally one of the following: continuous boron or graphite fibers or hard particles such as SiC and Al₂O₃ in discontinuous particulate or whisker morphology. The volume fraction of reinforced particles or whiskers is generally within the range of 10–30 %. Aluminum alloys, such as the 2000, 5000, 6000, and 7000 alloy series, are the most commonly used materials. Hypereutectic Al-Si-based composites such as A356 (Al, 7Si, 0.3Mg) containing Al₂O₃,

ZrO particles, or SiC particles are used. The wear resistance and operating properties of aluminum cast diesel pistons are enhanced by the use of aluminum-based composite piston ring inserts. These composite inserts are reinforced with Al₂O₃ whiskers or a combination of these whiskers (12 vol %) and carbon fibers (9 vol %). Aluminum-based composites have also been considered as substitute materials for use in the fabrication of brake rotors, pistons, cylinder liners, and cylinder heads.

The following factors were considered to be significant in influencing the wear rate of composites: second-phase particle dimension, interparticle spacing, and particle/matrix interfacial bond strength. It was stated that the wear rate decreased with an increase in the alumina volume fraction. The predominant wear mechanism was identified as delamination because of poor particle/matrix interfacial bonding. One of the earliest papers that reported the tribological properties of composites reinforced with various particulate types was that of Sato and Mehrabian [41]. Matrix alloys of Al-4Cu, Al, 4Cu, 0.75 Mg, and 6061 were reinforced with SiC, TiC, Si₃N₄, Al₂O₃, silica sand, MgO, mica, glass beads, and B₄N. The particulate size range (0.06–840 μm) and volume fraction (1–30 %) investigated were extensive. Adhesive wear tests (pin-on-disk) and the associated coefficient of friction data for a sliding velocity range of 0.05–0.46 m s⁻¹ were tabulated. In general, the friction coefficient decreased with increased sliding velocity for all of the composite combinations. For composites reinforced with more than 10 % of SiC, TiC, Si₃N₄, Al₂O₃, or silica sand, the wear rate was less than that of the unreinforced matrix. The correlation of the particulate volume fraction and size with these tribological properties by Sato and Mehrabian [41] was unfortunately not conducted in a very systematic manner. Therefore, the nature of the relationship between sliding wear and reinforcement volume fraction and size remained undefined in this study. Surappa et al. [42] noted that aluminum reinforced with 5 % alumina possessed an adhesive wear rate comparable to that of Al-11.8Si or Al-Si hypereutectic alloys. Other work published by the same workers [43] involving Al, Al-11.8Si, Al-16Si alloys, and Al reinforced with Al₂O₃ particles (5 %) indicated that increased silicon content reduced the wear rate.

Hosking et al. [44] reported a decrease in adhesive wear rate with increasing particle content (at constant particle size) and dimension (at constant volume fraction) for Al 2014 and 2024 alloys reinforced with Al₂O₃ and SiC particles (1–142 μm) of various weight fractions (2–30 %). SiC was shown to be more effective than alumina in resisting wear when tested in a ball-on-disk rig.

In the case of a high-performance combustion engine, the creep tendency of the aluminum piston head can be significantly decreased by the deposition of a thermal barrier in PSZ (partial stabilized zirconia). In this case, a bond coat (MCrAlY) is deposited [30].

To obtain the performance behavior of piston coatings, the scuffing and wear resistances of various piston coatings were evaluated and compared with tin plating and iron plating. The tested piston coatings included Ni-W plating, electroless Ni plating, Ni-P coatings with ceramic particles (BN, SiC and Si₃N₄), TiN by PVD coating, DLC coating, and hard anodizing. Simulation tests were performed with coatings against a 390 Al bore [45]. Results concluded that the coatings with very good scuffing resistance against 390 Al

included Ni-P-BN coating, iron plating, and Ni-W plating. A TiN PVD coating had marginal performance in terms of scuffing resistance when sliding against 309 Al and the most severe wear on 390 Al samples. Compared with TiN coating, hard anodizing, DLC, Ni-P-SiC, and Ni-P- Si_3N_4 coatings had less severe wear on the bore samples [45].

A plasma immersion ion implantation technique was used to develop a diamond-like hydrocarbon (DLHC) coating of 390 Al alloy, and the coating's performance was verified [46]. In this case, 390 Al, the processing temperature must be kept below 220°C so that the alloy does not lose its original metallurgical properties. Results show that DLHC performance is strongly dependent on the thickness and microstructure of the coating. Adhesion tests with coatings up to 7 μm indicated that sufficient performance should be achieved with relatively thick DLHC coatings [46].

19.3.3 Engine Bearings

In an operating engine, rotating journal bearings are used to support the camshaft, the crankshaft, and the connecting rod. The basic configuration is a split half-shell bearing fitted into a bore and incorporating some form of locating notch.

A conventional bearing is typically composed of a top layer of Pb-Sn-In or Pb-Sb-Cu plating of 10- to 25- μm thickness, a second 200- to 300- μm layer of Cu-Pb alloy or Al-Sn alloy, and a cold-rolled sheet as the backing metal [47].

Recent trends toward the higher power efficiency of engines mean that bearings should have a higher load-carrying capability and better antiseizure performance. One way to obtain these improvements is the dispersion hardening of hard particles in the soft metal overlay. Dispersion of 1.3–2.5 vol % Si_3N_4 fine powder in Pb-Sn-In alloy drastically improved the wear resistance. Dispersion of cobalt base hard powder in Cu-Sn-Pb alloy also gave better bearing performance [48]. In the near future, lead bearings will have to be substituted because of their toxicity.

Several studies have been performed for the development of polymer bearings. They were originally studied mainly for large marine vessel applications in which the white metal journal bearings cause serious problems of seizure between the journal and bearing when the lubricant film is broken under heavy load, low-velocity applications, or start-and-stop periods. To solve the seizure problem, polymers are widely used because their friction coefficients are much lower when compared with that of metallic materials because of their self-lubricating properties.

Among several types of plastic for bearings, phenolics are largely used because they operate satisfactorily with steel or bronze journals when lubricated with oil, water, or other liquids. One main disadvantage is their low thermal conductivity ($\sim 0.35 \text{ W/m K}$), which is approximately 1/150 of steel, which can result in bearing failure by charring. To overcome this problem, the polymer can be reinforced with high thermal conductivity fibers, which, at the same time, intrinsically also show a low friction coefficient.

Several investigations of composite journal bearings have been performed.

Zhang [49] manufactured three kinds of metal-plastic multilayer composite journal bearings that were composed of a steel backing, a middle layer of sintered porous bronze, and a surface layer of PTFE filled with Pb or Cu_2O

powders. S.S. Kim et al. [50] developed a specific carbon fiber-reinforced phenolic composite.

Shafts designed for running against engine bearings are generally made of heat-treated steels or spheroidal graphite irons, with hardness values approximately 3 times that of the principal bearing material. Lubricant is directed to the bearings by jet impingement or by passing through the bore of a hollow shaft. If the bearings are adequately lubricated, bearing wear is low after an initial stage of running in period. However, shaft misalignment or particulate contamination of the lubricant supply can lead to excessive wear. An additional failure mechanism is bearing corrosion. The tribology of journal bearings is complicated by issues such as lubricant supply, thermal effects, dynamic loading, and elasticity of the bounding solids.

19.3.4 Piston Rings

The heart of the internal combustion engine is the piston assembly, forming a critical linkage in transforming the energy generated by combustion of the fuel and air mixture into useful kinetic energy. The piston assembly includes the ring pack, which is essentially a series of metallic rings, the primary role of which is to maintain an effective gas seal between the combustion chamber and the crankcase. The rings of the piston assembly, which form a labyrinth seal, achieve this function by closely conforming to their grooves in the piston and to the cylinder wall. A secondary role of the piston ring is to transfer heat from the piston into the cylinder wall, and hence into the coolant, and to limit the amount of oil that is transported from the crankcase to the combustion chamber.

This flow path is probably the largest contributor to engine oil consumption and leads to an increase in harmful exhaust emissions as the oil mixes and reacts with the other contents of the combustion chamber. The objectives to extend engine service intervals and minimize harmful exhaust emissions for meeting more stringent legislative requirements are to reduce the permissible oil consumption to a lower level compared with their predecessors of 20 years ago.

From a tribological perspective, the main piston features are the grooves, which hold the piston rings, and the region of the piston below the ring pack (the piston skirt), which transmits the transverse loads on the piston to the cylinder wall. The top two piston rings are referred to as the compression rings. Firing pressure pushes these rings out until the whole ring face engages the cylinder wall. Gas pressure is provided to supplement the inherent elasticity of the ring and maintain an effective combustion chamber seal. The top compression ring is the major gas seal and encounters the highest loads and temperatures as the ring closest to the combustion chamber. The top compression ring usually has a barrel-faced profile with a wear-resistant coating such as flame-sprayed molybdenum on the periphery and occasionally on the flanks. The second compression ring, which is sometimes referred to as the scraper ring, is designed to assist in limiting upward oil flow in addition to providing a secondary gas seal. Because of these functions, the second compression ring has a taper-faced, downward-scraping profile that is not normally coated.

The bottom ring in the ring assembly is the oil-control ring, which has two running faces, or lands, and a spring element to enhance radial load. As its name defines, the role

of this ring is to limit the amount of oil transported from the crankcase to the combustion chamber, and it has no gas sealing ability.

The periphery of the lands and occasionally the flanks are often chromium plated. Some practical examples are the compression ring with tapered sides designed to prevent ring sticking due to deposit formation in the piston ring grooves of diesel engines; the internally stepped compression ring, which imposes a dishing on the ring when fitted to improve oil control; and the multipiece, steel rail, oil-control ring. In contrast to the one-piece oil-control ring, the multipiece oil-control ring has smaller land heights, which increases the conformability to the cylinder wall, and hence oil control, with reduced spring force.

The piston ring is the most complicated tribological component in the internal combustion engine to analyze because of large variations of load, speed, temperature, and lubricant availability. In one single stroke of the piston, the piston ring interface with the cylinder wall may experience boundary, mixed, and full fluid film lubrication.

Gray cast iron, malleable/nodular iron, and carbides/malleable iron are the most common base materials for all types of compression piston rings and single-piece oil-control rings. However, steel is becoming popular as a piston ring material because of its high strength and fatigue properties. Steel is used for top compression rings and the rails of multipiece oil-control rings. There are various surface treatments and coatings for piston ring running-in processes. Chromium plating and flame-sprayed molybdenum are the most common wear-resistant coatings, although plasma-sprayed molybdenum, MMCs, cermets, and ceramics are gaining popularity as their technology progresses.

Hard chrome plating is commercially used to produce wear-resistant coating. However, the plating bath contains hexavalent chromium, which has adverse health and environmental effects, and because of this it has been replaced. Thermal spray technologies, particularly HVOF spraying, have been accepted as capable of replacing hard chromium. The reason is because HVOF spraying produces low-porosity (<1 %), high-adherence (bond strength > 50 MPa) coatings that generally have an oxide content less than 1 % for reactive metals [51].

CrC-NiCr system coatings applied by HVOF spraying are used to improve the wear resistance and decrease the friction coefficient between various sliding components on automotive applications. In addition, they are also

corrosion resistant even for service temperatures up to 800–900°C. An interesting work comparing coating performance between hard chromium and Cr_{23}C_6 (75 %) + NiCr₂₀ (25 %) applied by HVOF spraying was presented by Picas et al. [51]. Three different CrC-NiCr powders were used as feedstock powders. Figure 19.6 shows the tribological results from pin-on-disk tests and hardness values for the studied coats. Results suggest that fine CrC-NiCr coatings have superior performance to hard chromium with regard to mechanical and tribological properties, becoming a good candidate to replace hard chromium in pistons and valves [51].

Other surface treatments and coatings for piston ring running-in processes in addition to chromium plating are flame-sprayed molybdenum and plasma-sprayed molybdenum. Molybdenum alloys provide self-lubricity whereas the hardface reinforcements provide wear resistance [28]. MMCs, cermets, and ceramics are also becoming popular as coatings [34].

Ceramic materials applied as thermal barrier coatings have been actively studied and developed since the 1960s. They are applied to combustion system components such as pistons, valves, and piston fire decks in diesel engines. Coatings made by zirconia and yttria as well as alumina zirconia composite exhibited excellent wear resistance. In those cases, before spray coating, a Ni-Cr-Al-Co-Y composite was applied as a bond coat to enhance adhesion and reduce thermal expansion mismatch between substrate and the coating layer [52].

By applying the coating on the liner and piston rings, the service life of the piston ring/cylinder liner pair and thermal efficiency of the engines are expected to be enhanced. Metal matrix carbide-containing coatings applied by plasma spray and HVOF spray processes are very efficient in piston rings, mainly for diesel engines [28,35,36].

There are various piston rings for different applications; therefore, different surface treatments are used depending on the substrate material and the required application. Figure 19.7 shows different piston ring treatments, engine applications, and tribological characteristics [30,31].

Piston rings are routinely surface hardened via gaseous nitriding, which is a well-known process promoting improved performance because of an increase in hardness and surface residual compressive stresses leading to fatigue life are increased. On the other hand, PVD coatings are more wear resistant. Japanese manufacturers were the first

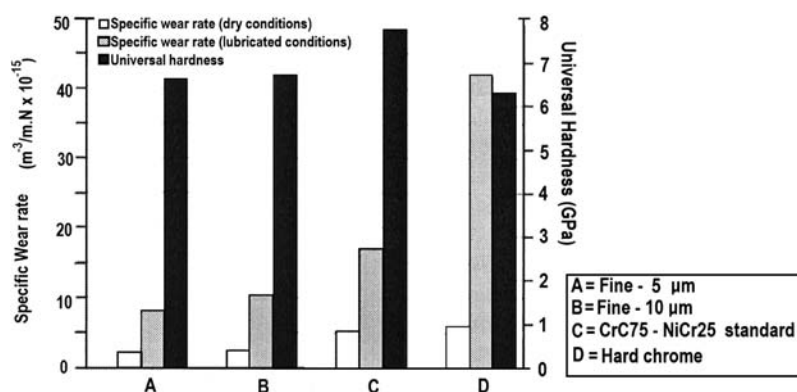


Figure 19.6—Tribological results from pin-on-disk tests and hardness values for three different CrC-NiCr powders and hard chromium used as coatings.

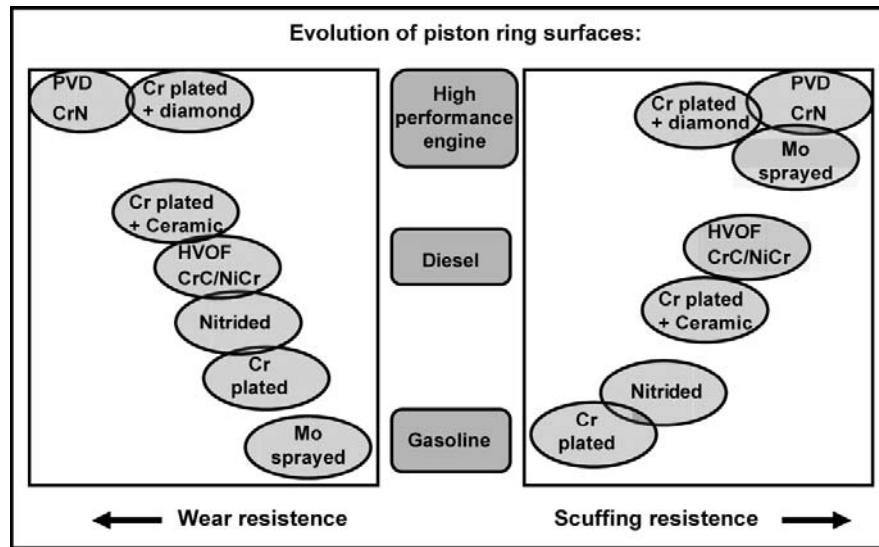


Figure 19.7—Piston ring treatments and engine applications. Source: Figure adapted from [30,31].

to apply PVD coating (Cr/N or Cr₂N or both) for piston rings in diesel engines and, according to Dearnley [4], European engine manufactures are now using CrN-coated piston rings in very significant quantities.

However, a combination of two processes (PVD and nitriding) will provide a superior performance of the component. Figure 19.8 provides a hardness variation among the three coating situations: PN treatment, CrN by PVD coating, and a combination of both. Nitriding before the deposition of the hard coating increases the load-bearing capacity of the coating-substrate system [30,31].

Skopp and collaborators [53] performed tribological tests in two thermally sprayed titanium suboxide coatings with different stoichiometries for the piston ring/cylinder liner system under conditions of mixed lubrication. Vacuum plasma spraying (VPS) promotes no reoxidation of the titanium oxide powders whereas in the APS process oxidation can occur. Using a mixture of argon and hydrogen as plasma-forming gases, the titanium oxide is slightly reduced during spraying, resulting in a decrease of the total

O/Ti ratio. The VPS titanium oxide and APS titanium oxide coatings showed a low porosity and excellent adherence to the gray cast iron substrate. On the basis of the piston ring/cylinder liner simulation tests, thermally sprayed titanium-oxide-based cylinder liner coating can substitute for the commonly used uncoated gray cast iron liner materials.

Surface texturing in general and laser surface texturing (LST) in particular have emerged in recent years as a potential new technology to reduce friction in mechanical components, including the piston/cylinder system [54]. Etsion et al. [55] presented a study evaluating the effect of partially laser surface-textured piston rings on the fuel consumption and exhausted gas composition of a compression-ignition internal combustion engine. LST was performed in cylindrical face rings in coated (Cr) and uncoated piston rings. Results showed that laser-texturing did not produce a significant change in the exhausted gas composition. However, a significant reduction of up to 4 % in fuel consumption was obtained.

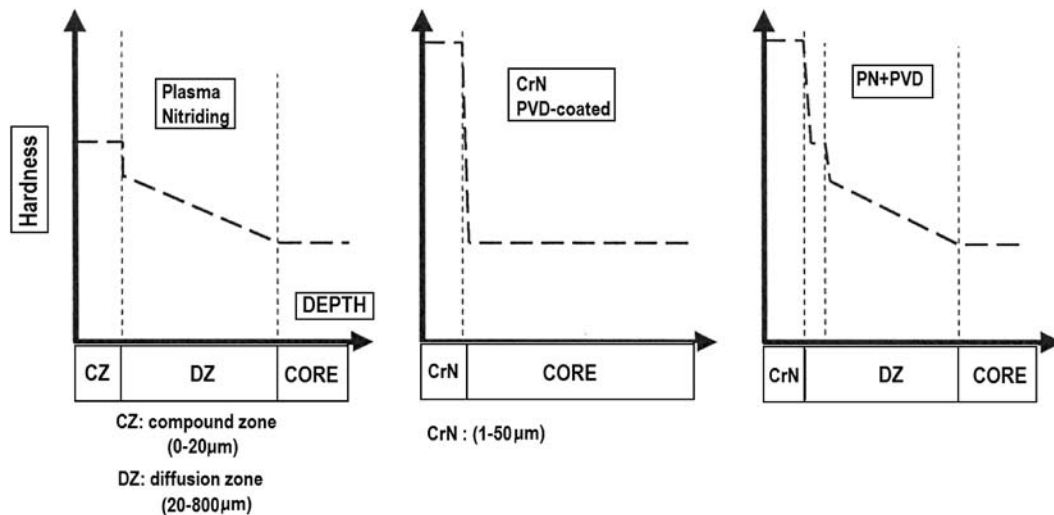


Figure 19.8—Hardness vs. distance from the surface for steels with three different coatings. Source: Figure adapted from [30,31].

Cr-plated plus ceramic particles by Federal Mogul (an electrolytic Cr + alumina [Al_2O_3] coating) are used widely on diesel engines. U.S. Patent No. 5,868,917 [56] mentions the European patent by Federal Mogul. It is called CKS (Chrom-Keramic-Schicht [chromium ceramic layer]) coating. By an electrolytic process, a protective coating based on chromium is deposited in which solid particles are distributed. It is thought that this process' better performance is obtained on wear and abrasive resistance as well as corrosion resistance [4,25]. Hardness is increased, and there is improvement of the friction coefficient. Chromium plating was obtained by the electrolysis of an aqueous trivalent chromium solution containing suspension particles of alumina (size between 0.2 and 0.6 μm). The characteristics of this coating show a homogeneous distribution of the particles throughout the plating as well as perfect adhesion to the substrate. Vickers microhardness values (100-g load) are between 1050 and 1100 HV [56]. In addition to Al_2O_3 , diamond particles also serve to promote the battle against abrasion. The Cr matrix mitigates the oxidative wear process by forming a stable and adherent chromium oxide layer during use. CKS coatings are now receiving significant competition from CrN/nitrided steel piston rings because the process as electroplating has been more rigorously examined by environmental legislation [4,25].

19.3.5 Valvetrain

A valvetrain system includes valves, the valve spring, valve spring retainers, valve keys, rocker arms, piston rods, lifter/tappets, and a camshaft. Valvetrain friction accounts for approximately 30 % of all engine friction.

19.3.5.1 ENGINE VALVE AND SEAT INSERT

The requirements for automotive engines in recent years (e.g., higher horsepower, lower fuel/oil consumption, and longer maintenance-free life) have increased the severity of wear to which valves and valve seat inserts are submitted. The valves impact against the valve seat inserts by the action of the valve springs at high temperature, and more the impacts often include a sliding phenomenon. Furthermore, combustion pressure is applied to the valves and valve seat inserts in an exhaust gas environment [57]. Therefore, the valves and valve seat inserts are submitted to a cycle impact load together with a sliding movement in a corrosive environment at elevated temperature.

Intake valve seat wear is generally thought to occur by three types of wear: adhesive wear, abrasive wear, and plastic deformation controlled wear [58–62]. High contact stresses, poor seat lubrication, relative sliding, and incompatible seat materials are thought to be the primary causes of adhesive wear. During engine operation, relative sliding of the surfaces enhances abrasive wear. In addition, hard carbides; trapped wear debris; combustion products; and contaminant particles from oil, fuel, and air are also influencing factors. The high coefficient of friction and sliding effect between the valve and insert seat contribute significantly to the seat surface deformation or radial flow, which subsequently results in wear. Corrosive wear occurs in exhaust valves because of the harsh chemical environment and high temperature and seldom occurs in intake valves [63–65]. It can result in valve guttering or burning [34,66,67].

Valves are generally made of forged alloy steel. Inlet valves in automobiles are generally made of low-alloy steels

whereas the exhaust valves are made of highly alloyed stainless steels depending on the operating temperature of the exhaust valves. Automobile exhaust valves operate at approximately 615°C whereas in buses and trucks they operate at 730–850°C. Inlet valves usually operate at approximately 320°C, thereby justifying the use of carbon steel. For inlet valves, the steel grades applied are carbon steels such as SAE 1041, 1050 and alloy steels such as SAE 3140, 5150, 6415, and 8645. For light-duty exhaust valves, medium carbon with high silicon (up to 4 %) and chromium (2.25–7.5 %) are applied. However, the high silicon reacts with lead oxide; hence, it is not suitable for leaded, high-octane gasoline engines. Heavy-duty exhaust valves are generally made of steels containing carbon (up to 0.4 %), manganese (7–9 %), chromium (21 %), nickel (4–5 %), and nitrogen (0.10–0.25 %) [68].

From the standpoint of the tribological behavior of the valves and valve seat inserts, engine engineers have begun to take the advantage of the application ceramic material [69]. In fact, ceramic materials, particularly silicon-based ceramics (e.g., silicon carbide, silicon nitride, and sialon), have a useful combination of properties, including low density, high corrosion resistance, low thermal expansion, chemical inertness, and high hardness over a wide range of temperatures. Moreover, it has been demonstrated that silicon-based ceramics, especially silicon nitride and sialon, can exhibit outstanding tribological performance in extreme conditions such as high temperatures, lubrication starvation, or corrosive environments [70]. Several studies in recent decades on actual engine valve and valve insert applications have been reported to be successful with silicon-based ceramics [71]. The major problem for their application to engine valves is often characterized by catastrophic failures, such as underhead and keeper fracture [72], which are caused by their low tensile strength.

Additionally, some powdered metal such as iron-based sintered alloy was applied on valve inserts [73]. With the trend of the cast iron engine head being replaced by an aluminum engine block, research [74] developed thermal-sprayed, composite $\text{Fe}/\text{Fe}_3\text{O}_4/\text{Ni}/\text{NiO}/\text{CrO}$ coatings on aluminum engine heads to replace powdered metal valve seat inserts.

Recently, Toyota developed a low-cost process that is based on powder metallurgy starting with sponge titanium boride powder to fabricate lightweight titanium valves for passenger cars [39].

Titanium aluminides such as TiAl (called gamma) have useful properties for engineering applications such as for automotive engine poppet valves [75]. Table 19.5 compares the properties of 21-2N (0.55C; 8.25Mn; 0.25Si; 20Cr; 2.25Ni), which is commonly used as material for exhausted valve steel and TiAl.

Calculations showed that the use of solid TiAl valves to replace solid steel valves would permit increasing the limiting speed of a push rod engine from 6000 to 6900 r/min in a large engine. In some cases, plasma carburizing was used to improve the wear resistance, but in others, the valves were tested uncoated. The tests show that the TiAl valves give a power increase over steel valves of approximately 8 % because of the increase in revolutions per minute allowed. If high load is applied on the valves, a hard coating on the valve tips and a wear coating on the valve stems can be necessary. There are various coatings that have been used,

TABLE 19.5—Comparative Properties between TiAl and 21-2N Steel

Properties	TiAl	21-2N
Density (g/cm ³)	3.9	7.7
Tensile strength (MPa)	560 (room temperature) 600 (760°C)	1090 (room temperature) 400 (760°C)
Thermal conductivity (W/m·K) at 760°C	28	25
Fatigue strength, 108 cycles 440°C (MPa) 816°C (MPa)	326 22	— 165
Hardness (BHN)	260 (room temperature) 240 (760°C)	300 (room temperature) 140 (760°C)
Modulus (GPa) at 24°C	170	200
Coefficient of thermal expansion (μm/m)	12.2	18.4

including nitriding, CVD coatings, plasma carburizing, and platings. Titanium aluminide is a promising material to be used in this application, although the price is still higher than that of 21-2N steel.

19.3.5.2 CAM AND FOLLOWER

Cams and tappets (or cam follower systems) are used to transform the camshaft's rotational movement to reciprocating movement of the inlet and exhaust valves in an automotive valvetrain. Several types of wear occur at the interface between the cam and sliding type follower where the most severe wear conditions such as higher contact pressure, presence of boundary lubrication, lower allowable wear limits, and other factors exist for engine components. The patterns and causes of wear can be broadly divided into two groups [76]. One is characterized by sliding contact, such as in the case of swing-arm- (end pivot) and rocker-arm-type followers, and shows mainly scuffing wear caused by adhesion. The other is characterized by rolling contact, which is dominant in the case of tappet- and roller-type followers and shows mainly pitting wear caused by fatigue. Therefore, under heavy duty, cam and tappets suffer from burnishing (because of adhesive/abrasive wear processes), scuffing (because of severe adhesive wear processes), and pitting (because of fatigue wear processes).

Cam, cam tappets, rocker arms, and camshaft materials are generally made of hardenable cast iron or forged steel. The most critical interface in the valvetrain is between the cam and follower, which usually are manufactured of iron and steel. Materials and surface treatments have been investigated to increase wear performance. Lubricant additives were developed to produce wear-resistant surface films by chemical reactions, including zinc dialkylphosphates (ZDDP or ZDTP) [34]. Phosphate coatings are commonly used for break-in.

Kano et al. [77] investigated the wear-resistant properties of several series of valvetrain materials, such as ferro-based sintered powder metals, alloyed cast irons, and silicon nitride ceramics. The results indicated that cam follower wear decreased as the matrix hardness, transverse strength,

the roundness ratio of the hard carbide shape, the hardness, and the hard carbide area ratio increased and the average particle size decreased. Therefore, the wear of cam and cam followers can be reduced considerably by selecting hard material combinations, by hardening the cam material by heat or thermochemical treatments, or by applying coatings. Tappet materials are usually made of hardened high carbon, chromium, or molybdenum types of carburized low-alloy steels. The most common tappet material in automotive applications is gray hardenable cast iron containing chromium, molybdenum, and nickel or chilled cast iron. Nowadays, many types of wear-resistant materials such as ferro-based powder metals with a high chromium content, high-chromium cast irons, and silicon nitride ceramics have been adopted for cam followers, especially for sliding rocker arm pads [78].

The contact at the cam/follower interface is the most important because this is where sliding-dominated motion takes place. Oil film thickness is very small (~1 μm), and direct contact between surface asperities can occur, leading to well-known damage in surfaces, including pitting and scuffing [3]. The most severe area in the operating conditions is the cam nose. Applying an antiwear low-friction coating would result in a friction reduction by 30 %, which implies a reduction of the fuel consumption on the order of 1 % [3].

19.4 DRIVETRAIN GROUP

19.4.1 Power Transmission Gears

Automotive powertrain requirements necessitate that individual components have mechanical properties adequate to ensure system reliability up to 250,000 km. Multiple requirements of high static strength, bending fatigue, and rolling contact fatigue durability led gear designers to use forged and machined wrought steels to ensure long-term vehicle reliability.

Moreover, transmission gears for automotive applications are complex in shape and require very high geometrical accuracy in terms of gear quality as well as very high mechanical performance in terms of durability of tooth flank and root.

Considerable research work is underway to explore the possibility of using high-density steels from powder metallurgy in applications traditionally fulfilled by wrought steels. Powder metallurgy is a processing technology that aims at obtaining metal products by the compaction of metal powders into desired shapes and then sintering at the proper temperature. Powder metallurgy sintered parts can be made from many different materials and can create parts in a wide choice of shapes and accurate dimensions. The strongest proficiencies that make powder metallurgy applications competitive compared with other technologies were recognized as self-lubrication, cost and energy effectiveness, near-net-shape products as an outcome, the possibility of porosity control, and material flexibility.

The mechanical properties of powder metallurgy ferrous materials are related to microstructure and density. In the as-sintered condition, most of the ipo-eutectoidic ferrous powder metallurgy materials show a ferritic-pearlitic microstructure, with different ratios depending on the carbon content. That is why a secondary heat treatment is suggested to obtain high mechanical properties with related problems such as an increase in component production cost and loss of part precision. Sinter hardening is a fast-growing

powder metallurgy process in which the cooling rate after sintering is fast enough to produce high-strength materials with an as-sintered martensitic microstructure [79–81]. The parts are “quenched” directly inside of the sintering furnace during the cooling stage. The cooling rate is high enough to prevent ferritic and pearlitic transformations, therefore allowing the transformation from austenite to martensite, or, in the long run, to bainite. The main benefits of this innovative process are

- Elimination of the secondary heat treatments, with considerable cost advantages;
- Reduced distortion of the parts, because of slower cooling rates, compared with oil quenching; and
- Oil-free parts, because cooling is performed in the same gaseous atmosphere used for sintering.

Powders formulated for sinter hardening must possess a hardenability that is high enough to prevent perlitic transformations (and bainitic as well) at the cooling rates usually achieved in suitable sintering furnaces (a few Celsius degrees per second, or between 850 and 400°C). The ability of these materials to form martensite during the cooling stage is related to their chemical composition and to the local cooling rate. The specific powder grades contain hardenability-enhancing elements (e.g., nickel, molybdenum, copper, and, in many cases, manganese and chromium) but in low percentages. The choice and the content of alloying elements depend on the application requirements. To increase hardenability, these alloying elements must be in solid solution. However, although beneficial to hardenability, the elements in solid solution reduce the compressibility because of the inevitable outcome of solid solution hardening. To optimize the manufacturing costs and performance of sinter-hardened parts, the combined effects of alloying elements, their content, and the nature of the base powder on compressibility and hardenability must be properly analyzed and balanced.

To increase the mechanical performance of the parts, new technologies were recently introduced (e.g., warm compaction and high-velocity compaction [82]) to increase the green density, high sintering temperature for increasing the sintering degree [83] and new heat and surface treatments for improving the bulk and surface mechanical properties [84–87]. Moreover, surface rolling and shot peening were proposed to increase the density of the parts surface and then thermochemical heat treatments such as nitriding or case-hardening were superimposed to increase the rolling fatigue strength [86,88–90].

19.4.2 Transmission

The tribological characteristics of the transmission clutch band are crucial because they control transmission shift performance and clutch durability. From a tribological standpoint, an automatic transmission clutch consists of two basic elements: the friction lined clutch plates and the steel reaction plates. The clutch plate assembly consists of three major components: a steel core, an adhesive coating, and the friction facings.

In most U.S. automotive clutches, the steel core is a part onto which the friction facings are bonded. The core is blanked from medium carbon steel with a Rockwell C hardness minimum of 24. The core hardness ensures maximum tooth contact area. The minimum compressive load requirement can reduce the potential for wear or fretting on

both spline surfaces. The friction facing is bonded to one or both sides of the steel core with an adhesive. The adhesive, a thermosetting organic resin, is selected to withstand high shear forces and a wide range of operating temperatures.

The friction material must have the required friction characteristics for effective engagement and a pleasing (to the customers) shifting of gears and durability. It also must withstand a broad range of operating temperatures as well as high shear forces and compressive loads.

19.4.3 Brakes

Performance of a brake system depends on the interaction of gray iron rotors (or drums) with brake linings at their sliding interfaces.

Car brakes experience dry sliding contact at roughly 50 % of the speed of the car. A typical front brake pad is approximately 8 cm long and 5 cm wide, and the brake disk has a diameter of 28 cm. The pad covers approximately 10–15 % of the corresponding rubbing surface of the disk. During normal, relatively soft brakings, the force pressing the pad against the disk is approximately 5 kN, resulting in a nominal pressure at the pad surface just above 1.2 MPa. In extreme situations, the pressure could be close to 10 MPa. During hard brakings, the power dissipation on a brake pad easily exceeds 30 kW. These high-power densities result in very high surface temperatures and thus put special demands on the friction materials.

The interaction between the two disparate materials involves mechanical and chemical actions on a molecular level, and the interaction at the rubbing surface is very complicated in nature. Gray cast iron with the microstructure of Type A graphite flakes in a predominantly perlitic matrix has long been used for brake rotors and drums since the early stage of vehicle development. On the other hand, the linings have experienced major changes in their formulations during the last 2 decades because of the health issues related to asbestos fibers, and there has been a significant effort to develop high-performance nonasbestos linings [91].

During the last several decades, a great deal of effort has been devoted to improve the friction performance of brake rotors (or drums). The effort includes the development of nonferrous materials such as copper alloys, aluminum MMCs, and carbon composites as new candidates. However, gray cast iron is mainly used for automotive brake rotors because of its excellent damping capacity, high thermal conductivity, easy fabrication, and, in particular, low cost.

Anderson [92] reported that fine graphite flakes reduced the wear of the rotor and lining. Zhang et al. [93] studied the tribological properties of cast iron in terms of phosphorus content and graphite morphology. They concluded that phosphorous containing cast iron having compacted graphite morphology showed the highest coefficient of friction and the lowest wear loss. Hecht et al. [94] found that the thermal diffusivity of gray iron is influenced by a change in chemical composition and showed a linear relationship between thermal diffusivity and carbon equivalent (or maximum flake length).

Cho et al. [91] demonstrated that the amount of free ferrite (and perlite) on the gray iron disk did not affect the coefficient of friction. Moreover, the coefficient of friction increased with the graphite area percentage on the gray iron disk samples, and the increment was more pronounced

in the case of using steel-containing linings. In the case of nonsteel linings, fade resistance was improved with increasing the graphite content on the gray iron disks, suggesting a possible overcoming of the inferior fade resistance of nonsteel linings by using gray iron rotors with a high graphite content.

The lining materials of automotive brakes are usually composites formed by hot compaction of coarse powders, including many different components [95]. These components include

- A binder, which keeps the other components together and forms a thermally stable matrix. Thermosetting phenolic resins are commonly used, often with the addition of rubber for increased damping properties.
- Structural materials, which provide mechanical strength. Metal, carbon, glass, or Kevlar® fibers, or a combination of any of these, are typically used. More rarely, different mineral and ceramic fibers can be used.
- Fillers, mainly to reduce cost but also to improve manufacturability. Different minerals such as mica and vermiculite are often used. Barium sulfate is another commonly used filler.
- Frictional additives, which are added to ensure stable frictional properties and to control wear rates of pad and disk. Solid lubricants such as graphite and different metal sulfides are used to stabilize the coefficient of friction, primarily at elevated temperatures. Abrasive particles, typically alumina and silica, increase the coefficient of friction and the disk wear. The purpose of the latter is to give a better defined rubbing surface by removing iron oxides and other undesired surface films from the disk.

Car manufacturers are tending to design more prestigious and sports-class vehicles, which require braking systems that provide more braking power than conventional braking systems. Accordingly, new materials are being introduced into braking systems (particularly in the case of disk materials; e.g., carbon-ceramic C/C SiC composites) that can provide more friction and can operate at higher temperatures. It is clear that new counter-pad materials that can resist higher temperatures compared with conventional organic-based materials need to be used with these ceramic-based materials (e.g., MMCs) [96,97].

In the last years some studies were performed to investigate the origin of the particulate emissions on paved roadways. Intensive mass and chemical measurements were performed at roadside locations in Reno, NV, and Durham/Research Triangle Park, NC [98], and they showed that resuspended road dust and tailpipe emissions are the dominant mechanisms contributing significantly to the total PM_{10} and $PM_{2.5}$ (particulate matter less than or equal to 10 and 2.5 μm in aerodynamic diameter, respectively) emission factors, respectively. No tirewear was seen at any sampling location, and only small contributions from brake wear were observed at locations where strong braking occurs.

19.5 NEW PROSPECTIVE MATERIALS: THE TRIBOACTIVE MATERIALS

Triboactive materials, or triboactive materials, is a term that describes a beneficial reaction between the surface and the lubricant or the ambient, thus indicating a more overall functional approach. Oxides, hydroxides, or hydrates cover this understanding [99].

They can be used potentially for automotive applications as cylinder liner or ring coatings or both.

Woydt and collaborators [99] describe results obtained from tribological tests, comparing the behaviors of cast iron versus triboactive materials. $Ti_{n-2}Cr_2O_{2n-1}$ and (Ti, Mo)(C,N)-23Ni Mo were applied as coating by plasma thermal spray. $Ti_{n-2}Cr_2O_{2n-1}$ showed an overall wear resistance comparable with gray cast iron with high carbon content and liner wear reduction when matched with molybdenum-based rings. However, the best wear performance was obtained for $Ti_{n-2}Cr_2O_{2n-1}$ coated rings with smooth machined HVOF (Ti,Mo)(C,N) liner coating.

Different plasma-sprayed triboactive coatings have been deposited on cast iron piston rings and the tribological properties were studied [100]. Lubricants formulated based on a blend of hydrocarbon with esters (HCEs) were used in this experiment. Oil A and oil B were HCEs based on the same base fluid composition but differed in additives. Water-soluble polyalkylene glycols (PAGs) and oil-soluble polypropylene glycols (PPGs) were also considered. Table 19.6 summarizes part of the results. Tests were performed under

TABLE 19.6—Cylinder Liner-Piston Rings Test Results

Piston Rings	Lubricants	Time to Failure (min)	The Highest Friction Load at Which No Failure Occurs (N)	Type of Failure
Chrome plated $Ti_{n-2}Cr_2O_{2n-1}$	Reference oil	28 36 29	1300 1800 1400	Stroke <0.3 mm Stroke <0.3 mm Stroke <0.3 mm
Chrome plated $Ti_{n-2}Cr_2O_{2n-1}$	Oil A	30 32 41	1400 1600 2000	Stroke <0.3 mm Stroke <0.3 mm No failure
Chrome plated $Ti_{n-2}Cr_2O_{2n-1}$	Oil B	32 31 36 38 41	1500 1500 1800 1900 2000	Stroke <0.3 mm Stroke <0.3 mm Stroke <0.3 mm Stroke <0.3 mm No failure
Chrome plated $Ti_{n-2}Cr_2O_{2n-1}$	PPG	29 35 34	1500 1700 1600	Stroke <0.3 mm Stroke <0.3 mm Stroke <0.3 mm
Chrome plated $Ti_{n-2}Cr_2O_{2n-1}$	PAG	24 25 41	1200 1200 2000	Stroke <0.3 mm Stroke <0.3 mm No failure

extreme pressure conditions and failure was considered when the first microwelding appeared.

$Ti_{n-2}Cr_2O_{2n-1}$ and $Ti_{n-2}O_{2n-1}$ coatings deposited by plasma showed good tribological properties in the piston ring/cylinder liner simulation tests. However, in the engine test, because of its brittleness, $Ti_{n-2}Cr_2O_{2n-1}$ coating was detached, therefore demonstrating for $Ti_{n-2}O_{2n-1}$ the best performance and potentially being more economical. The most important conclusions from this work are related to the combinations of lubricant and triboreactive coating materials. Triboreactive coatings with polar lubricants seem to be synergistic, improving the extreme pressure properties and wear resistance.

19.6 CONCLUSION

This chapter reviewed the bulk materials and engineered surfaces for tribology in automotive applications. It is well known that one of the most important contributions to engine efficiency can be achieved by reducing the weight of the rotating and reciprocating engine parts. This requirement justifies the selection of lighter materials for manufacturing engine components, such as aluminum, titanium, and magnesium alloys, which generally show poor tribological properties to resist to the high values of the local contact pressure that can be reached during operation. Hence, automotive engine components generally need specific surface modifications, which were described and discussed in this chapter for each specific application, also considering the characteristics of the working environment.

Moreover, the selection of materials for the power transmission group was introduced, with specific reference to gears and clutches. Finally, because car manufacturers are tending to design more prestigious vehicles requiring braking systems that provide more braking power, new materials for brakes, particularly for disks, were described.

In the last part of the chapter, tribo(re)active materials (i.e., the materials showing beneficial reactions between the surface and the lubricant or the ambient) were introduced. They can potentially be used for automotive applications as cylinder liner or ring coatings or both, and in the chapter, some experimental results of applications were presented.

REFERENCES

- [1] Andersson, B.S., 1991, "Company Perspectives in Vehicle Tribology—Volvo." In: *17th Leeds-Lyon Symposium on Tribology-Vehicle Tribology*, Tribology Series, 18, Elsevier, Oxford, UK, pp. 503–506.
- [2] Nakasa, M., 1995, "Engine Friction Overview." In *Proceedings of the International Tribology Conference*, Yokohama, Japan.
- [3] Merlo, A.M., 2003, "The Contribution of Surface Engineering to the Product Performance in the Automotive Industry," *Surf. Coat. Technol.*, Vol. 174–175, pp. 21–26.
- [4] Dearnley, P.A., Neville, A., Turner, S., Scheibe, H.-J., Tietema, R., Tap, R., Stüber, M., Hovsepian, P., Layyous, A., and Stenbom, B., 2010, "Coatings Tribology Drivers for High Density Plasma Technologies," *Surf. Eng.*, Vol. 26, pp. 80–96.
- [5] Bulloch, J.H., and Henderson, J.L., 1991, "Some Considerations of Wear and Hardfacing Materials," *Int. J. Pres. Ves. Piping*, Vol. 46, pp. 251–267.
- [6] "Types of Thermal Spray Coating Processes." Available at <http://www.thomasnet.com/articles/chemicals/process-of-thermal-spray-coatings> (accessed December 29, 2009).
- [7] Cabeo, E.R., Laudien, G., Biemer, S., Rie, K.T., and Hope, S., 1999, "Plasma-Assisted Boring of Industrial Components in a Pulsed DCC Glow Discharge," *Surf. Coat. Technol.*, Vol. 116–119, pp. 229–233.
- [8] ASM International, 1992, "Surface Treatment and Coatings for Friction and Wear." In *Friction, Lubrication and Wear Technology*, ASM Handbook 18, ASM International, Materials Park, OH, pp. 1686–1878.
- [9] ASM International, 1991, "Surface Hardening of Steel." In *Heat Treating*, ASM Handbook 4, ASM International, Materials Park, OH, pp. 606–1029.
- [10] DeKock, J., 2004, "Laser Heat Treating Advances for the Gear Industry," *Gear Solutions*, pp. 49–54.
- [11] Krauss, G., 1992, "Advanced Surface Modifications of Steels," *J. Heat Treating*, Vol. 9, pp. 81–89.
- [12] Herring, D.H., 2007, "Heat Treating Heavy Duty Gears," *Gear Solutions*, pp. 58–75.
- [13] Hoffmann, F.T., and Mayer, P., 1992, "Nitriding and Nitro-carburizing." In *Friction, Lubrication and Wear Technology*, ASM Handbook 18, ASM International, Materials Park, OH, pp. 1783–1796.
- [14] Chattopadhyay, R., 2001, *Surface Wear: Analysis, Treatment, and Prevention*, ASM International, Materials Park, OH.
- [15] Priotr, K., Konrad, R.P., Maciej, D., Józef, K., and Prenitlpc, O., 2009, "The Modern Technology for Automotive." In *Proceedings of New Challenges in Heat Treatment and Surface Engineering—Conference in Honor of Professor Bozidar Liscic*, Dubrovnik-Cavtat, Croatia, pp. 165–170.
- [16] Rodionov, A.V., Ryzhov, N.M., Fakhurtdinov, R.S., and Borisov, M.V., 1994, "Enhancement of Bending Strength of Heat-Resistance Steel by Ion Carbonitriding," *Metal Sci. Heat Treat.*, Vol. 36, 5–6, pp. 292–298.
- [17] Nan, C., Northwood, D., Bowers, R.J., and Sun, X., 2010, "Study on the Dimensional Changes and Residual Stresses in Carbonitrided and Ferritic Nitrocarburized SAE 1010 Plain Carbon Steel," *Mater. Sci. Forum*, Vol. 638–642, pp. 829–834.
- [18] Funatani, K., 2006, "Emerging Technology in Heat Treatment and Surface Engineering of Automotive Components," *La Metall. Ital.*, Vol. 2, pp. 67–73.
- [19] Bell, T., 1991, "Gaseous and Nitrocarburizing of Steels." In *Heat Treating*, ASM Handbook 4, ASM International, Materials Park, OH, pp. 954–977.
- [20] Bindumadhavan, P.N., Makesh S., Gowrishnkar, N., Wah, H.K., and Prabhakar, O., 2000, "Aluminizing and Subsequent Nitriding of Plain Carbon Low Alloy Steels for Piston Ring Applications," *Surf. Coat. Technol.*, Vol. 1272–1273, pp. 251–258.
- [21] Holmberg, K., and Matthews A., 1994, *Coatings Tribology*, Tribology Series 28, D. Dowson, Ed., Elsevier Science, Amsterdam, The Netherlands.
- [22] Budinski, K.G., 1996, "Overview of Surface Engineering and Wear." In *Effect of Surface Coatings and Treatments on Wear*, ASTM STP1278, S. Bahadur, Ed., ASTM International, West Conshohocken, PA, pp. 4–21.
- [23] Vinokurov, E.G., Arsenkin, A.M., Gricorovich, K.V., and Bondar, V.V., 2006, "Electrodeposition and Physico-Mechanical Properties of Chromium Coatings Modified with Disperse Particles." *Protect. Metals*, Vol. 42, pp. 290–294.
- [24] Tseluikin, V.N., 2009, "Composite Electrochemical Coatings: Preparation, Structure, Properties." *Protect. Metals Phys. Chem. Surf.*, Vol. 5, pp. 312–326.
- [25] Dearnley, P.A., 2007, "Meeting Tribological Challenges with Surface Engineered Materials," *Tribology*, Vol. 1, pp. 18–27.
- [26] Newby, K.R., 2000, "Functional Chromium Plating. Galvanic (Electrochemical) Coating Materials Furthermore Include Copper (Cu) and Tin (Sn) as Friction-Reducing Coatings for Piston Ring Face Surfaces," *Metal Finish.*, Vol. 98, pp. 223–224.
- [27] Qiu, X., Hamdi, A., Elmoursi, A., and Malaczynski, G., 1996, "Development of Bench Test Methods for the Evaluation of Ion-Implanted Materials: Piston/Bore Application," *Surf. Coat. Technol.*, Vol. 88, pp. 190–196.
- [28] Herman, H., Sampath, S., and McCune, R., 2000, "Thermal Spray: Current Status and Future Trends," *MRS Bull.*, July, pp. 17–25. Available at <http://www.mrs.org/publications/bulletin>.
- [29] Edrissy, A., Perry, T., and Alpas, A.T., 2005, "Investigation of Scuffing Damage in Aluminum Engines with Thermal Spray Coatings," *Wear*, Vol. 259, pp. 1056–1062.
- [30] Vetter, J., Crummenauer, J., Barbezat, G., and Avissar J., 2008, *Surface Treatments of Automotive Parts Research and*

- Applications. Vacuum's Best VIP.* Wiley-VCA Verlag, Weinheim, Germany, pp. 47–52.
- [31] Vetter, J., Barbezat, G., Crummenauer, J., and Avissar, J., 2005, "Surface Treatment Selections for Automotive Applications," *Surf. Coat. Technol.*, Vol. 200, pp. 1962–1968.
 - [32] Harrison, K., 2002, "Improved Performance in Car Engines through Plasma Sprayed Coatings," *Sulzer Metco*, June 1, 2002.
 - [33] Ootani, T., Yahata, N., Fujiki, A., and Ehira, A., 1995, "Impact Wear Characteristics of Engine Valve and Valve Seat Insert Materials at High Temperature," *Wear*, Vol. 188, pp. 175–184.
 - [34] Tung, S.C., and McMillan M.L., 2004, "Automotive Tribology Overview of Current Advances in Challenges for the Future," *Tribology Int.*, Vol. 37, pp. 517–536.
 - [35] Barbezat, G., 2006, "Application of Thermal Spraying in the Automotive Industry," *Surf. Coat. Technol.*, Vol. 201, pp. 2028–2031.
 - [36] Barbezat, G., 2006, "Thermal Spray Coatings for Tribological Applications in the Automotive Industry," *Adv. Eng. Mater.*, Vol. 8, pp. 678–681.
 - [37] Barbezat, G., 2001, "The State of the Art of Internal Plasma Spraying on Cylinder Bore in AlSi Cast Alloys," *Int. J. Auto. Technol.*, Vol. 2, pp. 47–52.
 - [38] Öner, C., Hazar, H., and Nursoy, M., 2009, "Surface Properties of CrN Coated Engine Cylinders," *Mater. Design*, Vol. 30, pp. 914–920.
 - [39] Funatani, K., 2004, "Heat Treatment of Automotive Components: Current Status and Future Trends," *Trans. Indian Inst. Met.*, Vol. 57, pp. 381–396.
 - [40] Chawla, N., 2006, "Metal Matrix Composites in Automotive Applications," *Adv. Mater. Process.*, pp. 29–31.
 - [41] Sato, A., and Mehrabian, R., 1976, "Aluminum Matrix Composites: Fabrication and Properties," *Metall. Trans. B*, Vol. 7, pp. 443–451.
 - [42] Surappa, M.K., Prasad, S.V., and Rohatgi, P.K., 1982, "Wear and Abrasion of Cast Al-Alumina Particle Composites," *Wear*, Vol. 77, pp. 295–312.
 - [43] Surappa, M.K., and Rohatgi, P.K., 1981, "Preparation and Properties of Cast Aluminum-Ceramic Particle Composites," *J. Mater. Sci.*, Vol. 16, pp. 983–993.
 - [44] Hosking, F.M., Portillo, F.F., Wunderlin, R., and Mehrabian, R., 1982, "Composites of Aluminum Alloys: Fabrication and Wear Behaviour," *J. Mater. Sci.*, Vol. 17, pp. 477–498.
 - [45] Wang, Y., and Tung, S.C., 1999, "Scuffing and Wear Behaviour of Aluminum Piston Skirt Coating against Aluminum Cylinder Bore," *Wear*, Vol. 225–229, pp. 1100–1108.
 - [46] Malaczynski, G.W., Handi, A.H., Elmoursi, A.A., and Qiu, X., 1997, "Diamond-Like Carbon Coating for Aluminum 390 Alloy-Automotive Application," *Surf. Coat. Technol.*, Vol. 93, pp. 280–286.
 - [47] Massey, I.D., MacQuarrie, N.A., Coston, N.F., and Eastham, D.R., 1990, "Development of Crankshaft Bearing Materials for Highly Loaded Applications. Vehicle Tribology." In *Proceedings of 17th Leeds-Lyon Symposium Tribology*, Leeds Tribology Series 18, pp. 43–52.
 - [48] Enomoto, Y., and Yamamoto, T., 1998, "New Materials in Automotive Tribology," *Tribology Lett.*, Vol. 5, pp. 13–24.
 - [49] Zhang, Z.Z., 1997, "Tribological Properties of Metal-Plastic Multilayer Composites under Oil Lubricated Conditions," *Wear*, Vol. 210, pp. 195–203.
 - [50] Kim, S.S., Park, D.C., and Lee, D.G., 2004, "Characteristics of Carbon Fiber Phenolic Composite for Journal Bearing Materials," *Composite Struct.*, Vol. 66, pp. 359–366.
 - [51] Picas, J.A., Forn, A., and Matthau, G., 2006, "HVOF Coatings As an Alternative to Hard Chrome for Piston and Valves," *Wear*, Vol. 261, pp. 477–484.
 - [52] Ahn, H.-S., Kim, J.-Y., and Lim, D.-S., 1997, "Tribological Behaviour of Plasma-Sprayed Zirconia Coatings," *Wear*, Vol. 203–204, pp. 77–87.
 - [53] Skopp, A., Kelling, N., Woydt, M., and Berger, L.M., 2007, "Thermally Sprayed Titanium Suboxide Coatings for Piston Ring/Cylinder Liners under Mixed Lubrication and Dry-Running Conditions," *Wear*, Vol. 262, pp. 1061–1070.
 - [54] Etsion I., 2005, "State of the Art in Laser Surface Texturing," *J. Tribol. Trans ASME*, Vol. 127, pp. 632–638.
 - [55] Etsion, I., and Sher E., 2009, "Improving Fuel Efficiency with Laser Surface Textured Piston Rings," *Tribology Int.*, Vol. 42, pp. 542–547.
 - [56] "Process for Electodeposition of a Chromium Coating Containing Solid Inclusions and Plating Solution Employed in this Process," U.S. Patent No. 5,868,917, 1999.
 - [57] Narasimhan, S.L., and Larson J.M., 1985, *Valve Gear Wear and Materials*, SAE Paper No. 851497, SAE, Warrendale, PA.
 - [58] Van Dissel, R., Barber, G.C., Larson, J.M., and Narasimhan, S.L., 1989, *Engine Valve Seat and Insert Wear*, SAE Paper No. 892146, SAE, Warrendale, PA.
 - [59] Wang, Y.S., Schaefer, S.K., Bennett, C., and Barber, G.C., 1995, *Wear Mechanisms of Valve Seat and Insert in Heavy Duty Diesel Engines*, SAE Paper No. 952476, SAE, Warrendale, PA.
 - [60] Godfrey, D., and Courtney, R.L., 1971, *Investigation of the Mechanism of Exhaust Valve Seat Wear in Engines Run on Unleaded Gasoline*, SAE Paper No. 710356, SAE, Warrendale, PA.
 - [61] Chaudhuri, A., 1973, *Hot Corrosion of Diesel Engine Exhaust Valves*, SAE Paper No. 730679, SAE, Warrendale, PA.
 - [62] Wang, Y.S., Narasimhan, S., Larson, J.M., Larson, J.E., and Barber, G.C., 1996, "The Effect of Operating Conditions on Heavy Duty Engine Valve Seat Wear," *Wear*, Vol. 201, pp. 15–25.
 - [63] National Institute of Science and Technology (NIST), 1995, *Engine Materials and Tribology Workshop*, Gaithersburg, MD, April 4–7.
 - [64] Ootani, T., Yahata, N., Fujiki, A., and Ehira, A., 1995, "Impact Wear Characteristics of Engine Valve and Valve Seat Insert Materials at High Temperature," *Wear*, Vol. 188, pp. 175–184.
 - [65] Narasimhan, S.L., and Larson, J.M., 1985, *Valve Gear Wear and Materials*, SAE Paper No. 851497, SAE, Warrendale, PA.
 - [66] Van Dissel, R., Barber, G.C., Larson, J.M., and Narasimhan, S.L., 1989, *Engine Valve Seat and Insert Wear*, SAE Paper No. 892146, SAE, Warrendale, PA.
 - [67] Wang, Y.S., Schaefer, S.K., Bennett, C., and Barber, G.C., 1995, *Wear Mechanisms of Valve Seat and Insert in Heavy Duty Diesel Engines*, SAE Paper No. 952476, SAE, Warrendale, PA.
 - [68] Raja, B.V.R., Pal, N., Talwar, P.L., and Jayaswal, N.P., 2005, *Engineering Steels for Automobile Applications*, Steel World, Mumbai, India.
 - [69] Wang, Y.S., Narasimhan, S., and Larson, J.M., 1996, "A Review of Ceramic Tribology and Application of Si-Based Ceramics to Engine Valves/Seat Inserts," *J. Auto. Eng.*, Vol. 304, pp. 330–342.
 - [70] Lumby, R.J., Hodgson, P., and Cother, N.E., 1985, *Syalon Ceramics for Advanced Engine Components*, SAE Paper No. 850521, SAE, Warrendale, PA.
 - [71] Kabat, D.M., Garwin, I.J., and Hartsock, D.L., 1988, *Ceramic Valve Analysis, Reliability and Test Results*, SAE Paper No. 880670, SAE, Warrendale, PA.
 - [72] Asnani, M., and Kuonen, F.L., 1985, *Ceramic Valve and Seat Insert Performance in a Diesel Engine*, SAE Paper No. 850358, SAE, Warrendale, PA.
 - [73] Rodrigues, H., 1997, "Sintered Valve Seat Inserts and Valve Guides: Factors Affecting Design, Performance and Machinability." In *Valve Train System Design and Materials*, ASM International, Materials Park, OH.
 - [74] Popoola, O.O., Reatherford, L.V., and McCune, R.C., 1998, "Process and Materials Development for Adherently Sprayed Valve Seats on Aluminum Engine Heads," *J. Auto. Eng.*, Vol. 329, pp. 201–208.
 - [75] Chandley, D., 2000, "Use of Gamma Titanium Aluminide for Automotive Engine Valves," *Metall. Sci. Technol.*, Vol. 18, pp. 8–11.
 - [76] Wang, Y.S., Narasimhan, S., Larson, J.M., Larson, J.E., and Barber, G.C., 1996, "The Effect of Operating Conditions on Heavy Duty Engine Valve Seat Wear," *Wear*, Vol. 201, pp. 15–25.
 - [77] Kano, M., and Tanimoto, I., 1991, "Wear Mechanism of High Wear-Resistant Materials for Automotive Valve Trains," *Wear*, Vol. 151, pp. 83–89.
 - [78] Kato, M., and Kimura, Y., 1993, "Quantitative Analysis of Cam Follower Wear in Relation to Various Material Properties," *Wear*, Vol. 162–164, pp. 897–905.
 - [79] Rivolta, B., Silva, G., Bocchini, G.F., Poggio, E., Pinasco, M.R., and Ienco, M.G., 2004, "Microstructural and Mechanical

- Characterization of Some Sinter Hardening Alloys and Comparisons with Heat Treated Pm Steels," Powder Metall., Vol. 47, pp. 343–351.
- [80] Bocchini, G.F., Pinasco, M.R., Rivolta, B., and Silva, G., 2007, "Sinter Hardening of Low-Alloy Steels: Influence of Part Geometry and Physical Properties of the Material," Int. J. Mater. Prod. Technol., Vol. 28, pp. 312–337.
- [81] Rivolta, B., Gerosa, R., Tavaschi, A., Silva, G., and Bergmark, A., 2008, "Crack Initiation and Propagation in Chromium Pre-Alloyed PM-Steel under Cyclic Loading," Eng. Fracture Mech., Vol. 75, pp. 750–759.
- [82] Skoglund, P., 2001, "High Density PM Parts by High Velocity Compaction," Powder Metall., Vol. 44, pp. 199–201.
- [83] Marcu, T., Molinari, A., Straffellini, G., and Berg, S., 2005, "Microstructure and Tensile Properties of 3%Cr-0.5%Mo High Carbon PM Sintered Steels," Powder Metall., Vol. 48, pp. 139–143.
- [84] Molinari, A., Tesi, B., Bacci, T., and Pradelli, G., 1993, "Low Temperature Ion-Nitriding of Fe-Mo-C Sintered Steels," J. Physique, Vol. 3, pp. 949–954.
- [85] Stagno, E., Pinasco, M.R., Palombarini, G., Ienco, M.G., and Bocchini, G.F., 1997, "Behaviour of Sintered 410 Low Carbon Steels Towards Ion Nitriding," J. Alloys Comp., Vol. 247, pp. 172–179.
- [86] Rivolta, B., Tavaschi, A., Alzati, L., and Engström, U., 2008, "Wear Resistance of Gas Nitrided Astaloy CrL™ Sintered Steel." Paper presented at the World Congress PM2008, Washington DC, June 8–12.
- [87] Menapace, C., Stoyanova, V., Cislighi, L., and Molinari A., 2008, "Effect of Plasma Nitrocarburising on Fatigue Resistance of Low Alloy Cr-Mo Sintered Steel," Powder Metal., Vol. 51, pp. 310–317.
- [88] Jandeska, J., Slattery, R.H., Haneiko, J.F., Rawlings, A., and King, P., 2006, "Rolling-Contact Fatigue: Performance Comparison of Surface-Densified, Powder-Forged, and Wrought Steels," Int. J. Powder Metal., Vol. 42, pp. 57–64.
- [89] Haneiko, F., Rawlings A., King P., and Poszmik G., 2007, "Surface Densification Coupled with Higher Density Processes Targeting High-Performance Gearing," Mater. Sci. Forum, Vol. 534–536, pp. 317–320.
- [90] Engstrom, U., Johansson, P., Bengtsson, S., Dizdar, S., and Molin L., 2007, "Opportunities for High Performance PM Gears in Automotive Applications." Paper presented at PMAsia2007, Shanghai, People's Republic of China.
- [91] Cho, M.H., Kim, S.J., Basch, R.H., Fash, J.W., and Jang, H., 2003, "Tribological Study of Gray Cast Iron with Automotive Brake Linings: The Effect of Rotor Microstructure," Tribology Int., Vol. 36, pp. 537–545.
- [92] Anderson, A.E., 1992, *Friction and Wear of Automotive Brakes*, ASM Handbook 18, ASM, Materials Park, OH.
- [93] Zhang, Y., Chen, Y., He, R., and Shen, B., 1993, "Investigation of Tribological Properties of Brake Shoe Materials-Phosphorous Cast Irons with Different Graphite Morphologies," Wear, Vol. 166, pp.179–186.
- [94] Hecht, R.L., Dinwiddie, R.B., Poter, W.D., and Wang, A.H., 1996, *Thermal Properties of Gray Cast Irons*, SAE Technical Paper 962126, SAE, Warrendale, PA.
- [95] Eriksson, M., Bergman, F., and Jacobson, S., 2002, "On the Nature of Tribological Contact in Automotive Brakes," Wear, Vol. 252, pp. 26–36.
- [96] Jacko, M.G., Tsang, P.H.S., and Rhee, S.K., 1984, "Automotive Friction Materials Evolution during the Past Decade," Wear, Vol. 100, pp. 503–515.
- [97] Kermc, M., Kalin, M., and Vizintin, J., 2005, "Development and Use of an Apparatus for Tribological Evaluation of Ceramic-Based Brake Materials," Wear, Vol. 259, pp. 1079–1087.
- [98] Abu-Allaban, M., Gillies, J. A., Gertler A. W., Clayton, R., and Proffitt D., 2003, "Tailpipe, Resuspended Road Dust, and Brake-Wear Emission Factors from on-Road Vehicles," Atmos. Environ., Vol. 37, pp. 5283–5293.
- [99] Woydt, M., Criqui, B., Desplanches, G., and Linneman, T., 2008, "Zero Wear Concept Using Bionotox and Polymer-Free Engine Oils with Triboreactive Materials," Ind. Lubric. Tribology, Vol. 60, pp. 14–23.
- [100] Igartua, A., Fernandez, X., Areitioaurtena, O., Seyfert, C., Rausch, J., Illarramendi, I., Berg, M., Schultheib, H., Duffau, B., Plouseau, S., and Woydt, M., 2009, "Biolubricants and Triboreactive Materials for Automotive Applications," Tribology Int., Vol. 42, pp. 561–568.

Surface Analysis and Tribochemistry of Automotive Engine Components

Ardian Morina¹ and Hongyuan Zhao¹

20.1 INTRODUCTION

20.1.1 Engine Efficiency and Surface Science

There are 820 million vehicles in the world today, and with the progressive growth of the automotive sector in developing countries such as Brazil, China, India, etc., the number of vehicles worldwide is predicted to reach 1 billion by 2020². Passenger cars and commercial light vehicles have been estimated¹ to account for 20 % of the total CO₂ delivered into the atmosphere from hydrocarbon sources in the United States and other developed countries, indicating the level of impact of the automotive sector on the environment. As such, the technological improvement on fuel economy will have a great impact in reducing the CO₂ emissions. Reduction of mechanical losses in internal combustion (IC) engines as prime drivers in the automotive industry is an action with immediate effect toward increasing the fuel economy through improving engine efficiency.

Powertrain optimization, such as the development of advanced valve train systems (cylinder deactivation, mechanically variable valve trains, etc.), advanced combustion strategies (i.e., controlled autoignition), downsizing engine designs (i.e., highly supercharged engines or displacement reduction), and engine weight reduction are regarded as some of the most viable short-/mid-term strategies toward improving automotive engine fuel economy and CO₂ emission reduction. These strategies require radical changes in the engine design that pose challenges for effective lubrication. As a result of the use of the technologies above, engines are expected to operate in higher temperatures, higher operating speeds, and with tighter mechanical tolerances. More engine components will operate in the boundary and mixed lubrication regime where the asperities of sliding components will come into contact producing wear debris and nascent surfaces that then interact, physically and chemically, with the lubricating oil chemistry. Chemical interaction of lubricated surfaces with the lubricant chemistry, known as tribochemistry [1], is essential for maintaining low friction and wear in the boundary/mixed lubrication regime. In addition, engine downsizing will require engine oils to lubricate nontraditional materials/coatings (nonferrous) with fewer amounts of engine oil and a longer oil drain interval. All of the above, coupled with the limitation by environmental legislations on using some well-proven chemical additives for engine oils and the require-

ment for increasing fuel economy, place much stress on the oil and require more superior performance from the whole powertrain system. The optimization of engine oil performance in future automotive engines requires a good understanding of the tribochemical processes that occur between its additives and lubricated surfaces.

Automotive engineers, coating developers, and lubricant formulators are increasingly required to be familiar with surface science fundamentals and surface analytical techniques that are used as the tools for determining the physical and chemical characteristics of surfaces, which are important for the optimization of engine lubrication. Therefore, this chapter focuses on reviewing the relevant fundamental information on surface analytical techniques as essential tools for understanding the tribofilm formation processes and their application on studying the tribochemical processes that occur in automotive engines. The objective of this chapter is to provide a valuable information resource for automotive engineers, material scientists, tribologists, and lubricant formulators in their attempt toward assessing the optimized performance of existing lubricants as well as developing new engine lubrication solutions.

20.1.2 Engine Tribology and Tribochemistry

Figure 20.1 shows the main components of a typical automotive engine. Friction reduction in bearings, piston ring/cylinder liner interface, and valve train systems are of great importance for reducing fuel energy losses.

These tribological systems operate in different kinematical conditions, and as such friction losses result in different amounts of power losses. Figure 20.2 shows the power losses in modern passenger cars [3]. The exact energy losses in the valve train and piston assembly vary with the engine model and operating conditions, but, in general, piston assembly friction accounts for 40–60 % of the total mechanical losses in an automotive engine [4]. This indicates the importance of friction reduction in the whole system for improving the engine fuel efficiency and economy. A comprehensive overview of the mechanics of these systems can be found in reference 5.

The role of the engine oil as a lubricant is significant in reducing the power losses and maintaining low wear rates. The functionality of the lubricant in reducing friction losses depends greatly on the lubrication regime in each tribological system. Figure 20.3 shows schematically the lubrication regimes in which the automotive engine tribological systems operate. Automotive bearings operate at high speeds, and as

¹ University of Leeds, UK

² Community Strategy to reduce CO₂ emissions from passenger cars and light-commercial vehicles, COM(2007) 19, http://ec.europa.eu/environment/co2/co2_home.htm.

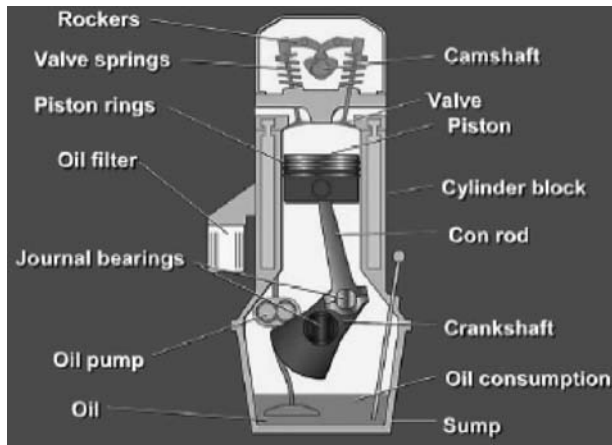


Figure 20.1—Main engine components in an IC engine [2].

a result, their lubrication is in the hydrodynamic regime. In this system, friction losses are mainly due to the lubricant's rheological properties (i.e., viscosity and pressure-viscosity coefficient). In boundary/mixed-lubricated systems (valve train and partly piston ring/liner system), the chemistry of the lubricant becomes of primary importance for maintaining the controlled wear rate and reducing friction. Current engine oils can contain 5–25 % of different chemical additives [6], which are used to enhance existing properties of the base oil or to give new properties. Chemical additives such antiwear, friction modifier, and detergent/dispersant will interact with the surfaces lubricated to form protective surface films called tribofilms. In these systems, the tribochemical processes between the lubricant and the lubricated surfaces will determine the properties of the tribofilms formed and consequently the friction and wear performance.

Because of the change of sliding speeds, lubrication of the piston assembly system varies from the hydrodynamic to the boundary regime [7]. At the middle point of the piston stroke, when the sliding speed reaches its maximum peak, lubricant will form a film for which the thickness and other properties are determined by the rheological properties of the lubricant. In this regime, the lubrication performance will be mainly a function of the viscosity. Toward the top dead center (TDC) and bottom dead center (BDC), the speed reduces and the lubrication now moves from full-film lubrication to the mixed and eventually boundary regime.

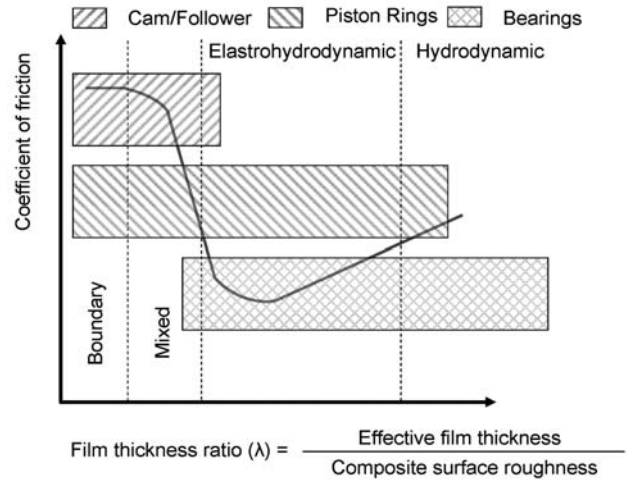


Figure 20.3—Automotive engine tribological systems in the modified Stribeck diagram [7].

Figure 20.4 shows the lubricant film thickness and friction coefficient as a function of the crank angle [7,8]. From the crank angle 0° to approximately 20° and from approximately 160° to 180°, the film thickness h_{min} is low, and the friction coefficient (Figure 20.4b) is high in this period. The friction coefficient is determined by the interface tribochemistry in the boundary lubrication regime. Therefore, the tribofilms on the piston ring and liner surfaces, which form by the additive packages in the lubricant, are essential to reduce the overall piston ring/liner friction.

The valve train is another important engine component and plays an important role in frictional energy loss (Figure 20.2). It is a mechanical system that contains a camshaft and followers and its function is to control the motion of the intake and exhaust valves. The energy loss due to valve train friction is quite significant, especially when the engine is idle or being used in urban conditions. The cam and follower system operates in much harsher tribological conditions than journal bearings and the piston ring/liner systems [9]. The contact pressure is high, speed is low, and as a result, its effective lubrication is more challenging. Figure 20.5 shows the lubricant film thickness and friction coefficient as a function of the cam angle [10,11]. Low sliding speeds as well as high contact pressures do not enable formation of a continuous lubricant film throughout

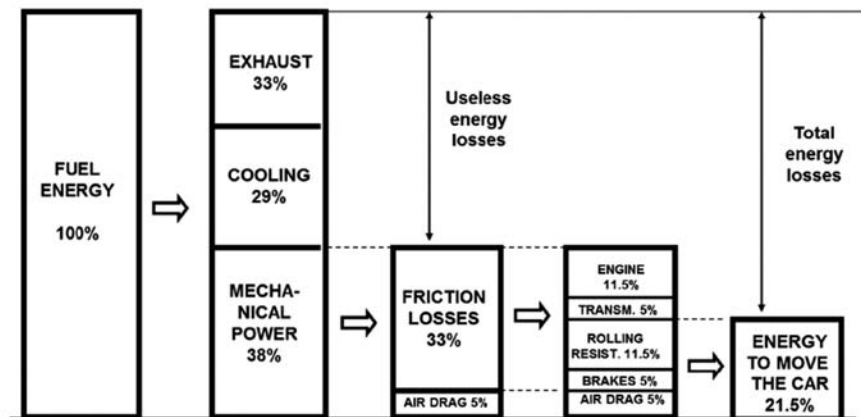


Figure 20.2—Breakdown of energy friction losses for an automotive engine [3].

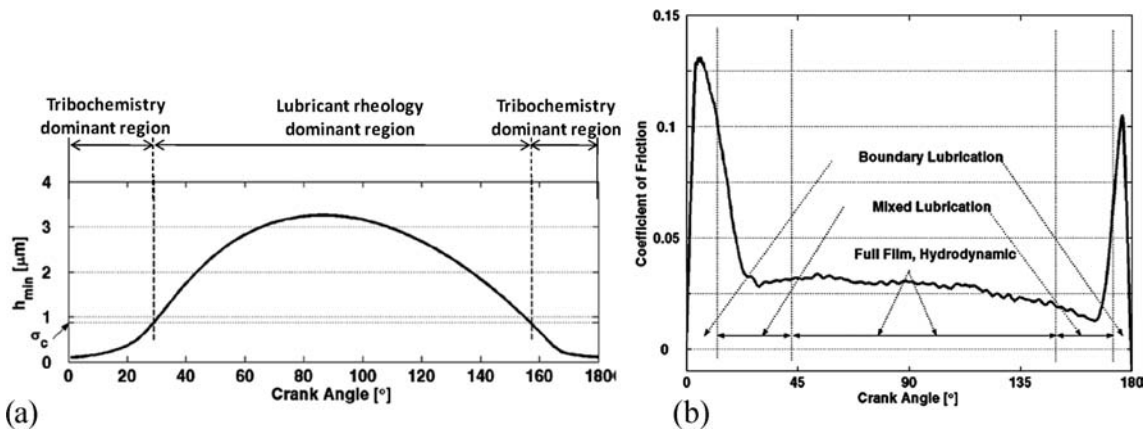


Figure 20.4—(a) Minimal lubricant film thickness and (b) friction coefficient variation over an expansion stroke in a piston ring/liner system. Source: Adapted from [8].

the contact interface. From the cam angle 45° to 135° (Figure 20.5), the film thickness is low, and the friction is mainly dominated by the boundary lubrication regime. Again, the tribofilm composition and friction reduction

property (in boundary lubrication) will be the key factors for overall engine efficiency. Therefore, the lubricant additives packages are important for friction reduction, especially for valve train and piston/liner systems.

The process of the development of a lubricant's additive package has historically always been a trial-and-error process. This is mainly due to the complexity of the engine lubrication, especially the lubrication of the systems that operate in boundary and mixed lubrication. The lack of complete understanding of how tribofilms form and then protect the surfaces from wear and high friction has restricted the development of lubricant technologies. Although the experimental studies on the lubricant chemistry effect on friction and wear in boundary lubricated systems are numerous, there is still a gap between the understanding obtained and the development of tools that could be useful to designers in industry. For example, although the theoretical aspect of valve train lubricants has been a subject of several studies as reviewed in [12], they are mainly based on equations that consider only the rheological properties of the lubricant and not the chemistry. A semiempirical work has only recently included chemical information in friction modeling of the cam/follower system [13], but there is still a lot of work to be done to achieve friction and wear modeling of valve train performance where the tribochemical processes are fully taken into consideration.

It is of high engineering importance to understand the mechanisms of formation of tribofilms from the lubricant additives to optimize a lubricant's performance. In this aspect, surface-sensitive analytical techniques are essential tools for understanding the tribochemical processes that lead to tribofilm formation, and as a result they are valuable tools for supporting the lubricant technology development. Using these techniques, the chemical and physical properties of the tribofilms formed can be investigated. The use of surface analytical techniques with all of the drawbacks discussed in Section 20.2 provides insight on how the lubricant additives behave in the surface chemistry process, enabling the lubricant formulators to promote synergistic performance or eliminate undesired effects. It is very important for the tribologist to have sufficient knowledge of the chosen surface analysis techniques to be able to obtain reliable data from the techniques and interpret them accurately.

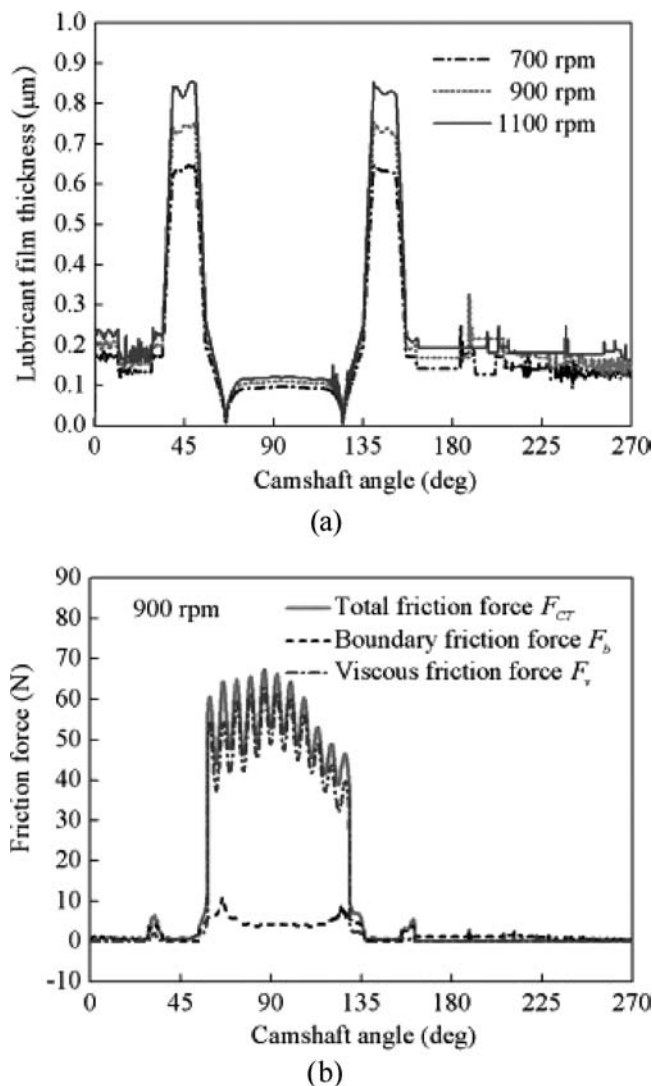


Figure 20.5—(a) Minimal lubricant film thickness and (b) friction force on the cam (900 r/min) [11].

20.2 SURFACE ANALYTICAL TECHNIQUES

To obtain the compositional information and physical properties of the tribofilm formed from lubricant additives, surface analytical techniques are applied. Techniques for surface analysis can be divided into two main categories: (1) those that assess physical and topographical properties and (2) those that assess chemical properties. The physical property analysis techniques are used to investigate the mechanical and physical properties [e.g., hardness, Young's modulus (E), Poisson ratio (ν), roughness etc.] of the tribofilms formed on the lubricated component surfaces. The chemical surface analysis techniques are used to obtain the chemical composition of the tribofilms. Figure 20.6 indicates the sensitivity of the main surface analytical techniques as well as their output.

20.2.1 Analysis of Physical and Topographical Properties

20.2.1.1 SCANNING ELECTRON MICROSCOPY

The scanning electron microscope (SEM) was developed in the 1930s and brought about a different way of imaging a solid [14]. By 1965, the first commercial instruments were in general use and this represented a revolution in microscopy. Using electrons to focus, it has the benefit of providing a great depth of field as well as extremely high-resolution images at magnification levels in excess of $\times 10,000$. The SEM is fully equipped with a range of secondary electron (SE) and back-scattered electron (BSE) detectors.

The SEM has been extensively used in analysis of the worn surface to obtain the wear mechanism. For example, Figure 20.7 shows clearly the extent of the surface damage of Al-Si alloy after different sliding distances [15]. The information obtained from SEM is normally qualitative—providing an image of the surface at very high magnification. However, some software can be used to determine quantitative surface properties such as average roughness (R_a), RMS roughness (R_{rms}), and fractal parameters.

BSE images are very helpful for obtaining high-resolution compositional maps of a sample and for quickly distinguishing different phases or elemental distributions. Backscattered electrons consist of high-energy electrons originating in the electron beam. Elastic scattering changes the trajectory of the incoming beam electrons when they interact with a target sample without significant change in their kinetic energy. The number of backscattered electrons reaching a BSE detector is proportional to the mean atomic number of the sample. Because heavy elements (high atomic number) backscatter electrons more strongly than light elements (low atomic number), they normally appear brighter in the image. Therefore, BSE images are usually used to identify the different compositional distribution on the surface. Figure 20.8 shows the BSE image of a zinc dialkyl dithiophosphate (generally referred to as ZDDP or ZDTP) tribofilm (area A) formed on the diamond-like carbon (DLC) coating surface (area B) whereas Table 20.1 gives the chemical element composition of both areas.

A very important development in the SEM came in the 1990s when the first environmental scanning electron microscope (ESEM) was developed. This was an important technological advance, especially in the area of polymer science, in which there were always the restrictions in SEM analysis of nonconductive samples. Before ESEM was introduced, to perform the examination of polymers using a SEM there was a need to apply a very thin sputtered layer of a metallic coating (normally gold) to provide a path for the discharge of electrons. Without this, the surface “charges” and the image quality is extremely poor. With the introduction of ESEM, the need for coating was reduced and sometimes eliminated because the accelerating voltage could be reduced. Figure 20.9 shows the high-resolution images of the paper-based clutch friction material before and after the tribological tests in SAE No. 2 rig obtained using the ESEM, illustrating the potential of this technique for studying the wear of clutch friction material.

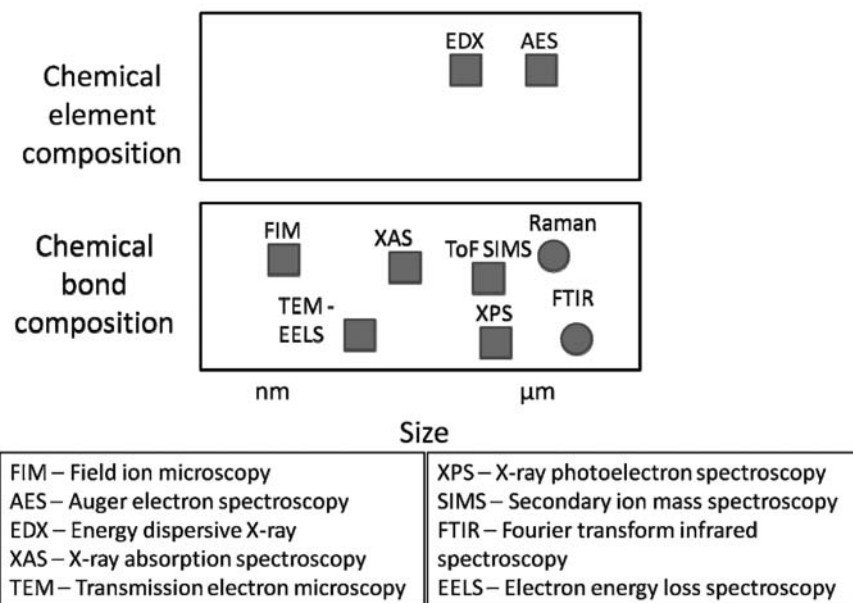


Figure 20.6—Schematic illustration of the lateral and chemical resolution of key surface analytical tools. Solid squared techniques require high vacuum whereas solid circled techniques can be used in air.

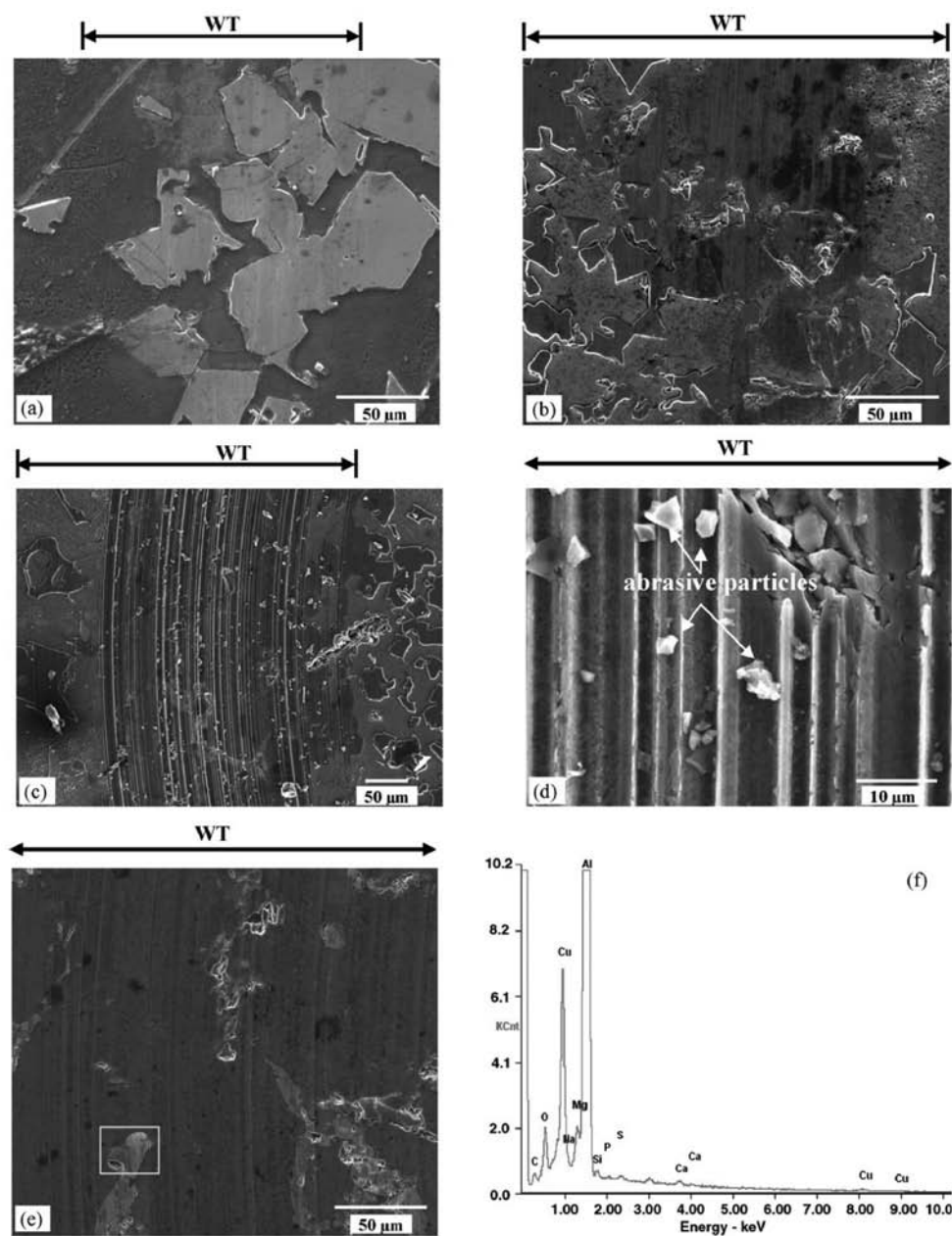


Figure 20.7—Wear images of Al-Si alloy (a–f) and EDS spectrum from the wear track [15].

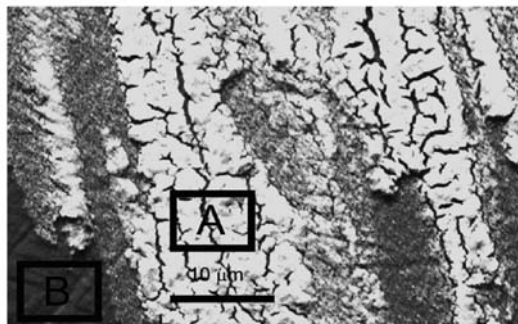


Figure 20.8—Backscattered electron image obtained with a SEM of the tribofilm formed from ZDDP on DLC [16].

TABLE 20.1—A and B Show That the Areas in Figure 20.8 Measured with EDX had Different Chemical Element Concentrations in A and B [16]

Element Concentration [at. %]		
	A	B
Carbon	77.4	91.2
Oxygen	13.5	7.9
Phosphorus	2.5	0.1
Sulphur	1	0.1
Iron	0.5	0.4
Zinc	5.1	0.3

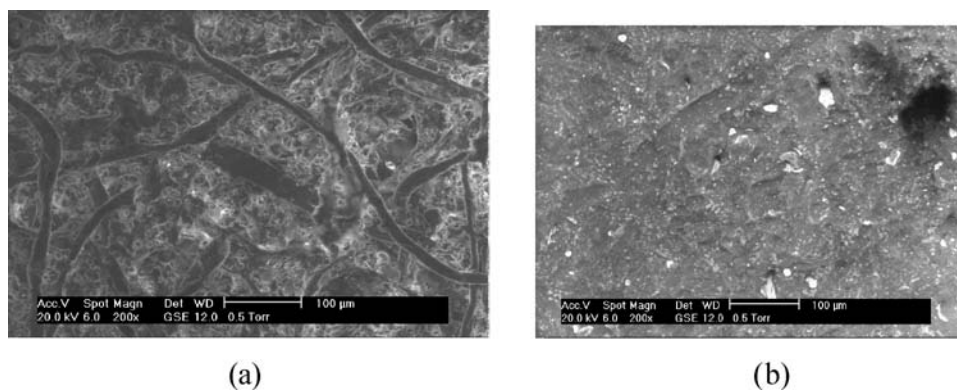


Figure 20.9—ESEM images of (a) the fresh clutch friction material and (b) clutch material following a SAE No. 2 test.

High-resolution images of the tribofilm cross-section can be obtained by combining the focused ion beam (FIB) material sputtering technique with the SEM. The high beam currents (normally Ga source) would result in surface collision with energetic ions leading to sputtered material, which leaves the surface either as secondary ions or neutral atoms (substrate milling). Figure 20.10 shows the ZDDP tribofilm cross-section image obtained with this technique [17].

In this technique, Ga ions are produced as a result of the high electric field caused by the Ga metal being placed in contact with a W needle. These ions are then accelerated and focused onto the surface by electrostatic lenses to sputter the top layer of the material. To avoid the surface damage from irradiated high-energy Ga ions, the surface is usually coated with a platinum layer of approximately 500-µm thickness.

20.2.1.2 TRANSMISSION ELECTRON MICROSCOPY

Another high-resolution visualizing technique used in tribology research is transmission electron microscopy (TEM). In this technique, the two-dimensional (2-D) internal structure images are obtained by transmitting a beam of high-energy electrons through the ultrathin solid sample [18]. Depending on the density of the material being tested, some of the electrons will scatter whereas the unscattered

electrons will hit a phosphor-coated screen, resulting in an image with bright and dark areas according to the material density. Crystalline samples, when analyzed in TEM, will diffract the incident electron beam and generate diffraction patterns that can be used to identify the material being analyzed.

In tribology research, TEM has been very useful to analyze the structure of wear particles produced from a tribology test [19–23]. In these studies, wear particles were collected at the end of the test and then analyzed using TEM. Figure 20.11a shows a typical TEM image of a wear particle collected from the wear scar and the corresponding electron diffraction pattern, indicating the amorphous character of the material [24]. The wear scar was produced from a lubricated test using a ZDDP-containing lubricant. The energy dispersive X-ray chemical analysis of this particle (Figure 20.11b) indicates that this particle is a fragment from the ZDDP tribofilm formed on the wear scar.

Although TEM has shown to be a good technique for characterizing the wear particles, analyzing the actual tribofilms formed on the wear scar with this technique is much more complex. This is due to the sample preparation needed before the TEM analysis. The process of getting ultrathin solid samples for TEM is based on ion bombardment and as a result can be time-consuming. In addition, not altering the microstructure of the sample

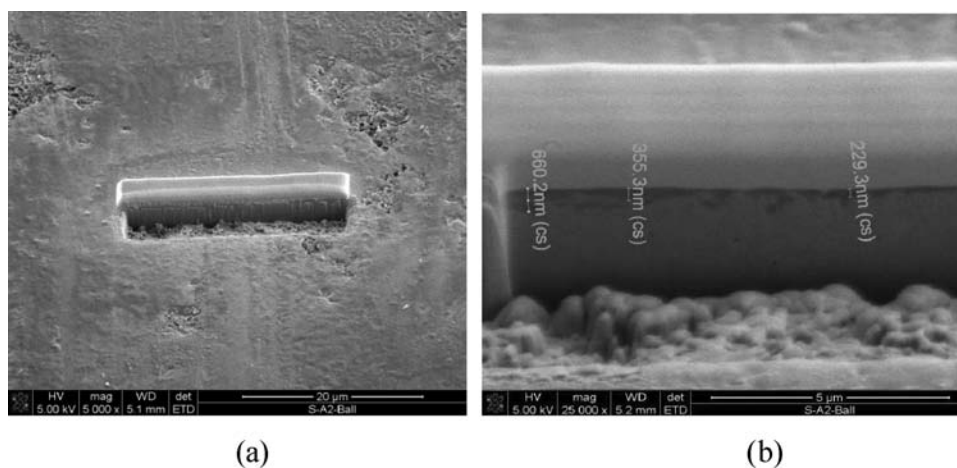


Figure 20.10—SEM images in (a) low and (b) high magnification showing the cross-section of a ZDDP tribofilm on steel.

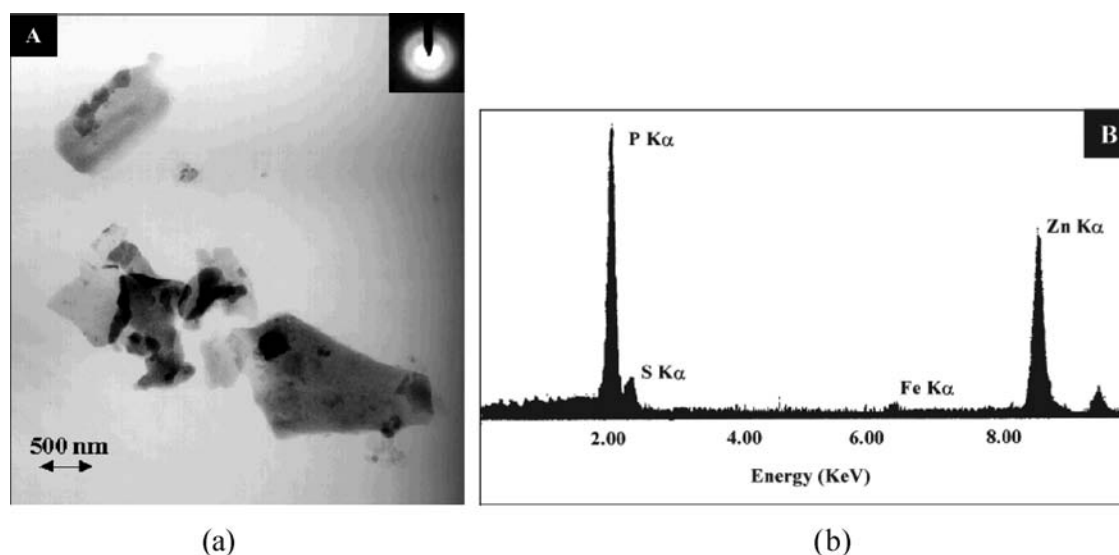


Figure 20.11—(a) Energy-filtering TEM analysis of ZDDP wear fragments originating from wear tests performed in mild wear conditions (SRV tribometer) and (b) its elemental chemical composition obtained with EDX [24].

while preparing the sample for TEM analysis [18] could be challenging.

20.2.1.3 ATOMIC FORCE MICROSCOPY

Atomic force microscopy (AFM) is probably the most commonly used surface analysis technique in the scanning probe microscopy (SPM) family for analysis of tribofilms formed from engine oil additives. Based on a relatively simple concept, the AFM has been partly responsible for the nanorevolution in material science. The AFM is an instrument that allows for the observation of topography of surfaces at very high resolution, helping to understand the tribofilm microstructure. The instrument comprises a cantilever that holds a tip made of silicon nitride. The tip is kept either in contact with the surface (contact mode) or a few nanometres away from the sample (noncontact mode). In a contact-mode AFM, also known as repulsive mode, an AFM tip makes soft “physical contact” with the sample. The tip is attached to the end of a cantilever with a low spring constant, lower than the spring constant holding the atoms of the sample together. The cantilever is typically Si or silicon nitride with a tip radius of curvature on the order of nanometres. Nowadays, most atomic force microscopes use a laser beam deflection system, introduced by Meyer and Amer [25], in which a laser is reflected from the back of the reflective AFM lever and onto a position-sensitive detector. As the scanner gently traces the tip across the sample, the contact force causes the cantilever to bend to accommodate changes in topography. The vertical and lateral deflection of the cantilever, which are used respectively to obtain topographic (AFM) and lateral force microscopy (LFM)/friction force microscopy (FFM) images, are detected by a quadrant photodetector via a laser light reflected from the back of the cantilever. The measured cantilever deflection in AFM is generated into a surface topography map of the sample. For LFM scanning the twisting or lateral forces experienced by the cantilever are usually caused by variations in surface friction and changes in slope. LFM scanning should be simultaneously performed with AFM to separate one effect

from the other. Figure 20.12 illustrates the principle of how AFM works. The force is not measured directly but calculated by measuring the deflection of the lever and knowing the stiffness of the cantilever. The ASTM work item (ASTM WK29480, New Practice for Size Measurement of Nanoparticles Using Atomic Force Microscopy) is currently being developed to provide guidelines on general AFM operation and size measurement of nanoparticles.

Pidduck and Smith [26] were the first authors to use AFM and LFM to examine the local topography and frictional properties of tribochemical ZDDP films formed during tribological testing using a reciprocating Amsler test and in a real engine component. AFM analyses of ZDDP tribofilms have shown clearly that ZDDP tribofilm is patchy in structure (Figure 20.13 and Figure 20.14a). Apart from the patchy ZDDP tribofilm formed on DLC, Topolovec-Miklozic, Lockwood, and Spikes also reported the low lateral force molybdenum dialkyl dithiocarbamate (MoDTC)

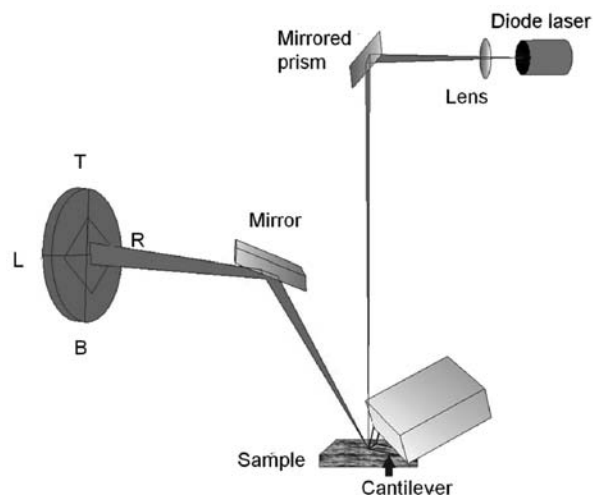


Figure 20.12—Schematic representation of the principles of operation of AFM.

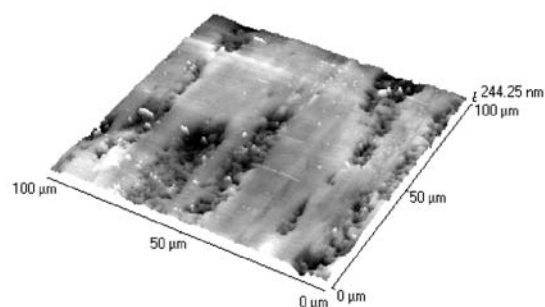


Figure 20.13—ZDDP tribofilm [28].

tribofilm formed only on the asperity peaks as shown in Figure 20.14b [27].

20.2.1.3.1 Noncontact-Mode AFM

Contact-mode applications of AFM are very useful in the molecular-scale measurement of a material surface, and some detailed surface changes can be investigated. However, in some cases, the contact with the AFM tip can alter or damage the surface being scanned. Noncontact-mode AFM provides a way to record the surface details without damaging the surface.

Wang [29] used ac noncontact-mode AFM to image the microliquid of sulfuric acid deposited on an SUS304 steel surface. Figure 20.15 shows the SUS304 surface with the ac noncontact mode of the AFM after pouring a macrodroplet of sulfuric acid and holding for 600 ks. It is observed that a typical particle of the size of 24-nm height and

2.58- μm radius (Figure 20.15a) was covered with small particles of 10-nm height and 55-nm diameter (Figure 20.15, c and d). However, the small particles are not shown in the contact-mode results whereas a hole is shown in the large particle (Figure 20.15b), indicating a surface damage from contact-mode AFM. All large and small particles should be corrosion products, but the small ones did not combine strongly with each other or with the large one, so the tip of the cantilever in contact-mode scanning could easily remove them.

For molecular-level research on the solid sample surface, the noncontact-mode AFM could keep the damage to the surface at a minimal level, which is considerably less detrimental than the contact mode.

20.2.1.4 NANOINDENTER

Because of the low indentation forces that can be used in this technique, the mechanical property measurement of very thin films can be achieved. This is achieved by indenting the surface with a diamond probe applying a controlled force [30]. Force, displacement, and time are recorded throughout the test. As a result of the measurement, the force-displacement curve is obtained (Figure 20.16). A process devised by Oliver and Pharr [31,32] can be used to obtain the modulus of elasticity by analyzing the slope of the unloading force-displacement curve whereas hardness can be obtained after calculating the indentation projected area. Hardness is obtained by measuring the depth of penetration of the indenter into the sample surface [33] and taking into consideration the known geometry of the

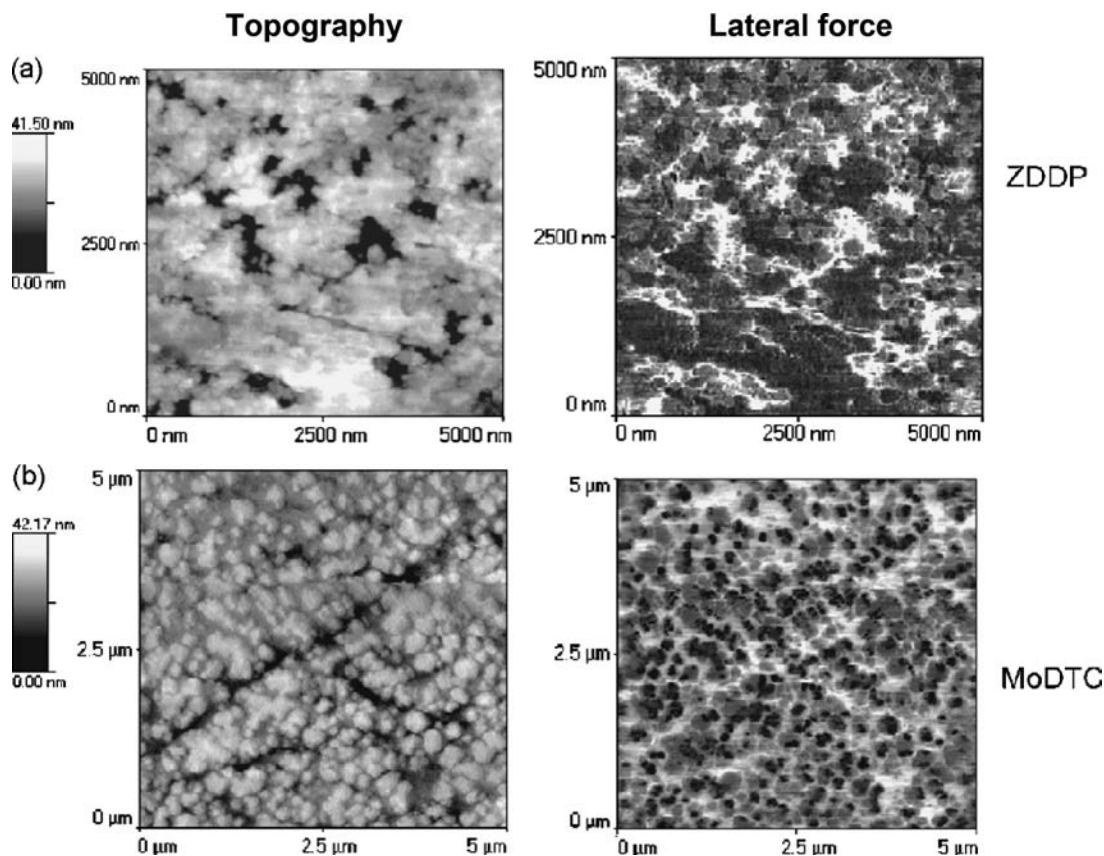


Figure 20.14—AFM topography and lateral force maps from rubbed track on g-DLC disc after 2 h of rubbing in two boundary lubricating additive solutions: (a) ZDDP and (b) MoDTC [27].

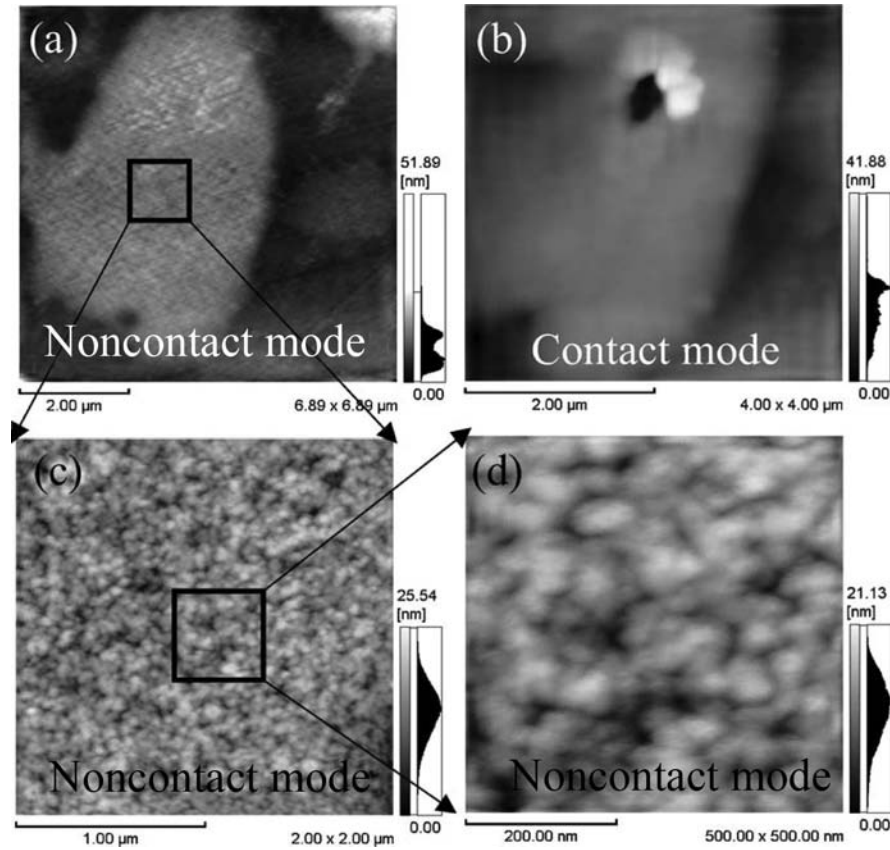


Figure 20.15—SUS304 steel surfaces observed with the ac noncontact mode of AFM after depositing microdroplets for 430 ks (a, c, and d). Panel b shows almost the same regions of panel a with the contact mode. Panels c and d show magnified morphologies in the frame region of panel a [29].

indenter. For example, for an indentation using a Berkovich indenter, which has a face angle of $\theta = 65.3^\circ$, the relationship between the projected area A of the indentation and the depth of penetration (h_p) is

$$A = 3\sqrt{3}h_p^2 \tan^2 65.3 = 24.5h_p^2 \quad (20.1)$$

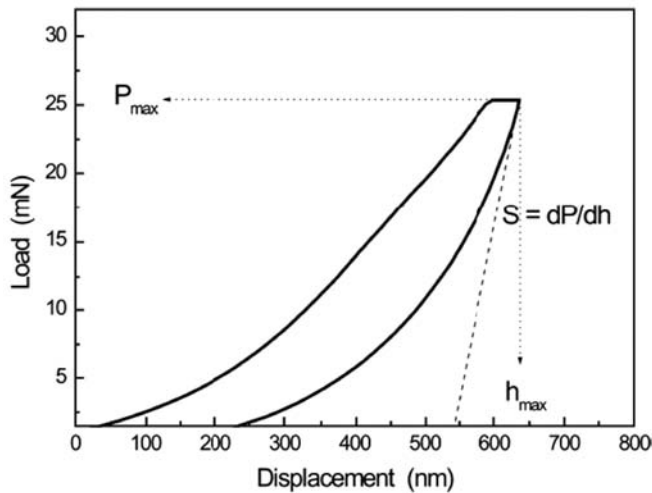


Figure 20.16—Force-displacement curve shows the typical load-unloading vs. displacement curve. The maximal tip penetration (h_{max}), the maximal applied load (P_{max}), the final depth (h_p), and the system stiffness (S) [35].

The calculated projected area A is then used in eq. 20.2 to obtain the hardness.

$$H = \frac{P}{A} \quad (20.2)$$

A is the projected area, P is the maximal applied load, and h_p is the depth of penetration.

The elastic modulus is a function of the unloading curve top 80 % slope, S , and of the projected area A , and can be obtained using eq. 20.3:

$$S = \frac{dP}{dh} = \frac{2}{\sqrt{\pi}} E_{eff} \sqrt{A} \quad (20.3)$$

where E_{eff} is the effective elastic modulus defined by

$$\frac{1}{E_{eff}} = \frac{1-\nu^2}{E} + \frac{1-\nu_i^2}{E_i} \quad (20.4)$$

where E_i and ν_i are the elastic modulus and Poisson's ratio of the indenter, respectively, and E and ν are the elastic modulus and Poisson's ratio of the analyzed sample, respectively. The E_i and ν_i values for the Berkovich indenter are 1141 GPa and 0.07, respectively.

The behavior of the material while increasing the indentation force, expressed by the force-displacement curve, will provide the information on ductility or brittleness, dislocation motion, and creep behavior of the

material [34,35]. An ASTM standard (ASTM E2546-07, Standard Practice for Instrumented Indentation Testing) on the indentation testing is available as a practical guide. In addition, the ISO 14577 standard titled “Metallic Materials—Instrumented Indentation Tests for Hardness and Materials Parameters” gives a description of the method and principles of the indentation tests and calibration procedures.

The reliability of nanoindenter tests depends on the ability to produce and measure very small forces and displacements [18]. Controlled forces can be achieved by different means: electromagnetic actuation, electrostatic actuation, and actuation through springs. Displacement is usually measured using capacitance displacement sensors. Figure 20.17 shows a typical nanoindenter result obtained from analyzing a ZDDP-derived tribofilm formed on steel components [36]. In this study, the averaged force-distance curves obtained on the tribofilm at the two extreme temperatures, 25 and 200°C, showed a significant decrease in modulus of the tribofilm at 200°C, indicating a change in mechanical properties of the tribofilm depending on the temperature.

Careful considerations need to be taken into account when analyzing mechanical properties of tribofilms to avoid the effect of substrate in the measurement. It is generally accepted that for thin films on a substrate, the maximal depth of penetration in a test should be restricted to no more than 10 % of the film thickness to avoid the substrate effect on the measurement [33]. This is challenging considering that the thickness of a typical ZDDP tribofilm is in the submicron region. However, there are several models available that can be used to extract the film properties from the composite ones [37,38].

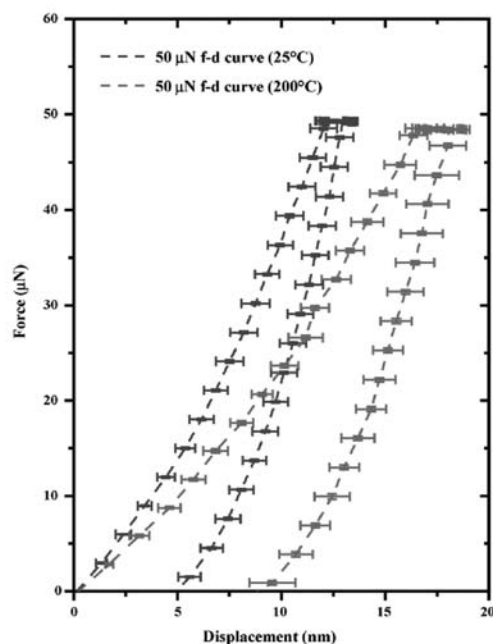


Figure 20.17—Representative 50- μ N force-displacement (f-d) curves obtained from the ZDDP-derived tribofilm heated at 25 and 200°C. Each f-d curve shown is an average of 25 f-d curves [36].

20.2.2 Analysis of Chemical Properties

The main advantage of a surface analytical technique for chemical analysis is the ability to obtain high-resolution data without interfering with the surface being analyzed. So far, this cannot be achieved comprehensively by applying only one technique. Although vacuum-based techniques provide good depth sensitivity for analysis of tribofilms, the surfaces need to be rinsed/cleaned before they are placed in the vacuum chamber. The cleaning process is shown to have the possibility of completely removing the top layers of the tribofilm [39] or it could affect the nature of the chemisorbed film. On the other hand, chemical bond vibrational techniques, such as Fourier transform infrared (FTIR) and Raman spectroscopy, can be used without any cleaning process of the surface and the analyses depth could go up to a micron on the surface, but the resolution of the thin tribofilm chemical characterization on the wear scar is normally not as good as on the vacuum analysis techniques. Figure 20.18 illustrates the depth sensitivity of several techniques in relation to the ZDDP tribofilm thickness. Combining the information obtained from several analytical techniques is probably the best approach for assessing the physical/chemical nature of the surface films. In the following sections, an overview of vacuum- and nonvacuum-based surface analytical techniques is given.

20.2.2.1 VACUUM-BASED TECHNIQUES

20.2.2.1.1 Energy-Dispersive X-Ray

The energy-dispersive X-ray (EDX) technique has a probing depth in excess of 1 μ m; hence, it will probe the substrate composition as well as the tribofilm itself. The use of this technique is important to obtain the elemental composition of the entire tribofilm, and it is useful to give the overall concentration of main elements in the tribofilm. When the incident electron beam hits the atoms of the sample, in addition to those SE and BSE that are emitted from the sample, energy in form of X-rays is released ($h\nu$) (Figure 20.19). This energy is released because the electron from the outer shells fills the holes in inner shells created with the release of SE to stabilize the atoms. The electrons in outer shells are at higher energy, so to drop into the lower

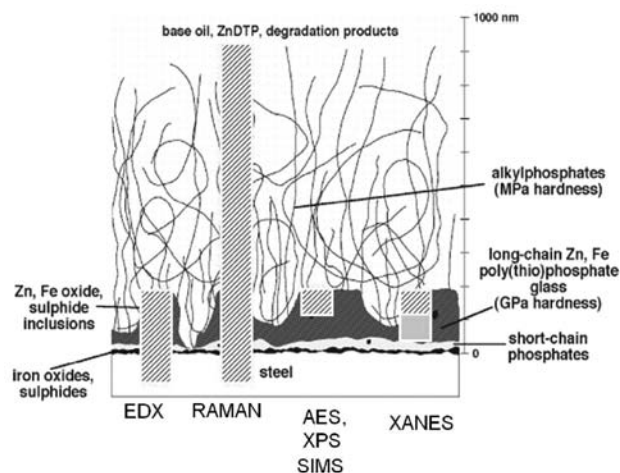


Figure 20.18—Schematic representation of the depth sensitivity of EDX, Raman, XPS/AES, and SIMS techniques in relation to the ZDDP tribofilm thickness.

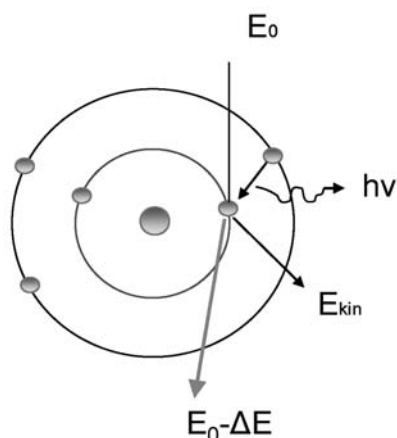


Figure 20.19—Basic principle of the EDX technique.

shells, they must lose some energy, which is released as X-ray energy. It can analyze the elements that are heavier than or equal to sodium in atomic weight. The ASTM standard E1508-98(2008) (Standard Guide for Quantitative Analysis by Energy-Dispersive Spectroscopy) provides guidelines on the quantitative analysis by this technique.

To illustrate the potential of the EDX technique for tribofilm chemical characterization, Figure 20.20 shows the typical EDX spectra taken from ZDDP and ZDDP/MoDTC tribofilms [40].

There are a few disadvantages of the EDX technique that need to be taken into account while discussing its spectra. One disadvantage of the EDX technique is that it cannot distinguish among the different chemical states of the same element, for example, whether P^{4+} or P^{6+} is formed in the tribofilm by ZDDP (Figure 20.20). The other disadvantage is the overlap of peaks; for example, overlap of Mo and S peaks makes it impossible to distinguish Mo and S species present in the tribofilm.

20.2.2.1.2 X-Ray Photoelectron Spectroscopy/Auger Electron Spectroscopy

X-ray photoelectron spectroscopy (XPS) and Auger electron spectroscopy (AES) are powerful techniques widely used for the surface analysis of materials. An important

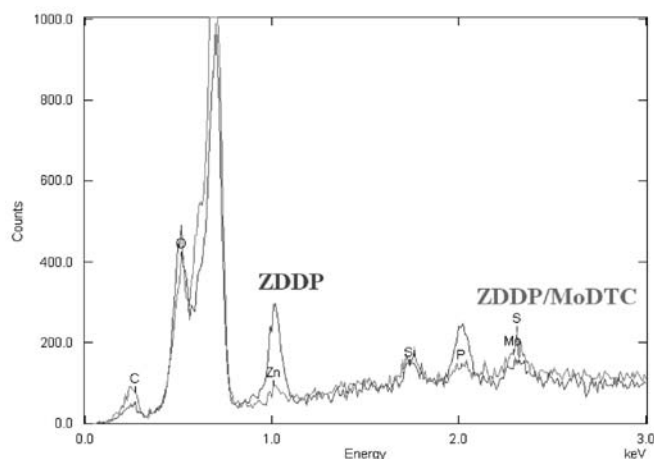


Figure 20.20—Comparison of typical EDX spectra obtained from ZDDP and ZDDP/MoDTC tribofilms formed at 100°C tests [40].

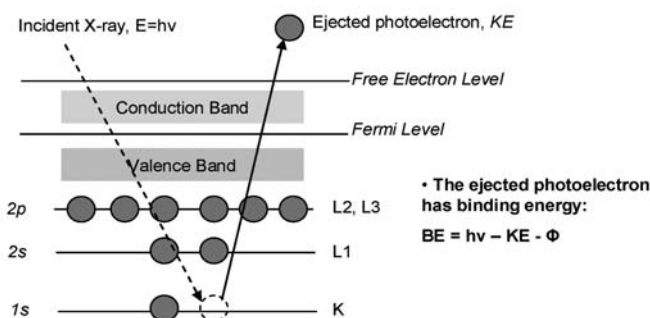


Figure 20.21—XPS principle.

characteristic of these techniques is their surface dependence; although X-rays penetrate to a depth of several micrometres, ejected photoelectrons generally come from only the first several nanometres of material. Considering that these two techniques are similar, the rest of this section focuses only on XPS. In XPS, the photon is absorbed by an atom in a molecule or solid, leading to ionization and the emission of a core (inner shell) electron as shown schematically in Figure 20.21. The binding energy (BE) is now taken to be a direct measure of the energy required to remove the electron concerned from its initial level to the vacuum level.

Before the XPS analysis, samples are suggested to be prepared according to the ASTM standard guides ASTM E1078 and ASTM E1829. In a typical XPS analysis, a survey scan is obtained first to identify elements present (Figure 20.22), and then the long scans of the selected peaks are obtained to determine a more comprehensive picture of the chemical composition. The realization of surface chemical-state microscopy by XPS requires the resolution of overlapped chemical states, an adequate background description, and the ability to quantify data. Whereas tribofilm quantification is done using peak area sensitivity factors, chemical species are determined after a curve-fitting procedure on the peaks obtained. For example, the curve-fitting results of Ca and C peaks (Figure 20.23) show clearly the formation of $CaCO_3$ in the tribofilm. The formation of $CaCO_3$ was confirmed by analyzing the Ca, C, and O peaks and then using stoichiometric analysis to determine the chemical species in the tribofilm.

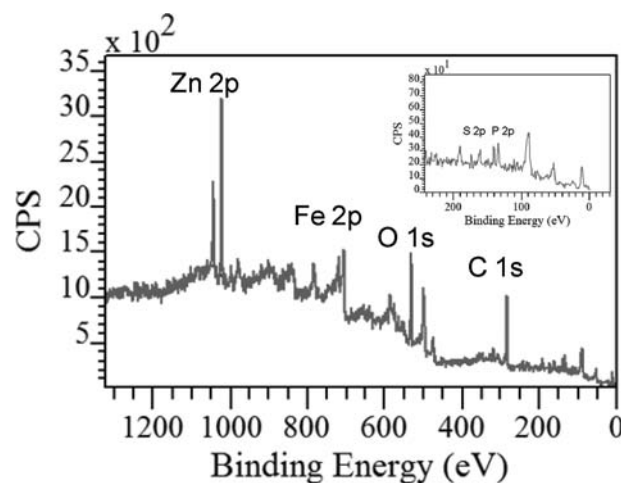


Figure 20.22—XPS survey scan of the ZDDP tribofilm. Inset shows low-BE elements.

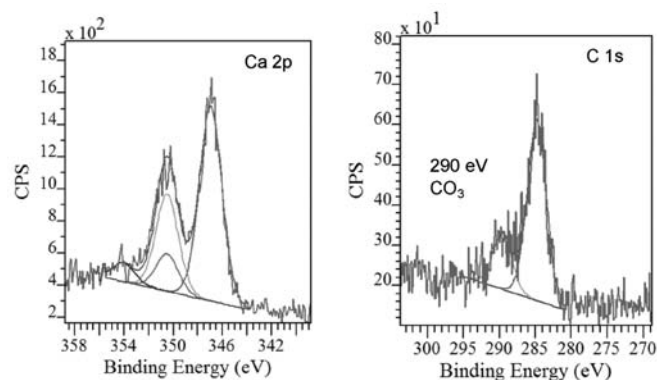


Figure 20.23—Ca 2p and C 1s XPS peaks obtained from analysis of piston ring after a fired engine test. By analyzing both peaks, formation of the CaCO_3 in the tribofilm is confirmed.

Chemical analyses as a function of depth are usually performed by using controlled etching of the surface by Ar ion sputtering. The etching process is a very useful technique to obtain the chemical composition depth profile of the tribofilm, but analysis is normally semiquantitative at best. For example, Unnikrishnan, Jain, Harinarayan, and Mehta used the XPS depth profile results to show that the tribofilm formed using a lubricant containing ZDDP and MoDTC (Figure 20.24b) has a higher Mo and S concentration than the tribofilm formed from lubricants containing MoDTC only (Figure 20.24a), indicating the effect of ZDDP additive on MoDTC tribofilm formation [41].

However, this procedure could be misleading because the sputtering rate could be different for different molecules present on the surface being analyzed, causing preferential etching, and this needs to be considered while using XPS. Another issue could be the change of XPS peak position due to the etching process. For example, the XPS analysis of MoS_2 powder (Figure 20.25) proves that the appearance of the 228.2-eV peak is due to the etching of the MoS_2 powder.

These need to be considered carefully when interpreting XPS results to avoid reaching the wrong conclusions.

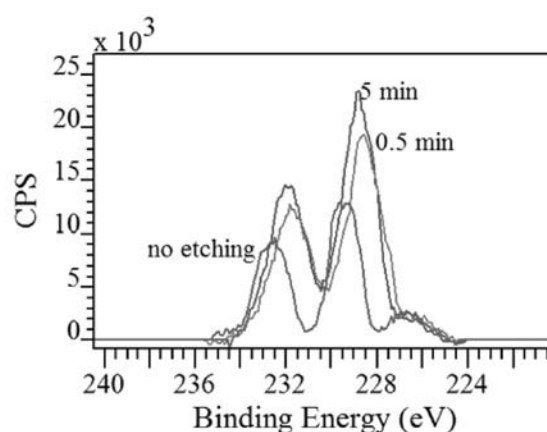


Figure 20.25—Mo 3d peak obtained from scanning of MoS_2 powder after 0, 0.5, and 5 min of etching.

20.2.2.1.3 X-Ray Absorption Near-Edge Structure Spectroscopy

X-ray absorption near-edge structure (XANES) spectroscopy has become a powerful analytical and research tool. The XANES spectroscopy data indicate the absorption peaks due to the photoabsorption cross-section in the X-ray absorption spectra (XAS) observed in the energy region, extending over a range of approximately 100 eV, between the edge region (up to approximately 5 eV) and the extended X-ray absorption fine structure (EXAFS) region (from approximately 150 eV) [42,43]. This technique is particularly useful for low-atomic-number elements such as C, N, P, O, and S.

By exciting an atom using an X-ray source, the electron configuration of the atom is changed; one (usually a core-shell) or more electrons populate unoccupied bound or continuum states. When the photon energy is large enough, the photoeffect in one of the core shells can occur. This results in the step-like shape of the absorption spectrum: The increased photoabsorption cross-section due to the

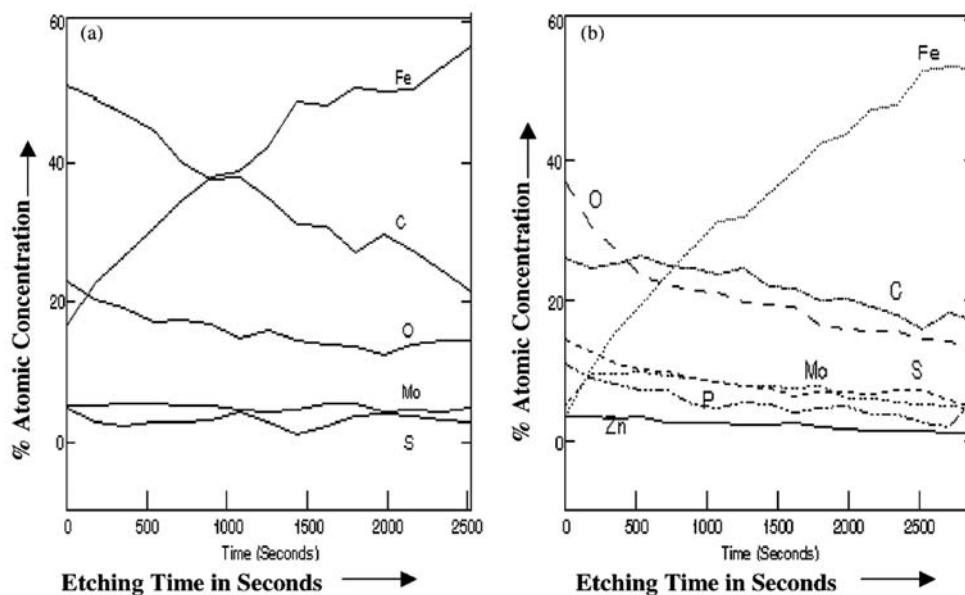


Figure 20.24—Surface depth profiles (XPS results) from the worn surface of the ball tested with (a) MoDTC- and (b) MoDTC + ZDDP-containing lubricant [41].

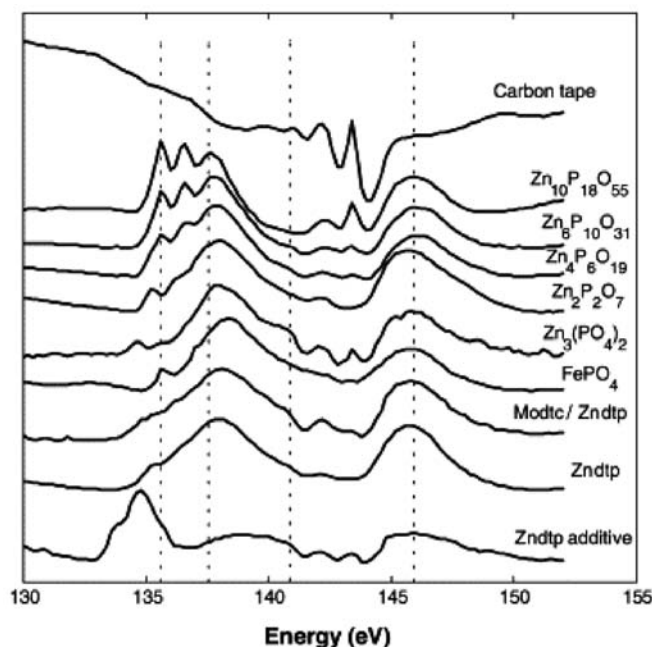


Figure 20.26—P L-edge XANES spectra of model compounds and tribofilms using the TEY mode [45].

knocking-out of an electron is called the “absorption edge” (Figure 20.26) [42,44,45]. The excitation of a bound atom can be understood by means of multiple scattering: The photoelectron’s wave is scattered on atoms surrounding the absorbing atom [43,46]. Figure 20.27 shows the different magnitude and position of the Fourier transform of $k^2\chi(k)$ spectra [47]. The absorption peaks of XANES spectra are determined by multiple scattering resonances of the photoelectron excited at the atomic absorption site and scattered by neighboring atoms.

When the photon energy ω is low, the photoelectrons can populate either unoccupied bound states or low-lying continuum states. This part of the spectrum (Figure 20.26)

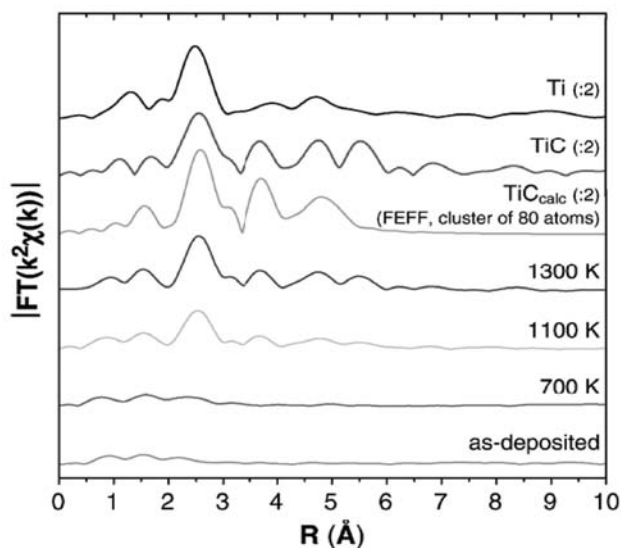


Figure 20.27—Magnitude of the non-phase-corrected Fourier transform of $k^2\chi(k)$ for a-C:Ti after different annealing temperatures (as-deposited, annealed to 700, 1100, and 1300 K) [47].

is called the XANES region. On its high-energy end, the XANES region extends up to the EXAFS region. In the XANES regime, the electron’s kinetic energy is small, and the scattering on the neighboring atoms tends to be strong for this reason whereas the effect of the scatterers becomes smaller at higher energies.

The XANES technique, in conjunction with XPS, is one of the most valuable tools used for chemical analysis of the tribofilms formed from engine oil additives. It uses soft X-ray for characterizing the P and S species on the surface. Two modes of the XANES technique—total electron yield (TEY) and fluorescence yield (FY)—enable depth chemical analysis without having to etch the sample with Ar as is a usual procedure in XPS. Depth sensitivities of the TEY and FY modes at the P L-edge are approximately 5 and 50 nm, respectively, which, considering the typical thickness of a tribofilm, are very useful for obtaining the bulk and top surface tribofilm chemical composition [48]. To illustrate the typical XANES spectra, Figure 20.28 shows the XANES TEY and FY spectra obtained from analyzing a ZDDP tribofilm formed from a fresh oil and from oils preheated at 150°C for different lengths of time [49]. Fuller et al. [49] reported that the thickness of the film, as indicated by the intensity of the FY peaks (Figure 20.28E–H), does not decrease with a decrease in ZDDP concentration or ZDDP oil soluble decomposition product concentration. On the basis of the work of Yin et al. [50,51], who reported that polyphosphate chain length increased with the intensity of peaks a and b, Fuller et al. [49] also found that polyphosphate chain length decreases with an increase in preheating time (the extent of ZDDP decomposition).

One advantage of X-ray absorption spectroscopy is that it can be used to study the electron transitions from atomic core levels to unoccupied molecular states below and above the vacuum level in the absorbing atom [49], enabling surface analysis under realistic pressures and temperatures [52]. Using monochromatized X-ray photons from synchrotron radiation, it is possible to tune the X-ray energies to probe the atomic species in which the excitation occurs. To identify the chemical nature of tribofilm species, the obtained spectra are compared with the spectra of different model compounds with known chemistry [49, 53–60].

20.2.2.1.4 X-Ray Photoemission Electron Microscopy

The lateral resolution of conventional XANES spectroscopy is on the order of several square millimetres, which is too large for analyzing microscale features or tribofilm distribution on the wear scar. The application of energy filtering in photoemission electron microscopy (PEEM)-based imaging methods has become popular in recent years with the availability of powerful instruments. X-PEEM is PEEM using X-rays as an excitation source and installed with an energy filter to select an X-ray photoelectron peak specific to the target atoms. X-PEEM can image the distribution of elements, chemical states, and chemical species at the working surface at a mesoscopic scale, enabling the acquisition of chemical information on the submicron scale. In addition, with X-PEEM, high-resolution XANES spectra can be obtained with very good spatial resolution. This gives the user the unique ability to visualize and then determine the chemical nature of the species present using X-ray absorption spectroscopy of small submicron features

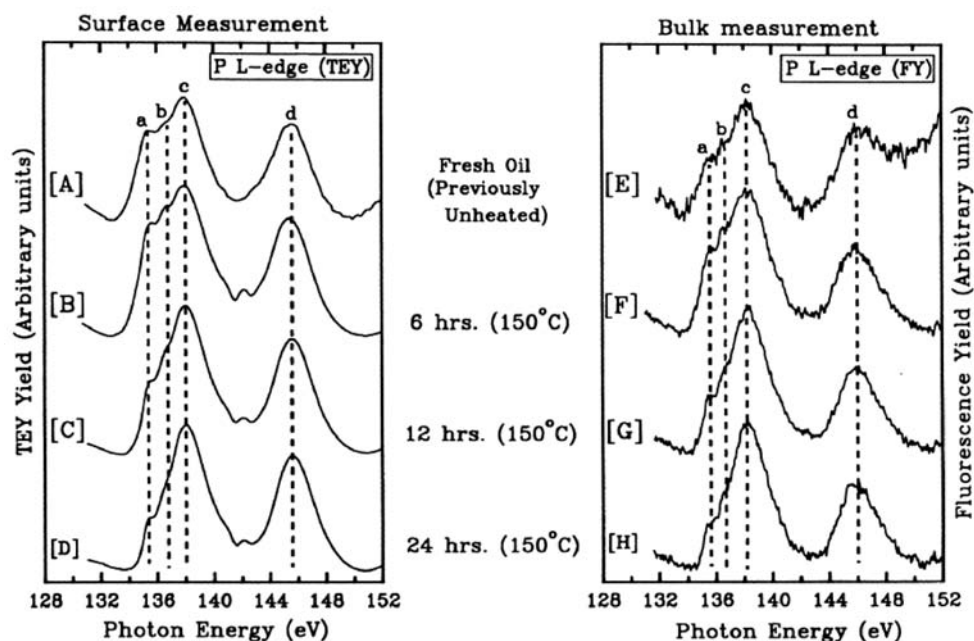


Figure 20.28—P L-edge surface (TEY) and bulk (FY) XANES spectra of antiwear films generated from ZDDP oil solutions preheated at 150°C for various lengths of time [49].

on a surface (down to 10-nm lateral resolution in the ideal case) with high-sensitivity depth of approximately 5 nm [61,62].

In terms of tribochemistry research, this technique has been very useful for analyzing the ZDDP tribofilm formation on Al-Si alloys [61,63]. Figure 20.29 shows a typical result obtained by combining X-PEEM imaging capabilities with the XANES spectroscopy chemical characterization of an organic sample on a Si surface [64].

Use of this high-resolution imaging technique has shown that the ZDDP antiwear pads are located on the hard Si grains and have a similar chemical structure to the tribofilm formed on steel surfaces [65].

20.2.2.1.5 Time of Flight–Secondary Ion Mass Spectroscopy

Secondary ion mass spectrometry (SIMS) is the mass spectrometry of ionized particles that are emitted from the surface when energetic primary particles bombard the surface. Figure 20.30 schematically illustrates the mechanism of time-of-flight (ToF)–SIMS [66]. In this technique, pulsed primary ions with energy of 1–25 keV, typically liquid metal ions such as Ga^+ , Cs^+ or O^- , are used to bombard the sample surface, causing the secondary elemental or cluster ions to be emitted from the surface. The secondary ions are then electrostatically accelerated into a field-free drift region with a nominal kinetic energy of $E_k = eV_0 = mv^2/2$, where V_0

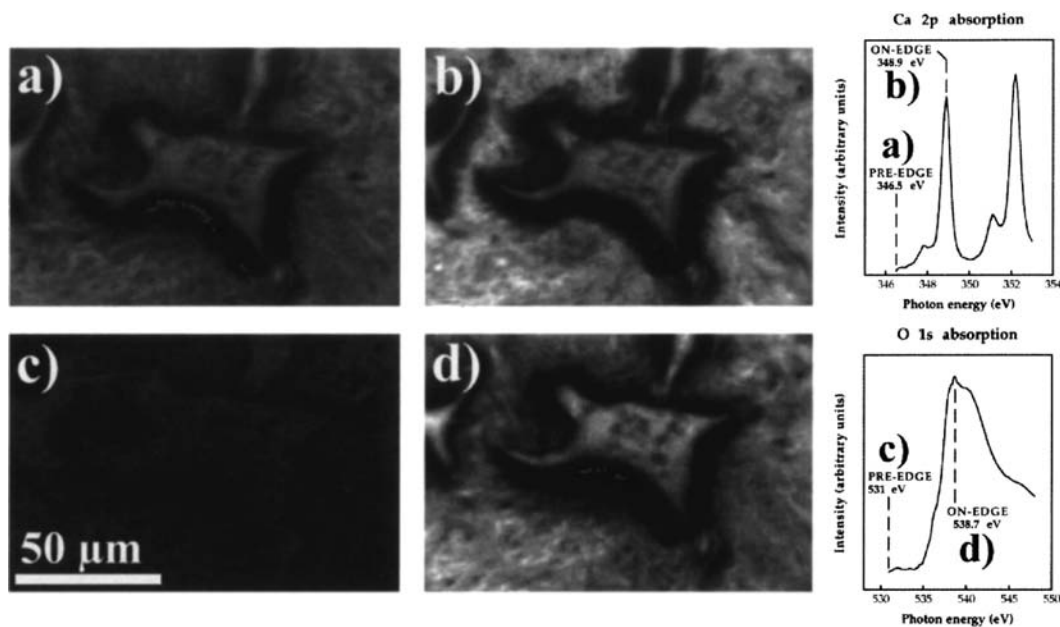


Figure 20.29—X-PEEM images of an organic sample on a Si surface [64].

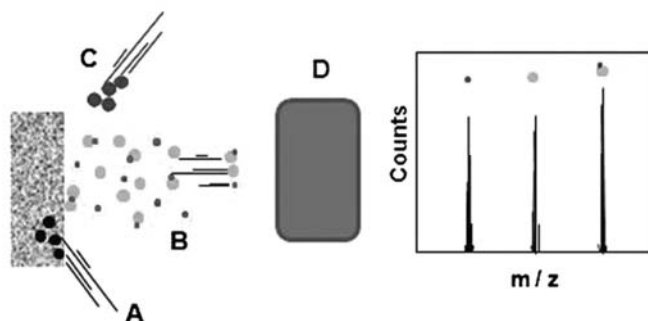


Figure 20.30—Schematic graph of the ToF-SIMS working mechanism, including the primary ion beam (A), the ejected secondary ions (B), the electron flood gun for charge compensation (C), and the mass analyzer (D) [66].

is the accelerating voltage, m is the mass of the ion, v is the flight velocity of the ion, and e is its charge. As can be seen from this formula, the ions with lower mass have higher flight velocity than those with higher mass. As a result, lower mass ions will reach the secondary ion detector earlier. The detector records various mass ions with the time sequence to give the SIMS spectrum. The data interpretation can follow ASTM standard E2695-09, “Standard Guide for Interpretation of Mass Spectral Data Acquired with Time-of-Flight Secondary Ion Mass Spectroscopy.”

Figure 20.31 shows a typical mass spectroscopy spectra obtained from analyzing tribofilms formed from engine oils on steel material [67]. ToF-SIMS analyses showed that for the engine oil A system (paraffinic base oil containing ZDDP, calcium sulfonate, and polyisobutenyl succinimide) a tribofilm containing Ca^+ and $\text{C}_8\text{H}_7\text{SO}_3^-$ (originating from calcium sulfonate additive), C_7H_7^+ , and CNO^- (originating from the succinimide) as well as Zn^+ and $\text{C}_9\text{H}_{20}\text{O}_2\text{PS}_2^-$ (originating from ZDDP) is formed on the friction surface. For the engine oil B system (oil A plus MoDTC), a tribofilm containing Mo^+ , MoO_3^- , and MoS_3^- (originating from the MoDTC additive) was clearly detected whereas sulfonate ions were not detected.

The ToF-SIMS technique is particularly useful to investigate the chemical nature of organic species formed in the

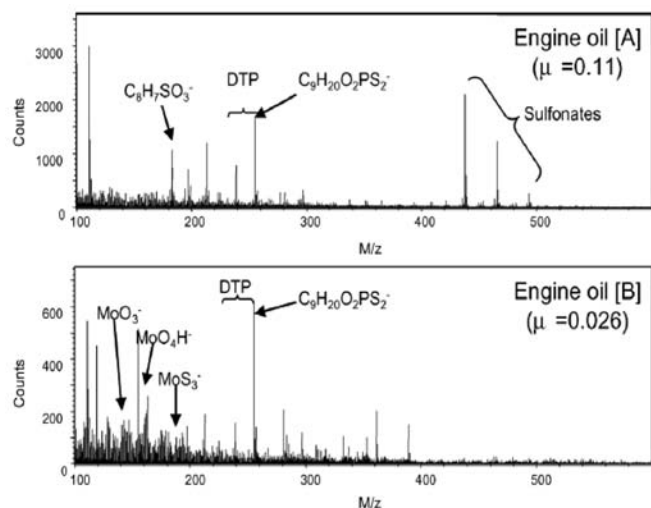


Figure 20.31—Negative ion spectra of friction surfaces of SUS, tested in engine oil [A] and [B] [67].

tribofilm [68], tribofilm formation on DLC coatings [16,69], and ionic liquid working mechanisms as a lubricant additive [70].

20.2.2.2 NONVACUUM-BASED TECHNIQUES

20.2.2.2.1 Raman Spectrometer

Raman scattering is a vibrational spectroscopy technique that provides information about the structure of the molecular species; however, different selection rules and sensitivity may reveal new component information for the films. Raman spectroscopy is concerned with the scattering of radiation by the sample rather than an absorption process. Rotational and vibrational Raman spectroscopies are possible. The energy of the exciting radiation will determine which type of transition occurs—rotational transitions are lower in energy than vibrational transitions. Moreover, Raman spectroscopy has specific advantages. The Raman technique is generally nondestructive and requires simple sample preparation. With a spatial resolution of approximately 1 μm , it is also capable of assessing heterogeneity in the film.

There has been a consistent interest in using Raman spectroscopy to investigate DLC coatings [71,72]. Raman spectroscopy is a comparatively simple, nondestructive analysis technique that, in principle, can be used as an in situ diagnostic technique. Hence, a Raman signature characteristic of DLC films of high sp^3 content could be very useful for future studies seeking to optimize DLC growth for the “best quality” (i.e., most diamond-like) films [73]. The first-order Raman spectrum of polycrystalline graphite consists of two peaks. The first, located at 1580–1590 cm^{-1} (the G peak), originates from lattice vibrations in the plane of the graphite-like rings. The second peak is located at approximately 1350 cm^{-1} (the D peak) and only occurs in graphite with small crystal sizes. This disorder-induced mode corresponds to a peak in the vibrational density of states (DOS) of graphite and is observed when the crystallite size is sufficiently small so that the selection rules are relaxed to allow phonons with non-zero wavevectors to contribute to the Raman spectrum. Indeed, for purely amorphous films, the Raman spectrum is expected to closely follow the vibrational DOS [73,74].

To demonstrate the potential of Raman spectroscopy for tribofilm characterization, Figure 20.32 shows the 488-nm Raman spectra of the antiwear tribofilms formed by fresh and aged oil after 1 h of sliding [75]. The film formed with 24-h aged lubricating oil appears to have a combination of the components present in the films formed with fresh and 47-h aged oil.

The assignments by Uy and his colleagues [75] of the peaks are as follows: the peaks at approximately 675 and 551 cm^{-1} are due to Fe_3O_4 ; the peak at 961 cm^{-1} is likely due to the symmetric P-O stretch of orthophosphate (PO_4^{3-}) species, and the 1089- cm^{-1} peak is due to the C-O symmetric stretch of CO_3^{2-} in calcium carbonate. The peak at approximately 1006 cm^{-1} in the films formed from aged oils may be due to a pyrophosphate ($\text{P}_2\text{O}_7^{4-}$), an orthophosphate, a sulfate (SO_4^{2-}), or a combination of these species.

20.2.2.2.2 FTIR Microscope Spectroscopy

FTIR is often used alongside XPS to provide a comprehensive analysis of how the surface of the polymer is changed

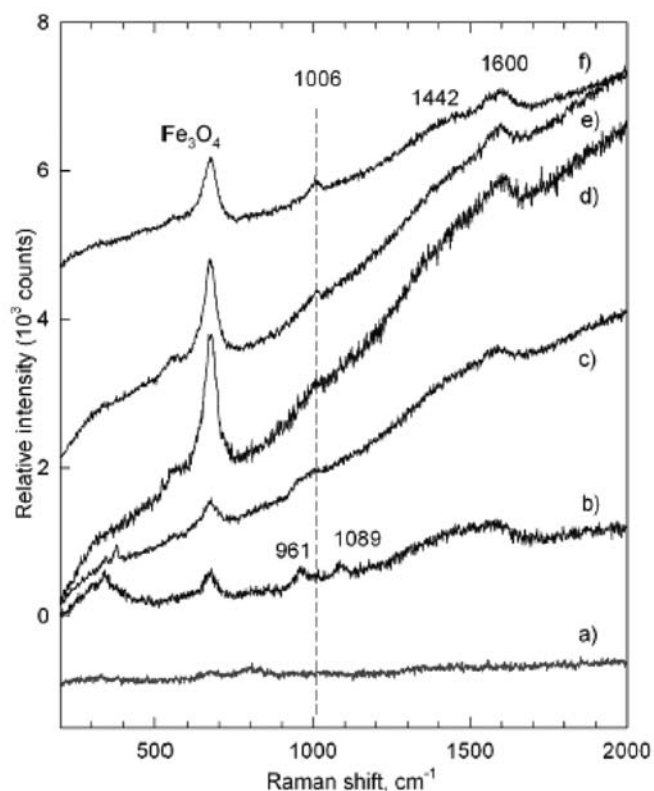


Figure 20.32—Raman spectra from a ball-on-flat experiment: (a) steel disk away from wear scar (i.e., no film); antiwear films formed after 1 h with (b) fresh oil and oil aged for (c) 24 h, (d) 47 h, (e) 50 h, and (f) 122 h [75]. Source: Reprinted with permission from [75].

as a result of plasma treatment. The vibrational spectroscopy enables important information on the C=C and C=O bonds to be determined as well as the presence of important functional groups such as -OH, COO-, -OOH, and -COOH, which can provide hydrophilic functionality at the surface. These groups have a fingerprint wavelength, and determination of the FTIR spectra enables the surface bonding characteristics to be determined. This complements the chemical speciation information usually obtained with the XPS. The analysis procedure can be found in detail in the ASTM standard E168-06 titled "Standard Practices for General Techniques of Infrared Quantitative Analysis." Figure 20.33 shows the typical FTIR spectra obtained from analyzing the fresh clutch friction material and the friction material after a SAE No. 2 clutch test.

The analysis approach in this technique is based on the fact that structural features of the molecule, whether they are the backbone of the molecule or the functional group attached to the molecule, produce a characteristic and reproducible peak in the spectrum. This information can indicate whether the backbone of the molecule consists of linear or branched chains, whether there are aromatic rings in the structure, and the nature of functional groups [76].

Attenuated total reflection (ATR) spectroscopy has also been widely used in surface engineering and polymer studies. The absorption spectra and ATR were explored and used as an analysis technique by Harrick [77] and Fahrenfort [78] in their separate studies. The infrared (IR) radiation propagating in the ATR optical element generates

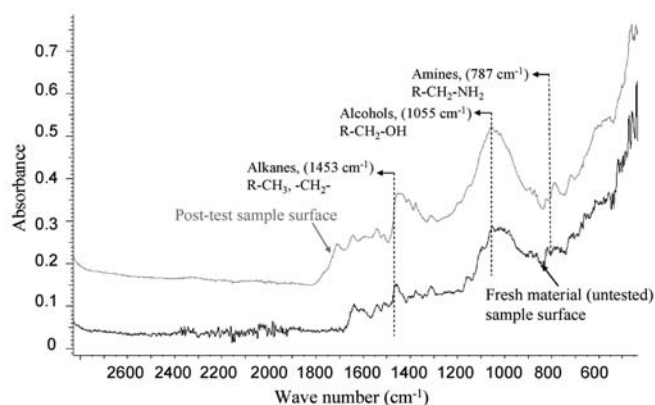


Figure 20.33—FTIR spectra of fresh and post-test friction material.

total internal reflection at the interface with the sample layer because of the different refractive indices of the two media. An exponentially decaying electromagnetic wave penetrates into the sample medium and interacts with molecules on the surface. The reflected wave intensity is thereby attenuated and yields an IR spectrum similar to the transmission IR spectra. Good contact between the sample and the internal reflection element (IRE) is required for good ATR spectroscopy, and samples such as viscous fluids or flexible solids are most appropriate to be analyzed by this technique. Piras, Rossi, and Spencer [79,80] reported that ZDDP decomposition and P-O-P species formation can be observed by ATR FTIR after tribological tests.

20.2.3 Surface Techniques for In Situ Chemical Characterization of Buried Surfaces

Most of the studies on tribofilm chemistry characterization, done as a first step to understand the material/lubricant tribochemistry processes, are mainly performed analyzing tribofilms formed in bench tribometers using ex situ surface analytical techniques, requiring pretest sample preparation. Tribofilms analyzed in this way are not necessarily representative of the films formed in their active state in the engine, and monitoring changes with time, temperature, or other variables becomes more difficult. In this section, the current techniques used for chemical characterization of buried surfaces are discussed.

Vibrational spectroscopies are of high importance for in situ surface analysis (reviewed recently in [81]). Post-test Raman analysis of tribofilms formed from fully formulated

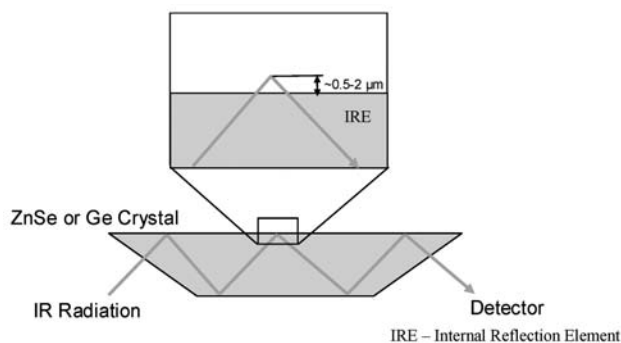


Figure 20.34—Schematic representation of ATR FTIR reflection-absorption microscopy.

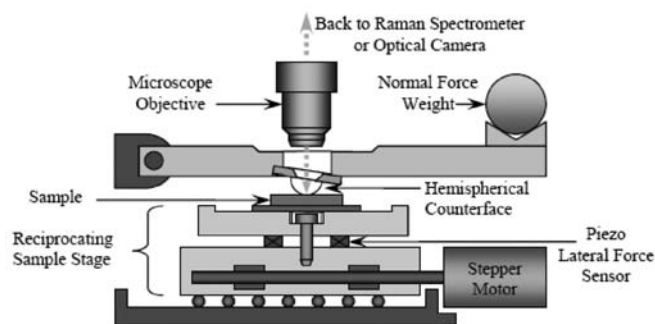


Figure 20.35—Schematic of an in situ Raman tribometer [85].

engine oils have shown formation of orthophosphates at 962 cm^{-1} , Fe_2O_3 at 677 cm^{-1} , CaCO_3 at 1090 cm^{-1} ; hydrocarbon at approximately 2930 cm^{-1} [82]; and MoS_2 and MoO_3 from MoDTC-containing oil at 405 and 951 cm^{-1} , respectively [83], indicating the potential of this technique for analyzing tribofilms formed when using typical engine oil additives. Raman spectroscopy has already been used to analyze materials at very high hydrostatic pressures using a diamond anvil cell [84]. Adapted by Singer, Dvorak, and Wahl [85] (Figure 20.35), it is mainly used to analyze tribological interfaces in dry sliding. The ASTM standard E1840-96 titled “Standard Guide for Raman Shift Standards for Spectrometer Calibration” provides the guideline for the Raman spectrometer calibration. In situ tribological studies using a Raman spectrometer have shown to be very useful in studying the tribological properties of solid lubricant coatings. In this equipment, the usually dry sample slides in a reciprocating way under a stationary hemispherical counterbody (glass or sapphire) whereas an Ar^+ laser beam from the Raman spectrometer travels through the transparent counterbody into the sliding contact area. The combination of Raman spectroscopy with friction sensing and contact visualization enables investigation of spatially resolved information on the friction and chemistry of the contact [86,87].

Other studies involving in situ analysis have involved optical methods and FTIR [88,89]. The drawback of using IR microreflection absorption spectroscopy is the large depth of the material analyzed making it unsuitable for analyzing tribofilms of approximately 200-nm thickness. Use of an ATR FTIR tribometer has increased the surface sensitivity of the FTIR [90]. Piras and colleagues reported on the application of the ATR FTIR spectrometer with a special tribometer (Figure 20.36) to analyze the buried

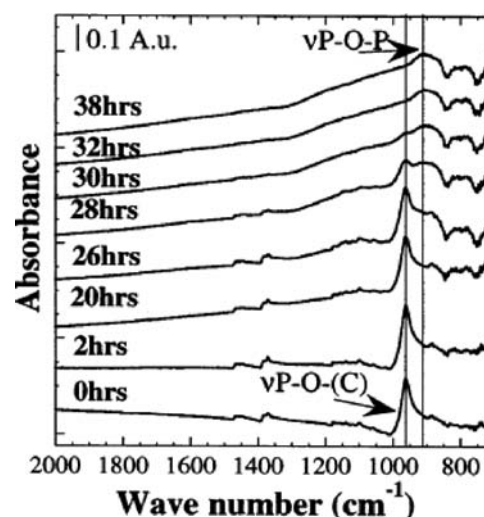


Figure 20.37—Commercial ZDDP ATR spectra collected during thermal tests at 150°C on Ge ATR crystals coated with Fe (10 nm) [80].

surface in situ [80]. Ge was chosen as the ATR element because of its favorable mechanical properties, high refractive index, and chemical resistance to many solvents. The advantage of this crystal is that it can be coated with different metals by magnetron sputtering. The moving part of the tribological system was a fixed cylinder (diameter 10 mm, width 7 mm) sliding in a reciprocating motion across the metal-coated Ge crystal surface.

Figure 20.37 shows a ZDDP ATR FTIR spectra collected at different times during a thermal test performed at a temperature of 150°C on a Ge crystal coated with Fe. The spectrum of commercial ZDDP at the beginning of the experiment (0 h) shows the P-O-(C) stretching vibration peak (961 cm^{-1}), which is the characteristic peak of the ZDDP molecule [79]. This peak was seen to decrease as the experiment progressed. Instead of the P-O-(C) peak, the (P-O-P) peak became more obvious after 2 h of testing.

20.3 APPLICATION OF SURFACE ANALYTICAL TECHNIQUES TO UNDERSTAND THE TRIBOCHEMISTRY OF AUTOMOTIVE ENGINE COMPONENTS

Surface analytical techniques have played an essential role in understanding the lubrication mechanisms of surface-active additives such as antiwear additives, detergents, dispersants, friction modifiers, etc. This section reviews the

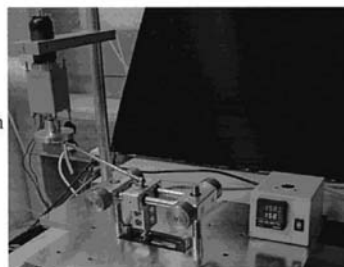
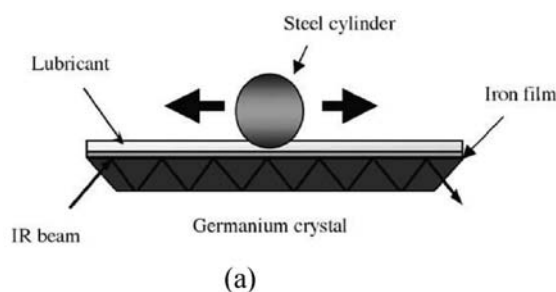


Figure 20.36—Schematic (a) and photograph (b) of the ATR tribometer (ETH, Switzerland) for the in situ chemical analysis of tribological films [80].

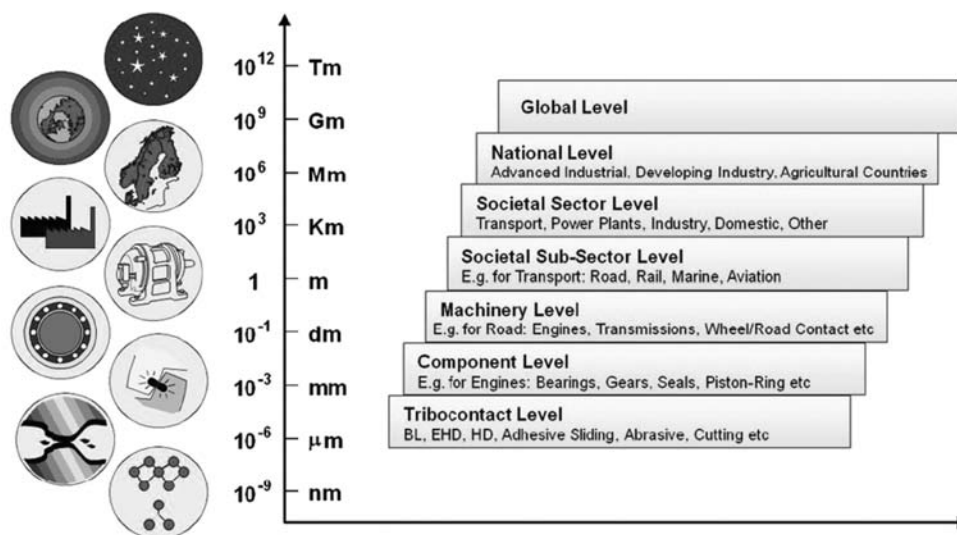


Figure 20.38—Key factors that determine the performance of tribological systems in passenger cars [3].

research on tribochemistry processes that lead to formation of ZDDP and MoDTC tribofilms on steel and Al-Si alloy, in which the use of the surface analytical techniques discussed in the previous section was of primary importance. Before that, a brief discussion on the relevance of bench tribometer tests in tribochemical studies and typical automotive engine oil chemical additives is presented.

20.3.1 Engine-Relevant Tribological Tests

Ideally, engine tests with absolute control of testing parameters are required for studying the tribology/tribochemistry of these systems. However, this is financially not sustainable because engine tests cost between €30,000 and €400,000 depending on the equipment, instrumentation, engine size, and test duration [91]. In addition, because the engine tests are complex, it is difficult to obtain any meaningful and statistically significant correlations between the testing parameters and tribological performance. Therefore, any valid results that can be achieved in much cheaper bench tribometers and that are of relevance to understanding the lubrication in real engine systems will not only have a significant financial effect by reducing the number of engine tests needed but will also enable development of fundamental friction and wear models relevant to the real system.

Figure 20.38 lists the key factors that determine the tribological performance of modern passenger car systems and that need to be considered when developing bench tribometer test methodologies for simulating these systems and engines [3,92].

Several experimental tribometers have been developed so far and used for simulating the tribological conditions of valve train or piston ring/liner systems. In designing tribometers, the focus was mainly in maintaining the mechanical and material parameters of the tribology system, aiming to achieve similar wear mechanisms to those observed in the engine [82, 91–97]. The current ASTM standard [98] recommends the conditioning of test oils before testing them on a ring-on-liner test to simulate the lubrication of the automotive engine piston ring/liner system. Most engine tribochemistry knowledge is developed by studying the lubrication in bench tribometer tests that are carefully

designed to simulate the material and mechanical properties of actual automotive engine tribological systems.

20.3.2 Automotive Engine Oils

To meet the ever-changing needs of the engine designers and of the consumers, increasingly with respect to environmental concerns, the additive industry puts major effort into developing new additives. The precise level of additives in the lubricants can be critical because the interactions between additives can be synergistic or antagonistic. The automotive crankcase lubricant additive package typically ranges from 5 to 25% [6]; therefore the optimization of the additive package is also very important.

Engine oil additives fall into two categories:

1. Those protecting metal surfaces in the engines, such as antiwear, antirust, and anticorrosion additives
2. Those reinforcing base stock performance, such as antioxidants, dispersants, viscosity modifiers, and pour-point depressants.

Antiwear additives are used to reduce wear, scuffing, and scoring under boundary lubrication conditions. The most common antiwear additives used in practice are organochlorine; organosulfur; organophosphorus (tricresyl phosphate [TCP] and dibutyl phosphite [DBP]); organometallic (ZDDP, MoDTP, and MoDTC); and organic borate compounds [99]. The most important class of antiwear additives remains the ZDDPs [100–102]. The ZDDP additive is one of the most widely used additives in engine oils. This is because it has shown to have multifunctional properties, providing several of the characteristics needed in a lubricant specification, namely antiwear, extreme pressure (EP), and antioxidant action. ZDDP additives are manufactured by reaction of alcohols, phosphorus pentasulfide, and zinc salts [103]. The type of ZDDP is defined by the organic alcohol used to synthesize it: alkylphenols for aryl ZDDP, primary alcohols for primary ZDDP ($\text{CH}_3\text{CH}_2\text{CH}_2\text{CH}_2\text{O}-$), and secondary alcohols for secondary ZDDP ($\text{CH}_3\text{CH}_2\text{CH}(\text{CH}_3)\text{O}-$). Primary and secondary alkyl ZDDPs are preferred for use in gasoline engines whereas the aryl ZDDPs are preferred for use in diesel engines [104]. It has been shown that primary ZDDP gives higher wear than secondary

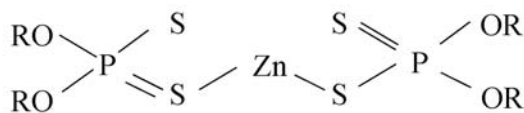


Figure 20.39—Molecular structure of ZDDP.

ZDDP, which is thought to be due to the different thermal stability of both additives, molecular weight, or concentration of unreacted acids used in the synthesis of the ZDDP [105]. Its molecular structure is shown in Figure 20.39.

Friction modifiers are surface-active agents closely related to EP additives in structure and mode of action. They are added to reduce friction in engine components for which the surfaces operate mainly under boundary lubrication conditions such as the valve train. The additives generally fall into two classes: the physically adsorbed molecules such as fatty acids and amides and the chemically reactive species such as molybdenum dithiocarbamates [100–102]. Of particular interest are the MoDTC and MoDTP additives [106–108]. The structures of these two compounds are shown in Figure 20.40.

Complete details on other typical automotive engine oils can be found in references 100–102.

20.3.3 Tribochemistry of the ZDDP Antiwear Additive

20.3.3.1 PHYSICAL PROPERTIES

The ability to have the detailed information on the tribofilm thickness and ultimately the chemical composition while in contact is of paramount importance to be able to understand the exact antiwear mechanism of the ZDDP tribofilm. Tribofilm thickness has been quantitatively estimated indirectly by using XANES spectroscopy combined with the particle-induced X-ray emission (PIXE) technique [109], EDX intensity [110,111], AES depth profiling [58,112], AFM [26], and optical interferometry-based techniques such as the spacer layer interferometry method (SLIM) [113,114]. Each of the methods above has its drawbacks that ultimately affect the accuracy of the measured film thickness. Most of the above techniques estimate the thickness of the tribofilm formed on one of the surfaces of the tribocouple. If the same tribofilm is formed on the counterbody surface, the overall layer in between the contacting surfaces will be greater than 1000 nm. At this stage, the technique that has shown the greatest potential for accurately measuring the tribofilm thickness is the SLIM [113,114]. The interference of the tribofilm is minimized using the SLIM, although the

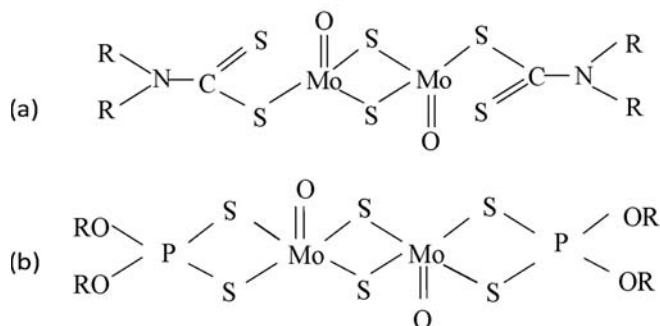


Figure 20.40—Molecular structure of (a) MoDTC and (b) MoDTP additives.

major drawback is having to stop the tribological process during measurement.

In terms of the mechanical properties, ZDDP tribofilms are very tenacious [109]. Fuller and colleagues [109] found that there is little to no change in the ZDDP tribofilm thickness when rubbed in base oil for 24 h in the same conditions when rubbed with ZDDP lubricant. Studies of the structure and rheological properties of the antiwear films formed from ZDDPs [39,115] have shown that the film has varying structure and properties with depth. The mechanical properties of the films after *n*-heptane washing and soft mechanical removal of alkyl phosphate indicated that the polyphosphate layer was damaged by solvent washing. In the case of soft mechanical removal of the alkyl phosphate layer, the polyphosphate layer was heterogeneous. Three values of reduced modulus of the film were recorded: 15, 27–30, and 40 GPa. The initial hardness was in the range of 1–1.5 GPa. In the case in which the films were washed with *n*-heptane, the reduced modulus was 30–40 GPa. The numerical application gave a viscosity value of approximately 10^8 Pa for the polyphosphate layer, clearly showing the solid nature of the film. The sulfide oxide layer properties were not affected by the cleaning procedure. They gave a reduced modulus of 90 GPa and an initial hardness of 4.7 GPa. It was found that the initial hardness increased with penetration depth, which suggests that the ZDDP surface film accommodates the pressure applied by the indenter by increasing the hardness. Figure 20.41 provides a TEM image of the ZDDP tribofilm layers [115].

20.3.3.2 CHEMICAL PROPERTIES

Through analyzing the cam and tappet engine components by XPS [116,117], it is found that practical surfaces lubricated using ZDDP-containing lubricants appear to consist of an iron oxide layer containing a minor proportion of zinc polyphosphate and iron sulfide. This led to the suggestion that zinc phosphates are physically adsorbed on the surface oxide layer whereas the iron sulfide is formed via the oxide layer and the elemental sulfur is generated from

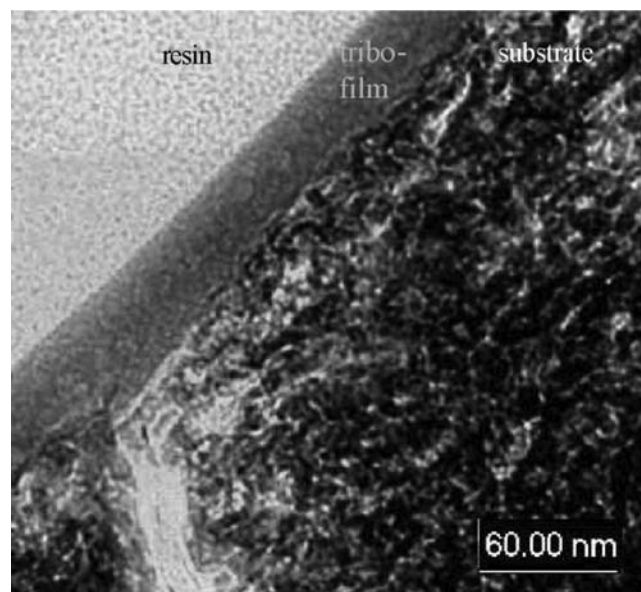


Figure 20.41—TEM observation of a FIB cross-section preparation of the ZDDP tribofilm [115].

alkyl sulfides. The composition of this surface film and its tribological performance are functions of the contact conditions. Sensitive analytical techniques such as XANES spectroscopy and XPS showed the effects of physical parameters on the composition and mechanism of ZDDP antiwear film formation [59,118]. High temperature, high load, and rubbing time increase the rate of ZDDP decomposition, resulting in a thicker tribofilm containing more long-chain polyphosphates on the topmost surface. This film covers a shorter chain polyphosphate ($\text{Zn}_7(\text{P}_5\text{O}_{16})_2$) layer in the bulk of the surface film [49]. XANES analyses of the ZDDP tribofilms indicate formation of a linkage isomer of ZDDP (LI-ZDDP) as an important precursor for the film formation. The complete proposed mechanism can be found in reference 49. Considering that friction is necessary to produce the speciation of phosphorus and sulfur, Martin [58,119] proposed a model for film formation with metal dithiophosphates in which chemical and mechanical aspects are linked together. After detailed analysis of the wear scar using AES, XPS, and XANES techniques, they proposed that ZDDP additives when lubricating steel components form a thin, long-chain zinc poly(thio)phosphate film superimposed on a thicker, short-chain mixed Fe/Zn polyphosphate film with some embedded ZnO and ZnS nanocrystallites [58]. A schematic graph of the possible pathway of ZnDTP (ZDDP) film formation, as suggested by De Barros [45], can be seen in Figure 20.42.

Freezing lubricated samples immediately after the test and subsequently analyzing the chemistry in the wear scar has enabled obtaining a clearer picture of the cleaning effect on the surface film composition. In the work by Bell, Delargy, and Seeney [120], the antiwear films formed from ZDDP were analyzed under cryogenic and solvent washed conditions using surface techniques such as SEM, ToF-SIMS, and for quantitative analysis XPS. In addition to phosphates in polymeric and glassy states, evidence of a significant concentration of organic material in the furthest layers of the film was found. This layer is believed to be removed as a result of the sample solvent washing [120].

In understanding the mechanism by which ZDDP additive controls wear, it is essential to characterize the chain length of the polyphosphate film that they form and the nature of the sulfur-containing film. Polyphosphates with

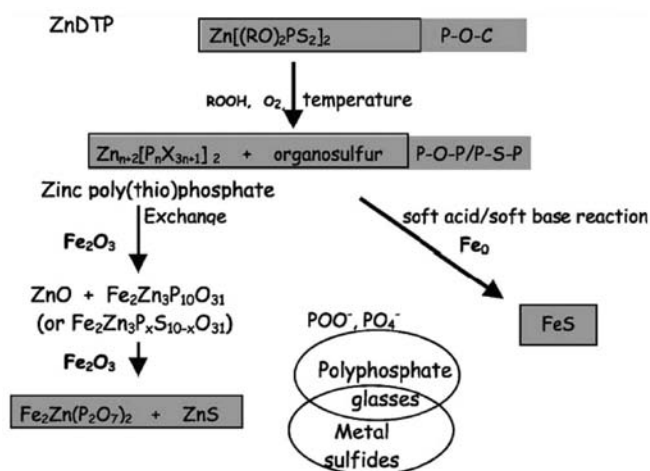


Figure 20.42—The different phosphates and sulfur species in AQ8 ZnDTP tribofilm [45].

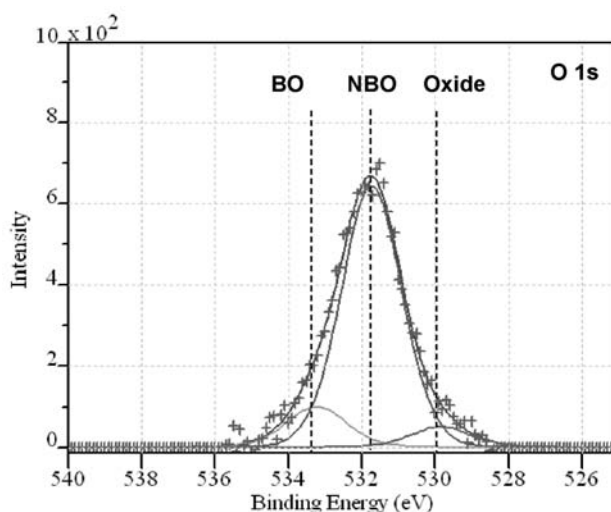


Figure 20.43—Curve-fitted oxygen 1s XPS peak obtained from the ZDDP tribofilm.

different chain lengths have different mechanical and rheological properties and as such are expected to have different tribological properties. In this aspect, the two most important parameters that need to be obtained are the P/O atomic ratio and the ratio of bridging oxygen (P–O–P) to nonbridging oxygen (–P=O and P–O–Zn). These two parameters determine the glass polymerization number, indicating the nature of the phosphate structure (ortho-, pyro-, or methaphosphate) and its polymeric chain length. XPS is a good technique to determine the above parameters; hence, it is very useful in analyzing the ZDDP tribofilm. Figure 20.43 shows a typical oxygen 1s XPS peak obtained from the wear scar produced after the test with ZDDP-containing lubricant, showing that oxide, nonbridging oxygen (NBO), and bridging oxygen (BO) are the surface reaction products.

For the fitting analysis of XPS results, it is important to accurately determine the full-width half maximum (FWHM) of the peaks and to carefully apply the XPS curve-fitting procedure for determining the chemical species formed [121–123]. In addition, in the case of ZDDP tribofilm, the film is not highly defined and as a result sulfur may partially replace oxygen in the polymer chain backbone (formation of O–P–S instead of O–P–O bond), altering the BO/NBO ratio [24,124]. Analysis of the sulfur peak clearly shows formation of sulfide (S^{2-}), but with XPS, it is difficult to determine which metal sulfide is formed or to separate it from the thiophosphate. Hence, it is important to analyze the tribofilms with other techniques to supplement the information obtained by XPS.

Use of the XANES technique has significantly improved the characterization of phosphate chain length [59,60]. The XANES P L-edge has shown to be very useful in characterizing the polyphosphates, mainly because of its sensitivity to small structural changes caused by bridging P–O bonds [125]. Figure 20.44 shows XANES P L-edge peaks obtained analyzing ZDDP tribofilm and thermal film as well as the model compounds ZDDP additive, Zn orthophosphate, and a long-chain Zn polyphosphate [49].

Because of the limitations of the XANES technique in quantitative analysis and lateral resolution, the most comprehensive results will be achieved by analyzing surface

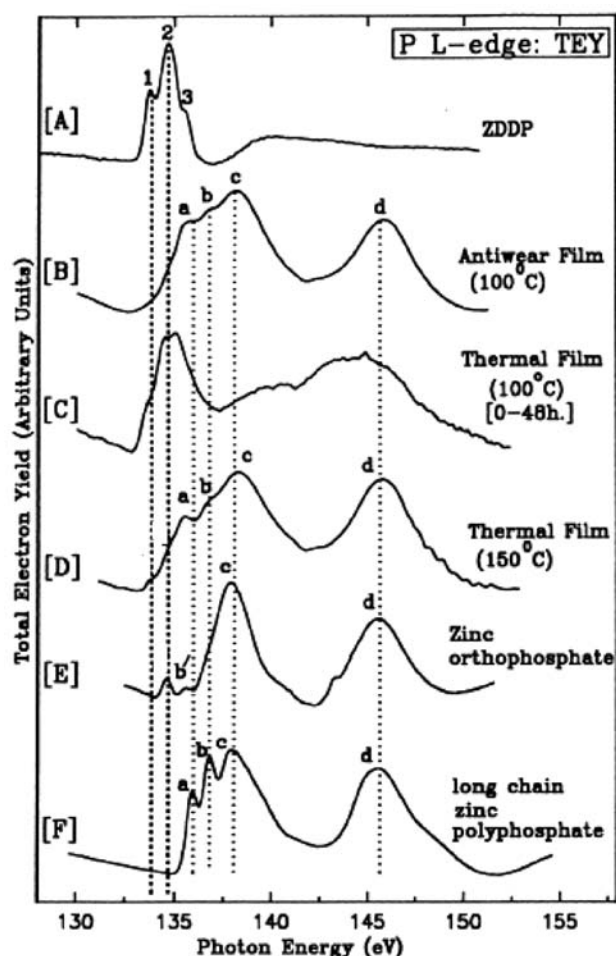


Figure 20.44—P L-edge XANES peaks obtained from the ZDDP tribofilm, thermal film, and model compounds [49]. Detailed analysis of position and intensity of peaks a, b, and c, after curve-fitting enables accurate determination of the polyphosphate chain length.

films in conjunction with other surface analytical techniques such as XPS, SIMS, or AES.

Figure 20.45 summarizes the understanding of physical appearance and the chemical composition of the ZDDP tribofilm obtained with a range of surface analytical techniques.

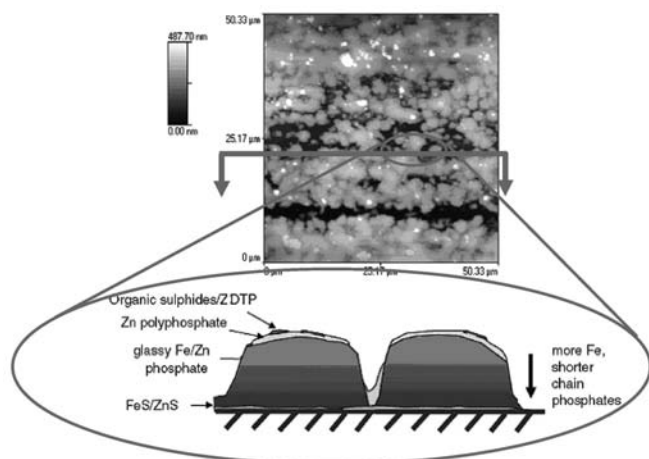


Figure 20.45—AFM image and schematic representation of the ZDDP antiwear pads [126].



Figure 20.46—The TEM of wear debris showing the presence of MoS₂ "eyelashes" [131].

20.3.4 Tribochemistry of the MoDTC Friction Modifier

Tribochemistry processes of friction modifiers used in engine oils are of particular interest because these additives directly influence the fuel economy and as a result of the vehicle emissions. Formation of low-friction tribofilms as a result of the interaction of engine oil friction modifiers such as MoDTC with the contact surface result in significant friction reduction in engines [127,128]. This is usually achieved by the formation of a low-shear tribofilm in the tribological systems that operate in the boundary/mixed lubrication regime. In the case of MoDTC, low friction is achieved by the formation of a MoS₂-containing tribofilm on the tribological contact [106–108,129–131]. TEM images (Figure 20.46) have shown that MoS₂ to be in the form of tiny, flake-like nanocrystals with diameters of 10–25 nm and heights of 1–2 nm [131,132]. The layer-lattice structure of the MoS₂ facilitates the low friction between the tribocouple components [133].

AFM images of the MoDTC tribofilm showed different features than the ones from ZDDP tribofilms. Figure 20.47 shows a typical AFM image of the MoDTC tribofilm [134].

Of great interest is the performance of friction modifiers when used in the additive package because their

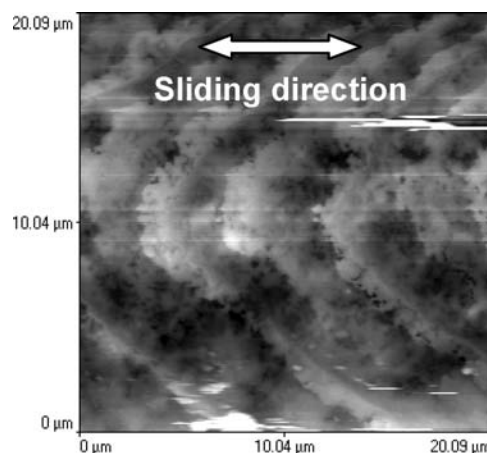


Figure 20.47—AFM image of MoDTC tribofilm [134]. Features oriented in the sliding direction can be observed.

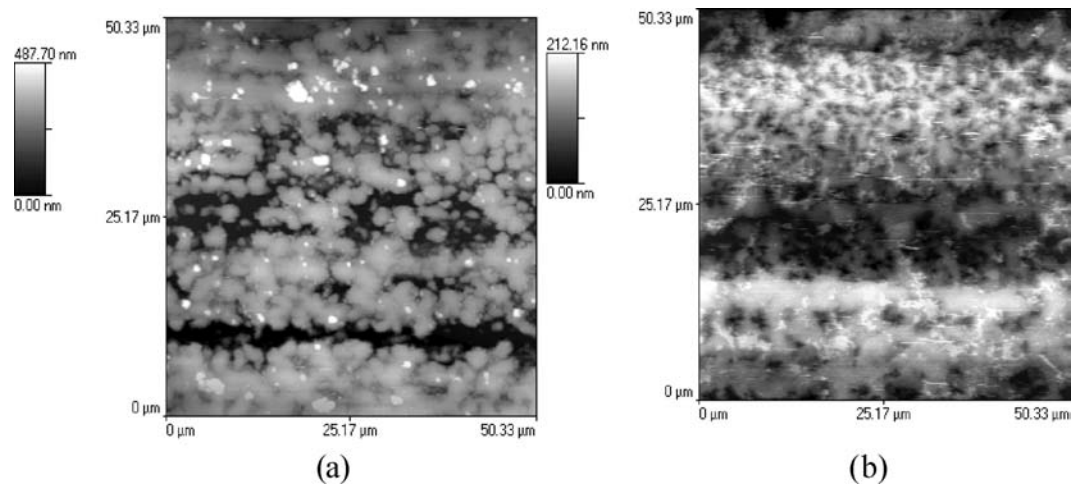


Figure 20.48—Tribofilm structures obtained using AFM: (a) ZDDP tribofilm and (b) ZDDP/MoDTC tribofilm [134]. Both tribofilms are formed following the same testing conditions.

effectiveness may be strongly affected by synergistic or antagonistic effects from the interactions with other additives [135]. A substantial number of studies have focused on the interactions between friction modifiers (MoDTC) and antiwear additives (ZDDP). It is important to optimize the performance of friction modifiers with the antiwear additives because both additives are surface active and compete for the active adsorption sites at the interface. Interactions between ZDDP and MoDTC additives in tribofilm formation and subsequently in tribological performance are shown to occur in the bulk oil [136] and in the tribofilm [137]. Detailed analyses of the tribofilms formed from oils containing ZDDP and MoDTC additives show that the ZDDP/MoDTC tribofilm is a two-phase composition: Zn/Mo phosphate glass and a carbon-rich amorphous phase with MoS₂ sheets embedded in the phosphate glass [40,54,138–141]. AFM images of this tribofilm (Figure 20.48b) show it being more uniform than the ZDDP tribofilm (Figure 20.48a) [134].

ZDDP is thought to promote formation of the MoS₂ from the MoDTC additive [142,143], and the possible mechanisms by which this is done is by providing the sulfur [54,144] or by preserving the pure MoS₂ from oxidation to MoO₃ [137].

20.3.5 Tribochemistry in Nonferrous Materials—Hypereutectic Al-Si Alloys

A wide range of tribomaterials, tribocoatings, and surface treatments for engine tribocomponents have been used in the last few decades. A comprehensive review of the conventional and novel materials being used in the IC engine can be found in reference 40. Table reviews all materials applied for piston assembly systems in IC engines.

For the engine block material, the cast iron is being substituted with lower density materials, such as Al-Si alloys, to reduce the weight of the engine. Other advantages of Al-Si alloys are good electrical and thermal conductivity and lower manufacturing costs compared with cast iron [145]. A high strength-to-weight ratio, high thermal conductivity, and low machining cost of these alloys have made this material a cost-effective replacement for heavy cast iron in engine blocks [145]. For diesel engines, because of the increasing demand of high cylinder pressure, com-

pacted graphitic iron (CGI) is being considered to replace cast iron [146].

Si, when used in Al alloys, will increase the overall strength of Al because of the solidification that occurs in the near-surface regions around the Si grains [147,148]. Figure 20.49 shows the Al-Si equilibrium diagram and different surface structure that can be achieved depending on the Si content [148]. In hypereutectic alloys, a hard phase of pure Si is formed when the melt is cooled after casting.

The resulting Si “islands” that are formed in the Al alloy matrix are often said to act as load-bearing/sliding surfaces, enabling the use of this material for cylinder liners in IC engines. Similar to cast iron liners, the friction and wear performance at the TDC and BDC will be greatly influenced by the tribochemistry processes occurring between the material surface and the lubricant chemistry as well as the mechanical properties of the tribofilm formed on the surface. In the hypereutectic Al-Si alloys, the distinct material phases make the determination of the tribochemical processes even more challenging.

TABLE 20.2—Tribomaterials for the Piston Assembly System [40]

	Piston Ring	Piston Skirt	Cylinder Bore/ Liner
Conventional materials	Gray CI	Gray CI	Monolithic gray CI
	Carbide CI Malleable/ nodular CI		
Recently used materials	Nitrided steel	Cu- and Ni-based Al alloy (e.g., Al 336)	Si-containing Al alloy (AA 390)
	Tool steel		Cast Al-based metal matrix composite
			Steel liner
			Compacted graphite iron

CI = cast iron.

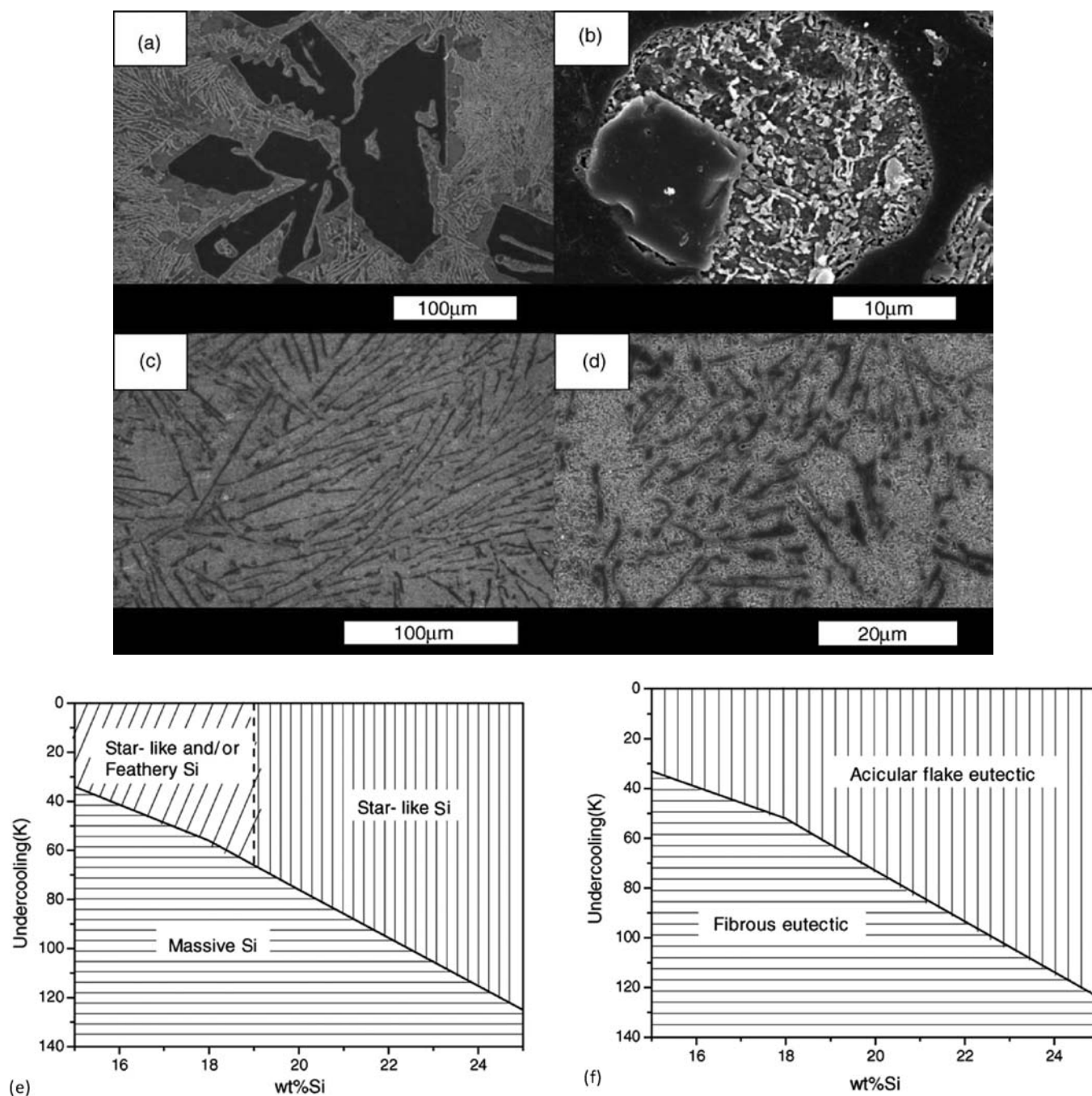


Figure 20.49—The effect of undercooling on the microstructures of Al-25 wt% Si (SEM image): (a) bulk (primary), (b) $\Delta T = 125$ K, (c) bulk (eutectic), and (d) $\Delta T = 124$ K. Microstructure selection maps of hypereutectic Al-Si alloys (e and f) [148].

Formation of the ZDDP tribofilm in Al-Si alloys has been recently studied [63,149,150] and, although the findings are still not conclusive, insight on the interaction between this additive and the Al-Si alloy has started to grow. It is demonstrated that amorphous polyphosphates form on both Al and Si material [150], and the higher Si content promotes formation of the polyphosphates from the ZDDP additive [63]. Formation of the phosphates is also supported by the authors' work using the SIMS analyses of Al-Si wear scars that were produced after lubricating with ZDDP-containing lubricants. Figure 20.50 shows the PO_2 peak depth profile obtained from the ZDDP tribofilms formed after different sliding time.

Although the ZDDP additive seems to form a phosphate film, its role on wear reduction is small [150,151]. The process of the tribofilm formation is a dynamic process that involves formation and removal of the tribofilm during the sliding process. Only a positive correlation between formation and removal of the phosphate film on the interface (i.e., higher formation rate than removal rate) will ensure its effectiveness on wear reduction. The reason why the phosphate film on the Al-Si alloy is not as effective on wear reduction as it is on steel seems to be related to the low tenacity of this film. Essential for formation of tenacious phosphate film on steel components is the interaction of the $\text{Zn}_3(\text{PO}_4)_2$ with the Fe_2O_3 , which results in the formation of Zn/Fe phosphates.

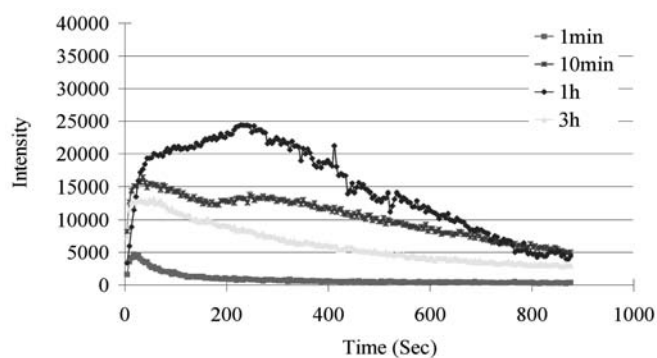
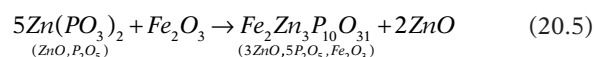


Figure 20.50— PO_2 SIMS peak depth profiling from the tribofilm formed using the ZDDP lubricant after different sliding time.

The tribochemical reaction, based on the Hard and Soft Acids and Bases (HSAB) principle [24], is



Al-Si alloy can not provide a thick oxide layer on the surface; therefore, the ZDDP film is unable to bind to the surface via oxide as it does on the steel surface [150].

In regard to friction reduction, effectiveness of the MoDTC additive on Al-Si surfaces and its interactions with the ZDDP still remain to be understood. As shown in the previous section, MoDTC is known as a good friction modifier for steel tribocouples lubricated in the boundary regime because of its decomposition to form MoS_2 sheets in the interface. In the case of the Al-Si alloy surfaces, the XANES technique [152] has shown that MoS_2 , ZnS, and sulfate were formed on the Al-Si plate wear scar when fully formulated oil was used for lubrication. Raman spectra of the surface films formed from model lubricating oil containing only ZDDP and MoDTC additives, as in Figure 20.51, have confirmed the formation of the MoS_2 on the wear scar. Raman spectrometer peaks at 405 and 379 cm^{-1} are observed at the wear scar formed after the test, indicating formation of the MoS_2 [129]. Rinsing with heptane removed the hydrocarbons from the wear scar but not the MoS_2 film. This film is seen to form on Al and Si phases of the alloy.

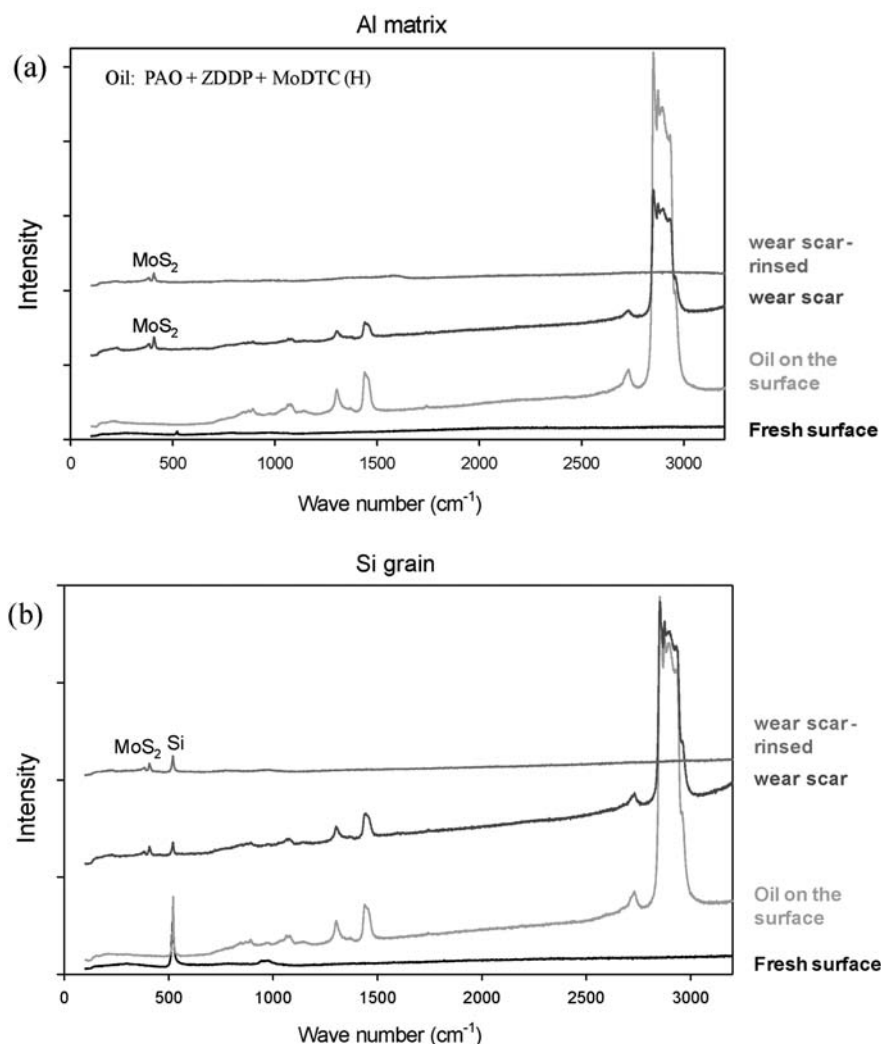


Figure 20.51—Raman spectra from the fresh Al-Si surface, PAO+ZDDP+MoDTC dispersed on the Al-Si surface, PAO+ZDDP+MoDTC wear scar, and PAO+ZDDP+MoDTC wear scar after rinsing with heptane: (a) Al phase and (b) Si phase of the Al-Si alloy.

Formation of the low-friction MoS₂ on both Al-Si material phases shows clearly that formation of the MoS₂ is not dependent on the substrate properties but mainly depends on the MoDTC concentration in the lubricating oil and the rubbing process.

20.4 CONCLUSION

Understanding the mechanisms of how engine oil additives interact with the lubricated surface is of great importance not only for engine lubricating oil formulation but also for the development of low-friction and low-wear functionalized materials/coatings to be used in automotive engine tribological systems. Surface analytical techniques are the essential tools to be used to study the physical, mechanical, and chemical properties of the lubricated surfaces. This chapter reviews some of the key surface techniques and their use for obtaining the properties of tribofilms formed from ZDDP and MoDTC engine oil additives. The common drawback of these techniques is the difficulty of measuring in situ tribofilms' physical properties such as its thickness, hardness, and viscosity as well as its chemical properties. This greatly limits the understanding of the phenomena related to the lubrication in the boundary regime. As a consequence, the current level of understanding of boundary/mixed lubricated tribological systems offers little predictive ability. Therefore, a detailed understanding of interface phenomena, especially of tribofilms' formation and removal kinetics, and their effect on friction and wear will significantly improve the process of designing new lubricants and coatings. Having the ability to characterize the tribofilm chemical composition in contact will inevitably facilitate the studies on tribofilm formation and removal kinetics far beyond what can be achieved currently. Future research in this area should use the latest development in ambient pressure surface analyses and applied physics to devise innovative experimental procedures that will make the analyses of the tribofilms while in contact possible.

REFERENCES

- [1] Kajdas, C., 2004, "Tribocchemistry." In *Surface Modification and Mechanisms*, G.E. Totten and H. Liang, Eds., Marcel Dekker, New York, pp. 99–165.
- [2] Tung, S.C., and McMillan, M.L., 2004, "Automotive Tribology Overview of Current Advances and Challenges for the Future," *Tribology Int.*, Vol. 37, pp. 517–536.
- [3] Holmberg, K., Andersson, P., and Erdemir, A., 2012, "Global Energy Consumption Due to Friction in Passenger Cars," *Tribology Int.*, Vol. 47, pp. 221–234.
- [4] Taylor, C.M., 1998, "Automobile Engine Tribology—Design Considerations for Efficiency and Durability," *Wear*, Vol. 221, pp. 1–8.
- [5] Dowson, D., 1993, "Piston Assemblies; Background and Lubrication Analysis." In *Engine Tribology*, C.M. Taylor, Ed., Elsevier: London, pp. 213–240.
- [6] Smith, G.C., 2000, "Surface Analytical Science and Automotive Lubrication," *J. Phys. D: Appl. Phys.*, Vol. 33, pp. R187–R197.
- [7] Priest, M., and Taylor, C.M., 2000, "Automobile Engine Tribology—Approaching the Surface," *Wear*, Vol. 241, pp. 193–203.
- [8] Bolander, N.W., Steenwyk, B.D., Sadeghi, F., and Gerber, G.R., 2005, "Lubrication Regime Transitions at the Piston Ring-Cylinder Liner Interface," *J. Eng. Tribology*, Vol. 219, pp. 19–31.
- [9] Taylor, C.M., ed. *Engine Tribology*. 1993, Elsevier: Amsterdam.
- [10] Mufti, R.A., and Priest, M., 2003, "Experimental and Theoretical Study of Instantaneous Engine Valve Train Friction," *Trans. ASME*, Vol. 125, pp. 628–637.
- [11] Guo, J., Zhang, W., and Zou, D., 2011, "Investigation of Dynamic Characteristics of a Valve Train System," *Mechan. Mach. Theory*, Vol. 46, pp. 1950–1969.
- [12] Green, J.H., Priest, M., Morina, A., and Neville, A., 2002, *Approaches to Sensitising Engine Valve Train Friction Models to Lubricant Formulation Characteristics*. in *Tribological Research and Design for Engineering Systems*, Proc. 29th Leeds-Lyon Symposium on Tribology. 2002. Leeds, Leeds, UK: Elsevier 2003, pp. 35–45.
- [13] Roshan, R., Priest, M., Neville, A., Morina, A., Xia, X., Green, J.H., Warrens, C.P., and Payne, M.J., 2008, "Friction Modelling of Tribofilm Performance in a Bench Tribometer for Automotive Engine Lubricants," *J. Tribology*, Vol. 222, pp. 357–367.
- [14] Knoll, M., 1935, "Aufladepotential und Sekundäremission Elektronenbestrahlter Körper," *Zeits. Tech. Physik*, Vol. 16, pp. 467–475.
- [15] Chen, M., and Alpas, A.T., 2008, "Ultra-Mild Wear of a Hyper-eutectic Al–18.5 wt.% Si Alloy," *Wear*, Vol. 265, pp. 186–195.
- [16] Equey, S., Roos, S., Mueller, U., Hauert, R., Spencer, N.D., and R. Crocket, 2008, "Tribofilm Formation from ZnDTP on Diamond-Like Carbon," *Wear*, Vol. 264, pp. 316–321.
- [17] Mistry, K., 2009, *The Tribocchemical Interactions at Lubricated Diamond-like-Carbon Interfaces under Extreme Pressure Conditions*, Ph.D. Thesis, University of Leeds, UK.
- [18] Stachowiak, G.W., Batchelor, A.W., and Stachowiak, G.B., 2004, "Experimental Methods in Tribology." In *Tribology Series* 44, D. Dowson, Ed., Elsevier, Amsterdam.
- [19] De Barros, M.I., Martin, J.M., LeMogne, Th., Bilas, P., Vacher, B., and Yamada, Y., 2005, "Mechanisms of MoS₂ formation by MoDTC in presence of ZnDTP: effect of oxidative degradation," *Wear*, Vol. 258, pp. 1643–1650.
- [20] De Barros Bouchet, M.I., Martin, J.M., Le-Mogne, T., and Vacher, B., 2005, "Boundary Lubrication Mechanisms of Carbon Coatings by MoDTC and ZDDP Additives," *Tribology Int.*, Vol. 38, pp. 257–264.
- [21] Grossiord, C., Martin, J.M., Le Mogne, Th., and Palermo, Th., 1998, "In Situ MoS₂ Formation and Selective Transfer from MoDTP Films," *Surface Coat. Technol.*, Vol. 108–109, pp. 352–359.
- [22] Martin, J.M., Grossiord, C., Le Mogne, T., and Igarashi, J., 2000, "Role of Nitrogen in Tribocchemical Interaction between ZnDTP and Succinimide in Boundary Lubrication," *Tribology Int.*, Vol. 33, pp. 453–459.
- [23] Varlot, K., Kasrai, M., Martin, J.M., Vacher, B., Bancroft, G.M., Yamaguchi, E.S., and Ryason, P.R., 2000, "Antiwear Film Formation of Neutral and Basic ZDDP: Influence of the Reaction Temperature and of the Concentration," *Tribology Lett.*, Vol. 8, pp. 9–16.
- [24] Martin, J.M., 1999, "Antiwear Mechanisms of Zinc Dithiophosphate: A Chemical Hardness Approach," *Tribology Lett.*, Vol. 6, pp. 1–8.
- [25] Grill, A., Patel, V., and Meyerson, M., 1991, "Tribological Behavior of Diamond-Like Carbon: Effects of Preparation Conditions and Annealing," *Surface Coat. Technol.*, Vol. 49, pp. 530–536.
- [26] Pidduck, A.J., and Smith, G.C., 1997, "Scanning Probe Microscopy of Automotive Antiwear Films," *Wear*, Vol. 212, pp. 254–264.
- [27] Topolovec-Miklozic, K., Lockwood, F., and Spikes, H., 2008, "Behaviour of Boundary Lubricating Additives on DLC Coatings," *Wear*, Vol. 265, pp. 1893–1901.
- [28] Morina, A., Green, J.H., Neville, A., and Priest, M., 2003, "Surface and Tribological Characteristics of Tribofilms Formed in the Boundary Lubrication Regime with Application to Internal Combustion Engines," *Tribology Lett.*, 2003, Vol. 15, pp. 443–452.
- [29] Wang, R., 2004, "An AFM and XPS Study of Corrosion Caused by Micro-Liquid of Dilute Sulfuric Acid on Stainless Steel," *Appl. Surface Sci.*, 2004, Vol. 227, pp. 399–409.
- [30] Fischer-Cripps, A.C., 2004, *Nanoindentation*, Springer, New York.
- [31] Oliver, W.C., and Pharr, G.M., 1992, "An Improved Technique for Determining Hardness and Elastic Modulus Using Load Displacement Sensing Indentation Experiments," *J. Mater. Res.*, Vol. 7, pp. 1564–1583.

- [32] Oliver, W.C., and Pharr, G.M., 2004, "Measurement of Hardness and Elastic Modulus by Instrumented Indentation: Advances in Understanding and Refinements to Methodology," *J. Mater. Res.*, Vol. 19, pp. 3–20.
- [33] Fischer-Cripps, A.C., 2002, *Nanoindentation*, Mechanical Engineering Series, F.F. Ling, Ed., Springer, New York.
- [34] Dickinson, M.E., and Schirer, J.P., 2009, "Probing More than the Surface," *Mater. Today*, Vol. 12, pp. 46–50.
- [35] Ballarre, J., Lapez, D.N.A., and Cavalieri, A.L., 2008, "Nano-Indentation of Hybrid Silica Coatings on Surgical Grade Stainless Steel," *Thin Solid Films*, Vol. 516, pp. 1082–1087.
- [36] Pereira, G., Munoz-Paniagua, D., Lachenwitzer, A., Kasra, M., Norton, P.R., Capehart, T.W., Perry, T.A., and Cheng, Y.-T., 2007, "A Variable Temperature Mechanical Analysis of ZDDP-Derived Antiwear Films Formed on 52100 Steel," *Wear*, Vol. 262, pp. 461–470.
- [37] Saha, R., and Nix, W.D., 2002, "Effects of the Substrate on the Determination of Thin Film Mechanical Properties by Nanoindentation," *Acta Mater.*, Vol. 50, pp. 23–38.
- [38] Rar, A., Song, H., and Pharr, G.M., 2002, "Assessment of New Relation for the Elastic Compliance of a Film-Substrate System," *Mater. Res. Soc. Symp. Proc.*, Vol. 695, pp. 431–436.
- [39] Bec, S., Tonck, A., Georges, J.M., Coy, R.C., Bell, J.C., and Roper, G.W., 1999, "Relationship between Mechanical Properties and Structures of Zinc Dithiophosphate Antiwear Films," *Proc. R. Soc. Lond. A*, Vol. 455, pp. 4181–4203.
- [40] Neville, A., Morina, A., Haque, T., and Voong, M., 2007, "Compatibility between Tribological Surfaces and Lubricant Additives—How Friction and Wear Reduction Can Be Controlled by Surface/Lube Synergies," *Tribology Int.*, Vol. 40, pp. 1680–1695.
- [41] Unnikrishnan, R., Jain, M.C., Harinarayan, A.K., and Mehta, A.K., 2002, "Additive-Additive Interaction: An XPS Study of the Effect of ZDDP on the AW/EP Characteristics of Molybdenum Based Additives," *Wear*, Vol. 252, pp. 240–249.
- [42] Ankoudinov, A.L., 1996, *Relativistic Spin-Dependent X-ray Absorption Theory*, Ph.D. Dissertation, University of Washington.
- [43] Koningsberger, D.C., and Prins, R., 1998, *X-Ray Absorption—Principles, Applications, Techniques of EXAFS, SEXAFS and XANES*. John Wiley, New York.
- [44] Sakurai, J.J., 1994, *Modern Quantum Mechanics*, Rev. Ed., Addison-Wesley, Boston.
- [45] De Barros, M.I., Bouchet, J., Raoult, I., Le Mogne, Th., Martin, J.M., Kasrai, M., and Yamada, Y., 2003, "Friction Reduction by Metal Sulfides in Boundary Lubrication Studied by XPS and XANES Analyses," *Wear*, Vol. 254, pp. 863–870.
- [46] Ankudinov, A.L., Ravel, B., Rehr, J.J., and Conradson, S.D., 1998, "Real-Space Multiple-Scattering Calculation and Interpretation of X-Ray-Absorption Near-Edge Structure," *Phys. Rev. B*, Vol. 58, pp. 7565–7576.
- [47] Adelhelm, C., Balden, M., and Sikora, M., 2007, "EXAFS Investigation of the Thermally Induced Structuring of Titanium-Doped Amorphous Carbon Films," *Mater. Sci. Eng. C*, Vol. 27, pp. 1423–1427.
- [48] Nicholls, M.A., Do, T., Norton, P.R., Kasrai, M., and Bancroft, G.M., 2005, "Review of the Lubrication of Metallic Surfaces by Zinc Dialkyl-Dithiophosphates," *Tribology Int.*, Vol. 38, pp. 15–39.
- [49] Fuller, M.L.S., Kasrai, M., Bancroft, G. M., Fyfe, K., and Tan, K.H., 1998, "Solution Decomposition of Zinc Dialkyl Dithiophosphate and Its Effect on Antiwear and Thermal Film Formation Studied by X-Ray Absorption Spectroscopy," *Tribology Int.*, Vol. 31, pp. 627–644.
- [50] Yin, Z., Kasrai, M., Bancroft, G. M., Fyfe, K., Colaianni, M. L., and Tan, K. H., 1997, "Application of Soft X-Ray Absorption Spectroscopy in Chemical Characterization of Antiwear Films Generated by ZDDP Part II: The Effect of Detergents and Dispersants," *Wear*, Vol. 202, pp. 192–201.
- [51] Yin, Z., Kasrai, M., and Bancroft, G.M., 1995, "X-Ray-Absorption Spectroscopic Studies of Sodium Polyphosphate Glasses," *Phys. Rev. B*, Vol. 51, p. 742.
- [52] Ferrari, E.S., Roberts, K.J., and Adams, D., 1999, "A Multi-Edge X-Ray Absorption Spectroscopy Study of the Reactivity of Zinc Di-Alkyl-Di-Thiophosphates (ZDDPS) Anti-Wear Additives: 1. An Examination of Representative Model Compounds," *Wear*, Vol. 236, pp. 246–258.
- [53] Bancroft, G.M., Kasrai, M., Fuller, M., Yin, Z., Fyfe, K., and Tan, K.H., 1997, "Mechanisms of Tribochemical Film Formation: Stability of Tribo- and Thermally-Generated ZDDP Films," *Tribology Lett.*, Vol. 3, pp. 47–51.
- [54] De Barros, M.I., Bouchet, J., Raoult, I., Le Mogne, Th., Martin, J.M., Kasrai, M., and Yamada, Y., 2003, "Friction Reduction by Metal Sulfides in Boundary Lubrication Studied by XPS and XANES Analyses," *Wear*, Vol. 254, pp. 863–870.
- [55] Belin, M., and Martin, J.M., 1995, "Local Order in Surface ZDDP Reaction Films Generated on Engine Parts, Using EXAFS and Related Techniques," *Lubr. Sci.*, Vol. 8, pp. 1–14.
- [56] Cizaire, L., Martin, J.M., Le Mogne, Th., and Gresser, 2004, "Chemical Analysis of Overbased Calcium Sulfonate Detergents by Coupling XPS, ToF-SIMS, XANES, and EFTEM," *Colloids Surf., A*, Vol. 238, pp. 151–158.
- [57] Kasrai, M., Fuller, M.S., Bancroft, G.M., Yamaguchi, E.S., Ryason, P.R., 2003, "X-Ray Absorption Study of the Effect of Calcium Sulfonate on Antiwear Film Formation Generated from Neutral and Basic ZDDPs: Part I—Phosphorus Species," *Tribology Trans.*, Vol. 46, pp. 534–542.
- [58] Martin, J.M., Grossiord, C., Le Mogne, Th., Bec, S., and Tonck, A., 2001, "The Two-Layer Structure of ZnDTP tribofilms Part I: AES, XPS and XANES Analyses," *Tribology Int.*, Vol. 34, pp. 523–530.
- [59] Yin, Z., Kasrai, M., Bancroft, G. M., Fyfe, K., Colaianni, M. L., and Tan, K. H., 1997, "Application of Soft X-Ray Absorption Spectroscopy in Chemical Characterisation of Antiwear Films Generated by ZDDP Part I: The Effects of Physical Parameters," *Wear*, Vol. 202, pp. 172–191.
- [60] Yin, Z., Kasrai, M., Bancroft, G. M., Fyfe, K., Colaianni, M. L., and Tan, K. H., 1997, "Application of Soft X-Ray Absorption Spectroscopy in Chemical Characterisation of Antiwear Films Generated by ZDDP Part II: The Effect of Detergents and Dispersants," *Wear*, Vol. 202, pp. 192–201.
- [61] Nicholls, M., Najman, M.N., Zhang, Z., Kasrai, M., Norton, P.R., and Gilbert, P.U.P.A., 2007, "The Contribution of XANES Spectroscopy to Tribology," *Can. J. Chem.*, 2007. 85: p. 816–830.
- [62] Sumant, A.V., Gilbert, P.U.P.A., Grierson, D.S., Konicek, A.R., Abrecht, M., Butler, J.E., Feygelson, T., Rotter, S.S. and Carpick, R.W., 2007, "Surface Composition, Bonding, and Morphology in the Nucleation and Growth of Ultra-Thin, High Quality Nanocrystalline Diamond Films," *Diamond Relat. Mater.*, Vol. 16, pp. 718–724.
- [63] Nicholls, M.A., Norton, P.R., Bancroft, G.M., and Kasrai, M., 2004, "X-Ray Absorption Spectroscopy of Tribofilms Produced from Zinc Dialkyl Dithiophosphates on Al-Si Alloys," *Wear*, Vol. 257, pp. 311–328.
- [64] Gilbert, B., Andres, R., Perfetti, P., Margaritondo, G., Rempfer, G., and De Stasio, G., 2000, "Charging Phenomena in PEEM Imaging and Spectroscopy," *Ultramicroscopy*, Vol. 83, pp. 129–139.
- [65] Nicholls, M.A., Bancroft, G.M., Norton, P.R., Kasrai, M., De Stasio, G., Frazier, B.H., and Wiese, L.M., 2004, "Chemomechanical Properties of Antiwear Films Using X-Ray Absorption Microscopy and Nanoindentation Techniques," *Tribology Lett.*, 2004, Vol. 17, pp. 245–259.
- [66] Barnes, T.J., Kempson, I.M., and Prestidge, C.A., 2011, "Surface Analysis for Compositional, Chemical and Structural Imaging in Pharmaceuticals with Mass Spectrometry: A ToF-SIMS Perspective," *Int. J. Pharm.*, Vol. 417, pp. 61–69.
- [67] Murase, A., Mori, H., and Ohmori, T., 2008, TOF-SIMS Analysis of Friction Surfaces of Hard Coatings Tested in Engine Oil," *Appl. Surf. Sci.*, Vol. 255, pp. 1494–1497.
- [68] Tohyama, M., Ohmori, T., Murase, A., and Masuko, M., 2009, "Friction Reducing Effect of Multiply Adsorptive Organic Polymer," *Tribology Int.*, Vol. 42, pp. 926–933.
- [69] Equey, S., Roos, S., Mueller, U., Hauert, R., Spencer, N.D., and Crockett, R., 2008, "Reactions of Zinc-Free Anti-Wear Additives in DLC/DLC and Steel/Steel Contacts," *Tribology Int.*, Vol. 41, pp. 1090–1096.
- [70] Kamimura, H., Kubo, T., Minami, I., and Mon, S., 2007, "Effect and Mechanism of Additives for Ionic Liquids As New Lubricants," *Tribology Int.*, Vol. 40, pp. 620–625.
- [71] Erdemir, A., and Donnet, C., 2001, "Tribology of Diamond, Diamond-Like Carbon and Related Films." In *Modern Tribology Handbook*, B. Bhushan, Ed., CRC Press, Boca Raton, FL.

- [72] Erdemir, A., and Donnet, C., 2006, "Tribology of Diamond-like Carbon Filmes: Recent Progress and Future Prospects. J. Phys. D: Appl. Phys., Vol. 39, pp. R1-R17.
- [73] Praver, S., Nugent, K.W., Lifshitz, Y., Lempert, G.D., Grossman, E., Kulik, J., Avigal, I., Kalish, R., 1996, "Systematic Variation of the Raman Spectra of DLC Films as a Function of sp²:sp³ Composition," *Diamond Relat. Mater.*, Vol. 5: p. 433-438.
- [74] Schwan, J., Ulrich, S., Batori, V., Ehrhardt, H., and Silva, S.R.P., 1996, "Raman Spectroscopy on Amorphous Carbon Films," *J. Appl. Physics*, Vol. 80, pp. 440-447.
- [75] Uy, D., Simko, S., O'Neill, A., Jensen, R., Gangopadhyay, A., Carter, R. O., 2006, *Raman Characterization of Anti-Wear Films Formed from Fresh and Aged Engine Oils*. SAE Technical Paper Series, 2006-01-1099, SAE, Warrendale, PA.
- [76] Atek, D., and Belhaneche-Bensemra, N., 2005, "FTIR Investigation of the Specific Migration of Additives from Rigid Poly(Vinyl Chloride)," *Eur. Polymer J.*, Vol. 41, pp. 707-714.
- [77] Harrick, N.J., 1967, *Internal Reflection Spectroscopy*, John Wiley & Sons, New York.
- [78] Fahrenfort, J., 1961 Attenuated Total Reflection: A New Principle for the Production of Useful Infra-Red Reflection Spectra of Organic Compounds," *Spectrochim. Acta*, Vol. 17, p. 698.
- [79] Piras, F.M., Rossi, A., and Spencer, N.D., 2002, "Growth of Tribological Films: In Situ Characterization Based on Attenuated Total Reflection Infrared Spectroscopy," *Langmuir*, Vol. 18, pp. 6606-6613.
- [80] Piras, F.M., Rossi, A., and Spencer, N.D., 2002, "In Situ Attenuated Total Reflection (ATR) Spectroscopic Analysis of Tribological Phenomena," *Tribology Ser. Vol. 40*, pp. 199-206.
- [81] Cann, P.M., 2008, "In-Contact Molecular Spectroscopy of Liquid Lubricant Films," *MRS Bull.*, Vol. 33, pp. 1151-1158.
- [82] Uy, D., Simko, S.J., Carter, R.O., III, Jensen, R.K., and Gangopadhyay, A.K., 2007, "Characterization of Anti-Wear Films Formed from Fresh and Aged Engine Oils," *Wear*, Vol. 263, pp. 1165-1174.
- [83] Jimenez, A.E., Morina, A., Neville, A., and Bermudez, M.D., 2008, "Surface Interactions and Tribochemistry in Boundary Lubrication of Hypereutectic Al-Si Alloys," *Proc. IMechE J: J. Tribology*, Vol. 223, pp. 593-601.
- [84] Gardiner, D.J., Bowden, M., Daymond, J., Gorvin, A.C., and Dare-Edwards, M.P., 1984, "A Raman Microscope Technique for Studying Liquids in a Diamond Anvil Cell," *Appl. Spectrosc.*, Vol. 38, pp. 282-284.
- [85] Singer, I.L., Dvorak, S.D., and Wahl, K.J., 2000, "Investigation of Third Body Processes by In Vivo Raman Tribometry." In *Conference Proceedings of NordTrib 2000*, Finland.
- [86] Singer, I.L., Dvorak, S.D., Wahl, K.J., and Scharf, T.W., 2003, "Role of Third Bodies in Friction and Wear of Protective Coatings," *J. Vacuum Sci. Technol. A*, Vol. 5, pp. S232-S240.
- [87] Scharf, T.W., and Singer, I.L., 2003, "Monitoring Transfer Films and Friction Instabilities with In Situ Raman Tribometer," *Tribology Lett.*, Vol. 14, p. 3.
- [88] Cann, P., and Spikes, H., 1991, "In Lubro Studies of Lubricants in EHD Contacts Using FTIR Absorption Spectroscopy," *Tribology Trans.*, Vol. 34, p. 248.
- [89] Westerfield, C., and Agnew, S., "IR Study of the Chemistry of Boundary Lubrication with High Temperature and High Pressure Shear," *Wear*, Vol. 181-183, p. 805.
- [90] Piras, F.M., Rossi, A., and Spencer, N.D., 2002, "Growth of Tribological Films," *Langmuir*, Vol. 2002, pp. 6606-6613.
- [91] Woydt, M., and Kelling, N., 2003, "Testing the Tribological Properties of Lubricants and Materials for the System "Piston Ring/Cylinder Liner" Outside of Engines," *Indust. Lubr. Tribology*, Vol. 55, pp. 213-222.
- [92] Blau, P.J., 2001, *A Review of Sub-Scale Test Methods to Evaluate the Friction and Wear of Ring and Liner Materials for Spark-and Compression Ignition Engines*, ORNL/TM-2001/184, Oak Ridge National Laboratory, Oak Ridge, TN.
- [93] Roper, G.W., and Bell, J.C., 1995, *Review and Evaluation of Lubricated Wear in Simulated Valve Train Contact Conditions*, SAE Paper 952473, SAE, Warrendale, PA, pp. 67-83.
- [94] Truhan, J.J., Qu, J., and Blau, P.J., 2005, "The Effect of Lubricating Oil Condition on the Friction and Wear of Piston Ring and Cylinder Liner Materials in a Reciprocating Bench Test," *Wear*, Vol. 259, pp. 1048-1055.
- [95] Truhan, J.J., Qu, J., and Blau, P.J., 2005, "A Rig Test to Measure Friction and Wear of Heavy Duty Diesel Engine Piston Rings and Cylinder Liners Using Realistic Lubricants," *Tribology Int.*, Vol. 38, pp. 211-218.
- [96] Li, S., Zhang, R., Jin, Y., Wang, Y.C., and Tung, S.C., 2003, "Competitive Surface Interactions of Critical Additives with Piston Ring/Cylinder Liner Components under Lubricated Breaking-in Conditions," *Tribology Trans.*, Vol. 46, pp. 200-205.
- [97] Tung, S.C., and Tseregounis, S.I., 2000, *An Investigation of Tribological Characteristics of Energy-Conserving Engine Oils Using a Reciprocating Bench Test*, SAE Paper 2000-01-1781, SAE, Warrendale, PA.
- [98] ASTM Standard G181-04, 2004: Practice for Conducting Friction Tests of Piston Ring and Cylinder Liner Materials under Lubricated Conditions, *Annual Book of ASTM Standards*, ASTM International, West Conshohocken, PA (reapproved 2009).
- [99] Wei, D., 1995, "Future Directions of Fundamental Research in Additive Tribochemistry," *Lubr. Sci.*, Vol. 7, pp. 211-232.
- [100] Rudnick, L., 2003, *Lubricant Additives: Chemistry and Applications*, Marcel Dekker, New York.
- [101] ATC, 1993, *Lubricant Additives and the Environment*, Document 49, ATC.
- [102] Mortier, R., 1999, "Gasoline Engine Lubricants." In *Modern Petroleum Technology: Downstream*, Vol. 2, A.G. Lucas, Ed., John Wiley & Sons, New York.
- [103] Barnes, A.M., Bartle, K.D., and Thibon, V.R.A., 2001, "A Review of Zinc Dialkyldithiophosphates (ZDDPs): Characterisation and Role in the Lubricating Oil," *Tribology Int.*, Vol. 24, pp. 389-395.
- [104] Khorramain, B.A., Iyer, G.R., Kodali, S., Natarajan, P., and Tupil, R., 1993, "Review of Antiwear Additives for Crankcase Oils," *Wear*, Vol. 169, pp. 87-95.
- [105] Sheasby, J.S., Caughlin, T.A., and Habeeb, J.J., 1991, "Observation of the Antiwear Activity of Zinc Dialkyldithiophosphate Additives," *Wear*, Vol. 150, pp. 247-257.
- [106] Yamamoto, Y., and Gondo, S., 1989, "Friction and Wear Characteristics of Molybdenum Dithiocarbamate and Molybdenum Dithiophosphate," *Tribology Trans.*, Vol. 32, pp. 251-257.
- [107] Davis, F.A., and Eyre, T.S., 1990, "The Effect of a Friction Modifier on Piston Ring and Cylinder Bore Friction and Wear," *Tribology Int.*, Vol. 23, pp. 163-171.
- [108] Martin, J.M., Mogne, Th., Grossiord, C., and Palermo, Th., 1996, "Tribochemistry of ZDDP and MoDDP Chemisorbed Films," *Tribology Lett.*, Vol. 2, pp. 313-326.
- [109] Fuller, M.L.S., Rodriguez Fernandez, L., Massoumi, G.R., Lennard, W.N., Kasrai, M., and Bancroft, G.M., 2000, "The Use of X-Ray Absorption Spectroscopy for Monitoring the Thickness of Antiwear Films from ZDDP," *Tribology Lett.*, Vol. 8, pp. 187-192.
- [110] Palacios, J.M., 1986, "Thickness and Chemical Composition of Films Formed by Antimony Dithiocarbamate and Zinc Dithiophosphate," *Tribology Int.*, Vol. 19, pp. 35-39.
- [111] Palacios, J.M., 1987, "Films Formed by Antiwear Additives and Their Incidence in Wear and Scuffing," *Wear*, Vol. 114, pp. 41-49.
- [112] Willermet, P.A., Dailey, D.P., R.O.C. III, Schmitz, P.J., Zhu, W., Bell, J.C. and Park, D., 1995, "The Composition of Lubricant-Derived Surface Layers Formed in a Lubricated Cam/Tapped Contact II. Effects of Adding Overbased Detergent Dispersant to a Simple ZDTP Solution," *Tribology Int.*, Vol. 28, pp. 163-175.
- [113] Fujita, H., and Spikes, H.A., 2004, "The Formation of Zinc Dithiophosphate Antiwear Films," *J. Eng. Tribology*, Vol. 218, pp. 265-277.
- [114] Fujita, H., Glovnea, R.P., and Spikes, H.A., 2005, "Study of Zinc Dialkyldithiophosphate Antiwear Film Formation and Removal Processes, Part I: Experimental," *Tribology Trans.*, Vol. 48, pp. 558-566.

- [115] Minfray, C., Esnouf, C., Le Mogne, T., Kersting, R., and Hagenhoff, B., 2004, "A Multi-Technique Approach of Tribofilm Characterisation," *Thin Solid Films*, Vol. 447–448, pp. 272–277.
- [116] Speeding, H., and Watkins, R.C., 1982, "The Antiwear Mechanism of ZDDP's Part I," *Tribology Int.*, Vol. 15, pp. 9–12.
- [117] Watkins, R.C., 1982, "The Antiwear Mechanism of ZDDP's Part II," *Tribology Int.*, Vol. 15, pp. 13–15.
- [118] Morina, A., Neville, A., Priest, M., and Green, J.H., 2006, "ZDDP and MoDTC Interactions in Boundary Lubrication—The Effect of Temperature and ZDDP/MoDTC Ratio," *Tribology Int.*, Vol. 39, pp. 1545–1557.
- [119] Martin, J.M., 1997, "Lubricant Additives and the Chemistry of Rubbing Surfaces: Metal Dithiophosphates Triboreaction Films Revisited," *Jap. J. Tribology*, Vol. 42, pp. 1–8.
- [120] Bell, J.C., Delargy, K.M., and Seeney, A.M., 1992, "The Removal of Substrate Material through Thick Zinc Dithiophosphate Antiwear Films." In *Tribology Series 21, Wear Particles: From the Cradle to the Grave*, D. Dowson, C.M. Taylor, T.H.C. Childs, M. Godet, and G. Dalmaz, Eds., Elsevier, New York.
- [121] Beamson, G., and Briggs, D., 1992, *High Resolution XPS of Organic Polymers, The Scienta ESCA300 Database*. Wiley, Chichester, UK.
- [122] Brow, R.K., 1996, "An XPS Study of Oxygen Bonding in Zinc Phosphate and Zinc Borophosphate Glasses," *J. Noncrystal. Solids*, Vol. 194, pp. 267–273.
- [123] Moulder, J.F., Stickle, W.F., Sobol, P.E., and Bomben, K.D., 1992, *Handbook of X-Ray Photoelectron Spectroscopy*. Perkin-Elmer Corporation, Eden Prairie, MN.
- [124] Minfray, C., 2004, "A Multi-Technique Approach of Tribofilm Characterisation," *Thin Solid Films*, Vol. 447, pp. 272–277.
- [125] Yin, Z., Kasrai, M., and Bancroft, G.M., 1995, "X-Ray Absorption Spectroscopic Studies of Sodium Polyphosphate Glasses," *Phys. Rev. B*, Vol. 51, pp. 742–750.
- [126] Spikes, H., 2004, "The History and Mechanisms of ZDDP," *Tribology Lett.*, Vol. 17, pp. 469–489.
- [127] Yamada, Y., Ishimaru, M., Yaguchi, A., Inoue, K., Akiyama, K., Kawai, H., 2000, *Retention of Friction Reducing Performance of MoDTC-Containing Fuel Efficient Gasoline Engine Oils during Use*, SAE 2000-01-2053, SAE, Warrendale, PA.
- [128] Lechner, G., Knafl, A., Assanis, D., Tseregounis, S.I., McMillan, M.L., Tung, S.C., Mulawa, P.A., Bardasz, E., and Cowling, S., 2002, *Engine Oil Effects on the Friction and Emission of a Light-Duty, 2.2L Direct-Injection-Diesel Engine, Part I—Engine Test Results*. SAE Paper 2002-01-2681, SAE, Warrendale, PA.
- [129] Graham, J., Spikes, H., and Korcek, S., 2001, "The Friction Reducing Properties of Molybdenum Dialkylthiocarbamate Additives: Part I—Factors Influencing Friction Reduction," *Tribology Trans.*, Vol. 44, pp. 626–636.
- [130] Graham, J., Spikes, H., and Jensen, R., 2001, "The Friction Reducing Properties of Molybdenum Dialkylthiocarbamate Additives: Part II—Durability of Friction Reducing Capability," *Tribology Trans.*, Vol. 44, pp. 637–647.
- [131] Grossiord, C., Varlot, K., Martin, J.-M., Le Mogne, Th., Esnouf, C., and Inoue, K., 1998, "MoS₂ Single Sheet Lubrication by Molybdenum Dithiocarbamate," *Tribology Int.*, Vol. 31, pp. 737–743.
- [132] Miklozic, K.T., Graham, J., and Spikes, H., 2001, "Chemical and Physical Analysis of Reaction Films Formed by Molybdenum Dialkyl-Dithiocarbamate Friction Modifier Additive Using Raman and Atomic Force Microscopy," *Tribology Lett.*, Vol. 11, pp. 71–81.
- [133] Lansdown, A.R., 1999, "Molybdenum Disulphide Lubrication," In *Tribology Series 35*, D. Dowson, Ed., Elsevier, New York.
- [134] Morina, A., Neville, A., Priest, M., and Green, J.H., 2006, "ZDDP and MoDTC Interactions and Their Effect on Tribological Performance—Tribofilm Characteristics and Its Evolution," *Tribology Lett.*, Vol. 24, pp. 243–256.
- [135] Korcek, S., Jensen, R.K., Johnson, M.D., and Sorab, J., 1999, "Fuel Efficient Engine Oils, Additive Interactions, Boundary Friction, and Wear," In *Proceedings of the 25th Leeds-Lyon Symposium on Tribology, Lubrication at the Frontier*. Elsevier, New York.
- [136] Johnson, M.D., Jensen, R.K., and Korcek, S., 1997, *Base Oil Effects on Friction Reducing Capabilities of Molybdenum Dialkylthiocarbamate Containing Engine Oils*, SAE Paper 972860, SAE, Warrendale, PA, pp. 37–47.
- [137] Martin, J.M., Grossiord, C., Le Mogne, Th., and Igarashi, J., 2000, "Transfer Films and Friction under Boundary Lubrication," *Wear*, Vol. 245, pp. 107–115.
- [138] Martin, J.M., Grossiord, C., Varlot, K., Vacher, B., and Igarashi, J., 2000, "Synergistic Effects in Binary Systems of Lubricant Additives: A Chemical Hardness Approach," *Tribology Lett.*, Vol. 8, pp. 193–201.
- [139] Grossiord, C., Martin, J.M., Varlot, K., Vacher, B., Le-Mogne, Th., Yamada, Y., 2000, "Tribocchemical Interactions between ZnDTP, MoDTC and Calcium Borate," *Tribology Lett.*, Vol. 8, pp. 203–212.
- [140] Bec, S., Tonck, A., Georges, J.M., Roper, G.W., 2004, "Synergistic Effects of MoDTC and ZDTP on Frictional Behaviour of Tribofilms at the Nanometer Scale," *Tribology Lett.*, Vol. 17, pp. 794–809.
- [141] Kasrai, M., Cutler, J.N., Gore, K., Canning, G., and Bancroft, G. M., 1998, "The Chemistry of Antiwear Films Generated by the Combination of ZDDP and MoDTC Examined by X-Ray Absorption Spectroscopy," *Tribology Trans.*, Vol. 41, pp. 69–77.
- [142] Muraki, M., Yanagi, Y., and Sakaguchi, K., 1997, "Synergistic Effect on Frictional Characteristics under Rolling-Sliding Condition Due to a Combination of Molybdenum Dialkylthiocarbamate and Zinc Dialkylthiophosphate," *Tribology Int.*, Vol. 30, pp. 69–75.
- [143] Muraki, M., and Wada, H., 1993, "Frictional Properties of Organo Molybdenum Compounds in Presence of ZnDTP under Sliding Conditions (Part I): Frictional Properties of MoDTC and MoDTP," *Jap. J. Tribology*, Vol. 38, pp. 1347–1359.
- [144] Sogawa, Y., Yoshimura, N., and Iwasaki, O.H., 2000, R&D on New Friction Modifier for Lubricant for Fuel Economy Improvement. Available at www.pecj.or.jp/gijutu-report/e-report/00E115e.pdf.
- [145] Donahue, R., and Fabiyi, P.A., 2000, *Manufacturing Feasibility of All-Aluminum Automotive Engines via Application of High Silicon Aluminum Alloy*. SAE Paper 2001-01-0061, SAE, Warrendale, PA.
- [146] McCune, R.C., and Weber, G.A. 2004, "Encyclopedia of Materials: Science and Technology," *Automotive Engine Materials*, <http://www.sciencedirect.com/science/article/pii/B0080431526000863>, pp. 426–434.
- [147] Warmuzek, M., 2004, *Aluminum-Silicon Casting Alloys: Atlas of Microfractographs*. ASM International, Materials Park, OH.
- [148] Kang, H.S., Yoon, W.Y., Kim, K.H., Kim, M.H., Yoon, Y.P., 2005, "Microstructure Selections in the Undercooled Hypereutectic Al-Si Alloys," *Mater. Sci. Eng. A*, Vol. 404, pp. 117–123.
- [149] Nicholls, M.A., Norton, P.R., Bancroft, G.M., Kasrai, M., De Stasio, G., and Wiese, L.M., 2005, "Spatially Resolved Nanoscale Chemical and Mechanical Characterisation of ZDDP Antiwear Films on Aluminum-Silicon Alloys under Cylinder/Bore Wear Conditions," *Tribology Lett.*, Vol. 18, pp. 261–278.
- [150] Pereira, G., Lachenwitzer, A., Kasrai, M., Norton, P.R., Capehart, T.W., Perry, T.A., and Gilbert, P.U.P.A., 2007, "A Multi-Technique Characterisation of ZDDP Antiwear Films Formed on Al (Si) Alloy (A383) under Various Conditions," *Tribology Lett.*, Vol. 26, pp. 103–117.
- [151] Xia, X., Morina, A., Neville, A., Priest, M., Roshan, R., Warrens, C.P., and Payne, M.J., 2008, "Tribological Performance of an Al-Si Alloy Lubricated in the Boundary Regime with ZDDP and MoDTC Additives," *J. Eng. Tribology*, Vol. 222, pp. 305–314.
- [152] Pereira, G., Lachenwitzer, A., Kasrai, M., Bancroft, G.M., Norton, P.R., Abrecht, M., Gilbert, P.U.P.A., Regier, T., Blyth, R.I.R., and Thompson, J., 2007, "Nanoscale Chemistry and Mechanical Properties of Tribofilms on an Al-Si alloy (A383): Interaction of ZDDP, Calcium Detergent and a Molybdenum Friction Modifier," *Tribology Mater. Surf. Interfaces*, Vol. 1, pp. 4–17.

21

Tribology and Fine Automotive Mechanical Systems

Werner Friedrich Stehr¹

21.1 PRECISION MECHANICS IN THE VEHICLE

The laws and findings of tribology as an applied science are also applicable to the entire field of mechanics, from the bearing arrangement of a brown coal excavator with a diameter of 1 m to the bearing in a miniature gear with a diameter of only 0.1 mm. According to one definition, precision mechanics begins with bearing diameters of less than 5 mm (Figure 21.1), but this definition is purely arbitrary. The difference between the classical mechanics of mechanical engineering and precision mechanics consists only of the dimensions of the components. However, downscaling creates typical problems and particulars. This is also true in the automobile.

21.2 TRIBOLOGICAL OPERATING STATE OF PRECISION MECHANICAL SYSTEMS

In the downsizing of bearings with ever-smaller diameters and bearing lengths, the manufacturing quantity and manufacturing precision remain the same. However, to achieve a hydrodynamic operating state even with extremely small bearing arrangements, the surface roughness and shaft/bearing conformity would have to be improved; however, that cannot be achieved for reasons based on manufacturing technology. There is a disproportionate decline in the hydraulic seal of the shaft/bearing system. Therefore, the pressure in the lubricant gap becomes progressively lower and tribological systems move from hydrodynamics into mixed friction.

21.3 APPLICATIONS

There are several hundred precision mechanical components in approximately 100 modules in an automobile.



Figure 21.1—Precision mechanical components. Bearing diameter less than 5 mm.



Figure 21.2—Bearing in a housing made of poly(butylene terephthalate) (PBT). Diameter 0,2 mm.



Figure 21.3—Sintered bronze bearing, 2 mm inside diameter. The pores are clearly visible.

Some typical systems are mentioned here as examples (Figure 21.2–21.14).

- *Bending light:* The headlight housing contains a mechanism that moves the halogen lamp in the aspherical mirror within 0.03 s and thus can change the direction of the beam toward the inner curve radius.
- *Electric motors and miniature gears:* Approximately 50 electric motors with an electric power of 0.5 W to 5 kW are installed in a top-of-the-line vehicle (Figures 21.4, 21.6, 21.7, and 21.9).
- *Rotary transducers in the steering wheel:* The steering wheel or steering column or both contain a high-resolution

¹ Dr. Tillwisch GmbH Werner Stehr, Germany



Figure 21.4—Miniature motors with planetary gears.



Figure 21.7—Miniature variant.



Figure 21.5—Miniature ball bearing.



Figure 21.8—Angle of rotation generator in the steering wheel.

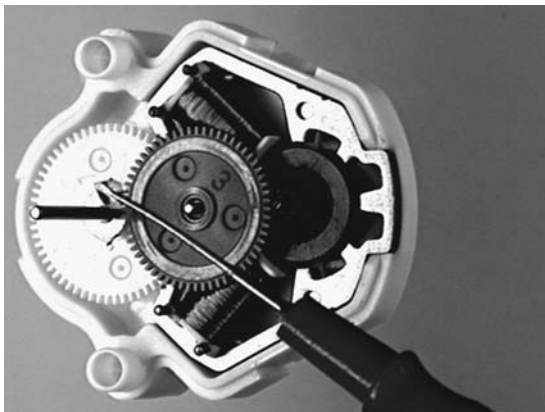


Figure 21.6—Stepping motor gear from a tachometer drive.

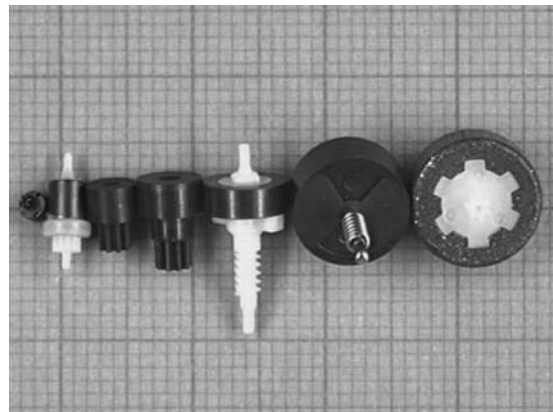


Figure 21.9—The smallest rotor at the far left rotates at 20,000 r/min and is made of a polymer-bonded magnet material.

mechanical rotary transducer (Figure 21.8) that measures the angle of rotation of the steering wheel and sends this value to the computer of the antilock brake system (ABS).

- *Steering and brakes:* Both areas are supported by electromechanical control elements and regulating elements in a fuel-saving manner. In many vehicles, the parking brake can be activated by push button (electric).
- *Engine compartment:* The engine compartment (Figure 21.11) contains many active control elements and electromechanical sensors (e.g., air choke mechanisms,

intake manifold damping, turbo-charger bypass, turbo-charger blade adjustment, wastegate, idling speed controller, servo pumps, valve systems for gas and exhaust gas, cooling water pump, and valves).

- *Motor:* Important precision mechanical modules include injection pumps, pistons, cylinders, bearings, actuators for camshaft adjustment and for ignition timing, fuel pumps, windshield cleaner pumps, cylinder



Figure 21.10—Polycarbonate gear wheel with diameter of 10 mm.

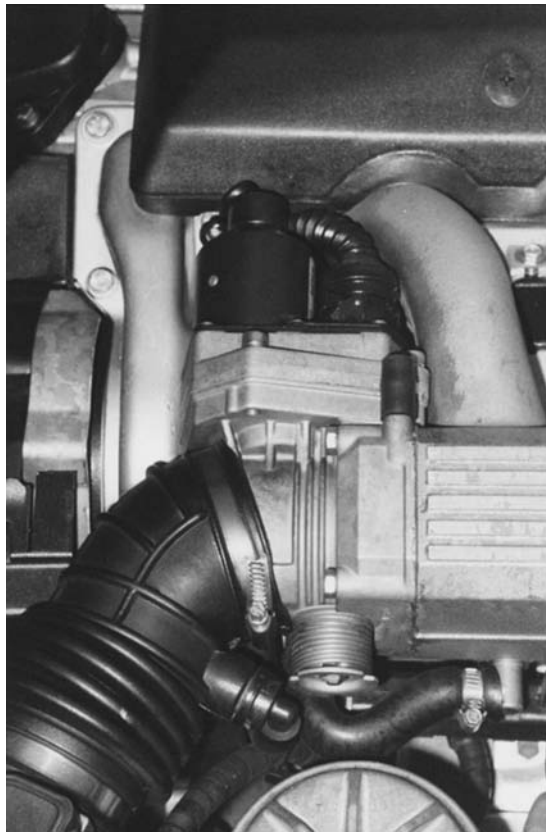


Figure 21.11—Air valve mechanism.

cutoffs, change in cross-section in the intake area, carburetor and gasoline injection control, injection pressure regulation, and pressure distributors.

- *Interior space:* In addition to fans in the air conditioner area, there are several large-area flaps, up to 100 electric switches, rockers and lever mechanisms, cupholder mechanisms, grip handle dampers, door props, and window-opening mechanisms. Up to 20 adjusting gears are required in the seat adjustment and adaptation. There are also haptic rotating actuators, sliding roof and convertible top mechanisms, display mechanisms, fans, fans for seat climate control, sensor fans, dashboard instruments, speedometers (Figure 21.13), revolutions-per-minute meters, fuel gauges, clocks, usage indicator



Figure 21.12—Part of the door lock mechanism.

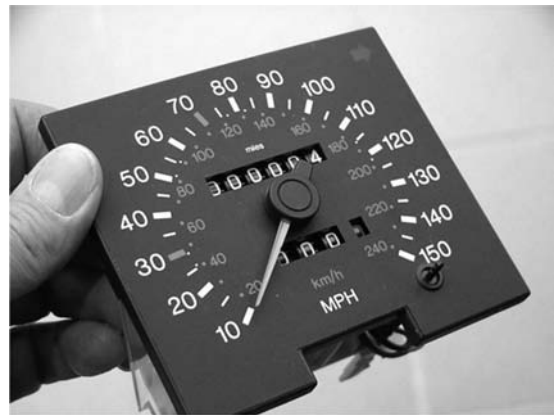


Figure 21.13—Speedometer out of the dashboard of a vehicle.

displays, voltmeters, oil pressure meters, tilt indicators, restraints and safety systems such as seat belt tighteners, and roll bar mechanisms. The electromechanical adjustment of the steering wheel position is accomplished by two servo drives with miniature gears.

- *Exterior area:* Lock and security mechanisms in doors (Figure 21.12), panic lock release, door hinges, mufflers, actuators for adjusting the shock absorbers and spring paths, actuators for raising and lowering the vehicle for getting in and out, actuators for changing the rear axle geometry involved in steering, and control elements in the differential and universal gear areas.
- *Trunk area:* Gas pressure springs (Figure 21.14) with complicated valve and sealing systems are used here in



Figure 21.14—Gas pressure spring.

the area of the trunk, the valve and hood, servo-assisted lifting and closing mechanisms, and rearview mirror adjustment. The two exterior mirrors and the interior mirror have electric adjusting drives that make the angle of the mirrors biaxially adjustable or additionally allow them to be folded in completely.

21.4 SPECIAL ASPECTS OF THE TRIBOLOGY OF PRECISION MECHANICS

21.4.1 Materials

Various different bearing and sliding surface materials are used, including steel and stainless steel; chrome-, nickel-, and copper-plated surfaces; aluminum with an oxidized surface; magnesium alloys; titanium; noble metals such as platinum, gold, silver, and beryllium; solid brass and bronze friction bearings; sintered bronze and sintered iron friction bearing materials; all conceivable polymers with various fillers and reinforcing materials such as glass, carbon, chalk, polytetrafluorethylene (PTFE), metals, compounds, and elastomers; tribological function layers such as physical vapor deposition, chemical vapor deposition, and diamond-like carbon layers; lubricant lacquers; sputtered surfaces with graphite and molybdenum disulfide (MoS_2); friction lacquer coatings; ceramic materials for shafts, bearings, and friction bearings; bearing blocks made of ruby and sapphire; and magnetic materials such as iron oxide, rare earths, and plastic-bonded magnetic materials. Polymer materials are used quite often in precision mechanics, including, among others, polystyrene and related polymers such as ABS (acrylonitrile/butadiene/styrene), ASA (acrylonitrile/styrene/acrylate), etc.; polyamides; polyesters such as poly(terephthalates) and polycarbonates; and polyoxides such as POM (polyoxymethylene) or PPOX (poly[propylene oxide]). Because of the inexpensive manufacturing method of the injection molding technology, even complex parts can be manufactured with a precision that is reproducible a thousand times over.

21.4.2 Integration

Today, in most cases, the construction material of the housing will also assume a bearing function (Figure 21.15). In mass production, this integration can lead to a substantial cost reduction because it is not necessary to install expensive sintered bearings or bearing bushings.



Figure 21.15—Housing with integrated friction bearings.

21.4.3 Thermal

If polymer materials are used as bearing materials, one fundamental point to consider is that many of their properties differ from those of metals. This includes as an important point their substantially inferior thermal conductivity. With the same friction loss and the same bearing geometry as with a metallic friction bearing, considerably higher contact temperatures occur in a corresponding polymer friction bearing. This behavior can lead to a thermal overload of the bearing system even at low bearing loads, especially in the event of dry running.

Even with relatively moderate $P \times V$ values, friction power is high (Figure 21.16). Because the thermal conductivity of plastics is approximately 100 times worse than that of metals, overheating of the friction site occurs very quickly (Figure 21.17).

The melt wear occurs spontaneously and is extremely dangerous, especially when the friction system moves from hydrodynamic to boundary lubrication because of a lack of lubricant (Figure 21.18).

If the friction point temperature at the friction contact exceeds the softening point or melting point, the bearing system dies a thermal death. High running speeds create this effect because the coefficient of friction increases with the running speed (Figure 21.19).

Contactless thermography is the only measurement method for determining the friction temperature (Figure 21.20). Even miniature thermal sensors withdraw too much heat from the friction site and falsify the measurement result.

21.4.4 Deformation

Polymer friction bearings are deformed to a greater extent by the applied bearing loads than comparable metal bearings. Superficial creep and flow of the materials may occur even with prolonged and higher loads. This behavior results in an improvement in the conformity of shaft and bearing: the true contact surface is greatly enlarged, and the actual surface pressure declines. A polymer bearing automatically adjusts its sliding surface within certain limits even without abrasive wear and needs a far shorter running-in time than a metal bearing of comparable dimensions.

Alignment errors that occur because of larger installation and manufacturing tolerances are more readily absorbed by polymer bearings. The edge pressure that is

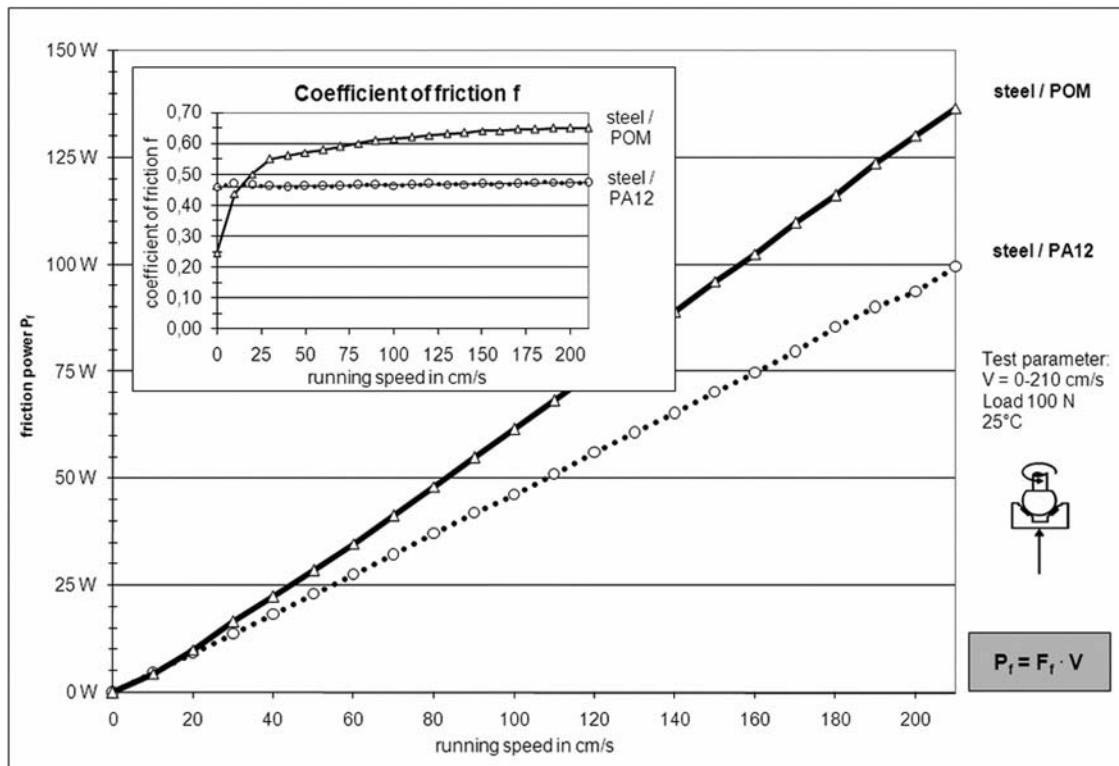


Figure 21.16—Relationship between coefficient of friction, f , and friction power: unlubricated steel/plastic friction pairings with different coefficient of friction curves.

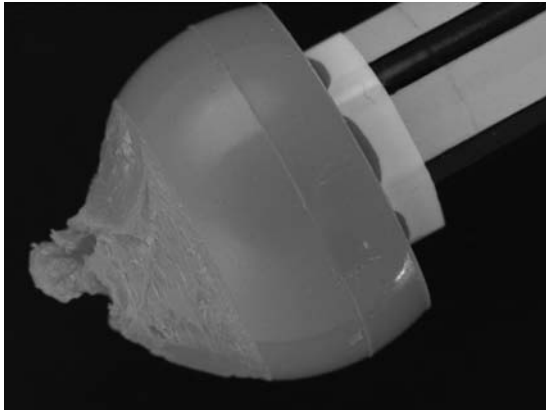


Figure 21.17—Test specimen of ABS (acrylonitrile/butadiene/styrene) after a 10-s friction test.

feared with metallic constructions almost never occurs with polymer bearings because high pressures lead to elastic deformation or to flow of the material.

One problem in using polymers is their great thermal expansion, which makes it necessary to equip the bearings with a larger play and larger tolerances (Figure 21.21). Furthermore, many polymers, in contrast with metals, are able to absorb and release substantial amounts of water, which may result in changes in shape and dimension of the components.

21.4.5 Power-On Time

A typical requirement of precision mechanical tribological systems is that they often have very long idle times and, associated with this, short power-on times. The mechanisms



Figure 21.18—Melt wear on polyimide (PI) surface.

of automatic restraint systems normally are not in tribological operation for the entire life of an automobile (average 12 years) and are not used until a crash event, which only occurs in 0.01 % of cases.

However, the requirements change with many systems having a short power-on time, for example, as in the case of ABS brake systems. The control and regulating mechanisms of the ABS system are never activated by many drivers, so they never respond to the maximum braking power and thus the deployment of the ABS mechanism. Because ABS or the components thereof or both are also used today for skid control, as a start-up aid on snow and icy roads as well as for traction control in off-road vehicles, this can often

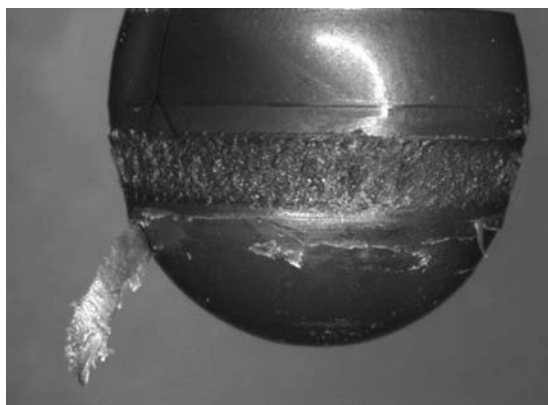


Figure 21.19—Test ball out of POM polyacetal with ring-shaped melt wear running against sodium chloride without lubrication: 3000 r/min, 30-N load, and ball rotating for 10 s.

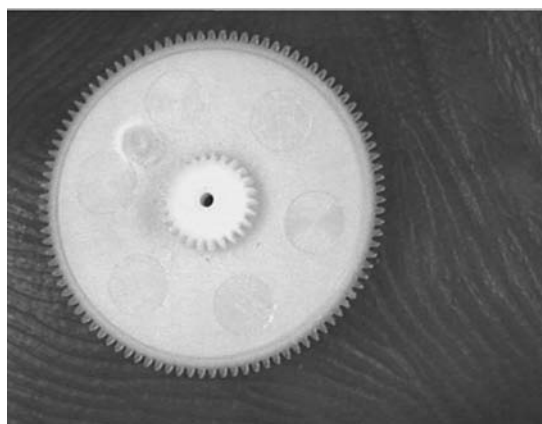


Figure 21.21—Gear wheel with bearing hole (diameter 0.2 mm).

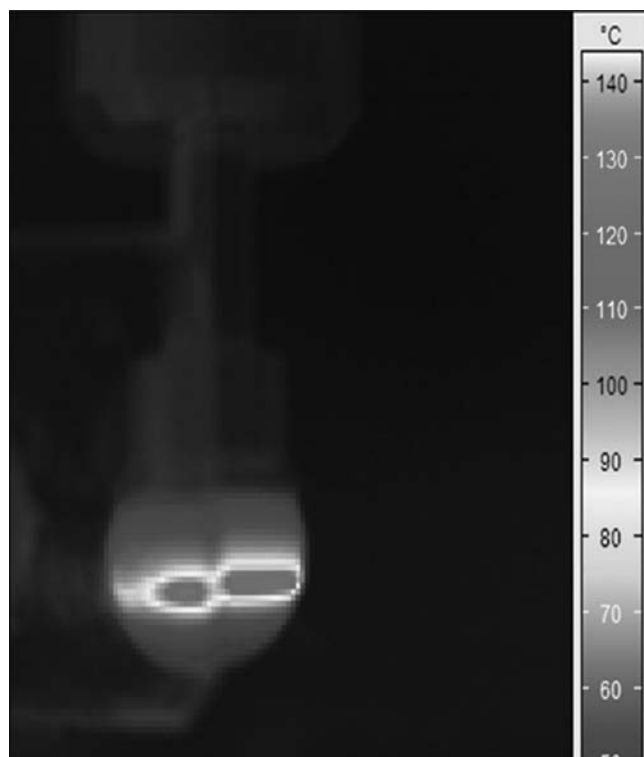


Figure 21.20—The thermograph indicates approximately 130°C.

mean a substantial increase in operating times. As of 2009, an operating life of 400 h is required for an ABS brake system and its other components. On the extreme other end, the mechanism of time display in a motor vehicle has a 100 % power-on time with an operating time of 100,000 h.

21.5 LUBRICANTS IN PRECISION MECHANICS

In precision mechanics, all conceivable lubricants are used. Because the volumes in the bearing sites usually amount to only a few microlitres, expensive or rare exotic lubricants such as ionic fluids may also be used. In special problem situations (e.g., in noise suppression of miniature gear wheels), the lubricant costs more than the components (Figure 21.22).

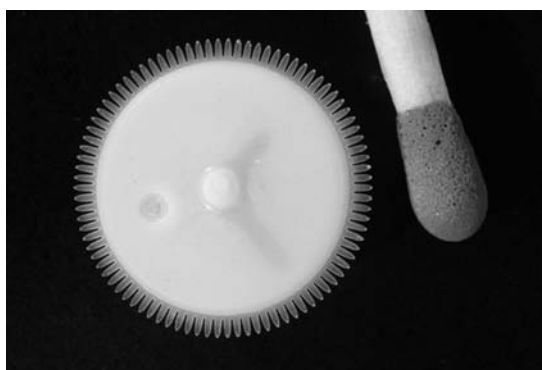


Figure 21.22—Gear wheel of thermoplastic polymer with “long” teeth for noise suppression.

The most important representatives of the basic oils used are synthetic hydrocarbons, synthetic esters, polyalkylene glycols, perfluoropolyalkyl ethers, and silicone oils. All types of metal soaps and organic and inorganic substances are used as grease thickeners. The solid lubricants include mainly MoS_2 , graphite, PTFE, and polymer powder.

21.5.1 Specific Requirements

- *Sliding speeds:* The sliding speed of precision mechanical systems covers several powers of 10, from 0.01 mm/day (indicator bearing in the fuel gauge) up to 100 m/s (pyrotechnic seat belt tightening mechanism). The surface pressure range is like that of classical mechanical engineering with a tendency toward higher pressures in small and very small bearing systems. The smallest friction bearings (automotive instruments) have a diameter of 0.1 mm. Because of the decline in overall precision when downscaling the parts, the actual bearing surfaces achieve only 10 % of the calculated values in these small structures, thus explaining the higher surface pressures.
- *Quantities of lubricant:* Almost all precision mechanical bearings receive only an initial lubrication at the time of production of the modules. The quantities of lubricant are usually very small, generally reaching only 75 % of the bearing gap volume. With friction bearings in dashboard instruments, the typical lubricant volume is 0.003 mL (10^{-6} L). With these small volumes of one droplet, abrasion particles very rapidly lead to thickening and a pasty consistency of the oils and greases.

- *Aging:* The smaller the amount of lubricant, the greater and the more rapid the reaction with the bearing materials. The increase in viscosity is a problem in particular. A 20 % increase in viscosity of the impregnating oil in the sintered bearing of an air conditioner sensor fan leads to final failure at -35°C (Figure 21.23). With some manufacturers, the stepping motor in the speedometer has a rotational speed of 20,000 r/min. The viscosity of the oil used there may deviate only $\pm 5\%$ from the specified value; otherwise, there are step losses and a malfunctioning display.
- *Interactions:* Because of the wide variety of bearing materials and all conceivable lubricants, physical and chemical interactions often occur in the bearing boundary layer. The lubricants may have a corrosive effect (Figure 21.24); they may plasticize polymers; or they may cause them to become brittle, develop stress cracking, or lead to swelling or shrinkage. The depth of action of these reactions of 0.01–0.1 mm is not relevant in classical mechanical engineering but is fatal for a bearing with a diameter of only 0.1 mm.
- *Spreading of lubricants:* Because of the very small quantities of lubricants, spreading and migration of oils and bleeding of greases lead to a loss of tribological function due to starved lubrication. This loss mechanism is typical of precision filigree components and is completely irrelevant in ordinary mechanical engineering. The rate of migration with a low-viscosity silicone oil may be 5 mm/h. In this example, the creep volume is

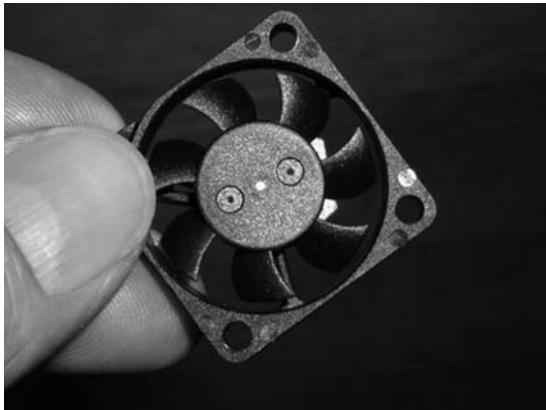


Figure 21.23—Miniature fan for air conditioner regulation.

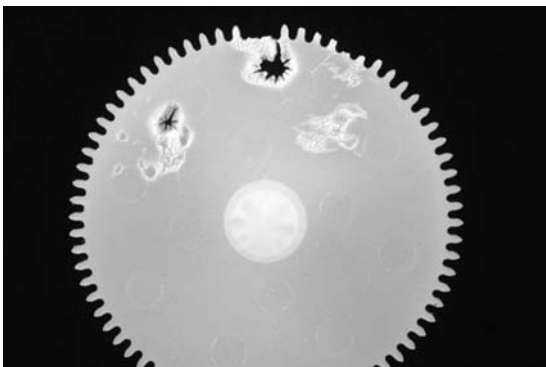


Figure 21.24—Pitting corrosion due to oleic acid and moisture. Notice the stress cracking in the toothed rim.

1 mm³/week. A lubricant volume of 5 mm³ in the bearing gap will disappear after 5 weeks. This results in dry running, increased wear, increased friction, failure, and at least noise production.

- *Contamination:* Creeping of the lubricants onto sensors or sensitive polymers may likewise lead to the feared failure. When using different lubricants, a migrating oil can completely displace a bearing impregnating oil and contaminate the bearing location. Fuel vapors or aerosols may flush out the small bearing oil volumes or dilute them until the lubricity is lost, and thus, they become ineffective.
- *Noise:* There are many precision mechanical systems in the interior of a motor vehicle. For example, in many vehicles, the miniature fan (sensor fan) in the air conditioner system is installed (invisibly) in the interior light only 20 cm away from the front passenger's ear. Friction noises of the bearings are audible and annoying here, which is no longer acceptable today. For these reasons, a lubricant must also provide noise-suppressing properties in addition to its tribological benefit.
- *Haptic demands:* Beverage holders, grip handles, ashtrays, shelf guides, and pop-up and display mechanisms and flaps should open and close slowly and smoothly. One effect that is feared here is stick-slip, which makes motion sequences jerky.
- *Attenuation:* For attenuation of the speed of motion sequences (e.g., in the case of grip handles), extremely viscous lubricants (silicones) up to 1,000,000 mm²/s are used. However, these lubricants must not cause soiling of the interior lining (often made of a light-colored leather) under any circumstances (forming oil spots).

21.5.2 Types of Lubricants

Lubricants based on natural raw materials (e.g., native oils or mineral oils) normally do not meet the high demands of precision technology in the automotive field, in particular with respect to lack of aging resistance, viscosity-temperature performance, high- and low-temperature usability, and the required tribological properties. Therefore, synthetic fluids with a defined profile of properties were already being used in this field at a very early point in time. However, there is still no fluid that combines all of the advantages. There are always some disadvantages in addition to the advantages.

Various groups of synthetic lubricants are differentiated depending on their chemical composition. They are normally obtained by chemical reaction of defined compounds with a uniform structure. The path to the desired end product frequently involves many steps. Synthesis is often very complex, which also explains the high price of such lubricants, in some cases up to \$3,000 (U.S.)/L.

21.5.2.1 SYNTHETIC HYDROCARBONS

The synthetic hydrocarbons used in precision mechanics include the large group of polyalphaolefins (PAOs). PAOs are branched paraffin hydrocarbons that differ essentially in their molecular size and the chain length of the branches [1]. They are similar in their chemical and physical properties to the paraffin-based mineral oils.

They are available in different viscosity levels, have good low-temperature and viscosity-temperature properties, and have a higher thermal and oxidative stability in comparison with natural mineral oils. They do not have a

corrosive effect on metals, where they exhibit their excellent friction-reducing and wear-reducing properties.

Their disadvantages lie in the incompatibility of many low-viscosity grades with polymers and their poor dissolving power for certain additives. In practice, PAOs are used for lubricating metal/metal and metal/thermoplastic worm gears and miniature ball bearings.

21.5.2.2 SYNTHETIC ESTERS

Fluids from the synthetic ester group are to be defined precisely in their chemical structure and composition. They are formed by reaction of acids with alcohols in the presence of catalysts, splitting off water. Organic and inorganic esters are essentially differentiated according to whether the acid is of organic or inorganic origin. The variety of different acids and alcohols has led to a wide range of offerings of esters having different properties [2]. Mainly carboxylic acid esters are used as lubricants for precision mechanical bearings.

Critical aspects in the use of ester oil include an excessively high tendency to evaporate in some cases and their incompatibility with respect to many polymers, on which they act as plasticizers. If synthetic ester oils are used successfully for lifetime lubrication in precision mechanical thermoplastic friction bearings, their compatibility with regard to the polymer materials must be tested carefully. Furthermore, they must be stable with respect to oxidation by atmospheric oxygen and hydrolysis (i.e., they must not split into alcohol and acid, their starting components, in the presence of water). Another disadvantage may be that in some cases they are available only as low-viscosity fluids with a viscosity of less than 50 mm²/s at 20°C.

What makes synthetic esters virtually predestined for use as lubricants is their excellent lubricity and load-carrying capacity, which is approximately twice as high as that of mineral oil, and the good stability of the oil droplets on metallic and polymer surfaces. In addition, they sometimes have extremely low pour points that conform to U.S. Military specifications.

Carboxylate esters are used as low-temperature oils and as lubricants for metal, stone, and polymer bearings that are subjected to high loads.

21.5.2.3 POLYALKYLENE GLYCOLS

Polyalkylene glycols or simple polyglycols are chemical compounds of carbon, hydrogen, and oxygen in various compositions. They are strongly polar, which leads to their various possible uses [3]. A distinction is made between water-miscible and non-water-miscible products, which have a low flammability and a high surface tension. The stability of the oil droplets on metals and polymers is good, but corrosion problems often occur on metals. Their viscosity may be varied from 50 to 20,000 mm²/s at 20°C depending on the intended purpose. Their viscosity-temperature behavior is good, and continuous low-temperature use at -35°C is possible in some cases. Their friction and wear-reducing properties must also be evaluated as quite positive.

One disadvantage is that they decompose easily at higher temperatures, forming acidic degradation products. They are incompatible with some polymer materials used in precision mechanics, so their stability must be tested with extreme care before they are used in practice. The main applications of polyglycols have proven to be as metal

working agents and as lubricants for textile fibers. In precision mechanics, they are used mainly as heating media and silicone-free damping fluids.

21.5.2.4 PERFLUOROPOLYALKYL ETHERS

In perfluoropolyalkyl ethers, the hydrogen atoms of traditional hydrocarbon ethers have been replaced completely by fluorine, thus yielding lubricants with the greatest thermal, oxidative, and chemical stability known so far [4]. Use temperatures up to +260°C are possible. A fundamental distinction is made between linear and branched types with different property profiles in some cases.

Branched perfluoropolyalkyl ethers may be used down to -30°C and have a viscosity-temperature behavior similar to that of mineral oils. Linear perfluoropolyalkyl ethers have extremely low pour points (in some cases below -65°C) and a good viscosity-temperature behavior, but they may decompose at higher temperatures, such as those occurring in friction contacts with metal friction bearings. Perfluoropolyalkyl ethers have a high density (~1.9 g/cm³) and a very low evaporation tendency. They can be used with most plastics and lacquers, are noncombustible, nonflammable, biologically neutral, and soluble only in fluorinated organic solvents.

Perfluoropolyalkyl ethers are very expensive, but they have gained a particular position as special lubricants because of their unique profile of properties. They are used wherever other lubricants can no longer be used (e.g., in aviation and space applications, in vacuum pumps, in oxygen-carrying systems, and in equipment in an aggressive environment). For lifetime lubrication of precision mechanical thermoplastic friction bearings, they are used wherever other lubricants fail because of incompatibility with the polymers used, because of inadequate oxidation stability at higher temperatures, or because of inadequate low-temperature use limits.

21.5.2.5 SILICONE OILS

Silicones or polysiloxanes are organic silicon compounds in which the silicon atoms are linked together by oxygen. Numerous liquids of different structures and different properties are available on the market [5]. However, dimethylpolysiloxanes essentially have the best viscosity-temperature performance of all fluids used as lubricants. They have excellent low-temperature properties, high temperature stability and oxidation stability, low evaporation tendency, a low surface tension, and their viscosity may be adjusted in a wide range (10–1,000,000 mm²/s) at 20°C.

From the position of these properties, silicone oils would be excellent lubricants, but their use is greatly limited, especially in terms of for-life lubrication of precision mechanical bearings. Under boundary and mixed lubrication conditions, they have poor shear stability and a low load-carrying capacity. This rules out lubrication of metal bearings or bearings under high loads. Furthermore, their spreading and creep tendencies do not allow their use for spot lubrication with only a little drop of oil, unless suitable measures are taken to prevent the spreading of the oils. In lubrication of polymers, it is important to note that certain low-viscosity grades are incompatible with amorphous thermoplastics and polyamides. Their use in many areas is restricted because silicones are electric contact poisons and very easily entrained.

The main use of silicone oils is as parting compounds and lubricants, heat transfer fluids, and damping fluids. To some extent, they are used as base oils for plastic lubricants. They are also incorporated in the form of microscopically small droplets into thermoplastics (e.g., polyamide PA66, polyacetal POM) where they act as “friction additives” and significantly improve the friction and wear behavior.

21.5.2.6 GREASES

Greases are lubricants with a consistency, composing 60–95 % of a basic fluid, which may be any base oil, plus a thickener. In the field of precision mechanics, mainly very soft greases and pastes are used. Inorganic substances (e.g., fumed silica); organic compounds (e.g., polyurea); metal soaps; and polymers (PTFE, PE, etc.) are used as thickeners.

If metal soap-thickened greases are used for lubrication of plastic friction bearings, the compatibility of the grease and the plastic must be tested because some polymers are not stable with respect to some of the soap thickeners that are used.

Fluid greases (oils containing only a very small amount of thickener, so they behave almost like fluids) or soft pastes are often used for lifetime lubrication in the field of precision mechanics. The adhesive ability of the basic oils on the material surfaces and thus the aspect of spot lubrication may thus be influenced in a positive sense.

21.5.2.7 SOLID LUBRICANTS

For some applications, liquid or pasty lubricants cannot be used (e.g., in the door lock mechanisms and seat adjustments where soiling of clothing or hands is to be prevented). Only “dry” or so-called “solid” lubricants are possible here. For example, this term includes fine powders of MoS_2 ; graphite; metal oxides; or thermoplastics (PTFE, PA, etc.). However, the amount used for lifetime lubrication of precision mechanical friction bearings tends to be low.

With friction lacquers, these solid lubricants are placed in a polymer matrix (e.g., a water-soluble acrylic basecoat). Then in the simplest case, the components are spray painted or coated as bulk material by the drum method. Even elastomers (e.g., door seals or o-rings) can be coated today with modern friction-reducing lacquers to yield designs that are free of rattling and clicking sounds.

21.5.3 Properties and Testing

21.5.3.1 SPREADING BEHAVIOR

A very important and essential requirement of for-life lubrication of precision mechanical bearings is that the tiny quantity of lubricant must not creep away from the friction site: The result would be loss of lubricant and starved lubrication with friction noises and increased wear. The increase of friction lowers efficiency and the increased wear rate leads to a loss of quality due to inadequate precision or even failure of the entire module. Furthermore, the migrating lubricant may cause failure of the device because of its incompatibility with respect to other parts of the module. This tendency to creep of the lubricant is especially pronounced on polymer materials.

One example should illustrate how rapidly such spreading effects can take place: One drop of a fluid grease, which is used for lubricating the sintered bearing surface there, is on an injection-molded housing surface of a component. The condition of the droplet of fluid grease

was documented in time-lapse photography over a 24-h period (Figures 21.25 and 21.26). Even after a very short period of only 1 h, a fine margin (corona) of bleeding oil develops around the drop of fluid grease, spreading more and more and ultimately wetting the entire component.

The spreading behavior of a lubricant is tested by placing small droplets of lubricant on the materials that are used in practice (Figures 21.27 and 21.28). The mate-

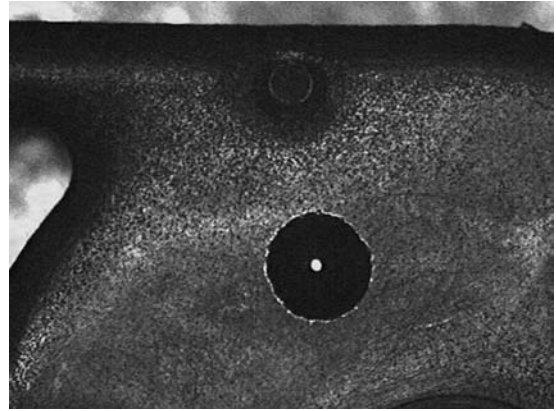


Figure 21.25—Time-lapse photograph of a sintered bearing impregnation fluid on an injection molded component surface (start of test).

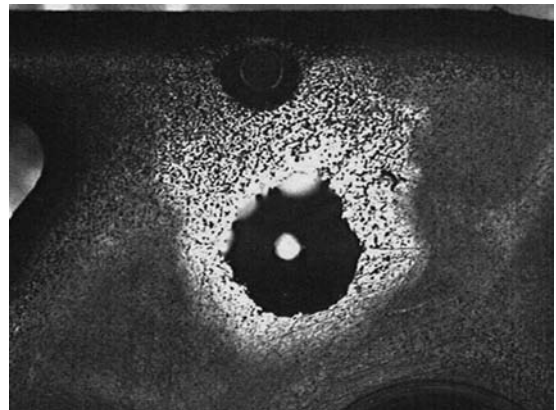


Figure 21.26—Time-lapse photograph of a sintered bearing impregnation fluid on an injection molded component surface (end of test).

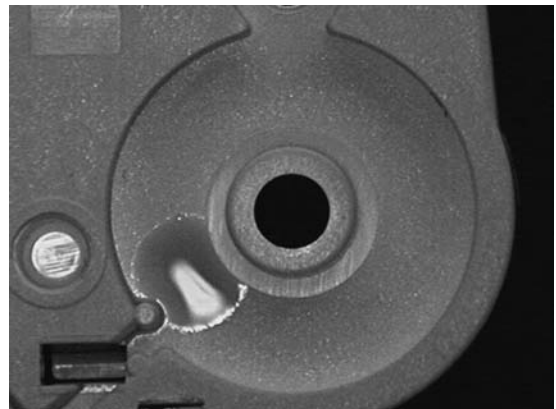


Figure 21.27—Time-lapse photograph of a lubricant drop on the surface of a component (start of test).

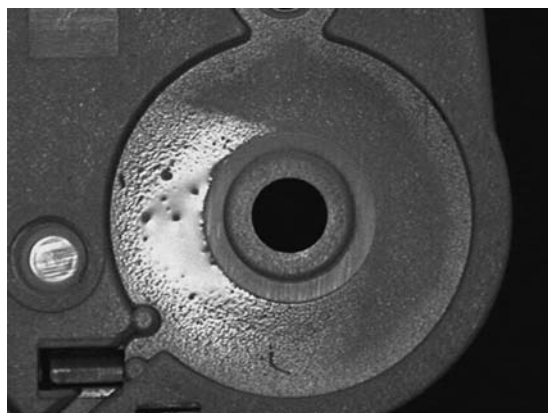


Figure 21.28—Time-lapse photography of spreading. The droplet of lubricant spreads over the complete surface of the component.

rial samples with the droplets placed on them are kept for 3 days in a drying cabinet at 85 or 120°C and evaluated visually for their spreading behavior each day. The changes in the contact angle or in the wetted surface are measured.

Strongly polar substances (e.g., polyglycols) have a high surface tension (~36 mN/m), forming droplets with a large contact angle. Nonpolar substances (e.g., silicone oils) have a low surface tension (~22 mN/m); they wet the surface very well but do not form a stable contact angle.

Various measures can be taken to reduce or prevent the migration of a lubricant:

- *Additivation of the lubricants with wetting modifiers:* These additives arrange themselves in the interface between the droplet of lubricant and the surface of the material and there form a “chemical” oil barrier beyond which the oil droplet cannot creep away. The efficacy of this method is limited to a few lubricant groups and materials.
- *Epilamization:* Epilamization agents (*epilam* is Greek for “little skin”) are very low-concentration solutions of special fluorinated plastics such as PTFE in a solvent that is also fluorinated. When the solvent evaporates, a fine invisible network of fluoroplastic molecules polymerizes on the surface of the material, lowering the apparent surface tension of the solid to such an extent that even an oil such as silicone oil with a high tendency to creep will remain in the same location for years. This method may be applied to both metallic surfaces and polymer surfaces. If a POM surface is epilamized, even a silicone oil that would tend to creep away under these conditions remains unchanged. Methods of epilamization include coating by immersion, spraying, and drop-wise application of epilamization fluid and by printing or stamping. When the solvent evaporates, the active ingredient polymerizes on the surfaces. The layer thicknesses are extremely thin, with 0.0001–0.00001 mm being sufficient. The friction and wear properties are not affected by epilamization.
- *Design measures for reducing spreading:* Retention of the oil can also be improved through design measures in the component. Sharp protruding edges act as barriers beyond which the lubricant cannot creep. Indented edges and boreholes hold the oil securely and create a depot. On smooth surfaces, lubricants tend to form

droplets with a high contact angle, but on rough surfaces, they spread to a greater extent (capillarity of the surface roughness).

21.5.3.2 EVAPORATION BEHAVIOR

A very low tendency to evaporate is the condition for the usability of a lubricant in a precision mechanical application. Especially with the very small volumes and long years of use, there must not be starved lubrication due to evaporation of lubricant. The evaporation properties of a lubricant are tested according to FTMS Method No. 3480.1, in which the weight loss of 1 g lubricant on a defined surface area is determined after 24 h at 105°C. This method reveals how strongly a lubricant evaporates under these defined conditions. The percentage weight loss provides an indication of the usability of a lubricant in practice, but in any case, it must not be used as an absolute value for the practical application. The highest evaporation losses are measured for polyglycols and synthetic esters. These oils should not be used at temperatures above 100°C. Almost no evaporation is detectable with perfluoropolyalkyl ethers, which may be used at temperatures up to 260°C. Silicone oils and PAOs have only a low evaporation tendency, but the values of low-viscosity grades are somewhat higher than those of high-viscosity variants. Their use range is from 120 to 150°C.

21.5.3.3 AGING

The lubricant is in extremely close contact with the material of the shaft (usually steel) and the bearing itself in the bearing gap. The surface roughness makes the reaction surface many times larger and leads to chemical aging reactions, which in some cases take place rapidly and violently (Figure 21.29).

Therefore, a high chemical stability of the lubricant is an important aspect of for-life lubrication and is thus also an important point in the laboratory simulation. The aging resistance or oxidation stability of a lubricant is usually determined by its chemical structure and the amount of protective stabilizers. Bearing metals, polymers, higher ambient temperatures, wear particles, or aggressive ambient media accelerate the aging of the lubricant. The testing of the aging resistance should be designed in such a manner that inferences can be made about the long-term behavior in practice or the suitability of a lubricant for use in precision mechanics or both.

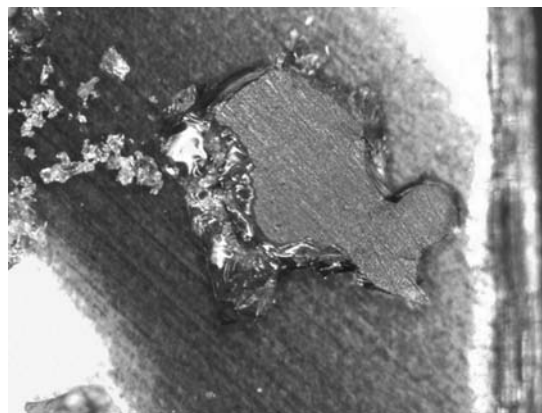


Figure 21.29—Resinified oil in the sliding contact of a brass bearing/steel shaft after an accelerated aging test.

One method that has particular relevance in practice is the testing of the aging resistance of lubricants in thin layers under the influence of catalytic nonferrous and ferrous metals [6]. Brass rounds and fine steel shavings are covered with a thin layer of oil and exposed to a temperature of 120 or 150°C in a heating cabinet (Figure 21.30).

The ratio of metal surface area to the amount of lubricant is adapted to practical conditions. The lubricants are exposed to very rapid oxidative attack and resinify because of the influence of heat and metals, which act as catalysts (Figure 21.31). Aging processes in the lubricant are tracked by changes in viscosity, formation of acids, degradation of additives, or oxidation of the base oils. In general, one can say that the longer any oil persists under these conditions, the better its aging performance will be under practical conditions.

Calculation of the expected lifetime according to the so-called reaction rate-temperature rule evaluated by van't Hoff and Arrhenius also provides indications of the practical performance of a lubricant. This rule states that the reaction rate of a chemical reaction varies with temperature, such that an increase in temperature by 10 K results in a reaction rate that is approximately doubled to tripled. For example, if a lubricant has already formed aging products to a significant extent after 24 h at 120°C, the same thing would occur after 2 days at 110°C, 4 days at 100°C, etc., and only after 17 months at 30°C accordingly. The lubricant would then have an expected lifetime of approximately 1.5 years at room temperature (20–30°C).

The results of the aging experiments in thin layers of the most important precision mechanical lubricants are summarized and compared in Figure 21.32. This shows the days until collapse or resinification of the oil or both at the test temperature of 120°C.

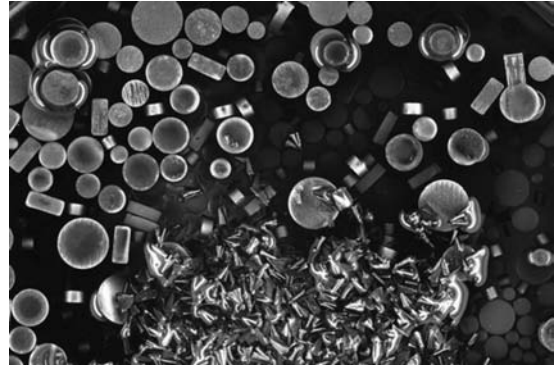


Figure 21.30—Accelerated aging in laboratory simulation. Lubricant in contact with brass and steel at elevated temperatures.



Figure 21.31—Oxidation converts the low-viscosity oil to a mass resembling asphalt.

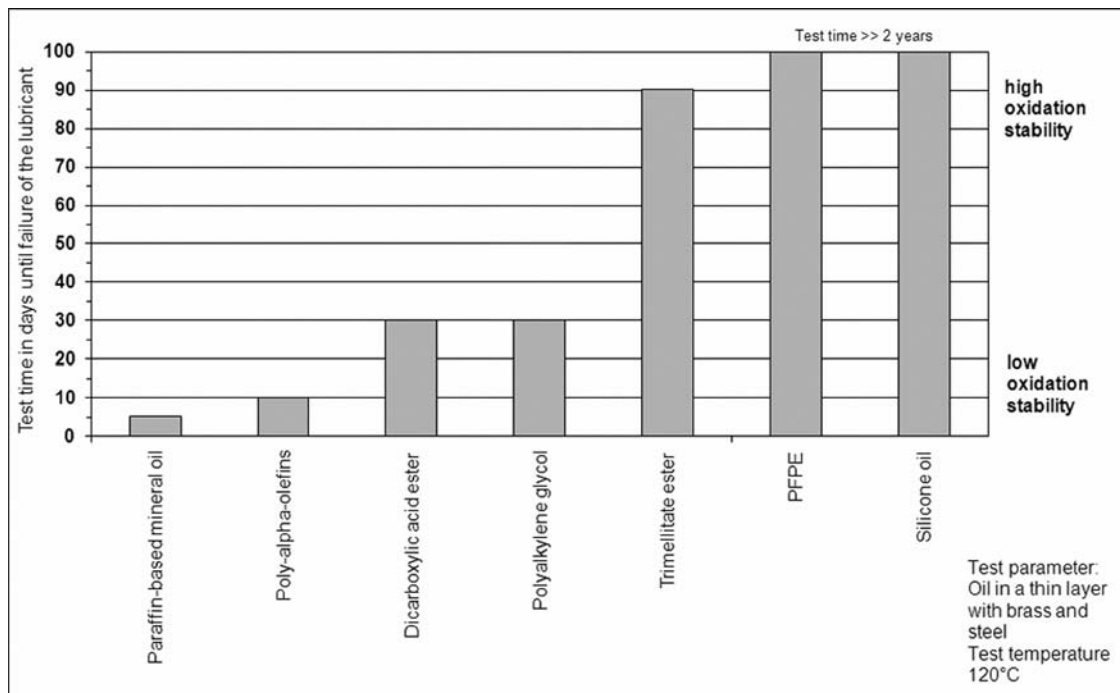


Figure 21.32—Aging performance of lubricants. Comparison of laboratory test results with most common base oils for precision mechanic lubricants.

The aging stability of oils based on natural ingredients (e.g., a paraffin-based mineral oil) is very low. After only 5 days at 120°C, the oil samples are completely resinified, although they have already been furnished with special oxidation inhibitors.

With this test method, PAOs last for approximately 10 days at 120°C. On the basis of our experience, the expected lifetime in practical use at an operating temperature of 40°C is approximately 6–7 years. Polyalkylene glycols have a much better aging behavior; when equipped with an optimized additive package, they are destroyed under these test conditions after approximately 20–30 days. Theoretically, they can be used for 15–20 years at an operating temperature of 40°C.

Equally good results are obtained with well-stabilized dicarboxylate esters, which resinify after 20–30 days at a test temperature of 120°C. This would correspond to a lifetime of approximately 15–20 years at an operating temperature of 40°C. However, if the operating temperature is raised to 80°C, the lifetime is shortened to only 1–2 years, although some trimellitate esters have a much higher aging resistance.

The best aging results are obtained with perfluoropolyalkyl ethers and silicone oils. Even at 120 or 150°C, they are not destroyed under the selected test conditions over a period of more than 2 years. Only the viscosity of the silicone oils increases in the range from 1 to 10 % in comparison with the initial value. Depending on their chemical structure, silicone oils can be exposed to continuous operating temperatures between 120 and 150°C and even up to 260°C in the case of perfluoropolyalkyl ethers.

21.5.3.4 INTERACTIONS OF LUBRICANTS WITH POLYMERS AND LACQUERS

In 80 % of all applications, polymer materials are used as construction materials in precision mechanical engineering. Because interactions occur especially with the polymers, compatibility testing of lubricants with the polymers and lacquers used is an important aspect of the laboratory simulation. Unfortunately, these reactions proceed very slowly, so that in practical application there may be long-term failures with substantial economic damage. These reactions include embrittlement or swelling of the plastic surfaces and development of stress cracking in parts under stress. These reactions are simulated in two different laboratory test methods, the so-called “static compatibility testing” and the test under static stress conditions.

Static compatibility testing should test whether interaction occurs simply because of the contact between the lubricant and the polymer. Therefore, plastic granulates and lubricants are kept for 28 days at 85°C in a heating cabinet. After the end of the experiment, the changes in the lubricant are determined by measuring the viscosity and the neutralization value. Chemical changes in the lubricant (e.g., dissolving of the plasticizer out of the polymer) are determined by infrared spectroscopic investigations.

A polymer test rod immersed completely in oil is kept under the same test conditions. After the end of the test, the changes in the plastic are determined by measurement of torsion, Shore D hardness, and cross-sectional area. Chemical changes in the polymer (e.g., because of diffusion of the lubricant into the polymer) are also determined here by infrared spectroscopic analysis, if possible.

In practical use of polymer components, it has repeatedly been found that the compatibility of plastics and lubricants was different from that determined in the laboratory test. The difference between a laboratory test and a practical application is that in a laboratory test, the interactions between the plastic and the lubricant are tested under purely static conditions. In the modules, the components (bearings, gear wheels, clip connections of housings, etc.) are under mechanical load and stress. The influence of lubricant may definitely turn out to be more critical here.

In the static stress test, the polymer test rods therefore are subjected to different strain stress stages (0.6, 1, 2, and 3 %) in contact with lubricants (Figure 21.33). The influence of the strain stress on the stress cracking susceptibility of polymers in contact with the respective lubricant can be determined in this way. After even a short test time of 7 days at 85°C in a heating cabinet, it is possible to reliably evaluate whether or not a particular polymer/lubricant combination leads to stress cracking (Figure 21.34).

In general, it can be stated that the various lubricant groups show different compatibility properties with respect to the various polymer groups. Actually, only the perfluoropolyalkyl ethers are stable in the presence of all of the thermoplastics tested. All other oil groups are less stable. The synthetic ester group is probably the most critical from the point of view of the oils; they can be used as plastic

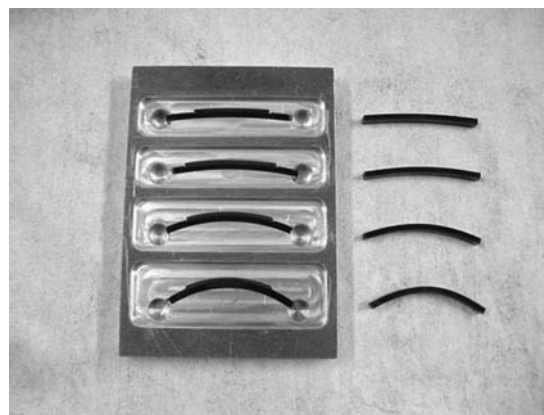


Figure 21.33—Method of testing of stress cracking.

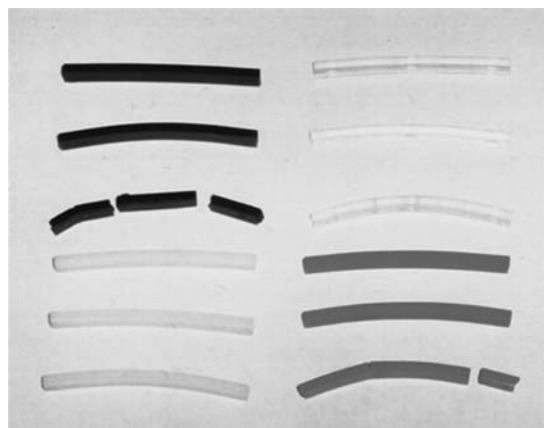


Figure 21.34—Test results after 7 days at 85°C and 0.6, 1, and 3 % strain.

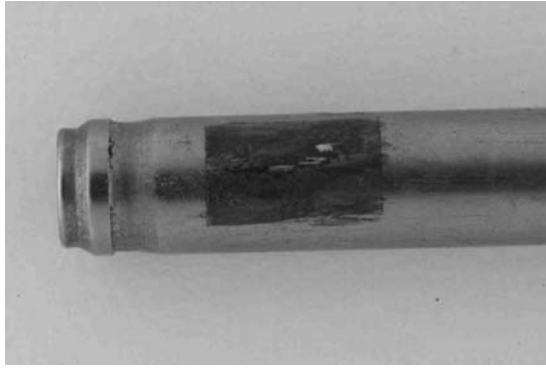


Figure 21.35—Corrosion on a steel shaft of a fan (diameter 5 mm) in the contacting area with the lubricated sintered iron bearing.

lubricants only after making a careful selection. Lubrication of amorphous thermoplastics is critical from the point of view of plastics; many lubricants cause stress cracking here.

21.5.3.5 CORROSION

Metals are used as shaft or bearing materials in many precision mechanical bearings (Figure 21.35). Therefore, the lubricants must not cause any rusting of iron alloys, corrosion, or discoloration of nonferrous metals (brass, bronze). The corrosion effect of lubricants on metals is therefore tested and evaluated in contact with moisture.

One test method is emulsification of 10 % water in the lubricant in which, for example, steel balls and brass rounds are stored at 85°C. After only 24 and 48 h, the anti-corrosion properties of the lubricant can be evaluated reliably because metals can undergo a great deal of corrosion in this period of time.

Another method of assessing the anticorrosion properties of a lubricant is by coating metal parts with a thin layer of oil, which is then exposed to a relative atmospheric humidity of almost 100 % at 40°C.

As a rule, precision mechanical instrument oils and plastic lubricants are furnished today with suitable inhibitors to ensure adequate corrosion protection.

21.5.3.6 VISCOSITY-TEMPERATURE BEHAVIOR

The viscosity of a lubricant is an important factor in the lubrication of bearings, most especially in bearings used in precision mechanical engineering, in which relatively low-viscosity oils (viscosity ~ 100 – 150 mm²/s at 20°C) are used because of the drive power and torque, which are usually low. If lubricants are to be used additionally or exclusively as noise-damping fluids (e.g., in plastic gears of stepping motors), the viscosity of the lubricant may vary between 500 and 10,000 mm²/s at 20°C, depending on the desired damping result.

If the application range of precision mechanical devices (e.g., from -40°C to $+120^{\circ}\text{C}$ in the automotive industry) is considered from the point of for-life lubrication, then the viscosity characteristic of the lubricant should remain largely constant over this temperature range. However, the viscosity of a fluid depends to a great extent on the temperature: With a rise in temperature, there is a definite decline in viscosity, and with a reduction in temperature there is a definite increase in viscosity. A change in temperature has a much greater influence on viscosity than most other

physical properties. One example is a PAO that has a viscosity of 300 mm²/s at 20°C, but at -10°C , it is approximately 2400 mm²/s, and at 50°C it is only approximately 75 mm²/s.

To investigate the viscosity-temperature behavior of a lubricant, its viscosity is determined at different temperatures, preferably at -20 , 0 , 20 , and 40°C . These values are then plotted in a viscosity-temperature chart, in which the viscosity is plotted in a log-log plot as a function of the log of the absolute temperature. This graphic plot of viscosity values as a function of temperature almost yields a straight line (VT line) from which viscosity values can be determined in first approximation at measured temperatures by interpolation. The steeper the VT line, the greater is the viscosity-temperature dependence of the lubricant. An almost horizontal VT line would be desirable.

Another conventional method of mathematically characterizing the viscosity-temperature behavior of lubricants is to calculate the viscosity index (VI) according to ISO 2909. A very complex calculation is performed here using two measured viscosity values at different temperatures to determine a characteristic number, which allows a comparison of different oils. For example, mineral oils have a VI of approximately 100. This corresponds to a lubricant with a great dependence of viscosity on temperature (steep VT line). However, silicones have one of the highest VIs of all known fluids (i.e., ~ 450), so there is only a slight dependence of viscosity on temperature (flat VT line).

21.5.3.7 LOW-TEMPERATURE BEHAVIOR

To evaluate the use limit of lubricants in the low-temperature range, long-term cold tests must be conducted. The practice of reporting a pour point, as is customary in general, provides only limited information about the usability of lubricants at low temperatures because in these tests the lubricant samples are cooled within a relatively short period of time until they solidify. However, crystallization processes in lubricants proceed very slowly in some cases. Depending on the complexity of the molecular chain, a longer or shorter amount of time is needed for the molecules to assume an ordered structure. Long-term cold tests are therefore absolutely mandatory.

According to FTMS Method No. 3458.1, the lubricant samples are always stored for 72 h at a certain temperature and then are tested for cloudiness and solidification. The test is begun at 0°C. After storing for 72 h at this temperature and then evaluating, the temperature is lowered by 5 K and the test is continued at the lower temperature. This procedure is repeated until the lubricant has solidified. The lowest temperature at which the lubricant is still liquid after 72 h is reported as the result of this test. This indicates the lower use limit temperature of the lubricant.

Analog to test results with this method, PAOs may be used at low temperatures in the range of -20°C to -40°C ; polyglycols instead may be used only from -20 to -30°C . Linear perfluoropolyalkyl ethers may be used down to -60°C , but branched ones can be used only down to approximately -30°C . In the case of silicone oils, the long-term low-temperature use limit is between -10 and -45°C , depending on chemical structure and viscosity. The lowest temperatures down to -70°C are reached by only a few special synthetic low-viscosity ester oils. Otherwise, the low-temperature use limit of synthetic esters is between -20 and -50°C , depending on the chemical structure and viscosity.

21.6 TRIBOLOGICAL SIMULATION OF PRECISION MECHANIC PARTS

21.6.1 Model Test Systems

To investigate and optimize tribological systems, many different test setups and model test systems may be used, all of them with the goal of making a preliminary choice of materials and, optionally, lubricants in the laboratory. Therefore, operational life cycle experiments with original parts can be greatly reduced or shortened to some extent, but they can never be replaced entirely.

Even the lubricant supply of the tribological contact, which is comparable to that in the actual component, is extremely difficult. There may be starved lubrication because the lubricant is pushed away or even dry running, or the system is in a hydrodynamic operating state when, for example, the pin surface stands obliquely in the sliding direction in a pin-on-disc system. Then the model system is somewhat better when a test ball of the same material as in the original component is used instead of a pin. This prevents lubricants from being pushed out of the sliding contact.

ISO 7148/2 describes various tribological model test systems (Figure 21.36) with their advantages and disadvantages, namely for polymer materials here.

For the choice of the model system for tribological investigations, it is important for the model system to approximate practical conditions as closely as possible. Figure 21.37 is an example.

If a plain bearing is going to be simulated, a test system in which wear leads to a decline in surface pressure is needed. In the real radial plain bearing, the final operating friction surface is achieved only through the running-in wear. Because of the increase in the contact area and the associated decline in surface pressure, the lubricated bearing enters the hydrodynamic stage only during or after the running-in process.

21.6.2 Friction Behavior

Friction reduces the efficiency of modules and destroys energy. The goal of any lubrication is therefore to reduce

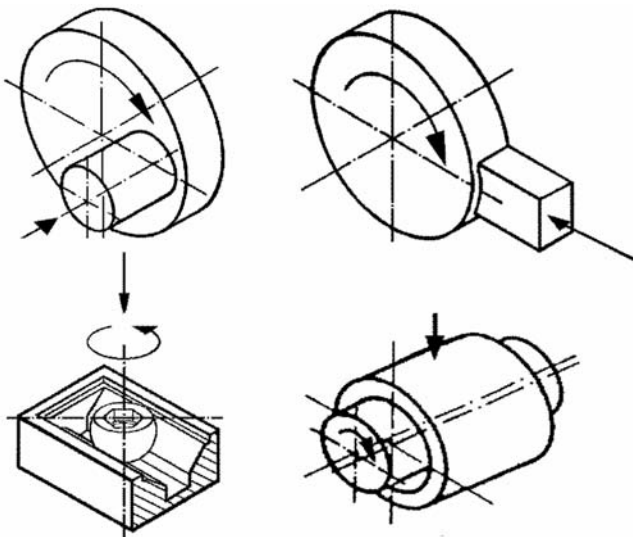


Figure 21.36—Model test systems according to ISO 7148-2 pin-on-disc, block-on-ring, sphere-on-prism, and plain bearing-on-shaft.

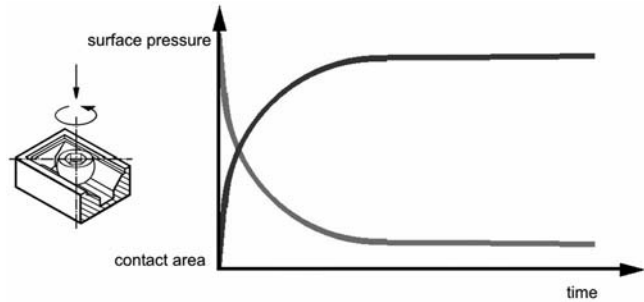


Figure 21.37—Model system sphere-on-prism: Development of surface pressure and contact area with wear.

friction. Friction depends on, among other things, the dimensions of the bearing (e.g., the bearing diameter and the bearing clearance), the material combination of the bearing materials, and naturally and most especially the lubricant. Other parameters such as surface roughness, surface pressure, sliding speed, and ambient temperature also influence the friction behavior. A variety of different tests are required to investigate the friction-reducing properties of a lubricant because all important influencing parameters are to be included in the assessment.

In the sphere-on-prism test (Figure 21.38), the sphere rotates and initially has point contact. Surface pressure then declines because of wear because the contact surface increases. Lubricant and wear particles remain in the test body. The test specimens are “disposable parts” (Figure 21.39).

The result of the friction simulation in the sphere-on-prism model system according to ISO 7148-2 is a three-dimensional graph that shows the friction coefficient, f , at three load levels dependent on sliding speed. The example in Figure 21.40 shows the typical friction behavior of a steel/steel sliding combination with no lubrication (dry), which shows a high coefficient of friction f with no dependence on either speed or load.

Under lubricated conditions the friction depends on sliding speed. The example in Figure 21.41 shows the friction behavior of a sliding combination steel against polyamide 66, which has been lubricated by a perfluoropolyalkyl ether with a viscosity of 300 mm²/s at 20°C. Typical Stribeck

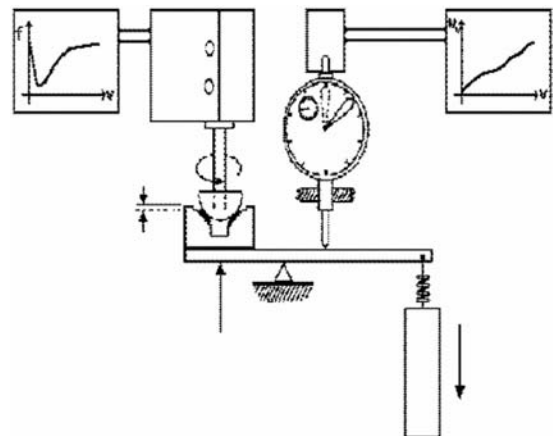


Figure 21.38—Torque measurement system with sphere-on-prism test bench (ISO 7148-2).

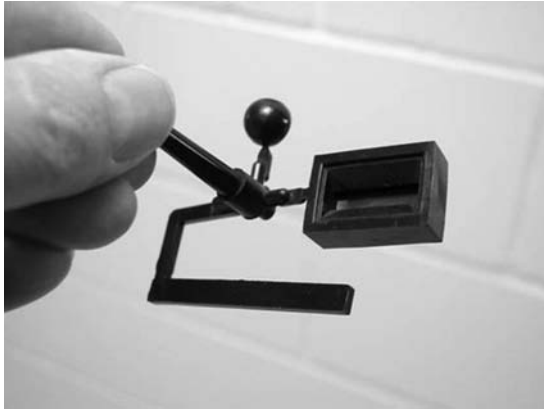


Figure 21.39—Injection molded test specimens out of thermoplastics for sphere-on-prism tests.

curves are obtained. The friction diagram differs from sliding combination and lubricant, as may be seen in Figure 21.42, steel versus camrider, lubricated with diesel oil.

21.6.3 Static Friction

In the friction behavior, low static friction is normally required. However, many modules (e.g., window-opening mechanisms) require a defined high-static friction to

prevent the window from opening because of gravity or vibrations. With the electromechanical parking brake, a tribological self-locking of the brake shoe system is required.

A static friction tribometer (Figures 21.43 and 21.44) has been developed to allow determination of the transitional range between sticking and slipping.

In addition to tribological effects such as wear and friction with different loads, sliding speeds, and temperatures, which are largely understood, static friction or friction at rest is a borderline field, but is a common tribological operating state, especially in precision mechanics. This is mainly due to the complex measurement setup required to measure static friction (i.e., friction at rest). In the transitional range between static friction and kinetic friction, complex stick-slip effects occur, but the cause and sequence of these effects have not yet been researched much. The Stribeck curve provides some striking information about the sliding of polymers in the range of extremely low sliding speeds (0–0.001 mm/s).

21.6.3.1 TRIBOLOGICAL SIMULATION OF START-STOP FRICTION

The sphere-on-three plates tribometer (static friction tribometer) is used to investigate the friction pairing of steel against polycarbonate lubricated with a silicone oil with a viscosity of 5000mm²/s at 20°C. The design and control of

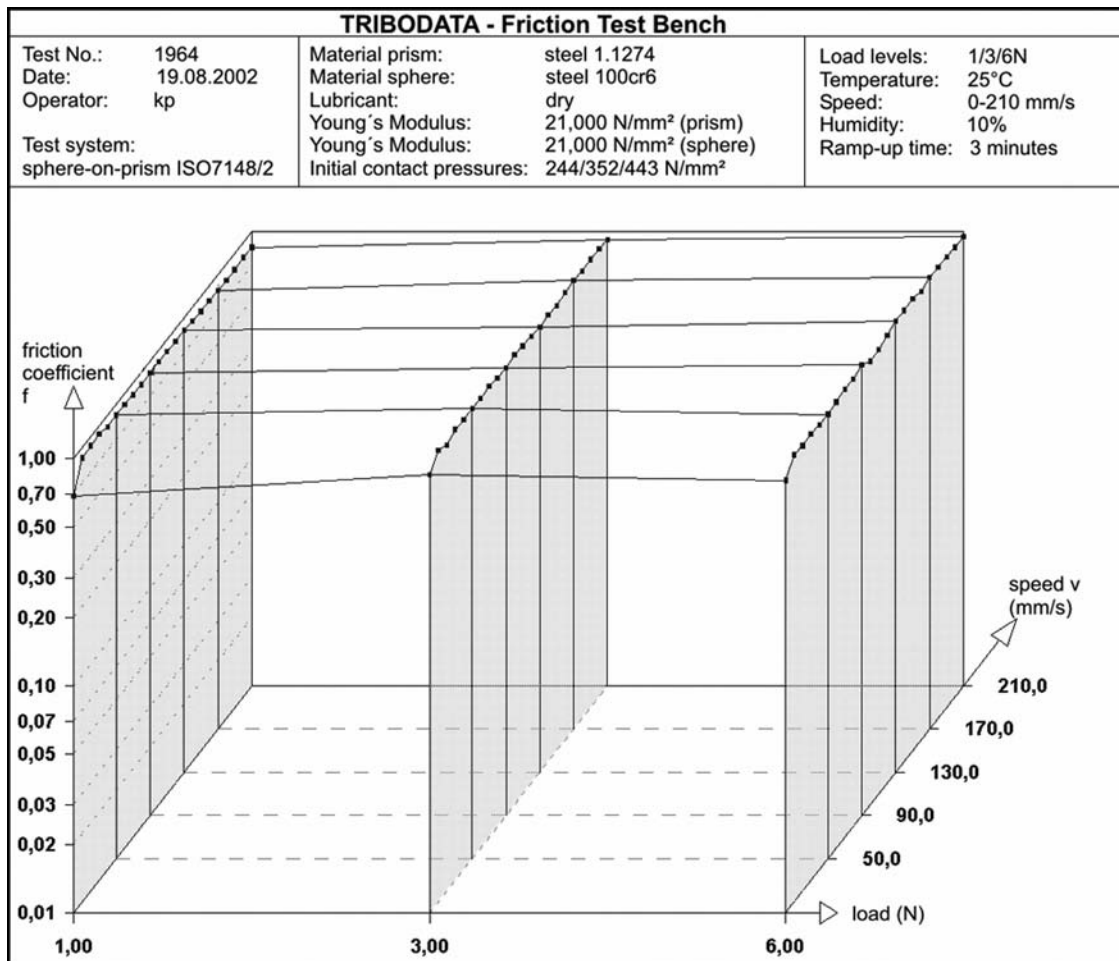


Figure 21.40—Three-dimensional friction diagram. f is dependent on load and speed. Sliding combination steel/steel, no lubrication.

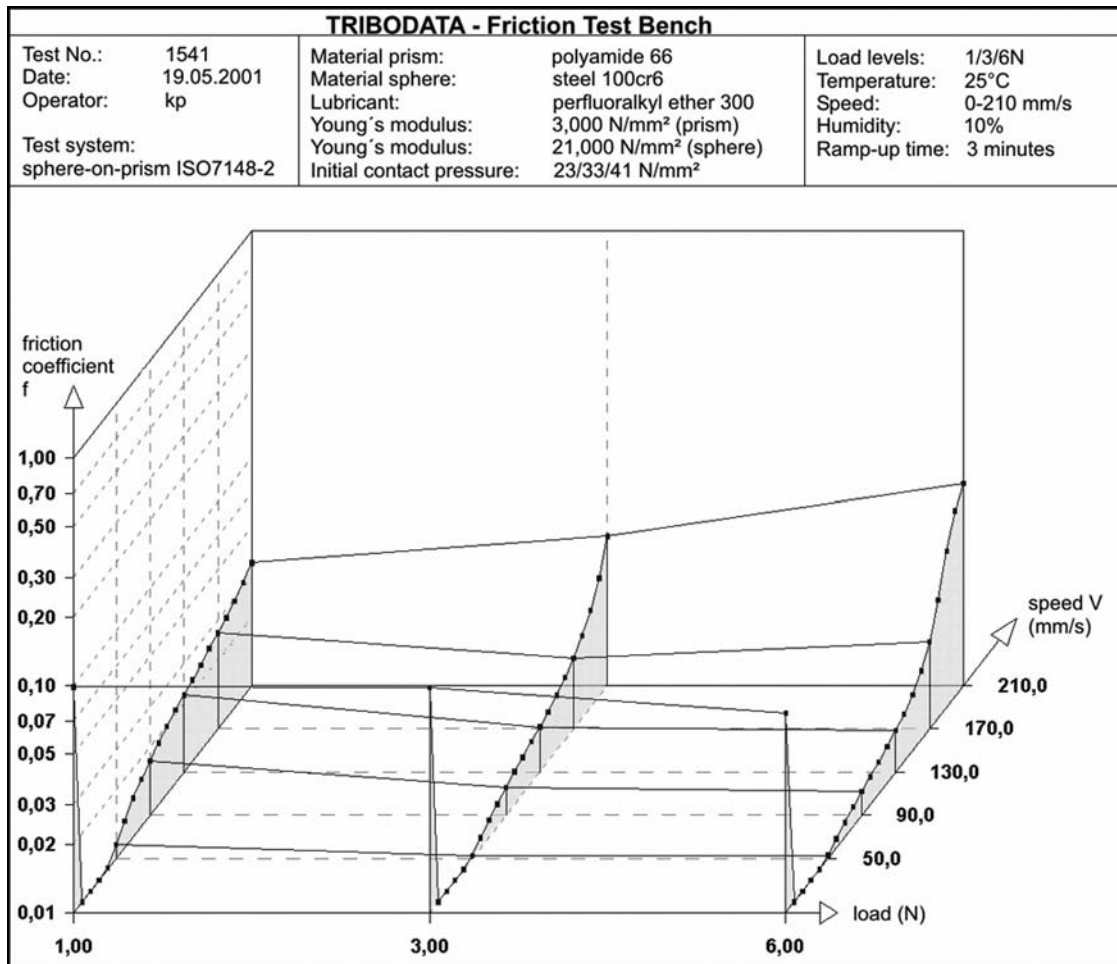


Figure 21.41—Three-dimensional friction diagram. f is dependent on load and speed. Sliding combination of steel/polyamide 66 lubricated with a perfluoropolyalkyl ether (viscosity 300mm²/s at 20°C).

the tribometer allow an investigation of starting and stopping friction. To obtain more detailed information about the starting friction behavior, the downtimes between the individual experiments can be selected freely.

Unique phenomena have been discovered. Before a friction system reaches a state of sliding, the static friction must be overcome. A body is in a stage of static friction or at rest or both when there is no relative speed between its contact face and the substrate. In other words, the sliding speed in this case is zero. At the moment when a relative movement begins because of an acting force, the measured coefficient of friction is referred to as starting friction. The opposite process occurs when a body comes to rest from a sliding state or from movement and then stopping friction is measured. The sliding speed approaches zero. One should now assume that both static friction states are represented by the same frictional forces or coefficients of friction or both. In experiments and in practice we find substantial differences between starting friction and stopping friction in lubricated systems (Figure 21.45).

With many polymer friction pairings (e.g., POM/steel), the coefficient of friction depends on the speed. It is interesting to note that the static friction is then lower than the kinetic friction. This behavior is explained by the fact that the polymer molecules are linked together visco-elastically.

At a higher deformation rate of the molecular network because of lateral friction forces, there is a greater uptake of energy or at a higher deformation rate there is an increase in damping energy or both. This is also zero at a speed of zero.

21.6.4 Wear Behavior

When solid bodies are in sliding contact with one another, in addition to the resulting friction, it always leads to wear. The magnitude of the wear depends on numerous parameters. The most important of these are load per unit surface area (surface pressure), sliding speed, and sliding distance. The basic formula is wear equals surface pressure times sliding speed, $W = P \times V$. However, this formula has limited application in the area of precision bearings. Above all, the sliding speed often makes it impossible to predict the rate of wear.

An example: On a nonlubricated (i.e., dry running) plain polymer bearing, wear only follows the equation if the resulting friction heat does not lead to softening of the bearing material. If it does, wear dramatically increases.

In the case of an optimally designed plain bearing with little bearing play provided with a lubricant of well-matched viscosity, an increase in sliding speed actually reduces the wear rate. The goal of attaining a hydrodynamic operating state is also an important goal in precision bearings.

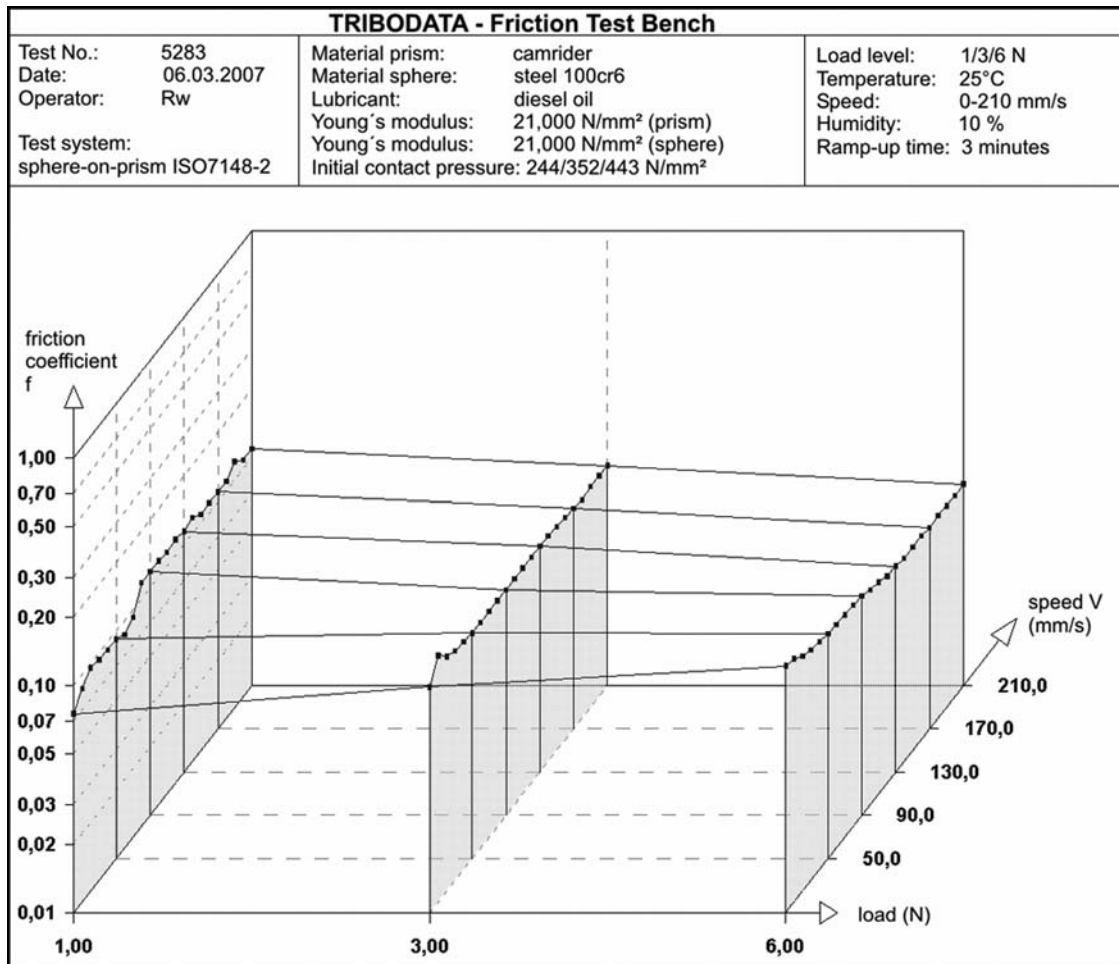


Figure 21.42—Three-dimensional friction diagram for sliding combination steel versus camrider lubricated with diesel oil.

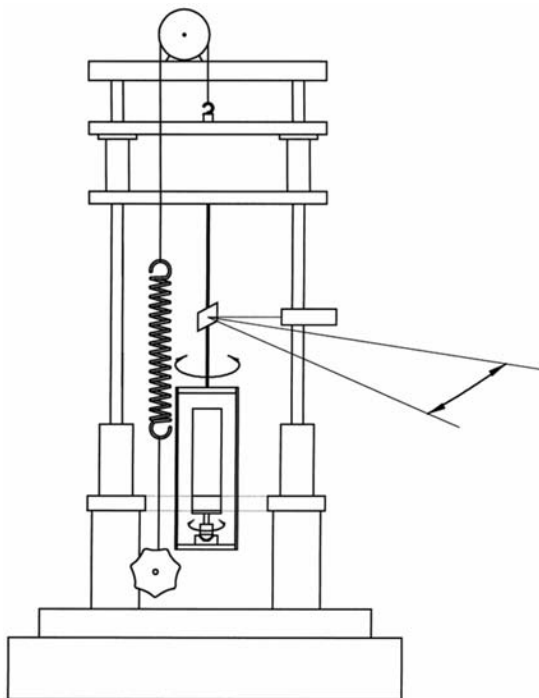


Figure 21.43—Function principle of static friction tribometer.

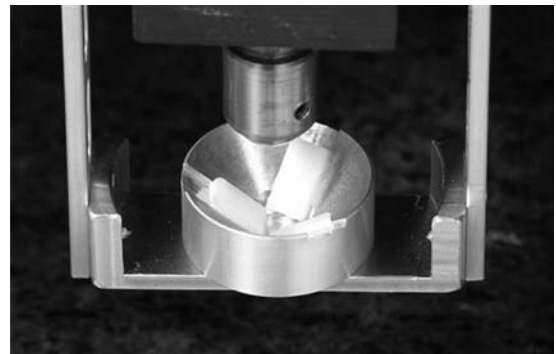


Figure 21.44—Test specimen of static friction tribometer: rotating sphere in a pyramid with three plates.

The material combination, surface roughness, and hardness all have a significant impact on wear. A high ambient temperature reduces oil viscosity and can cause the friction system to transition from a hydrodynamic state to a mixed friction state. This also leads to a dramatic increase in wear. The effects of air humidity on the wear behavior of polymers is material-specific. In the case of POM, wear increases with higher air humidity. However, some polyamides need humidity for good tribological

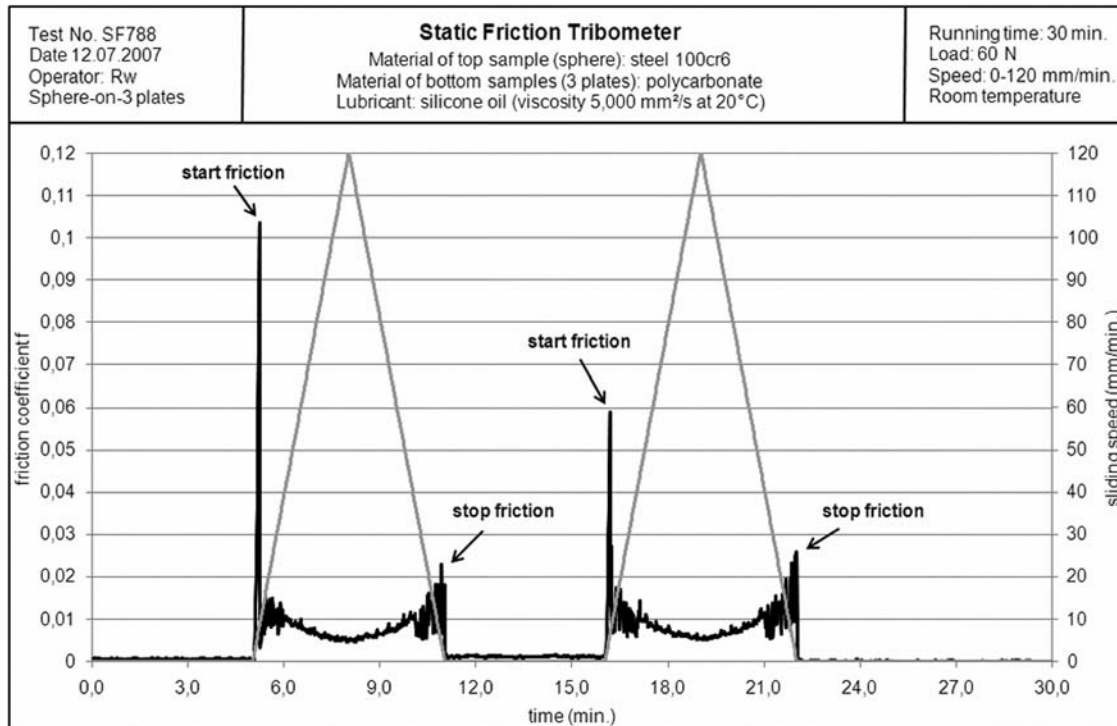


Figure 21.45—When a system comes to a stop, the friction is much lower than when breaking out from a standstill. The x-axis is time. The y-axis is sliding speed and coefficient of friction.

operation. For example, PTFE friction ring seals will fail in a very dry ambient atmosphere (relative humidity < 5 %).

On plain polymer bearings, the type of movement also has a decisive effect on wear. In contrast to metal plain bearings, reversing or oscillating operation can multiply wear. Alternating directions of the sliding movement weaken the inner structure of the polymers.

Movement types can be ranked in order of relevance to wear:

- *Low wear*: Unidirectional rotation (motor bearing);
- *Moderate wear*: Reversing rotation (window lifts, wipers);
- *High wear*: Oscillating motion (doors, actuators); and
- *Very high wear*: Drilling motion (axial bearing, shaft end bearing).

21.6.4.1 EFFECTS OF THE INJECTION MOLDING SKIN

In thin-walled components of precision bearings, the sliding surface frequently exhibits an amorphous structure. Because of the high cooling rate (e.g., in the case of POM), no spheruliths are created in the outer areas of the parts any longer. Its tribological behavior depends to a great extent on the crystalline, semicrystalline, or amorphous structure of the bearing surface.

Often, amorphous materials have worse wear behavior than crystalline or semicrystalline materials.

The morphology and size of the wear particle is extremely crucial in attaining reliable operation when bearing diameters are small. At the same rate of wear, either very small powder-like particles (<1 μm) or macroscopic agglomerates up to 100 μm in size might be produced. Large particles lead to shaft seizing in the bearing gap. The

same applies to the resulting transfer layers and material fusing in nonpolymeric bearings. Layer thicknesses that are considered negligible on bearings greater than 5 mm in size may cause a 0.5-mm bearing to seize.

21.6.4.2 SIMULATION OF WEAR BEHAVIOR

Wear has a direct effect on a device's performance and life. Prediction of these properties requires tribological simulation. Because testing of assemblies is very complicated and expensive, simplified model-based tests are used to save on time and costs. Nonetheless, even precise simulation of tribological processes in model systems is known to lead to faulty conclusions or results.

More than 150 different model test systems are used worldwide (Figure 21.46). The following example will illustrate the types of results attainable today in such a system. The friction and wear behavior of materials and

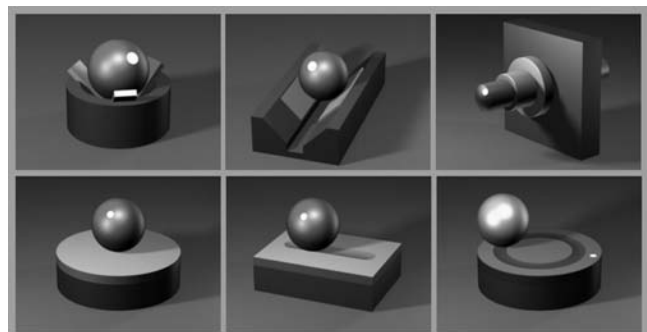


Figure 21.46—Different model test systems for the simulation of wear behavior of materials.



Figure 21.47—Oscillating friction tribometer.

lubricants can be studied on an oscillating friction tribometer (Figure 21.47). The type of movement is back and forth (oscillating). All test parameters are adjustable over broad ranges. Load is 100–2000 N, sliding speed is 0.01–1 m/s, temperature is –20 to 200°C, and test time is 10 s to 200 h.

Different model systems can be studied on this universal test bench: pin/disc, sphere/plate, plate/plate, cylinder/plate, o-ring/plate, piston/cylinder, sphere/prism, and spherical cap/plate. The model test system should approximate the practical application as closely as possible. Examples are given in Figures 21.48–21.51 of o-ring seals in the piston/cylinder system of a gas spring, back and forth type of movement.

In studying the wear behavior of o-rings, the simplified system of o-ring on plate may be used to approximate the practical application of shaft/o-ring. Test parameters measured in preliminary studies can be used to obtain very good findings on the comparative behavior of the wear properties of different o-ring coatings. The friction counterpart (plate) uses the same materials with the same characteristics as those of the actual part.

When studying plain bearing materials of lubricated bearing sleeves, the system of a pin with spherical cap on



Figure 21.48—Specimen holder for different types of o-rings.

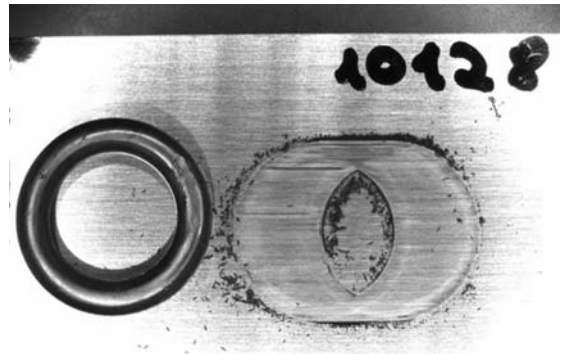


Figure 21.49—Result of a wear test with an o-ring material on a steel plate under oscillating conditions.

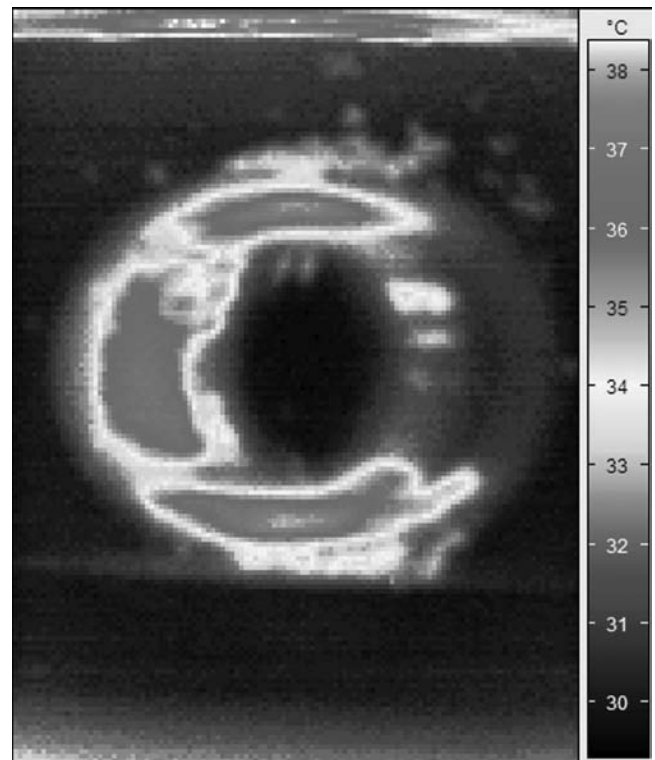


Figure 21.50—Thermography of the contact area of an o-ring oscillating against a steel plate.

plate makes sense. The curved surface closely produces hydrodynamic processes that are similar to those of a lubricated plain bearing.

If the wear behavior of an unidirectionally rotating plain bearing (e.g., in a fan motor) is to be simulated, the oscillating test is generally too severe. The test bench must allow a rotational movement. A good model system here is the sphere-on-prism model simulation of ISO 7148/2.

The results of a model simulation only lend themselves to making a comparative assessment. Only a rough estimate can be made of the predicted life of the real part. If the comparative wear results of two plain bearing lubricants differ by more than 40 %, then it can be expected that use of the one lubricant in the actual part will yield reliable operation over a significantly longer time period.

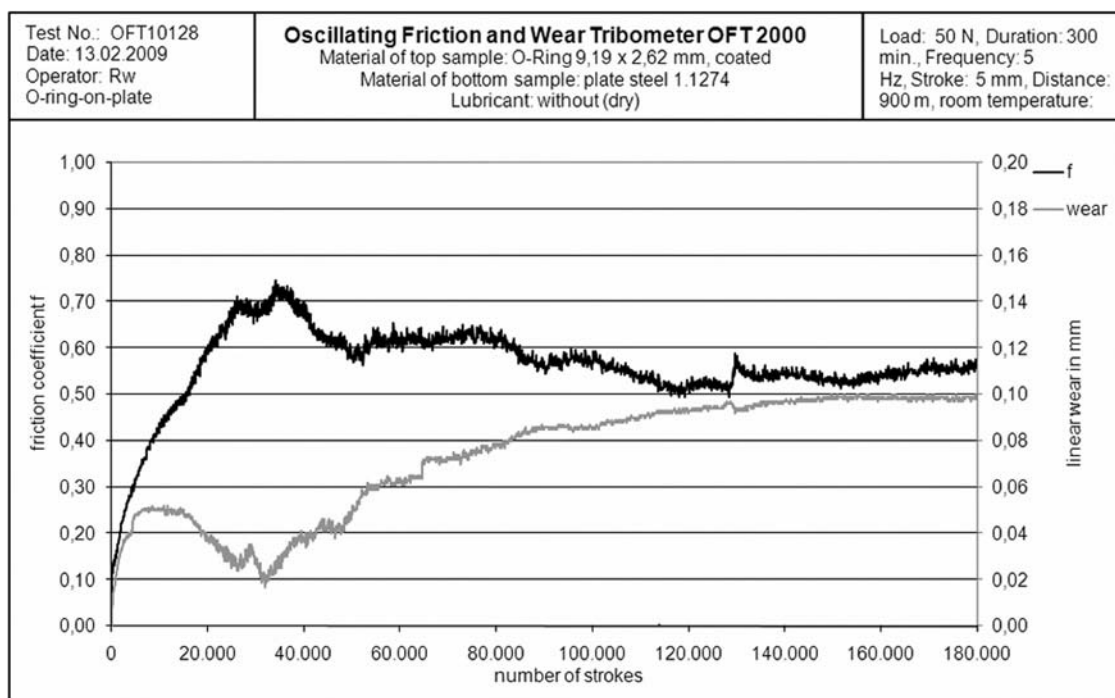


Figure 21.51—Development of friction coefficient and linear wear over number of strokes in oscillating model simulation of an o-ring-seal against a steel plate.

21.7 CONCLUSIONS

The tribology of precision systems in automotive applications differs significantly from the teachings of classic mechanical engineering in some areas. The small size of the parts amplifies the effects of roughness, bearing geometry, and bearing design. The often high-power density of precision assemblies also creates thermal problems, especially when polymer materials are used. The very small volumes of the lubricants used and their mutual interactions with the friction materials assume tremendous significance and can lead to damage in production parts. Loss of lubricant by migration is a typical problem that generally only occurs in precision mechanical systems.

References

- [1] Nagdi, K., 1990, "Polyalphaolefine (PAO)—die Dichtungsfreundlichen Flüssigkeiten," *Tribologie Schmierungstechnik*, Vol. 37, pp. 281–288.
- [2] Wildersohn, M., 1985, "Esteröle—Struktur und Chemisch-Physikalische Eigenschaften," *Tribologie Schmierungstechnik*, Vol. 32, pp. 70–78.
- [3] Kussi, S., 1985, "Chemical, Physical and Technological Properties of Polyethers as Synthetic Lubricants," *J. Synth. Lub.*, Vol. 2, pp. 63–89.
- [4] Wunsch, F., 1991, "Perfluoralkylether," *Tribologie Schmierungstechnik*, Vol. 38, pp. 130–136.
- [5] Huber, P., and Kaiser, W., 1986, "Silicone Fluids—Synthesis, Properties and Applications," *J. Synth. Lub.*, Vol. 3, pp. 105–120.
- [6] Beyer-Faiss, S., 2005, "Test Method for Simulating the Aging and Oxidation Stability of Lubricants," *Practicing Oil Analysis*, Vol. 7, pp. 23–30.

Analysis of In-Service Automotive Engine Oils

Jim C. Fitch

22.1 INTRODUCTION

Most oil analysis performed in North America is done on diesel engine crankcase oils, primarily for large fleets in the transportation and off-road equipment industries. Ranking second would be the analysis of lubricants used in stationary industrial machinery including compressors, turbines, gearing, bearing lubes, and hydraulics. Far down the list is engine oil analysis performed on crankcase lubes from automotive fleets or privately owned cars and trucks.

Although there are a few isolated exceptions, condition monitoring of passenger car motor oils (PCMOs) has not yet emerged as a strong market. There are several understandable reasons for this. One is the fact that most car owners are not interested in paying a premium to extend engine life. Most car owners seem to be satisfied with the current engine life expectancy. This is evidenced by the fact that less than 10 % of PCMOs in use are synthetic formulations despite their widely promoted benefits.

Unlike commercial and industrial applications, in which machine owners often run equipment to their end of useful life, car owners are more commonly enticed to sell earlier for newer models. After all, why invest in engine life extension when the benefit of the investment would only be gained by the next owner of the vehicle?

Sampling is another impediment. Automobiles are not fitted with convenient oil sampling valves, nor are these valves easy to retrofit on engines. The only practical alternative is to obtain a sample from the dipstick port by drop-tube vacuum sampling or from the oil pan drain port. Neither of these locations is suitable for obtaining a representative sample.

The other factor is the cost and turnaround time of getting the data. Although laboratory automation has increasingly enabled basic tests to be performed quickly and with minimal cost of labor, routine oil analysis is still expensive for personal car owners. Some instruments are actually an integration of several conventional oil analysis sensors and often include viscometry, molecular spectroscopy, and atomic spectroscopy, typically with no needed glassware or sample preparation steps. So too, many new onboard sensors have been introduced that monitor key oil properties in real time. They displace the need for oil sampling and can alert the car owner to the optimal timing of an oil change or the presence of aberrant oil properties and wear metals.

22.2 OIL SAMPLING METHODS

Oil sampling is a critical component of a high-quality and effective oil analysis program regardless of the machine

involved. Errors in obtaining a representative sample impair all further oil analysis efforts. There are two primary goals in obtaining a representative oil sample [1,2]:

1. *Maximize data density:* Samples should be taken in such way that meaningful properties of the oil can be extracted with sufficient discriminant validity; restated, we want the most meaningful information per millilitre of oil possible. This information relates to such properties as cleanliness and dryness of the oil, depletion of additives, and the presence of wear particles being generated by the engine. For example, sampling oil from a cold engine would fail to capture a representative concentration of particles, sludge, water, and other contaminants prone to stratification by gravity and time.
2. *Minimize data disturbance:* Samples should be extracted in such a way that the concentration of information is uniform; consistent; and unaltered by the sampling process, hardware used, or location. For example, it is important to make sure that the sample does not become contaminated during the sampling process. This can occur by using dirty sample bottles, unclean or unflushed sampling valves, and other exposures that alter the target properties of the sample.

To ensure good data density and minimum data disturbance in oil sampling, one should consider the following factors, each of which is discussed in detail later in the chapter [1,2]:

- *Sampling location:* In engines, live zone sampling will produce the best results. Sampling from dipstick ports or oil pan drain ports should be avoided.
- *Sampling procedure:* The quality of the procedure by which a sample is drawn is critical to the success of oil analysis.
- *Sampling hardware:* The hardware used (valves, pumps, probes, tubing, pressure regulators, etc.) to extract the sample should not disturb sample quality but should aid it. It should be clean, easy to use, rugged, and cost-effective.
- *Sample bottle:* The type, size, and cleanliness of the oil sample bottle help to ensure that a representative sample is achieved.

22.2.1 Sampling from Oil Pressure Line

When a sample is taken from a line in a circulating system, it is referred to as a live zone sample. On an automobile engine, the best location for obtaining such a sample is on the pressure line between the pump and the filter (Figure 22.1). As previously noted, for most engine types, this is not an easy option for locating a sampling valve,

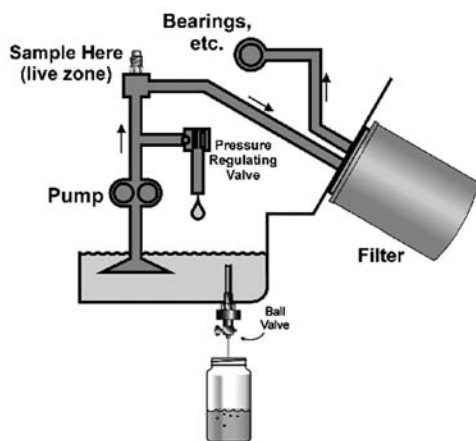


Figure 22.1—Sampling location on an engine wet-sump circulating system.

although with special hardware and adapters such valves can be installed successfully. There are measures that can be taken during the sampling process that improve the quality and effectiveness of the live zone sample. The following is a summary of recommended sampling practices [1,2]:

1. Sample from turbulent zones where the fluid is moving and the oil is well mixed (i.e., from circulating fluid).
2. Sample after the oil has completed its primary function(s). In an engine, the oil that lubricates cylinders, gearing, and bearings falls by gravity back to the sump and is quickly picked up by the suction strainer and pump. Contaminants and wear debris introduced by the engine are infused in this fluid. Sampling from a valve between the pump and the filter during engine operation enables a live zone sample to be obtained.
3. Sample engines during typical working conditions and while the engine is running and the fluid is hot. Try not to sample after an oil change, filter change, after long-idle times, or at some time when the fluid would not represent typical conditions.

22.2.2 Drain Port Sampling

The most basic method for sampling is to remove the drain plug from the bottom of the sump, allowing an amount of fluid to flow into the sample bottle. For many reasons, this is not an ideal sampling method or location. Most important is the fact that bottom sediment, debris, and particles (including water) enter the bottle in concentrations that are not representative of what is experienced near or around where the oil lubricates the engine. Because of this stratification, the drain port sampling method should be avoided if at all possible (except for the purpose of inspecting for free water, coolant, and sediment).

Drain port sampling can be greatly improved by using a short length of stainless steel tubing, extending inward and up into the active moving zone of the sump (Figure 22.1) [1–3]. In many cases, this ball valve and tube assembly can be threaded into the drain port without interfering with the use of the plug for periodic draining of the oil.

A third option is called drain port vacuum sampling. With this method, a minimess or similar valve is installed as previously described using an inward-directed pilot tube, but instead of fluid passing into a sample bottle by gravity, it is assisted by a vacuum sampler (Figure 22.2) [1–3].

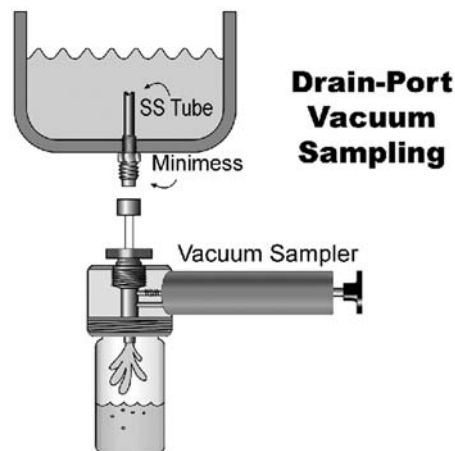


Figure 22.2—Drain port sampling aided by a vacuum pump.

This is particularly helpful when the oil is highly viscous (cold temperature) or otherwise difficult to sample by gravity alone. During the sampling process, the connector on the end of the plastic tube of the vacuum pump is threaded onto the minimess valve. A vacuum is produced by the pump pulling oil downward into the sample bottle.

22.2.3 Drop-Tube Vacuum Sampling

One of the most common methods for sampling an engine sump is to use the drop-tube vacuum sample method. With this method, a tube is inserted through the dipstick port and lowered into the sump cavity. For the best results, the tube should be cut approximately 10 in. longer than the dipstick and inserted approximately 0.24 in. shorter than the dipstick [3]. This sampling method has several drawbacks and should be avoided if other sampling methods, as previously described, can be used instead. The following is a summary of the risks and problems associated with drop-tube vacuum sampling:

- *Tube location:* A tube that is inserted into a dipstick port is extremely difficult to control. The tube's final resting place is hard to predict, resulting in samples being taken from different locations each time. There is always a risk of the tube actually going all of the way to the bottom of the sump where debris and sediment are picked up (not representative of circulating fluid).
- *Drop-tube contamination:* There is considerable concern that the tube will scoop up debris from the sides of the casing as it is being inserted. Also, the tube itself may be contaminated because of poor cleanliness control during handling and storage.
- *Large flush volume:* The drop-tube method substantially increases the volume of fluid that must be flushed through the sampling hardware (in advance) to obtain a representative sample.
- *Machine intrusion:* The drop-tube method is intrusive. The engine must be invaded to draw a sample. This intrusion introduces the risk of contamination, and there is always the concern that the engine might not be properly restored to run-ready condition before startup.

22.2.4 Sampling Bottles and Hardware

An important factor in obtaining a representative sample is to make sure the sampling hardware is completely flushed

before obtaining the sample. This is usually accomplished using a spare bottle to catch the purged fluid. It is important to flush the dead sampling pathway volume five to ten times before obtaining the sample. All hardware that the oil comes into contact with is considered dead volume and must be flushed, including

- Sampling ports, valves, and adapters,
- Probe-on sampling devices,
- Adapters for using vacuum sample extraction pumps,
- Plastic tubing used for vacuum pumps (this tubing should not be reused to avoid cross-contamination between oils).

There is an assortment of sampling bottles that are commonly used in oil analysis. An appropriate bottle needs to be selected for the application and the tests that are planned. The following parameters should be considered when selecting sample bottles [1–3]:

- **Size:** There are several different sizes of sample bottles that are available. They vary from 50-mL (or ~2 oz of fluid) to 200-mL bottles. The most common bottle size is 100 mL, which is generally suitable for automotive engine oil analysis.
- Another consideration in selecting the bottle size is the fact that the entire volume of the bottle should not be filled with oil during the sampling process. Only a portion of the sample bottle should be filled. The unfilled portion, called the ullage, is needed to allow proper fluid agitation by the laboratory to restore even distribution of suspended particles and water in the sample. It is advised to only fill the bottle approximately three-quarters full.
- **Material:** Modern sample bottles are made of polyethylene terephthalate (PET) plastic because of (1) their chemical compatibility with most base oils and additives, (2) the fact that they are clear, (3) their strength (fracture resistance), (4) their wide availability, and (5) their low cost. The primary disadvantage of using PET is the risk that the sample bottles will melt or become soft when sampling high-temperature engine oils (above 200°F).
- **Cleanliness:** One of the most important considerations in selecting a sample bottle is to make sure it is sufficiently clean [4,5]. The bottle's required cleanliness level should be determined in advance. The bottle supplier should provide a certificate of cleanliness that is based on random testing of the bottles per ISO 3722. Bottles can be classified according to their contribution to the particle count into the following cleanliness categories:
 - **Clean:** Fewer than 100 particles, greater than 10 μm /mL fluid.
 - **Super clean:** Fewer than 10 particles, greater than 10 μm /mL fluid.
 - **Ultraclean:** Less than 1 particle, greater than 10 μm /mL fluid.

The selection of the bottle cleanliness depends heavily on the target cleanliness of the fluids being sampled. Engine oils sampled for particle counting should generally use bottles 10 times cleaner than the fluid target cleanliness for the same volume. A clean or super clean sample bottle is typically sufficient for most automotive oil analyses.

22.2.5 Oil Sampling Frequency

The objective of oil analysis, like engine condition monitoring in general, is incipient (early) detection of root causes

or impending failure conditions. The engine and oil will generally give off silent alarms when problems first occur. In time, as the severity increases, these alarms are no longer silent and even the most rudimentary condition monitoring methods can reveal the problem. Of course, at this point, a great deal of damage may have already occurred. It is also likely too late to arrest the problem on the run; the engine may require a major repair or need to be rebuilt.

One of the greater benefits of oil analysis is its sensitivity to these silent alarms and the detection of incipient failures and faults. The method of doing this successfully is discussed further in this chapter. Scheduled sampling intervals are common in oil analysis. The sample frequency is typically just before the drain intervals for gasoline and diesel engines [3]. However, it is important that the interval be consistently maintained based on engine run time (e.g., hours or kilometres). Loosely regulated drain intervals (and sampling intervals) will result in erratic data behavior (untrendable) unless mathematically normalized.

22.3 OIL TESTING AND ANALYSIS

In used oil analysis, testing plans are defined based on the specific questions that need to be answered about the lubricant, the engine, and the operating conditions. Because there are many possible tests, these questions need to be given careful consideration to optimize results and keep costs streamlined. Because lubricant testing involves specific costs to the vehicle owner, the value gained in getting specific answers to the questions must be weighed against these costs. The following are examples of questions that may need to be answered [3]:

- **Lubricant type/quality questions:**
 - Is the specified lubricant being used?
 - Have two incompatible lubricants been mixed?
- **Lubricant health/condition questions:**
 - Have any critical additives become depleted or impaired?
 - Has the base oil been damaged by oxidation, hydrolysis, or thermal degradation?
 - Has the oil's viscosity changed because of evaporation, shear, contamination, or various chemical reactions?
 - What is the residual life of the lubricant?
- **Lubricant contamination questions:**
 - Has the lubricant been cross-contaminated (mixed) with other vehicle fluids?
 - Has the lubricant become contaminated with fuel, soot, dirt, water, or coolant?
- **Wear and fault detection questions:**
 - Is there incipient evidence of abnormal wear?
 - Which engine surface is generating the wear?
 - What is the tribological, chemical, or mechanical cause of the wear?
 - How severe (advanced) or threatening is the wear?
- **Maintenance, operations, and commissioning questions:**
 - Does a filter need to be changed?
 - Is there internal or external leakage?
 - Is there evidence of abnormal operating temperatures, pressures, or duty cycle?
 - Has the engine been improperly repaired or rebuilt?

In its simplest and most basic form, lubricant analysis is performed to improve the quality of lubrication maintenance decisions. When well designed and implemented,

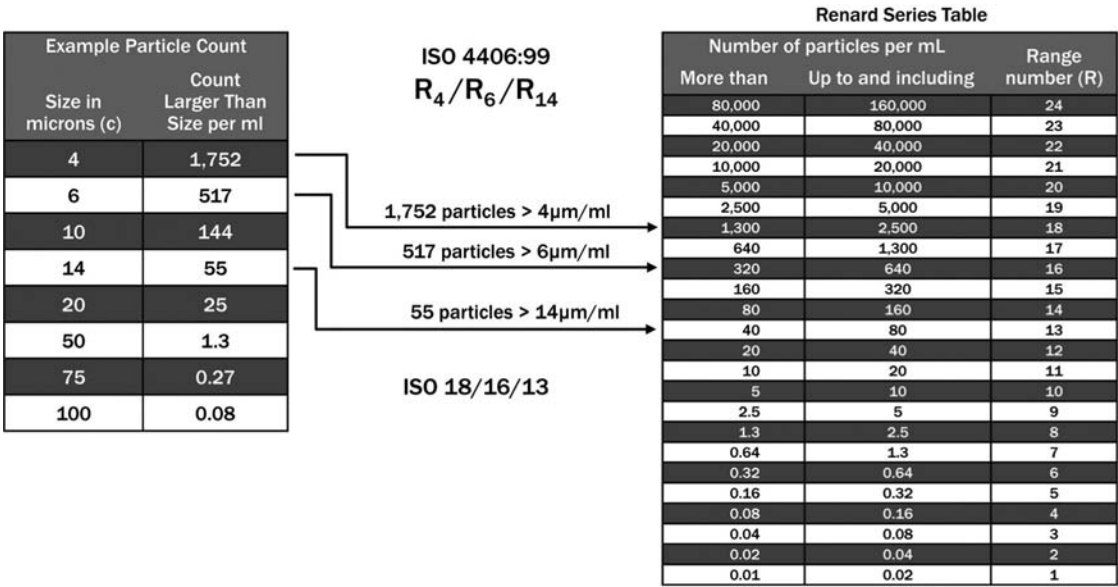


Figure 22.3—Under ISO 4406:99, a sample is given a fluid cleanliness rating using the above table. To do this, the number of particles greater than three size ranges—4, 6, and 14 µm—are determined in the equivalent of 1 mL of sample. In the above example, the particle count distribution shown in the table on the left translates to an ISO 4406:99 rating of 18/16/13.

many of the questions listed above can be answered without excessive expense or complexity. This is best accomplished by directing the testing program around three important categories of lubricant analysis:

- 1. *Fluid properties analysis:* This category of oil analysis deals with the assessment of the chemical, physical, and additive properties of the oil. Its primary goals are to define the remaining useful life (RUL) of the lubricant as well as to confirm that the correct lubricant is currently in use. It can also detect improperly mixed lubricants (e.g., a motor oil and a differential gear lube).
- 2. *Contamination analysis:* Contaminants are foreign energy or substances that enter a lubricant and engine from the environment or are generated internally. Contamination compromises engine reliability and promotes premature lubricant failure. Oil analysis can be effective at ensuring that goal-driven targets for contamination control are maintained.
- 3. *Wear debris analysis:* When components wear, they generate debris in the form of small particles (typically from 1 to 100 µm in size). The lubricant is usually the first recipient of this wear debris because of its close proximity to the frictional surfaces where the debris was formed. Monitoring and analyzing the generated debris enables technologists to detect and evaluate abnormal conditions such that effective and timely maintenance decisions can be made and implemented.

22.3.1 Review of Common Used Oil Analysis
22.3.1.1 PARTICLE COUNTING

Particle counting is a common oil analysis test that reports the number of particles above specified size ranges (in micrometres) per fluid volume (usually per 1 or 100 mL). Also, particle concentration and distribution data may be expressed in terms of ISO 4406:99 Cleanliness Codes (Figure 22.3). Particles can be manually counted using optical microscopy (ISO 4407 and ASTM F312-97). In this method, an aliquot of fluid is passed through a membrane. Afterward, particles on the membrane are manually counted under a

microscope. The method is similar to the patch test procedure discussed in Section 22.3.1.8. There are also commercial methods available that enable membranes to be optically scanned and digitally analyzed for particle size, count, and shape (ISO 16232-7). This method is referred to as particle micropatch imaging.

Most laboratories use automatic particle counters, which can report a particle count or ISO Code in just a couple of minutes. The two methods are laser optical (ISO 11500 and ASTM D7647) particle counters and pore-blockage (BS 3406) particle counters. Optical particle counters direct a laser light source at passing particles in the sensor cell (Figure 22.4). The amount and frequency of light blockage is measured by a photodiode. This signal is converted to particle size and count by the use of standardized calibration methods [4,6].

Because in-service engine oil is heavily loaded with soot (a combustion byproduct), the ability to use optical methods has limited application. However, a modified method using particle resuspension has been met with considerable success. This method filters the particle from the oil using a standard patch test procedure (5-µm pore size). Next, the filtered particles are backwashed into a superclean hydraulic fluid (or similar fluid). The soot particles pass through the membrane so that only those particles resuspended in the hydraulic fluid (>5 µm) are seen by the particle counter [4].

Pore-blockage particle counters use calibrated screens through which the sample flows during a test (Figure 22.5). The profile of the pressure rise or flow decay, caused by particle blockage of the screen’s pores, is measured. This

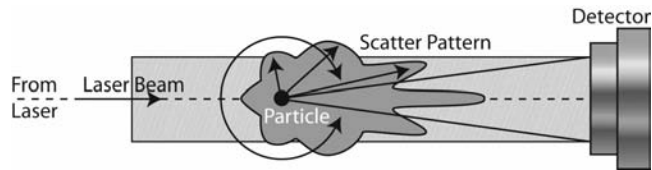


Figure 22.4—Light-blockage particle counter.

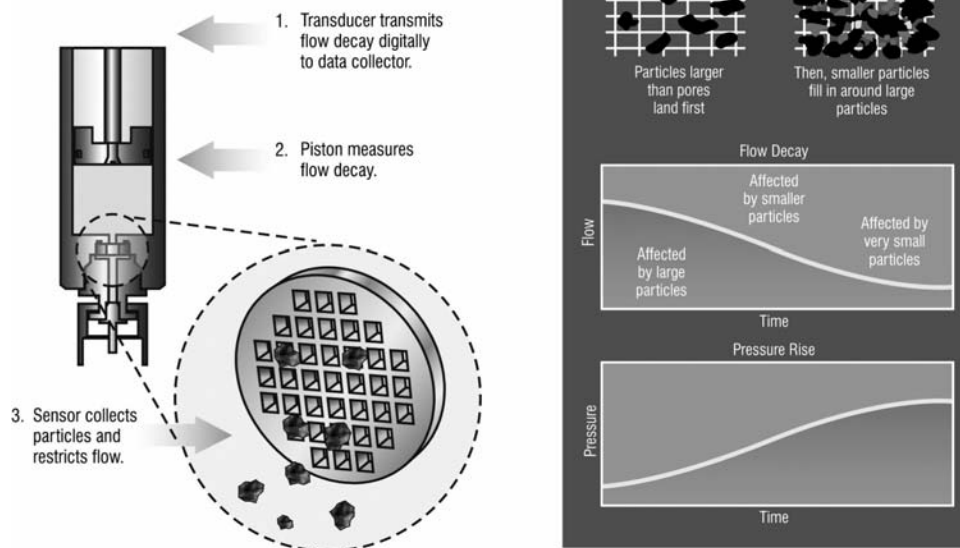


Figure 22.5—Pore-blockage particle counter.

profile is mathematically converted to an estimated particle count or ISO Code on the basis of calibration standards. Pore blockage is popular with laboratories testing engine oils because it is not hampered by soot [7,8].

Some modern optical particle counting technologies also have the ability to characterize particle shape. This is referred to as direct image particle counting (ASTM D7596). With this added information, interpretation of the source, type, and severity of the particles can be estimated [9,10].

Summary of applicable particle count standards: ISO 11171, ISO 4406, ISO 11500, ASTM D7647, ASTM D6786, FTM 3012, FTM 3010, ISO 4407, BS 3406, ISO/DIS 21018, ISO 16232-7, and ASTM D7596.

22.3.1.2 VISCOSITY

Kinematic viscosity is a measure of a fluid's internal (molecular) resistance to flow (shear) under gravitational forces. It is determined by measuring the time, in seconds, required for a fixed volume of fluid to flow a known distance by gravity through a capillary within a calibrated viscometer at a closely controlled temperature (ASTM D445 or ISO 3105). This value is converted to standard units such as centistokes (cSt) or square millimetres per second (mm^2/sec). Viscosity reporting is only relevant when the temperature at which the test was conducted is also reported (e.g., 12 cSt at 100°C).

Viscosity affects engine operation, energy losses, and the oil film thickness in bearings, cylinders, valves, cams, gearing, and other frictional zones. Therefore, its measurement and trending is critical to used engine oil analysis. Even modest changes in viscosity may adversely influence the lubricant's performance and stability, possibly causing metal-to-metal contact and accelerated wear [11]. Change in a lubricant's viscosity is also a common symptom of a host of other problems. As such, a viscosity trend excursion may be the first symptom of a far more serious problem.

The rate of viscosity change from oil oxidative degradation depends on the presence of pro-oxidation stressing agents that are in the oil. This can be sharply intensified

in internal combustion engines. These include heat, water contamination, agitation, oil pressure, acidic combustion byproducts, metal particles (metal catalysts), entrained air, and degraded remnants of previously used oil. Oil oxidation causes viscosity to increase from synthesis and polymerization. Given enough time, oxidation can transform an oil into a tar-like substance.

A change in viscosity can result from a host of other root causes such as the following [3] (Figure 22.6):

- Excessive amounts of contamination such as water, fuel, glycol, and solvents;
- Hydrolysis (from water contamination) of ester-based synthetic lubricants (some API Group V base oils);
- Volatilization of the light ends of the basestock (increases the viscosity);
- Topping up with the incorrect viscosity grade; and
- Severe mechanical shearing of the oil (lowers viscosity).

Applicable viscosity standards: ASTM D445, SAE J300, ISO 3105, ASMT D6971, ASTM D6810, ASTM D7590-09, and ISO 3448.

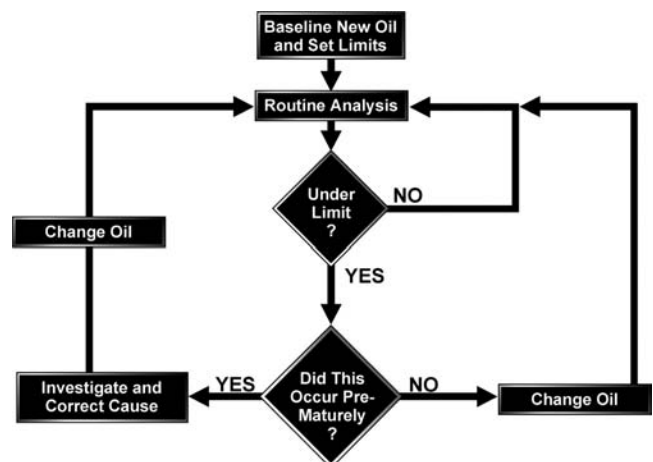


Figure 22.6—Viscosity diagnostics.

22.3.1.3 BASE NUMBER

Primarily for engine crankcase applications, the base number (BN) measures the reserve alkalinity of an oil. Engine oils are formulated with overbased additives (high alkalinity) such as calcium sulfonate, which can neutralize the acids that enter an oil from combustion blowby, base oil oxidation, and environmental contamination. Once the reserve alkalinity has depleted through normal consumption (neutralization) as the oil ages, the oil can subsequently become highly corrosive to bearings, valves, pistons, and cylinder walls as acid ingress continues.

The BN test is performed by colorimetric or potentiometric titration (usually potentiometric because of the opaqueness of used engine oil) (Figure 22.7). During the test, the alkaline oil is titrated (neutralized) with hydrochloric (HCl; preferred for used oil analysis) or perchloric acid (risk of false positives on alkalinity). Results are reported in milligrams of potassium hydroxide (KOH) per gram of oil. The result is actually a derived value that represents the volume of KOH that is required to neutralize the volume of BN reagent acid (HCl) that is required to neutralize the reserve alkalinity of the sample being tested. In this way, the units are balanced, (i.e., 1 unit of BN neutralizes 1 unit of acid number [AN]).

BN numbers trend steadily downward as the oil's reserve alkalinity is depleted by the progressive neutralization of acids from combustion and base oil oxidative. A rapid change in BN may be caused by one or more of the following [3]:

- Burning high-sulfur fuel,
- Abnormal fuel dilution,
- Poor combustion,
- Excessive blowby,
- Hot running conditions,
- Severe oxidation,
- Overextended drain interval,
- Wrong oil addition, and
- Glycol contamination.

If BN numbers change rapidly, the root cause should be determined and corrective actions should be taken.

Applicable standards: ASTM D974, ASTM D2896, ASTM D4739, and ASTM D5984-96.



Figure 22.7—Potentiometric titrometer used to determine ANs and BNs.

22.3.1.4 ACID NUMBER

This method is primarily used for non-crankcase industrial lubricants, although many laboratories will perform BN and AN tests on gasoline and diesel engine oils. AN is a measure of the acid concentration of the oil. It does not measure acid strength (like pH). AN is a titration test method, and results are expressed as the volume (milligrams) of KOH required to neutralize the acidic components in 1 g of sample oil. The reported unit is milligrams of KOH per gram of oil. AN can be quantified by colorimetric (color change) or potentiometric (electrical voltage change) titration methods (Figure 22.7). For dark-colored engine oils, the latter method should be used.

As motor oil ages, becomes contaminated with combustion blowby, or oxidizes, small amounts of organic acids begin to accumulate in the oil causing the AN to increase. These acidic constituents will initially be neutralized by the overbase detergent and other overbase formulation constituents. For diesel engine motor oils with BNs starting at 9–10, the BN will trend downward to 5–5.5 before the AN starts to rise. By the time the BN falls to 3–3.5, the AN will have risen by 1 to 1.5 (indicating increasing corrosion risk) [3].

A high AN typically indicates the oil's useful life has expired and it needs to be changed. For mineral oils and many synthetics, an AN above 4.0 is highly corrosive, risking attack of metal surfaces leading to pitting, etching, and permanent damage. Strong acids can enter an oil from external contamination sources; these include sulfuric, nitric, HCl, hydrofluoric, and phosphoric acids. Corrosive damage risk is increased in the presence of water contamination, which strengthens the corrosive potential of acids.

A slow increase in AN over a long period of use is considered normal for certain lubricants. However, once an upper limit is reached, the oil will need to be changed. Rapid change in AN may be due to one or more of the following events:

- Severe oxidation of oil,
- Depletion of overbase additives, or
- Large makeup of an incorrect oil such as antiwear hydraulic oils or gear oils that have high baseline AN values

Applicable standards: ASTM D664, ASTM D974, ASTM D1534 (transformer oils), and ASTM D3339.

22.3.1.5 FOURIER TRANSFORM INFRARED SPECTROSCOPY

Fourier transform infrared spectroscopy (FTIR) is a method that provides a rapid means to simultaneously monitor the molecular components of multiple oil parameters. In one common instrument configuration, a fixed thickness of oil (path length) is applied to the FTIR instrument's test cell through which infrared energy is passed. Numerous oil properties, additives, and contaminants absorb infrared energy at particular infrared spectral bands (similar to frequency). A fast Fourier transform is applied to create a wavelength spectrum of attenuated (absorbed and reflected) infrared energy (attenuated total reflectance [ATR] cell) or transmitted infrared energy (transmission cell).

The spectrum of the used oil is generally compared to the baseline of the new oil for analysis to identify certain contaminants (e.g., soot, water, glycol, and fuel) and certain oil degradation products (e.g., oxides, nitrates, and sulfates)

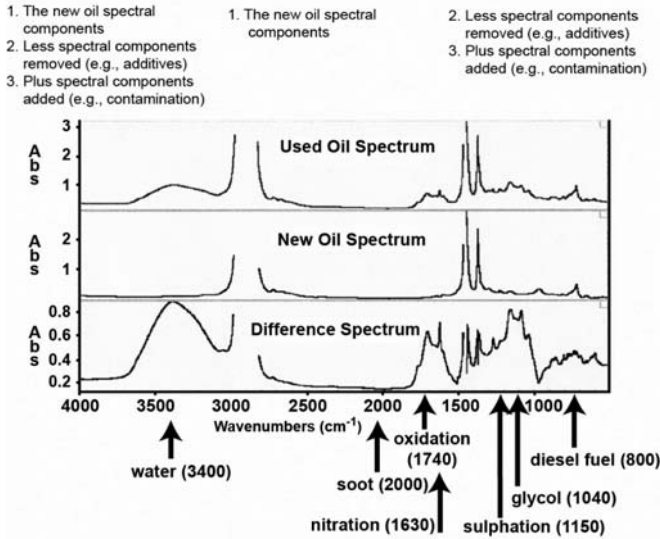
Used Oil Spectrum - New Oil Spectrum = Difference Spectrum

Figure 22.8—Spectral subtraction method for infrared spectroscopy.

and additives (e.g., zinc dialkyldithiophosphate [ZDDP] and phenols) (Figure 22.8) [3].

Infrared spectroscopy is unique in that it assesses the constituent components of the oil sample at the molecular level. This information is very useful when the existence of compounds such as additives and oxidation byproducts (which are often difficult to measure and trend by other means) are of interest.

Oil contamination by water, soot, glycol, incorrect make-up oils, and chemical solvents can all be monitored using FTIR. The analyst or instrument software looks for discrepancies in spectral features, or bands, at specific wavenumbers (WN or cm⁻¹) (Figure 22.9) [11–13]. Soot produces a broadband spectrum shift so a wavenumber where no other significant spectral activity occurs is selected for soot measurement (typically 2000 WNs). Wavenumbers refer to the number of spectral waves per centimetre of path length.

Overall lubricant health can also be monitored using FTIR. Oil degradation caused by oxidation and nitration

results in unique wavenumber-specific absorption features (e.g., centering at 1750 and 1630 cm⁻¹). A decrease in absorption at spectral bands relating to certain additives can also be observed.

Applicable standards: ASTM D7214-07a, ASTM D7412-09, ASTM D7414-09, ASTM D7415-09, ASTM D7416-09, ASTM D7418-07, and ASTM E2412-04.

22.3.1.6 FERROUS DENSITY

A significant increase in the population of large (>5 µm) ferrous particles usually suggests the presence of an abnormal wear condition and should serve as a warning of impending engine failure. Several methods are available for determining the concentration of large ferrous debris. The severity of the wearing event is generally proportional to step changes in generation rate of large particles. The ferrous density instruments report results in different measurement units established by the instruments' manufacturer. These instruments are not currently standardized, although they are widely used.

Contamination, poor lubrication, and adverse mechanical conditions are the usual causes of high ferromagnetic particles. In automotive engines as well as most other types of machinery, at least one surface in a frictional pair is typically ferrous (iron or steel), and it is usually the surface most critical to reliability. For this reason the monitoring of ferrous density in used lubricants can provide valuable engine health information and an early warning to failure. The need for ferrous density readings is further magnified by the fact that elemental analysis becomes less accurate with larger size particles (>5 µm), which is usually the critical size range in monitoring and detecting impending failure [3].

Some ferrous density instruments use powerful rare-earth magnets to separate ferromagnetic particles from all other particles. Once these particles are separated, their density or concentration can be estimated using various means (optical, particle count method, magnetic flux method, Hall effect, etc.) [14]. It should be noted that some ferrous particles are generally not magnetic. These include corrosion debris (red-iron oxide) and high-alloy stainless steel. Figure 22.10 shows the measurement units for direct reading ferrography, which is perhaps the most commonly used ferrous density instrument by commercial laboratories.

Parameter	Wavenumber (cm ⁻¹)
Oxidation:	
• Mineral oil	1750
• Organic ester	3540
• Phosphate ester	815
Sulfation	1150
Nitration	1630
Soot	2000
Water:	
• Mineral oil	3400
• Organic ester	3625
Glycol	880, 3400 1040, 1080
Fuel dilution:	
• Diesel	800
• Gasoline	750
• Jet fuel	795-815
Phenol oxidation inhibitors	3650
ZDDP antiwear/antioxidant	980

Figure 22.9—Common spectral search areas used in infrared spectroscopy.

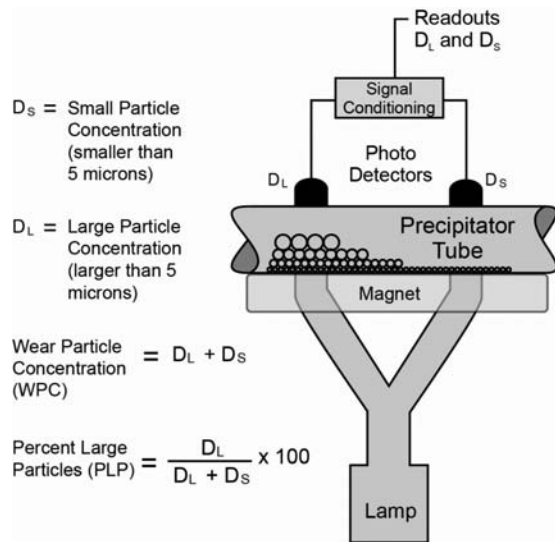


Figure 22.10—Direct reading ferrography.

An increase in the generation of ferrous particles can be brought about by several factors, including

- Load changes (e.g., hauling conditions, mountain terrain);
- Eccentric shaft loads caused by imbalance or misalignment;
- Insufficient lubrication caused by wrong lubricant, starvation, additive depletion, or lubricant degradation;
- Contamination by particles, water, air, coolant, fuel, solvents, etc.; and
- Component fatigue and wear.

The plot in Figure 22.11 shows three engines with different abnormal wear conditions as measured with direct reading ferrography [15]. The wear index is a cumulative score for the severity (large particles) and density (number of particles) of ferromagnetic wear debris.

Applicable standards: Specific to equipment supplier.

22.3.1.7 MICROSCOPIC CONTAMINANT AND WEAR PARTICLE IDENTIFICATION

When abnormal wear metals have been identified by other methods, including particle counting, elemental spectroscopy, or ferrous density analysis, a common and important

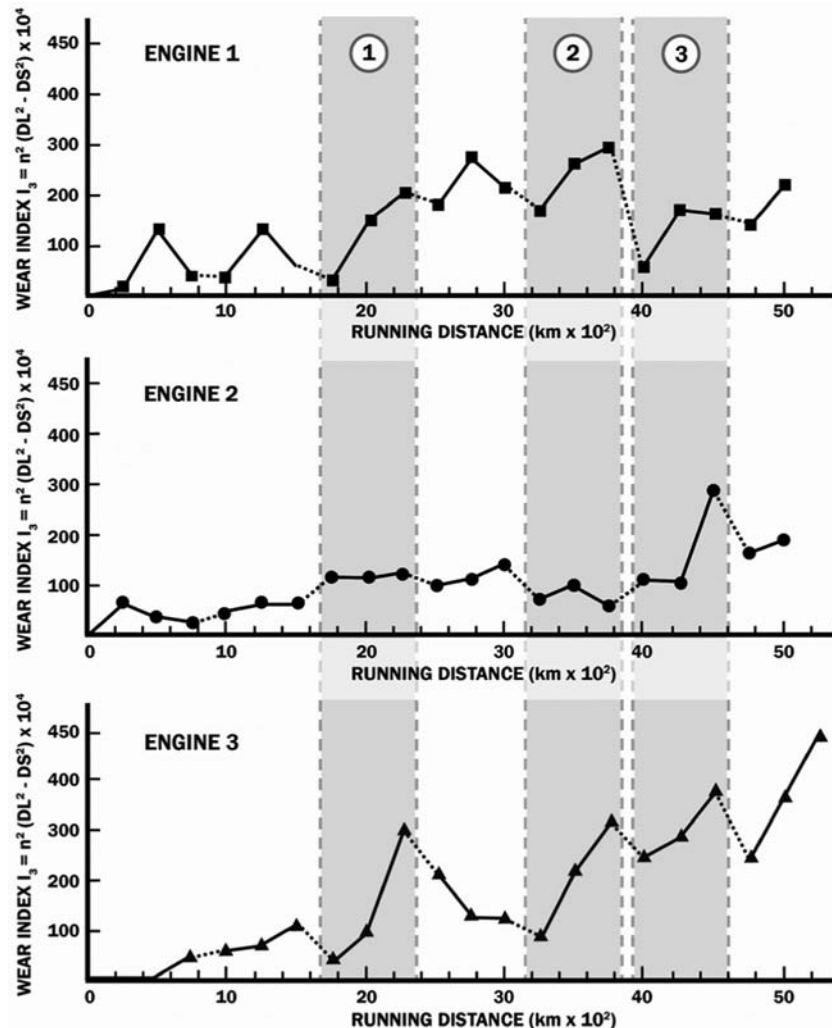


Figure 22.11—Comparison of wear index trends for three engines showing abnormal wear of the following components (1) cam and tappet wear (engine 1); (2) valve spring, piston pins, and tappets wear (engines 1 and 2); and valve spring wear (engines 1 and 3).

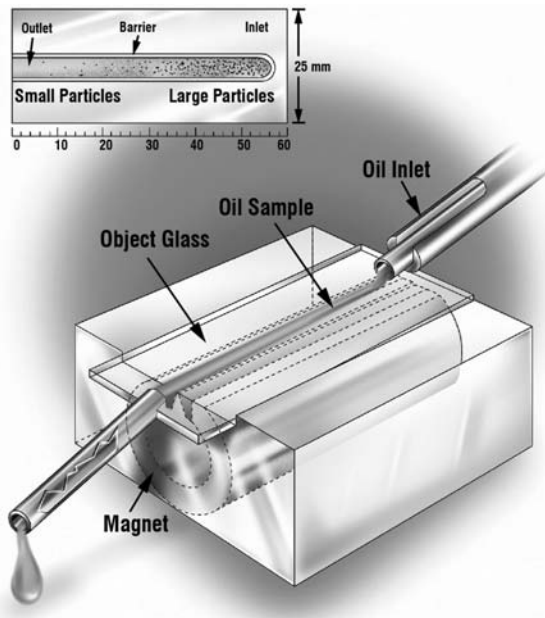


Figure 22.12—Particles are pinned down to the ferrogram by a high-gradient magnetic field.

exception test that should follow is microscopic particle examination and identification. The most common version of the procedure is referred to as analytical ferrography [14]. Analytical ferrography involves the analysis of debris deposited onto a ferrogram slide (aided by a magnet) or alternatively a filtergram membrane (Figure 22.12).

Using an optical microscope (typically bichromatic with bottom and top lighting), the particle morphology (shape), color, size, reflectivity, surface appearance, edge detail, angularity, and relative concentration provide the analyst with clues about the nature, severity, and root cause of the contaminant ingress or wear problem [14]. Scanning electron microscopy can also be used to examine particles as well as their elemental composition using an energy-dispersive spectroscopy feature. Ferrograms can be heated on a hot plate to 330°C to help reveal the composition of particles. The heat can alter the color of the particle by forming an oxide film that can help reveal its composition. The following describes how some particles change in color from heat exposure according to composition differences [15]:

- *Copper alloy (bushings)*: Yellow before and after heat treatment.
- *Aluminum alloy (piston, bearings)*: Heat treat does not affect.
- *Stainless steel*: Slight straw color when heated.
- *Lead/tin babbitt (bearings)*: White color; mottled blue, purple when heated.
- *Copper/lead babbitt (bearings)*: Yellow color; becomes yellow with blue/purple mottling when heated.
- *Low-alloy steel (connecting rod, valve springs)*: Exposed to progressive heating, light tan → straw color → blue/violet → pale blue.
- *Cast iron (cylinders, crankshaft, camshaft)*: yellow-brown.

Although largely a qualitative technique, the analyst typically reports the presence and concentration of wear particles, friction polymers, dirt and sand, fibers, and other solid contaminants on a scale of 1–10 or 1–100 to describe

the severity or concentration of the debris field. Descriptive text and photomicrographs usually accompany the enumerated values to clarify conclusions and recommend corrective measures.

It is important to determine the root cause of impending engine failure and abnormal wear problems so they can be eliminated to preclude recurrence. By combining information from analytical ferrography with other lubricant analysis and maintenance technology evaluations, the analyst attempts to answer the following questions:

- Where in the engine does the contaminant or wear debris originate?
- What is causing it?
- How severe or threatening is it (residual life)?
- Can the condition be mitigated or arrested without downtime or production loss?

Applicable standards: ASTM D7684 (patch ferrography) and ISO 16232 7&8.

22.3.1.8 Patch Test

This method is similar to the microscopic contaminant and wear particle identification previously described. Using a vacuum pump (either manual or electric), a small amount of sample is pulled through a porous membrane (typically ~5 µm) to enable suspended particles to become deposited on the membrane's surface. A solvent is used to rinse any residual oil from the surface of the membrane. Afterward, the membrane can be visually inspected for overall particle density and color. If an abnormal debris field is encountered, the membrane can be placed under a top-lit microscope for detailed analysis and characterization of the particles (Figures 22.13 and 22.14) [3].

Many analysts estimate the fluid's ISO Code (ISO 4406:99) on the basis of the overall appearance of particles, sometimes using comparator standards. One such comparator standard used in the patch analysis of aviation fuels is ASTM D2276, which is also easily adapted to lubricants. However, unlike optical particle counters, patch testing allows particle shape, color, edge detail, and organic particles to be inspected. Unlike analytical ferrography, patch testing is a relatively inexpensive screening procedure and can easily be performed in the field.

Applicable standards: ASTM D7670 and SAE ARP 4285.

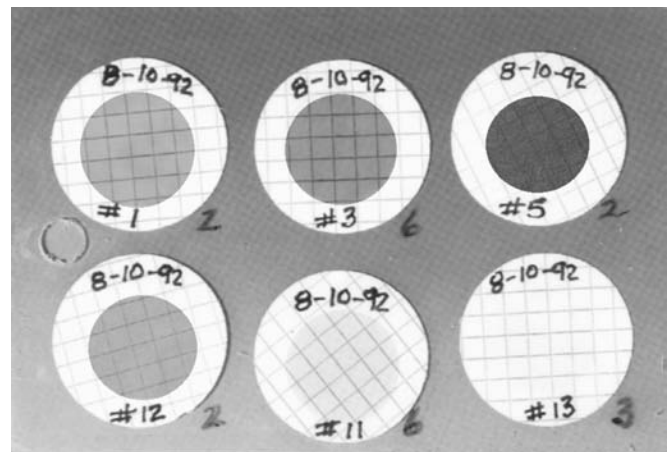


Figure 22.13—Patches of varying colors and densities.

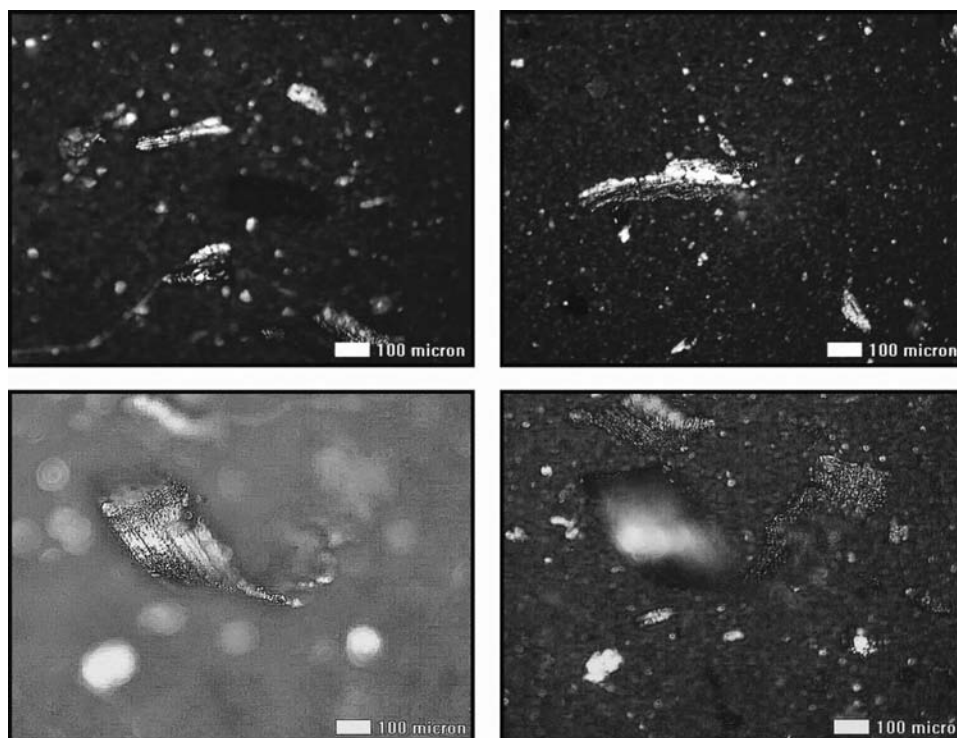


Figure 22.14—Patch images under magnification.

22.3.1.9 WATER CONTENT BY KARL FISCHER TEST

The Karl Fischer test is a titration method to measure the water concentration in oil. It is usually performed after the sample is screened with the hot plate “crackle test” or by FTIR. Karl Fischer reports water concentration in percentage or parts per million (ppm) of the “total” water (free, emulsified, and dissolved) in the oil sample.

In the volumetric test, the oil is titrated with a standard iodine-containing Fischer reagent to an electrometric end point. The accuracy of the test is affected by the presence of sulfur-containing additives such as detergents, antiwear agents, rust inhibitors, and antiscuffing agents. Many laboratories prefer the coulometric method combined with co-distillation to eliminate the risk of additive interferences [16].

Water corrodes iron and steel surfaces, accelerates corrosion, depletes and degrades additives, promotes base oil oxidation, and alters lubricant film strength. Large amounts of water form persistent emulsions in motor oils that join with insoluble oxidation products to form sludge and may significantly impair engine reliability. In addition, free water may cause the formation of hard, brittle deposits on bearing surfaces.

The following are common causes of elevated water content in engine oil:

- Oil cooler leak,
- Atmospheric condensation,
- Intermittent running conditions, and
- Cold-temperature service.

Applicable Karl Fischer standards: ASTM D1744-volumetric (withdrawn but still in active use) and ASTM D6304-98-coulometric.

22.3.1.10 ELEMENTAL SPECTROSCOPY

Elemental spectroscopy quantifies the presence of dissolved and some undissolved inorganic materials by element in

the oil. Nearly all elemental spectrometers used today for oil analysis are of the atomic emission type. One such instrument works by exposing the sample to extreme temperatures generated by arcing electrodes commonly referred to as rotating disc electrodes (RDEs).

Another common method uses an argon plasma torch to vaporize the sample. This is known as an inductively coupled plasma (ICP) spectrometer. The extreme heat excites the atoms in the sample causing them to emit energy in the form of light. Atomic elements emit light at specific frequencies. The spectrometer quantifies the amount of light generated at these frequencies to estimate the concentration of each element (iron, lead, tin, etc.) in parts per million by weight.

Atomic emission spectroscopy is particle-size limited. Dissolved metals and suspended particles up to approximately 2 μm are detected with high accuracy. The accuracy diminishes (lower recovery) as particle size increases up to 5 μm . Elemental concentrations can be greatly understated for particles larger than 5 μm .

Increasing or decreasing elemental concentration can signal a change in the generation of wear debris, the ingress of contaminants, and the addition or depletion of additives. The table in Figure 22.15 generally categorizes the common elements observed with oil analysis as wear, contamination, or additives.

The following should be considered when diagnosing nonconforming elemental data [3,11]:

- An increase in the concentration of elements such as iron, copper, chromium, tin, aluminum, and lead suggests that abnormal wear is occurring. Further steps should include analysis of the debris with complementary testing to determine its severity, nature, origin, and root cause.
- Increasing concentrations of silicon, sodium, boron, calcium, and magnesium can signal the ingress of

Element	Wear	Contamination	Additive
Iron (Fe)	X	X	
Copper (Cu)	X	X	X
Chromium (Cr)	X		
Tin (Sn)	X		
Aluminum (Al)	X	X	
Lead (Pb)	X		
Silicon (Si)		X	X
Sodium (Na)		X	X
Boron (B)		X	X
Calcium (Ca)		X	X
Magnesium (Mg)		X	X
Zinc (Zn)	X		
Phosphorous (P)		X	X
Molybdenum (Mo)			X
Potassium (K)		X	

Figure 22.15—Common elements and their sources.

contamination. A lock-step increase in silicon and aluminum typically suggests dirt ingress, although silicon is also the primary element found in antifoaming additives (silicone), which can cause confusing results. Increasing levels of sodium and boron may signal the ingestion of glycol-based coolant. Calcium and magnesium are often present when hard water is ingested (e.g., from cooling system leaks), but they are also common elements found in engine oil additives.

- Numerous elements are used in a multitude of additives. For example, zinc and phosphorous are common in antiwear additives; sulfur, phosphorous, and molybdenum are common components of extreme pressure (e.g., from a differential lubricant) and friction modifier additives; and calcium and magnesium are frequent components of engine oil alkalinity improvers. Knowledge of the new oil baseline is critical to trending additive depletion with elemental spectroscopy.

Applicable standards: ASTM D4951 (ICP, additives); ASTM D5185 (ICP, additives, wear metals, and contaminants); ASTM D6595 (RDE, additives, wear metals, and contaminants) and ASTM D7303-06 (metals in grease by ICP).

22.3.1.11 FLASH POINT TEST AND FUEL DILUTION INSTRUMENTS

The flash point, when used to analyze used oils, can identify the presence of volatile molecules from fuel and other

flammable contaminants. A lubricant's flash point is the lowest temperature at which an ignition source (small flame) applied to the oil's surface causes the vapors of the lubricant to ignite under specified conditions. The oil is said to have "flashed" when a blue flame appears and instantaneously propagates over the oil's entire surface. The oil flashes because a flammable mixture results when it is heated sufficiently, causing vapors to emerge and mix with oxygen in the air. The flash point temperature of an oil corresponds roughly to a vapor pressure of 3–5 mm Hg. Figure 22.16 shows the contaminants and other influencing conditions that can alter the flash point in used oils.

Many laboratories simply test up to a specified temperature (e.g., 20°C below the oil's normal flash point). If the oil flashes at this lower temperature it can be reliably assumed that it has been diluted with fuel or other low-boiling point flammable liquid. This pass/fail use of the flash point test reduces the time to perform the test as well as its cost. Those oils that fail can then be analyzed further to determine the specific flash point to estimate the total contaminant level (e.g., fuel contamination) [17].

This test is commonly used with engine oils (diesel, gasoline, and natural gas) and occasionally with natural gas compressor lubricants to detect excessive gas solubility. The closed-cup flash point test is the most widely used method for fuel dilution testing because of its sensitivity to low concentrations of fuel. Fuel or chemical dilution severely impairs the lubricant's effectiveness and can cause fire or explosion hazard [17].

	Decreases Flash Point	Increases Flash Point
Changes in oil chemistry	<ul style="list-style-type: none"> • Thermal cracking • Radiation (cracking by γ rays) • Microdieseling 	<ul style="list-style-type: none"> • Polymerization
Additions to the oil	<ul style="list-style-type: none"> • Diesel fuel • Gasoline • Natural gas • Solvents • Wrong make-up oil • Water (instrument interference) 	<ul style="list-style-type: none"> • Water • Coal dust • Glycol/antifreeze • Wrong make-up oil
Subtractions from the oil		<ul style="list-style-type: none"> • Thermal evaporation (boiling point off of light ends) • Vacuum dehydration

Figure 22.16—Contaminants and factors that influence flash point.

Applicable flash point standards: ASTM D92 (Cleveland open cup), ASTM D93 (Pensky-Marten closed cup), and ASTM D3828-97 (small-scale closed cup).

22.3.1.12 OTHER USED OIL ANALYSIS TESTS

The previously described tests represent the core analytical methods used in the analysis of in-service lubricating oils. There are many instruments and methods that are emerging onto the market that show considerable promise. Likewise, there are others that serve niche applications and still others that are slowly being phased out to make room for new technology. It is not possible to discuss all of these technologies and analytical methods. However, there are a few that fall outside of the mainstream that, for various reasons, are worth noting.

22.3.1.12.1 Optical Soot Meters

Whereas some laboratories commonly use infrared spectroscopy to estimate the percentage soot in engine oil (described previously), other laboratories prefer to use single-channel optical devices (either white light or infrared) to quantify the amount of nontransmitted light through a fixed path length or they use an ATR cell. The nontransmitted light fraction is defined as the soot load of the oil and is often reported as percentage soot. This is a nonstandardized test method.

22.3.1.12.2 Blotter Spot Testing

This simple test, also known as paper chromatography or radial planar chromatography, is used to examine soft insoluble suspensions in oil using blotter paper to which a small aliquot of sample is applied. Varnish and sludge-producing impurities will form distinct deposits and rings on the blotter paper as the oil wicks outward in a radial direction by capillary action. These impurities include carbon insolubles, oxide insolubles, additive degradation products, and glycol contamination. This is a good field and laboratory test and is nonstandardized.

22.3.1.12.3 Glycol Reagent Method

The Schiff's reagent method (ASTM D2982) is a colorimetric method for detecting trace amounts of glycol in lubricating oils. In this method, a solution of HCl and periodic acid is introduced to the oil to oxidize any glycol that may be present. The reaction produces an aldehyde, which in turn reacts with the Schiff's reagent, yielding a positive color change from colorless to pink/purple—the darker the color, the more glycol present.

22.3.1.12.4 Crackle Test

The crackle test is a noninstrument method of determining the presence of water in oil, and in some instances, estimating its concentration. The usual procedure is to place a couple drops of oil on the surface of a hot plate (320°F) and then visually examine the response of the oil to the heat. Oil with no free or emulsified water will become thin and spread because of the heat. Free and emulsified water will result in vapor bubbles and scintillation (crackling sound). With practice, the concentration of water can be estimated when compared to known levels of water. This is a nonstandardized method.

22.3.1.12.5 Fuel Dilution Meter

One other instrument of note is the fuel dilution meter that uses surface acoustic wave technology to detect and quantify fuel contamination in motor oil. It samples the "head space" in a bottle of oil on the basis of Henry's law to assess fuel vapor concentration. Fuel vapor concentration correlates to fuel dilution in the oil. This is a nonstandardized method.

22.4 SETTING LIMITS AND TARGETS

Oil analysis alarms serve as a "trip-wire" to tell the analyst that a threshold has been passed and that action is required. Some data parameters have only upper limits, such as particle counts or wear debris levels. A few data parameters use lower limits, such as BN, additive elements, flash point, oxidation stability, and FTIR (additive). Other data parameters such as viscosity and FTIR use upper and lower limits. These generally relate to important chemical and physical properties of the lubricant in which stability of these properties is desired.

Alarming techniques vary to fulfill the requirements of different oil analysis objectives. These techniques can be generally categorized as proactive and predictive alarms.

22.4.1 Proactive Alarms

Proactive alarms alert the user to abnormal conditions associated with root causes of engine wear, operating faults, and lubricant degradation. They are keyed to the proactive maintenance philosophy of setting targets and stabilizing lubricant conditions within those targets. A strategic premise of proactive alarms is that they be set to levels that will generate improvement over past performance (e.g., cleaner, dryer, etc.) or ensure that conditions are maintained to within levels that have previously been optimized relative to organizational objectives. Within the proactive domain, the following types of alarms and limits are used:

- *Goal-based targets:* Goal-based targets are used to reduce stress (e.g., contamination) on the oil and engine to extend service life (Figure 22.17).
- *Aging limits:* Aging limits alert car owners to the approaching end of the service life of the oil or engine component (Figure 22.18).

22.4.2 Predictive Alarms

Predictive alarms signal the presence of abnormal engine conditions or the onset of wear and failure. They are aligned with the goals of predictive maintenance (i.e., the early

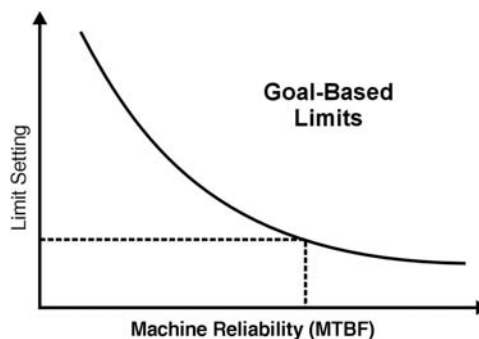


Figure 22.17—Goal-based limits are used on the oil and engine to extend service life.

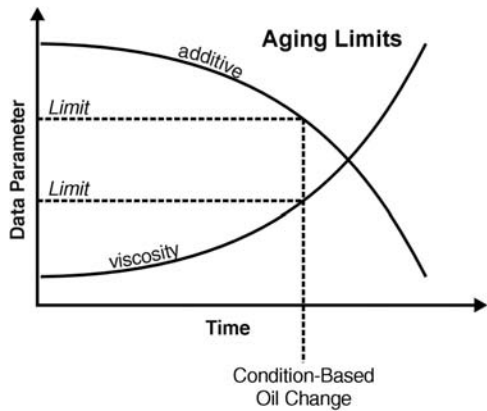


Figure 22.18—Aging limits alert to the approaching end of the service life of the oil or engine.

detection of engine failure symptoms as opposed to failure root causes [proactive maintenance]). Within the predictive domain, the following oil analysis alarming techniques can be used:

- **Rate-of-change-based alarms:** Rate of change alarms are typically set to measure properties that are being progressively introduced into the oil, such as wear debris (Figure 22.19). The add rate (change) can be calculated per unit of time, hours, cycles, etc. For example, a 100-ppm increase in iron over a period of 100 operating hours could be stated as 1 ppm/h operation. Rate-of-change limits are effectively applied to particle counting, elemental wear metals, ferrous density, and BN. It can also be effectively applied to monitor abnormal degradation of additives using elemental analysis, linear sweep voltammetry, and FTIR spectroscopy.
- **Statistical alarms:** This practice requires the availability of a sufficient quantity of historical data for the particular type of engine and type of service. A population mean and associated standard deviation are generated from the available data. The data from a sample of used oil are compared to the mean of the population. If the value falls within 1 standard deviation of the mean, then it is considered normal. If it falls outside of 1 standard deviation from the mean, but within 2 standard deviations, then it is considered a caution. If the result

exceeds 2 standard deviations, the value is considered in critical alarm.

22.5 INTERPRETING AND APPLYING OIL ANALYSIS RESULTS

Interpreting oil analysis data requires an understanding of the specific oil analysis tests and an understanding of how these tests interrelate when oil and engine conditions change. Reference the table in Figure 22.20 during the discussion of the primary and secondary oil analysis indications for typical abnormal conditions.

22.5.1 Solid Particle Contamination

An alarm on particle contamination signals an increase in suspended particles due to such occurrences as the failure of the lube oil filter, abnormal ingestion of contaminants from the engine air induction system, contaminated new oil, or an increase in the internal generation of wear debris.

- **Primary test:**
 - **Particle count:** Use suitable automatic particle counting or microscopic particle counting methods. Report ISO code, or particle count (at different sizes in micrometres), or both.

Oil Analysis Tests	Lube/Machine Conditions											
	Particle Contamination	Wear Debris Detection	Wear Debris Analysis	Abnormal Viscosity	Moisture Contamination	Additive Depletion	Oxidation Stability	Glycol Contamination	Fuel Dilution	Soot Load	Alkalinity Reserve	Wrong Oil
Particle Count	P	S	S									
Viscosity				P	S		S	S	S	S		P
AN/BN				S		S	P				P	S
FTIR Spectroscopy				S	P	P	P	S	P	P		P
Ferrous Density		P	S									
Analytical Ferrography	S		P									
RPVOT							P				S	
Moisture Tester					P							S
Elemental Spectroscopy	S	P	P		S	P		P	S		P	S
Flash Point Test				S				P			S	P

Figure 22.20—Table of commonly used primary and secondary (confirming) oil analysis indicators.

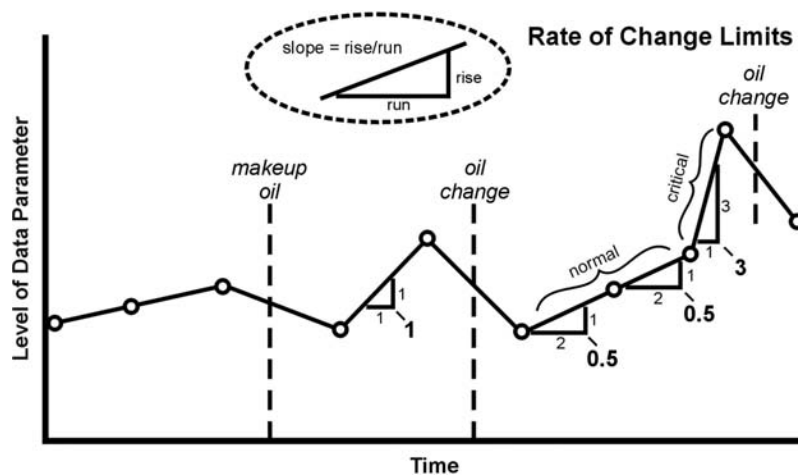


Figure 22.19—Trend-line slope is a visual indication of rate-of-change and parameter severity.

- *Secondary tests:*
 - *Elemental spectroscopy:* Often, when a particle count increases the elemental levels of the particles present increase. For dirt contaminated oil, silicon and aluminum typically increase. Likewise, wear metal elements may increase depending upon the metallurgy of the failing components.
 - *Wear particle identification:* Although expensive and time-consuming, examining individual particles onto a slide or membrane and viewing them under a microscope will reveal an increase in particle count and information on the particle source. Quantification of the particulate is limited with this technique.

22.5.2 Wear Debris Detection

When engines are operating abnormally because of lubrication failure, contamination, corrosive conditions, thermal distress, etc., a message is sent into the oil in the form of wear debris.

- *Primary tests:*
 - *Ferrous density:* Measuring an increase in the production of ferrous debris is a good indication of abnormal wear because so many engine components and frictional surfaces are constructed of steel or iron. These tests are biased against nonmagnetic wear debris generated from brass, bronze, aluminum, lead, tin, and stainless steel surfaces.
 - *Elemental analysis:* A rise in the level of elemental metals is an indication of the presence of an abnormal engine condition. By comparing results to component metallurgy records, the abnormal condition can often be qualified.
- *Secondary test:*
 - *Particle count:* Any wear that is generated will result in an increase in particle count. However, particle count reports no differentiation between ingested debris such as dirt and generated wear particles.

22.5.3 Wear Debris Analysis

When an abnormal wearing condition is encountered, it can be analyzed to provide an indication of the nature, severity, and root cause of the problem. This requires an investigation of the wear particles themselves along with a review of collateral information such as engine acoustics, exhaust smoke color, computer diagnostics, operational information, etc.

- *Primary tests:*
 - *Analytical ferrography:* This microscopic technique provides an abundance of information about the wear debris and the wearing event. By evaluating particle size, dimension, shape, and appearance, the analyst can often determine what wear mechanism generated the debris. By manipulating the particles with light, heat, and chemicals, the metallurgy of the particles can often be defined.
 - *Elemental spectroscopy:* When engine component metallurgy is known, elemental spectroscopy proves invaluable for localizing wearing components.
- *Secondary tests:*
 - *Ferrous density:* Trending an increase in the rate at which ferrous particles are generated provides

important information about the severity of a failure event. Also, some ferrous density testers provide large and small ferrous particle differentiation. A rising “percentage large particles” reading (from direct reading ferrography) suggests increased severity. These devices are biased toward magnetic particles.

- *Particle count:* The rate at which particle count increases is indicative of the severity of the problem. Also, most particle counters sort the particles by size range. An increasing generation of large particles suggests high urgency. Particle counters lack the ability to differentiate particles by type (dirt or wear).

22.5.4 Abnormal Viscosity

Viscosity can increase for several reasons. Oxidation, thermal failure, water/glycol contamination, soot loading, and wrong oil are the most common reasons. Fuel dilution, viscosity index improver (additive) shear-down, and base oil cracking all reduce viscosity.

- *Primary test:*
 - *Viscosity:* Viscosity is the “catch all” test for several abnormal lubricant or contaminant conditions. Changes in viscosity are often an early indicator of other problems that involve the need for an expanded scope of analysis.
- *Secondary tests:*
 - *AN:* If the increase in viscosity is associated with oxidative failure, the AN will typically increase. AN sometimes increases or decreases when the wrong oil (and wrong viscosity) has been added to the sump because of the influence of the additive package on the AN.
 - *FTIR spectroscopy:* When viscosity changes because of thermal failure, oxidation, fuel dilution, or glycol contamination, the FTIR spectrum tends to change at certain bands. If the wrong or mixed oil is being used, numerous spectral features will also tend to change.
 - *Flash point test:* When the oil has been contaminated with fuel or solvents, the flash point will drop.

22.5.5 Moisture Contamination

Moisture in all of its forms brings nothing but trouble to the lubricant and engine. It rusts iron and steel surfaces, promotes corrosion on other metal surfaces, and over time can destroy the lubricant. Moisture can enter the oil from many places, including coolant leaks and combustion blowby. It is common for moisture generated by engine combustion to condense in the crankcase because of wintertime and short-distance driving conditions.

- *Primary tests:*
 - *Moisture tester:* Water can be screened to approximately 500–1000 ppm with the crackle test depending on the exact procedure used and the type of oil. Quantification of the moisture content (if required) is best accomplished using the standard Karl Fischer titration procedure.
 - *FTIR spectroscopy:* FTIR serves as an effective screen for moisture above approximately 1000 ppm for mineral oils, depending on the instrument’s signal-to-noise ratio. FTIR will also signal the

presence of glycol if leakage is from a cooler that uses glycol-based antifreeze.

- **Secondary tests:**

- **Viscosity:** When high levels of water contaminate oil, an emulsion is often formed. The viscosity, as measured by traditional viscometers, will increase under these conditions.
- **Elemental spectroscopy:** Often, metals accompany the ingested water. For example, hard water brings calcium. Salt water brings sodium. Water and glycol (coolant) bring sodium, boron, and potassium depending on the corrosion inhibitors used in the antifreeze. The source of the water can often be localized by examining the relative concentration of these trace metals.

22.5.6 Additive Depletion

Additives are among the most difficult parameters to measure using oil analysis. The additives exist as organic, inorganic, or organometallic compounds that improve base oil performance. Often, it is easier to assess the performance characteristic than the additive itself. Still it is possible to estimate the RUL of certain additives using conventional oil analysis techniques. New technologies have greatly expanded this capability.

- **Primary tests:**

- **Elemental spectroscopy:** Many additives are organometallic compounds using zinc, phosphorous, magnesium, calcium, silicon, etc. These levels can be effectively assessed using elemental spectroscopy. The technique has two primary limitations:
 1. Additives can be decomposed and their constituent elements transformed into other molecules with no visible change in elemental concentration. These are often referred to as dead additives or additive floc; their mass still exists in the oil but they are no longer functional. For certain additives, a loss of elemental concentration of just 25 % is enough to merit concern for the remaining 75 % additive mass (that may be dead). Some additives lose mass by precipitation (drop out), water washing, particle scrubbing, filtration, etc.

2. Many additives have elements similar to wear metals and contaminants. For example, dirt and some antifoaming agents appear on the oil analysis report as silicon.

- **FTIR spectroscopy:** FTIR spectroscopy can to a certain extent measure the presence of active additive molecules, including organic molecules (see Figure 22.21) [18]. It is limited by (1) its poor ability to quantify additives in low concentrations and (2) interferences that might occur.
- **BN:** The oil's reserve alkalinity (detergent additive) is measured using the BN test. As BN declines, the oils' ability to counteract the ingress of combustion acids is weakened. A loss of BN signals the need for an oil change or make-up oil.
- **Blotter spot test:** The blotter spot test is extremely effective at assessing the condition of motor oil dispersancy.

22.5.7 Oxidation Stability

Oxidation stability is an indication of the oil's residual ability to resist oxidation. Some oil analysis tests measure the byproducts of oxidation whereas others attempt to measure the oil's ability to resist oxidation. Figure 22.22 plots the pre- and postoxidation physical and chemical oil properties that can be monitored by routine oil analysis [19].

- **Primary tests:**

- **AN:** As an oil oxidizes, organic acids (formic, carboxylic, etc.) are produced. Measuring the concentration of these acids is a measure of oxidative damage that has occurred. Not all acids found in oil relate to oxidation.
- **FTIR spectroscopy:** During oxidation, the oil's base molecules (hydrocarbon) are turned into ketones, aldehydes, carboxylates, and other transition molecules. Many of these new molecules have ester functional groups and can be measured with FTIR spectroscopy.

- **Secondary tests:**

- **Viscosity:** As the oil oxidizes, its viscosity typically increases. As such, viscosity trending is not a good forecasting technique for oxidation stability but is rather a positive indication of the onset of oxidation.

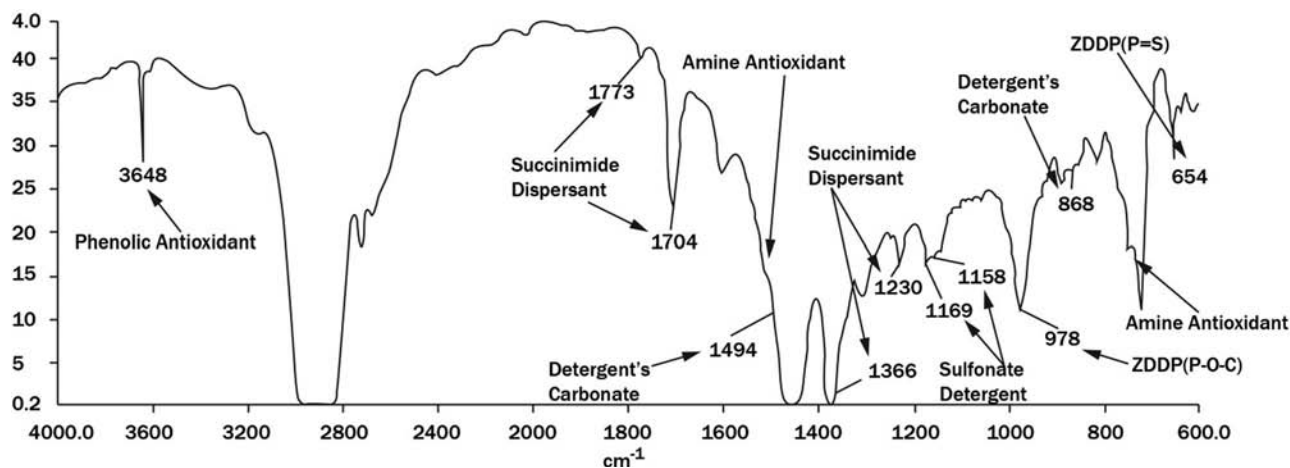


Figure 22.21—FTIR spectrum showing spectral bands of common motor oil additives.

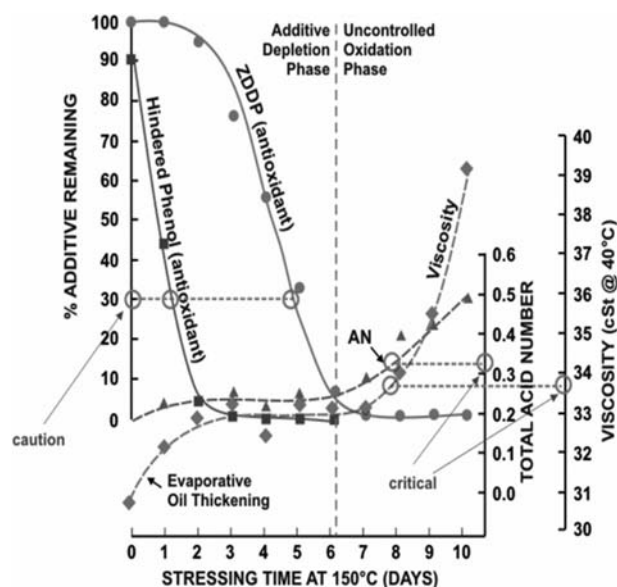


Figure 22.22—Oil analysis properties that characterize pre- and postoxidation physical and chemical oil properties [19].

22.5.8 Glycol Contamination

Glycol (antifreeze) enters lubricating oils from the cooler. Leakage from corrosion, seal failure, cooler core damage, and cavitation are the most common causes of glycol contamination. Glycol is extremely harmful to (1) the lubricant base oil (promotes oxidation and deposit formation), (2) additives (additive reactions forms abrasive oil balls), (3) filtration (plugs pores prematurely), and (4) the engine (corrosion, wear, etc.).

- **Primary tests:**
 - **Elemental spectroscopy:** Most commercial anti-freeze formulations include corrosion inhibitors that contain sodium, boron, or potassium, or a combination of these, among other elements. The inhibitors transfer into the oil with coolant (glycol) contamination. As such, they can be detected elementally by trending boron, sodium, or potassium, or a combination of these. The presence of these elements effectively serves as “markers” in detecting and quantifying glycol contamination.
- **Secondary tests:**
 - **Viscosity:** When a significant amount of glycol is present in used oil there will typically be an increase in oil viscosity. Therefore, an increase in oil viscosity should be investigated as possible antifreeze contamination.
 - **Water testers:** While not all coolant leaks result in the prolonged presence of water in the crankcase oil (water boils off quickly at normal engine running temperatures) some amount of water is not uncommon.
 - **Schiff's reagent method:** This is a colorimetric procedure used in the field and in the laboratory. If there is antifreeze in the oil there will be a distinctive color produced by the chemical change of the glycol-contaminated oil when mixed with the Schiff's reagent. Often glycol transforms rapidly into other chemicals after it contacts the oil. This condition frequently results in a false negative from this test.

- **Blotter spot test:** By placing a couple drops of oil on common blotter paper or card stock a qualitative assessment of glycol contamination can be obtained.

22.5.9 Fuel Dilution

Fuel typically gets into the crankcase as an incomplete combustion byproduct (blowby) or by leakage. Either way, the influence of the fuel on lubrication can be substantial. For instance, just 10 % fuel dilution can be enough to reduce an SAE 30 viscosity to an SAE 20. The reduced oil viscosity can alter critical oil film thickness in engine components. Additionally, the fuel dilutes additive concentrations. If excessive fuel levels are measured (>3 %); the source of the fuel needs to be determined and remedied.

- **Primary tests:**
 - **Flash point testing:** When a lubricant is properly baselined, a sudden drop in flash point is a positive indication of fuel dilution.
 - **FTIR spectroscopy:** There are specific search areas in the infrared spectra that can be used to assess the presence of gasoline and diesel in lubricants.
 - **Fuel dilution meter:** This instrument uses a head-space sampler to measure fuel vapor. This correlates well with fuel dilution using Henry's law.
- **Secondary tests:**
 - **Viscosity:** Fuel contamination of crankcase oils sharply influences the blended viscosity. Fuel that enters the crankcase through the combustion chamber (blowby) may only consist of the heavier molecules (i.e., reducing the resultant viscosity effect). However, raw fuel from leakage will sharply lower viscosity and oil film thickness.

22.5.10 Soot and Lost Dispersancy

Soot enters crankcase oil from combustion blowby. Excessive amounts occur when oil drains are overextended, air cleaners are plugged, rings/liners are worn, or overfueling conditions occur, or any combination of these. As soot builds in the oil, the performance of the oil can degrade to eventually impair lubrication and result in the formation of sludge and deposits. Soot load and the quality of soot dispersancy (influenced by additives) affect the timing of a condition-based oil change for crankcase lubricants. Dispersancy is considered impaired when soot particles coagulate, forming carbon suspensions larger than 1 μm . Depending on the grade of oil and engine type, soot concentrations in the range of 2–5 % are typically flagged as abnormal.

- **Primary tests:**
 - **FTIR spectroscopy:** Infrared provides a reliable, time-efficient test for soot load. However, it does not evaluate the quality of dispersancy. Because soot absorbs infrared energy across the full spectrum, its concentration is quantified by the resulting baseline shift (spectral shift). It is typically presented as percentage soot or percentage transmittance (for infrared).
 - **Optical soot meters:** These can provide a quick and reliable determination of soot concentration.
- **Secondary tests:**
 - **Viscosity:** Viscosity will generally increase somewhat with increasing concentrations of soot. There is

even a sharper effect on viscosity when dispersancy is lost.

- *Blotter spot test:* In addition to soot load, the appearance of well-defined annular structure (rings, halos, dark center spot, etc.) points to loss of dispersancy.

22.5.11 Alkalinity Reserve

Monitoring and controlling the reserve alkalinity of crankcase oils is key to any extended, condition-based oil drain strategy. Certain fuels (e.g., high in sulfur) and operating conditions (cold climates, short trips, etc.) contribute to loss of alkalinity reserve. High blowby from worn engines can also lead to corrosive conditions.

- *Primary test:*
 - *BN:* This particular test has been performed for many years to assess alkalinity reserve by oil laboratories. The preferred procedure is ASTM D4739 or ASTM D5984-96. Typically, crankcase oils are scheduled for change when BN drops to 50 % of the original, new-oil BN. BN results less than 2 are considered critical (corrosive).

REFERENCES

- [1] Fitch, J.C., 2000, "Sampling Methods for Used Oil Analysis," *Lubric. Eng.*, pp. 40–47.
- [2] Fitch, J.C., 1998, "Elements of a Successful Oil Analysis Program—Part I Oil Sampling," *Lubric. Eng.*, pp. 33–36.
- [3] Fitch, J.C., and Troyer, D., 2010. *Oil Analysis Basics* (2nd ed.), Noria Corporation, Tulsa, OK.
- [4] Fitch, E.C., 1988, *Fluid Contamination Control*. FES, Inc., Stillwater, OK.
- [5] Fitch, J.C., 1999, "The Influence of Bottle Cleanliness and Sample Agitation on Particle Count Trends," *Practicing Oil Analysis Magazine*, March.
- [6] Sommer, H.T., 1999, "Advancements in Oil Condition Monitoring," Paper presented at the Practicing Oil Analysis Conference, Tulsa, OK, October 26–27.
- [7] Fitch, J.C., 1986, *Theory, Design, and Performance Characteristics of a Direct-Reading Portable Solid Contaminant Analyzer*, SAE Paper 860738, SAE, Warrendale, PA.
- [8] Fitch, J.C., 2005, "The Agony of Diesel Engine Oil Particle Counts," *Practicing Oil Analysis Magazine*, March.
- [9] Barraclough, T.G., and Walsh, D.P., *Establishing Wear Particle Limits Using the Theory of Dynamic Equilibrium Together with the LaserNet Fines Q200 to Predict when Abnormal Wear Modes Are Taking Place in Machinery*, Spectro, Inc., Littleton, MA.
- [10] Reintjes, J., Tucker, J.E., Thomas, S.E., Schultz, A.V., Tankersley, L.L., Lu, C., Howard, P.L., Sebok, T., and Holloway, C., 2001, "The Application of LaserNet Fines for the Detection of Mechanical Wear and Hydraulic Contamination for CBM Systems." Paper presented at the ASNE Fleet Maintenance Symposium, San Diego, CA, August 28–30.
- [11] Fitch, J.C., 1996, "Elements of an Oil Analysis Program." In *STLE/CRC Tribology Data Handbook*, E.R. Booser, Ed., CRC Press, Boca Raton, FL.
- [12] Fox, M.F., 2006, "The Degradation of Lubricants in Service Use." In *Handbook of Lubrication and Tribology. Volume 1: Application and Maintenance*, G. Totten, Ed., CRC Press, Boca Raton, FL.
- [13] Fitch, J.C., and Barnes, M., 2003, "Hydrocarbon Analysis." In *ASTM Fuels and Lubricants Manual*, G. Totten, Ed., ASTM International, West Conshohocken, PA.
- [14] Anderson, D.P., 1982, *Wear Particle Atlas (Revised)*. Report Prepared for Advanced Technology Office, Naval Air Engineering Center, NJ, 1982.
- [15] Belmondo, A., Giuggioli, F., and Giorgi, B., 1983, "Optimization of Ferrographic Oil Analysis for Diesel Engine Wear Monitoring," *Wear*, Vol. 90, pp. 49–61.
- [16] Gebarin, S., 2004, "A Closer Look at Karl Fischer," *Practicing Oil Analysis Magazine*, March.
- [17] Fitch, J.C., 2000, "The Enduring Flash Point Test," *Practicing Oil Analysis Magazine*, March.
- [18] Wooton, D., 2003, "Trending Additive Depletion," Paper presented at the Lubrication Excellence Conference, Nashville, TN, March 23–25.
- [19] Kauffman, R.E., 1995, "Remaining Useful Life Measurements of Diesel Engine Oils, Automotive Engine Oils, Hydraulic Fluids, and Greases Using Cyclic Voltammetric Methods," *J. Soc. Tribologists Lubric. Eng.*, Vol. 51, pp. 223–229.

Diesel Fuel Lubrication and Testing

Jun Qu¹

23.1 INTRODUCTION

Diesel engine fuel pump and fuel injection system components rely for lubrication on the fuels that are generally not good lubricants. Diesel fuels have low viscosities and are composed almost entirely of nonpolar hydrocarbons with intrinsically poor boundary lubricating properties. To achieve relatively complete combustion to reduce exhaust emissions, fuel injection pressures in diesel engines of recent manufacture are becoming very high (~200 MPa) to achieve fine atomization of the fuel. The tolerances between the plungers and the bores in fuel injectors (e.g., Figure 23.1) must be extremely tight, typically 2–4 μm , to seal the pressure between the top and bottom ends [1]. The combination of the low fuel lubricity and tight geometric clearance makes the diesel fuel injector operate at boundary lubrication and vulnerable to scuffing damage that would cause the injector plunger to stick or seize, leading to an engine failure.

The fuel lubricity problems have historically occurred when a more refined fuel was introduced. This issue started to draw attention in the 1960s when a series of aviation engines failed because of fuel pump problems. These included pump failures caused by excessive bore wear, seizure of pistons, the hang-up of fuel control valves, and gear scuffing. One principal reason was found to be the substantial reduction in fuel lubricity caused by hydrotreatment (HT) of aviation kerosine, a refinement process that was introduced in the preceding years to enhance fuel stability. Interest in fuel lubricity was regained in the late 1980s and early 1990s as a result of diesel fuel delivery system failures experienced in Sweden and Canada. Driven by environmental concerns about the toxic and harmful emissions from diesel engines, these countries introduced low-sulfur fuels. Many failures were characterized by adhesive sliding wear due to inadequate fuel lubricity. These two practical problems were eventually overcome by a combination of changes to pump design and by the widespread addition of boundary lubricating additives to enhance their depleted natural lubricity due to refinement.

Diesel engine emissions have been significantly reduced in the last 20 years. This has come with the combination of using “cleaner” diesel fuels and improvements to the fuel system, including the fuel injector hardware, the use of electronic actuation, and the improved combustion chamber design. The lubricity of current diesel fuels would be acceptable if the more stringent limit of sulfur content were not introduced recently. In 2000, the U.S. Environmental Protection Agency released the Highway Diesel Rule (updated in October 2006) [2]. Beginning in September 2006, EPA required a 97 % reduction in the

sulfur content of highway diesel fuel from its current level of 500 ppm (low-sulfur diesel, or LSD) to 15 ppm (ultralow sulfur diesel, or ULSD). The detailed specifications for diesel fuels can be found in ASTM D975 [3]. The European Union applied the Euro IV standard in 2005, which specifies a 50-ppm maximum quantity of sulfur in diesel fuel for most highway vehicles, and enforced the maximum sulfur content down to 10 ppm from December 31, 2008 upon the entry of the Euro V fuel standard [4].

In general, low-sulfur fuels have exhibited deteriorated fuel lubricity [5–8]. However, research has revealed that it was not the reduction of sulfur that degrades the fuel lubricity but the loss of the polar oxygenated compounds and polycyclic aromatics, which are believed to provide good boundary lubrication, through the more severe refinement [9–11]. Sulfur level is just a convenient means of measuring the degree of refinement. In the meantime, more complete combustion and finer atomization of the fuel are being sought for higher engine efficiency, which leads to higher operating pressure in the fuel injector and tighter geometric clearance between the plunger and the bore. The further fuel refinement and more stringent operation conditions are expected to increase the vulnerability of diesel fuel injection systems. Two approaches are being sought to solve this issue:

1. Increasing fuel lubricity by introducing effective additives or alternative fuels, and
2. Improving the scuffing-resistance of the fuel injector by introducing advanced materials or surface engineering techniques or both.

Gasoline fuel injection systems inject fuel upstream of the inlet valves and operate at much lower pressures than diesel fuel injectors; thus, the lubricity of gasoline is generally a less critical issue compared with that of diesel. Gasoline lubricity, although not being emphasized in this chapter, can be an important issue in certain circumstances, such as for direct injection gasoline engines with relatively high pressure [12]. Wei et al. [13] provided a review of gasoline lubricity.

23.2 DISCUSSION

23.2.1 Diesel Fuel Lubricity Additives and Alternative Fuels

23.2.1.1 DIESEL FUEL LUBRICITY ORIGINS AND LUBRICITY ADDITIVES

For developing fuel lubricity additives, it is essential to gain a fundamental understanding of the fuel lubricity origins and their functional mechanisms. The lubricity of diesel fuels has been linked to the concentrations of polyaromatics, saturates, and polar compounds, such as

¹ Oak Ridge National Laboratory, Materials Science and Technology Division, Oak Ridge, TN, USA

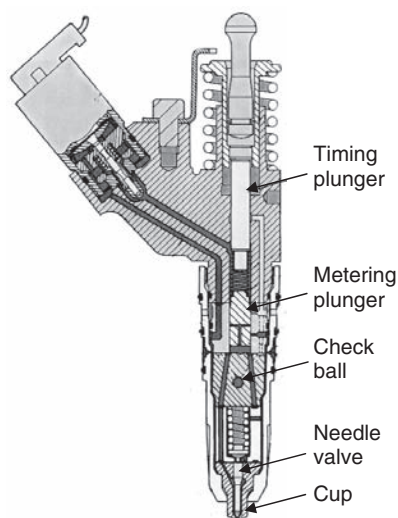


Figure 23.1—Schematic drawing of the Cummins Select unit fuel injector [1].

phenols and aromatics [9–11]. The length of hydrocarbon chains largely determines the viscosity, a key factor of fuel lubricity. The presence of oxygen atoms provides the polarity that is critical for the fuel lubricity. Lubricity is proposed to be strongly dependent on how oxygen atoms are bound in the molecule and the number of these moieties [11]. For example, the lubricity of esters is mainly introduced by the carbonyl moiety aided by ether linkage. The functional group $-\text{COOH}$ effectively enhances lubricity. A short-chain compound (e.g., glycerol) could also exhibit good lubricity as long there are sufficient oxygenated moieties [11].

In the production of LSD fuels, HT has commonly been used to remove the sulfur contents, but this also removes polyaromatic, polar, and unsaturated compounds—the lubricating essentials. Hughes et al. [10] analyzed the compositional changes induced by a series of HTs for several commercial diesel fuels and investigated their effects on the fuel lubricity using three ASTM standard tests: ball-on-cylinder lubricity evaluator (BOCLE) [14], scuffing load ball-on-cylinder lubricity evaluator (SLBOCLE) [15], and high-frequency reciprocating rig (HFRR) [16]. Selected results for hydrotreated No. 2 diesel fuels are displayed in Figure 23.2. Each HT process effectively reduced the sulfur concentration by approximately one order of magnitude. At the same time, the concentration of aromatics was also reduced significantly, from 25.2 to 3.9 vol %, after the four HTs, and the saturated compounds increased from 73.0 to 94.4 vol %. As shown in Figure 23.2, the BOCLE test results showed a corresponding increase in wear scar size for the cleaner fuels, and all hydrotreated fuels failed to pass the lubricity criterion.

To restore the fuel lubricity, several types of lubricity additives (e.g., formulations involving fatty acid esters, unsaturated fatty acids dimers, aliphatic amines, and long-chain monocarboxylic acids) have been developed and their effectiveness has been studied [17–21]. Research has shown hydroxylated fatty acid methyl esters (FAMES) possessing better lubricating properties than nonhydroxylated FAMES [9]. Geller and Goodrum [22] investigated the effects of

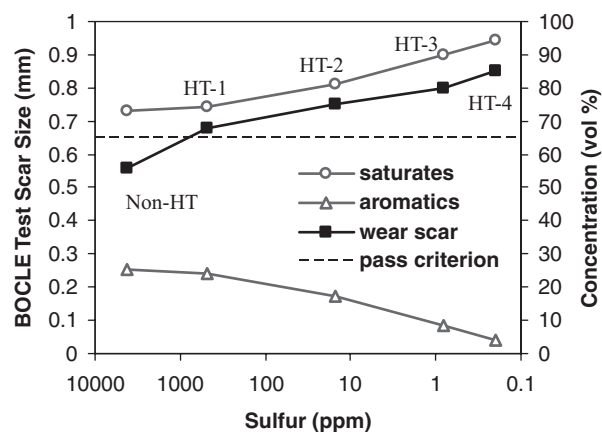


Figure 23.2—Concentrations of aromatics and saturates in a hydrotreated No. 2 diesel fuel and their effects on fuel lubricity [10].

individual component FAMES and suggested little correlation between FAME chain length and lubricity enhancing properties but a rough correlation between saturation and lubricity enhancement. The identification of the types and concentrations of lubricity improver additives in a diesel fuel can be realized using gas chromatography–mass spectrometry [23].

23.2.1.2 ALTERNATIVE FUELS

The tightening environmental regulations along with recent high fuel prices have recently renewed the interest in alternative fuels such as biodiesel, ethanol-diesel blend fuels, and dimethyl ether [24,25].

23.2.1.2.1 Biodiesel

As renewable energy sources, biomass-based biodiesel fuels can potentially reduce the dependence on imported oil. Biodiesel is nontoxic and biodegradable. Using biodiesel can significantly reduce emissions of sulfur oxides (SO_x), particulates, soot, and polycyclic aromatic hydrocarbons, although it will typically increase the nitrogen oxide (NO_x) exhaust emissions [5,24]. Other issues with biodiesel include lower energy density, lower oxidation stability, and poorer low-temperature flow characteristics than conventional petroleum-based diesel (petrodiesel) fuels [5,24]. Vegetable oils without proper treatments have been reported to be unsuitable for compression ignition engines [26]. There are various long-term problems such as poor atomization characteristics, ring sticking, injector choking, injector deposits, injector pump failure, and lube oil dilution by crankcase polymerization [26]. To avoid these problems, transesterification has been widely used to split the glycerides in vegetable oils because the glycerides cause an excess of carbon in comparison [27]. Transesterification basically substitutes the glycerol of the mono-, di-, and triglycerides with up to three molecules of primary alcohols to form alkyl esters. A blend of transesterified linseed oil methyl ester (20 %) and petroleum diesel has demonstrated good compatibility with a compression ignition engine and passed a 512-h duration engine test with lower engine wear and emissions compared with the neat petroleum diesel [28].

Biodiesels have been reported to possess higher lubricity than petrodiesel fuels [5,29]. Using biodiesel [30] or biodiesel-derived FAMES [9,22,31–35] to blend with or as additives for low-sulfur petrodiesel fuels may effectively restore their lubricity. For example, Figure 23.3 compares the sizes of the wear scars produced in HFRR tests lubricated by blends of a petrodiesel and four biodiesels with various biodiesel concentrations [33]. Any biodiesel content showed improvement on the fuel lubricity to some extent. A higher concentration of a biodiesel generally yielded a smaller wear scar, but the first 20 wt % appeared to have the largest effects. Studies have revealed that the methyl esters and monoacylglycerols contained in biodiesel are the main lubricity improvers and the free fatty acids and diacylglycerols also contribute to the fuel lubricity [11,36].

23.2.1.2.2 Ethanol-Diesel Blends (E-Diesel)

E-diesel, as an alternative renewable energy, offers a significant opportunity to produce cleaner, more energy-efficient cars and trucks. An E-diesel with 15 % ethanol could reduce particulate and NO_x emissions by 30–41 % and 4–5 %, respectively, although it may release higher total hydrocarbons (THC) [24,37,38]. An E-diesel has different physicochemical properties than the conventional petrodiesel, with reduced density, cetane number, viscosity, lubricity, heat content, and flash point [38–40], as shown in Table 23.1. The reduced viscosity and lubricity limit the ethanol content to 18.5 vol % for the No. 2 diesel fuel, as illustrated in Figure 23.4 [41], to meet the ASTM minimum viscosity requirement [42]. Higher ethanol concentration may be a pathway to increase domestic renewable fuel

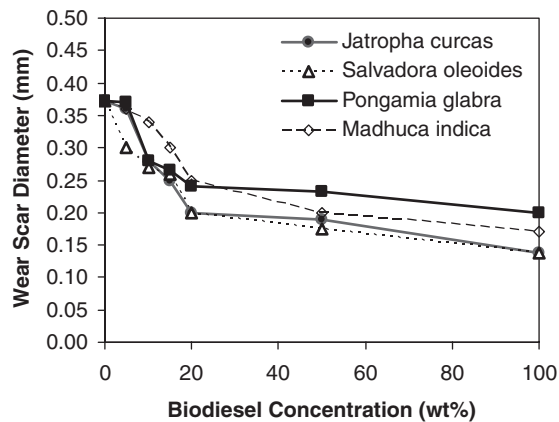


Figure 23.3—Comparison of the sizes of the wear scars produced in HFRR tests lubricated by a petrodiesel blended with various concentrations of four biodiesels [33].

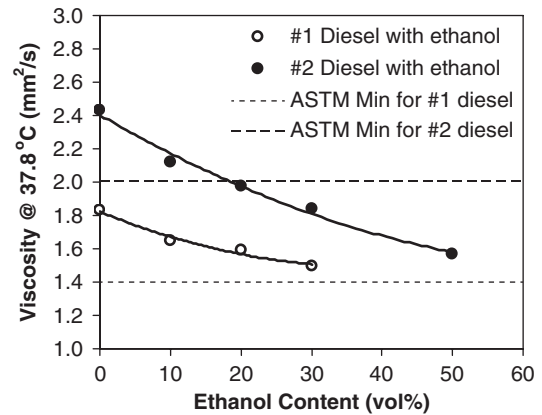


Figure 23.4—Effect of ethanol content on diesel fuel viscosity. Source: Figure modified after [41].

content in diesel and to meet more and more stringent EPA emission regulations, but the resulting insufficient fuel lubricity may cause problems with existing diesel fuel injectors.

Additives have been considered to restore the viscosity and lubricity for E-diesel. Some ethanol-1-butanol-diesel (1:2:3 and 1:2.5:5.5) microemulsions have exhibited similar viscosity and gross heat of combustion compared to petrodiesel fuels [43] and an ethanol-biodiesel-diesel blend (EB-diesel) in the volumetric ratio of 20:4:76 has shown significantly higher lubricity than the neat petrodiesel in HFRR tests [44]. In addition to the lubricity issue, the corrosiveness and compatibility of E-diesel to engine materials have yet to be systematically studied and require further investigations for E-diesels.

Although millions of cars powered by ethanol-blended fuels are on U.S. roads, and ethanol-blended gasoline fuels (primarily E10 up to 10 vol % ethanol) sales represent more than 11 % of all automotive fuels sold in the United States, the usage of E-diesel blends is limited to prototype applications. A limited range of durability tests have been conducted on E-diesel blends in the laboratory [45–49] and in the field [50,51], including two fleets of urban transit buses at Lincoln, NE, and Chicago, IL, respectively. With correctly adjusted injection timing, no abnormal wear or deterioration was detected for the engine or fuel injection system in laboratory durability engine tests for E-diesel with up to 30 vol % ethanol. No abnormal maintenance or fuel-related problems were encountered in the over-the-road tests, including one case in which a diesel engine accumulated 434,500 km of running mileage on a E-diesel fuel with 15 % ethanol [51].

TABLE 23.1—Physicochemical Properties of No. 2 Diesel and Anhydrous Ethanol

	Formula	Mole Weight	Density at 20°C (g/cm ³)	Boiling Point (°C)	Pour Point (°C)	Flash Point (°C)	Viscosity at 20°C (mPa·s)	Heat Content (MJ/kg)	Cetane Number
No. 2 diesel	C _x H _y	190–220	0.829	180–360	–1 to 3	65–88	3.35	42.5	45–50
Ethanol	CH ₃ –CH ₂ OH	46.1	0.789	78.4	–117.3	13–14	1.20	26.8	5–8

Source: Table modified after [38].

23.2.1.3
DIESEL FUEL LUBRICITY TESTS

Field tests and dynamometer tests to measure wear in engine components are very costly and time-consuming; thus, there was a need for generally accepted bench tests that the petroleum industry could use to evaluate diesel fuel lubricity. Many bench tests have been nonexclusively used to quantify lubricity for aviation and diesel fuels including the four-ball test, Timken test, Falex pin-on-Vee, Falex BOTS test, BOCLE, SLBOCLE, U.S. Army scuffing load test (based on the BOCLE), Shell Thornton aviation fuel lubricity evaluator, Bosch 2000-h pump test, Bosch ball-on-disc test, Plint TE-77 roller on flat high-frequency reciprocating test, and HFRR [5,6]. However, most tests were designed primarily for lubricating oils and were too severe to distinguish the relatively subtle difference of lubricity among the fuels. So far, only three have been widely accepted and adopted as ASTM standards: BOCLE (ASTM D5001) [14], SLBOCLE (ASTM D6078) [15], and HFRR (ASTM D6079) [16]. Their applicability, test materials, test conditions, and pass criteria are compared in Table 23.2.

HFRR is also a standard diesel fuel lubricity test certified by ISO (ISO 12156) [52,53] and CEC (CEC F-06-96) [54]. ISO and CEC jointly launched an extensive round-robin program in the early 1990s to compare laboratory fuel lubricity tests including HFRR, two variants of BOCLE, and Falex BOTS tests. Round-robin field tests were simultaneously performed by industry contributors including Bosch, Lucas, and Stanadyne with the support of oil and additive companies. On the basis of the results, HFRR received the highest recommendation by the round-robin program committee and was eventually adopted by ISO and CEC.

23.2.2
Diesel Fuel Injector Materials

23.2.2.1
BACKGROUND

Fuel injectors in diesel engines usually contain cylindrical plungers that rapidly move up and down to supply pressurized fuel to the injector nozzle and to the combustion chamber. The fuel itself lubricates the plungers. Plungers

and bores are carefully finished so that a tight seal is maintained while still allowing the plungers to move up and down without binding. The tight clearance between the plunger and the bore (2–4 μm) makes it difficult to supply lubricating fluid between them. Thus, any error in plunger fit, excessive side load, or inadequate fuel lubricity may cause scuffing damage on the plunger and the bore. Scuffing in a diesel fuel injector, once initiated, would rapidly propagate because of the tight geometric clearance and easily lead to a plunger seizure and engine failure. The use of ULSD fuels, which possess lower lubricity, makes the fuel injector system more vulnerable to scuffing. Developing advanced materials or surface treatments or both for diesel fuel injectors is an important alternative approach to seeking new fuel lubricity additives to solve this critical issue.

23.2.2.2
SCUFFING DEFINITION

The term “scuffing” has been used to describe surface damage in various contexts throughout the field of engineering, and there is no simple definition for the term that can fit all situations. Even the definition of scuffing presented in the ASTM Wear and Erosion Terminology Standard G-40 [55] is so broadly worded that the attributes of the phenomenon are not uniquely identifiable from other forms of contact damage. A narrower definition specifically for fuel injector scuffing was proposed by P.J. Blau [56]:

Scuffing—a form of sliding-induced contact damage to a bearing surface, usually associated with asperity-scale plastic deformation, that results in localized and perceptible changes in roughness or appearance without significantly altering the geometric form of the part on which the damage occurs.

Scuffing may occur either with or without the generation of wear particles, and it may result in either smoothing or roughening of the surface [56]. The primary point is that

TABLE 23.2—Comparison of Three ASTM Standards for Testing Fuel Lubricity [14–16]

	BOCLE	SLBOCLE	HFRR
Applicable	Middle distillate fuels including diesel and aviation fuels		
Configuration	Ball-on-cylinder		Ball-on-flat
Materials	Ball: AISI 52100 steel, 64-66 HRC Ring: SAE 8720 steel, 58-62 HRC		Ball: AISI 52100 steel, 58-66 HRC Ring: SAE 8720 steel, 58-62 HRC
Fluid volume (mL)	50 \pm 1.0	50 \pm 1.0	2 \pm 0.2
Fluid temperature ($^{\circ}\text{C}$)	25 \pm 1	25 \pm 1	25 \pm 2
Relative humidity	10 \pm 0.2	50 \pm 1	>30 %
Applied load (g-f)	1000	Break-in: 500 Incremental-load test: 500–5000 Single-load test: user defined	200 \pm 1
Cylinder rotational speed (r/min)	240 \pm 1	525 \pm 1	Ball oscillation frequency: 50 \pm 1 Hz Stroke length: 1 \pm 0.02 mm
Test duration (min)	30 \pm 0.1	Break-in: 0.5 Wear test: 1.0	75 \pm 0.1
Criterion for No. 2 diesel	Wear scar size <0.65 mm	Scuffing load >3100 g	Wear scar size <0.45 mm

the occurrence of scuffing generally degrades the tribological or cosmetic functionality or both of a surface without necessarily producing gross amounts of wear or surface damage.

23.2.2.3 SCUFFING DETECTION

For diesel fuel injectors, once scuffing is underway, it can quickly lead to an engine failure. Therefore, detecting the onset of scuffing is more critical than the scuffing-associated progressive wear emphasized by the current standard tests [14–16] and many literatures [57–59]. Much less attention has been paid to predicting or monitoring the onset of scuffing. Wood et al. [60–62] reported using electrostatic charge monitoring for the early stage of scuffing in unidirectional sliding. However, their method was less reliable for reciprocating sliding (like the fuel injector) because of vibration and oil flow fluctuations, and an averaging approach was used [62]. The prediction of scuffing failure on the basis of oxide formation and removal measurements was made for steel sliding against steel [63]. Infrared and visual monitoring systems were applied to study the onset of scuffing [64], and in other work, the contact temperature and friction coefficient were tracked to reveal the initial scuffing and recovery [65]. All of these studies of scuffing detection were conducted in the oil-lubricated condition, and their applicability to diesel fuels has yet to be confirmed.

A sudden rise of the friction force is well known to reflect an increased incidence of surface deformation and is used by the ASTM SLBOCLE test [15] as an indicator of scuffing for unidirectional sliding. For reciprocating sliding, which better simulates the movement of a fuel injector plunger, a macroscopic trend by averaging out the small frictional variations within each stroke is usually used [56,62]. Using this technique, some success was achieved for capturing severe scuffing in diesel fuels for metals with relatively low scuffing resistance, such as annealed steel [56]. An example is shown in Figure 23.5 [56], on which the trace of the average friction coefficient for the self-mated annealed AISI 52100 steel reciprocating sliding lubricated by a Jet A fuel (a surrogate for ULSD fuel) showed a dramatic transition at 10- to 15-m sliding distance implying the onset of scuffing. However, this averaging approach has been proved to not be sensitive enough for high scuffing-resistant materials, such as hardened steel and ceramics [66].

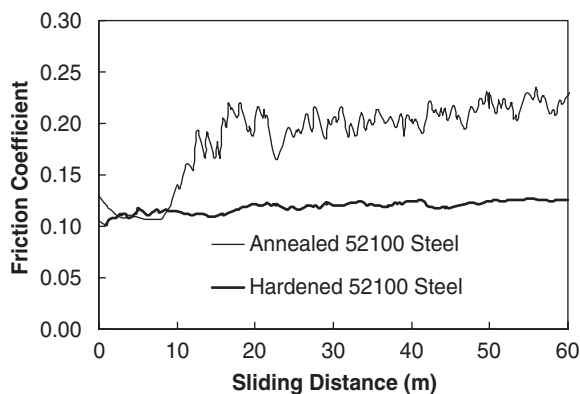


Figure 23.5—Average friction coefficient traces for annealed and hardened 52100 steel. *Source:* Figure modified after [66].

As shown in Figure 23.5, there was no apparent friction transition for the hardened 52100 steel experiencing the same fuel-lubricated sliding test as the annealed version. During the post-test analysis, the worn surfaces on the hardened steel clearly showed localized, moderate scuffing features, but damage was not severe enough to be reflected by the average friction coefficient of the entire reciprocating stroke [66].

More recently, Qu et al. [66–68] have demonstrated the capability of capturing the onset of localized scuffing and its propagation in space and time domains by analyzing the progressive changes in the friction traces of individual strokes for reciprocating sliding in a fuel-lubricated environment. The concept is that a significant change of the friction force at a certain location corresponds to the surface scuffing there. The friction trace analysis is illustrated schematically in Figure 23.6. Figure 23.6, a and b, shows the hypothetical friction traces μ_1 and μ_n , for the first and the n th reciprocating stroke, respectively. The sign of the friction coefficient merely reflects the sliding direction. The sinusoidally oscillating sliding velocity is also plotted in Figure 23.6a. The sliding speed starts at zero at the turnaround points (stroke ends) and reaches a maximum at the stroke midpoint. The change in friction coefficient ($\Delta\mu_n$) is obtained by subtracting the friction trace of the first cycle from that of n th cycle, as plotted in Figure 23.6c. The friction coefficient increases at the stroke ends first, indicating that scuffing starts there. Little change in the friction in the middle of the stroke implies that the scuffing damage has not occurred there yet. This actually is often observed in reciprocating sliding because the lubricant film thickness at the interface is proportional to the sliding velocity [69].

A three-dimensional visualization of this scuffing detection method can be implemented by plotting the friction change versus the location and time. For example, Figure 23.7 shows the friction change captured in a reciprocating sliding of self-mated hardened 52100 steel lubricated by Jet A fuel [68]. It clearly shows when (90 s) and where (stroke locations 0, 1, 9, and 10) the scuffing initiated and how the scuffing damage propagated (gradually from the stroke

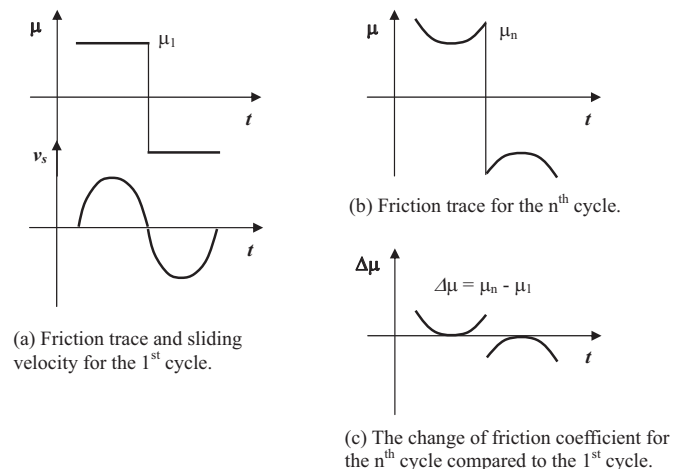


Figure 23.6—Detecting localized scuffing by examining the change of friction traces at individual stroke cycles. *Source:* Figure modified after [66].

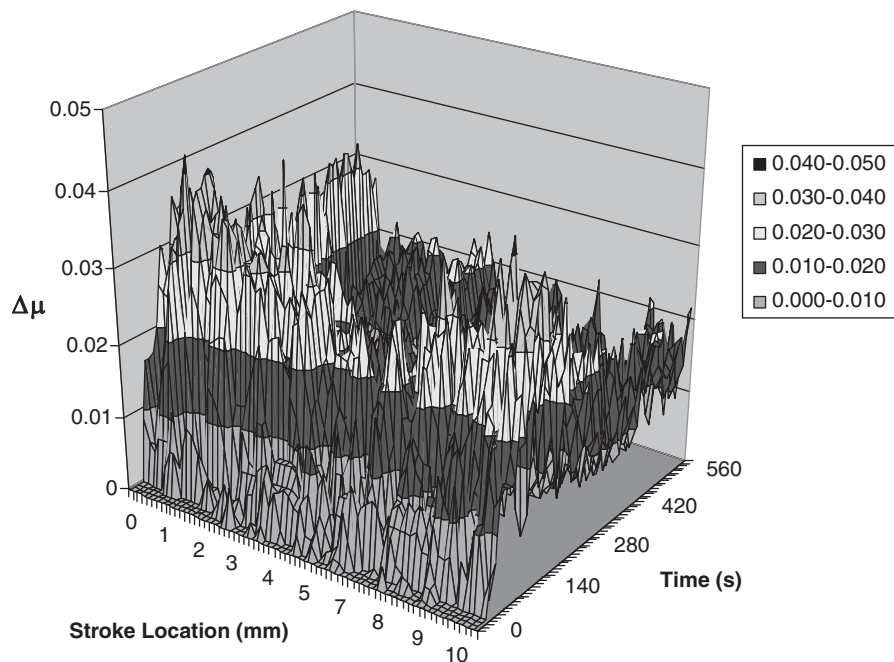


Figure 23.7—A three-dimensional map of the change of friction coefficient in space and time domains revealing scuffing initiation and propagation. *Source:* Figure modified after [68].

ends to the stroke center). This enables one to quickly visualize aspects of the different progressive stages of localized, moderate scuffing that are usually experienced by high scuffing-resistant materials.

23.2.2.4 EVALUATION OF FUEL INJECTOR MATERIALS

Issues associated with evaluating diesel fuel injector materials include the determination of an appropriate surface finish, the suitability of using hard coatings, the proper relative hardness of the mating materials, the compatibility of materials with fuels, and the effects of applied load and speed on the propensity of materials to scuff. The portrayal of scuffing characteristics of materials for engine components is not straightforward because

- Scuffing damage is localized and generally nonuniform across the affected surface.
- Unlike other types of wear, scuffing may not generate a net loss of material and therefore cannot be measured simply by mass loss.

- The development of quantitative criteria for whether a material has or has not scuffed is not trivial. Visual inspection is often used in practice, but that does not lend itself to quantification.
- Scuffing is a function of the lubrication regime, surface finish, and material characteristics; thus, displaying all of the key variables in a meaningful scuffing map is not straightforward.

Ceramics, cermets, and hard coatings have been developed for modern fuel injectors to achieve superior scuffing resistance and they have achieved success in industry to various extents [1]. Laboratory evaluation [67] of the scuffing characteristics of selected diesel fuel injector materials using the individual stroke-based friction analysis [66] showed reasonably good agreement with industrial field experience [1], as shown in Table 23.3. Generally, the zirconia plunger against steel bore exhibited the better scuffing resistance than the cermet-steel and titanium nitride coating-steel pairs that, in turn, showed improved performance over the conventional steel-steel

TABLE 23.3—Comparison of the Scuffing Characteristics of Diesel Fuel Injector Plunger Materials Lubricated by No. 2 Diesel Fuel in Laboratory Tests and Industrial Field Experience		
Plunger Material	Laboratory Test	Field Experience
Zirconia	No scuffing	Extremely high scuffing resistance
Cermets	High resistance to both scuffing initiation and propagation	Unavailable
TiN coatings	Low resistance to scuffing initiation, moderate resistance to scuffing propagation	High scuffing resistance
AISI 52100 steel	Moderate resistance to scuffing initiation, low resistance to scuffing propagation	Moderate scuffing resistance

Source: Table modified after [67].

combination. Results also suggested higher vulnerability to scuffing for all test materials in the cleaner Jet A aviation fuel compared with the No. 2 diesel fuel [67]. Zirconia plungers have achieved a big success in industrial diesel engines [1], but they did not pass the scuffing tests lubricated by Jet A fuel. The composite surface roughness of a production zirconia plunger and steel bore is $0.27\text{ }\mu\text{m}$. Rougher surfaces (in the test range of $0.04\text{--}0.4\text{ }\mu\text{m}$) were found to help increase the resistance to scuffing initiation and propagation, as shown in Figure 23.8 [68]. However, to meet the stricter diesel engine emissions standards, superior surface finish and tighter tolerances are required to seal the higher injection pressures. This dilemma necessitates the investigation of new materials or surface engineering processes to resist scuffing in the more stringent operating conditions.

23.3 CONCLUSIONS

Stricter diesel emission regulations and higher engine efficiency requirements are pushing the need for ULSD fuels and more complete combustion. The fuel refinement processes for reducing the sulfur contents have also been found to remove the fuel lubricity components and thus reduce the fuel lubricity. More efficient combustion requires higher injection pressures and tighter geometric tolerances. This combination increases the vulnerability of the diesel fuel injection system to scuffing damage that can cost a catastrophic engine failure. This chapter discussed two different approaches to deal with this issue:

1. *Fuel lubricity additives and alternative fuels:* Various lubricity improvers have been used with a certain degree of success for LSD fuels, but they may require further development for ULSD fuels. Alternative fuels such as biodiesel and E-diesel are currently of particular interest because of their renewable nature and potential in emission reductions, although concerns are yet to be fully resolved, such as the aging (oxidation) of biodiesel and the low viscosity of E-diesel.

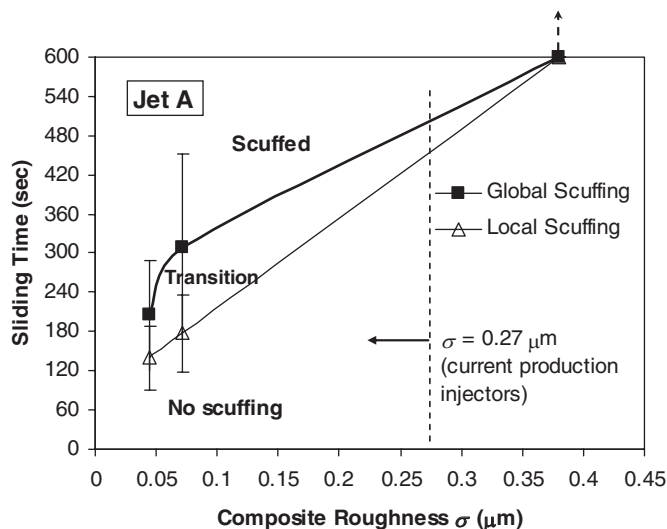


Figure 23.8—Scuffing transition diagrams for zirconia against 52100 steel with different surface finish lubricated by Jet A fuel (a surrogate for ULSD fuel). *Source:* Figure modified after [68].

2. *High scuffing-resistant fuel injector materials or surface engineering processes or both:* Given various advanced materials, coatings, and surface treatments already available and many emerging, a reliable testing methodology to assess the scuffing characteristics is essential for material evaluation and further development if needed. One technique was highlighted in the discussion because of its superior capability of detecting the onset of scuffing in reciprocating systems and its good correlation to industrial field experience with injector wear.

ACKNOWLEDGMENTS

The author thanks Drs. P.J. Blau and J.M. Storey from Oak Ridge National Laboratory and Dr. J.J. Truhan from Caterpillar, Inc. for their valuable inputs and comments. The writing of this chapter was supported by the U.S. Department of Energy, Assistant Secretary for Energy Efficiency and Renewable Energy, Vehicle Technologies Program, under contract DE-AC05-00OR22725 with UT-Battelle LLC.

References

- [1] Naylor, M.G., Kodali, P., and Wang, J.C., 2000, "Diesel Engine Tribology." In *Modern Tribology Handbook*, B. Bhushan, Ed., CRC Press, Boca Raton, FL.
- [2] U.S. Environmental Protection Agency (EPA), 2006, *Introduction of Cleaner-Burning Diesel Fuel Enables Advanced Pollution Control for Cars, Trucks and Buses*, EPA420-F-06-064, EPA Office of Transportation and Air Quality, Washington, DC.
- [3] ASTM Standard D975-08a, 2008: Standard Specification for Diesel Fuel Oils, *Annual Book of ASTM Standards*, ASTM International, West Conshohocken, PA.
- [4] "Stricter Fuel Standards to Combat Climate Change and Reduce Air Pollution, European Commission," IP/07/120, January 31, 2007, available at <http://europa.eu/rapid/pressReleasesAction.do?reference=IP/07/120>.
- [5] Margaroni, D., 1998, "Fuel Lubricity," *Ind. Lub. Tribology*, Vol. 50, pp. 108–118.
- [6] Wilson, B., 1996, "Fuel Lubricity," *Ind. Lub. Tribology*, Vol. 48, pp. 10–14.
- [7] Lacey, P.I., 1993, "Wear with Low-Lubricity Fuels, I. Development of a Wear Mapping Technique," *Wear*, Vol. 160, pp. 325–332.
- [8] Lacey, P.I., 1993, "Wear with Low-Lubricity Fuels, II. Correlation between Wear Maps and Pump Components," *Wear*, Vol. 160, pp. 333–343.
- [9] Anastopoulos, E.L., Zannikos, F., Kalligeros, S., and Teas, C., 2001, "Influence of Aceto Acetic Esters and Di-Carboxylic Acid Esters on Diesel Fuel Lubricity," *Tribology Int.*, Vol. 34, pp. 749–755.
- [10] Hughes, J.M., Mushrush, G.W., and Hardy, D.R., 2003, "The Relationship between the Base Extractable Species Found in Middle Distillate Fuel and Lubricity," *Energy & Fuels*, Vol. 17, pp. 444–449.
- [11] Knothe, G., and Steidley, K.R., 2005, "Lubricity of Components of Biodiesel and Petrodiesel. The Origin of Biodiesel Lubricity," *Energy & Fuels*, Vol. 19, pp. 1192–1200.
- [12] Anderson, R.W., Brehob, D.D., Yang, J., Valiance, J.K., and Whiteaker, R.M., 1996, *Understanding the Thermodynamics of Direct Injection Spark Ignition (DISI) Combustion Systems: An Analytical and Experimental Investigation*, SAE Technical Paper 962018, SAE, Warrendale, PA.
- [13] Wei, D.P., Spikes, H.A., and Korcek, S., 1999, "The Lubricity of Gasoline," *Tribology Trans.*, Vol. 42, pp. 813–823.
- [14] ASTM Standard D5001-08, 2008: Standard Test Method for Measurement of Lubricity of Aviation Turbine Fuels by the Ball-on-Cylinder Lubricity Evaluator (BOCLE), *Annual Book of ASTM Standards*, ASTM International, West Conshohocken, PA.

- [15] ASTM Standard D6078-04, 2004, Standard Test Method for Evaluating Lubricity of Diesel Fuels by Scuffing Load Ball-on-Cylinder Lubricity Evaluator (SLBOCLE), *Annual Book of ASTM Standards*, ASTM International, West Conshohocken, PA.
- [16] ASTM Standard D6079-04e1, 2004: Standard Test Method for Evaluating Lubricity of Diesel Fuels by the High-Frequency Reciprocating Rig (HFRR), *Annual Book of ASTM Standards*, ASTM International, West Conshohocken, PA.
- [17] Perilstein, W.L., 1980, "Diesel Fuel Compositions Having Anti-Wear Properties," U.S. Patent 4,185,594.
- [18] Malec, R.E., 1980, "Fuel Lubricity from Blends of a Diethanolamine Derivative and Biodiesel," U.S. Patent 4,204,481.
- [19] Malec, R.E., 1980, "Diesel Fuels Having Anti-Wear Properties," U.S. Patent 4,208,190.
- [20] Eber, D., Germanaud, L., and Maldonado, P., 2003, "Additive for Fuel Oiliness," EP 6511520.
- [21] Bernasconi, C., Germanaud, L., Laupie, J.-M., and Maldonado, P., 2008, "Fuel with Low Sulphur Content for Diesel Engines," EP 7374589.
- [22] Geller, D.P., and Goodrum, J.W., 2004, "Effects of Specific Fatty Acid Methyl Esters on Diesel Fuel Lubricity," *Fuel*, Vol. 83, pp. 2351–2356.
- [23] Rezende, M.J.C., Perruso, C.R., Azevedo, D.A., and Pinto, A.C., 2005, "Characterization of Lubricity Improver Additive in Diesel by Gas Chromatography–Mass Spectrometry," *J. Chrom. A*, Vol. 1063, pp. 211–215.
- [24] Ribeiro, N.M., Pinto, A.C., Quintella, C.M., da Rocha, G.O., Teixeira, L.S.G., Guarieiro, L.L.N., do Carmo Range, M., Veloso, M.C.C., Rezende, M.J.C., Serpa da Cruz, R., Maria de Oliveira, A., Torres, E.A., and de Andrade, J.B., 2007, "The Role of Additives for Diesel and Diesel Blended (Ethanol or Biodiesel) Fuels: A Review," *Energy & Fuels*, Vol. 21, pp. 2433–2445.
- [25] Arcoumanis, C., Bae, C., Crookes, R., and Kinoshita, E., 2008, "The Potential of Di-Methyl Ether (DME) as an Alternative Fuel for Compression-Ignition Engines: A Review," *Fuel*, Vol. 87, pp. 1014–1030.
- [26] Krawczyk, T., 1996, "Biodiesel: Alternative Fuel Makes Inroads but Hurdles Remain," *Inform*, Vol. 7, pp. 801–814.
- [27] Van Dyne, D.L., Weber, J.A., and Braschler, C.H., 1996, "Macroeconomic Effects of a Community Based Biodiesel Production System," *Bioresource Technol.*, Vol. 56, pp. 1–6.
- [28] Agarwal, A.K., Bijwe, J., and Das, L.M., 2003, "Wear Assessment in a Biodiesel Fueled Compression Ignition Engine," *J. Engineer. Gas Turbines Power*, Vol. 125, pp. 820–826.
- [29] Wain, K.S., Perez, J.M., Chapman, E., and Boehman, A.L., 2005, "Alternative and Low Sulfur Fuel Options: Boundary Lubrication Performance and Potential Problems," *Tribology Int.*, Vol. 38, pp. 313–319.
- [30] Hughes, J.M., Mushrush, G.W., and Hardy, D.R., 2002, "Lubricity-Enhancing Properties of Soy Oil When Used as a Blending Stock for Middle Distillate Fuels," *Ind. Eng. Chem. Res.*, Vol. 41, pp. 1386–1388.
- [31] Dmytryshyn, S.L., Dalai, A.K., Chaudhari, S.T., Mishra, H.K., and Reaney, M.J., 2004, "Synthesis and Characterization of Vegetable Oil Derived Esters: Evaluation for Their Diesel Additive Properties," *Bioresource Technol.*, Vol. 92, pp. 55–64.
- [32] Karonis, D., Anastopoulos, G., Lois, E., Stournas, S., Zannikos, F., and Serdari, A., 1999, *Assessment of the Greek Road Diesel and the Effect of the Addition of Specific Types of Biodiesel*, SAE Technical Paper 1999-01-1471, SAE, Warrendale, PA.
- [33] Bhatnagar, A.K., Kaul, S., Chhibber, V.K., and Gupta, A.K., 2006, "HFRR Studies on Methyl Esters of Nonedible Vegetable Oils," *Energy & Fuels*, Vol. 20, pp. 1341–1344.
- [34] Lang, X., Dalai, A.K., Bakhshi, N.N., Reaney, M.J., and Hertz, P.B., 2001, "Preparation and Characterization of Bio-Diesels from Various Bio-Oils," *Bioresource Technol.*, Vol. 80, pp. 53–62.
- [35] Kulkarni, M.G., Dalai, A.K., and Bakhshi, N.N., 2007, "Transesterification of Canola Oil in Mixed Methanol/Ethanol System and Use of Esters As Lubricity Additive," *Bioresource Technol.*, Vol. 98, pp. 2027–2033.
- [36] Hu, J., Du, Z., Li, C., and Min, E., 2005, "Study on the Lubrication Properties of Biodiesel As Fuel Lubricity Enhancers," *Fuel*, Vol. 84, pp. 1601–1606.
- [37] Kass, M.D., Thomas, J.F., Storey, J.M., Domingo, N., Wade, J., and Kenreck, G., 2001, *Emissions from a 5.9 Liter Diesel Engine Fueled with Ethanol Diesel Blends*, SAE Technical Paper 2001-01-2018, SAE, Warrendale, PA.
- [38] Li, D., Zhen, H., Lu, X., Zhang, W., and Yang, J., 2005, "Physico-Chemical Properties of Ethanol-Diesel Blend Fuel and Its Effect on Performance and Emissions of Diesel Engines," *Renewable Energy*, Vol. 30, pp. 967–976.
- [39] Satge de Caro, P., Mouloungui, Z., Vaitilingom, G., and Berge, J.C., 2001, "Interest of Combining an Additive with Diesel–Ethanol Blends for Use in Diesel Engines," *Fuel*, Vol. 80, pp. 565–574.
- [40] Hansen, A.C., Zhang, Q., and Lyne, P.W.L., 2005, "Ethanol-Diesel Fuel Blends—A Review," *Bioresource Technol.*, Vol. 96, pp. 277–285.
- [41] Wrage, K.E., and Goering, C.E., 1980, "Technical Feasibility of Diesohol," *Trans. ASABE*, Vol. 23, pp. 1338–1343.
- [42] ASTM Standard D975-08a, 2008: "Standard Specification for Diesel Fuel Oils," *Annual Book of ASTM Standards*, ASTM International, West Conshohocken, PA.
- [43] Bhattacharya, T.K., Chatterjee, S., and Mishra, T.N., 2004, "Performance of a Constant Speed CI Engine on Alcohol-Diesel Microemulsions," *Appl. Eng. Ag.*, Vol. 20, pp. 253–257.
- [44] Fernando, S., and Hanna, M., 2004, "Development of a Novel Biofuel Blend Using Ethanol-Biodiesel-Diesel Microemulsions: EB-Diesel," *Energy & Fuels*, Vol. 18, pp. 1695–1703.
- [45] Hansen, A.C., Vosloo, A.P., Lyne, P.W.L., and Meiring, P., 1982, "Farm-scale Application of an Ethanol–Diesel Blend," *Ag. Eng. South Africa*, Vol. 16, pp. 50–53.
- [46] Hashimoto, I., Nakashima, H., Komiyama, K., Maeda, Y., Hamaguchi, H., Endo, M., and Nishi, H., 1982, *Diesel–Ethanol Fuel Blends for Heavy Duty Diesel Engines—A Study Of Performance And Durability*, SAE Technical Paper 820497, SAE, Warrendale, PA.
- [47] Meiring, P., Allan, R.S., Hansen, A.C., and Lyne, P.W.L., 1983, "Tractor Performance and Durability with Ethanol–Diesel Fuel," *Trans. ASAE*, Vol. 26, pp. 59–62.
- [48] Meiring, P., Hansen, A.C., Vosloo, A.P., and Lyne, P.W.L., 1983, *High Concentration Ethanol–Diesel Blends for Compression-Ignition Engines*, SAE Technical Paper No. 831360, SAE, Warrendale, PA.
- [49] Hansen, A.C., Mendoza, M., Zhang, Q., and Reid, J.F., 2000, *Evaluation of Oxydiesel as a Fuel for Direct-Injection Compression-Ignition Engines*, Final Report, Contract IDCCA 96-32434, Illinois Department of Commerce and Community Affairs, Springfield, IL.
- [50] Hansen, A.C., Hornbaker, R.H., Zhang, Q., and Lyne, P.W.L., 2001, *On Farm Evaluation of Diesel Fuel Oxygenated with Ethanol*, ASAE Paper No. 01-6173, ASAE, St. Joseph, MI.
- [51] Marek, N., and Evanoff, J., 2001, "The Use of Ethanol Blended Diesel Fuel in Unmodified, Compression Ignition Engines: An Interim Case Study," In *Proceedings of the Air and Waste Management Association 94th Annual Conference and Exhibition*, Orlando, FL.
- [52] ISO 12156-1:2006, 2006: Diesel Fuel—Assessment of Lubricity Using the High-Frequency Reciprocating Rig (HFRR)—Part 1: Test Method, TC 22/SC 7, ISO, Geneva, Switzerland.
- [53] ISO 12156-2:2007, 2007: Diesel Fuel—Assessment Lubricity Using the High-Frequency Reciprocating Rig (HFRR)—Part 2: Limit, TC 22/SC 7, ISO, Geneva, Switzerland.
- [54] CEC F-06-96, 2007: Measurement of Diesel Fuel Lubricity (HFRR Fuel Lubricity Tester).
- [55] ASTM Standard G40-05, 2005: Wear and Erosion Terminology Standard, *ASTM Annual Book of Standards*, Vol. 03.02, ASTM International, West Conshohocken, PA.
- [56] Qu, J., Truhan, J.J., Blau, P.J., and Ott, R., 2007, "The Development of a Pin-on-Twin Scuffing Test to Evaluate Materials for Heavy Duty Diesel Fuel Injectors," *Tribology Trans.*, Vol. 50, pp. 50–57.
- [57] Dyson, A., 1975, "Scuffing—A Review," *Tribology Int.*, Vol. 8, pp. 77–87.
- [58] Ludema, K.C., 1984, "A Review of Scuffing and Running-In of Lubricated Surfaces, with Asperities and Oxides in Perspective," *Wear*, Vol. 100, pp. 315–331.

- [59] Lee, S.C., and Cheng, H.S., 1991, "Scuffing Theory Modeling and Experimental Correlations," *J. Tribology*, Vol. 113, pp. 327–334.
- [60] Tasbaz, O.D., Wood, R.J.K., Browne, M., Powrie, H.E.G., and Denuault, G., 1999, "Electrostatic Monitoring of Oil Lubricated Sliding Point Contacts for Early Detection of Scuffing," *Wear*, Vol. 230, pp. 86–97.
- [61] Morris, S., Wood, R.J.K., Harvey, T.J., and Powrie, H.E.G., 2002, "Use of Electrostatic Charge Monitoring for Early Detection of Adhesive Wear in Oil Lubricated Contacts," *J. Tribology*, Vol. 124, pp. 288–296.
- [62] Morris, S., Wood, R.J.K., Harvey, T.J., and Powrie, H.E.G., 2003, "Electrostatic Charge Monitoring of Unlubricated Sliding Wear of a Bearing Steel," *Wear*, Vol. 255, pp. 430–443.
- [63] Cutiongco, E.C., and Chung, Y.W., 1994, "Prediction of Scuffing Failure Based on Competitive Kinetics of Oxide Formation and Removal: Application to Lubricated Sliding of AISI 52100 Steel on Steel," *Tribology Trans.*, Vol. 37, pp. 622–628.
- [64] Enthoven, J., and Spikes, H.A., 1996, "Infrared and Visual Study of the Mechanisms of Scuffing," *Tribology Trans.*, Vol. 39, 441–447.
- [65] Odi-Owei, S., Roylance, B.J., and Xie, L.Z., 1987, "An Experimental Study of Initial Scuffing and Recovery in Sliding Wear Using a Four-Ball Machine," *Wear*, Vol. 117, pp. 267–287.
- [66] Qu, J., Truhan, J.J., and Blau, P.J., 2005, "Detecting the Onset of Localized Scuffing with the Pin-on-Twin Fuel-Lubricated Test for Heavy Duty Diesel Fuel Injectors," *Int. J. Engine Res.*, Vol. 6, pp. 1–9.
- [67] Qu, J., Truhan, J.J., and Blau, P.J., 2005, "Evaluating Candidate Materials for Heavy Duty Diesel Fuel Injectors Using a 'Pin-On-Twin' Scuffing Test," *Tribology Int.*, Vol. 38, pp. 381–390.
- [68] Qu, J., Truhan, J.J., Blau, P.J., Meyer III, H.M., 2005, "Scuffing Transition Diagrams for Heavy Duty Diesel Fuel Injector Materials in Ultra Low-Sulfur Fuel-Lubricated Environment," *Wear*, Vol. 259, pp. 1031–1040.
- [69] Hamrock, B.J., and Dowson, D., 1981, *Ball Bearing Lubrication—The Elastohydrodynamics of Elliptical Contacts*, John Wiley, New York.

Filters and Filtration Testing of Automotive Fuels and Lubricants

Gary Bessee¹ and Erica Clark-Heinrich²

24.1 INTRODUCTION

This chapter provides an introduction to automotive petroleum filtration—fuels and lubricants. This chapter is not intended to provide the reader with in-depth guidance, but rather to provide a general introduction to automotive fuel and lubricant filtration.

This information is intended to explain why filters are required as well as describe the differences in design for various filtration devices, the types of media used in fuel and lubricant filtration, the contaminants used in standardized test methods to evaluate filtration products, the methods for measuring filtration efficiency and capacity, some of the common fuel and lubricant test methods, and future filtration challenges to the automotive industry.

24.1.1 Why Filters Are Needed

Fuel and lubricant filters are required to remove contamination either generated by the engine or ingested from the environment (dirt and water). Fuel and lubricants have different filtration requirements because of the sensitivity of the components. It should be noted that when filters plug, it does not indicate a bad filter but rather a dirty system. Often the users will encounter short filter life and blame it on the filter. If the filter were not present, the user most likely would be replacing an engine, injectors, or other major components rather than a fuel or lubricant filter.

24.1.2 Lubricant Filters

Engine oil is intended to not only lubricate rotating parts, but also to cool, clean, and seal critical engine components. It also aids in suspending wear metals and hard particles such as soot that is produced in the combustion process. If used properly, a lube oil and filter combination can prolong the life of an engine and its components. Full-flow filters are needed to capture manufacturing and wear metal debris from rotating engine parts. Filters do not plug (creating high restriction) during normal operation and recommended service intervals. If the filter does plug, it is functioning as it was designed. The two main test methods used by the automobile industry for evaluating full-flow oils filters are SAE HS806 and ISO 4548 [1].

Bypass oil filters are used to provide fine filtration to the oil to extend oil drain intervals. Bypass oils typically filter 2–5 % of the oil and return this “clean” oil back to the oil sump. The main contaminants removed with bypass oil filters are soot and wear metals. The test method for evaluating soot removal efficiency is ISO/TS 23556.

24.1.3 Fuel Filters

Fuel filters are required to remove abrasive contaminants and water. This filtration system can consist of a single filter or multiple elements. Fuel filtration systems typically provide finer filtration than oil filters because of the tight clearance requirements to produce injection pressure to meet current and future emission requirements. Current injection pressure can exceed 1600 bar.

24.2 FILTERS

24.2.1 Construction

The original lube filter was a metal screen placed at the intake of the oil pump to catch large debris inherent from manufacturing (Figure 24.1). The first mass-produced lube filter was a cotton fleece “sock” that would later contain a bypass section full of woodchips, shredded newspaper, or any other matter that could possibly slow the flow of oil to catch smaller particles and increase efficiency. The “spin-on” design with a steel canister was developed in the 1950s. These early spin-on filters used resin-impregnated pleated paper, otherwise known as cellulose paper. This paper proved more efficient, in general, because the media pore size was easier to control, as were the paper properties. Cellulose gave way to polyester fiber paper, which was more resilient to continuous pressure pulses. Soon after, microglass fiber was introduced. With a reduced media pore size, consumers experienced better performance and could maintain higher flow rates across the filter. The 1980s filter media research introduced an all-synthetic microglass with better permeability, smaller pore sizes, and longer filter life. With a more efficient media, manufacturers could provide better filtration in a smaller package. Today, filters are made of any combination of the aforementioned media to produce efficient full-flow filters, bypass filters, or a combination thereof. Some are full of all synthetic plastic fibers (e.g., melt blown or nonwovens) and are provided at a lower cost with a higher performance level. Most filters are still manufactured using a steel canister; however, disposal costs, higher steels costs, and landfill and environmental regulations are forcing engineering innovations. Some filter manufacturers are developing all engineered material composite filters that totally incinerate and therefore do not contribute to landfill waste. U.S. environmental concerns will continue to drive the market to use recyclable or incinerable materials [2].

Another ongoing filtration concern is oil stability. As combustion byproducts migrate into the oil (e.g., acids, oxidation, and hydrocarbons from fuel), the oil chemistry

¹ Southwest Research Institute, San Antonio, TX, USA

² Advanced Engineering, Components Development, Cummins Filtration Inc., Cookeville, TN, USA

Filter Media Timeline

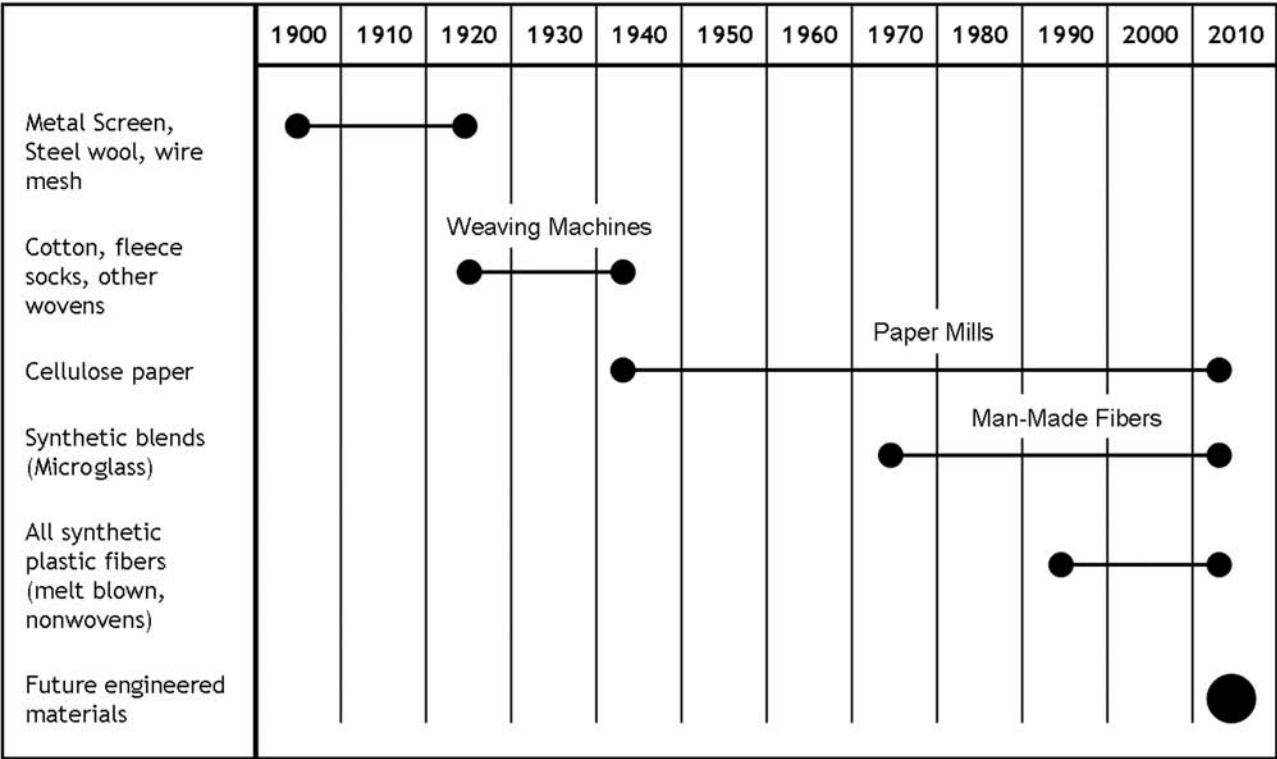


Figure 24.1—Basic timeline of filter media development.

turns sour. The overbase additive is meant to neutralize acids that migrate, but there is currently nothing to strip water or light hydrocarbons (fuel) from the oil. Filter manufacturers will continue to investigate methods to completely strip water from lube and fuel applications and search to develop media with better chemical compatibilities. The filters of the future are expected to be smaller, less expensive, mostly composite materials that are able to withstand higher pressures and temperatures, all of the while providing a negligible decrease to engine performance.

24.2.2 Properties

The design of automotive filters is a complex process that requires incorporating the available volume for installation on the vehicle, the expected life of the filter, the required efficiency and micron rating required to protect the system, an understanding of the environment and challenges the filter will likely encounter during operation, the duty cycle, and the minimizing the cost.

24.2.3 Coarse Versus Fine Filtration

Coarse filtration (large pore sized media) is meant to catch the “rocks” and “rabbits” or rather large particles in a fuel or lube system. Fine filtration is meant to more stringently filter a system. Very fine pore-sized media, or bypass filters, are commonly used to better filter the system. In some cases a filter within a filter is needed to remove tiny particles. This is especially important in fuel filtration when dealing with a high-pressure common rail application. Any

particles that escape filtration have the potential to damage the high-pressure injection system.

24.2.4 Water Separation

Water can enter the fuel system externally but usually is a result of dissolved water falling out of the fuel because of temperature changes. Dissolved water is a function of temperature—the higher the temperature, the more water can be dissolved in the fuel. However, as the temperature drops, the fuel can no longer carry this water and it falls out as free water. Free water—not dissolved water—is the concern for the fuel injection system. It can cause corrosion and is a breeding ground for microbial growth. The two main technologies used to separate water are coalescing or repelling. Glass media is typically used to act as a coalescer whereas silicon-treated cellulose is used to repel water. The repellent media is most often used because of cost constraints. One current issue that will continue to be a challenge in the future is the effect of additives and alternatives on water separation characteristics. The use of lubricity additives is required because of the poor lubricity characteristics of ultralow-sulfur diesel fuel (S15). Biodiesel fuel blends will become more prevalent in the field, and they have been shown to have poor water removal characteristics.

24.2.5 Full-Flow Oil

Oil filtration is often taken for granted, but this small, inexpensive part of your vehicle’s lubrication system plays

a vital role in protecting the engine from premature wear. Each moving part in the engine and cylinder walls requires clean oil for proper lubrication and lasting life. The full-flow oil filter removes the larger debris from the oil that can cause abrasive engine wear. Typical full-flow oil filters have micron ratings of approximately 30 μm . This porosity is required to ensure that enough oil reaches the engine to provide the required lubrication. If the filter restriction exceeds a high enough pressure, the bypass valve will open, allowing unfiltered oil to lubricate the engine. Technology is allowing manufacturers to develop tighter oil filters (10 μm) and still achieve the required flow rates to provide enough oil to the engine.

24.2.6 Bypass Oil (Combo Filters and Centrifugal Filters)

Bypass filters are designed to remove very small particles suspended in the engine oil. A bypass filter is intended to slow the flow of oil to increase the chance of catching finer particles. Typical particles include soot, wear metals, and spent oil additives. Used in conjunction with a full-flow filter, a typical bypass device will draw approximately 10 % of the oil flow from the lube circulation loop. Some bypass filters are incorporated into full-flow filters whereas others are standalone units (e.g., centrifuges). Internal centrifuge rotor design and rotational frequency determine overall soot removal efficiency. At 50 psi, a typical rotor will spin between 5000 and 8000 r/min depending on the design. Figure 24.2 shows two different centrifuge rotor designs at the completion of a 300-h soot draw-down test. Figures 24.3 and 24.4 illustrate the quantity of debris removed by centrifuges used in the field. The soot is collected from the outside in and forms the sludge wall shown at the bottom of the figure.

24.3 CONTAMINANTS

Contaminants in lube oil consist primarily of three types: organic, inorganic, and harmful acids. Organic contamination consists of the byproduct of the combustion process and includes unburned fuel, fuel resin/deposits, solvents, water, and soot (carbon particulate).

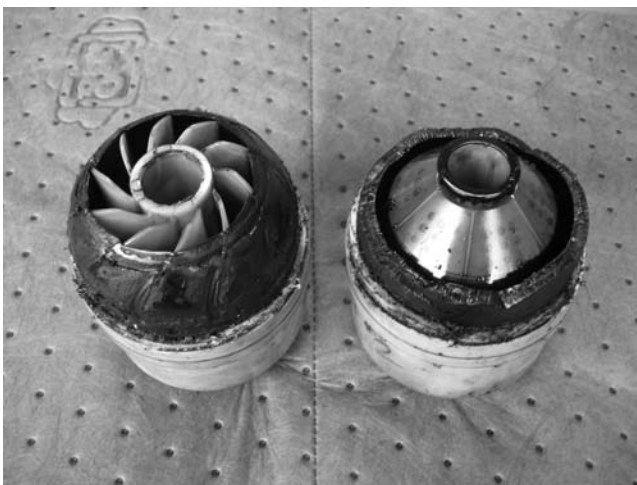


Figure 24.2—Soot collected inside of centrifuge rotors (sectioned view).



Figure 24.3—Sectioned view of a centrifuge field return from Saudi Arabia (contained 75 % sand).

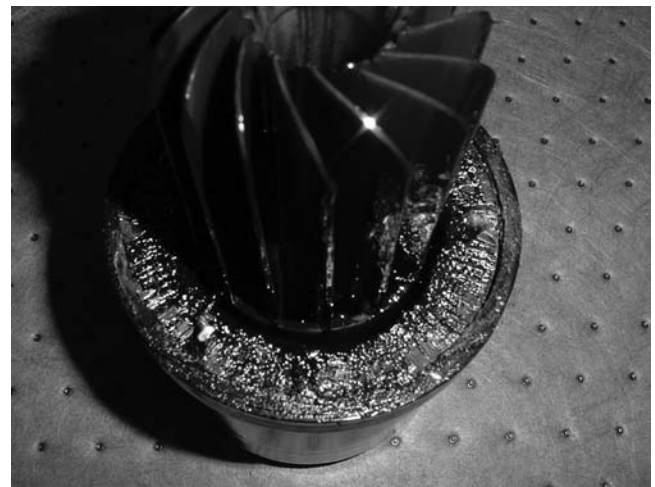


Figure 24.4—Sectioned view from a common on-highway diesel. Cake/sludge thickness is 15 mm.

Organic contamination is commonly referred to as sludge and is similar in density to that of lube oil. Sludge typically increases in quantity as engine hours are accumulated. As organic contamination increases in the lube system, the viscosity of the oil increases, causing a greater chance for filter plugging. High lube oil viscosity can be detrimental to the engine. Some of the adverse effects include: hard start-up conditions due to reduced oil flow, excessive engine component wear, lack of proper lubrication to crucial components, and reduced fuel economy. Organic contamination typically makes up 75 % of the contamination in the lube oil system. As the service interval is extended, the overall organic contamination increases. If organic contamination levels are high enough to plug the filter, a bypass valve opens, sending sludge oil straight to the engine. It is important to note that filter plugging is a result, not a cause, of a lubrication problem.

Inorganic contamination is also troublesome to the lubrication system and typically makes up approximately 25 % of the overall contaminant. Inorganic contamination can include dust, dirt, wear metals from engine components (iron, copper, etc.), gasket material, spent oil additives, and core sand (a common engine casting process uses sand cores).

Acids are another form of engine lubrication system contaminant. As a result of the combination of the combustion byproducts and heat from the combustion process,

acids (e.g., sulfuric and nitric) form in the oil. Some oils contain acid inhibitors (e.g., overbase) that help with overall oil stability, prevent rust, and prevent acids from attacking metal surfaces. Some typical additives include sulfur, phosphorous, calcium, and zinc.

24.3.1 ISO 12103-1 Tests Dusts [3]

Dust is an easily obtainable testing contaminant and is used to produce repeatable laboratory tests, such as dust holding capacity, single- or multipass dust removal efficiencies, and dust collapse (i.e., measuring differential pressure across a filter until it plugs). Dust particle size and distribution of particles is extremely important for repeatable laboratory testing.

The most common types of ISO 12103-1 test dust are ISO 12103-1, A1 ultra fine test dust, A2 fine test dust; ISO 12103-1, A3 medium dust; and ISO 12103-1, A4 coarse dust.

The dust is used with filter testing to perform dust holding capacity, single pass, multipass, dust removal efficiencies, collapse, beta testing, and accelerated filter plugging. Powder Technology, Inc. has been the main source of test dust for several years that has proven to be a consistent medium with good control from batch to batch. Because on-engine field tests are rather lengthy and expensive, the standards committees developed standardized test methods to use the test dust most relevant to the application to compare filtration performance in the laboratory.

The contaminants that occur naturally in today's environment may be of much smaller particle size (again depending on where an engine is located) and may have different elemental composition.

24.3.2 SOFTC 2A

Synthetic Oil Filter Test Contaminant (SOFTC) 2A is an older test contaminant consisting of an oil carrier containing carbon black and wear metals to simulate used oil contaminant. SOFTC 2A is used to determine the life of oil filters. The average carbon black particle size is approximately 750 nm. Specifics on this contaminant are provided in SAE HS 806 [4].

24.3.3 ISO/TS 23556 Soot [5]

The test contaminant specified in ISO/TS 23556 is based on a literature search that better defines the soot particle size distribution in used oils. This distribution varies greatly and is dependent on the following variables, among others: duty cycle, fuel type and source, and engine. As with SOFTC 2A, the contaminant is produced using carbon black. The average soot particle size is approximately 120 nm and contains trace metals. Mitsubishi produces this oil filter contaminant. The SAE Filter Test Methods Committee is evaluating other contaminants that can meet the specification as potential alternatives.

Soot dispersion for testing is created by combining carbon black with motor oil. The overall soot percentage level is determined by the amount of carbon black added to the mixture. Overall stability of the mixed dispersion is the most important characteristic of a good test fluid. In other words, if you are adding a 5 % soot dispersion to a clean sump system over time, it is important that the dirty dispersion stays as close as possible to the original 5 % soot level. Soot is an inherent byproduct of the combustion process and is especially prominent in diesel engines. Engine

inefficiencies lead to an incomplete combustion process, which can result in soot particle formation between the cylinder walls and rings. Newer exhaust gas recirculation diesel engines are designed to route a portion of the exhaust back through the intake manifold, which is meant to reduce nitrogen oxide emissions but, in turn, increases soot formation. Soot particles are mostly carbon and therefore very hard particles. High soot content in the lube system can lead to increased injector and ring/liner wear, poor oil viscosity, and filter plugging.

24.3.4 Water

Water is a common contaminant used in fuel filter laboratory testing. Deionized water is used as the standardized water contaminant because tap water composition varies greatly. This scenario creates the optimal test conditions for the filter because "hard" water creates lower interfacial tensions (IFTs) that indicate the water is more difficult to separate.

For testing purposes, water is defined as coarse or emulsified water. The water used for the test is dependent on the filter's application. Suction-side filters usually encounter coarse water whereas pressure-side applications are challenged with emulsified water. Coarse water droplets are in the range of 200–250 μm , and emulsified water droplets average approximately 10–15 μm .

24.4 METHODS OF QUANTIFYING PERFORMANCE

24.4.1 Gravimetric

Gravimetric analysis determines the mass of debris passing through the test filter. Comparing the upstream and downstream mass, the dirt removal efficiency can be determined for the filter. This method is used in many test methods but is not the most accurate. The weight could consist of many small particles or one large particle, and the efficiencies would be the same. However, for some test methods, it is the best method because of limitations in instrumentation.

24.4.2 Particle Count

Particle count analysis is used for more current test methods. Particle counting allows better definition of the distribution of the debris passing through the test filters and allows the users to have a micron rating for the filter at a certain efficiency. Care needs to be taken in verifying that the instrumentation is properly calibrated to ISO 11171 [6], and if the counters are used in a test stand, the system needs to be verified by ISO 11943 [7].

24.4.3 Karl Fischer Titration

Karl Fischer (KF) titration is a commonly accepted and used analytical method to quantify the amount of water by weight in a specified fluid or product. It is widely accepted among filter manufacturers to validate/qualify new designs or changes in design when determining fuel water separation efficiency. In short, a known water add rate is injected upstream of the filter, and a sample is taken downstream of the filter. The titrator slowly injects a reagent that absorbs water, and a calculation is performed to determine the total water content of the sample (usually specified in parts per million). An example of a KF titrator is shown in Figure 24.5.

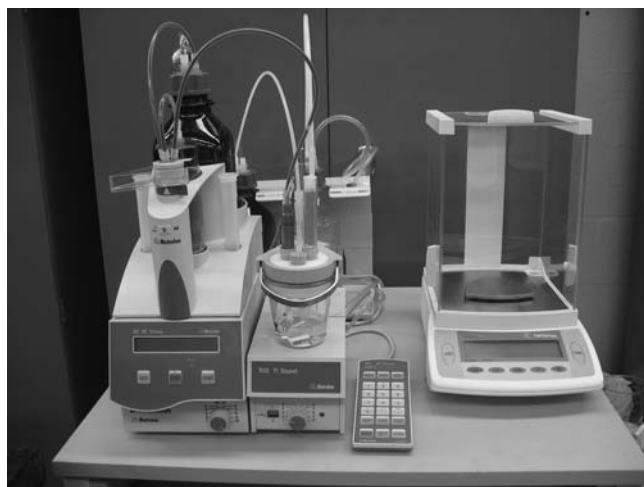


Figure 24.5—KF titrator.

24.4.4 Thermogravimetric Analysis for ISO 23556

Thermogravimetric analysis (TGA) is an analytical method used to determine minute changes in weight in relation to a change in temperature. This analysis relies heavily on precise measurements in weight, temperature, and temperature change rate. This method is used to determine

a material's thermal stability and its fraction of volatile components (i.e., soot content) by monitoring the weight change that occurs as the specimen is heated. Usually, TGA is performed in an air (oxygen) and inert gas mixture with a linear temperature ramp. A maximum temperature is selected so that the specimen weight is stable at the end of the experiment, implying that all of the carbon is burnt off, leaving only metal oxides. This approach provides the ash content (residual mass) and oxidation temperature. The TGA method is also commonly used to determine the soot content (percentage) in a sample. A typical TGA graph is shown in Figure 24.6.

24.5 FUEL FILTRATION TEST METHODS

24.5.1 SAE J905—Fuel Filter Test Methods [8]

The purpose of SAE J905 is to provide standardized methods for evaluating the performance characteristics of fuel filters by bench test methods. This method is an older method, but it is still used by many in the automotive industry because of the large database generated over the years of use. Chapter 2 uses gravimetric analysis to provide efficiency and capacity values for the fuel filters. A more current method discussed later in this chapter uses online particle counting to determine the efficiency of the filter at a particular particle size. For SAE and ISO test methods, no minimal performance requirements for filters have been specified because that is the requirement of the OEM and

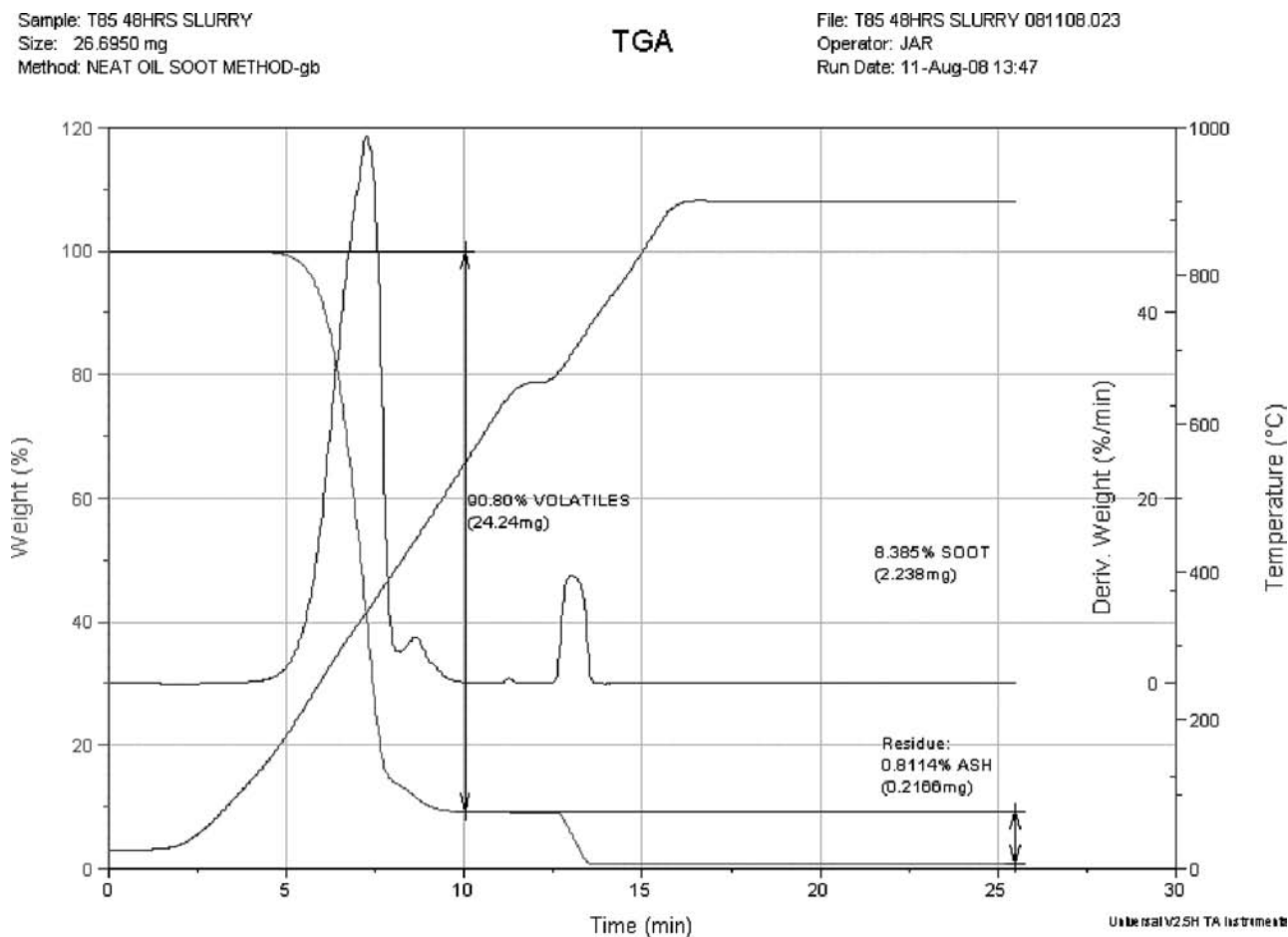


Figure 24.6—Example of actual TGA results.

user. Only the methods of determining, interpreting, and reporting performance characteristics are the proper province of this SAE Recommended Practice.

Separate chapters cover the test methods that are necessary to evaluate the several functional capabilities and mechanical properties of the filter. Each chapter is complete with recommended materials, apparatuses, and procedures for testing and evaluation. The chapters are as follows:

- *Chapter 1: Resistance to Flow* (Section 3)
- *Chapter 2: Filter Capacity and Contaminant Removal Characteristics* (Section 4)
- *Chapter 3: Media Migration Test* (Section 5)
- *Chapter 4: Collapse Test* (Section 6)
- *Chapter 5: Ability to Meet Environmental Conditions* (Section 7)
- *Chapter 6: Installation and Removal* (Section 8)
- *Chapter 7: Mechanical Tests* (Section 9).

24.5.2 ISO 4020 (Road Vehicles—Fuel Filters for Diesel Engines Test Methods) [9]

ISO 4020 is very similar to SAE J905 with multiple chapters to evaluate various filter parameters. These chapters include

- Test for Cleanliness of New Filters
- Fabrication Integrity Test
- Test for Differential Pressure of New Filters
- Test for Instantaneous Filtration Efficiency and Filter Life
- Test for Water Separation Efficiency
- Collapse/Burst Test of the Filter Element
- Burst Test of Complete Filters
- Pulsating Pressure Fatigue Test
- Vibration Resistance Fatigue Test

Although the chapter titles between ISO 4020 and SAE J905 may be the same or very similar, the test methods need to be compared to determine the differences among them. Industry is attempting to harmonize documents, therefore, it is the responsibility of the user to stay abreast of the methods.

24.5.3 SAE J1985—Fuel Filter Initial Single-Pass Efficiency Test Method [10]

SAE J1985 determines the efficiency of the fuel filter at various particle sizes using online particle counting. It uses ISO 12103-1 A2 fine test dust as the dust challenge. As the name implies, the contaminated fuel is passed through the filter only one time. A clean-up filter is typically used downstream of the test filter to remove any contaminant not removed by the test filter.

24.5.4 SAE J1488—Emulsified Water/Fuel Separation Test Procedure [11]

Why are fuel/water separators needed in the automotive industry? Water in fuels is one of the major causes of diesel engine maintenance problems. The effects of water in fuel are characterized by corrosion of fuel system parts; plugging of filters and orifices; and, in some cases, failure of fuel injection equipment. Water in fuel often dissolves sulfur compounds, becomes acidic, and enhances corrosion in fuel injection systems as well as in the engine itself. The presence of water also encourages microbiological growth, which generates orifice- and filter-restricting sludge. Furthermore, because of displacement of fuel lubrication in close tolerance injector parts and rapid expansion of heated

water at the fuel injector tip, galling and more serious failure may also occur. With the automotive and heavy-duty industry moving toward high-pressure common rail fuel systems, the removal of free water will become more important.

The SAE J1488 emulsified water/fuel separation test method is a severe evaluation of the fuel/water separator's capabilities. The test filter is challenged with finely dispersed water that is approximately 10–15 μ m in mean droplet size. The fuel/water separator is challenged with a 2500-ppm emulsion, and samples are obtained upstream and downstream to determine the water removal efficiency. The emulsion is generated using a 3500-r/min centrifugal pump. The test is performed for 150 min with the time-weighted efficiency reported.

Several variables exist that create differences in results, including IFT of the fuel, suitability of the fuel, lubricity and corrosion inhibitor additives, biodiesel fuels, and the crude source (other additives and surfactants). All of these parameters affect the water droplet distribution and coalescing properties. The SAE Filter Test Methods Committee is working with the industry to develop a reference diesel fuel to allow direct performance comparison between fuel/water separators. Currently, nothing has been developed that properly simulates diesel fuel fuel/water separation characteristics.

24.5.5 SAE J1839—Coarse Droplet Water/Fuel Separation Test Procedure [12]

SAE J1839 is relevant to coarsely dispersed water separation devices whether applied on the suction or discharge side of engine fuel transfer pumps. This procedure recommends pressure-side location of the test unit for ease and convenience of testing only. A water dispersing technique simulating the water droplet sizes experienced drawing fuel/water mixtures through fuel lines and fittings (180–260 μ m mean droplet size) is used to reproduce field conditions in which coarse droplets predominate. The test method is performed essentially the same as described in SAE J1488; the only difference is emulsified water challenge versus coarse water challenge.

24.5.6 ISO/TS 13353—Diesel Fuel and Petro Filters for Internal Combustion Engines—Initial Efficiency by Particle Counting, Retention Capacity and Gravimetric Efficiency (Withdrawn) [13]

The technical specification specified a test procedure for evaluating the initial efficiency, the efficiency evolution during clogging, and the retention capacity of a fuel filter for internal combustion engines. This test method is no longer valid and has been replaced with ISO 19438—Diesel Fuel and Petro Filters for Internal Combustion Engines—Filtration Efficiency Using Particle Counting and Contaminant Retention Capacity.

24.5.7 ISO 19438—Diesel Fuel and Petro Filters for Internal Combustion Engines—Filtration Efficiency Using Particle Counting and Contaminant Retention Capacity [14]

This international standard specifies a multipass filtration test method, with continuous contaminant injection, using online particle counting meeting ISO 11171 and 11943

specifications, for evaluating the performance of diesel and petroleum fuel filters. The test method determines the capacity or life of the filter, the particle efficiency at various particle sizes, and the differential pressure. The test method uses ISO 12103-1 A3 medium test dust and MIL-H-5606 hydraulic fluid as the test fluid.

24.5.8 SAE J2793—Fuel Dispensing Filter Test Method [15]

SAE J2793 is a new test method being developed for fuel dispensing pumps. The objective of this test method is to determine particle efficiency, capacity, and media migration for dispensing filters using gasoline, ethanol, diesel, and biodiesel-type fuels. ISO 19438 will be used to determine the particle removal efficiency and filter life. Because these types of filters will often use super absorbent polymers (SAPs) to remove free water, this test method will incorporate new methodologies to determine SAP media migration.

24.5.9 ISO/TS 16332—Diesel Fuel Filters—Method for Evaluating Fuel/Water Separation Efficiency [16]

This technical specification specified a fuel/water test method to evaluate the water removal characteristics of automotive and heavy-duty diesel fuel systems. Whereas SAE specifies two separate test methods for emulsified and coarse water droplets, ISO/TS 16332 incorporates both methods into one document. This method is designed to replace ISO 4020, Section 6.5.

ISO/TS 16332 is attempting to develop a test method that incorporates more real-world parameters that include lower IFT values (15 mN/m) and generate the water emulsion using an orifice plate. As with the SAE Filter Test Methods Committee, ISO TC 22/SC7/WG1 is working with the industry to develop a reference diesel fuel to allow direct performance comparison between fuel/water separators. Currently, nothing has been developed that properly simulates diesel fuel fuel/water separation characteristics.

24.5.10 SwRI Wear Index [17]

The SwRI Wear Index was developed through a cooperative research and development project involving diesel engine and filter manufacturers. The goal was to develop a methodology to improve differentiating between fuel filters that correlate to real-world applications. This method is able to better rate fuel filters because it includes the real-world operating parameters of vibration, diesel fuel, and heat. This provides a realistic challenge for the fuel filters. The test engine is shown in Figure 24.7.

The Wear Index is a test method that evaluates the filtration performance for a fuel filter or fuel filtration system using real-world operating conditions. A Caterpillar 3406E test engine is used to provide the vibration and heat generated during steady-state operations. Diesel fuel is used as the test fluid with ISO 12103 A3 medium test dust used as the particulate challenge. The test engine is operated at 1210 r/min with the inlet fuel temperature maintained at 90°F. Online particle counting is used upstream and downstream of the test filtration system.

The test filtration system upstream particulate challenge is maintained at 450 ± 50 counts/mL at 10 mm (c).

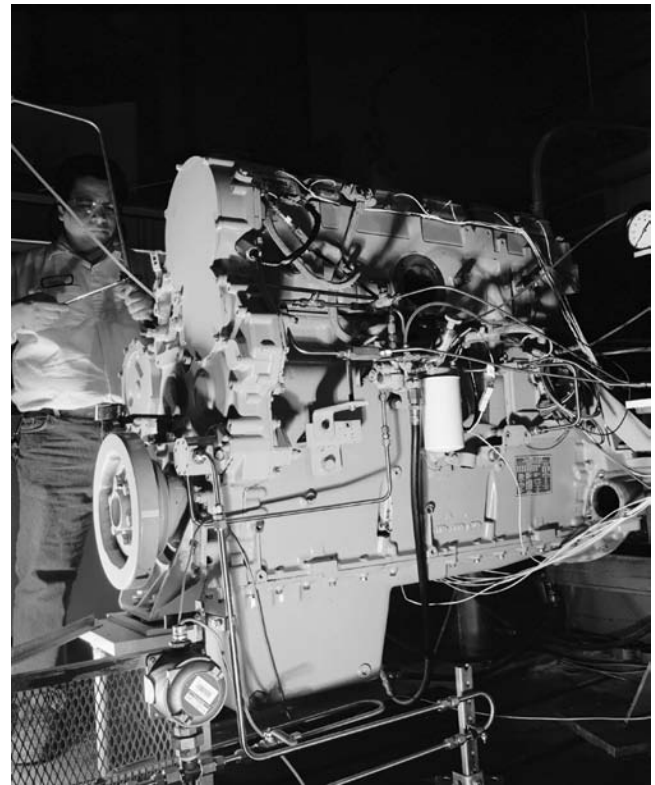


Figure 24.7—Wear Index test engine.

The effluent particle counts at 6, 10, and 14 mm (c) are obtained every 5 min inserted into the Wear Index formula

$$\text{Wear Index} = (14 * X + 71.13 * (Y)^2 + 112.6 * (Z)^3) / 1,000,000 \quad (24.1)$$

where:

$X = \geq 6$ m (c) counts/100 mL,

$Y = \geq 10$ m (c) counts/100 mL, and

$Z = \geq 14$ m (c) counts/100 mL

The Wear Index is determined for 25 datapoints that are averaged and reported as the Wear Index for the filtration system. A Wear Index value of 2 or less is the minimum value that would protect a unit injector fuel system.

Why is this method better than the standardized test methods? The incorporation of vibration provides the largest impact. As shown in Table 24.1, particle count data illustrate the difference between vibration and no vibration using the same test fuel filter.

To verify that the Wear Index test method provides a realistic operational environment, the two test engine vibrations were compared with the vibration generated by a Caterpillar 3406 operating during on-highway operations. To measure the vibration spectra on the fuel filters, three accelerometers were mounted orthogonally on the fuel filter assemblies. The vibration measurements were gathered for frequencies ranging up to 5000 Hz with a bandwidth resolution of 2 Hz. Figure 24.8 provides a summary of the data verifying that the test engines are generating vibration profiles similar to what would be experienced on the highway.

TABLE 24.1—The Effects of Vibration on Filtration Performance						
Time (h)	Engine Mounted Filter—Vibration			Isolated Filter—No Vibration		
	6 μm (c)	10 μm (c)	14 μm (c)	6 μm (c)	10 μm (c)	14 μm (c)
5	254,496	10,996	648	162,052	5704	200
10	272,980	17,120	1212	191,076	8164	376
15	233,468	16,464	1188	170,536	8392	648

24.6 OIL FILTRATION TEST METHODS

24.6.1 ISO 4548—Methods of Test for Full-Flow Lubricating Oil Filters [18]

For internal combustion engines, this specification provides a way of measuring full-flow oil filter performance. The standard is broken into several different sections or parts. Refer to the standard for test rig diagrams for each specific test. Note that Parts 8 and 10 are obsolete from the standard.

- *Part 1—Differential Pressure/Flow Characteristics:* This test is performed across the complete filter assembly at all ranges of possible flow rates. At engine rated flow, the difference between inlet and outlet pressure should not exceed a customer-specified ΔP .
- *Part 2—Element Bypass Valve Characteristics:* The purpose of a filter bypass valve is to ensure an adequate supply of oil to the engine, especially in the event of

filter plugging or cold-start conditions. To prevent dirty, unfiltered oil from entering the engine, a typical bypass valve is designed to only open under a certain ΔP , as specified by the customer.

- *Part 3—Resistance to High Differential Pressure and Elevated Temperature:* Because a full-flow filter will build restriction over time, this test is meant to simulate this restriction by subjecting the full-flow filter to high differential pressures and elevated temperatures.
- *Part 4—Initial Particle Retention Efficiency, Life, and Cumulative Efficiency:* Using the gravimetric method, the initial particle retention efficiency (probable retention efficiency for any particle size can be derived) for the full-flow filter can be determined. This part of the standard also helps determine probable filter life and cumulative efficiency.

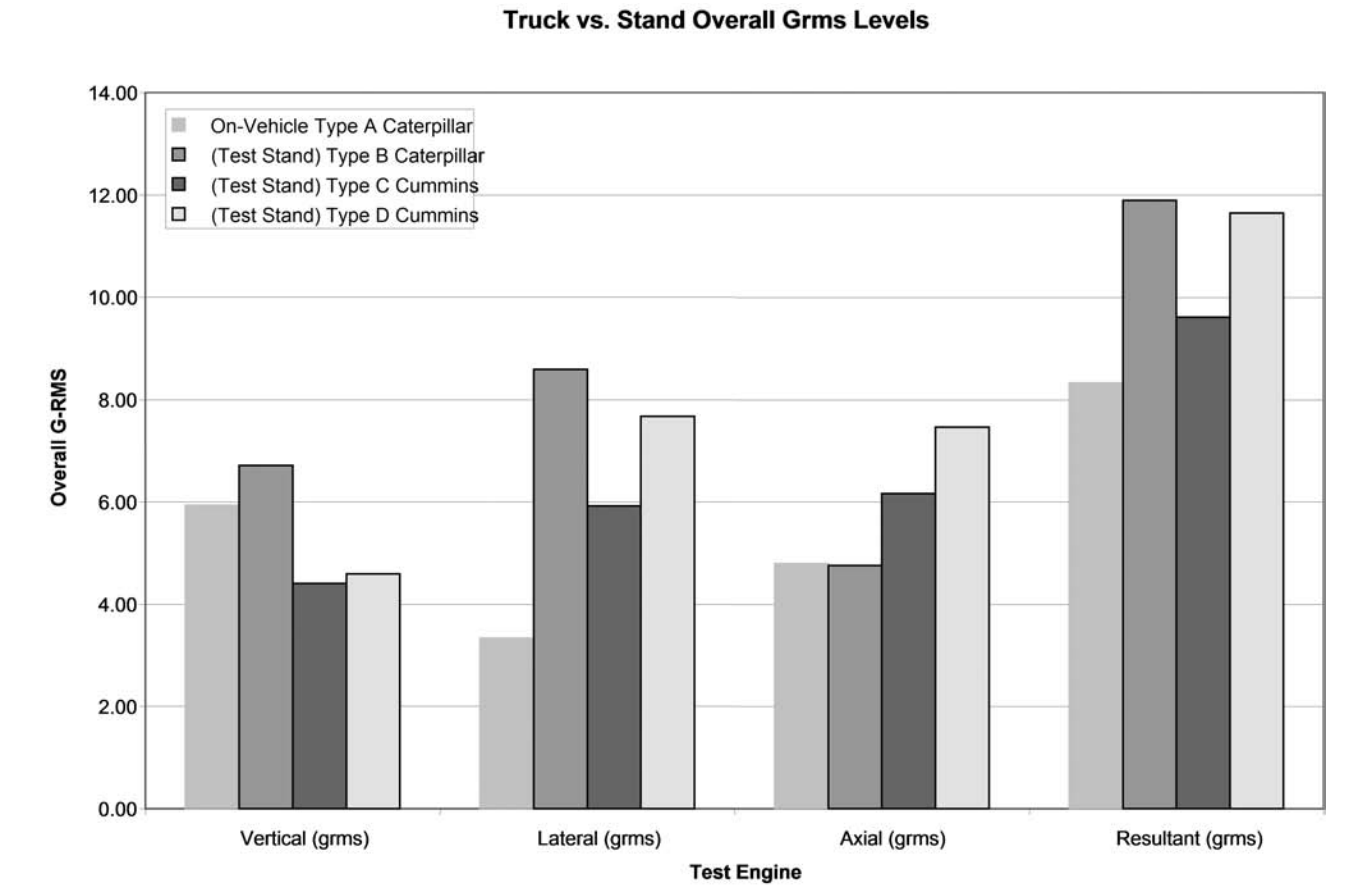


Figure 24.8—Vibration comparison between the laboratory and the field.

- *Part 5—Cold-Start Simulation and Hydraulic Pulse Durability Test:* During cold weather conditions, the engine oil is typically much thicker and exerts much higher pressure on the filtration system. This part of the standard simulates high-pressure surges and pressure variations experienced during cold engine starts by pressurizing the full-flow filter to higher-than-normal pressures for a given number of cycles. In addition, the filter must undergo a series of hydraulic pressure pulses for a customer-specified number of cycles.
- *Part 6—Static Burst Pressure:* This test is performed to determine the filter's ability to withstand burst pressure and determine probable failure modes. During accelerated life testing, an average filter burst pressure must be frequently determined before filter life acceleration factors can be applied.
- *Part 7—Vibration Fatigue Test:* To verify structural integrity of a new filter design or changes to a current design, the assembly must undergo vibration fatigue. A vibration sweep is performed first to determine the resonant frequency. If only one resonance exists, the part is vibrated at that frequency for a given amount of time or a number of cycles. If more than one resonance exists, the standard recommends using the one that gives the highest displacement. The peak input acceleration must be agreed upon between the engine and filter manufacturer.
- *Part 9—Inlet and Outlet Antidrain Valve Tests:* This part of the test specification measures the overall effectiveness of fitting an inlet/outlet antidrain valve to a full-flow filter assembly. The procedure describes methods of monitoring basic valve performance to serve as an antidrain back feature. It is only meant to monitor the performance of the valve itself within the full-flow filter.
- *Part 11—Self-Cleaning Filters (Continuous or Intermittent):* This part of ISO 4548 describes methods of monitoring filter element performance under customer-specified operating conditions and to measure its ability to withstand reversal of flow (backflush) and pressure/temperature variations. For self-cleaning filtration systems, the element is intended to be permanent.
- *Part 12—Contaminant Holding Capacity Using Particle Counting:* Part 12 of the standard details a full-flow filter multipass test. The intent is to develop a test rig with continuous contaminant injection and online particle counters. The results of the test are ΔP , overall contaminant capacity, and particulate removal characteristics. The test rig should also be designed with several test loops to cover all desired flow ranges.
- *HS 806, Section 6: Filter Capacity and Contaminant Removal:* This portion of the standard describes the method for measuring contaminant holding capacity and contaminant (dust) removal characteristics. This test can help determine filter life and total amount of contaminant removed by the filter (expressed in either capacity or efficiency).
- *HS 806, Section 7: Single Pass Particle Retention Capability Test:* For a specific size and size range of contaminant, this test determines the filter media percentage efficiency after a contaminant single-pass flow. Results are in test filter single-pass efficiency (%).
- *HS 806, Section 8: Media Migration Test:* The purpose of the media migration test is to measure the amount of inherent contaminant introduced by the filter itself. The test method requires flowing clean oil through the filter while catching all contaminants on a very fine wire cloth screen. The screen is then thoroughly washed with a prefiltered solvent and weighed to determine the amount of contamination.
- *HS 806, Section 9: Collapse Test:* The element collapse strength test is designed to ensure that a filter will not fail because of high differential pressures and cause a bypass. The test is performed by flowing contaminated (dust) oil through the filter until the element collapses or a specified ΔP is reached. The results should describe the maximum ΔP achieved, reasons for test termination (e.g., collapse), and post-test filter condition.
- *HS 806, Section 10: Inlet/Outlet Antidrain Valve Test:* If inherent to a full-flow filter, this test describes the method for measuring the performance of the inlet/outlet antidrain valve and its effectiveness to serve as an antidrain back feature.
- *HS 806, Section 11: Ability to Meet Environmental Conditions:* This test method details the evaluation of several environmental conditions such as the effect of water in the oil on filter capacity, the effect of high oil temperature on the integrity and collapse strength of the filter, oil additive removal tendencies of the filter (only for ash type additives), and the effect of low temperatures on filter gasket characteristics (simulating cold-start conditions).
- *HS 806, Section 12: Installation and Removal:* This test method measures how well the filter will remain sealed at the gasket during environmental conditions and normal operating vibrations.
- *HS 806, Section 13: Mechanical Tests:* To simulate real on-engine conditions, filters are subject to vibration fatigue, dynamic pressure impulse fatigue, and hydrostatic burst pressure strength. All parameters should correspond to actual engine data such as measured oil pressure and measured vibration data.
- *HS 806, Section 14: Relief Valve Performance:* The purpose of this performance test is to measure the full-flow filter relief valve leak rate, cracking pressure, and resistance to flow.

24.6.2 SAE HS 806—Oil Filter Test Procedure, Full-Flow Filters for Internal Combustion Engines [4]

This test method is meant to closely mimic the operating conditions of an in-service oil filter with several detailed tests:

- *HS 806, Section 5: Resistance to Flow:* This is a test to determine pressure drop/loss through a filter. It can also be used to determine flow capacities. The result of this test is a flow versus pressure loss curve.

24.6.3 SAE J1260—Standard Oil Filter Test Oil [19]

SAE J1260 is a short document that specifies all requirements for the oil that should be used in HS806 (above) and other standards.

24.6.4 SAE J1858—Full-Flow Lubricating Oil Filters Multipass Method for Evaluating Filtration Performance (Cancelled June 2003, Superseded by ISO 4548-12) [20]

SAE J1858 describes a multipass filter performance test with a continuous contaminant injection system. It also describes methods for determining filter contaminant holding capacity. The intent of this standard is to provide a method that will yield reproducible test results from laboratory to laboratory. This document has been harmonized with ISO 4548-12.

24.6.5 ISO/TS 23556—Performance Test Method for Diesel Engine Soot-Removal Devices in Lubricating Oils—Initial Filtration Efficiency [5]

This test method is intended to accelerate a soot draw-down test by adding a known concentration of soot dispersion at a given rate to clean engine oil. A bypass or full-flow filter is used to measure the time-rated efficiency of soot removal. TGA is used to determine changes in the soot content of the clean oil sump.

ACKNOWLEDGMENTS

The authors thank Southwest Research Institute and Cummins Filtration for allowing them to use company time and resources to generate this summary of liquid filtration tests and test methods. The authors also thank ASTM for including this topic in this book, and Ms. Rebecca Emmot and Ms. Dianna Barrera for editing and formatting the document.

References

- [1] Cummins Filtration, "Engine Lube System and Low Ash Oil," Available at http://www.cumminsfiltration.com/files/lube_training.pdf.
- [2] Hutzler, S.A., and Bessee, G.B., 2008, "The Effects of Biodiesel Fuels of Water Separation Performance in Diesel Fuel," Presented at World Filtration Congress 10, Leipzig, Germany, April 15–18.
- [3] ISO 12103-1: Road Vehicles—Test Dust for Filter Evaluation—Part 1: Arizona Test Dust, ISO, Geneva, Switzerland.
- [4] SAE HS 806: Oil Filter Test Method, SAE International, Troy, MI.
- [5] ISO/TS 23556: Performance Test Method for Diesel Engine Soot-Removal Devices in Lubricating Oils—Initial Filtration Efficiency, ISO, Geneva, Switzerland.
- [6] ISO 11171: Hydraulic Fluid Power—Calibration of Automatic Particle Counters for Liquids, ISO, Geneva, Switzerland.
- [7] ISO 11943: Hydraulic Fluid Power—On-line Automatic Particle-Counting Systems for Liquids—Methods of Calibration and Validation, ISO, Geneva, Switzerland.
- [8] SAE J905: Fuel Filter Test Methods, SAE International, Troy, MI.
- [9] ISO 4020: Road Vehicles—Fuel Filters for Diesel Engines—Test Methods, ISO, Geneva, Switzerland.
- [10] SAE J1985: Fuel Filter—Initial Single Pass Efficiency Test Method, SAE International, Troy, MI.
- [11] SAE J1488: Emulsified Water/Fuel Separation Test Procedure, SAE International, Troy, MI.
- [12] SAE J1839: Coarse Droplet Water/Fuel Separation Test Procedure, SAE International, Troy, MI.
- [13] ISO/TS 13351: Diesel Fuel and Petro Filters for Internal Combustion Engines—Initial Efficiency by Particle Counting, Retention Capacity and Gravimetric Efficiency (Withdrawn), ISO, Geneva, Switzerland.
- [14] ISO 19438: Diesel Fuel and Petro Filters for Internal Combustion Engines—Filtration Efficiency Using Particle Counting and Contaminant Retention Capacity, ISO, Geneva, Switzerland.
- [15] SAE J2793: Fuel Dispensing Filter Test Method, SAE International, Troy, MI.
- [16] ISO/TS 16332: Diesel Fuel Filters—Method for Evaluating Fuel/Water Separation Efficiency, ISO, Geneva, Switzerland.
- [17] Bessee, G., 2001 "Wear Index Test Method," Presented at the Fourth International Filtration Conference, San Antonio, TX, January 16–18.
- [18] ISO 4548: Methods of Test for Full-Flow Lubricating Oil Filters for Internal Combustion Engines, ISO, Geneva, Switzerland.
- [19] SAE J1260: Standard Oil Filter Test Oil, SAE International, Troy, MI.
- [20] SAE J1858: Full-Flow Lubricating Oil Filters Multipass Method for Evaluating Filtration Performance (Cancelled June 2003, Superseded by ISO 4548-12), SAE International, Troy, MI.

Dynamic Friction Characterization and Modeling of Tripod Constant Velocity Joints

Chul-Hee Lee¹ and Andreas A. Polycarpou²

NOMENCLATURE

a	half-width of elliptical or line contact
b	transverse contact width of elliptical contact
BCD	ball circular diameter at the housing-end view
c_{si} ($i = 1-9$)	empirical constant coefficients in static friction model, eqs. 25.8 and 25.9
c_{di} ($i = 1-2$)	empirical constant coefficients in dynamic friction model, eq. 25.11
F_x, y, z	measured triaxial friction forces inside of CV joint
GAF	generated axial force
l	transverse contact width of line contact
n	number of pade trunnions
P	resultant normal force inside of the CV joint (in housing coordinates)
P_n	general contact normal load
Q	resultant friction force inside of the CV joint (in housing coordinate)
R	combined radius in the direction of rolling
R_c	contact radius from the CV joint center
R_s	slip ratio
T_d	CV joint applied torque
α	hysteresis loss factor
β	CV joint articulation angle
φ	CV joint rotational phase angle
λ	pure rolling friction coefficient
μ	friction coefficient
μ_{avg}	average friction coefficient
μ_{dyn}	dynamic friction coefficient
$\mu_{dyn,in}$	positive dynamic friction coefficient (inward direction)
$\mu_{dyn,out}$	negative dynamic friction coefficient (outward direction)
μ_{GAFi}	GAF friction coefficient model at a trunnion
μ_{res}	resultant friction coefficient combining the three trunnions
$\mu_{S/R}$	slip-to-roll friction coefficient
μ_{slp}	pure sliding friction coefficient
μ_{sta}	CV joint static (or stationary) friction coefficient
μ_{tot}	total CV joint internal friction coefficient
$\mu_{tot,in}$	total CV joint internal friction coefficient (inward direction)
$\mu_{tot,out}$	total CV joint internal friction coefficient (outward direction)

25.1 INTRODUCTION

Constant velocity (CV) joints are an integral part of modern vehicles. CV joints exhibit superior vibration performance

compared with universal joints because they eliminate uneven rotating torque via their self-centering ability. CV joints provide coupling forces and moments between connected substructures as well as localized damping dissipation [1,2]. In modern vehicles, CV joints have become a standard design of driveshaft for front-wheel-drive (FWD) passenger cars. Figure 25.1 shows a typical FWD configuration in a vehicle with driveshaft installations. Each driveshaft comprises two types of CV joints—namely fixed (outboard) and plunging (inboard) types—connected via a shaft, and their primary function is to transmit the engine torque to the wheels with CV. In this work, the emphasis is on a class of plunging CV joints called tripod CV joints, as shown in Figure 25.2, which have been especially favored for automatic transmission vehicles. This is because of their noise and vibration advantages because they offer lower plunging resistance compared with ball-type joints [1]. Note that tripod CV joints also fulfill the conditions of CV operation [1].

Although CV joints are standard design components attached to torque-transmitting shafts in vehicles, there are certain aspects of their friction and contact dynamics that are not understood or modeled. For example, a main CV joint-related problem in vehicles is the so-called “take off shudder,” which occurs when a vehicle moves abruptly. This problem is related to the internal friction in a CV joint, which consequently generates an axial force known as generated axial force (GAF). Another problem causing undesirable vehicle vibration is what is referred as “idle boom,” which is due to the fact that the plunging joint is directly connected to the transmission, which is excited by the engine, and there is a transfer of vibration to driveshafts via the CV joints [2].

Extensive testing with all new model vehicles is undertaken to avoid potential vehicle problems, which lead to longer and costly development periods. Better understanding of the nonlinear dynamic friction behavior of CV joints and the development of a CV joint friction model can provide powerful design tools and shorter development efforts. Current research in modeling CV joint effects on vehicle performance assumes constant empirical friction coefficient values [4]. However, such models are long known to be inaccurate, especially under dynamic conditions, which is the case for tripod CV joints [5]. High-speed and sport utility vehicles with large joint articulation angles demand lower plunging friction inside of their CV joints to meet noise and vibration requirements, thus requiring a more thorough understanding of their internal friction characteristics and mechanisms.

¹ Inha University, Incheon, Korea

² University of Illinois at Urbana-Champaign, USA

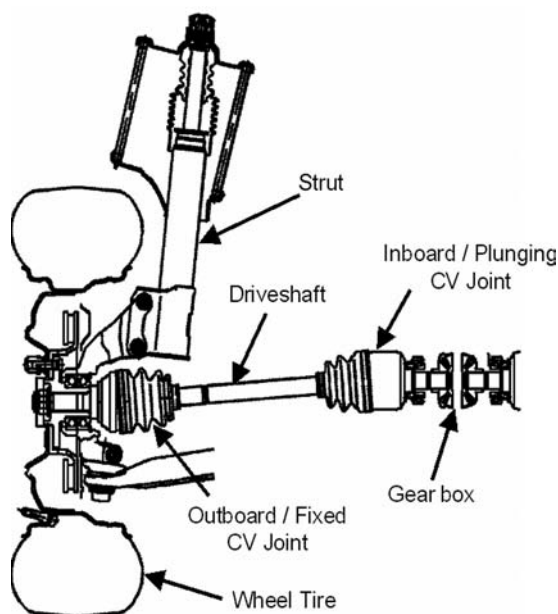


Figure 25.1—FWD configuration showing typical CV joints in a vehicle.

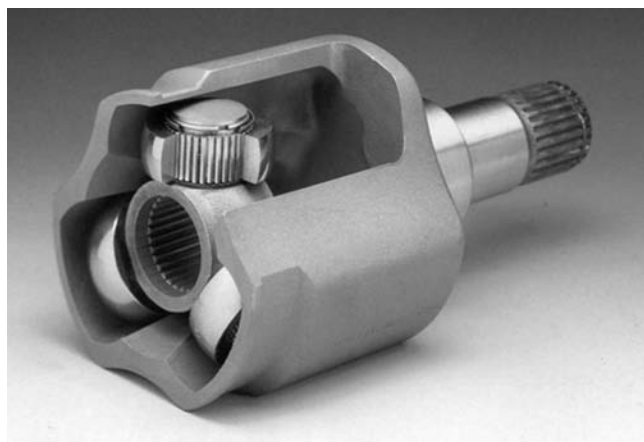


Figure 25.2—Typical tripod CV joint [3].

In this research, a prototype advanced and well-instrumented CV joint apparatus was designed and constructed to experimentally measure the internal friction in CV joints under simulated vehicle operating conditions and correlate them with the externally and readily measured GAF. A unique feature of the apparatus is that an actual CV joint is retrofitted with a three-axis piezoelectric force transducer for in situ measurements of the internal CV joint friction and normal forces. By using the designed experimental setup, detailed experiments were conducted under different realistic operating conditions of oscillatory speeds, CV joint articulation angles, lubrication, and torque. The obtained experimental data were used to develop a physics-based semiempirical CV joint internal friction model as a function of different CV joint operating parameters. In addition, the proposed friction coefficient model was used to develop a model for the GAF. On the basis of the friction and GAF models, one can establish a better understanding of CV

joint friction and use these models for designing vehicle components with improved performance.

25.2 EXPERIMENTAL SETUP

25.2.1 CV Joint Apparatus

Because of the importance of CV joints as well as their complexity, specialized CV joint apparatuses have been presented in the literature to measure different aspects of CV joint behavior. For example, Philpott et al. [6] developed a tester and implemented a two-phase surface fitting regression algorithm to quantify the racetrack wear in ball-type CV joints. Bierman [7] designed an apparatus to accurately measure the efficiency of CV joints by recording power and heat losses. Kernizan et al. [8] developed a tester to assess the performance of grease by measuring the temperature rise in CV joints. Jia et al. [9] investigated the dynamic performance of tripod-type CV joints and designed an experimental tester to measure the effect of the clearance on their dynamic response. Watanabe et al. [10] conducted kinematic and static analyses of tripod CV joints, especially for spherical-end spider-type joints. Kochersberger [11] patented an apparatus to detect defects in CV joints by measuring irregular vibration patterns during CV joint operation. Despite these advances in measuring CV joint parameters, none of these works directly measures internal CV joint friction, and this is what was undertaken in the study presented here. In this research, an advanced well-instrumented CV joint apparatus to experimentally investigate the internal friction in CV joints is presented. Specifically, an instrumented CV joint apparatus was designed and constructed that is capable of testing actual CV joints to measure their internal friction characteristics under simulated vehicle operating conditions. The test apparatus and instrumentation used in this work is described in detail in Lee and Polycarpou [12].

Figure 25.3 shows a photograph of the CV joint friction measurement apparatus. The apparatus uses actual CV joint assemblies and consists of dynamic sliding and height adjustment mechanisms and a static torque generator. The sliding motion and height/angle adjustment mechanism was designed to provide a plunging motion (stroke) using a linear actuator and a servomotor control drive. The linear plunging motion was controlled by a linear brushless servocontroller using programmable-logic-control and programmed sequential codes. A fixture was also designed to directly attach the ball joint part of the CV joint assembly to the linear actuator. This fixture can adjust the height of one of the ends of the CV joint, thus being able to change the CV joint articulation angle, which is a major factor affecting the plunging joint friction during tests. In actual vehicles, this mechanism simulates the articulation angle and plunging motions in the CV joint due to wheel bouncing as well as steering motion and engine movement. The apparatus can supply a maximum articulation angle of 15° , a plunging force of 100 N, and a maximum oscillation frequency of 25 Hz.

The static torque is applied manually with a hand crank and gear box mechanism to simulate the abrupt start of vehicles. It uses a worm gear mechanism and a reduction gear with a flexible coupling. The design is such that it can generate a maximum static torque of 1000 Nm, which covers the maximum torque applied to each driveshaft at the maximum engine torque by using the reduction gear

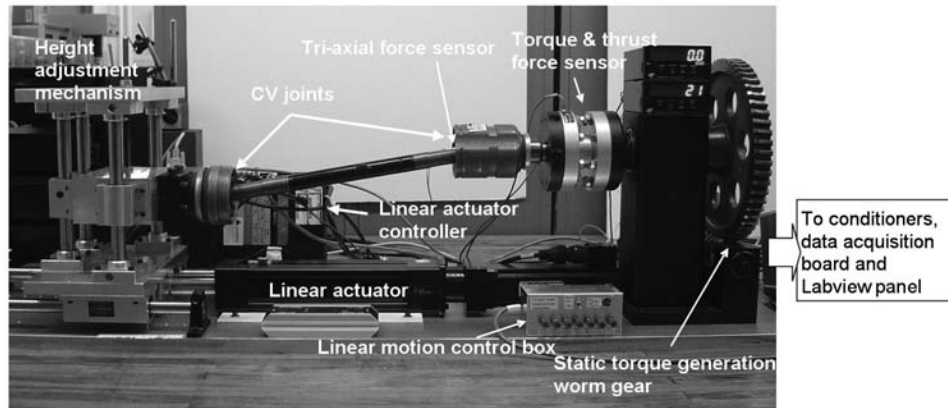


Figure 25.3—Photograph of CV joint friction measurement apparatus.

box. This mechanism was also used to attach the tripod joint to the static torque generator. The applied torque and generated thrust force are measured directly using a dual force/torque strain gage transducer attached between the CV joint and the torque mechanism. Thus, the apparatus is capable of conducting controlled experiments to measure the internal and external friction of actual CV joints.

25.2.2 Instrumentation Development

In typical CV joint tests, CV joint friction is typically measured externally using a thrust load cell at the end of the CV joint. However, the complexities of the sliding and rolling interfaces in a typical tripod CV joint are such that the overall external axial force is inadequate to reveal details of the internal CV joint forces, including friction. To this extent, and to directly measure the internal friction components during the experiments, a triaxial force transducer was installed inside of the spider assembly as shown in Figure 25.4. A possible concern in this triaxial force transducer design was the crosstalk between each orthogonal force axis, which was measured and in all cases found to be less than 2 %. The force transducer assembly accurately measures the internal frictional forces that occur along each axis of the CV joint. On the basis of its method of attachment, one of the transducer output directions is exactly parallel to the shaft axis. Thus, the directions of the three orthogonal axes of measurement were precisely known at any instance during an experiment.

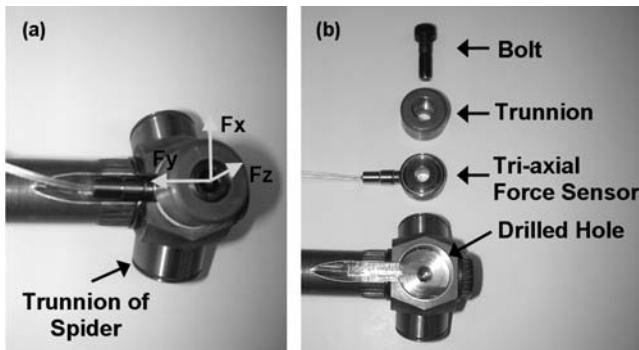


Figure 25.4—Installation of triaxial force transducer inside of a CV joint: (a) assembled and (b) disassembled.

Once all of the different apparatus components were designed, constructed, and assembled, they were accurately aligned using a digital level gage. Subsequently, a Labview® master control program was designed and implemented. Such a master control program provides accurate triggering and synchronizing of the apparatus components and at the same time precisely captures and digitally records all measurements. The linear actuator, which generates the force to linearly move the CV joint, is controlled by the computer via a drive/controller. To precisely measure the torque applied to the CV joint with the static torque generator, a two-axis strain-gage force/torque sensor was installed, and the outputs were displayed on digital meters and fed to the computer for digital recording. The thrust GAF force output, which is typically measured in such experiments, represents the combined CV joint frictional and other internal forces. The internal triaxial friction forces were measured directly using the embedded force transducer. Moreover, the linear motion information from the encoder, which is part of the servomotor and linear actuator, in the form of displacement and velocity were also recorded. Thus, the instrumented CV joint apparatus enables the measurement of key performance parameters, such as internal friction forces inside of a CV joint, and under different realistic operating conditions.

25.3 MEASUREMENT OF FRICTION

25.3.1 Experimental Procedure

A fully assembled tripod CV joint was securely installed on the apparatus using a machined spline on the side of the height adjustment mechanism and a tight-fit clamping interference with a key on the side of torque/thrust force sensor (see Figure 25.3). The ball-joint side of the CV joint is clamped to the apparatus using a machined spline whereas the tripod-joint side is clamped using a tight-fit interference with secure clamping. After secure clamping, the CV joint angular position was articulated to a specified angle by adjusting the static height mechanism and verifying the articulation angle using a precise digital level gage. Because the tests were under loaded conditions, a static torque was applied to the CV joint using the worm gear mechanism. The preset static torque values were measured on the digital display of the torque transducer with typical values used in this work being up to 160 Nm.

Once the CV joint assembly was secured and adjusted on the apparatus, dynamic experiments were performed by plunging the CV joint two full cycles of ± 15 mm from the joint center position with a velocity of 2 mm/s. The 30-mm travel distance is typical in actual automotive CV joints and simulates the wheel bouncing and steering motions. Experiments were repeated at two different extreme articulation angles: $\beta = 0^\circ$ representing idealistic conditions with minimal internal friction and GAF and $\beta = 15^\circ$ representing aggressive conditions with significant CV joint friction and GAF. Experiments were performed under grease-lubricated conditions with two types of grease (designated as greases A and grease B) as well as under dry conditions to simulate extreme cases. The greases used in this research are typical CV joint greases used in North American vehicles, and their properties are summarized in Table 25.1. Both greases are polyurea-thickened greases with different additives; grease A contains organomolybdenum and is designed to have better friction performance whereas grease B contains solid extreme pressure (EP) additives for enhanced durability. The greases can also be classified as containing chemical (grease A) and physical (grease B) additives [12]. All experiments were performed under laboratory conditions at a temperature of 22.5°C and a relative humidity of 45 %.

During the experiments, the in situ internal triaxial CV joint forces were measured using the embedded triaxial

TABLE 25.1—Properties of Typical CV Joint Greases Used in This Study

Properties	Grease A	Grease B
Type	Polyurea	Polyurea
NLGI grade	2	2
Base oil	Mineral/synthetic	Mineral
Viscosity at 100°C , η (mPa·s)	12	12
Representative additives	Organomolybdenum	Solid EP
Color	Green	Blue

force transducer and designated as F_x , F_y , and F_z . The applied torque and the axial thrust force were also recorded. The coordinates of the three orthogonal force components measured with the triaxial force transducer installed inside of the CV joint are depicted in Figure 25.5a, and further details of these force measurements can be found in reference [13]. F_x represents the measured normal force, also designated as P , and is directly related to the applied torque. F_y and F_z represent the axial and vertical friction forces, respectively, which are the source of the total combined friction force, Q . Figure 25.5b defines the CV joint rotational phase angle ϕ from the housing-end view.

25.3.2 CV Joint Friction Coefficient

As shown in Figure 25.6, from the measurement of internal friction forces, one can calculate the net friction coefficient at the CV joint by the following equation:

$$\mu = \frac{Q}{P} = \frac{F_y \cos \beta + F_z \sin \beta}{F_x} \quad (25.1)$$

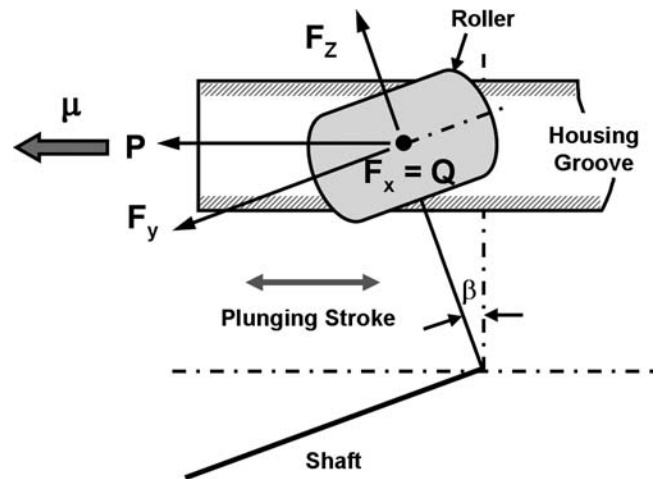


Figure 25.6—Internal friction forces and friction coefficient at a single trunnion inside of a tripod CV joint.

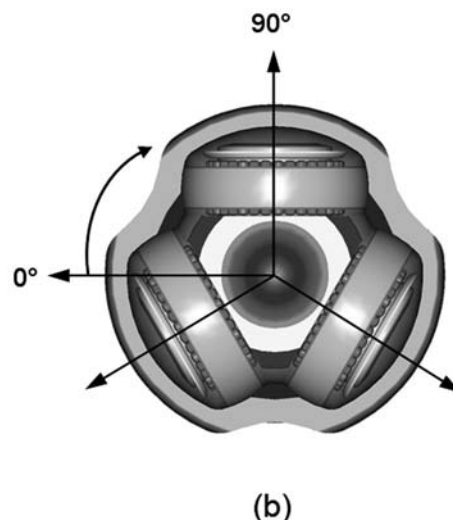
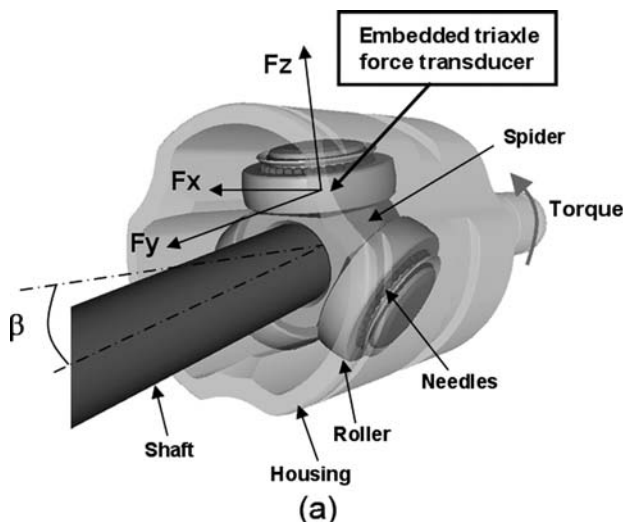


Figure 25.5—Definitions used in tripod CV joint friction measurements: (a) orthogonal triaxial force coordinates and (b) rotational phase angle.

where β is the CV joint articulation angle, as also depicted in Figure 25.5a. Notice that this equation is only valid when the trunnion with the triaxial force sensor is in the top position, which is defined as 90° of the rotational phase angle φ in Figure 25.5b.

Thus, to calculate the internal friction coefficient that is present under all CV joint conditions, one needs to find a universal equation to cover all articulation angles and rotational phase angles. This is accomplished by introducing a coordinate transformation matrix on the basis of Euler angles representing articulation angle β and rotational phase angle φ . Using the defined coordinates of the

triaxial forces shown in Figure 25.5a, one can obtain the combined rotational transformation matrix by performing rotation α first, articulation β second, and rotation $-\alpha$ third as illustrated in Figure 25.7. If the measurement of friction forces occurs at a 210° phase, by following steps a, b, and c in Figure 25.7, one can finally position the triaxial force components to be aligned to the housing coordinates. By multiplying each individual transformation matrix and replacing α with $\varphi = 90^\circ$ in sequence, the following equation that relates the measured internal forces to the global forces in accordance with the housing coordinate can be obtained:

$$\begin{bmatrix} F_x''' \\ F_y''' \\ F_z''' \end{bmatrix} = \begin{bmatrix} \cos^2(\varphi - 90^\circ) + \cos\beta \sin^2(\varphi - 90^\circ) & -\sin(\varphi - 90^\circ)\sin\beta & \cos(\varphi - 90^\circ)\sin(\varphi - 90^\circ)[-1 + \cos\beta] \\ \sin(\varphi - 90^\circ)\sin\beta & \cos\beta & \cos(\varphi - 90^\circ)\sin\beta \\ \cos(\varphi - 90^\circ)\sin(\varphi - 90^\circ)[-1 + \cos\beta] & -\cos(\varphi - 90^\circ)\sin\beta & \cos^2(\varphi - 90^\circ)\cos\beta + \sin^2(\varphi - 90^\circ) \end{bmatrix} \begin{bmatrix} F_x \\ F_y \\ F_z \end{bmatrix} \quad (25.2)$$

Thus, by using the relationship of eq. 25.1, one can calculate the net friction coefficient along the housing groove using the following relationship:

$$\mu = \frac{Q}{P} = \frac{[\sin(\varphi - 90^\circ)\sin\beta]F_x + [\cos\beta]F_y + [\cos(\varphi - 90^\circ)\sin\beta]F_z}{[\cos^2(\varphi - 90^\circ) + \cos\beta \sin^2(\varphi - 90^\circ)]F_x + [-\sin(\varphi - 90^\circ)\sin\beta]F_y + [\cos(\varphi - 90^\circ)\sin(\varphi - 90^\circ)[-1 + \cos\beta]]F_z} \quad (25.3)$$

25.3.3 Typical Experimental Results

Once the CV joint assembly was in place, friction measurements were conducted under various experimental conditions. To investigate experimental repeatability, several experiments under identical test conditions were performed and it was confirmed that the experiments were highly repeatable [12]. In the experiments reported herein, the rubber boot that seals the grease in a CV joint housing was removed for easy accessibility and visualization as well as to minimize additional sources of friction thus not included in the CV joint internal friction model.

Typical experimental data captured over two complete cycles (60 s) under 160-Nm static torque are depicted in Figure 25.8 at the two extreme articulation angles of 0° and 15° . As shown in Figure 25.8a, which depicts the CV joint stroke, the experiments start with the CV joint spider in the center position of the housing and continue with it moving inward and then outward in the housing for ± 15 mm at a 2-mm/s velocity. The static applied torque was constant during the experiment as shown in Figure 25.8b, except for small changes attributed to irregularities in the housing surface. Figure 25.8c shows the external thrust force acting

in the horizontal axial direction, which is the main force that affects the external friction force. For the case of $\beta = 0^\circ$, the thrust force is zero, implying zero external friction and zero GAF whereas for $\beta = 15^\circ$ the thrust force fluctuates significantly. The internal forces measured with the embedded triaxial force transducer on one of the spider legs (Figure 25.5a) are depicted in Figure 25.8, d–f. F_x is related to the normal force P and shows fluctuation depending on the direction of stroke motion. The main source of friction, the F_y force, is nominally constant at the articulation angle $\beta = 0^\circ$ and fluctuates with an amplitude of approximately 200 N at $\beta = 15^\circ$. F_z acts perpendicular to the CV joint shaft and is negative during the inward stroke, which means that the force is acting downward, or in compression in regards to the spider assembly whereas it is positive during the outward stroke at both articulation angles. By directly substituting the measured triaxial forces into eq. 25.3, the resultant friction force Q , normal force P , and friction coefficient μ were obtained and shown in Figure 25.8, g–i, respectively. As schematically explained in Figure 25.5b, 90° of the rotational phase angle normal force P (Figure 25.8h) is exactly the same as the force component F_x , and the

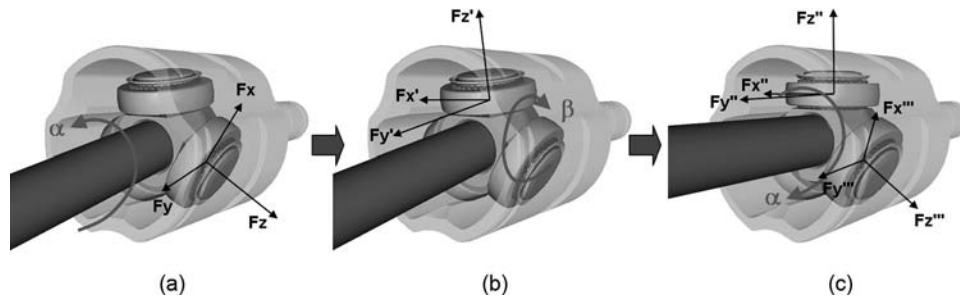


Figure 25.7—Coordinate transformation from the coordinate of triaxial force sensor to the housing coordinate.

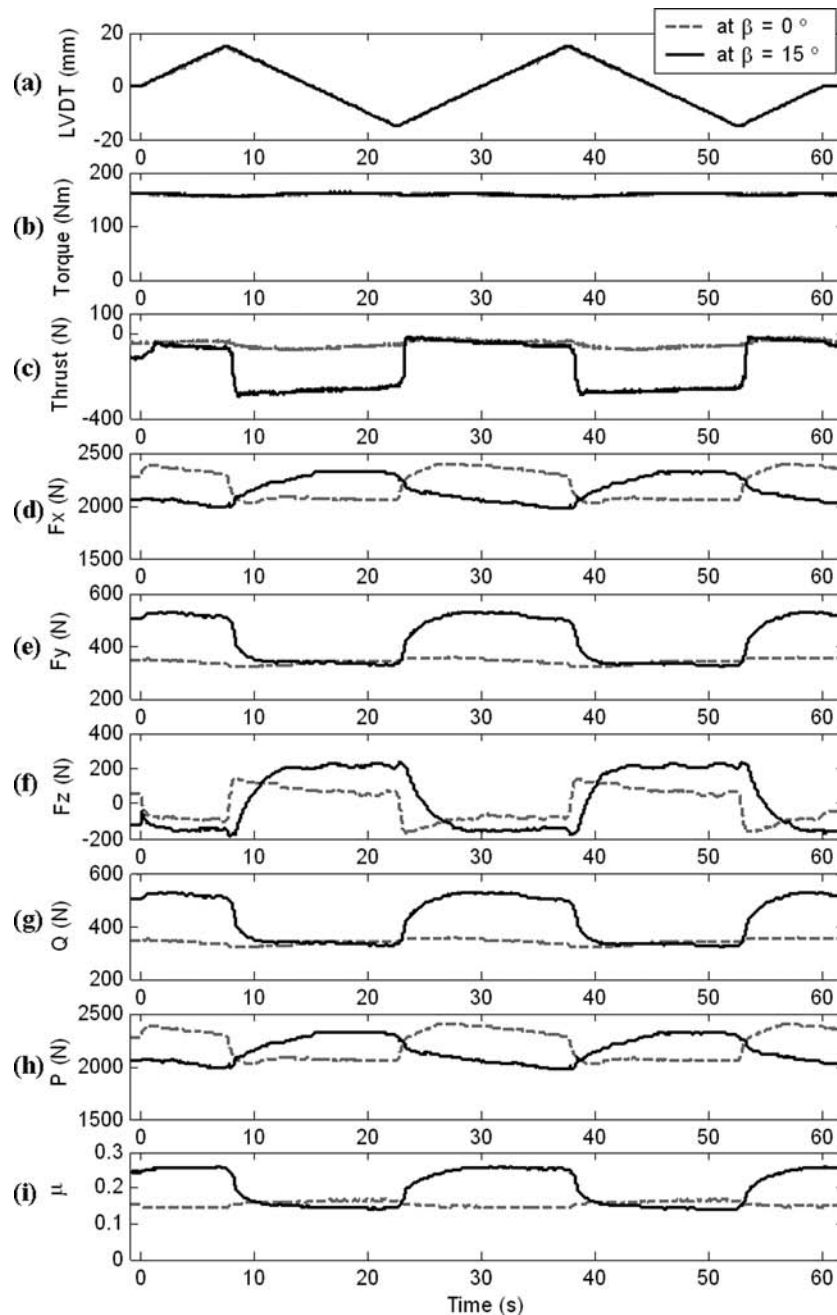


Figure 25.8—Typical measurement data during two CV joint strokes at two extreme articulation angles.

resultant friction force Q (Figure 25.8g) is the combination of the F_y and F_z force components. The large articulation angle of 15° shows the friction fluctuation, thus showing a larger variation of friction coefficient compared with the zero angle case, as shown in Figure 25.8i. The main source of this difference is due to the slippage of the roller because the rolling direction is different from the plunging direction when the CV joint is articulated. Thus, the slip ratio will be increased with increasing the articulation angle, which generates larger friction.

The measured friction coefficient versus stroke is plotted in Figure 25.9 for the two cases of extreme articulation angles presented in Figure 25.8. It is seen that the size of the hysteresis loops as well as the absolute mean value for

the resultant friction coefficient increase with the higher articulation angle of 15° . Moreover, the friction loops show that the inward stroke friction is more dependent on the articulation angle compared with the outward stroke friction. However, the friction loops never reach negative values during motion reversals. This seems counterintuitive because the friction coefficient is always positive even when motion is reversed. This is because that initial static friction exists because of significant torque loading, even before the stroking motion.

25.4 FRICTION CHARACTERIZATION

Under ideal conditions, a CV joint should only experience rolling motion without any sliding or slipping. However,

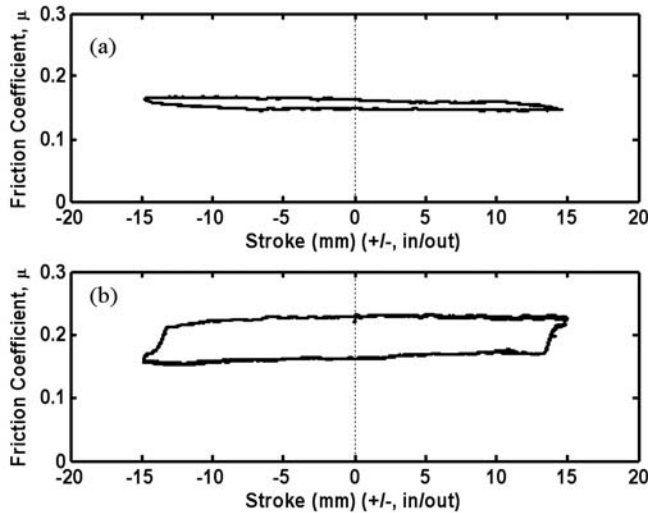


Figure 25.9—Comparison of internal friction coefficient loops (hysteresis) for two different articulation angles: (a) $\beta = 0^\circ$ and (b) $\beta = 15^\circ$.

sliding friction occurs due to kinematic effects at the articulation angles and because of microslip in the contact zone. Thus, the combination of sliding and rolling friction affects the friction performance in CV joints and needs to be better understood.

25.4.1 Slip-to-Roll Ratio

As discussed in the introduction, in addition to pure sliding friction, there is also rolling friction during CV joint operation. The slip-to-roll ratio between roller and housing is very important because (1) at $\beta = 0^\circ$, GAF is zero because the slip-to-roll ratio is zero (which means that all friction is due to rolling friction); and (2) as the CV joint angle increases, the GAF and the possibility for “shudder” increases. On the basis of the above argument, the slip-to-roll ratio must be increasing with increasing articulation angle, which is experimentally investigated.

To measure the slip-to-roll ratio, videorecording was performed using the CV joint apparatus, where part of the housing was cut open to videorecord the internal rolling motion of the roller, as shown in the inset of Figure 25.10. Thus, from several tests under different articulation angles, one can obtain the slip ratio, as depicted in Figure 25.10. The relationship between slip ratio (%) and articulation angle $\beta (^\circ)$ is approximately linear, described by the following simple relationship:

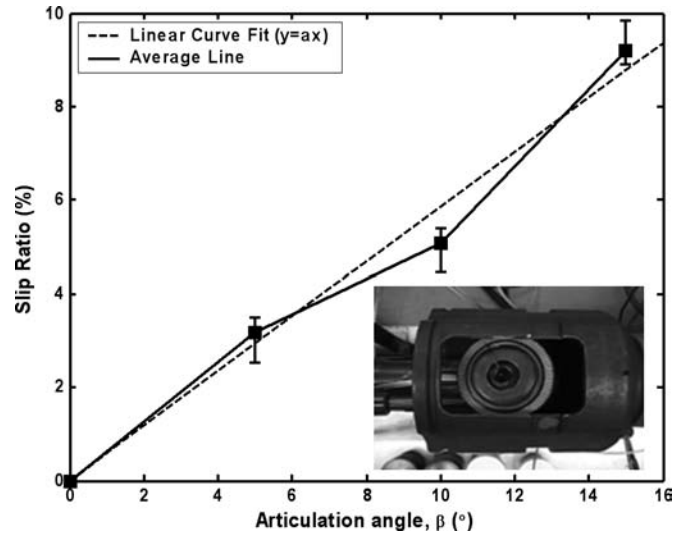


Figure 25.10—Measured slip ratio and linear curve-fit in terms of articulation angle. (Error bars show minimum-maximum values from multiple measurements.)

$$\text{Slip Ratio}(\%) = 0.585\beta \quad (25.4)$$

This relationship will be incorporated in the CV joint friction model to represent the proportion of pure sliding and rolling friction.

25.4.2 Pure Sliding Friction

Before proceeding to develop a comprehensive CV joint friction model, pure sliding friction experiments in the presence of grease (see Table 25.1) with actual CV joint samples were performed using a versatile pin-on-disk tribometer. Specifically, 412-H modified steel disks were procured under the same conditions as in an actual CV joint housing and were tested against 52100 steel pins (3.2 mm diameter) simulating the rollers. For the experiments, the actual driving conditions in terms of CV joint contact were estimated from typical vehicle specifications, and actual materials for the roller ball and housing track were obtained (using the same surface treatments as the actual parts). Measured surface roughness and hardness data confirm that the sample properties match those of the actual CV joint parts, as indicated in Table 25.2. The R_q of the disks and housing ranged from 1.90 to 2.35 μm , and the R_q of the pins and rollers ranged from 0.10 to 0.16 μm . The tribometer applies a normal force through a stationary pin to a rotating disk. In addition, the tribometer is equipped with computer control of the axial

TABLE 25.2—CV Joint Material Properties and Surface Roughness

Samples	Material	Surface Treatment	$R_a (\mu\text{m})$	$R_q (\mu\text{m})$	E (GPa)	ν	H (HRc)
Disks ^a	4121-H steel	Forged (as-formed)	1.50–1.91	1.90–2.35	206.9	0.29	60–62
Housing ^b			1.72–1.90	2.08–2.27			61–62
Pins ^a	52100 steel	Fine machined	0.11–0.13	0.14–0.16	206.9	0.29	60–61
Roller ^b			0.06–0.10	0.10–0.14			59–60

^aExperimental specimen; ^bOriginal CV joint specimen.

load and rotational velocity of the specimen and can measure in situ the friction force, normal load, and near-contact temperature at 2 mm below the interface with a miniature thermocouple. Before and after testing, all specimens were ultrasonically cleaned in acetone, rinsed with alcohol (2-propanol), and immediately dried using warm air.

The evolutionary nature of the friction coefficient with respect to load was determined with the use of step-loading experiments at a CV of 0.5 m/s as depicted in Figure 25.11. For the grease-lubricated experiments, an initial normal load of 178 N (resulting in a nominal contact pressure of 22 MPa) was applied for 30 min followed by stepping up the load to 445 N (55.4 MPa) with subsequent step loadings of 445 N every 5 min to a maximum of 4448 N (554 MPa) for a total test duration of 70 min. The sliding velocity was constant at 0.5 m/s. For the unlubricated experiments, an initial normal load of 178 N (22 MPa) for 30 min with step loading of 44.5 N (5.5 MPa) every 10 min was applied to a maximum of 445 N (55.4 MPa). The dry experiments could not be performed at higher loads because of high friction forces demanding torque greater than the capacity of the tribometer.

The results showed that the friction coefficient decreased slightly with increasing normal contact pressure. The error bars shown in Figure 25.11a for grease A are typical minimum-maximum values obtained from repeatability experiments. Specifically, grease A exhibits slightly higher friction coefficients than grease B at contact pressures below 300 MPa, but above this pressure, the relative trends

are reversed. This phenomenon is due to the pressure-sensitive additives in grease A that require higher contact pressures to be activated and thus cause lower friction. This particular additive, organomolybdenum, is designed to reduce friction significantly through chemical reaction, and the test results show that it can attain values as low as 0.035, which is in agreement with published literature [14]. The friction coefficient for grease B is relatively stable as compared with grease A, which often exhibits high fluctuations. It is assumed that the physical additives (or particles) in grease B help to produce smoother transitions than the chemical reactions produced by the additives in grease A. As the surfaces of the disks become smoother because of wear and burnishing of the asperities, the physical particles of grease B have less surface interaction than grease A, in which chemical reactions are still taking place. Testing of conventional, multipurpose grease under identical step-loading conditions exhibits similar friction coefficient values at low pressures, but become much higher at elevated pressures compared with both CV joint greases. This clearly confirms the superiority of the specifically formulated CV joint greases at very high contact pressures.

For the purpose of developing a comprehensive CV joint friction model, the measured pure sliding friction coefficient values at 400 MPa of contact pressure (corresponding to 160-Nm CV joint torque) of 0.06, 0.09, and 0.3 for grease A, grease B, and unlubricated surfaces, respectively, were used in the model.

25.4.3 Rolling Friction

Generally, most CV joints contain ball and roller bearing designs, thus involving rolling motion. Although rolling friction inside of a CV joint is smaller in magnitude than sliding friction and is the “preferred” friction mode, rolling motion and the associated rolling friction occur throughout the CV joint operation and it also needs to be investigated and included in the friction model. Rolling motion ideally should not have any kind of resistance during motion, but in reality, rolling friction occurs through various energy dissipation mechanisms in the contact zone.

When the CV joint is transmitting the engine torque to the wheels, the tangential compressive load, P , is transferred by the pade trunnions (a tripod CV joint has three trunnions) through the input shaft via the needle bearing and rollers to the tracks of the output housing. The tripod-type CV joints have three contacting positions inside of each trunnion, as shown in the section view of Figure 25.12, where elliptical contact occurs at point 1 between the rollers and the housing tracks and line or cylindrical contact occurs at point 2 between the needle bearings and rollers as well as at point 3 between the needle bearings and the trunnions [1].

For a CV joint contact, the source of energy dissipation (under rolling conditions) is due to elastic hysteresis and the so-called Heathcote microslip at the contact interface. Using the concept that the work done by the Hertzian pressure on the contact is equal to the energy dissipated with a hysteresis loss factor, α , one can obtain the sliding resistance during rolling, λ , as [15]

$$\begin{aligned} \text{Line Contact : } \lambda &= \alpha \frac{2a}{3\pi R} \\ \text{Elliptical Contact : } \lambda &= \alpha \frac{3a}{16R} \end{aligned} \quad (25.5)$$

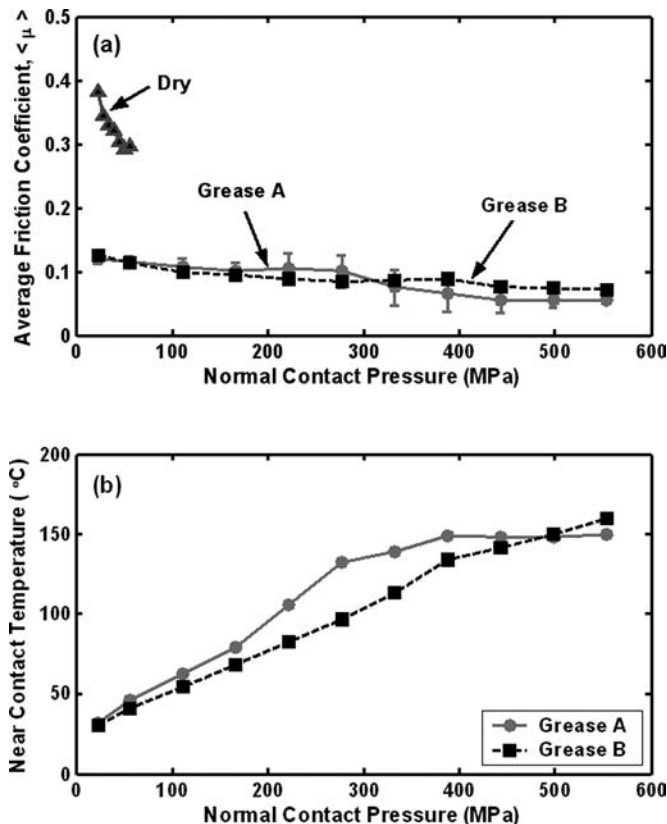


Figure 25.11—(a) Average friction coefficient and (b) near-contact temperature in terms of normal contact pressure (at 0.5 m/s linear velocity). Experiments performed using a pin-on-disk tribometer and samples/conditions as listed in Table 25.2.

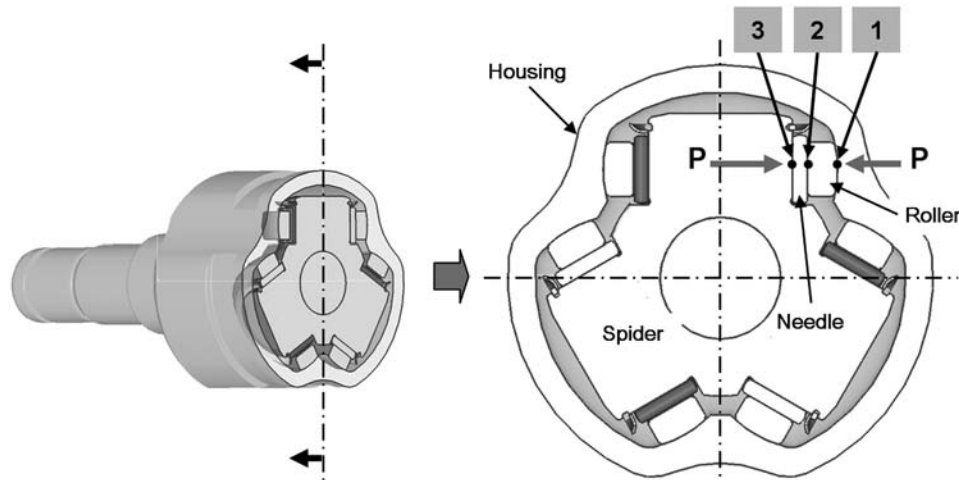


Figure 25.12—Cross-section view of tripod CV joint indicating contact locations.

where the rolling resistance λ has an analogous meaning to the coefficient of sliding friction μ , a is the semicontact width of the contact patch, and R is the combined radius in the direction of rolling. For most metals stressed within the elastic limit, α values are usually less than 1 % [16]. However, according to reference 15, α values should be 3 times the usual hysteresis loss factor obtained from simple tensile tests because the rolling contact process is a complex phenomenon. Thus, using the line contact equation in eq. 25.5, one can estimate the rolling friction between the needle and spider and needle and roller contacts.

Intuitively, when a ball or roller rolls along the track of a groove, it must be rotated about an instantaneous axis of rotation, and it follows that the contact zone remotely from the axis should slip. Unlike a typical contact zone being in a single plane, for the case of a roller bearing in a groove under normal compressive forces, their cross-sectional radii of curvature are very close to each other (conformal). Thus, the contact area is not planar, but it shares the transverse curvature of the roller and groove. Therefore, the contact points in the roller show different peripheral velocity of rotation, which leads to microslip. Heathcote introduced a theory (referred to as Heathcote slip) predicting that the rotation of the ball would be resisted by a frictional moment and is given by the following equation [15]:

$$\lambda = 0.08\mu \frac{b^2}{R^2} \quad (25.6)$$

where $2b$ is the transverse width of the contact ellipse ($b \gg a$). μ represents the pure sliding friction coefficient

where for CV joints it was measured using pure sliding experiments (Section 25.4.2) for two different lubricants. The Heathcote slip theory is only applicable for conformal contacts such as the ball-in-groove contact. When two bodies fit closely (close conformal) as in the case of the contact between the roller and the grooved track, the rolling resistance becomes significant because the contact size is larger than the nonconformal contact.

In general, tripod CV joints have three contacting positions on each trunnion as can be seen in Figure 25.12. The contact geometry between rollers and housing is elliptical, between needle bearings and rollers is line or cylindrical, and between the needle bearings and the trunnions is also line or cylindrical [1]. Using Hertzian theory one can readily obtain the contact dimensions (see Table 25.3) at the experimental conditions of CV applied torque, $T_d = 160$ Nm. Normal load P_n can be obtained from T_d (driveshaft torque) with the following relationship [1]:

$$T_d = nP_n R_c \quad (25.7)$$

where:

n = number of pade trunnions and

R_c = contact radius from the CV joint center (in this case, $R_c = 24$ mm).

The individual rolling resistance for each contact location in the CV joints can be calculated using eqs. 25.5 and 25.6.

Considering all 33 needle contacts at a trunnion, one can combine the total rolling resistance in a trunnion, and

TABLE 25.3—Hertzian Contact Dimensions and Parameters for Rolling Friction

Contact	Mechanism	a (mm)	b or l (mm)	R (mm)
Elliptical contact (roller vs. housing)	Heathcote slip	0.23	7.85	21.53
Line contact (needle vs. spider)	Elastic hysteresis	0.02	11.59	1.25
Line contact (needle vs. roller)	Elastic hysteresis	0.02	11.59	1.52
There are 33 needles in a trunnion of a CV joint.				

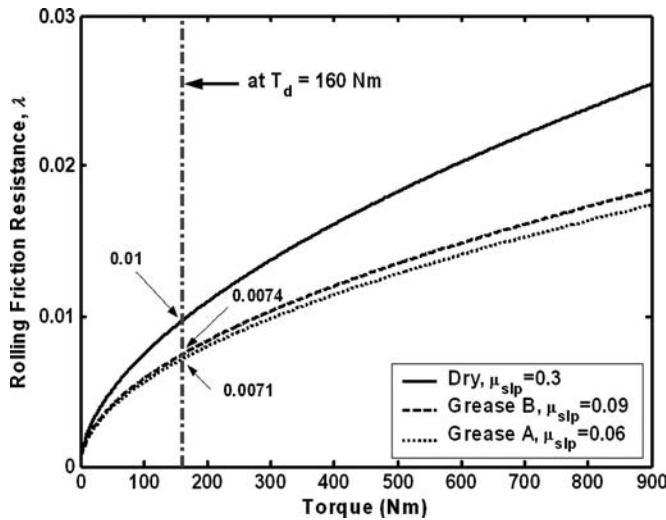


Figure 25.13—Modeled total rolling friction at a single trunnion as a function of applied torque.

the result is depicted in Figure 25.13. The calculated results show the combined rolling resistance, λ , at a trunnion versus torque, up to 900 Nm, which is the maximum value at the maximum engine torque. To compare the rolling resistance under different lubrication conditions, pure sliding friction coefficient values measured with the tribometer were used in eq. 25.6 as $\mu_{slp} = 0.06$ (grease A), $\mu_{slp} = 0.09$ (grease B), and $\mu_{slp} = 0.3$ (dry). Under the experimental conditions of $T_d = 160$ Nm, the total rolling friction for the dry, grease A, and grease B cases are 0.011, 0.0071, and 0.0074, respectively, and their values are approximately 10 % of the pure sliding friction measurement results. However, because the rolling friction is dominant in the CV joint friction with a minimum of 91 % of the total friction, as shown in Figure 25.10, it cannot be ignored.

25.5 FRICTION MODELING

During the development of new vehicles, extensive testing with all new model vehicles is undertaken to avoid potential vehicle problems, which leads to longer and costly development periods. Better understanding of the nonlinear dynamic interfacial friction behavior of CV joints and the development of a CV joint friction model can provide powerful design tools and shorter development efforts.

As observed during the experiments, the total friction consists of static (stationary) and dynamic (stroking) components, and the phenomenological model should specifically include both components. The static friction part of the model includes static friction behavior while applying torque but without stroking motion. The dynamic friction model is related to the fluctuating friction behavior during the stroking motion under the applied torque. Thus, a semiempirical model that is based on realistic CV joint experiments as well as basic friction model results was developed to capture realistic CV joint friction behavior. Note that one could directly curve-fit the experimental data of Figure 25.8 to develop a fully empirical friction model; however, the physics of the problem will not be captured because the individual contributions from roll-to-slip, rolling, and sliding friction will not be accounted for.

The terminology used in this work to describe the different types of friction coefficients as used to develop the CV joint friction model is explained in Figure 25.14, in which raw data obtained during a dynamic experiment are depicted. The test was conducted at $T_d = 160$ Nm and $\beta = 15^\circ$. Figure 25.14a shows the friction coefficient versus time, and Figure 25.14b shows the friction coefficient versus stroke for the same experimental data. From both plots, one can clearly see that μ_{sta} represents the friction coefficient before motion initiates (at $t = 0$ s) and μ_{avg} is the average value of the friction coefficient during dynamic motion. It is also seen that inward and outward dynamic friction coefficients, $\mu_{dyn,in}$ and $\mu_{dyn,out}$, respectively, are distinct and follow a hysteretic “loop.” As illustrated in Figure 25.14, one can represent each test with an “error bar” and a solid circle to represent the amplitude fluctuation and average values of the dynamic friction coefficient.

25.5.1 Static Friction Model

The initial static friction coefficient, μ_{sta} , represents the friction behavior that occurs during static experiments by applying a static torque without any stroking of the CV joint. This phenomenon arises because of the complex CV joint kinematics. To establish a relationship among the initial static friction coefficient, μ_{sta} , articulation angle, β , and applied static torque, T_d , experiments under variations of these parameters were conducted and the following function was fitted to the experimental data in a least-square sense:

$$\mu_{sta} = c_{s1} + (c_{s2} + c_{s3}\beta)(1 - e^{-c_{s4}T_d}) \quad (25.8)$$

where c_{si} are constant coefficients fitted to the experimental data and are as follows: $c_{s1} = 3.86 \times 10^{-2}$, $c_{s2} = 1.34 \times 10^{-1}$, $c_{s3} = 4.50 \times 10^{-3}$, and $c_{s4} = 2.35 \times 10^{-2}$. Equation 25.8 is valid for a wide range of practical β and T_d values. On the basis of the functional form of eq. 25.8, it can be seen that the initial static friction coefficient reaches a constant value with increasing torque. Figure 25.15 clearly shows this trend and shows how well the model fits the experimental data. These experiments were conducted without any stroking motion and using grease B. On the basis of the model and the test results (reaching steady-state values at some torque value), it could be assumed that conducting experiments at a steady-state torque of 160 Nm is sufficiently large to estimate the static frictional behavior, although actual mid-size passenger cars can generate up to a maximum of 900 Nm of torque in CV joints.

As illustrated in Figure 25.14, each test can be represented with an error bar and a solid circle for the amplitude of friction fluctuation and average friction values. Figure 25.16 shows the average friction coefficient at four representative articulation angles exhibiting a proportional relationship with the initial static friction coefficient. This means that the average friction coefficient value is related to the static friction behavior and not the dynamic plunging motion. Thus, to represent the average friction coefficient value, the average friction coefficient μ_{avg} can be represented by using the static friction coefficient μ_{sta} . Moreover, the average friction coefficient μ_{avg} shows sinusoidal behavior as a function of the rotational phase angle, and a simple sine function was added to the

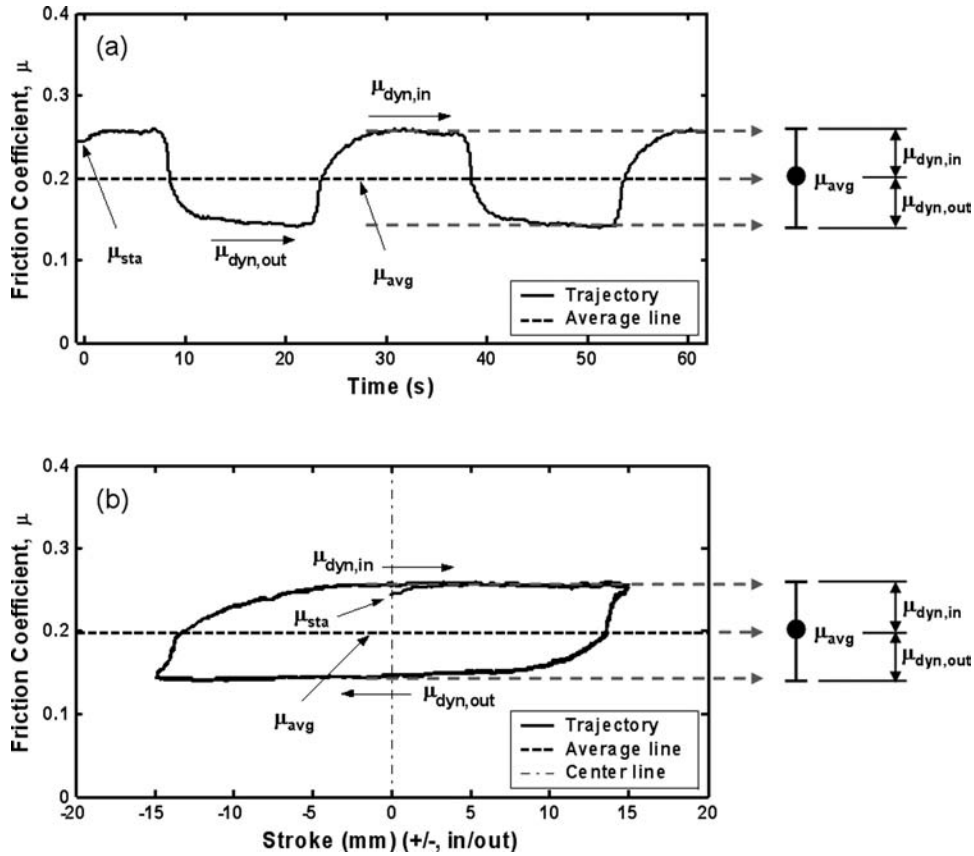


Figure 25.14—Friction coefficient measurements during a typical trajectory in a CV joint: (a) vs. time and (b) vs. plunging stroke ($T_d = 160$ Nm, $\beta = 15^\circ$, $\varphi = 90^\circ$).

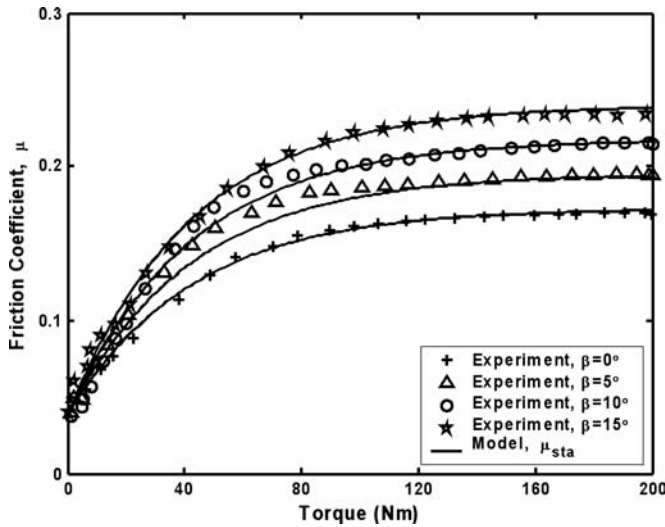


Figure 25.15—Comparison of initial internal static friction model at a single trunnion with experimental results at different articulation angles and torque values (grease B lubricated, $\varphi = 90^\circ$).

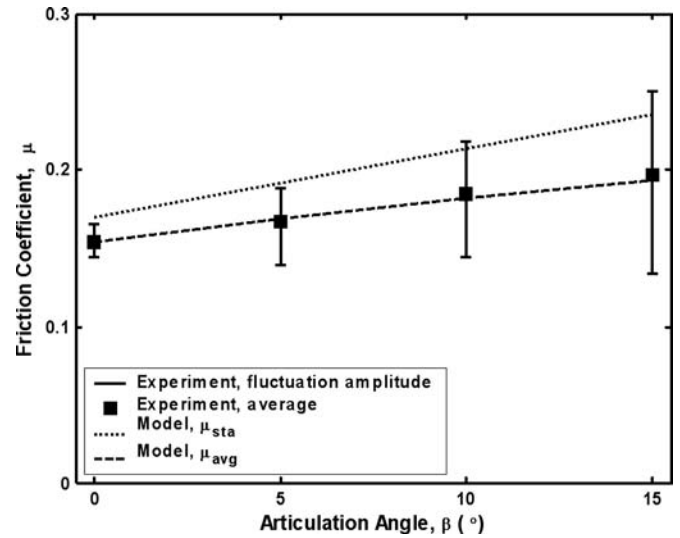


Figure 25.16—Model of static and average friction coefficient compared to the dynamic friction measurements at different articulation angles ($T_d = 160$ Nm, $\varphi = 90^\circ$).

static friction model to capture this behavior. The empirical constant coefficients were obtained by curve-fitting the experimental data for different φ , β , and pure sliding friction coefficient μ_{slp} values. The average friction model is given by

$$\mu_{avg} = \mu_{sta}(1 + (c_{s5}\mu_{slp} - c_{s6})\beta) + c_{s7}\mu_{slp} - c_{s8} + \frac{\beta}{15}c_{s9}(\sin \varphi - 1) \quad (25.9)$$

where $c_{s5} = 3.33 \times 10^{-2}$, $c_{s6} = 1.04 \times 10^{-2}$, $c_{s7} = 1.00 \times 10^{-1}$, $c_{s8} = 2.47 \times 10^{-2}$, and $c_{s9} = 4.25 \times 10^{-2}$.

Figure 25.16 also shows the models of the static and average friction coefficients compared with the actual dynamic measurements at different CV joint articulation angles. The test results were conducted with $T_d = 160$ Nm and phase angle $\varphi = 90^\circ$. The results clearly show that the average friction model matches the average values of the friction coefficient measurements and that the model can capture the increment of average friction coefficient when the articulation angle increases.

Figure 25.17 shows the average friction coefficient variation compared with the actual measurement results during one complete revolution of the CV joint (using grease B). In this model, the pure sliding friction coefficient μ_{slp} is obtained from the basic pin-on-disk experiments as explained in Section 25.4.2. The experimental contact pressure is estimated from Hertzian theory for the elliptical contact between housing and roller and is found to be 400 MPa at the test condition of 160 Nm applied torque. At a 400-MPa contact pressure, the pure sliding friction coefficient value was found earlier to be 0.09 (grease B). The experimental results depicted in Figure 25.17 show the coefficient fluctuation with “error bars” and its average value with a solid circle at each rotational phase (obtained from the raw data as shown in Figure 25.8). The friction measurements were recorded while stroking the CV joint with the test conditions at the articulation angle $\beta = 15^\circ$ and $T_d = 160$ Nm. The results clearly show that the average friction model captures the sinusoidal behavior of the averaged dynamic friction coefficient values quite well.

Using this static friction model at a trunnion as a function of the rotational phase angle, one can obtain the resultant static friction by combining the friction from all three trunnions that are a 120° phase angle apart. Thus, the sinusoidal friction variation from each trunnion is canceled out and the combined resultant static friction $\mu_{avg,res}$ is constant, as shown in Figure 25.18 and given by the following equation:

$$\begin{aligned}\mu_{avg,res} &= [\mu_{avg}(\varphi) + \mu_{avg}(\varphi + 120^\circ) + \mu_{avg}(\varphi + 240^\circ)] / 3 \\ &= \mu_{sta} (1 + (c_{s5}\mu_{slp} - c_{s6})\beta) + c_{s7}\mu_{slp} - c_{s8} - \frac{\beta}{15}c_{s9}\end{aligned}\quad (25.10)$$

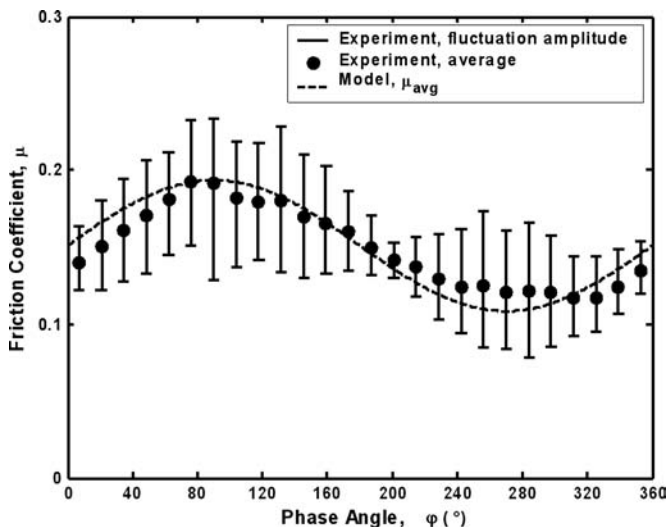


Figure 25.17—Model of average friction coefficient compared to dynamic friction experiments in terms of rotational phase angle ($\beta = 15^\circ$, $T_d = 160$ Nm).

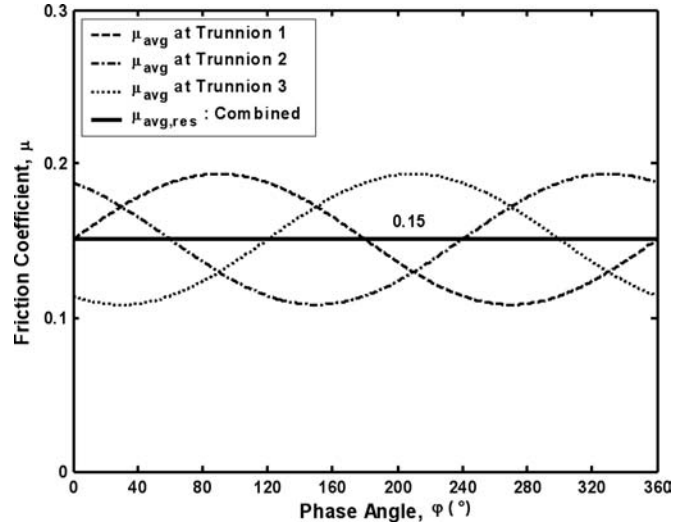


Figure 25.18—Simulation of combined average friction coefficient from all three CV joint trunnions in terms of the rotational phase angle ($\beta = 15^\circ$, $T_d = 160$ Nm).

In this case, the combined friction coefficient is constant with a value of 0.15, although the individual μ values (for each trunnion) exhibit sinusoidal fluctuations. Although the average friction model is for the average value of the dynamic friction coefficient, it nonetheless represents the static friction behavior for a CV joint because μ_{avg} is dependent on μ_{sta} , which is related to the applied torque rather than the dynamic plunging motion. The consequence of this finding is that the external friction measurements, which can only capture the combined effects, are unable to measure the internal sinusoidal friction behavior. More importantly, it means that the sinusoidal fluctuation of the internal static friction behavior does not affect the external vibration problem because it always acts as a combined constant friction. Thus, one can conclude that the static friction behavior occurs because of the inherent CV joint kinematics and does not relate to the dynamic GAF in vehicles. However, the internal friction behavior is still important, for example in the design of a CV joint, because it can be used to estimate the strength and fatigue life of a CV joint.

25.5.2 Dynamic Friction Model

A dynamic friction model was developed to capture the friction fluctuation behavior during the CV joint stroking (or plunging) motion. Subsequently, this model was directly related to the external GAF, which is practically and readily measured by CV joint manufacturers. On the basis of the dynamic experiments under different articulation and phase angles as well as contact conditions, the following friction coefficient model for the dynamic (or fluctuating) part well captures the data:

$$\mu_{dyn} = \pm \frac{\beta}{15} [(c_{d1}\mu_{slp} - c_{d2})|\sin \varphi|] \pm \mu_{S/R} \quad (25.11)$$

where

$$\mu_{S/R} = R_s \beta \mu_{slp} + (1 - R_s \beta) \lambda. \quad (25.12)$$

The empirical constants, obtained by curve-fitting the pure dynamic terms in the experimental results, are $c_{d1} = 4.00 \times 10^{-1}$ and $c_{d2} = 8.40 \times 10^{-3}$.

Examining eqs. 25.11 and 25.12, the semiempirical dynamic friction coefficient model μ_{dyn} is related to the articulation angle β , rotational phase angle ϕ , slip ratio R_s , pure sliding friction coefficient μ_{slp} , and pure rolling friction coefficient λ via the slip-to-roll friction coefficient $\mu_{s/R}$. The value of the slip ratio R_s is 5.85×10^{-3} from eq. 25.4, which is the slope of the slip-to-roll ratio measured data. The model correctly predicts that dynamic friction $\mu_{dyn} = \mu_{s/R} = \lambda$ at $\beta = 0^\circ$, thus confirming that rolling friction is dominant at $\beta = 0^\circ$. In the dynamic friction model, the pure rolling friction coefficient λ was estimated by analyzing the CV joint rolling friction mechanism. As explained in Section 25.4.3, elastic hysteresis is the source of rolling friction for all needle contacts, and Heathcote microslip is the source of rolling friction for the contact between the roller and housing. Thus, by combining all rolling resistance components from the 33 needle contacts, the total rolling friction resistance or rolling coefficient at a trunnion is estimated to be approximately 0.0071–0.0074 in the presence of CV joint grease and 0.01 at dry conditions with an applied static torque T_d of 160 Nm (refer to Figure 25.13). A sinusoidal function in the dynamic friction model was added to capture the experimental variation during the rotational angle changes. In the proposed dynamic friction model, “+” represents the positive friction coefficient during the inward stroke motion $\mu_{dyn,in}$, and “−” represents the negative friction coefficient during the outward stroke motion, $\mu_{dyn,out}$.

Figure 25.19 shows the comparison of the dynamic friction model and experimental data for one complete revolution of a single trunnion. The experimental results are the same as the results shown in Figure 25.17 except that the average values are set to zero and show only the fluctuating terms. The results clearly show that the model well captures the inward and outward dynamic friction coefficient values. Although the results shown in Figure 25.19 are for one trunnion, using the same methodology for the combined static friction coefficient (see eq. 25.10), the combined resultant

dynamic friction could also be obtained. Unlike the static case of constant combined friction, it shows that the combined friction coefficient is fluctuating with an approximate average friction coefficient value of 0.043. Thus, one can readily see that the dynamic friction terms are a source of external fluctuation, and it may potentially cause vehicle vibration problems.

25.5.3 Total Friction Model

Having developed the different components of the friction model on the basis of the physics of the problem as well as curve-fitting the experiments, the total friction coefficient inside of a CV joint can be obtained by combining the average friction model including the static friction model and the dynamic friction model in the following form:

$$\mu_{tot} = \mu_{avg} + \mu_{dyn} = \mu_{avg}(\mu_{sta}, \beta, \phi, \mu_{slp}, T_d) + \mu_{dyn}(\beta, \phi, \mu_{slp}, \lambda, R_s) \quad (25.13)$$

where μ_{avg} and μ_{dyn} are given by eqs. 25.9 and 25.11, respectively. Note that μ_{avg} is dependent on the articulation angle β , phase angle ϕ , pure sliding friction coefficient, applied static torque (although it becomes independent of torque after 160 Nm), and static friction model μ_{sta} . μ_{dyn} also depends on β and ϕ , the pure sliding and rolling friction coefficient, respectively, and the slip ratio; however, it is independent of the applied static torque T_d . In addition, it was found that the proposed friction model is not dependent on the sliding velocity in agreement with experiments [13].

Figure 25.20 shows the comparison between the proposed model and experimental results with grease B in terms of applied torque. Specifically, Figure 25.20a depicts the comparison of the static and total friction model and experimental results at $\beta = 0^\circ$ and 15° . Figure 25.20b shows the comparison of the dynamic friction model and the fluctuating terms in the experiments at $\beta = 0^\circ$ and $\beta = 15^\circ$. From Figure 25.20a, the total friction model captures the test results very well at $\beta = 0^\circ$ but not as well for $\beta = 15^\circ$, especially at low torque values. However, one can argue that the model is sufficiently accurate because it captures the measured friction coefficient at high torque levels (in the steady state range), which from a practical point of view is more relevant. Moreover, when observing only the dynamic terms as shown in Figure 25.20b, the model well captures all of the data (i.e., for the overall torque range); thus, it shows that the dynamic friction is independent of the torque load.

As the model was curve-fitted to experimental data, it is important to ensure that the fitting parameters are valid for all of the experimental conditions examined in this work. Figure 25.21 shows the comparison between the modeled and measured friction coefficient values inside of the CV joint to investigate the robustness of the friction model to different lubrication conditions. All tests were conducted at the rotational phase angle $\phi = 90^\circ$, which is when the trunnion with the built-in force sensor was positioned at the top of the CV joint. The test results in Figure 25.21, a and b, were obtained by applying a torque of 160 Nm and changing the CV joint articulation angle up to 15° . The test for the dry condition, Figure 25.21c, was conducted at 50-Nm static torque and up to $\beta = 10^\circ$ because of the

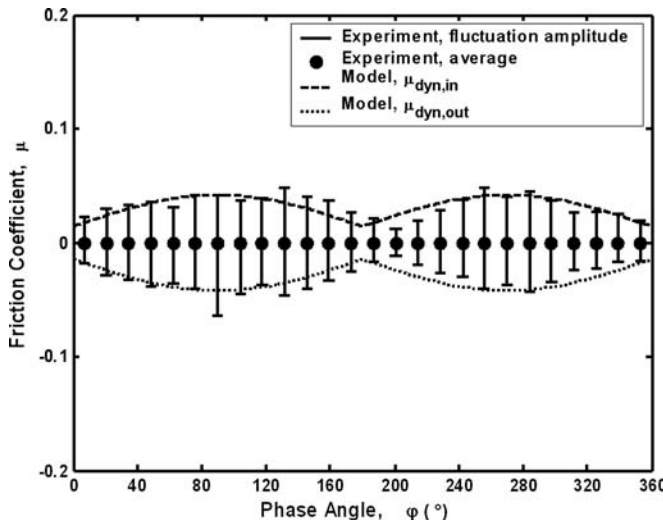


Figure 25.19—Simulation of dynamic friction coefficient, μ_{dyn} , by comparing to the actual CV joint internal friction coefficient after setting the average value to zero ($\beta = 15^\circ$, $T_d = 160$ Nm).

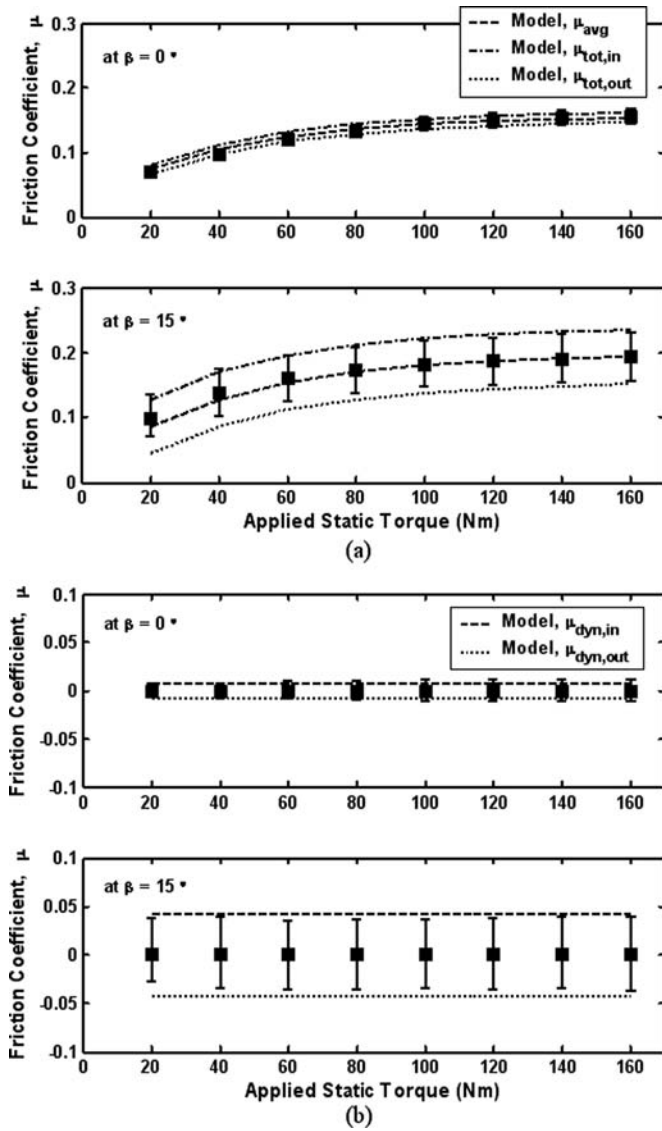


Figure 25.20—Comparison of experimental data and proposed friction model in terms of applied static torque at two different extreme articulation angles: (a) average and total friction coefficient and (b) dynamic friction coefficient.

generation of very high friction. For the grease-lubricated cases in Figure 25.21a (grease A) and Figure 25.21b (grease B), pure sliding and rolling friction coefficient values for the friction model were measured and calculated at $T_d = 160$ Nm as $\mu_{slp} = 0.06$, $\lambda = 0.0071$, $\mu_{slp} = 0.09$, and $\lambda = 0.0074$, respectively. For the nonlubricated (or dry) case, $\mu_{slp} = 0.30$, which is the closest value under 50-Nm applied torque, and $\lambda = 0.01$. All constants and parameters for the friction model simulation (determined earlier) are summarized in Table 25.4. From the results, it is evident that the proposed model very well captures the test results (the average and fluctuating behavior) in terms of articulation angle changes even for the dry surface condition as well as the grease-lubricated cases. Note that the empirical constants listed in Table 25.4 are the same for all experimental conditions described in this work and the physical parameters can readily be obtained. Moreover, because the two greases investigated as well as the dry condition cover a large range of frictional

conditions, it is believed that the model could readily be applied to other types of greases as used in CV joints. For example, such greases include lithium-based greases that are used in European cars.

25.5.4 GAF Friction Model

The dynamic friction model was obtained by conducting stroking experiments at each rotational phase angle without dynamic rotation. However, in actual vehicle applications, CV joints are rotating by generating one stroking motion for every revolution of each trunnion. Thus, by using this concept, one can obtain the actual GAF by considering a stroke motion inside of a CV joint during one revolution. Knowledge of GAF is extremely important because it directly relates to vehicle performance and a model to predict it would be extremely useful.

Figure 25.22 shows the trajectory of the friction coefficient for the developed dynamic friction model and the proposed GAF friction model during one revolution. As explained by the arrows on the trajectory for μ_{GAF} in Figure 25.22, when the CV joint is rotating clockwise (refer to the definition of rotational phase angle in Figure 25.5b) from $\varphi = 90^\circ$ to 270° via $\varphi = 0^\circ$ (or 360°), the top trunnion is moving inward until it is positioned on the bottom at 270° . At the same time, the bottom trunnion is moving outward when the CV joint is rotating from $\varphi = 270^\circ$ to 90° . Thus, the actual trajectory of the friction coefficient for GAF follows the trajectory of $\mu_{dyn,in}$ from $\varphi = 90^\circ$ to 270° and $\mu_{dyn,out}$ from $\varphi = 270^\circ$ to 90° , which is plotted with a thick solid line in Figure 25.22. The actual trajectory of the friction coefficient for GAF can be expressed with the following equation relating directly to the dynamic friction model:

$$\mu_{GAFi} = \text{sgn}[\sin(\varphi_i + 90^\circ)] |\mu_{dyn}| \quad (25.14)$$

where sgn is a sign function that extracts the sign of $\sin(\varphi_i + 90^\circ)$.

By using this individual GAF friction coefficient at a single trunnion, one can readily obtain the combined GAF friction coefficient by combining it from all three trunnions that are 120° apart. The individual and combined GAF friction coefficients are plotted in Figure 25.23 for grease B at $\beta = 15^\circ$ and $T_d = 160$ Nm. The maximum peak value of the combined friction coefficient was 0.062. It clearly shows that the combined GAF friction coefficient has a modified square waveform with a frequency of 3 times the rotational speed, which is in agreement with the literature [2]. Thus, it confirms that the internal dynamic friction force of a tripod CV joint produces a cyclic axial force or GAF along the axis of the housing axle. By using the GAF friction coefficient model, the following equation is proposed to estimate the GAF in actual vehicle applications:

$$GAF = \frac{2T_d}{3BCD} \left[\sum_{i=1}^3 \mu_{GAFi} \right] \quad (25.15)$$

where BCD is the ball circular diameter at the housing-end view, and one may need to consider the eccentricity or offset from the geometrical center to accurately calculate the GAF. Thus, GAF represents the axial friction force with the normal force of $2T_d / BCD$ under the friction coefficient of $\frac{1}{3} \sum_{i=1}^3 \mu_{GAFi}$ at each trunnion.

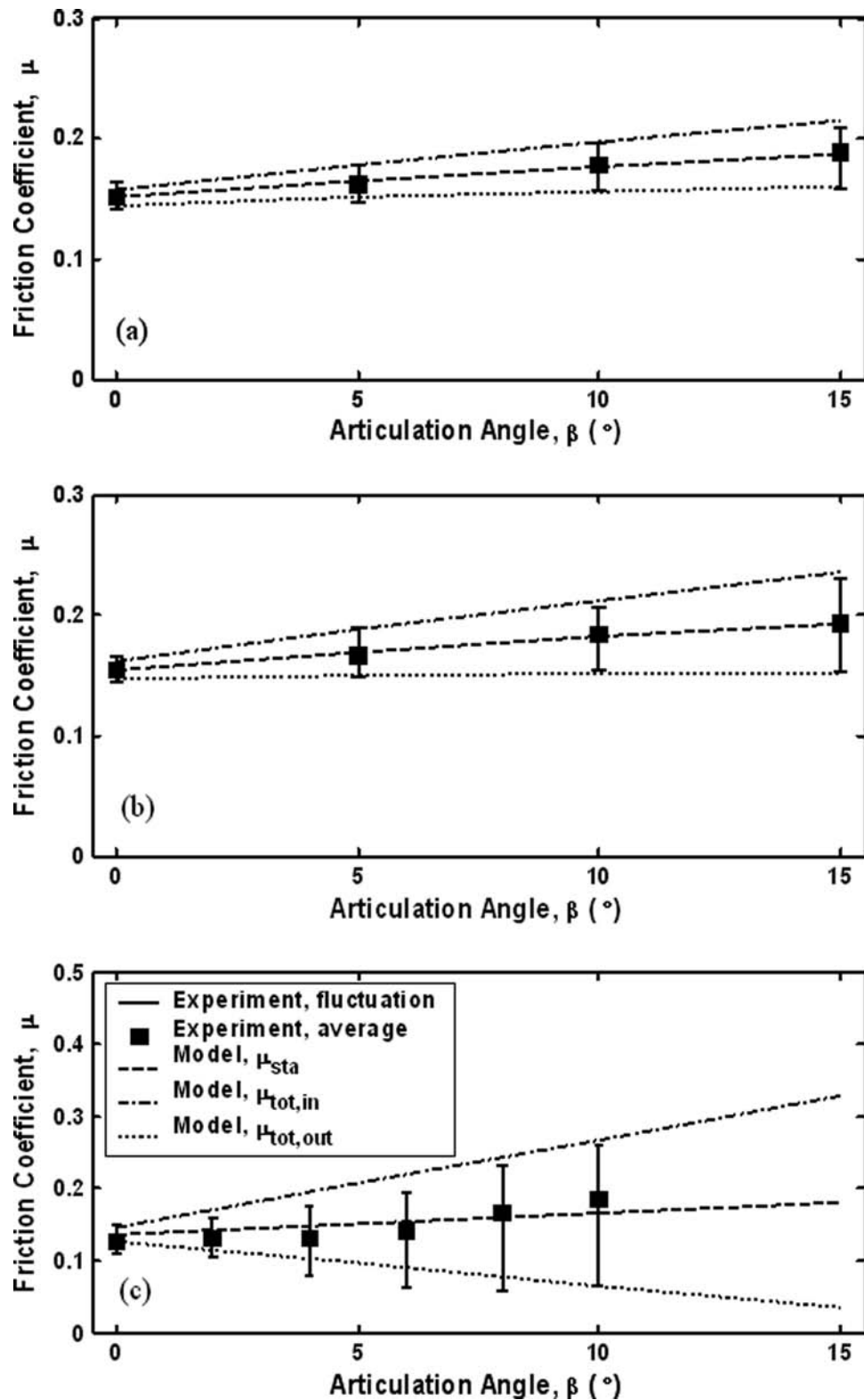


Figure 25.21—Comparison of friction model with experimental results in terms of articulation angle for different CV joint greases ($\varphi = 90^\circ$): (a) grease A ($\mu_{slp} = 0.06$, $\lambda = 0.0071$, $T_d = 160$ Nm), (b) grease B ($\mu_{slp} = 0.09$, $\lambda = 0.0074$, $T_d = 160$ Nm), and (c) dry ($\mu_{slp} = 0.30$, $\lambda = 0.01$, $T_d = 50$ Nm).

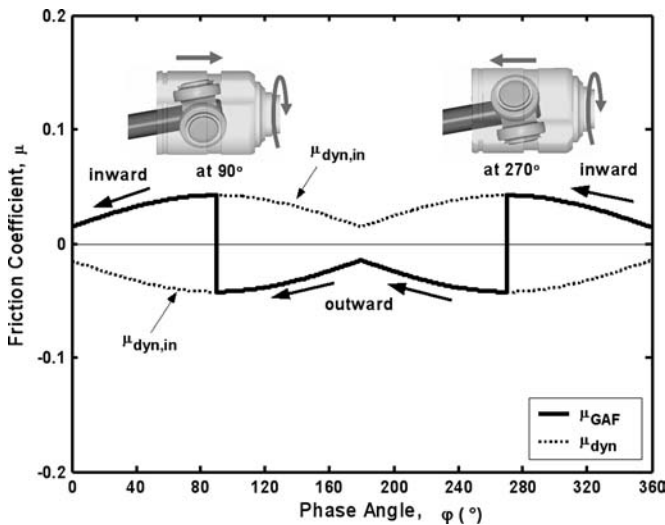
25.6 CONCLUSIONS

A physics-based phenomenological CV joint internal friction model has been presented as a function of different CV joint operating parameters. The internal CV joint friction

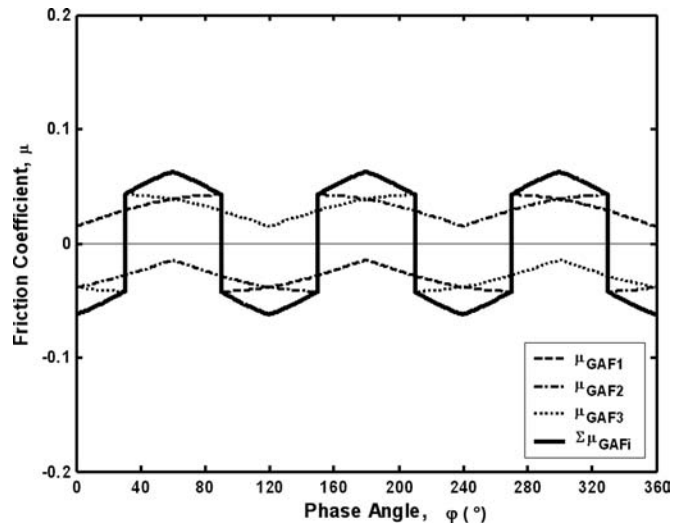
model was developed based on experimental results under grease-lubricated conditions. To measure the internal CV joint friction forces, an advanced CV joint friction apparatus was designed and constructed to perform realistic

TABLE 25.4—Empirical Constants and Physical Parameters Used in the Friction Model

Empirical Constants			
Average friction model	C_{s1}	3.86×10^{-2}	
	C_{s2}	1.34×10^{-1}	
	C_{s3}	4.50×10^{-3}	
	C_{s4}	2.35×10^{-2}	
	C_{s5}	3.33×10^{-2}	
	C_{s6}	1.04×10^{-2}	
	C_{s7}	1.00×10^{-1}	
	C_{s8}	2.47×10^{-2}	
	C_{s9}	4.25×10^{-2}	
Dynamic friction model	C_{d1}	4.00×10^{-1}	
	C_{d2}	8.40×10^{-3}	
Physical Parameters (at $T_d = 160$ Nm)			
Properties	Grease A	Grease B	Dry
μ_{slp}	0.06	0.09	0.30
λ	0.0071	0.0074	0.01
R_s	5.85×10^{-3}	5.85×10^{-3}	5.85×10^{-3}

**Figure 25.22—Trajectory of μ_{GAF} per revolution at a single trunnion using the dynamic friction model.**

CV joint tests using a triaxial force transducer attached inside of the CV joint. Experiments were performed under different articulation angles, rotational phase angles, lubrication conditions, and applied torque values. As observed during the experiments, there are static (stationary) and dynamic (stroking) friction components, and the proposed total friction coefficient model was divided into static and dynamic friction terms. The static friction model was derived from the inherent CV joint kinematics

**Figure 25.23—Combination of μ_{GAF} using individual μ_{GAF} values at a trunnion (grease B, $\beta = 15^\circ$, $T_d = 160$ Nm).**

while applying the static torque, and it is important in the design of CV joints because it can be used to estimate its strength and life. The dynamic friction model is due to the stroking motion of the CV joint, so it is directly related to the external GAF, which is the main source of friction force in CV joints and is related to vehicle vibration problems. The proposed friction model that is based on physical parameters (i.e., pure rolling and sliding friction coefficient values as well as curve-fitted parameters) is in good agreement with experimental results under grease-lubricated and unlubricated conditions. The internal dynamic friction model was then directly related to the practical GAF by considering a stroke motion inside of a CV joint during one revolution. No similar model exists in the literature, and it is believed that the proposed model can accurately predict the external GAF over a wide range of operating conditions, which is very important for the design of future CV joints.

ACKNOWLEDGMENTS

The authors thank Delphi Saginaw Steering Systems for their funding of this project. Special thanks to William P. Skvarla and Dave Litter for coordinating the project and supplying the samples and to Mark W. McPherson for providing useful advice and information in the design of the CV joint friction apparatus. Some parts of the work presented in this chapter have also been published by the authors in references 12, 13, and 17.

References

- [1] Schmelz, F., Seher-Thoss, C.H.-C., and Aucktor E., 1992, *Universal Joints and Driveshafts: Analysis, Design, Applications*, S.J. Hill and J.A. Tipper, Trans., Springer-Verlag, New York.
- [2] Wagner, E.R., 1979, *Universal Joint and Driveshaft Design Manual: Advances in Engineering*, Series No. 7., SAE, Warrendale, PA.
- [3] Delphi Steering Systems, 2001, *Constant-Velocity Joint Manuals*, Delphi Steering Systems, Troy, MI.
- [4] Hayama, Y., 2001, *Dynamic Analysis of Forces Generated on Inner Parts of a Double Offset Constant Velocity Universal Joint (DOJ): Non-Friction Analysis*, SAE Technical Paper 2001-01-1161, SAE, Warrendale, PA.

- [5] Polycarpou, A.A., and Soom, A., 1995, "Boundary and Mixed Friction in the Presence of Dynamic Normal Loads: Part 1—System Model," *ASME J. Tribol.*, Vol. 117, pp. 255–260.
- [6] Philpott, M.L., Welcher, B.P., Pankow, D.R., and Vandenberg, D., 1996, "Two Phase Circular Regression Algorithm for Quantifying Wear in CV Joint Ball Race Tracks," *Wear*, Vol. 199, pp. 160–168.
- [7] Bierman, J., 1999, *Measurement System for CV Joint Efficiency*, SAE Technical Paper 1999-01-0936, SAE, Warrendale, PA.
- [8] Kernizan, C., Jacobs, R.P., and Whitticar, D.J., 2002, "Development of a Constant Velocity Joint, CVJ, Test Stand to Assess the Performance of a Series of Greases," *NLGI Spokesman*, Vol. 66, pp. 26–32.
- [9] Jia, X., Jin, D., Ji, L., and Zhang, J., 2002, "Investigation on the Dynamic Performance of the Tripod-Ball Sliding Joint with Clearance in a Clank-Slider Mechanism. Part1. Theoretical and Experimental Results," *J. Sound Vibration*, Vol. 252, pp. 919–933.
- [10] Watanabe, K., Kawakatsu, T., and Nakao, S., 2005, "Kinematic and Static Analysis of Tripod Constant Velocity Joints of the Spherical End Spider Type," *ASME J. Mech. Design*, Vol. 127, pp. 1137–1144.
- [11] Kochersberger, K.B., 2002, "Apparatus for Testing a Constant Velocity Joint and a Method Thereof," U.S. Patent, 6,378,374 B2.
- [12] Lee, C.-H., and Polycarpou, A.A., 2005, "Development of an Apparatus to Investigate Friction Characteristics of Constant-Velocity Joints," *Tribology Trans.*, Vol. 48, pp. 505–514.
- [13] Lee, C.-H., and Polycarpou, A.A., 2007, "Experimental Investigation of Tripod Constant Velocity (CV) Joint Friction," *SAE Trans.*, Vol. 115, pp. 475–482.
- [14] Fish, G., and Jisheng, E., 2002, "The Effect of Friction Modifier Additives on CVJ Grease Performance," *NLGI Spokesman*, Vol. 66, pp. 22–31.
- [15] Halling, J., 1975, *Principles of Tribology*, 1st ed., Macmillan, London.
- [16] Johnson, K.L., 1985, *Contact Mechanics*, 1st ed., Cambridge University Press, Cambridge, UK.
- [17] Lee, C.-H., and Polycarpou, A.A., 2010, "A Phenomenological Friction Model of Tripod for Constant Velocity (CV) Joints," *Tribology Int.*, Vol. 43, pp. 844–858.

Biobased Automotive Lubricants

Lou A. Honary¹

26.1 INTRODUCTION

There is a new impetus for the use of vegetable oils or renewable oils in automotive applications. The environmental factor promises to be a more steady and persistent force in promoting the use of these products than the fluctuating availability of petroleum. However, increased demand for petroleum by emerging economies has led to an increase in the need for petroleum substitutes. Either because of imposed environmental regulations or society's desire for a more environmentally friendly lubricant, the interest and increased use of vegetable-based engine oils and industrial lubricants will continue. Every year in the United States nearly 2.5 billion gallons of lubricants are manufactured; 1.4 % are automotive-related lubricants, and the rest are considered industrial lubricants. Therefore, the automotive engineer should become familiar with greases and oils and their characteristics as they relate to automotive use. Because this chapter deals with automotive lubricants, the emphasis will be placed on the use of vegetable oils within automotive systems. Furthermore, the chapter provides information on the chemistry of vegetable oils, the general performance requirement of lubricants and greases, standard test procedures required for the oil testing, and the issues of biodegradability and toxicity.

26.2 USES OF VEGETABLE OILS IN AUTOMOTIVE APPLICATIONS

Vegetable oils have been a source for lubricants throughout history. As such, the use of vegetable-based lubricant or fuel is not new, and since the invention of the wheel, animal fats and vegetable oils have been used to lubricate the wheel and its axle. In more recent history, in the 1900s during a power show in Paris, Rudolf Diesel used peanut oil to power one of his diesel engines. However, the use of biolubricants and biofuels was put on hold because of the abundance and low cost of petroleum.

Henry Ford I, automotive industrialist, and Dr. George Washington Carver pioneered agricultural research for industrial purposes. Henry Ford had a vision of using crop-based materials in making cars as well as tractors and to create a closed circle of cradle-to-grave renewable products. George Washington Carver's research resulted in many products from peanuts, sweet potatoes, and pecans.

Henry Ford was supportive of George Washington Carver's research, recognizing their mutual visions. They shared a vision of a future in which agricultural products would be put to new uses to create what today we refer to as biobased products and industries. Ford believed that agriculture could be the source of chemicals and raw materials for industrial uses. He paid attention to the mechanization of farm machinery and was convinced that farmers could become self-sufficient

in creating their own food, fuels, and lubricants from their farm-renewable products. Toward that end, Ford sponsored the research activities of Carver, whom he considered another visionary in the use of biobased products. He even manufactured biobased plastic car bodies to show the potential of renewable products. When Ford began to manufacture tractors, he included bioplastic seats for the tractors to eliminate the hot metal seats in the summer and cold metal seat in the winter. The bioplastic seat idea had to be abandoned when rodents and cows began to chew on the seat.

During the 1980s, encouraged by the agriculture community in Europe, European researchers began to explore the use of vegetable oils as hydraulic fluids and for other industrial lubricants. The concern for the environment and lobbying by farmers' organizations led to mandates for the use of biodegradable products in certain parts of Europe. As an example, in the 1980s the German government required the use of biodegradable hydraulic oils in some parts of Germany. During this period, the European community created environmental seals and emblems to identify the "Environmentally Aware" lubricants.

The efforts toward a biodegradable lubricant in North America began in the 1990s with many U.S. companies following the Europeans' leads on creating biodegradable products. In the 1990s, during the meetings of ASTM in the United States, over 40 North American companies had representatives present to discuss their efforts in creating biodegradable products and to help establish standards.

The U.S.-based chemical additive company, the Lubrizol Corporation, invested significant amounts of resources in creating additive packages for vegetable oil (specifically sunflower oil) lubricants. The list of additive packages and products from the Lubrizol Corporation was comprehensive and included food-grade products, two-stroke-cycle engine oils, and universal tractor hydraulic fluids. Neither the Lubrizol Corporation nor other companies ventured into the concept of developing engine oils made of vegetable oils. Small entrepreneurial companies in the U.S. experimented by using small percentages of 5–10 % vegetable oils in engine oils and then testing that oil in post office trucks and family vehicles. However, a lack of industry-approved standards from API or SAE doomed their efforts of creating commercially successful engine oil. Other U.S. companies such as Cargill also invested heavily in the testing of vegetable-oil-based engine oils but abandoned the concept after facing difficulty meeting the requirements of various standards while creating economical engine oil.

The continued low price of petroleum and a lack of mandates for using biodegradable or renewable products eventually diminished the investments in research and

¹ University of Northern Iowa, Waterloo, IA, USA

development by U.S. companies for these products. By the late 1990s, only farmers groups such as the United Soybean Board, representing U.S. soybean farmers, or the U.S. Department of Agriculture were continuing to fund the research and developmental activities of industrial products and lubricants made from renewable biomass materials.

In the United States, the Farm Bill passed in the year 2000. It was a 5-year plan for advancement of agriculture, including provisions for the promotion and use of biodegradable and renewable products. In an attempt to avoid mandates and to allow the free market enterprise to bring about the success of renewable products, the U.S. government selected a “leadership by example” approach. This required the federal agencies to give purchase preference and use biobased products so as to prove viability of performance and eventually lead to commercial success in competitive private sector markets. Biobased and renewable-based lubricants now have a presence in the world market and are anticipated to significantly grow in technology and use.

To better understand the future of biobased lubricants vis-à-vis petroleum lubricants, it is important to understand the nature and types of plant oils and petroleum oils. Within that context, basic concepts relating to these two oils will be covered.

26.3 VEGETABLE OILS

26.3.1 Triglycerides

The basic structure of vegetable oils is an ester between glycerol and three fatty acids. Depending on the length of the carbon chain making up the fatty acid, the resulting fat can be either liquid (oil) or solid (fat or butter). Because glycerol is capable of bonding with three molecules of fatty acid, the result is referred to as a triglyceride (Figure 26.1).

A triglyceride, also called triacylglycerol (TAG), is a chemical compound formed from one molecule of glycerol (also called glycerin) and three fatty acids. The structure of glycerol is shown in Figure 26.2.

Glycerol is a trihydric alcohol (containing three $-OH$, or hydroxyl groups) that can combine with up to three fatty acids. Fatty acids may combine with any of the three hydroxyl groups to create a wide diversity of compounds. Monoglycerides, diglycerides, and triglycerides are classified as esters, which are compounds created by the reaction between (fatty) acids and alcohols (glycerol) that release water (H_2O) as a byproduct.

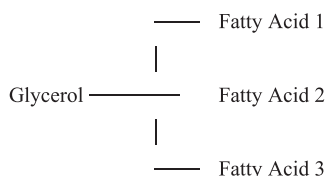


Figure 26.1—Structure of a triglyceride.

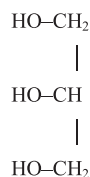


Figure 26.2—Structure of glycerol or glycerin.

Fatty acids contain a chain of carbon atoms combined with hydrogen, forming a hydrocarbon. They terminate in a carboxyl group. If the three fatty acids are alike, the molecule is a simple triglyceride; if they are different, it is a mixed triglyceride.

26.3.2 Saturated Fatty Acids

Each carbon atom along the chain has the ability to hold two hydrogen atoms. The fatty acid is said to be saturated if there are no double- or triple-bonded carbon atoms in the chain.

26.3.3 Unsaturated Fatty Acids

If a fatty acid chain contains double bonds it is said to be unsaturated. In other words, by breaking the double or triple bonds, more hydrogen can be added to the molecule. An unsaturated carbon chain can be saturated by adding hydrogen to the multiple bonds in the chain in a process referred to as hydrogenation.

Saturation and unsaturation affect the liquidity of the vegetable oil. Unsaturation is directly related to the liquidity of the oil as well as its solubility and chemical reactivity. With an increase in unsaturation, the melting point goes down and liquidity increases while solubility in certain solvents and chemical reactivity also increases. This usually results in oxidation and thermal polymerization. In general, saturated oils show more oxidation stability but have high melting points (lower liquidity), such as palm oil, which has high oxidation stability but is solid at room temperature. This limits its use for liquid lubricant applications unless modified.

When considering the fatty acids' molecular formation in a normal single-bond atom, there is freedom of rotation around the bond, but there is rigidity at the site of a double bond. Thus, two fixed positions of cis (meaning on same side) and trans (meaning across) are possible. Trans forms of fatty acids “pack” much closer together than the cis forms. Therefore, the trans forms more closely resemble the saturated fatty acids making “trans fat” undesirable as a food oil. Because the saturated fatty acids have no double bonds to distort the chain, they pack more easily into crystal forms and therefore have higher melting points than unsaturated fatty acids of the same length. They are also less vulnerable to oxidation. This property also allows for winterization of the vegetable oils described later.

26.4 VEGETABLE OIL PROPERTIES

Vegetable oils have many advantages as well as some shortcomings when considered for their use in automotive lubricants and hydraulic fluids. Most importantly, unless they are modified they lack oxidation stability. The oxidative stability of vegetable oils is dependent on the position and degree of unsaturation of the fatty acids that are attached to the glycerol molecule. For example, most soybean oil fatty acid composition comprises conjugated carbon-to-carbon double bonds that make it more susceptible to oxidation. “Conjugated” is a term used to describe a condition in which the double bonds in a carbon chain alternate with single bonds. Conventional soybean oil contains approximately 52 % linoleic acid, which has two conjugated double bonds, and 7–8 % α -linolenic acid, which contains three conjugated double bonds. If left untreated the use of these oils could lead to increased oxidation and consequently increased viscosity.

In extreme cases, if the oil continues to oxidize during use it could lead to polymerization and formation of polymer films in the oil. To avoid oxidation in use, the vegetable oil is either chemically modified or antioxidants are used to increase oxidation stability or both. Hydrogenation, in which hydrogen is chemically added to the double bonds, is one method used to chemically modify the oil and increase its oxidation stability. Unfortunately, hydrogenation also increases the melting point, and full hydrogenation will result in a product that is solid or semisolid at room temperature. Oilseeds that are genetically enhanced and have higher oxidation stability are more conducive for use in industrial lubricants and hydraulic oils.

26.4.1 Cold-Temperature Properties of Vegetable Oils

The longer the fatty acid carbon chain, the higher the melting point of the oil will be. Double bonds within the carbon chain significantly lower the melting point. Vegetable oils, because of their fatty acid structure, tend to freeze at relatively higher temperatures than their mineral oil counterparts. A pour-point comparison of hydraulic fluid using mineral and soybean oil as base fluid is shown in Table 26.1. For applications in which hydraulic oil or industrial lubricants are exposed to subzero temperatures, a mixture of vegetable oils and mineral or synthetic oils could be used. However, mixing affects other properties of vegetable oils, including the viscosity index (VI), flash/fire points, compatibility with elastomers, and other components including biodegradability.

Vegetable oils, because of their relative polarity, adhere to metal surfaces for better metal-to-metal separation. In addition, because of a higher VI relative to petroleum oils, they are more stable as the temperature changes. For example, soybean oil has a VI of approximately 222, with a viscosity of 31.69 cSt at 40°C (104°F) and a viscosity of 7.589 cSt at 100°C (212°F). For comparison, naphthenic base oil with a viscosity of 37.95 cSt at 40°C (104°F) and a viscosity of 5.295 cSt at 100°C (212°F) would have a VI of 53. Because the high VI results in a more stable viscosity when temperatures change, lower viscosity vegetable-oil-based fluids could be used in applications in which higher viscosity petroleum oil is required. As an example, an SAE 30 oil made from vegetable oil may be suitable for applications in which an SAE 40 from petroleum oil is specified. The difference in VI is significant with most vegetable oils having almost 4 times higher VIs than the petroleum mineral oils.

The flash and fire points of vegetable oils are consistently and considerably higher than equivalent viscosity

mineral oils. Fire points of vegetable oils are typically greater than 300°C (572°F). This property is suitable for the creation of industrial or automotive lubricants that could meet some fire retardancy standards, including those of the Factory Mutual standards in the U.S. metalworking fluids made from vegetable oils, which show less tendency to burn in addition to hydraulic applications such as in building elevators, which could benefit from the fire safety aspect of this property of vegetable oils. Table 26.2 presents a recent report on viscosity and the VI of Groups I, II, and III for comparison [1].

There are many factors that affect the fatty acid makeup of vegetable oils. In addition to their natural structure, changes in the growing conditions and geographic location and factors such as exposure to daylight, light intensity, and quality affect the properties of vegetable oils. Because the fatty acid composition of oils and fats are unique, their characteristics are different. One important process that can be used to affect the types of fatty acid present is partial hydrogenation, in which only some of the double bonds present in the carbon chain are given their full complement of hydrogen.

26.4.2 Oxidation Stability

Vegetable oils are used for frying applications, but exposure to heat as well as moisture from food, light and air causes them to oxidize. Oxidation of frying oil is accompanied by rancidity and an increase in viscosity. Most materials will have some degree of reaction with oxygen resulting in oxidation. For frying applications, attempts are made to stabilize the oil through hydrogenation or use of more saturated oils, such as palm oil. One indication of oxidation is the onset of rancidity, which can be recognized by smell. In industrial applications, as indicated earlier, increased viscosity could be used to note the onset of oxidation.

The change in viscosity mentioned above is irreversible. This is different from when the oil thickens because of exposure to cold temperatures such as when cooking oil becomes solid at room temperatures. In the latter case, heating the oil reverses it back to its original viscosity. In the case of oxidation thickening, a change in molecular structure takes place resulting in the initiation of the polymerization process. Once initiated, larger molecules continue to form, propagating the entire volume of the product. This will then continue until terminated by intervention or by completion of the full polymerization.

Figure 26.3 shows crude soybean oil that was exposed to air and ambient temperatures that fully polymerized over the period of a few months. This phenomenon

TABLE 26.1—Viscosity, VI, and Pour Points of Selected Oils and Identical Hydraulic Fluids Using Soybean- and Mineral-Oil-Based Fluids

Description	Pour Point (°C) ASTM D6749	Viscosity at 40°C ASTM D445	Viscosity at 100°C ASTM D445	VI ASTM D2270
Crude conventional soybean oil	−6	31.69	7.589	222
Mineral oil	−49	37.95	5.295	53
Hydraulic fluid with crude conventional soy	−4	32.26	7.592	217
Hydraulic fluid with mineral oil blend	−11	25.24	4.248	46

TABLE 26.2—Viscosity Characteristics of ISO VG32 for Groups I, II, and III Base Oil

Properties	ISO VG32 Group I	ISO VG32 Group II	ISO VG32 Group III
Appearance	Clear yellowish liquid	Colorless liquid	Colorless liquid
Kinematic Viscosity at 40°C (cSt)	29.15	29.65	37.55
Kinematic Viscosity at 100°C (cSt)	5.14	5.37	6.43
Viscosity Index	105	116	123

**Figure 26.3—Soybean oil naturally oxidized and polymerized.**

should be taken into consideration when formulating vegetable-oil-based engine oils. Even small quantities of vegetable oil in an engine could result in the formation of polymer films in oil galleries or on crankcase walls. Unless the amount of vegetable oil used in an engine oil is small, higher quantities of detergents may be required to clean any potential polymer, gum, or other byproduct of oxidation.

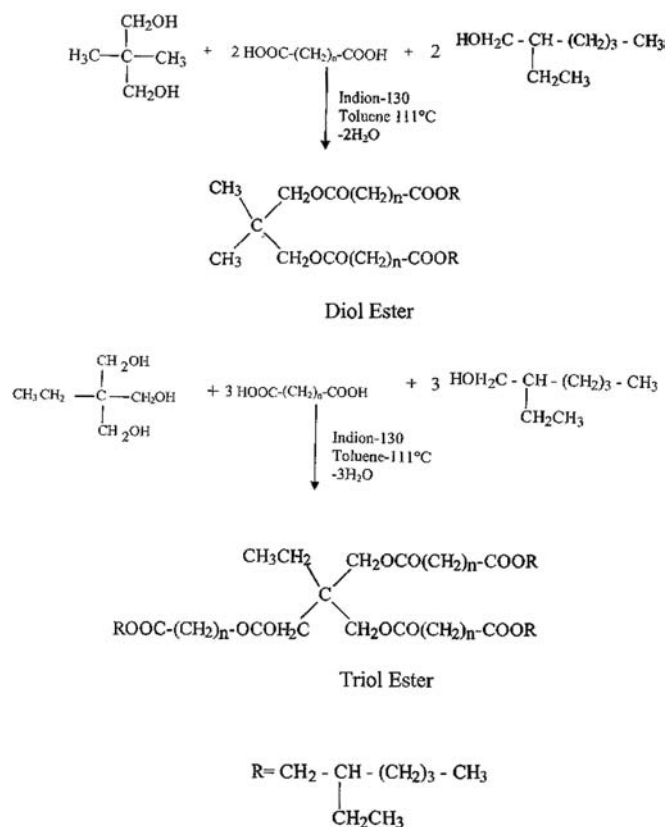
26.4.3 Esters

Esters can have various molecular weights offering advantages for some applications. The *Journal of Synthetic Lubrication* has published numerous papers on synthetic esters. For example, some of the complex esters may be made via the reaction of a polyol, dicarboxylic acid, and monoalcohol as an end-capping agent. Key structural features of these esters and the basic structure of an alcoxy group from the end-capping monoalcohols are presented in Figure 26.4 [2].

26.4.4 Estolides

Estolides are designed with the idea of being able to use various vegetable oils or animal fats as starting materials. A patent by Steve Cermak et al. [3] describes the creation of estolides for industrial and automotive lubricants.

These estolides showed pour points of -30°C (-22°F) for the unsaturated oleic estolides and -40°C (-40°F) for the saturated ones. “They also showed oxidative breakdown of 200 and 400 minutes respectively in the Rotary Bomb Oxidation Test (RBOT), compared with 200 minutes for comparable mineral engine oil.” [3]. Note that ASTM

**Figure 26.4—Key structural features of these esters and basic structure of alcoxy group from the end-capping monoalcohols.**

has a new name for this test, which is now referred to as the Rotary Pressure Vessel Oxidation Test (RPVOT), ASTM D942.

Table 26.3 shows the oxidation stability and viscosity-related data for three commercially supplied estolides: distilled oleic estolide 2-ethylhexyl ester, oleic estolide 2-ethylhexyl ester and monomer, and distilled coco-oleic estolide 2-ethylhexyl ester.

Cermak and Isbell [3] provided comparative data on commercial petroleum-based hydraulic oils, regular soybean oil, and estolides (Table 26.4). The estolides without property-enhancing additives show comparable VIs and lower cloud and pour point formulated products.

Estolides are one example of chemical modification schemes that provide flexibility in the raw input materials and base oils with high oxidation stability and low pour point.

TABLE 26.3—Oxidation Stability and Viscosity Data of Three Estolides

ID #	Estolide Type	OSI Time (h)	Viscosity at 40°C (cSt)	Viscosity at 100°C (cSt)	VI
1	Oleic estolide	18.18	98.17	15.40	167
2	Coco-oleic estolide	22.25	76.58	12.59	165
3	Oleic estolide with monomer	15.45	40.30	8.20	185

TABLE 26.4—Comparison of Low-Temperature Properties and VIs of Coconut-Oleic Estolide 2-Ethylhexyl Esters to That of Commercial Lubricants

Lubricant	Pour Point (°C)	Cloud Point (°C)	Viscosity at 40°C (cSt)	VI
Commercial petroleum oil	−27	2	66	152
Commercial synthetic oil	−21	−10	60.5	174
Commercial soy-based oil	−18	1	49.6	220
Commercial hydraulic fluid	−33	1	56.6	146
Coco-oleic estolide	−33	−26	55.2	162
Oleic estolide	−33	−33	92.8	170

26.4.5 Other Chemical Modifications

There are many other processes being explored to modify the properties of fats or fatty acids and add value for industrial application. An example of such a process is metathesis. A simple definition of the word means to change places. In an example when two electrolytes are mixed together, the ions exchange place or exchange partners. When two solutions are mixed, positive ions of one electrolyte encounter anions of the other. If this new pairing forms a more stable substance such as a solid or neutral molecule, the reaction is said to go to completion. Products that would lead to completion in a metathesis include formation of a solid, formation of water, or formation of a gas.

More detailed information on catalytic metathesis is beyond the scope of this chapter. Its importance in creating new base oils for industrial lubricants needs to be emphasized.

26.4.6 Enzymatic Hydrolysis of Fatty Acids

The use of enzymes to mimic the digestive system's breakdown of fats and triglycerides has been reported. Triglycerides can be enzymatically hydrolyzed to fatty acids and glycerol by the use of lipases. Most industrial hydrolyses involve high-pressure steam stripping to hydrolyze the triglyceride esters. Unfortunately this process destroys some of the more useful fatty acids found in the more exotic plant oils. The use of lipases for enzymatic hydrolysis of oils can provide a more efficient approach that is less energy-intensive and does not alter the fatty acids that result.

U.S. Patent No. 5089403 by Hammond and Lee [4] describes using moistened, dehulled oat seeds or oat caryopses, which contain lipases. When the oil is exposed to the moistened caryopsis, the fatty acids dissolve in the oil phase and the glycerol is absorbed into the moist dehulled oil seeds. According to Hammond and Lee, in a single cycle, approximately 20 % of the oil can be catalyzed. Increasing the number of contact cycles will result in the hydrolysis of more oil.

Using lipases to split triglycerides into free fatty acids and glycerin will have potential for the creation of better lubricants and greases. The removal of glycerin from the fatty acids could reduce the hydrophilic properties of the formulated product. Also, if the free fatty acids are further processed into individual free fatty acids, more uniform grease soaps could be manufactured with predictable performance.

26.5 GENETICS AND INDUSTRIAL CROPS

Other promising technologies include genetic modification of crops, which was initially used primarily as a means of creating healthier oils. Because hydrogenation to stabilize vegetable oils for cooking results in unhealthy trans fats, the genetic modification of crops has taken a new direction with new and diverse goals. Genetic modification is considered for creating crops that are resistant to pests or herbicides or both or for including vitamins and pharmaceutical properties. Modification is also considered for including transgenic properties for drought resistance or for season or climate independence. Agronomists and food scientists, working on the genetics of the oilseeds for the development of healthier food, may have contributed to the increased potential for use of oilseeds in industrial and automotive lubricant applications. It is now clear that through genetic modification of the seeds, the fatty acid profile of the oil can be altered with great benefits in terms of stability, cold temperature flowability, and reduced need for chemical additives. This concept eliminates the need for hydrogenation or other chemical modification and thus reduces the cost of the base oil and finished products for use in industrial applications.

Genetic modification has been accomplished for some of the vegetable oils, including rapeseed, sunflower, and soybean. Salunkhe et al. [5] reported on the changes in the genetic makeup of rapeseed oil starting in the late 1960s. Accordingly, before the 1970s, the rapeseed oil contained 20–50 % erucic acid. The first Canadian low-erucic-acid variety, containing about approximately 3 % erucic acid, was licensed in 1968. In 1974, a lower acid variety containing less than 0.3 % erucic acid was introduced following the Canadian government's encouragement to switch to low-acid varieties. Canola is the Canadian version of the rapeseed with distinctly low erucic acid and low glucosinolate. It has a linoleic/linolenic acid ratio of 2:1. In the United States, various genetically modified seeds for canola, sunflower, and soybean have been developed by major seed and chemical companies. Currently, the availability of these oils with high oleic acid content of 80–90 % and excellent oxidation stability promises to create many new opportunities for vegetable-based automotive and industrial lubricants.

Perhaps the most promising new research advance to date is the development of new mutant lines of soybeans, which lead to new lines of high-oleic soybeans. These mutant lines with improved fatty acid profiles of the oil

can be cloned and then integrated into high-yielding elite lines by providing molecular markers. Cloned genes are introduced into soybeans to create transgenic lines with increased lysine, oleic, or stearic acid contents. These are oils with a very low content of polyunsaturated fatty acids and show high oxidative stability. Initially designed to replace hydrogenated oil, these oils, although more stable for frying and healthier in food, are also stable for use in many automotive and industrial lubricant and grease applications.

26.6 BIOBASED LUBRICANT TECHNOLOGY

The initial technology for biobased lubricants, primarily referred to as biodegradable lubricants, was based on vegetable oils with minor chemical modification and performance-enhancing additives. Because vegetable oils generally face inherent challenges when it comes to automotive or industrial lubricant uses, their performance properties must be carefully studied. For example, soybean oil shows a significant lack of oxidation stability, with an oil stability index (OSI) value of approximately 7 h. In one case, this oil was partially hydrogenated to improve its oxidation stability and then winterized to improve its pour-point performance. Addition of hydraulic oil additive packages, antioxidants, and pour-point depressants resulted in hydraulic oils capable of working in high-performance hydraulic systems.

Perhaps one the most important developments for U.S. biobased lubricants was the introduction of high-oleic-acid soybeans by the DuPont Corporation in the early 1990s. This genetically enhanced soybean had oil with a fatty acid profile considerably superior to conventional soybean oils. Originally designed for frying applications, this oil showed an OSI value of 192 h, approximately 27 times more stable than conventional soybean oils. This helped in the creation of several highly successful lubricants and greases. The Lubrizol Corporation had built its additive and lubricant technology on the basis of high-oleic and ultrahigh-oleic sunflower oils. Today, for many automotive and industrial lubricant applications, high-oleic soybean oil, high-oleic sunflower oil, and high-oleic canola oils are base oils of choice [6].

26.6.1 Oxidation Stability

Oxidation stability refers to the ability of the oil to maintain its properties, mainly its viscosity, when exposed to specific operating conditions. Because vegetable oils have been a main ingredient in the food industry, most methods dealing with their oxidation stability have been created through the efforts of the food industry, and by association, the chemical industry. Oxidation stability methods used in the lubricant and grease industry are based on petroleum and its derivative oils and are often not able to determine the stability of vegetable oils. Biobased lubricant researchers and developers have been relying on the use of standards created by the American Oil Chemist Society (AOCS) as well modified versions of standards created by ASTM. Others at the University of Northern Iowa National Ag-Based Lubricants (NABL) center have used hydraulic pump tests and field evaluations to create reference materials for possible use with vegetable-based lubricants. Below are examples of some of the test methods used to determine the oxidation stability of vegetable oils [6].

26.6.1.1 ACTIVE OXYGEN METHOD (AOCS CD 12-57)

In the active oxygen method (AOM), oxygen is bubbled through an oil or fat, which is held at 36.6°C (97.8°F). Oil samples are withdrawn at regular intervals and the peroxide value (PV) is determined. Expressed in hours, AOM is based on the length of time needed for the PV to reach a certain level. AOM is used as a specification for fats and oils. AOM hours tend to increase with the degree of saturation or hardness. This method has been largely replaced with the oxidative stability index [6].

26.6.1.2 PEROXIDE VALUE (AOCS CD 8B-90)

This test, designed to measure oxidation in fresh oils, is highly sensitive to temperature. Peroxides are unstable radicals formed from triglycerides. A PV more than 2 is an indicator that the product has a high rancidity potential and could fail on the shelf.

26.6.1.3 OIL STABILITY INDEX (AOCS METHOD CD 12B-92)

In the OSI method, instead of pure oxygen, regular shop air is used, which is one of the reasons the OSI method is simpler to operate than the AOM. A conductivity probe monitors the conductivity of deionized water as the evaporates from the test oil are emitted into the deionized water (Figure 26.5).

OSI values are expressed in hours; the lower the number of hours, the lower the stability of the oil. For lubricants such as hydraulic fluids that tend to reside in the system for hundreds or thousands of hours, a high OSI value for the base oil and yet a higher value for the formulated products will be needed. OSI values can be correlated with other oxidation tests, but for vegetable-oil-based lubricants, it is best to establish a relationship between field test results and the OSI values. Table 26.5 shows the OSI values for selected vegetable oils.

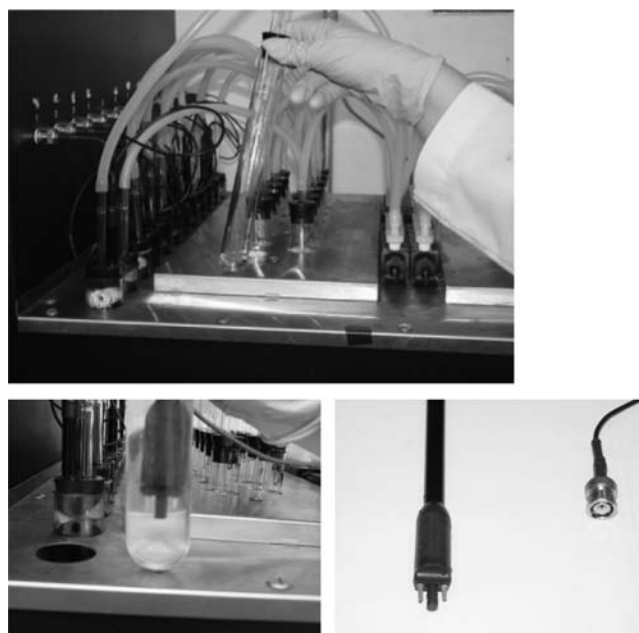


Figure 26.5—Oxidation stability instrument (top) and conductivity sensor in deionized water [6].

TABLE 26.5—OSI Values for Selected Vegetable Oils

Oil	OSI (h)
Apricot kernel	23.42
Avocado	18.53
Babassu	57.8
Castor	105.13
Coconut	75.38
Flaxseed	1.17
Hempseed	0.10
Jobba—refined	42.15
Jobba—golden	38.3
Macadamia	6.87
Ricebran	20.82
Ricinoleic acid	117.1
Safflower	17.98

26.6.1.4 RANCIMAT

Rancimat is a test that provides similar information to what one gets from the OSI test. It was recently approved by ASTM as a part of the Biodiesel Standard Test, ASTM D6751.

Honary [7] reported that using a hydraulic pump test would expose the vegetable oil to industrial conditions that are difficult to duplicate in many standard test methods. For example, he reported that most untreated vegetable oils meet ASTM wear protection requirements for hydraulic pumps because they naturally adhere better to metal surfaces preventing boundary lubrication, but the oil also breaks down and oxidizes. In ASTM D2882, currently designated as ASTM D7043, the untreated crude soybean oil showed 40 mg of wear, which is under the 50-mg passing maximum level. However, the lack of oxidation stability resulted in increased viscosity of the oil and, in extreme cases, led to polymerization.

As a result, in studying the performance of vegetable oil vis-à-vis resistance to oxidation, some hydraulic pump tests could be used with the primary purpose of monitoring the changes in viscosity. Empirical research and field test observations indicate that an increase of less than 10 % in viscosity for an oil tested in an ASTM D2271 (modified ASTM D7043) or equivalent is desirable. It is also observed that although the addition of additive packages to vegetable oils improves many of the oils' characteristics, it could negatively affect its natural lubricity.

The Eaton (Vickers) Pump Test procedure for evaluation of antiwear fluids for mobile systems has been replaced by the modified ASTM D7043 (Figure 26.7). This test method is used to evaluate the ability of a hydraulic fluid to provide acceptable fluid pump antiwear characteristics. Total weight loss of all vanes from individual cartridges tested should be less than 50 mg (not including intravanes). Weight loss of rings from individual cartridges tested should be less than 50 mg.

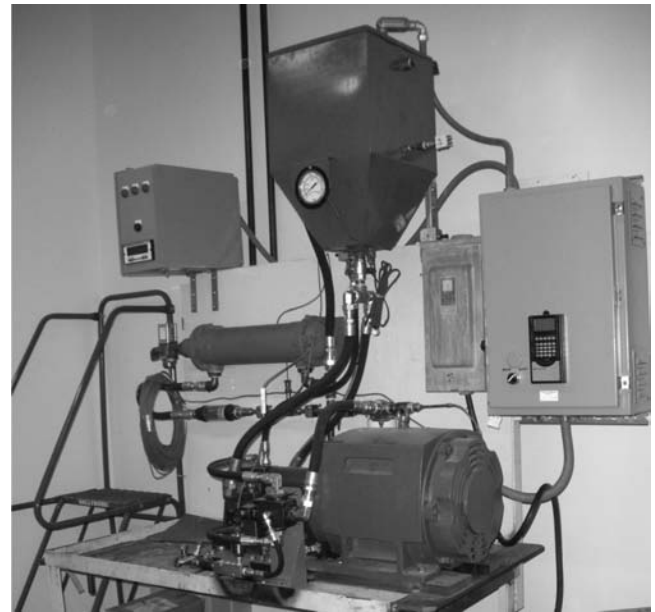


Figure 26.6—Pump testing setup for ASTM D7043.

26.7 BIOBASED ENGINE OILS [8]

Over the last 20 years, for researchers and biobased oil formulators, searching for a biobased engine oil has been a figurative searching for the Holy Grail. During this period, various small and large entities have been experimenting with biobased engine oils. Large entities abandoned the search after numerous trials and the ever-changing specifications. Other smaller groups created ventures and drove a truck filled with “biobased engine oil,” licking the dipstick at various stops to make a point for “environmental friendliness” of the product with no success. Other groups in Europe experimented with the Continuous Oil Recycling concept in diesel passenger cars. Although complex esters derived from vegetable oils can become economical and stable enough to handle the engine lubrication environment, many of the current vegetable-oil-based technologies have lacked the necessary stability and cold-temperature flowability to perform in the engines the way mature and perfected petroleum engine oils do.

As of this writing, claims for biobased engine oils are viewed with suspicion. Some have included small quantities of biobased oils in conventional engine oils and claimed the oil to be biobased. It is likely that eventually the biobased engine oils will be based on biobased-derived synthetic base oils. Using vegetable oils, even in small quantities, could still result in the oxidation of the oil and possible formation of polymer films within the oil galleries or exposed surfaces of the oil pan.

A design by the NABL center that involves a new approach to using biobased engine oils was described in the May 2009 issue of the *OEM Off-Highway Magazine* as follows:

26.7.1 The Continuous Oil Recycling System

The Continuous Oil Recycling System (CORS) as a concept has been tried as an aftermarket product that was added to a diesel engine to continuously steal a small amount of engine oil and feed it into the fuel line of the engine. The driver would then add in a small quantity of oil to the engine at every refueling. As a result, after a certain number of

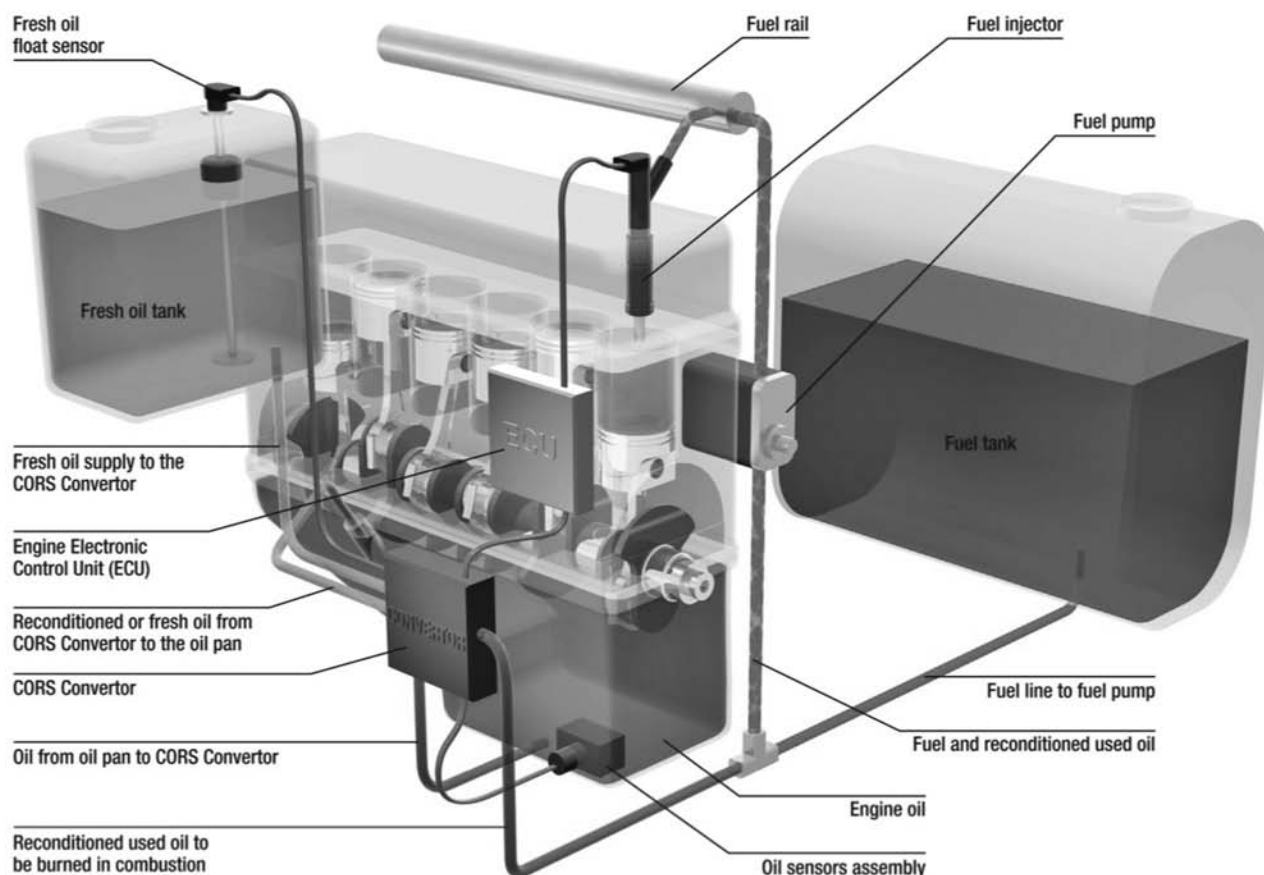


Figure 26.7—Conceptual representation of the CORS components plus the engine ECU and injector.

refuelings, the operator would purchase oil for the add-on oil tank. The main problem with this approach was that the burning of used engine oil resulted in a significant, negative effect on the already hard to achieve emission standards.

The author and a team of researchers modified the CORS concept to use vegetable-oil-based engine oils and created a sophisticated “black box” called the CORS converter. The CORS converter not only communicates with the main processor of the engine, but it also has its own sensors and transducers to monitor the conditions of the engine oil and engine fuel before introducing the oil into the fuel line. The CORS converter is an add-on unit that conceptually resides between the crankcase and the fuel injectors and ensures that the recycling of the oil as fuel is performed in a way that is beneficial to the engine Figure 26.7.

26.7.2 The CORS Converter

The CORS converter comprises an array of sensors plugged into the crankcase to monitor the physiochemical conditions of the engine oil, which is made of a mixture of modified vegetable oils and minimal amount of performance-enhancing additives. The CORS converter continuously draws oil samples from the crankcase; in addition to evaluating the oil, it conditions it as needed to be used as fuel. In effect the CORS converter is expected to act like an onboard fluid conditioner that ensures what is fed into the fuel system is cleansed of harmful constituents and is only sent to the fuel system when the engine conditions indicate the best time to use this oil as fuel. As an example, a cold

engine would receive zero to a small amount of vegetable-based engine oil into its fuel system, and the amount of oil that is fed into the fuel system is varied based on the ability of the engine’s combustion process to provide the cleanest combustion possible. Thus, during this time, when the engine is running at operating temperature and coasting, larger quantities of oil are fed into the fuel line to burn.

Whereas the original idea of feeding used petroleum-based engine oil into the fuel system had a negative effect on the emissions, the CORS combined with the CORS converter can actually improve exhaust emissions when using biobased oils.

In U.S. Patent No. 6,532,918, Meng and Luther [9] described a process lubricating and simultaneously supplying fuel in a vegetable-oil-operated combustion engine. In this process using an oil “suction pump,” a specific quantity of engine oil is siphoned off from the engine to be burned with the fuel. The same quantity of fresh oil corresponding to the amount that is siphoned off is then added to the crankcase. In this patented process, provisions are made for injecting additives into the crankcase oil [9].

26.7.3 CORS for Stationary Engines

The best place to start the platform for CORS-based engine oils are with stationary diesel engines in which the addition of an oil tank next to the fuel tank does not present the logistic problems of dealing with mobile equipment. To test the concept, three John Deere diesel engines were prepared and instrumented for testing using an eddy current dynamometer to test the engine under various load conditions.

Figure 26.8 shows the engine, dynamometer, and monitoring equipment associated with the data collection system.

All sensor and transducers were interfaced with a data monitoring system to allow monitoring of the engine performance. For each test, the maximum load and horsepower setting were selected to accelerate the degradation of the oil. The four-cylinder engine was rated at 120 hp, and the test parameters were set to simulate the full load at approximately 120 ± 5 hp (Figure 26.9).

Because these engines were used with a dynamometer, it is assumed that data gathered using these diesel engines will be transferable to the stationary engines. Such engines are used as back-up or small-scale electric generators for utility companies, hospitals, and any place that may use a diesel engine for electric generation or for pumping.

During the start-up process, regular diesel engine fuel is used without any mixing with the engine oil. In the meantime, the CORS converter draws small quantities of the oil from the engine via a positive displacement pump. The physiochemical properties of this oil are constantly monitored by an array of sensors placed in the crankcase oil. The CORS converter receives the oil and, depending on its conditions, sends it through several conditioning steps based on a design that could include physical and chemical

filtration, addition of chemical catalysts, heating, cooling, etc. Some of this “conditioned” oil will remain in the CORS converter in a small reservoir ready to be sent into the fuel system whereas some of it may return back to the engine crankcase if not needed at that moment.

The CORS converter has four oil lines attached to it: one for bringing in the engine oil from the crankcase for analysis and conditioning; one from the fresh oil reservoir for preparation for injection into the crankcase to replenish the used oil; one to the crankcase for injection of fresh oil, excess reconditioned oil, or a mixture of fresh and reconditioned oil back into the crankcase; and one connected into the fuel line of the engine so that conditioned oil can be fed into the fuel system.

When the data from the engine electronic control unit (ECU) and the engine sensors from CORS indicate that the conditions are right to feed the oil into the fuel, a small but varying quantity, currently not exceeding an average 2 % of the weight of the fuel being consumed, is sent into the inlet side of the fuel injector pump. For example, at 2 %, the diesel fuel could be considered a B-2 biodiesel fuel, and because the vegetable oils have shown to improve the lubricity of low-sulfur fuels, the result is a tribologically more effective fuel. The conditioned oil is void of most of the impurities often found in the used engine oils. In addition, the oil is conditioned to proper temperature, and at 2 % level it is highly diluted in the fuel. Although the vegetable oils have a lower British thermal unit/volume content than diesel fuels, the effect on the power output of the engine would be minimal.

26.7.4 Observed Results

A comparison of several diesel engines, commonly used for agricultural machinery, was used to determine the time residency of the oil in the crankcase at different oil consumption rates. Table 26.6 shows the reservoir sizes and the percentage of the oil that has to be removed from the crankcase to meet the desired residency time.

In the initial test, a pure vegetable base oil was prepared with a viscosity of 107 cSt at 40°C as a replacement for 10W-40 diesel engine oil that has a viscosity of 120 cSt at 40°C. A lower viscosity vegetable-oil-based engine oil was chosen because the vegetable base oil has a much higher VI of approximately 220, as compared with the equivalent petroleum oil with a VI of approximately 100. This allows the use of thinner oil and less starting torque requirement while maintaining the viscosity of the oil at the operating temperatures.

During the test, the viscosity of the oil was checked every hour, knowing that an increase in viscosity is a sign of oxidation. After some initial shearing of the oil, the viscosity was stable for approximately 10 h and then began to increase rapidly because of oxidation. During this test, the CORS was turned off and no oil was being removed from the crankcase for burning as fuel. The untreated vegetable oil showed stable viscosity for approximately 10 h at full load and the test was terminated after 14 h. This viscosity increase was not unexpected because similar viscosity changes had been observed in high-pressure/high-temperature hydraulic pump tests but after longer hours of operation. Because the engine was running at full load, it is anticipated that a lower level of engine load could increase this operational performance to several hours more than

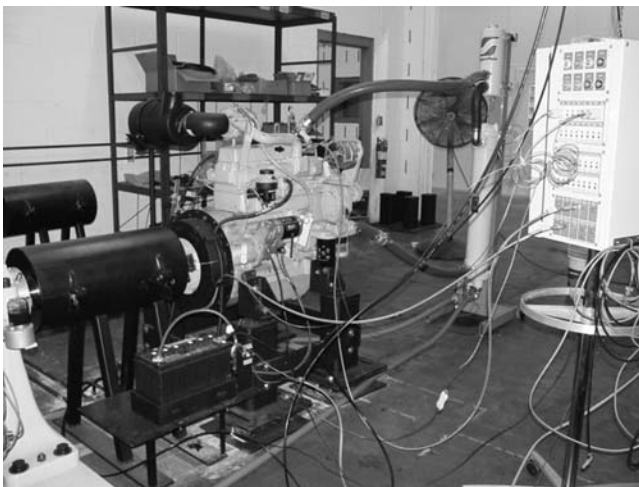


Figure 26.8—John Deere diesel engine (120 hp).

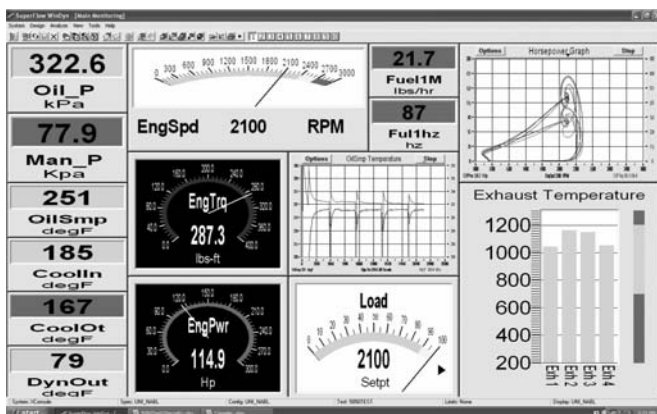


Figure 26.9—A screen shot of the parameters set for the engine tests.

TABLE 26.6—Example of Different Drain Intervals on the Basis of Burn Rate of Selected Diesel Engines

Engine Data	Agriculture Engine 1	Agriculture Engine 2	Agriculture Engine 3	Agriculture Engine 4
Engine power (kW)	93	138	150	360
Oil reservoir capacity (L)	13	20	28	42
Amount of fuel use (kg/h)	20	31	34	67
Drain rate at 0.25 % burn rate (in hours)	225	232	296	226
Drain rate at 1 % burn rate (in hours)	113	116	148	113
Drain rate at 5 % burn rate (in hours)	11	12	15	11
Drain rate at 10 % burn rate (in hours)	6	6	7	6

the observed 10 h. The time to rapid increase in viscosity corresponds to the OSI time for the oil.

In the next test, the same vegetable oil was mixed with an SAE 10W-40 conventional oil at a ratio of 75/25 vegetable oil/petroleum. This mixture oil was tested with the engine at full load, and the viscosity of the oil remained flat for the entire 100 h with the CORS on. All other variables in the engine indicated that the mixture could be run in the engine indefinitely as long as oil volume equal to 2 % of the fuel consumption is removed and replaced with fresh oil. Because similar tests have been performed on the fuel using 2 % purified vegetable oil in the fuel system without any effect on the engine performance, the researchers were convinced that CORS is viable and will indefinitely run a clean engine and a clean combustion. These are still considered experimental products at the time of this publication. The developmental activities are ongoing for optimizing the size and components of the CORS Converter, improving the accuracy of the sensors assembly and optimizing the algorithm used on the CORS processor. The engine oil is undergoing further improvements to replace the 25 % petroleum portion of the blend with additives in the 75 % vegetable oil portion. Although the engine tests are continuing in the laboratory, field test sites are being run for long-term tests.

Economically, when the oil is consumed at the rate of 2 % of the fuel consumption, its residency in the engine would range from 57 to 64 h depending on the size of the engine and crankcase as appeared in Table 26.7. Because the residency of the oil is limited, there is reasonably little need for and as a result little cost for the performance enhancing additives. Because the oil would be used as a lubricant first and then burned with almost par value for the fuel, the cost of the lubrication could almost be eliminated. The inconvenience of having to resupply the fresh oil tank would be compensated for with the elimination for the need to change the engine oil. Understandably, CORS is still in developmental stage, but it could deliver the first real biobased oil based engine lubricant technology based on vegetable oils.

26.8 BIOBASED AUTOMOTIVE GREASES

Greases provide an effective means of delivering lubrication to the machine component being lubricated. Where liquid lubricants flow easier, they require a reservoir to contain their volume. On the other hand, solid lubricants require direct contact to the point of lubrication for effective lubrication delivery. Greases are semisolid and can deliver the benefits of liquid lubricants without requiring a reservoir as well as the benefits of solid lubricants by

TABLE 26.7—ASTM Test Methods Required for ASTM D4950

1. <i>ASTM D212</i> : Test Method for Cone Penetration of Lubricating Greases
2. <i>ASTM D566</i> : Test Method for Dropping Point of Lubricating Greases
3. <i>ASTM D1264</i> : Test Method for Water Washout Characteristics of Lubricating Greases
4. <i>ASTM D1742</i> : Test Method for Oil Separation from Lubricating Greases during Storage
5. <i>ASTM D1743</i> : Test Method for Corrosion Prevention Properties of Lubricating Greases
6. <i>ASTM D2265</i> : Test Method for Dropping Point of Lubricating Greases over Wide Temperature Range
7. <i>ASTM D2266</i> : Test Method for Wear Preventive Characteristics of Lubricating Greases (Four-Ball Method)
8. <i>ASTM D3527</i> : Test Method for Life Performance Automotive Wheel-Bearing Grease
9. <i>ASTM D4170</i> : Test Method for Fretting Wear Protection by Lubricating Grease
10. <i>ASTM D4289</i> : Test Method for Compatibility of Lubricating Grease with Elastomers
11. <i>ASTM D4290</i> : Test Method for Leakage Tendencies of Automotive Wheel-Bearing Grease under Accelerated Conditions
12. <i>ASTM D4693</i> : Test Method for Low-Temperature Torque of Grease Lubricated Wheel Bearings

maintaining their body structure. In applications such as the wheel bearing of an automobile where excessive heat is generated, liquid lubricants would thin down and can leak out of the bearing seals. The wheel bearing is a good example for using grease.

Grease as a semisolid lubricant is made of a mixture of soap (solid) and oil (liquid). Compared with liquid lubricants, grease maintains its body within the wheel bearing, filling all of the bearing cavities while at the same time allowing the oil in the grease to lubricate the bearing.

By definition, grease is a solid or semisolid fluid made of a thickening agent in a liquid lubricant and other ingredients that impart special properties (ASTM D4175) [10]. The body of the grease is formed by the soap, which forms a matrix structure similar in detail to that of a sponge, thus allowing the voids within the matrix to be filled with the lubricating oil. The soap provides the body to keep the grease in place while the oil delivers the lubricity. An important benefit of the soap in the grease is that it provides the ability to seal and prevent the oil from leaking out or dirt from getting in. The soap's matrix acts as a reservoir for the oil in providing delivery of the lubricants and performance additives at the point of contact. As indicated earlier, grease is then made up of soap, which acts as a reservoir for the liquid oil, and its chemical performance enhancers (additives). The additives are used to match the performance requirements and could be used for wear protection, extreme pressure (EP), corrosion resistance, antirust, and tackiness [7].

26.8.1 Lithium Hydroxide Soap-Based Greases

Simple and complex lithium greases make the largest portion of the worldwide grease produced. The process of making such grease could simply be explained as follows: The lithium hydroxide as a base is reacted with oil, fat, and fatty acid to make soap. Some water may be added, and the lithium hydroxide may absorb water or be made into slurry to avoid exposure to its dust; the water is boiled off during the process. The initial process may require the oil to be heated to approximately 135°C (275°F) and then introduced to the lithium hydroxide. Excessive foaming is possible during this reaction. High-pressure vessels, antifoam agents, or slowing of the reaction could be used to reduce or control foaming. A neutralized soap would have a pH of approximately 7, indicating all of the base has reacted with the acids. After the reaction is completed, the soap is heated further to approximately 200°C (392°F) to evaporate the resulting water from the reaction. At this stage the lubricating (cooling) oil is added, and the product is mixed, cooled, and milled until homogenized. When the product temperature is low enough to add the chemical additives, they are then added to finish the product.

Lithium grease has a fibrous structure that is effective in entraining the lubricating oil. Each grease made from different thickener has a different structure. Some, such as the organoclay grease, is very smooth and creamy with little fibrous structure as compared with soap-based greases.

26.8.2 Nonsoap-Based Greases

Some greases are made without the use of soap as their thickener to overcome the limitations of various soap-thickened greases. Specifically, soap-based greases have

limitations when exposed to extreme cold or hot temperatures. For example, aircraft greases are exposed to extreme cold temperatures at a high altitude. Chains on conveyors used in bakery ovens or foundry furnaces require greases with a high tolerance to heat. The presence of soap in grease makes the grease vulnerable to hardening at extreme cold temperatures or liquefying at extreme high temperatures. Examples of nonsoap greases include clay-, polyurea-, and polymer-based greases. Vegetable oils can be used as the base oil to make any such nonsoap greases.

26.8.3 Biobased Greases

Renewable oils can be used as a substitute for petroleum base oil in the conventional grease manufacturing equipment. For simple lithium soap grease, the reactor could be charged with the choice vegetable oil and heated to approximately 60°C (140°F) to melt the stearic acid and then heat the mixture to 130°C (266°F). At this temperature, the lithium hydroxide is added to react with the stearic acid. When the reaction is completed, the resulting soap (having water as a byproduct) is heated while mixing to temperatures of approximately 204.4°C (400°F) to evaporate the water. Then, an equal or less volume of cooling oil, depending on the desired consistency, is introduced into the soap to make the grease, which is then milled to homogenize. The grease has to be cooled down to appropriately low enough temperatures so that the additives that are added to the final product are not damaged.

During the conventional petroleum-based grease-making process the fatty acids to be reacted with lithium do not interact with the mineral oil. However, with vegetable oils, because of the presence of fatty acids in their makeup, the level of other fatty acids may be reduced or eliminated. Nevertheless, the process yield is approximately the same as making grease with mineral-oil-based greases. Vegetable oils may absorb the atmospheric moisture, especially during the summer, which results in more water that will need to be boiled off in the process. Because vegetable oils generally range in viscosity from 35 to 45 cSt at 40°C (104°F), some processes have included the introduction of higher viscosity vegetable oils as a viscosity modifier. This could be the inclusion of blown vegetable oils or naturally higher viscosity oils mixed with the base oil. High viscosity vegetable oils at 1500 cSt at 40°C (104°F) are commercially available for mixing to increase the viscosity of base vegetable oils.

Renewable oils have a uniquely different behavior when exposed to high temperatures. In the case of some vegetable oils, once the oil temperature exceeds 150°C (302°F), it begins to oxidize rapidly. If steps are not taken to remedy this rapid oxidation, the product will begin to polymerize, resulting in irreversible structural change. In such cases, the product could partially or fully polymerize or change its state from a soap into a polymer with little or no lubrication value. Several methods exist for stabilizing soybean or other vegetable oils so they can be reacted with lithium hydroxide and produce stable greases. The use of high-oleic vegetable oils, is often used to improve the oxidation stability of the final product. Vegetable oils, because of their higher VI, present a more stable body when exposed to high temperatures. As a result, properly formulated vegetable-oil-based grease shows a more stable body in usage and will not thin down as fast as comparable mineral-oil-based greases when exposed to high temperatures.

Because vegetable oils are made up of a mixture of fatty acids, they present another challenge in grease-making. Different fatty acids have different melting points, so when reacted with lithium, the fatty acids with the lower melting point react faster than the fatty acids with the higher melting point or longer carbon chain. It can be conceptualized that the vegetable-oil-based grease can be considered a mixture of several different greases, such as lithium oleate, lithium linoleate, lithium stearate, lithium palmitate, and the like. These greases behave differently at different operating temperatures; the high oleic vegetable oils provide the advantage of making the final grease more uniform.

26.8.4 Specifications for Greases

Most of today's grease specifications are set by the National Lubricating Grease Institute (NLGI) in the United States. This is the primary body of experts focused on supporting the grease industry. Working with existing standards as developed by the ASTM, NLGI continues to create new information that is useful for improving the performance standards of greases.

The key grease standard (ASTM D4950) was created based on the request from SAE, to the ASTM with input from NLGI. ASTM D4950 is "the Standard Classification and Specifications for Automotive Service Greases." It includes specifications for two categories of greases:

(1) chassis lubricants (with letter designation L) and (2) wheel-bearing lubricants (with letter designation G). Performance classifications within these categories result in two letter designations for chassis greases (LA and LB) and three for wheel-bearing greases (GA, GB, and GC). The automotive industry is in agreement that the highest performance classification in each group is LB and GC. This is typically shown as LB-GC, which is also suitable for service relubrication for automotive and truck shops.

Later, NLGI developed the service categories for automotive greases to include LA (chassis grease with frequent lubrication requirement), LB (chassis grease with infrequent lubrication requirement), GA (wheel-bearing grease with frequent lubrication requirement), GB (wheel-bearing grease with less frequent relubrication), and GC (wheel-bearing grease for mild to severe duty) applications. A combination of these classifications is also used with the GC-LB as one of the highest classifications, normally used as a single grease that is suitable for all grease points of cars and trucks [7].

26.8.5 ASTM D4950 Method

ASTM D4950 is based on a set of 12 other ASTM tests as appear in Table 26.8:

The categories for each service class are shown as follows:

1. **Service Category "L" Chassis (and Universal Joint) Grease**

TABLE 26.8—Requirements for the LA Service Category

Property	Requirement	Property	Requirement
Worked penetration	220–340	Elastomer compatibility	
Dropping point (°C)	80	3217/3B CR (%) volume change	0 to 40
Four-ball wear (mm) maximum	0.9	3217/3B CR hardness change	–15 to 0
Four-ball EP		3217/2B NBR-L volume change (%)	–
LWI (kg) minimum	–	3217/2B NBR-L hardness change	–
Weld point (kg) minimum	–	Low-temperature torque at –40°C (Nm)	–
Oil separation (%) maximum	–	Water resistance at 80°C (%) maximum	–
Rust (maximum)	–	High-temperature life (h) minimum	–
Fretting protection (mg loss) maximum	–	Leakage tendency (g) maximum	–

TABLE 26.9—Requirements for the Service Category GA

Property	Requirement	Property	Requirement
Worked penetration	220–340	Elastomer compatibility	
Dropping point (°C)	80	3217/3B CR (%) volume change	–
Four-ball wear (mm) maximum	–	3217/3B CR hardness change	–
Four-ball EP		3217/2B NBR-L volume change (%)	–
LWI (kg) minimum	–	3217/2B NBR-L hardness change	–
Weld point (kg) min	–	Low-temperature torque at –40°C (Nm)	15.5
Oil separation (%) maximum	–	Water resistance at 80°C (%) maximum	–
Rust (maximum)	–	High-temperature life (h) minimum	–
Fretting protection (mg loss) max	–	Leakage tendency (g) maximum	–

TABLE 26.10—Requirements for the Service Category GC-LB

Property	Requirement	Property	Requirement
Worked penetration	220–340	Elastomer compatibility	
Dropping point (°C)	220	3217/3B CR (%) volume change	0 to 40
Four-ball wear (mm) maximum	0.6	3217/3B CR hardness change	–15 to 0
Four-ball EP		3217/2B NBR-L volume change (%)	–5 to 30
LWI (kg) minimum	30	3217/2B NBR-L hardness change	–15 to 2
Weld point (kg) minimum	200	Low-temperature torque at –40°C (Nm)	15.5
Oil separation (%) maximum	6	Water resistance at 80°C (%) maximum	15
Rust (maximum)	Pass	High-temperature life (h) minimum	80
Fretting protection (mg loss) maximum	10	Leakage tendency (g) maximum	10
The NLGI symbols specifying the categories of grease are used for identifications by grease manufacturers under the NLGI license.			

LA—Mild-duty or noncritical applications. For use under highly loaded conditions with frequent relubrication (≤ 2000 mi). Table 26.9 shows the requirements for the service category LA.

LB—Mild to severe duty (high loads, vibration, exposure to water). Usable temperature of -40°C to 120°C (-40 to 248°F) with relubrication intervals greater than 2000 mi.

2. Service Category “G” Wheel-Bearing Grease

GA—Mild duty or noncritical applications. For use over limited temperature range with frequent relubrication. Table 26.10 shows the requirements for the service category GA.

GB—Mild to moderate duty (cars, trucks in urban and highway service). For use over a wide temperature range of -40 to 120°C (-40°F to 248°F) and occasional spikes to 160°C (320°F).

GC—Mild to severe duty (frequent stop-and-go service, trailer-hauling, mountain driving, etc.). For use over a wide temperature range of -40°C to 120°C (-40°F to 320°F) and occasional spikes to 160°C (320°F).

3. Multipurpose Category

GC-LB—Multipurpose combined wheel-bearing and chassis grease. For example, there are soybean-oil-based greases that meet these requirements.

References

- [1] Nynas, A.B., 2009, *Handbook of Naphthenic Specialty Oils for Greases*, Nynas Corporation, Stockholm, Sweden.
- [2] Nagendramma, P., and Kaul, S., 2008, “Study of Synthetic Complex Esters As Automotive Gear Lubricants,” *J. Synth. Lub.*, Vol. 25, pp. 131–136.
- [3] Cermak, S.C. and Isbel, T.A., 2003, “Synthesis and Physical Properties of Estolide-Based Functional Fluids,” *J. Ind. Crops Products*, Vol. 18, pp. 183–196.
- [4] Hammond, E.G., and Lee, I., 1992, “Process for Enzymatic Hydrolysis of Fatty Acid Triglycerides with Oat Caryopses,” U.S. Patent No. 5089403.
- [5] Salunkhe, J.K., Chavan, J.K., Adsule, R.N., and Kadem, S.S., 1992, *World Oilseeds: Chemistry, Technology, and Utilization*, Van Nostrand Reinhold, New York.
- [6] Honary, L.A.T., and Richter, E., 2011 *Biobased Lubricants and Greases—Technology and Products*, Wiley and Sons, London.
- [7] Honary, L.A.T., 1995, *Performance of Selected Vegetable Oils in ASTM Hydraulic Tests*, SAE Technical Paper 952075, SAE, Warrendale, PA.
- [8] Honary, L.A., 2009, “OEM Biobased Engine Oils,” *OEM Off-Highway Magazine*, Sygnus, Fort Atkinson, WI.
- [9] Meng, T., and Luther, R., 2003, “Method and Device for Lubricating and Simultaneously Supplying Fuel in a Vegetable Oil-Operated Combustion Engine,” U.S. Patent No. 6,532,918.
- [10] National Lubricating Grease Institute (NLGI), 1984, *Lubricating Grease Guide*, NLGI, Kansas City, MO.

Appendix

List of Referenced Documents

The following tables include all ASTM reference documents and updated standard test methods for engine oils, transmission lubricants, gear lubricants, and grease.

TABLE 1—Definition of Terms and Abbreviations	
AAMA	American Automobile Manufacturers Association
AMS	Aerospace Materials Specification
ANSI	American National Standards Institute
API	American Petroleum Institute
ASTM	American Society for Testing and Materials
CEC	Coordinating European Council
CF, CF-2, CF-4, CG, CG-4, CH-4, CI-4, CJ-4	“C” represents a category for engine oils that are used in compression-ignition (diesel) engines. CF, CF-2, CF-4, CG, CG-4, CH-4, CI-4, and CJ-4, all represent a particular oil quality at different time frames used for different diesel engines. After 2006, the current diesel engine specification is CJ-4 for high-speed four-stroke engines to meet 2007 emission standards.
CR	Chloroprene Rubber
CRC	Coordinating Research Council
CRC Press	Chemical Rubber Company Press
CVT	Continuously Variable Transmission
cSt	Centistokes, a measure of viscosity
DIN	Deutsch Industries Norm (German industry standard)
EMA	Engine Manufacturers Association
EOAT	Engine Oil Aeration Test
EOFT	Engine Oil Filterability Test
EOWTT	Engine Oil Water Tolerance Test
EP	Extreme Pressure (used for lubricants that experience high pressure or high temperature)
FZG	Fahrzeug (German word for motor vehicle)
GF-1, GF-2, GF-3, GF-4, GF-5	Terms represent an engine oil quality that is defined by a series of tests that the oil must pass. GF-X series indicates the evolved engine oils performance specifications that were specified by ILSAC. At present, the ILSAC GF-5 represents the new engine oil performance requirements that aim to improve fuel economy, protection for emission control systems, and lubricant robustness for petroleum engines.
GF-5 and API SN	ILSAC GF-5 and API SN represent almost a convergence of two engine oil series in lubricant performance specifications after many years. The current ILSAC GF-5 and API SN represent the new engine oil performance requirements which aim to improve fuel economy, protection for emission control systems, and lubricant robustness for petroleum engines. It only applies to 0W(X), 5W(X), and 10W(X).
ILSAC	International Lubricant Standardization and Approval Committee
ISA	Instrument Society of America
ISO	Represents a standard from the American National Standards Institute
JAMA	Japan Automobile Manufacturers Association
MIL	Military specification

(Continued)

TABLE 1— Definition of Terms and Abbreviations (Continued)

NBR-L	Acrylonitrile-Butadiene Rubber with Low Acrylonitrile
PC	Pre-chamber, associated with engine oil tests for diesel engines
SAE	Society of Automotive Engineers
API SF, SG, SH,	"S" represents a category for engine oils that are used in spark ignition engines. Each successive final letter represents a more recent category.
API SJ, SL, SN	SN is more recent than the others listed. It represents the new API category for improving engine oil performance like ILSAC GF-5.
TEOST	Thermo Oxidation Engine Oil Simulation Test
ZDP or ZDDP	Zinc dialkyl-dithio phosphate, an antioxidant and an anti-wear agent used as an additive in engine oil

TABLE 2—Referenced Documents in ASTM Standard Test Methods Related to Engine Oil

ASTM No.	Test Method or Document Title
C1109	Analysis of Aqueous Leachates from Nuclear Waste Materials Using Inductively Coupled Plasma-Atomic Emission Spectrometry
D16	Definitions of Terms Relating to Paint, Varnish, Lacquer, and Related Products
D56	Flash Point by Tag Closed Tester
D86	Distillation of Petroleum Products
D91	Acidity of Hydrocarbon Liquids and Their Distillation Residues
D92	Flash and Fire Points by Cleveland Open Cup
D93	Flash Point by Penske-Martens Closed Tester
D97	Pour Point of Petroleum Products
D117	Guide to Sampling Test Methods, Standard Practices, and Guides for Electrical Insulating Oils of Petroleum Origin
D129	Sulfur in Petroleum Products (General Bomb Method)
D130	Detection of Copper Corrosion from Petroleum Products by the Copper Strip Tarnish Test
D140	Practice for Sampling Bituminous Materials
D156	Saybolt Color of Petroleum Products (Saybolt Chromometer Method)
D235	Specification for Mineral Spirits (Petroleum Spirits) (Hydrocarbon Dry-cleaning Solvent)
D240	Heat of Combustion of Liquid Hydrocarbon Fuels by Bomb Calorimeter
D287	API Gravity of Crude Petroleum and Petroleum Products (Hydrometer Method)
D323	Vapor Pressure of Petroleum Products (Reid Method)
D341	Viscosity-Temperature Charts for Liquid Petroleum Products
D381	Existent Gum in Fuels by Jet Evaporation
D445	Kinematic Viscosity of Transparent and Opaque Liquids (the Calculation of Dynamic Viscosity)
D446	Standard Specifications and Operating Instructions for Glass Capillary Kinematic Viscometers
D482	Ash from Petroleum Products
D524	Ramsbottom Carbon Residue of Petroleum Products
D525	Oxidation Stability of Gasoline (Induction Period Method)
D613	Cetane Number of Diesel Fuel Oil
D664	Acid Number of Petroleum Products by Potentiometric Titration
D850	Acidity of Hydrocarbon Liquids and Their Distillation Residues
D873	Oxidation Stability of Aviation Fuels (Potential Residue Method)
D892	Foaming Characteristics of Lubricating Oils
D893	Insolubles in Used Lubricating Oils

TABLE 2—Referenced Documents in ASTM Standard Test Methods Related to Engine Oil (Continued)	
ASTM No.	Test Method or Document Title
D974	Acid and Base Number by Color-Indicator Titration
D1078	Distillation Range of Volatile Organic Liquids
D1093	Acidity of Hydrocarbon Liquids and Their Distillation Residues
D1133	Kauri-Butanol Value of Hydrocarbon Solvents
D1193	Specification for Reagent Water
D1217	Density and Relative Density (Specific Gravity) of Liquids by Bingham Pycnometer
D1250	Standard Guide for Petroleum Measurement Tables
D1266	Sulfur in Petroleum Products (Lamp Method)
D1298	Density, Relative Density (Specific Gravity), or API Gravity of Crude Petroleum and Liquid Petroleum Products by Hydrometer Method
D1310	Flash Point and Fire Point of Liquids by Tag Open-Cup Apparatus
D1319	Hydrocarbon Types in Liquid Petroleum Products by Fluorescent Indicator Adsorption
D1353	Nonvolatile Matter in Volatile Solvents for Use in Paint, Lacquer, and Related Products
D1480	Density and Relative Density (Specific Gravity) of Viscous Materials by Bingham Pycnometer
D1481	Density and Relative Density (Specific Gravity) of Viscous Materials by Lipkin Bicapillary Pycnometer
D1552	Determination of Additive Elements in Lubricating Oils by Inductively Coupled Plasma Atomic Emission Spectrometry
D2170	Kinematic Viscosity of Asphalts (Bitumens)
D2171	Viscosity of Asphalts by Vacuum Capillary Viscometer
D2422	Standard Classification of Industrial Fluid Lubricants by Viscosity System
D2500	Cloud Point of Petroleum Products
D2509	Measurement of Load-Carrying Capacity of Lubricating Grease (Timken Method)
D2622	Sulfur in Petroleum Products by X-ray Spectrometry
D2699	Research Octane Number of Spark-Ignition Engine Fuel
D2700	Motor Octane Number of Spark-Ignition Fuel
D2709	Water and Sediment in Distillate Fuels by Centrifuge
D2782	Measurement of Extreme-Pressure Properties of Lubricating Fluids (Timken Method)
D2887	Boiling Range Distribution of Petroleum Fractions by Gas Chromatography
D2896	Base Number of Petroleum Products by Potentiometric Perchloric Acid Titration
D2982	Detecting Glycol-Base Antifreeze in Used Lubricating Oils
D3120	Trace Quantities of Sulfur in Light Liquid Petroleum Hydrocarbons by Oxidative Microcoulometry
D3231	Phosphorus in Gasoline
D3237	Lead in Gasoline by Atomic Absorption Spectrometry
D3244	Standard Practice for Utilization of Test Data to Determine Conformance with Specifications
D3338	Estimation of Heat of Combustion of Aviation Fuels
D3339	Acid Number of Petroleum Products by Semi-Micro Color Indicator Titration
D3525	Gasoline Diluent in Used Gasoline Engine Oils by Gas Chromatography
D3606	Determination of Benzene and Toluene in Finished Motor and Aviation Gasoline by Gas Chromatography
D3829	Predicting the Borderline Pumping Temperature of Engine Oils
D3941	Flash Point by the Equilibrium Method with a Closed-Cup Apparatus
D4052	Density and Relative Density of Liquids by Digital Density Meter

(Continued)

TABLE 2—Referenced Documents in ASTM Standard Test Methods Related to Engine Oil (Continued)

ASTM No.	Test Method or Document Title
D4057	Standard Practice for Manual Sampling of Petroleum and Petroleum Products
D4175	Standard Terminology Relating to Petroleum, Petroleum Products, and Lubricants
D4177	Standard Practice for Automatic Sampling of Petroleum and Petroleum Products
D4206	Sustained Burning of Liquid Mixtures by the Setaflash Tester (Open Cup)
D4294	Sulfur in Petroleum Products by Energy-Dispersive X-ray Fluorescence Spectroscopy
D4307	Determination of Additive Elements in Lubricating Oils by Inductively Coupled Plasma Atomic Emission Spectrometry
D4485	Standard Specification for Performance of Engine Oils
D4626	Calculation of Gas Chromatographic Response Factors
D4628	Analysis of Barium, Calcium, Magnesium, and Zinc in Unused Lubricating Oils by Atomic Absorption Spectrometry
D4636	Corrosiveness and Oxidation Stability of Hydraulic Oils, Aircraft Turbine Engine Lubricants, and Other Highly Refined Oils
D4683	Measuring Viscosity at High Shear Rate and High Temperature by Tapered Bearing Simulator
D4684	Determination of Yield Stress and Apparent Viscosity of Engine Oils at Low Temperature
D4737	Calculated Cetane Index by Four Variable Equation
D4739	Base Number Determination by Potentiometric Titration
D4741	Measuring Viscosity at High Temperature and High Shear Rate by Tapered-Plug Viscometer
D4863	Determination of Lubricity of Two-Stroke-Cycle Gasoline Engine Lubricants
D4927	Elemental Analysis of Lubricant and Additive Components—Barium, Calcium, Phosphorus, Sulfur, and Zinc by Wave-length-Dispersive X-ray Fluorescence Spectroscopy
D4951	Determination of Additive Elements in Lubricating Oils by Inductively Coupled Plasma Atomic Emission Spectrometry
D5119	Test Method for Evaluation of Automotive Engine Oils in the CRC L-38 Spark-Ignition Engine
D5133	Low Temperature, Low Shear Rate, Viscosity/Temperature Dependence of Lubricating Oils Using a Temperature Scanning Technique
D5134	Detailed Analysis of Petroleum Naphthas Through n-Nonane by Capillary Gas Chromatography
D5185	Determination of Additive Elements, Wear Metals and Contaminants in Used Lubricating Oils by Inductively-Coupled Plasma Atomic Emission Spectrometry
D5186	Determination of the Aromatic Content and Polynuclear Content of Diesel Fuels and Aviation Turbine Fuels by Supercritical Fluid Chromatography
D5290	Measurement of Oil Consumption, Piston Deposits, and Wear in a Heavy-Duty High-Speed Diesel Engine-NTC-400 Procedure
D5302	Evaluation of Automotive Engine Oils for Inhibition of Deposit Formation and Wear in a Spark-Ignition Internal Combustion Engine Fueled with Gasoline and Operated Under Low-Temperature, Light-Duty Conditions
D5480	Engine Oil Volatility by Gas Chromatography
D5481	Measuring Apparent Viscosity at High-Temperature and High-Shear Rate by Multicell Capillary Viscometer
D5533	Evaluation of Automotive Engine Oils in the Sequence IIIE, Spark-Ignition Engine
D5800	Evaporation Loss of Lubricating Oils by the Noack Method
D5844	Evaluation of Automotive Engine Oils for Inhibition of Rusting (Sequence IID)
D5862	Evaluation of Engine Oils in Two-Stroke Cycle Turbo-Supercharged 6V92TA Diesel Engine
D5966	Evaluation of Diesel Engine Oils for Roller Follower Wear in Light-Duty Diesel Engine
D5967	Evaluation of Diesel Engine Oils in the T-8 Diesel Engine
D5968	Evaluation of Corrosiveness of Diesel Engine Oil at 121°
D6074	Guide for Characterizing Hydrocarbon Lubricant Base Oils

TABLE 2—Referenced Documents in ASTM Standard Test Methods Related to Engine Oil (Continued)	
ASTM No.	Test Method or Document Title
D6082	High Temperature Foaming Characteristics of Lubricating Oils
D6202	Measurement of the Effects of Automotive Engine Oils on the Fuel Economy of Passenger Cars and Light-Duty Trucks in the Sequence VIA Spark Ignition Engine
D6278	Shear Stability of Polymer Containing Fluids Using a European Diesel Injector Apparatus
D6299	Applying Statistical Quality Assurance Techniques to Evaluate Analytical Measurement System Performance
D6300	Determination of Precision and Bias Data for Use in Test Methods for Petroleum Products and Lubricants
D6335	Determination of High Temperature Deposits by Thermo-Oxidation Engine Oil Simulation Test
D6417	Estimation of Engine Oil Volatility by Capillary Gas Chromatography
D6483	Evaluation of Diesel Engine Oils in the T-9 Diesel Engine
D6557	Evaluation of Rust Preventative Characteristics of Automotive Engine Oils
D7097	Standard Test Method for Determination of Moderately High Temperature Piston Deposits by Thermo-Oxidation Engine Oil Simulation Test (TEOST MHT1)
D7528	Standard Test Method for Bench Oxidation of Engine Oils by ROBO Apparatus
E1	Specification for ASTM Thermometers
E29	Standard Practice for Using Significant Digits in Test Data to Determine Conformance with Specifications
E77	Inspection and Verification of Thermometers
E128	Maximum Pore Diameter and Permeability of Rigid, Porous Filters for Laboratory Use
E135	Terminology Relating to Analytical Chemistry for Metals, Ores, and Related Materials
E178	Practice for Dealing with Outlying Observations
E191	Specification for Apparatus for Microdetermination of Carbon and Hydrogen in Organic and Organo-Metallic Compounds
E270	Terminology Relating to Liquid Penetrant Examination
E300	Practice for Sampling Industrial Chemicals
E344	Terminology Relating to Thermometry and Hydrometry
E355	Gas Chromatographic Terms and Relationships
E380	Use of the International System of Units (SI) (The Modernized Metric System)
E473	Terminology Relating to Thermal Analysis
E502	Selection and Use of ASTM Standards for the Determination of Flash Point of Chemicals by the Closed Cup Method
E594	Testing Flame Ionization Detectors Used in Gas Chromatography
E691	Conducting an Inter-laboratory Study to Determine the Precision of a Test Method
E1119	Specification for Industrial Grade Ethylene Glycol
E1500	Installing Fused Silica Open Tubular Capillary Columns in Gas Chromatographs
G40	Terminology Relating to Wear and Erosion

TABLE 3—Referenced Documents to Non-ASTM Methods for Engine Oils	
Organization	Test Method or Document Title
ANSI (American National Standards Institute)	Standard MC96.1 Temperature Measurement—Thermocouples
API (American Petroleum Institute) Standard	API 1509 Engine Service Classification and Guide to Crankcase Oil Selection
Chemical Manufacturers Association	CMA Petroleum Additives Product Approval Code of Practice
Coordinating Research	CRC Rust Rating (CRC Manual No. 7)

(Continued)

TABLE 3—Referenced Documents to Non-ASTM Methods for Engine Oils (Continued)

Organization	Test Method or Document Title
Council (CRC) Motor Rating	CRC Sludge Rating Manual (CRC Manual No. 12)
Method Manuals	CRC Varnish Rating Manual (CRC Manual No. 14) CRC Techniques for Valve Rating (CRC Manual No. 16)
Deutsches Institut für Normung (DIN)	DIN 51.581 Noack Evaporative Test DIN 1725 Specification for Aluminum Alloys DIN 12785 Specification for Glass Thermometers
Federal Test Method Standard	No. 791b—Lubricants Liquid Fuels and Related Products, Methods of Testing No. 791c—Method 3470 and No. 791, Method 5308.7
General Motors Corporation	GM9099-P Engine Oil Filterability Test (EOFT)
IEEE/ASTM (Institute of Electrical and Electronic Engineers)	SI-10 Standard for Use of International System of Units (SI): The Modern Metric System
Institute of Petroleum (IP)	IP 17 Color by the Lovibond Tintometer IP 139 Neutralization Number by Color Indicator Titration IP 146 Test for Foaming Characteristics of Lubricating Oil
ISO	Guide 25 General Requirements for the Calibration and Testing Laboratories Guide 34 Quality Systems Guidelines for the Production of Reference Materials Guide 35 Certification of Reference Material—General and Statistical Principles ISO 3104 Petroleum Products—Transparent and Opaque Liquids—Determination of Kinematic Viscosity and Calculation of Dynamic Viscosity ISO 3105 Glass Capillary Kinematic Viscometers—Specification and Operating Instructions ISO 3696 Water for Analytical Laboratory Use—Specification and Test Methods ISO 9000 Quality Management and Quality Assurance Standards—Guidelines for Selection and Use
Military Specification	MIL-L-2104, Lubricating Oil, Internal Combustion Engine, Combat/Tactical Services
SAE (Society of Automotive Engineers) Standards	J183, Engine Oil Performance and Engine Service Classification (Other Than “Energy Conserving”) J254, Instrumentation and Techniques for Exhaust Gas Emissions Measurement J300, Engine Oil Classification and J304, Engine Oil Tests J726, Air Cleaner Test Code (Includes Piezometer Ring Specifications) J1423, Passenger Car and Light-Duty Truck Energy-Conserving Engine Oil Classification J1995, Engine Power Test Code—Spark Ignition and Compression Ignition—Gross Power Rating
U.S. Federal Test Method	No. 791, Method 5308.7 Corrosiveness and Oxidative Stability of Light Oils (Metal Squares)
Standards	No. 791b Lubricants Liquid Fuels and Related Products; Methods of Testing

TABLE 4—Referenced Documents in ASTM Standard Test Methods for Transmission Fluids

ASTM No.	Test Method or Document Title
A108	Specification for Steel Bars, Carbon, Cold-Finished, Standard Quality
A109	Specification for Steel, Strip, Carbon, Cold-Rolled
A240/A240 M	Specification for Heat-Resisting Chromium and Chromium-Nickel Stainless Steel Plate, Sheet, and Strip for Pressure Vessels
B224	Classification of Coppers
D91	Precipitation Number of Lubricating Oils
D130	Detection of Copper Corrosion from Petroleum Products by the Copper Strip Tarnish Test
D235	Specification for Mineral Spirits (Petroleum Spirits) (Hydrocarbon Dry-cleaning Solvent)
D396	Specification for Fuel Oils
D412	Vulcanized Rubber and Thermoplastic Rubbers and Thermoplastic Elastomers—Tension
D445	Kinematic Viscosity of Transparent and Opaque Liquids (and the Calculation of Dynamic Viscosity)
D471	Test Method for Rubber Property—Effect of Liquids
D512	Chloride Ion in Water

TABLE 4—Referenced Documents in ASTM Standard Test Methods for Transmission Fluids (Continued)	
ASTM No.	Test Method or Document Title
D516	Sulfate Ion in Water
D664	Acid Number of Petroleum Products by Potentiometric Titration
D892	Foaming Characteristics of Lubricating Oils
D893	Insolubles in Used Lubricating Oils
D975	Specification for Diesel Fuel Oils
D1193	Specification for Reagent Water
D1217	Density and Relative Density (Specific Gravity) of Liquids by Bingham Pycnometer
D1401	Water Separability of Petroleum Oils and Synthetic Fluids
D1480	Density and Relative Density (Specific Gravity) of Viscous Materials by Bingham Bicapillary Pycnometer
D1481	Density and Relative Density (Specific Gravity) of Viscous Materials by Lipkin Bicapillary Pycnometer
D1655	Specification for Aviation Turbine Fuels
D1838	Copper Strip Corrosion by Liquefied Petroleum (LP) Gases
D2170	Test Method for Kinematic Viscosity of Asphalts (Bitumens)
D2171	Viscosity of Asphalts by Vacuum Capillary Viscometer
D2240	Rubber Property—Durometer Hardness
D2422	Classification of Industrial Fluid Lubricants by Viscosity System
D3603	Rust-Preventing Characteristics of Steam Turbine Oil in the Presence of Water (Horizontal Disk Method)
D4057	Manual Sampling of Petroleum and Petroleum Products
D4175	Terminology Relating to Petroleum, Petroleum Products, and Lubricants
D4177	Automatic Sampling of Petroleum and Petroleum Products
D5182	Evaluating the Scuffing (Scoring) Load Capacity of Oils (FZG Visual Method)
D5579	Evaluating the Thermal Stability of Manual Transmission Lubricants in a Cyclic Durability Test
D5662	Determining Automotive Gear Oil Compatibility with Typical Oil Seal Elastomers
D5704	Evaluation of the Thermal and Oxidative Stability of Lubricants Used for Manual Transmissions and Final Drive Axles
D5760	Performance of Manual Transmission Gear Lubricants
D6074	Guide for Characterizing Hydrocarbon Lubricant Base Oils
E1	Specification for ASTM Thermometers
E77	Inspection and Verification of Thermometers
E527	Practice for Numbering Metals and Alloys
G40	Terminology Relating to Erosion and Wear
ASTM Adjuncts	ASTM Copper Strip Corrosion Standard Engineering Drawings PCN ADJD5704

TABLE 5—Additional Standards and Specifications Related to Transmission Fluids	
Organization	Test Method or Document Title
ANSI/ISA (Instrument Society of America)-S7.3	Quality Standard for Instrument Air
DIN 51 354 Teil 1	FZG Zahnrad Verspannungs Prüf Maschine—Allgemeine Arbeitsgrundlagen
Federal Specification	RRS-366 (Method 5329 of VV-L-791e) Test Sieve Sizes QQ-S-698 Steel Sheet and Strip, Low Carbon PD-680 Standard Solvent JAN-H-792 Operations of Humidity Cabinet

(Continued)

TABLE 5—Additional Standards and Specifications Related to Transmission Fluids (Continued)

Organization	Test Method or Document Title
Federal Specifications Standard No. 791C	Method 3430.2 Compatibility Characteristics of Universal Gear Lubricants Method 3440.1 Storage Solubility Characteristics of Universal Gear Lubricants
Federal Standard No. 791C, Method 3440.1	Storage Solubility Characteristics of Universal Gear Lubricants
Institute of Petroleum (IP)	Specifications—IP Standard Thermometers, Appendix A Specifications for IP Standard Reference Liquids, Appendix B BS 871 Specification for Abrasive Papers and Cloths BS 970: Part 1: Carbon and Carbon Manganese Steels Including Free Cutting Steels
ISO	Guide 25—General Requirements for the Calibration and Testing Laboratories 3104 Petroleum Products—Transparent and Opaque Liquids—Determination of Kinematic and Calculation of Dynamic Viscosity 3105 Glass Capillary Kinematic Viscometers—Specification and Operating Instructions 3696 Water for Analytical Laboratory Use—Specification and Test Methods 4021 Hydraulic Fluid Power—Particulate Contamination Analysis—Extraction of Fluid Samples from Lines of an Operating System 4406 Hydraulic Fluid Power—Fluids—Method for Coding Level of Contamination by Solids Particles 9000 Quality Management and Quality Assurance Standards—Guidelines for Selection and Use
Mack Trucks Oil, Gear	Multipurpose (GO-H)
Military Standard	MIL-L-2105 and 2105D, Lubricating Oil, Gear, Multipurpose MIL-C-15074C, Corrosion Preventive Compound Finger Print Remover MIL-C-16173D Corrosion Preventive Compound, Solvent Compound Cutback, Cold Application
SAE Standard	1009C Tee Reducer, Bulkhead on Side, Flareless Tube

TABLE 6—Referenced Documents in ASTM Standard Tests for Greases

ASTM No.	Test Method or Document Title
D88	Saybolt Viscosity
D95	Water in Petroleum Products and Bituminous Materials by Distillation
D97	Pour Point for Petroleum Oils
D130	Detection of Copper Corrosion from Petroleum Products by the Copper Strip Tarnish Test
D156	Saybolt Color of Petroleum Products (Saybolt Chromometer Method)
D217	Cone Penetration of Lubricating Grease
D235	Specifications for Mineral Spirits (Petroleum Spirits) Hydrocarbon Dry-cleaning Solvent
A240/A240M	Specification for Heat-Resisting Chromium and Chromium-Nickel Stainless Steel Plate, Sheet, and Strip for Pressure Vessels
D297	Rubber Products—Chemical Analysis
D329	Specification for Acetone
D412	Vulcanized Rubber and Thermoplastic Elastomers-Tension
D445	Kinematic Viscosity of Transparent and Opaque Liquids (the Calculation of Dynamic Viscosity)
D446	Specifications and Operating Instructions for Glass Capillary Kinematic Viscometers
D471	Rubber Property—Effect of Liquids
D473	Sediment in Crude Oils and Fuel Oils by the Extraction Method
D566	Dropping Point of Lubricating Grease
D770	Specification for Isopropyl Alcohol

TABLE 6—Referenced Documents in ASTM Standard Tests for Greases (Continued)	
ASTM No.	Test Method or Document Title
D785	Rockwell Hardness of Plastics and Electrical Insulating Materials
D937	Cone Penetration of Petrolatum
D972	Evaporation Loss of Lubricating Greases and Oils
D1078	Distillation Range of Volatile Organic Liquids
D1193	Specification for Reagent Water
D1217	Density and Relative Density (Specific Gravity) of Liquids by Bingham Pycnometer
D1310	Flash Point and Fire Point of Liquids by Tag Open-Cup Apparatus
D1353	Nonvolatile Matter in Volatile Solvents for Use in Paints, Varnish, Lacquer, and Related Products
D1403	Cone Penetration of Lubricating Grease Using One-Quarter and One-Half Scale Cone Equipment
D1480	Density and Relative Density (Specific Gravity) of Viscous Materials by Bingham Pycnometer
D1481	Density and Relative Density (Specific Gravity) of Viscous Materials by Lipkin Bicapillary Pycnometer
D2170	Kinematic Viscosity of Asphalts (Bitumens)
D2171	Viscosity of Asphalts by Vacuum Capillary Viscometer
D2240	Rubber Property—Durometer Hardness
D2265	Dropping Point of Lubricating Grease Over Wide Temperature Range
D2500	Cloud Point of Petroleum Oils
D2595	Evaporation Loss of Lubricating Greases Over Wide Temperature Range
D2714	Calibration and Operation of the Falex Block-on-Ring Friction and Wear Testing Machine
D3182	Practice for Rubber—Materials, Equipment, and Procedures for Mixing Standard Compounds and Preparing Standardized Vulcanized Sheets
D3183	Practice for Rubber—Preparation of Pieces for Test Purposes from Products
D3244	Practice for Utilization of Test Data to Determine Conformance with Specifications
D3527	Life Performance of Automotive Wheel Bearing Grease
D4175	Terminology Relating to Petroleum, Petroleum Products, and Lubricants
D4289	Elastomer Compatibility of Lubricating Greases and Fluids
D4290	Determining the Leakage Tendencies of Automotive Wheel Bearing Grease under Accelerated Conditions
D4693	Low-Temperature Torque of Grease-Lubricated Wheel Bearings
D4950	Classification of and Specification for Automotive Service Greases
D5483	Oxidation Induction Time of Lubricating Greases by Pressure Differential Scanning Calorimetry
D5706	Determining Extreme Pressure Properties of Lubricating Greases Using a High-Frequency, Linear Oscillation (SRV) Test Machine
D5707	Measuring Friction and Wear Properties of Lubricating Grease Using a High-Frequency, Linear Oscillation (SRV) Test Machine
D5969	Corrosion-Preventive Properties of Lubricating Greases in Presence of Dilute Synthetic Sea-Water Environments
D6074	Guide for Characterizing Hydrocarbon Lubricant Base Oils
D6138	Corrosion-Preventive Properties of Lubricating Greases Under Dynamic Wet Conditions (Emcor Test)
D6184	Oil Separation from Lubricating Grease (Conical Sieve Method)
D6185	Practice for Evaluating Compatibility of Binary Mixtures of Lubricating Greases
E1	Specification for ASTM Thermometers
E11	Specification for Wire-Cloth Sieves for Testing Purposes

(Continued)

TABLE 6—Referenced Documents in ASTM Standard Tests for Greases (Continued)

ASTM No.	Test Method or Document Title
E77	Inspection and Verification of Thermometers
E220	Calibration of Thermocouples by Comparison Techniques
E230	Temperature-Electromotive Force (EMF) Tables for Standardized Thermocouples
E563	Practice for Preparation and Use of Freezing Point Reference Baths
E585	Specification for Sheathed Base-Metal Thermocouple Materials
E608	Specification for Metal-Sheathed Base-Metal Thermocouples
E691	Practice for Conducting an Interlaboratory Study to Determine the Precision of a Test Method
G15	Terminology Related to Corrosion and Corrosion Testing
Adjunct	ASTM Adjunct: Copper Strip Corrosion Standard, Adjunct PCN 12-401300-00
ASTM	Test Methods for Rating Motor, Diesel, and Aviation Fuels; Motor Fuels (Section I), Reference Materials and Blending Accessories (Annex 2), Reference Materials (A2.7), and Table 32; (Specification for ASTM Knock Test Reference Fuel, n-heptane)

TABLE 7—Additional Standards and Specifications Related to Greases

Organization	Test Method or Document Title
ABMA (American Bearing Manufacturers Association)	Standard 4. Tolerance Definitions and Gaging Practices for Ball and Roller Bearings
AFBMA (Anti-Friction Bearing Manufacturers Association)	Standard 19 1974 (available from ANSI, American National Standards Institute, B.3.19-1975)
ANSI (American National Standards Institute)	Specification B3.12 for Metal Balls ANSI/AFBMA Standard 20–1987 Radial Bearings of Ball, Cylindrical, Roller, and Spherical-Roller Type–Metric Designs (AFBMA Code 20BCO2JO)
British Standards Institute	BS970: 1983 Part I, Section 5
Compressed Gas Association	Booklets G-4 and G-4-1
Federal Test Method	Standard 791C, Method 3603.5, Swelling of Synthetic Rubbers
IP (Institute of Petroleum)	Specification for Standard IP Thermometers IP 50, Method of Testing for Cone Penetration of Lubricating Grease
ISO (American National Standards Institute)	Guide 25–General Requirements for the Calibration and Testing Laboratories 3104 Petroleum Products–Transparent and Opaque Liquids–Determination of Kinematic Viscosity and Calculation of Dynamic Viscosity 3105 Glass Capillary Kinematic Viscometers–Specification and Operating Instructions 3696 Water for Analytical Laboratory Use–Specification and Test Methods 9000 Quality Management and Quality Assurance Standards–Guidelines for Selection and Use
Military Standard	MIL-G-10924F, Specification for Automotive and Artillery
NLGI (National Lubricating Grease Institute)	Grease Consistency Specification
SAE (Society of Automotive Engineers) Standard	AMS (Aerospace Materials Specification) 3217A Standard Elastomer Stocks-Test Slabs AMS 3217/2A Test Slabs, Acrylonitrile AMS 3217/3A Test Slabs, Chloroprene (CR)-65-75 Butadiene (NBR-L)-Low Acrylonitrile, 65-75
U.S. Air Force	Specification 539, Specification Bulletin for Standard Elastomer Stocks

TABLE 8—Referenced Documents in ASTM Standards Related to Gear Lubricants	
ASTM No.	Test Method or Document Title
B16	Specification for Free-Cutting Brass Rod, Bar, and Shapes for Use in Screw Machines
D96	Water and Sediment in Crude Oil by Centrifuge Method (Field Procedure)
D130	Detection of Copper Corrosion from Petroleum Products by the Copper Strip Tarnish Test
D235	Specification for Mineral Spirits (Petroleum Spirits) (Hydrocarbon Dry-cleaning Solvents)
D329	Specification for Acetone
D341	Viscosity-Temperature Charts for Liquid Petroleum Products
D396	Specification for Fuel Oils
D412	Vulcanized Rubber and Thermoplastic Rubbers and Thermoplastic Elastomers—Tension
D446	Specifications and Operating Instructions for Glass Capillary Kinematic Viscometers
D471	Rubber Property—Effect of Liquids
D484	Specification for Hydrocarbon Dry-cleaning Solvents
D892	Foaming Characteristics of Lubricating Oils
D975	Specification for Diesel Fuel Oils
D1193	Specification for Reagent Water
D1217	Density and Relative Density (Specific Gravity) of Liquids by Bingham Pycnometer
D1480	Density and Relative Density (Specific Gravity) of Viscous Materials by Bingham Pycnometer
D1481	Density and Relative Density (Specific Gravity) of Viscous Materials by Lipkin Bicapillary Pycnometer
D1655	Specification for Aviation Turbine Fuels
D1796	Water and Sediment in Fuel Oils by Centrifuge Method (Laboratory Procedure)
D1838	Copper Strip Corrosion by Liquefied Petroleum (LP) Gases
D2170	Viscosity of Asphalts (Bitumens)
D2171	Viscosity of Asphalts by Vacuum Capillary Viscometer
D2240	Rubber Property—Durometer Hardness
D2266	Wear Preventive Characteristics of Lubricating Fluid (Four-Ball Method)
D2509	Measurement of Load-Carrying Capacity of Extreme Lubricating Grease (Timken Method)
D2670	Wear Properties of Fluid Lubricants (Falex Pin and Vee Block Method)
D2783	Measurement of Extreme Pressure Properties of Lubricating Fluids (Four-Ball Method)
D4175	Terminology Relating to Petroleum, Petroleum Products, and Lubricants
D5182	Evaluating the Scuffing (Scoring) Load Capacity of Oils
D5579	Evaluating the Thermal Stability of Manual Transmission Lubricants In a Cyclic Durability Test
D5662	Determining Automotive Gear Oil Compatibility with Typical Oil Seal Elastomers
D5704	Evaluation of the Thermal and Oxidative Stability of Lubricating Oils Used for Manual Transmissions and Final Drive Axles
D5760	Specification for Performance of Manual Transmission Gear Lubricants
D6074	Guide for Characterizing Hydrocarbon Lubricant Base Oils
D7450	Standard Specification for Performance of Rear Axle Gear Lubricants Intended for API Category GL-5 Service 1
E1	Specification for ASTM Thermometers
E128	Maximum Pore Diameter and Permeability of Rigid, Porous Filters for Laboratory Use
G40	Terminology Relating to Erosion and Wear
ASTM	Three Glossy Prints of Test Blocks Showing Scars (D 2780)
Adjuncts	ASTM Copper Strip Corrosion Protection

TABLE 9—Additional Standards Related to Gear Lubricants

Organization and Test No.	Test Method or Document Title
ANSI (American National Standards Institute) B3.12	Specification for Metal Balls
DIN (Deutsch Industries Norm)	FZG Zahnrad Verspannungs Pruef Maschine—Allgemeine Arbeitsgrundlagen
51 354 Teil (Part)	1
Federal Standard No 791 C	Method 3430.2 Compatibility Characteristics of Universal Gear Lubricants Method 3440.1 Storage Solubility Characteristics of Universal Gear Lubricants
Institute of Petroleum Standards	Color measured using the Lovibond Tintometer
ISO	Guide 25—General Requirements for the Calibration and Testing Laboratories 3104 Petroleum Products—Transparent and Opaque Liquids—Determination of Kinematic Viscosity and Calculation of Dynamic Viscosity 3105 Glass Kinematic Capillary Viscometers—Specifications and Operating Instructions 3696 Water for Analytical Laboratory Use—Specification and Test Methods 9000 Quality Management and Quality Assurance Standards—Guidelines for Selection and Use
Mack Trucks, Inc.	GO-H, Oil, Gear: Multipurpose
Military Standard	MIL-L-2105, Lubricating Oil, Gear, Multipurpose
SAE (Society of Automotive Engineers)	J308 Axle and Manual Transmission Lubricants

TABLE 10—ASTM Standard Test Methods Related to Brake Fluids

D91	American Automobile Manufacturers Association
D260	Standard Recommended Practice for General Gas Chromatography Procedure
D344	Method of Test for Relative Dry Hiding Power of Paints
D395	Aerospace Materials Specification
D412	Rubber Properties in Tension
D445	Kinematic Viscosity of Transparent and Opaque Liquids (and the Calculation of Dynamic Viscosity)
D664	Neutralization Number of Potentiometric Titration
D746	Brittleness
D1120	Method of Test for Boiling Point of Engine Antifreezes
D1209	Color of Clear Liquids (Platinum-Cobalt Pigments)
D1364	Water in Volatile Solvents (Fischer Reagent Titration Method)
D1415	Method of Test for International Hardness of Vulcanized Natural Rubber and Synthetic Rubbers
D2240	Rubber Property—Durometer Hardness
D3182	Recommended Practice for Rubber-Materials, Equipment and Procedures for Mixing Standard Compounds and Preparing Standard Vulcanized Sheets
D3185	Methods for Rubber-Evaluation of SBR (Styrene-Butadiene Rubber) including Mixtures with Oil
E1	Specification for ASTM Thermometers
E145	Specification for Gravity-Convection and Forced-Ventilation Ovens
E260–73	Standard Recommended Practice for General Gas Chromatography Procedure

Index

A

- A/B petrol and diesel engine, 233, 234 (table), 235 (table), 236 (table)
- ABDT. *See* sealed bearing simulation tester
- ABFT. *See* accelerated life tester (ABFT)
- abnormal sound, 144, 146, 148 (table)
- abrasive wear, 296–299, 298 (figure)
- abuse testing, 289
- accelerated aging test, 388–390, 388 (figure), 389 (figure)
- accelerated life tester (ABFT), 149–150, 149 (figure), 150 (figure), 151 (figure)
- accelerated tests, 146, 276–277, 388–390, 388 (figure), 389 (figure)
- ACEA C (X), 82, 233
- ACEA C4-08, 75, 76, 77, 78
- ACEA E (X), 233–237, 238 (table), 239 (table)
- ACEA E9-08, 68–69, 70, 71, 72, 74, 78–79
- ACEA Heavy-Duty Diesel (HDD), 232–233, 241 (table), 241–242
- ACEA performance standards, 34, 36, 233–237, 234 (table), 235 (table), 236 (table). *See also* European Automobile Manufacturers' Association (ACEA); *specific standards*
- acid number (AN), 404, 412, 413
- acids, 206, 429–430
- acrylonitrile/butadiene/styrene (ABS), 383 (figure)
- additive company, 259
- additives, 23, 34–35, 111, 200 (table), 207 (table), 252, 353, 368–369, 413 (figure)
 - alternative depletion, 413
 - antiwear, 29 (figure), 29–30, 48, 108, 198–201, 202, 209, 220, 224, 247, 368–371, 369 (figure), 370 (figure), 371 (figure)
 - atomic force microscopy (AFM) and, 358 (figure)
 - bulk fluid property, 261
 - detergents, 31, 33 (figure), 34 (table)
 - dispersants, 30–33, 298
 - friction and, 22, 29, (figure), 224, 352, 362 (figure), 369 (figure), 371–372, 371 (figure), 372 (figure)
 - extreme pressure and, 30, 31 (table), 261
 - fuel and, 317–318, 321, 325
 - functions, 198–201
 - gears and, 170
 - grease, 41
 - lubricity and, 417–418, 423
 - protective, 27–28, 29 (figure), 261
 - performance, 23–26, 261
 - soot and, 298
 - surface analytical techniques and, 367–368
 - transmissions and, 262–266
 - tribology and, 319–332, 347–348, 369–372
 - viscosity modification and, 111
- See also* molybdenum dithiocarbamate (MoDTC); *specific additives*; *specific components*; *specific materials*; zinc dialkyl dithiophosphate ZDDP
- adhesive wear, 296, 298 (figure)
- A/8.3/90, 180, 181
- aging, 385
 - accelerated, 388–390, 388 (figure), 389 (figure)
 - limits, 410, 411 (figure)
 - See also* accelerated aging tests; oxidative stability
- air retention, 284
- air-fuel ratio, 122–123
- alignment errors, 382–383
- alkalinity, 404, 415
- all-wheel drive, 160 (figure), 164
- Al-Si alloy, 338–339, 355 (figure), 364 (figure), 368–375
- alternative fluids, 320–321, 328–329
 - film forming and, 321–324
 - fuel, 82, 218, 228–229
 - shear thinning and, 323–324
 - wear tests and, 323–328
 - See also* biofuel; vegetable oil
- aluminizing, 335
- aluminum, 335, 340. *See also* aluminum alloy
- aluminum alloy, 107, 108, 109, 125, 215, 338, 407
- Aluminum Beaker Oxidation Test (ABOT), 266
- aluminum oxide, 227–228
- American Chemistry Council Product Approval Code of Practice, 227
- American Oil Chemist Society (AOCS), 460
- American Petroleum Institute (API), 64, 68, 226. *See also* API performance standards; *specific standards*
- American Society for Testing and Materials (ASTM), 64, 217, 226, 231. *See also* ASTM test methods; performance standard, organizations; *specific test methods*
- ammonia (NH₃), 127, 209
- angular velocity, 122, 123
- anhydrous ethanol, 419 (table)
- antifoam agents, 26, 48, 200 (table). *See also* foam control
- antioxidant, 26–27, 27 (figure), 48, 200 (table)
- antioxidant reserve test, 71
- antitrust agent, 200 (table)
- antiwear agent, 29–30, 29 (figure), 31 (table), 48, 200 (table), 333–337, 338–345. *See also* additives, antiwear
- APEA performance requirements, 36
- API basestock classification system, 47, 48 (table)
- API C series specifications, 240–241. *See also* *specific specifications*
- API C (X), 242–243
- API CI-4, 36, 68, 232–233
 - engine tests, 72–74, 241 (table)
 - laboratory tests and, 70–72
- API CJ-4, 243 (table)
- API gear oil designations, 38
- API GL-4, 181, 288
- API GL-5, 181, 288 *See also* ILSAC GL-5
- API performance standards, 34, 36. *See also* *specific standards*
- API S (X), 243–244, 245 (table)
- API SM, 243–244, 245 (table), 246 (table)
- API SN, 245, 249 (table)

API Tripartite Sequences, 237–244. *See also specific sequences*
 API Tripartite System, 64–65, 82
 aromatic base oil, 261
 ash, 247, 250 (table). *See also soot*
 ashless dispersants, 47
 Asia, 259
 asperities, 3, 5 (figure), 7–8, 120
 asperity contact model, 18
 Association for Petroleum and Explosives
 Administration (APEA). *See* APEA performance standards; *specific standards*
 ASTM test methods, 290–291, 420 (table), 421. *See also specific test methods*
 ASTM Wear and Erosion Terminology Standard G-40, 420
 atom force microscopy (AFM), 357–358, 357 (figure), 358 (figure), 359 (figure), 371 (figure)
 atomic emission spectroscopy, 408
 ATR FTIR spectrometer, 366 (figure), 367 (figure)
 ATR tribometer, 367
 attenuated total reflection (ATR) spectroscopy, 366
 attenuation, 385
 Auger electron spectroscopy (AES), 361
 autocorrelation function, 5
 automatic dinematic viscometer, 49
 automatic transmission fluid (ATF), 37, 255, 261 (table), 266–267
 chemical construction of, 259–266
 planetary gear and, 257
 automotive bearing vibration. *See* bearing vibration test
 automotive exterior, 381
 automotive fluid test. *See specific lubricants; specific standards; specific tests*
 automotive gear oil tests, 38, 39 (table)
 automotive grease. *See* grease
 automotive service grease, 43–45, 137–138. *See also* grease
 auxiliary engine parts, 142 (table), 143 (table)
 average Reynolds equation. *See* Reynolds equation
 aviation fuel, 417
 AW agent, 263–264, 318
 axle, 36, 38, 159–160, 165 (figure), 166 (figure). *See also* axle fluid
 axle lubricant, 288
 axle fluid, 38–39, 38 (table)
 axle tests, 288

B

ball bearing, 153 (table)
 ball joint, 140
 Ball Rust Test (BRT), 81, 112, 193 (table), 226
 BAM test, 325–326
 band clutches, 256–257, 257 (figure)
 base number (BN) test, 413
 base oil, 23, 24 (figure), 35 (table), 111, 317
 grease and, 142
 transmission fluid and, 259–261, 260 (figure), 260 (table)
 See also basestock
 basestock, 47, 260 (table). *See also* base oil
 bathtub curve, 62

bearing, 109 (figure), 131 (figure), 132–133, 134, 168
 auxiliary, 142
 ball, 153 (table)
 damage and, 77, 134–135
 electrical part, 142
 grease and, 42
 hub, 137–139, 138 (table), 139 (figure)
 inserts, 107–108
 journal, 18, 19, 129–132, 130 (figure), 131 (figure)
 material for, 132–133, 382, 395–396
 non-automotive, 379 (figure)
 shells, 130 (figure), 131, 134 (figure)
 sliding, 106
 speed, 262
 surface treatment and, 133
 temperature and, 129
 See also bearing design; bearing tests; *specific bearings*
 bearing tests, 133–134, 134 (figure), 146–154. *See also* bearing vibration tests
 bearing vibration test (BVT), 144–146. *See also* bearing vibration tester
 bearing vibration tester, 144–146, 144 (figure), 145 (figure), 146 (table), 147 (table)
 Beilby layer, 3
 belt arrangement, 259 (figure)
 bench scuffing wear simulation test, 98
 bench test rigs, 97, 178
 bench tests, 94, 96 (table), 99 (table), 111–114, 134 (figure), 287
 alternative fuel and, 218, 228–229
 API CJ-4, 195–197 (table), 199 (table)
 cylinder components and, 218–219, 223–224
 diesel fuel and, 420
 friction and, 393 (figure)
 ILSAC GF-5 and, 248–249 (table)
 industrial standards and, 95
 material and, 215, 216 (figure), 216–218, 217 (table), 218 (figure), 226
 pistons and, 218–219, 220–223
 test method and, 97–98. *See specific methods*
 valve train subsystems and, 218–219
 See also laboratory tests; *specific tests*; tribological bench tests
 biofuel, 82, 209, 232, 237, 253–254. *See also* alternative fluid; vegetable oil
 bio-no-tox, 317, 318, 319. *See also* alternative fluid; biofuel
 black sludge test, 78
 block wear, 97
 block-on-ring tester, 218 (figure)
 Blok's solution, 15
 blotter spot testing, 410
 BOCLE (Ball-on-Cylinder Lubricity Evaluator), 420
 bore shape, 131
 boriding treatment, 335
 boundary film, 19, 204
 boundary friction coefficient, 206. *See also* friction coefficient
 boundary lubrication, 19, 204, 263, 301, 352, 353 (figure). *See also specific systems*
 Boussinesq equation, 6–7, 14

brake mechanisms, 42, 346–347, 380
 breathers, 284
 bridge phenomena, 208
 bridging oxygen (BO), 370
 bulk oil, 261–262
 buried surface, 366–367
 bypass oil filters, 427, 429, 434

C

calcium, 139
 cam and follower, 352–353, 353 (figure)
 cam follower system, 219, 220, 345
 Cameron-Plint high frequency friction machine, 96, 97 (figure), 97–98, 219 (figure)
 camshaft, 108–109, 223
 camshaft tests, 223–225, 224 (figure)
 capacitance method, 85
 carbon, 334, 335
 carbon monoxide (CO), 126
 carbon polymer tails, 31 (figure)
 carbonitriding, 335
 carburizing, 64, 334
 cast iron, 125, 245, 338, 340, 342, 407
 Castrol. *See* Greentec LS 5W-30
 catalytic converter, 78, 127, 128 (figure), 209
 Caterpillar C13, 195 (table), 198, 199, 242 (table)
 Caterpillar 1N, 74, 195 (table), 198, 199, 242 (table)
 CCMC (Comite des Constructeurs du Marché Commun), 65
 centerline average, 4, 16 (figure)
 ceramic material, 342, 344
 C-GFKT/8.3/90, 184
 chassis system, 43–44
 chemical bond vibrational techniques, 360
 chemical limits, 71–72, 241 (table), 242
 chemical properties, 360–367, 360 (figure)
 chemically inert additive, 41
 Chevron Test, 181
 chlorine, 82
 chromium, 335, 342, 344
 Chrysler, 266–267
 CI compounds, 30
 circular point contact, 302 (figure), 302–303
 CJ-4. *See* API CJ-4
 Cleveland open cup (COC), 56
 clip ratio, 443 (figure)
 closed loop testing, 276
 cloud point, 52
 clutch friction specifications, 251 (table), 252 (table)
 clutch, 251 (table), 252 (table), 262, 346, 356 (figure)
 coated surfaces, 8–9. *See also specific surfaces*
 cold crank simulator (CCS), 49, 80
 cold-scuffing, 221, 225–227, 226 (table), 227 (table)
 cold-start simulation, 435
 collapse test, 435
 color, 56
 colorimetric interferometry technique, 86
 combustion, 105, 106, 119
 commercial engine, 43, 119
 combustion engine architecture, 124
 compression, 105, 119, 120
 compression ring, 341, 342
 computer models, 284
 conformal contact, 5, 18–19
 conformal engine, 19
 connecting rod, 125–126
 constant velocity (CV) joint, 421, 437–439, 445 (figure)
 apparatus, 438–439
 friction characterization and, 442–446
 friction coefficient and, 440–441, 440 (figure), 441 (figure), 443 (figure), 444 (figure), 446–448, 447 (figure), 448 (figure), 449 (figure), 450, 452 (figure)
 friction measurement and, 439–442, 442 (figure), 438, 439 (figure)
 friction modeling, 446–452, 452 (figure)
 grease and, 140–142, 141 (figure)
 contact analysis, 5–9, 217 (figure), 302–304. *See also specific engine components*
 contact mechanics, 302, 304, 303 (figure). *See also specific mechanisms*
 contact pressure, 217 (table)
 contaminant capacity, 435
 contamination, 23, 205, 384, 402, 409 (figure)
 moisture and, 412–413
 filtration and, 429–430, 429 (figure), 435
 solid particle, 411–412
 continuous oil recycling system, 461, 463, 462 (table)
 continuously slipping torque converter clutches (CSTCCs), 257
 continuously variable transmission (CVT), 258–259, 259 (figure)
 continuously variable transmission (CVT) fluid, 37, 258–259
 cooling circuit, 126. *See also* continuously variable transmission (CVT) fluid
 cooling tests, 277–278
 Coordinating European Council for the Development of Performance Tests for Transportation Fuels, Lubricants, and Other Fluids (CEC), 65–66
 copper alloy, 407
 copper corrosion inhibitor, 264, 265
 Cooper Strip Corrosion Standard, 56
 CORES converter, 462 (figure), 462–463
 corporate average fuel economy (CAFE), 201, 254
 corrosion, 56, 300, 385 (figure), 391 (figure)
 corrosion inhibitor, 33, 200 (table), 264–265, 265 (figure)
 corrosive wear, 300
 counterformal contact, 5, 18
 counterformal engine, 19
 coupling greases, 43
 course filtration, 428
 crackle test, 410
 crank angle, 121–122, 131
 crankcase lubricants, 199 (table)
 cranking viscosity, 49–50
 crankshaft, 105, 106, 107–108, 121, 125
 crankshaft-rod-piston connecting system, 124
 CrC-NiCr coating, 342
 CrN coating material, 339
 C-type gears (C-PT), 185 (figure), 186, 187
 Cu, 33–34
 Cummins Bearing Corrosion Test and the Corrosion Bench Test (CBT), 56, 73
 Cummins fuel injector, 418 (figure)

Cummins ISB, 195 (table), 198, 199, 242 (table)
 Cummins ISM, 195 (table), 198, 199, 237, 242 (table)
 Cummins M-11, 299
 cumulative distribution function, 4
 cumulative plastic deformation, 110
 CVD, 336
 cylinder, 105, 120, 124–128
 elastic, 6
 materials and, 339 (figure), 339–340, 347 (table)
 multi-, 124, 125
 See also combustion engine architecture
 cylinder bore, 108, 338–339. *See also* cylinder bore tests
 cylinder bore tests, 218–219, 220–223, 224 (figure), 225 (figure)
 cylinder liner tests, 223–224, 319, 347
 C/0.05/120/12, 182
 C/0.05/90/12, 182

D

D1217, 55
 D130, 56
 D1480, 55
 D1481, 55
 D1500, 56
 D2240, 193 (table), 194 (table)
 D2266, 286 (table)
 D2500, 52
 D2603, 52
 D2782, 286 (table)
 D2893, 286 (table)
 D2983, 51
 D3427, 286 (table)
 D3527, 286 (table)
 D4052, 55
 D412, 193 (table), 194 (table)
 D4289, 286 (table)
 D445, 49
 D4485, 49
 D4624, 323
 D4683, 68, 69–70, 238, 232
 D4684, 51, 238
 D471, 193 (table), 194 (table)
 D4741, 323
 D4857, 252
 D4858, 252
 D4863, 252
 D4950, 139 (table), 140 (table), 464 (table), 466–467, 466 (table)
 D4951, 54, 71 (table), 192 (table)
 D4998, 181
 D5133, 50, 51, 192 (table)
 D5158, 54–55
 D5183, 286
 D5275, 51, 52
 D5579, 288
 D5662, 57
 D5704, 287 (table)
 D5706, 324–325, 326 (figure)
 D5800, 53, 71, 192 (table)
 D5949, 52
 D5950, 52
 D5966, 74

D5968, 56
 D5985, 52
 D6082, 53, 193 (table)
 D6278, 52
 D6335, 57
 D6417, 53, 192 (table)
 D6425, 286 (table)
 D6557, 193 (table)
 D6593, 192 (table), 194
 D6594, 56
 D665, 286 (table)
 D6709, 51, 52, 80, 192 (table). *See also* Sequence VIII
 D6749, 52
 D6794, 56–57, 193 (table)
 D6795, 56, 193 (table)
 D6821, 51
 D6837, 194
 D6891, 77, 192 (table), 194. *See also* Sequence IVA
 D6892, 52
 D6894, 53–54, 71 (table)
 D6895, 51
 D6896, 70 (table)
 D6922, 81, 193 (table)
 D6984, 74
 D7038, 288
 D7097, 57, 192 (table)
 D7109, 69
 D7146, 197
 D7156, 70 (table)
 D7216, 57
 D7320, 76, 192 (table). *See also* Sequence III-GB
 D7450, 39 (table), 43, 288
 D7452, 288
 D7528, 193 (table)
 D7563, 193 (table)
 D7589, 192 (table). *See also* Sequence VID
 D8696, 197
 D874, 55, 71 (table)
 D892, 53, 71, 193 (table), 286 (table)
 D97, 52
 damage accumulation, 110
 deep-groove ball bearings, 153 (table), 167
 deformations, 6–7, 7 (figure), 302
 degradation, 61–63, 62 (figure), 207
 biodiesel and, 237
 performance specifications and, 63–66
 testing and, 66–67
 demulsifiers, 200 (table)
 density, 11, 55
 density-pressure relationship, 11, 13
 deposits, 73–74, 76, 79, 206, 237
 design life, 274
 design tools, 313
 detergents, 31, 33 (figure), 34 (figure), 47–48, 206, 263, 264 (figure)
 deterministic modeling, 15, 18
 DEXRON®, 266, 267 (table)
 DI package, 47
 diamond-like carbon (DLC) coating, 97, 133, 224
 diesel catalyzed particle filters (DCPF), 209–210
 diesel engine oil, 194, 197. *See also* diesel engine tests
 diesel engine tests, 194, 195–197 (table), 197–198

- diesel engine
 - emissions control and, 127–128
 - lubrication, 231–232, 232 (figure)
 - material and, 372
 - pistons and, 340
 - powertrain and, 120, 122–124, 123 (figure)
 - See also* A/B petrol and diesel engine; diesel fuel
 - diesel fuel, 68, 75, 120, 417–423, 418 (figure)
 - fuel filters and, 432–433
 - sulfur in, 239–240
 - See also* biofuel; ethanol-diesel; vegetable oil
 - diesel ideal cycles, 120 (figure)
 - diesel particulate filters (DPFs), 127–128, 231
 - differential, 282
 - differential assembly, 167 (figure)
 - differential pressure, 434, 435
 - diffuse reflectance infrared Fourier transform (DRIFT) spectroscopy, 209
 - dimethylpolysiloxanes, 386
 - DIN 51819, 151–152
 - Direct Injection Diesel Poston Cleanliness and Ring Sticking test, 72, 78
 - discharge-voltage method, 85
 - dispersant, 30–33, 31 (figure), 32 (figure), 33 (figure), 34 (table), 47, 263 (figure), 298; ashless, 47
 - dispersant viscosity modifier (DVM), 31
 - displacement, 105, 121, 122, 359 (figure), 360 (figure)
 - distribution system, 126
 - Doolittle parameter, 10
 - door hinges, 42
 - Dowson-Higgison's solution, 15
 - drain port sampling, 400
 - drive bearings, accessory, 42
 - drive gears, 281
 - drive units. *See* final drive units
 - driveline. *See* drivetrain
 - driveline fluid, 35–38, 39 (table)
 - driveshaft, 42, 165–166, 285, 286 (table), 437
 - drivetrain, 157–160, 158 (figure), 171–175, 345–347.
 - See also* drivetrain tests; gear box; transmission
 - drivetrain tests, 275–279. *See also* transmission; transmission tests
 - drop-tube vacuum sampling, 400–401 (figure)
 - dual clutch gear box, 164
 - dual-clutch transmission (DCTs), 258–259, 259 (figure).
 - See also* dual-clutch transmission (DCT) fluid
 - dual-clutch transmission (DCT) fluid, 37, 258
 - durability tests, 275–276, 328 (figure). *See also specific tests*
 - dustproof head test, 148, 149 (figure)
 - dynamic friction model, 448–449, 449 (figure), 448–449, 452 (figure)
 - dynamic viscosity, 49
 - dynamometer, 225, 309, 463
- E**
- E1078, 361
 - E1829, 361
 - E1840, 367
 - E2695, 365
 - E6-03. *See* ACEA E6-08
 - e-diesel. *See* ethanol-diesel
 - efficiency standards. *See* performance standards
 - efficiency test, 186–188, 187 (figure), 282–284, 283 (table)
 - elastohydrodynamics lubrication film tests, 85, 87 (figure), 91 (figure), 92 (figure), 92 (table), 93 (figure), 94 (figure), 101–102
 - fluid behavior and, 87–88
 - measurement techniques and, 85–87
 - surface lubrication and, 89–90, 89 (figure), 91–93
 - thickness and, 85–87, 87 (figure)
 - See specific techniques*
 - elastic cylinders, 6
 - elastohydrodynamic contact, 86
 - elastohydrodynamic lubrication, 13, 14, 15, 301
 - Elastomer Compatibility Test, 209
 - elastomer, 57, 81 (table), 115, 193 (table)
 - elasto-plastic contact, 9
 - elastoviscous effect, 10
 - electric motors, 379
 - electrical contact switch, 42
 - electrical part bearings, 142 (table), 143 (table), 143–144 (figure)
 - electrochemical coating, 335
 - elemental spectroscopy, 409–410, 412, 413, 414
 - elements, 54, 409 (figure). *See specific elements*
 - elliptical contact. *See* point contact
 - embedability, 107
 - EMCO rust test, 139
 - emissions, 71–72, 318
 - diesel, 417
 - particulate, 231
 - regulation of, 61–62, 126–127, 227, 231, 253
 - improvements, 110
 - See also* environmental effect
 - emulsion retention test, 81
 - energy dispersive x-ray (EDX), 360–361, 361 (figure)
 - engine, 105, 119, 124, 352 (figure)
 - block, 125, 372
 - characterization, 105–106, 351
 - components of, 215, 338–345, 379–382, 379 (figure), 380 (figure), 381 (figure), 382 (figure), 385 (figure)
 - friction loss and, 351–352
 - non-automotive, 252–253
 - See also* engine material; heavy-duty diesel; internal combustion engine; passenger cars; *specific components*; *specific engines*; triboactive material
 - engine architecture, 124
 - engine bearing. *See* bearings
 - engine block, 125, 372
 - engine deposits. *See* deposits
 - engine dynamometer test, 98
 - engine material, 106, 107, 110, 333, 372–375
 - behavior, 336 (table), 390–391, 390 (figure), 427
 - candidate, 217 (table)
 - follower, 220, 222 (figure)
 - polymer, 382–383
 - precision mechanics and, 382
 - Engine Oil Aeration Test (EOAT), 53–54, 71 (table), 195 (table), 197–198. *See also* ASTM D6894
 - Engine Oil Licensing Certification System (EOLCS), 64–65

- engine oil, 34–35, 34 (figure), 35 (figure), 36 (figure), 207–209, 318 (figure), 410–411
 additives and, 368. *See also* additives
 aeration, 242 (table)
 alternative, 320 (table), 320–321, 461–465
 analysis of, 401–410, 411–415, 411 (figure), 414 (figure)
 compression band, 108
 diesel, 194, 197
 gear boxes and, 162, 163
 precision mechanics and, 384–391, 387 (figure), 388 (figure)
 specifications and, 318–319, 323 (table)
 tests, 38, 39 (table)
See also alternative fluids; oil; oil filter; oil sampling methods; *specific engine types*; *specific oils*
- engine seal. *See* seal
- engine tests, 36, 62, 64–65, 66–67, 111, 225–226
 accelerated, 66, 388–390, 388 (figure), 389 (figure)
 ACEA C and, 36 (table), 133, 236 (table)
 API CJ-4 and, 36 (table), 195–197 (table), 199 (table)
 alternative fluid and, 323–328
 bearings and, 144–154
 biobased lubricants and, 461–464. *See also* biobased lubricant; *specific test methods*
 gear oil and, 38, 39 (table)
 grease and, 44 (table)
 performance specifications and, 61, 62 (figure), 62–63
 precision mechanics parts and, 392–398, 392 (figure). *See also* friction, precision mechanics and; wear, precision mechanics and
 requirements, 112–113. *See also* bench tests; performance standards
 stability and, 51
 tribological, 368
 valves and, 344
 wear and, 73, 76, 78
See also bearing tests; bearing vibration tests; bench tests; elastohydrodynamics lubrication film (EHL) tests; engine material; laboratory tests; performance standards; tribological bench tests; *specific tests*
- engineering surface, 3–9
- environmental effect, 110, 209–210, 285, 317, 320–321
- environmental scanning electron microscope (ESEM), 354
- environmental standard, 61–62, 231
- environmental stress stimulation test, 152
- enzymatic hydrolysis, 49
- EOWTT, 80
- epilamization, 388
- equation of motion, 11–12
- EREBIO, 326–327, 327 (figure), 328 (figure)
- esters, 320, 321, 323, 386, 458 (figure)
- estolides, 458, 459 (table)
- ESW M2C138-CJ, 266, 267 (table)
- ESW M2C33, 266, 267 (table)
- ethanol-biodiesel-diesel blend, 419
- ethanol-diesel blend, 419 (figure)
- ethyl alcohol, 254
- ethylene acrylic rubber (AEM-1), 194 (table)
- Europe, 259, 417
- European Automobile Manufacturers' Association (ACEA), 65–66, 68, 232. *See also* European performance standards; *specific standards*
- European performance standards, 62, 64, 65–66, 67, 232–237, 234 (table), 235 (table), 236 (table). *See also specific ACEA standards*
- evaporation behavior, 388
- exhaust, 105
- exhaust gas recirculation (EGR), 73, 127, 194–195, 195 (table), 197, 198, 206, 209–210, 231, 297–298
- extended service intervals, 254
- extended x-ray absorption fine structure (EXAFS), 362
- extreme operating conditions, 278–279
- extreme pressure (EP) agent, 30, 31 (table), 200 (table), 201, 263–264, 318, 324–325
- Eyring-Ewell equation, 9
- ## F
- factory-fill hydrocarbon based oil, 320–321
- FAG FE8, 151, 152 (figure)
- FAG FE9, 152 (figure)
- Falex BOTS, 420
- Falex-type block-on-ring friction and wear tester, 96, 97 (figure), 218 (figure)
- Farm Bill, 456
- fatigue life, 149–150, 150 (table), 153 (table)
- fatty acid methyl esters (FAMES), 209, 237
- fatty acids, 459
- ferrography, 406 (figure), 412. *See also* ferrous density
- ferromolybdenum, 327
- ferrous density, 405–406, 406 (figure), 412
- field testing, 215. *See also* bench tests; engine tests
- fill-for-life fluids, 273, 289, 317
- film thickness, 106 (figure), 132 (figure), 133 (figure), 216 (figure), 353 (figure)
 additives and, 369
 elastohydrodynamic solutions and, 13, 14–15, 15 (figure), 85–87, 87 (figure)
 measurement, 18, 200 (table)
 oil and, 321–323, 322 (figure)
- film-forming behavior, 320 (table), 321, 321–323. *See also* film thickness
- filterability, 56–57, 79–80, 193 (table), 435
- filters, 427–429, 428 (figure)
 capacity, 435
 performance qualifications and, 430–431, 434
 test methods and, 431–433
See also fuel filter; oil filter
- final drive units, 166, 167 (figure)
- fine filtration, 428
- five speed automatic transmission, 255
- fixed ball joint, 140
- flammability, 55
- flash point, 55–56. *See also* flash point test
- flash point test, 409–410, 409 (figure), 412, 414
- flat plate clutch, 256–257, 257 (figure)
- “flexible fuel,” 228
- fluorescence, 54
- flow characteristics, 16–17, 18, 248 (figure), 434, 435
- fluid behavior, 87–88
- fluid cleanliness rating, 402
- fluorocarbon rubber (FKM-1), 115 (figure), 194 (table)

foam control, 207, 265. *See also* foaming
 foaming, 53, 70, 80, 193 (table), 196 (table), 241 (table).
See also antifoam agents; foam control
 focused ion beam (FIB) material sputtering technique, 356
 force-displacement, 359 (figure), 360 (figure)
 Ford, 266–267
 Fourier transform infrared (FTIR) spectroscopy, 360, 365–366, 366 (figure), 404–405, 412, 413 (figure), 414
 four-square test rig, 279 (figure)
 four-stroke engine, 119, 251–252
 fractal contact, 9
 France, 319
 free-volume viscosity model, 10
 friction
 alternative oils and, 325–327
 precision mechanics and, 392–394, 393 (figure), 394 (figure), 395 (figure)
 static, 395 (figure)
 torque and, 149
 See also friction coefficient; friction loss; friction modifier; friction tests
 friction coefficient, 262, 352, 353 (figure), 383 (figure), 421–422, 421 (figure), 422 (figure), 440
 friction force microscopy (FFM), 357
 friction loss, 172, 333, 351, 352 (figure)
 friction model, 448–440, 449 (figure), 452 (figure)
 friction modifier (FM), 27–28, 28 (figure), 29 (figure), 31 (table), 48
 additives and, 29, (figure), 224, 362 (figure), 369 (figure), 371–372, 371 (figure), 372 (figure)
 performance criteria, 262–263
 friction tests, 96 (table), 96–97, 217–219, 219 (figure), 356 (figure), 369
 friction-sliding-elastic contact, 304
 friction-temperature regime, 334 (figure)
 front-wheel drive, 159 (figure)
 FTMS Method No. 3458.1, 391
 F2G gear test rig, 100, 181, 182, 188
 Fuchs. *See* Titan GT1 0W-20
 fuel
 alternative, 218, 228–229
 diesel, 68, 75, 120, 239–240, 417–423, 418 (figure), 432–433
 dilution of, 409, 410, 414
 lubricity and, 417–418, 418 (figure). *See also* lubricity tests
 quality of, 239–240. *See also* biodiesel
 hydrocarbons in, 105, 106, 226
 See also additives; fuel economy; fuel efficiency; *specific types*
 fuel consumption, 61, 77, 123 (figure). *See also* oil consumption
 fuel economy, 227–228, 317, 351
 fuel efficiency, 77, 78, 105, 110–111, 113, 192 (table), 202
 fuel filter, 431–433
 fuel injector, 418 (figure), 422–423, 422 (table)
 full-flow oil, 428–429
 full-scale mixed EHL model, 89, 90
 FZG back-to-back rig, 178–179, 179 (figure), 181
 FZG-type test rig, 279 (figure)

G

Ga ions, 356
 galvanic coating, 335
 gas chromatography (CGD), 53
 gas discharge, 119, 120
 gasoline, 417. *See also* fuel
 gasoline engine tests, 191–194. *See also* engine tests
 Gatto, V. J., 201
 Gaussian asperity-height distribution, 4, 5, 17
 Ge, 367
 gear box, 159, 160, 161–164, 161 (figure), 162 (figure), 163 (figure), 164 (figure), 165 (figure). *See also* gear box tests; in-line gear box; synchromesh testing
 gear box tests, 287–288
 gear oil, 178, 181, 288 (figure)
 gear oil screen tests, 177 (table), 178, 180–186
 gear selection, 274 (figure)
 gears
 lubricants and, 182, 183 (table), 288
 mesh, 169
 miniature, 379; 167–168, 180 (figure)
 test, 179 (table), 179–180, 180 (figure)
 transmission, 345–346; wheel, 38
 See also gear box; *specific gears*
 gelation index, 50, 75 (table), 75–76, 192 (table)
 General Motors, 266, 267
 generated axial force (GAF), 437, 438, 450
 gerotor pump, 110 (figure)
 GF-4, 192–194 (table)
 GL-1, 38
 GL-2, 38
 GL-3, 38
 GL-4, 38
 GL-5, 38, 69 (table). *See also* ILSAC GF-5
 GL-6, 38–39
 global elasticity, 18–19
 glycol reagent method, 410
 GM-9099P, 56
 government regulations, 227. *See also* environmental standards
 gravimetric analysis, 430
 grease, 40–45, 137, 138 (table), 142–143, 143 (figure), 387
 auxiliary parts and, 14
 biobased, 464–466
 constant velocity universal joints and, 140–142, 141 (figure)
 electrical parts and, 142, 143
 hub bearings and, 137–139, 138 (table), 139 (figure)
 life of, 151–152
 measurement technology and, 144–146, 145 (figure), 146 (table)
 requirements, 137–138
 Green's functions, 5
 Greentec LS 5W-30, 320 (table), 321, 323 (table), 324

H

haptic demands, 385
 hardness, 358–359
 heat capacity, 108. *See also* temperature
 heavy-duty diesel, 82, 159, 232
 API and, 240–241

- lubricants for, 233–234, 237
 - See also diesel engine
 - heavy-duty trailer-towing, 278
 - helical gears, 167, 168
 - Herrebrugh's solution, 15
 - Hersey number, 13
 - Hertz theory of elastic contact, 7, 302
 - Hertzian formulas, 7, 8, 9, 19
 - HFRR, 420
 - high-frequency reciprocating rig (HFRR), 204
 - high-shear viscometer, 323
 - high shear viscosity, 50, 68–70, 196 (table), 319, 321–323
 - high-temperature corrosion bench test, 196 (table), 241 (table)
 - high-temperature deposit, 57
 - high-temperature test life, 1369
 - high-temperature viscosity, 50
 - high-temperature, high-shear (HTHS) viscosity, 50, 68–70, 196 (table), 319, 321–323
 - Hooke's joints, 42
 - hot-scuffing, 225
 - HTHS stability, 69 (table)
 - HTX 822 15W-50, 320 (table), 321, 323, 324, 325
 - Hu, Y. Z., 89, 90
 - hub bearing, 137–139, 138 (table), 139 (figure), 149. See also hub bearing tests
 - hub bearing tests, 149. See also ABFT
 - hybrid thickeners, 41
 - hybrid vehicles, 160, 254
 - hydraulic pulse durability, 435
 - hydrocarbon (HC), 27–28, 126, 262
 - hydrodynamic lubrication, 11, 12, 15–19
 - hydrogenated nitrile rubber (HNBR-1), 115 (table), 194 (table)
 - hydrogenated radial isoprenes (RIs), 25
 - hydrogenated styrene butadiene copolymers (SBCs), 24 (figure), 25
 - hydrogenated styrene isoprene copolymers (SICs), 24 (figure), 25
 - hydraulic valve lifters, 109
 - hydroxide, 263
- I**
- ICOT (isothermal corrosion oxidation test), 219, 323–324, 325 (figure)
 - ignition timing, 231
 - ILSAC. See International Lubricants Standardization and Approval Committee (ILSAC) ILSAC GF-4, 227
 - ILSAC GF-5, 49, 64, 65, 74–82, 110–111, 227
 - requirements, 112–114, 115 (table), 244–245, 248–249 (table)
 - test methods, 192–194 (table)
 - viscosity and, 246 (table)
 - See also API GF-5
 - indirect laser transmission method, 86
 - inductively coupled plasma (ICP) spectrometer, 408
 - industrial applications, 180 (figure), 180–181
 - industrial crops, 456
 - infinite life, 275
 - infrared spectroscopy, 405 (figure)
 - injection molding skin, 396
 - injection system, 417
 - injection timing, 237
 - inlet antidrain, 435
 - in-line gear box, 13 (figure), 163–164
 - inorganic contamination, 429
 - intake, 105
 - interactive deterministic-stochastic modeling, 15
 - internal combustion engine, 105–106, 106 (figure), 119–120
 - ILSAC GF-5 and, 110–115
 - lubrication requirements of, 106–110, 107 (figure), 109 (figure), 110 (figure)
 - mechanisms of wear, 110
 - pollutant emissions and, 126–127
 - powertrain and, 124–126
 - See also combustion engine architecture; engine; engine tests; gasoline engine tests; *specific components*; *specific tests*
 - International Council of Marine Industry Associations (INCOMIA), 253
 - International Lubricants Standardization and Approval Committee (ILSAC), 64, 65, 217, 226, 244. See also *specific specifications*
 - involute curve, 168 (figure)
 - IP Method, 56
 - iron liners, 372
 - ISO 12103-1, 430
 - ISO 19438, 432–433
 - ISO 4020, 432
 - ISO 4406:99, 402 (figure)
 - ISO 4548, 434–435
 - ISO/TS 16332, 433
 - ISO/TS, 13353, 432
 - ISO/TS 23556, 436
 - ISO 7148-2, 392
 - isothermal contact simulations, 8
 - isotropic, 5 (figure)
- J**
- Japan, 67
 - JASO, 246–247, 250 (table), 251–252, 253
 - Johnson et al., 90–91, 91 (figure), 91 (table)
 - journal bearings, 18, 19, 129–132, 130 (figure), 131 (figure), 341. See also bearings
- K**
- Kaneta et al, 91–93, 92 (figure), 92 (table), 93 (figure), 94 (figure)
 - Karl Fischer Titration, 408, 430, 431 (figure)
 - Kégresse, Adolphe, 37
 - kinematic viscosity, 49
 - kinematics, 121–122
 - kurtosis, 4, 5
- L**
- laboratory tests, 62, 218
 - ACEA and, 232–237, 234 (figure), 235 (table)
 - API and, 238–244
 - heavy duty diesel lubricants and, 70–72
 - ILSAC and, 245
 - performance standards and, 61, 62–63, 62 (figure), 233 (table)
 - screening test, 64

wear and, 307–308, 308 (figure), 309
See also bench tests; engine tests; specific performance standards; specific tests
 laser transmission method, 86
 lateral force microscopy (LFM), 357
 layered materials, 3, 9
 layshaft, 169
 lead, 407
 lean mixtures, 126–127
 leptokurtic, 5
 life tester, 147, 149
 light vehicle. *See* passenger cars
 Lim and Ashby wear map, 304, 305 (figure)
 line contact, 5, 6 (figure), 303 (figure)
 linear curve-fit, 443 (figure)
 linear wear coefficient C_{L} , 183 (figure)
 lithium, 142
 lithium hydroxide soap-based grease, 465
 load carrying, 14, 178, 179, 181–188, 181 (table), 186 (figure), 341
 load loss factor, 188 (figure)
 low temperature, 20, 261 (figure), 391. *See also* temperature
 low-sulfur fuel, 417, 418. *See also* alternative fluid
 lubricant, 40–41, 217 (table)
 components of, 47–48
 degradation and, 61–63, 66–67. *See also* degradation
 gear, 182, 183 (table)
 physical properties of, 45–57
 in precision mechanics, 384–391, 387 (figure), 388 (figure)
 requirements, 106–110
 solid, 387
 See also additive; axle fluid, grease; engine oil; grease;
 specific performance standards; specific properties;
 specific test methods; transmission fluid
 lubricating grease life test rig, 151 (figure)
 lubricious oxides (LOs), 319
 lubricity tests, 420 (figure). *See also* bench tests; engine
 tests; laboratory tests; *specific tests*
 Lubrizol Corporation, 455
 Luk continuously variable transmission chain, 259 (figure)

M

M2C166-H, 266, 267 (table)
 M85, 228
 Mack T-11, 73, 195 (table), 197, 199 (table), 242 (table)
 Mack T-12, 73 (table), 197, 199 (table), 242 (table)
 macrogeometry, 217 (table)
 macrotribosystem, 293–294, 295 (figure)
 manual transmission (MT), 267, 279–282. *See also* dual-
 clutch transmission (DTC); gear box; synchromesh;
 synchromesh testing
 materials. *See* engine materials
 manual transmission fluid (MTF), 37, 289
 maximum specific load (MSL), 129
 Maxwell model, 10
 medium-temperature dispersivity, 78
 melt wear, 383 (figure), 384 (figure)
 MERCON®, 266–267, 267 (table)
 metal content, 54–55
 metal matrix composites (MMCs), 340

metal oxide, 1263
 metal passivators, 48
 metal salts or organic acids (soaps), 263, 264 (figure)
 methanol, 228
 MHT-4, 79
 microgeometry, 217 (table)
 micropitting test, 183–185, 184 (figure), 185 (figure)
 microscopic contaminant, 406–407
 microtribosystem, 293–294, 295 (figure)
 mineral oil, 11, 35, 183 (figure), 187, 259–260, 260 (table)
 miniature gears, 379
 mini-rotary viscometer (MRV), 50, 51
 Mini-Traction Machine (MTM®), 204–205
 miscibility, 57, 81
 mixed lubrication, 12–13, 19, 301. *See also* biofuel
 modeling, 15, 304–305
 constant velocity joints (CVJ) and, 446–452, 452 (figure)
 wear and, 294, 304–305, 305 (table), 310–311, 314
 MoDTC. *See* molybdenum dithiocarbamate (MoDTC)
 moisture contamination, 412–413
 molybdenum dithiocarbamate (MoDTC), 29, (figure),
 224, 362 (figure), 369 (figure), 371–372, 371 (figure),
 372 (figure), 374
 molybdenum oxide, 327
 motor, 380–381, 380 (figure)
 motorcycle engine lubrication, 251–252, 253
 movable glass plate, 86
 MS-4228, 266
 multicylinder configurations, 124, 125
 multiple test acceptance criteria (MTAC), 64

N

nanoindenter, 358–360
 naphthenic oil, 41, 261
 Natural Marine Manufacturing Association (NMMA),
 252, 253 (table)
 neutral detergent, 33, 34 (table), 47. *See also* detergent
 Newton ideology, 49, 202
 nitriding, 334–335, 343
 nitrocarburizing, 335
 nitrogen oxides (NOs), 126, 231
 NLGI certification marks, 45
 NOACK Volatility Test, 71 (table), 196 (table), 241 (table)
 noise suppression, 385
 non-automotive engine, 252–253
 nonbridgine oxygen (NBO), 370
 nonconformal contact, 5
 non-soap thickened grease, 41
 nonsoap-based grease, 465
 nonvacuum-based technique, 365–366
 normal fatigue loading, 275
 North American performance standards, 64. *See also*
 American Performance Institute (API); American So-
 ciety for Testing and Materials (ASTM); API Tripartite
 system; *specific performance standards*
 Novack volatility method, 53
 numerical surface, 3–4, 8

O

off-road tests, 277, 282
 off-road vehicle, 160 (figure), 166, 173, 278–279

- oil
 - protection additives, 23, 26–27, 41
 - robustness, 111
 - sampling methods, 399–401, 400 (figure), 462
 - stability, 427–428
 - supply, 131–132
 - thickening, 24, 76, 132 (figure), 133 (figure), 244. *See also* film thickness; soot
 - viscosity, 115
 - See* lubricants; engine oil
 - oil aeration, 71 (table)
 - oil analysis. *See* engine oil, analysis
 - oil consumption, 73–74, 341. *See also* fuel consumption; fuel efficiency
 - oil control ring, 108
 - oil filter, 207–208, 208 (figure), 427, 434–436
 - oil filter tests, 429–430, 435–436. *See also* oil filter tests
 - oil pump, 109–110, 110 (figure), 126, 284 (figure)
 - gear boxes and, 164
 - starvation of, 74, 76
 - spark ignition, 244. *See also* ISLAC GF-5
 - oil-out testing, 278
 - olefin copolymers (OCPs), 24 (figure), 24–25
 - OM646 engine test, 232, 233–237
 - open loop tests, 275–276
 - optical interferometry, 86–87
 - optical microscopy, 402, 407
 - optical soot meter, 410, 414
 - organic contamination, 429
 - original equipment manufacturers (OEM) standards, 34, 36, 233, 266
 - degradation and, 64
 - fuel efficiency and, 257
 - grease and, 43
 - o-rings, 397 (figure), 398 (figure)
 - oscillating friction tribometer, 397
 - Otto cycle, 119, 120 (figure)
 - outlet antidrain, 435
 - overbased detergents, 34 (table)
 - overload, 275
 - oxidation, 26–29, 68, 201, 337, 389 (figure), 403. *See also* oxidative stability
 - oxidation inhibitor, 26, 201
 - oxidative catalytic converter, 127
 - oxidative stability, 260, 319, 323–324, 325 (figure), 388, 413, 414 (figure), 456–457, 459, 460. *See also* aging
 - oxidative wear, 300
- P**
- P/O atomic ratio, 370
 - PAG46-4, 320 (table), 321, 322, 323 (table), 323–324, 325, 326
 - paraffinic oil, 41
 - parasitic loss, 172
 - partial-load performance, 124
 - particle count, 402–403, 411, 412
 - filtration and, 430, 432–433, 434, 435
 - wear and, 405–407, 407 (figure)
 - See also* particle counter
 - particle counter, 402–403, 402 (figure), 403 (figure)
 - particulate emissions, 126, 231
 - particulate filter, 318
 - passenger cars
 - drain intervals, 371
 - engine tests, 74–76, 243–244, 245 (table)
 - fuel and, 333, 432
 - grease and, 41–43
 - lubricant performance and, 62
 - motor oil monitoring, 399
 - precision mechanics and, 381–382
 - patch test, 407 (figure), 408 (figure)
 - pedal mechanism, 42
 - Peklenik number, 5
 - Pensky Martens Closed Cup (PMCC), 56
 - percussive impact, 299 (figure)
 - performance additive. *See* additive, performance
 - performance specification. *See* performance standard
 - performance standard organizations, 217, 226. *See also* American Society for Testing and Materials (ASTM); American Petroleum Institute (API); European Automobile Manufacturers' Association (ACEA); International Lubrication Standardization and Approval Committee (ILSAC); *specific organizations*
 - performance standards, 61, 62 (figure), 75, 289–290
 - automatic transmission fluid (ATF) and, 266–26
 - bearings and, 139
 - biobased lubricants and, 466–467, 464 (table), 466 (table)
 - engine oils and, 34–36, 36 (table), 225–227, 226 (table), 227 (table)
 - heavy duty engines and, 233, 237
 - manual transmission and, 289
 - methods and, 95, 430–431
 - organizations, 66–67, 231–232, 237, 239–240, 244. *See also specific organizations*
 - passenger cars and, 233
 - small-engine, 245–247, 250 (table), 250–251. *See also* motorcycle engine lubrication
 - systems of, 63–66
 - See also* ACEA performance standards; API performance standards; *specific specifications*
 - phenates, 34 (table)
 - phosphates, 369, 370 (figure), 373
 - phosphoric acid derivatives, 202
 - phosphorus, 78 (table) 78–79, 194, 209, 318
 - photoemission electron microscopy (PEEM), 363
 - physical vapor deposition (PVD), 336, 342–343
 - pinion, 179 (table), 180 (figure), 185
 - damage and, 180, 184 (figure), 185
 - tests and, 181, 182, 186
 - torque and, 181 (figure)
 - piston, 105, 108, 122, 125–126
 - assembly, 338; 351, 352
 - coating, 340–341
 - deposits, 74
 - scuffing, 220–223, 224–225
 - sets, 106
 - velocity and, 122
 - See also* piston ring; piston skirt
 - piston pin joint, 108, 129
 - piston ring, 108, 109 (figure), 341–344, 343 (figure)
 - material, 126
 - See also* piston ring tests
 - piston ring tests, 218–219, 219 (figure), 223–224, 225 (figure), 228–229, 319, 347 (table)

piston scuffing test, 220–223
 piston skirt, 109 (figure), 220–223, 338, 340–341
 piston-rings-to-cylinder block, 108
 piston-skirt-to-cylinder block, 108
 pitch point, 168, 169 (figure)
 pitting tests, 185 (figure), 185–186, 186 (figure), 187
 planetary gears, 256 (figure), 380 (figure). *See also*
 automatic transmission fluid (ATF), planetary
 gears and
 plasma spray coating, 338, 339
 plastic contact, 302, 304
 plastic deformation, 110, 309
 plasticizer, 261, 265
 plunge, 165–166
 plunging joint, 140
 pneumatic loader, 146 (figure)
 point contact, 5, 6–7, 6 (figure), 303 (figure)
 point-contact elastohydrodynamic lubrication (EHL),
 15, 87–88
 polar head groups, 262, 263
 pollution control, 61–62. *See also* emissions; environ-
 mental standards
 polutetrafluoroethylene (PTFE), 340
 polyacrylate rubber, 115 (table)
 polyalkyleneglycols (PAGs), 321, 386
 polyalphaolefin (PAO), 35, 385
 polyglycols, 320, 321, 323, 325–326. *See also* PPG32-2;
 PPG46-4
 polyimide (PI) surface, 383 (figure)
 polyinternal olefin (PIO), 35
 polyisobutene (PIB), 24 (figure), 250
 polyisobutene (PIB) succinate, 31
 polyisobutylene succinic anhydride (PIBSA), 31
 polymer material, 382–383, 390–391, 390 (figure)
 polymers, 261–262, 394. *See also* polymer material
 polymethacrylates (PMAs), 24 (figure), 25
 polymethylsiloxane antifoam, 26 (figure)
 polypropylene-glycol monobutylethers (PPGs), 321.
 See also specific polyglycols
 polytetrafluoroethylene (PTFE), 144
 polyurea, 142, 144
 poppet valve, 107 (figure), 109
 pore-blockage particle counter, 402–403, 403 (figure)
 pour point, 25 (figure), 52, 111, 200 (table), 262 (figure),
 457
 pour point depressant (PPD), 207
 powder metallurgy, 346
 power, 105, 122, 123, 124, 169, 186, 187
 power-law relationship, 87–88, 89 (figure)
 power-on time, 383–384
 powertrain, 124–126, 157, 159, 351
 precision mechanics, 379–384
 lubricants and, 384–391, 387 (figure), 388 (figure)
 tribological simulation and, 392–398
 predictive alarms, 411–412
 pressure, 10, 11, 16–17, 126, 319, 322
 proactive alarms, 410
 probability density function (PDF), 4
 propeller (“PROP”) shafts, 166
 propshaft, 42–43
 pumping viscosity, 50
 pure sliding friction, 443

R

radial isoprenes (RIs), 25
 radial loader pneumatic mechanism (BVT-5), 147
 (figure)
 radiation scattering, 365
 Raman spectrometer, 360, 365, 366 (figure). 366–367,
 374 (figure)
 rancimat, 461
 rate-of-change-based alarms, 411
 RECESS, 311
 reciprocating engine, 119, 121. *See also* internal combus-
 tion engine; engine
 reciprocating test method, 97–98
 resource conservation requirement, 245, 249 (table).
 See also environmental standards
 reduction gears, 166
 reflection technique, 87
 reliability. *See* fatigue life
 reliability environmental tester (RET), 149–152
 renewable oil. *See* biofuel; mineral oil; vegetable oil
 re-refined oil, 41
 resistance method, 85
 resistance-capacitance oscillation, 86
 Reynolds equation, 11–12, 13, 16, 19, 90, 129, 131, 323
 rig/bench test, 134 (figure)
 ring coating, 327–328
 ring wear, 96
 road test, 273 dry-sump lubrication, 274, 276–278, 126
 Romaszewski oil bench oxidation (ROBO) test, 61, 80,
 193 (table)
 ROBO test, 61, 80, 193 (table)
 roller follower wear test, 74, 197 (table), 198, 242 (table)
 rolling, 296, 297 (table)
 Rolling Bearing–Test and Assessment for Life and
 Reliability, 149
 rolling element bearings, 149–152, 167, 172, 173.
 See also hub bearings;
 rolling friction, 444–445, 445 (table), 446 (figure)
 rolling speed, 87 (figure), 89 (figure), 91
 rotary bench test methods, 96–97
 rotary engine, 121, 379–380
 rotation generator, 380 (figure)
 rotation speed, 121
 rotor, 380 (figure)
 roughness, 4, 91–92, 92 (figure)
 effect, 16, 18
 lubrication and, 89–90
 route mean square (RMS), 4, 5
 surface and, 7, 9–10, 301 (figure), 304, 443 (table)
 round-robin field tests, 420
 route mean square (RMS) roughness, 4, 5. *See also*
 roughness
 rubber, 115 (figure)
 rust inhibitor, 33, 48, 206–207, 264–265, 265 (figure)

S

SAE, 64, 237–239
 SAE HS 806, 435
 SAE J1260, 435
 SAE J1488, 432
 SAE J1839, 432
 SAE J1858, 436

- SAE J1985, 432
 SAE J2793, 433
 SAE J300, 49, 67, 192, 238, 251 (table)
 SAE J306, 38 (table), 52
 SAE J310, 40
 SAE J905, 431–432
 salicylates, 34 (table)
 sampling. *See* oil sampling methods
 sampling hardware, 400–401
 Scanning Brookfield method, 50, 51
 scanning electron microscopy (SEM), 354–355, 355 (figure), 356 (figure). *See also* transmission electron microscopy
 scanning probe microscopy (SPM), 357
 Schiff's reagent method, 414
 scuff tests, 180–181, 181 (table), 220–225
 scuffing, 19, 420–422, 422 (table), 423
 cold, 221, 225–227, 226 (table)
 failures and, 180 (figure)
 gears and, 178 (figure), 179 (figure)
 measurement, 224–225, 421 (figure)
 resistance, 327–328, 340–341
 test, 98–100, 100–101, 181 (figure). *See also* scuff tests
 seal, 72, 106, 171 (figure), 196 (table), 285
 seal compatibility, 228, 242 (table), 260–261
 seal swell agents, 48, 265
 sealed bearing simulation tester (ABDT), 152, 153 (figure)
 sealed bearings, 147–149
 seat adjuster, 43
 seat insert valve, 344
 seizure, 19
 selective catalytic reduction (SCR) device, 127
 self-cleaning filters, 435
 Sequence IIIF, 196 (table), 197
 Sequence IIIF, 242 (table)
 Sequence IIIG, 191, 196 (table), 197
 Sequence III-GA, 191, 194, 193 (table)
 Sequence III-GB, 76, 111
 Sequence IVA, 111, 192 (table), 194
 Sequence IVA, 77
 Sequence VG, 194
 Sequence VIB, 194
 Sequence VID, 111, 192
 Sequence VIII, 192, 193 (table), 194
 service intervals, 254, 293, 298
 service life, 410 (figure), 410–411
 shear loss, 251 (table)
 shear rate, 49, 50–52, 68, 203 (figure), 324 (figure)
 shear stability, 69 (table), 80–81, 193 (table), 204, 241 (table)
 shear stress, 10–11, 49, 50–51
 shear thinning, 10, 323
 shear-flow factors, 17 (table), 18 (table)
 shear-thinning model, 10
 shifting clutch systems, 257
 shock absorber, 42
 silicone oils, 71, 386–387
 silicone rubber (VMQ-1), 115 (figure), 193 (table)
 silicon-based ceramics, 344
 simulation reliability test, 152
 skewness, 4–5
 SKF ROF, 151 (figure)
 SLBOCLE, 420
 sliding bearings, 106
 sliding splines, 43
 sliding, 296, 297 (table), 304, 352, 384
 slip-to-roll ratio, 443
 slow-speed wear test, 181–183
 sludge, 76 (table), 205–206, 208–209, 208 (figure), 429 (figure)
 smooth surface lubrication, 89
 soap-thickened grease, 41
 SOFTC 2A, 430
 solid lubricant, 387
 solubility relationships, 228
 solvent, 250
 soot, 30–31, 32, 51, 231
 contamination, 296–299
 dispersancy, 414
 tests and, 244 (table), 429 (figure), 430
 See also ash; sooted oil
 sooted oil mini-rotary viscometer, 197 (table)
 sooted oil, 72 (table), 72–73, 197 (table), 241 (table)
 soybean oil, 457, 455, 457, 459–460
 spacer layer, 86
 spark ignited engine, 119, 120, 122, 123–125, 123 (figure), 126, 127 (figure)
 specimen, 101 (figure), 102 (figure), 393 (figure)
 specimen holders, 100 (figure), 220, 222 (figure)
 spherical contacts, 7
 spindle hydraulic mechanism, 145 (figure)
 Splash lubrication, 126, 129
 spreading behavior, 387–388, 387 (figure), 388 (figure)
 spur gear, 110 (figure), 167, 168
 square rig testing, 279
 SRV 4, 20 (table), 97–98, 220 (table), 221 (figure)
 SRV EP step-load test, 326
 SRV test, 319, 324–325
 stainless steel, 407
 starter motors, 42
 start-stop-friction, 393–394
 static burst pressure, 435
 static compatibility tests, 390
 static friction, 393, 395 (figure)
 static friction model, 446–448, 447 (figure)
 static stress test, 390
 statistical alarms, 411
 steel, 342, 343 (figure), 359 (figure), 368, 407
 steering, 380
 stochastic modeling, 15
 STP512, 289
 stress cracking, 390 (figure)
 Stribeck curve, 13 (figure), 14 (figure), 106 (figure), 215, 301, 352 (figure)
 stylus profilometer, 3
 substitution cycle, 120
 sulfated ash, 55, 72, 82
 sulfonates, 34 (table)
 sulfur, 78 (table) 78–79, 209, 239, 318, 370 (figure).
 See also low-sulfur fuel
 surface, 3–5, 6, 16 (figure)
 deviation, 16 (figure)
 irregularities, 3, 4, 343

modification, 333–338, 334 (figure), 338 (table).
 342–344. *See also specific engine components*
 protection additive, 27–33, 41
See also surface analysis; surface coating; surface treatment
 surface analysis, 3–5, 351–352, 353, 375
 application of, 367–375. *See also specific applications*
 chemical properties and, 360 (figure), 361 (figure), 362 (figure), 364 (figure), 367 (figure)
 techniques, 354–367, 355 (figure), 356 (figure), 358 (figure). *See also specific techniques*
 tools, 354 (figure), 355 (figure). *See also specific tools*
 surface coating, 8–9, 313, 333–337
 cylinders and, 338–430
 pistons and, 340–344
See also specific coating; specific treatments; surface treatment
 surface treatment, 133, 313 (figure), 333–336. *See also surface coating*
 SwRI Wear Index, 433 (figure)
 synchromesh gear boxes, 161–164, 162 (table), 163 (figure), 167, 169–171, 170 (figure). *See also synchromesh testing*
 synchromesh testing, 279–280, 280 (figure)
 synthetic esters. *See esters*
 synthetic hydrocarbons, 385–387
 Synthetic Oil Filter Contaminant (SOFTC) 2A, 430
 synthetic oil, 35. *See also engine oil*

T

tachometer drive, 380 (figure)
 temperature, 9, 10, 23
 additives and, 23, 30
 aging and, 390
 bearings and, 129, 133 (figure)
 corrosion and, 241 (table)
 deposits and, 57, 79
 drive train performance and, 171–172, 172 (figure)
 effects, 61, 62, 75, 80–81, 388
 engine performance and, 124 (figure)
 flash point and, 55–56
 friction and, 333, 334 (figure)
 oil and, 131–132, 260, 261 (figure)
 seals and, 285
 surface treatments and, 333–336, 334 (figure); 336 (table)
 synthetic hydrocarbons and, 385–387
 viscosity and, 50–51, 67–70, 203–204, 204 (figure)
See also cooling tests; high-temperature corrosion bench test; low temperature
 temperature programmed desorption (TPD), 209
 TEOST MHT, 192 (table)
 TEOST-33C, 57, 79, 111–112, 192 (table)
 test components, 64, 65, 148, 149 (figure), 150. *See also specific test methods; specific tests; specimens*
 test gears, 179 (table), 179–180, 180 (figure), 185 (figure)
 test head, 148, 149 (fatigue), 150
 test methods, 49–57, 225–227, 226 (table), 227 (table).
See also specific ASTM methods performance standards
 test requirements. *See engine tests*
 test rig, 179, 282, 307, 309, 310 (figure)
 test sponsors, 64
 tester. *See bearing vibration tester; block-on-ring tester; specific test; specific tool; test rig; wear tester*
 testing organizations. *See specific organizations*
 thermal conductivity, 382
 thermal degradative conditions, 61
 thermal spray technology, 336 (table), 338, 339, 342
 thermal wear, 300
 thermal-mechanical contact analysis, 8
 thermodynamics, 119–121
 thermoelasto hydrodynamic lubrication (TEHL), 131
 thermogravimetric analysis (TGA), 431 (figure)
 Thermo-Oxidation Engine Oil Simulation Test (TEOST-33C), 57
 thickener, 24, 41, 76
 three-body abrasive wear, 296, 298 (figure)
 time of flight-secondary ion mass spectroscopy (ToF)-SiMS, 364–365, 365 (figure), 370
 Timken antiwear test, 139
 tin, 407
 Titan GT1 0W-20, 320, 321, 323 (table), 324, 325
 titanium aluminides, 344
 topographic structure, 5
 torque, 12, 123 (figure), 124, 125, 160, 274 (figure)
 measurement, 392 (figure)
 static, 446–448, 447 (figure), 450 (figure)
 transmission and, 437–439
See also constant velocity CV joint. See also rolling element bearings
 torque converter, 56 (figure), 257, 259
 total base number (TBN), 82
 total friction model, 449–450
 Total. *See HTX 822 15W-50*
 transducer positioning device, 145 (figure)
 transfer gear box, 164
 transmission, 36, 157, 255–259, 258 (figure), 274, 289–290, 346
 applied stress and, 275–276
 efficiency, 171–172, 186
 fluid, 37, 258–259. *See also automatic transmission fluid (ATF); manual transmission; transmission fluid;*
 gears and, 345–346
 load and, 173–174
 manual, 274–282
 transverse, 162 (figure)
 trends and, 160–161
See also drivetrain; specific components; specific types; transmission tests
 transmission electron microscopy (TEM), 356–357, 357 (figure), 371 (figure)
 transmission fluids, 36–39, 40 (table). *See also automatic transition fluid (ATF); manual transmission fluid (MTF)*
 transmission tests
 ASTM specification and, 286–287 (table)
 individual components, 279–287
 as a whole unit, 273–279
 transverse, 5 (figure), 162 (figure)
 trials. *See bench tests; engine tests; laboratory tests; road tests; specific tests*
 triaxial force transducer, 339 (figure), 340 (figure)

tribochemistry, 369–375, 372 (figure), 373 (figure), 376 (figure)
 tribological bench tests, 93–100, 96 (figure), 216 (figure), 216–218; 217 (figure), 218 (figure). *See also* bench testing; engine tests; laboratory tests; *specific test methods* wear tests
 tribotest categories, 306 (table)
 trunk, 381
 tryglycerides, 456
 turbodiesel, 233
 two-body abrasive wear, 296, 298 (figure)
 two-stroke engine, 119, 252–253
 two-wheel drive, 159

U

Ueda et al., 209
 unburnt hydrocarbons (HCs), 126
 United States, 455
 United States government, 110
 universal joints (UJs), 43
 University of Northern Iowa National Ag-Based Lubricants (NABL), 460, 461–462
 unsaturated fatty acids, 456

V

vacuum plasma spraying (VPS), 343
 vacuum sampling, 400–401 (figure)
 vacuum-based technique, 360–365
 valve, 105–106, 107 (figure), 109, 308–311, 309 (figure), 311 (figure), 312 (figure)
 valvetrain, 106, 107, 216 (figure), 344–345
 friction loss and, 352–353, 352 (figure)
 relief, 435
 wear, 73 (table), 77
 Van Doorne push belt, 259 (figure)
 varnish, 205
 varnish test, 76 (table)
 Veeco software, 101, 102 (figure)
 vegetable oil, 41, 254, 455–459
 genetic modification and, 459–460
 temperature and, 459, 465
 See also biofuel
 velocity. *See* angular velocity
 velocity joints. *See* constant velocity joints (CVJ)
 velocity tests, 144–146, 144 (figure), 145 (figure), 146 (table), 147 (table)
 vibration, 434 (table), 434 (figure), 435, 437
 vibration fatigue test, 435
 vibrational spectroscopy technique, 365–367, 367 (figure)
 VII, 48, 49, 51, 204
 viscoelastic constitutive equation, 10
 viscosimetrics, 24, 49, 319
 viscosity, 202 (figure), 267 (table), 403
 classification and, 237–239, 412
 control, 202–203, 200 (table)
 cranking, 49–50
 diesel fuel and, 419 (figure)
 loss, 262
 measurements, 67–69, 324 (figure)
 relationships, 9–11
 requirements, 78–82, 112

 of sooted oil, 51
 temperature and, 23–24, 51, 203–204, 204 (figure)
 test methods and, 49–52, 193 (table)
 See also specific viscosity aspects. viscosity modifier (VM)
 viscosity grades, 35 (table), 38 (table), 69, 205 (table), 288–289
 API and, 241
 in basestock, 47
 SAE and, 240 (table)
 viscosity index (VI), 203, 259, 260 (table), 261–262, 317, 321. *See also* viscosity modifier
 viscosity laminar flow, 203 (figure)
 viscosity modifier (VM), 23–26, 24 (figure), 25 (figure), 111, 259, 261–262
 viscosity tests, , 49–52, 193 (table), 244 (table), 412, 413, 414–415
 viscosity-pressure relationship, 9–10, 11, 13
 viscosity-temperature relationship, 9, 261 (figure), 391
 viscosity-temperature-pressure relationship, 10
 Viscous drag, 201
 viscous stress tensor, 11
 volatility, 53, 78, 79
 volumetric compression ratio, 120

W

wall slip, 10
 Walther equation, 9
 Wankel engine, 121
 warranty, 215, 273
 water contamination, 408, 430, 432–433
 water immersion, 278
 water separation, 428
 water tester, 414
 water tolerance, 56–57
 wax crystals, 262
 wax formation, 207
 wear, 192 (table), 297 (table), 301 (table)
 alternative fluids and, 325–326, 328
 analysis, 293–295, 294 (figure), 294 (table), 295 (table), 297 (table)
 bearings and, 134–135, 135 (figure)
 coefficients, 306 (figure), 306 (table)
 contact mechanics and, 302–304, 305 (figure)
 control, 198–201. *See also* zinc dialkyl dithiophosphate (ZDDP)
 debris, 402, 412
 engine, 73, 76, 78
 failures, 182
 ferrous density and, 405–406, 406 (figure)
 map, 304–305, 305 (figure)
 mechanisms of, 110
 modeling, 294, 304–305, 305 (table), 310–311, 314
 particles and, 405–407, 406 (figure), 412
 pistons and, 340
 precision mechanics and, 394–396, 396 (figure), 397 (figure), 398 (figure)
 rate, 300–301, 300 (figure), 327
 reduction, 312 (table), 312–313, 313 (figure)
 scar, 370
 tester, 96–97, 97 (figure), 98 (figure), 100
 valvetrain, 73 (table), 77, 295 (figure)
 See also wear tests

wear test rig, 97, 100

wear tests, 305–308, 307 (figure), 307 (table), 308 (figure)
 analysis, 293–295, 294 (figure), 294 (table), 295 (figure)
 measurement and, 218 (figure), 223–224, 223 (figure),
 307
 pistons and, 218–219, 220, 225 (figure)
 in service oil, 406 (figure)
 slow speed, 181–183, 182 (table), 183 (figure)
 test methods and, 96–102, 298–299

See also slow-speed wear test

Weierstrass-Mandelborot (M-W), 10

wet clutch performance, 251

wet-stump circulating system, 400 (figure)

wetting modifiers, 38

wheel bearing, 42, 43, 44

wheel bearing grease, 467

white-light interferometer, 3

window winder, 42

World War II, 64

X

x-ray absorption near-edge structure (XANES), 362–363,
 363 (figure), 364 (figure), 370–371, 371 (figure)

x-ray absorption near-edge structure (XANES)
 spectroscopy, 199, 200

x-ray absorption spectra (XAS), 362

x-ray photoelectron spectroscopy (XPS), 361 (figure),
 361–362, 362 (figure), 369

x-ray photoemission electron microscopy (X-PEEM),
 363–364, 364 (figure)

x-ray transmission method, 85

Z

Zhu, D., 89, 90

zinc dialkyl dithiophosphate (ZDDP), 30, 48, 198–201,
 369–371, 369 (figure), 370 (figure), 371 (figure)

 biodiesel and, 209

 corrosion and, 207

 diesel engines and, 191

 friction modification and, 220

 MoDTC and, 202, 206, 224

 phosphorus and, 191, 194

 Al-Si alloy and, 373–374

zinc phosphates, 369–370, 370 (figure). *See also* zinc
 dialkyl dithiophosphate (ZDDP)



Simon C. Tung

Dr. Simon C. Tung has become an internationally recognized leader in the field of tribology and lubrication engineering as a result of 26 years of industrial applied research and project management with General Motors and through his service to the tribology technical community. Tung has been involved in the original engine manufacturers (OEM) and automotive industry since joining General Motors Research laboratories in 1982.

While there he led pioneering research and development on automotive powertrain tribology and lubrication engineering and was appointed a technical fellow at the General Motors Research and Development Center in 2003. In 2008, he joined the Industrial Technology Research Institute (ITRI) as General Director, where he was responsible for managing all research and development programs in the green energy and environmental research laboratories. He made significant contributions in the research areas of green energy, energy storage systems, hydrogen energy, energy efficient fuels and lubricants, and greenhouse emissions reduction. Dr. Tung's technical expertise includes energy technology, environmental engineering, lubrication, and automotive systems. He has over 180 published works and holds more than 30 U.S. and international patents on novel methods of improving energy efficiency and environmental protection.

Dr. Tung has received many distinguished honors, including being named Fellow of the Society of Automotive Engineers (SAE) and Fellow in the Society of Tribologists and Lubrication Engineers (STLE), as well as receiving the highest honor of Gold Award from the Engineering Society of Detroit (ESD). In addition, he has received 25 professional outstanding achievements awards during his career. He was recently honored with SAE International's Edward N. Cole Award for Automotive Engineering Innovation during the SAE 2011 World Congress.

In August 2011, Dr. Tung was appointed the global OEM industry liaison manager by R.T. Vanderbilt. In this new capacity, Dr. Tung leads global OEM liaison activities by developing and disseminating global OEM advanced lubricant requirements and energy resources technologies. In addition, he assists in advancing tribology and lubricant technology programs at R.T. Vanderbilt. He is also responsible for developing methods and providing technical input for the testing and evaluation of fuel efficient lubricant products for potential commercialization.

Dr. Tung holds a Ph.D. in chemical engineering from Rensselaer Polytechnic Institute. He also received an MBA from University of Michigan-Ann Arbor.



George E. Totten

Dr. George E. Totten is president of G.E. Totten & Associates, LLC, a research, sales, and consulting firm specializing in thermal processing, industrial lubrication problems, and equipment supply. In addition, he is a visiting professor at the University of Sao Paulo, an adjunct professor at Texas A&M University, and a research professor at Portland State University. Until his retirement in 2001, Dr. Totten was a senior research scientist at

Union Carbide Corporation, where he was responsible for their research and development programs in metalworking quenchants, hydraulic fluids, and exploratory research programs in lubrication fundamentals. Dr. Totten is the section chairman of ASTM D02 L.06 on Non-Lubricating Oils and is a member of the ASTM committee on publications.

Dr. Totten has published over 600 patents, technical papers, and books, including: *Handbook of Quenchants and Quenching Technology*, *Steel Heat Treating Handbook* (volumes 1 and 2), *Handbook of Residual Stress and Deformation of Steel*, *Fire Resistance of Industrial Fluids* (ASTM STP 1284), *Tribology of Hydraulic Pump Testing* (ASTM STP 1310), *Handbook of Hydraulic Fluid Technology and Hydraulic Failure Analysis: Fluids, Components and System Effects* (ASTM STP 1339), *Bench Testing of the Lubrication and Wear Properties of Industrial Fluids Used in Machinery Applications* (ASTM STP 1404), and *Handbook of Aluminum: Physical Metallurgy and Processes* (Volumes 1 and 2, and volume one of *Handbook of Lubrication and Tribology: Application and Maintenance*, Second Edition.

Dr. Totten received B.S. and M.S. degrees in chemistry from Fairleigh Dickinson University in New Jersey and a Ph.D. in physical organic chemistry from New York University. Dr. Totten is past president of the International Federation for Heat Treatment and Surface Engineering (IFHTSE), a fellow of ASM International, SAE International, and IFHTSE, and a founding fellow of AMME (World Academy of Materials Manufacturing Engineering). Currently, Dr. Totten is the co-editor of ASTM's *Journal of Materials Performance and Characterization* (MPC) with Professor Richard Neu.

R-428



www.astm.org

ISBN: 978-0-8031-7036-0

Stock #: MNL62